OPEN ACCESS

University of BRISTOL

This electronic thesis or dissertation has been downloaded from Explore Bristol Research, http://research-information.bristol.ac.uk

Author:
Boonrod, Pongsathon

Title:
Synthetic and Computational Study Leading Towards Structure-Property Relationships in Poly(aniline)-Based Conjugated Microporous Polymers

General rights
Access to the thesis is subject to the Creative Commons Attribution - NonCommercial-No Derivatives 4.0 International Public License. A copy of this may be found at https://creativecommons.org/licenses/by-nc-nd/4.0/legalcode This license sets out your rights and the restrictions that apply to your access to the thesis so it is important you read this before proceeding.

Take down policy
Some pages of this thesis may have been removed for copyright restrictions prior to having it been deposited in Explore Bristol Research. However, if you have discovered material within the thesis that you consider to be unlawful e.g. breaches of copyright (either yours or that of a third party) or any other law, including but not limited to those relating to patent, trademark, confidentiality, data protection, obscenity, defamation, libel, then please contact collections-metadata@bristol.ac.uk and include the following information in your message:

• Your contact details
• Bibliographic details for the item, including a URL
• An outline nature of the complaint

Your claim will be investigated and, where appropriate, the item in question will be removed from public view as soon as possible.

Synthetic and Computational Study Leading Towards Structure-Property Relationships in Poly(aniline)-Based Conjugated Microporous Polymers

Pongsathon Boonrod

School of Chemistry

University of Bristol

A dissertation submitted to the University of Bristol in on accordance with the requirements for award of the degree of Doctor of Philosophy in Chemistry in the Faculty of Science.

July 2022

Word count: 75773

Abstract

Poly(aniline)-based conjugated microporous polymers (PANI-CMPs) have been developed over the past decade, combining the properties from the parent materials. In this thesis, both theoretical and experimental approaches have been applied to better understand the structure-property relationships for the design of PANI-CMPs. Several descriptors have been designed based on previous publications and newly created in this study for systematic descriptions of PANI-CMP structures. Meanwhile, this study has also covered various aspects of material properties including spectroscopic properties, porosities, and interactions with CO_2 molecules. On the theoretical side, DFT and TD-DFT calculations have been applied to simulate properties of different models at several levels of complexities. Data from experiments and from calculation then have been compared.

Various PANI-CMPs have been prepared from different starting monomers, with three core monomer units (triphenylamine, 1,3,5-triphenylbenzene, and 2,4,6-triphenyl-1,3,5-triazine) and two linker (1,4-phenylene and 2,7-fluorenylene) monomer units used in this study. Other factors that can affect properties of resulting PANI-CMPs, namely functionality pathways, functional group ratios, and solubility tuning, have also been varied. In total, 72 different syntheses have been attempted, and 47 attempts have successfully produced polymers. Structure-property relationships in PANI-CMPs have been found to be complicated, with some factors being affected simultaneously by multiple preceding factors.

It is also established in this study that structures of polymers including PANI-CMPs are hierarchical with four different levels of structures. The simplest level of structures concerns repeating units, the higher levels concern arrangements of structures of lower levels, and the highest level of structures is the bulk polymers. This study has found that properties of bulk polymers may not be described correctly by computational models of lower levels.

While a full structure-property relationship cannot be completely formulated based on this study, this study should lead to new systematic approaches to determining structure-property relationships in PANI-CMPs.

Acknowledgments

Throughout the span of my PhD study in the University of Bristol, there are many entities and people that have provided both academic and non-academic supports. Without helping hands from these people, my PhD study would not have progressed as it is in the current form.

First of all, I would like to express my greatest gratitude to Prof Charl FJ Faul and Dr Natalie Fey, my great supervisors who have provided the greatest supports over the course of my PhD study. My two supervisors have not only offered academic supports but also taken care of my wellbeing, especially during the hard time when the pandemic has halted research processes for a long while. It would not be an exaggeration at all if I say that my thesis and my study could not be successful without their valuable helps.

I would also like to deliver my gratitude to members of the Faul research group which I have spent most of my time in the University of Bristol with since I joined the group in April 2017. There are a lot of great memories happening among us during my time I have been physically with them, and even after I left the UK for the write-up at the end of my funding, fellow Faul research group members are still helpful and ready to help me out even when we are now thousands of kilometers apart. I would cherish our time together for as long as I can. Meanwhile, although I have not spent as much time with fellow members of the Fey research group due to the nature of my research, there are significant memories of me in this research group as well. I could say that I am really proud to be part of both research groups.

I would also like to give the big thanks to the Bristol Centre for Functional Nanomaterials (BCFN) for the important trainings during my MSc year and my first PhD year which have led their way to my current PhD project. Besides the training, the BCFN, especially Dr Annela Seddon and Dr Ian Lindsay, also provided additional supports for me regardless of being academic or personal issues. I have also owed a lot to members of 2016 and 2017 cohorts of BCFN students. Although as our studies progress, we might have spent less time together than in our first years, these folks would still be in my memories as my group of first friends in Bristol.

I would like to thank Dr Richard Wingad, Dr Hsuan-Hung Liao, and Dr Claire Webster who has provided technical supports and discussions during the development of synthesis techniques for PANI-CMPs. On the same note, I would like to thank various facilities in the School of Chemistry, University of Bristol for helps regarding analyses of synthesised PANI-CMPs, their related oligomers, and their precursors. I would also like to thank the Advanced Computing Research Centre (ACRC) for allowing me to use their high-performance computing facilities for my calculations.

Doing a postgraduate research study abroad is a challenging task, especially when it has been later found out that besides the depression, I also have autism spectrum disorder (ASD) which have been undetected for about two and a half decades. For these reasons, I would like to thank various entities, both within and outside the university, namely the Student Counselling Service (especially Ms Helen who pointed out for the first time in my life that I might have ASD), the Students' Health Service, the Bristol Autism Spectrum Service (BASS, who performed the diagnosis and ran the post-diagnosis support group which helped me understanding my conditions greatly), the Disability Services, and Randstad Student Support (in particular, Ms Donna-Marie Lane).

I would also like to express the great gratitude to the Royal Thai Government Scholarship for the financial support and the preparation prior to travelling to the UK, to the National Nanotechnology Center for the support during the writing-up process, and to the Office of the

Educational Affairs, the Royal Thai Embassy, London for supports, visits, and check-ups I have got since the first day I arrived in the UK.

I would like to thank my brother for not only financially supporting me during the write-up process after the end of funding but also for taking care of some issues, giving some suggestions, and for understanding my gender identity. I would also like to thank other people whose names or mentions might have been omitted, including several business establishments who have let me use their facilities to finish my thesis.

Finally, this paragraph is dedicated to both of my late parents.

Author’s Declaration

I declare that the work in this dissertation was carried out in accordance with the requirements of the University's Regulations and Code of Practice for Research Degree Programmes and that it has not been submitted for any other academic award. Except where indicated by specific reference in the text, the work is the candidate's own work. Work done in collaboration with, or with the assistance of, others, is indicated as such. Any views expressed in the dissertation are those of the author.

SIGNED: ..... DATE:.....

Table of Contents

ABSTRACT ..... **I**

ACKNOWLEDGMENTS ..... **II**

AUTHOR'S DECLARATION ..... **IV**

TABLE OF CONTENTS ..... **V**

LIST OF TABLES ..... **XII**

LIST OF FIGURES ..... **XX**

LIST OF SCHEMES ..... **XXXI**

LIST OF ABBREVIATIONS ..... **XXXIV**

CHAPTER 1 INTRODUCTION **1**

1.1 Porosity and Porous Materials 1
1.1.1 Conjugated Microporous Polymers *2*
1.1.2 Poly(aniline)-based Conjugated Microporous Polymers (PANI-CMPs) *5*
1.1.3 Adsorption Analyses for Porous Materials *12*
1.1.3.1 Brunauer-Emmett-Teller (BET) Analysis of N_2 Adsorption Isotherm Data at 77 K 13
1.1.3.2 Additional Analyses from Nitrogen Adsorption Isotherm Data at 77 K 17
1.1.3.3 Carbon Dioxide Adsorption Isotherms 19
1.2 Structure-Property Relationships 21
1.3 Computational Chemistry 23
1.3.1 Levels of Theory *24*
1.3.1.1 Classical Mechanics Path: Molecular Mechanics 24
1.3.1.2 Quantum Mechanics Path: Hartree-Fock (HF) Methods and Density Functional Theory (DFT) Methods 26
1.3.2 Computational Chemistry for the Study of Poly(aniline)s and Oligo(aniline)s *31*
1.3.3 Computational Chemistry for the Study of Conjugated Microporous Polymers *33*
1.4 Aim, Objectives, and Thesis Outline 34
1.5 References 35

CHAPTER 2 METHODOLOGY **41**

2.1 Monomers Chosen for Studies of PANI-CMPs 41
2.2 Chemical Syntheses 42
2.2.1 Syntheses of PANI-CMPs by BH.BXJ Methods *42*
*2.2.2 Syntheses of 2,4,6-Triphenyl-1,3,5-triazine Core Monomers (**TPT**-Br_3 and **TPT**-$(NH_2)_3$)* *45*
2.2.3 Chemical and Equipment Suppliers *45*
2.3 Spectroscopic Analyses of Obtained Products 46
2.4 Morphological Analyses on PANI-CMPs 46
2.5 Computational Studies 46
2.6 References 47

CHAPTER 3 MODELLING OLIGO(ANILINE)S TOWARDS PANI-CMPS **51**

3.1 Structure Descriptors for the Study of Poly(aniline)s, Oligo(aniline)s, and PANI-CMPs 51
3.1.1 Descriptors for Primary Structures (BQ Units) *54*
3.1.1.1 Enumerations of Electron Delocalisation Patterns in Conjugated Systems 56
3.1.2 Descriptors for Secondary Structures *60*
3.1.3 Electronic Structure Descriptors *62*
3.2 Theoretical Studies of Oligo(aniline)s with Different Topologies 66
3.2.1 Structures of Branched and Unbranched Oligo(aniline)s *67*
3.2.2 Structures of PANI-CMP Oligomeric Models *77*
3.2.2.1 Geometric Structural Parameters for PANI-CMPs 77
3.2.2.2 Structures of **OTPA-BZN-210** and **OTPA-BZN-221** Models 79

3.2.2.3 Structures of **OTPA-FLR-210** Oligomers 85
3.2.2.4 Structures of **OTPB-BZN-210** and **OTPB-FLR-210** Oligomers 87
3.2.2.5 Structures of **OTPT-BZN-210** and **OTPT-FLR-210** Oligomers 91
3.2.2.6 Overall Effects of Monomer Units 94
3.3 Electronic Structures and Optical Spectra of PANI-CMP Oligomers 96
*3.3.1 Optical Spectra of **210** Oligomer Models 98*
3.3.1.1 Optical Spectra of **OTPA-BZN-210** and **OTPA-FLR-210** 98
3.3.1.2 Optical Spectra of **OTPB-BZN-210** and **OTPB-FLR-210** 106
3.3.1.3 Optical Spectra of **OTPT-BZN-210** and **OTPT-FLR-210** 109
3.3.1.4 Effects of Core Units on Electronic Transition Energies 112
3.3.2 Effects of Topologies and Strains 115
3.3.2.1 Optical Spectra of **OTPA-BZN-221** and **OTPA-FLR-221** 115
3.3.2.2 Optical Spectra of **OTPB-BZN-221** and **OTPB-FLR-221** 123
3.3.2.3 Optical Spectra of **OTPT-BZN-221** and **OTPT-FLR-221** 131
3.3.3 Comparisons between Theoretical and Experimental Spectra 139
3.4 Conclusions and Remarks 144
3.5 References 145

CHAPTER 4 SYNTHESES OF PANI-CMPS AND PROPERTIES OF PREPARED MATERIALS 149

4.1 Tuning Properties of PANI-CMPs 149
4.1.1 Effects of Monomer Unit Structures 149
4.1.2 Effects from Monomer Functionalities 151
4.1.3 Previous Property Tuning Attempts of PANI-CMPs 152
4.1.4 PANI-CMPs Studied in This Project 154
4.2 Studies of PANI-CMPs Prior to the BXJ Publication 154
4.3 Syntheses of PANI-CMPs by BH.BXJ Method 156
4.3.1 Factors to Consider for the Synthesis 156
4.3.2 Synthesis Outcomes 157
4.4 FT-IR Spectroscopic Analyses of PANI-CMPs 163
4.5 Porosity and Morphology Analyses of PANI-CMPs 169
4.5.1 Nitrogen Adsorption Isotherm Analyses at 77 K 169
4.5.2 Electron Microscope Imaging of Selected PANI-CMPs 171
4.5.3 Powder X-Ray Diffraction (XRD) of Selected PANI-CMPs 172
4.6 Carbon Dioxide Adsorption at Ambient Temperatures 173
4.6.1 CO_2 Uptake Performances at 273 K of PANI-CMPs 173
4.6.2 Thermodynamics of CO_2 Adsorptions of PANI-CMPs 177
4.7 Conclusions and Remarks 180
4.8 References 181

CHAPTER 5 COMPUTATIONAL STUDIES OF ADSORPTION PERFORMANCES OF PANI-CMPS 183

5.1 Non-Covalent Interactions for the Studies of Adsorptions 183
5.1.1 General Concepts about Non-Covalent Interactions 183
5.1.2 Studies of Non-Covalent Interactions between Aromatic Systems and CO_2 185
5.2 Studies of CO_2 Interactions on **OTPA-BZN-210** Models 189
*5.2.1 Binding Sites on **OTPA-BZN-210** Models 189*
5.2.2 Effects of Conformers 196
5.2.3 Effects of Oxidation States 199
5.3 Effects of Monomer Units 200
5.3.1 Geometries of Imine Binding Sites 201
5.3.2 Geometries of Linker Binding Sites 202
5.3.3 Geometries of Core Binding Sites 203
5.4 Computational Studies on Adsorption of **OTPA-BZN-430** Models 206
*5.4.1 Star-Shaped **OTPA-BZN-430** Oligomer 207*
*5.4.2 Linear **OTPA-BZN-430** Oligomer 209*
5.5 Conclusions and Remarks 210
5.6 References 211

CHAPTER 6 CONCLUSIONS AND FURTHER OPPORTUNITIES 213

6.1 THEORETICAL STUDIES OF PANI-CMPS 213
6.1.1 Modelling Structures of PANI-CMPs 213
6.1.1.1 Modelling Tertiary and Quaternary Structures of PANI-CMPs 213
6.1.1.2 Gaps in Theoretical Studies of PANI-CMP Secondary Structures 215
6.1.2 Interactions between PANI-CMPs and Adsorbate Molecules 216
6.2 EXPERIMENTAL STUDIES OF PANI-CMPS 216
6.2.1 Systematic Studies of Structure-Property and Property-Property Relationships 217
6.2.2 Further Explorations of PANI-CMP Properties 218
6.2.2.1 Different Synthesis Methods of PANI-CMPs 218
6.2.2.2 Further Analyses of PANI-CMPs 218
6.2.2.3 Explorations of Other Adsorbates 218
6.3 REFERENCES 218

APPENDIX A DETAILS RELATED TO DFT OPTIMISATIONS AND MICROSCOPIC STRUCTURES 221

A.1 OPTIMISED STRUCTURES OF TANI AND BRANCHED DERIVATIVES FOR MICROSCOPIC STRUCTURE ANALYSES 221
A.1.1 Optimised Structures of TANI 221
A.1.1.1 TANI, **LEB** State 221
A.1.1.2 TANI, ^{1}**ES** State 222
A.1.1.3 TANI, ^{3}**ES** State 223
A.1.2 Optimised Structures of TANI-2 224
A.1.2.1 TANI-2, **LEB** State 224
A.1.2.2 TANI-2, ^{1}**ES** State 225
A.1.2.3 TANI-2, ^{3}**ES** State 227
A.1.3 Optimised Structures of TANI-23 228
A.1.3.1 TANI-23, **LEB** State 228
A.1.3.2 TANI-23, ^{1}**ES** State 230
A.1.3.3 TANI-23, ^{3}**ES** State 231
A.1.4 Optimised Structures of TANI-14 233
A.1.4.1 TANI-14, **LEB** State 233
A.1.4.2 TANI-14, ^{1}**ES** State 235
A.1.4.3 TANI-14, ^{3}**ES** State 236
A.1.5 Microscopic Structures of TANI and Branched Derivatives 237
A.2 OPTIMISED STRUCTURES OF PANI-CMP OLIGOMERIC MODELS FOR PRIMARY AND SECONDARY STRUCTURE ANALYSES 238
*A.2.1 Optimised Structures of **OTPA-BZN-210** Oligomers 238*
A.2.1.1 **OTPA-BZN-210**, **LEB** State 238
A.2.1.2 **OTPA-BZN-210**, ^{1}**ES** State 239
A.2.1.3 **OTPA-BZN-210**, ^{3}**ES** State 241
A.2.1.4 **OTPA-BZN-210**, **EB** State 242
*A.2.2 Optimised Structures of **OTPA-BZN-221** Oligomers 243*
A.2.2.1 **OTPA-BZN-221**, **LEB** State 243
A.2.2.2 **OTPA-BZN-221**, ^{1}**ES** State 245
A.2.2.3 **OTPA-BZN-221**, ^{5}**ES** State 246
A.2.2.4 **OTPA-BZN-221**, **EB** State 248
*A.2.3 Optimised Structures of **OTPA-FLR-210** Oligomers 249*
A.2.3.1 **OTPA-FLR-210**, **LEB** State 249
A.2.3.2 **OTPA-FLR-210**, ^{1}**ES** State 251
A.2.3.3 **OTPA-FLR-210**, ^{3}**ES** State 252
A.2.3.4 **OTPA-FLR-210**, **EB** State 254
*A.2.4 Optimised Structures of **OTPA-FLR-221** Oligomers 255*
A.2.4.1 **OTPA-FLR-221**, **LEB** State 255
A.2.4.2 **OTPA-FLR-221**, ^{1}**ES** State 257
A.2.4.3 **OTPA-FLR-221**, ^{5}**ES** State 259
A.2.4.4 **OTPA-FLR-221**, **EB** State 261
*A.2.5 Optimised Structures of **OTPB-BZN-210** Oligomers 263*
A.2.5.1 **OTPB-BZN-210**, **LEB** State 263

A.2.5.2 **OTPB-BZN-210**, **^{1}ES** State 264
A.2.5.3 **OTPB-BZN-210**, **^{3}ES** State 266
A.2.5.4 **OTPB-BZN-210**, **EB** State 267
*A.2.6 Optimised Structures of **OTPB-BZN-221** Oligomers 269*
A.2.6.1 **OTPB-BZN-221**, **LEB** State 269
A.2.6.2 **OTPB-BZN-221**, **^{1}ES** State 271
A.2.6.3 **OTPB-BZN-221**, **^{5}ES** State 272
A.2.6.4 **OTPB-BZN-221**, **EB** State 274
*A.2.7 Optimised Structures of **OTPB-FLR-210** Oligomers 276*
A.2.7.1 **OTPB-FLR-210**, **LEB** State 276
A.2.7.2 **OTPB-FLR-210**, **^{1}ES** State 278
A.2.7.3 **OTPB-FLR-210**, **^{3}ES** State 279
A.2.7.4 **OTPB-FLR-210**, **EB** State 281
*A.2.8 Optimised Structures of **OTPB-FLR-221** Oligomers 283*
A.2.8.1 **OTPB-FLR-221**, **LEB** State 283
A.2.8.2 **OTPB-FLR-221**, **^{1}ES** State 285
A.2.8.3 **OTPB-FLR-221**, **^{5}ES** State 287
A.2.8.4 **OTPB-FLR-221**, **EB** State 289
*A.2.9 Optimised Structures of **OTPT-BZN-210** Oligomers 291*
A.2.9.1 **OTPT-BZN-210**, **LEB** State 291
A.2.9.2 **OTPT-BZN-210**, **^{1}ES** State 293
A.2.9.3 **OTPT-BZN-210**, **^{3}ES** State 294
A.2.9.4 **OTPT-BZN-210**, **EB** State 296
*A.2.10 Optimised Structures of **OTPT-BZN-221** Oligomers 297*
A.2.10.1 **OTPT-BZN-221**, **LEB** State 297
A.2.10.2 **OTPT-BZN-221**, **^{1}ES** State 299
A.2.10.3 **OTPT-BZN-221**, **^{5}ES** State 300
A.2.10.4 **OTPT-BZN-221**, **EB** State 302
*A.2.11 Optimised Structures of **OTPT-FLR-210** Oligomers 304*
A.2.11.1 **OTPT-FLR-210**, **LEB** State 304
A.2.11.2 **OTPT-FLR-210**, **^{1}ES** State 305
A.2.11.3 **OTPT-FLR-210**, **^{3}ES** State 307
A.2.11.4 **OTPT-FLR-210**, **EB** State 309
*A.2.12 Optimised Structures of **OTPT-FLR-221** Oligomers 310*
A.2.12.1 **OTPT-FLR-221**, **LEB** State 310
A.2.12.2 **OTPT-FLR-221**, **^{1}ES** State 312
A.2.12.3 **OTPT-FLR-221**, **^{5}ES** State 314
A.2.12.4 **OTPT-FLR-221**, **EB** State 316
A.3 OPTIMISED STRUCTURES OF PANI-CMP OLIGOMERIC MODELS FOR NON-COVALENT INTERACTIONS WITH CO_2 318
*A.3.1 Optimised Structures of **OTPA-BZN-210** Oligomers 318*
A.3.1.1 **OTPA-BZN-210**, **EB** State, trans-syn Conformer (Default Conformer) 318
A.3.1.2 **OTPA-BZN-210**, **EB** State, trans-anti Conformer 320
A.3.1.3 **OTPA-BZN-210**, **EB** State, cis-syn Conformer 321
A.3.1.4 **OTPA-BZN-210**, **EB** State, cis-anti Conformer 322
A.3.1.5 **OTPA-BZN-210**, **LEB** State, trans-syn Conformer 323
*A.3.2 Optimised Structures of Other **210** Oligomers 325*
A.3.2.1 **OTPA-FLR-210**, **EB** State 325
A.3.2.2 **OTPB-BZN-210**, **EB** State 326
A.3.2.3 **OTPB-FLR-210**, **EB** State 328
A.3.2.4 **OTPT-BZN-210**, **EB** State 330
A.3.2.5 **OTPT-FLR-210**, **EB** State 331
*A.3.3 Optimised Structures of **OTPA-BZN-430** Oligomers 333*
A.3.3.1 Star-Shaped **OTPA-BZN-430**, **EB** State 333
A.3.3.2 Linear/Coiled **OTPA-BZN-430**, **EB** State 335
A.4 OPTIMISED STRUCTURES OF ADDUCTS BETWEEN PANI-CMP OLIGOMERS AND CO_2 338
*A.4.1 Optimised Structures of Adducts between **OTPA-BZN-210** Oligomers and CO_2 ..... 338*
A.4.1.1 **OTPA-BZN-210**, **EB** State, with CO_2 Binding on Imine Nitrogen Atom 338
A.4.1.2 **OTPA-BZN-210**, **EB** State, with CO_2 Binding on Core Unit, near Hydrogen Atoms 339

A.4.1.3 **OTPA-BZN-210**, **EB** State, with CO_2 Binding on Core Unit, away from Hydrogen Atoms 341
A.4.1.4 **OTPA-BZN-210**, **EB** State, with CO_2 Binding on Linker Unit, near Hydrogen Atoms 342
A.4.1.5 **OTPA-BZN-210**, **EB** State, with CO_2 Binding on Linker Unit, away from Hydrogen Atoms 344
A.4.1.6 **OTPA-BZN-210**, **LEB** State, with CO_2 Binding on Imine Nitrogen Atom 345
A.4.1.7 **OTPA-BZN-210**, **LEB** State, with CO_2 Binding on Core Unit 346
A.4.1.8 **OTPA-BZN-210**, **LEB** State, with CO_2 Binding on Linker Unit 348
*A.4.2 Optimised Structures of Adducts between **OTPA-FLR-210** Oligomers and CO_2 ..... 349*
A.4.2.1 **OTPA-FLR-210**, **EB** State, with CO_2 Binding on Imine Nitrogen Atom 349
A.4.2.2 **OTPA-FLR-210**, **EB** State, with CO_2 Binding on Core Unit 351
A.4.2.3 **OTPA-FLR-210**, **EB** State, with CO_2 Binding on Linker Unit 352
*A.4.3 Optimised Structures of Adducts between **OTPB-BZN-210** Oligomers and CO_2 ..... 354*
A.4.3.1 **OTPB-BZN-210**, **EB** State, with CO_2 Binding on Imine Nitrogen Atom 354
A.4.3.2 **OTPB-BZN-210**, **EB** State, with CO_2 Binding on Core Unit 355
A.4.3.3 **OTPB-BZN-210**, **EB** State, with CO_2 Binding on Linker Unit 357
*A.4.4 Optimised Structures of Adducts between **OTPB-FLR-210** Oligomers and CO_2 ..... 358*
A.4.4.1 **OTPB-FLR-210**, **EB** State, with CO_2 Binding on Imine Nitrogen Atom 358
A.4.4.2 **OTPB-FLR-210**, **EB** State, with CO_2 Binding on Core Unit 360
A.4.4.3 **OTPB-FLR-210**, **EB** State, with CO_2 Binding on Linker Unit 362
*A.4.5 Optimised Structures of Adducts between **OTPT-BZN-210** Oligomers and CO_2 ..... 364*
A.4.5.1 **OTPT-BZN-210**, **EB** State, with CO_2 Binding on Imine Nitrogen Atom 364
A.4.5.2 **OTPT-BZN-210**, **EB** State, with CO_2 Binding on Core Unit 365
A.4.5.3 **OTPT-BZN-210**, **EB** State, with CO_2 Binding on Linker Unit 367
*A.4.6 Optimised Structures of Adducts between **OTPT-FLR-210** Oligomers and CO_2 ..... 368*
A.4.6.1 **OTPT-FLR-210**, **EB** State, with CO_2 Binding on Imine Nitrogen Atom 368
A.4.6.2 **OTPT-FLR-210**, **EB** State, with CO_2 Binding on Core Unit 370
A.4.6.3 **OTPT-FLR-210**, **EB** State, with CO_2 Binding on Linker Unit 372
*A.4.7 Microscopic Structures of the Adducts between **210** Oligomers and CO_2 ..... 374*
A.4.7.1 Microscopic Structures of Imine/Amine Binding Sites 375
A.4.7.2 Microscopic Structures of **BZN** Linker Binding Sites 382
A.4.7.3 Microscopic Structures of **FLR** Linker Binding Sites 387
A.4.7.4 Microscopic Structures of **TPA** Core Binding Sites 391
A.4.7.5 Microscopic Structures of **TPB** Linker Binding Sites 394
A.4.7.6 Microscopic Structures of **TPT** Core Binding Sites 397
A.4.7.7 Detailed Discussions of Geometries in PANI-CMPs–CO_2 Non-Covalent Interactions 398
*A.4.8 Optimised Structures of Adducts between **OTPA-BZN-430** Oligomers and CO_2 ..... 401*
A.4.8.1 Optimisation Processes of Adducts between Linear/Coiled **OTPA-BZN-430** Studies and CO_2 401
A.4.8.2 Star-Shaped **OTPA-BZN-430**, **EB** State, with CO_2 Binding on Inner Imine Nitrogen Atom, Branch 1 405
A.4.8.3 Star-Shaped **OTPA-BZN-430**, **EB** State, with CO_2 Binding on Outer Imine Nitrogen Atom, Branch 1 408
A.4.8.4 Star-Shaped **OTPA-BZN-430**, **EB** State, with CO_2 Binding on Inner Core Unit, Branch 1 411
A.4.8.5 Star-Shaped **OTPA-BZN-430**, **EB** State, with CO_2 Binding on Outer Core Unit, Branch 1 414
A.4.8.6 Star-Shaped **OTPA-BZN-430**, **EB** State, with CO_2 Binding on Linker Unit, Branch 1 416
A.4.8.7 Star-Shaped **OTPA-BZN-430**, **EB** State, with CO_2 Binding on Inner Imine Nitrogen Atom, Branch 2 419
A.4.8.8 Star-Shaped **OTPA-BZN-430**, **EB** State, with CO_2 Binding on Outer Imine Nitrogen Atom, Branch 2 422
A.4.8.9 Star-Shaped **OTPA-BZN-430**, **EB** State, with CO_2 Binding on Inner Core Unit, Branch 2 425
A.4.8.10 Star-Shaped **OTPA-BZN-430**, **EB** State, with CO_2 Binding on Outer Core Unit, Branch 2 427
A.4.8.11 Star-Shaped **OTPA-BZN-430**, **EB** State, with CO_2 Binding on Linker Unit, Branch 2 430
A.4.8.12 Star-Shaped **OTPA-BZN-430**, **EB** State, with CO_2 Binding on Inner Imine Nitrogen Atom, Branch 3 433
A.4.8.13 Star-Shaped **OTPA-BZN-430**, **EB** State, with CO_2 Binding on Outer Imine Nitrogen Atom, Branch 3 436
A.4.8.14 Star-Shaped **OTPA-BZN-430**, **EB** State, with CO_2 Binding on Inner Core Unit, Branch 3 438
A.4.8.15 Star-Shaped **OTPA-BZN-430**, **EB** State, with CO_2 Binding on Outer Core Unit, Branch 3 441
A.4.8.16 Star-Shaped **OTPA-BZN-430**, **EB** State, with CO_2 Binding on Linker Unit, Branch 3 444
A.4.8.17 Linear/Coiled **OTPA-BZN-430**, **EB** State, with CO_2 Binding, Mode 1 447
A.4.8.18 Linear/Coiled **OTPA-BZN-430**, **EB** State, with CO_2 Binding, Mode 2 449
A.4.8.19 Linear/Coiled **OTPA-BZN-430**, **EB** State, with CO_2 Binding, Mode 3 452

A.4.8.20 Linear/Coiled **OTPA-BZN-430**, **EB** State, with CO_2 Binding, Mode 4 455
A.4.8.21 Linear/Coiled **OTPA-BZN-430**, **EB** State, with CO_2 Binding, Mode 5 457

APPENDIX B DETAILED THEORETICAL STUDY OF VIBRATIONAL SPECTRA 461

B.1 VIBRATIONAL MODES OF SIX-MEMBERED RINGS 461
B.2 IDENTIFICATION OF MONOMER VIBRATIONAL PEAKS 463
B.2.1 Full Lists of DFT-Calculated Vibrational Peak Positions 475
B.3 REFERENCES 494

APPENDIX C TD-DFT CALCULATED ELECTRONIC TRANSITIONS IN OLIGO(ANILINE) MODELS 495

C.1 ELECTRONIC TRANSITIONS IN TANI AND BRANCHED DERIVATIVES 495
C.1.1 Electronic Transitions in TANI 495
C.1.1.1 TANI, **LEB** State 495
C.1.1.2 TANI, **^{1}ES** State 496
C.1.1.3 TANI, **^{3}ES** State 497
C.1.2 Electronic Transitions in TANI-2 504
C.1.2.1 TANI-2, **LEB** State 504
C.1.2.2 TANI-2, **^{1}ES** State 506
C.1.2.3 TANI-2, **^{3}ES** State 509
C.1.3 Electronic Transitions in TANI-23 520
C.1.3.1 TANI-23, **LEB** State 520
C.1.3.2 TANI-23, **^{1}ES** State 522
C.1.3.3 TANI-23, **^{3}ES** State 525
C.1.4 Electronic Transitions in TANI-14 537
C.1.4.1 TANI-14, **LEB** State 537
C.1.4.2 TANI-14, **^{1}ES** State 538
C.1.4.3 TANI-14, **^{3}ES** State 540
C.2 ELECTRONIC TRANSITIONS IN PANI-CMP OLIGOMERIC MODELS 552
*C.2.1 Electronic Transitions in **OTPA-BZN-210** Oligomers 552*
C.2.1.1 **OTPA-BZN-210**, **LEB** State 552
C.2.1.2 **OTPA-BZN-210**, **^{1}ES** State 554
C.2.1.3 **OTPA-BZN-210**, **^{3}ES** State 557
C.2.1.4 **OTPA-BZN-210**, **EB** State 568
*C.2.2 Electronic Transitions in **OTPA-BZN-221** Oligomers 571*
C.2.2.1 **OTPA-BZN-221**, **LEB** State 571
C.2.2.2 **OTPA-BZN-221**, **^{1}ES** State 574
C.2.2.3 **OTPA-BZN-221**, **^{5}ES** State 579
C.2.2.4 **OTPA-BZN-221**, **EB** State 590
*C.2.3 Electronic Transitions in **OTPA-FLR-210** Oligomers 595*
C.2.3.1 **OTPA-FLR-210**, **LEB** State 595
C.2.3.2 **OTPA-FLR-210**, **^{1}ES** State 598
C.2.3.3 **OTPA-FLR-210**, **^{3}ES** State 601
C.2.3.4 **OTPA-FLR-210**, **EB** State 615
*C.2.4 Electronic Transitions in **OTPA-FLR-221** Oligomers 619*
C.2.4.1 **OTPA-FLR-221**, **LEB** State 619
C.2.4.2 **OTPA-FLR-221**, **^{1}ES** State 622
C.2.4.3 **OTPA-FLR-221**, **^{5}ES** State 628
C.2.4.4 **OTPA-FLR-221**, **EB** State 654
*C.2.5 Electronic Transitions in **OTPB-BZN-210** Oligomers 661*
C.2.5.1 **OTPB-BZN-210**, **LEB** State 662
C.2.5.2 **OTPB-BZN-210**, **^{1}ES** State 664
C.2.5.3 **OTPB-BZN-210**, **^{3}ES** State 667
C.2.5.4 **OTPB-BZN-210**, **EB** State 679
*C.2.6 Electronic Transitions in **OTPB-BZN-221** Oligomers 681*
C.2.6.1 **OTPB-BZN-221**, **LEB** State 681
C.2.6.2 **OTPB-BZN-221**, **^{1}ES** State 684
C.2.6.3 **OTPB-BZN-221**, **^{5}ES** State 689
C.2.6.4 **OTPB-BZN-221**, **EB** State 699

*C.2.7 Electronic Transitions in **OTPB-FLR-210** Oligomers* *703*
C.2.7.1 **OTPB-FLR-210**, **LEB** State 703
C.2.7.2 **OTPB-FLR-210**, **^{1}ES** State 705
C.2.7.3 **OTPB-FLR-210**, **^{3}ES** State 708
C.2.7.4 **OTPB-FLR-210**, **EB** State 728
*C.2.8 Electronic Transitions in **OTPB-FLR-221** Oligomers* *730*
C.2.8.1 **OTPB-FLR-221**, **LEB** State 731
C.2.8.2 **OTPB-FLR-221**, **^{1}ES** State 734
C.2.8.3 **OTPB-FLR-221**, **^{5}ES** State 741
C.2.8.4 **OTPB-FLR-221**, **EB** State 772
*C.2.9 Electronic Transitions in **OTPT-BZN-210** Oligomers* *778*
C.2.9.1 **OTPT-BZN-210**, **LEB** State 779
C.2.9.2 **OTPT-BZN-210**, **^{1}ES** State 782
C.2.9.3 **OTPT-BZN-210**, **^{3}ES** State 788
C.2.9.4 **OTPT-BZN-210**, **EB** State 798
*C.2.10 Electronic Transition in **OTPT-BZN-221** Oligomers* *803*
C.2.10.1 **OTPT-BZN-221**, **LEB** State 803
C.2.10.2 **OTPT-BZN-221**, **^{1}ES** State 807
C.2.10.3 **OTPT-BZN-221**, **^{5}ES** State 814
C.2.10.4 **OTPT-BZN-221**, **EB** State 823
*C.2.11 Electronic Transitions in **OTPT-FLR-210** Oligomers* *829*
C.2.11.1 **OTPT-FLR-210**, **LEB** State 830
C.2.11.2 **OTPT-FLR-210**, **^{1}ES** State 834
C.2.11.3 **OTPT-FLR-210**, **^{3}ES** State 839
C.2.11.4 **OTPT-FLR-210**, **EB** State 863
*C.2.12 Electronic Transitions in **OTPT-FLR-221** Oligomers* *869*
C.2.12.1 **OTPT-FLR-221**, **LEB** State 869
C.2.12.2 **OTPT-FLR-221**, **^{1}ES** State 874
C.2.12.3 **OTPT-FLR-221**, **^{5}ES** State 883
C.2.12.4 **OTPT-FLR-221**, **EB** State 919

APPENDIX D ADSORPTION ISOTHERMS AND OTHER RELATED DATA 929

D.1 Nitrogen Adsorption Isotherm Analyses of PANI-CMPs at 77 K 929
D.1.1 Isotherm Plots *929*
D.1.2 BET Analysis Plots *937*
D.1.3 NLDFT Pore Size Distribution Plots *945*
D.2 Carbon Dioxide Adsorption Isotherm Analyses of PANI-CMPs 960
D.2.1 Isotherm Plots *960*
D.2.2 Langmuir Fitting Plots *967*
D.2.3 Virial Analysis Fitting Plots *975*
D.2.4 Isosteric Enthalpy of Adsorption Plots *983*

APPENDIX E MISCELLANEOUS DATA 995

E.1 Material Appearances 995
E.1.1 Polymers *995*
E.1.2 Oligomers *997*
E.2 Additional Powder XRD Analysis Results 999

List of Tables

TABLE 1-1 CLASSIFICATIONS OF POROUS MATERIALS BASED ON PORE SIZES AS DEFINED BY THE IUPAC, TAKEN FROM THOMMES ET AL.[20] 2
TABLE 1-2 MAIN FEATURES OF ADSORPTION ISOTHERM PLOTS AS PROPOSED BY THOMMES ET AL.[20] 14
TABLE 2-1 MASSES OF MONOMERS FOR SYNTHESES OF PANI-CMPS WITH DIFFERENT MONOMER UNITS WITH STOICHIOMETRIC RATIOS (**S**) BETWEEN AMINO AND BROMO GROUPS THROUGH DIFFERENT PATHWAYS 43
TABLE 2-2 MASSES OF MONOMERS FOR SYNTHESES OF PANI-CMPS WITH DIFFERENT MONOMER UNITS WITH AMINO-EXCESS RATIOS (**A**) BETWEEN AMINO AND BROMO GROUPS THROUGH DIFFERENT PATHWAYS 44
TABLE 2-3 MASSES OF MONOMERS FOR SYNTHESES OF PANI-CMPS WITH DIFFERENT MONOMER UNITS WITH BROMO-EXCESS RATIOS (**B**) BETWEEN AMINO AND BROMO GROUPS THROUGH DIFFERENT PATHWAYS 44
TABLE 3-1 STRUCTURE DESCRIPTORS BEING USED IN PREVIOUS THEORETICAL STUDIES OF POLY(ANILINE)S AND RELATED MATERIALS, SEE THE MAIN TEXT FOR FURTHER EXPLANATIONS 53
TABLE 3-2 BOND LENGTHS OF DFT-OPTIMISED **BZN**-$(NH_2)_2$ IN DIFFERENT STRUCTURES AND THEIR CHANGES UPON OXIDATION FROM **BZ** FORM. BLAS OR BOND LENGTH ALTERNATIONS ARE CALCULATED FROM THE DIFFERENCE BETWEEN AVERAGE C_{IPSO}–C_{ORTHO} AND C_{ORTHO}–C_{ORTHO} LENGTHS. COMPUTATIONAL CONDITIONS: B3LYP FUNCTIONAL,[18-20] 6-31G(D) BASIS SET,[21-30] D3(BJ) EMPIRICAL DISPERSION,[31] ACETONITRILE POLARISABLE CONTINUUM MODEL,[32-35] GAUSSIAN 09[32-35] 55
TABLE 3-3 HARMONIC OSCILLATOR MEASURE OF HETEROCYCLIC ELECTRON DELOCALISATION (HOMHED) AND HARMONIC OSCILLATOR MEASUREMENT FOR BENZENOID-QUINOID CHARACTERISTICS (HOMBQ) INDICES CALCULATED FROM DFT-OPTIMISED BOND LENGTHS IN TABLE 3-2 59
TABLE 3-4 CHARGE DISTRIBUTIONS ON DIFFERENT ATOMS AND ATOM GROUPS IN **BZN**-$(NH_2)_2$ MONOMER OF DIFFERENT OXIDATION AND SPIN MULTIPLICITY STATES. COMPUTATIONAL CONDITIONS: B3LYP FUNCTIONAL,[18-20] 6-31G(D) BASIS SET,[21-30] D3(BJ) EMPIRICAL DISPERSION,[31] ACETONITRILE POLARISABLE CONTINUUM MODEL,[32-35] NATURAL BOND ORBITAL ANALYSIS (NBO) VERSION 3,[53-60] GAUSSIAN 16 (C.01),[51] GEOMETRIES BASED ON THOSE IN TABLE 3-2 65
TABLE 3-5 CHARACTERISTICS OF BQ UNITS IN THREE DIFFERENT FORMS AS DESCRIBED BY HOMBQ INDICES AND NBO CHARGES 66
TABLE 3-6 HOMBQ INDICES OF TANI IN THE EMERALDINE SALT STATES (SINGLET AND TRIPLET) COMPARED TO THE LEUCOEMERALDINE STATE 68
TABLE 3-7 SECONDARY STRUCTURE DESCRIPTORS OF TANI IN THE EMERALDINE SALT STATES COMPARED TO THE LEUCOEMERALDINE STATE 68
TABLE 3-8 NBO PARTIAL CHARGES ON RINGS B, C, AND D AND ON NITROGEN ATOMS N^1 TO N^4 IN TANI FROM DFT CALCULATIONS 68
TABLE 3-9 ENERGIES OF TANI AND BRANCHED TANI DERIVATIVES IN SINGLET AND TRIPLET **ES** STATES, DETERMINED FROM THE DFT OPTIMISATION EARLIER MENTIONED (B3LYP-D3(BJ)/6-31G(D)/ACETONITRILE PCM/GAUSSIAN 09) 70
TABLE 3-10 HOMBQ INDICES OF TANI-2 IN THE EMERALDINE SALT STATES (SINGLET AND TRIPLET) COMPARED TO THE LEUCOEMERALDINE STATE 70
TABLE 3-11 SECONDARY STRUCTURE DESCRIPTORS OF TANI-2 IN THE EMERALDINE SALT STATES COMPARED TO THE LEUCOEMERALDINE STATE 70
TABLE 3-12 NBO PARTIAL CHARGES ON RINGS B, C, AND D AND ON NITROGEN ATOMS N^1 TO N^4 IN TANI-2 FROM DFT CALCULATIONS 71
TABLE 3-13 HOMBQ INDICES OF TANI-23 IN THE EMERALDINE SALT STATES (SINGLET AND TRIPLET) COMPARED TO THE LEUCOEMERALDINE STATE 73
TABLE 3-14 SECONDARY STRUCTURE DESCRIPTORS OF TANI-23 IN THE EMERALDINE SALT STATES COMPARED TO THE LEUCOEMERALDINE STATE 73
TABLE 3-15 NBO PARTIAL CHARGES ON RINGS B, C, AND D AND ON NITROGEN ATOMS N^1 TO N^4 IN TANI-23 FROM DFT CALCULATIONS 74
TABLE 3-16 HOMBQ INDICES OF TANI-14 IN THE EMERALDINE SALT STATES (SINGLET AND TRIPLET) COMPARED TO THE LEUCOEMERALDINE STATE 75
TABLE 3-17 SECONDARY STRUCTURE DESCRIPTORS OF TANI-14 IN THE EMERALDINE SALT STATES COMPARED TO THE LEUCOEMERALDINE STATE 75
TABLE 3-18 NBO PARTIAL CHARGES ON RINGS B, C, AND D AND ON NITROGEN ATOMS N^1 TO N^4 IN TANI-14 FROM DFT CALCULATIONS 76

TABLE 3-19 SELECTED GEOMETRIC STRUCTURE PARAMETERS FROM THE DFT-OPTIMISED STRUCTURES OF MONOMERS IN THIS STUDY (B3LYP-D3(BJ)/6-31G(D)/1,4-DIOXANE PCM/GAUSSIAN 16 (A.03)) 78
TABLE 3-20 HOMBQ INDICES OF BQ UNITS IN THE CORE AND LINKER UNITS OF **OTPA-BZN-210** IN THE EMERALDINE SALT AND EMERALDINE BASE STATES (SINGLET AND TRIPLET) COMPARED TO THE LEUCOEMERALDINE STATE 80
TABLE 3-21 C–N–C ANGLES AND DIHEDRAL ANGLES OF **OTPA-BZN-210** IN THE EMERALDINE SALT AND EMERALDINE BASE STATES COMPARED TO THE LEUCOEMERALDINE STATE 80
TABLE 3-22 NBO PARTIAL CHARGES ON C_6H_4 RINGS OF BQ UNITS, ON HUB PARTS OF CORE UNITS, AND ON NITROGEN ATOMS IN **OTPA-BZN-210** FROM DFT CALCULATIONS 80
TABLE 3-23 HOMBQ INDICES OF BQ UNITS IN THE CORE AND LINKER UNITS OF **OTPA-BZN-221** IN THE EMERALDINE SALT AND EMERALDINE BASE STATES (SINGLET AND TRIPLET) COMPARED TO THE LEUCOEMERALDINE STATE 82
TABLE 3-24 C–N–C ANGLES AND DIHEDRAL ANGLES OF **OTPA-BZN-221** IN THE EMERALDINE SALT AND EMERALDINE BASE STATES COMPARED TO THE LEUCOEMERALDINE STATE 82
TABLE 3-25 NBO PARTIAL CHARGES ON C_6H_4 RINGS OF BQ UNITS, ON HUB PARTS OF CORE UNITS, AND ON NITROGEN ATOMS IN **OTPA-BZN-221** FROM DFT CALCULATIONS 82
TABLE 3-26 HOMBQ INDICES OF BQ UNITS IN THE CORE AND LINKER UNITS OF **OTPA-FLR-210** IN THE EMERALDINE SALT AND EMERALDINE BASE STATES (SINGLET AND TRIPLET) COMPARED TO THE LEUCOEMERALDINE STATE 85
TABLE 3-27 C–N–C ANGLES AND DIHEDRAL ANGLES OF **OTPA-FLR-210** IN THE EMERALDINE SALT AND EMERALDINE BASE STATES COMPARED TO THE LEUCOEMERALDINE STATE 85
TABLE 3-28 NBO PARTIAL CHARGES ON RINGS OF BQ UNITS, ON HUB PARTS OF CORE UNITS, AND ON NITROGEN ATOMS IN **OTPA-FLR-210** FROM DFT CALCULATIONS 85
TABLE 3-29 HOMBQ INDICES OF BQ UNITS IN THE CORE AND LINKER UNITS OF **OTPB-BZN-210** IN THE EMERALDINE SALT AND EMERALDINE BASE STATES (SINGLET AND TRIPLET) COMPARED TO THE LEUCOEMERALDINE STATE 87
TABLE 3-30 C–N–C ANGLES AND DIHEDRAL ANGLES OF **OTPB-BZN-210** IN THE EMERALDINE SALT AND EMERALDINE BASE STATES COMPARED TO THE LEUCOEMERALDINE STATE 87
TABLE 3-31 NBO PARTIAL CHARGES ON C_6H_4 RINGS OF BQ UNITS, ON HUB PARTS OF CORE UNITS, AND ON NITROGEN ATOMS IN **OTPB-BZN-210** FROM DFT CALCULATIONS 88
TABLE 3-32 HOMBQ INDICES OF BQ UNITS IN THE CORE AND LINKER UNITS OF **OTPB-FLR-210** IN THE EMERALDINE SALT AND EMERALDINE BASE STATES (SINGLET AND TRIPLET) COMPARED TO THE LEUCOEMERALDINE STATE 89
TABLE 3-33 C–N–C ANGLES AND DIHEDRAL ANGLES OF **OTPB-FLR-210** IN THE EMERALDINE SALT AND EMERALDINE BASE STATES COMPARED TO THE LEUCOEMERALDINE STATE 89
TABLE 3-34 NBO PARTIAL CHARGES ON RINGS OF BQ UNITS, ON HUB PARTS OF CORE UNITS, AND ON NITROGEN ATOMS IN **OTPB-FLR-210** FROM DFT CALCULATIONS 90
TABLE 3-35 HOMBQ INDICES OF BQ UNITS IN THE CORE AND LINKER UNITS OF **OTPT-BZN-210** IN THE EMERALDINE SALT AND EMERALDINE BASE STATES (SINGLET AND TRIPLET) COMPARED TO THE LEUCOEMERALDINE STATE 91
TABLE 3-36 C–N–C ANGLES AND DIHEDRAL ANGLES OF **OTPT-BZN-210** IN THE EMERALDINE SALT AND EMERALDINE BASE STATES COMPARED TO THE LEUCOEMERALDINE STATE 92
TABLE 3-37 NBO PARTIAL CHARGES ON C_6H_4 RINGS OF BQ UNITS, ON HUB PARTS OF CORE UNITS, AND ON NITROGEN ATOMS IN **OTPT-BZN-210** FROM DFT CALCULATIONS 92
TABLE 3-38 HOMBQ INDICES OF BQ UNITS IN THE CORE AND LINKER UNITS OF **OTPT-FLR-210** IN THE EMERALDINE SALT AND EMERALDINE BASE STATES (SINGLET AND TRIPLET) COMPARED TO THE LEUCOEMERALDINE STATE 93
TABLE 3-39 C–N–C ANGLES AND DIHEDRAL ANGLES OF **OTPT-FLR-210** IN THE EMERALDINE SALT AND EMERALDINE BASE STATES COMPARED TO THE LEUCOEMERALDINE STATE 93
TABLE 3-40 NBO PARTIAL CHARGES ON RINGS OF BQ UNITS, ON HUB PARTS OF CORE UNITS, AND ON NITROGEN ATOMS IN **OTPT-FLR-210** FROM DFT CALCULATIONS 93
TABLE 3-41 PEAK POSITIONS IN ABSORPTION SPECTRA CALCULATED FROM TD-DFT CALCULATIONS OF **OTPA-BZN-210** AND **OTPA-FLR-210** IN DIFFERENT OXIDATION, DOPING, AND SPIN STATES 99
TABLE 3-42 DETAILS RELATED TO ELECTRONIC TRANSITIONS INVOLVED IN THE ABSORPTION PEAKS FROM TD-DFT CALCULATIONS OF **OTPA-BZN-210** OLIGOMERS IN DIFFERENT OXIDATION, DOPING, AND SPIN STATES. ONLY EXCITED STATES WITH OSCILLATOR STRENGTHS GREATER THAN 0.2 ARE CONSIDERED, AND FOR EACH EXCITED STATE, ONLY ELECTRONIC TRANSITIONS CONTRIBUTING AT LEAST 10% ARE LISTED 100
TABLE 3-43 STRUCTURES OF MAIN MOLECULAR ORBITALS INVOLVED IN ELECTRONIC TRANSITIONS OF **OTPA-BZN-210** IN **LEB** STATE 101
TABLE 3-44 STRUCTURES OF MAIN MOLECULAR ORBITALS INVOLVED IN ELECTRONIC TRANSITIONS OF **OTPA-BZN-210** IN **^{1}ES** STATE 101

TABLE 3-45 STRUCTURES OF MAIN MOLECULAR ORBITALS INVOLVED IN ELECTRONIC TRANSITIONS OF **OTPA-BZN-210** IN **^{3}ES** STATE 102
TABLE 3-46 STRUCTURES OF MAIN MOLECULAR ORBITALS INVOLVED IN ELECTRONIC TRANSITIONS OF **OTPA-BZN-210** IN **EB** STATE 103
TABLE 3-47 STRUCTURES OF GROUND STATE AND EXCITED STATE MOLECULAR ORBITALS FROM THE NTO ANALYSES OF CTBQ EXCITED STATES OF **OTPA-BZN-210** OLIGOMERS 104
TABLE 3-48 DETAILS RELATED TO ELECTRONIC TRANSITIONS INVOLVED IN THE CTBQ ABSORPTION PEAKS FROM TD-DFT CALCULATIONS OF **OTPA-FLR-210** OLIGOMERS IN DIFFERENT OXIDATION, DOPING, AND SPIN STATES. ONLY ELECTRONIC TRANSITIONS CONTRIBUTING AT LEAST 10% ARE LISTED. 105
TABLE 3-49 STRUCTURES OF GROUND STATE AND EXCITED STATE MOLECULAR ORBITALS FROM THE NTO ANALYSES OF CTBQ EXCITED STATES OF **OTPA-FLR-210** OLIGOMERS 105
TABLE 3-50 COMPARISONS BETWEEN CTBQ PEAK POSITIONS AND CORRESPONDING ENERGIES FOR **OTPA-BZN-210** AND **OTPA-FLR-210** IN DIFFERENT DOPING AND SPIN STATES FROM TD-DFT CALCULATIONS 106
TABLE 3-51 DETAILS RELATED TO ELECTRONIC TRANSITIONS INVOLVED IN THE CTBQ ABSORPTION PEAKS FROM TD-DFT CALCULATIONS OF **OTPB-BZN-210** AND **OTPB-FLR-210** OLIGOMERS IN DIFFERENT OXIDATION, DOPING, AND SPIN STATES. ONLY ELECTRONIC TRANSITIONS CONTRIBUTING AT LEAST 10% ARE LISTED. 107
TABLE 3-52 COMPARISONS BETWEEN CTBQ PEAK POSITIONS AND CORRESPONDING ENERGIES FOR **OTPB-BZN-210** AND **OTPB-FLR-210** IN DIFFERENT DOPING AND SPIN STATES FROM TD-DFT CALCULATIONS 108
TABLE 3-53 STRUCTURES OF GROUND STATE AND EXCITED STATE MOLECULAR ORBITALS FROM THE NTO ANALYSES OF CTBQ EXCITED STATES OF **OTPB-BZN-210** OLIGOMERS 109
TABLE 3-54 STRUCTURES OF GROUND STATE AND EXCITED STATE MOLECULAR ORBITALS FROM THE NTO ANALYSES OF CTBQ EXCITED STATES OF **OTPB-FLR-210** OLIGOMERS 109
TABLE 3-55 DETAILS RELATED TO ELECTRONIC TRANSITIONS INVOLVED IN THE CTBQ ABSORPTION PEAKS FROM TD-DFT CALCULATIONS OF **OTPT-BZN-210** AND **OTPT-FLR-210** OLIGOMERS IN DIFFERENT OXIDATION, DOPING, AND SPIN STATES. ONLY ELECTRONIC TRANSITIONS CONTRIBUTING AT LEAST 10% ARE LISTED. 111
TABLE 3-56 COMPARISONS BETWEEN CTBQ PEAK POSITIONS AND CORRESPONDING ENERGIES FOR **OTPT-BZN-210** AND **OTPT-FLR-210** IN DIFFERENT DOPING AND SPIN STATES FROM TD-DFT CALCULATIONS 111
TABLE 3-57 STRUCTURES OF GROUND STATE AND EXCITED STATE MOLECULAR ORBITALS FROM THE NTO ANALYSES OF CTBQ EXCITED STATES OF **OTPT-BZN-210** OLIGOMERS 112
TABLE 3-58 STRUCTURES OF GROUND STATE AND EXCITED STATE MOLECULAR ORBITALS FROM THE NTO ANALYSES OF CTBQ EXCITED STATES OF **OTPT-FLR-210** OLIGOMERS 112
TABLE 3-59 ABSORPTION PEAK POSITIONS OF **OTPA-BZN-221** OLIGOMERS IN DIFFERENT STATES SHOWN IN FIGURE 3-38 115
TABLE 3-60 DETAILS RELATED TO ELECTRONIC TRANSITIONS INVOLVED IN THE ABSORPTION PEAKS FROM TD-DFT CALCULATIONS OF **OTPA-BZN-221** OLIGOMERS IN DIFFERENT OXIDATION, DOPING, AND SPIN STATES. ONLY EXCITED STATES WITH ENERGIES IN THE VISIBLE-NEAR INFRARED REGION AND WITH OSCILLATOR STRENGTHS GREATER THAN 0.2 ARE CONSIDERED, AND FOR EACH EXCITED STATE, ONLY ELECTRONIC TRANSITIONS CONTRIBUTING AT LEAST 10% ARE LISTED. 117
TABLE 3-61 STRUCTURES OF GROUND STATE AND EXCITED STATE MOLECULAR ORBITALS FROM THE NTO ANALYSES OF EXCITED STATES OF **OTPA-BZN-221** OLIGOMERS IN THE **^{1}ES** STATE AS LISTED IN TABLE 3-60 118
TABLE 3-62 STRUCTURES OF GROUND STATE AND EXCITED STATE MOLECULAR ORBITALS FROM THE NTO ANALYSES OF EXCITED STATES OF **OTPA-BZN-221** OLIGOMERS IN THE **^{5}ES** STATE AS LISTED IN TABLE 3-60 118
TABLE 3-63 STRUCTURES OF GROUND STATE AND EXCITED STATE MOLECULAR ORBITALS FROM THE NTO ANALYSES OF EXCITED STATES OF **OTPA-BZN-221** OLIGOMERS IN THE **EB** STATE AS LISTED IN TABLE 3-60 119
TABLE 3-64 ABSORPTION PEAK POSITIONS OF **OTPA-FLR-221** OLIGOMERS IN DIFFERENT STATES SHOWN IN FIGURE 3-40 120
TABLE 3-65 DETAILS RELATED TO ELECTRONIC TRANSITIONS INVOLVED IN THE ABSORPTION PEAKS FROM TD-DFT CALCULATIONS OF **OTPA-FLR-221** OLIGOMERS IN DIFFERENT OXIDATION, DOPING, AND SPIN STATES. ONLY EXCITED STATES WITH ENERGIES IN THE VISIBLE-NEAR INFRARED REGION AND WITH OSCILLATOR STRENGTHS GREATER THAN 0.2 ARE CONSIDERED, AND FOR EACH EXCITED STATE, ONLY ELECTRONIC TRANSITIONS CONTRIBUTING AT LEAST 10% ARE LISTED. 120
TABLE 3-66 STRUCTURES OF GROUND STATE AND EXCITED STATE MOLECULAR ORBITALS FROM THE NTO ANALYSES OF EXCITED STATES OF **OTPA-FLR-221** OLIGOMERS IN THE **^{1}ES** STATE AS LISTED IN TABLE 3-65 121
TABLE 3-67 STRUCTURES OF GROUND STATE AND EXCITED STATE MOLECULAR ORBITALS FROM THE NTO ANALYSES OF EXCITED STATES OF **OTPA-FLR-221** OLIGOMERS IN THE **^{5}ES** STATE AS LISTED IN TABLE 3-65 122

TABLE 3-68 STRUCTURES OF GROUND STATE AND EXCITED STATE MOLECULAR ORBITALS FROM THE NTO ANALYSES OF EXCITED STATES OF **OTPA-FLR-221** OLIGOMERS IN THE **EB** STATE AS LISTED IN TABLE 3-65 123
TABLE 3-69 PEAK POSITIONS IN ABSORPTION SPECTRA CALCULATED FROM TD-DFT CALCULATIONS OF **OTPB-BZN-221** AND **OTPB-FLR-221** IN DIFFERENT OXIDATION, DOPING, AND SPIN STATES 124
TABLE 3-70 DETAILS RELATED TO ELECTRONIC TRANSITIONS INVOLVED IN THE ABSORPTION PEAKS FROM TD-DFT CALCULATIONS OF **OTPB-BZN-221** OLIGOMERS IN DIFFERENT OXIDATION, DOPING, AND SPIN STATES. ONLY EXCITED STATES WITH ENERGIES IN THE VISIBLE-NEAR INFRARED REGION AND WITH OSCILLATOR STRENGTHS GREATER THAN 0.2 ARE CONSIDERED, AND FOR EACH EXCITED STATE, ONLY ELECTRONIC TRANSITIONS CONTRIBUTING AT LEAST 10% ARE LISTED 125
TABLE 3-71 STRUCTURES OF GROUND STATE AND EXCITED STATE MOLECULAR ORBITALS FROM THE NTO ANALYSES OF EXCITED STATES OF **OTPB-BZN-221** OLIGOMERS IN THE **^{1}ES** STATE AS LISTED IN TABLE 3-70 126
TABLE 3-72 STRUCTURES OF GROUND STATE AND EXCITED STATE MOLECULAR ORBITALS FROM THE NTO ANALYSES OF EXCITED STATES OF **OTPB-BZN-221** OLIGOMERS IN THE **^{5}ES** STATE AS LISTED IN TABLE 3-70 127
TABLE 3-73 STRUCTURES OF GROUND STATE AND EXCITED STATE MOLECULAR ORBITALS FROM THE NTO ANALYSES OF EXCITED STATES OF **OTPB-BZN-221** OLIGOMERS IN THE **EB** STATE AS LISTED IN TABLE 3-70 128
TABLE 3-74 DETAILS RELATED TO ELECTRONIC TRANSITIONS INVOLVED IN THE ABSORPTION PEAKS FROM TD-DFT CALCULATIONS OF **OTPB-FLR-221** OLIGOMERS IN DIFFERENT OXIDATION, DOPING, AND SPIN STATES. ONLY EXCITED STATES WITH ENERGIES IN THE VISIBLE-NEAR INFRARED REGION AND WITH OSCILLATOR STRENGTHS GREATER THAN 0.2 ARE CONSIDERED, AND FOR EACH EXCITED STATE, ONLY ELECTRONIC TRANSITIONS CONTRIBUTING AT LEAST 10% ARE LISTED 129
TABLE 3-75 STRUCTURES OF GROUND STATE AND EXCITED STATE MOLECULAR ORBITALS FROM THE NTO ANALYSES OF EXCITED STATES OF **OTPB-FLR-221** OLIGOMERS IN THE **^{1}ES** STATE AS LISTED IN TABLE 3-74 129
TABLE 3-76 STRUCTURES OF GROUND STATE AND EXCITED STATE MOLECULAR ORBITALS FROM THE NTO ANALYSES OF EXCITED STATES OF **OTPB-FLR-221** OLIGOMERS IN THE **^{5}ES** STATE AS LISTED IN TABLE 3-74 130
TABLE 3-77 STRUCTURES OF GROUND STATE AND EXCITED STATE MOLECULAR ORBITALS FROM THE NTO ANALYSES OF EXCITED STATES OF **OTPB-FLR-221** OLIGOMERS IN THE **EB** STATE AS LISTED IN TABLE 3-74 130
TABLE 3-78 PEAK POSITIONS IN ABSORPTION SPECTRA CALCULATED FROM TD-DFT CALCULATIONS OF **OTPT-BZN-221** AND **OTPT-FLR-221** IN DIFFERENT OXIDATION, DOPING, AND SPIN STATES 132
TABLE 3-79 DETAILS RELATED TO ELECTRONIC TRANSITIONS INVOLVED IN THE ABSORPTION PEAKS FROM TD-DFT CALCULATIONS OF **OTPT-BZN-221** OLIGOMERS IN DIFFERENT OXIDATION, DOPING, AND SPIN STATES. ONLY EXCITED STATES WITH ENERGIES IN THE VISIBLE-NEAR INFRARED REGION AND WITH OSCILLATOR STRENGTHS GREATER THAN 0.2 ARE CONSIDERED, AND FOR EACH EXCITED STATE, ONLY ELECTRONIC TRANSITIONS CONTRIBUTING AT LEAST 10% ARE LISTED 133
TABLE 3-80 DETAILS RELATED TO ELECTRONIC TRANSITIONS INVOLVED IN THE ABSORPTION PEAKS FROM TD-DFT CALCULATIONS OF **OTPT-FLR-221** OLIGOMERS IN DIFFERENT OXIDATION, DOPING, AND SPIN STATES. ONLY EXCITED STATES WITH ENERGIES IN THE VISIBLE-NEAR INFRARED REGION AND WITH OSCILLATOR STRENGTHS GREATER THAN 0.2 ARE CONSIDERED, AND FOR EACH EXCITED STATE, ONLY ELECTRONIC TRANSITIONS CONTRIBUTING AT LEAST 10% ARE LISTED 134
TABLE 3-81 STRUCTURES OF GROUND STATE AND EXCITED STATE MOLECULAR ORBITALS FROM THE NTO ANALYSES OF EXCITED STATES OF **OTPT-BZN-221** OLIGOMERS IN THE **^{1}ES** STATE AS LISTED IN TABLE 3-79 134
TABLE 3-82 STRUCTURES OF GROUND STATE AND EXCITED STATE MOLECULAR ORBITALS FROM THE NTO ANALYSES OF EXCITED STATES OF **OTPT-FLR-221** OLIGOMERS IN THE **^{1}ES** STATE AS LISTED IN TABLE 3-80 135
TABLE 3-83 STRUCTURES OF GROUND STATE AND EXCITED STATE MOLECULAR ORBITALS FROM THE NTO ANALYSES OF EXCITED STATES OF **OTPT-BZN-221** OLIGOMERS IN THE **^{5}ES** STATE AS LISTED IN TABLE 3-79 136
TABLE 3-84 STRUCTURES OF GROUND STATE AND EXCITED STATE MOLECULAR ORBITALS FROM THE NTO ANALYSES OF EXCITED STATES OF **OTPT-FLR-221** OLIGOMERS IN THE **^{5}ES** STATE AS LISTED IN TABLE 3-80 137
TABLE 3-85 STRUCTURES OF GROUND STATE AND EXCITED STATE MOLECULAR ORBITALS FROM THE NTO ANALYSES OF EXCITED STATES OF **OTPT-BZN-221** OLIGOMERS IN THE **EB** STATE AS LISTED IN TABLE 3-79 138
TABLE 3-86 STRUCTURES OF GROUND STATE AND EXCITED STATE MOLECULAR ORBITALS FROM THE NTO ANALYSES OF EXCITED STATES OF **OTPT-FLR-221** OLIGOMERS IN THE **EB** STATE AS LISTED IN TABLE 3-80 138
TABLE 3-87 COMPARISONS BETWEEN CALCULATED AND MEASURED PEAK POSITIONS IN THE VISIBLE REGION OF PANI-CMP MODELS, OLIGOMERS, AND POLYMERS 142
TABLE 3-88 ABSORPTION PEAKS MEASURED FROM SYNTHESISED OLIGOMERS (REF [47]) AND POLYMERS. IN THE CASE OF POLYMERS, THERE CAN BE MORE THAN ONE CTBQ PEAK. ITALICISED NUMBERS REFER TO PEAKS WHICH POSITIONS CANNOT BE CLEARLY DETERMINED 144

TABLE 4-1 FUNCTIONAL GROUPS R_1 AND R_2 OF FUNCTIONALISED **CMP-1** MATERIALS AND THEIR SPECIFIC SURFACE AREAS STUDIED BY DAWSON, ADAMS, AND COOPER TAKEN FROM REFERENCE [7] 151
TABLE 4-2 PREVIOUSLY DEVELOPED PANI-CMPS IN THE FAUL RESEARCH GROUP FROM MONOMERS COMPILED IN SCHEME 4-6 153
TABLE 4-3 SPECIFIC SURFACE AREAS AND MICROPOROUS SURFACE AREAS FROM NITROGEN ISOTHERM ANALYSES AT 77 K OF **TPA**-BASED PANI-CMPS SYNTHESISED IN THE FIRST TWO SERIES 155
TABLE 4-4 SPECIFIC SURFACE AREAS OF **PTPA-BZN** PREPARED FROM DIFFERENT SYNTHESIS METHODS. ALL REACTIONS WERE CARRIED OUT IN TOLUENE (B.P. 110 °C) UNLESS STATED OTHERWISE 156
TABLE 4-5 RATIOS OF SPECIES INVOLVED IN THE SYNTHESIS OF PANI-CMPS USING DIFFERENT FUNCTIONAL GROUP RATIOS AND SYNTHETIC PATHWAYS 157
TABLE 4-6 SUMMARY OF SYNTHESIS OUTCOMES FOR PANI-CMP ATTEMPTS WITH DIFFERENT MONOMER UNITS AND SYNTHESIS INITIAL CONDITIONS. BLACK SQUARES (■) REFER TO SUCCESSFUL SYNTHESES WITH HIGH AMOUNTS OF POLYMERS OBTAINED, WHILE WHITE SQUARES (□) REFER TO UNSUCCESSFUL SYNTHESES WHERE PRODUCTS OBTAINED ARE MOSTLY SOLUBLE OLIGOMERS. "ON" REFERS TO THE SYNTHESIS ATTEMPTS WITH ADDITIONAL NABR, WHILE "OFF" REFERS TO SYNTHESIS ATTEMPTS WITHOUT ADDITIONAL NABR 158
TABLE 4-7 THEORETICAL M/Z VALUES OF DIFFERENT OLIGOMERS IN THE SERIES OF MASS SPECTROMETRY PEAKS FROM THE ANALYSES OF **PTPB-BZN-AR** AND **PTPB-FLR-AR** 160
TABLE 4-8 EXPECTED RANGES AND POSITIONS FOR FT-IR TRANSMISSION PEAKS OF FUNCTIONAL GROUPS IN PANI-CMPS AND THEIR MONOMERS. VIBRATIONS RELATED TO THE FUNCTIONAL GROUPS ARE SHOWN AS **BOLD**, AND THEIR CORRESPONDING PEAKS ARE SHOWN IN THE LAST TWO COLUMNS 164
TABLE 4-9 POROSITY DATA OF PANI-CMPS PREPARED FROM DIFFERENT MONOMERS, APPROACHES, AND SOLUBILITY TUNINGS, OBTAINED FROM NITROGEN ADSORPTION ISOTHERM AT 77 K. GREY ROWS REFER TO MATERIALS THAT FAILED TO BE OBTAINED IN SUITABLE AMOUNTS FOR POROSITY DETERMINATIONS (> 50 MG). ISOTHERM TYPES MARKED WITH A PRIME (') MARK MEAN THAT THE ISOTHERM PLOT SLIGHTLY DIFFER FROM THE IUPAC CLASSIFICATIONS 170
TABLE 4-10 POROSITY DATA OF PANI-CMPS PREPARED FROM DIFFERENT MONOMERS, APPROACHES, AND SOLUBILITY TUNINGS, OBTAINED FROM CARBON DIOXIDE ADSORPTION ISOTHERM AT **273 K**. 174
TABLE 4-11 SUMMARY OF CO_2 UPTAKE OF PANI-CMPS SYNTHESISED FROM DIFFERENT MONOMER UNITS, PATHWAYS, AND SOLUBILITY TUNING 176
TABLE 4-12 CO_2 UPTAKES OF PANI-CMPS AT TWO DIFFERENT TEMPERATURES, 273 K AND 298 K, THE RANGE OF CALCULATED ΔH_{ADS} FROM FREUNDLICH-LANGMUIR ADSORPTION MODEL AND CLAUSIUS-CLAPEYRON EQUATION, AND THE PREDICTED ISOSTERIC ENTHALPIES OF ADSORPTION AT ZERO COVERAGE ($\Delta H°_{ADS}$) 178
TABLE 5-1 BINDING ENERGIES OF CO_2 ONTO DIFFERENT HETEROATOM-CONTAINING AROMATIC MOLECULES FROM COMPUTATIONAL STUDIES (M06-2X/AVDZ) BY LEE ET AL.[29] 187
TABLE 5-2 BINDING ENERGIES AND DISTANCES BETWEEN CO_2 MOLECULES AND **OTPA-BZN-210** FRAGMENTS FROM DFT OPTIMISATION, WITH THE RELATIVE ENERGIES COMPARED TO THE MOST STABLE BINDING SITES GIVEN IN THE PARENTHESES. CO_2 DISTANCES ARE MEASURED AS EITHER C–N DISTANCES (FOR IMINE BINDING SITE) OR THE AVERAGE DISTANCES OF CO_2 ATOMS FROM THE BQ UNIT PLANE (FOR OTHER BQ UNIT BINDING SITES). O···H DISTANCES ARE MEASURED BETWEEN EACH OXYGEN ATOM AND THE NEAREST HYDROGEN ATOM 191
TABLE 5-3 COMPARISONS BETWEEN STRUCTURAL PARAMETERS BEFOR AND AFTER A CO_2 MOLECULE IS BOUND TO THE IMINE BINDING SITE FROM DFT-OPTIMISESD STRUCTURES. 193
TABLE 5-4 COMPARISON OF STRUCTURAL PARAMETERS BEFORE AND AFTER A CO_2 MOLECULE IS BOUND TO THE LINKER UNIT BINDING SITE FROM DFT-OPTIMISED STRUCTURES. 194
TABLE 5-5 COMPARISON OF STRUCTURAL PARAMETERS BEFORE AND AFTER A CO_2 MOLECULE IS BOUND TO THE CORE UNIT BINDING SITE FROM DFT-OPTIMISED STRUCTURES 196
TABLE 5-6 COMPARISON OF DFT-CALCULATED RELATIVE ENERGIES OF TETRA(ANILINE) AND **OTPA-BZN-210** IN **EB** STATE RESPECTIVE TO THE CONFORMER WITH LOWEST ENERGY (CIS-SYN IN BOTH CASES). CALCULATED ENERGIES OF TETRA(ANILINE) ARE TAKEN FROM THOMAS ET AL.[42] 197
TABLE 5-7 BINDING ENERGIES OF DIFFERENT BINDING MODES ON THE LINKER UNIT BINDING SITES OF **OTPA-BZN-210** OLIGOMERS IN DIFFERENT CONFORMERS. ITALICISED NUMBERS MEAN THAT THE OPTIMISATION PROCESS ENDED IN ERROR AND FAILED TO RESTART. 199
TABLE 5-8 BINDING ENERGIES OF CO_2 ON **OTPA-BZN-210** IN **LEB** AND **EB** STATES, AS DETERMINED FROM DFT-OPTIMISED STRUCTURES 200
TABLE 5-9 BINDING ENERGIES ON DIFFERENT BINDING SITES OF **210** OLIGOMERS FROM DIFFERENT CORE AND LINKER UNIT COMBINATIONS 201

TABLE 5-10 KEY PARAMETERS RELATED TO BINDING OF CO_2 ONTO IMINE BINDING SITES OF **210** OLIGOMERS FROM ALL SIX CORE AND LINKER UNIT COMBINATIONS. SEE THE MAIN TEXT FOR MEANINGS OF SIGNS FOR ANGLE DIFFERENCES....201
TABLE 5-11 KEY PARAMETERS RELATED TO BINDING OF CO_2 ONTO LINKER BINDING SITES OF **210** OLIGOMERS FROM ALL SIX CORE AND LINKER UNIT COMBINATIONS.....202
TABLE 5-12 KEY PARAMETERS RELATED TO BINDING OF CO_2 ONTO **TPA** CORE BINDING SITES OF **210** OLIGOMERS LINKED BY **BZN** AND **FLR** LINKERS.....204
TABLE 5-13 KEY PARAMETERS RELATED TO BINDING OF CO_2 ONTO **TPB** CORE BINDING SITES OF **210** OLIGOMERS LINKED BY **BZN** AND **FLR** LINKERS. FOR O···H DISTANCES, OXYGEN AND HYDROGEN ATOMS INVOLVED ARE NUMBERED AS IN FIGURE 5-14.....204
TABLE 5-14 KEY PARAMETERS RELATED TO BINDING OF CO_2 ONTO **TPT** CORE BINDING SITES OF **210** OLIGOMERS LINKED BY **BZN** AND **FLR** LINKERS.....205
TABLE 5-15 BINDING ENERGIES OF CO_2 ON THE DIFFERENT BINDING SITES ON STAR-SHAPED **OTPA-BZN-430** OLIGOMER COMPARED TO THOSE BINDING ON CORRESPONDING SITES ON **OTPA-BZN-210**.....208
TABLE 5-16 BINDING ENERGIES OF CO_2 ONTO COILED **OTPA-BZN-430** OLIGOMER FRAGMENT CALCULATED FROM OPTIMISED STRUCTURES OF THE OLIGOMER BEFORE BINDING (SECOND COLUMN) AND FROM SINGLE-POINT ENERGY (SPE, SEE MAIN TEXT) OF THE OPTIMISED STRUCTURES OF THE OLIGOMER AFTER BINDING WITH CO_2 MOLECULE REMOVED (THIRD COLUMN) ALONG WITH DIFFERENCES BETWEEN BINDING ENERGIES CALCULATED FROM THE TWO METHODS.....210
TABLE A-1 NBO PARTIAL CHARGES OF NITROGEN ATOMS IN TANI AND BRANCHED TANI DERIVATIVES IN THE EMERALDINE SALT STATES COMPARED TO THE LEUCOEMERALDINE STATE FROM DFT CALCULATIONS.....237
TABLE A-2 NBO PARTIAL CHARGES OF CARBON AND HYDROGEN ATOMS IN TANI AND BRANCHED TANI DERIVATIVES IN THE EMERALDINE SALT STATES COMPARED TO THE LEUCOEMERALDINE STATE FROM DFT CALCULATIONS.....238
TABLE A-3 STRUCTURAL PARAMETERS RELATED TO THE INTERACTIONS BETWEEN A CO_2 MOLECULE AND A **210** PANI-CMP FRAGMENT IN THE **EB** STATE WITH DIFFERENT CORE AND LINKER COMBINATIONS ON DIFFERENT BINDING SITES. CO_2 DISTANCES ARE MEASURED AS C···N DISTANCES FOR IMINE NITROGEN BINDING SITES AND MEASURED AS THE AVERAGE DISTANCES OF CO_2 ATOMS FROM THE BQ UNIT PLANE FOR CORE AND LINKER UNIT BINDING SITES. ONLY ONE N···H DISTANCE CAN BE FOUND FOR **TPT**-BASED OLIGOMER FRAGMENTS DUE TO THEIR FLAT D_{3H} GEOMETRY. 374
TABLE A-4 COMPARISONS BETWEEN STRUCTURAL PARAMETERS BEFORE AND AFTER A CO_2 MOLECULE IS BOUND TO THE IMINE BINDING SITE FROM DFT-OPTIMISESD STRUCTURES OF **EB OTPA-BZN-210**–CO_2 COMPLEX.....375
TABLE A-5 COMPARISONS BETWEEN STRUCTURAL PARAMETERS BEFORE AND AFTER A CO_2 MOLECULE IS BOUND TO THE IMINE BINDING SITE FROM DFT-OPTIMISESD STRUCTURES OF **EB OTPA-FLR-210**–CO_2 COMPLEX.....376
TABLE A-6 COMPARISONS BETWEEN STRUCTURAL PARAMETERS BEFORE AND AFTER A CO_2 MOLECULE IS BOUND TO THE IMINE BINDING SITE FROM DFT-OPTIMISESD STRUCTURES OF **EB OTPB-BZN-210**–CO_2 COMPLEX.....377
TABLE A-7 COMPARISONS BETWEEN STRUCTURAL PARAMETERS BEFOR AND AFTER A CO_2 MOLECULE IS BOUND TO THE IMINE BINDING SITE FROM DFT-OPTIMISESD STRUCTURES OF **EB OTPB-FLR-210**–CO_2 COMPLEX.....378
TABLE A-8 COMPARISONS BETWEEN STRUCTURAL PARAMETERS BEFORE AND AFTER A CO_2 MOLECULE IS BOUND TO THE IMINE BINDING SITE FROM DFT-OPTIMISESD STRUCTURES OF **EB OTPT-BZN-210**–CO_2 COMPLEX.....379
TABLE A-9 COMPARISONS BETWEEN STRUCTURAL PARAMETERS BEFORE AND AFTER A CO_2 MOLECULE IS BOUND TO THE IMINE BINDING SITE FROM DFT-OPTIMISESD STRUCTURES OF **EB OTPT-FLR-210**–CO_2 COMPLEX.....380
TABLE A-10 COMPARISONS BETWEEN STRUCTURAL PARAMETERS BEFORE AND AFTER A CO_2 MOLECULE IS BOUND TO THE AMINE BINDING SITE FROM DFT-OPTIMISESD STRUCTURES OF **LEB OTPA-BZN-210**–CO_2 COMPLEX.....381
TABLE A-11 COMPARISONS BETWEEN STRUCTURAL PARAMETERS BEFORE AND AFTER A CO_2 MOLECULE IS BOUND TO THE **BZN** LINKER UNIT BINDING SITE FROM DFT-OPTIMISESD STRUCTURES OF **EB OTPA-BZN-210**–CO_2 COMPLEX.382
TABLE A-12 COMPARISONS BETWEEN STRUCTURAL PARAMETERS BEFORE AND AFTER A CO_2 MOLECULE IS BOUND TO THE **BZN** LINKER UNIT BINDING SITE FROM DFT-OPTIMISESD STRUCTURES OF **LEB OTPA-BZN-210**–CO_2 COMPLEX. 383
TABLE A-13 COMPARISONS BETWEEN STRUCTURAL PARAMETERS BEFORE AND AFTER A CO_2 MOLECULE IS BOUND TO THE **BZN** LINKER UNIT BINDING SITE FROM DFT-OPTIMISESD STRUCTURES OF **EB OTPB-BZN-210**–CO_2 COMPLEX.385
TABLE A-14 COMPARISONS BETWEEN STRUCTURAL PARAMETERS BEFORE AND AFTER A CO_2 MOLECULE IS BOUND TO THE **BZN** LINKER UNIT BINDING SITE FROM DFT-OPTIMISESD STRUCTURES OF **EB OTPT-BZN-210**–CO_2 COMPLEX.386
TABLE A-15 COMPARISONS BETWEEN STRUCTURAL PARAMETERS BEFORE AND AFTER A CO_2 MOLECULE IS BOUND TO THE **FLR** LINKER UNIT BINDING SITE FROM DFT-OPTIMISESD STRUCTURES OF **EB OTPA-FLR-210**–CO_2 COMPLEX..387
TABLE A-16 COMPARISONS BETWEEN STRUCTURAL PARAMETERS BEFORE AND AFTER A CO_2 MOLECULE IS BOUND TO THE **FLR** LINKER UNIT BINDING SITE FROM DFT-OPTIMISESD STRUCTURES OF **EB OTPB-FLR-210**–CO_2 COMPLEX..388

TABLE A-17 COMPARISONS BETWEEN STRUCTURAL PARAMETERS BEFORE AND AFTER A CO_2 MOLECULE IS BOUND TO THE **FLR** LINKER UNIT BINDING SITE FROM DFT-OPTIMISESD STRUCTURES OF **EB OTPT-FLR-210**–CO_2 COMPLEX..389
TABLE A-18 COMPARISONS BETWEEN STRUCTURAL PARAMETERS BEFORE AND AFTER A CO_2 MOLECULE IS BOUND TO THE **TPA** CORE UNIT BINDING SITE FROM DFT-OPTIMISESD STRUCTURES OF **EB OTPA-BZN-210**–CO_2 COMPLEX. ...391
TABLE A-19 COMPARISONS BETWEEN STRUCTURAL PARAMETERS BEFORE AND AFTER A CO_2 MOLECULE IS BOUND TO THE **TPA** CORE UNIT BINDING SITE FROM DFT-OPTIMISESD STRUCTURES OF **LEB OTPA-BZN-210**–CO_2 COMPLEX..392
TABLE A-20 COMPARISONS BETWEEN STRUCTURAL PARAMETERS BEFORE AND AFTER A CO_2 MOLECULE IS BOUND TO THE **TPA** CORE UNIT BINDING SITE FROM DFT-OPTIMISESD STRUCTURES OF **EB OTPA-FLR-210**–CO_2 COMPLEX.....393
TABLE A-21 COMPARISONS BETWEEN STRUCTURAL PARAMETERS BEFORE AND AFTER A CO_2 MOLECULE IS BOUND TO THE **TPB** CORE UNIT BINDING SITE FROM DFT-OPTIMISESD STRUCTURES OF **EB OTPB-BZN-210**–CO_2 COMPLEX. ...394
TABLE A-22 COMPARISONS BETWEEN STRUCTURAL PARAMETERS BEFORE AND AFTER A CO_2 MOLECULE IS BOUND TO THE **TPB** CORE UNIT BINDING SITE FROM DFT-OPTIMISESD STRUCTURES OF **EB OTPB-FLR-210**–CO_2 COMPLEX.....395
TABLE A-23 COMPARISONS BETWEEN STRUCTURAL PARAMETERS BEFORE AND AFTER A CO_2 MOLECULE IS BOUND TO THE **TPT** CORE UNIT BINDING SITE FROM DFT-OPTIMISESD STRUCTURES OF **EB OTPT-BZN-210**–CO_2 COMPLEX. ...397
TABLE A-24 COMPARISONS BETWEEN STRUCTURAL PARAMETERS BEFORE AND AFTER A CO_2 MOLECULE IS BOUND TO THE **TPT** CORE UNIT BINDING SITE FROM DFT-OPTIMISESD STRUCTURES OF **EB OTPT-FLR-210**–CO_2 COMPLEX.....398
TABLE A-25 ANGLES INVOLVED IN THE DISCUSSION OF GEOMETRIES INVOLVED IN THE BINDING OF CO_2 ONTO IMINE AND AMINE GROUP BINDING SITES (Θ_0, Θ_1, AND Θ_2) AND THEIR LINEAR COMBINATIONS 399
TABLE A-26 NUMBERS OF STEPS AND OPTIMISATION TIMES FOR THE OPTIMISATION PROCESSES OF **OTPA-BZN-430**–CO_2 COMPLEXES. NUMBERS OF OPTIMISATION STEPS ARE BROKEN DOWN BY THE INITIAL SUBMISSION AND THE SUCCESSIVE SUBMISSIONS FROM UNFINISHED OPTIMISATIONS, IF APPLICABLE, AND OPTIMISATION TIMES ARE GIVEN IN THE FORM OF DAY:HOUR:MINUTE:SECOND. 402
TABLE B-1 COMPARISON OF SCALING FACTOR IN THIS WORK FOR PANI-CMPS SYSTEMS WITH OTHER REPORTED VALUES FOR B3LYP FUNCTIONAL AND 6-31G(D) BASIS SET 469
TABLE B-2 ASSIGNMENTS FOR ABSORPTION MAXIMA IN THE 1700-1100 CM^{-1} OF THE FT-IR SPECTRUM OF **TPA**-BR_3 CORE MONOMER 470
TABLE B-3 ASSIGNMENTS FOR ABSORPTION MAXIMA IN THE 1700-1100 CM^{-1} OF THE FT-IR SPECTRUM OF **TPA**-$(NH_2)_3$ CORE MONOMER 471
TABLE B-4 ASSIGNMENTS FOR ABSORPTION MAXIMA IN THE 1700-1100 CM^{-1} OF THE FT-IR SPECTRUM OF **TPB**-BR_3 CORE MONOMER 471
TABLE B-5 ASSIGNMENTS FOR ABSORPTION MAXIMA IN THE 1700-1100 CM^{-1} OF THE FT-IR SPECTRUM OF **TPB**-$(NH_2)_3$ CORE MONOMER 472
TABLE B-6 ASSIGNMENTS FOR ABSORPTION MAXIMA IN THE 1700-1100 CM^{-1} OF THE FT-IR SPECTRUM OF **TPT**-BR_3 CORE MONOMER 472
TABLE B-7 ASSIGNMENTS FOR ABSORPTION MAXIMA IN THE 1700-1100 CM^{-1} OF THE FT-IR SPECTRUM OF **TPT**-$(NH_2)_3$ CORE MONOMER 473
TABLE B-8 ASSIGNMENTS FOR ABSORPTION MAXIMA IN THE 1700-1100 CM^{-1} OF THE FT-IR SPECTRUM OF **BZN**-BR_2 LINKER MONOMER.....473
TABLE B-9 ASSIGNMENTS FOR ABSORPTION MAXIMA IN THE 1700-1100 CM^{-1} OF THE FT-IR SPECTRUM OF **BZN**-$(NH_2)_2$ LINKER MONOMER.....474
TABLE B-10 ASSIGNMENTS FOR ABSORPTION MAXIMA IN THE 1700-1100 CM^{-1} OF THE FT-IR SPECTRUM OF **FLR**-BR_2 LINKER MONOMER.....474
TABLE B-11 ASSIGNMENTS FOR ABSORPTION MAXIMA IN THE 1700-1100 CM^{-1} OF THE FT-IR SPECTRUM OF **FLR**-$(NH_2)_2$ LINKER MONOMER.....475
TABLE B-12 ALL VIBRATIONAL PEAK POSITIONS (RAW DATA AND CORRECTED DATA WITH SCALING FACTOR OF 0.9650) FROM DFT CALCULATIONS OF **TPA**-BR_3 CORE MONOMER 475
TABLE B-13 ALL VIBRATIONAL PEAK POSITIONS (RAW DATA AND CORRECTED DATA WITH SCALING FACTOR OF 0.9650) FROM DFT CALCULATIONS OF **TPA**-$(NH_2)_3$ CORE MONOMER 477
TABLE B-14 ALL VIBRATIONAL PEAK POSITIONS (RAW DATA AND CORRECTED DATA WITH SCALING FACTOR OF 0.9650) FROM DFT CALCULATIONS OF **TPB**-BR_3 CORE MONOMER 479
TABLE B-15 ALL VIBRATIONAL PEAK POSITIONS (RAW DATA AND CORRECTED DATA WITH SCALING FACTOR OF 0.9650) FROM DFT CALCULATIONS OF **TPB**-$(NH_2)_3$ CORE MONOMER 482
TABLE B-16 ALL VIBRATIONAL PEAK POSITIONS (RAW DATA AND CORRECTED DATA WITH SCALING FACTOR OF 0.9650) FROM DFT CALCULATIONS OF **TPT**-BR_3 CORE MONOMER 485

TABLE B-17 ALL VIBRATIONAL PEAK POSITIONS (RAW DATA AND CORRECTED DATA WITH SCALING FACTOR OF 0.9650) FROM DFT CALCULATIONS OF **TPT**-$(NH_2)_3$ CORE MONOMER 487
TABLE B-18 ALL VIBRATIONAL PEAK POSITIONS (RAW DATA AND CORRECTED DATA WITH SCALING FACTOR OF 0.9650) FROM DFT CALCULATIONS OF **BZN**-Br_2 LINKER MONOMER 490
TABLE B-19 ALL VIBRATIONAL PEAK POSITIONS (RAW DATA AND CORRECTED DATA WITH SCALING FACTOR OF 0.9650) FROM DFT CALCULATIONS OF **BZN**-$(NH_2)_2$ LINKER MONOMER 490
TABLE B-20 ALL VIBRATIONAL PEAK POSITIONS (RAW DATA AND CORRECTED DATA WITH SCALING FACTOR OF 0.9650) FROM DFT CALCULATIONS OF **FLR**-Br_2 LINKER MONOMER 491
TABLE B-21 ALL VIBRATIONAL PEAK POSITIONS (RAW DATA AND CORRECTED DATA WITH SCALING FACTOR OF 0.9650) FROM DFT CALCULATIONS OF **FLR**-$(NH_2)_2$ LINKER MONOMER 493
TABLE C-1 ATTRIBUTES OF TANI IN **LEB** AND **ES** (SINGLET AND TRIPLET) STATES RELATED TO ELECTRONIC STRUCTURES 495
TABLE C-2 ATTRIBUTES OF TANI-2 IN **LEB** AND **ES** (SINGLET AND TRIPLET) STATES RELATED TO ELECTRONIC STRUCTURES 504
TABLE C-3 ATTRIBUTES OF TANI-23 IN **LEB** AND **ES** (SINGLET AND TRIPLET) STATES RELATED TO ELECTRONIC STRUCTURES 520
TABLE C-4 ATTRIBUTES OF TANI-14 IN **LEB** AND **ES** (SINGLET AND TRIPLET) STATES RELATED TO ELECTRONIC STRUCTURES 537
TABLE C-5 ATTRIBUTES OF **OTPA-BZN-210** IN **LEB**, **ES** (SINGLET AND TRIPLET), AND **EB** STATES RELATED TO ELECTRONIC STRUCTURES 552
TABLE C-6 ATTRIBUTES OF **OTPA-BZN-221** IN **LEB**, **ES** (SINGLET AND QUINTET), AND **EB** STATES RELATED TO ELECTRONIC STRUCTURES 571
TABLE C-7 ATTRIBUTES OF **OTPA-FLR-210** IN **LEB**, **ES** (SINGLET AND TRIPLET), AND **EB** STATES RELATED TO ELECTRONIC STRUCTURES 595
TABLE C-8 ATTRIBUTES OF **OTPA-FLR-221** IN **LEB**, **ES** (SINGLET AND QUINTET), AND **EB** STATES RELATED TO ELECTRONIC STRUCTURES 619
TABLE C-9 ATTRIBUTES OF **OTPB-BZN-210** IN **LEB**, **ES** (SINGLET AND TRIPLET), AND **EB** STATES RELATED TO ELECTRONIC STRUCTURES 661
TABLE C-10 ATTRIBUTES OF **OTPB-BZN-221** IN **LEB**, **ES** (SINGLET AND QUINTET), AND **EB** STATES RELATED TO ELECTRONIC STRUCTURES 681
TABLE C-11 ATTRIBUTES OF **OTPB-FLR-210** IN **LEB**, **ES** (SINGLET AND TRIPLET), AND **EB** STATES RELATED TO ELECTRONIC STRUCTURES 703
TABLE C-12 ATTRIBUTES OF **OTPB-FLR-221** IN **LEB**, **ES** (SINGLET AND QUINTET), AND **EB** STATES RELATED TO ELECTRONIC STRUCTURES 730
TABLE C-13 ATTRIBUTES OF **OTPT-BZN-210** IN **LEB**, **ES** (SINGLET AND TRIPLET), AND **EB** STATES RELATED TO ELECTRONIC STRUCTURES 778
TABLE C-14 ATTRIBUTES OF **OTPT-BZN-221** IN **LEB**, **ES** (SINGLET AND QUINTET), AND **EB** STATES RELATED TO ELECTRONIC STRUCTURES 803
TABLE C-15 ATTRIBUTES OF **OTPT-FLR-210** IN **LEB**, **ES** (SINGLET AND TRIPLET), AND **EB** STATES RELATED TO ELECTRONIC STRUCTURES 829
TABLE C-16 ATTRIBUTES OF **OTPT-FLR-221** IN **LEB**, **ES** (SINGLET AND QUINTET), AND **EB** STATES RELATED TO ELECTRONIC STRUCTURES 869
TABLE D-1 PARAMETERS RELATED TO THE BET ANALYSIS OF NITROGEN ADSORPTION ISOTHERM DATA AT 77 K OF PANI-CMPS 937
TABLE D-2 FITTING PARAMETERS FOR LANGMUIR ISOTHERM ADSORPTION MODELS OF PANI-CMPS FOR CO_2 ADSORPTION 967
TABLE D-3 FITTING PARAMETERS FOR VIRIAL ANALYSES OF PANI-CMPS CO_2 ADSORPTION ISOTHERMS 975

List of Figures

FIGURE 1-1 POLYMER GEL FORMED DURING THE SYNTHESIS OF PANI-CMPS 5
FIGURE 1-2 UV-VIS-NIR ABSORPTION SPECTRA OF PH/PH TANI, 0.15 MM IN THF, WITH DIFFERENT CONCENTRATION OF PERCHLORIC ACID AS A DOPANT, TAKEN FROM MILLS ET AL.[62] 9
FIGURE 1-3 COMPARISON BETWEEN SIX TYPES OF ADSORPTION ISOTHERM PLOTS IN THE 1985 IUPAC RECOMMENDATION[19] (LEFT) AND THE 2015 IUPAC TECHNICAL REPORT[20] (RIGHT) 15
FIGURE 1-4 EXAMPLES OF PSD PLOTS OF MATERIALS WITH RELATIVELY HIGH MICROPOROSITY (LEFT PLOTS) AND RELATIVELY HIGH MESOPOROSITY (RIGHT PLOTS). BLUE PLOTS ARE THE F(D) VS D PLOTS, AND RED PLOTS ARE THE **CUMULATIVE** F(D) VS D PLOTS. IN BOTH GRAPHS, THE D_{MIN} IS APPROXIMATELY 7 Å. 17
FIGURE 1-5 THE V_{ADS}-T PLOT FOR MESOPOROUS AL-MCM-41(C16) (LEFT) AND MICROPOROUS FAU ZEOLITE (RIGHT) ILLUSTRATING HOW THE MICROPOROUS AND MESOPOROUS VOLUMES CAN BE DETERMINED FROM THE T-PLOT METHOD, TAKEN FROM GALARNEAU ET AL.[21] IN BOTH CASES, MICROPOROUS VOLUMES ARE THE DISTANCES BETWEEN THE Y-INTERCEPT OF THE PRE-DEVIATION LINEAR REGRESSION (BLUE LINE) AND THE ORIGIN, WHILE MESOPOROUS VOLUMES ARE THE DISTANCES BETWEEN THE Y-INTERCEPTS OF THE PRE-DEVIATION (BLUE LINE) AND THE POST-DEVIATION LINEAR REGRESSION (RED LINE). THE BLACK DOTTED LINES REFER TO THE ACTUAL VALUES COMPARED TO THE VALUES FROM THE T-PLOT METHOD. 18
FIGURE 1-6 THE DEFINITION OF THE THICKNESS FUNCTION T(P/P°) OF MCM-41 REFERENCE MATERIALS, CITED IN GALARNEAU ET AL.[21] 19
FIGURE 1-7 THE METAPHORICAL JACOB'S LADDER SUMMARISING PROGRESSES IN DFT FUNCTIONAL DEVELOPMENTS, ADAPTED FROM PENG, DUARTE, AND PATON[88] 27
FIGURE 1-8 DIFFERENT REGIONS OF THE BULK SOLVENT REGARDING THE SOLVATED CHEMICAL SYSTEM 29
FIGURE 1-9 COMPARISONS BETWEEN TD-DFT-CALCULATED TRANSITION ENERGIES (LEFT) AND ABSORPTION MAXIMA (RIGHT) OF OLIGO(ANILINE)S USING CAM-B3LYP AND B3LYP FUNCTIONALS, TAKEN FROM MILLS ET AL.[62] 31
FIGURE 3-1 CALCULATED HOMHED AND HOMBQ INDICES OF DFT-CALCULATED 1,4-PHENYLENEDIAMINE STRUCTURES IN DIFFERENT STATES. STRUCTURES FOR BQ UNITS IN THESE STATES CAN BE FOUND IN SCHEME 3-4 60
FIGURE 3-2 AN EXAMPLE OF A RESULT FROM A TD-DFT CALCULATION USING GAUSSIAN 16 REVISION A.03[49] 63
FIGURE 3-3 VISUALISATIONS OF CHARGE DISTRIBUTIONS FROM TABLE 3-4 (GAUSSVIEW 6.1.1[61]) 65
FIGURE 3-4 COMPARISON BETWEEN ESP MAPS OF **BZN**-$(NH_2)_2$ IN QUINOIDAL DICATION (**QDC**) AND DIRADICAL CATION (**DRC**) FORMS FROM THE SAME CALCULATIONS AS IN TABLE 3-4 (VISUALISED USING GAUSSVIEW 6.1.1[61]) 65
FIGURE 3-5 ELECTROSTATIC POTENTIAL (ESP) SURFACE OF TANI IN ^{1}**ES** AND ^{3}**ES** STATES 69
FIGURE 3-6 SPIN DENSITY SURFACE OF TANI IN THE ^{3}**ES** STATE 69
FIGURE 3-7 ELECTROSTATIC POTENTIAL (ESP) SURFACE OF TANI-2 IN ^{1}**ES** AND ^{3}**ES** STATES 72
FIGURE 3-8 SPIN DENSITY SURFACE OF TANI-2 IN THE ^{3}**ES** STATE 72
FIGURE 3-9 ELECTROSTATIC POTENTIAL (ESP) SURFACE OF TANI-23 IN ^{1}**ES** AND ^{3}**ES** STATES 74
FIGURE 3-10 SPIN DENSITY SURFACE OF TANI-23 IN THE ^{3}**ES** STATE 74
FIGURE 3-11 ELECTROSTATIC POTENTIAL (ESP) SURFACE OF TANI-14 IN ^{1}**ES** AND ^{3}**ES** STATES 76
FIGURE 3-12 SPIN DENSITY SURFACE OF TANI-14 IN THE ^{3}**ES** STATE 76
FIGURE 3-13 ELECTROSTATIC POTENTIAL (ESP) SURFACE OF **OTPA-BZN-210** IN FOUR DIFFERENT STATES. NEUTRAL STATES **LEB** AND **EB** ARE COLOURED ACCORDING TO THE MIDDLE SCALE BAR, WHILE +2 STATES ^{1}**ES** AND ^{3}**ES** ARE COLOURED ACCORDING TO THE BOTTOM SCALE BAR. 81
FIGURE 3-14 SPIN DENSITY SURFACE OF **OTPA-BZN-210** IN THE ^{3}**ES** STATE 81
FIGURE 3-15 A STRUCTURE OF SINGLET **OTPA-BZN-221**$^{4+}$, WITH THE CYCLIC HEXA(ANILINE) MOIETY SHOWN IN RED 82
FIGURE 3-16 ELECTROSTATIC POTENTIAL (ESP) SURFACE OF **OTPA-BZN-221** IN FOUR DIFFERENT STATES. NEUTRAL STATES **LEB** AND **EB** ARE COLOURED ACCORDING TO THE MIDDLE SCALE BAR, WHILE +4 STATES ^{1}**ES** AND ^{5}**ES** ARE COLOURED ACCORDING TO THE BOTTOM SCALE BAR. 83
FIGURE 3-17 SPIN DENSITY SURFACE OF **OTPA-BZN-221** IN THE ^{5}**ES** STATE 83
FIGURE 3-18 ELECTROSTATIC POTENTIAL (ESP) SURFACE OF **OTPA-FLR-210** IN FOUR DIFFERENT STATES. NEUTRAL STATES **LEB** AND **EB** ARE COLOURED ACCORDING TO THE MIDDLE SCALE BAR, WHILE +2 STATES ^{1}**ES** AND ^{3}**ES** ARE COLOURED ACCORDING TO THE BOTTOM SCALE BAR. 86
FIGURE 3-19 SPIN DENSITY SURFACE OF **OTPA-FLR-210** IN THE ^{3}**ES** STATE 86
FIGURE 3-20 ELECTROSTATIC POTENTIAL (ESP) SURFACE OF **OTPB-BZN-210** IN FOUR DIFFERENT STATES. NEUTRAL STATES **LEB** AND **EB** ARE COLOURED ACCORDING TO THE MIDDLE SCALE BAR, WHILE +2 STATES ^{1}**ES** AND ^{3}**ES** ARE COLOURED ACCORDING TO THE BOTTOM SCALE BAR. 90

FIGURE 3-21 ELECTROSTATIC POTENTIAL (ESP) SURFACE OF **OTPB-FLR-210** IN FOUR DIFFERENT STATES. NEUTRAL STATES **LEB** AND **EB** ARE COLOURED ACCORDING TO THE MIDDLE SCALE BAR, WHILE +2 STATES ^{1}**ES** AND ^{3}**ES** ARE COLOURED ACCORDING TO THE BOTTOM SCALE BAR. 91
FIGURE 3-22 SPIN DENSITY SURFACE OF **OTPB-BZN-210** (LEFT) AND **OTPB-FLR-210** (RIGHT) IN THE ^{3}**ES** STATE .. 91
FIGURE 3-23 ELECTROSTATIC POTENTIAL (ESP) SURFACE OF **OTPT-BZN-210** IN FOUR DIFFERENT STATES. NEUTRAL STATES **LEB** AND **EB** ARE COLOURED ACCORDING TO THE MIDDLE SCALE BAR, WHILE +2 STATES ^{1}**ES** AND ^{3}**ES** ARE COLOURED ACCORDING TO THE BOTTOM SCALE BAR. 94
FIGURE 3-24 ELECTROSTATIC POTENTIAL (ESP) SURFACE OF **OTPT-FLR-210** IN FOUR DIFFERENT STATES. NEUTRAL STATES **LEB** AND **EB** ARE COLOURED ACCORDING TO THE MIDDLE SCALE BAR, WHILE +2 STATES ^{1}**ES** AND ^{3}**ES** ARE COLOURED ACCORDING TO THE BOTTOM SCALE BAR. 94
FIGURE 3-25 SPIN DENSITY SURFACE OF **OTPT-BZN-210** (LEFT) AND **OTPT-FLR-210** (RIGHT) IN THE ^{3}**ES** STATE .. 94
FIGURE 3-26 THREE-DIMENSIONAL PLOTS COMPARING HOMBQ INDICES OF BQ UNITS OF **BZN**-LINKED (RED SPHERES) AND **FLR**-LINKED (BLUE SPHERES) OLIGOMERS IN DIFFERENT OXIDATION AND DOPING STATES 95
FIGURE 3-27 THREE-DIMENSIONAL PLOTS COMPARING SELECTED BOND ANGLES AND DIHEDRAL ANGLES OF **BZN**-LINKED (RED SPHERES) AND **FLR**-LINKED (BLUE SPHERES) OLIGOMERS IN DIFFERENT OXIDATION AND DOPING STATES..... 95
FIGURE 3-28 THREE-DIMENSIONAL PLOTS COMPARING NBO CHARGES OF **BZN**-LINKED (RED SPHERES) AND **FLR**-LINKED (BLUE SPHERES) OLIGOMERS IN DIFFERENT OXIDATION AND DOPING STATES 96
FIGURE 3-29 NORMALISED CALCULATED OPTOELECTRONIC SPECTRA OF **OTPA-BZN-210** MODELS IN DIFFERENT OXIDATION, DOPING, AND SPIN STATES FROM TD-DFT CALCULATIONS (250 TO 1400 NM) 98
FIGURE 3-30 NORMALISED CALCULATED OPTOELECTRONIC SPECTRA OF **OTPA-FLR-210** MODELS IN DIFFERENT OXIDATION, DOPING, AND SPIN STATES FROM TD-DFT CALCULATIONS (250 TO 1400 NM) 99
FIGURE 3-31 NORMALISED CALCULATED OPTOELECTRONIC SPECTRA OF **OTPB-BZN-210** MODELS IN DIFFERENT OXIDATION, DOPING, AND SPIN STATES FROM TD-DFT CALCULATIONS (250 TO 1400 NM) 106
FIGURE 3-32 NORMALISED CALCULATED OPTOELECTRONIC SPECTRA OF **OTPB-FLR-210** MODELS IN DIFFERENT OXIDATION, DOPING, AND SPIN STATES FROM TD-DFT CALCULATIONS (250 TO 1400 NM) 107
FIGURE 3-33 NORMALISED CALCULATED OPTOELECTRONIC SPECTRA OF **OTPT-BZN-210** MODELS IN DIFFERENT OXIDATION, DOPING, AND SPIN STATES FROM TD-DFT CALCULATIONS (250 TO 1400 NM) 110
FIGURE 3-34 NORMALISED CALCULATED OPTOELECTRONIC SPECTRA OF **OTPT-FLR-210** MODELS IN DIFFERENT OXIDATION, DOPING, AND SPIN STATES FROM TD-DFT CALCULATIONS (250 TO 1400 NM) 110
FIGURE 3-35 COMPARISONS OF CTBQ ABSORPTION WAVELENGTHS (LEFT) AND TRANSITION ENERGIES (RIGHT) OF OXIDISED **210** OLIGOMERS IN DIFFERENT DOPING AND SPIN STATES. RED SPHERES REPRESENT DATA OF **BZN**-LINKED OLIGOMERS, AND BLUE SPHERES REPRESENT DATA OF **FLR**-LINKED OLIGOMERS. 113
FIGURE 3-36 RELATIONSHIPS BETWEEN THE DECREASES IN HOMBQ INDICES OF LINKER UNITS AND THE ENERGIES OF CTBQ TRANSITIONS OF **210** OLIGOMERS IN THE ^{1}**ES** AND THE **EB** STATES 114
FIGURE 3-37 RELATIONSHIPS BETWEEN THE DECREASES IN HOMBQ INDICES OF CORE UNITS AND THE ENERGIES OF CTBQ TRANSITIONS OF **210** OLIGOMERS IN THE ^{3}**ES** STATE.....114
FIGURE 3-38 NORMALISED CALCULATED OPTOELECTRONIC SPECTRA OF **OTPA-BZN-221** MODELS IN DIFFERENT OXIDATION, DOPING, AND SPIN STATES FROM TD-DFT CALCULATIONS (250 TO 1400 NM) 115
FIGURE 3-39 STRUCTURES OF LOWEST UNOCCUPIED MOLECULAR ORBITALS (LUMOS) OF **OTPA-BZN-210** (TOP) AND **OTPA-BZN-221** (BOTTOM), TAKEN FROM THE **EB** STATE OLIGOMERS 116
FIGURE 3-40 NORMALISED CALCULATED OPTOELECTRONIC SPECTRA OF **OTPA-FLR-221** MODELS IN DIFFERENT OXIDATION, DOPING, AND SPIN STATES FROM TD-DFT CALCULATIONS (250 TO 1400 NM) 119
FIGURE 3-41 NORMALISED CALCULATED OPTOELECTRONIC SPECTRA OF **OTPB-BZN-221** MODELS IN DIFFERENT OXIDATION, DOPING, AND SPIN STATES FROM TD-DFT CALCULATIONS (250 TO 1400 NM) 124
FIGURE 3-42 NORMALISED CALCULATED OPTOELECTRONIC SPECTRA OF **OTPB-FLR-221** MODELS IN DIFFERENT OXIDATION, DOPING, AND SPIN STATES FROM TD-DFT CALCULATIONS (250 TO 1400 NM) 124
FIGURE 3-43 NORMALISED CALCULATED OPTOELECTRONIC SPECTRA OF **OTPT-BZN-221** MODELS IN DIFFERENT OXIDATION, DOPING, AND SPIN STATES FROM TD-DFT CALCULATIONS (250 TO 1400 NM) 131
FIGURE 3-44 NORMALISED CALCULATED OPTOELECTRONIC SPECTRA OF **OTPT-FLR-221** MODELS IN DIFFERENT OXIDATION, DOPING, AND SPIN STATES FROM TD-DFT CALCULATIONS (250 TO 1400 NM) 132
FIGURE 3-45 NORMALISED ABSORPTION SPECTRA OF **TPA-BZN** (TOP) AND **TPA-FLR** (BOTTOM) FROM CALCULATIONS (SQUARES FOR THE **210 EB** MODEL AND CIRCLES FOR THE **221 EB** MODEL) AND FROM MEASUREMENTS (UP TRIANGLES FOR OLIGOMERS AND DOWN TRIANGLES FOR POLYMERS WHERE APPLICABLE) 140

FIGURE 3-46 NORMALISED ABSORPTION SPECTRA OF **TPB-BZN** (TOP) AND **TPB-FLR** (BOTTOM) FROM CALCULATIONS (SQUARES FOR THE **210 EB** MODEL AND CIRCLES FOR THE **221 EB** MODEL) AND FROM MEASUREMENTS (UP TRIANGLES FOR OLIGOMERS AND DOWN TRIANGLES FOR POLYMERS WHERE APPLICABLE) 141
FIGURE 3-47 NORMALISED ABSORPTION SPECTRA OF **TPT-BZN** (TOP) AND **TPT-FLR** (BOTTOM) FROM CALCULATIONS (SQUARES FOR THE **210 EB** MODEL AND CIRCLES FOR THE **221 EB** MODEL) AND FROM MEASUREMENTS (UP TRIANGLES FOR OLIGOMERS AND DOWN TRIANGLES FOR POLYMERS WHERE APPLICABLE) 142
FIGURE 3-48 COMPARIONS BETWEEN CALCULATED AND MEASURED PEAK POSITIONS IN THE VISIBLE REGION OF PANI-CMP MODELS, OLIGOMERS, AND POLYMERS 143
FIGURE 4-1 THIN-LAYER CHROMATOGRAPHY (TLC) ANALYSES OF SUPERNATANT OBTAINED (**RXN**) AFTER SYNTHESES COMPARED TO MONOMERS, VIEWED UNDER SHORT WAVELENGTH UV (LEFT) AND LONG WAVELENGTH UV (RIGHT) LAMPS. THESE ANALYSES WERE PERFORMED FROM SUPERNATANTS OF **PTPB-BZN-AR** (LEFT SHEET) AND **PTPB-FLR-AR** (RIGHT SHEET), WHICH BOTH FAILED TO PRODUCE POLYMERS 158
FIGURE 4-2 MASS SPECTROMETRY ANALYSES OF THE OLIGOMERIC PRODUCTS FROM THE FAILED SYNTHESES OF **PTPB-BZN-AR** (TOP) AND **PTPB-FLR-AR** (BOTTOM). SQUARES, CIRCLES, AND TRIANGLES DENOTES PEAKS WITH CONSTANT DISTANCES, SEE THE MAIN TEXT FOR DISCUSSIONS. 159
FIGURE 4-3 FT-IR TRANSMISSION SPECTRA OF **BROMINATED** CORE AND LINKER MONOMERS. REDDISH BROWN TRIANGLES MARK THE POSITIONS OF C–BR STRETCHING ABSORPTION PEAKS. 164
FIGURE 4-4 FT-IR TRANSMISSION SPECTRA OF **AMINATED** CORE AND LINKER MONOMERS. BLUE SQUARES MARK THE POSITIONS OF N–H STRETCHING ABSORPTION PEAKS, AND BLUE CIRCLES DENOTE THE POSITIONS OF NH_2 WAGGING ABSORPTION PEAKS. 165
FIGURE 4-5 DISPLACEMENT VECTORS OF ATOMS INVOLVED IN VIBRATIONAL MODE N_{12} (LEFT) AND N_{18} (RIGHT) OF **BZN-**Br_2, DEPICTED USING GAUSSVIEW 6.1.1[16] 166
FIGURE 4-6 MEASURED FT-IR TRANSMISSION SPECTRA OF A) **PTPA-BZN-BN**, B) **PTPA-BZN-BR**, C) **PTPA-FLR-SN**, AND D) **PTPA-FLR-SR** COMPARED TO MEASURED SPECTRA OF CORRESPONDING MONOMERS. REDDISH BROWN TRIANGLES MARK THE POSITIONS OF C–BR STRETCHING ABSORPTION PEAKS. BLUE SQUARES MARK THE POSITIONS OF N–H STRETCHING ABSORPTION PEAKS (FILLED FOR NH_2, EMPTY FOR NH), AND BLUE CIRCLES DENOTE THE POSITIONS OF NH_2 WAGGING ABSORPTION PEAKS. 167
FIGURE 4-7 MEASURED FT-IR TRANSMISSION SPECTRA OF A) **PTPB-BZN-SN**, B) **PTPB-BZN-SR**, C) **PTPB-FLR-SN**, AND D) **PTPB-FLR-SR** COMPARED TO MEASURED SPECTRA OF CORRESPONDING MONOMERS. REDDISH BROWN TRIANGLES MARK THE POSITIONS OF C–BR STRETCHING ABSORPTION PEAKS. BLUE SQUARES MARK THE POSITIONS OF N–H STRETCHING ABSORPTION PEAKS (FILLED FOR NH_2, EMPTY FOR NH), AND BLUE CIRCLES DENOTE THE POSITIONS OF NH_2 WAGGING ABSORPTION PEAKS. 168
FIGURE 4-8 MEASURED FT-IR TRANSMISSION SPECTRA OF A) **PTPT-BZN-SN**, B) **PTPT-BZN-SR**, C) **PTPT-FLR-SN**, AND D) **PTPT-FLR-SR** COMPARED TO MEASURED SPECTRA OF CORRESPONDING MONOMERS. REDDISH BROWN TRIANGLES MARK THE POSITIONS OF C–BR STRETCHING ABSORPTION PEAKS. BLUE SQUARES MARK THE POSITIONS OF N–H STRETCHING ABSORPTION PEAKS (FILLED FOR NH_2, EMPTY FOR NH), AND BLUE CIRCLES DENOTE THE POSITIONS OF NH_2 WAGGING ABSORPTION PEAKS. 169
FIGURE 4-9 SEM IMAGES OF **PTPB-FLR-SN** (LEFT, BET SURFACE AREAS 721.0 $m^2 \cdot g^{-1}$) AND **PTPB-FLR-SR** (RIGHT, BET SURFACE AREAS 12.7 $m^2 \cdot g^{-1}$). SCALE BARS = 1 MM. 172
FIGURE 4-10 XRD ANALYSIS RESULTS OF **PTPB-FLR-SN** AND **PTPB-FLR-SR** 173
FIGURE 4-11 RELATIONSHIPS BETWEEN SURFACE AREAS, FROM MONTE CARLO ANALYSES OF CO_2 ADSORPTION ISOTHERM AT 273 K (TOP) AND FROM BET ANALYSES OF N_2 ADSORPTION ISOTHERM AT 77 K (BOTTOM), AND CO_2 UPTAKE AT 273 K OF PANI-CMPS 175
FIGURE 4-12 A LINEAR PLOT BETWEEN CO_2 ADSORPTION AT $P/P°$ 0.95 AT 273 K AND 298 K OF PANI-CMPS 179
FIGURE 4-13 THE RELATIONSHIP BETWEEN THE PREDICTED $\Delta H°_{ADS}$ FROM VIRIAL ANALYSES AND THE UPTAKES OF CO_2 OF PANI-CMPS IN THIS STUDY 179
FIGURE 4-14 A THREE-DIMENSIONAL PLOT FOR THE RELATIONSHIPS AMONG BET SURFACE AREAS, $\Delta H°_{ADS}$, AND THE CO_2 UPTAKES AT 273 K 180
FIGURE 5-1 AN EXAMPLE OF QUADRUPOLE ILLUSTRATION, WITH POSITIVE CHARGES DISTRIBUTED ALONG THE C_N ROTATIONAL AXIS (VERTICAL) AND NEGATIVE CHARGES DISTRIBUTED ALONG THE Σ_H PLANE (HORIZONTAL). QUADRUPOLES CAN ALSO BE REPRESENTED IN THE OTHER WAY ROUND (NEGATIVE CHARGES ALONG THE PLANE, POSITIVE CHARGES ALONG THE AXIS). 184
FIGURE 5-2 QUADRUPOLE-QUADRUPOLE INTERACTIONS BETWEEN CO_2 AND C_2H_2 ALONG WITH ESP SURFACES OF BOTH MOLECULES, ADAPTED FROM LEGON[5] 184
FIGURE 5-3 TWO MODES OF INTERACTIONS BETWEEN PYRIDINE AND CO_2, TAKEN FROM LEE ET AL.[29] 186

FIGURE 5-4 DFT-OPTIMISED STRUCTURES OF PER-HYDROXYLATED PILLAR[6]ARENE WITH ONE TO FOUR CO_2 MOLECULES HELD INSIDE, TAKEN FROM SAHU ET AL.[35] 188
FIGURE 5-5 A CHEMICAL STRUCTURE FOR **OTPA-BZN-210** IN THE **EB** STATE 189
FIGURE 5-6 DFT-OPTIMISED STRUCTURES (B3LYP-D3(BJ)/6-31G(D)/THF PCM) OF **OTPA-BZN-210** IN **EB** STATE (TAKEN FROM CHAPTER 3) AND THE ESP SURFACES. ARROWS MARK THREE POSSIBLE BINDING SITES ON THE MOLECULE OF **EB OTPA-BZN-210**. 189
FIGURE 5-7 ALIGNMENTS OF CO_2 MOLECULES ON THREE DIFFERENT BINDING SITES; **A)** IMINE NITROGEN ATOM, **B)** AND **C)** LINKER UNIT, **D)** AND **E)** CORE UNIT 190
FIGURE 5-8 THE ALIGNMENT OF THE CO_2 MOLECULE BOUND TO THE IMINE NITROGEN ATOM OF **OTPA-BZN-210** FRAGMENT FROM DFT OPTIMISATION (B3LYP-D3(BJ)/6-31G(D)/ANILINE PCM, VISUALISED IN GAUSSVIEW 6.1.1), VIEWED THROUGH THE TETREL BOND BETWEEN CO_2 CARBON ATOM (NUMBER 79) AND THE IMINE NITROGEN ATOM (OBSCURED BLUE ATOM BEHIND CARBON ATOM NUMBER 79) 192
FIGURE 5-9 THE ALIGNMENT OF THE CO_2 MOLECULE BOUND TO THE LINKER UNIT BINDING SITE OF **OTPA-BZN-210** OLIGOMER FRAGMENT FROM DFT OPTIMISATION (B3LYP-D3(BJ)/6-31G(D)/ANILINE PCM, VISUALISED IN GAUSSVIEW 6.1.1) 193
FIGURE 5-10 THE ALIGNMENT OF THE CO_2 MOLECULE BOUND TO THE CORE UNIT BINDING SITE OF **OTPA-BZN-210** OLIGOMER FRAGMENT FROM DFT OPTIMISATION (B3LYP-D3(BJ)/6-31G(D)/ANILINE PCM, VISUALISED IN GAUSSVIEW 6.1.1) 195
FIGURE 5-11 DIFFERENT POSITIONS OF CO_2 ON THE FRAGMENT OF THE **OTPA-BZN-210** OLIGOMER IN THE CIS-SYN CONFORMER. THESE INITIAL SET-UPS ARE ALSO APPLIED FOR THE TRANS-SYN CONFORMER, WHILE ONLY L1 AND L2 MODES ARE APPLICABLE FOR THE ANTI CONFORMERS. 198
FIGURE 5-12 BINDING GEOMETRIES OF CO_2 ONTO THE AMINE GROUP OF **OTPA-BZN-210** IN THE **LEB** STATE FROM TOP AND TILT FRONT VIEWS 200
FIGURE 5-13 BINDING GEOMETRIES OF CO_2 ONTO **BZN** (TOP) AND **FLR** (BOTTOM) LINKER UNITS OF THE RESPECTIVE **210** OLIGOMERS WITH **TPA** CORE UNITS FROM TOP AND TILT FRONT VIEWS (DFT-OPTIMISED, B3LYP-D3(BJ)/6-31G(D)/ANILINE PCM, VISUALISED IN GAUSSVIEW 6.1.1) 203
FIGURE 5-14 BINDING GEOMETRIES OF CO_2 ONTO **TPB** CORE UNITS OF **OTPB-BZN-210** (TOP) AND **OTPB-FLR-210** (BOTTOM) FROM TOP AND TILT FRONT VIEWS (DFT-OPTIMISED, B3LYP-D3(BJ)/6-31G(D)/ANILINE PCM, VISUALISED IN GAUSSVIEW 6.1.1) 204
FIGURE 5-15 BINDING GEOMETRIES OF CO_2 ONTO THE **TPT** CORE UNIT OF **OTPT-BZN-210** FROM TOP AND TILT FRONT VIEWS (DFT-OPTIMISED, B3LYP-D3(BJ)/6-31G(D)/ANILINE PCM, VISUALISED IN GAUSSVIEW 6.1.1) 205
FIGURE 5-16 DFT-OPTIMISED STRUCTURES OF LINEAR (TOP) AND STAR-SHAPED (BOTTOM) **OTPA-BZN-430** OLIGOMERS 207
FIGURE 5-17 DIFFERENT BINDING SITES ON THE STRUCTURE OF STAR-SHAPED **OTPA-BZN-430** OLIGOMER 208
FIGURE 5-18 OPTIMISED STRUCTURES OF OLIGOMER–CO_2 FROM COILED **OTPA-BZN-430** OLIGOMER IN FIVE DIFFERENT MODES 209
FIGURE A-1 RELATIVE ENERGIES OF THE LAST 10 OPTIMISATION STEPS FOR THE BINDING OF CO_2 ONTO THE INNER CORE UNITS OF THE **EB** STATE STAR-SHAPED **OTPA-BZN-430**, WITH N BEING THE NUMBER OF STEPS TAKEN IN THE **FIRST** OPTIMISATION SUBMISSION REGARDLESS WHETHER THE OPTIMISATION PROCESS HAS FINALISED WITHIN THE TIME LIMIT OR NOT. THE LOWEST ENERGY FOR EACH MODE IS SET TO BE 10^{-5} KJ·MOL^{-1} 403
FIGURE A-2 RELATIVE ENERGIES OF THE LAST 10 OPTIMISATION STEPS FOR THE BINDING OF CO_2 ONTO THE OUTER CORE UNITS OF THE **EB** STATE STAR-SHAPED **OTPA-BZN-430**, WITH N BEING THE NUMBER OF STEPS TAKEN IN THE **FIRST** OPTIMISATION SUBMISSION REGARDLESS WHETHER THE OPTIMISATION PROCESS HAS FINALISED WITHIN THE TIME LIMIT OR NOT. THE LOWEST ENERGY FOR EACH MODE IS SET TO BE 10^{-5} KJ·MOL^{-1} 403
FIGURE A-3 RELATIVE ENERGIES OF THE LAST 10 OPTIMISATION STEPS FOR THE BINDING OF CO_2 ONTO THE LINKER UNITS OF THE **EB** STATE STAR-SHAPED **OTPA-BZN-430**, WITH N BEING THE NUMBER OF STEPS TAKEN IN THE **FIRST** OPTIMISATION SUBMISSION REGARDLESS WHETHER THE OPTIMISATION PROCESS HAS FINALISED WITHIN THE TIME LIMIT OR NOT. THE LOWEST ENERGY FOR EACH MODE IS SET TO BE 10^{-5} KJ·MOL^{-1} 404
FIGURE A-4 RELATIVE ENERGIES OF THE LAST 10 OPTIMISATION STEPS FOR THE BINDING OF CO_2 ONTO THE INNER IMINE GROUPS OF THE **EB** STATE STAR-SHAPED **OTPA-BZN-430**, WITH N BEING THE NUMBER OF STEPS TAKEN IN THE **FIRST** OPTIMISATION SUBMISSION REGARDLESS WHETHER THE OPTIMISATION PROCESS HAS FINALISED WITHIN THE TIME LIMIT OR NOT. THE LOWEST ENERGY FOR EACH MODE IS SET TO BE 10^{-5} KJ·MOL^{-1} 404
FIGURE A-5 RELATIVE ENERGIES OF THE LAST 10 OPTIMISATION STEPS FOR THE BINDING OF CO_2 ONTO THE OUTER IMINE GROUPS OF THE **EB** STATE STAR-SHAPED **OTPA-BZN-430**, WITH N BEING THE NUMBER OF STEPS TAKEN IN THE

FIRST OPTIMISATION SUBMISSION REGARDLESS WHETHER THE OPTIMISATION PROCESS HAS FINALISED WITHIN THE TIME LIMIT OR NOT. THE LOWEST ENERGY FOR EACH MODE IS SET TO BE 10^{-5} KJ·MOL^{-1} 405
FIGURE A-6 RELATIVE ENERGIES OF THE LAST 10 OPTIMISATION STEPS FOR THE BINDING OF CO_2 ONTO THE **EB** STATE LINEAR/COILED **OTPA-BZN-430**, WITH N BEING THE NUMBER OF STEPS TAKEN IN THE **FIRST** OPTIMISATION SUBMISSION REGARDLESS WHETHER THE OPTIMISATION PROCESS HAS FINALISED WITHIN THE TIME LIMIT OR NOT. THE LOWEST ENERGY FOR EACH MODE IS SET TO BE 10^{-5} KJ·MOL^{-1} 405
FIGURE B-1 COMPARISON BETWEEN CALCULATED AND MEASURED FT-IR SPECTRA OF **TPA**-Br_3 (TOP) AND **TPA**-$(NH_2)_3$ (BOTTOM) 464
FIGURE B-2 COMPARISON BETWEEN CALCULATED AND MEASURED FT-IR SPECTRA OF **TPB**-Br_3 (TOP) AND **TPB**-$(NH_2)_3$ (BOTTOM) 465
FIGURE B-3 COMPARISON BETWEEN CALCULATED AND MEASURED FT-IR SPECTRA OF **TPT**-Br_3 (TOP) AND **TPT**-$(NH_2)_3$ (BOTTOM) 466
FIGURE B-4 COMPARISON BETWEEN CALCULATED AND MEASURED FT-IR SPECTRA OF **BZN**-Br_2 (TOP) AND **FLR**-$(NH_2)_2$ (BOTTOM) 467
FIGURE B-5 COMPARISON BETWEEN CALCULATED AND MEASURED FT-IR SPECTRA OF **FLR**-Br_2 (TOP) AND **FLR**-$(NH_2)_2$ (BOTTOM) 468
FIGURE B-6 LINEAR PLOT BETWEEN CALCULATED AND MEASURED FT-IR TRANSMISSION SPECTRA OF MONOMERS IN THE 1700-1000 CM^{-1} 469
FIGURE C-1 EXCITED STATES AND NORMALISED ABSORPTION SPECTRA FROM TD-DFT CALCULATIONS OF **OTPA-BZN-210** IN **LEB** STATE. THE AREAS OF EXCITED STATE DOTS ARE PROPORTIONAL TO THEIR OSCILLATOR STRENGTHS. 552
FIGURE C-2 EXCITED STATES AND NORMALISED ABSORPTION SPECTRA FROM TD-DFT CALCULATIONS OF **OTPA-BZN-210** IN **^{1}ES** STATE. THE AREAS OF EXCITED STATE DOTS ARE PROPORTIONAL TO THEIR OSCILLATOR STRENGTHS... 554
FIGURE C-3 EXCITED STATES AND NORMALISED ABSORPTION SPECTRA FROM TD-DFT CALCULATIONS OF **OTPA-BZN-210** IN **^{3}ES** STATE. THE AREAS OF EXCITED STATE DOTS ARE PROPORTIONAL TO THEIR OSCILLATOR STRENGTHS... 557
FIGURE C-4 EXCITED STATES AND NORMALISED ABSORPTION SPECTRA FROM TD-DFT CALCULATIONS OF **OTPA-BZN-210** IN **EB** STATE. THE AREAS OF EXCITED STATE DOTS ARE PROPORTIONAL TO THEIR OSCILLATOR STRENGTHS.... 568
FIGURE C-5 EXCITED STATES AND NORMALISED ABSORPTION SPECTRA FROM TD-DFT CALCULATIONS OF **OTPA-BZN-221** IN **LEB** STATE. THE AREAS OF EXCITED STATE DOTS ARE PROPORTIONAL TO THEIR OSCILLATOR STRENGTHS. 571
FIGURE C-6 EXCITED STATES AND NORMALISED ABSORPTION SPECTRA FROM TD-DFT CALCULATIONS OF **OTPA-BZN-221** IN **^{1}ES** STATE. THE AREAS OF EXCITED STATE DOTS ARE PROPORTIONAL TO THEIR OSCILLATOR STRENGTHS... 574
FIGURE C-7 EXCITED STATES AND NORMALISED ABSORPTION SPECTRA FROM TD-DFT CALCULATIONS OF **OTPA-BZN-221** IN **^{5}ES** STATE. THE AREAS OF EXCITED STATE DOTS ARE PROPORTIONAL TO THEIR OSCILLATOR STRENGTHS... 579
FIGURE C-8 EXCITED STATES AND NORMALISED ABSORPTION SPECTRA FROM TD-DFT CALCULATIONS OF **OTPA-BZN-221** IN **EB** STATE. THE AREAS OF EXCITED STATE DOTS ARE PROPORTIONAL TO THEIR OSCILLATOR STRENGTHS.... 590
FIGURE C-9 EXCITED STATES AND NORMALISED ABSORPTION SPECTRA FROM TD-DFT CALCULATIONS OF **OTPA-FLR-210** IN **LEB** STATE. THE AREAS OF EXCITED STATE DOTS ARE PROPORTIONAL TO THEIR OSCILLATOR STRENGTHS. 595
FIGURE C-10 EXCITED STATES AND NORMALISED ABSORPTION SPECTRA FROM TD-DFT CALCULATIONS OF **OTPA-FLR-210** IN **^{1}ES** STATE. THE AREAS OF EXCITED STATE DOTS ARE PROPORTIONAL TO THEIR OSCILLATOR STRENGTHS... 598
FIGURE C-11 EXCITED STATES AND NORMALISED ABSORPTION SPECTRA FROM TD-DFT CALCULATIONS OF **OTPA-FLR-210** IN **^{3}ES** STATE. THE AREAS OF EXCITED STATE DOTS ARE PROPORTIONAL TO THEIR OSCILLATOR STRENGTHS... 601
FIGURE C-12 EXCITED STATES AND NORMALISED ABSORPTION SPECTRA FROM TD-DFT CALCULATIONS OF **OTPA-FLR-210** IN **EB** STATE. THE AREAS OF EXCITED STATE DOTS ARE PROPORTIONAL TO THEIR OSCILLATOR STRENGTHS.... 615
FIGURE C-13 EXCITED STATES AND NORMALISED ABSORPTION SPECTRA FROM TD-DFT CALCULATIONS OF **OTPA-FLR-221** IN **LEB** STATE. THE AREAS OF EXCITED STATE DOTS ARE PROPORTIONAL TO THEIR OSCILLATOR STRENGTHS. 619
FIGURE C-14 EXCITED STATES AND NORMALISED ABSORPTION SPECTRA FROM TD-DFT CALCULATIONS OF **OTPA-FLR-221** IN **^{1}ES** STATE. THE AREAS OF EXCITED STATE DOTS ARE PROPORTIONAL TO THEIR OSCILLATOR STRENGTHS... 622
FIGURE C-15 EXCITED STATES AND NORMALISED ABSORPTION SPECTRA FROM TD-DFT CALCULATIONS OF **OTPA-FLR-221** IN **^{5}ES** STATE. THE AREAS OF EXCITED STATE DOTS ARE PROPORTIONAL TO THEIR OSCILLATOR STRENGTHS... 628
FIGURE C-16 EXCITED STATES AND NORMALISED ABSORPTION SPECTRA FROM TD-DFT CALCULATIONS OF **OTPA-FLR-221** IN **EB** STATE. THE AREAS OF EXCITED STATE DOTS ARE PROPORTIONAL TO THEIR OSCILLATOR STRENGTHS.... 654
FIGURE C-17 EXCITED STATES AND NORMALISED ABSORPTION SPECTRA FROM TD-DFT CALCULATIONS OF **OTPB-BZN-210** IN **LEB** STATE. THE AREAS OF EXCITED STATE DOTS ARE PROPORTIONAL TO THEIR OSCILLATOR STRENGTHS. 662
FIGURE C-18 EXCITED STATES AND NORMALISED ABSORPTION SPECTRA FROM TD-DFT CALCULATIONS OF **OTPB-BZN-210** IN **^{1}ES** STATE. THE AREAS OF EXCITED STATE DOTS ARE PROPORTIONAL TO THEIR OSCILLATOR STRENGTHS... 664

FIGURE C-19 EXCITED STATES AND NORMALISED ABSORPTION SPECTRA FROM TD-DFT CALCULATIONS OF **OTPB-BZN-210** IN ^{5}**ES** STATE. THE AREAS OF EXCITED STATE DOTS ARE PROPORTIONAL TO THEIR OSCILLATOR STRENGTHS...667
FIGURE C-20 EXCITED STATES AND NORMALISED ABSORPTION SPECTRA FROM TD-DFT CALCULATIONS OF **OTPB-BZN-210** IN **EB** STATE. THE AREAS OF EXCITED STATE DOTS ARE PROPORTIONAL TO THEIR OSCILLATOR STRENGTHS....679
FIGURE C-21 EXCITED STATES AND NORMALISED ABSORPTION SPECTRA FROM TD-DFT CALCULATIONS OF **OTPB-BZN-221** IN **LEB** STATE. THE AREAS OF EXCITED STATE DOTS ARE PROPORTIONAL TO THEIR OSCILLATOR STRENGTHS. 681
FIGURE C-22 EXCITED STATES AND NORMALISED ABSORPTION SPECTRA FROM TD-DFT CALCULATIONS OF **OTPB-BZN-221** IN ^{1}**ES** STATE. THE AREAS OF EXCITED STATE DOTS ARE PROPORTIONAL TO THEIR OSCILLATOR STRENGTHS...684
FIGURE C-23 EXCITED STATES AND NORMALISED ABSORPTION SPECTRA FROM TD-DFT CALCULATIONS OF **OTPB-BZN-221** IN ^{5}**ES** STATE. THE AREAS OF EXCITED STATE DOTS ARE PROPORTIONAL TO THEIR OSCILLATOR STRENGTHS...689
FIGURE C-24 EXCITED STATES AND NORMALISED ABSORPTION SPECTRA FROM TD-DFT CALCULATIONS OF **OTPB-BZN-221** IN **EB** STATE. THE AREAS OF EXCITED STATE DOTS ARE PROPORTIONAL TO THEIR OSCILLATOR STRENGTHS....699
FIGURE C-25 EXCITED STATES AND NORMALISED ABSORPTION SPECTRA FROM TD-DFT CALCULATIONS OF **OTPB-FLR-210** IN **LEB** STATE. THE AREAS OF EXCITED STATE DOTS ARE PROPORTIONAL TO THEIR OSCILLATOR STRENGTHS. 703
FIGURE C-26 EXCITED STATES AND NORMALISED ABSORPTION SPECTRA FROM TD-DFT CALCULATIONS OF **OTPB-FLR-210** IN ^{1}**ES** STATE. THE AREAS OF EXCITED STATE DOTS ARE PROPORTIONAL TO THEIR OSCILLATOR STRENGTHS...705
FIGURE C-27 EXCITED STATES AND NORMALISED ABSORPTION SPECTRA FROM TD-DFT CALCULATIONS OF **OTPB-FLR-210** IN ^{3}**ES** STATE. THE AREAS OF EXCITED STATE DOTS ARE PROPORTIONAL TO THEIR OSCILLATOR STRENGTHS...708
FIGURE C-28 EXCITED STATES AND NORMALISED ABSORPTION SPECTRA FROM TD-DFT CALCULATIONS OF **OTPB-FLR-210** IN **EB** STATE. THE AREAS OF EXCITED STATE DOTS ARE PROPORTIONAL TO THEIR OSCILLATOR STRENGTHS....728
FIGURE C-29 EXCITED STATES AND NORMALISED ABSORPTION SPECTRA FROM TD-DFT CALCULATIONS OF **OTPB-FLR-221** IN **LEB** STATE. THE AREAS OF EXCITED STATE DOTS ARE PROPORTIONAL TO THEIR OSCILLATOR STRENGTHS. 731
FIGURE C-30 EXCITED STATES AND NORMALISED ABSORPTION SPECTRA FROM TD-DFT CALCULATIONS OF **OTPB-FLR-221** IN ^{1}**ES** STATE. THE AREAS OF EXCITED STATE DOTS ARE PROPORTIONAL TO THEIR OSCILLATOR STRENGTHS...734
FIGURE C-31 EXCITED STATES AND NORMALISED ABSORPTION SPECTRA FROM TD-DFT CALCULATIONS OF **OTPB-FLR-221** IN ^{5}**ES** STATE. THE AREAS OF EXCITED STATE DOTS ARE PROPORTIONAL TO THEIR OSCILLATOR STRENGTHS...741
FIGURE C-32 EXCITED STATES AND NORMALISED ABSORPTION SPECTRA FROM TD-DFT CALCULATIONS OF **OTPB-FLR-221** IN **EB** STATE. THE AREAS OF EXCITED STATE DOTS ARE PROPORTIONAL TO THEIR OSCILLATOR STRENGTHS....772
FIGURE C-33 EXCITED STATES AND NORMALISED ABSORPTION SPECTRA FROM TD-DFT CALCULATIONS OF **OTPT-BZN-210** IN **LEB** STATE. THE AREAS OF EXCITED STATE DOTS ARE PROPORTIONAL TO THEIR OSCILLATOR STRENGTHS. 779
FIGURE C-34 EXCITED STATES AND NORMALISED ABSORPTION SPECTRA FROM TD-DFT CALCULATIONS OF **OTPT-BZN-210** IN ^{1}**ES** STATE. THE AREAS OF EXCITED STATE DOTS ARE PROPORTIONAL TO THEIR OSCILLATOR STRENGTHS...782
FIGURE C-35 EXCITED STATES AND NORMALISED ABSORPTION SPECTRA FROM TD-DFT CALCULATIONS OF **OTPT-BZN-210** IN ^{3}**ES** STATE. THE AREAS OF EXCITED STATE DOTS ARE PROPORTIONAL TO THEIR OSCILLATOR STRENGTHS...788
FIGURE C-36 EXCITED STATES AND NORMALISED ABSORPTION SPECTRA FROM TD-DFT CALCULATIONS OF **OTPT-BZN-210** IN **EB** STATE. THE AREAS OF EXCITED STATE DOTS ARE PROPORTIONAL TO THEIR OSCILLATOR STRENGTHS....798
FIGURE C-37 EXCITED STATES AND NORMALISED ABSORPTION SPECTRA FROM TD-DFT CALCULATIONS OF **OTPT-BZN-221** IN **LEB** STATE. THE AREAS OF EXCITED STATE DOTS ARE PROPORTIONAL TO THEIR OSCILLATOR STRENGTHS. 803
FIGURE C-38 EXCITED STATES AND NORMALISED ABSORPTION SPECTRA FROM TD-DFT CALCULATIONS OF **OTPT-BZN-221** IN ^{1}**ES** STATE. THE AREAS OF EXCITED STATE DOTS ARE PROPORTIONAL TO THEIR OSCILLATOR STRENGTHS...807
FIGURE C-39 EXCITED STATES AND NORMALISED ABSORPTION SPECTRA FROM TD-DFT CALCULATIONS OF **OTPT-BZN-221** IN ^{5}**ES** STATE. THE AREAS OF EXCITED STATE DOTS ARE PROPORTIONAL TO THEIR OSCILLATOR STRENGTHS...814
FIGURE C-40 EXCITED STATES AND NORMALISED ABSORPTION SPECTRA FROM TD-DFT CALCULATIONS OF **OTPT-BZN-221** IN **EB** STATE. THE AREAS OF EXCITED STATE DOTS ARE PROPORTIONAL TO THEIR OSCILLATOR STRENGTHS....823
FIGURE C-41 EXCITED STATES AND NORMALISED ABSORPTION SPECTRA FROM TD-DFT CALCULATIONS OF **OTPT-FLR-210** IN **LEB** STATE. THE AREAS OF EXCITED STATE DOTS ARE PROPORTIONAL TO THEIR OSCILLATOR STRENGTHS. 830
FIGURE C-42 EXCITED STATES AND NORMALISED ABSORPTION SPECTRA FROM TD-DFT CALCULATIONS OF **OTPT-FLR-210** IN ^{1}**ES** STATE. THE AREAS OF EXCITED STATE DOTS ARE PROPORTIONAL TO THEIR OSCILLATOR STRENGTHS...834
FIGURE C-43 EXCITED STATES AND NORMALISED ABSORPTION SPECTRA FROM TD-DFT CALCULATIONS OF **OTPT-FLR-210** IN ^{3}**ES** STATE. THE AREAS OF EXCITED STATE DOTS ARE PROPORTIONAL TO THEIR OSCILLATOR STRENGTHS...839
FIGURE C-44 EXCITED STATES AND NORMALISED ABSORPTION SPECTRA FROM TD-DFT CALCULATIONS OF **OTPT-FLR-210** IN **EB** STATE. THE AREAS OF EXCITED STATE DOTS ARE PROPORTIONAL TO THEIR OSCILLATOR STRENGTHS....863
FIGURE C-45 EXCITED STATES AND NORMALISED ABSORPTION SPECTRA FROM TD-DFT CALCULATIONS OF **OTPT-FLR-221** IN **LEB** STATE. THE AREAS OF EXCITED STATE DOTS ARE PROPORTIONAL TO THEIR OSCILLATOR STRENGTHS. 869

FIGURE C-46 EXCITED STATES AND NORMALISED ABSORPTION SPECTRA FROM TD-DFT CALCULATIONS OF **OTPT-FLR-221** IN **^{1}ES** STATE. THE AREAS OF EXCITED STATE DOTS ARE PROPORTIONAL TO THEIR OSCILLATOR STRENGTHS...874
FIGURE C-47 EXCITED STATES AND NORMALISED ABSORPTION SPECTRA FROM TD-DFT CALCULATIONS OF **OTPT-FLR-221** IN **^{5}ES** STATE. THE AREAS OF EXCITED STATE DOTS ARE PROPORTIONAL TO THEIR OSCILLATOR STRENGTHS...883
FIGURE C-48 EXCITED STATES AND NORMALISED ABSORPTION SPECTRA FROM TD-DFT CALCULATIONS OF **OTPT-FLR-221** IN **EB** STATE. THE AREAS OF EXCITED STATE DOTS ARE PROPORTIONAL TO THEIR OSCILLATOR STRENGTHS....919
FIGURE D-1 NITROGEN ADSORPTION ISOTHERM AT 77 K OF **PTPA-FLR-SN** 929
FIGURE D-2 NITROGEN ADSORPTION ISOTHERM AT 77 K OF **PTPA-FLR-SNx**....930
FIGURE D-3 NITROGEN ADSORPTION ISOTHERM AT 77 K OF **PTPA-FLR-SR** 930
FIGURE D-4 NITROGEN ADSORPTION ISOTHERM AT 77 K OF **PTPB-FLR-SN** 931
FIGURE D-5 NITROGEN ADSORPTION ISOTHERM AT 77 K OF **PTPB-FLR-SNx**....931
FIGURE D-6 NITROGEN ADSORPTION ISOTHERM AT 77 K OF **PTPB-FLR-SR** 932
FIGURE D-7 NITROGEN ADSORPTION ISOTHERM AT 77 K OF **PTPB-FLR-SRx**....932
FIGURE D-8 NITROGEN ADSORPTION ISOTHERM AT 77 K OF **PTPT-BZN-SN**....933
FIGURE D-9 NITROGEN ADSORPTION ISOTHERM AT 77 K OF **PTPT-BZN-SNx** 933
FIGURE D-10 NITROGEN ADSORPTION ISOTHERM AT 77 K OF **PTPT-BZN-SR**....934
FIGURE D-11 NITROGEN ADSORPTION ISOTHERM AT 77 K OF **PTPT-BZN-SRx**....934
FIGURE D-12 NITROGEN ADSORPTION ISOTHERM AT 77 K OF **PTPT-FLR-SN**....935
FIGURE D-13 NITROGEN ADSORPTION ISOTHERM AT 77 K OF **PTPT-FLR-SNx** 935
FIGURE D-14 NITROGEN ADSORPTION ISOTHERM AT 77 K OF **PTPT-FLR-SR**....936
FIGURE D-15 NITROGEN ADSORPTION ISOTHERM AT 77 K OF **PTPT-FLR-SRx** 936
FIGURE D-16 BET ANALYSIS PLOT FOR **PTPA-FLR-SN**....937
FIGURE D-17 BET ANALYSIS PLOT FOR **PTPA-FLR-SNx**....938
FIGURE D-18 BET ANALYSIS PLOT FOR **PTPA-FLR-SR**....938
FIGURE D-19 BET ANALYSIS PLOT FOR **PTPB-FLR-SN**....939
FIGURE D-20 BET ANALYSIS PLOT FOR **PTPB-FLR-SNx**....939
FIGURE D-21 BET ANALYSIS PLOT FOR **PTPB-FLR-SR**....940
FIGURE D-22 BET ANALYSIS PLOT FOR **PTPB-FLR-SRx**....940
FIGURE D-23 BET ANALYSIS PLOT FOR **PTPT-BZN-SN** 941
FIGURE D-24 BET ANALYSIS PLOT FOR **PTPT-BZN-SNx**....941
FIGURE D-25 BET ANALYSIS PLOT FOR **PTPT-BZN-SR** 942
FIGURE D-26 BET ANALYSIS PLOT FOR **PTPT-BZN-SRx**....942
FIGURE D-27 BET ANALYSIS PLOT FOR **PTPT-FLR-SN**....943
FIGURE D-28 BET ANALYSIS PLOT FOR **PTPT-FLR-SNx**....943
FIGURE D-29 BET ANALYSIS PLOT FOR **PTPT-FLR-SR**....944
FIGURE D-30 BET ANALYSIS PLOT FOR **PTPT-FLR-SRx**....944
FIGURE D-31 NLDFT PORE SIZE DISTRIBUTIONS IN **PTPA-FLR-SN**, ANALYSED FROM SURFACE AREA, AND CUMULATIVE SURFACE AREA PLOT....945
FIGURE D-32 NLDFT PORE SIZE DISTRIBUTIONS IN **PTPA-FLR-SN**, ANALYSED FROM PORE VOLUME, AND CUMULATIVE PORE VOLUME PLOT....945
FIGURE D-33 NLDFT PORE SIZE DISTRIBUTIONS IN **PTPA-FLR-SNx**, ANALYSED FROM SURFACE AREA, AND CUMULATIVE SURFACE AREA PLOT....946
FIGURE D-34 NLDFT PORE SIZE DISTRIBUTIONS IN **PTPA-FLR-SNx**, ANALYSED FROM PORE VOLUME, AND CUMULATIVE PORE VOLUME PLOT....946
FIGURE D-35 NLDFT PORE SIZE DISTRIBUTIONS IN **PTPA-FLR-SR**, ANALYSED FROM SURFACE AREA, AND CUMULATIVE SURFACE AREA PLOT....947
FIGURE D-36 NLDFT PORE SIZE DISTRIBUTIONS IN **PTPA-FLR-SR**, ANALYSED FROM PORE VOLUME, AND CUMULATIVE PORE VOLUME PLOT....947
FIGURE D-37 NLDFT PORE SIZE DISTRIBUTIONS IN **PTPB-FLR-SN**, ANALYSED FROM SURFACE AREA, AND CUMULATIVE SURFACE AREA PLOT....948
FIGURE D-38 NLDFT PORE SIZE DISTRIBUTIONS IN **PTPB-FLR-SN**, ANALYSED FROM PORE VOLUME, AND CUMULATIVE PORE VOLUME PLOT....948
FIGURE D-39 NLDFT PORE SIZE DISTRIBUTIONS IN **PTPB-FLR-SNx**, ANALYSED FROM SURFACE AREA, AND CUMULATIVE SURFACE AREA PLOT....949

FIGURE D-40 NLDFT PORE SIZE DISTRIBUTIONS IN **PTPB-FLR-SNX**, ANALYSED FROM PORE VOLUME, AND CUMULATIVE PORE VOLUME PLOT 949
FIGURE D-41 NLDFT PORE SIZE DISTRIBUTIONS IN **PTPB-FLR-SR**, ANALYSED FROM SURFACE AREA, AND CUMULATIVE SURFACE AREA PLOT 950
FIGURE D-42 NLDFT PORE SIZE DISTRIBUTIONS IN **PTPB-FLR-SR**, ANALYSED FROM PORE VOLUME, AND CUMULATIVE PORE VOLUME PLOT 950
FIGURE D-43 NLDFT PORE SIZE DISTRIBUTIONS IN **PTPB-FLR-SRX**, ANALYSED FROM SURFACE AREA, AND CUMULATIVE SURFACE AREA PLOT 951
FIGURE D-44 NLDFT PORE SIZE DISTRIBUTIONS IN **PTPB-FLR-SRX**, ANALYSED FROM PORE VOLUME, AND CUMULATIVE PORE VOLUME PLOT 951
FIGURE D-45 NLDFT PORE SIZE DISTRIBUTIONS IN **PTPT-BZN-SN**, ANALYSED FROM SURFACE AREA, AND CUMULATIVE SURFACE AREA PLOT 952
FIGURE D-46 NLDFT PORE SIZE DISTRIBUTIONS IN **PTPT-BZN-SN**, ANALYSED FROM PORE VOLUME, AND CUMULATIVE PORE VOLUME PLOT 952
FIGURE D-47 NLDFT PORE SIZE DISTRIBUTIONS IN **PTPT-BZN-SNX**, ANALYSED FROM SURFACE AREA, AND CUMULATIVE SURFACE AREA PLOT 953
FIGURE D-48 NLDFT PORE SIZE DISTRIBUTIONS IN **PTPT-BZN-SNX**, ANALYSED FROM PORE VOLUME, AND CUMULATIVE PORE VOLUME PLOT 953
FIGURE D-49 NLDFT PORE SIZE DISTRIBUTIONS IN **PTPT-BZN-SR**, ANALYSED FROM SURFACE AREA, AND CUMULATIVE SURFACE AREA PLOT 954
FIGURE D-50 NLDFT PORE SIZE DISTRIBUTIONS IN **PTPT-BZN-SR**, ANALYSED FROM PORE VOLUME, AND CUMULATIVE PORE VOLUME PLOT 954
FIGURE D-51 NLDFT PORE SIZE DISTRIBUTIONS IN **PTPT-BZN-SRX**, ANALYSED FROM SURFACE AREA, AND CUMULATIVE SURFACE AREA PLOT 955
FIGURE D-52 NLDFT PORE SIZE DISTRIBUTIONS IN **PTPT-BZN-SRX**, ANALYSED FROM PORE VOLUME, AND CUMULATIVE VOLUME PLOT 955
FIGURE D-53 NLDFT PORE SIZE DISTRIBUTIONS IN **PTPT-FLR-SN**, ANALYSED FROM SURFACE AREA, AND CUMULATIVE SURFACE AREA PLOT 956
FIGURE D-54 NLDFT PORE SIZE DISTRIBUTIONS IN **PTPT-FLR-SN**, ANALYSED FROM PORE VOLUME, AND CUMULATIVE PORE VOLUME PLOT 956
FIGURE D-55 NLDFT PORE SIZE DISTRIBUTIONS IN **PTPT-FLR-SNX**, ANALYSED FROM SURFACE AREA, AND CUMULATIVE SURFACE AREA PLOT 957
FIGURE D-56 NLDFT PORE SIZE DISTRIBUTIONS IN **PTPT-FLR-SNX**, ANALYSED FROM PORE VOLUME, AND CUMULATIVE PORE VOLUME PLOT 957
FIGURE D-57 NLDFT PORE SIZE DISTRIBUTIONS IN **PTPT-FLR-SR**, ANALYSED FROM SURFACE AREA, AND CUMULATIVE SURFACE AREA PLOT 958
FIGURE D-58 NLDFT PORE SIZE DISTRIBUTIONS IN **PTPT-FLR-SR**, ANALYSED FROM PORE VOLUME, AND CUMULATIVE PORE VOLUME PLOT 958
FIGURE D-59 NLDFT PORE SIZE DISTRIBUTIONS IN **PTPT-FLR-SRX**, ANALYSED FROM SURFACE AREA, AND CUMULATIVE SURFACE AREA PLOT 959
FIGURE D-60 NLDFT PORE SIZE DISTRIBUTIONS IN **PTPT-FLR-SRX**, ANALYSED FROM PORE VOLUME, AND CUMULATIVE PORE VOLUME PLOT 959
FIGURE D-61 CARBON DIOXIDE ADSORPTION ISOTHERM AT 273 K (BLUE) AND 298 K (RED) OF **PTPA-FLR-SN** 960
FIGURE D-62 CARBON DIOXIDE ADSORPTION ISOTHERM AT 273 K (BLUE) AND 298 K (RED) OF **PTPA-FLR-SNX** 960
FIGURE D-63 CARBON DIOXIDE ADSORPTION ISOTHERM AT 273 K (BLUE) AND 298 K (RED) OF **PTPA-FLR-SR** 961
FIGURE D-64 CARBON DIOXIDE ADSORPTION ISOTHERM AT 273 K (BLUE) AND 298 K (RED) OF **PTPB-FLR-SN** 961
FIGURE D-65 CARBON DIOXIDE ADSORPTION ISOTHERM AT 273 K (BLUE) AND 298 K (RED) OF **PTPB-FLR-SNX** 962
FIGURE D-66 CARBON DIOXIDE ADSORPTION ISOTHERM AT 273 K (BLUE) AND 298 K (RED) OF **PTPB-FLR-SR** 962
FIGURE D-67 CARBON DIOXIDE ADSORPTION ISOTHERM AT 273 K (BLUE) AND 298 K (RED) OF **PTPB-FLR-SRX** 963
FIGURE D-68 CARBON DIOXIDE ADSORPTION ISOTHERM AT 273 K (BLUE) AND 298 K (RED) OF **PTPT-BZN-SN** 963
FIGURE D-69 CARBON DIOXIDE ADSORPTION ISOTHERM AT 273 K (BLUE) AND 298 K (RED) OF **PTPT-BZN-SNX** 964
FIGURE D-70 CARBON DIOXIDE ADSORPTION ISOTHERM AT 273 K (BLUE) AND 298 K (RED) OF **PTPT-BZN-SR** 964
FIGURE D-71 CARBON DIOXIDE ADSORPTION ISOTHERM AT 273 K (BLUE) AND 298 K (RED) OF **PTPT-BZN-SRX** 965
FIGURE D-72 CARBON DIOXIDE ADSORPTION ISOTHERM AT 273 K (BLUE) AND 298 K (RED) OF **PTPT-FLR-SN** 965
FIGURE D-73 CARBON DIOXIDE ADSORPTION ISOTHERM AT 273 K (BLUE) AND 298 K (RED) OF **PTPT-FLR-SNX** 966

FIGURE D-74 CARBON DIOXIDE ADSORPTION ISOTHERM AT 273 K (BLUE) AND 298 K (RED) OF **PTPT-FLR-SR** 966
FIGURE D-75 CARBON DIOXIDE ADSORPTION ISOTHERM AT 273 K (BLUE) AND 298 K (RED) OF **PTPT-FLR-SRx** 967
FIGURE D-76 LANGMUIR FITTING PLOT FOR **PTPA-FLR-SN** CO_2 ADSORPTION ISOTHERM 968
FIGURE D-77 LANGMUIR FITTING PLOT FOR **PTPA-FLR-SNx** CO_2 ADSORPTION ISOTHERM 968
FIGURE D-78 LANGMUIR FITTING PLOT FOR **PTPA-FLR-SR** CO_2 ADSORPTION ISOTHERM 969
FIGURE D-79 LANGMUIR FITTING PLOT FOR **PTPB-FLR-SN** CO_2 ADSORPTION ISOTHERM 969
FIGURE D-80 LANGMUIR FITTING PLOT FOR **PTPB-FLR-SNx** CO_2 ADSORPTION ISOTHERM 970
FIGURE D-81 LANGMUIR FITTING PLOT FOR **PTPB-FLR-SR** CO_2 ADSORPTION ISOTHERM 970
FIGURE D-82 LANGMUIR FITTING PLOT FOR **PTPB-FLR-SRx** CO_2 ADSORPTION ISOTHERM 971
FIGURE D-83 LANGMUIR FITTING PLOT FOR **PTPT-BZN-SN** CO_2 ADSORPTION ISOTHERM 971
FIGURE D-84 LANGMUIR FITTING PLOT FOR **PTPT-BZN-SNx** CO_2 ADSORPTION ISOTHERM 972
FIGURE D-85 LANGMUIR FITTING PLOT FOR **PTPT-BZN-SR** CO_2 ADSORPTION ISOTHERM 972
FIGURE D-86 LANGMUIR FITTING PLOT FOR **PTPT-BZN-SRx** CO_2 ADSORPTION ISOTHERM 973
FIGURE D-87 LANGMUIR FITTING PLOT FOR **PTPT-FLR-SN** CO_2 ADSORPTION ISOTHERM 973
FIGURE D-88 LANGMUIR FITTING PLOT FOR **PTPT-FLR-SNx** CO_2 ADSORPTION ISOTHERM 974
FIGURE D-89 LANGMUIR FITTING PLOT FOR **PTPT-FLR-SR** CO_2 ADSORPTION ISOTHERM 974
FIGURE D-90 LANGMUIR FITTING PLOT FOR **PTPT-FLR-SRx** CO_2 ADSORPTION ISOTHERM 975
FIGURE D-91 VIRIAL ANALYSIS FITTING PLOT FOR **PTPA-FLR-SN** CO_2 ADSORPTION ISOTHERM 976
FIGURE D-92 VIRIAL ANALYSIS FITTING PLOT FOR **PTPA-FLR-SNx** CO_2 ADSORPTION ISOTHERM 976
FIGURE D-93 VIRIAL ANALYSIS FITTING PLOT FOR **PTPA-FLR-SR** CO_2 ADSORPTION ISOTHERM 977
FIGURE D-94 VIRIAL ANALYSIS FITTING PLOT FOR **PTPB-FLR-SN** CO_2 ADSORPTION ISOTHERM 977
FIGURE D-95 VIRIAL ANALYSIS FITTING PLOT FOR **PTPB-FLR-SNx** CO_2 ADSORPTION ISOTHERM 978
FIGURE D-96 VIRIAL ANALYSIS FITTING PLOT FOR **PTPB-FLR-SR** CO_2 ADSORPTION ISOTHERM 978
FIGURE D-97 VIRIAL ANALYSIS FITTING PLOT FOR **PTPB-FLR-SRx** CO_2 ADSORPTION ISOTHERM 979
FIGURE D-98 VIRIAL ANALYSIS FITTING PLOT FOR **PTPT-BZN-SN** CO_2 ADSORPTION ISOTHERM 979
FIGURE D-99 VIRIAL ANALYSIS FITTING PLOT FOR **PTPT-BZN-SNx** CO_2 ADSORPTION ISOTHERM 980
FIGURE D-100 VIRIAL ANALYSIS FITTING PLOT FOR **PTPT-BZN-SR** CO_2 ADSORPTION ISOTHERM 980
FIGURE D-101 VIRIAL ANALYSIS FITTING PLOT FOR **PTPT-BZN-SRx** CO_2 ADSORPTION ISOTHERM 981
FIGURE D-102 VIRIAL ANALYSIS FITTING PLOT FOR **PTPT-FLR-SN** CO_2 ADSORPTION ISOTHERM 981
FIGURE D-103 VIRIAL ANALYSIS FITTING PLOT FOR **PTPT-FLR-SNx** CO_2 ADSORPTION ISOTHERM 982
FIGURE D-104 VIRIAL ANALYSIS FITTING PLOT FOR **PTPT-FLR-SR** CO_2 ADSORPTION ISOTHERM 982
FIGURE D-105 VIRIAL ANALYSIS FITTING PLOT FOR **PTPT-FLR-SNx** CO_2 ADSORPTION ISOTHERM 983
FIGURE D-106 ISOSTERIC ENTHALPY OF ADSORPTION OVER THE VALID RANGE OF **PTPA-FLR** FROM DIFFERENT APPROACHES. **SN** AND **SR** REFER TO NORMAL AND REVERSED APPROACHES, RESPECTIVELY, AND LETTER **X** REFERS TO THE SYNTHESES WITHOUT ADDED SODIUM BROMIDE. 983
FIGURE D-107 ISOSTERIC ENTHALPY OF ADSORPTION OVER THE VALID RANGE OF **PTPB-FLR** FROM DIFFERENT APPROACHES. **SN** AND **SR** REFER TO NORMAL AND REVERSED APPROACHES, RESPECTIVELY, AND LETTER **X** REFERS TO THE SYNTHESES WITHOUT ADDED SODIUM BROMIDE. 984
FIGURE D-108 ISOSTERIC ENTHALPY OF ADSORPTION OVER THE VALID RANGE OF **PTPT-BZN** FROM DIFFERENT APPROACHES. **SN** AND **SR** REFER TO NORMAL AND REVERSED APPROACHES, RESPECTIVELY, AND LETTER **X** REFERS TO THE SYNTHESES WITHOUT ADDED SODIUM BROMIDE. 984
FIGURE D-109 ISOSTERIC ENTHALPY OF ADSORPTION OVER THE VALID RANGE OF **PTPT-FLR** FROM DIFFERENT APPROACHES. **SN** AND **SR** REFER TO NORMAL AND REVERSED APPROACHES, RESPECTIVELY, AND LETTER **X** REFERS TO THE SYNTHESES WITHOUT ADDED SODIUM BROMIDE. 985
FIGURE D-110 COMPARISON BETWEEN ISOSTERIC ENTHALPIES OF ADSORPTION FROM LANGMUIR MODEL (RED) AND VIRIAL ANALYSIS (BLUE) IN THE RANGE FROM ZERO ADSORPTION TO MAXIMUM ADSORPTION AT RELATIVE PRESSURE 0.95 AND 273 K (GREY LINE) FOR **PTPA-FLR-SN**. THE BLUE NUMBER ON THE Y-AXIS IS THE ESTIMATED ISOSTERIC ENTHALPY OF ADSORPTION AT ZERO COVERAGE ($\Delta H°_{ADS}$). 985
FIGURE D-111 COMPARISON BETWEEN ISOSTERIC ENTHALPIES OF ADSORPTION FROM LANGMUIR MODEL (RED) AND VIRIAL ANALYSIS (BLUE) IN THE RANGE FROM ZERO ADSORPTION TO MAXIMUM ADSORPTION AT RELATIVE PRESSURE 0.95 AND 273 K (GREY LINE) FOR **PTPA-FLR-SNx**. THE BLUE NUMBER ON THE Y-AXIS IS THE ESTIMATED ISOSTERIC ENTHALPY OF ADSORPTION AT ZERO COVERAGE ($\Delta H°_{ADS}$). 986
FIGURE D-112 COMPARISON BETWEEN ISOSTERIC ENTHALPIES OF ADSORPTION FROM LANGMUIR MODEL (RED) AND VIRIAL ANALYSIS (BLUE) IN THE RANGE FROM ZERO ADSORPTION TO MAXIMUM ADSORPTION AT RELATIVE PRESSURE 0.95

and 273 K (grey line) for **PTPA-FLR-SR**. The blue number on the y-axis is the estimated isosteric enthalpy of adsorption at zero coverage ($\Delta H°_{ADS}$). 986
Figure D-113 Comparison between isosteric enthalpies of adsorption from Langmuir model (red) and virial analysis (blue) in the range from zero adsorption to maximum adsorption at relative pressure 0.95 and 273 K (grey line) for **PTPB-FLR-SN**. The blue number on the y-axis is the estimated isosteric enthalpy of adsorption at zero coverage ($\Delta H°_{ADS}$). 987
Figure D-114 Comparison between isosteric enthalpies of adsorption from Langmuir model (red) and virial analysis (blue) in the range from zero adsorption to maximum adsorption at relative pressure 0.95 and 273 K (grey line) for **PTPB-FLR-SNx**. The blue number on the y-axis is the estimated isosteric enthalpy of adsorption at zero coverage ($\Delta H°_{ADS}$). 987
Figure D-115 Comparison between isosteric enthalpies of adsorption from Langmuir model (red) and virial analysis (blue) in the range from zero adsorption to maximum adsorption at relative pressure 0.95 and 273 K (grey line) for **PTPB-FLR-SR**. The blue number on the y-axis is the estimated isosteric enthalpy of adsorption at zero coverage ($\Delta H°_{ADS}$). 988
Figure D-116 Comparison between isosteric enthalpies of adsorption from Langmuir model (red) and virial analysis (blue) in the range from zero adsorption to maximum adsorption at relative pressure 0.95 and 273 K (grey line) for **PTPB-FLR-SRx**. The blue number on the y-axis is the estimated isosteric enthalpy of adsorption at zero coverage ($\Delta H°_{ADS}$). 988
Figure D-117 Comparison between isosteric enthalpies of adsorption from Langmuir model (red) and virial analysis (blue) in the range from zero adsorption to maximum adsorption at relative pressure 0.95 and 273 K (grey line) for **PTPT-BZN-SN**. The blue number on the y-axis is the estimated isosteric enthalpy of adsorption at zero coverage ($\Delta H°_{ADS}$). 989
Figure D-118 Comparison between isosteric enthalpies of adsorption from Langmuir model (red) and virial analysis (blue) in the range from zero adsorption to maximum adsorption at relative pressure 0.95 and 273 K (grey line) for **PTPT-BZN-SNx**. The blue number on the y-axis is the estimated isosteric enthalpy of adsorption at zero coverage ($\Delta H°_{ADS}$). 989
Figure D-119 Comparison between isosteric enthalpies of adsorption from Langmuir model (red) and virial analysis (blue) in the range from zero adsorption to maximum adsorption at relative pressure 0.95 and 273 K (grey line) for **PTPT-BZN-SR**. The blue number on the y-axis is the estimated isosteric enthalpy of adsorption at zero coverage ($\Delta H°_{ADS}$). 990
Figure D-120 Comparison between isosteric enthalpies of adsorption from Langmuir model (red) and virial analysis (blue) in the range from zero adsorption to maximum adsorption at relative pressure 0.95 and 273 K (grey line) for **PTPT-BZN-SRx**. The blue number on the y-axis is the estimated isosteric enthalpy of adsorption at zero coverage ($\Delta H°_{ADS}$). 990
Figure D-121 Comparison between isosteric enthalpies of adsorption from Langmuir model (red) and virial analysis (blue) in the range from zero adsorption to maximum adsorption at relative pressure 0.95 and 273 K (grey line) for **PTPT-FLR-SN**. The blue number on the y-axis is the estimated isosteric enthalpy of adsorption at zero coverage ($\Delta H°_{ADS}$). 991
Figure D-122 Comparison between isosteric enthalpies of adsorption from Langmuir model (red) and virial analysis (blue) in the range from zero adsorption to maximum adsorption at relative pressure 0.95 and 273 K (grey line) for **PTPT-FLR-SNx**. The blue number on the y-axis is the estimated isosteric enthalpy of adsorption at zero coverage ($\Delta H°_{ADS}$). 991
Figure D-123 Comparison between isosteric enthalpies of adsorption from Langmuir model (red) and virial analysis (blue) in the range from zero adsorption to maximum adsorption at relative pressure 0.95 and 273 K (grey line) for **PTPT-FLR-SR**. The blue number on the y-axis is the estimated isosteric enthalpy of adsorption at zero coverage ($\Delta H°_{ADS}$). 992
Figure D-124 Comparison between isosteric enthalpies of adsorption from Langmuir model (red) and virial analysis (blue) in the range from zero adsorption to maximum adsorption at relative pressure 0.95 and 273 K (grey line) for **PTPT-FLR-SRx**. The blue number on the y-axis is the estimated isosteric enthalpy of adsorption at zero coverage ($\Delta H°_{ADS}$). 993
Figure E-1 Appearances of **PTPA-BZN** materials. **PTPA-BZN-BNox** refers to a failed batch of **PTPA-BZN-BNx** in which material was accidentally oxidised during synthesis. 995
Figure E-2 Appearances of **PTPA-FLR** materials 995
Figure E-3 Appearances of **PTPB-BZN** materials 995
Figure E-4 Appearances of **PTPB-FLR** materials 996

FIGURE E-5 APPEARANCES OF **PTPT-BZN** MATERIALS....996
FIGURE E-6 APPEARANCES OF **PTPT-FLR** MATERIALS....996
FIGURE E-7 APPEARANCES OF **OTPA-BZN** MATERIALS. **OTPA-BZN-BNOX** REFERS TO A FAILED BATCH OF **OTPA-BZN-BNX** IN WHICH MATERIAL WAS ACCIDENTALLY OXIDISED DURING SYNTHESIS....997
FIGURE E-8 APPEARANCES OF **OTPA-FLR** MATERIALS....997
FIGURE E-9 APPEARANCES OF **OTPB-BZN** MATERIALS....997
FIGURE E-10 APPEARANCES OF **OTPB-FLR** MATERIALS....998
FIGURE E-11 APPEARANCES OF **OTPT-BZN** MATERIALS....998
FIGURE E-12 APPEARANCES OF **OTPT-FLR** MATERIALS....998
FIGURE E-13 XRD ANALYSIS RESULT OF AN EMPTY AMORPHOUS SILICON SAMPLE HOLDER (RED) AND A SAMPLE HOLDER WITH VASELINE (BLUE) FROM THE 2θ OF 5° TO 35°....999
FIGURE E-14 XRD ANALYSIS RESULT OF **TPB**-Br_3 CORE MONOMER FROM THE 2θ OF 5° TO 60°....999
FIGURE E-15 XRD ANALYSIS RESULT OF **TPB**-$(NH_2)_3$ CORE MONOMER FROM THE 2θ OF 5° TO 60°....1000
FIGURE E-16 XRD ANALYSIS RESULT OF **FLR**-Br_2 LINKER MONOMER FROM THE 2θ OF 5° TO 60°....1000
FIGURE E-17 XRD ANALYSIS RESULT OF **FLR**-$(NH_2)_2$ LINKER MONOMER FROM THE 2θ OF 5° TO 60°....1001

List of Schemes

Scheme 1-1 Classification of porous materials based on chemical components and syntheses with further classifications of porous organic materials (POMs) 2

Scheme 1-2 Examples of porous organic materials of each type, **COF-1** for COFs,[29] propylene-crosslinked PANI for HCPs (crosslinking propylene groups shown in bold),[30] **CMP-1** for CMPs,[5, 31] **PIM-1** for PIMs,[32] and cage 1 for POCs[33] 3

Scheme 1-3 Polyaddition reactions between two monomers, red A_3 and blue B_2, showing different possible reactions taking place during the first three steps of the polymerisation process. Not all possible reactions are shown. Polycondensation reactions can be considered in the similar manner with the formation of smaller molecules. 4

Scheme 1-4 Examples of tetra(aniline)s with different functionalities; Ph/Ph (top), Ph/NH_2 (middle), and NH_2/NH_2 (bottom) 6

Scheme 1-5 Structures of five oxidation states of octa(aniline) as proposed by Green and Woodhead in early 1910s, benzenoid and quinoid units are shown in red and blue, respectively[49, 50] 6

Scheme 1-6 General representation of poly(aniline) structures[4] 6

Scheme 1-7 Relationship diagram of poly(aniline)s in different oxidation and doping states, adapted from Wei and Faul[3] 7

Scheme 1-8 Poly(aniline) doping process as proposed by Stafström et al.[56] 8

Scheme 1-9 Polaron lattice model (top) and four-ring BQ derivatives model (bottom) 8

Scheme 1-10 Relationship diagram of poly(aniline)s in different oxidation and doping states with regards to spin multiplicities 10

Scheme 1-11 Synthesis of 4-methoxyphenyl-capped octa(aniline) using palladium-catalysed coupling reactions published by Singer, Sadighi, and Buchwald.[63] Amino groups are protected by tert-butoxycarbonyl (Boc) groups to prevent oxidation. 10

Scheme 1-12 Examples of new materials based on structures of poly(aniline)s by replacing aromatic systems[1, 2, 65, 66] 11

Scheme 1-13 Factors in the study of PANI-CMPs from design to applications 22

Scheme 1-14 Structure of acetic acid, with numbering for explanation of different interactions being used in molecular mechanics 25

Scheme 1-15 Structure of acetic acid, redrawn in Newman projection viewing through C2–C1 bond 25

Scheme 1-16 Structures of **ES** state poly(aniline) chains in bipolaron (top) and polaron (bottom) forms 32

Scheme 2-1 Formation of phenazine moieties from the oxidative polymerisation of aniline formed via Michael addition of aniline end group as proposed by Ćirić-Marjanović[4] 41

Scheme 2-2 Structures of core (top row) and linker (bottom row) monomers being used for the syntheses of PANI-CMPs in this study 42

Scheme 3-1 A diagram showing four levels of poly(aniline) structures from smallest units to bulk polymers 51

Scheme 3-2 An example of poly(aniline) secondary structures consisting of multiple BQ units as primary units 52

Scheme 3-3 Structures of benzenoid (left) and quinoid (right) BQ units with three different types of bonds and atoms illustrated (see main text) 54

Scheme 3-4 Five possible structures of BQ units that can be found in poly(aniline)s and oligo(aniline)s. Bonds and hydrogen atoms in blue can be replaced with oligo(aniline) chains. 54

Scheme 3-5 Resonance structures of **BZN**-$(NH_2)_2$ in **BZ** form, illustrating delocalisation of non-bonding electron pairs from amino groups 55

Scheme 3-6 Two different ways to mitigate the steric hindrance between two ortho hydrogen atoms in a geminal diaryleneamine system 61

Scheme 3-7 Geometric descriptors for angles between two adjacent BQ units, **a)** C–N–C angle, **b)** N···N···N angle, **c)** C–C–N–C dihedral angle, and **d)** C–C···C–C dihedral angle. Bold bonds represent bonds between pairs of chemically bonded atoms, and dashed lines represent imagination connections between pairs of non-chemically-bonded atoms. Only one sequence is shown for **c)** while there are two sequences, see main text 61

Scheme 3-8 Structures of TANI and branched derivatives chosen for comparative study, as well as numbering and naming conventions for amino groups, carbon rings, and BQ units 67

Scheme 3-9 Structures of TANI in **^{1}ES** (left) and **^{3}ES** (right) states, as published by Mills et al.[13] 68
Scheme 3-10 Structures of TANI-2 in **^{1}ES** (left) and **^{3}ES** (right) states 72
Scheme 3-11 Structures of TANI-23 in **^{1}ES** (left) and **^{3}ES** (right) states 75
Scheme 3-12 Structures of TANI-14 in **^{1}ES** (left) and **^{3}ES** (right) states 76
Scheme 3-13 The comparison between two different approaches for the consideration of branched oligo(aniline)s (left) and PANI-CMP oligomeric model (right) with the same chemical component 77
Scheme 3-14 Hub (red) and blade (blue) parts of the three core monomer units, **TPA** (left), **TPB** (middle), and **TPT** (right) 78
Scheme 3-15 Structures of **OTPA-BZN-221** in **^{1}ES** (left) and **^{5}ES** (right) states 84
Scheme 3-16 Structures of **FLR** BQ units in the benzenoid (**BZ**, left) and quinoid (**QN**, right) forms 85
Scheme 3-17 Structures of **OTPA-FLR-210** in **^{1}ES** (top) and **^{3}ES** (bottom) states 87
Scheme 3-18 Structures of **TPA** (left) and **TPB** (right) core units showing two hydrogen atoms causing steric hindrances 88
Scheme 3-19 Structures of oligomers and polymers in the comparison between absorption spectra 144
Scheme 4-1 Structures of poly(aryleneethylnylene) materials (**CMP-0** to **CMP-5**, excluding **CMP-4**) studied by Jiang, Cooper, and co-workers [5] 150
Scheme 4-2 Structures of two fluorine-containing materials **NWPTPE** and **NWPPYR** studied by Hayashi et al.[6] 150
Scheme 4-3 Structures of functionalised **CMP-1** materials studied by Dawson, Adams, and Cooper[7] 151
Scheme 4-4 Retrosynthesis analyses for the synthesis of N-phenyl-2-naphthylamine using BH cross-coupling reaction 151
Scheme 4-5 Monomers used in the syntheses of **CMP-1** (the left pathway) and **CMP-4** (the right pathway)[3] 152
Scheme 4-6 Structures of brominated core (top) and aminated linker (bottom) monomers in the designs of PANI-CMPs in the Faul Research Group[8, 9, 11] 153
Scheme 4-7 Structures of core and linker monomers used in the studies of PANI-CMPs in the first series 154
Scheme 4-8 Structures of core and linker monomers used in the studies of PANI-CMPs in the second series 154
Scheme 4-9 Structures of **110** oligomeric fragments from **TPB**-$(NH_2)_3$ core monomer and **BZN**-Br_2 (left) or **FLR**-Br_2 (right) linker monomer in unoxidised form (top row) and oxidised form (bottom row) 160
Scheme 4-10 Reactions taking place in the first few steps of the polymerisation process towards the formation of PANI-CMPs from **NORMAL** functionality pathway. Chemical species shown in these steps are denoted by three-digit codes representing, from the first to the third digit, the number of core units, the number of linker units, and the number of cycles. Not all possible reactions and not all possible isomers, if applicable, are listed. 161
Scheme 4-11 Reactions taking place in the first few steps of the polymerisation process towards the formation of PANI-CMPs from **REVERSED** functionality pathway. Chemical species shown in these steps are denoted by three-digit codes representing, from the first to the third digit, the number of core units, the number of linker units, and the number of cycles. Not all possible reactions and not all possible isomers, if applicable, are listed. 162
Scheme 5-1 Numbering of atoms involved in the geometries of imine binding site 192
Scheme 5-2 Numbering of atoms involved in the geometries of linker unit binding site, matching Figure 5-9 193
Scheme 5-3 Numbering of atoms involved in the geometries of core unit binding site, matching Figure 5-10 194
Scheme 5-4 Four different conformers of two adjacent BQ units respective to the middle BQ unit 197
Scheme 5-5 Structures of linear (top) and star-shaped (bottom) **OTPA-BZN-430** in **EB** state, compared to two corresponding isomers of butane 206
Scheme 6-1 Oligo(aniline)s containing different topological features, namely branches and cycles. Unbranched cyclic oligomers (an example of which encased in a dashed frame) are not discussed in this thesis. 215
Scheme 6-2 A structure of **OTPA-BZN-320** in the singlet **ES** state 216
Scheme A-1 General numbering of atoms involved in the geometries of imine binding site 375

SCHEME A-2 NUMBERING OF ATOMS INVOLVED IN THE GEOMETRIES OF AMINE BINDING SITE. THE UNNUMBERED HYDROGEN ATOM HAS DIFFERENT NUMBERINGS IN THE OPTIMISED STRUCTURES BEFORE AND AFTER BINDING AND THUS WILL ONLY BE REFERRED TO SIMPLY AS H.....380
SCHEME A-3 NUMBERING OF ATOMS INVOLVED IN THE GEOMETRIES OF **BZN** LINKER UNIT BINDING SITE.....382
SCHEME A-4 NUMBERING OF ATOMS INVOLVED IN THE GEOMETRIES OF **FLR** LINKER UNIT BINDING SITE 387
SCHEME A-5 NUMBERING OF ATOMS INVOLVED IN THE GEOMETRIES OF **TPA** CORE UNIT BINDING SITE 391
SCHEME A-6 NUMBERING OF ATOMS INVOLVED IN THE GEOMETRIES OF **TPB** CORE UNIT BINDING SITE 394
SCHEME A-7 NUMBERING OF ATOMS INVOLVED IN THE GEOMETRIES OF **TPT** CORE UNIT BINDING SITE 397
SCHEME A-8 TWO POSSIBLE WAYS FOR A CO_2 MOLECULE TO BEND UPON BINDING ONTO AN IMINE BINDING SITE. SOLID LINES REPRESENT COVALENT BONDS (REGARDLESS OF BEING SINGLE OR DOUBLE), AND DASHED LINES REPRESENT NON-COVALENT INTERACTIONS.....399
SCHEME B-1 ELEMENTARY VIBRATIONAL MODES OF SIX-MEMBERED AROMATIC SYSTEMS 461
SCHEME B-2 GRAPHIC REPRESENTATION OF VIBRATIONAL MODES OF BENZENE, SHOWING DIRECTIONS OF MOVEMENTS WITHOUT MAGNITUDES, REPRODUCED FROM WILSON,[3] PREUSS AND BECHSTEDT,[4] AND WANG[2].....462
SCHEME B-3 GRAPHIC REPRESENTATION OF VIBRATIONAL MODES OF TRIAZINE, SHOWING DIRECTIONS OF MOVEMENTS WITHOUT MAGNITUDES, REPRODUCED FROM LARKIN ET AL.[1] 463

List of Abbreviations

AMB-$(NH_2)_2$ 4,4'-Diamino-3,3'-dimethylbiphenyl

ATC 9,10-Anthracenylene

ATC-Br_2 9,10-Dibromoanthracene

ATR Attenuated total reflectance

B3LYP Becke's three-parameter hybrid functional with Lee-Yang-Parr correlation

BBLP Backbone bond length pattern

BET Brunauer-Emmett-Teller [analysis of isotherm adsorption]

BH Buchwald-Hartwig [cross-coupling reaction]

BH.BXJ Buchwald-Hartwig cross-coupling reaction with Bristol-Xi'an Jiaotong method of solubility tuning

BLA Bond length alteration

BPE-$(NH_2)_2$ 1,2-Bis(4-aminophenyl)ethane

BPH Biphenyl-4,4'-diyl

BPH-Br_2 4,4'-Dibromobiphenyl

BQ Benzenoid/quinoid [unit]

BSSE Basis set superposition error

BXJ Bristol-Xi'an Jiaotong [method of solubility tuning]

BZ Benzenoid

BZN 1,4-Phenylene

BZN-Br_2 1,4-Dibromobenzene

BZN-$(NH_2)_2$ 1,4-Phenylenediamine

CAM-B3LYP Becke's three-parameter hybrid functional with Lee-Yang-Parr correlation with Coulomb-attenuating method

CCU Carbon capture and utilisation

CLBQ Conjugated core-linker benzenoid-quinoid units

CMP Conjugated microporous polymer

COF Covalent organic framework

CT Charge transfer

CTBQ Charge transfer between benzenoid-quinoid units

CTF Covalent triazine framework

D3(BJ) Grimme's dispersion correction D3 with Becke-Johnson damping

DFT	Density functional theory
DPA-$(NH_2)_2$	4,4'-Diaminodiphenylamine
DPE-$(NH_2)_2$	4,4'-Diaminodiphenyl ether
DPPD	*N*,*N*-diphenyl-1,4-phenylenediamine
DRC	Diradical cation
EB	Emeraldine base
ES	Emeraldine salt
ES*n*	Excited state *n*, when *n* is an integer
ESP	Electrostatic potential
FF	Force field
FLR	2,7-Fluorenylene
FLR-Br_2	2,7-Dibromofluorene
FLR-$(NH_2)_2$	2,7-Diaminofluorene
FMO	Frontier molecular orbital
FT-IR	Fourier-transform infrared [spectroscopy]
FTMW	Fourier-transform microwave [spectroscopy]
GGA	Generalised gradient approximation
HCP	Highly-crosslinked polymer
HF	Hartree-Fock
HOF	Hydrogen-bonded organic framework
HOMA	Harmonic oscillator model of aromaticity
HOMBQ	Harmonic oscillator measurement for benzenoid-quinoid characteristics
HOMED	Harmonic oscillator measure of electron delocalisation
HOMHED	Harmonic oscillator measure of heterocycle electron delocalisation
HOMO	Highest occupied molecular orbital
HPB-Br_6	Hexakis(4-bromophenyl)benzene
HPLC	High-performance liquid chromatography
HSP	Hansen solubility parameter
IUPAC	International Union of Pure and Applied Chemistry
KS-DFT	Kohn-Sham density functional theory
LDA	Local density approximation
LEB	Leucoemeraldine base

LRS	Long-range correlated [exchange-correlation functional]
LR-TD-DFT	Linear-response time-dependent density functional theory
LUMO	Lowest unoccupied molecular orbital
MALDI	Matrix-assisted laser desorption/ionisation
MC	Monte Carlo
MD	Molecular dynamics
MESP	Molecular electrostatic potential (*see* ESP)
MM	Molecular mechanics
MMFF94	Merck molecular force field
MNDO	Modified neglect of differential overlap
MO	Molecular orbital
MOF	Metal-organic framework
MS	Mass spectrometry
m/z	Mass per charge
NaO^{t}Bu	Sodium tert-butoxide
NBO	Natural bond orbital [analysis]
NCI	Non-covalent interaction
NICS	Nucleus-independent chemical shift
NPH	1,4-Naphthalenylene
NPH-Br_2	1,4-Dibromonaphthalene
NPT	2,6-Naphthalenylene
NPT-Br_2	2,6-Dibromonaphthalene
NLDFT	Non-local density functional theory
NTO	Natural transition orbital
OANI	Octa(aniline)
PANI	Poly(aniline)
PANI-CMP	Poly(aniline)-based conjugated microporous polymer
PB	Pernigraniline base
PBC	Periodic boundary condition
PCM	Polarisable continuum model of solvation
$Pd(dba)_2$	Bis(dibenzylideneacetone)palladium(0)
PIM	Polymer of intrinsic microporosity

POC	Porous organic cage
POM	Porous organic material
POP	Porous organic polymer
$p/p°$	Relative pressure
PSD	Pore size distribution
PYR-$(NH_2)_2$	2,6-Diaminopyridine
QDC	Quinoidal dication
QM/MM-MD	hybrid quantum mechanics/molecular mechanics-molecular dynamics
QN	Quinoid
QSDFT	Quenched solid density functional theory
RC	Radical cation
R_f	Retention factor
RPA	Random phase approximation
SEM	Scanning electron microscope
SPE	Single-point energy
SPR	Structure-property relationship
STB-$(NH_2)_2$	4,4'-Diaminostilbene
TANI	Tetra(aniline)
TD-DFT	Time-dependent density functional theory
THF	Tetrahydrofuran
TLC	Thin-layer chromatography
TOF	Time-of-flight
TPA	Triphenylamine
TPA-Br_3	Tris(4-bromophenyl)amine
TPA-$(NH_2)_3$	Tris(4-aminophenyl)amine
TPB	1,3,5-Triphenylbenzene
TPB-Br_3	1,3,5-Tris(4-bromophenyl)benzene
TPB-$(NH_2)_3$	1,3,5-Tris(4-aminophenyl)benzene
TPE-Br_4	1,1,2,2-Tetrakis(4-bromophenyl)ethene
TPT	2,4,6-Triphenyl-1,3,5-triazine
TPT-Br_3	2,4,6-Tris(4-bromophenyl)-1,3,5-triazine
TPT-$(NH_2)_3$	2,4,6-Tris(4-aminophenyl)-1,3,5-triazine

UV-Vis-NIR	Ultraviolet, visible, and near infrared
XPhos	2-Dicyclohexylphosphino-2',4',6'-triisopropylbiphenyl
XPS	X-ray photoelectron spectroscopy
ΔH_{ads}	Isosteric enthalpy of adsorption
$\Delta H°_{ads}$	Isosteric enthalpy of adsorption at zero adsorption

Chapter 1 Introduction

This research project aims to establish structure-property relationships for the designs of poly(aniline)-based conjugated microporous polymers (PANI-CMPs). This project uses both theoretical and experimental studies to assess spectroscopic properties, porosity, and CO_2 adsorption of these materials.

PANI-CMPs are a group of conjugated microporous polymers which are developed from poly(aniline)s or PANIs.[1, 2] These materials, therefore, have the properties of both poly(aniline)s and conjugated microporous polymers. Chemical properties of PANI-CMPs can be altered by redox reactions or by doping with acids, properties that are inherited from PANIs.[3, 4] Meanwhile, they possess highly crosslinked structures, which result in high porosities, making these materials useful for adsorption-based applications.[5, 6] The presence of both aromatic systems and nitrogenous functional groups also contribute to high affinities towards CO_2, which means that materials in this family can be good candidates for carbon capture and utilisation (CCU) applications.[7] Therefore, structure-property relationships of PANI-CMPs are worth studying in detail.

PANI-CMPs have been developed for less than a decade. Therefore, while several studies, both experimental and theoretical, have been reported of poly(aniline)s or porous materials before, there are some challenging aspects emerging from the unique chemical structures and designs of PANI-CMPs. This report is a summary of attempts that have been applied to the study of PANI-CMPs with various degree of success.

This chapter will discuss the general scientific background information such as principles of techniques being used during the studies and earlier studies on similar chemical systems or materials. Scientific background related to more specific aspects of the study can be found in the early parts of the respective chapters. At the end of this chapter, the aim and objectives of this study along with an overview of other chapters will be given.

1.1 Porosity and Porous Materials

In material sciences, porosity is the possession of cavities or holes in material structures, and materials that have this property are known as porous materials. The most obvious example of porous materials is a sponge, with holes that can hold water inside because of capillary properties. The sizes of holes or cavities can vary from less than one nanometre in ultramicroporous polymers to a few centimetres in a slab of Emmental cheese. Materials with pore sizes in the ranges of up to hundreds of nanometres are of interest because their pores can interact with small molecules, which lead to various interesting applications. These applications include adsorption,[8-12] catalysis,[13, 14] sensing,[15, 16] and even electronics.[17, 18]

Pores can be categorised into different groups based on their sizes. According to IUPAC, there are three main categories, namely macropores (> 50 nm in diameters), mesopores (2 – 50 nm in diameters), and micropores (< 2 nm in diameters).[19, 20] The term “nanopore” covers both micropores and mesopores along with macropores up to 100 nm in diameters. These terms can be derived further analogously such as microporous and microporosity, for example. Meanwhile, micropores can be divided further into supermicropores (0.7 – 2 nm in diameters) and ultramicropores (< 0.7 nm in diameters). Pore sizes are usually reported either in nanometre or angstrom (Å) which equals to 0.1 nm. In this work, pore sizes will be discussed in angstrom for convenience because this unit is also the default unit of pore size in the analysis software and being generally used, despite being a non-SI unit. Classifications of pore sizes are summarised in Table 1-1.

Table 1-1 Classifications of porous materials based on pore sizes as defined by the IUPAC, taken from Thommes et al.[20]

Category		Pore Size	
		in Nanometre	**in Angstrom**
Micropore	Ultramicropore	< 0.7	< 7
	Supermicropore	0.7 – 2	7 – 20
Mesopore		2 – 50	20 – 500
Macropore		> 50	> 500

In the following section, the general concept of conjugated microporous polymers or CMPs will be discussed first. The chemistry of poly(aniline)s and the development of PANI-CMPs, i.e., CMPs designed based on poly(aniline)s, will be explained in Section 1.1.2. Finally, techniques for the analysis of porous materials along with parameters to be obtained will be discussed in Section 1.1.3.

1.1.1 Conjugated Microporous Polymers

Porous materials can be divided into four categories based on their chemical components (Scheme 1-1), namely non-carbonaceous materials, metal-organic frameworks (MOFs), porous carbon materials, and porous organic materials (POMs). Non-carbonaceous materials, as the name suggests, do not contain carbon and therefore are inorganic. Examples of these porous materials are zeolites, silicas, and perovskites.[11, 21-24] MOFs, on the other hand, are crystalline materials with organic molecules bridging between metal atoms forming large lattices.[14, 25] They contain both organic part (organic linkers or struts) and inorganic part (metal nodes). Next, porous carbon materials are prepared from carbonisation of other carbon-containing materials, including other porous organic materials.[26, 27] The main component of these materials is carbon. However, other elements such as nitrogen, oxygen, or hydrogen can also exist depending on conditions during carbonisation and components of original materials. The example of these materials is charcoal, which has been used as a household adsorbent for odour removals. The last category is porous organic materials (POMs). These materials can be divided further into many categories depending on structures, components, and synthesis methods. Further categorisations of these materials are challenging because new POMs have been developed over the past two decades from different components and using different synthesis pathways, creating materials with different properties and requiring different names. Materials of these types have also been referred to as porous organic polymers (POPs),[7, 28] among other names, in the literature. It should be noted, however, that POMs cover slightly more than POPs because there are organic materials that are porous but not technically polymers, which will be discussed later.

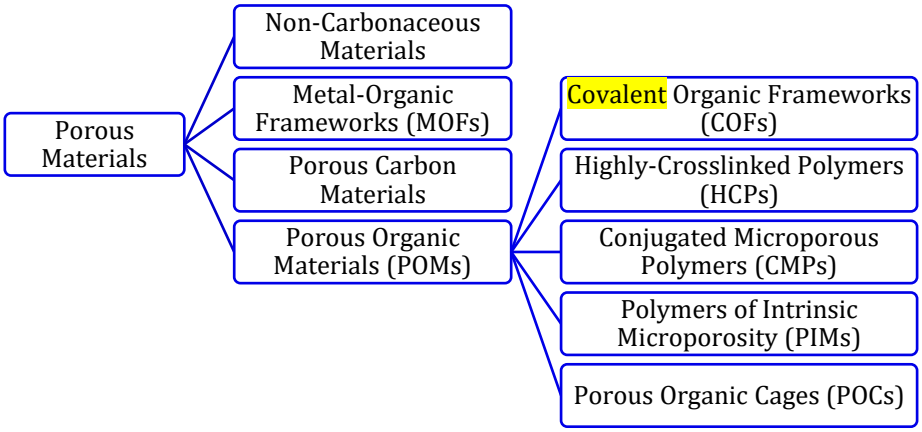

Scheme 1-1 Classification of porous materials based on chemical components and syntheses with further classifications of porous organic materials (POMs)

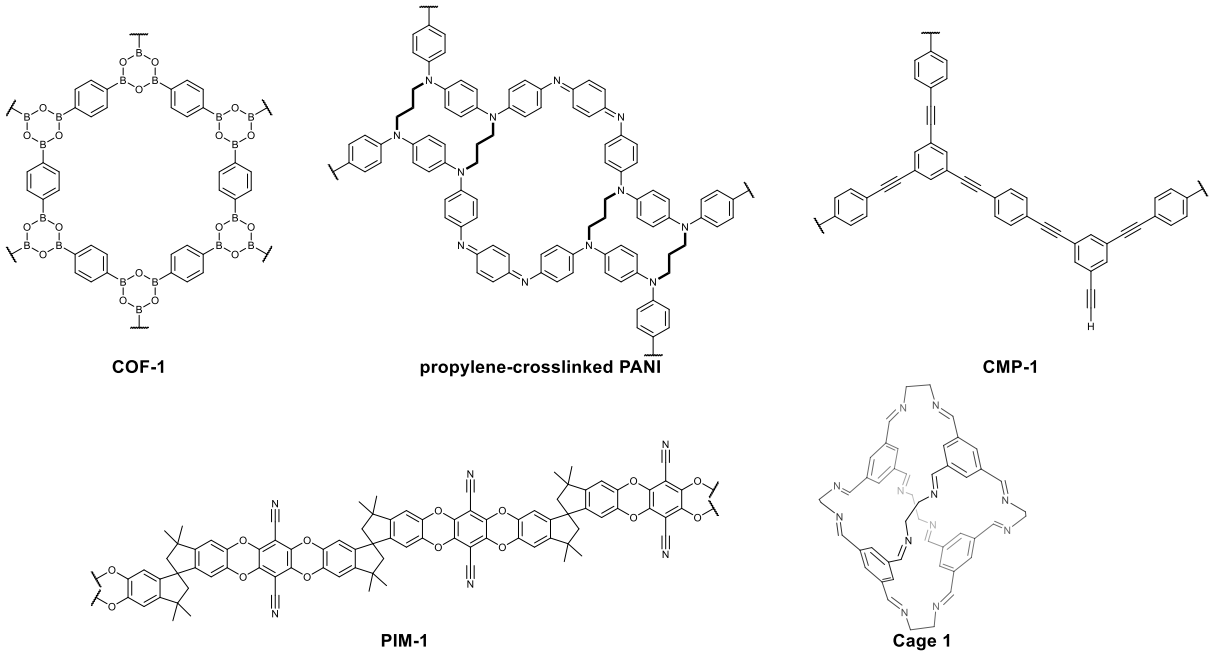

*Scheme 1-2 Examples of porous organic materials of each type, **COF-1** for COFs,[29] propylene-crosslinked PANI for HCPs (crosslinking propylene groups shown in bold),[30] **CMP-1** for CMPs,[5, 31] **PIM-1** for PIMs,[32] and cage 1 for POCs[33]*

While further classifications of POMs are complicated, only five categories will be described in this section, namely covalent organic frameworks (COFs), highly crosslinked polymers (HCPs), conjugated microporous polymers (CMPs), polymers of intrinsic microporosity (PIMs), and porous organic cages (POCs) as shown in Scheme 1-1. Examples of these POMs are shown in Scheme 1-2.

COFs can be considered as the all-organic analogues of MOFs, with organic moieties being linked together by newly formed functional groups instead of metal ions. These functional groups are formed from chemical reactions of functional groups from monomers. Chemical reactions for the formation of COFs are reversible, making their structures crystalline,[34, 35] which are different from other types of porous organic materials.

Meanwhile, HCPs and CMPs are also polymer networks with highly crosslinked structures, without crystallinity as present in COFs. While CMPs were considered as a subcategory of HCPs,[34] the main difference between CMPs and HCPs is that HCPs are constructed from crosslinking synthesised polymers to create porous structures. CMPs, however, can be synthesised directly from monomers in a single step without the need for further crosslinking.[5, 36] Also, as the name suggests, structures of CMPs also contain extended π-conjugations, which can be useful for many applications, such as catalysis and sensing. Their structural characteristics will be discussed further.

PIMs,[37] meanwhile, differ from POMs of the three earlier-mentioned groups because they normally do not possess highly crosslinked networks. Instead, porosities of PIMs come from the inclusions of rigid and non-planar moieties such as spirobisindane (as shown in **PIM-1** in Scheme 1-2) and triptycene. These moieties disrupt the packing of polymer chains and create porous networks. In fact, PIMs can be classified as one-dimensional based on how polymer chains propagate,[38] compared to those of three aforementioned categories of which polymer growth is in three dimensions. Meanwhile, porous organic cages (POCs)[33, 39] differ the most from the rest of mentioned subcategories because they are not polymers. Instead, they are finite-sized molecules that have rigid structures and permanent cavities, see Cage 1 in Scheme 1-2. They are considered as zero-dimensional porous materials because of the lack of further propagation in any

direction.[38] Because structures of PIMs and POCs do not have high-degree networks, they are easier to dissolve in organic solvents and therefore easier to process into films or coatings.

While five categories of POMs/POPs have been discussed so far, there are other categories of POMs or POPs existing in the literature, including covalent triazine frameworks (CTFs),[40] which can arguably be a triazine-based subcategory of CMPs,[36] or hydrogen-bonded organic frameworks (HOFs),[41] which are linked together with hydrogen bonds instead of covalent bonds. Discussions about these materials are beyond the scope of this study, so further details of these materials will not be presented here.

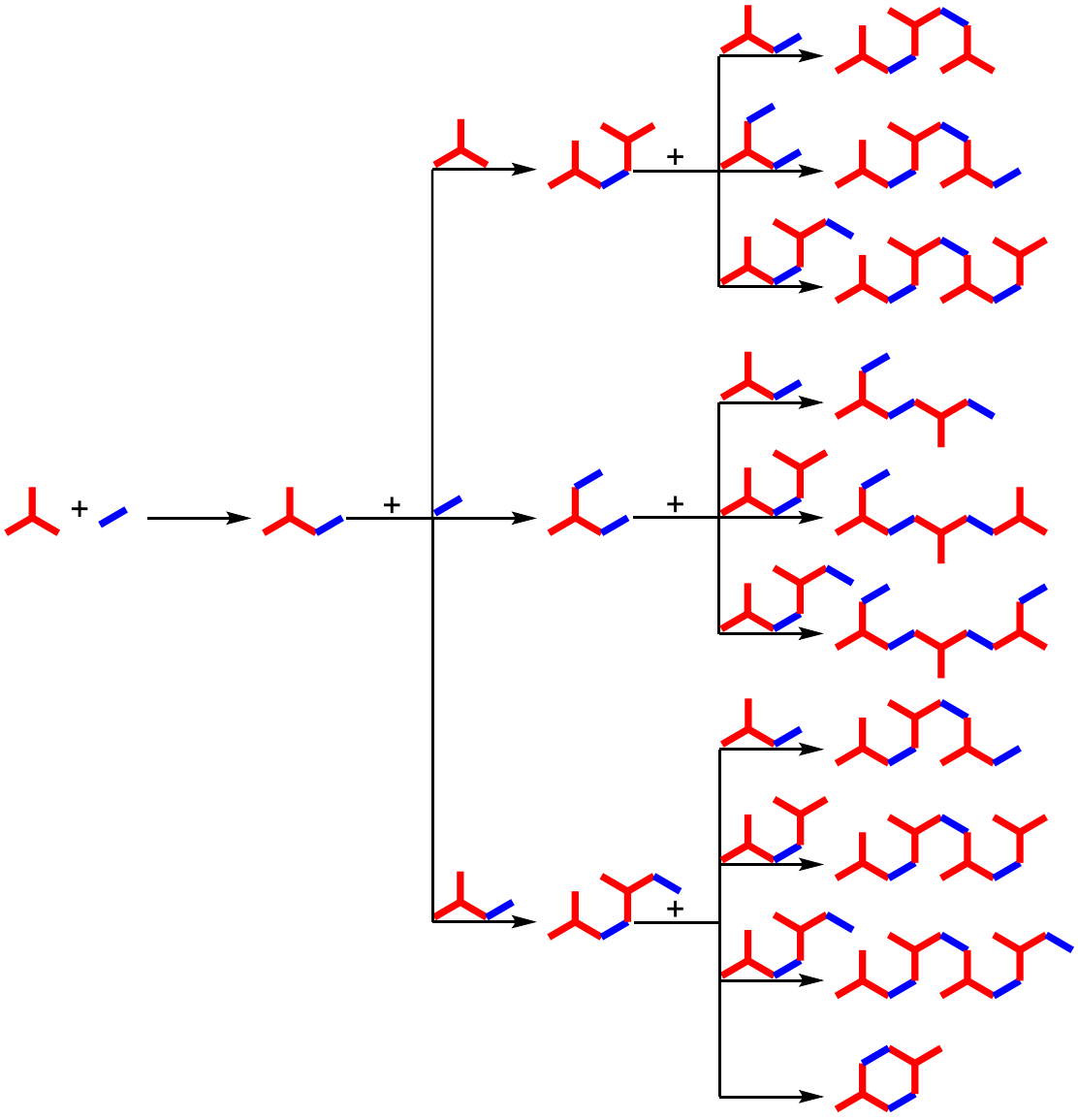

Scheme 1-3 Polyaddition reactions between two monomers, red A_3 and blue B_2, showing different possible reactions taking place during the first three steps of the polymerisation process. Not all possible reactions are shown. Polycondensation reactions can be considered in the similar manner with the formation of smaller molecules.

Most polymerisation reactions towards the formations of CMPs can be considered as step-growth or polyaddition/polycondensation. The usage of latter terms is more encouraged by the IUPAC,[42, 43] with the difference between polyaddition and polycondensation being the presence (in polyaddition) and the absence (in polycondensation) of smaller molecules produced. Nonetheless, both polyaddition and polycondensation involve the polymerisation reactions between oligomers at any stage, as opposed to chain polymerisations in which individual

monomer molecules are added to the reactive ends of polymer chains. The whole process initiates when the first two molecules of monomers react, forming an oligomer molecule. This molecule then reacts further with another monomer or oligomer molecule forming a larger oligomer molecule, and so on, as illustrated in Scheme 1-3. As the oligomer molecules grow larger. At one point, a gel is formed, in which the polymer network acting as a matrix while the solvent system dispersing thoroughly, as the polymerisation process progresses further.[31] This gel system acts as a template for the polymerisation to create highly crosslinked and interpenetrated networks, as shown in Figure 1-1, which are important for the microporosity of resulting polymers.

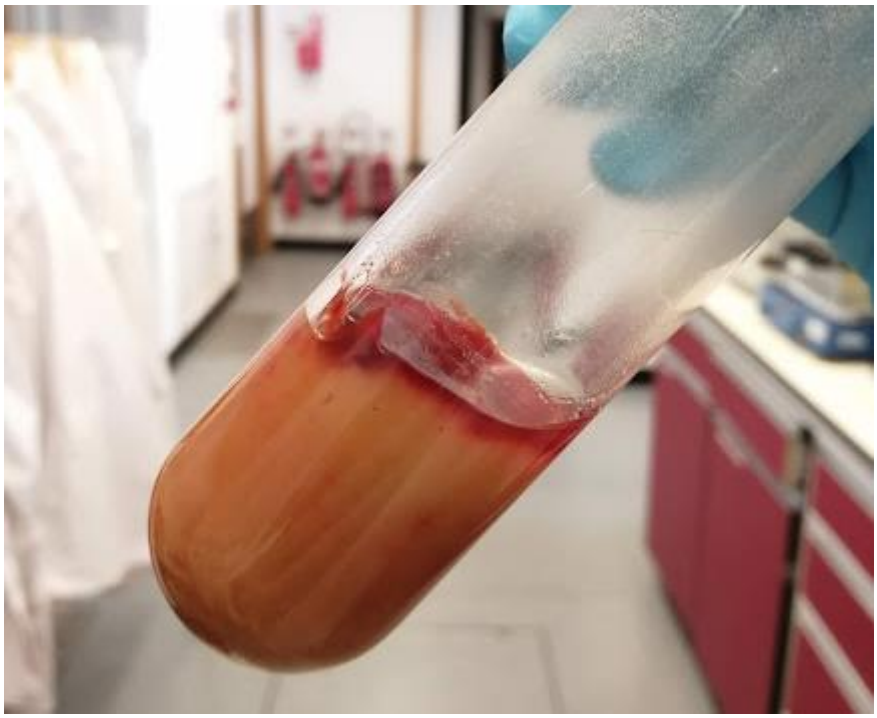

Figure 1-1 Polymer gel formed during the synthesis of PANI-CMPs

The matches between solubility parameters of formed polymers and liquid matrices have been the basis for the Bristol-Xi'an Jiaotong (BXJ) approach[44, 45] for the use of salt for tuning the solubility parameters. This approach is explained in detail in the next section.

1.1.2 Poly(aniline)-based Conjugated Microporous Polymers (PANI-CMPs)

Poly(aniline)s (PANIs) are a group of polymers in which repeating units are aniline units, with one benzene ring and one imine/amine group per each unit. Oligo(aniline)s, meanwhile, are compounds with limited number of aniline units. They can be named based on number of aniline units such as tetra(aniline)s (TANIs) and octa(aniline)s (OANIs) for oligo(aniline)s with four and eight aniline units, respectively. For oligo(aniline)s with no further functionalisation, the amino group on each end can also either be capped with phenyl group or not. This results in three different functionalities, Ph/Ph, Ph/NH_2, and NH_2/NH_2.[3] Scheme 1-4 illustrates structures of tetra(aniline)s or TANIs with three different functionalities. These oligomers are considered tetra(aniline)s because there are four complete aniline units (benzene rings and imino groups) in each of them.

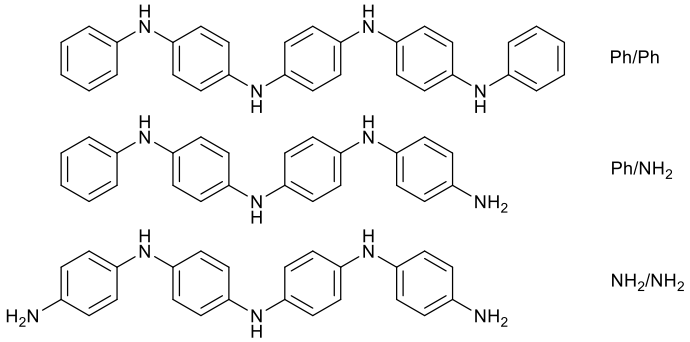

Scheme 1-4 Examples of tetra(aniline)s with different functionalities; Ph/Ph (top), Ph/NH_2 (middle), and NH_2/NH_2 (bottom)

Poly(aniline)s have been discovered in the nineteenth century, and several studies on different oxidation states have been published over the following decades.[46-48] In the early 1910s, Green and Woodhead proposed five different oxidation states of Ph/NH_2 octa(aniline) as a model for poly(aniline)s.[49, 50] These five states are, from fully reduced to fully oxidised, leucoemeraldine, protoemeraldine, emeraldine, nigraniline, and pernigraniline, with their proposed structures shown in Scheme 1-5. However, these oxidation states have been re-examined in 1991 by Masters *et al.*[51] During the gradual oxidation of poly(aniline) solutions in *N*-methylpyrrolidone and the measurement of absorption spectra, unique spectra for protoemeraldine and nigraniline could not be found. They have concluded that the two non-existent states are actually mixtures of emeraldine state with either leucoemeraldine or pernigraniline state. Following this study, general structures of poly(aniline)s are usually represented with regards to oxidation states as shown in Scheme 1-6.[4]

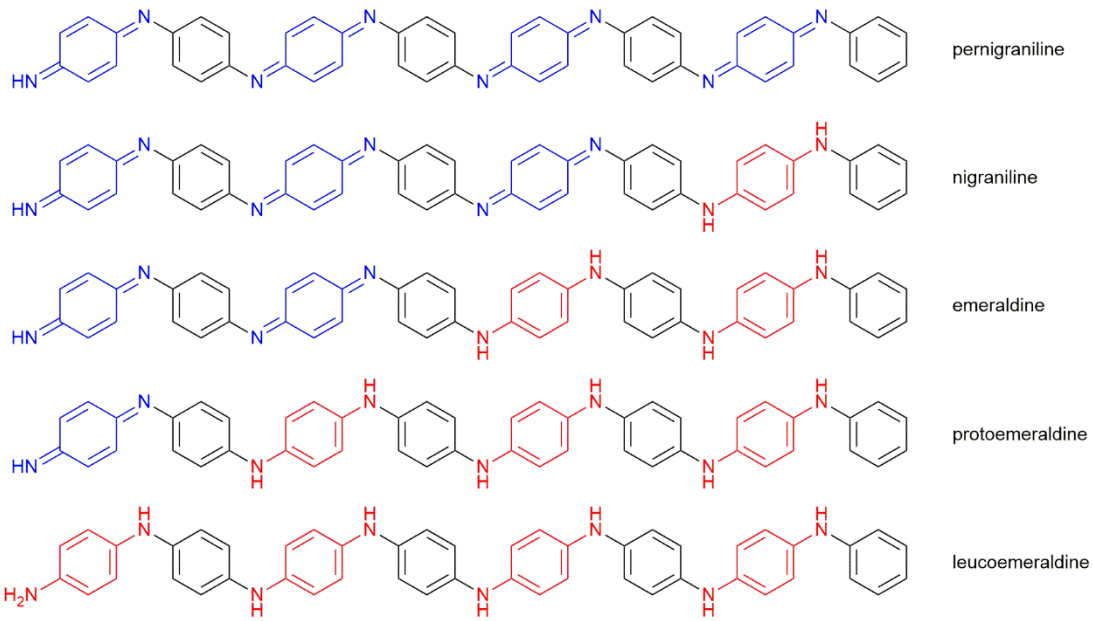

Scheme 1-5 Structures of five oxidation states of octa(aniline) as proposed by Green and Woodhead in early 1910s, benzenoid and quinoid units are shown in red and blue, respectively[49, 50]

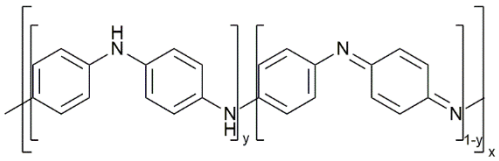

Scheme 1-6 General representation of poly(aniline) structures[4]

By definitions, repeating units of poly(aniline)s and oligo(aniline)s are aniline units. However, as hinted in Scheme 1-5 and Scheme 1-6, it would make more chemical sense to consider these polymers and oligomers as copolymers between 1,4-phenylene units and imino-1,4-phenyleneimino units. The latter are more conventionally referred to simply as benzenoid units, while the oxidised counterpart, nitrilocyclohexa-2,5-diene-1,4-diylnitrilo units, are referred to as quinoid units. Structures of benzenoid and quinoid units are illustrated in Scheme 1-5 and Scheme 1-7. Meanwhile, Scheme 1-6 depicts general representation of poly(aniline) structures, with each unit consist of one 1,4-phenylene unit and one benzenoid or quinoid unit. Consider the three oxidation states, they are different in ratio of oxidised units. In leucoemeraldine state, none of these units are oxidised. The ratio of oxidised unit increased to half in emeraldine and whole in pernigraniline states. Therefore, depictions of poly(aniline) structures as in Scheme 1-6 consider each repeating unit with subscripts *x* to contain two subunits of di(aniline)s, which can be in either reduced (left) or oxidised (right) form. Meanwhile, subscripts *y* and 1-*y* refer to ratios of reduced and oxidised forms of the di(aniline) units. The values of *y* are 1 for fully reduced leucoemeraldine, 0.5 for half-oxidised emeraldine, and 0 for fully oxidised pernigraniline states.

Despite their long existence, properties of poly(aniline)s as conductive polymers were not studied until the publication of Shirakawa, Heeger, and MacDiarmid's work on poly(acetylene) in 1977[46, 52] (the authors won the 2000 Nobel Prize in Chemistry for their pioneering work on conductive polymers).[53] Generally, insulative polymers can be transformed into conductive polymers by the process known as "doping", which can be done by either introducing substances or "dopants" or performing electronic alterations such as radiation and charge-injection.[4, 54] Dopants in the case of poly(aniline)s can be oxidising agents, reducing agents, and acids. While poly(aniline)s in the emeraldine state, as well as other oxidation states of uncharged poly(aniline)s, are insulators, acid doping increases conductivities by 10 orders of magnitudes, yielding conductive polymers.[4, 55] To distinguish between two forms with the same oxidation state but different conductive properties, the protonated form from acid doping is called the emeraldine salt (**ES**) form, and the non-protonated insulative form is called the emeraldine base (**EB**) form. Relationships among different forms of poly(aniline)s are illustrated in Scheme 1-7.

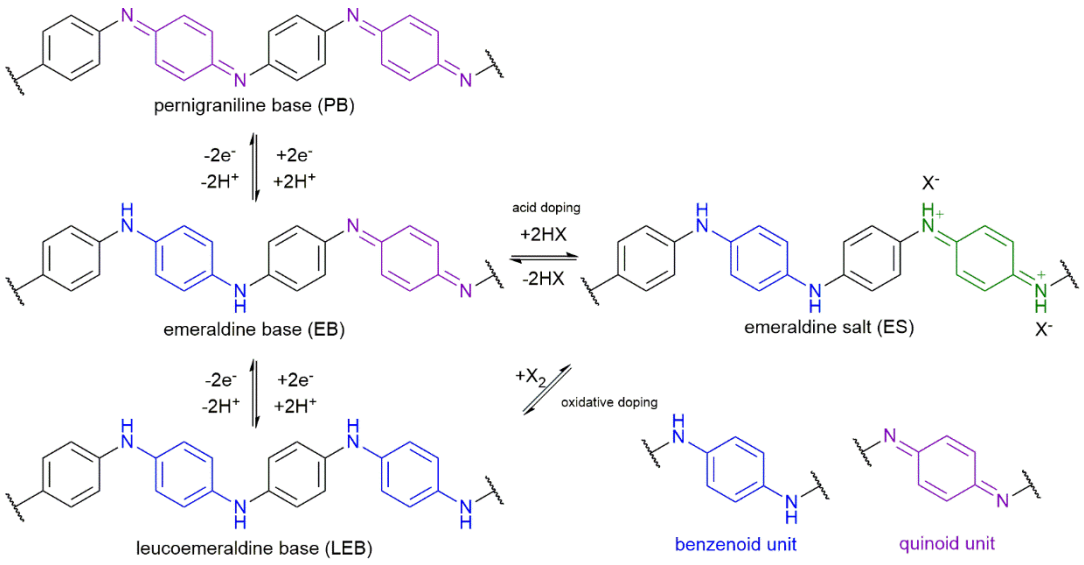

Scheme 1-7 Relationship diagram of poly(aniline)s in different oxidation and doping states, adapted from Wei and Faul[3]

From Scheme 1-7, the conductive **ES** form of poly(aniline)s can be achieved from two different pathways. One pathway is from the protonation of **EB** poly(aniline)s as explained earlier.

Another pathway is from direct oxidation of poly(aniline)s in **LEB** form, known as oxidative doping, which is in line with other conductive polymers.[4, 54]

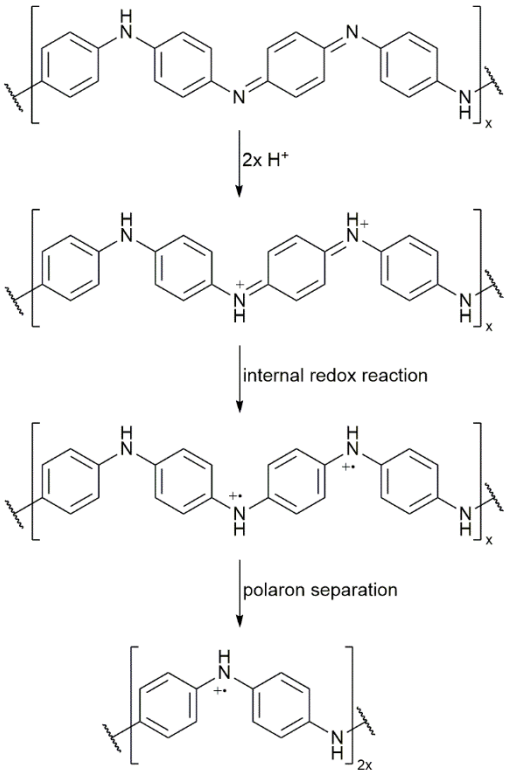

Scheme 1-8 Poly(aniline) doping process as proposed by Stafström et al.[56]

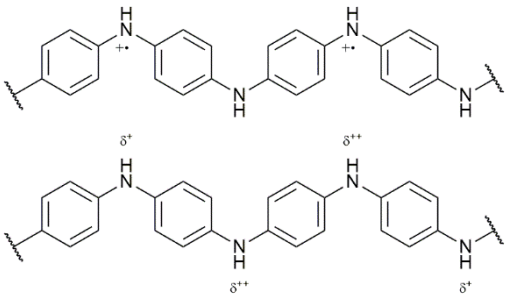

Scheme 1-9 Polaron lattice model (top) and four-ring BQ derivatives model (bottom)

Electronic structures of conductive **ES** poly(aniline)s are complicated. Earlier proposal made by Stafström, MacDiarmid, and co-workers[56] (Scheme 1-8) suggested that the first step is the protonation of quinoid units, producing a singlet bipolaron state. This newly formed singlet bipolaron state then undergoes internal redox reactions to yield a triplet bipolaron state, and then the triplet bipolaron state undergoes another step called polaron separation to become the polaron state. In this proposal, **ES** state poly(aniline)s contain radical cations located on every second amino group. Despite being backed by optical spectroscopic data and MNDO (modified neglect of differential overlap) semi-empirical self-consistent-field calculations, this proposed structure does not match with ^{1}H NMR spectra of poly(aniline)s.[57] Based on ^{1}H NMR spectra of poly(2,5-dimethylaniline) and *N*,*N*-diphenyl-1,4-phenylenediamine (DPPD, Ph/Ph di(aniline)), Jing *et al.* have proposed the four-ring BQ derivatives model.[58] As compared in Scheme 1-9, the four-ring BQ derivatives model suggests more continuous distribution of positive charges across imine nitrogen atoms compared to the polaron lattice model. Each region with more partial positive charges in the four-ring BQ derivatives model covers two consecutive imino groups,

which is closer to the bipolaron lattice model (Scheme 1-8, the second structure) with more delocalisation. These findings become important for combined experimental and computational studies of both geometric and electronic structures of oligo(aniline)s, encouraging experimental data to be integrated into considerations towards more accurate models for these oligomeric and polymeric systems. Later computational studies of poly(aniline)s in the **ES** state have also tended to suggest bipolaronic models rather than polaronic models.[59-61] Computational studies of poly- and oligo(aniline)s will be discussed in Section 1.3.2. Nonetheless, it is not until recently that poly(aniline)s in the **ES** state have been proven to be in either polaronic or bipolaronic forms, depending on dopant concentrations.[62]

Absorption spectra of Ph/Ph TANI doped with different concentration of dopants are shown in Figure 1-2.[62] Addition of perchloric acid as a dopant initially decreases the absorbance at approximately 600 nm, corresponding to the absorption of **EB** quinoid units, and new peaks have emerged at approximately 800 nm and 1000 nm. Absorbance values of both peaks increase over the initial span. However, the absorbance of the 800 nm peak reaches its peak as the concentration of the dopant reaches 0.25 mM. Beyond this point, the absorbance of the 800 nm peak decreases while the absorbance of the 1000 nm peak remains increasing. These results suggest that both polaron and bipolaron forms exist in the doped state, and the ratio between concentrations of the two forms appears to be a function of the dopant concentration.

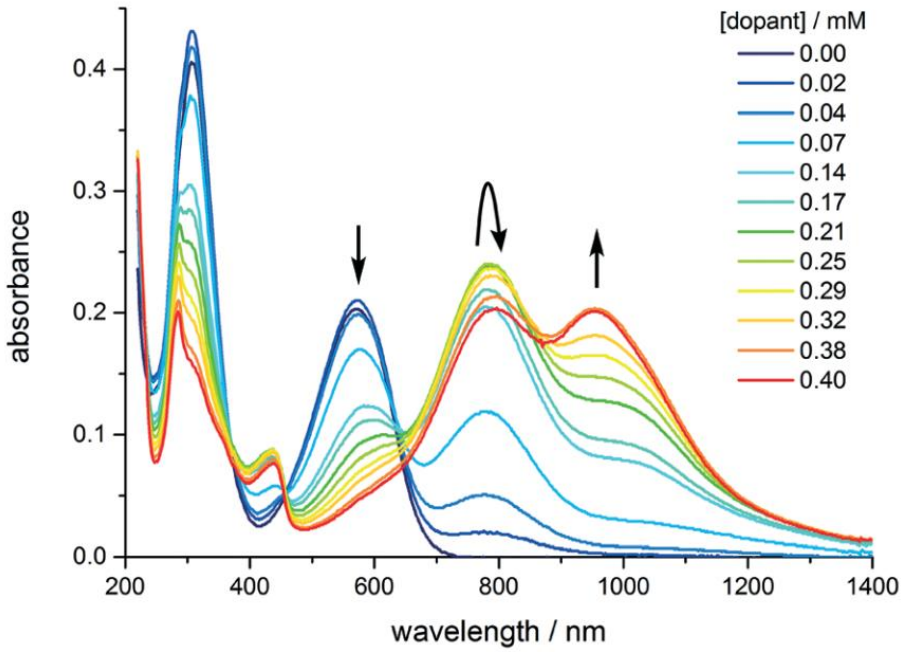

Figure 1-2 UV-Vis-NIR absorption spectra of Ph/Ph TANI, 0.15 mM in THF, with different concentration of perchloric acid as a dopant, taken from Mills et al.[62]

Following the discovery of polaron-bipolaron balance, the relationship diagram of PANIs in different forms can then be rewritten, taking interchangeability between singlet and triplet forms into account, as in Scheme 1-10. The presence of multiple forms in these materials is important because it creates further complications for the study by adding more factors to consider. If a chemical species is not a single species but instead a mixture of forms or states that can easily interchange between each other, and if these forms or states have different properties, then properties of the chemical species cannot be explained by properties of just one form or state anymore. Instead, these properties are now a combination of properties of each form or state, weighted by the molar proportion of that form or state. To properly compare different sets of data related to properties of such chemical species, either from experiments or from theoretical

determinations, the ratios need to either be deduced or be controlled. Meanwhile, consideration of ideal cases, where only one component exists in the system, in computational studies may be useful to identify the likely components of such mixtures.

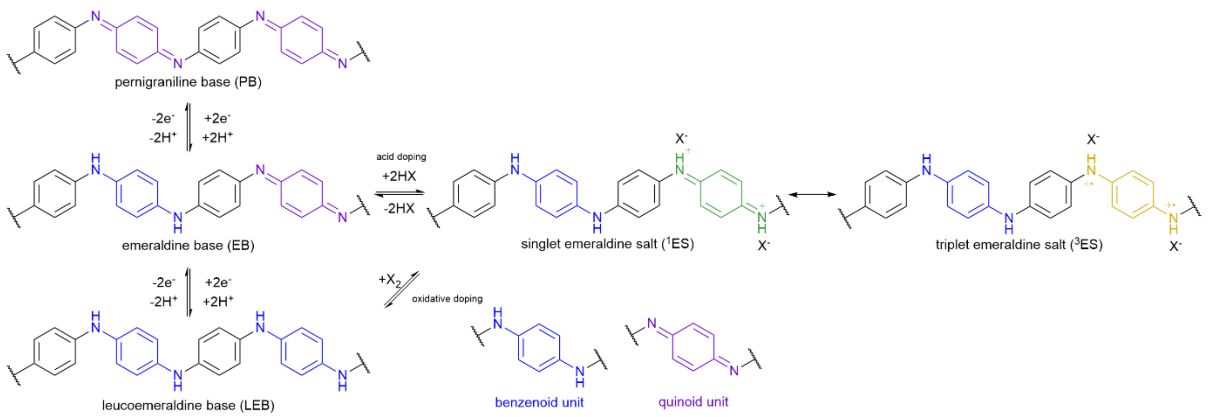

Scheme 1-10 Relationship diagram of poly(aniline)s in different oxidation and doping states with regards to spin multiplicities

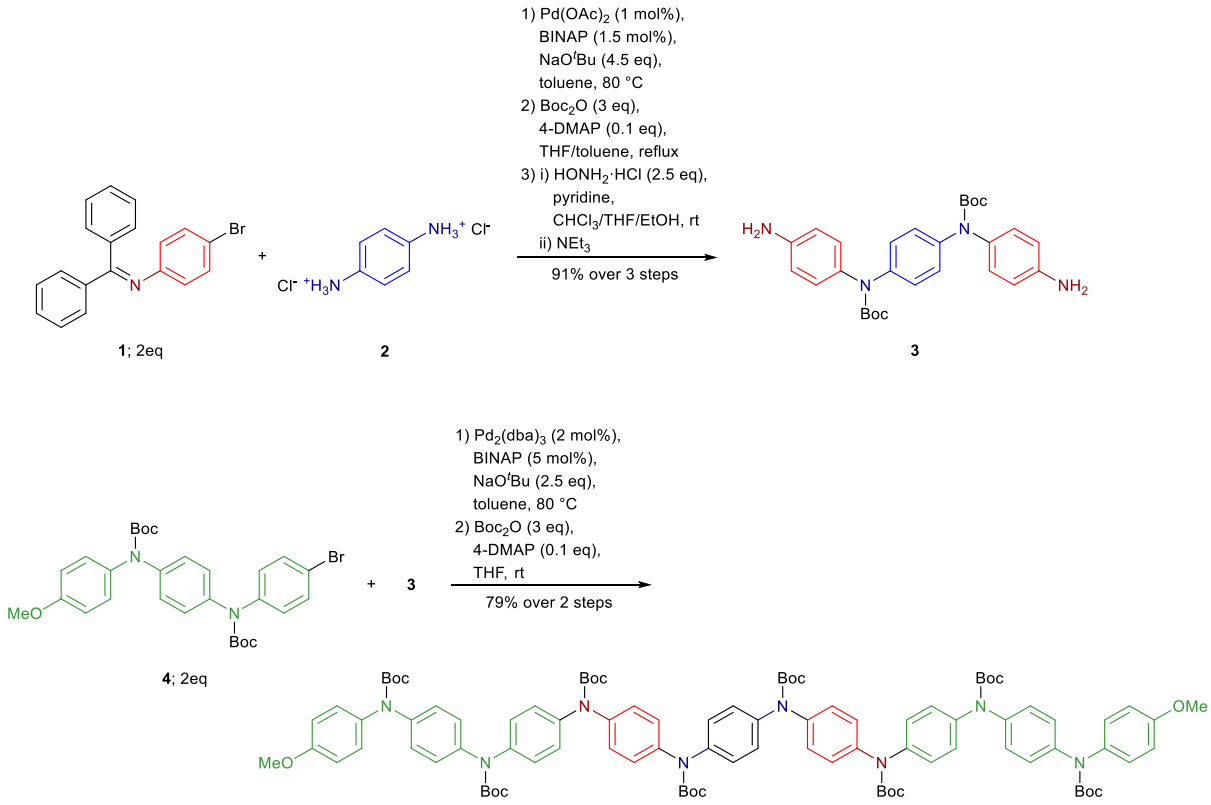

Scheme 1-11 Synthesis of 4-methoxyphenyl-capped octa(aniline) using palladium-catalysed coupling reactions published by Singer, Sadighi, and Buchwald.[63] Amino groups are protected by tert-butoxycarbonyl (Boc) groups to prevent oxidation.

As discussed, structures of poly(aniline)s can be viewed as a copolymer of 1,4-phenylene and benzenoid/quinoid units. This consideration allows poly(aniline)s and oligo(aniline)s to be synthesised using Buchwald-Hartwig (BH) cross-coupling reactions between bromoarenes and aminoarenes.[63, 64] An example of the synthesis of a functionalised octa(aniline) is shown in Scheme 1-11. Synthesis of poly(aniline)s from BH cross-coupling reactions in turn enables their structures to be tuned by replacing either the 1,4-phenylene unit or the imino-1,4-phenyleneimino unit with different aromatic systems.[1, 2, 44, 65, 66] Three-dimensional networks can

also be achieved by increasing the numbers of reactive functional groups (connectivities) in either one of or both monomers from two to three, four, or six,[1, 2, 67] leading to the development of poly(aniline)-based conjugated microporous polymers (PANI-CMPs). It should be noted, however, that poly(aniline)s have been applied for porous polymers before; instead of being made directly from monomers, polymers were used as starting materials for HCPs by modification with crosslinkable alkylene groups (Scheme 1-2).[30]

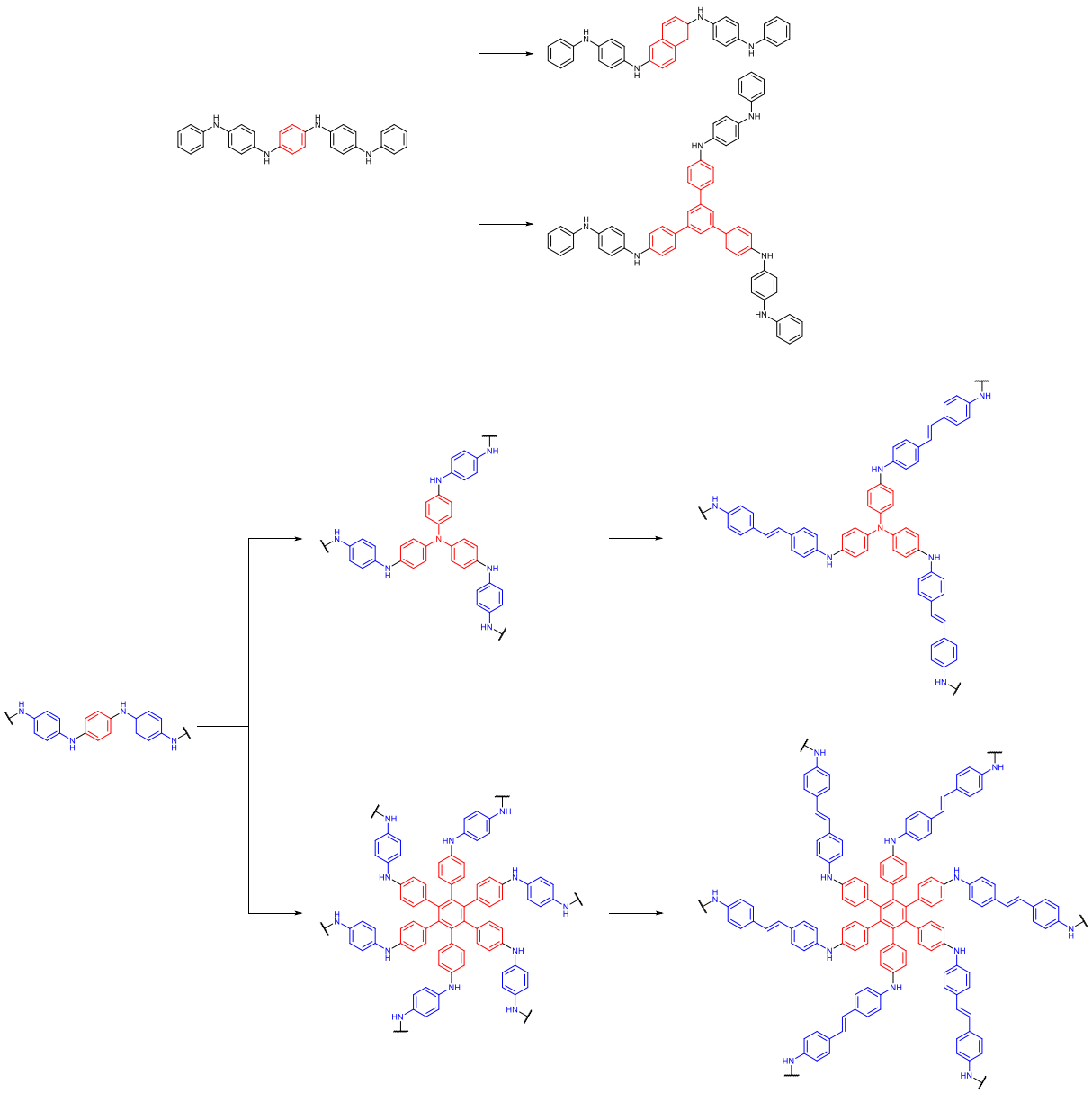

Scheme 1-12 Examples of new materials based on structures of poly(aniline)s by replacing aromatic systems[1, 2, 65, 66]

Many publications have shown the strong influences of synthetic methods on properties of the resulting CMPs, implying the opportunities for fine-tuning properties of these materials. This aspect will be discussed in detail in Section 4.1. As Laybourn *et al.* have concluded, the key to the formation of highly microporous materials is the formation of a gel,[31] which can be achieved when the solubility parameters of the solid polymer particles and the liquid matrix match. This concept has led to the development of the Bristol-Xi'an Jiaotong (BXJ) approach in which an

appropriate ionic salt such as sodium fluoride or sodium bromide is added to alter the solubility parameters of the solvent.[44, 45]

Hansen solubility parameters (HSPs), which are the main idea for the BXJ approach, consist of three components for each substance. These three-dimensional components are dispersion, polarity, and hydrogen bonding.[68] Each solubility parameter is defined as in Equation 1-1.

$$\delta = \sqrt{\frac{-e^{\circ}}{V_m}} \qquad 1\text{-}1$$

The solubility parameter is represented with the Greek letter δ, while $-e^{\circ}$ and V_m stand for the molar potential energy and the molar volume, respectively. In this case, the molar potential energy is replaced with ΔE for the evaporation energy, which can then be partitioned into three aforementioned components, namely ΔE_d for dispersion, ΔE_p for polarity, and ΔE_h for hydrogen bonding. Therefore, the relationship between total solubility parameter δ and its components δ_d, δ_p, and δ_h can be written as:

$$\delta^2 = \delta_d^2 + \delta_p^2 + \delta_h^2. \qquad 1\text{-}2$$

The idea of separating three different components is a development from the previously proposed Hilderbrand solubility parameters because each of the three components contributes towards the solubility or the compatibility to a different extent from others. For two different substances, the HSP distance (R_a) between them can be calculated using differences between the corresponding pairs of solubility parameters ($\Delta\delta$). The equation is given as:[69]

$$R_a^2 = 4(\Delta\delta_d)^2 + (\Delta\delta_p)^2 + (\Delta\delta_h)^2. \qquad 1\text{-}3$$

The factor of 4 in front of $(\Delta\delta_d)^2$ is empirically determined from experiments.[70] The value of R_a or HSP distance between two species, solvent and solute, can determine whether the two species will be compatible or miscible. The smaller the R_a value, the more likely for solvent and solute to be miscible. In a study by Diehn *et al.* for the relationship between R_a and gelation,[71] they have found that there are four end scenarios for gelation based on the R_a values, from smallest to largest, solution, slow gel (not immediately formed after heating up for initiation), immediate gel, and suspension. While solubility tuning is not an objective in this study, the issues of HSP distance and compatibility can still affect properties of synthesised PANI-CMPs, which will be discussed in detail in Chapter 4.

1.1.3 Adsorption Analyses for Porous Materials

Contents in this section are mostly based on the IUPAC Technical Report in 2015.[20] This report has been prepared as a revision of the IUPAC Recommendation published earlier in 1985.[19]

The uptake of molecules onto the surface of materials is called adsorption, which differs from absorption in which molecules are taken into the structure of materials. Consider a person and a plate of food. The absorption process is analogous to the person eating the plate of food, while the adsorption process is analogous to someone else pouring the content of the plate over the head of the person. Collectively, both processes are considered as sorption. This term is useful in some cases when adsorption and absorption can occur simultaneously. The person-and-plate-

of-food analogy is when small bits of food accidentally get into the oral cavity of the person while having the content poured over themselves.

Adsorbents, adsorbates, and adsorptives are terms used to describe the species involved in the adsorption process. Adsorbents refer to materials (or the person) of which surfaces take part in the uptakes. Meanwhile, adsorbates and adsorptives refer to the same substance (gas, liquid, or the food) to be taken onto the surface of adsorbents. If such substance remains in the bulk and yet to be on the adsorbent surfaces, like the food remained on the plate, it is referred to as an adsorptive. However, if the substance has already been in contact with the adsorbent surfaces, or the person's surfaces, it is referred to as an adsorbate. Meanwhile, the opposite process of the adsorption process is the desorption process.

Isotherm adsorptions are the most utilised analytical techniques for the study of porous materials. In these techniques, materials are put in a vessel with a certain volume at a certain temperature, and the amount of adsorptive being adsorbed onto the surfaces are measured as the adsorptive being gradually introduced into (adsorption branch) and subsequently removed from (desorption branch) the vessel. Isotherm plots are plots of the amounts of adsorptive being adsorbed per material weight against the relative pressures, which are ratios of the pressure or partial pressure (p) of the adsorptive to the saturate pressure ($p°$) of adsorptive.

In cases of gaseous adsorptives such as nitrogen or carbon dioxide, the vessel along with the analysing material will first be evacuated. The dead volume, which is the volume of the vessel not occupied with the material, will then be determined using non-sorptive gases such as helium. After the non-sorptive gas has been removed and the vessel has been returned to vacuum and placed at a certain temperature using a temperature-controlling bath along with the $p°$ tube, the adsorptive gas will then be introduced for adsorption branch measurements. For each pre-determined data point, the gas will be filled into the vessel until the $p/p°$ reaches the desired value. The gas admitted into the vessel is either adsorbed onto material surfaces, become adsorbate, or remained as adsorptive filling up the dead volume in the vessel. Therefore, the difference between the amount of gas admitted to fill the vessel to reach $p/p°$ value and the amount of gas required to fill the dead volume is the amount of gas adsorbed, and this amount will be recorded and plotted against the $p/p°$ value, yielding the adsorption branch. The measurements for the desorption branch are performed in the same manner, but their data will be plotted as another branch. Typically, for the same $p/p°$, the adsorbed amount on the desorption branch will be higher than or equal to the amount on the adsorption branch due to the nature of porosity of the material. The phenomena of the desorption branch being above the adsorption branch is called hysteresis which, along with the shape of the adsorption branch itself, relates to the porosity of the material. The relationship between the shape of isotherm plots and material pore morphologies will be explained further in Section 1.1.3.1. Meanwhile, the following sections will discuss further analyses of surface morphologies (Section 1.1.3.2) and CO_2 adsorption isotherm analyses for thermodynamics of adsorptions (Section 1.1.3.3).

1.1.3.1 Brunauer-Emmett-Teller (BET) Analysis of N_2 Adsorption Isotherm Data at 77 K

Properties related to surface of porous materials can be studied by the means of isotherm adsorption of inert gas at low temperature. The most commonly used gases are nitrogen (at 77 K) and argon (at 87 K) although nitrogen is far more common due to the lower cost compared to argon. Many porosity-related properties can be obtained from these low-temperature isotherm analyses, namely pore morphologies, specific surface areas, pore size distributions, and microporous surface areas.

Table 1-2 Main features of adsorption isotherm plots as proposed by Thommes et al.[20]

Type	Main Feature
I	• Found in microporous materials with small external surfaces. • The low $p/p°$ region shows steep increase due to enhanced interaction. • There is almost no increase after the initial steep increase. • Narrower pores cause stronger adsorbent-adsorptive interaction and, therefore, faster filling in Type I(a).
II	• Found for macroporous materials. • An inflection point can be seen as an indication of the completion of monolayers. • Multilayers can be formed beyond the knee point and can be observed as the amount of adsorptive taken increase infinitely.
III	• The interaction between adsorbent and adsorptive is weak. • There is no sign of an inflection point indicating the completion of monolayers. • The increase at high $p/p°$ appears more finite.
IV	• Found for mesoporous materials. • A knee point, similar to Type II, can also be observed. • Pore condensations at moderate to high $p/p°$ cause the steep increase. • The plot plateaus or inflects at high $p/p°$. • A hysteresis can be seen if the pores are wider than the critical width for specific adsorptive (4 nm for nitrogen at 77 K or argon at 87 K, for example), in Type IV(a).
V	• This type is a hybrid between Type III and Type IV. • The initial, low pressure region resembles Type III. • The moderate to high pressure region resembles Type IV with plateau/inflection and hysteresis loop.
VI	• Found for microporous materials with hierarchical structures. • Multiple knee points denote the layer-by-layer filling.

Six different types of adsorption isotherm plots have been proposed.[19, 20] Main features of these proposed six types of these isotherm plots are summarised in Table 1-2. There is no significant change to definitions provided in the 2015 report compared to the 1985 report. However, Type I and Type IV in the 2015 report have been divided further into two subtypes, denoted by (a) and (b). Isotherm plots from both references are shown comparatively in Figure 1-3.

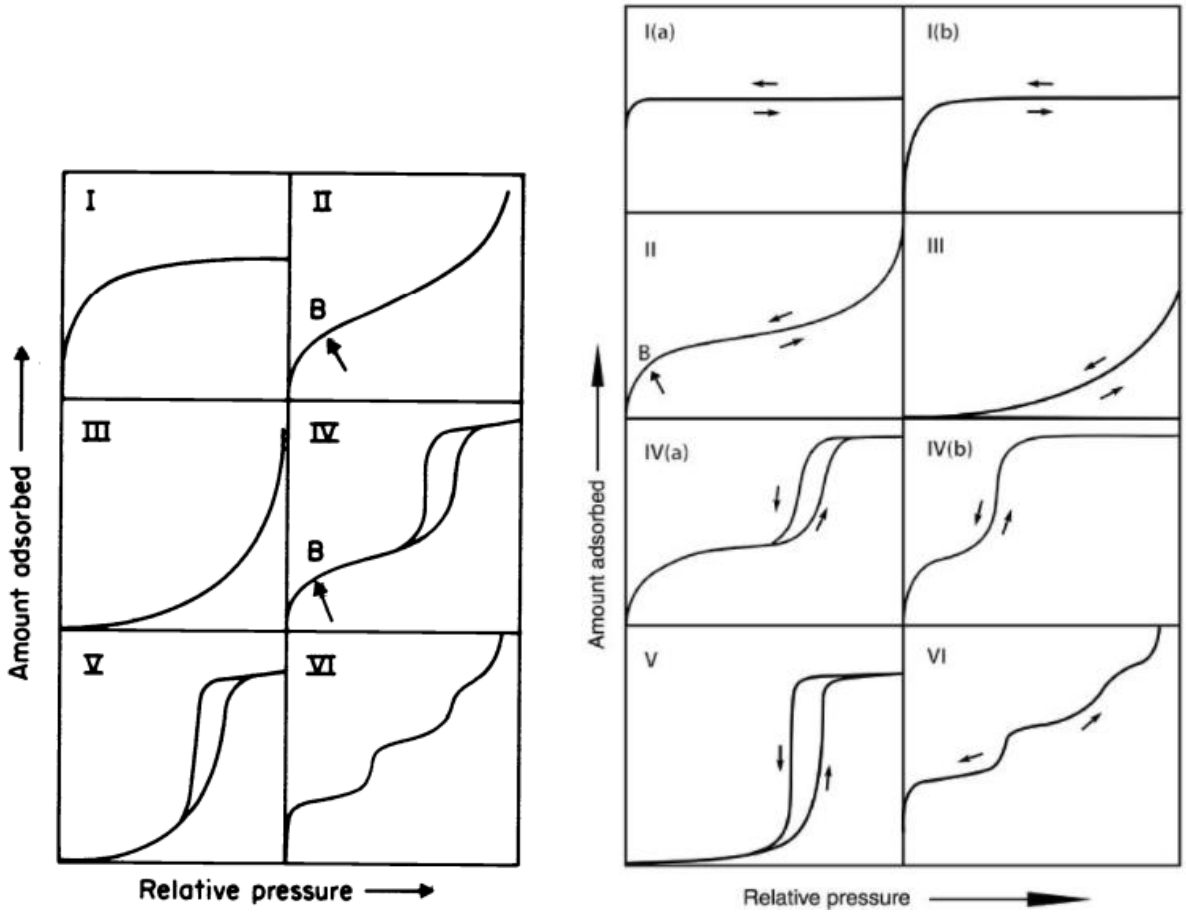

Figure 1-3 Comparison between six types of adsorption isotherm plots in the 1985 IUPAC Recommendation[19] (left) and the 2015 IUPAC Technical Report[20] (right)

Surface areas are usually determined from these types of isotherm analyses using the Brunauer-Emmett-Teller (BET) adsorption model.[72] This model concerns the adsorption of gases or vapours at the temperatures near their condensation or boiling points, and it is based on the Langmuir monolayer adsorption model. The main assumptions for this model are that the energy required for the formation of second layer onwards is of the same magnitude as the energy required for condensation process and that the adsorption is on the free surface, where formation of infinite layers is possible.[72] Under these assumptions, the total volume of gas adsorbed v as a function of pressure p can be written as:[72]

$$v = \frac{v_m c p}{(p^\circ - p)[1+(c-1)(p/p^\circ)]}. \qquad 1\text{-}4$$

In Equation 1-4, v_m is the volume of the monolayer, p° is the pressure at the saturation point, which is the reference pressure in practice, and c is essentially a constant. The scientific meaning of c relates to the difference between the energy for the formation of the monolayer and the energy for the formation of the multilayer with regards to the Langmuir adsorption model.[72] This equation can be algebraically rewritten to the more useful form.

$$\frac{p}{v(p^\circ - p)} = \frac{c-1}{v_m c} \cdot \frac{p}{p^\circ} + \frac{1}{v_m c} \qquad 1\text{-}5$$

Equation 1-5 is in the linear equation form, $y = Mx + C$, between $\frac{p}{v(p°-p)}$ and $\frac{p}{p°}$, with the slope and y-intercept being $\frac{c-1}{v_m c}$ and $\frac{1}{v_m c}$ respectively. Therefore, values of monolayer volume v_m and constant c can be calculated from the slope and y-intercept of the plot. Generally, the practical range of $p/p°$ has the lower boundary around 0.05 and the upper boundary around 0.30-0.35.[20, 72] The lower boundary is determined by the completion of the monolayer, noted as point B in Type II adsorption isotherm (Figure 1-3). Meanwhile, the upper boundary is determined from where the BET equation in linear form (Equation 1-5) starts to deviate from linearity.[72] Although v and v_m parameters are related to volumes, in practice, any pair of properties that are proportional to volumes can be used, including masses and amounts in mole. In both IUPAC reports,[19, 20] the amount adsorbed n^a is used instead of v, and its monolayer counterpart $n^a{}_m$ is used instead of v_m. In this case, Equation 1-5 using amounts instead of volumes will look like this:

$$\frac{p}{n^a(p°-p)} = \frac{c-1}{n^a{}_m c} \cdot \frac{p}{p°} + \frac{1}{n^a{}_m c}. \qquad 1\text{-}6$$

$$c = \frac{M}{C} + 1 \qquad 1\text{-}7$$

$$n^a{}_m = \frac{1}{M+C} \qquad 1\text{-}8$$

$$a_s = \frac{n^a{}_m N_A \sigma_m}{m} \qquad 1\text{-}9$$

Equations 1-7 and 1-8 show how values of c and $n^a{}_m$ can be determined from slope M and y-intercept C from Equation 1-6. (Note the difference between uppercase C representing y-intercepts and lowercase c representing the constant in the BET equations.) In turn, the value of monolayer amount adsorbed $n^a{}_m$ is then be used to calculated specific surface area a_s (Equation 1-9), with N_A representing Avogadro constant, σ_m representing the molecular cross-sectional area, and m representing mass of the material to be analysed. The term "specific" in specific surface area refers to the surface area per mass unit, while the surface area A_s is the total surface area of material of mass m.[20] However, in this thesis, the term corresponding to A_s will not be used, and the terms "specific surface area" and "surface area" are used interchangeably.

As mentioned previously, values of constant c are related to the difference between monolayer and multilayer formations, which means that higher values of c also mean the larger magnitudes of monolayer formation energy compared to multilayer formation energy. It has been determined that the c value of 80 or higher relates to the clearly defined point B of monolayer completion,[20] and the v_m values determined from linear BET plot and directly from the isotherm plot (i.e., the v_m value at point B) are not significantly different.[72] If the c value is around 50, this means that the energy of monolayer and multilayer formations are close, and point B cannot be clearly determined. If the value of c is lower than 2, this means that the BET model is not an appropriate model for the adsorption isotherm of that material.[20]

It is also worth noting that in the case of BET plots with very low y-intercept, the y-intercept C can be slightly below zero due to experimental noises. Since the BET constant c is calculated from Equation 1-7, this small negative y-intercept C can lead to large negative constant c.

1.1.3.2 Additional Analyses from Nitrogen Adsorption Isotherm Data at 77 K

Specific surface areas on their own are not enough to describe adsorptive properties of materials. For CO_2 adsorptions, for example, there are several publications exhibiting positive links between microporosity and CO_2 adsorption.[73-76] This means that pore sizes and their distributions are also important factors for adsorption-based applications. Several conventional models such as BET[72] and BJH[77] still have limitations for the explanation of microporosity and pore size distributions.[78] Seaton *et al.*[79] have later proposed the molecular model methods for the study of pore size distributions (PSDs) in porous materials. Such methods for determining PSDs are later known as DFT methods.[78] These methods use the density of adsorbates in material cavities in a similar way to how DFT calculations use the density of electrons to model electron movements in molecules. (The concept of DFT calculations itself will be explained in detail in Section 1.3.1.2.) DFT methods can then be classified into two types, non-local DFT (NLDFT) and quenched solid DFT (QSDFT). NLDFT methods[80-82] are the first generation of DFT-based calculations of PSDs which consider material surfaces to be smooth and homogeneous, while QSDFT methods, later developed from NLDFT, have taken the molecular roughness of material surfaces into account and therefore have become more practical for analyses of silicas and carbons.[78]

While the DFT methods have been developed over the past decades and regarded as standard methods, there are still flaws in these techniques.[78] For example, both NLDFT and QSDFT consider the material surfaces to be rigid and remain unchanged. This, however, is not the case for many materials, including CMPs, that have been reported to swell upon the uptake of adsorbates. Landers *et al.* have reviewed the accuracy of DFT methods in various porous materials in their 2013 review,[78] so this issue will not be further discussed here.

Nonetheless, both NLDFT and QSDFT rely on the same principle:

$$N_{\text{exp}}(p/p^{\circ}) \quad = \quad \int_{D_{min}}^{D_{max}} N_{DFT}(p/p^{\circ}, D)\, f(D) dD. \qquad \textit{1-10}$$

Equation 1-10 is the main equation for the determination of PSDs, represented as $f(D)$, a function of pore width D.[78] N_{exp} and N_{DFT} are adsorption isotherm from the experiment and from the calculating kernel, respectively. An isotherm adsorption analysis software can either use pore volumes or surface areas as parameters for $f(D)$. The kernel for these calculation methods consists of a list of pore widths, between D_{min} and D_{max}, and their specific adsorption isotherm. Despite the representation in Equation 1-10, there are a finite number of pore widths in a kernel. Each pore width value has its specific N_{DFT} for it. Hence, the N_{DFT} term is shown as a function of both p/p° and D, unlike N_{exp}.

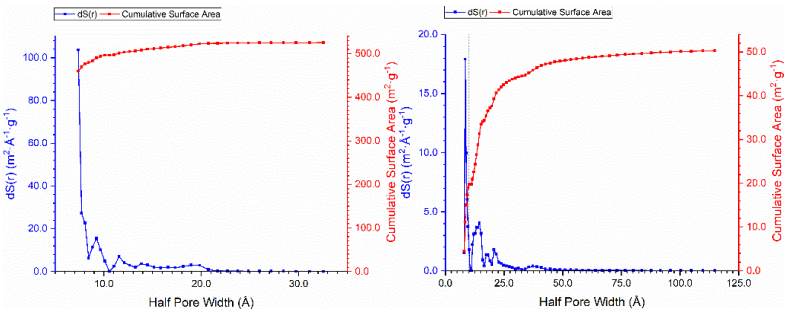

*Figure 1-4 Examples of PSD plots of materials with relatively high microporosity (left plots) and relatively high mesoporosity (right plots). Blue plots are the f(D) vs D plots, and red plots are the **cumulative** f(D) vs D plots. In both graphs, the D_{min} is approximately 7 Å.*

PSDs of a material can be represented in two ways (Figure 1-4), either as a plot of $f(D)$ against D or as a plot of cumulative $f(D)$ against D, which is the summation of data from the pores of smaller sizes than or equal sizes to D. Both plots can give the idea how PSD of the material of interest would look like. The $f(D)$ vs D plot, obviously, tells how much pores of each certain size range contribute to the overall porosity of the material. Meanwhile, the cumulative $f(D)$ vs D plot can also visually tell how much the porosity is contributed by microporosity or mesoporosity. For materials with high micropore ratios, the cumulative $f(D)$ vs D plots would climb steeply near the origin (pore widths < 20 Å) because micropores have already contributed greatly to the overall porosity of these materials. Meanwhile, for materials with fairly high mesopore ratios, the cumulative $f(D)$ vs D plots would continue to climb beyond the microporosity region.

For the analysis of microporosity, one of the most popularly used methods is the *t*-plot method.[21, 83, 84] The name *t*-plot comes from the use of a plot of the volume of adsorbate (V_{ads}), usually nitrogen, against the thickness function $t(p)$ or $t(p/p°)$. If the adsorbent surface is flat without any pores, the V_{ads}-t plot will be linear and intercepting the axes at the origin. The deviation from the $y = mx$ relationship occurs with the presence of mesoporosity and microporosity. For materials with meso- and microporosity, the adsorption process at lower $p/p°$ has the filling of the pores alongside normal depositions of adsorbate molecules on the surface. The pore filling also involves condensation of materials if the pores are of the appropriate sizes, in the mesopore region. As a result, the V_{ads}-t plot is steeper in the initial stage compared to the stage after the pore condensation has finished, causing the deviation from a straight line. Meanwhile, filling of micropores takes place at the very early stage, mostly lower than the first $p/p°$ for the isotherm adsorption data to be recorded. Therefore, the plot will appear *as if* it has started from a positive V_{ads} at zero thickness. These understandings can be used to determine the volume contributed by micropores and mesopores, as shown in Figure 1-5, which can be later converted to respective microporous and mesoporous surface areas.

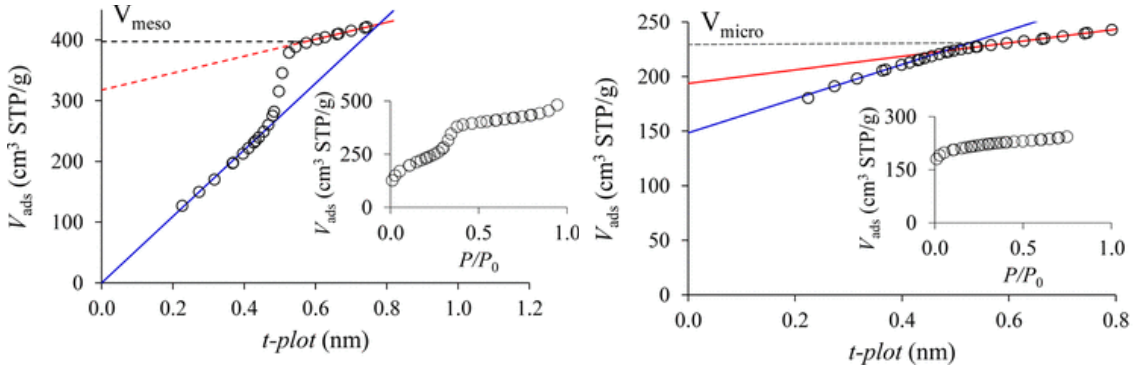

Figure 1-5 The V_{ads}-t plot for mesoporous Al-MCM-41(C16) (left) and microporous FAU zeolite (right) illustrating how the microporous and mesoporous volumes can be determined from the t-plot method, taken from Galarneau et al.[21] In both cases, microporous volumes are the distances between the y-intercept of the pre-deviation linear regression (blue line) and the origin, while mesoporous volumes are the distances between the y-intercepts of the pre-deviation (blue line) and the post-deviation linear regression (red line). The black dotted lines refer to the actual values compared to the values from the t-plot method.

While being regarded as a sensible analytical technique, the accuracy of the *t*-plot method is still limited by the accuracy of the thickness function *t*.[21] Different thickness functions are required, depending on the nature of materials to be analysed, to ensure the reasonable accuracy. An example of such thickness function is shown in Figure 1-6 which shows how complicated the thickness function can be. The function is defined over five subintervals, with 18 parameters in total. These parameters are defined, quoted directly from Galarneau *et al.*,[21] as following.

"…where A_1 = 0.1887299 nm, A_2 = -481.3, A_3 = 0.182099 nm, A_4 = -23.78, B_1 = 0.5675647 nm, B_2 = 0.199735, B_3 = 0.4116168 nm, B_4 = 2.00834, C_1 = 0.1423566, C_2 = 0.1078, C_3 = 0.4888, D_1 = 0.08309076, D_2 = 0.02995, D_3 = 0.369, E_1 = 1.268066 nm, E_2 = 1.931, E_3 = 0.76934 nm, and E_4 = 51.09. If used as such, this equation provides the film thickness in nm."

$$t(P/P_0)\ (\text{in nm}) = \begin{cases} A_1[1-\exp(A_2P/P_0)] + A_3[1-\exp(A_4P/P_0)] & (P/P_0 < 0.03) \\ B_1(P/P_0)^{B_2} + B_3(P/P_0)^{B_4} & (0.03 \le P/P_0 < 0.25) \\ \left[\frac{C_1}{C_2 - \log(P/P_0)}\right]^{C_3} & (0.25 \le P/P_0 < 0.6) \\ \left[\frac{D_1}{D_2 - \log(P/P_0)}\right]^{D_3} & (0.6 \le P/P_0 < 0.9) \\ E_1(P/P_0)^{E_2} + E_3(P/P_0)^{E_4} & (0.9 \le P/P_0) \end{cases}$$

Figure 1-6 The definition of the thickness function t(p/p°) of MCM-41 reference materials, cited in Galarneau et al.[21]

Galarneau *et al.*, in the same article, have discussed the validity of this analysis method in hierarchically micro- and mesoporous materials by analysing mixtures of standard porous materials, MCM-41 silica and FAU zeolite.[21] They have found the reliability of the *t*-plot method to be questionable for materials which microporosity contributes for at least 20% of overall porosity. The issue has been found to be systematic, and the correction formula has been given in the article.

1.1.3.3 Carbon Dioxide Adsorption Isotherms

General adsorption isotherms of CO_2 and other adsorptive gases are performed at more ambient temperatures such as ice-water (0 °C; 273 K) or room temperature (298 K). At these temperatures, the isotherm graphs have different shapes from the six types mentioned in the previous section. Isotherm plots of CO_2 at ambient temperature show the increase throughout the relative pressure range from 0 to 1, with the rates of increase become slower as the relative pressure values become closer to 1. The plots resemble Type I isotherm but without the plateau. One mathematical model for the fitting of these isotherm plots is the Freundlich-Langmuir model, which is presented in Equation 1-11.

$$n_s(p) = \frac{abp^c}{1+bp^c} \qquad 1\text{-}11$$

The Freundlich-Langmuir model represents the specific amount of adsorptive being adsorbed (n_s) as a function of pressure (p), or relative pressure.[85] There are three parameters in this equation, namely a, b, and c. Parameter a is the maximum adsorption of CO_2, which can be approached at the infinitely high pressure ($p \rightarrow \infty$). Parameters b and c are the affinity constant and the heterogeneity exponent, respectively. Usually, parameter a has the same unit as n_s, while the term bp^c is dimensionless. Some publications use the form $(bp)^c$ instead of bp^c, which would affect the unit of parameter b. Another factor that can affect the unit of parameter b is the unit of p itself.[85] However, if relative pressure ($p/p°$), which is already dimensionless, is used instead of pressure, the parameter b will also become dimensionless. Nonetheless, these parameters can be obtained by fitting data from experiments with the given equation using the data analysis software.

Thermodynamic data regarding the adsorption of CO_2 on the material surfaces can also be obtained by measuring the isotherm adsorption at two or more different temperatures and using the Clausius-Clapeyron equation, Equation 1-12.

$$\Delta H_{\text{ads}}(n_s) = -R \ln\left(\frac{p_{T_2}}{p_{T_1}}\right)\frac{T_1 T_2}{T_2 - T_1} \quad \textit{1-12}$$

This equation represents the isosteric enthalpy of adsorption (ΔH_{ads}) as a function of the specific amount of CO_2 adsorbed on the surface. Pressure values p_{T_1} and p_{T_2} are (relative) pressures at temperatures T_1 and T_2 where the amount of CO_2 adsorbed equals n_s. These pressure values can be calculated as an inverse function of Equation 1-11, as shown in Equation 1-13.

$$p(n_s) = \sqrt[c]{\frac{n_s}{b(a - n_s)}} \quad \textit{1-13}$$

It is worth noting that Equation 1-12 has a limited range, which is determined from experimental data, and cannot be used for prediction beyond that range. A mathematical function has *domain* and *range*, which define the span of independent and dependent factor values where the function can be validly defined. Consider the isotherm plot and the eventual Freundlich-Langmuir-fitted function (Equation 1-11) as a mathematical function, the *domain* of this function is the (relative) pressure span predetermined in the experiments, and the *range* of this function is the span of amounts of adsorptive being adsorbed onto surfaces over the aforementioned *domain*. Since Equation 1-13, which is the basis of Equation 1-12, is an inverse function of Equation 1-11, the *range* of Equation 1-11 has become the *domain* of Equation 1-13, and *vice versa*. This means that at a given temperature, Equation 1-13 can be validly defined only over the n_s values ranged from the lowest measurable amount to the highest measurable amount. In addition, Equation 1-12 requires data measured at two different temperatures, which means that, in this case, the valid range of n_s is the overlapped range between the aforementioned valid range from each temperature. Therefore, it is recommended that the two selected temperatures should be different enough to measure their differences in amounts taken accurately and should be close enough to ensure the significant range where the Equation 1-12 is still practically defined. Nuhnen and Janiak have recommended to use the gap of 20 K (273 K and 293 K, for example) or less for more accurate determinations of ΔH_{ads}, and they also recommended against estimating ΔH_{ads} values beyond the valid range.[85]

Another way to determine the values of ΔH_{ads} is to use the virial method, which has the form as shown in Equation 1-14.[85] The virial method equation has both terms for amount adsorbed n_s and temperature T and uses polynomial expressions for fitting, one for the temperature-dependent term and another for the temperature-independent term. The inclusion of temperature as a parameter allows data from multiple sets to be fitted simultaneously, with the same set of a_i and b_i parameters can be obtained for all data sets. In their article, Nuhnen and Janiak have recommended to have 5 a_i parameters (a_0 to a_4; $m_a = 4$) and 2 b_i parameters (b_0 and b_1; $m_b = 1$) and then add more parameters if needed (i.e., if the fitting is not good enough).[85]

$$\ln(p) = \ln n_s + \frac{1}{T}\left(\sum_{i=0}^{m_a} a_i {n_s}^i\right) + \sum_{i=0}^{m_b} b_i {n_s}^i \quad \textit{1-14}$$

While the virial method equation is more empirical compared to the Freundlich-Langmuir model mentioned earlier, the advantage of the virial method is that the fitting can be closer to

experimental data, especially at the lower pressure or adsorbed amount.[85] Also, unlike in the previous method, the pressure as a function of n_s is no longer an inverse function. Therefore, it does not have the mathematical restriction and can be applicable over the whole range of n_s. If p_{T_1} and p_{T_2} are substituted into Equation 1-12 in the same way, the ΔH_{ads} at amount adsorbed n_s can then be written as:

$$\Delta H_{\text{ads}}(n_s) = R\left(a_0 + a_1 n_s + \cdots + a_{m_a} {n_s}^{m_a}\right). \quad 1\text{-}15$$

$$\Delta H°_{\text{ads}} = R a_0 \quad 1\text{-}16$$

Equation 1-15 can also be applicable over the whole range of n_s, and therefore, it can be used to predict the value beyond the range of n_s obtained from experiments. This way, the value of ΔH_{ads} as n_s approaches 0 (zero coverage) can be determined. The value is called the isosteric enthalpy of adsorption at zero coverage or $\Delta H°_{\text{ads}}$, which can be calculated from Equation 1-16.

In this work, both methods will be used to determine the isosteric enthalpies of adsorption, and their validities will be discussed and compared in Chapter 4.

1.2 Structure-Property Relationships

The concept of structure-property relationships (SPRs) is straightforward. Properties of chemical systems such as chemical compounds, polymers, or solutions are ultimately governed by the chemical structures of their components. This project aims to understand how structures of monomers affect the properties of the resulting PANI-CMPs, using both computational and experimental approaches to aid each other for further understanding.

Factors related to the study of PANI-CMPs and other functional porous materials in general can be divided into four levels from design of materials to applications of these materials, as shown in Scheme 1-13: independent factors, dependent factors, translational factors, and applicative factors.

Independent Factors. Independent factors are factors which can be directly varied either in experiments or in calculations. There are two aspects for these factors, intrinsic and extrinsic. Intrinsic independent factors refer to any factors related to intrinsic properties of chemical moieties or starting materials involved in the synthesis of PANI-CMPs. This also includes oxidation states and doping states. On the other hand, extrinsic independent factors are related to additional factors that are not directly related to chemical components. Examples of these extrinsic factors are synthesis conditions such as temperatures, solvents, concentrations, or atmospheres.

Dependent Factors. These factors cannot be tuned directly without changing any of the independent factors. These factors or properties can be separated into two main groups by scale: microscopic and macroscopic. Microscopic properties concern properties related to atomic arrangements and their subsequent results. These structural properties can be separated further into two groups, geometric structures and electronic structures. Geometric structures concern coordinates of atoms in the chemical space and related properties such as bond lengths or bond angles, while electronic structures concern properties related to electron arrangements and positions respective to the geometric structures.

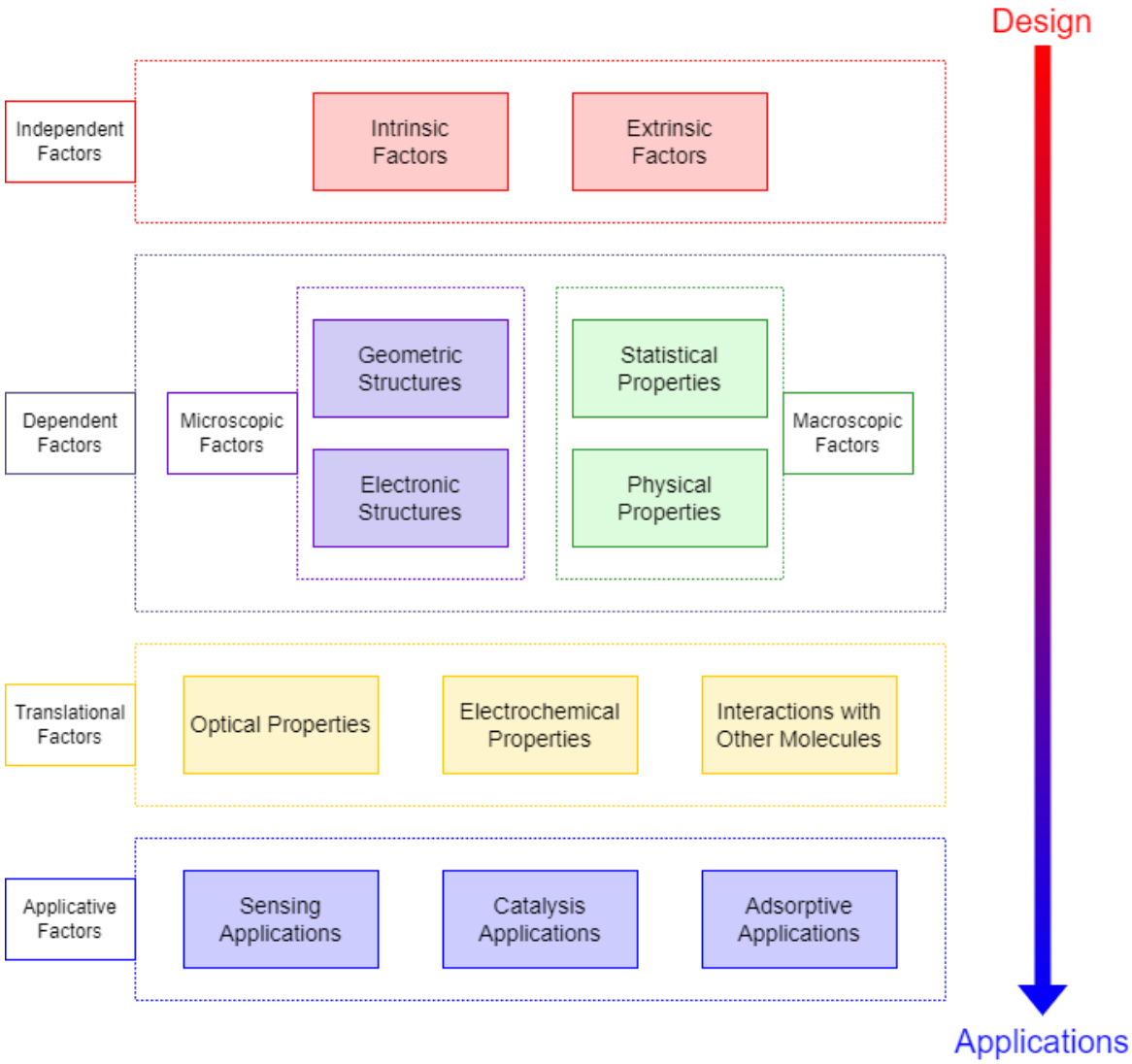

Scheme 1-13 Factors in the study of PANI-CMPs from design to applications

Macroscopic properties focus on properties of bulk materials such as morphological properties or solubilities. Bulk properties of materials can be categorised further depending on how these properties are considered. They can be considered as an overall contribution from smaller parts with different properties and appearing in different ratios. In this case, statistical distribution of different states with different properties become important. These are called statistical properties. Meanwhile, they can also be considered as a single property of the whole bulk material. These are called physical properties. Examples of physical properties in the studies of porous materials are surface areas and solubilities.

Translational Factors and Applicative Factors. Factors in these two categories can also be included as dependent factors. However, they are separated from the "dependent" category because factors of both groups are related to their further applications, while dependent factors are related to the particular materials on their own. Translational factors are related to the *potential* for applications, i.e., to how materials *can be used* for applications. On the other hand, applicative factors are related to the *performance* for such applications, i.e., how materials *perform* for particular applications.

To explain these different levels of factors and their relationships, consider the design of PANI-CMPs for CO_2 adsorption. The ultimate goal as an application for these materials is to have

materials that can adsorb high amounts of CO_2 compared to their own masses. The amount of CO_2 uptake per unit mass of material is then the applicative factor. To achieve this high amount, materials should have properties that allow a high amount of CO_2 to be stored inside. This can be fulfilled in at least 2 ways, either having materials that attract CO_2 molecules strongly or having materials that have high surface areas. The property of attracting CO_2 molecules strongly is the translational factor because it does not indicate directly that the material will take up high amounts of CO_2 but indicates its potential for CO_2 adsorptive applications. Meanwhile, surface area is less specific to CO_2 adsorption since it can be related to other applications including catalysis, sensing, or even adsorption of other gases. Therefore, surface area is the dependent factor. From the translational factor of strong affinity towards CO_2, it can be considered further for relating dependent factors. The material needs to, for example, either have functional groups that can bind CO_2 molecules or have pores with appropriate sizes to those of CO_2 molecules. (It should also be noted that there are more factors related to the uptake of CO_2 besides the aforementioned.) Deductive analysis can be performed further and further until independent factors are reached. This factor chain is unique for one particular application, and to achieve novel materials as strong candidates for a certain application, these contributing factors need to be delineated and understood.

In this work, structure-property relationships for the design of PANI-CMPs will be explored by replacing different aromatic groups as monomer units. Details for monomer units being used, as independent factors, will be discussed in Chapter 2, while the resulting properties as dependent, translational, and applicative factors will be discussed in following chapters, respectively.

1.3 Computational Chemistry

Computational chemistry is a field of chemistry aiming to study properties of chemical systems using mathematical models. In general, chemical systems involve a group of atoms bonded together in specific ways. These atoms also contain protons, neutrons, and electrons, which are the elementary particles building up these chemical systems. Therefore, the main foci of these mathematical models are on the atoms and their elementary particles.

$$\hat{H}\Psi = E\Psi \qquad 1\text{-}17$$

The Schrödinger equation, Equation 1-17, is the most well-known equation affiliated with quantum chemistry and quantum physics. The Greek letter Ψ, psi, refers to the wave function for the particular system of interest. These wave functions can be either time-independent or time-dependent. Time-independent wave functions are in the form of functions of spatial coordinates such as (x, y, z) in three-dimensional Cartesian coordinates or (r, θ, φ) in polar coordinates. On the other hand, time-dependent wave functions have time, t, as another variable. The symbol $\hat{H}$ on the left-hand side refers to the Hamiltonian operator, which is a mathematical operation acting upon the wave function. Such operation can result in the form written on the right-hand side, with a constant E multiplied to the original wave function.[86] To understand the meaning of Equation 1-17, the concepts of eigenfunction and eigenvalue need to be explained.

In mathematics, an eigenfunction is a mathematical operator that, when applied to a function, yields the result in the form of a constant multiplied to the same function. For example, when the derivative operation, d/dx, is applied to the function $y = e^{2x}$, the result is $2e^{2x}$ or $2y$. In this case, the derivative operation d/dx is the eigenfunction, and the constant 2 is the eigenvalue for the function $y = e^{2x}$. Therefore, in the case of the Schrödinger equation, the Hamiltonian operator is the eigenfunction, and the constant E is the eigenvalue, and the purpose of "solving"

the Schrödinger equation is to find the wave function that satisfies the mathematical criteria in Equation 1-17. These criteria come from the properties of the system of interest, and if solved correctly and explicitly, the wave function for that system should be obtained.

Wave functions for simple systems such as particle-in-a-box, harmonic oscillator, or hydrogen-like atoms can be solved explicitly, with the solutions clearly defined. For more complicated systems, however, their solutions may not be practically obtained. These unfortunate cases also include systems with multiple electrons, which include almost every chemical system. Therefore, a sensible approximation technique must be applied to provide sensible mathematical models for these systems.

The following sections are aimed to provide background information relevant to methods used for theoretical studies in this work. Details for comparable methods are also given wherever relevant to the discussions.

1.3.1 Levels of Theory

As earlier explained, wave functions for most chemical systems involving more than one electron cannot be solved from their Schrödinger equations explicitly, and a proper approximation is required. The Born-Oppenheimer approximation has been proposed and is one of the best-regarded approximation techniques for theoretical studies of chemical systems.[86] Since protons and neutrons, two types of elementary particles in the nuclei, are around 1800 times heavier than electrons, the Born-Oppenheimer approximation considers the kinetic energies of nuclei and those of electrons to be separable. On one hand, when focusing on nuclei, electrons can be deemed as too light to have any effects on them. On the other hand, when focusing on electrons, movements of nuclei can also be deemed as negligible, and they can be considered as static. This principle allows chemical systems to be viewed from two separate points, classical mechanics and quantum mechanics. As should be expected from approximations, mathematical models from both classical and quantum mechanics come with their own limitations.

1.3.1.1 Classical Mechanics Path: Molecular Mechanics

On the classical mechanics branch from the Born-Oppenheimer approximation, chemical systems can be considered as groups of balls connected with springs. Atoms are viewed as charged balls, similar to the Dalton's atomic model which considered atoms to be the identity particles for elements, while springs in this case represent chemical bonds. This consideration leads to the development of molecular mechanics (MM) methods. In molecular mechanics, the energy of a particular chemical system can be written as:[86, 87]

$$E_{\text{sys}} = E_{\text{van de Waals}} + E_{\text{stretching}} + E_{\text{bending}} + E_{\text{dihedral}} + E_{\text{out-of-plane}} + E_{\text{dipole}} + E_{\text{cross-term}}. \quad (1\text{-}18)$$

Each of the seven terms on the right-hand side of Equation 1-18 represents energy from different interactions being considered; van der Waals force between two atoms, stretching of chemical bonds, bending or changes in angles between chemical bonds, dihedral interactions, out-of-plane or "improper" dihedral interactions, interactions between dipole moments, and cross-term and other non-bonding interactions.

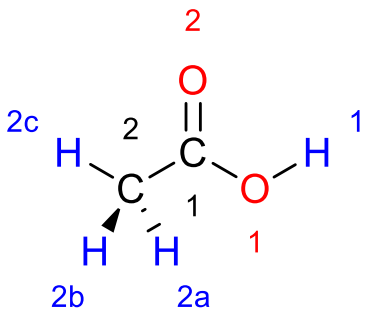

Scheme 1-14 Structure of acetic acid, with numbering for explanation of different interactions being used in molecular mechanics

Consider the structure of acetic acid, Scheme 1-14, with two carbon atoms (1 and 2, black), four hydrogen atoms (1, 2a, 2b, and 2c, blue), and two oxygen atoms (1 and 2, red). This molecule has eight atoms, and therefore there are C(8, 2) or 28 pairs of atoms to be considered for van der Waals interactions. Some pairs, such as H2c and H1, can sometimes be deemed as too far apart, and therefore, their van de Waals interactions contribute negligibly to the overall $E_{\text{van de Waals}}$ term. Setting the cut-off distance to rule out atom pairs that are "too far apart" might not be that helpful for small molecules such as acetic acid. However, it would improve the calculation time greatly in the case of larger molecules with more number of atoms, given that for a system with n atoms, there are C(n, 2) or (n^2 - n)/2 pairs. In the case of tris(4-aminophenyl)amine, the core monomer **TPA**-$(NH_2)_3$ in this work, there are 40 atoms, which is equivalent to 780 atom pairs, with only 42 of these pairs being actually chemically bonded.

Definitions of bond stretching, bond angle bending, and dihedral angle are straightforward compared to the following terms in Equation 1-18. Stretching and bending are vibrational modes, and energy contributions from these modes ($E_{\text{stretching}}$ and E_{bending}) are written as harmonic oscillations, as functions of the deviation from the equilibrium values, combined with further terms from Taylor expansions.[86] Dihedral angles, on the other hands, are slightly different from the former two. They are defined upon sequences of four atoms, in which the first atom is bound to the second atom, the second atom is bound to the third atom, and the third atom is bound to the fourth atom. In the case of acetic acid, examples of such sequences are (C2, C1, O1, H1), (H2a, C2, C1, O2), and (O2, C1, O1, H1). (In mathematics, a sequence is similar to a set, but unlike in a set, the member positions matter. For example, sets {1, 2, 3} and {1, 3, 2} are the same, but sequence (1, 2, 3) and sequence (1, 3, 2) are not the same.) For a four-atom sequence, their dihedral angle is defined as the angle between projections of the first-atom–second-atom bond and third-atom–fourth-atom bond upon the plane perpendicular to the bond between the second and the third atom.

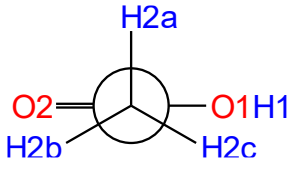

Scheme 1-15 Structure of acetic acid, redrawn in Newman projection viewing through C2–C1 bond

For the better visualisation of dihedral angles, Newman projection is used for illustration. Considering the (H2a, C2, C1, O2) sequence, the second and the third atoms are C2 and C1 carbon atoms, respectively. Therefore, this molecule should be viewed through C2–C1 bond, with the atom C2 obscuring the atom C1 completely. The page is now the plane perpendicular to the C2–C1 bond, and other bonds involving either C2 (the front atom) or C1 (the back atom) are now

projected onto the aforementioned plane. In this case, the dihedral angle of (H2a, C2, C1, O2) is the angle between the line pointing towards H2a and another line pointing towards O2.

There is another type of dihedral angles that is defined to take the out-of-plane bending into account. They are focused on a subunit of four coplanar atoms such as the carbonyl carbon (C1) in acetic acid. The difference between dihedral angles for systems like this and the previously discussed dihedral angles is that the fourth atom is bound to the second atom, rather than to the third atom in the normal dihedral angles, which also means that the second atom bond with all other three atoms in the sequence. Therefore, they can sometimes be called "improper dihedral angles".[86] In acetic acid, there is only one atom with this property, C1, and therefore, there are three atom sequences that can be used to define out-of-plane bending angles, (C2, C1, O1, O2), (O1, C1, O2, C2), and (O2, C1, C2, O1). The out-of-plane bending angle is defined to be the angle between the second-atom–fourth-atom and the plane of the first three atoms.

The sixth term, E_{dipole}, emerges from the interactions between dipoles, polar bonds between atom pairs with significant difference in electronegativities. Electronegativity is an index number of an element related to the ability to attract electron densities towards itself. When chemical bonds are formed between atoms of different elements, atoms with higher electronegativity will pull the electron density towards itself more strongly, causing the area around it to be partially more negatively charged. This has created a dipole, with the partially more positive side lying on an atom with lower electronegativity. In the case of acetic acid, since electronegativities of carbon and hydrogen are close, there are only three bonds that can be dipoles, C1–O1, C1=O2, and O1–H1.

The last term considers the effects from one term against another which might cause some deviations and therefore might need some corrections.[86] This term also involves other interactions that are not involved in the previous six terms for the similar purpose of corrections.

A set of parameters available for the modelling of chemical systems is called a force field (FF).[86] Each force field contains elements, bonding modes for available elements, and sets of constants and formulae for the energy calculations. Various force fields have been developed for different chemical systems and purposes.

Molecular mechanics calculations, in general, use classical mechanics to consider chemical systems by viewing molecules as groups of charged balls connected together with springs. The classical-mechanics approach simplifies chemical systems significantly, which then allows large systems to be studied at reasonable computational costs. However, such simplifications lead to the inferior performances compared to quantum-mechanics-led Hartree-Fock or DFT methods in terms of accuracies, especially properties related to energies.

In this thesis, molecular mechanics calculations have been applied during the conformation screening prior to DFT optimisations. While not being as accurate as quantum mechanics in terms of electronic energies, their speed can be helpful for screening for various possible local minima, which can then be used as starting points for further optimisations with higher-level methods. Molecular mechanics screening can also reveal the existence of multiple conformers with similar energies but different properties, see Section 1.1.2 for a relevant discussion.

1.3.1.2 Quantum Mechanics Path: Hartree-Fock (HF) Methods and Density Functional Theory (DFT) Methods

Computing methods based on quantum mechanics implement the Born-Oppenheimer approximation by focusing only on electrons while treating nuclei as static positive charges. Attempts to simulate multiple-electron chemical systems using available quantum mechanics

tools over the past decades can be divided into two groups with different main principles, namely Hartree-Fock (HF) methods and density functional theory (DFT) methods. While HF methods are based on approximations, DFT methods are exact methods, at least in theory.[86] The different between the two groups will be explained further.

The main principle of Hartree-Fock methods is to approximate the potential solution of the Schrödinger equation for the multiple-electron chemical system using existing wave functions. Developments of approximation techniques can also be further divided into two groups based on how approximations are improved, semiempirical methods and *ab initio* methods. Semiempirical methods rely on experimental data to adjust parameters for better approximations, while *ab initio* or "from the start" methods concentrate on making newer sets of wave functions to yield better approximations. While Hartree-Fock methods are not used in this study, they are included in this background theory discussion because of their historical importance in the development of DFT methods. It should also be noted that there are post-HF methods as well, which are not discussed here.

DFT methods take a different approach from HF methods by using density functionals instead of wave functions for the modelling of chemical systems. A functional, in mathematics, is a function of which the argument is also a function. Therefore, density functionals are functions of the electron density, which in turn is a function of spatial coordinates describing the molecular structure. Using density functionals allows the equations describing the systems of interest to be written in the same mathematical forms as in the *ab initio* HF methods. This allows DFT calculations to be performed in the same manner as *ab initio* HF methods such as using basis sets and being performed using the same software.[86] The DFT concept is also used to determine pore size distributions in porous materials, see Section 1.1.3.2.

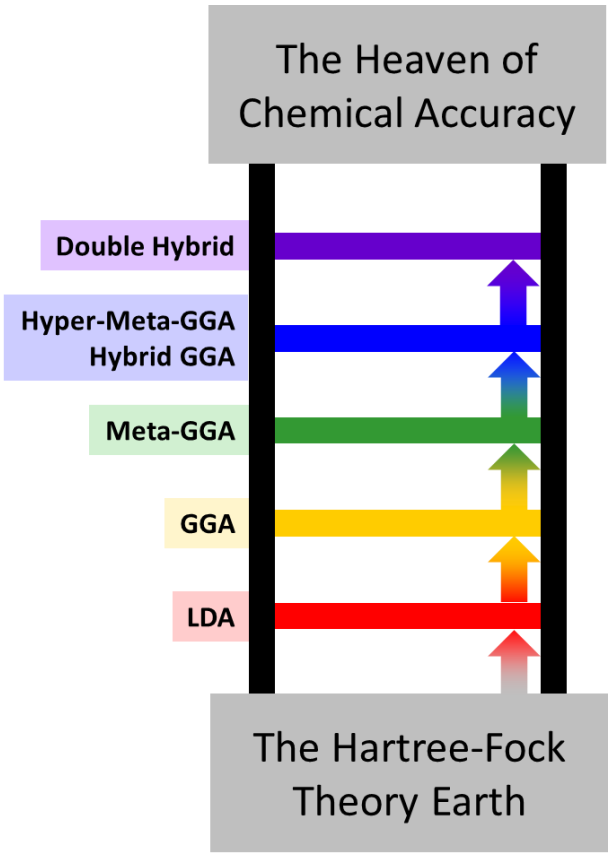

Figure 1-7 The metaphorical Jacob's Ladder summarising progresses in DFT functional developments, adapted from Peng, Duarte, and Paton[88]

Developments of functionals for DFT calculations are usually compared to the Jacob's Ladder, a biblical ladder linking heaven and earth,[88-92] with heaven being the ideal chemical accuracy and earth being the Hartree-Fock methods, as shown in Figure 1-7. This concept has been first proposed by Perdew and Schmidt[89] at the DFT2000 Symposium, and this metaphorical ladder has been updated in 2009 to reflect the progress in DFT developments.[91] Going up each rung represents the improvement of functionals by adding further corrections to close the gap between theoretical and actual chemical systems. Developments of DFT functionals will be then discussed loosely based on this model ladder which structures a discussion of the development of DFT in general since the crucial part for achieving so-called chemical accuracies is the functional itself, as discussed next.

Early DFT computational methods have been developed by Kohn and Sham in early 1960s[93] based on the Hohenberg–Kohn theorem.[94] The basic DFT calculations, without further modifications, will be referred to as Kohn-Sham DFT calculations or KS-DFT in this discussion. In KS-DFT calculations, the energy E of a chemical system of interest can be calculated from the electron density $\rho(r)$. The electronic energy functional $E[\rho]$ can be written as a summation of four mathematical terms, with each term representing the kinetic energy of non-interacting electrons, the potential energy resulting from electron–nucleus interactions, the potential energy from electronic repulsions, and the exchange-correlation energy $E^{XC}[\rho]$. The last term is the most important for the accuracy of each computational method, and therefore, developments of functionals for KS-DFT calculations are focus on formulating $E^{XC}[\rho]$.[90]

The exchange-correlation energy functional $E^{XC}[\rho]$ can be formulated in two different ways, local density approximation (LDA) and generalised gradient approximation (GGA).[90] LDA and GGA differ in the assumption regarding the nature of electron densities. On the one hand, LDA considers electron densities to be homogeneous. On the other hand, GGA considers them to be non-homogeneous, and the gradient of electron density $\Delta\rho(r)$ is also considered in addition. GGA methods are regarded as improvements from LDA methods. As a result, LDA methods are placed on the first step on the Jacob's Ladder while GGA methods are placed on the second step. GGA methods generally perform better in calculations for total energies, atomisation energies, structural energy differences, and energy barriers. However, both LDA and GGA methods still struggle to describe properties in solid state systems or non-covalent interactions.[90]

Beyond LDA and GGA, improvements of DFT functionals have taken several routes.[90] One such route is the development of meta-GGA functionals (the third rung of the Jacob's Ladder, Fig. 1-7) which include higher orders of electron density gradient in addition to $\Delta\rho(r)$. The other way is the development of hybrid GGA functionals. The term "hybrid" refers to the inclusion of Hartree-Fock elements for the exchange part of the exchange-correlation functional. Hybrid GGA functionals, including the B3LYP[95-97] or Becke three-parameter hybrid functional[95] with Lee-Yang-Parr correlation functionals,[96, 97] have become popular since the mid-2000s[90, 98] due to their accuracy compared to experimental data. However, it can be argued that such accuracy might result from errors in different approximations which cancel each other out.[99, 100] Hybrid meta-GGA[90] or hyper-meta-GGA[88] functionals, named differently in published literatures, can also be developed from corresponding meta-GGA functionals in the same way as hybrid GGA functionals arise from GGA functionals.

The fifth rung is called as generalised random phase approximation (RPA) in the 2009 updated version of the Jacob's Ladder by Perdew *et al.*[91] However, it is referred to as double hybrid functionals in other review publications.[88, 92] Regardless, the fifth rung development adds virtual unoccupied orbitals to hybrid functionals. Several double hybrid or RPA functionals have been available in many computational chemistry software packages.

It is worth noting, however, that the Jacob's Ladder concept only concerns functionals for KS-DFT, or more specifically, the developments of exchange-correlation functions. This concept does not include other modifications such as dispersion models, solvation models, or time-dependent DFT, which will be discussed later in this section. Also, we are aware that machine learning has been used for the development of DFT methods over the past few years.[101] However, this topic has exceeded the scope of this study, and therefore it will not be discussed here.

While developments of functionals for Kohn-Sham DFT have reached the fifth rung along the metaphorical Jacob's Ladder so far, KS-DFT calculation methods still have limitations. For example, while KS-DFT calculations perform well for molecules in the gaseous state, they cannot explain the properties of chemical systems in solution or in the solid state.[90] KS-DFT methods also fail to take the effects from non-covalent interactions into account.[102, 103] To improve the accuracy of DFT calculations, dispersion models and solvation models have been developed.

Non-covalent interactions (NCIs) are interactions between chemical moieties that do not form covalent bonds. Their strengths vary from miniscule London dispersions to very strong ionic interactions. These interactions are important in the discussions regarding higher-level structures in macromolecules such as DNAs or polymers[104] and physisorption of gas molecules, with the latter being discussed in detail in Chapter 5. Therefore, the failure to capture these properties can be a major concern in the studies of chemical systems where NCIs can affect chemical structures and properties. The issue generally emerges from the way the exchange-correlation functionals are approximated.[102, 103] With the general approximations used in KS-DFT, the electron density in the space between two chemical moieties distanced beyond the sum of van der Waals radii is almost zero,[102] which means that KS-DFT methods underestimate NCIs in general.

Different methods have been proposed to correct the this over recent decades. One of the early methods is called the DFT-D approach, with the term $C_6 \cdot r^{-6}$ being included in the exchange-correlation functional $E^{XC}[\rho]$.[102, 103] The coefficient C_6 in this case is the dispersion coefficient for the term with the exponent of (minus) six in the mathematical expression of electron dispersion in the series expansion form, which also has terms with the exponents of eight, ten, and so on. These coefficients can be determined both experimentally and theoretically.[103] Other methods have been proposed, taking more factors into account. These correction methods have been discussed in detail in the 2016 review article[105] by Grimme *et al.* published in *Chemical Reviews* and therefore will not be discussed here.

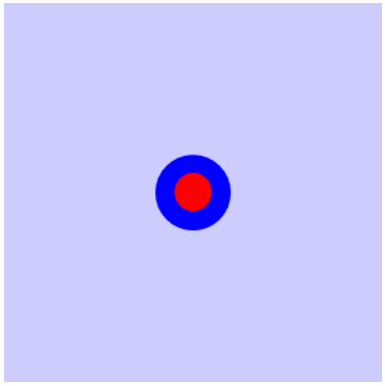

Figure 1-8 Different regions of the bulk solvent regarding the solvated chemical system

KS-DFT methods also have accuracy problems when used to study chemical systems in the solvated state.[90] In this case, the issue is the result of further complications regarding the interactions between molecules in the systems of interest and solvent molecules. One way to

improve the solvation is to separate the bulk solvent into two regions, the main region and the remainder region.[106] Figure 1-8 illustrates the simple model of a chemical system of interest (red inner circle) being solvated in the bulk solvent (blue regions). The main region (blue outer circle) is where most solvent-solute interactions take place, while the rest of the bulk solvent other than the main region will be described as the remainder region. Interactions between the chemical system and solvent in the two regions will be modelled differently.

Another issue with KS-DFT is that these methods are focusing on ground state systems, which means that properties involving excited states or excitation may not be portrayed properly.[90] These properties include spectroscopic properties such as optoelectronic or vibrational absorption spectra. Therefore, time-dependent density functional theory (TD-DFT, sometimes also referred to as TDDFT without a hyphen in literature) has been proposed to mitigate this issue. For TD-DFT calculations, time-dependent forms of Schrödinger equation and eventually wave functions are used for the determinations of dynamic response to external factors.[92, 107, 108] The application of time-dependent aspect of quantum mechanics leads to further applications regarding excited states such as electronic transitions and fluorescence properties, for example.[107, 109]

The conventional TD-DFT methods, known as linear-response TD-DFT (LR-TD-DFT) methods,[92, 108] are attributed to the proposal of four theorems for TD-DFT by Runge and Gross in 1984.[110] The main proposals are the use of time-dependent charge density function and the adiabatic approximation. The latter proposal means that the reactions towards the external factors happen "instantaneously and without memory to any temporal change in the charge density".[108]

Like their non-TD predecessors, while LR-TD-DFT methods are popular choices for theoretical studies related to electronic ground and excited states, they are not flawless. Casida *et al.* have summarised four categories of problems from LR-TD-DFT usages, and it is concluded that LR-TD-DFT methods "[work] best for (*a*) low-energy, (*b*) one-electron excitations involving (*c*) little or no charge transfer and (*d*) that are not too delocalised".[92, 108]

Among the four categories of LR-TD-DFT failures, the underestimation of excitation energies for charge transfer (CT) transitions is the biggest challenge in the study of poly- and oligo(aniline)s. As shown in previously published work,[62, 65] electronic transitions in oligo(aniline)s are charge transfer in nature. The issues related to CT transitions are not limited to the excitation energies, however, since there are reports of other problems for the use of LR-TD-DFT in chemical systems with charge transfers such as geometric structures of molecules in ground and excited states[111] and emergences of "ghost" CT states.[112] The latter issue is yet to be found in poly- and oligo(aniline) studies. Nonetheless, one way to mitigate the CT-related errors in LR-TD-DFT studies is to use long-range separated (LRS) exchange-correlation functionals.[111] Mills *et al.*[62] have compared two functionals, hybrid-GGA B3LYP and LRS-modified CAM-B3LYP, in their studies of oligo(aniline)s with various numbers of aniline units and have found that CAM-B3LYP yields closer results to experimental data for both transition energies and absorption maxima, as shown in Figure 1-9.

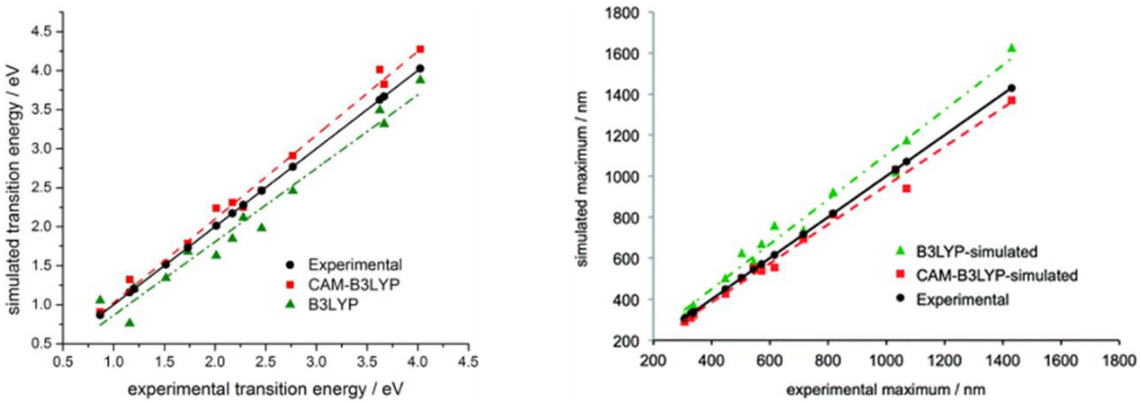

Figure 1-9 Comparisons between TD-DFT-calculated transition energies (left) and absorption maxima (right) of oligo(aniline)s using CAM-B3LYP and B3LYP functionals, taken from Mills et al.[62]

While the use of LRS-modified functionals can improve the CT-related errors in LR-TD-DFT studies, at least for poly- and oligo(aniline) systems, the fundamentals of TD-DFT themselves are also being improved with other approaches. They can be either further improvements from adiabatic approximations or other methods entirely.[92, 108]

One major difference between HF and DFT methods for the studies of long π-conjugated systems such as those in conductive polymers is the issue of localisation/delocalisation error,[98] which has stemmed from how the two streams of method were initiated. On the one hand, HF methods are based on the approximations of molecular orbitals from atomic orbitals, while on the other hand, DFT methods are based on the use of electron densities and their gradients (from the second rung onwards). Therefore, HF methods tend to favour localisation of electrons within the atomic realms, but DFT methods tend to favour delocalisation of electrons throughout the molecule realms. The two extreme cases of errors are referred to in the *Accounts of Chemical Research* article by Körzdörfer and Brédas[98] as the localisation error (for HF methods) and the delocalisation error (for DFT methods). The effects from localisation/delocalisation error on the study of poly- and oligo(aniline) systems will be discussed in the next section.

DFT methods have been developed based on the principle that the energy of a chemical system of interest can be determined from the electron density of that system, with the electronic exchange-correlation functionals playing the most crucial role in the accuracy. Different approximation methods have been applied for the development of functionals to improve accuracies. While the Jacob's Ladder model might imply that we have become closer to chemical accuracy with the developments of hybrid functionals, there are other issues outside the metaphorical ladder that are affecting the chemical accuracy, including non-covalent interactions, solvation, and excited states. These issues cannot be resolved only by the improvement of better estimations but also by taking these issues into account.

In this project, DFT and TD-DFT methods are applied for the theoretical studies of PANI-CMP oligomeric models, based on the methods previously published by our group.[62, 65] Optimisation of these models are performed using DFT calculations, and TD-DFT calculations will be used for the studies of electronic transitions.

1.3.2 Computational Chemistry for the Study of Poly(aniline)s and Oligo(aniline)s

While poly(aniline)s are a group of polymers containing only light elements namely carbon, hydrogen, and nitrogen, comparable to poly(styrene)s, poly(methyl methacrylate)s, or polyurethanes, their conductive properties in doped states make them stand out from other polymers. This difference has led to a surge in theoretical studies of these polymers and their

oligomeric counterparts, with the most important question being which form is responsible for the conductivity, polaron or bipolaron.

The terms polaron and bipolaron are classifications of different types of excitations for discussions in photochemistry. According to the IUPAC Glossary of Terms Used in Photochemistry,[113] "polaron" refers to the lattice distortion or polarisation caused by photoexcitation, while "bipolaron" refers to two polarons bound together to one lattice distortion. For poly(aniline)s, the corresponding structures for polaron and bipolaron are shown in Scheme 1-16. The bipolaron structure (top) has two +1 charges on both nitrogen atoms of one protonated quinoid unit, while the polaron structure (bottom) has two +1 charges on nitrogen atoms of different benzenoid units.

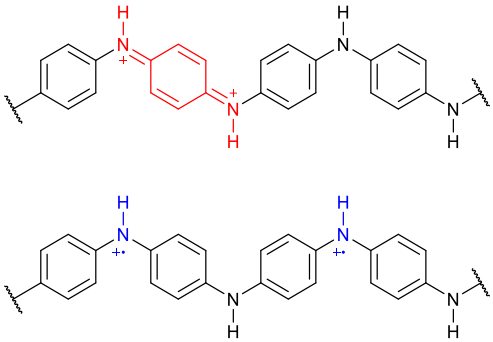

*Scheme 1-16 Structures of **ES** state poly(aniline) chains in bipolaron (top) and polaron (bottom) forms*

The polaron form is proposed to be responsible for the conductive properties in acid-doped poly(aniline)s by Stafström and co-workers,[56] see Scheme 1-9 in Section 1.1.2, in 1987. The polaron model proposal was supported by spectroscopic data (XPS and optical absorption) and computational data. However, the computational method in the 1987 publication was the MNDO (modified neglect of differential overlap) semi-empirical self-consistent-field Hartree-Fock technique.[56] In fact, most of the earlier studies using semi-empirical techniques tend to suggest the polaron model to be the more stable structure than the bipolaron model.[114] However, later studies using DFT methods tend to suggest otherwise.[59, 114-118] In the 2010 publications,[115, 116] Romanova and co-workers have compared the Hartree-Fock method with three other hybrid functionals for DFT methods, namely BH&H, B3LYP, and BLYP. They have found that HF calculations provide inaccurate geometric structures of poly(aniline) models[115] and fail to describe the effects of protonation upon doping from **EB** to **ES** state.[116] The disadvantage of HF methods against DFT methods is that HF methods tend to localise charge perturbations,[115] which can be traced back to the tendency of HF methods to localise charges onto nuclei.[98] The HF tendency towards localisation is also observed among the hybrid functionals. Structural parameters from BLYP calculations suggest strongest delocalisation effects, followed by those from B3LYP and BH&H, which is the same order as the proportion of HF exchange included in the functional, from lowest to highest. These DFT-derived structures, especially with B3LYP and BLYP functionals, are also in better agreements with experimental data.[115] Therefore, it is sensible to conclude that earlier proposals were based on the less accurate computational methods for poly(aniline)s, and later DFT-based studies have suggested that the bipolaron model is closer to the actual conductive structures. It is also worth noting that in the study by Canales *et al.* of long-chain poly(aniline) models in solid state using molecular dynamics (MD), with parameters specifically designed for poly(aniline) systems, and hybrid quantum mechanics/molecular mechanics-molecular dynamics (QM/MM-MD),[61] both methods also suggest that the bipolaron model is more stable.

Another important aspect in computational studies of poly(aniline)s is the use of polarisable continuum models of solvation (PCM). Romanova and co-workers also compared the effects from the presence and the absence of PCM (i.e., in vacuum)[116] and the effects from different PCMs[119] on geometric and electronic structures of poly(aniline)s in different states. They have found that these structures are affected by the dielectric constants of the media, which is important because many of poly(aniline) chemistry phenomena occur in solutions.

Because, as illustrated in Scheme 1-16, most poly(aniline) structures are represented as a four-unit structures, the models being used for the computational studies of poly(aniline)s mostly contain numbers of aniline units in multiples of four, namely tetra(aniline)s (4 units), octa(aniline)s (8 units), dodeca(aniline)s (12 units), and hexadeca(aniline)s (16 units). In the study of **EB** state oligo(aniline)s, in which two hydrogen atoms are removed from the **LEB** state oligo(aniline)s upon oxidations, with the number of aniline units varied from 5 to 13,[118] the defects in geometric and electronic structures tend to be centralised around the five middle units.

These polymers and their subsequent oligomers are also known to have strong and distinctive colours, and these colours can also change upon chemical changes such as doping.[49-51, 56, 62, 65, 66] Therefore, these materials can potentially be used for many applications including sensing. The optoelectronic spectroscopy, corresponding to the electromagnetic wave in the UV-Vis-NIR region, has then become one of the most important properties for the study of these materials.

Unlike the aforementioned properties such as geometric structures or electronic structures, optoelectronic properties involve the electronic transition from ground to excited state, with the absorbed wavelengths being affected by the energies between ground state and excited state molecular orbitals (MOs). Earlier studies, published in the late 2000s to early 2010s, usually used band gap energies between highest occupied MOs (HOMOs) and lowest unoccupied MOs (LUMOs) as a main descriptor.[99, 100, 118] However, as time-dependent DFT methods have been developed, getting the bigger pictures of absorption spectra has been more sophisticated. A full spectrum can be calculated, and MOs involved in contributing electronic transitions can be identified for each transition state, for example. Therefore, TD-DFT methods have become popular in the study of optoelectronic properties in poly(aniline)s and derivatives.[62, 65, 66]

As functional materials with distinctive and interesting properties, poly(aniline)s and their derivatives have attracted a great number of theoretical studies as well as experimental studies. Theoretical studies have been involved strongly in the delineation of geometric and electronic structures of species involved in conductive and optoelectronic properties, and development of better computational techniques have led to better understanding of properties of these materials and potentially can predict properties of materials yet to be produced.

1.3.3 Computational Chemistry for the Study of Conjugated Microporous Polymers

Since structures of CMPs are amorphous, creating accurate models for these polymers is the most challenging part in computational studies of these materials, compared to metal-organic frameworks (MOFs) or even covalent organic frameworks (COFs) with well-defined crystalline structures. Theoretical studies for structure-property relationships in these amorphous materials can be done in two different approaches, direct and indirect. The direct approach attempts to create the CMP structures as accurate as possible, while the indirect approach uses relatively smaller chemical species as representatives for CMP structures. Both approaches have their own advantages and disadvantages.

Accurate structures of amorphous materials can be either obtained from published reports or deducted from mechanistic studies. The former option is more applicable for more well-known materials with known structures such as amorphous silica.[120] Meanwhile, the latter method have been developed over the past years using the combination of formation mechanisms of polymer structures and computational chemistry aided with programming to create the structures of amorphous polymers.[121-124]

While three-dimensional structures of amorphous polymers can be theoretically deducted, many studies have used smaller fragments for studies of interactions with adsorbate molecules.[27, 125-130] Using less numbers of atoms allows computations with higher level of theories to be used, which are helpful for understanding interactions in microscopic levels. One work used DFT calculations to screen substructures in a carbon material based on analysis of X-ray photoelectron spectroscopic data.[27] While the findings from theoretical screenings are comparable to the experimental data, the use of small fragments to represent macromolecular systems is still questionable. The issue will be discussed in detail in Chapter 5.

The amorphous nature of CMPs and other porous organic materials in general has become a big challenge for the theoretical studies of their properties. Various top-down and bottom-up approaches have been applied for modelling of these materials with different advantages and drawbacks. Therefore, there is still a big gap for the theoretical studies of porous organic materials.

1.4 Aim, Objectives, and Thesis Outline

The aim of this project is to understand the structure-property relationships in the design of PANI-CMPs. Both theoretical and experimental approaches have been applied to explore properties of PANI-CMPs constructed from different building blocks. These properties will then be compared to see the properties that are common among different PANI-CMPs and the properties that depend on the different monomer unit structures.

To achieve the aim, several objectives have been identified as listed below:

Theoretical Studies

- Optimise structures of PANI-CMP oligomeric models with different monomer units and in different oxidation, doping, and spin states using DFT calculations. Geometric and electronic structures of resulting optimised PANI-CMP models are analysed, and the results are compared across different monomer units and different oxidation, doping, and spin states.
- Calculate electronic excitations of PANI-CMP oligomeric models with different monomer units and in different oxidation, doping, and spin states using time-dependent DFT calculations. Resulting oxidation states and corresponding absorption spectra are analysed and compared to data obtained from experimental studies.
- Optimise structures of the complex between PANI-CMP oligomeric models and CO_2 using DFT calculations. Geometric structures and binding energies obtained are analysed and discussed.

Experimental Studies

- Synthesise different PANI-CMPs from different A_3 core and B_2 linker monomers using Buchwald-Hartwig (BH) coupling reactions with Bristol-Xi'an Jiaotong (BXJ) method of solubility tuning (referred to as BH.BXJ). Different initial conditions, namely functionalities of monomers, stoichiometric ratios of monomers, and the addition of sodium bromide are varied.

- Analyse spectroscopic properties, namely optical and vibrational spectroscopies, of resulting PANI-CMP materials.
- Analyse for surface areas, other porosity properties, and CO_2 adsorption properties of PANI-CMP materials.

The work towards the realisations of these objectives will be discussed in the following chapters:

In Chapter 2, methodological details are given along with rationales behind for both theoretical and experimental studies. For theoretical studies, conditions for setting up both DFT optimisations and TD-DFT calculations together with details regarding data visualisations are listed along with names of software packages and computational facilities involved. For experimental studies, conditions for BH coupling reactions towards PANI-CMPs are given along with syntheses of some core monomers and further analyses for resulting materials.

In Chapter 3, structures of PANI-CMP oligomeric models are discussed. Various structure descriptors, for both geometric and electronic structures, both used in the previous studies of poly- and oligo(aniline)s and newly created for this project are listed. This chapter discuss the effects from various structural independent factors, namely oligomer topologies (branching and cyclisation), monomer units, and chemical structures (oxidation, doping, and spin states), on geometric and electronic structures of the resulting models. Discussions related to optoelectronic spectra, as results from electronic structures, including the comparisons with experimental data can also be found in this chapter.

In Chapter 4, the syntheses and properties of resulting PANI-CMP materials are discussed. Different attempts for the syntheses and property tunings prior to the publication of the BXJ method of solubility tunings are listed, and properties of resulting materials are compared. Later BH.BXJ attempts are discussed separately and more systematically. Properties of materials to be discussed are spectroscopic, morphological, and porosity properties, with larger emphasis on porosity properties including surface areas, pore size distributions, and uptakes of CO_2.

In Chapter 5, non-covalent interactions (NCIs) between PANI-CMP fragments and CO_2 molecules are theoretically discussed. Effects of binding positions and monomer units on binding energies of CO_2 onto material fragments are compared, and the possibility of using larger models for NCIs between the fragment and a CO_2 molecule is explored.

Finally, in Chapter 6 the findings and conclusions drawn across the previous chapters are discussed. Possible future studies for further understanding of structure-property relationships based on what is missing from the current set of data are also proposed.

1.5 References

1. Y. Liao, J. Weber and C. F. J. Faul, *Chem. Commun.*, 2014, **50**, 8002-8005.
2. Y. Liao, J. Weber, B. M. Mills, Z. Ren and C. F. J. Faul, *Macromolecules*, 2016, **49**, 6322-6333.
3. Z. X. Wei and C. F. J. Faul, *Macromol. Rapid Commun.*, 2008, **29**, 280-292.
4. A. G. MacDiarmid, *Angew. Chem. Int. Ed.*, 2001, **40**, 2581-2590.
5. J. Jiang, F. Su, A. Trewin, C. D. Wood, N. L. Campbell, H. Niu, C. Dickinson, A. Y. Ganin, M. J. Rosseinsky, Y. Z. Khimyak and A. I. Cooper, *Angew. Chem. Int. Ed.*, 2007, **46**, 8574-8578.
6. R. Dawson, A. Laybourn, Y. Z. Khimyak, D. J. Adams and A. I. Cooper, *Macromolecules*, 2010, **43**, 8524-8530.
7. L. Zou, Y. Sun, S. Che, X. Yang, X. Wang, M. Bosch, Q. Wang, H. Li, M. Smith, S. Yuan, Z. Perry and H. C. Zhou, *Adv. Mater.*, 2017, **29**.
8. D. Ramimoghadam, E. M. Gray and C. J. Webb, *Int. J. Hydrogen Energy*, 2016, **41**, 16944-16965.

9. D. S. Ahmed, G. A. El-Hiti, E. Yousif, A. A. Ali and A. S. Hameed, *J. Polym. Res.*, 2018, **25**.
10. Y. B. Sun, L. Wang, W. A. Amer, H. J. Yu, J. Ji, L. Huang, J. Shan and R. B. Tong, *J. Inorg. Organomet. Polym. Mater.*, 2013, **23**, 270-285.
11. A. Alonso, J. Moral-Vico, A. Abo Markeb, M. Busquets-Fite, D. Komilis, V. Puntes, A. Sanchez and X. Font, *Sci. Total Environ.*, 2017, **595**, 51-62.
12. N. Huang, G. Day, X. Y. Yang, H. Drake and H. C. Zhou, *Sci. China: Chem.*, 2017, **60**, 1007-1014.
13. C. C. Wang, J. R. Li, X. L. Lv, Y. Q. Zhang and G. S. Guo, *Energy Environ. Sci.*, 2014, **7**, 2831-2867.
14. S. Bhattacharjee, Y. R. Lee, P. Puthiaraj, S. M. Cho and W. S. Ahn, *Catal. Surv. Asia*, 2015, **19**, 203-222.
15. K. Muller-Buschbaum, F. Beuerle and C. Feldmann, *Microporous Mesoporous Mater.*, 2015, **216**, 171-199.
16. D. Y. Chen, C. Liu, J. T. Tang, L. F. Luo and G. P. Yu, *Polym. Chem.*, 2019, **10**, 1168-1181.
17. L. Wang, Y. Z. Han, X. Feng, J. W. Zhou, P. F. Qi and B. Wang, *Coord. Chem. Rev.*, 2016, **307**, 361-381.
18. H. Bildirir, V. G. Gregoriou, A. Avgeropoulos, U. Scherfd and C. L. Chochos, *Mater. Horiz.*, 2017, **4**, 546-556.
19. K. S. W. Sing, D. H. Everett, R. A. W. Haul, L. Moscou, R. A. Pierotti, J. Rouquerol and T. Siemieniewska, *Pure Appl. Chem.*, 1985, **57**, 603-619.
20. M. Thommes, K. Kaneko, A. V. Neimark, J. P. Olivier, F. Rodriguez-Reinoso, J. Rouquerol and K. S. W. Sing, *Pure Appl. Chem.*, 2015, **87**, 1051-1069.
21. A. Galarneau, F. Villemot, J. Rodriguez, F. Fajula and B. Coasne, *Langmuir*, 2014, **30**, 13266-13274.
22. S. Builes and L. F. Vega, *J. Phys. Chem. C*, 2012, **116**, 3017-3024.
23. J.-J. Xu, D. Xu, Z.-L. Wang, H.-G. Wang, L.-L. Zhang and X.-B. Zhang, *Angew. Chem. Int. Ed.*, 2013, **52**, 3887-3890.
24. W. Qin, Z. Yuan, Y. Shen, R. Zhang and F. Meng, *Chem. Eng. J.*, 2022, **431**, 134280.
25. R. M. Guo, J. Q. Bai, H. Zhang, Y. B. Xie and J. R. Li, *Prog. Chem.*, 2016, **28**, 232-243.
26. Y. Liao, Z. Cheng, W. Zuo, A. Thomas and C. F. J. Faul, *ACS Appl. Mater. Interfaces*, 2017, **9**, 38390-38400.
27. M. Wang, X. Fan, L. Zhang, J. Liu, B. Wang, R. Cheng, M. Li, J. Tian and J. Shi, *Nanoscale*, 2017, **9**, 17593-17600.
28. A. Trewin and A. I. Cooper, *Angew. Chem. Int. Ed.*, 2010, **49**, 1533-1535.
29. A. P. Côté, A. I. Benin, N. W. Ockwig, M. O'Keeffe, A. J. Matzger and O. M. Yaghi, *Science*, 2005, **310**, 1166-1170.
30. J. Germain, J. M. J. Fréchet and F. Svec, *J. Mater. Chem.*, 2007, **17**, 4989-4997.
31. A. Laybourn, R. Dawson, R. Clowes, T. Hasell, A. I. Cooper, Y. Z. Khimyak and D. J. Adams, *Polym. Chem.*, 2014, **5**, 6325-6333.
32. M. Carta, K. J. Msayib and N. B. McKeown, *Tetrahedron Lett.*, 2009, **50**, 5954-5957.
33. T. Tozawa, J. T. A. Jones, S. I. Swamy, S. Jiang, D. J. Adams, S. Shakespeare, R. Clowes, D. Bradshaw, T. Hasell, S. Y. Chong, C. Tang, S. Thompson, J. Parker, A. Trewin, J. Bacsa, A. M. Z. Slawin, A. Steiner and A. I. Cooper, *Nat. Mater.*, 2009, **8**, 973-978.
34. R. Dawson, A. I. Cooper and D. J. Adams, *Prog. Polym. Sci.*, 2012, **37**, 530-563.
35. K. Geng, T. He, R. Liu, S. Dalapati, K. T. Tan, Z. Li, S. Tao, Y. Gong, Q. Jiang and D. Jiang, *Chem. Rev.*, 2020, **120**, 8814-8933.
36. A. I. Cooper, *Adv. Mater.*, 2009, **21**, 1291-1295.
37. P. M. Budd, B. S. Ghanem, S. Makhseed, N. B. McKeown, K. J. Msayib and C. E. Tattershall, *Chem. Commun.*, 2004, 230-231.
38. A. Thomas, *Nat. Commun.*, 2020, **11**, 4985.
39. T. Hasell and A. I. Cooper, *Nat. Rev. Mater.*, 2016, **1**, 16053.
40. H. Wang, D. N. Jiang, D. L. Huang, G. M. Zeng, P. Xu, C. Lai, M. Chen, M. Cheng, C. Zhang and Z. W. Wang, *J. Mater. Chem. A*, 2019, **7**, 22848-22870.
41. R.-B. Lin, Y. He, P. Li, H. Wang, W. Zhou and B. Chen, *Chem. Soc. Rev.*, 2019, **48**, 1362-1389.

42. A. D. Jenkins, P. Kratochvíl, R. F. T. Stepto and U. W. Suter, *Pure Appl. Chem.*, 1996, **68**, 2287-2311.
43. R. G. Jones, E. S. Wilks, W. Val Metanomski, J. Kahovec, M. Hess, R. Stepto and T. Kitayama, *Compendium of Polymer Terminology and Nomenclature: IUPAC Recommendations 2008*, Royal Society of Chemistry, Cambridge, 2009.
44. J. Chen, W. Yan, E. J. Townsend, J. Feng, L. Pan, V. Del Angel Hernandez and C. F. J. Faul, *Angew. Chem. Int. Ed.*, 2019, **58**, 11715-11719.
45. J. Chen, T. Qiu, W. Yan and C. F. J. Faul, *J. Mater. Chem. A*, 2020, **8**, 22657-22665.
46. E. M. Geniès, A. Boyle, M. Lapkowski and C. Tsintavis, *Synth. Met.*, 1990, **36**, 139-182.
47. F. F. Runge, *Ann. Phys. Chem.*, 1834, **107**, 513-524.
48. H. Letheby, *J. Chem. Soc.*, 1862, **15**, 161-163.
49. A. G. Green and A. E. Woodhead, *J. Chem. Soc. Trans.*, 1910, **97**, 2388-2403.
50. A. G. Green and A. E. Woodhead, *J. Chem. Soc. Trans.*, 1912, **101**, 1117-1123.
51. J. G. Masters, Y. Sun, A. G. MacDiarmid and A. J. Epstein, *Synth. Met.*, 1991, **41**, 715-718.
52. H. Shirakawa, E. J. Louis, A. G. MacDiarmid, C. K. Chiang and A. J. Heeger, *J. Chem. Soc. Chem. Commun.*, 1977, 578-580.
53. B. Nordén and E. Krutmeijer, The Nobel Prize in Chemistry, 2000: Conductive polymers, https://www.nobelprize.org/uploads/2018/06/advanced-chemistryprize2000.pdf, (accessed 25 June, 2021).
54. A. J. Heeger, *J. Phys. Chem. B*, 2001, **105**, 8475-8491.
55. J. C. Chiang and A. G. MacDiarmid, *Synth. Met.*, 1986, **13**, 193-205.
56. S. Stafstrom, J. L. Bredas, A. J. Epstein, H. S. Woo, D. B. Tanner, W. S. Huang and A. G. MacDiarmid, *Phys. Rev. Lett.*, 1987, **59**, 1464-1467.
57. Z. C. Sun, X. B. Jing, X. H. Wang, J. Li and F. S. Wang, *Synth. Met.*, 2001, **119**, 313-314.
58. Y. H. Geng, X. B. Jing, J. Li and F. S. Wang, *Macromol. Rapid Commun.*, 1997, **18**, 73-81.
59. A. Varela-Alvarez, J. A. Sordo and G. E. Scuseria, *J. Am. Chem. Soc.*, 2005, **127**, 11318-11327.
60. Y. H. Zhang, Q. Xi, J. L. Chen and Y. P. Duan, *J. Clust. Sci.*, 2014, **25**, 1501-1510.
61. M. Canales, J. Torras, G. Fabregat, A. Meneguzzi and C. Aleman, *J. Phys. Chem. B*, 2014, **118**, 11552-11562.
62. B. M. Mills, Z. Shao, S. R. Flynn, P. Rannou, D. M. Lindsay, N. Fey and C. F. J. Faul, *Mol. Syst. Des. Eng.*, 2019, **4**, 103-109.
63. J. P. Sadighi, R. A. Singer and S. L. Buchwald, *J. Am. Chem. Soc.*, 1998, **120**, 4960-4976.
64. R. A. Singer, J. P. Sadighi and S. L. Buchwald, *J. Am. Chem. Soc.*, 1998, **120**, 213-214.
65. B. M. Mills, N. Fey, T. Marszalek, W. Pisula, P. Rannou and C. F. J. Faul, *Chem. - Eur. J.*, 2016, **22**, 16950-16956.
66. Z. Shao, P. Rannou, S. Sadki, N. Fey, D. M. Lindsay and C. F. J. Faul, *Chem. - Eur. J.*, 2011, **17**, 12512-12521.
67. L. Pan, Z. Liu, M. Tian, B. C. Schroeder, A. E. Aliev and C. F. J. Faul, *ACS Appl. Mater. Interfaces*, 2019, **11**, 48352-48362.
68. C. M. Hansen, Doctoral, The Technical University of Denmark, 1967.
69. D. Rabelo and F. M. B. Coutinho, *Polym. Bull.*, 1994, **33**, 479-486.
70. C. M. Hansen, The Famous Factor of 4 - Dr Hansen's View, https://www.hansen-solubility.com/HSP-science/4factor.php, (accessed 2 March, 2022).
71. K. K. Diehn, H. Oh, R. Hashemipour, R. G. Weiss and S. R. Raghavan, *Soft Matter*, 2014, **10**, 2632-2640.
72. S. Brunauer, P. H. Emmett and E. Teller, *J. Am. Chem. Soc.*, 1938, **60**, 309-319.
73. J. H. Zhu, Q. Chen, Z. Y. Sui, L. Pan, J. G. Yu and B. H. Han, *J. Mater. Chem. A*, 2014, **2**, 16181-16189.
74. C. J. Sun, X. Q. Zhao, P. F. Wang, H. Wang and B. H. Han, *Sci. China: Chem.*, 2017, **60**, 1067-1074.
75. L. S. Shao, M. Q. Liu, Y. F. Sang and J. H. Huang, *Microporous Mesoporous Mater.*, 2019, **285**, 105-111.
76. K. X. Shi, H. Y. Yao, Y. C. Zou, Y. F. Wei, N. N. Song, S. Zhang, Y. Tian, S. Y. Zhu, B. Zhang and S. W. Guan, *Microporous Mesoporous Mater.*, 2019, **287**, 246-253.

77. E. P. Barrett, L. G. Joyner and P. P. Halenda, *J. Am. Chem. Soc.*, 1951, **73**, 373-380.
78. J. Landers, G. Y. Gor and A. V. Neimark, *Colloids Surf., A*, 2013, **437**, 3-32.
79. N. A. Seaton, J. P. R. B. Walton and N. Quirke, *Carbon*, 1989, **27**, 853-861.
80. C. Lastoskie, K. E. Gubbins and N. Quirke, *J. Phys. Chem.*, 1993, **97**, 4786-4796.
81. J. P. Olivier, W. B. Conklin and M. v. Szombathely, in *Studies in Surface Science and Catalysis*, eds. J. Rouquerol, F. Rodríguez-Reinoso, K. S. W. Sing and K. K. Unger, Elsevier, 1994, vol. 87, pp. 81-89.
82. P. I. Ravikovitch, S. C. O. Domhnaill, A. V. Neimark, F. Schueth and K. K. Unger, *Langmuir*, 1995, **11**, 4765-4772.
83. B. C. Lippens and J. H. de Boer, *J. Catal.*, 1965, **4**, 319-323.
84. J. H. de Boer, B. C. Lippens, B. G. Linsen, J. C. P. Broekhoff, A. van den Heuvel and T. J. Osinga, *J. Colloid Interface Sci.*, 1966, **21**, 405-414.
85. A. Nuhnen and C. Janiak, *Dalton Trans.*, 2020, **49**, 10295-10307.
86. C. J. Cramer, *Essentials of Computational Chemistry: Theories and Models*, John Wiley & Sons Ltd., United Kingdom, 2 edn., 2004.
87. F. Jensen, *Introduction to Computational Chemistry*, John Wiley & Sons, Ltd, United Kingdom, 3 edn., 2017.
88. Q. Peng, F. Duarte and R. S. Paton, *Chem. Soc. Rev.*, 2016, **45**, 6093-6107.
89. J. P. Perdew and K. Schmidt, *AIP Conf. Proc.*, 2001, **577**, 1-20.
90. S. F. Sousa, P. A. Fernandes and M. J. Ramos, *J. Phys. Chem. A*, 2007, **111**, 10439-10452.
91. J. P. Perdew, A. Ruzsinszky, L. A. Constantin, J. Sun and G. I. Csonka, *J. Chem. Theory Comput.*, 2009, **5**, 902-908.
92. M. E. Casida, *J. Mol. Struct.: THEOCHEM*, 2009, **914**, 3-18.
93. W. Kohn and L. J. Sham, *Phys. Rev.*, 1965, **140**, 1133-1138.
94. P. Hohenberg and W. Kohn, *Phys. Rev. B: Condens. Matter Mater. Phys.*, 1964, **136**, B864.
95. A. D. Becke, *J. Chem. Phys.*, 1993, **98**, 5648-5652.
96. C. Lee, W. Yang and R. G. Parr, *Phys. Rev. B: Condens. Matter Mater. Phys.*, 1988, **37**, 785-789.
97. B. Miehlich, A. Savin, H. Stoll and H. Preuss, *Chem. Phys. Lett.*, 1989, **157**, 200-206.
98. T. Korzdorfer and J. L. Bredas, *Acc. Chem. Res.*, 2014, **47**, 3284-3291.
99. S. S. Zade, N. Zamoshchik and M. Bendikov, *Acc. Chem. Res.*, 2011, **44**, 14-24.
100. S. S. Zade and M. Bendikov, *Org. Lett.*, 2006, **8**, 5243-5246.
101. J. T. Margraf and K. Reuter, *Nat. Commun.*, 2021, **12**, 344.
102. S. Grimme, J. Antony, T. Schwabe and C. Muck-Lichtenfeld, *Org. Biomol. Chem.*, 2007, **5**, 741-758.
103. E. R. Johnson, I. D. Mackie and G. A. DiLabio, *J. Phys. Org. Chem.*, 2009, **22**, 1127-1135.
104. P. Hobza, *Acc. Chem. Res.*, 2012, **45**, 663-672.
105. S. Grimme, A. Hansen, J. G. Brandenburg and C. Bannwarth, *Chem. Rev.*, 2016, **116**, 5105-5154.
106. J. Tomasi, R. Cammi, B. Mennucci, C. Cappelli and S. Corni, *Phys. Chem. Chem. Phys.*, 2002, **4**, 5697-5712.
107. C. Adamo and D. Jacquemin, *Chem. Soc. Rev.*, 2013, **42**, 845-856.
108. M. E. Casida and M. Huix-Rotllant, *Ann. Rev. Phys. Chem.*, 2012, **63**, 287-323.
109. A. D. Laurent, C. Adamo and D. Jacquemin, *Phys. Chem. Chem. Phys.*, 2014, **16**, 14334-14356.
110. E. Runge and E. K. U. Gross, *Phys. Rev. Lett.*, 1984, **52**, 997-1000.
111. J. Plötner, D. J. Tozer and A. Dreuw, *J. Chem. Theory Comput.*, 2010, **6**, 2315-2324.
112. M. Campetella, F. Maschietto, M. J. Frisch, G. Scalmani, I. Ciofini and C. Adamo, *J. Comput. Chem.*, 2017, **38**, 2151-2156.
113. S. E. Braslavsky, *Pure Appl. Chem.*, 2007, **79**, 293-465.
114. J. N. Petrova, J. R. Romanova, G. K. Madjarova, A. N. Ivanova and A. V. Tadjer, *J. Phys. Chem. B*, 2011, **115**, 3765-3776.
115. J. Romanova, J. Petrova, A. Ivanova, A. Tadjer and N. Gospodinova, *J. Mol. Struct.: THEOCHEM*, 2010, **954**, 36-44.
116. J. Romanova, J. Petrova, A. Tadjer and N. Gospodinova, *Synth. Met.*, 2010, **160**, 1050-1054.

117. A. Varela-Alvarez and J. A. Sordo, *J. Chem. Phys.*, 2008, **128**, 174706.
118. C. Alemán, C. A. Ferreira, J. Torras, A. Meneguzzi, M. Canales, M. A. S. Rodrigues and J. Casanovas, *Polymer*, 2008, **49**, 5169-5176.
119. J. Romanova, G. Madjarova, A. Tadjer and N. Gospodinova, *Int. J. Quantum. Chem.*, 2011, **111**, 435-443.
120. G. Gatti, D. Costenaro, C. Vittoni, G. Paul, V. Crocella, E. Mangano, S. Brandani, S. Bordiga, M. Cossi, L. Marchese and C. Bisio, *Phys. Chem. Chem. Phys.*, 2017, **19**, 14114-14128.
121. L. J. Abbott and C. M. Colina, *Macromolecules*, 2011, **44**, 4511-4519.
122. L. J. Abbott, N. B. McKeown and C. M. Colina, *J. Mater. Chem. A*, 2013, **1**, 11950-11960.
123. J. M. H. Thomas and A. Trewin, *J. Phys. Chem. C*, 2014, **118**, 19712-19722.
124. P. Fayon and A. Trewin, *Phys. Chem. Chem. Phys.*, 2016, **18**, 16840-16847.
125. F. Jiang, T. Jin, X. Zhu, Z. Q. Tian, C. L. Do-Thanh, J. Hu, D. E. Jiang, H. L. Wang, H. L. Liu and S. Dai, *Macromolecules*, 2016, **49**, 5325-5330.
126. S. Aparicio, C. T. Yavuz and M. Atilhan, *ChemistrySelect*, 2018, **3**, 8294-8305.
127. D. Dey and P. Banerjee, *New J. Chem.*, 2019, **43**, 3769-3777.
128. Y. Wang, X. Hu, J. Hao, R. Ma, Q. Guo, H. Gao and H. Bai, *Ind. Eng. Chem. Res.*, 2019, **58**, 13390-13400.
129. Z. Yang, S. Wang, Z. Zhang, W. Guo, K. Jie, M. I. Hashim, O. Š. Miljanić, D. e. Jiang, I. Popovs and S. Dai, *J. Mater. Chem. A*, 2019, **7**, 17277-17282.
130. C. Lin, Z. Cheng, B. Li, T. Chen, W. Zhang, S. Chen, Q. Yang, L. Chang, G. Che and H. Ma, *ACS Appl. Mater. Interfaces*, 2019, **11**, 40970-40979.

Chapter 2 Methodology

2.1 Monomers Chosen for Studies of PANI-CMPs

In this work, poly(aniline)-based conjugated microporous polymers (PANI-CMPs) have been synthesised by the Buchwald-Hartwig coupling reaction. This coupling reaction allows structures of PANI-CMPs to be tuned by using other aromatic or conjugated systems. This work focuses on A_3 + B_2 polymerisations, following earlier publications on PANI-CMPs in which trifunctional A_3 core monomers are coupled with bifunctional B_2 linker monomers.[1, 2] In contrast to typical poly(aniline) syntheses, the purpose of A_3 + B_2 Buchwald-Hartwig coupling approaches is to introduce branched network. Although poly(aniline)s prepared from oxidation reactions of aniline are also known to possess branched structures,[3, 4] these branched moieties are formed through competing reactions. As proposed by Ćirić-Marjanović, branch formations in acidic oxidative polymerisation of aniline occur via Michael additions of aniline or aniline end groups to the 1,4-benzoquinonediimine moieties.[4] These side reactions usually end up producing phenazines as oligomeric products, see Scheme 2-1. As a result, while the formation of branched moieties in poly(aniline) chains is theoretically possible, branched structures in poly(aniline)s prepared from oxidation of anilines are less frequent. Meanwhile, the A_3 + B_2 polymerisation reactions allow greater extents of branching, which then can create interpenetrating network of polymers. Buchwald-Hartwig coupling reactions also facilitate controlled syntheses of oligo(aniline)s and poly(aniline)s,[5, 6] which means easier controls of product chemical structures. As a result, conjugated microporous polymers can be formed in a controlled manner, which can then be used for other applications including adsorption of CO_2 gas, iodine vapour, and water contaminants.[1, 2, 7, 8]

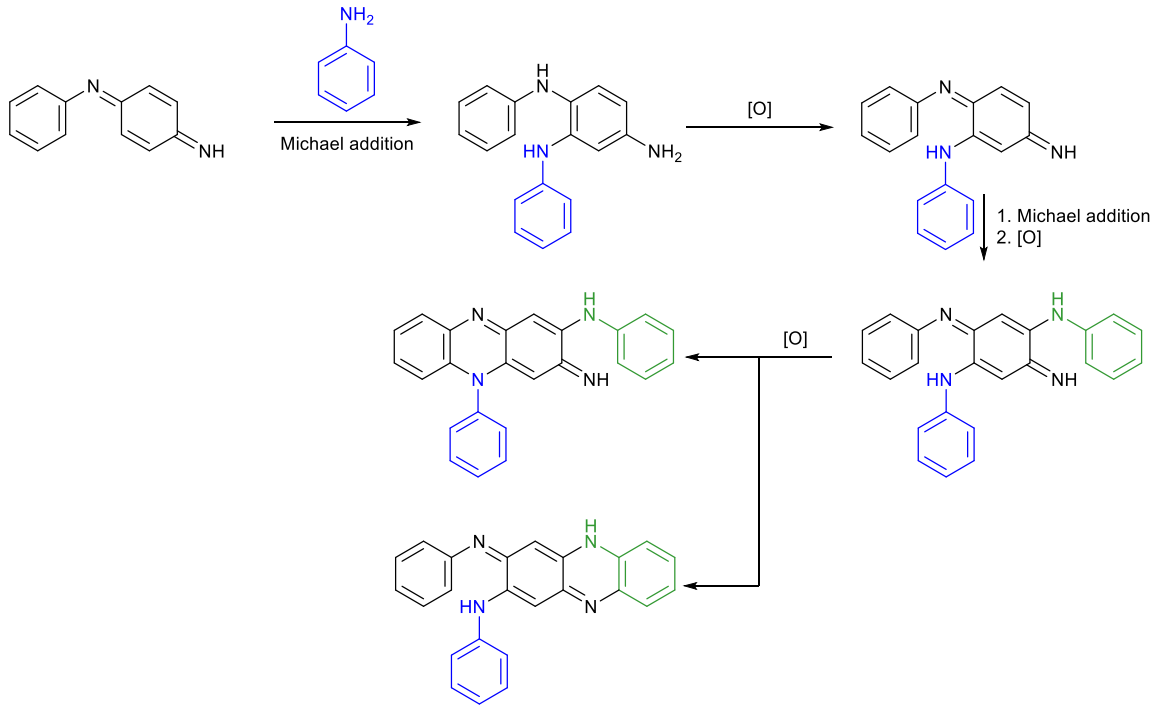

Scheme 2-1 Formation of phenazine moieties from the oxidative polymerisation of aniline formed via Michael addition of aniline end group as proposed by Ćirić-Marjanović[4]

Five conjugated systems have been chosen, three core units with connectivity of three (A_3) and two linker units with connectivity of two (B_2). Structures of these conjugated core and linker

units are shown in Scheme 2-2. The first core unit, tris(1,4-phenylene)amine or **TPA**, and the first linker unit, 1,4-phenylene or **BZN**, are based on 1,4-phenylene units, which are the majority of aromatic units in poly(aniline)s. These two monomeric units have been used for the earlier published syntheses of PANI-CMPs.[1, 2] To study structure-property relationships for further modification of PANI-CMPs, two additional core units, 1,3,5-tris(1,4-phenylene)benzene (**TPB**) and 2,4,6-tris(1,4-phenylene)-1,3,5-triazine (**TPT**) along with one additional linker unit, 2,7-fluorenylene (**FLR**), have been selected. Several published studies suggest relationships between structural factors of monomers, such as sizes and rigidities, and porosity of resulting materials,[1, 7, 9-14] which will be discussed in detail in Section 4.1. Besides, triazine and fluorene moieties have been used in many functional porous materials for important applications including gas adsorption and fluorescent sensing.[15-27] Moieties with high nitrogen contents such as triazines have also been found to correlate with high CO_2 adsorptions and good selectivity towards CO_2.[17, 25, 28-30] Therefore, these structural modifications could lead to new materials with interesting properties and eventually applications.

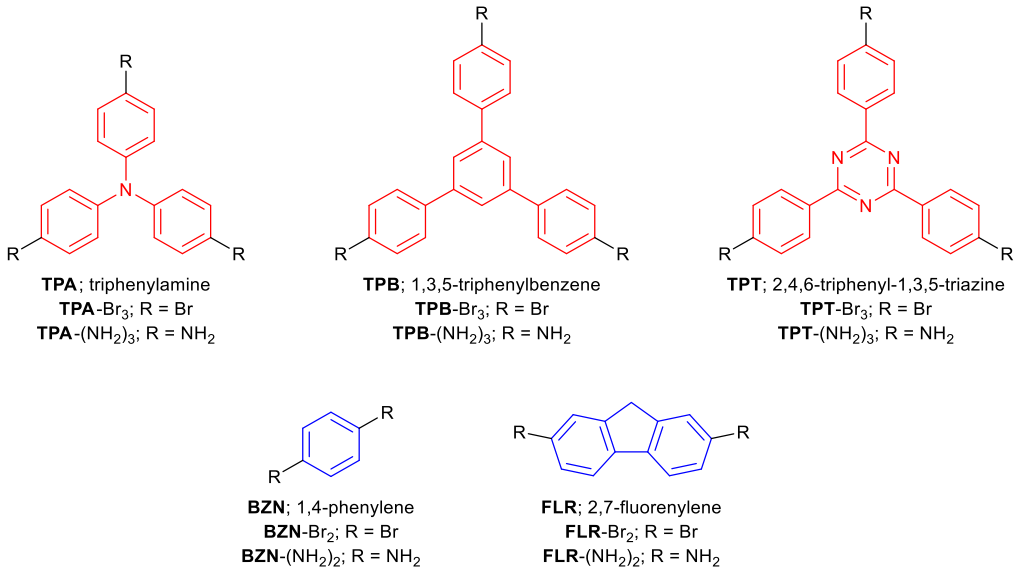

Scheme 2-2 Structures of core (top row) and linker (bottom row) monomers being used for the syntheses of PANI-CMPs in this study

2.2 Chemical Syntheses

2.2.1 Syntheses of PANI-CMPs by BH.BXJ Methods

General syntheses of PANI-CMPs follow the BH.BXJ methods published earlier, with Buchwald-Hartwig (BH) coupling reactions[1, 2, 7, 8] and Bristol-Xi'an Jiaotong (BXJ) solubility tuning methods.[2] A typical reaction at the stoichiometric ratio between bromo and amino groups is described here: a dry Schlenk flask was charged with monomers equivalent to 1.0 mmol of respective amino or bromo functional groups, bis(dibenzylidineacetone)palladium(0) ($Pd(dba)_2$, 0.030 mmol, 17.3 mg), 2-dicyclohexylphosphino-2',4',6'-triisopropylbiphenyl (XPhos, 0.045 mmol, 21.5 mg), sodium *tert*-butoxide (NaO^tBu, 3.5 mmol, 336.4 mg), and sodium bromide (0.50 mmol, 51.4 mg), and then placed under flowing nitrogen atmosphere. 1,4-dioxane (30 mL) was added, and the mixture was stirred and heated to 65 °C for 48 hours. Once cooled, solid products were collected via filtration, washed by Soxhlet extraction with chloroform, THF, and methanol (250 mL, 24 hours for each solvent), and dried under vacuum. Meanwhile, the remaining filtrates were evaporated, redissolved in THF until saturated, and then precipitated in methanol (1:4 by volume saturated THF solution:methanol). Precipitates were then collected by centrifugation.

Solid products obtained after filtration are referred to as "polymers", while solid products obtained after precipitation and subsequent centrifugation are referred to as "oligomers".

Two different pathways of polymerisations have been studied, depending on the functional group connected to each monomer. Polymerisations between brominated A_3 cores and aminated B_2 linkers are referred as "normal" (**N**) since this is the same approach as in earlier publications on PANI-CMPs.[1, 2, 7] Meanwhile, polymerisations between aminated A_3 cores and brominated B_2 linkers are referred to as "reversed" (**R**). Monomers equivalent to 1.0 mmol of functional groups mentioned in the previous paragraph refer to 0.33 mmol of brominated A_3 core and 0.50 mmol of aminated B_2 linker for the normal pathway **N** and refer to 0.33 mmol of aminated A_3 core and 0.50 mmol of aminated B_2 linker for the reversed pathway **R**. Masses of monomers for syntheses of PANI-CMPs with different monomer units and through different pathways are listed in Table 2-1.

Other ratios between amino and bromo groups have also been attempted, with masses of monomers for the amino-excess and bromo-excess ratios being listed in Table 2-2 and Table 2-3, respectively. For the excess ratios, the amounts of the excess functional groups were increased to 1.5 mmol, while the amounts of the limited functional groups were decreased to 0.66 mmol.

*Table 2-1 Masses of monomers for syntheses of PANI-CMPs with different monomer units with stoichiometric ratios (**S**) between amino and bromo groups through different pathways*

Core (A_3) Monomers				
Unit	**Brominated A_3 Monomer (Normal Pathway)**		**Aminated A_3 Monomer (Reversed Pathway)**	
	Monomer	**Mass (g)**	**Monomer**	**Mass (g)**
TPA	Tris(4-bromophenyl)amine (**TPA**-Br_3)	160.7	Tris(4-aminophenyl)amine (**TPA**-$(NH_2)_3$)	96.8
TPB	1,3,5-tris(4-bromophenyl)benzene (**TPB**-Br_3)	181.0	1,3,5-tris(4-aminophenyl)benzene (**TPB**-$(NH_2)_3$)	117.2
TPT	2,4,6-tris(4-bromophenyl)-1,3,5-triazine (**TPT**-Br_3)	182.0	2,4,6-tris(4-aminophenyl)-1,3,5-triazine (**TPT**-$(NH_2)_3$)	118.1
Linker (B_2) Monomers				
Unit	**Aminated B_2 Monomer (Normal Pathway)**		**Brominated B_2 Monomer (Reversed Pathway)**	
	Monomer	**Mass (g)**	**Monomer**	**Mass (g)**
BZN	1,4-phenylenediamine (**BZN**-$(NH_2)_2$)	54.1	1,4-dibromobenzene (**BZN**-Br_2)	118.0
FLR	2,7-diaminofluorene (**FLR**-$(NH_2)_2$)	98.1	2,7-dibromofluorene (**FLR**-Br_2)	162.0

*Table 2-2 Masses of monomers for syntheses of PANI-CMPs with different monomer units with amino-excess ratios (**A**) between amino and bromo groups through different pathways*

Core (A_3) Monomers				
Unit	**Brominated A_3 Monomer (Normal Pathway)**		**Aminated A_3 Monomer (Reversed Pathway)**	
	Monomer	**Mass (g)**	**Monomer**	**Mass (g)**
TPA	Tris(4-bromophenyl)amine (**TPA**-Br_3)	106.0	Tris(4-aminophenyl)amine (**TPA**-$(NH_2)_3$)	145.2
TPB	1,3,5-tris(4-bromophenyl)benzene (**TPB**-Br_3)	119.4	1,3,5-tris(4-aminophenyl)benzene (**TPB**-$(NH_2)_3$)	175.8
TPT	2,4,6-tris(4-bromophenyl)-1,3,5-triazine (**TPT**-Br_3)	120.1	2,4,6-tris(4-aminophenyl)-1,3,5-triazine (**TPT**-$(NH_2)_3$)	177.1
Linker (B_2) Monomers				
Unit	**Aminated B_2 Monomer (Normal Pathway)**		**Brominated B_2 Monomer (Reversed Pathway)**	
	Monomer	**Mass (g)**	**Monomer**	**Mass (g)**
BZN	1,4-phenylenediamine (**BZN**-$(NH_2)_2$)	81.1	1,4-dibromobenzene (**BZN**-Br_2)	77.9
FLR	2,7-diaminofluorene (**FLR**-$(NH_2)_2$)	147.2	2,7-dibromofluorene (**FLR**-Br_2)	106.9

*Table 2-3 Masses of monomers for syntheses of PANI-CMPs with different monomer units with bromo-excess ratios (**B**) between amino and bromo groups through different pathways*

Core (A_3) Monomers				
Unit	**Brominated A_3 Monomer (Normal Pathway)**		**Aminated A_3 Monomer (Reversed Pathway)**	
	Monomer	**Mass (g)**	**Monomer**	**Mass (g)**
TPA	Tris(4-bromophenyl)amine (**TPA**-Br_3)	241.0	Tris(4-aminophenyl)amine (**TPA**-$(NH_2)_3$)	63.9
TPB	1,3,5-tris(4-bromophenyl)benzene (**TPB**-Br_3)	271.5	1,3,5-tris(4-aminophenyl)benzene (**TPB**-$(NH_2)_3$)	77.4
TPT	2,4,6-tris(4-bromophenyl)-1,3,5-triazine (**TPT**-Br_3)	273.0	2,4,6-tris(4-aminophenyl)-1,3,5-triazine (**TPT**-$(NH_2)_3$)	77.9
Linker (B_2) Monomers				
Unit	**Aminated B_2 Monomer (Normal Pathway)**		**Brominated B_2 Monomer (Reversed Pathway)**	
	Monomer	**Mass (g)**	**Monomer**	**Mass (g)**
BZN	1,4-phenylenediamine (**BZN**-$(NH_2)_2$)	35.7	1,4-dibromobenzene (**BZN**-Br_2)	177.0
FLR	2,7-diaminofluorene (**FLR**-$(NH_2)_2$)	64.7	2,7-dibromofluorene (**FLR**-Br_2)	243.0

Products are named in the format **XCOR-LKR-YZ(x)**.

X refers to product types (polymers **P** or oligomers **O**).

COR refers to the core unit (**TPA**, **TPB**, or **TPT**).

LKR refers to the linker unit (**BZN** or **FLR**).

Y refers to the ratio between bromo and amino groups (amino-excess **A**, bromo-excess **B**, or stoichiometric **S**).

Z refers to the synthetic pathway (normal **N** or reversed **R**).

x refers to the addition of sodium bromide (omitted if added, included if not added).

For example, **PTPA-FLR-SNx** refers to a polymer (**P**) product of **TPA** core unit and **FLR** linker unit prepared from the stoichiometric (**S**) ratio between amino and bromo groups and the normal (**N**) functionality pathway, i.e., from **TPA**-Br_3 and **FLR**-$(NH_2)_2$ monomers, without (**x**) additional sodium bromide.

2.2.2 Syntheses of 2,4,6-Triphenyl-1,3,5-triazine Core Monomers (**TPT**-Br_3 and **TPT**-$(NH_2)_3$)

The synthesis of **TPT**-Br_3 was adapted from a published procedure.[31] A 100-mL round bottom flask was charged with trifluoromethanesulfonic acid (9.99 g, 5.89 mL, 66.6 mmol) and placed in an ice bath at 0 °C. 4-Bromobenzonitrile (3.57 g, 19.6 mmol) was then added slowly under stirring, and the mixture was stirred while maintaining temperature in an ice bath. After 30 minutes the reaction mixture was allowed to warm to ambient temperature. The reaction was left running for 24 hours. After 24 hours, water (50 mL) was added to the reaction mixture, followed by sodium hydroxide solution (2 M) until the solution became neutral. Some product precipitated out and was collected by filtration. The rest of product was collected from extraction by 1:1 chloroform/acetone.

The synthesis of **TPT**-$(NH_2)_3$ was adapted from a published procedure.[32] A 100-mL two-necked round bottom flask was charged with 4-aminobenzonitrile (772 mg, 6.53 mmol), placed under flowing nitrogen atmosphere and cooled with an ice bath (0 °C). Trifluoromethanesulfonic acid (3.39 g, 2 mL, 22.6 mmol) was slowly added through a syringe and a needle, and the mixture was stirred using a magnetic stirrer. The ice bath was left for 20 minutes, when the reaction mixture was allowed to warm to ambient temperature. The reaction was left running for 24 hours. After 24 hours, water (20 mL) was added to the reaction mixture. The mixture occasionally solidified and needed to be broken down using physical agitation. Sodium hydroxide solution (2 M) was subsequently added dropwise until the solution became neutral. As pH value increased, the reaction mixture turned from yellow suspension to bright orange solution, and then turned further to pale yellow suspension. The resulting precipitate was filtered using celite and collected using tetrahydrofuran.

Both products were used for further syntheses without further purifications.

2.2.3 Chemical and Equipment Suppliers

Chemicals were ordered from their respective chemical providers and used without further purifications. Grinding was required for some chemicals to break down clumps and aid the solubility. Trifluoromethanesulfonic acid, 4-bromobenzonitrile, 4-aminobenzonitrile, sodium *tert*-butoxide, sodium bromide, and bis(dibenzylidineacetone)palladium(0) ($Pd(dba)_2$) were ordered from Sigma-Aldrich. 2-Dicyclohexyl-phosphino-2',4',6'-triisopropylbiphenyl (XPhos) was ordered from either Alfa Aesar or Sigma-Aldrich. 1,4-Dioxane was ordered from Fisher Scientific. Tris(4-bromophenyl)amine (**TPA**-Br_3) was ordered from Santa Cruz Biotechnology. Tris(4-aminophenyl)amine (**TPA**-$(NH_2)_3$), 1,3,5-tris(4-bromophenyl)benzene (**TPB**-Br_3), 1,4-dibromobenzene (**BZN**-Br_2), 1,4-phenylenediamine (**BZN**-$(NH_2)_2$), and 2,7-diaminofluorene

(**FLR**-$(NH_2)_2$) were ordered from Alfa Aesar. 1,3,5-Tris(4-amino-phenyl)benzene (**TPB**-$(NH_2)_3$) was ordered from Tokyo Chemical Industry. 2,7-dibromofluorene (**FLR**-Br_2) was ordered from either Alfa Aesar or Acros Chemicals.

2.3 Spectroscopic Analyses of Obtained Products

Mass Spectrometry. Mass spectrometry (MS) analyses of soluble oligomeric products were recorded on the Bruker Daltonics UltrafleXtreme™ MALDI/TOF-TOF mass spectrometer in the Mass Spectrometry Facility in the School of Chemistry, University of Bristol. Samples were prepared as a solution in HPLC grade THF and were run using dithranol as the matrix for MALDI.

FT-IR Spectroscopy. FT-IR spectra of synthesised materials were recorded as neat solid samples using attenuated total reflectance (ATR) setup on a PerkinElmer Spectrum 100 FT-IR spectrometer in the Teaching Facility in the School of Chemistry over the range from 4000 to 400 cm^{-1}.

UV-Vis-NIR Spectroscopy. UV-vis-NIR transmittance spectra were recorded either as solutions (for oligomers) or suspensions (for polymers) in HPLC grade THF. Suspensions of polymers were prepared by sonication for 2.5 hours. Measurements were performed on a Shimadzu UV-2600 spectrometer over the range from 250 to 1400 nm.

2.4 Morphological Analyses on PANI-CMPs

Electron Microscopy Imaging. Scanning Electron Microscope (SEM) imaging was performed on a JEOL IT300 Scanning Electron Microscope in the Electron and Scanning Probe Microscopy Unit in the School of Chemistry. Samples were coated with a 15-nm layer of silver by plasma sputtering prior to imaging.

X-Ray Diffraction Analysis. Powder X-ray diffraction analyses were performed on a Bruker D8 Advance analysis instrument in the X-Ray Crystallography Unit in the School of Chemistry. The source of X-ray for the analysis is a copper Kα source with the wavelength of 1.5406 Å. The sample holders used in the analysis are amorphous silicon sample holders, and samples are attached onto the sample holders using Vaseline. Samples were set to spin at approximately 60 rounds per minute. Measurements were performed for the 2θ angles in the range between 5° and 60°, with a step size of 0.02° and the measurement time of one second for each step.

Adsorption Isotherm Analysis. Adsorption isotherm analysis of polymers was performed on a Quantachrome Autosorb iQ analyser. Prior to analysis, materials were pre-degassed under vacuum at 150 °C for at least 20 hours. Liquid nitrogen cooling bath (77.35 K) was used for nitrogen adsorption analysis. For CO_2 adsorption analysis, an ice water bath (273.15 K) and a room temperature water bath (298.15 K) were used.

2.5 Computational Studies

Details given in this section are generalised. Any deviations from the details given in this section will be explicitly listed.

Pre-Optimisation. Possible conformations were screened using the software *Spartan '14*.[33] Distributions of conformations were determined using molecular mechanics calculations (Merck Molecular Force Field; MMFF94),[34, 35] and the structures with lowest energies were used as starting points for DFT optimisation.

Optimisation and Frequency Calculation. Optimisation of structures along with frequency calculations were performed at the density functional theory (DFT) level.[36-39] Becke's three-parameter hybrid functionals[40] with Lee-Yang-Parr expressions[41, 42] (B3LYP), 6-31G(d)

basis set[43-52], and Grimme's dispersion correction D3 with Becke-Johnson damping (D3(BJ))[53] have been used during optimisation. To simulate the solvation of oligo(aniline)s, a polarisable continuum model (PCM)[54-57] with either acetonitrile or tetrahydrofuran as the solvent has been used during the optimisation process. Natural Bond Orbital analysis version 3[58-65] has been applied for partial charge analysis. All DFT calculations have been executed using either *Gaussian 09* revision D.01[66] or *Gaussian 16* revision A.03[67] on the Grendel, the Blue Pebble, or the Blue Crystal 4 high-performance computing cluster at the University of Bristol, unless stated otherwise. Structural and electronic data of oligo(aniline)s have been obtained either directly from Gaussian log output files or through visualisation using *GaussView* software, version 6.1.1.[68]

Time-Dependent DFT Calculation. Time-dependent DFT (TD-DFT)[69-75] have been carried out to simulate electronic properties of oligo(aniline)s using B3LYP functional with Coulomb-attenuation method[76] (CAM-B3LYP). Other computational keywords remain the same as for the optimisation step. The discussion between CAM-B3LYP and B3LYP functionals for the TD-DFT studies of oligo(aniline)s can be found in Section 1.3.1.2. Software used for calculations and visualisations are the same as DFT calculations.

Oligomer-Adsorptive Interaction Study. Optimisation of structures were performed at the density functional theory (DFT) level.[36-39] Becke's three-parameter hybrid functionals[40] with Lee-Yang-Parr expressions[41, 42] (B3LYP), 6-31G(d) basis set[43-52], and Grimme's dispersion correction D3 with Becke-Johnson damping (D3(BJ))[53] have been used during optimisation. A polarisable continuum model (PCM)[54-57] of aniline has been used during the optimisation process to simulate the environment of other polymer fragments. For systems with an oligomer fragment and an adsorptive molecule, the initial structures were created so that the adsorptive molecule is 3 Å away from either the centre of the BQ unit or the imine nitrogen atom of interest.

2.6 References

1. Y. Liao, J. Weber and C. F. J. Faul, *Chem. Commun.*, 2014, **50**, 8002-8005.
2. J. Chen, W. Yan, E. J. Townsend, J. Feng, L. Pan, V. Del Angel Hernandez and C. F. J. Faul, *Angew. Chem. Int. Ed.*, 2019, **58**, 11715-11719.
3. J. Stejskal, I. Sapurina and M. Trchová, *Prog. Polym. Sci.*, 2010, **35**, 1420-1481.
4. G. Ćirić-Marjanović, *Synth. Met.*, 2013, **177**, 1-47.
5. R. A. Singer, J. P. Sadighi and S. L. Buchwald, *J. Am. Chem. Soc.*, 1998, **120**, 213-214.
6. J. P. Sadighi, R. A. Singer and S. L. Buchwald, *J. Am. Chem. Soc.*, 1998, **120**, 4960-4976.
7. Y. Liao, J. Weber, B. M. Mills, Z. Ren and C. F. J. Faul, *Macromolecules*, 2016, **49**, 6322-6333.
8. L. Pan, Z. Liu, M. Tian, B. C. Schroeder, A. E. Aliev and C. F. J. Faul, *ACS Appl. Mater. Interfaces*, 2019, **11**, 48352-48362.
9. S. Hayashi, Y. Togawa, S. I. Yamamoto, T. Koizumi, K. Nishi and A. Asano, *J. Polym. Sci., Part A: Polym. Chem.*, 2017, **55**, 3862-3867.
10. K. X. Shi, H. Y. Yao, Y. C. Zou, Y. F. Wei, N. N. Song, S. Zhang, Y. Tian, S. Y. Zhu, B. Zhang and S. W. Guan, *Microporous Mesoporous Mater.*, 2019, **287**, 246-253.
11. D. Y. Chen, Y. Fu, W. G. Yu, G. P. Yu and C. Y. Pan, *Chem. Eng. J.*, 2018, **334**, 900-906.
12. J. Jiang, F. Su, A. Trewin, C. D. Wood, N. L. Campbell, H. Niu, C. Dickinson, A. Y. Ganin, M. J. Rosseinsky, Y. Z. Khimyak and A. I. Cooper, *Angew. Chem. Int. Ed.*, 2007, **46**, 8574-8578.
13. J. Jiang, F. Su, A. Trewin, C. D. Wood, N. L. Campbell, H. Niu, C. Dickinson, A. Y. Ganin, M. J. Rosseinsky, Y. Z. Khimyak and A. I. Cooper, *Angew. Chem. Int. Ed.*, 2008, **47**, 1167-1167.
14. J. Jiang, F. Su, A. Trewin, C. D. Wood, H. Niu, J. T. Jones, Y. Z. Khimyak and A. I. Cooper, *J. Am. Chem. Soc.*, 2008, **130**, 7710-7720.
15. D. Y. Chen, C. Liu, J. T. Tang, L. F. Luo and G. P. Yu, *Polym. Chem.*, 2019, **10**, 1168-1181.
16. T. Senthilkumar and S. K. Asha, *Macromolecules*, 2013, **46**, 2159-2171.
17. N. Popp, T. Homburg, N. Stock and J. Senker, *J. Mater. Chem. A*, 2015, **3**, 18492-18504.
18. H. Li, Q. Pan, Y. Ma, X. Guan, M. Xue, Q. Fang, Y. Yan, V. Valtchev and S. Qiu, *J. Am. Chem. Soc.*, 2016, **138**, 14783-14788.

19. S. Bhunia, P. Bhanja, S. K. Das, T. Sen and A. Bhaumik, *J. Solid State Chem.*, 2017, **247**, 113-119.
20. H. Singh, V. K. Tomer, N. Jena, I. Bala, N. Sharma, D. Nepak, A. De Sarkar, K. Kailasam and S. K. Pal, *J. Mater. Chem. A*, 2017, **5**, 21820-21827.
21. Q. Zhang, S. Yu, Q. Wang, Q. Xiao, Y. Yue and S. Ren, *Macromol. Rapid Commun.*, 2017, **38**.
22. S. K. Das, X. B. Wang and Z. P. Lai, *Microporous Mesoporous Mater.*, 2018, **255**, 76-83.
23. T. Geng, W. Zhang, Z. Zhu, G. Chen, L. Ma, S. Ye and Q. Niu, *Polym. Chem.*, 2018, **9**, 777-784.
24. Y. Lu, J. He, Y. Chen, H. Wang, Y. Zhao, Y. Han and Y. Ding, *Macromol. Rapid Commun.*, 2018, **39**.
25. G. Wang, K. Leus, S. Zhao and P. Van Der Voort, *ACS Appl. Mater. Interfaces*, 2018, **10**, 1244-1249.
26. S. Krishnan and C. V. Suneesh, *J. Photoch. Photobiol., A*, 2019, **371**, 414-422.
27. H. Wang, D. N. Jiang, D. L. Huang, G. M. Zeng, P. Xu, C. Lai, M. Chen, M. Cheng, C. Zhang and Z. W. Wang, *J. Mater. Chem. A*, 2019, **7**, 22848-22870.
28. J. Huang and S. R. Turner, *Polym. Rev.*, 2018, **58**, 1-41.
29. S.-C. Qi, J.-K. Wu, J. Lu, G.-X. Yu, R.-R. Zhu, Y. Liu, X.-Q. Liu and L.-B. Sun, *J. Mater. Chem. A*, 2019, **7**, 17842-17853.
30. X. Y. Wang, Y. Zhao, L. L. Wei, C. Zhang and J. X. Jiang, *J. Mater. Chem. A*, 2015, **3**, 21185-21193.
31. H. Tanaka, K. Shizu, H. Nakanotani and C. Adachi, *Chem. Mater.*, 2013, **25**, 3766-3771.
32. R. Gomes, P. Bhanja and A. Bhaumik, *Chem. Commun.*, 2015, **51**, 10050-10053.
33. Spartan'14, Wavefunction, Inc., Irvine, CA, 2014
34. T. A. Halgren, *J. Comput. Chem.*, 1996, **17**, 490-519.
35. T. A. Halgren, *J. Comput. Chem.*, 1996, **17**, 520-552.
36. P. Hohenberg and W. Kohn, *Phys. Rev. B: Condens. Matter Mater. Phys.*, 1964, **136**, B864.
37. W. Kohn and L. J. Sham, *Phys. Rev.*, 1965, **140**, 1133-1138.
38. R. G. Parr and Y. Weitao, *Density-Functional Theory of Atoms and Molecules*, Oxford University Press, New York, 1995.
39. D. R. Salahub and M. C. Zerner, *The Challenge of d and f Electrons : Theory and Computation*, American Chemical Society, Washington, 1989.
40. A. D. Becke, *J. Chem. Phys.*, 1993, **98**, 5648-5652.
41. C. Lee, W. Yang and R. G. Parr, *Phys. Rev. B: Condens. Matter Mater. Phys.*, 1988, **37**, 785-789.
42. B. Miehlich, A. Savin, H. Stoll and H. Preuss, *Chem. Phys. Lett.*, 1989, **157**, 200-206.
43. R. Ditchfield, D. P. Miller and J. A. Pople, *J. Chem. Phys.*, 1971, **54**, 4186-4193.
44. W. J. Hehre, R. Ditchfield and J. A. Pople, *J. Chem. Phys.*, 1972, **56**, 2257-2261.
45. P. C. Hariharan and J. A. Pople, *Theor. Chim. Acta*, 1973, **28**, 213-222.
46. P. C. Hariharan and J. A. Pople, *Mol. Phys.*, 1974, **27**, 209-214.
47. M. S. Gordon, *Chem. Phys. Lett.*, 1980, **76**, 163-168.
48. M. M. Francl, W. J. Pietro, W. J. Hehre, J. S. Binkley, M. S. Gordon, D. J. DeFrees and J. A. Pople, *J. Chem. Phys.*, 1982, **77**, 3654-3665.
49. R. C. Binning Jr. and L. A. Curtiss, *J. Comput. Chem.*, 1990, **11**, 1206-1216.
50. J. P. Blaudeau, M. P. McGrath, L. A. Curtiss and L. Radom, *J. Chem. Phys.*, 1997, **107**, 5016-5021.
51. V. A. Rassolov, J. A. Pople, M. A. Ratner and T. L. Windus, *J. Chem. Phys.*, 1998, **109**, 1223-1229.
52. V. A. Rassolov, M. A. Ratner, J. A. Pople, P. C. Redfern and L. A. Curtiss, *J. Comput. Chem.*, 2001, **22**, 976-984.
53. S. Grimme, S. Ehrlich and L. Goerigk, 2011, **32**, 1456-1465.
54. S. Miertuš, E. Scrocco and J. Tomasi, *Chem. Phys.*, 1981, **55**, 117-129.
55. S. Miertuš and J. Tomasi, *Chem. Phys.*, 1982, **65**, 239-245.
56. J. L. Pascual-ahuir, E. Silla and I. Tuñon, *J. Comput. Chem.*, 1994, **15**, 1127-1138.
57. J. Tomasi, B. Mennucci and R. Cammi, *Chem. Rev.*, 2005, **105**, 2999-3093.
58. J. P. Foster and F. Weinhold, *J. Am. Chem. Soc.*, 1980, **102**, 7211-7218.

59. A. E. Reed and F. Weinhold, *J. Chem. Phys.*, 1983, **78**, 4066-4073.
60. A. E. Reed and F. Weinhold, *J. Chem. Phys.*, 1985, **83**, 1736-1740.
61. A. E. Reed, R. B. Weinstock and F. Weinhold, *J. Chem. Phys.*, 1985, **83**, 735-746.
62. J. E. Carpenter, Doctor of Philosophy, University of Wisconsin, Madison, 1987.
63. J. E. Carpenter and F. Weinhold, *J. Mol. Struct.: THEOCHEM*, 1988, **46**, 41-62.
64. A. E. Reed, L. A. Curtiss and F. Weinhold, *Chem. Rev.*, 1988, **88**, 899-926.
65. F. Weinhold and J. E. Carpenter, in *The Structure of Small Molecules and Ions*, eds. R. Naaman and Z. Vager, Springer US, Boston, MA, 1988, ch. Chapter 24, pp. 227-236.
66. M. J. Frisch, G. W. Trucks, H. B. Schlegel, G. E. Scuseria, M. A. Robb, J. R. Cheeseman, G. Scalmani, V. Barone, B. Mennucci, G. A. Petersson, H. Nakatsuji, M. Caricato, X. Li, H. P. Hratchian, A. F. Izmaylov, J. Bloino, G. Zheng, J. L. Sonnenberg, M. Hada, M. Ehara, K. Toyota, R. Fukuda, J. Hasegawa, M. Ishida, T. Nakajima, Y. Honda, O. Kitao, H. Nakai, T. Vreven, J. J. A. Montgomery, J. E. Peralta, F. Ogliaro, M. Bearpark, J. J. Heyd, E. Brothers, K. N. Kudin, V. N. Staroverov, T. Keith, R. Kobayashi, J. Normand, K. Raghavachari, A. Rendell, J. C. Burant, S. S. Iyengar, J. Tomasi, M. Cossi, N. Rega, J. M. Millam, M. Klene, J. E. Knox, J. B. Cross, V. Bakken, C. Adamo, J. Jaramillo, R. Gomperts, R. E. Stratmann, O. Yazyev, A. J. Austin, R. Cammi, C. Pomelli, J. W. Ochterski, R. L. Martin, K. Morokuma, V. G. Zakrzewski, G. A. Voth, P. Salvador, J. J. Dannenberg, S. Dapprich, A. D. Daniels, O. Farkas, J. B. Foresman, J. V. Ortiz, J. Cioslowski and D. J. Fox, Gaussian 09, Revision D.01, Gaussian, Inc., Wallingford, CT, 2013
67. M. J. Frisch, G. W. Trucks, H. B. Schlegel, G. E. Scuseria, M. A. Robb, J. R. Cheeseman, G. Scalmani, V. Barone, G. A. Petersson, H. Nakatsuji, X. Li, M. Caricato, A. V. Marenich, J. Bloino, B. G. Janesko, R. Gomperts, B. Mennucci, H. P. Hratchian, J. V. Ortiz, A. F. Izmaylov, J. L. Sonnenberg, D. Williams-Young, F. Ding, F. Lipparini, F. Egidi, J. Goings, B. Peng, A. Petrone, T. Henderson, D. Ranasinghe, V. G. Zakrzewski, J. Gao, N. Rega, G. Zheng, W. Liang, M. Hada, M. Ehara, K. Toyota, R. Fukuda, J. Hasegawa, M. Ishida, T. Nakajima, Y. Honda, O. Kitao, H. Nakai, T. Vreven, K. Throssell, J. J. A. Montgomery, J. E. Peralta, F. Ogliaro, M. J. Bearpark, J. J. Heyd, E. N. Brothers, K. N. Kudin, V. N. Staroverov, T. A. Keith, R. Kobayashi, J. Normand, K. Raghavachari, A. P. Rendell, J. C. Burant, S. S. Iyengar, J. Tomasi, M. Cossi, J. M. Millam, M. Klene, C. Adamo, R. Cammi, J. W. Ochterski, R. L. Martin, K. Morokuma, O. Farkas, J. B. Foresman and D. J. Fox, Gaussian 16, Revision A.03, Gaussian, Inc., Wallingford, CT, 2016
68. R. D. Dennington, II, T. A. Keith and J. M. Millam, GaussView Version 6.1.1, Semichem Inc., Shawnee Mission, KS, 2019
69. R. Bauernschmitt and R. Ahlrichs, *Chem. Phys. Lett.*, 1996, **256**, 454-464.
70. M. E. Casida, C. Jamorski, K. C. Casida and D. R. Salahub, *J. Chem. Phys.*, 1998, **108**, 4439-4449.
71. R. E. Stratmann, G. E. Scuseria and M. J. Frisch, *J. Chem. Phys.*, 1998, **109**, 8218-8224.
72. C. Van Caillie and R. D. Amos, *Chem. Phys. Lett.*, 1999, **308**, 249-255.
73. C. Van Caillie and R. D. Amos, *Chem. Phys. Lett.*, 2000, **317**, 159-164.
74. F. Furche and R. Ahlrichs, *J. Chem. Phys.*, 2002, **117**, 7433-7447.
75. G. Scalmani, M. J. Frisch, B. Mennucci, J. Tomasi, R. Cammi and V. Barone, *J. Chem. Phys.*, 2006, **124**, 94107.
76. T. Yanai, D. P. Tew and N. C. Handy, *Chem. Phys. Lett.*, 2004, **393**, 51-57.

Chapter 3 Modelling Oligo(aniline)s towards PANI-CMPs

This chapter aims to discuss modelling and theoretical studies of PANI-CMP structures. The discussion will start at the general concepts by introducing structure hierarchy of polymers, specifically poly(aniline)s and the related PANI-CMPs, and descriptors used in previous theoretical studies of poly(aniline)s and oligo(aniline)s.

The second part of this chapter will discuss effects from the introductions of different topologies into the structures of oligo(aniline)s on geometric and electronic structures. Different topologies to be discussed are branches and cycles, which have rarely been discussed in the theoretical studies of poly(aniline)s and their related oligomers. DFT methods have been applied for structure optimisations of selected models. The discussion will cover structures of oligo(aniline)s in four different oxidation, doping, and spin states, namely the fully reduced **LEB** state, the half-oxidised **EB** state, and the doped **ES** +2 states in two different spin states, singlet and triplet. Later in this section, further modifications of PANI-CMP models with different core and linker models will be discussed.

In the third part, optoelectronic properties, represented by UV-Vis-NIR absorption spectra, will be discussed as the direct translations from electronic structures to measurable properties. TD-DFT calculations have been applied to predict the absorption spectra and delineate contributing electronic transfers. The predicted spectra will then be compared to the spectra recorded from products obtained from the syntheses of PANI-CMPs, and the validity of models selected for the studies will then be evaluated.

3.1 Structure Descriptors for the Study of Poly(aniline)s, Oligo(aniline)s, and PANI-CMPs

Parameters that explain or describe properties numerically are known as descriptors. Different descriptors have been selected for theoretical studies of poly(aniline)s and oligo(aniline)s. They can be separated into two categories depending on focused aspects, geometric and electronic. Geometric structure descriptors focus on geometric structures of chemical systems such as bond lengths and bond angles, which are directly related to positions of atoms or alignments of moieties in the systems, while electronic structure descriptors focus on electronic structures or distribution.

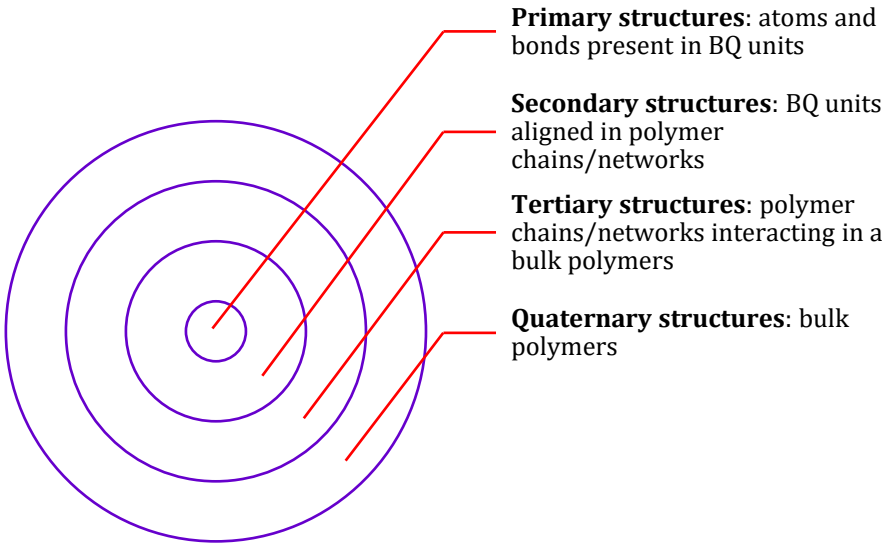

Scheme 3-1 A diagram showing four levels of poly(aniline) structures from smallest units to bulk polymers

Structures of poly(aniline)s, and any polymers in general, and oligo(aniline)s can be considered in the same way as protein structures, with hierarchical structures ranging from the simplest arrangements of subunits to the most complicated networks. Polymer structures can be classified into four levels, where structures of higher levels can be viewed as assemblies of structures of lower levels, as illustrated in Scheme 3-1.

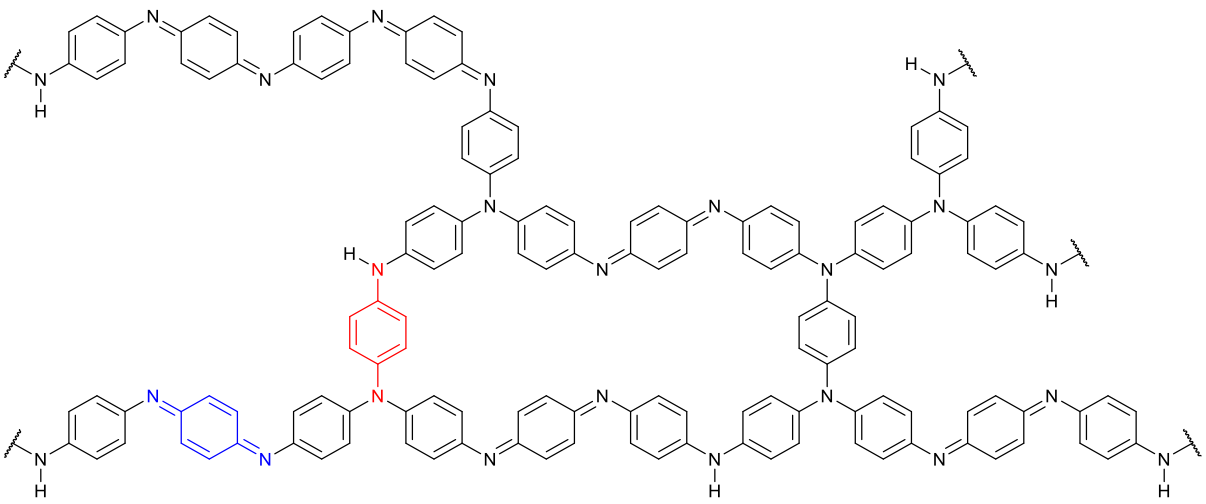

Scheme 3-2 An example of poly(aniline) secondary structures consisting of multiple BQ units as primary units

For PANIs and PANI-derived materials, benzenoid/quinoid or BQ units are the most elementary units, see the relevant discussion in Chapter 1. Therefore, in this study, these units will be considered as primary structures (individual units coloured red and blue in Scheme 3-2, for example). Primary structures concern atoms and bonds involved in BQ units. Geometric structure descriptors for primary structures will be discussed in Section 3.1.1.

The next level of complexity, secondary structures, concerns arrangements of these primary units along the direction of polymer network propagation. Polymers in this work are produced from coupling reactions, classified as polycondensation, which means that network-propagating coupling reactions can occur between any pair of moieties, regardless of respective positions on the polymer network. Therefore, there are possibilities that branched or cyclic structures can be formed (Scheme 3-2). In other words, different topologies can be found in these polymer structures. Polymer topologies have been found to affect the optical spectroscopic properties of polymers,[1] the effects of which will be explained in detail in Section 3.3. Meanwhile, geometric structure descriptors related to secondary structures will be discussed in Section 3.1.2. It should also be noted that PANIs and their derivatives that are prepared from non-BH methods or designed differently from PANI-CMPs discussed in this thesis might have other issues regarding their secondary structures such as the statistical arrangements of BQ units, which are beyond the scope of this study.

Tertiary structures are related to the larger scope of polymer structures in which different polymer chains or networks non-covalently interact. While detailed discussions about non-covalent interactions can be found in Chapter 5, it should be noted that the interactions between polymer chains in bulk structures are beyond the scope of this work partially because of the current limitation of theoretical studies. Finally, quaternary structures are the bulk structures of poly(aniline)s themselves. Discussions regarding morphologies or porosities of PANI-CMPs, in Chapter 4, are therefore related to the quaternary structures of PANI-CMPs.

Table 3-1 Structure descriptors being used in previous theoretical studies of poly(aniline)s and related materials, see the main text for further explanations

Study	Geometric Structural Parameter												Electronic Structural Parameter							
	Primary Structure				Secondary Structure															
	C_{ipso}–N Bond Length	C_{ipso}–C_{ipso} Bond Length	C_{ipso}–C_{ortho} Bond Length	Bond Length Alternation (BLA)	C_{ipso}–N–C_{ipso} Bond Angle	C$_{ipso}$–N–H Bond Angle	N···N···N Angle	C_{ortho}–C_{ipso}–N–C_{ipso} Dihedral Angle	C_{ipso}–N–C_{ipso}–C_{ortho} Dihedral Angle	C_{ortho}–C_{ipso}···C_{ipso}–C_{ortho} Dihedral Angle	C_{ipso}···H···C_{ipso}–N Improper Dihedral Angle	Backbone Bond Length Patterns (BBLP)	Band Gap Energy	Mulliken Charge	NBO Charge	Optical Absorption Peak Position	Electronic Transition Energy	Frontier Molecular Orbital	Spin Density	Electrostatic Potential Mapping
de Oliveira and dos Santos (2000)[2]	✓	✓	✓	×	✓	×	×	✓	✓	×	×	×	×	×	×	✓	×	×	×	×
Varela-Álvarez *et al.* (2005)[3]	✓	✓	×	×	✓	×	×	×	×	✓	×	×	×	×	×	×	×	×	×	×
Alemán *et al.* (2008)[4]	✓	×	×	×	✓	✓	✓	✓	✓	✓	×	✓	✓	✓	×	×	×	×	✓	×
Yang *et al.* (2008)[5]	×	×	×	×	✓	×	×	?	?	?	×	✓	×	?	?	×	×	×	×	×
Romanova *et al.* (2010)[6]	✓	✓	✓	×	×	×	×	×	×	×	×	×	×	×	✓	×	×	×	×	×
Petrova *et al.* (2011)[7]	×	×	×	✓	×	×	×	✓	✓	×	×	×	×	×	✓	×	×	✓	×	×
Romanova *et al.* (2011)[8]	×	×	×	✓	×	×	×	×	×	×	×	×	×	×	✓	×	×	×	×	×
Petrova *et al.* (2012)[9]	×	×	×	×	×	×	×	×	×	×	×	×	×	×	×	✓	✓	✓	✓	×
Canales *et al.* (2014)[10]	✓	✓	✓	×	✓	×	×	✓	✓	✓	✓	×	×	×	×	×	×	×	×	×
Zhang *et al.* (2014)[11]	×	×	×	✓	✓	×	×	?	?	?	×	×	×	×	✓	×	×	✓	×	×
Mills *et al.* (2016)[12]	×	×	×	×	×	×	×	×	×	×	×	×	×	×	×	✓	✓	×	✓	×
Mills *et al.* (2019)[13]	✓	✓	✓	×	✓	✓	×	×	×	✓	×	×	×	×	✓	✓	✓	✓	✓	✓

Note: "✓" means descriptor was used, "×" means descriptor was not used, and "?" means descriptor was used but was not explicitly reported whether which one was used.

Several structure descriptors have been applied for theoretical studies of poly(aniline)s and oligo(aniline)s, as listed in Table 3-1. As explained earlier, geometric and electronic structure descriptors focus on the different aspects of poly/oligo(aniline) systems as the name of each category suggests. For geometric structures, their descriptors can be subdivided further into primary (BQ units) and secondary structure descriptors. These descriptors will be discussed in detail over the next subsections.

3.1.1 Descriptors for Primary Structures (BQ Units)

As primary structures of poly(aniline)s and their derivative materials, structures of BQ units need thorough consideration. This section aims to discuss the geometric structures of BQ units in different oxidation states.

In general, there are eight atoms and eight bonds involved in the conjugated system of each BQ unit (Scheme 3-3). Each unit consists of one six-membered ring and two substituents on the *para* positions, mostly amino or imino groups for PANI-CMPs and derivatives, which are labelled in green. The differences between BQ units in these two oxidation states are bond lengths. As BQ units are oxidised from benzenoid to quinoid forms, two C–N bonds (green) become shorter and more resemble double bonds.

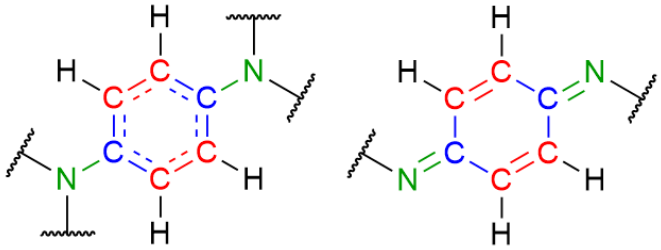

Scheme 3-3 Structures of benzenoid (left) and quinoid (right) BQ units with three different types of bonds and atoms illustrated (see main text)

For the central carbon ring, carbon atoms can be divided into two groups based on their respective position to either of the two substituents, *ipso* carbon atoms (blue) and *ortho* carbon atoms (red). Therefore, six C–C bonds can then be divided into two groups, C_{ipso}–C_{ortho} (blue) and C_{ortho}–C_{ortho} (red). Although in the older publications, C–N bonds were usually more frequently used as descriptors that the other C–C bonds, all three bonds are used alongside each other in more recent publications, see Table 3-1.

It is worth noting that some research articles also use bond length alterations (BLAs) which are defined differently for C–N bonds and C–C bonds. For C–C bonds in the ring, BLAs are calculated from the differences between average C_{ipso}–C_{ortho} and average C_{ortho}–C_{ortho} bond lengths of the same ring. However, for C–N bonds, they are calculated from the differences between the C–N bond lengths of the current unit and those of the previous unit in the chain.

Scheme 3-4 Five possible structures of BQ units that can be found in poly(aniline)s and oligo(aniline)s. Bonds and hydrogen atoms in blue can be replaced with oligo(aniline) chains.

There are more possible forms other than benzenoid and quinoid forms, depending on oxidation states, protonation patterns, and spin multiplicities. Five of these possible forms are listed in Scheme 3-4, based on 1,4-phenylenediamine or **BZN**-$(NH_2)_2$ monomer as an arbitrary model. The first form, the benzenoid or **BZ** form, is **BZN**-$(NH_2)_2$ prior to oxidation or other chemical reactions. As **BZN**-$(NH_2)_2$ in **BZ** form is being oxidised, removal of one electron yields the radical cation (**RC**) form. Further removal of the second electron can yield two different products with different spin multiplicities, either the diradical cation (**DRC**) form, which is a triplet or the quinoidal dication (**QDC**) form, which is a singlet. Finally, removal of two protons from oxidised **BZN**-$(NH_2)_2$ yields the quinoid (**QN**) form. In theory, there are other possible

oxidation, doping, and spin states such as the triplet equivalent of the **QN** form. However, these are not considered in this study due to the lack of reports regarding their existences.

To illustrate different bond lengths in these five forms, structures of **BZN**-$(NH_2)_2$ in these forms have been optimised using density functional theory (DFT) level calculations.[14-17] Table 3-2 lists lengths of these bonds from DFT calculations.

*Table 3-2 Bond lengths of DFT-optimised **BZN**-$(NH_2)_2$ in different structures and their changes upon oxidation from **BZ** form. BLAs or bond length alternations are calculated from the difference between average C_{ipso}–C_{ortho} and C_{ortho}–C_{ortho} lengths. Computational conditions: B3LYP functional,[18-20] 6-31G(d) basis set,[21-30] D3(BJ) empirical dispersion,[31] acetonitrile polarisable continuum model,[32-35] Gaussian 09[32-35]*

Structure	Bond Length (Å)				Bond Length Change (Å)		
	C_{ipso}–C_{ortho}	C_{ortho}–C_{ortho}	BLA	C–N	C_{ipso}–C_{ortho}	C_{ortho}–C_{ortho}	C–N
BZ	1.403	1.393	+0.010	1.410			
RC	1.428	1.367	+0.061	1.342	+0.025	-0.026	-0.068
DRC	1.425	1.419	+0.006	1.328	+0.022	+0.026	-0.081
QDC	1.461	1.344	+0.117	1.297	+0.058	-0.050	-0.112
QN	1.470	1.345	+0.125	1.292	+0.067	-0.048	-0.118

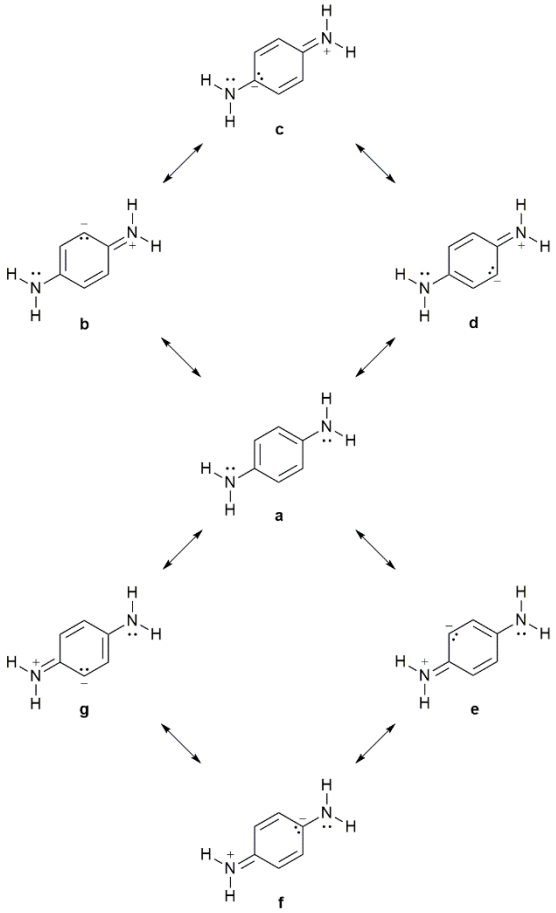

*Scheme 3-5 Resonance structures of **BZN**-$(NH_2)_2$ in **BZ** form, illustrating delocalisation of non-bonding electron pairs from amino groups*

From Table 3-2, C_{ipso}–C_{ortho} bonds from DFT-calculated **BZN**-$(NH_2)_2$ in all states have been found to be longer than C_{ortho}–C_{ortho} bonds. This can be explained by considering their resonance structures, with those of **BZ** form given in Scheme 3-5. As illustrated, after the donation from

either of the amino groups, the resulting negative charges can be on all six carbon atoms, in theory. However, structures **c** and **f** with negative charges located on either of the C_{ipso} atoms are energetically unfavourable due to the proximity of carbanion to another amino group, which also has a non-bonding electron pair. Therefore, the electron density over the four *ortho* carbon atoms is then higher than over the two *ipso* carbon atoms. In other words, the electron cloud, referring to the chance of finding electrons, is denser on *ortho* carbon atoms and thinner on *ipso* carbon atoms. This means that electrons tend to be more *localised* on C_{ortho}–C_{ortho} bonds, making them shorter than C_{ipso}–C_{ortho} bonds. This trend is also in line with the NBO charges (Table 3-4 and Figure 3-3), the discussions of which are in Section 3.1.3.

The effects from amino group delocalisation are more pronounced in the oxidised forms, considering that C–N bonds become shorter (**BZ** > **RC**$^{+}$ > **DRC**$^{2+}$ > **QDC**$^{2+}$ > **QN**). However, the outlier in this case is the diradical cation form if considering C–C bond lengths. While carbon-carbon bond lengths in **RC** and **QDC** forms follow the same trend with longer C_{ipso}–C_{ortho} and shorter C_{ortho}–C_{ortho} bonds, the different changes are observed in the **DRC** form. Although their C_{ipso}–C_{ortho} bonds become longer, their C_{ortho}–C_{ortho} bonds are also longer than in the **BZ** form. Interestingly, C_{ipso}–C_{ortho} and C_{ortho}–C_{ortho} bond lengths in the **DRC** form become closer in length. It is possible that this structure, where all six C–C bonds have almost the same length while radical cations are separated from the ring system, is favoured because of the aromaticity within the six-membered ring.

Bond lengths can be used to compare the differences between BQ units in different states. Oxidation of BQ units in general leads to decreases in C–N bond lengths, elongations of C_{ipso}–C_{ortho} bonds, and (with the exception of the **DRC** form) decreases in C_{ortho}–C_{ortho} bond lengths. However, while the changes in bond lengths are understandable, there are still three different types of bonds to consider. It would be convenient if there is a descriptor that can unify the variations in these three bond types, the proposal of which will be discussed in the following subsection.

3.1.1.1 Enumerations of Electron Delocalisation Patterns in Conjugated Systems

In organic chemistry, conjugated systems are systems of multiple π-bonds or orbitals that are capable of overlapping to create extended chains of delocalised molecular orbitals. BQ units, in both benzenoid and quinoid forms, are examples of conjugated systems, as well as poly(aniline)s. Their differences in aromaticity properties between BQ units in different oxidation states can be demonstrated by their variations in bond lengths. However, there are three types of bonds in each BQ units, and the changes in bond lengths are arguably direct results from the changes in aromaticity properties. As the BQ unit being oxidised from the **BZ** form to the **QDC** or **QN** form, its structure is changed from 1,4-phenylenediamine, which is more aromatic, to 1,4-benzoquinone diamine, which is less aromatic. Therefore, it is possible that the change in structures upon oxidation from the **LEB** state can be described by only one descriptor directly related to aromaticity.

Attempts have been made to enumerate aromaticity of chemical structures, with various methods have been proposed over several decades. These enumerating methods are related to the chemistry of BQ units since there are certain dearomatising changes upon variation of chemical structures away from the **BZ** or benzenoid BQ structure. These proposed methods include nucleus-independent chemical shifts (NICS), based on the calculations of ^{1}H NMR chemical shifts to determine the shielding or deshielding effects, and geometry-based calculations. The major limitation of NICS compared to geometry-based methods is that NICS indices are mostly useful for individual rings rather than extended conjugated systems.[36]

Therefore, for the study of these polymeric material models, with infinitely expanding structures, geometry-based methods are more suitable. Over the past decades, several calculation

methods have been proposed. Most of these proposed rely on the concept of harmonic oscillations, with general mathematical expressions in the form of:

$$A_{\text{system}} = 1-\frac{1}{n}\sum_{\text{all bonds}} k\left(R_{\text{ref, bond}}-r_{\text{bond}}\right)^2. \quad \textit{3-1}$$

A_{system} refers to the index of aromaticity or electron delocalisation, as being included in later expansion proposals. The number of bonds involving in the conjugated system is represented by n. Normalisation factors k and reference bond lengths $R_{\text{ref, bond}}$ depend on the types of atoms involved in each bond. Reference bond lengths can be divided into two groups based on the scope of definitions, either specifically defined for particular systems or universally defined for all conjugated systems, which will be an important issue later in the application for this particular work. To be in line with other publications, the unit of bond lengths discussed in this work is Angstrom (Å). The first reported equation for the calculation of aromaticity was proposed in 1967 by Julg and Françoise, applied to the study of aromatic hydrocarbons.[37]

$$A_{\text{J-F}} = 1-\frac{225}{n}\sum_{\text{all bonds}}\left(1-\frac{r_{\text{bond}}}{\bar{r}}\right)^2 \quad \textit{3-2}$$

In Equation 3-2, the reference bond length is the average length of bonds in that system, $\bar{r}$, rather than a universal set of bond lengths. The idea of having a single set of values that can be used across all aromatic hydrocarbon systems was introduced by Kruszewski and Krygowski in 1972 in their proposal of the harmonic oscillator model of aromaticity (HOMA).[38] The reference bond length is calculated using following equation.

$$R_{\text{ref}} = \frac{(R_{\text{s}}+\omega R_{\text{d}})}{1+\omega} \quad \textit{3-3}$$

R_{s} and R_{d} in Equation 3-3 refer to lengths of "pure single bond" and "pure double bond", which were taken from C–C bond lengths in ethane (1.524 Å) and ethylene (1.334 Å), respectively. The constant ω in Equation 3-3 is the ratio between stretching force constants for double and single bonds, which is generally assumed as 2.[36, 39] Therefore, the reference bond length for C–C bonds are 1.397 Å. The normalisation constant is set to 98.89 Å^{-1} to calibrate the scale so that the HOMA value of fully delocalised benzene is 1, and that of Kekulé benzene (cyclo-1,3,5-hexatriene) becomes 0. The HOMA equation is proposed as following.

$$\text{HOMA} = 1-\frac{98.89}{n}\sum_{\text{all bonds}}(1.397-r_{\text{bond}})^2 \quad \textit{3-4}$$

It should be noted that the original proposal for HOMA was also focusing on hydrocarbons. Heteroatom-containing systems have been included for the enumeration of aromaticity for the first time in the later update of Julg-Françoise model in 1971,[36] and the HOMA method has been expanded to include heteroatoms in the 1993 publication.[40] The 1993 improvement of HOMA integrated 6 more types of bonds (C–N, C–O, C–P, C–S, N–N, and N–O) in addition to the original C–C bonds. Also, the concept has also been expanded to include acyclic systems although the name still retains the term "aromaticity". Reference single and double bonds for C–C bonds were also changed from ethane and ethylene to 1,3-butadiene, 1.467 Å and 1.349 Å, respectively. With a smaller gap between reference single and double bonds, the normalisation constant for C–C bonds was then increased from 98.89 Å^{-1} to 257.7 Å^{-1}. The new method to calculate normalisation

constants α, functionally the same as parameter k in Equation 3-1, was also proposed as shown in Equation 3-5.

$$\alpha = \frac{2}{\left(R_{opt}\text{-}R_s\right)^2+\left(R_{opt}\text{-}R_d\right)^2} \qquad 3\text{-}5$$

$$\alpha = \frac{n_s+n_d}{n_s\left(R_{opt}\text{-}R_s\right)^2+n_d\left(R_{opt}\text{-}R_d\right)^2} \qquad 3\text{-}6$$

Further improvements of harmonic oscillator aromaticity enumeration include harmonic oscillator measure of electron delocalisation (HOMED) in 2007 by Raczynska *et al.*,[41] and harmonic oscillator measure of heterocycle electron delocalisation (HOMHED) in 2012 by Frizzo and Martins.[39] The difference between these two proposals is that parameters in HOMED are based on computational data, while parameters in HOMHED are based on experimental data. Also, normalisation factor α in HOMED is calculated with regards to the numbers of single bonds (n_s) and double bonds (n_d) in the case of systems with odd numbers of bonds involved (Equation 3-6). It should be noted that in their original publication, only cases with the differences between n_s and n_d being 1 are discussed. However, there are cases where the differences between the numbers of single and double bonds are more than one, including the **FLR**-$(NH_2)_2$ monomer, or 2,7-diaminofluorene, in this work with 6 double bonds and 9 single bonds. Nonetheless, this mathematical expression should apply to these cases. In fact, mathematically, Equation 3-5 is the specific case of Equation 3-6 where n_s and n_d are equal. Meanwhile, HOMHED calculations do not differentiate systems with odd or even numbers of bonds. A thorough review of geometric enumeration methods of aromaticity and electron delocalisation including other proposed models with slightly different mathematical expressions can be found in the 2014 *Chemical Reviews* article by Krygowski *et al*.[36] So far, harmonic oscillator calculations have yet to be applied for the study of poly(aniline) systems.

Considering the general form of harmonic oscillator models in Equation 3-1, the general mathematical expression on the right-hand side is the subtraction of an average contribution from each bond in the conjugated system from one. For each bond, the contribution is similar to the potential energy equation of a harmonic oscillator, which is proportional to the square of the displacement from the equilibrium length of that oscillator. If the oscillator is at its equilibrium length, there is no potential energy stored in that oscillator. Therefore, bonds at their optimum lengths do not contribute to the deviation from equilibrium. Meanwhile, when the length of a bond changes, the potential energy stored depends on the spring constant of that bond. Normalisation factors are then introduced to calibrate the scale from one to zero, as explained earlier, under the assumption that all bonds involved contribute equally to the decrease in electron delocalisation index.[40] All models mentioned earlier use the same form, as in Equation 3-1. The only thing that differs among these models are the values of parameter k for each type of bonds. This can be seen in the similar way as force fields for molecular mechanics (MM) calculations; each of them is created for a group of specific chemical systems of interest, with appropriate parameters suitable for its dedicated group. In other words, different harmonic-oscillation-based models for aromaticity are the same in principle. The only difference is the parameters for each type of bonds being considered. It is also worth noting that MM methods also rely on harmonic oscillations to calculate energies of chemical systems.

Usually, scales of aromaticity or electron delocalisation indices are set so that the value of "absolute aromatic" or "fully delocalised" system becomes one, while that of "absolute non-

aromatic" or "fully localised" system becomes zero. In theory, this concept of setting a range from one constant to another constant can be applied to any property which two opposite ends of the spectrum are defined. Herein, the harmonic oscillator model will be applied to benzenoid and quinoid forms of BQ units, with the benzenoid unit arbitrarily set as "one" and the quinoid unit set as "zero", and this model will be called HOMBQ or harmonic oscillator measurement for benzenoid-quinoid characteristics.

Since the benzenoid unit is set to have HOMBQ index of one, the reference bond lengths in the Equation 3-1 in this case are bond lengths from the benzenoid unit. Therefore, in the BQ unit with *n* bonds,

$$\text{HOMBQ} \quad = \quad 1-\frac{1}{n}\sum_{i=1}^{n}\alpha_i(R_{\text{B}i}-r_i)^2 \,, \tag{3-7}$$

when $R_{\text{B}i}$ and r_i refer to lengths of the *i*th bond in the BQ unit in the true benzenoid form and the actual system, respectively. Normalisation factors are also a function of the bond index number *i*. Meanwhile, the quinoid unit is set to have HOMBQ index of zero. If the length of the *i*th bond in the quinoid BQ unit is $R_{\text{Q}i}$, substituting r_i with $R_{\text{Q}i}$ in Equation 3-7 and subsequent transforming yield:

$$1 \quad = \quad \frac{1}{n}\sum_{i=1}^{n}\alpha_i\left(R_{\text{B}i}-R_{\text{Q}i}\right)^2 . \tag{3-8}$$

To fulfil mathematical conditions in Equation 3-8 and the assumption of equal contribution, the term $\alpha_i(R_{\text{B}i}-R_{\text{Q}i})^2$ for bond *i* is set to one. This means that the normalisation factor α_i, as a function of *i*, equals to the reciprocal of the square of the difference between lengths of bond *i* or $\frac{1}{\left(R_{\text{B}i}-R_{\text{Q}i}\right)^2}$ in benzenoid and quinoid units. Therefore, HOMBQ in this work will be defined as:

$$\text{HOMBQ} \quad = \quad 1-\frac{1}{n}\sum_{i=1}^{n}\frac{(R_{\text{B}i}-r_i)^2}{\left(R_{\text{B}i}-R_{\text{Q}i}\right)^2} . \tag{3-9}$$

Having enumerating models which allow data specific for a particular aromatic system to be used allows the scale to be specifically set, which is useful for the comparison of BQ units in PANI-CMP models with different chemical properties because variations in HOMBQ indices are related to π-electron conjugations between core and linker units in PANI-CMP models, which is to be explained later. HOMHED, with universally set parameters, and HOMBQ indices of **BZN**-$(NH_2)_2$ in five different chemical structures are shown comparatively in Table 3-3 and Figure 3-1.

Table 3-3 Harmonic oscillator measure of heterocyclic electron delocalisation (HOMHED) and harmonic oscillator measurement for benzenoid-quinoid characteristics (HOMBQ) indices calculated from DFT-optimised bond lengths in Table 3-2

Structure	***ipor* C–C (Å)** 4 bonds	***oror* C–C (Å)** 2 bonds	**C–N (Å)** 2 bonds	**HOMHED**	**HOMBQ**
BZ	1.403	1.393	1.410	0.879	1.000
RC	1.428	1.367	1.342	0.926	0.773
DRC	1.425	1.419	1.328	0.920	0.754
QDC	1.461	1.344	1.297	0.710	0.131
QN	1.470	1.345	1.292	0.646	0.000

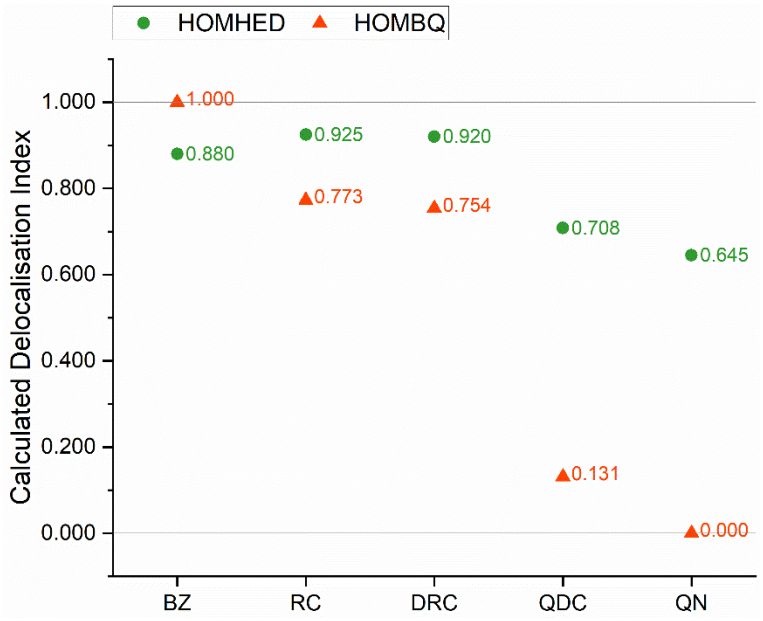

Figure 3-1 Calculated HOMHED and HOMBQ indices of DFT-calculated 1,4-phenylenediamine structures in different states. Structures for BQ units in these states can be found in Scheme 3-4.

It is obvious that values of HOMBQ indices distribute more throughout the range between 0 and 1 than values of HOMHED indices which scatter over the range of only 0.280 (0.645 for **QN** and 0.925 for **RC**). Also, HOMHED indices of **RC** and **DRC** forms are beyond the range between **BZ** and **QN** forms, which are the two extreme forms for the chemistry of BQ units. Therefore, for the characterisation of BQ units, using HOMBQ indices with more specific parameters provide better differentiation than HOMHED that are using generally defined parameters. This is also similar to the original proposal by Julg and Françoise to use the average bond lengths within the system itself to calculate aromaticity of aromatic hydrocarbons.[37] Nonetheless, the concept of using harmonic oscillators to enumerate degrees or extents of electron delocalisation for comparison is still relevant and reliable.

However, as the later proposals and also this work have illustrated, the most important part of an appropriate scale for comparison of characteristics is the selection of reference bond lengths. It should also be noted that since this work involves structure modifications of PANI-CMPs by changing aromatic systems, BQ units can take different structures if their phenylene units are replaced. Therefore, comparisons of BQ units across different aromatic building blocks are less straightforward yet achievable, nonetheless. For BQ units derived from a certain aromatic system, the scale of HOMBQ is set to be from zero (in a **QN** unit) to one (in a **BZ** unit). The oxidation of unbound BQ units from **BZ** form to **QN** form therefore reduce the HOMBQ indices from one to zero when the pattern of electron delocalisation changes from benzenoid to quinoid. However, for bound BQ units, there is π-conjugation from neighbouring aromatic systems, allowing electrons to delocalise into these units. This prevents the HOMBQ indices from being reduced all the way down to zero. This will be explained further in the discussion of PANI-CMPs with different core or linker units in Section 3.2.

3.1.2 Descriptors for Secondary Structures

Secondary structures of PANI-CMPs and corresponding oligomers concern arrangements of BQ units within the polymer or oligomer structures. In this thesis, two aspects of secondary structures in the studies of PANI-related systems are focused, namely alignments of two adjacent BQ units and the topology of polymer chains. According to Table 3-1, most studies involving secondary structures focus on alignments of two adjacent BQ units, with only two publications

consider larger structures. Both of the topology-focusing publications used backbone bond length patterns (BBLPs) to exhibit the patterns of C–C and C–N bond lengths throughout the structure.

Alignments of two adjacent BQ units have gathered more interest from researchers because they dictate how polymer chains or networks propagate. General structures of poly- and oligo(aniline)s contain units of geminal diaryleneamine, with two arylene units attached on an -NH- group. These two aromatic units cannot be on the same plane due to the steric effect from hydrogen atoms on the *ortho* positions, as illustrated in Scheme 3-6. To compensate for these repulsions, the two aromatic systems have to move away from each other. With respect to the propagation of polymer structures, these movements can either be parallel, by adjusting the Ar-N-Ar angles (the bottom branch in Scheme 3-6), or perpendicular, by twisting away from the plane (the top branch in Scheme 3-6). Adjustments of Ar-N-Ar angles distort these bond angles from 120°, the ideal bond angle for atoms in sp^2 hybridisation. Meanwhile, twisting aromatic systems away from each other reduces the ability for π-conjugated systems and the nonbonding *p* orbital of the connecting nitrogen atom to overlap. Either way, the two actions also decrease the stability of the whole system. Therefore, these destabilising effects need to be balanced against each other.

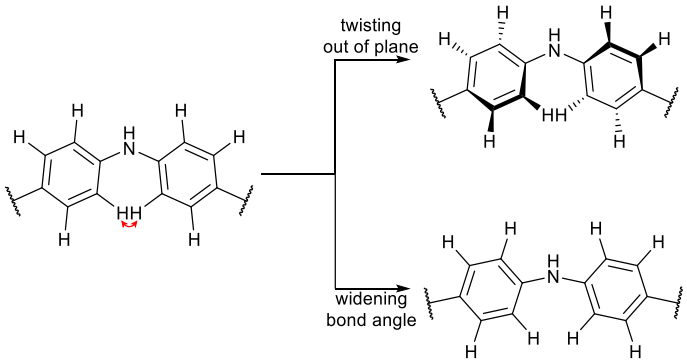

Scheme 3-6 Two different ways to mitigate the steric hindrance between two ortho hydrogen atoms in a geminal diaryleneamine system

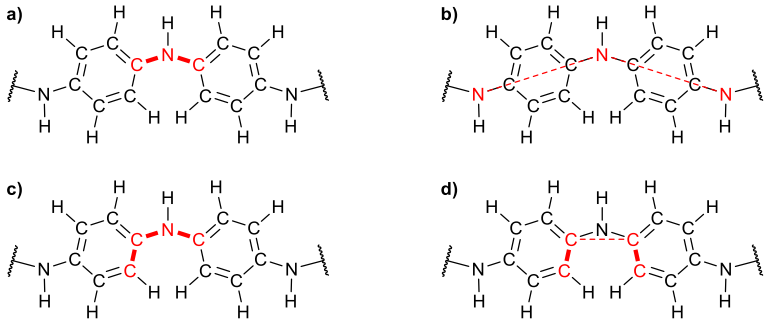

Scheme 3-7 Geometric descriptors for angles between two adjacent BQ units, ***a)*** *C–N–C angle,* ***b)*** *N···N···N angle,* ***c)*** *C–C–N–C dihedral angle, and* ***d)*** *C–C···C–C dihedral angle. Bold bonds represent bonds between pairs of chemically bonded atoms, and dashed lines represent imagination connections between pairs of non-chemically-bonded atoms. Only one sequence is shown for* ***c)*** *while there are two sequences, see main text.*

Various descriptors have been chosen for the thorough studies of adjacent BQ unit alignments in poly(aniline) and oligo(aniline) structures, see Table 3-1. The most popularly used descriptors can be divided into two groups based on two modes of structural adjustments explained earlier, namely bond angles parallel to the polymer propagations and dihedral angles perpendicular to the polymer propagations, as shown in Scheme 3-7. C–N–C angles are the most obvious and generally used bond angles in these studies.[2, 4, 5, 10, 11] In addition, Alemán *et al.* have used angles formed from three consequent nitrogen atoms bridging adjacent BQ units or N···N···N

angles.[4] However, unless the oligomer fragments are in highly strained conditions such as small rings, the difference between C–N–C and N···N···N angles should not be significant.

Meanwhile, ring dihedral angles between adjacent rings, as representations of adjustments perpendicular to the propagation, can be divided further into two different groups, C–C–N–C and C–C···C–C dihedrals. The difference between the two groups is the selection of atom 2 and atom 3 to define dihedrals. C–N–C–C dihedrals are defined with a C–N bond as a source for atoms 2 and 3, while C–C···C–C dihedrals are defined using both C_{ipso} atoms on both sides of the C–N–C bonds as atoms 2 and 3 although they are not directly bound. While data of C–N–C–C dihedrals can be directly obtained from the log files after the optimisation processes have been finished, the fact that there are two C–N bonds concerning two adjacent rings or BQ units means that two C–N–C–C dihedral angles have to be combined to describe the twisting of one adjacent unit pair. Therefore, the use of C–C···C–C would be more practical as a descriptor.

It should be noted that one previous study also used an improper dihedral angle related to the planarity of the amino group as a structure descriptor.[10] However, the geometry of the amino group itself can be affected by computational procedures to dictate whether it is closer to sp^2 or sp^3. Meanwhile, this descriptor obviously is not applicable for oligomers in the **EB** state. For these reasons, this improper dihedral angle would be omitted in this study.

Another aspect that has never been implemented before in the previous theoretical studies is the topology of poly(aniline) chains. Many theoretical studies focus on the question whether the structure of the conductive emeraldine salt form of poly(aniline)s is polaronic or bipolaronic, see the discussion in Section 1.1.2. The proposed structures are based on unbranched oligo(aniline)s (Scheme 1-8), so are the following theoretical studies. However, as Ćirić-Marjanović has proposed,[42] branched structures can be formed as side reactions during the oxidative polymerisation towards PANI. Branched moieties, where nitrogen atoms are connected to three non-hydrogen groups, are even more common in poly(aniline)-based porous materials. However, so far, models deliberately created to be branched are still limited.

Another possible topology that can theoretically be found in poly(aniline)s is cyclic topologies, which occurs when, for materials prepared from Buchwald-Hartwig coupling reactions, the coupling reaction happens intramolecularly. While cyclic moieties in poly(aniline)s have yet to be reported in literature, mass spectrometry analyses of products from synthesis attempts reveal that it is possible to form cyclic structures (see relevant discussions in Section 4.3.2). Considering the adjustments of two adjacent BQ units, cyclisation leads to more restriction along the propagational direction and limits the adjustment of C–N–C angles. To counteract, BQ units have to be twisted further from the plane of polymer propagation, and the overlap between molecular orbitals of adjacent units becomes more disrupted. It has been found that strains in cyclic structures can affect absorption spectra of oligomers.[1] Branched structures can also cause similar restrictions in C–N–C angle adjustments due to additional steric effects. Therefore, it is important for the studies of oligo(aniline)s and poly(aniline)s to take the issue of branched and cyclic structures into account.

In this study, two descriptors, C–N–C angles and C–C···C–C dihedral, will be used for the discussions regarding alignments of two neighbouring BQ units. Meanwhile, effects from branching and cyclisation in PANI-CMPs will also be discussed.

3.1.3 Electronic Structure Descriptors

Electronic structures of chemical systems focus on configurations and distributions of electrons throughout those systems. From Table 3-1, descriptors related to electronic structures can be subdivided into four groups based on the aspects of electronic structures being described.

The first group of descriptors consists of only one descriptor, band gap energy (ε_g). It should be noted that the estimation of ε_g based on the difference between highest occupied molecular orbitals (HOMOs) and lowest unoccupied molecular orbitals (LUMOs) of chemical systems at the ground state was popular before the development of time-dependent DFT (TD-DFT) methods. Band gap energies of π-conjugated polymers can be extrapolated from the linear ε_g vs $1/n$ plot when n is the number of repeating units.[4, 43] However, the relationship between ε_g and $1/n$ tends to deviate from linearity at high n values, and the prediction can be improved either by using second-order polynomial equations or periodic boundary conditions.[43, 44] Nonetheless, the later development of TD-DFT methods means that electronic excited states can be simulated better. TD-DFT calculations can tell not only energies of electronic transitions but also their intensities. The development of TD-DFT methods therefore has rendered the use of band gap energy as a descriptor obsolete, and it is now replaced by transition-based descriptors, which will be discussed later in this section.

The second group consists of atomic charges, which are Mulliken and NBO (natural bond orbital) charges. Mulliken charges have been known to be dependent on computational methods, while NBO charges are less affected and have become more popularly used. For the studies of poly- and oligo(aniline)s, atomic charges are considered on nitrogen atoms and on carbon rings. Charges of hydrogen atoms are usually integrated into those of heavier atoms they are bound to.[6-8, 11, 13] These atomic charges can give the ideas whether which area will be more positively or negatively charges. However, it should be noted that charges on *ipso* and *ortho* carbon atoms can be different because of atoms they are bound to; *ipso* carbon atoms are bound to more electronegative nitrogen atoms while *ortho* carbon atoms are bound to hydrogen atoms.

The third group can be considered as the development from the first group, and descriptors of this group are translatable to physical properties. These are descriptors related to electronic transitions which have become popular in the studies of poly- and oligo(aniline) systems thanks to the development of TD-DFT calculations. Electronic transitions in turn also relate to optoelectronic properties because the energy gap between ground state and excited state for electronic transitions are roughly in the near ultraviolet to near infrared range, which means that data from descriptors of this type are comparable to those recorded from UV-Vis-NIR spectroscopy, which have been one of the popular analytical methods for experimental studies of poly- and oligo(aniline)s.[2, 10, 12, 13, 45-48]

```
Excitation energies and oscillator strengths:

Excited State   1:  3.061-B      1.3425 eV  923.52 nm  f=1.1538  <S**2>=2.093
   154B ->157B       -0.44034
   155B ->156B        0.87919
This state for optimization and/or second-order correction.
Total Energy, E(TD-HF/TD-DFT) =  -1838.50892756
Copying the excited state density for this state as the 1-particle RhoCI density.

Excited State   2:  3.047-A      1.7181 eV  721.64 nm  f=0.1130  <S**2>=2.071
   154B ->156B       -0.59415
   155B ->157B        0.76103
```

Figure 3-2 An example of a result from a TD-DFT calculation using Gaussian 16 revision A.03[49]

As explained, TD-DFT methods can be used to calculate electronic transitions within the chemical system and can provide several data pieces for each electronic transition. For example, TD-DFT calculations using *Gaussian*[49-51] series of software can provide results as shown in Figure 3-2. For each transition, the energy for that transition is given (in eV in the example) along with the corresponding wavelength (in nm). Another parameter, oscillator strength (*f*), is also given. This parameter is related to the intensity of the corresponding absorption. The higher the oscillator strength, the more intense the absorption, in theory. Besides energy and intensity, TD-

DFT calculations can also give the molecular orbitals involving in electronic transitions. For example, for the result in Figure 3-2, Excited State 1 is contributed by two transitions. The major transition is from molecular orbital (MO) 155B to MO 156B, and the minor transition is from MO 154B to MO 157B.

Data from descriptors of the third group can be represented in two ways. They can be plotted or listed as energy, wavelength, and oscillator strength, or they can be converted into an absorption spectrum. Providing data as a list or a scatter plot can delineate the most important electronic transitions and the MOs involved. However, converting data into absorption spectra can provide absorption maxima which can then be compared to data obtained from experiments. In most cases, there should be no difference between the two ways of representation. However, a new absorption maximum can emerge if two or more excited states are of the similar intensity and have an energy gap of appropriate size.

The fourth group of descriptors are surface plots. These plots include frontier molecular orbitals (FMOs), natural transition orbitals[52] (NTOs, not featured in Table 3-1 due to no usage record), spin density surfaces, and electrostatic potential (ESP) maps. These plots can either be isovalue plots or projection plots onto total density surface.

An ESP map, sometimes referred to as a molecular electrostatic potential (MESP) map, is a plot of electrostatic potentials projected onto the electron density surface. It can be used for visualisations of nucleophilic or electrophilic regions on the structures, which can be useful for further applications related to interactions such as adsorption or catalysis. The discussion regarding ESP and non-covalent interactions can be found in Chapter 5.

In terms of structural hierarchy discussed earlier, atomic charges are applicable for the discussion regarding primary or secondary structures. However, descriptors of the third and the fourth group are more related to higher levels of PANI-CMP structures. This section will continue to discuss atomic charges, especially NBO charges, for BQ units in different forms in addition to earlier discussions regarding primary structures in Section 3.1.1. TD-DFT calculations have been performed with **BZN**-$(NH_2)_2$ monomer in difference forms shown in Scheme 3-4.

Charge distributions on atoms in the monomer at different states are listed in Table 3-4 and visualised in Figure 3-3. In addition to atomic charges, three types of atom groups are also considered, namely CH, NH, and C_6H_4 ring. A CH charge is calculated from a sum of a C_{ortho} and a H_{ortho} charge, an NH charge is calculated from a sum of a N charge and a H_N charge, and a C_6H_4 ring charge is calculated from a sum of six carbon and four hydrogen atoms in the phenyl ring. C_6H_4 ring charges and NH group charges are obvious because they have also been used in previous publications (see the discussion earlier). It should be noted that only one H_N atom is integrated into each NH group although, in all cases except **QN** form, there are two hydrogen atoms attached to one nitrogen atom.

*Table 3-4 Charge distributions on different atoms and atom groups in **BZN**-$(NH_2)_2$ monomer of different oxidation and spin multiplicity states. Computational conditions: B3LYP functional,[18-20] 6-31G(d) basis set,[21-30] D3(BJ) empirical dispersion,[31] acetonitrile polarisable continuum model,[32-35] natural bond orbital analysis (NBO) version 3,[53-60] Gaussian 16 (C.01),[51] geometries based on those in Table 3-2*

Form	Atomic Charge					Atom Group Charge		
	C_{ipso}	C_{ortho}	N	H_{ortho}	H_N	CH	NH	C_6H_4 Ring
^{1}**BZ**^{0}	+0.130	-0.274	-0.862	+0.238	+0.403	-0.036	-0.460	+0.116
^{2}**RC**$^+$	+0.216	-0.228	-0.691	+0.269	+0.447	+0.041	-0.244	+0.596
^{1}**QDC**$^{2+}$	+0.347	-0.117	-0.565	+0.303	+0.483	+0.126	-0.082	+1.198
^{3}**DRC**$^{2+}$	+0.162	-0.033	-0.636	+0.302	+0.469	+0.269	-0.167	+1.400
^{1}**QN**^{0}	+0.202	-0.244 -0.211	-0.620	+0.253 +0.257	+0.363	+0.009 +0.046	-0.257	+0.514

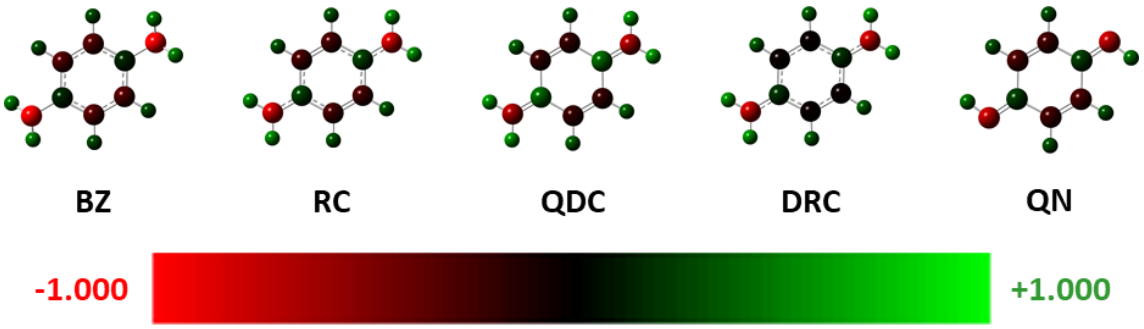

Figure 3-3 Visualisations of charge distributions from Table 3-4 (Gaussview 6.1.1[61])

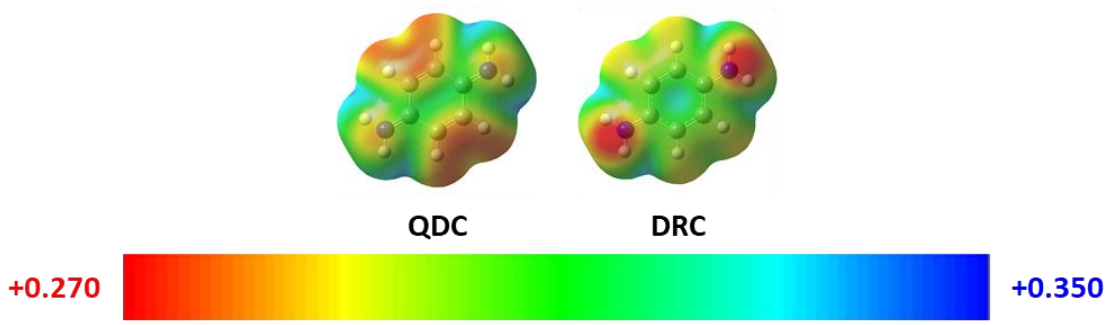

*Figure 3-4 Comparison between ESP maps of **BZN**-$(NH_2)_2$ in quinoidal dication (**QDC**) and diradical cation (**DRC**) forms from the same calculations as in Table 3-4 (visualised using Gaussview 6.1.1[61])*

Oxidations of the benzenoid BQ unit to radical cation (**RC**$^+$) leads to stronger positive changes were observed around C_{ipso}–N bonds (+0.257 for each, +0.514 overall) compared to CH groups in the ring (+0.077 for each, +0.308 overall). The similar trend is also observed in quinoidal dication (**QDC**$^{2+}$), +0.514 for each C_{ipso}–N bond (+1.028 overall) compared to +0.162 for each C_{ortho}–H bond (+0.648 overall). However, oxidation towards diradical cation (**DRC**$^{2+}$), the triplet state counterpart of the **QDC**$^{2+}$ form, shows the opposite trend, with more pronounced positive changes being observed around CH groups (+0.305 for each, +1.220 overall) than around C–N bonds (+0.258 for each, +0.516 overall). It should be noted that changes on charges on the hydrogen atoms on their own are less significant. Therefore, charges on hydrogen atoms are not good descriptors for electronic properties since they cannot aid the differentiations between different oxidised forms. This might be the reason why hydrogen atom charges are usually integrated into heavier atoms or moieties rather than used as descriptors on their own.

Differences between **QDC** and **DRC** forms of **BZN**-$(NH_2)_2^{2+}$ species can also be seen in their electrostatic potential (ESP) maps, Figure 3-4. The **QDC** form has two areas with more electron density (less positive) around both C_{ortho}–C_{ortho} bonds, while the **DRC** form appears to be more uniform and more positive throughout the six-membered ring. Overall, the C_6H_4 ring charge in the **DRC** form is also more positive (+1.400) compared to that in the **QDC** form (+1.198).

This relatively higher uniformity also corresponds to data in Table 3-4, with the gaps between *ortho* and *ipso* carbon charges become closer in the **DRC** form (-0.033 and 0.162, a gap of 0.195) than in other forms. In fact, the **DRC** is the only charged oxidised form in which charge differences between *ortho* and *ipso* carbon atoms decrease from 0.404 in the **BZ** form, with the differences in the **RC** and **QDC** forms increasing to 0.444 and 0.464 respectively. Compared data with earlier discussions regarding geometric structures, data in Table 3-3 and Table 3-4 show good agreements that the **DRC** form is more aromatic and more benzenoid-like compared to the **QDC** form.

Table 3-5 Characteristics of BQ units in three different forms as described by HOMBQ indices and NBO charges

Form	HOMBQ Index	NBO Charge
^{2}RC$^+$	0.773 (more benzenoid-like)	more positive around C–N bonds
^{1}QDC^{2+}	0.131 (more quinoid-like)	
^{3}DRC^{2+}	0.754 (more benzenoid-like)	more positive and uniform throughout the C_6H_4 ring

To determine the structure of BQ units in oligo(aniline)s and poly(aniline)s in positively charged states with uncoupled electrons, HOMBQ indices and NBO charges might be used in combination. Table 3-5 listed characteristics of BQ units in the three positively charged forms. It should also be noted that both changes in HOMBQ indices and NBO charges are the result of oxidation, or in a more literal context, the removal of electrons.

3.2 Theoretical Studies of Oligo(aniline)s with Different Topologies

The main difference between unbranched and branched oligo(aniline)s is the existence of tertiary amino groups. Unbranched oligo(aniline)s contain mainly secondary amino groups and can include primary amino groups if either or both ends are not capped with phenyl groups. However, if branching occurs at any secondary amino groups, tertiary amino groups can be formed. Theoretically, this could cause a difference in their secondary structures. Since the third polymer branch is more sterically hindered than a hydrogen atom, C–N–C angles around the tertiary amino group are more restricted. To reduce this destabilising effect, aromatic units are twisted away further from the propagation plane, which could lead to larger dihedral angles. In turn, overlap and eventual conjugation with non-bonding nitrogen atoms are reduced. The decrease in conjugation affects delocalisation of electrons within benzenoid/quinoid units, which can alter the geometric structures of such units. Meanwhile, electronic structures of branched oligo(aniline)s are also affected since more aryl groups attached to the amino group mean more stabilisations, which allow more positive charges to be located around that amino group. Therefore, it is sensible to suggest that oligo(aniline)s with different topologies will have both different geometric and different electronic structures. These structural differences have been found to affect optical properties,[1] which in turn can be related to various applications of poly(aniline)-based materials including catalysis and adsorption.

Discussions in this section will cover two different aspects. In the first section, the changes in geometric and electronic structures of oligo(aniline)s upon the introduction of tertiary amine groups will be discussed since this concept has rarely been discussed before. The second section

will then focus on the effects from different monomer units when they are introduced into PANI-CMP structures.

3.2.1 Structures of Branched and Unbranched Oligo(aniline)s

To study the effects of branching in these structural parameters of oligo(aniline)s, Ph/Ph capped tetra(aniline) (TANI) has been chosen along with branched derivatives. Branched TANI is named by the positions of tertiary nitrogen atoms. For example, TANI-23 refers to TANI where the second and the third nitrogen atoms are tertiary amines. In this section, three branched structures, TANI-2, TANI-23, and TANI-14 (Scheme 3-8) have been chosen for the study. The numbers of units in branches are set to be symmetric with the original TANI chains to avoid effects from asymmetry. For TANI-2 and TANI-23, since there is an equivalent of two aniline units from the branching nitrogen atom and the nearest end of main TANI chain, the branches are set to be at the same length. On the other hand, for TANI-14, there is only a phenyl ring between the branching nitrogen atom and the nearest end. Therefore, the branches also consist of one phenyl ring. These branches are coloured red in Scheme 3-8.

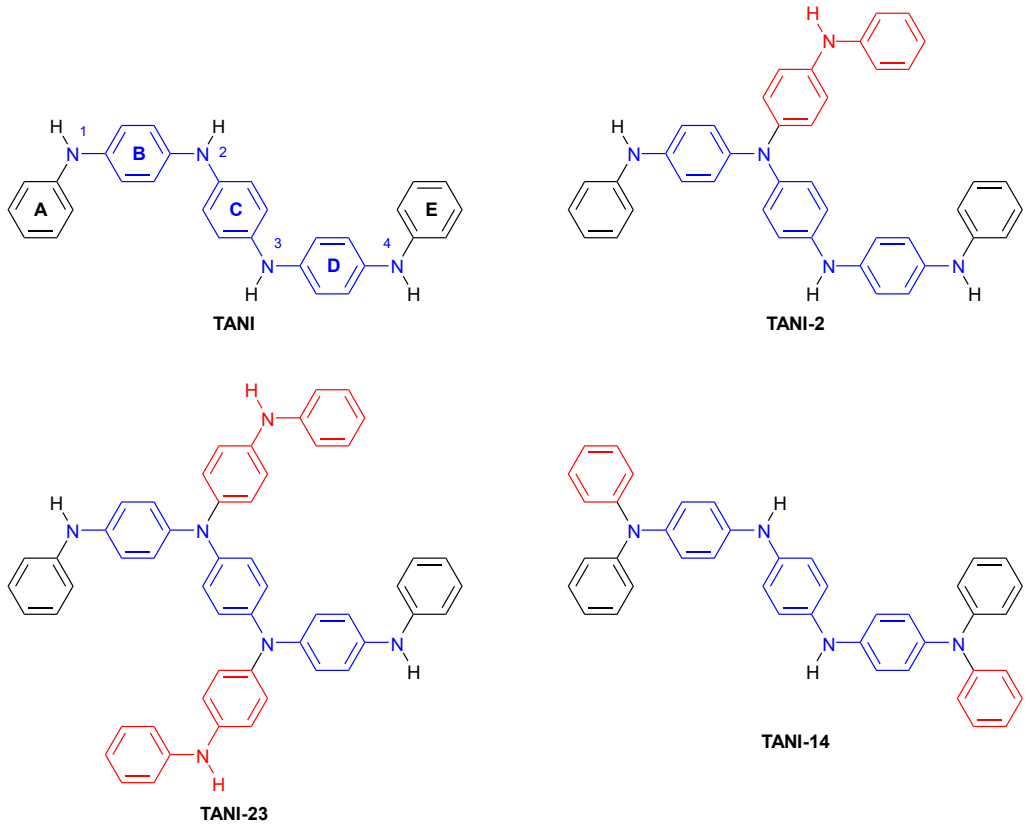

Scheme 3-8 Structures of TANI and branched derivatives chosen for comparative study, as well as numbering and naming conventions for amino groups, carbon rings, and BQ units

The studies of structures for these four oligo(aniline) models will focus on nitrogen atoms and BQ units on the main chain, coloured blue in Scheme 3-8. Nitrogen atoms are numbered 1 to 4 from the left end to the right end, and the benzene rings are named Ring A to Ring E from the left end to the right end. Since there is only one amino group connected to Ring A and Ring E (Scheme 3-8), they cannot be considered as BQ units. Therefore, they are omitted from the considerations, and only Ring B, Ring C, and Ring D are concerned. The BQ units are named in the same way as benzene rings but combined with the two amino groups. Thus, for each oligomeric model, three BQ units (Unit B, Unit C, and Unit D) and four nitrogen atoms (N^1, N^2, N^3, and N^4) will be discussed.

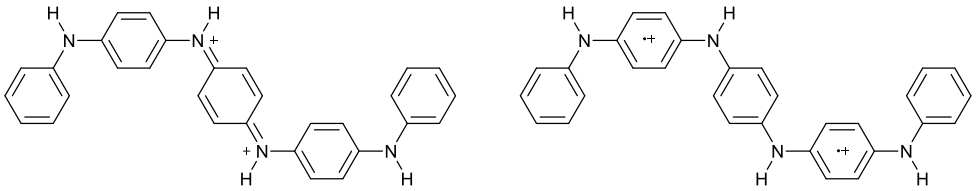

*Scheme 3-9 Structures of TANI in **¹ES** (left) and **³ES** (right) states, as published by Mills et al.[13]*

Oxidations of TANI to **¹ES** and **³ES** states have been a subject of many studies, with known structures of $TANI^{2+}$ in singlet and triplet states in the recent publication given in Scheme 3-9.[13] In short, the difference between structures of singlet and triplet states $TANI^{2+}$ is that in the singlet state, Ring C is less aromatic and more quinoid-like compared to Ring B and Ring D, while in the triplet state, Ring B and Ring D are less aromatic and more quinoid-like instead. While their structures might have been delineated in literature already, structures of TANI in different states will still be explored in this study as the basis for comparison with their branched derivatives.

In this section, the optimisation processes have been performed at the DFT level using the B3LYP functional,[18-20] 6-31G(d) basis set,[21-30] D3(BJ) empirical dispersion,[31] acetonitrile polarisable continuum (PCM) model,[32-35] *Gaussian* 09,[50] while electronic structure analyses have been performed at the DFT level using the same conditions but in *Gaussian* 16 (revision A.03).[49] Both sets of conditions will be applied to TANI and all three branched derivatives in this section. Visualisations of data were done using *GaussView* version 6.1.1.[61]

Table 3-6 HOMBQ indices of TANI in the emeraldine salt states (singlet and triplet) compared to the leucoemeraldine state

State	Unit B		Unit C		Unit D	
	HOMBQ	**ΔHOMBQ**	**HOMBQ**	**ΔHOMBQ**	**HOMBQ**	**ΔHOMBQ**
LEB	0.998		0.997		0.998	
¹ES	0.905	-0.093	0.838	-0.160	0.905	-0.093
³ES	0.868	-0.130	0.995	-0.002	0.868	-0.130

Table 3-7 Secondary structure descriptors of TANI in the emeraldine salt states compared to the leucoemeraldine state

State	C–N–C Angles (A; °)								Dihedral Angles (D; °)							
	Atom N¹		**Atom N²**		**Atom N³**		**Atom N⁴**		**Atom N¹**		**Atom N²**		**Atom N³**		**Atom N⁴**	
	A	**ΔA**	**A**	**ΔA**	**A**	**ΔA**	**A**	**ΔA**	**D**	**ΔD**	**D**	**ΔD**	**D**	**ΔD**	**D**	**ΔD**
LEB	127.7		128.1		128.2		127.8		43.1		43.5		43.4		43.1	
¹ES	128.8	+1.1	130.9	+2.8	130.9	+2.7	128.8	+1.0	41.8	-1.3	34.3	-9.2	34.3	-9.1	41.9	-1.2
³ES	129.1	+1.4	128.7	+0.6	128.7	+0.5	129.1	+1.3	41.2	-1.9	42.1	-1.4	42.1	-1.3	41.2	-1.9

Table 3-8 NBO partial charges on Rings B, C, and D and on nitrogen atoms N^1 to N^4 in TANI from DFT calculations

State	Ring NBO Charge						Nitrogen NBO Charge							
	Ring B		**Ring C**		**Ring D**		**Atom N¹**		**Atom N²**		**Atom N³**		**Atom N⁴**	
	q	**Δq**	**q**	**Δq**	**q**	**Δq**	**q**	**Δq**	**q**	**Δq**	**q**	**Δq**	**q**	**Δq**
LEB	+0.206		+0.203		+0.208		-0.613		-0.612		-0.612		-0.613	
¹ES	+0.524	+0.318	+0.610	+0.407	+0.524	+0.316	-0.522	+0.091	-0.454	+0.158	-0.454	+0.158	-0.522	+0.091
³ES	+0.577	+0.371	+0.444	+0.241	+0.577	+0.369	-0.481	+0.132	-0.504	+0.108	-0.504	+0.108	-0.481	+0.132

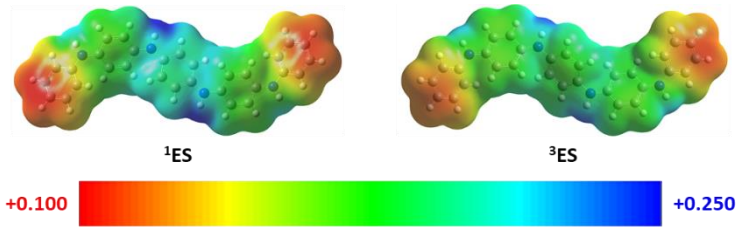

*Figure 3-5 Electrostatic potential (ESP) surface of TANI in **¹ES** and **³ES** states*

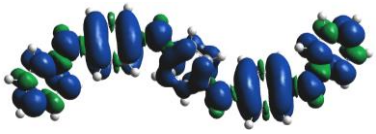

*Figure 3-6 Spin density surface of TANI in the **³ES** state*

Table 3-6 and Table 3-7 list geometric structure descriptors for TANI in three states, while Table 3-8 lists partial charges calculated using natural bond orbital (NBO) analysis.[53-60] As clearly illustrated in Scheme 3-9, the difference between structures of singlet and triplet **ES** TANI, besides the presence or the absence of unpaired electrons, is the position of positive charges. In **¹ES** TANI, the structure of Unit C has become closer to **QDC** form of the BQ unit. It should be noted, however, that the change in HOMBQ index of Unit C is not as strong as in the **QDC** BQ unit (0.160 for **¹ES** TANI Unit C compared to 0.869 in free **BZN**-$(NH_2)_2^{2+}$, see Table 3-5). Meanwhile, in **³ES** TANI, the positive charges are located on Units B and D, and their HOMBQ indices are decreased by 0.130, with structures of both units becoming more like the **RC** form of the BQ unit. Again, the decreases in HOMBQ indices are smaller than that of **RC** BQ unit (0.227). These smaller decreases in bound BQ units, as in TANI, compared to free units can be explained by the fact that there are additional π-conjugations, subduing the effect from oxidation reactions. Therefore, the dearomatising effects in BQ units are then reduced.

The quinoid-like nature of Unit C in **¹ES** TANI can also be seen in the secondary structures. Since both C–N bonds of the Unit C have become more like double bonds, the out-of-plane adjustment has become more restricted. The dihedral angles surrounding nitrogen atoms N^2 and N^3 therefore decreased by approximately 9°. As a result, the corresponding C–N–C angles become widened by 2° approximately. Meanwhile, secondary structures of **³ES** TANI are less changed compared to the **LEB** state, reflecting the more benzenoid-like natures in contrast to those in the singlet counterpart.

Positive charge positions can also be determined by NBO charges and ESP mapping (Figure 3-5) in combination. Both data sets agree that in the case of **¹ES** TANI, Unit C is the most positive region. The NBO charge of Ring C is +0.610, an increase of 0.407 from the **LEB** state, compared to +0.524 for both Ring B and Ring D, and the partial charges on nitrogen atoms N^2 and N^3 in the singlet **ES** state are also less negative than the other two atoms. In contrast, NBO charges of Ring B and Ring D (+0.577) are more positive that that of Ring C (+0.444) in **³ES** TANI. The more positive charges near Ring B and Ring D together with the spin density surface, Figure 3-6, implying that the radical cation should be around both rings. Structures of the two spin isomers are therefore concluded as given in Scheme 3-9.

Structure analyses of branched TANI derivatives from DFT-optimised structures will follow the same discussion as earlier to determine the effects from branching. Table 3-9 lists the energies of the oxidised states relative to their **LEB** states and to each other. They might not be immediately related to the current discussion but will be referred to later in corresponding discussions related to each TANI derivative.

*Table 3-9 Energies of TANI and branched TANI derivatives in singlet and triplet **ES** states, determined from the DFT optimisation earlier mentioned (B3LYP-D3(BJ)/6-31G(d)/acetonitrile PCM/Gaussian 09)*

Model	Energy Relative to the LEB State (kJ·mol^{-1})		^{1}ES-^{3}ES Difference (kJ·mol^{-1})	% ^{1}ES Form at 298 K
	^{1}ES	^{3}ES		
TANI	862.25	861.10	+1.15	38.55
TANI-2	835.95	846.67	-10.73	98.70
TANI-23	820.56	831.90	-10.33	98.98
TANI-14	870.10	862.78	+7.32	4.96

The first branched TANI derivative, TANI-2, has another chain with two aniline units connected to the nitrogen atom N^2, see Scheme 3-8. Geometric structural descriptors for TANI-2 are listed in Table 3-10 and Table 3-11, and electronic structural descriptors are listed in Table 3-12.

Branching at the nitrogen atom N^2 does not affect the primary structure in the **LEB** state, as the HOMBQ indices of all three units remain at 0.999 or almost perfect benzenoid-like. However, for the secondary structure, the difference can be clearly seen around the branching atom N^2. Due to more steric hindrance from the third aryl group, instead of a hydrogen atom as in TANI, the C–N–C angle decreases to only 119.9°, compared to 128.3°-128.7° for other C–N–C angles. Because the in-plane adjustment to avoid *ortho* hydrogen atom repulsions has become more restricted at the branching point, the dihedral angle becomes larger as a result (69.9° compared to 41.6°-43.4°).

The effect from branching is also seen in the electronic structure (Table 3-12). The NBO charge on the nitrogen atom N^2 has become less negative, -0.445 compared to approximately -0.61 for the other three atoms. The neighbouring rings also observe more positive charges although the magnitude of change is smaller than in nitrogen atoms (+0.247 for Ring B and +0.238 for Ring C compared to +0.216 for Ring D). This has concluded that the introduction of branching at the imine/amine nitrogen atom causes significant changes in structures of resulting oligo(aniline)s, both geometrically and electronically.

Table 3-10 HOMBQ indices of TANI-2 in the emeraldine salt states (singlet and triplet) compared to the leucoemeraldine state

State	Unit B		Unit C		Unit D	
	HOMBQ	ΔHOMBQ	HOMBQ	ΔHOMBQ	HOMBQ	ΔHOMBQ
LEB	0.999		0.999		0.998	
^{1}ES	0.934	-0.065	0.884	-0.115	0.958	-0.039
^{3}ES	0.953	-0.046	0.996	-0.003	0.866	-0.132

Table 3-11 Secondary structure descriptors of TANI-2 in the emeraldine salt states compared to the leucoemeraldine state

State	C–N–C Angles (A; °)								Dihedral Angles (D; °)							
	Atom N^1		Atom N^2		Atom N^3		Atom N^4		Atom N^1		Atom N^2		Atom N^3		Atom N^4	
	A	ΔA	A	ΔA	A	ΔA	A	ΔA	D	ΔD	D	ΔD	D	ΔD	D	ΔD
LEB	128.7		119.9		128.3		128.4		41.6		69.9		43.4		42.9	
^{1}ES	128.7	0.0	120.4	+0.5	129.8	+1.5	128.9	+0.5	42.6	+1.0	61.0	-8.9	37.2	-6.2	41.7	-1.2
^{3}ES	128.8	+0.1	119.6	-0.3	128.7	+0.4	129.1	+0.7	41.9	+0.3	66.7	-3.2	42.5	-0.9	41.2	-1.7

Table 3-12 NBO partial charges on Rings B, C, and D and on nitrogen atoms N^1 to N^4 in TANI-2 from DFT calculations

State	Ring NBO Charge						Nitrogen NBO Charge							
	Ring B		Ring C		Ring D		Atom N^1		Atom N^2		Atom N^3		Atom N^4	
	q	Δq	q	Δq	q	Δq	q	Δq	q	Δq	q	Δq	q	Δq
LEB	+0.247		+0.238		+0.216		-0.607		-0.445		-0.609		-0.610	
^{1}ES	+0.506	+0.259	+0.570	+0.332	+0.416	+0.200	-0.539	+0.068	-0.285	+0.160	-0.488	+0.121	-0.554	+0.056
^{3}ES	+0.450	+0.203	+0.468	+0.230	+0.582	+0.366	-0.548	+0.059	-0.328	+0.117	-0.507	+0.102	-0.477	+0.133

Upon the oxidation of TANI-2 to the **^{1}ES** state, the overall changes are similar to that of TANI, with the Unit C becoming more quinoidal. The decreases in dihedral angles surrounding nitrogen atoms N^2 and N^3, the relatively larger decrease in HOMBQ index for Unit C, and the larger increases in NBO charges of moieties related to the Unit C are all present in the case of TANI-2 as well as of TANI. Therefore, it can be concluded that the structure of singlet TANI-2^{2+} should be similar to that of the TANI counterpart (Scheme 3-10).

One clear difference between structures of **^{1}ES** TANI and **^{1}ES** TANI-2 can be seen in their electronic structures. Unit D in TANI-2 is obviously less positive compared to the other two units, as can be observed in the ESP maps (Figure 3-7, left). It should also be noted that the least positive regions can be found at the ends of the three branches. It is possible that electronic structures of the oligo(aniline)s in singlet +2 states tend to be more positive in the centre and become less positive around the peripheral parts. The positive central region tends to surround Unit C and especially on the N^2 end of the unit C where the branching happens. It is arguable that Unit D therefore lies further than the positive region compared to Unit B and Unit C, and as a result, Unit D becomes less positive compared to the other two units.

It should also be noted that in a study involving longer unbranched oligo(aniline) chains (8, 12, and 16 units), the local maxima in ring NBO charge plots tend to be four units apart.[7] The distances between local maxima in those models are longer than any of the branches on TANI-2. Therefore, it is possible that a study on larger models with two branching points located at different distances from each other might lead to different electronic structures. However, studies on larger models are beyond the scope of the current study.

For **^{3}ES** TANI-2, the changes in primary structure follow the same trend as in the TANI counterpart, with the dearomatisation effects being stronger surrounding Units B and D. However, the change in Unit D is stronger, with the decrease in HOMBQ index being 0.132 compared to 0.046 for Unit B. Unit C, same as in TANI, remains benzenoidal. For the secondary structure, its changes upon the oxidation towards the triplet **ES** are less significant than those upon the triplet **ES** state, same as in TANI.

For electronic structures, the increase in ring NBO charge of Ring D is also stronger than those of the other rings (0.366 for Ring D compared to 0.230 for Ring C and 0.203 for Ring B). The trend is also similar for the nitrogen atom charge, with more intense increases for N^4 (0.133) and N^2 (0.117) than for N^3 (0.102) and N^1 (0.059). The least negative nitrogen atom, however, is still the N^2 (-0.328) followed by N^4 (-0.477). This is possibly because the effect from branching which still remains influential. Combining these facts and the spin density surface (Figure 3-8), it can be concluded that the radical cations should be located around the tertiary nitrogen atom N^2 and around Unit D, as shown in Scheme 3-10.

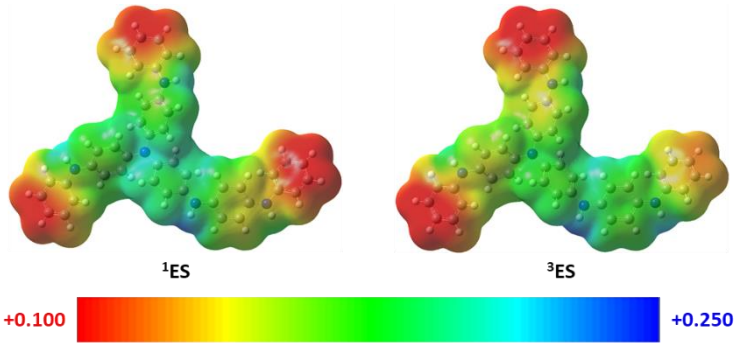

*Figure 3-7 Electrostatic potential (ESP) surface of TANI-2 in **¹ES** and **³ES** states*

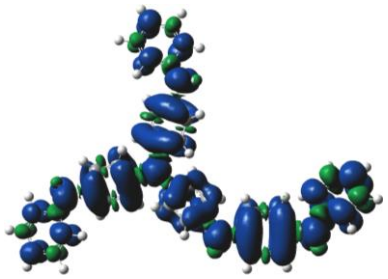

*Figure 3-8 Spin density surface of TANI-2 in the **³ES** state*

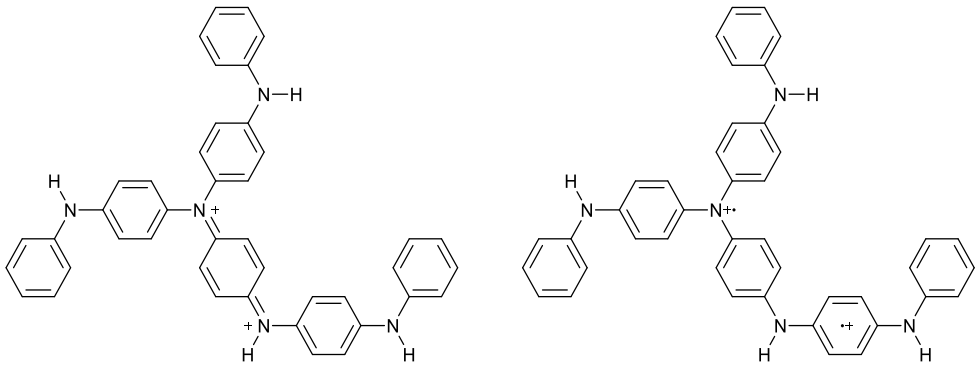

*Scheme 3-10 Structures of TANI-2 in **¹ES** (left) and **³ES** (right) states*

Comparing **³ES** TANI and **³ES** TANI-2, both triplet structures tend to place the radical cations distributed throughout the structure. In the previously mentioned study,[7] distances between local maxima of NBO plots in the case of fully polaronic structures are two units apart, as is the case with TANI in this study. However, for TANI-2, the position of one radical cation has moved from Unit B to nitrogen atom N². Arguably, having three aryl groups connected to the nitrogen atom can stabilise the radical cation better than having only two groups as in unbranched TANI amine moieties.

The introduction of branching, as the extensions of π-conjugations, has led to more stabilisation of the resulting cations from oxidation. These stabilisations can be observed as the relative energies of both singlet and triplet **ES** states, compared to their **LEB** state, of TANI-2 are significantly less than those of TANI, see Table 3-9. However, another significant difference can be seen in the comparison between energies of **ES** TANI or TANI-2 in singlet and triplet states. In the case of TANI, the singlet-triplet energy difference is only 1.15 kJ·mol^{-1} favouring the triplet state, while that in the case of TANI-2, the difference becomes 10.73 kJ·mol^{-1}, with the singlet state becoming more energetically favoured instead. It could be argued that since the radical cations

are essentially pushed closer to each other (Unit B and Unit D in TANI, atom N^2 and Unit D in TANI-2), the closer distance between the two radical cations creates destabilisation effects for the triplet state.

Structural analyses of TANI-2 in **LEB** and **ES** states have revealed that branching can create significant differences in the resulting oligo(aniline) structures compared to the unbranched ones. These differences can be observed in both geometric and electronic structures. Two more branched TANI oligomers have been studied, namely TANI-23 and TANI-14. Both of them feature two branches rather than one as in TANI-2, but branch positions are different. The structure of TANI-23 oligomers in general has the second branch located on the nitrogen atom N^3 in addition to the previously discussed branch on atom N^2. Introducing the new branch at this position can potentially push the two radical cations to be even closer than in the case of TANI-2. Meanwhile, the structure of TANI-14 oligomers features two branches at the nitrogen atoms N^1 and N^4, which resembles the PANI-CMP oligomer from **TPA** and **BZN** monomer units. Therefore, this TANI-14 can lead to further studies on PANI-CMP oligomers from other monomer unit combinations.

For TANI-23 (Table 3-13, Table 3-14, and Table 3-15), similar effects from branching can still be observed around nitrogen atoms N^2 and N^3. Rings bound to these nitrogen atoms are twisted further from the plane compared to other rings as expected. Oxidation reactions towards **ES** states also lead to the same decreases in HOMBQ indices as seen in TANI (more in Unit C in singlet oxidation, more in Units B and D in triplet oxidation) albeit less intense, and secondary structures of TANI-23 are less affected by the oxidation towards ^{3}**ES** state as well. However, the difference in the case of TANI-23 from the previously mentioned TANI and TANI-2 can be seen in electronic structures. In this case, oxidation reactions towards both **ES** state lead to the same trend in NBO charges.

Table 3-13 HOMBQ indices of TANI-23 in the emeraldine salt states (singlet and triplet) compared to the leucoemeraldine state

State	Unit B		Unit C		Unit D	
	HOMBQ	ΔHOMBQ	HOMBQ	ΔHOMBQ	HOMBQ	ΔHOMBQ
LEB	0.999		0.998		0.999	
^{1}ES	0.963	-0.036	0.902	-0.096	0.963	-0.036
^{3}ES	0.954	-0.045	0.993	-0.005	0.954	-0.045

Table 3-14 Secondary structure descriptors of TANI-23 in the emeraldine salt states compared to the leucoemeraldine state

State	C–N–C Angles (A; °)								Dihedral Angles (D; °)							
	Atom N^1		Atom N^2		Atom N^3		Atom N^4		Atom N^1		Atom N^2		Atom N^3		Atom N^4	
	A	ΔA	A	ΔA	A	ΔA	A	ΔA	D	ΔD	D	ΔD	D	ΔD	D	ΔD
LEB	128.7		120.0		120.0		128.7		42.0		68.8		68.8		42.0	
^{1}ES	128.8	+0.1	120.4	+0.4	120.4	+0.4	128.8	+0.1	41.9	-0.1	61.8	-7.0	61.8	-7.0	41.9	-0.1
^{3}ES	128.7	0.0	119.3	-0.7	119.3	-0.7	128.7	0.0	42.2	+0.2	68.1	-0.7	68.1	-0.7	42.2	+0.2

Table 3-15 NBO partial charges on Rings B, C, and D and on nitrogen atoms N^1 to N^4 in TANI-23 from DFT calculations

State	Ring NBO Charge						Nitrogen NBO Charge							
	Ring B		Ring C		Ring D		Atom N^1		Atom N^2		Atom N^3		Atom N^4	
	q	Δq	q	Δq	q	Δq	q	Δq	q	Δq	q	Δq	q	Δq
LEB	+0.251		+0.278		+0.251		-0.607		-0.444		-0.444		-0.607	
^{1}ES	+0.440	+0.189	+0.578	+0.300	+0.440	+0.189	-0.557	+0.050	-0.310	+0.134	-0.310	+0.134	-0.557	+0.050
^{3}ES	+0.452	+0.201	+0.494	+0.216	+0.452	+0.201	-0.548	+0.059	-0.329	+0.115	-0.329	+0.115	-0.548	+0.059

In the case of TANI-23, both nitrogen atoms N^2 and N^3 are affected by more conjugations, with the NBO charges for both atoms being -0.444 compared to -0.607 for the other two atoms. The effects remain influential upon oxidations, and more conjugations also lead to stronger increases in NBO charges for both Ring C and tertiary nitrogen atoms compared to the rest of the molecule. ESP maps of both singlet and triplet **ES** TANI-23 (Figure 3-9) are almost identical, and the spin density surface (Figure 3-10) confirms that the radical cations are indeed on both N^2 and N^3 atoms as expected. Structures of **ES** state TANI-23 are given in Scheme 3-11, and it should be noted that both structures now have cations positioned on the same nitrogen atoms.

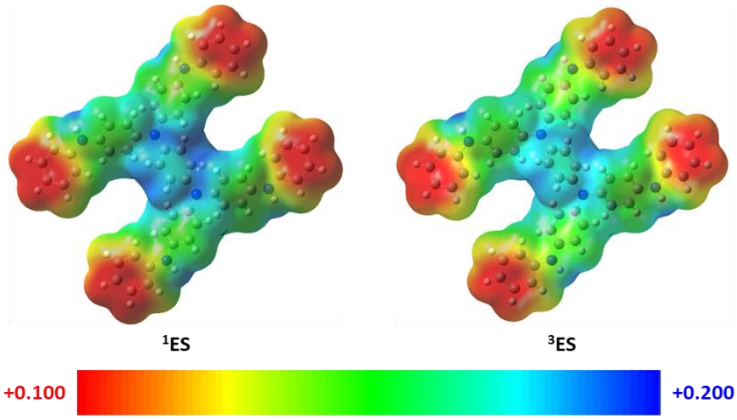

*Figure 3-9 Electrostatic potential (ESP) surface of TANI-23 in ^{1}**ES** and ^{3}**ES** states*

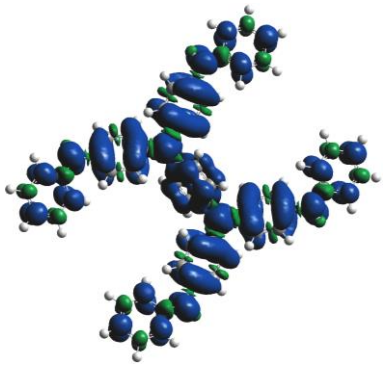

*Figure 3-10 Spin density surface of TANI-23 in the ^{3}**ES** state*

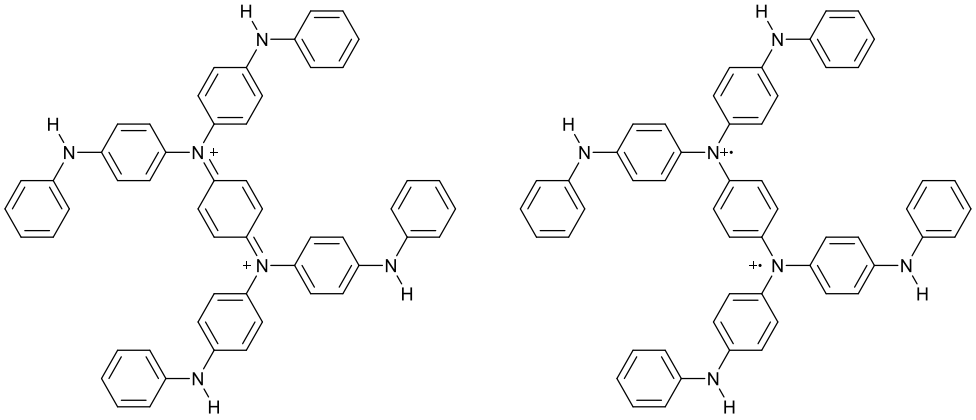

Scheme 3-11 Structures of TANI-23 in ^{1}***ES*** *(left) and* ^{3}***ES*** *(right) states*

The introduction of additional branching leads to further stabilisation of the resulting **ES** TANI-23 (Table 3-9). The destabilisation effect from the closer radical cation distance as in TANI-2 is also observed in TANI-23, with the energy difference of 10.33 kJ·mol^{-1}. Overall, there is no significant difference in terms of energies between TANI-2 and TANI-23.

For TANI-14, overall changes upon oxidation from the **LEB** state to the **ES** states do not differ much from those for unbranched TANI in terms of both geometric and electronic structures. While the dihedral angles surrounding the branching atoms N^1 and N^4 are arguably larger, and their changes in magnitudes upon oxidation are also larger (approximately 10°-11°), these might be the result of initially larger dihedral angles in the **LEB** state, which in turn are results of smaller benzene rings compared to dianiline branches allowing more freedom for out-of-plane adjustments. These changes are not really significant to the general chemistry of TANI-14 compared to TANI.

Table 3-16 HOMBQ indices of TANI-14 in the emeraldine salt states (singlet and triplet) compared to the leucoemeraldine state

State	Unit B		Unit C		Unit D	
	HOMBQ	ΔHOMBQ	HOMBQ	ΔHOMBQ	HOMBQ	ΔHOMBQ
LEB	0.999		0.998		0.999	
^{1}**ES**	0.923	-0.076	0.864	-0.134	0.923	-0.076
^{3}**ES**	0.905	-0.094	0.995	-0.003	0.905	-0.094

Table 3-17 Secondary structure descriptors of TANI-14 in the emeraldine salt states compared to the leucoemeraldine state

State	C–N–C Angles (A; °)								Dihedral Angles (D; °)							
	Atom N^1		Atom N^2		Atom N^3		Atom N^4		Atom N^1		Atom N^2		Atom N^3		Atom N^4	
	A	ΔA	A	ΔA	A	ΔA	A	ΔA	D	ΔD	D	ΔD	D	ΔD	D	ΔD
LEB	119.3		128.4		128.4		119.3		72.5		42.8		42.8		72.5	
^{1}**ES**	121.0	+1.7	130.6	+2.2	130.6	+2.2	121.0	+1.7	62.0	-10.5	35.6	-7.2	35.6	-7.2	62.0	-10.5
^{3}**ES**	120.8	+1.5	128.8	+0.4	128.8	+0.4	120.8	+1.5	62.4	-10.1	41.7	-1.1	41.7	-1.1	62.4	-10.1

Table 3-18 NBO partial charges on Rings B, C, and D and on nitrogen atoms N^1 to N^4 in TANI-14 from DFT calculations

State	Ring NBO Charge						Nitrogen NBO Charge							
	Ring B		Ring C		Ring D		Atom N^1		Atom N^2		Atom N^3		Atom N^4	
	q	Δq	q	Δq	q	Δq	q	Δq	q	Δq	q	Δq	q	Δq
LEB	+0.252		+0.222		+0.252		-0.444		-0.608		-0.608		-0.444	
^{1}ES	+0.536	+0.284	+0.580	+0.358	+0.536	+0.284	-0.359	+0.085	-0.464	+0.144	-0.464	+0.144	-0.359	+0.085
^{3}ES	+0.561	+0.309	+0.424	+0.202	+0.561	+0.309	-0.314	+0.130	-0.517	+0.091	-0.517	+0.091	-0.314	+0.130

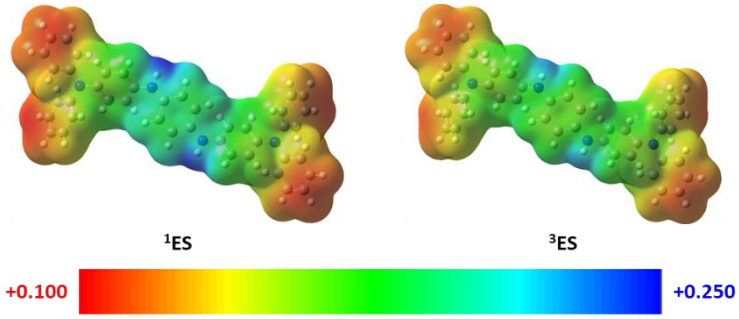

*Figure 3-11 Electrostatic potential (ESP) surface of TANI-14 in **^{1}ES** and **^{3}ES** states*

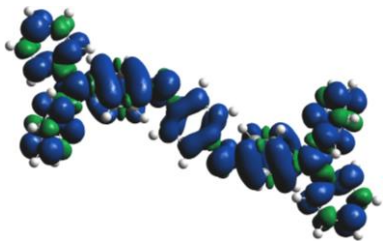

*Figure 3-12 Spin density surface of TANI-14 in the **^{3}ES** state*

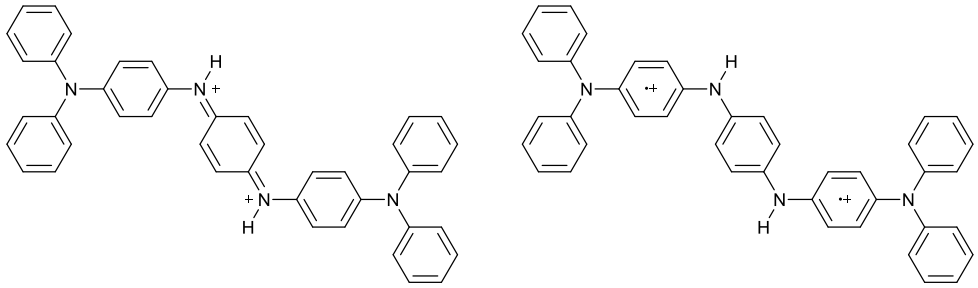

*Scheme 3-12 Structures of TANI-14 in **^{1}ES** (left) and **^{3}ES** (right) states*

The major difference of TANI-14 from TANI-2 and TANI-23 is that the branching atoms are not related to Unit C, which is the BQ unit to become more quinoidal upon the oxidation towards the **^{1}ES** state. This difference from TANI-2 and TANI-23 and the larger resemblance to unbranched TANI mean that the stabilising effects are not seen in the case of TANI-14. Instead, the gap between **LEB** TANI-14 and **^{1}ES** TANI-14 are even wider. It is possible that the introduction of branches at nitrogen atoms N^1 and N^4 has somehow either destabilised the **^{1}ES** state or stabilised the **LEB** state, but a clear conclusion cannot be drawn.

Meanwhile, for the triplet **ES** state, there is also no significant change between TANI and TANI-14 for radical positions or energies. Positions or radical cations might have shifted closer to the two branching nitrogen atoms (Figure 3-12). However, they still remain on their respective units rather than being completely on the nitrogen atoms.

Geometric and electronic structures of three branched TANI derivatives are discussed in comparison with those of unbranched TANI based on DFT calculations. The introduction of branching can alter structures of the singlet or the triplet **ES** state of oligo(aniline)s, which potentially can affect the relative stability of polaronic or bipolaronic structures, depending on the positions and distances between branching points. However, for TANI-14, the PANI-CMP analogue, the effects of branching on their structures are relatively less significant compared to TANI-2 and TANI-23. Nevertheless, the uses of primary and secondary structure concepts are still a logical way for the discussions of these oligomeric structures.

3.2.2 Structures of PANI-CMP Oligomeric Models

PANI-CMPs in this study are prepared from A_3+B_2 polymerisation reactions, i.e., with trifunctional core and bifunctional linker units. While the resulting structures of PANI-CMPs can be likened to branched poly(aniline)s, the design process itself is different. Therefore, for the structure-property relationship, a slightly different approach or consideration is required to suit the design process. This section explores the relationship between different monomers and structures of resulting oligomers, focusing on three core units, two linker units, and two different oligomer topologies.

The discussion in this section will start from establishing the primary and secondary structures of PANI-CMP oligomers which are slightly different from those of TANI derivatives in the previous section. Then the structure of **OTPA-BZN-210**, the most basic PANI-CMP oligomer which still holds a fair resemblance to TANI-14 will be discussed first as a starting point. Further discussions will be made as structures of PANI-CMPs are being modified further.

3.2.2.1 Geometric Structural Parameters for PANI-CMPs

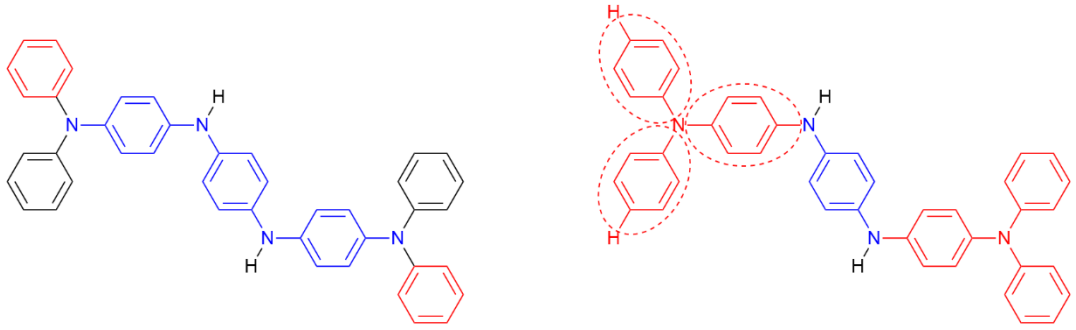

Scheme 3-13 The comparison between two different approaches for the consideration of branched oligo(aniline)s (left) and PANI-CMP oligomeric model (right) with the same chemical component

The structure of TANI-14 in the previous section is essentially the same as that of **OTPA-BZN-210**, with Unit C of TANI-14 being similar to the 1,4-phenylene BQ linker unit. Meanwhile, nitrogen atoms N^1 and N^4 are analogous to the tertiary nitrogen atoms in the two triphenylamine core units. Therefore, TANI-14/**OTPA-BZN-210** model will be used to demonstrate different dissections for two different aspects of geometric structures in this section and the previous section, as shown in Scheme 3-13. The difference between TANI-14 and **OTPA-BZN-210** emerges from the different chemical natures of the two species. TANI-14 is created to be a branched derivative of TANI and therefore can be considered in the same way as oligo(aniline)s, with the BQ units being the primary structure units. However, **OTPA-BZN-210** is a model created for PANI-CMP discussions, which in principle are synthesised either from **TPA**-Br_3 and **BZN**-$(NH_2)_2$ or from **TPA**-$(NH_2)_3$ and **BZN**-Br_2 depending on the synthesis pathway.

Because PANI-CMPs in this study are prepared from A_3 core monomers and B_2 linker monomers, linker units bear more resemblance to BQ units than core units. Therefore, in further discussions, the terms “BQ units” and “HOMBQ” will be used for the discussions regarding **FLR**

linker despite structural differences. Scaling of HOMBQ for **FLR** linkers will be calibrated using structures of **FLR** linker in **LEB** and **EB** states, respectively as "one" and "zero" in the same manner as **BZN** linker. However, the structures of core units are less straightforward.

Three core units chosen for this study are triphenylamine (**TPA**), 1,3,5-triphenylbenzene (**TPB**), and 2,4,6-triphenyl-1,3,5-triazine (**TPT**). The common characteristic among the three core units is that they all resemble a tri-blade propeller consisting of a *hub* and three *blades*. The hub in this case is where the three units differ (a nitrogen atom for **TPA**, a benzene-1,3,5-triyl group for **TPB**, and a 1,3,5-triazine-2,4,6-triyl group of **TPT**), while the blades for all three monomers are **BZN** BQ units. Therefore, the geometric structures of core units can be divided into three parts, namely the hubs, the blades, and the hub-blade connections. Hubs and blades of core monomer units are divided as shown in Scheme 3-14.

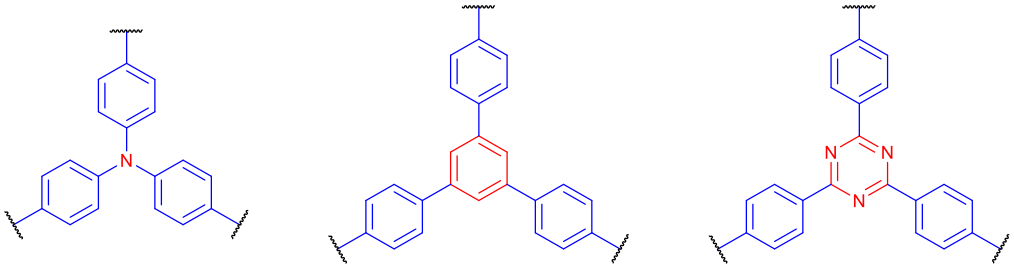

*Scheme 3-14 Hub (red) and blade (blue) parts of the three core monomer units, **TPA** (left), **TPB** (middle), and **TPT** (right)*

Since the hub of a **TPA** core unit is essentially a nitrogen atom, there is no importance for describing the hub geometry of this core unit. Meanwhile, while the other two core units may have multiple atoms and bonds, there is no practical way to establish a scale for aromaticity indices or any other geometry-related descriptors. Besides, models being used in this study only have one branch that forms further conjugations with linker units, which means that any structural influences that might be observed may not be found in the actual PANI-CMPs. Therefore, geometric structural parameters of the hub parts will not be discussed in this study. However, NBO charges of these units may be used in the same way as NBO charges on nitrogen atoms in the previous section.

For the blades, the previously discussed primary structure descriptors can be used for the discussions in this section as well. However, as mentioned earlier, not all blades are forming further conjugations with linker units. Therefore, the discussions will focus only on the blades that are connected or bound to linker units.

Table 3-19 Selected geometric structure parameters from the DFT-optimised structures of monomers in this study (B3LYP-D3(BJ)/6-31G(d)/1,4-dioxane PCM/Gaussian 16 (A.03))

Core Unit / Functionality	BQ Blade HOMBQ Index			Hub-Blade Dihedral Angle		
	TPA	TPB	TPT	TPA	TPB	TPT
Aminated	0.999	0.951	0.954	41.6°	35.5°	0.2°
Brominated	-1.276	-1.326	-1.291	40.4°	36.9°	0.0°

Table 3-19 lists the HOMBQ indices of BQ blades from DFT-optimised structures of the three aminated core monomers. Calculations were performed on the **LEB** equivalents for all three monomers. HOMBQ indices of BQ units in **TPB**-$(NH_2)_3$ and **TPT**-$(NH_2)_3$ are deviated slightly from unity to approximately 0.95 because for each BQ unit in both core monomers, one C–N bond is replaced by one C–C bond. The differences between these BQ units and original **BZN** BQ units are

too miniscule to justify recalibrating a separate scale for core blade BQ units. Meanwhile, the indices of brominated core monomers are approximately -1.3 because C–Br bonds are clearly longer than C–N or C–C bonds. The staggering differences skew the indices vastly.

The hub-blade connections are also as important as the blades themselves due to the potential steric hindrances that cannot be explained solely by the hub or blade geometries. The three "blades" in **TPA** monomers cannot be coplanar because of steric hindrances between hydrogen atoms in *ortho* positions. Similar behaviours can be seen in **TPB** monomers although through slightly different explanations. The "hub" and "blade" benzene rings can be considered as similar to biphenyls, with two rings also twisting out of the plane to reduce *ortho*-induced hindrances.[62] However, the triazine "hub" of **TPT** monomers lacks hydrogen atoms in *ortho* positions as these CH units have been replaced by nitrogen atoms. Therefore, while steric hindrance renders **TPA** and **TPB** units to be in D_3 symmetry, **TPT** units can be in D_{3h} symmetry due to the lack of such hindrance. This can be observed in dihedral angles of the "blade" against its "hub" in DFT-optimised structures listed in Table 3-19. These dihedral angles are defined using the chemical bond between the hub and the blade moieties as the second and the third atoms.

Secondary geometric structures of these PANI-CMP models concern the C–N–C angles and the dihedral angles at the junction between core and linker units, similar to the branched TANI models. There is no significant difference between secondary structures of PANI-CMPs and TANI derivatives.

This section has aimed to establish the basic understanding for primary and secondary structures of PANI-CMPs which are different from those of TANI derivatives mentioned in the previous chapter. For PANI-CMPs, monomer units have to be considered instead of the BQ units, and structures of core monomer units are slightly more complicated due to their geometries. Nonetheless, structures of these oligomers should not be significantly different in principle.

*3.2.2.2 Structures of **OTPA-BZN-210** and **OTPA-BZN-221** Models*

The simplest PANI-CMP oligomers in terms of similarity to oligo(aniline)s are **OTPA-BZN** oligomers. Synthetically, they are prepared from the BH coupling reactions between **TPA** (triphenylamine) and **BZN** (phenylene) monomers. Structures of **TPA** core monomer units can be described as three **BZN** BQ units attached to a nitrogen atom.

To keep the following discussions simple, there will be no complete distinction between primary and secondary structures. Instead, data tabulations will be done in a similar manner as in Section 3.2.1, with one table for HOMBQ indices, one table for C–N–C and dihedral angles, and one table for NBO charges. The hub-blade dihedral angles for describing the structures of **TPA** core units are listed together with other C–N–C and dihedral angles. However, the hub-blade dihedral angles are defined using the bond directly linked between the phenyl ring and the hub nitrogen atom, which are different from the ring dihedral angles defined by the imaginary bond between two *ortho* carbon atoms of the adjacent units. Due to the symmetry of these models, the differences between geometric and electronic structures of both core units present are miniscule. Therefore, only one data value will be given for each core unit entry.

In addition to **OTPA-BZN-210** models, with two core units, one linker unit, and no cyclisation, **OTPA-BZN-221** models with two core units, two linker units, and one cycle are also included for comparison. These two models represent the two extreme cases of strains, one with no strain at all, another with the smallest ring possible and subsequently highest strain, resulting from the copolymerisation between the two monomers. Since each **OTPA-BZN-221** model has two linker units instead of one, to ensure that both units are oxidised, the emeraldine salt states

are set to have the oxidation state of +4. For spin isomers, singlet and quintet are used for **221** models instead of singlet and triplet as for **210** models.

Another inclusion for discussions in this section is the emeraldine base or **EB** state. This state has become more of interest due to its prevalence in actual synthesised polymers, which can be useful for further discussions regarding adsorption properties, which can be found in Chapter 5.

Optimisation processes for PANI-CMP models were performed slightly differently from those of TANI derivatives. They were done using the *Gaussian* 16 (revision A.03)[49] with tetrahydrofuran PCM while the same functional, basis set, and dispersion model were used. The changes should not result in significant differences in addition to those emerging from the nature of chemical systems themselves. This fact can be proven by comparing data for **OTPA-BZN-210** to the corresponding data for TANI-14 (Table 3-20 to Table 3-16, Table 3-21 to Table 3-17, and Table 3-22 to Table 3-18). The two data sets differ only slightly.

*Table 3-20 HOMBQ indices of BQ units in the core and linker units of **OTPA-BZN-210** in the emeraldine salt and emeraldine base states (singlet and triplet) compared to the leucoemeraldine state*

State	Core Unit		Linker Unit	
	HOMBQ	ΔHOMBQ	HOMBQ	ΔHOMBQ
LEB	0.993		0.998	
^{1}ES	0.922	-0.071	0.886	-0.112
^{3}ES	0.910	-0.083	0.996	-0.002
EB	0.985	-0.008	0.314	-0.684

*Table 3-21 C–N–C angles and dihedral angles of **OTPA-BZN-210** in the emeraldine salt and emeraldine base states compared to the leucoemeraldine state*

State	C–N–C Angles (A; °)		Dihedral Angles (D; °)			
	Nitrogen Atom		Nitrogen Atom		Hub-Blade	
	A	ΔA	D	ΔD	D	ΔD
LEB	128.3°		43.1°		49.9°	
^{1}ES	130.5°	+2.2°	36.0°	-7.1°	25.3°	-24.6°
^{3}ES	128.8°	+0.5°	41.9°	-1.2°	27.8°	-22.1°
EB	123.0°	-5.3°	43.7°	+0.6°	35.0°	-14.9°

*Table 3-22 NBO partial charges on C_6H_4 rings of BQ units, on hub parts of core units, and on nitrogen atoms in **OTPA-BZN-210** from DFT calculations*

State	Ring NBO Charge				Core Unit Hub NBO Charge		Nitrogen NBO Charge	
	Core Ring		Linker Ring					
	q	Δq	q	Δq	q	Δq	q	Δq
LEB	+0.253		+0.224		-0.444		-0.607	
^{1}ES	+0.534	+0.281	+0.550	+0.326	-0.353	+0.091	-0.472	+0.135
^{3}ES	+0.548	+0.295	+0.414	+0.190	-0.310	+0.134	-0.522	+0.085
EB	+0.300	+0.047	+0.476	+0.252	-0.434	+0.010	-0.433	+0.174

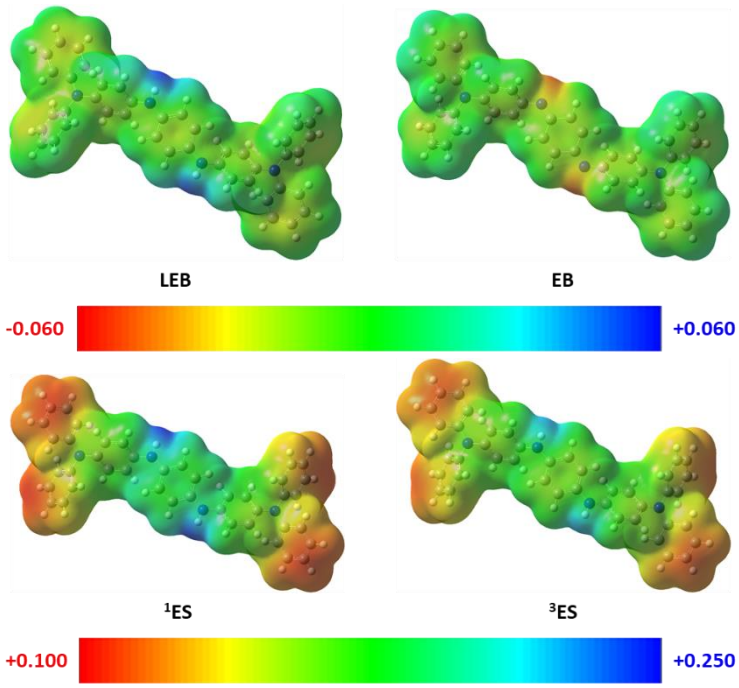

*Figure 3-13 Electrostatic potential (ESP) surface of **OTPA-BZN-210** in four different states. Neutral states **LEB** and **EB** are coloured according to the middle scale bar, while +2 states **¹ES** and **³ES** are coloured according to the bottom scale bar.*

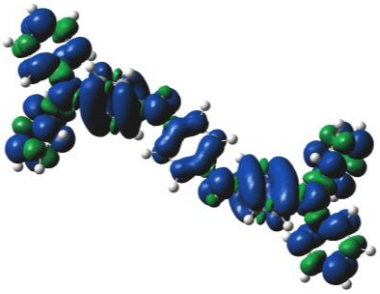

*Figure 3-14 Spin density surface of **OTPA-BZN-210** in the **³ES** state*

As also illustrated in Figure 3-13 and Figure 3-14, the ESP maps and the spin density surface of **OTPA-BZN-210** do not differ much from those of TANI-14. Therefore, chemical structures given in Scheme 3-12 should also apply to those of **OTPA-BZN-210** as well.

For the **EB** state of **OTPA-BZN-210**, the HOMBQ index of the linker BQ unit decreases, as expected, by 0.684 to only 0.314, while those of the core BQ units only decrease slightly (by 0.008). The NBO charge on the linker phenylene ring has increased by 0.252 to 0.476, while those of the core units only increase by 0.047 to 0.300. This, together with the larger increases in nitrogen atom NBO charges surrounding the linker unit, should also be expected for the BQ unit with essentially higher oxidation state.

For **OTPA-BZN-221**, oxidations of this oligomer from the **LEB** state to the **ES** states lead to totally opposite changes in HOMBQ indices (Table 3-23). The oxidation of **OTPA-BZN-221** to the **¹ES** state leads to larger decreases of HOMBQ indices in core units (by 0.143) than in linker units (by only 0.006). Such large decreases of core unit HOMBQ indices in combination with drastic increases in C_6H_4 ring NBO charges in bound core units (+0.419, compared to +0.284 for linker units) imply that the effects from oxidation reactions should be observed around the core units, not the linker units.

*Table 3-23 HOMBQ indices of BQ units in the core and linker units of **OTPA-BZN-221** in the emeraldine salt and emeraldine base states (singlet and triplet) compared to the leucoemeraldine state*

State	Core Unit		Linker Unit	
	HOMBQ	ΔHOMBQ	HOMBQ	ΔHOMBQ
LEB	0.996		0.999	
^{1}ES	0.853	-0.143	0.993	-0.006
^{5}ES	0.994	-0.002	0.855	-0.144
EB	0.991	-0.005	0.268	-0.731

*Table 3-24 C–N–C angles and dihedral angles of **OTPA-BZN-221** in the emeraldine salt and emeraldine base states compared to the leucoemeraldine state*

State	C–N–C Angles (A; °)		Dihedral Angles (D; °)			
	Nitrogen Atom		Nitrogen Atom		Hub-Blade	
	A	ΔA	D	ΔD	D	ΔD
LEB	125.1°		44.8°		53.2°	
^{1}ES	128.0°	+2.9°	36.1°	-8.7°	40.2°	-13.0°
^{5}ES	127.2°	+2.1°	41.6°	-3.2°	49.1°	-4.1°
EB	121.9°	-3.2°	43.0°	-1.8°	51.9°	-1.3°

*Table 3-25 NBO partial charges on C_6H_4 rings of BQ units, on hub parts of core units, and on nitrogen atoms in **OTPA-BZN-221** from DFT calculations*

State	Ring NBO Charge				Core Unit Hub NBO Charge		Nitrogen NBO Charge	
	Core Ring		Linker Ring					
	q	Δq	q	Δq	q	Δq	q	Δq
LEB	+0.267		+0.208		-0.447		-0.618	
^{1}ES	+0.686	+0.419	+0.492	+0.284	-0.260	+0.187	-0.496	+0.122
^{5}ES	+0.560	+0.293	+0.662	+0.454	-0.266	+0.181	-0.493	+0.125
EB	+0.320	+0.053	+0.518	+0.310	-0.439	+0.008	-0.425	+0.193

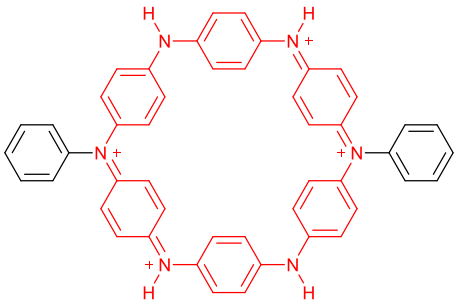

*Figure 3-15 A structure of singlet **OTPA-BZN-221^{4+}**, with the cyclic hexa(aniline) moiety shown in red*

One plausible way to explain the unexpected changes is to consider the structure of **OTPA-BZN-221** as a branched cyclic hexa(aniline), as in Figure 3-15. As being the case with branched TANI derivatives, namely TANI-2 and TANI-23, the quinoidal form with the third aryl group bound to a nitrogen atom tend to be more stable due to further conjugations. Therefore, it is more likely for any of the core BQ units to become quinoidal rather than any of the linker BQ units. However, Figure 3-15 is still not an accurate representation for the structure of the **^{1}ES** form of **OTPA-BZN-221** due to the lack of symmetry. The ESP map of **^{1}ES** form (Figure 3-16) reveals that all four core C_6H_4 rings in the cyclohexa(aniline) ring should be equally positive, while

the structure shown in Figure 3-15 implies that for a core unit, one phenylene ring is more positive and quinoidal than another.

Structural data discussed agree that the relatively positive regions should be surrounding both core units. This is also supported by the decreases in hub-blade dihedral angles for core units by 13°, implying more quinoidal characteristics. Therefore, the structure of **OTPA-BZN-221** in the singlet +4 state should be better represented as in Scheme 3-15. However, this structure is still not the best representation because it still puts the linker unit nitrogen atoms to be more positive, which disagrees with the ESP map (Figure 3-16) which shows that the core unit nitrogen atoms are more positive.

For the quintet state, the opposite trends are observed. Linker BQ units become more dearomatised with the decreases in HOMBQ indices of 0.144 compared to only 0.002 for core BQ units. Meanwhile, the NBO charges on the linker C_6H_4 rings also increase to the larger extents (+0.454 compared to +0.293 for the core rings). The charges on core nitrogen atoms, however, increase by larger margins than those on linker nitrogen atoms, +0.181 compared to +0.125. Therefore, combining these facts with the spin density surface (Figure 3-17), two of the four radical cations should be placed on the linker units, and the other two should be on the nitrogen atoms in the core units, as shown in Scheme 3-15. There is no significant difference between ESP maps of the **221** oligomers in both +4 states as shown in Figure 3-16.

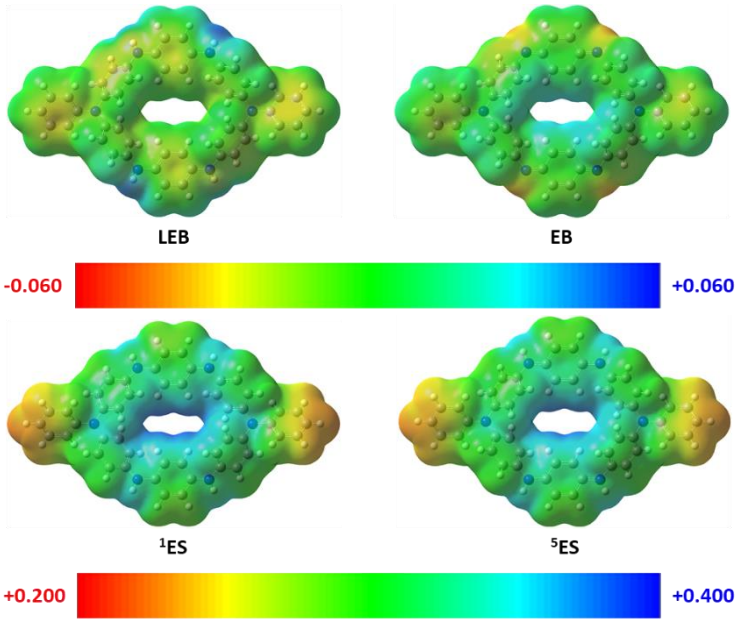

*Figure 3-16 Electrostatic potential (ESP) surface of **OTPA-BZN-221** in four different states. Neutral states **LEB** and **EB** are coloured according to the middle scale bar, while +4 states **¹ES** and **⁵ES** are coloured according to the bottom scale bar.*

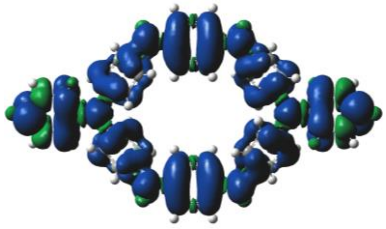

*Figure 3-17 Spin density surface of **OTPA-BZN-221** in the **⁵ES** state*

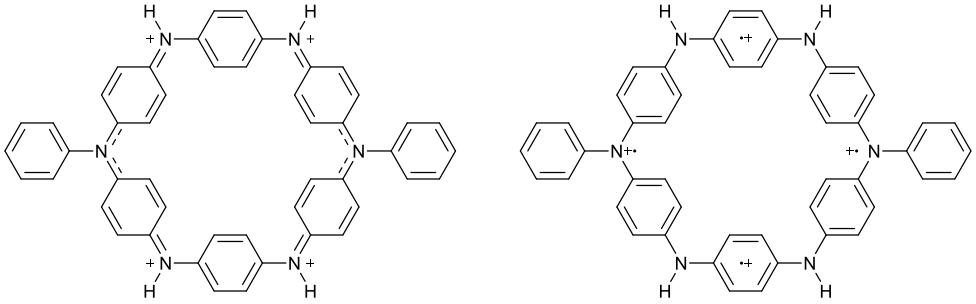

*Scheme 3-15 Structures of **OTPA-BZN-221** in **¹ES** (left) and **⁵ES** (right) states*

The similarity in charge distributions of the two spin isomers might be from the size of the main oligo(aniline) chains and the magnitude of charges. For **OTPA-BZN-221** in the singlet form, there are two bipolarons (+2 charge for each), and they have to be situated furthest away from each other. Since tertiary amine groups of the core units can stabilise the bipolarons better, each of the bipolarons tend to straddle over two core BQ units. Meanwhile, for the quintet form, there are four polarons (+1 charge for each) which also have to be separated from each other. Two of them are on the two core unit nitrogen atoms for the similar reason as their bipolaron counterparts, and the other two, as a result, are located on the two linker units. While NBO charges on C_6H_4 rings can distinguish the two spin isomers apart, the limited space on the cyclohexa(aniline) ring means that these local charge maxima are not far apart, and they can influence the neighbouring areas on the molecules, resulting in almost identical electrostatic potential surfaces between the two spin isomers.

It should also be noted that the +4 oxidation states in the case of **OTPA-BZN-221** is actually slightly higher than the normal **ES** states found in poly(aniline)s. Generally, poly(aniline)s in the fully oxidised state, pernigraniline base or **PB**, consist of BQ units in benzenoid and quinoid forms in equal numbers, while those in the emeraldine *base* or **EB** state, which is the half-oxidised form, have three quarters of BQ units being in the benzenoid form. Poly(aniline)s in the emeraldine *salt* or **ES** state, which is the protonated or acid-doped form of the **EB** state, have three quarters of BQ units in the benzenoid form and one quarter in either polaron or bipolaron form. However, if both linker units in the **221** models become oxidised, the ratio between polaron/bipolaron BQ units to all BQ units will be one third, which is more than one fourth as in typical **ES** poly(aniline)s. This fact means that the +4 oxidation states might be rare, given that oxidising poly- and oligo(aniline)s beyond the **ES** or **EB** state usually require strong oxidising agents such as Ag_2O.[12, 13] However, these **221** models are chosen as one extreme case for ring strain, which is already less likely to happen, and the +4 state is chosen to ensure that both linker units are oxidised and reduce further possibilities for partial oxidations.

Deprotonation of +4 state **OTPA-BZN-221** to the **EB** state leads to the similar result as in **OTPA-BZN-210**, with the NBO charges being greater on the linker BQ units for both phenylene rings and nitrogen atoms. It should also be noted that the four protons to be removed are all attached to secondary amine groups and are the only acidic protons connected to electronegative atoms.

Structures of oligo(aniline) models with cyclic topology at various oxidation states have been delineated and compared against those of the open-chain oligo(aniline)s. The structure of both cyclic and open-chain oligomers in both the **LEB** and the **EB** states are similar, with the linker units being oxidised to the quinoid form. However, for the **ES** states, further complications from cyclic structures and the higher oxidation states than typical **ES** oligo(aniline)s cause the structures of **ES** cyclic oligo(aniline)s to differ from those of open-chain oligomers. It has become more challenging to pinpoint structural features of these oligomers in detail. Therefore,

structures of **221** oligomers will not be discussed in detail for other core-linker combinations. However, their optoelectronic spectra will still be discussed in comparison with those of the **210** counterparts.

*3.2.2.3 Structures of **OTPA-FLR-210** Oligomers*

Fluorenyl and fluorenylene moieties have been studied and applied for various functional materials due to their tuneable fluorescent properties. Therefore, 2,7-fluorenylene (**FLR**) group has been selected as an additional linker unit in this study.

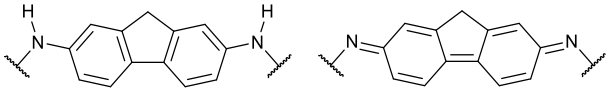

*Scheme 3-16 Structures of **FLR** BQ units in the benzenoid (**BZ**, left) and quinoid (**QN**, right) forms*

Structures of BQ units for **FLR** linker units in **BZ** and **QN** forms are shown in Scheme 3-16, while those of other forms can also be defined similarly to Scheme 3-4. HOMBQ indices for **FLR** linker units are calibrated based on structures of **FLR**-$(NH_2)_2$ and the oxidised form, **FLR**=$(NH)_2$.

*Table 3-26 HOMBQ indices of BQ units in the core and linker units of **OTPA-FLR-210** in the emeraldine salt and emeraldine base states (singlet and triplet) compared to the leucoemeraldine state*

State	Core Unit		Linker Unit	
	HOMBQ	ΔHOMBQ	HOMBQ	ΔHOMBQ
LEB	0.995		0.999	
^{1}ES	0.943	-0.052	0.855	-0.144
^{3}ES	0.905	-0.090	0.996	-0.003
EB	0.979	-0.016	0.370	-0.629

*Table 3-27 C–N–C angles and dihedral angles of **OTPA-FLR-210** in the emeraldine salt and emeraldine base states compared to the leucoemeraldine state*

State	C–N–C Angles (A; °)		Dihedral Angles (D; °)			
	Nitrogen Atom		Nitrogen Atom		Hub-Blade	
	A	ΔA	D	ΔD	D	ΔD
LEB	128.9°		42.6°		48.2°	
^{1}ES	130.7°	+1.8°	35.8°	-6.8°	26.1°	-22.2°
^{3}ES	129.1°	+0.2°	41.6°	-1.0°	27.8°	-20.4°
EB	123.3°	-5.6°	43.4°	+0.8°	36.2°	-12.0°

*Table 3-28 NBO partial charges on rings of BQ units, on hub parts of core units, and on nitrogen atoms in **OTPA-FLR-210** from DFT calculations*

State	Ring NBO Charge				Core Unit Hub NBO Charge		Nitrogen NBO Charge	
	Core Ring		Linker Ring					
	q	Δq	q	Δq	q	Δq	q	Δq
LEB	+0.262		+0.182		-0.444		-0.603	
^{1}ES	+0.494	+0.232	+0.755	+0.573	-0.366	+0.078	-0.485	+0.118
^{3}ES	+0.542	+0.280	+0.502	+0.320	-0.322	+0.122	-0.511	+0.092
EB	+0.294	+0.032	+0.538	+0.356	-0.432	+0.012	-0.458	+0.145

Overall, geometric and electronic structures of **OTPA-FLR-210** are almost the same as those of the **BZN**-linked counterparts. These similar characteristics include the variations in

HOMBQ indices upon oxidations to different states (Table 3-26), the change in C–N–C and dihedral angles (Table 3-27), and NBO charges (Table 3-28). It should be noted as well that the linker ring NBO charges and their margins of increases are larger in the case of **FLR** BQ units compared to the **BZN** BQ units in all oxidised states. This can be simply because there are more atoms in each **FLR** BQ unit (13 carbon atoms and 8 hydrogen atoms) than in each **BZN** BQ unit (6 carbon atoms and 4 hydrogen atoms).

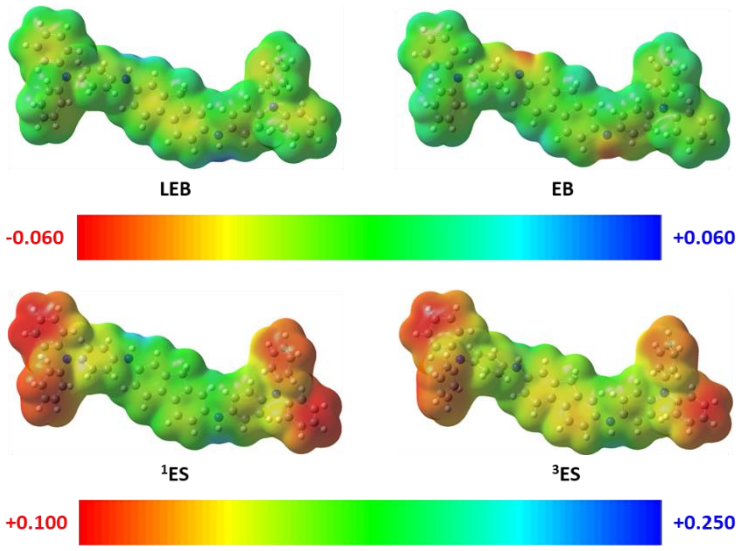

*Figure 3-18 Electrostatic potential (ESP) surface of **OTPA-FLR-210** in four different states. Neutral states **LEB** and **EB** are coloured according to the middle scale bar, while +2 states **¹ES** and **³ES** are coloured according to the bottom scale bar.*

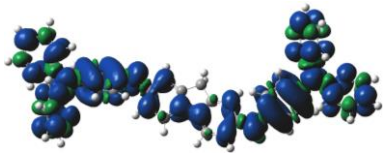

*Figure 3-19 Spin density surface of **OTPA-FLR-210** in the **³ES** state*

Electrostatic potential maps of **OTPA-FLR-210** in different states are shown in Figure 3-18. These surfaces are also similar to those of **OTPA-BZN-210** that the **FLR** BQ units are more positive in the singlet bipolaron form, which in good agreement with the NBO data. Meanwhile, the ESP surfaces imply that the **FLR** BQ units are less positive than the **BZN** BQ units, while the NBO charges on the **FLR** moieties (+0.755 in **¹ES** and +0.502 in **³ES**) are larger than on the **BZN** moieties (+0.550 in **¹ES** and +0.414 in **³ES**). However, if the charges were calculated per atom instead of total charges, NBO charges for each atom in the **FLR** unit will be +0.0360 for the singlet and +0.0239 for the triplet state. For each atom in the **BZN** unit, NBO charges will be +0.0550 for the singlet and +0.0414 for the triplet state, which are larger than those in the **FLR** unit. The fact that there are more atoms in one **FLR** BQ unit than in one **BZN** BQ unit causes the discrepancy between NBO charges and ESP maps.

The spin density surface of **³ES OTPA-FLR-210** (Figure 3-19) is also similar to that of the **BZN**-linked oligomer, with the largest lobes surrounding the bound BQ units from both core units. Therefore, structures of both spin isomers can be deducted in the same ways as those of **OTPA-BZN-210**, as shown in Scheme 3-17. The lack of drastic differences between oligomers with these two different linker units is probably because both **BZN** and **FLR** are aromatic hydrocarbon groups. There are no heteroatoms such as oxygen or nitrogen which might alter the electronic structures either by their electronegativities or by involvements of lone pair electrons in the

conjugation. Therefore, substitution of **BZN** units with **FLR** units would not cause significant changes to either geometric or electronic structures.

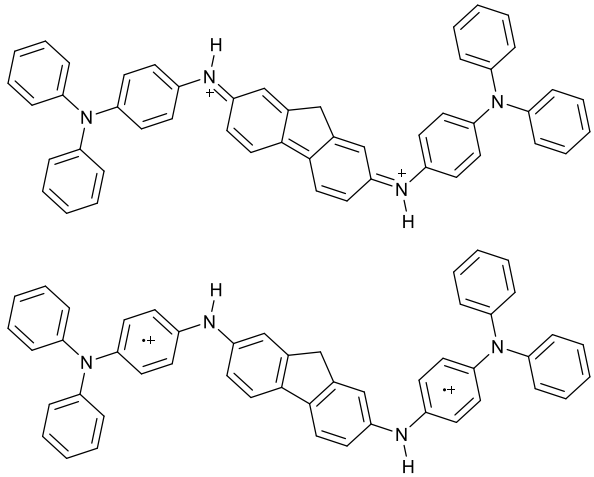

*Scheme 3-17 Structures of **OTPA-FLR-210** in **^{1}ES** (top) and **^{3}ES** (bottom) states*

Structures of **FLR**-linked PANI-CMP oligomers have been studied for comparison with those of **BZN**-linked. Overall, there is no significant difference between structures of **FLR**-linked and **BZN**-linked oligomers due to the fact that both linker units are hydrocarbon and do not have electronegative heteroatoms. Further studies can be performed on heteroatom-containing linker units to see their effects on electronic structures and possibly geometric structures.

*3.2.2.4 Structures of **OTPB-BZN-210** and **OTPB-FLR-210** Oligomers*

This section is intended to discuss the structures of PANI-CMP oligomers with **TPB** or 1,3,5-tris(1,4-phenylene)benzene as a core monomer instead of the original core unit, **TPA** or tris(1,4,-phenylene)amine. The difference between the two core units is that the **TPB** core unit has a benzene ring as the hub part instead of a nitrogen atom as in the **TPA** core unit.

*Table 3-29 HOMBQ indices of BQ units in the core and linker units of **OTPB-BZN-210** in the emeraldine salt and emeraldine base states (singlet and triplet) compared to the leucoemeraldine state*

State	Core Unit		Linker Unit	
	HOMBQ	ΔHOMBQ	HOMBQ	ΔHOMBQ
LEB	0.949		0.998	
^{1}ES	0.934	-0.015	0.743	-0.255
^{3}ES	0.874	-0.075	0.991	-0.007
EB	0.948	-0.001	0.228	-0.770

*Table 3-30 C–N–C angles and dihedral angles of **OTPB-BZN-210** in the emeraldine salt and emeraldine base states compared to the leucoemeraldine state*

State	C–N–C Angles (A; °)		Dihedral Angles (D; °)			
	Nitrogen Atom		Nitrogen Atom		Hub-Blade	
	A	ΔA	D	ΔD	D	ΔD
LEB	128.5°		42.7°		33.9°	
^{1}ES	131.4°	+2.9°	33.2°	-9.5°	28.6°	-5.3°
^{3}ES	129.4°	+0.9°	39.6°	-3.1°	24.8°	-9.1°
EB	122.7°	-5.8°	47.1°	+4.4°	34.3°	+0.4°

*Table 3-31 NBO partial charges on C_6H_4 rings of BQ units, on hub parts of core units, and on nitrogen atoms in **OTPB-BZN-210** from DFT calculations*

State	Ring NBO Charge				Core Unit Hub NBO Charge		Nitrogen NBO Charge	
	Core Ring		Linker Ring					
	q	Δq	q	Δq	q	Δq	q	Δq
LEB	+0.087		+0.236		-0.037		-0.603	
^{1}ES	+0.427	+0.340	+0.756	+0.520	+0.094	+0.131	-0.432	+0.171
^{3}ES	+0.499	+0.412	+0.524	+0.288	+0.160	+0.197	-0.472	+0.131
EB	+0.151	+0.064	+0.546	+0.310	-0.019	+0.018	-0.419	+0.184

Structure descriptors of **OTPB-BZN-210** are listed in Table 3-29, Table 3-30, and Table 3-31. Overall, the same characteristics observed in structures of **OTPA-BZN-210** and the changes as the oligomer undergoes oxidation reactions are also observed in **OTPB-BZN-210**. The key differences between oligomers in these two series, as expected, are related to the core unit structures. First, the hub-blade dihedral angles are not affected by oxidation as much as those in **TPA** core units. The decreases in these **TPB** dihedral angles are 5.3° upon oxidation towards the **^{1}ES** state and 9.1 upon oxidation towards the **^{3}ES** state, compared to 24.6° (singlet) and 22.1° (triplet) observed in **TPA** core units, see Table 3-21. However, the magnitude of hub-blade dihedral angles themselves for the **ES** states are not significantly different, 25.3° (singlet) and 27.8° (triplet) in **OTPA-BZN-210** compared to 28.6° (singlet) and 24.8° (triplet) in **OTPB-BZN-210**.

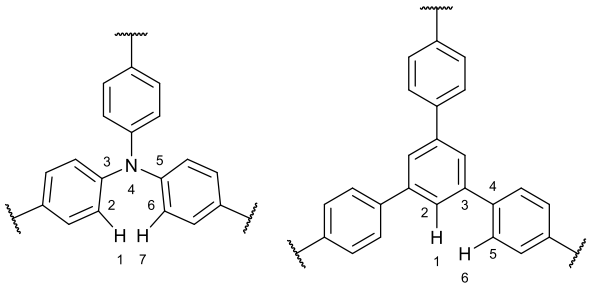

*Scheme 3-18 Structures of **TPA** (left) and **TPB** (right) core units showing two hydrogen atoms causing steric hindrances*

The similarity between hub-blade dihedral angles is also the case for the **EB** state, with the hub-blade dihedral angles being 35.0° for **TPA** oligomer and 34.3° for **TPB** oligomer. The cause for the difference therefore comes from the structures of core units at the **LEB** state. In the case of **TPA**, the hub-blade dihedral angle at the **LEB** state is 49.9°, while the value for the **TPB** oligomer is only 33.9°. This can be explained by considering the structures of **TPA** and **TPB** core units (Scheme 3-18). Both core units have steric hindrances from hydrogen atoms in the *ortho* positions, but the patterns between the two core units are different. For the **TPB** core, the two hydrogen atoms are in the 1,6-pattern, while those in the **TPA** core are in the 1,7-pattern. In both environments, bond angles are generally 120° approximately, which means that for the 1,6-pattern as in **TPB** cores, the two hydrogen atoms will be coplanar and close together enough to cause the repulsive non-covalent interactions. However, for the 1,7-pattern as in **TPA** cores, these two hydrogen atoms will be not only coplanar but also almost at the same position. The 1,7-pattern therefore causes stronger repulsions, and as a result, the two hydrogen atoms have to be pushed away further.

In the case of oxidised states **ES** and **EB**, the alignments between adjacent units may be more governed by the participations in the π-conjugations across neighbouring units. Tilting the

rings away too far from the coplanarity can interrupt the π-overlapping and therefore is unfavourable.

Because the hub of a **TPB** core unit is a benzene ring, which does not contain any heteroatoms, the total NBO charges on the hub part are less negative (-0.035 to +0.106 over 9 atoms, or -0.0039 to +0.0118 per atom) than those of **TPA** nitrogen atom hubs (-0.444 to -0.310, Table 3-25). The lack of heteroatoms also causes the BQ blade of **TPB** core units to be less positive (+0.096 to +0.455) than those of **TPA** core units (+0.253 to +0.548). Meanwhile, for the linker BQ units, NBO charges are larger in **OTPB-BZN-210** (+0.236 to +0.756) compared to those in **OTPA-BZN-210** (+0.224 to +0.550). The differences are less significant in the two neutral states, with NBO charges in the **LEB** state being +0.236 (for **TPB**) and +0.224 (for **TPA**) and in the **EB** state being +0.546 (for **TPB**) and +0.476 (for **TPA**). However, the linker NBO charges for **ES** state **TPB** oligomers are +0.756 (singlet) and +0.524 (triplet) compared to +0.550 (singlet) and +0.414 (triplet) for **TPA** oligomers.

Larger increases in NBO charges of linker units also correspond to larger decreases in HOMBQ indices. The HOMBQ index of the linker BQ unit of **OTPB-BZN-210** decreases from 0.998 upon the oxidation reactions to 0.743 (**^{1}ES**) and 0.228 (**EB**). For comparisons, in the case of **OTPA-BZN-210**, the index decreases from 0.998 to 0.886 (**^{1}ES**) and 0.314 (**EB**). However, as expected, the oxidation towards the triplet state does not cause any decrease in linker HOMBQ indices in both cases.

For **OTPB-FLR-210**, the effects of replacing **TPA** core units with **TPB** core units can still be observed. The **FLR** linker rings observe greater increases in ring NBO charges (0.925 for **LEB** to **^{1}ES** in the **TPB**-linked oligomer compared to 0.573 in the **TPA**-linked oligomer, 0.539 for **TPB** compared to 0.320 for **TPA** for **LEB** to **^{3}ES**, and 0.850 for **TPB** compared to 0.356 for **TPA** for **LEB** to **EB**). Meanwhile, HOMBQ indices also decreases to further extents in **^{1}ES** (0.396 compared to 0.144 for **TPA**) and **EB** (0.745 compared to 0.629 for **TPB**) oxidation states compared to the **LEB** state.

*Table 3-32 HOMBQ indices of BQ units in the core and linker units of **OTPB-FLR-210** in the emeraldine salt and emeraldine base states (singlet and triplet) compared to the leucoemeraldine state*

State	Core Unit		Linker Unit	
	HOMBQ	ΔHOMBQ	HOMBQ	ΔHOMBQ
LEB	0.950		0.999	
^{1}ES	0.949	-0.001	0.603	-0.396
^{3}ES	0.896	-0.054	0.981	-0.018
EB	0.944	-0.006	0.254	-0.745

*Table 3-33 C–N–C angles and dihedral angles of **OTPB-FLR-210** in the emeraldine salt and emeraldine base states compared to the leucoemeraldine state*

State	C–N–C Angles (A; °)		Dihedral Angles (D; °)			
	Nitrogen Atom		Nitrogen Atom		Hub-Blade	
	A	ΔA	D	ΔD	D	ΔD
LEB	128.9°		42.0°		34.3°	
^{1}ES	130.4°	+1.5°	37.9°	-4.1°	32.1°	-2.2°
^{3}ES	129.7°	+0.8°	39.4°	-2.6°	26.9°	-7.4°
EB	122.8°	-6.1°	47.1°	+5.1°	34.8°	+0.5°

*Table 3-34 NBO partial charges on rings of BQ units, on hub parts of core units, and on nitrogen atoms in **OTPB-FLR-210** from DFT calculations*

State	Ring NBO Charge				Core Unit Hub NBO Charge		Nitrogen NBO Charge	
	Core Ring		Linker Ring					
	q	Δq	q	Δq	q	Δq	q	Δq
LEB	+0.096		+0.196		-0.035		-0.600	
^{1}ES	+0.345	+0.249	+1.121	+0.925	+0.044	+0.079	-0.458	+0.142
^{3}ES	+0.455	+0.359	+0.735	+0.539	+0.106	+0.141	-0.455	+0.145
EB	+0.136	+0.040	+0.640	+0.444	-0.022	+0.013	-0.446	+0.154

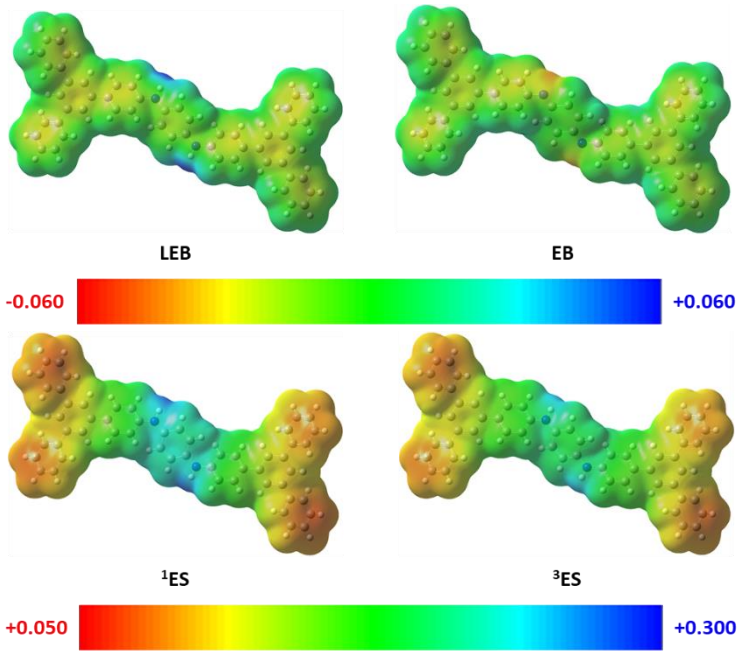

*Figure 3-20 Electrostatic potential (ESP) surface of **OTPB-BZN-210** in four different states. Neutral states **LEB** and **EB** are coloured according to the middle scale bar, while +2 states **^{1}ES** and **^{3}ES** are coloured according to the bottom scale bar.*

Replacing the linker unit from **BZN** to **FLR** also changes the structure descriptors in the similar way as in **OTPA-FLR-210**. NBO charges on **FLR** linker units of **OTPB-FLR-210^{2+}** are overall greater than on **BZN** linker units of **OTPB-BZN-210^{2+}**, but the increases per atoms are smaller. For the singlet state, the NBO charge on the linker unit of the **FLR**-linked oligomer is +1.121 for 21 atoms or +0.0534 on average, while that of the **BZN**-linked is +0.756 for 10 atoms or +0.0756 on average. Meanwhile, for the triplet state, NBO charges are +0.735 (+0.0350 per atom) for the **FLR**-linked oligomer and +0.524 (+0.0524 per atom) for the **BZN**-linked oligomer.

ESP surfaces of **OTPB-BZN-210** in different oxidation and spin states are shown in Figure 3-20, while those of **OTPB-FLR-210** are shown in Figure 3-21. There is no significant difference between these ESP surfaces and those of previously discussed PANI-CMP **210** oligomers. This is also the case for the spin density surface (Figure 3-22) as well, with the bound BQ unit from the core moieties being the most likely positions of radical cations.

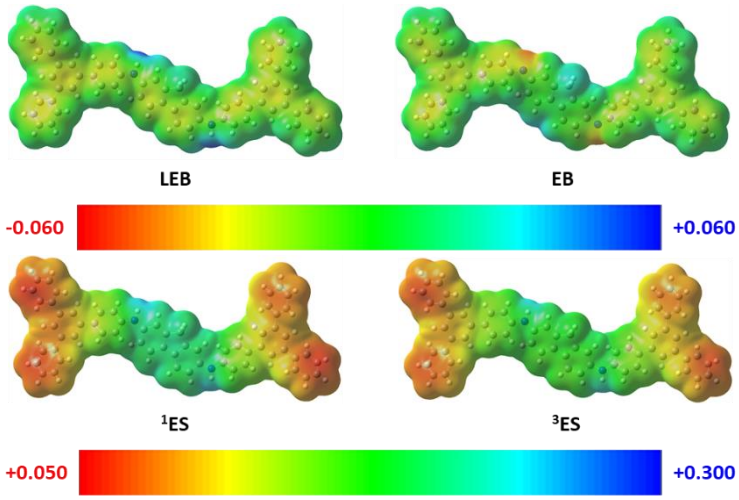

*Figure 3-21 Electrostatic potential (ESP) surface of **OTPB-FLR-210** in four different states. Neutral states **LEB** and **EB** are coloured according to the middle scale bar, while +2 states **¹ES** and **³ES** are coloured according to the bottom scale bar.*

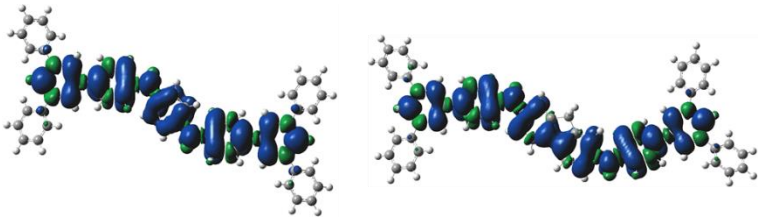

*Figure 3-22 Spin density surface of **OTPB-BZN-210** (left) and **OTPB-FLR-210** (right) in the **³ES** state*

Structures of **OTPB-BZN-210** and **OTPB-FLR-210** have been compared to structures of those previously discussed **TPA**-based oligomers. Overall, replacing the **TPA** moieties with **TPB** groups lead to more intense effects of oxidations on the linker units. The main cause of these differences may be the lack of heteroatoms in the **TPB** core units, leading to smaller changes in electronic structures in the core units. As a result, the changes in electronic structures upon oxidations are more concentrated on the linker unit regions.

*3.2.2.5 Structures of **OTPT-BZN-210** and **OTPT-FLR-210** Oligomers*

Another core unit selected for the study is 2,4,6-tris(1,4-phenylene)-1,3,5-triazine or **TPT**. The structure of a **TPT** core unit is similar to that of a **TPB** core unit for having three phenylene groups attached to a six-membered hub on the 1,3,5-pattern. However, the three CH groups in the hub ring are replaced by nitrogen atoms in a **TPT** core unit structure. The disappearance of hydrogen atoms which are the sources of steric hindrances in **TPB** core units means that all four rings can be coplanar. Meanwhile, since the hub of a **TPT** core unit now contain heteroatoms, differences in core unit electronic properties should be expected.

*Table 3-35 HOMBQ indices of BQ units in the core and linker units of **OTPT-BZN-210** in the emeraldine salt and emeraldine base states (singlet and triplet) compared to the leucoemeraldine state*

State	Core Unit		Linker Unit	
	HOMBQ	ΔHOMBQ	HOMBQ	ΔHOMBQ
LEB	0.951		0.999	
¹ES	0.936	-0.015	0.604	-0.395
³ES	0.848	-0.103	0.992	-0.007
EB	0.952	+0.001	0.200	-0.799

*Table 3-36 C–N–C angles and dihedral angles of **OTPT-BZN-210** in the emeraldine salt and emeraldine base states compared to the leucoemeraldine state*

State	C–N–C Angles (A; °)		Dihedral Angles (D; °)			
	Nitrogen Atom		Nitrogen Atom		Hub-Blade	
	A	ΔA	D	ΔD	D	ΔD
LEB	128.7°		42.3°		0.8°	
^{1}ES	130.6°	+1.9°	37.0°	-5.3°	4.4°	+3.6°
^{3}ES	129.4°	+0.7°	40.6°	-1.7°	4.4°	+3.6°
EB	122.8°	-5.9°	50.0°	+7.7°	0.3°	-0.5°

*Table 3-37 NBO partial charges on C_6H_4 rings of BQ units, on hub parts of core units, and on nitrogen atoms in **OTPT-BZN-210** from DFT calculations*

State	Ring NBO Charge				Core Unit Hub NBO Charge		Nitrogen NBO Charge	
	Core Ring		Linker Ring					
	q	Δq	q	Δq	q	Δq	q	Δq
LEB	+0.134		+0.270		-0.204		-0.591	
^{1}ES	+0.452	+0.318	+0.906	+0.636	-0.131	+0.073	-0.411	+0.180
^{3}ES	+0.606	+0.472	+0.598	+0.328	-0.118	+0.086	-0.431	+0.160
EB	+0.185	+0.051	+0.578	+0.308	-0.178	+0.026	-0.412	+0.179

The coplanarity within the core units can be seen in hub-blade dihedral angles (Table 3-36 and Table 3-39), with the largest dihedral angles being only 4.4° in both **ES** states of **OTPT-BZN-210**. Meanwhile, the NBO charges on the hub part of core units have become more negative (-0.204 to -0.118) compared to **TPB** core units (-0.037 to +0.160) from the previous section, but these charges are still less negative than those of **TPA** core units (-0.444 to -0.310, for **210** oligomers only). Indeed, the existence of nitrogen atoms leads to more overall negativity within the hub region.

The increases in magnitudes of negative partial charges on the hub of core units also correlate with the increases in magnitudes of positive partial charges on the blade of core units. The blade NBO charges for **TPT** cores in **LEB**, **^{1}ES**, and **EB** states are between +0.134 and +0.452, which are larger than those for **TPB** cores (+0.087 to +0.427) but still lower than those for **TPA** cores (+0.253 to +0.534). For oligomers in the triplet state, however, different trends are observed between **OTPT-BZN-210** and **OTPT-FLR-210**. For **OTPT-FLR-210**, the NBO charges of core unit blades are +0.490, which are between those of **OTPA-FLR-210** (+0.542) and **OTPB-FLR-210** (+0.455). However, the NBO charges of **TPT** blades in **OTPT-BZN-210** are as high as +0.606, which are more than those of **TPA** (+0.548) and **TPB** (+0.499) counterparts. In correspondence, the HOMBQ indices of core unit blades of **OTPT-BZN-210** decrease by 0.103, more than those of **OTPT-FLR-210** (by 0.051) and both **BZN**-linked oligomers of the other two core units (**OTPA-BZN-210** by 0.083 and **OTPB-BZN-210** by 0.075).

Since the NBO charges of **TPT** and **TPA** core units are in the similar trends and are larger in magnitudes compared to those of **TPB** core units, it should be expected that the NBO charges on linker units of **TPT** oligomers should be similar to those of **TPA** oligomers. However, this is not the case. Instead, the increases are even larger in the case of **TPT** oligomers compared to those of the other two linkers. While it is tempting to conclude that these discrepancies might be the results of the planar geometries of **TPT** core units, the data may be too few to draw a clear conclusion, and further studies may be required.

*Table 3-38 HOMBQ indices of BQ units in the core and linker units of **OTPT-FLR-210** in the emeraldine salt and emeraldine base states (singlet and triplet) compared to the leucoemeraldine state*

State	Core Unit		Linker Unit	
	HOMBQ	ΔHOMBQ	HOMBQ	ΔHOMBQ
LEB	0.952		1.000	
^{1}ES	0.946	-0.006	0.474	-0.526
^{3}ES	0.901	-0.051	0.969	-0.031
EB	0.947	-0.005	0.233	-0.767

*Table 3-39 C–N–C angles and dihedral angles of **OTPT-FLR-210** in the emeraldine salt and emeraldine base states compared to the leucoemeraldine state*

State	C–N–C Angles (A; °)		Dihedral Angles (D; °)			
	Nitrogen Atom		Nitrogen Atom		Hub-Blade	
	A	ΔA	D	ΔD	D	ΔD
LEB	129.0°		42.0°		1.2°	
^{1}ES	129.7°	+0.7°	40.8°	-1.2°	0.4°	-0.8°
^{3}ES	129.9°	+0.9°	39.5°	-2.5°	1.0°	-0.2°
EB	123.0°	-6.0°	49.1°	+7.1°	0.4°	-0.8°

*Table 3-40 NBO partial charges on rings of BQ units, on hub parts of core units, and on nitrogen atoms in **OTPT-FLR-210** from DFT calculations*

State	Ring NBO Charge				Core Unit Hub NBO Charge		Nitrogen NBO Charge	
	Core Ring		Linker Ring					
	q	Δq	q	Δq	q	Δq	q	Δq
LEB	+0.136		+0.259		-0.202		-0.589	
^{1}ES	+0.354	+0.218	+1.269	+1.010	-0.146	+0.056	-0.454	+0.135
^{3}ES	+0.490	+0.354	+0.888	+0.629	-0.135	+0.067	-0.424	+0.165
EB	+0.173	+0.037	+0.694	+0.435	-0.186	+0.016	-0.442	+0.147

Surface plots for electronic properties are shown in Figure 3-23, Figure 3-24, and Figure 3-25. There is no general difference between these surface plots and those of other **210** oligomers discussed in previous sections.

Structures of **OTPT-BZN-210** and **OTPT-FLR-210** are not significantly different from those of the previously mentioned oligomers other than the planar geometry of **TPT** core units. However, there are differences in details regarding NBO charges which may be resulted from the different geometry of the core units themselves, but further studies are still required to form clear conclusions.

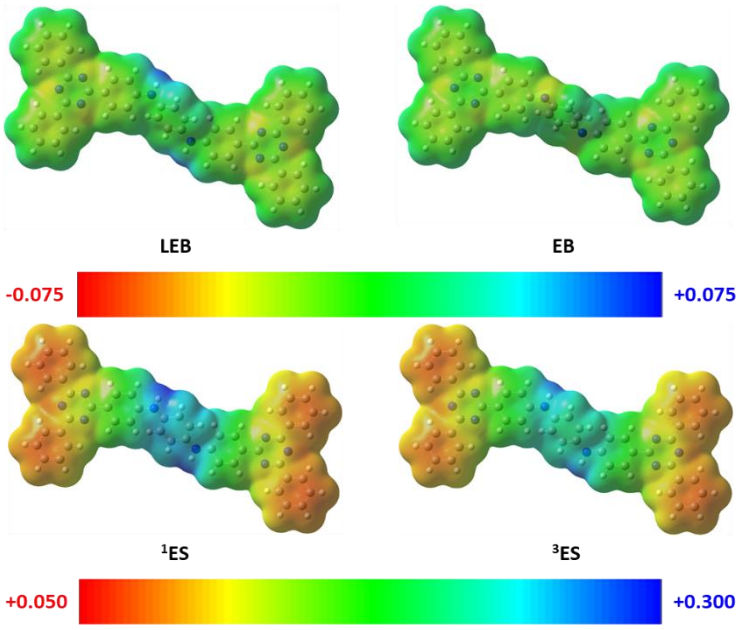

*Figure 3-23 Electrostatic potential (ESP) surface of **OTPT-BZN-210** in four different states. Neutral states **LEB** and **EB** are coloured according to the middle scale bar, while +2 states **¹ES** and **³ES** are coloured according to the bottom scale bar.*

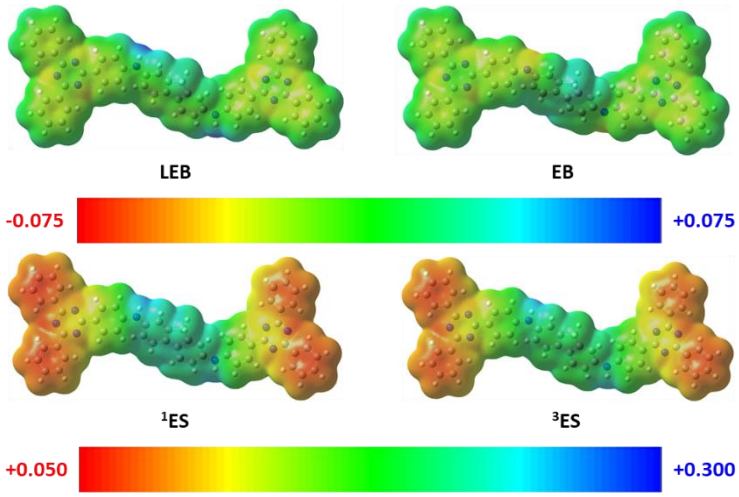

*Figure 3-24 Electrostatic potential (ESP) surface of **OTPT-FLR-210** in four different states. Neutral states **LEB** and **EB** are coloured according to the middle scale bar, while +2 states **¹ES** and **³ES** are coloured according to the bottom scale bar.*

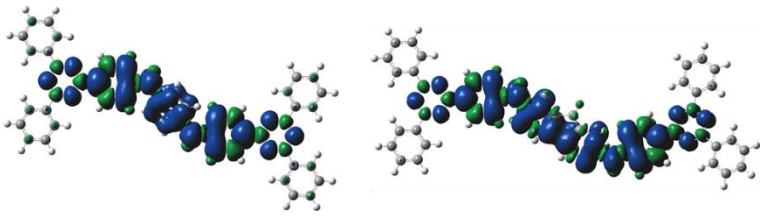

*Figure 3-25 Spin density surface of **OTPT-BZN-210** (left) and **OTPT-FLR-210** (right) in the **³ES** state*

3.2.2.6 Overall Effects of Monomer Units

In this study, three core units and two linker units have been chosen, and their effects on geometric and electronic structures are discussed. This subsection is intended to summarise the effects of monomer units on structures of resulting oligomers.

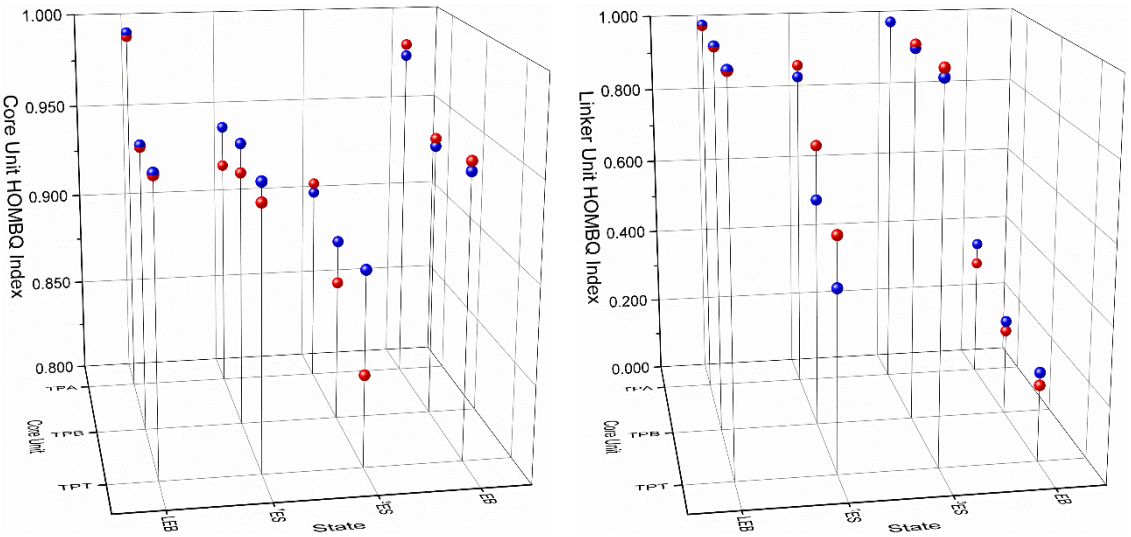

*Figure 3-26 Three-dimensional plots comparing HOMBQ indices of BQ units of **BZN**-linked (red spheres) and **FLR**-linked (blue spheres) oligomers in different oxidation and doping states*

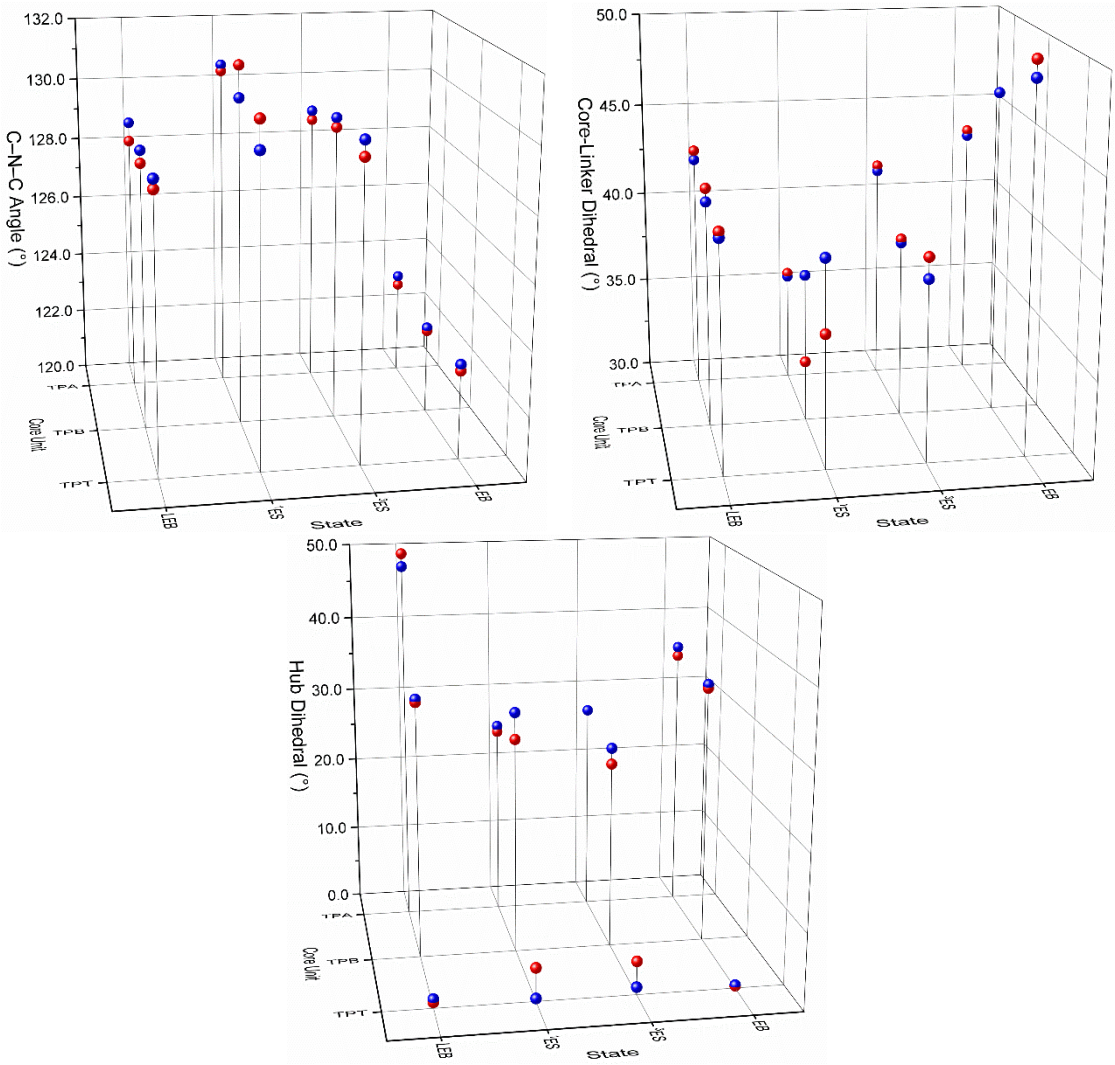

*Figure 3-27 Three-dimensional plots comparing selected bond angles and dihedral angles of **BZN**-linked (red spheres) and **FLR**-linked (blue spheres) oligomers in different oxidation and doping states*

Structural parameters of PANI-CMP oligomers are graphically compared in Figure 3-26, Figure 3-27, and Figure 3-28. General structures of these **210** oligomers are systematically similar, with the linker BQ unit being more dearomatised and becoming more quinoidal in the ^{1}**ES** and **EB** states. Meanwhile, the ^{3}**ES** state structures tend to have radical cations situated on the bound blade part of the core monomers as analysed from the spin density surfaces.

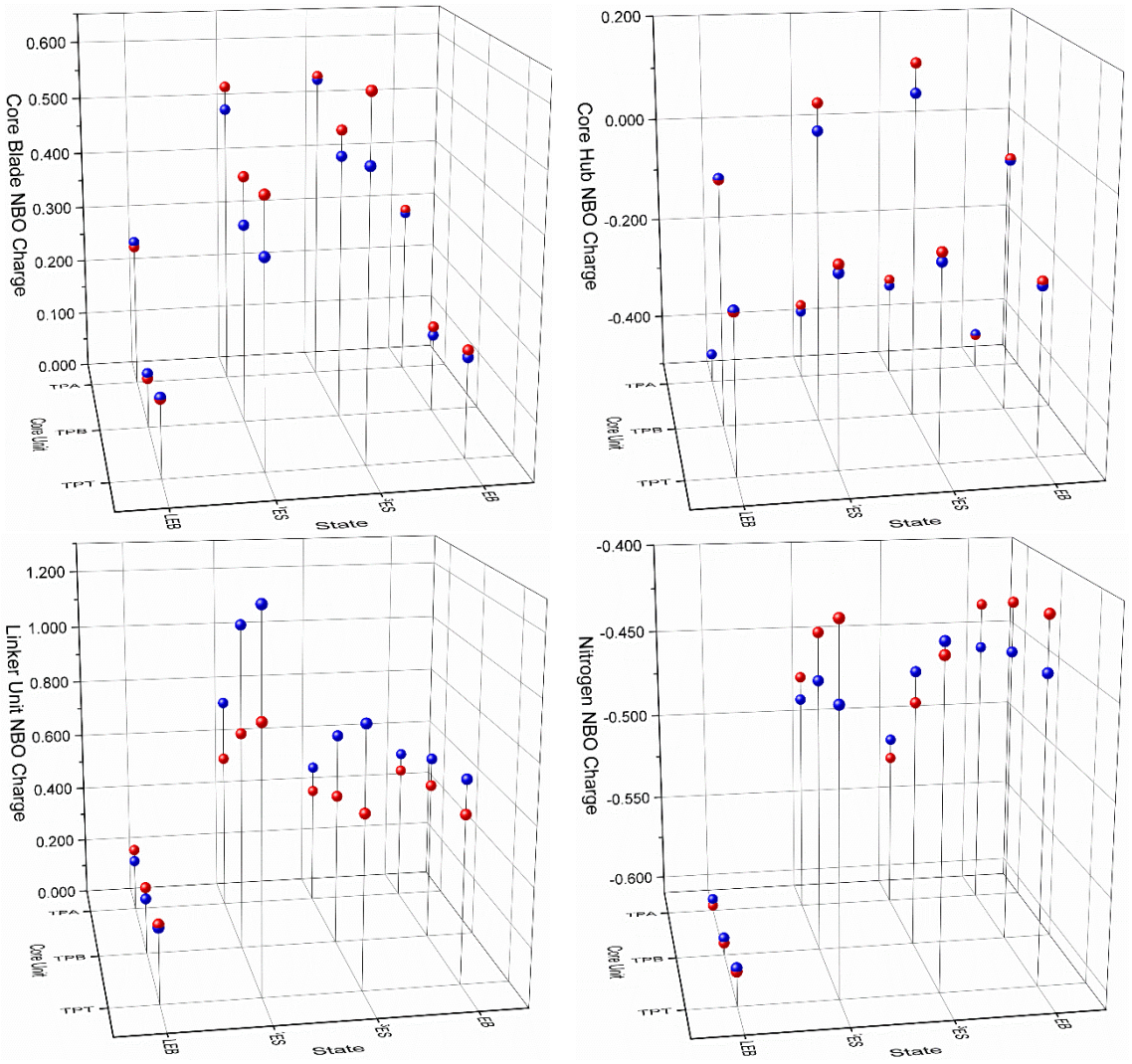

*Figure 3-28 Three-dimensional plots comparing NBO charges of **BZN**-linked (red spheres) and **FLR**-linked (blue spheres) oligomers in different oxidation and doping states*

Several structure descriptors, both geometric and electronic, have been applied for detailed comparisons among oligomers of different monomer unit combinations. Generally, linker units are affected more significantly by redox reactions than core units, and their structural changes can be used for the identification of doping or spin states. The attempts to delineate the relationship between structures of core units and linker units are, however, less successful.

3.3 Electronic Structures and Optical Spectra of PANI-CMP Oligomers

Optical absorption spectra can reflect the electronic structures of chemical systems to certain extents. Vision of colours happens when the cone cells in eyes detect lights of different wavelengths and convert the signals received into colours. As the surfaces of non-light-emitting are illuminated, some of lights illuminated on the surfaces will be absorbed to different extents

depending on their energies. A relationship plot between the extent of absorption and the energy of light is called a spectrum. A spectrum of a material is unique to that material, and different materials appear in different colours because of their different spectra. Meanwhile, as materials absorb light, molecules within materials absorb the energy of that light and become excited. Eventually, the excited molecules return to their ground states and emit energies through several processes including fluorescence and phosphorescence.[63] The range of energies involved in processes between ground and excited states cover ultraviolet, visible, and near infrared radiations, which also coincide with the energy differences between molecular orbitals.[64]

As a family of analytical techniques, they are known collectively as optical spectroscopy or UV-Vis-NIR spectroscopy. However, these techniques can be further divided by phenomena of interest such as optical absorption spectroscopy or fluorescence spectroscopy. Different measurements require different instrumentations or settings.[65] In this study, only optical absorption spectroscopy is discussed.

Optical spectroscopy is one of the most important analytical techniques to study and delineate properties of many chemical species including poly- and oligo(aniline)s. In fact, poly(aniline)s have been known to have strikingly intense colours since their early published reports,[66, 67] so are PANI-CMPs developed after.[68, 69] Absorption spectroscopy was also used to confirm that poly(aniline)s have only three neutral (undoped) oxidation states, namely **LEB**, **EB**, and **PB** (pernigraniline base) and rule out the existence of the in-between protoemeraldine base and nigraniline base states.[45] Meanwhile, these properties have also been used for the verifications of theoretical models or computational methods.[2, 12, 13, 45, 70]

Generally, each absorption peak in the optoelectronic spectra is related to either one or several electronic transitions. Theoretical studies of these spectra aim to identify electronic transitions responsible for major peaks to understand their properties further. Among important data obtained for each transition are structures of ground state molecular orbital (or "hole") and excited state molecular orbital (or "electron"), which can be determined in several ways. They can be deduced directly from their computational log files which list electronic transitions contributed to each excited state, which pair of molecular orbitals involve in each transition, and how much each transition contributes. However, in some cases where multiple transitions contribute to an excited state without clear major contributors, this can cause complications. To overcome such complications, natural transition orbital (NTO) analysis has been proposed to simplify determinations of "hole" and "electron" structures.[52] Meanwhile, while it is helpful to determine the highest occupied molecular orbitals (HOMOs) and the lowest unoccupied molecular orbitals (LUMOs) and to relate the involved MOs to HOMO and LUMO, in this work, where different analogous chemical systems are compared, this might cause confusion. HOMOs and LUMOs of these analogues might be completely different due to their differences in electronic structures of different chemical building blocks, as to be explained further. Therefore, structures of "hole" and "electron" will be obtained from NTO analysis, with relevant MOs given either accompanying the NTO structures or in the appendix.

Discussions in this section will be divided into three parts. The first part will discuss the absorption spectra of **210** oligomer models with different core-linker unit combinations, aiming to delineate the effects from different core and linker units. The second part will discuss the effects of oligomer topologies by comparing **221** oligomer models against their corresponding **210** models. Finally, the third part will discuss the differences between theoretical and measured spectra and further opportunities for improvements.

3.3.1 Optical Spectra of **210** Oligomer Models

To compare electronic structures of PANI-CMP models with different core and linker units, the **210** models with two core units and one linker unit will be discussed first. Compared with the **221** models with cyclisation, these **210** models do not have issues regarding strains. Effects of strains and oligomer topologies will be discussed further in the next section.

TD-DFT calculations for electronic transitions and optical spectra in this subsection and the next subsection are performed on the structures optimised as described in Section 3.2.2. Calculations were performed using CAM-B3LYP[71] functional (B3LYP functional[18-20] with Coulomb-attenuating method[72]), 6-31G(d) basis set,[21-30] D3(BJ) empirical dispersion,[31] tetrahydrofuran (THF) polarisable continuum (PCM) model,[32-35] *Gaussian* 16 (A.03).[49] Visualisations of computational data were done using *GaussView* version 6.1.1.[61]

*3.3.1.1 Optical Spectra of **OTPA-BZN-210** and **OTPA-FLR-210***

Theoretical spectra of **OTPA-BZN-210** in four oxidation, doping, and spin states are shown in Figure 3-29, while those of **OTPA-FLR-210** are shown in Figure 3-30. Peak positions for both oligomers are tabulated in Table 3-41. The absorption peak of ^{3}**ES OTPA-FLR-210** is 1447 nm, but the spectra are listed only to 1400 nm due to the limitation of the measuring instrument.

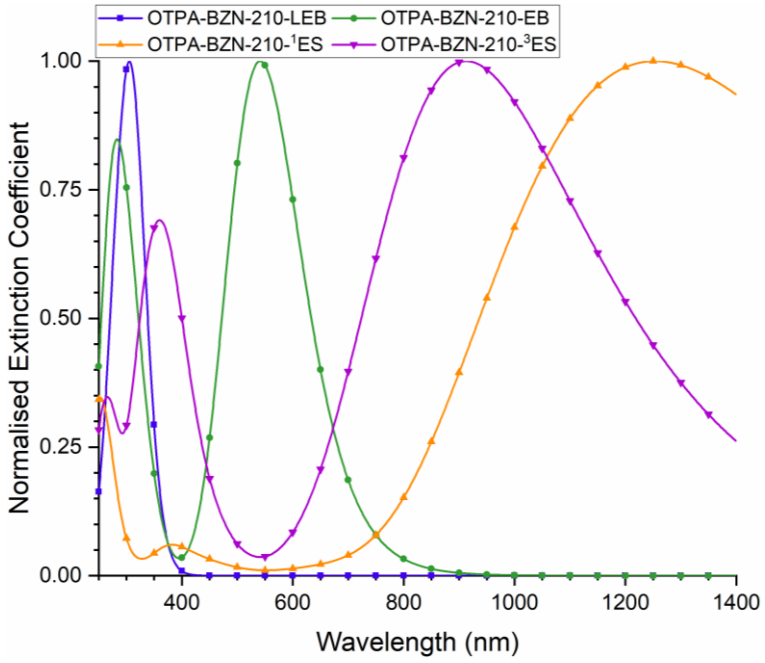

*Figure 3-29 Normalised calculated optoelectronic spectra of **OTPA-BZN-210** models in different oxidation, doping, and spin states from TD-DFT calculations (250 to 1400 nm)*

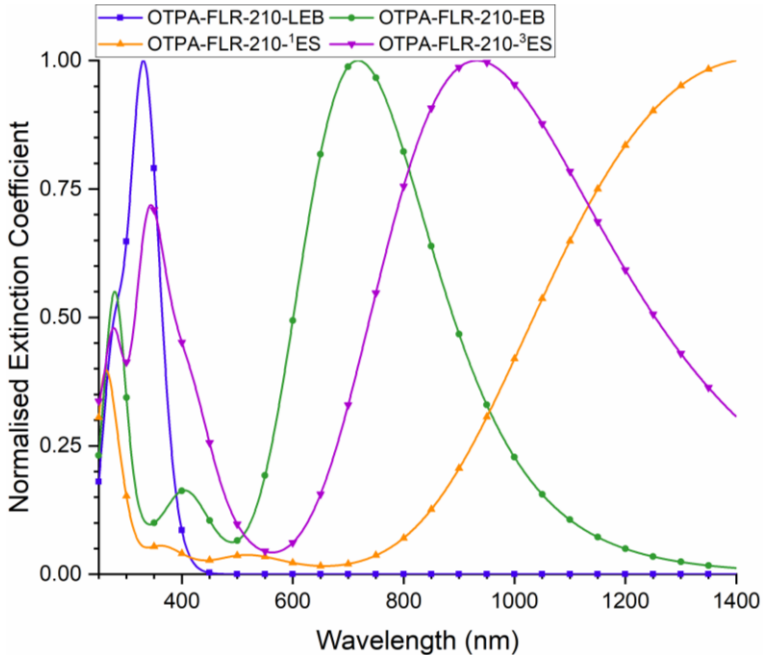

*Figure 3-30 Normalised calculated optoelectronic spectra of **OTPA-FLR-210** models in different oxidation, doping, and spin states from TD-DFT calculations (250 to 1400 nm)*

*Table 3-41 Peak positions in absorption spectra calculated from TD-DFT calculations of **OTPA-BZN-210** and **OTPA-FLR-210** in different oxidation, doping, and spin states*

State	Absorbance Peak Position (nm)	
	OTPA-BZN-210	**OTPA-FLR-210**
LEB	305	*285* (obscured), 330
^{1}ES	253, 382, 1253	263, 362, 517, 1447
^{3}ES	266, 360, 913	277, 344, 932
EB	283, 541	279, 405, 718

Absorption spectra of **OTPA-BZN-210** of different states will be discussed in detail because, as explained earlier, their structures are closer to those of oligo(aniline)s than other oligomers. Details related to electronic transitions, namely energies, corresponding wavelengths, oscillator strengths, and molecular orbitals involved along with percentage of contributions are compiled in Table 3-42. Usually, TD-DFT calculations would produce excited states with different oscillator strengths *f*. These parameters are roughly related to the extinction coefficients which in turn are related to absorption intensities. These relationships mean that excited states with low oscillator strengths do not contribute much to the absorption spectra and therefore can be neglected. As a result, some peaks with relatively low absorptions may be neglected entirely because there is no excited state with high enough oscillator strength.

*Table 3-42 Details related to electronic transitions involved in the absorption peaks from TD-DFT calculations of **OTPA-BZN-210** oligomers in different oxidation, doping, and spin states. Only excited states with oscillator strengths greater than 0.2 are considered, and for each excited state, only electronic transitions contributing at least 10% are listed.*

Excited State	Energy (eV)	Wavelength (nm)	Oscillator Strength *f*	Contributing Electronic Transition
LEB State				
ES1	3.9412	314.59	1.6679	157 (HOMO) → 158 (LUMO) (38.1%)
ES7	4.4067	281.36	0.5778	156 (HOMO-1) → 162 (LUMO+4) (18.9%)
				157 (HOMO) → 161 (LUMO+3) (15.1%)
^{1}**ES** State				
ES1	0.9891	1253.51	2.2435	156 (HOMO) → 157 (LUMO) (51.5%)
ES19	4.5649	271.61	0.2861	156 (HOMO) → 162 (LUMO+5) (31.8%)
				155 (HOMO-1) → 158 (LUMO+1) (10.3%)
ES22	4.9104	252.49	0.4484	156 (HOMO) → 163 (LUMO+6) (36.2%)
				155 (HOMO-1) → 164 (LUMO+7) (10.3%)
^{3}**ES** State				
ES1	1.3425	923.52	1.1538	155B (βHOMO) → 156B (βLUMO) (77.3%)
				154B (βHOMO-1) → 157B (βLUMO+1) (19.4%)
ES13	3.3061	375.01	0.5400	157A (αHOMO) → 158A (αLUMO) (40.5%)
ES State				
ES1	2.2896	541.50	1.5080	156 (HOMO) → 157 (LUMO) (43.6%)
ES3	3.7692	328.94	0.3103	144 (HOMO-12) → 157 (LUMO) (15.7%)
				154 (HOMO-2) → 157 (LUMO) (12.6%)
ES5	4.1352	299.83	0.6387	154 (HOMO-2) → 157 (LUMO) (30.6%)
				144 (HOMO-12) → 157 (LUMO) (10.0%)
ES10	4.4824	276.60	0.5580	156 (HOMO) → 161 (LUMO+4) (23.3%)
				155 (HOMO-1) → 162 (LUMO+5) (19.6%)
ES14	4.6677	265.62	0.2657	155 (HOMO-1) → 158 (LUMO+1) (19.9%)
				156 (HOMO) → 163 (LUMO+6) (19.5%)

For each excited state, a list of contributing electronic transitions is given (see Figure 3-2). These transitions are listed with ground state MOs, excited state MOs, and coefficients *x*. Ratios of contributions towards excited state are roughly x^2. Molecular orbitals involved are referred to by numbers, which can be then visualised using specific software such as *GaussView*.[61] Molecular orbitals significantly involved in absorption of **OTPA-BZN-210** oligomers are listed in Table 3-43 (**LEB** state), Table 3-44 (^{1}**ES** state), Table 3-45 (^{3}**ES** state), and Table 3-46 (**EB** state).

*Table 3-43 Structures of main molecular orbitals involved in electronic transitions of **OTPA-BZN-210** in **LEB** state*

Occupied Molecular Orbital	Unoccupied Molecular Orbital	
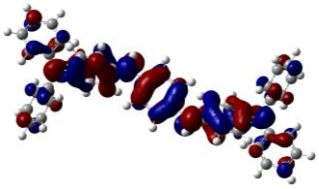 157 (HOMO)	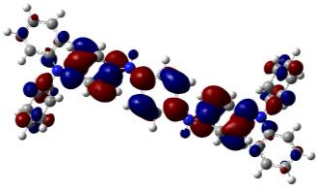 158 (LUMO)	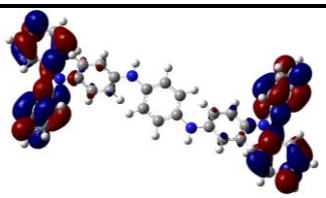 162 (LUMO+4)
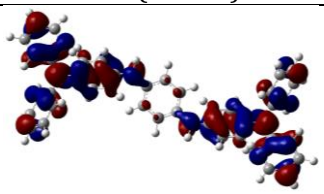 156 (HOMO-1)	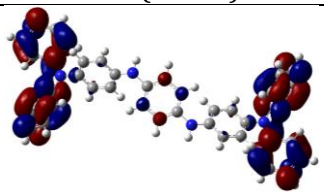 161 (LUMO+3)	

For **OTPA-BZN-210** in the fully reduced **LEB** state, its absorption spectrum contains only one peak at 305 nm. However, this peak is contributed by two major excited states, ES1 (314.59 nm, f = 1.6679) and ES7 (281.36 nm, f = 0.5778), along with several minor excited states. This is one example where one absorption peak is related to multiple excited states with similar energies, and theoretical studies can help with delineating different contributing electronic transitions. ES1 is a typical HOMO-LUMO transition. Meanwhile, ES7 involves the charge transfer from either the core moieties or core-linker bound moieties to the two unbound core blades. As discussed in Section 3.2.2 regarding bound and unbound core unit blades, unbound core blades are less likely to be found in the structure of PANI-CMPs. Therefore, peaks involved these moieties can potentially cause discrepancies between theoretical and experimental spectra.

*Table 3-44 Structures of main molecular orbitals involved in electronic transitions of **OTPA-BZN-210** in **^{1}ES** state*

Occupied Molecular Orbital	Unoccupied Molecular Orbital	
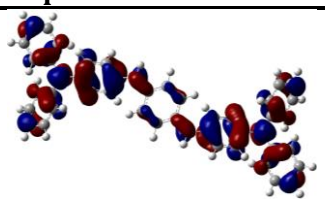 156 (HOMO)	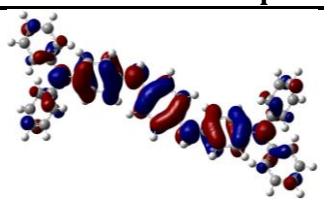 157 (LUMO)	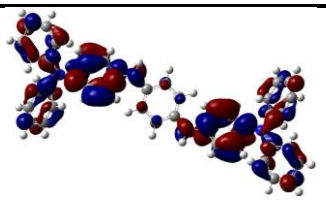 162 (LUMO+5)
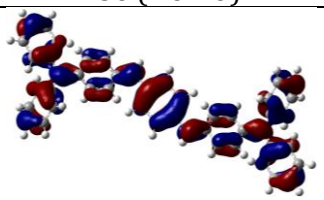 155 (HOMO-1)	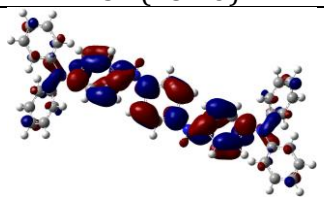 158 (LUMO+1)	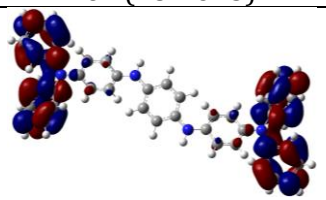 163 (LUMO+6)
		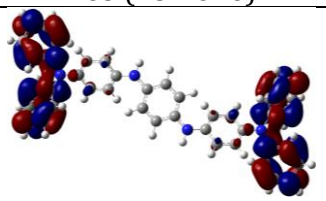 164 (LUMO+7)

*Table 3-45 Structures of main molecular orbitals involved in electronic transitions of **OTPA-BZN-210** in **^{3}ES** state*

Occupied Molecular Orbital	Unoccupied Molecular Orbital
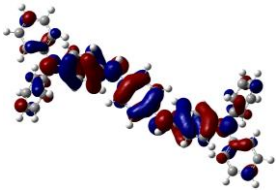 157A (αHOMO)	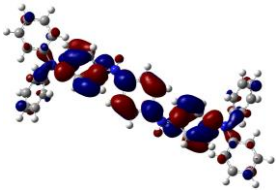 158A (αLUMO)
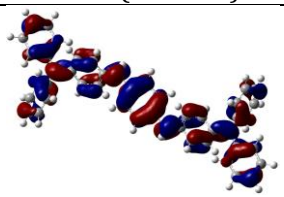 155B (βHOMO)	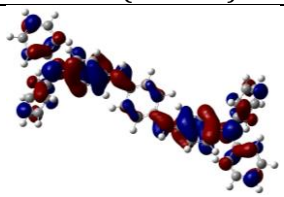 156B (βLUMO)
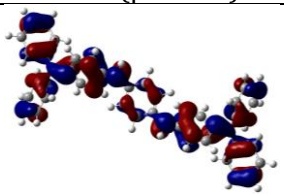 154B (βHOMO-1)	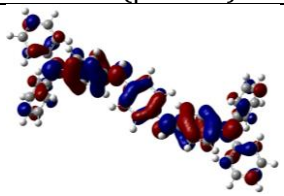 157B (βLUMO+1)

For **OTPA-BZN-210** oligomers in oxidised states, multiple absorption peaks are predicted. Excluding peaks with low intensities and oscillator strengths, two peaks can be observed for each state, which corresponds to previous studies on **EB** state oligo(aniline)s.[13, 47] Meanwhile, the issue of electronic transitions involving unbound core blades can still be observed in **^{1}ES** and **EB** states around the ultraviolet region, which will be discussed next.

OTPA-BZN-210 in the **^{1}ES** state has three excited states contributing to the absorption spectrum, namely ES1, ES19, and ES22. ES22 involves the transfer of charges to the unbound core blades, however, and therefore will be excluded. Meanwhile, ES19 has two major electronic transitions contributing, 156 to 162 (31.8%) and 155 to 158 (10.3%). The former focuses around the bound core BQ units, while the latter is concentrated around the whole core units, see MOs in Table 3-44. Nonetheless, both contributors involve the π-π* transitions within the core units themselves. ES1, similar to the **LEB** state, is also a HOMO-LUMO transition. However, while the HOMO is concentrated around the core units as mentioned earlier, the LUMO is now concentrated around the linker units, which means that the HOMO-LUMO is now also a charge transfer from the core to the linker units.

*Table 3-46 Structures of main molecular orbitals involved in electronic transitions of **OTPA-BZN-210** in **EB** state*

Occupied Molecular Orbital	Unoccupied Molecular Orbital	
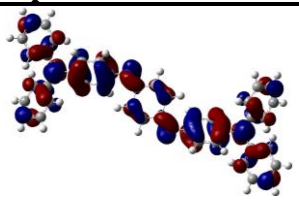 156 (HOMO)	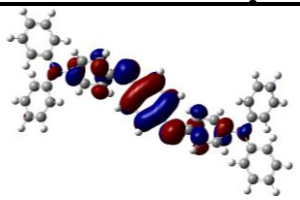 157 (LUMO)	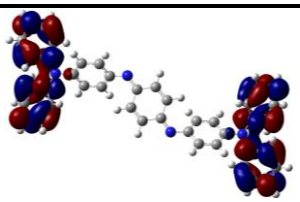 161 (LUMO+4)
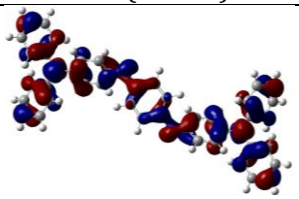 155 (HOMO-1)	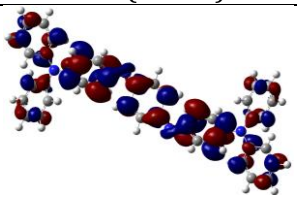 158 (LUMO+1)	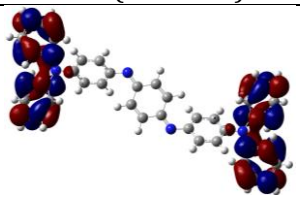 162 (LUMO+5)
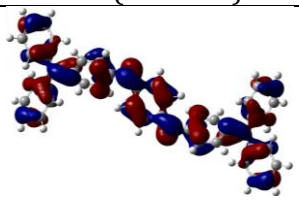 154 (HOMO-2)		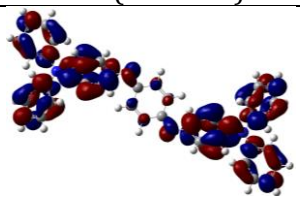 163 (LUMO+6)
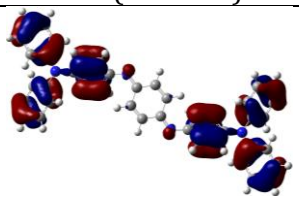 144 (HOMO-12)		

For the triplet **ES** state, because the system now contains unpaired electrons, each molecular orbital is now split into alpha and beta. The absorption spectrum of **^{3}ES OTPA-BZN-210** have two major excited states, ES1 and ES13. Both of these involve HOMO-LUMO transitions of alpha orbitals and beta orbitals. ES13 is a HOMO-LUMO transition for alpha orbitals happening around the core-linker conjugated moiety, which is similar to ES1 of the **LEB** state mentioned earlier. Meanwhile, ES1 is a HOMO-LUMO transition for beta orbitals. It is also a transition from the core to the linker units similar to ES1 of the **^{1}ES** state.

Five excited states are significantly involved in the absorption spectrum of **OTPA-BZN-210** in **EB** state, namely ES1, ES3, ES5, ES10, and ES14. Again, ES10 is excluded because it involves the transfer to the unbound core blades. For ES14, two major transitions contribute equally to this excited state, 155 to 158 (19.9%) and 156 to 163 (19.5%). The former transition is the π-π* transition happening throughout the whole oligomer molecule, while the latter transition is also the π-π* transition but happening mainly around core moieties. Meanwhile, both ES3 and ES5 involve the same two transitions, 144 to 157 and 154 to 157, with different contribution ratios. They are both charge transfers towards the core-linker conjugated moiety but originated from the different parts, with MO 144 being around the core units while MO 154 being spread throughout the whole oligomer molecule. For the least energetic state, ES1, it is also a charge transfer from core to linker units, same as in the other two oxidised states.

Overall, electronic transitions involved in the absorption spectra of **OTPA-BZN-210** in different states can be categorised into three major groups. The first group is the transition from

the core unit to the linker unit, which can only be found in the three oxidised states. They can be found in the visible (for the **EB** state) or the near infrared (for the **ES** states) region, and they are also the most intense peaks in their respective spectra. The second group is the transition happening within the core-linker conjugated moiety. These moieties usually consist of the linker BQ unit and both of the bound core blades. They can also include the hub parts of core units and even unbound core blades. Their positions are around the near ultraviolet region (approximately 300 to 400 nm). Finally, the last group contains the miscellaneous peaks such as transitions within core units or transitions towards the unbound core blades.

Transitions of the first group will be called **c**harge **t**ransfer between **BQ** units (CTBQ) because they involve the transfer of charges between core and linker BQ units. Meanwhile, transitions of the second group will be called conjugated **c**ore-**l**inker **BQ** units (CLBQ) because they happen in the conjugated core-linker regions. While transitions of both groups are important contributors to peaks in the absorption spectra, CLBQs are more complicated as seen in the case of **EB** state **OTPA-BZN-210** where four excited states, at least, contribute to the same CLBQ peak. Also, these CLBQ peaks can also be contaminated by transitions that can only be found in the oligomer models and not actual polymers, which might hinder further translational studies. Therefore, CTBQ peaks will be the main point for discussions.

Since it is possible to have many molecular orbitals involved in electronic transitions, the use of molecular orbitals for the identification of electronic transitions involved in absorption spectra can be confusing. To ease the analyses and the following discussions, natural transition orbitals (NTOs)[52] will be used instead of molecular orbitals. A natural transition orbital analysis is applied to a selected excited state, and it returns surface plots similar to molecular orbitals.

*Table 3-47 Structures of ground state and excited state molecular orbitals from the NTO analyses of CTBQ excited states of **OTPA-BZN-210** oligomers*

Oligomer State	Ground State MO	Excited State MO
^{1}ES	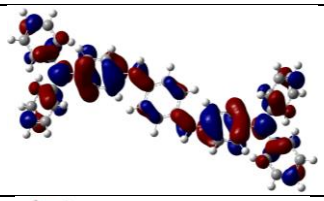	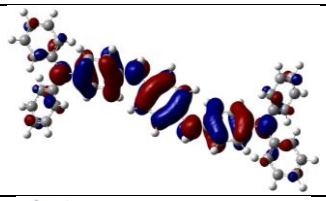
^{3}ES	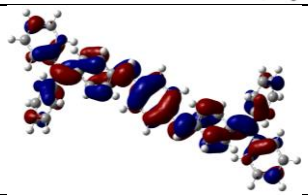	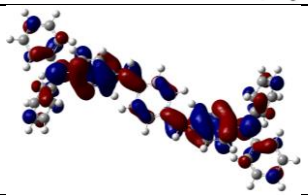
EB	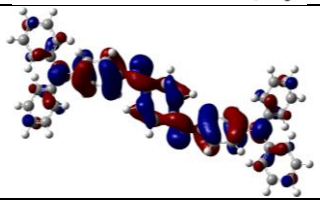	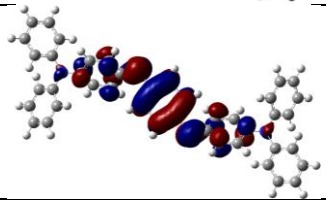

Structures of ground state and excited state molecular orbitals from NTO analyses of excited states related to the CTBQ electronic transitions of the three oxidised states are shown in Table 3-47. These molecular orbitals structures are slightly different from those of their respective HOMO and LUMO structures due to the integration of other minor contributors beside the main ones discussed earlier. However, despite the slight differences, these NTO molecular

orbitals are still in agreement with the frontier MOs regarding the core-linker charge transfer natures.

Excited states and electronic transitions for **OTPA-FLR-210** oligomers related to their CTBQ absorption peaks are listed in Table 3-48, while structures of molecular orbitals from corresponding NTO analyses are shown in Table 3-49. The structures of molecular orbitals involved in the CTBQ electronic transitions are similar to those of the **BZN** counterparts, which agrees with the discussions in the previous section regarding the electronic structures for the lack of significant differences between geometric and electronic structures of oligomers with **BZN** and **FLR** linker units.

*Table 3-48 Details related to electronic transitions involved in the CTBQ absorption peaks from TD-DFT calculations of **OTPA-FLR-210** oligomers in different oxidation, doping, and spin states. Only electronic transitions contributing at least 10% are listed.*

State	Energy (eV)	Wavelength (nm)	Oscillator Strength *f*	Contributing Electronic Transition
^{1}ES	0.8586	1444.07	2.5784	179 (HOMO) → 180 (LUMO) (51.7%)
^{3}ES	1.3081	947.78	1.2576	178B (βHOMO) → 179B (βLUMO) (69.2%)
				177B (βHOMO-1) → 180B (βLUMO+1) (25.1%)
EB	1.7261	718.28	2.3499	179 (HOMO) → 180 (LUMO) (47.6%)

*Table 3-49 Structures of ground state and excited state molecular orbitals from the NTO analyses of CTBQ excited states of **OTPA-FLR-210** oligomers*

Oligomer State	Ground State MO	Excited State MO
^{1}ES	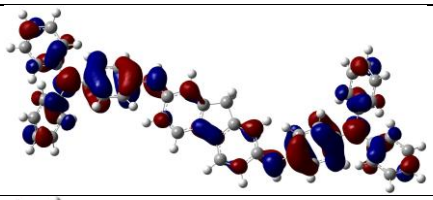	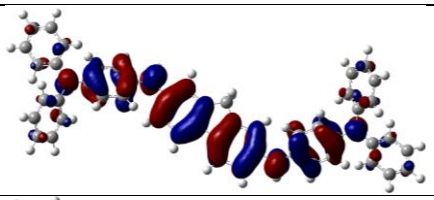
^{3}ES	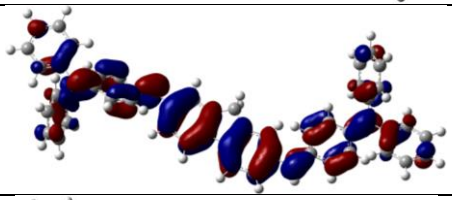	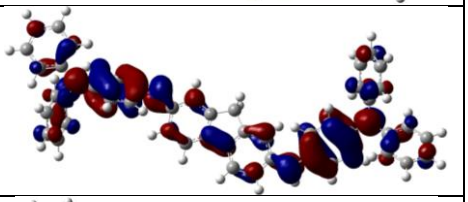
EB	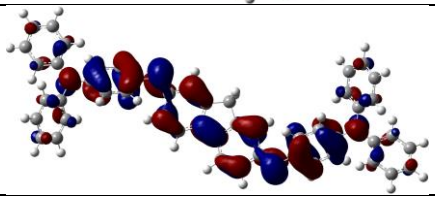	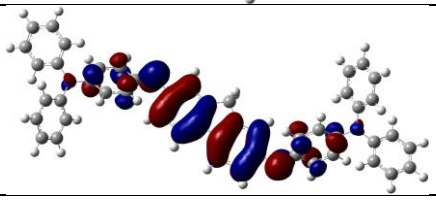

The effects of oxidation states on CTBQ peak positions are similar for oligomers with both linker units and therefore can be discussed simultaneously. These peaks appear at longer wavelengths, lower energies, for doped oligomers than for the oligomers in the **EB** state. For oligomers in the doped **ES** states, the CTBQ peaks appear far in the infrared region, while those peaks of oligomers in the undoped state are in the visible region. Meanwhile, doped oligomers in the singlet **ES** state also have their CTBQ peaks appear at longer wavelengths than those in the triplet **ES** state.

*Table 3-50 Comparisons between CTBQ peak positions and corresponding energies for **OTPA-BZN-210** and **OTPA-FLR-210** in different doping and spin states from TD-DFT calculations*

State	OTPA-BZN-210			OTPA-FLR-210		
	CTBQ Peak Position (nm)		Calculated Energy (eV)	CTBQ Peak Position (nm)		Calculated Energy (eV)
	Spectrum	Excited State		Spectrum	Excited State	
^{1}ES	1253	1253.51	0.9891	1447	1444.07	0.8586
^{3}ES	913	923.52	1.3425	932	947.78	1.3081
EB	541	541.50	2.2896	718	718.28	1.7261

The effect of linker unit can be seen as the CTBQ peak positions of oxidised **OTPA-FLR-210** are at the longer wavelengths than those of oxidised **OTPA-BZN-210** (Table 3-50). These red-shift phenomena can be the results of longer conjugation systems due to the longer size of **FLR** linker units compared to **BZN** linker units. However, the effects of **FLR** linker units appear to be more complicated than just longer size alone. For oligomers in the **^{1}ES** state, the calculated energies for the CTBQ excited states differ by 0.1305 eV. The difference decreases to only 0.0344 eV for **^{3}ES** state oligomers but increases to 0.5635 eV for **EB** state oligomers. This variety in energy differences between these two sets of oligomers implies more complications than just longer conjugation systems.

*3.3.1.2 Optical Spectra of **OTPB-BZN-210** and **OTPB-FLR-210***

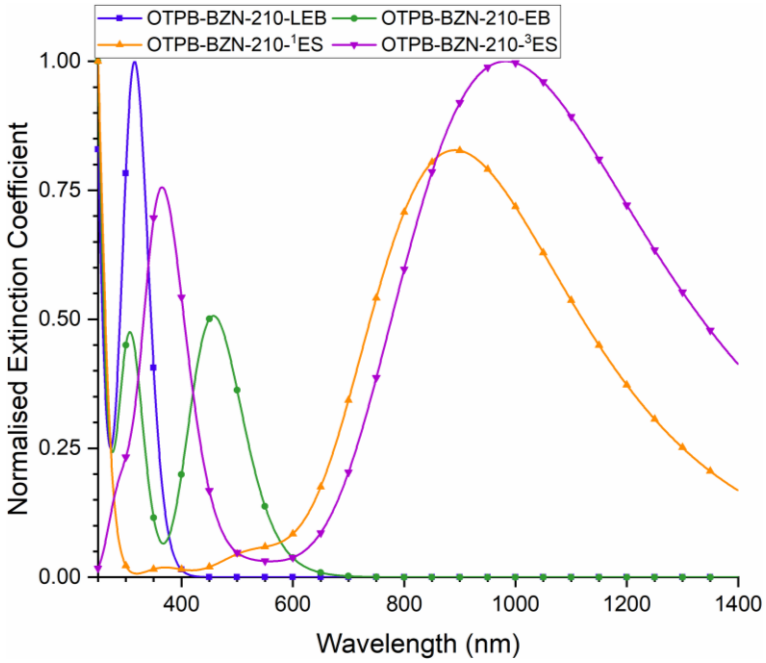

*Figure 3-31 Normalised calculated optoelectronic spectra of **OTPB-BZN-210** models in different oxidation, doping, and spin states from TD-DFT calculations (250 to 1400 nm)*

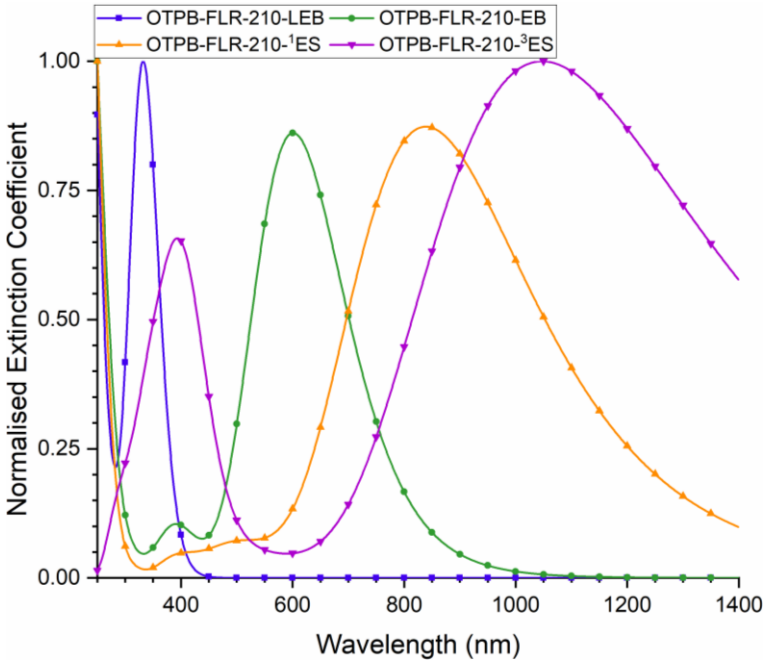

*Figure 3-32 Normalised calculated optoelectronic spectra of **OTPB-FLR-210** models in different oxidation, doping, and spin states from TD-DFT calculations (250 to 1400 nm)*

*Table 3-51 Details related to electronic transitions involved in the CTBQ absorption peaks from TD-DFT calculations of **OTPB-BZN-210** and **OTPB-FLR-210** oligomers in different oxidation, doping, and spin states. Only electronic transitions contributing at least 10% are listed.*

State	Energy (eV)	Wavelength (nm)	Oscillator Strength *f*	Contributing Electronic Transition
OTPB-BZN-210				
^{1}ES	1.3905	891.66	2.2626	188 (HOMO) → 189 (LUMO) (46.2%)
^{3}ES	1.2618	982.62	1.3281	185B (βHOMO-2) → 188B (βLUMO) (59.4%)
				179B (βHOMO-8) → 188B (βLUMO) (23.5%)
EB	2.7109	457.35	1.3686	188 (HOMO) → 189 (LUMO) (42.9%)
OTPB-FLR-210				
^{1}ES	1.4763	839.83	2.4576	211 (HOMO) → 212 (LUMO) (46.5%)
^{3}ES	1.1813	1049.58	1.4902	210B (βHOMO) → 211B (βLUMO) (49.3%)
				209B (βHOMO-1) → 211B (βLUMO) (20.1%)
				206B (βHOMO-4) → 211B (βLUMO) (13.7%)
EB	2.0622	601.21	2.4635	211 (HOMO) → 212 (LUMO) (47.6%)

Calculated absorption spectra of PANI-CMP oligomers with **TPB** core units are shown in Figure 3-31 (for **OTPB-BZN-210**) and Figure 3-32 (for **OTPB-FLR-210**), while Table 3-51 lists details for the CTBQ absorption peaks of oxidised oligomers. The trends for **ES** state oligomers are different from those in oligomers with **TPA** core units. For singlet **ES** oligomers, the CTBQ transition energy of the **FLR**-linked oligomer (1.4763 eV) is greater than that of the **BZN**-linked oligomer (1.3905 eV). This is opposite to the trend observed for **^{1}ES TPA** oligomers, with the

CTBQ transition energy of **OTPA-FLR-210** (0.8586 eV) being less than that of **OTPA-BZN-210** (0.9891 eV).

For **ES** oligomers in the triplet state, the CTBQ transition energies follow the same trend as **TPA** oligomers, with the energies being greater for **BZN**-linked oligomers than **FLR**-linked oligomers (1.3425 eV to 1.3081 eV for **OTPA** series, 1.2618 eV to 1.1813 eV for **OTPB** series). However, there are stronger contributions from non-HOMO-LUMO transitions in **TPB** oligomers. For **OTPB-FLR-210**, two major contributions are from the second (20.1%) and the fifth (13.7%) highest occupied MOs alongside the HOMO itself (49.3%). While the HOMO-LUMO transition is still the main contributor for **^{3}ES OTPB-FLR-210**, however, the contribution from the same transition for **OTPB-BZN-210** is negligible (see Section C.2.5.3 in the Appendix).

Nonetheless, the NTO analyses for both CTBQ excited states of singlet and triplet (Table 3-53 and Table 3-54) still demonstrate the charge transfer natures. The differences between oligomers of **OTPA** and **OTPB** series in singlet states, however, may imply that introducing new aromatic core units can create more complications in electronic structures and resulting electronic transitions.

For oligomers in the **EB** state, the CTBQ transition energies are also higher than those of the doped oligomers, and therefore their peaks appear at the shorter wavelengths. Meanwhile, oligomers with **TPB** core units have their CTBQ peaks appearing at shorter wavelengths compared to those with **TPA** core units. For **BZN**-linked oligomers, the peak positions are 457 nm for **OTPB-BZN-210** and 541 nm for **OTPA-BZN-210**, while for **FLR**-linked oligomers, the peak positions are 601 nm for **OTPB-FLR-210** and 718 nm for **OTPA-FLR-210**. In fact, the same trend also applies for **^{1}ES** oligomers but not for **^{3}ES** oligomers where the opposite applies instead. The full comparison can be seen between Table 3-50 (for **OTPA** series) and Table 3-52 (for **OTPB** series). The opposite trend for the triplet **ES** state, with CTBQ peaks for **TPB** oligomers are at longer wavelengths instead, can be the result of more significant contributions from the non-HOMO-LUMO transitions.

*Table 3-52 Comparisons between CTBQ peak positions and corresponding energies for **OTPB-BZN-210** and **OTPB-FLR-210** in different doping and spin states from TD-DFT calculations*

State	OTPB-BZN-210			OTPB-FLR-210		
	CTBQ Peak Position (nm)		Calculated Energy (eV)	CTBQ Peak Position (nm)		Calculated Energy (eV)
	Spectrum	Excited State		Spectrum	Excited State	
^{1}ES	891	891.66	1.3905	839	839.83	1.4763
^{3}ES	982	982.62	1.2618	1047	1049.58	1.1813
EB	457	457.35	2.7109	601	601.21	2.0622

The common theme between NTO ground state and excited state MOs of **EB** and **ES** states in both oligomer series is that **EB** state transitions involve other moieties of the core units, other than the bound BQ units, to a lesser extent than those of either of the two **ES** states, see Table 3-47 and Table 3-49 for NTO results of the **OTPA** series and Table 3-53 and Table 3-54 for NTO results of the **OPTB** series. As discussed in Section 3.2.2, the core units in **EB** state oligomers are geometrically less flat (larger hub-blade dihedral angles) compared to those in the **ES** states. The less flat geometries might have disrupted the overlapping between π-systems of core-linker conjugated moiety and of the other core unit moieties.

*Table 3-53 Structures of ground state and excited state molecular orbitals from the NTO analyses of CTBQ excited states of **OTPB-BZN-210** oligomers*

Oligomer State	Ground State MO	Excited State MO
^{1}ES	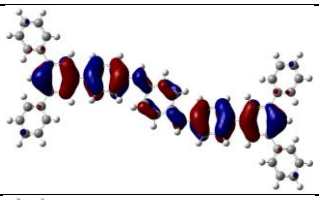	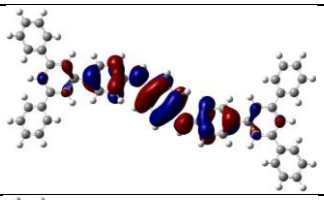
^{3}ES	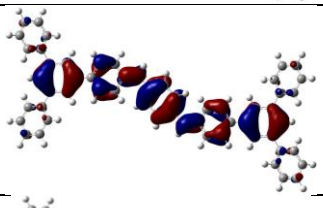	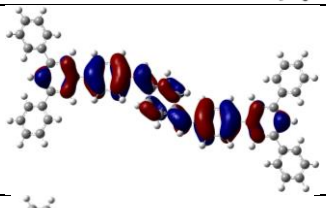
EB	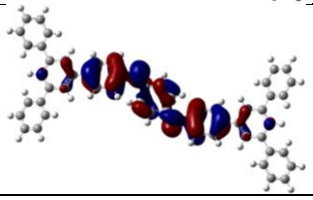	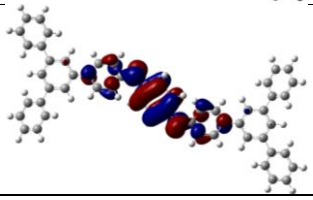

*Table 3-54 Structures of ground state and excited state molecular orbitals from the NTO analyses of CTBQ excited states of **OTPB-FLR-210** oligomers*

Oligomer State	Ground State MO	Excited State MO
^{1}ES	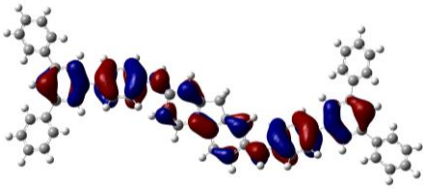	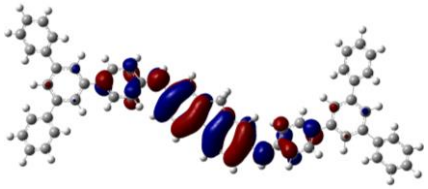
^{3}ES	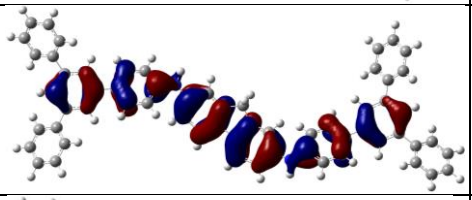	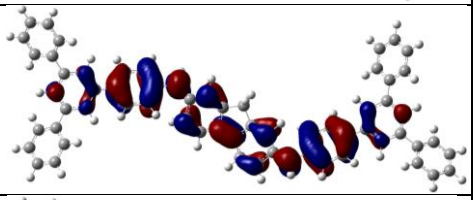
EB	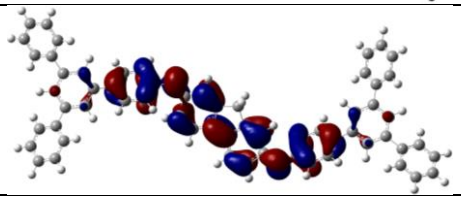	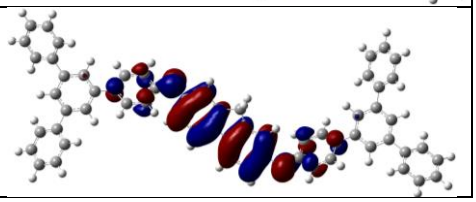

The less flat geometries can also explain less significant involvements of unbound core moieties in oligomers of the **OTPB** series compared to those of the **OTPA** series. Since the structures of **TPB** core units are generally less flat than those of **TPA** core units due to stronger steric hindrances, the resulting disruptions are more drastic.

*3.3.1.3 Optical Spectra of **OTPT-BZN-210** and **OTPT-FLR-210***

For the **OTPT** series, replacing **TPA** core units with **TPT** units leads to the same trend in terms of CTBQ transition energies as shown in Table 3-55 and Table 3-56. Transitions energies are smaller in **FLR**-linked oligomers than in **BZN**-linked oligomers, and they are also largest in **EB** state, followed by the **^{1}ES** state and the **^{3}ES** state, respectively.

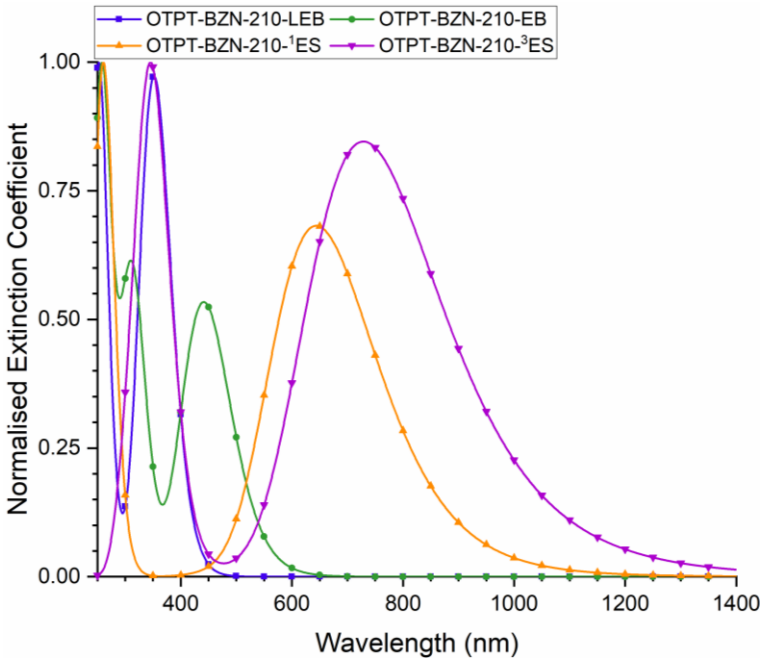

*Figure 3-33 Normalised calculated optoelectronic spectra of **OTPT-BZN-210** models in different oxidation, doping, and spin states from TD-DFT calculations (250 to 1400 nm)*

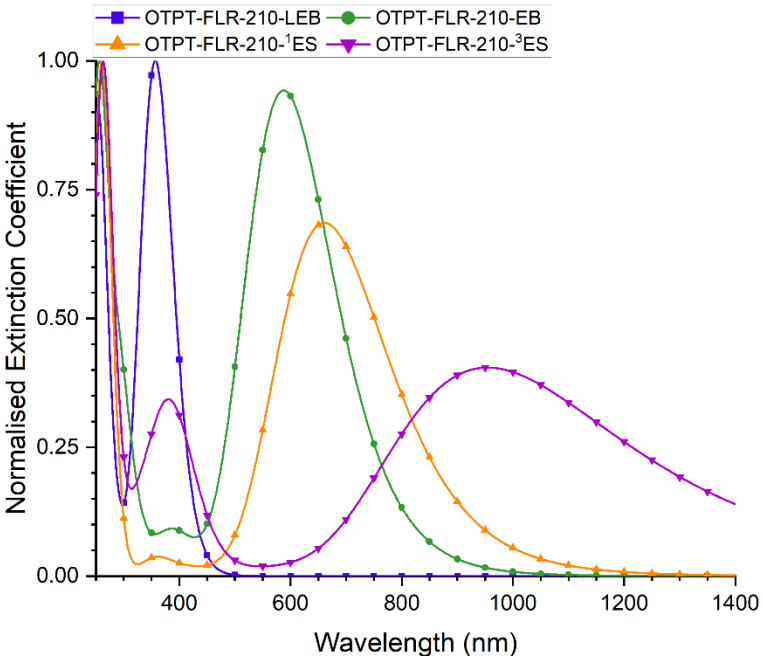

*Figure 3-34 Normalised calculated optoelectronic spectra of **OTPT-FLR-210** models in different oxidation, doping, and spin states from TD-DFT calculations (250 to 1400 nm)*

However, in terms of the contributing electronic transitions, they follow the same trend as in the **OTPB** series instead, with more contributions from non-HOMO-LUMO transitions in the triplet **ES** state. In fact, HOMO-LUMO transitions almost do not contribute to the CTBQ absorption peaks at all (see full list of contributions in Section C.2.9.3 for **OTPT-BZN-210** and Section C.2.11.3 for **OTPT-FLR-210**). For **OTPT-BZN-210**, the major contribution (80.3%) comes from the transition from the ninth highest occupied MO, while for the **FLR** counterpart, two major contributions come from those of the fifth (54.2%) and the third (28.1%) highest occupied MOs.

This theme also applies to **OTPT-BZN-210** in the **^{1}ES** state as well, with the major contribution (37.7%) also coming from the transition from the ninth highest occupied MO.

*Table 3-55 Details related to electronic transitions involved in the CTBQ absorption peaks from TD-DFT calculations of **OTPT-BZN-210** and **OTPT-FLR-210** oligomers in different oxidation, doping, and spin states. Only electronic transitions contributing at least 10% are listed.*

State	Energy (eV)	Wavelength (nm)	Oscillator Strength *f*	Contributing Electronic Transition
OTPT-BZN-210				
^{1}ES	1.9237	644.50	2.0870	180 (HOMO-8) → 189 (LUMO) (37.7%)
^{3}ES	1.6969	730.64	0.9955	179B (βHOMO-8) → 188B (βLUMO) (80.3%)
EB	2.8090	441.37	1.4379	188 (HOMO) → 189 (LUMO) (43.5%)
OTPT-FLR-210				
^{1}ES	1.8762	660.83	2.5056	211 (HOMO) → 212 (LUMO) (47.3%)
^{3}ES	1.2981	955.10	1.2434	206B (βHOMO-4) → 211B (βLUMO) (54.2%)
				208B (βHOMO-2) → 211B (βLUMO) (28.1%)
EB	2.1092	587.82	2.6422	211 (HOMO) → 212 (LUMO) (47.2%)

*Table 3-56 Comparisons between CTBQ peak positions and corresponding energies for **OTPT-BZN-210** and **OTPT-FLR-210** in different doping and spin states from TD-DFT calculations*

State	OTPT-BZN-210			OTPT-FLR-210		
	CTBQ Peak Position (nm)		Calculated Energy (eV)	CTBQ Peak Position (nm)		Calculated Energy (eV)
	Spectrum	Excited State		Spectrum	Excited State	
^{1}ES	644	644.50	1.9237	661	660.83	1.8762
^{3}ES	729	730.64	1.6969	955	955.10	1.2981
EB	441	441.37	2.8090	588	587.82	2.1092

*Table 3-57 Structures of ground state and excited state molecular orbitals from the NTO analyses of CTBQ excited states of **OTPT-BZN-210** oligomers*

Oligomer State	Ground State MO	Excited State MO
^{1}ES	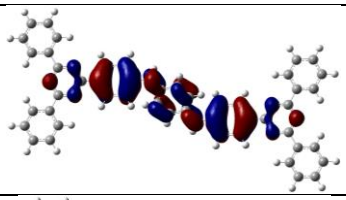	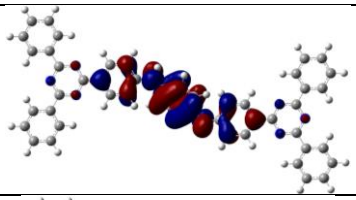
^{3}ES	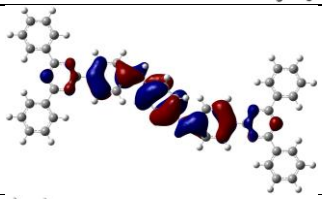	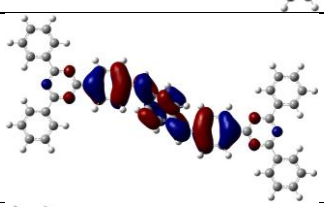
EB	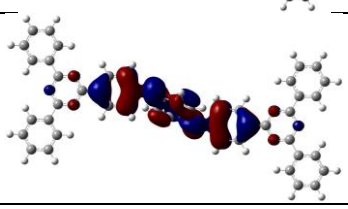	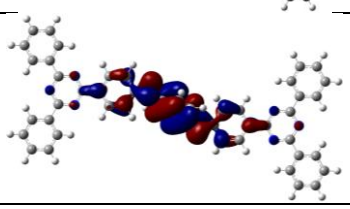

*Table 3-58 Structures of ground state and excited state molecular orbitals from the NTO analyses of CTBQ excited states of **OTPT-FLR-210** oligomers*

Oligomer State	Ground State MO	Excited State MO
^{1}ES	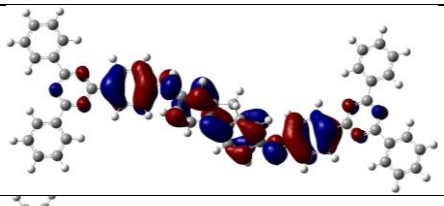	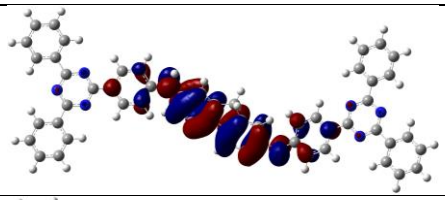
^{3}ES	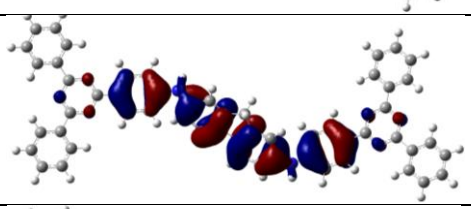	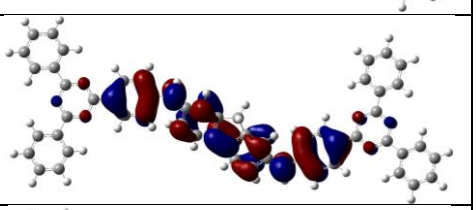
EB	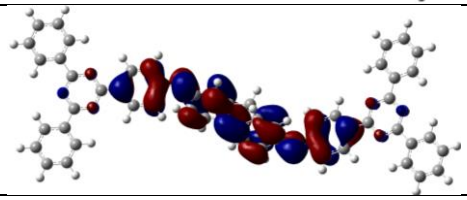	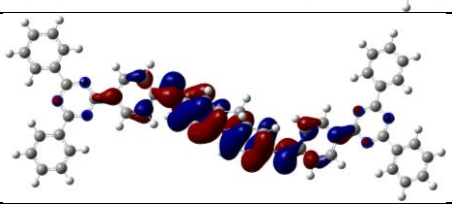

For NTO molecular orbitals, the large core-linker dihedral angles appear to have more influence on the disruption of π-overlapping than the flat geometry of **TPT** core units. In all six cases of state and linker unit combinations (Table 3-57 and Table 3-58) this analysis illustrates that there is no contribution from unbound core blades at all, and the contributions from the core hubs are small.

3.3.1.4 Effects of Core Units on Electronic Transition Energies

This section aims to summarise the effects observed across all **210** oligomeric models with different core and linker units discussed in the previous three sections.

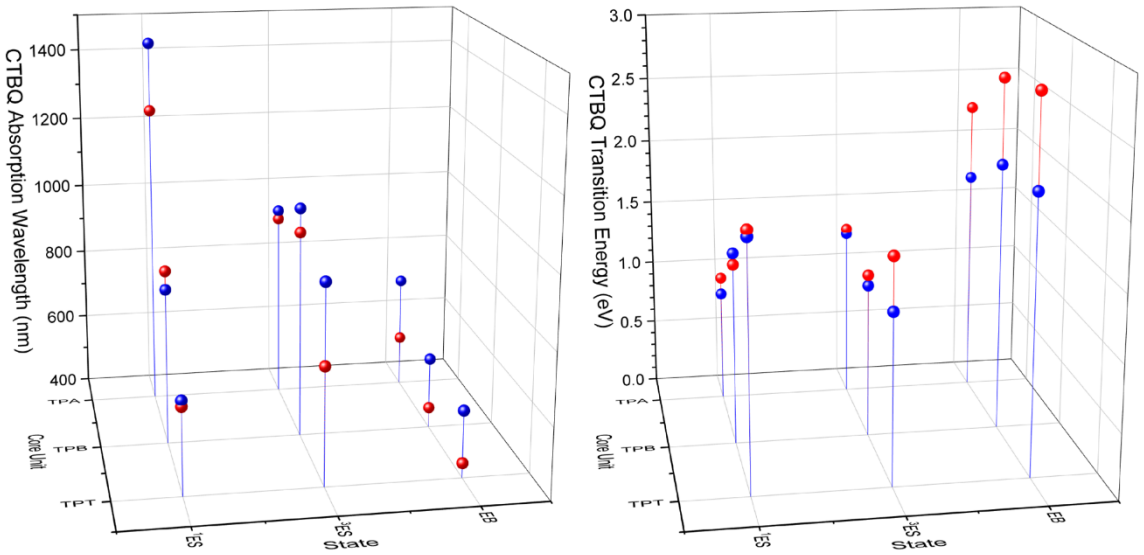

*Figure 3-35 Comparisons of CTBQ absorption wavelengths (left) and transition energies (right) of oxidised **210** oligomers in different doping and spin states. Red spheres represent data of **BZN**-linked oligomers, and blue spheres represent data of **FLR**-linked oligomers.*

Data related to CTBQ transitions, namely absorption wavelengths and transition energies, calculated from TD-DFT calculations of oxidised **210** oligomers in different doping and spin states are shown in Figure 3-35. The trends can be clearly seen in the ^{1}**ES** and **EB** states compared to the ^{3}**ES** state, with the transitions in oligomers of **OTPA** series happening at lower energies and longer wavelengths than those of **OTPB** and **OTPT** series, respectively. In both ^{1}**ES** and **EB** states, the electronic transitions are the charge transfer processes from the bound core blades to the linker units within the oligomer molecules, while in the ^{3}**ES** state, the charge transfer processes happen in the other way round, as illustrated in the respective NTOs.

To compare the effects from core units in the more quantitative way, decreases in the HOMBQ indices of linker units have been chosen as descriptors for core units. Because the HOMBQ index is a measurement for electron delocalisation characteristics of BQ units relatively to the **LEB** (HOMBQ index of 1) and the **EB** (HOMBQ index of 0) forms of unbound BQ units, the oxidation of a BQ unit leads to a decrease in HOMBQ index of that unit. Also, as discussed, the linker units of **210** oligomers are where the most intense effects from oxidation can be observed, and these effects can be counteracted by electron delocalisation from neighbouring BQ units, the bound core blades in these cases. The whole argument means that the linker unit HOMBQ index decreases are the results of core-linker conjugations, and this is the rationale for the use of these numbers as descriptors.

Figure 3-36 shows the relationships between the linker unit HOMBQ index decreases and the transition energies for the CTBQ process. Data are divided into four sets based on doping states and linker units, since the scales for HOMBQ indices are calibrated specifically for individual linker units. Indeed, the relationships between the decreases in HOMBQ indices and the transition energies are linear. This fact, if confirmed by further calculations for more oligomers with different core and linker units, can be used for the tuning of optoelectronic properties in TANIs and their derivatives.

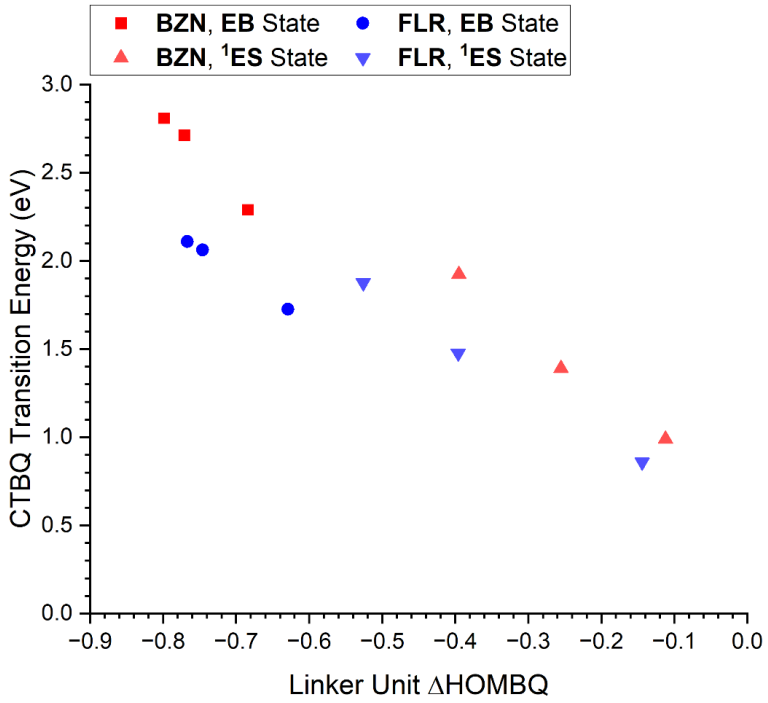

*Figure 3-36 Relationships between the decreases in HOMBQ indices of linker units and the energies of CTBQ transitions of **210** oligomers in the **¹ES** and the **EB** states*

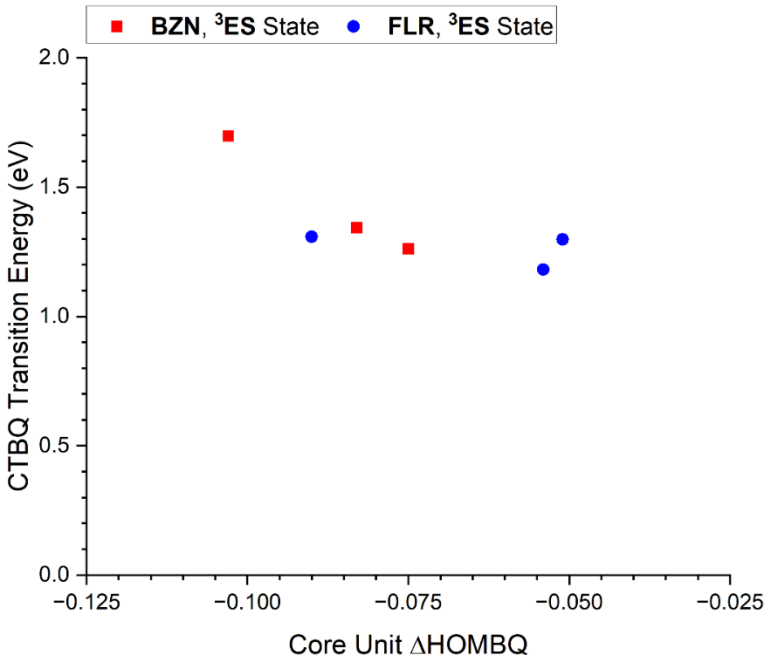

*Figure 3-37 Relationships between the decreases in HOMBQ indices of core units and the energies of CTBQ transitions of **210** oligomers in the **³ES** state*

For the **³ES** state, the changes in HOMBQ indices are more intense in the bound core units instead of the linker units, and the CTBQ transitions take place from the linker units to the core units instead. Therefore, the equivalent comparisons are performed using the decreases in HOMBQ indices from the core units instead, as shown in Figure 3-37. However, a linear relationship cannot be found in this case. It is possible that in the case of the triplet **ES** state, the decreases in HOMBQ indices are relatively small compared to those in the other two states, and therefore, they cannot be used as proper descriptors to represent effects of core-linker unit conjugations.

Overall, there is a significant relationship between the electron delocalisation from the core unit to the linker unit of a **210** modified tetra(aniline) and the optoelectronic properties of the singlet oxidised states (**^{1}ES** and **EB**) of the tetra(aniline). Such relationship can be realised by illustrating the relationship between the decreases in HOMBQ indices of the linker units and the electronic transition energies. However, for the triplet state, the similar relationship cannot be established yet, possibly because the descriptors that can represent the electron delocalisation in the triplet state are yet to be found.

3.3.2 Effects of Topologies and Strains

In the synthesis of PANIs and PANI-CMPs, formations of cyclic oligomer are possible. This is suggested by the mechanism of oligomer formations and confirmed by the analysis of oligomer by-products by MS (see Section 4.4 for the detailed discussion of mass spectrometry analyses of oligomeric products). Therefore, it is possible that different oligomers with different topologies, ring existences and sizes, exist in the oligomers or the polymers. Since these oligomers can have different optoelectronic spectra,[1] it is worth investigating these differences.

*3.3.2.1 Optical Spectra of **OTPA-BZN-221** and **OTPA-FLR-221***

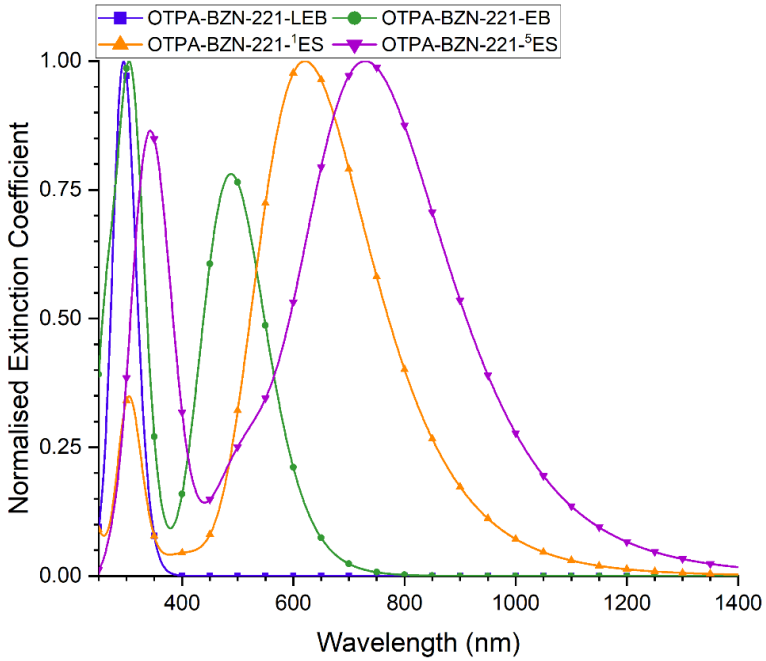

*Figure 3-38 Normalised calculated optoelectronic spectra of **OTPA-BZN-221** models in different oxidation, doping, and spin states from TD-DFT calculations (250 to 1400 nm)*

*Table 3-59 Absorption peak positions of **OTPA-BZN-221** oligomers in different states shown in Figure 3-38*

Oligomer State	Peak Position (nm)	
	Ultraviolet Region	Visible-Near IR Region
LEB	295	-
^{1}ES	305	621
^{5}ES	343	*516* (obscured), 729
EB	305	488

Figure 3-38 shows the absorption spectra of **OTPA-BZN-221** in different states. Overall, the spectrum of **OTPA-BZN-221** in the **LEB** state shows only one peak in the ultraviolet region, while the rest of oxidised oligomers have at least one peak in the visible-near infrared region. While the CTBQ absorption peaks of **ES** state **OTPA-BZN-221** oligomers are still at the longer

wavelengths compared to that of the **EB** state oligomer (Table 3-59), positions of these **ES** state peaks are at higher energies and shorter wavelengths compared to those of the **OTPA-BZN-210** oligomers (Table 3-41).

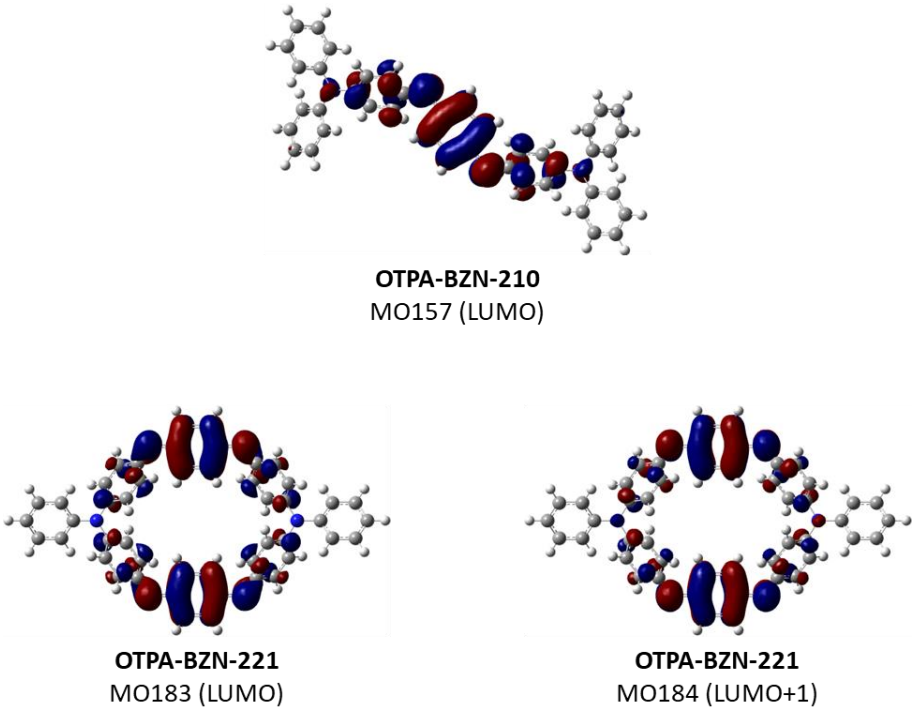

*Figure 3-39 Structures of lowest unoccupied molecular orbitals (LUMOs) of **OTPA-BZN-210** (top) and **OTPA-BZN-221** (bottom), taken from the **EB** state oligomers*

Introduction of the second linker unit also brings more complications into electronic structures. While the comparisons of molecular orbitals between **OTPA-BZN-210** and **OTPA-BZN-221** can be challenging, the most obvious difference can be seen in the structure of lowest unoccupied molecular orbitals (LUMOs). For the open-chain **210** oligomer, the LUMO (MO157) is concentrated around the linker unit, with three lateral nodes passing through both C–N bonds (one node for each bond) and both C_{ortho}–C_{ortho} bonds (one node across both bonds). For the cyclic **221** oligomer, the LUMO (MO183) have the same structures as described earlier for both linker units, and the same also applies to the LUMO+1 (MO184). The difference between the LUMO and the LUMO+1 is the symmetry against the medial line, the line passing through both core units, with the LUMO being antisymmetric and the LUMO+1 being symmetric. The two molecular orbitals are almost similar in energies (degenerate). It should be noted that molecular symmetries were not enforced during the optimisation process. If symmetries were implemented, the two molecular orbitals would likely be degenerate.

Additional data related to contributing electronic transitions are listed in Table 3-60. It is clearly demonstrated that contributions of electronic transitions in the case of cyclised 221 models are more complicated than in the uncyclised 210 models. None of the listed contributions is from HOMO-LUMO transitions, and absorption peaks are contributed by multiple electronic transitions or even multiple excited states entirely. The latter is the case for both 1ES state and EB state oligomers.

*Table 3-60 Details related to electronic transitions involved in the absorption peaks from TD-DFT calculations of **OTPA-BZN-221** oligomers in different oxidation, doping, and spin states. Only excited states with energies in the visible-near infrared region and with oscillator strengths greater than 0.2 are considered, and for each excited state, only electronic transitions contributing at least 10% are listed.*

Excited State	Energy (eV)	Wavelength (nm)	Oscillator Strength *f*	Contributing Electronic Transition
^{1}ES State				
ES2	1.7511	708.04	0.9118	182 (HOMO) → 184 (LUMO+1) (50.3%)
ES3	2.0257	612.05	2.0394	181 (HOMO-1) → 183 (LUMO) (45.8%)
ES4	2.2075	561.64	0.5832	180 (HOMO-2) → 183 (LUMO) (47.3%)
^{5}ES State				
ES2	1.6898	733.73	1.4934	180B (βHOMO) → 181B (βLUMO) (63.1%)
				178B (βHOMO-2) → 182B (βLUMO+1) (16.3%)
				179B (βHOMO-1) → 183B (βLUMO+2) (12.6%)
ES7	2.4057	515.39	0.2888	179B (βHOMO-1) → 182B (βLUMO+1) (48.8%)
				173B (βHOMO-7) → 181B (βLUMO) (29.5%)
EB State				
ES2	2.5051	494.93	1.4442	182 (HOMO) → 184 (LUMO+1) (36.6%)
ES3	2.7662	448.21	0.3111	181 (HOMO-1) → 183 (LUMO) (39.6%)

For **^{1}ES** oligomer, three excited states (ES2, ES3, and ES4) contribute towards the absorption peak at 621 nm. In terms of energy, ES2 and ES4 differ quite significantly from ES3, with the energy difference between ES2 and ES3 being 0.2746 eV and between ES3 and ES4 being 0.1818 eV. However, since the oscillator strength of ES3 (2.0394) is greater than those of ES2 (0.9118) and ES4 (0.5832), the peaks of ES2 and ES4 are being obscured by that of ES3. Both ES2 and ES3 are charge transfers between the linker units and the bound core BQ units (Table 3-61). However, ES3 also involves the unbound blade of **TPA** core units as well, which, again, make the validity of these **221** models questionable for translational studies towards the PANI-CMP systems. Meanwhile, NTO analysis results for ES4 can imply either electronic transitions within the core units themselves or charge transfers between two core units on the opposite ends. Regardless of which transition contributes to the excited state, neither of these is a charge transfer transition.

It should also be noted that while both the excited states ES2 and ES3 of **OTPA-BZN-221** and the excited state ES1 of **OTPA-BZN-210** (Table 3-41) contribute to the visible-to-near-infrared region absorption peak and involve charge transfers between core and linker monomer units, the transfers go in the opposite directions for different oligomer topologies. For **OTPA-BZN-210**, the transfer takes place from the bound core blade to the linker unit, while in the case of **OTPA-BZN-221**, it happens in the other way round.

*Table 3-61 Structures of ground state and excited state molecular orbitals from the NTO analyses of excited states of **OTPA-BZN-221** oligomers in the **^{1}ES** state as listed in Table 3-60*

Excited State	Ground State MO	Excited State MO
ES2	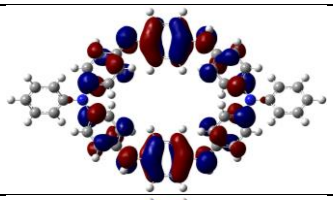	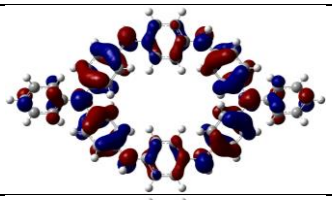
ES3	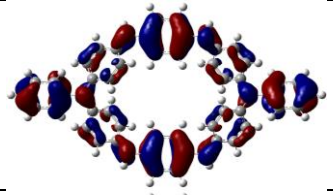	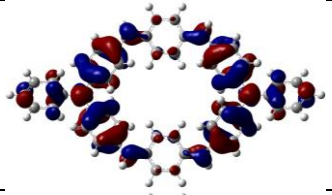
ES4	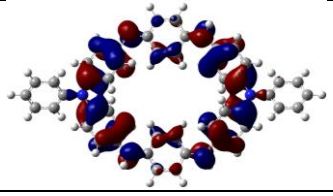	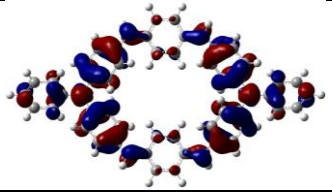

For the quintet state oligomer, two peaks can be seen in the visible-near infrared region, with the less intense peak at 516 nm being obscured by the main peak at 729 nm. These two peaks are corresponding to the excited states ES7 (515.39 nm) and ES2 (733.73 nm), respectively. As shown in Table 3-62, the ES7 is a charge transfer from the bound blades of core units to the unbound blades which, again, is inconclusive whether to be of the same or the different core unit. Meanwhile, the ES2 is a transfer from the core units to the linker units. It appears, however, that the unbound core blades are also involved in the transfer.

*Table 3-62 Structures of ground state and excited state molecular orbitals from the NTO analyses of excited states of **OTPA-BZN-221** oligomers in the **^{5}ES** state as listed in Table 3-60*

Excited State	Ground State MO	Excited State MO
ES2	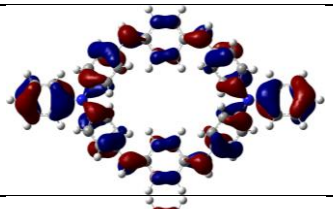	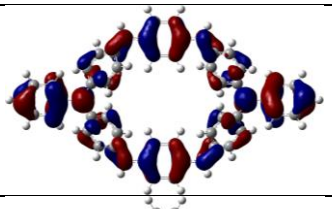
ES7	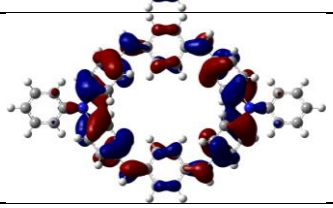	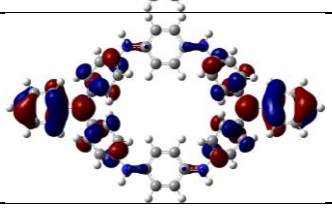

For **OTPA-BZN-221** in the **EB** state, two excited states, ES2 (494.93 nm) and ES3 (448.21 nm), contribute to the absorption peak at 488 nm. NTO analyses of both excited states (Table 3-63) found that the molecular orbitals are almost identical. However, the difference between the two sets of molecular orbitals is the symmetry relative to the medial line, the line that passing through both core units. Both ES2 molecular orbitals are symmetric, while both ES3 molecular orbitals are antisymmetric. The difference is also similar to the LUMO and the LUMO-1 shown in Figure 3-39.

*Table 3-63 Structures of ground state and excited state molecular orbitals from the NTO analyses of excited states of **OTPA-BZN-221** oligomers in the **EB** state as listed in Table 3-60*

Excited State	Ground State MO	Excited State MO
ES2	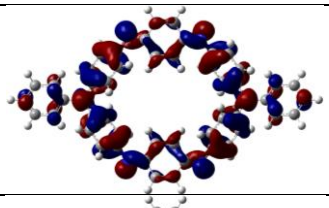	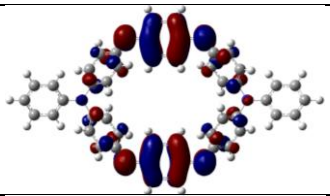
ES3	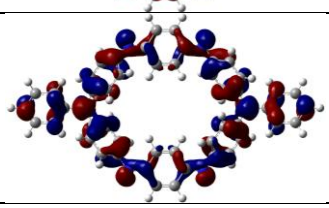	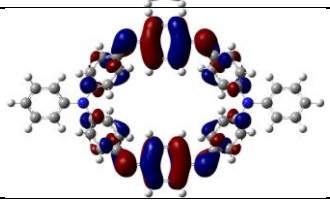

Overall, the cyclic **OTPA-BZN-221** oligomers have their absorption peaks in the visible to near infrared region appearing at the shorter wavelengths, higher energies than the open chain **OTPA-BZN-210** oligomers. While the charge transfers between core and linker units are still prevalent in the singlet **ES** and **EB** states, such characteristics have become recessive in the triplet **ES** state. Meanwhile, electronic transitions involving the unbound core blades have low enough energies to interfere with the CTBQ absorption peaks. These interferences might lead to discrepancies between oligomeric models and the PANI-CMPs in translational studies.

Calculated absorption spectra of **OTPA-FLR-221** in different states are plotted in Figure 3-40, and their peak positions are listed in Table 3-64. Visible and near infrared peaks of **OTPA-FLR-221** appear at the longer wavelengths and lower energies than those of **OTPA-BZN-221**, which follow the same trend as in the **210** oligomeric models. However, while these peaks for **^{1}ES** and **EB** states appear at shorter wavelengths than those of the **OTPA-FLR-210** oligomers, the absorption peak of the triplet state **OTPA-FLR-221** oligomer appears at slightly longer wavelength (942 nm) than that of the triplet state **OTPA-FLR-210** oligomer (932 nm).

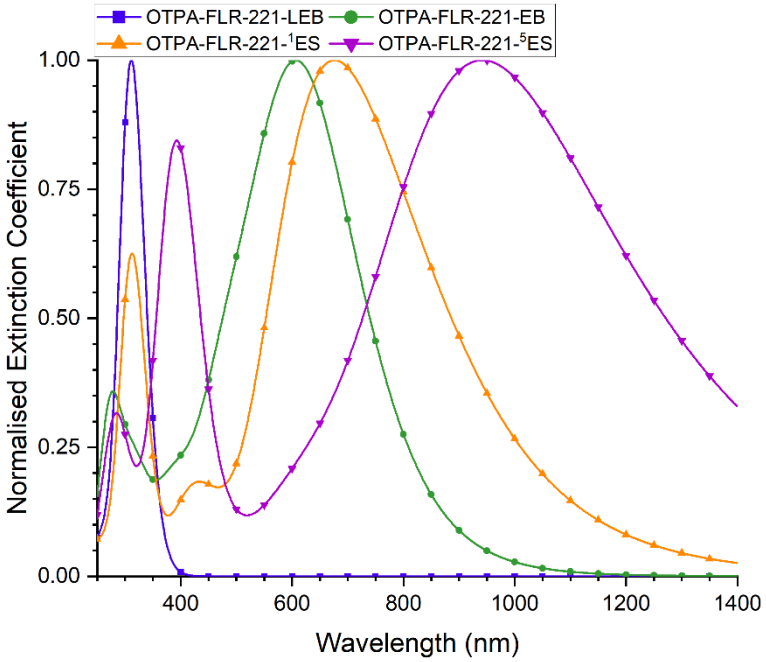

*Figure 3-40 Normalised calculated optoelectronic spectra of **OTPA-FLR-221** models in different oxidation, doping, and spin states from TD-DFT calculations (250 to 1400 nm)*

*Table 3-64 Absorption peak positions of **OTPA-FLR-221** oligomers in different states shown in Figure 3-40*

Oligomer State	Peak Position (nm)	
	Ultraviolet Region	Visible-Near IR Region
LEB	311	-
^{1}ES	313	433, 676
^{5}ES	285	393, 942
EB	278	*392* (obscured), 607

*Table 3-65 Details related to electronic transitions involved in the absorption peaks from TD-DFT calculations of **OTPA-FLR-221** oligomers in different oxidation, doping, and spin states. Only excited states with energies in the visible-near infrared region and with oscillator strengths greater than 0.2 are considered, and for each excited state, only electronic transitions contributing at least 10% are listed.*

Excited State	Energy (eV)	Wavelength (nm)	Oscillator Strength *f*	Contributing Electronic Transition
^{1}ES State				
ES2	1.5592	795.20	1.1562	228 (HOMO) → 230 (LUMO+1) (45.1%)
ES3	1.9058	650.56	1.8230	227 (HOMO-1) → 229 (LUMO) (46.5%)
ES4	2.1162	585.88	0.4086	226 (HOMO-2) → 229 (LUMO) (40.8%)
ES10	2.8308	437.98	0.2546	219 (HOMO-9) → 229 (LUMO) (13.0%)
^{5}ES State				
ES2	1.3054	949.81	2.1238	225B (βHOMO-1) → 227B (βLUMO) (53.5%)
				226B (βHOMO) → 229B (βLUMO+2) (30.5%)
ES23	3.1138	398.18	0.6587	225B (βHOMO-1) → 230B (βLUMO+3) (37.1%)
				239A (αHOMO-1) → 231A (αLUMO) (13.1%)
				230A (αHOMO) → 232A (αLUMO+1) (12.9%)
ES24	3.1390	394.97	0.9074	225B (βHOMO-1) → 230B (βLUMO+3) (23.1%)
				230A (αHOMO) → 232A (αLUMO+1) (20.0%)
				229A (αHOMO-1) → 231A (αLUMO) (18.7%)
EB State				
ES2	1.9849	624.63	2.7706	228 (HOMO) → 230 (LUMO+1) (43.9%)
ES3	2.2435	552.65	0.2051	227 (HOMO-1) → 229 (LUMO) (42.6%)
ES5	2.5402	488.09	1.1905	226 (HOMO-2) → 229 (LUMO) (44.2%)

Table 3-65 list details related to electronic transitions involved in absorption peaks of **OTPA-FLR-221** oligomers in oxidised states. There are several similarities between contributing electronic transitions of **OTPA-FLR-221** and of **OTPA-BZN-221** (Table 3-60). For example, three excited states with different energies appear together as one broad peak in the **^{1}ES** state. The same peak of the **EB** state oligomer is also contributed by several excited states although there is a third excited state with oscillator strength *f* high enough to be considered significant in addition to the similar ES2 and ES3. However, there are differences between electronic transitions involved in spectra of **FLR**-linked and **BZN**-linked **221** oligomers, which will be explored over the next paragraphs.

Three excited states with similar energies, namely ES2 (1.5592 eV, 795.20 nm), ES3 (1.9058 eV, 650.56 nm), and ES4 (2.1162 eV, 585.88 nm), contribute towards the absorption peak of ^{1}**ES** state **OTPA-FLR-221**. These three states are the same as in the ^{1}**ES** state **OTPA-BZN-221**, which are reflected by the similar structures of NTO molecular orbitals (Table 3-66, compared to Table 3-61 for the **BZN**-linked counterpart). Again, excited states ES2 and ES3 are related to charge transfer transitions, while ES4 only involves bound core units. The only difference between these three excited states of **FLR**-linked and **BZN**-linked oligomers in the singlet **ES** state is the linker unit structures.

Another peak can also be observed in the visible region of the singlet **ES** state **OTPA-FLR-221** absorption spectrum at 433 nm. This peak is chiefly arising from excited state ES10 (2.8308 eV, 437.98 nm). This 433 nm peak is comparable to the two peaks at 362 and 517 nm in the corresponding spectrum of the ^{1}**ES** state **OTPA-FLR-210** oligomer, only with significant intensity (f = 0.2546). ES10 is similar to ES4 for involving only core unit, albeit ES10 involves all three blades, bound and unbound, rather than only bound blades as in ES4. For ES10, two pairs of molecular orbitals, instead of just one pair, contribute dominantly towards the absorption, but there is no significant difference between the two pairs other than symmetry against the medial and the lateral lines.

*Table 3-66 Structures of ground state and excited state molecular orbitals from the NTO analyses of excited states of **OTPA-FLR-221** oligomers in the ^{1}**ES** state as listed in Table 3-65*

Excited State	Ground State MO	Excited State MO
ES2	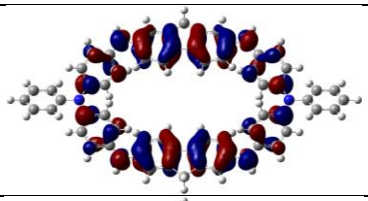	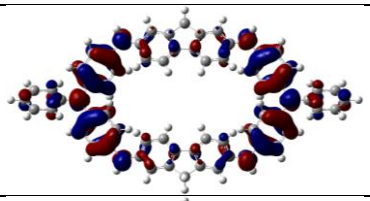
ES3	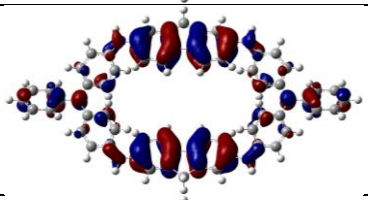	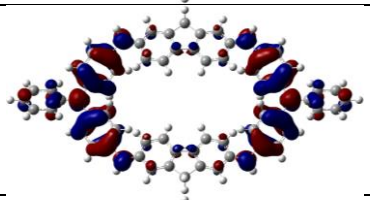
ES4	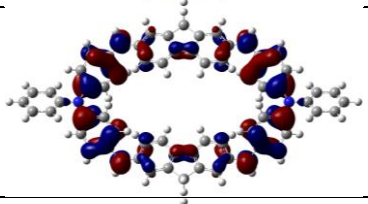	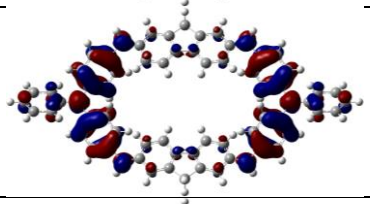
ES10	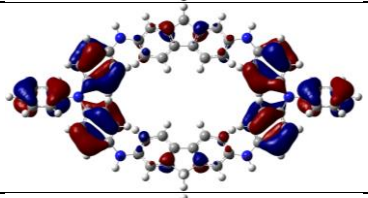 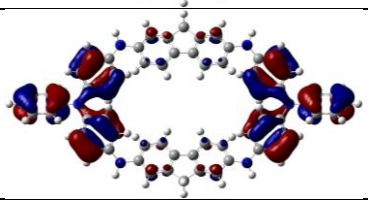	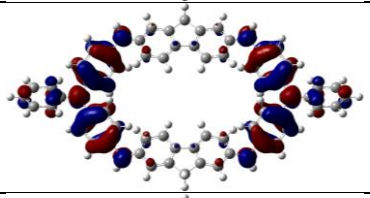 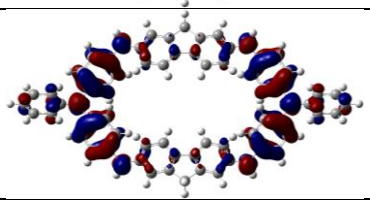

NTO analyses of ^{5}**ES** state **OTPA-FLR-221** (Table 3-67) are similar to those of the **BZN**-linked oligomer for not being CTBQ in nature. However, the difference between NTO molecular orbitals of **OTPA-FLR-221** and **OTPA-BZN-221** is the location of transitions. While the NTO molecular orbitals from the analyses of **OTPA-BZN-221** (Table 3-62, ES2) involve the whole molecule, the orbitals from the analyses of **OTPA-FLR-221** (also ES2) are more focused on the **FLR** linker units. It is worth noting that although the energy and position of the infrared absorption peaks of the two polaronic **OTPA-FLR** oligomers (triplet **210** and quintet **221**) are similar, the contributing electronic transitions are different since the transition taking place in **OTPA-FLR-210** appears to be charge transfer, unlike in the **OTPA-FLR-221**.

There is another peak appearing around the ultraviolet-visible borderline region (393 nm) contributed by excited states ES23 (398.18 nm) and ES24 (394.17 nm). Both states arise, meanwhile, mainly from the same three electronic transitions but with different ratios. These electronic transitions consist of both alpha and beta orbitals, and they appear to be the mixtures of the transition within the core-linker conjugated BQ units (CLBQ) and the transition from **FLR** linkers to the whole structure.

For the undoped **EB** state, there are two excited states that are similar to those of **OTPA-BZN-221**, namely ES2 (1.9849 eV, 624.63 nm) and ES3 (2.2435 eV, 552.65 nm) contributing to the main peak at 607 nm. The energy gap between the two states (0.2586 eV) is also comparable to that between those energies of **OTPA-BZN-221** (0.2611 eV), and the molecular orbitals from NTO analyses, shown in Table 3-68, are also similar to those of the **BZN**-linked counterparts (Table 3-63). Again, NTO molecular orbitals of ES2 and ES3 only differ by symmetry, and the electronic transitions corresponding to these two states are charge transfer in nature.

*Table 3-67 Structures of ground state and excited state molecular orbitals from the NTO analyses of excited states of **OTPA-FLR-221** oligomers in the ^{5}**ES** state as listed in Table 3-65*

Excited State	Ground State MO	Excited State MO
ES2	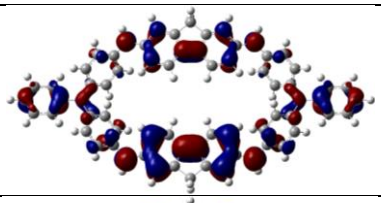	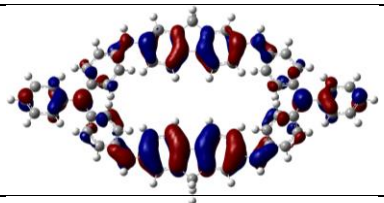
ES23	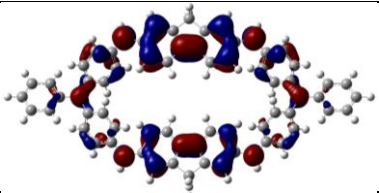	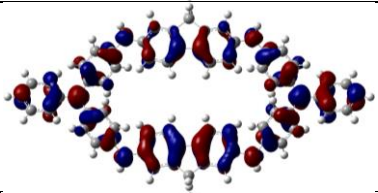
ES24	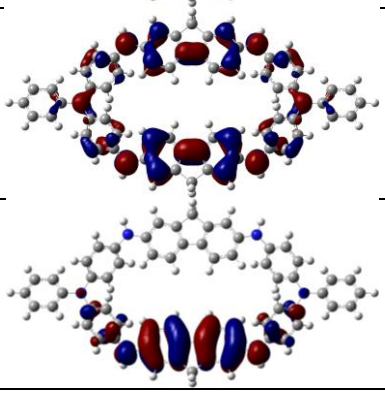	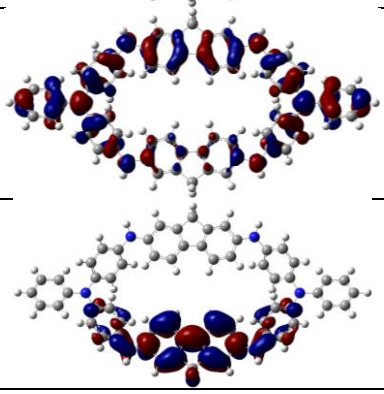

*Table 3-68 Structures of ground state and excited state molecular orbitals from the NTO analyses of excited states of **OTPA-FLR-221** oligomers in the **EB** state as listed in Table 3-65*

Excited State	Ground State MO	Excited State MO
ES2	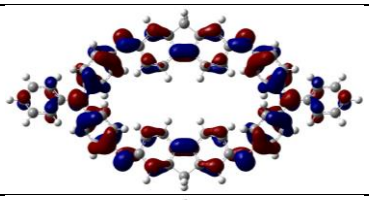	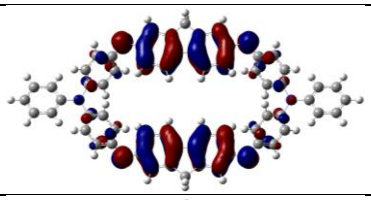
ES3	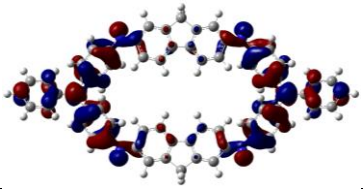	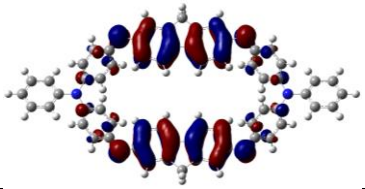
ES5	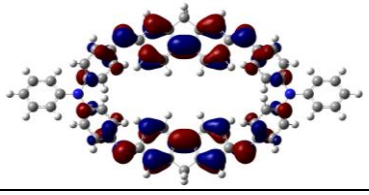	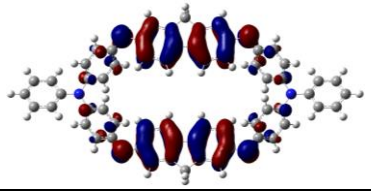

The peak at 607 nm also obscures a peak at approximately 393 nm, contributed by the excited state ES5. This peak is a CLBQ peak in nature, considering that the NTO molecular orbitals are concentrated around **FLR** linker units.

*3.3.2.2 Optical Spectra of **OTPB-BZN-221** and **OTPB-FLR-221***

Optical absorption spectra of **OTPB-BZN-221** and **OTPB-FLR-221** are shown in Figure 3-41 and Figure 3-42, respectively, with their peak positions listed in Table 3-69. Overall, the situations are similar to the **TPA** cyclic oligomers as all spectra of oxidised **221** oligomers become more complicated than those of oxidised **210** oligomers. The clear difference between **OTPB-BZN-221** absorption spectra and **OTPB-FLR-221** absorption spectra is the peak positions in visible region of the doped oligomers. For the **FLR**-linked oligomers in the **ES** states, the absorption peak of the polaron quintet oligomer appears at a longer wavelength (818 nm) than that of the bipolaron singlet oligomer (677 nm). However, in the case of **BZN**-linked oligomers, absorption peaks of both spin isomers appear at almost the same position, with the peak position being 678 nm for ^{1}**ES** oligomer and 685 nm for ^{5}**ES** oligomer.

Meanwhile, for the absorption spectra of **EB** state oligomers, the absorption peak of **OTPB-BZN-221** appears at a shorter wavelength (434 nm) than that of **OTPB-FLR-221** (558 nm). These peak positions follow the same trend as the other comparisons between **BZN**-linked and **FLR**-linked oligomers. For example, for the open chain **TPB** oligomers, the absorption peaks are at 457 nm for **OTPB-BZN-210** and 601 nm for **OTPB-FLR-210**, and for the cyclic oligomers of the **OTPA** series, the absorption peaks are at 488 nm for **OTPA-BZN-221** and 607 nm for **OTPA-FLR-221**.

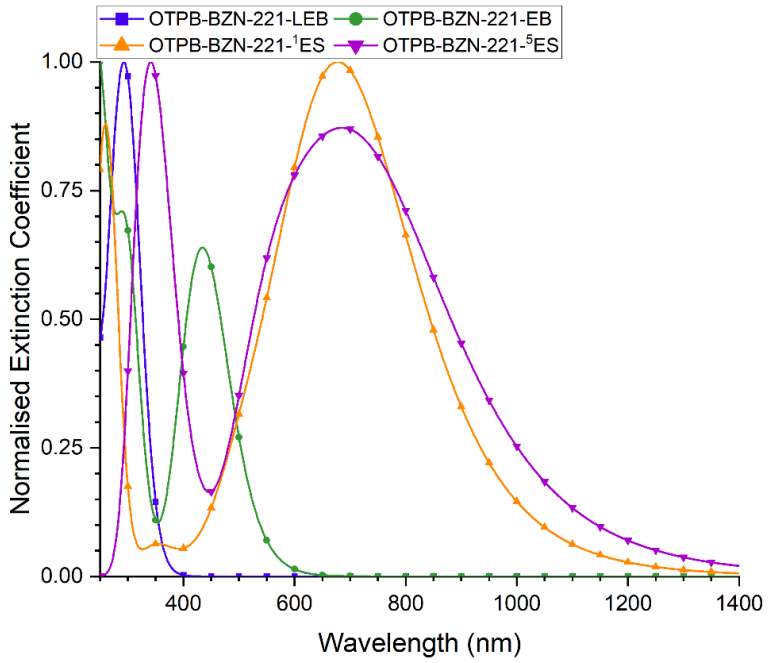

*Figure 3-41 Normalised calculated optoelectronic spectra of **OTPB-BZN-221** models in different oxidation, doping, and spin states from TD-DFT calculations (250 to 1400 nm)*

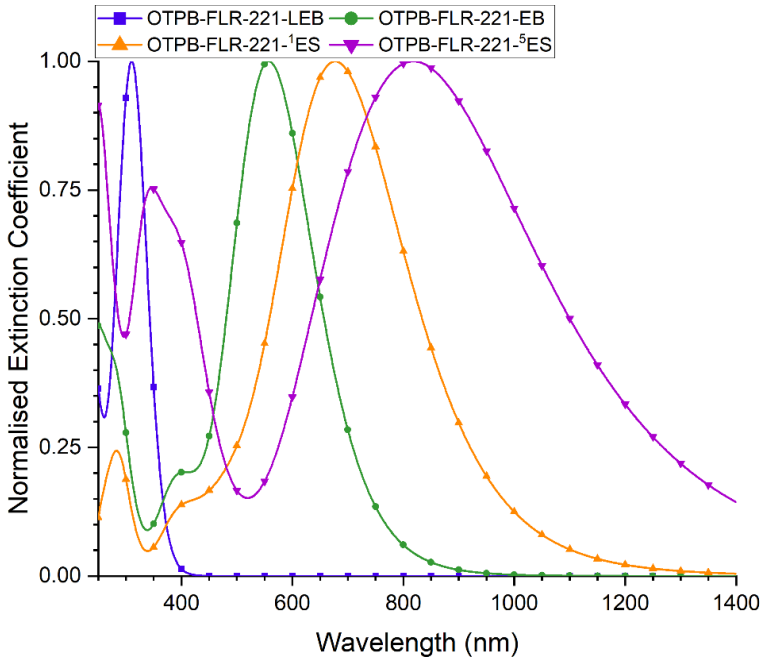

*Figure 3-42 Normalised calculated optoelectronic spectra of **OTPB-FLR-221** models in different oxidation, doping, and spin states from TD-DFT calculations (250 to 1400 nm)*

*Table 3-69 Peak positions in absorption spectra calculated from TD-DFT calculations of **OTPB-BZN-221** and **OTPB-FLR-221** in different oxidation, doping, and spin states*

Oligomer State	Peak Position (nm)	
	OTPB-BZN-221	**OTPB-FLR-221**
LEB	293	310
^{1}ES	260, 354, 678	*413* (obs.), 677
^{5}ES	341, 685	346, *395* (obs.), 818
EB	289, 434	*283* (obs.), 406, 558

Table 3-70 listed details about electronic transitions and excited states involved in the visible-NIR absorption peaks of oxidised **OTPB-BZN-221**. For all three oxidised states, only one peak can be observed beyond 400 nm in each state. However, all these peaks are arisen from several excited states. In the cases of singlet **ES** and **EB** states, the absorption peak arises mainly from one excited state obscuring the smaller peaks, while in the case of the quintet **ES** state, two main excited states contribute almost equally.

*Table 3-70 Details related to electronic transitions involved in the absorption peaks from TD-DFT calculations of **OTPB-BZN-221** oligomers in different oxidation, doping, and spin states. Only excited states with energies in the visible-near infrared region and with oscillator strengths greater than 0.2 are considered, and for each excited state, only electronic transitions contributing at least 10% are listed.*

Excited State	Energy (eV)	Wavelength (nm)	Oscillator Strength *f*	Contributing Electronic Transition
^{1}ES State				
ES2	1.7755	698.32	2.2673	212 (HOMO-2) → 216 (LUMO+1) (26.5%)
				214 (HOMO) → 215 (LUMO) (14.5%)
ES7	2.2472	551.72	0.5484	209 (HOMO-5) → 215 (LUMO) (41.8%)
ES9	2.4901	497.91	0.2833	208 (HOMO-6) → 215 (LUMO) (40.9%)
^{5}ES State				
ES2	1.6103	769.94	0.8778	212B (βHOMO) → 213B (βLUMO) (38.5%)
				208B (βHOMO-4) → 214B (βLUMO+1) (24.1%)
				207B (βHOMO-5) → 213B (βLUMO) (19.2%)
ES3	1.7916	692.03	0.3315	211B (βHOMO-1) → 214B (βLUMO+1) (61.6%)
				212B (βHOMO) → 216B (βLUMO+3) (23.1%)
ES6	1.9662	630.57	0.2285	212B (βHOMO) → 213B (βLUMO) (39.3%)
				208B (βHOMO-4) → 214B (βLUMO+1) (30.7%)
ES11	2.2209	558.26	0.7303	208B (βHOMO-4) → 215B (βLUMO+2) (38.7%)
				206B (βHOMO-6) → 213B (βLUMO) (30.5%)
EB State				
ES2	2.8391	436.70	1.7473	214 (HOMO) → 215 (LUMO) (23.8%)
				213 (HOMO-1) → 216 (LUMO+1) (19.2%)
ES3	3.0042	412.70	0.2149	212 (HOMO-2) → 216 (LUMO+1) (19.8%)
				211 (HOMO-3) → 215 (LUMO) (12.5%)

For the **^{1}ES** state **OTPB-BZN-221**, the absorption peak arises mostly from excited state ES2 (1.7755 eV, 698.32 nm, f = 2.2673). While the NTO analyses of this excited state revealed that there are two major pairs of molecular orbitals contributing (Table 3-71), they are both still charge transfers from the core units to the linker units. The other two excited states, namely ES7 (2.2472 eV, 551.72 nm, f = 0.5484) and ES9 (2.4901 eV, 497.91 nm, f = 0.2833), are also charge transfers but only originated from the different parts of core units.

*Table 3-71 Structures of ground state and excited state molecular orbitals from the NTO analyses of excited states of **OTPB-BZN-221** oligomers in the **^{1}ES** state as listed in Table 3-70*

Excited State	Ground State MO	Excited State MO
ES2	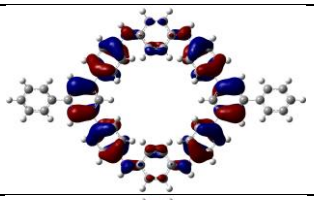	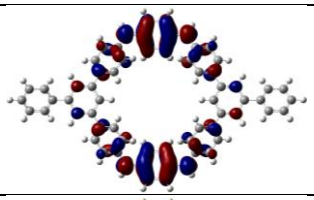
	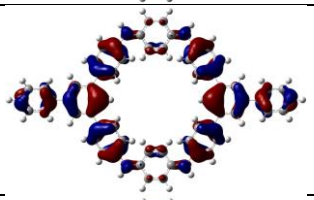	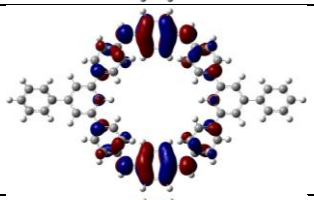
ES7	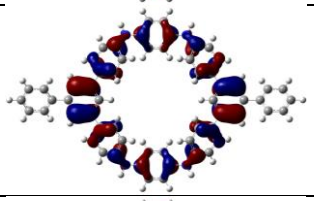	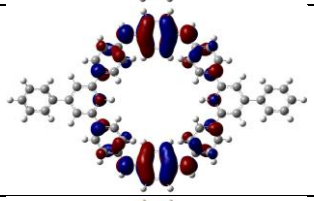
ES9	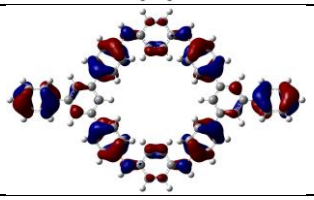	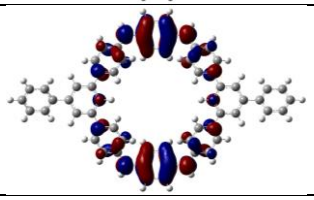

For the quintet state, NTO molecular orbitals are listed in Table 3-72. While only one peak at 685 nm is also observed in the absorption spectra, there are four excited states involved, namely ES2 (1.6103 eV, 769.94 nm), ES3 (1.7916 eV, 692.03 nm), ES6 (1.9662 eV, 630.57 nm), and ES11 (2.2209 eV, 558.26 nm). ES2 (f = 0.8778) and ES11 (f = 0.7303) are the major contributors. While the absorption peaks of the singlet state (678 nm) and the quintet state (685 nm) are close in wavelength, this should be considered coincidental because the quintet state absorption peak arises from two major excited states and at least two minor excited states while the singlet state peak is mainly coming from one intense excited state.

In the case of ES2, the transition involved is a charge transfer, with the origin of the transfer being the core hub rings coupled with the unbound core blade rings along with the linker units and the destination of the transfer being the bound core blade rings. As the main cyclic part of the **OTPB-BZN-221** contains eight aromatic rings, it has become more obvious that both structures of ground state and excited states molecular orbitals have positive charges (refers to the lack of electrons) located on every other ring, compared to the six-ring cycle in **OTPA-BZN-221**. Meanwhile, ES11 is similar to ES2 for origins and destinations of charge transfers. It differs from ES2 only by symmetries.

For the two minor contributors, ES3 (f = 0.3315) and ES6 (f = 0.2285), they are also charge transfers. However, origins of transfers in these two cases are couples between unbound core blades and core hubs. Arguably, because of the 1,6-pattern of steric hindrance between the two *ortho* hydrogen atoms of the blade and the hub ring of **TPB** core units (see Scheme 3-18), the dihedral angles between adjacent rings are small enough to aid the overlapping between their π-systems. However, it should also be reminded that the unbound core units might be rare in the

structures of PANI-CMPs, which may not affect ES3 and ES6 much due to their relatively smaller contributions, but it might affect ES2 (one of the major contributors) as well.

*Table 3-72 Structures of ground state and excited state molecular orbitals from the NTO analyses of excited states of **OTPB-BZN-221** oligomers in the ^{5}**ES** state as listed in Table 3-70*

Excited State	Ground State MO	Excited State MO
ES2	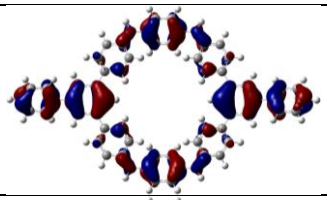	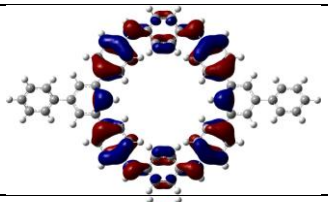
ES3	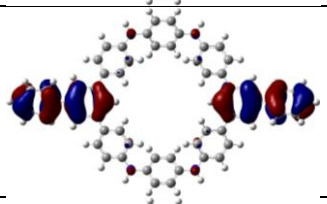	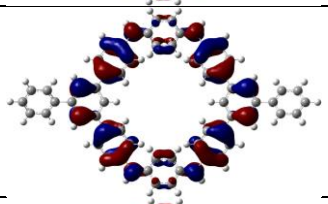
ES6	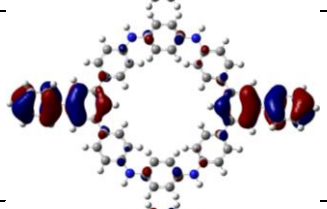	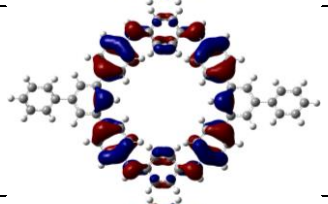
ES11	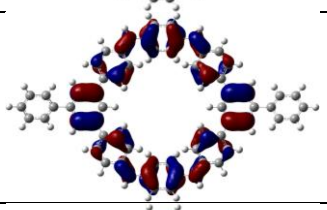	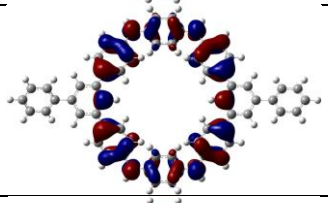
	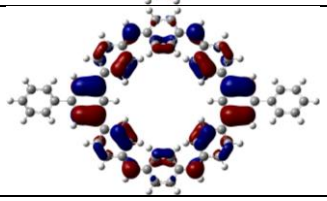	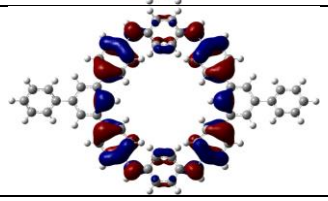

For the **EB** state, the absorption peak is at 434 nm. The majorly contributing excited state is ES2 (2.8391 eV, 436.70 nm, f = 1.7473), while another contributor is ES3 (3.0042 eV, 412.70 nm, f = 0.2149). NTO molecular orbitals for both excited states are shown in Table 3-73. Overall, molecular orbitals for both excited states still have the same characteristics as the previously mentioned **EB** state molecular orbitals. The related electronic transitions are still charge transfers from the bound blades of core units to the linker BQ units of different symmetries. The notable difference from the **TPA** counterpart is the blueshift from 488 nm in **OTPA-BZN-221**, which is again the same trend as in the uncyclised **210** oligomers (541 nm for **OTPA-BZN-210** and 457 nm for **OTPB-BZN-210**). The blueshift phenomenon as a result from cyclisation can also be observed (541 nm to 488 nm for **OTPA** series and 457 nm to 434 nm for **OTPB** series).

Across all three oxidised states, a common theme that can be observed as a result of cyclisation is the greater prevalence of non-HOMO-LUMO electronic transitions. Although this issue has already been discussed for the absorption peak of triplet **OTPB-BZN-210** (Table 3-51), the HOMO-LUMO transitions are still the major contributors for the open chain **OTPB-BZN-210** oligomers in ^{1}**ES** and **EB** states. However, for the **221** oligomers, non-HOMO-LUMO transitions can be found in all three states. The increased significance of non-HOMO-LUMO transitions can

be the result of more complexed electronic structures due to symmetries which in turn are the results of cyclisation and the inclusion of a second linker unit.

*Table 3-73 Structures of ground state and excited state molecular orbitals from the NTO analyses of excited states of **OTPB-BZN-221** oligomers in the **EB** state as listed in Table 3-70*

Excited State	Ground State MO	Excited State MO
ES2	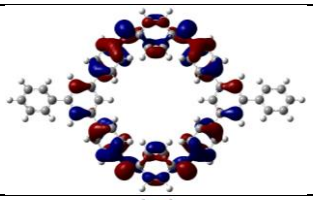	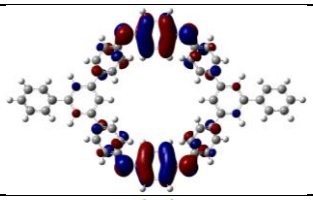
	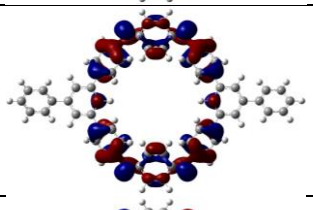	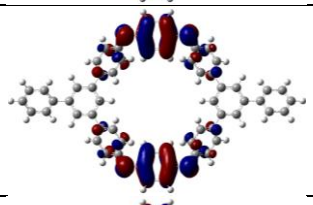
ES3	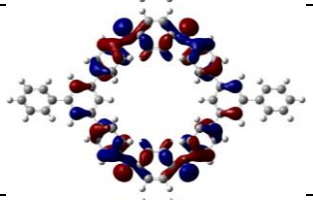	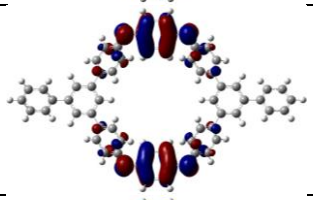
	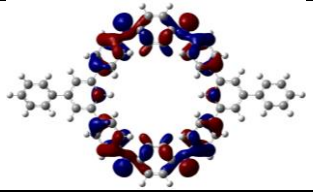	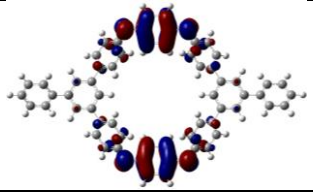

For **OTPB-FLR-221** oligomers, the details about electronic transitions involved in absorption spectra are listed in Table 3-74. While the emergences of non-HOMO-LUMO transitions are observed in all three states, and contributions from multiple excited states are also seen in both singlet and quintet spin isomers of the **ES** state, it is notable that only one excited state contributes to the absorption peak of **EB** state **OTPB-FLR-221**.

Three excited states contribute to the absorption peak at 677 nm of ^{1}**ES** state **OTPB-FLR-221**, namely ES2 (1.8094 eV, 685.21 nm), ES3 (2.1114 eV, 587.22 nm), and ES9 (2.5099 eV, 493.98 nm). Like in **OTPB-BZN-221**, ES2 is also the main contributor with the oscillator strength of 3.3711, compared to 0.2558 for ES3 and 0.4937 for ES9. All three states are, again, charge transfers from core units to linker units, and their NTO molecular orbitals (Table 3-75) are roughly comparable to those of **OTPB-BZN-221** (Table 3-71). The major similarity between the ES2 states in both oligomers is that the origins of charge transfers in both cases are the three-ring moieties consisting of the two bound core blades and the core hub rings. For minor contributors, the origins may be different between the two oligomers due to the differences in oscillator strengths, but they are still located within the core units. Interestingly, the ES2 energy of **OTPB-FLR-221** (1.8094 eV) is also similar to that of **OTPB-BZN-221** (1.7755 eV), only slightly larger by 0.0339 eV.

*Table 3-74 Details related to electronic transitions involved in the absorption peaks from TD-DFT calculations of **OTPB-FLR-221** oligomers in different oxidation, doping, and spin states. Only excited states with energies in the visible-near infrared region and with oscillator strengths greater than 0.2 are considered, and for each excited state, only electronic transitions contributing at least 10% are listed.*

Excited State	Energy (eV)	Wavelength (nm)	Oscillator Strength *f*	Contributing Electronic Transition
^{1}ES State				
ES2	1.8094	685.21	3.3711	259 (HOMO-1) → 262 (LUMO+1) (30.5%)
				260 (HOMO) → 261 (LUMO) (10.1%)
ES3	2.1114	587.22	0.2558	258 (HOMO-2) → 262 (LUMO+1) (25.6%)
				257 (HOMO-3) → 261 (LUMO) (16.5%)
ES9	2.5099	493.98	0.4937	256 (HOMO-4) → 261 (LUMO) (36.5%)
^{5}ES State				
ES2	1.4040	883.09	1.5092	256B (βHOMO-2) → 260B (βLUMO+1) (28.2%)
				255B (βHOMO-3) → 259B (βLUMO) (21.8%)
				258B (βHOMO) → 259B (βLUMO) (20.6%)
				257B (βHOMO-1) → 260B (βLUMO+1) (12.5%)
ES3	1.7615	703.87	0.8459	256B (βHOMO-2) → 261B (βLUMO+2) (22.3%)
				258B (βHOMO) → 262B (βLUMO+3) (17.8%)
				252B (βHOMO-6) → 259B (βLUMO) (16.6%)
EB State				
ES2	2.2182	558.94	3.8979	260 (HOMO) → 262 (LUMO+1) (25.3%)
				259 (HOMO-1) → 261 (LUMO) (22.1%)

*Table 3-75 Structures of ground state and excited state molecular orbitals from the NTO analyses of excited states of **OTPB-FLR-221** oligomers in the **^{1}ES** state as listed in Table 3-74*

Excited State	Ground State MO	Excited State MO
ES2	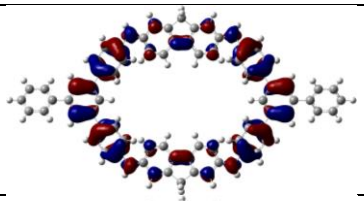	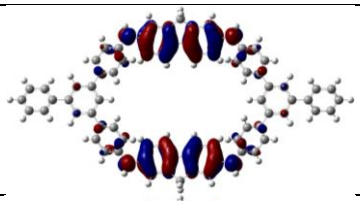
ES3	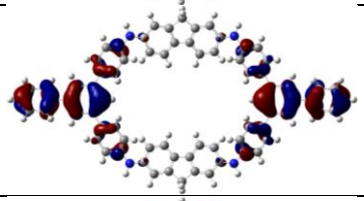	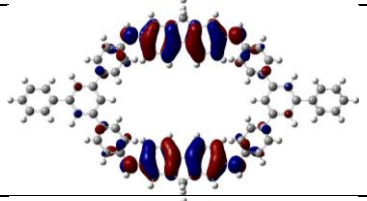
ES9	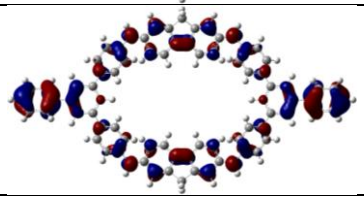	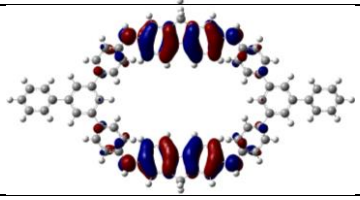

*Table 3-76 Structures of ground state and excited state molecular orbitals from the NTO analyses of excited states of **OTPB-FLR-221** oligomers in the ^{5}**ES** state as listed in Table 3-74*

Excited State	Ground State MO	Excited State MO
ES2	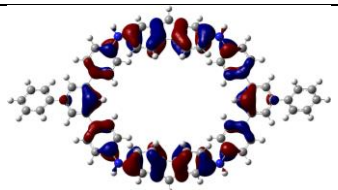	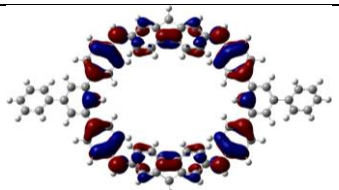
	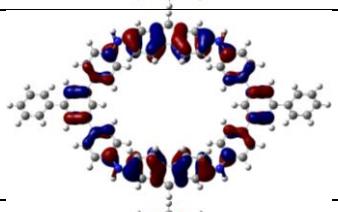	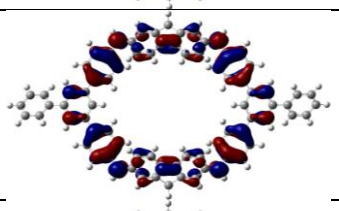
ES3	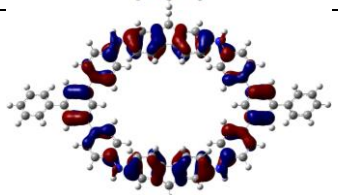	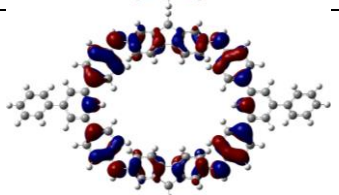
	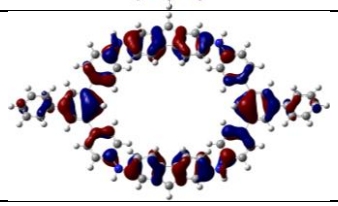	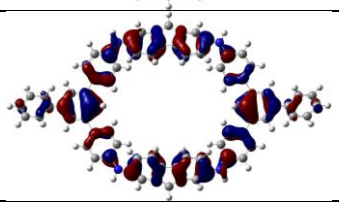

For the quintet state, the absorption peak at 818 nm is a result of two major excited states, ES2 (1.4040 eV, 883.09 nm) and ES3 (1.7615 eV, 703.87 nm), which is the same as in the quintet **OTPB-BZN-221**$^{4+}$ (Table 3-70). However, the contributing electronic transitions of ^{5}**OTPB-FLR-221**$^{4+}$ have become more complicated. A similar pattern as discussed for **OTPB-BZN-221** in the NTO molecular orbitals of ground and excited states can also be seen in **OTPB-FLR-221** (Table 3-76).

*Table 3-77 Structures of ground state and excited state molecular orbitals from the NTO analyses of excited states of **OTPB-FLR-221** oligomers in the **EB** state as listed in Table 3-74*

Excited State	Ground State MO	Excited State MO
ES2	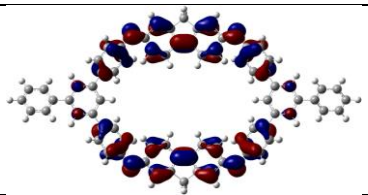	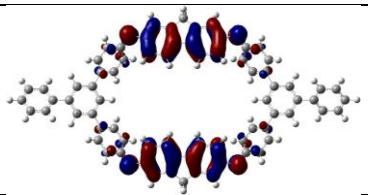
	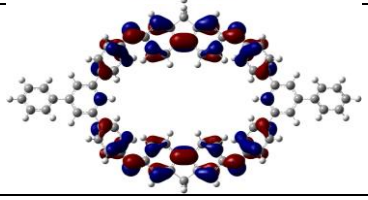	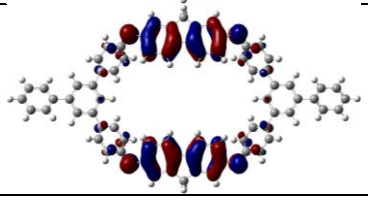

For **OTPB-FLR-221** in the **EB** state, the peak position in the visible region is at 558 nm. There is a clear difference between the contributing electronic transitions, however. Typically, electronic transitions involved in the visible-near-IR absorption peak of **EB** state oligomers are

CTBQ transitions. However, as shown in Table 3-77, the transitions involved are more CLBQ in nature.

*3.3.2.3 Optical Spectra of **OTPT-BZN-221** and **OTPT-FLR-221***

Absorption spectra of **OTPT-BZN-221** and **OTPT-FLR-221** are shown in Figure 3-43 and Figure 3-44, respectively, with peaks listed in Table 3-78. The major difference between spectra of these oligomers and spectra of previously discussed **221** oligomers can be seen in the quintet state. These visible-NIR peaks now appear clearly as two overlapped peaks rather than combined peaks as in the **OTPB** series. Besides the transition energies and subsequent peak positions, detailed related to absorption of the two oligomers are almost similar. Therefore, absorption data of both oligomeric models will be discussed together.

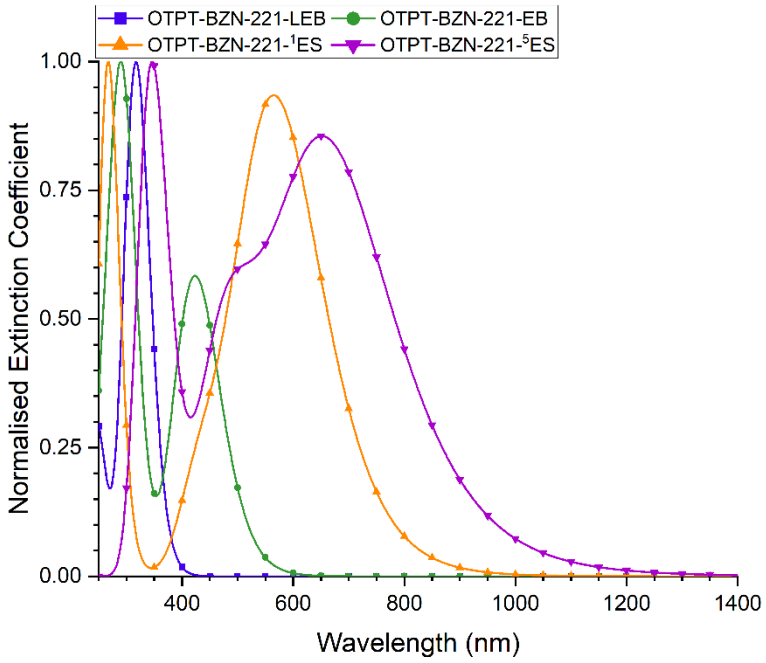

*Figure 3-43 Normalised calculated optoelectronic spectra of **OTPT-BZN-221** models in different oxidation, doping, and spin states from TD-DFT calculations (250 to 1400 nm)*

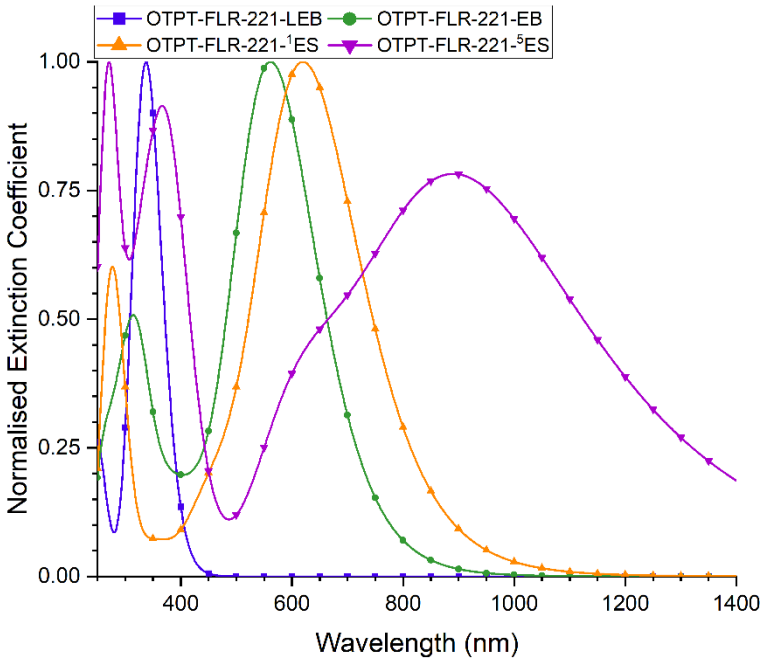

*Figure 3-44 Normalised calculated optoelectronic spectra of **OTPT-FLR-221** models in different oxidation, doping, and spin states from TD-DFT calculations (250 to 1400 nm)*

*Table 3-78 Peak positions in absorption spectra calculated from TD-DFT calculations of **OTPT-BZN-221** and **OTPT-FLR-221** in different oxidation, doping, and spin states*

Oligomer State	Peak Position (nm)	
	OTPT-BZN-221	**OTPT-FLR-221**
LEB	317	337
^{1}ES	267, 565	274, 620
^{3}ES	346, *515* (obs.), 651	271, 366, *633* (obs.), 890
EB	290, 423	254, 314, 562

For oxidised **OTPT-BZN-221** oligomers, details related to electronic transitions and absorption peaks are listed in Table 3-79. It is clearly shown that electronic transitions involved in the absorption spectra of **OTPT-BZN-221** are more complicated than those of **OTPB-BZN-221**. Meanwhile, there is no HOMO-LUMO transition significantly contributing towards absorption peaks at all. This further complication can also be the result of the structures of **TPT** core units.

For the **^{1}ES** state, the absorption peak of **OTPT-BZN-221** appears at 565 nm. The same pattern of electronic transitions as previously mentioned for **OTPB** series of cyclic oligomers can also be seen in **OTPT-BZN-221**, with the main contributor being ES2 (2.1762 eV, 569.73 nm). This excited state also corresponds to the core-to-linker charge transfer transitions, with the NTO molecular orbitals shown in Table 3-81. Meanwhile, the transitions for minor contributors (ES13 and ES15) also originate from the other moieties of the core units towards the linker units.

In the case of **FLR**-linked oligomeric model, the corresponding peak appears slightly redshifted at 620 nm, while the main contributing electronic transition (ES2) is at 622.13 nm (1.9929 eV). The peak also obscures another contribution from ES5 (2.6568 eV, 466.67 nm). Both ES2 and ES5 are similar to the ES2 of the **BZN**-linked counterpart, with the transitions being the transfers from bound core units to the linker units (Table 3-82).

*Table 3-79 Details related to electronic transitions involved in the absorption peaks from TD-DFT calculations of **OTPT-BZN-221** oligomers in different oxidation, doping, and spin states. Only excited states with energies in the visible-near infrared region and with oscillator strengths greater than 0.2 are considered, and for each excited state, only electronic transitions contributing at least 10% are listed.*

Excited State	Energy (eV)	Wavelength (nm)	Oscillator Strength *f*	Contributing Electronic Transition
^{1}ES State				
ES2	2.1762	569.73	2.5389	210 (HOMO-4) → 215 (LUMO) (24.6%)
				209 (HOMO-5) → 216 (LUMO+1) (21.3%)
ES13	2.7563	449.82	0.2153	211 (HOMO-3) → 216 (LUMO+1) (28.7%)
ES15	2.8336	437.55	0.4055	208 (HOMO-6) → 216 (LUMO+1) (18.0%)
				211 (HOMO-3) → 216 (LUMO+1) (16.2%)
^{5}ES State				
ES2	1.8290	677.87	0.4641	207B (βHOMO-5) → 214B (βLUMO+1) (21.1%)
				208B (βHOMO-4) → 213B (βLUMO) (17.9%)
				200B (βHOMO-12) → 213B (βLUMO) (17.6%)
				199B (βHOMO-13) → 214B (βLUMO+1) (14.2%)
ES6	1.8948	654.35	0.4844	208B (βHOMO-4) → 213B (βLUMO) (27.0%)
				207B (βHOMO-5) → 214B (βLUMO+1) (18.7%)
				199B (βHOMO-13) → 214B (βLUMO+1) (15.7%)
				200B (βHOMO-12) → 213B (βLUMO) (13.6%)
ES15	2.5371	488.69	0.2855	208B (βHOMO-4) → 216B (βLUMO+3) (20.1%)
				207B (βHOMO-5) → 215B (βLUMO+2) (17.8%)
				204B (βHOMO-8) → 213B (βLUMO) (13.9%)
				203B (βHOMO-9) → 214B (βLUMO+1) (11.1%)
ES18	2.5730	481.87	0.2903	204B (βHOMO-8) → 213B (βLUMO) (18.0%)
				203B (βHOMO-9) → 214B (βLUMO+1) (17.3%)
				208B (βHOMO-4) → 216B (βLUMO+3) (15.1%)
				207B (βHOMO-5) → 215B (βLUMO+2) (14.2%)
EB State				
ES2	2.9092	426.18	1.8131	213 (HOMO-1) → 215 (LUMO) (22.5%)
				214 (HOMO) → 216 (LUMO+1) (21.2%)
ES3	3.0749	403.21	0.2625	211 (HOMO-5) → 215 (LUMO) (21.5%)
				212 (HOMO-4) → 216 (LUMO+1) (19.3%)

*Table 3-80 Details related to electronic transitions involved in the absorption peaks from TD-DFT calculations of **OTPT-FLR-221** oligomers in different oxidation, doping, and spin states. Only excited states with energies in the visible-near infrared region and with oscillator strengths greater than 0.2 are considered, and for each excited state, only electronic transitions contributing at least 10% are listed.*

Excited State	Energy (eV)	Wavelength (nm)	Oscillator Strength *f*	Contributing Electronic Transition
^{1}ES State				
ES2	1.9929	622.13	3.7983	260 (HOMO) → 261 (LUMO) (26.0%)
				259 (HOMO-1) → 262 (LUMO+1) (22.8%)
ES5	2.6568	466.67	0.6250	254 (HOMO-6) → 262 (LUMO+1) (23.4%)
				253 (HOMO-7) → 261 (LUMO) (20.5%)
^{3}ES State				
ES2	1.3560	914.31	1.5538	256B (βHOMO-2) → 259B (βLUMO) (42.5%)
				255B (βHOMO-3) → 260B (βLUMO+1) (37.8%)
ES3	1.9593	632.80	0.6506	256B (βHOMO-2) → 262B (βLUMO+3) (19.8%)
				252B (βHOMO-6) → 260B (βLUMO+1) (18.8%)
				255B (βHOMO-3) → 261B (βLUMO+2) (18.7%)
				251B (βHOMO-7) → 259B (βLUMO) (14.0%)
EB State				
ES2	2.1996	563.67	3.8554	259 (HOMO-1) → 261 (LUMO) (24.4%)
				260 (HOMO) → 262 (LUMO+1) (23.3%)
ES3	2.7876	444.77	0.4019	257 (HOMO-3) → 261 (LUMO) (23.0%)
				258 (HOMO-2) → 262 (LUMO+1) (20.2%)

*Table 3-81 Structures of ground state and excited state molecular orbitals from the NTO analyses of excited states of **OTPT-BZN-221** oligomers in the **^{1}ES** state as listed in Table 3-79*

Excited State	Ground State MO	Excited State MO
ES2	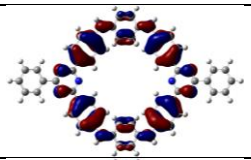	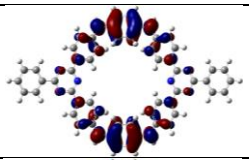
	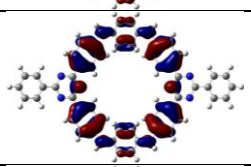	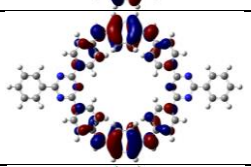
ES13	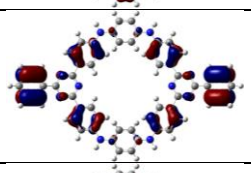	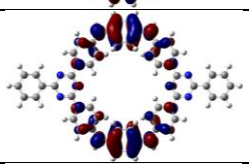
ES15	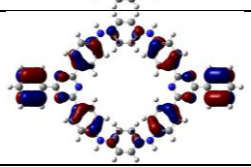	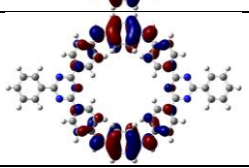

*Table 3-82 Structures of ground state and excited state molecular orbitals from the NTO analyses of excited states of **OTPT-FLR-221** oligomers in the **[1]ES** state as listed in Table 3-80*

Excited State	Ground State MO	Excited State MO
ES2	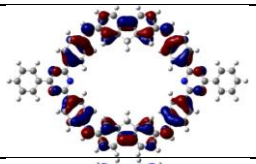	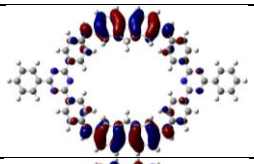
	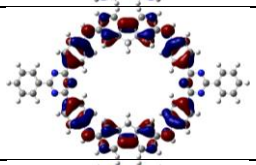	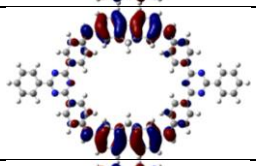
ES5	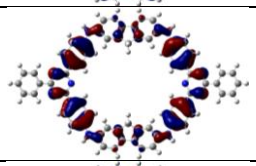	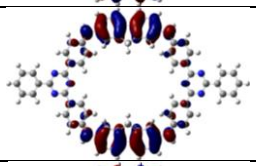
	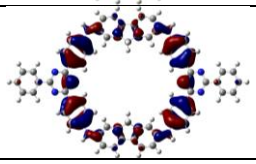	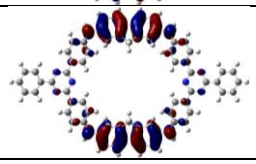

For the **[5]ES** state **OTPT-BZN-221**, there are two peaks overlapping, with the more intense peak appearing at 651 nm and the obscured peak appearing at approximately 515 nm. Meanwhile, the four majorly contributing excited states are indeed two pairs of excited states with similar energies and oscillator strengths. The first pair, with higher intensity, consists of ES2 (1.8290 eV, 677.87 nm, f = 0.4641) and ES6 (1.8948 eV, 654.35 nm, f = 0.4844), while another pair for the obscured peak consists of ES15 (2.5371 eV, 488.69 nm, f = 0.2855) and ES18 (2.5730 eV, 481.87 nm, f = 0.2903). The effects from overlapping between the two peaks move the positions on the absorption spectra closer.

For each of the four excited states, there are four significant electronic transitions involved, and the transitions for excited states in the same pair are also the same set but with different ratios of contributions. As a result, the NTO analysis results are also similar for excited states in the same pair (Table 3-83).

The first pair, ES2 and ES6, appear to be more CLBQ in nature than CTBQ, with the lobes being concentrated around the bound core blades and the linker units. Meanwhile, the second pair, ES15 and ES18, are clearly CTBQ, with the ground state MOs being around the linker units while the excited state MOs are more distributed throughout the core-linker conjugation moieties.

*Table 3-83 Structures of ground state and excited state molecular orbitals from the NTO analyses of excited states of **OTPT-BZN-221** oligomers in the ^{5}**ES** state as listed in Table 3-79*

Excited State	Ground State MO	Excited State MO
ES2	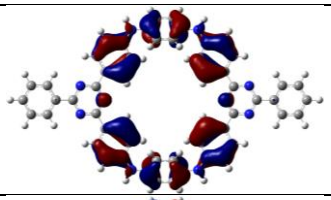	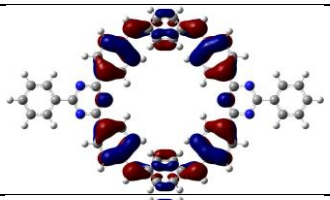
	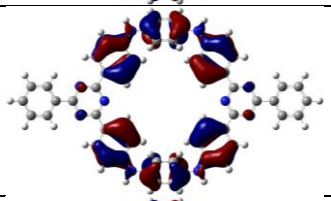	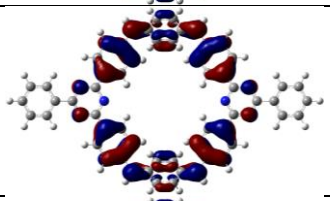
ES6	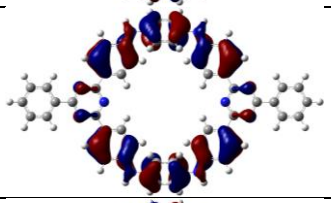	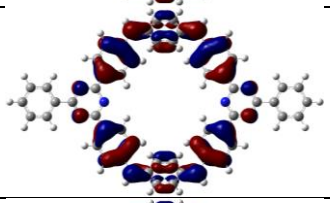
	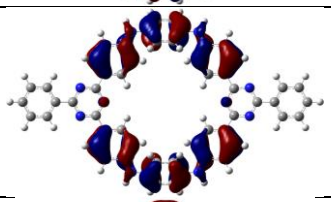	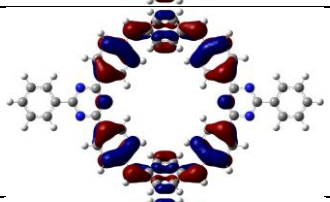
ES15	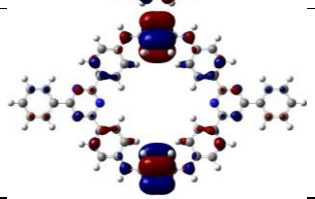	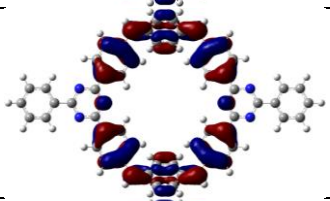
	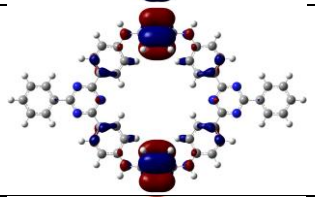	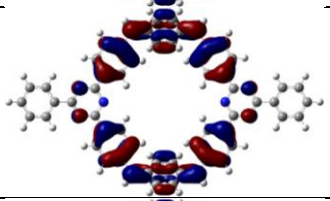
ES18	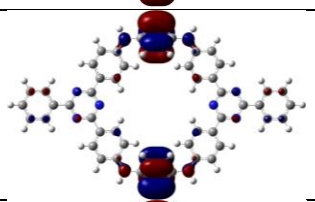	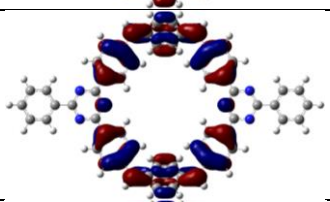
	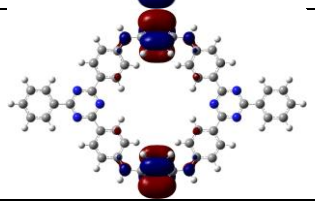	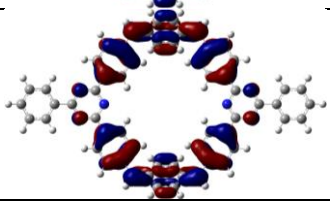

*Table 3-84 Structures of ground state and excited state molecular orbitals from the NTO analyses of excited states of **OTPT-FLR-221** oligomers in the ^{5}**ES** state as listed in Table 3-80*

Excited State	Ground State MO	Excited State MO
ES2	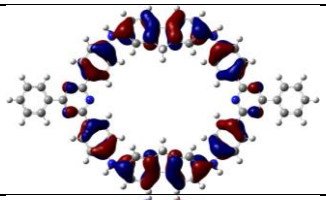	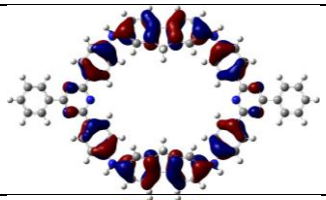
	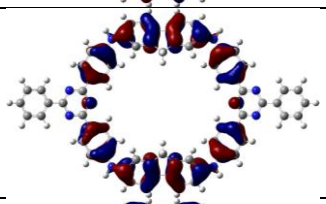	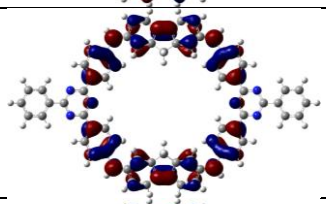
ES3	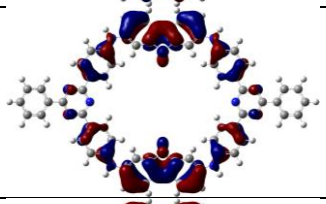	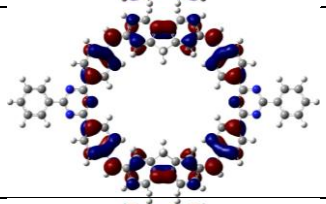
	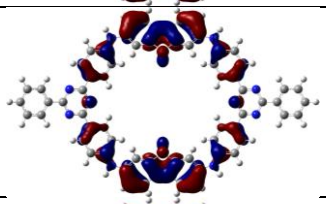	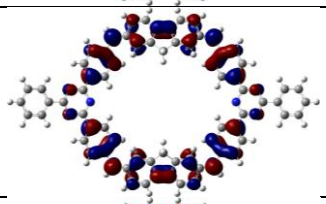
	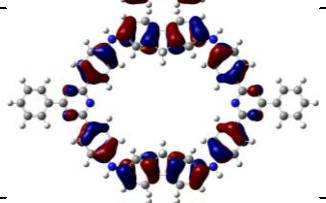	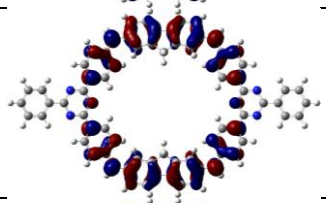
	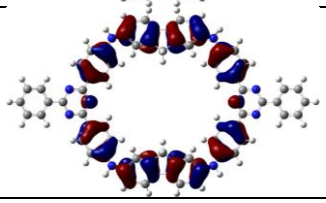	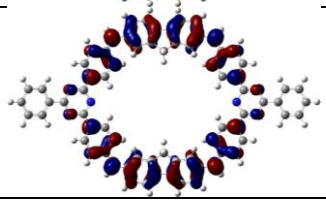

While the main cyclic structure of **OTPT-BZN-221** also contains eight rings like that of **OTPB-BZN-221**, the alternative characteristics observed in the quintet state **OTPB-BZN-221**$^{4+}$ is not seen in the **TPT** counterpart. Instead, the triazine hub moieties contribute almost nothing to the absorption spectra. It is possible that the different cyclic structures play a role in the difference between absorption spectra of the polaron form of the **221** oligomers.

The absorption peak of quintet state **OTPT-FLR-221**$^{4+}$ also has the same feature as that of quintet state **OTPT-BZN-221**$^{4+}$, albeit at longer wavelengths, with the main peak (890 nm) partially hiding a smaller peak (633 nm, approximately) at its shoulder. Both peaks are contributed by only one excited state (ES2 for the main peak, ES3 for the obscured peak, see Table 3-80) instead of two in the case of the **BZN**-linked oligomer. Again, both ES2 and ES3 of the ^{5}**ES** state **OTPT-FLR-221** have less charge transfer character in nature and appear more like CLBQs.

*Table 3-85 Structures of ground state and excited state molecular orbitals from the NTO analyses of excited states of **OTPT-BZN-221** oligomers in the **EB** state as listed in Table 3-79*

Excited State	Ground State MO	Excited State MO
ES2	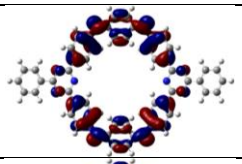	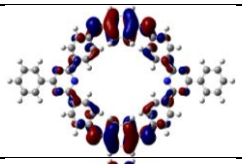
	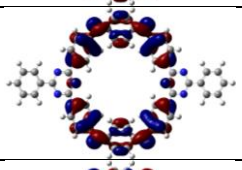	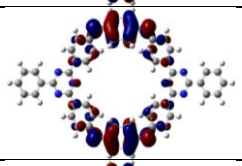
ES3	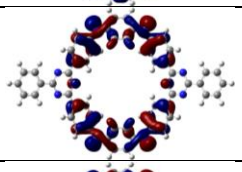	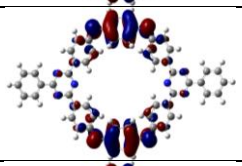
	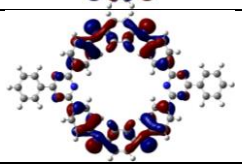	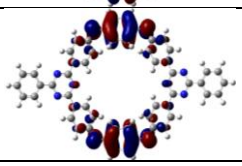

*Table 3-86 Structures of ground state and excited state molecular orbitals from the NTO analyses of excited states of **OTPT-FLR-221** oligomers in the **EB** state as listed in Table 3-80*

Excited State	Ground State MO	Excited State MO
ES2	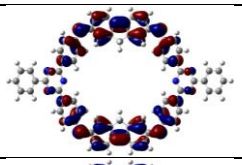	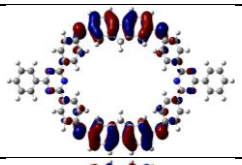
	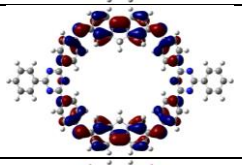	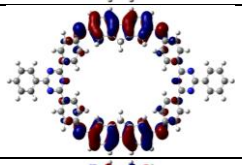
ES3	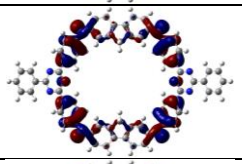	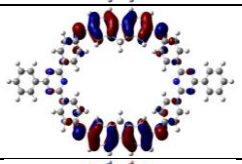
	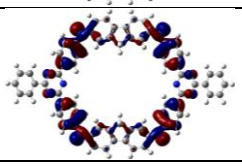	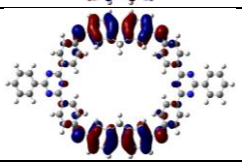

The visible range absorption peaks in the spectra of both **EB** state **OTPT-BZN-221** (423 nm) and **OTPT-FLR-221** (562 nm) appear as single peaks without any obvious sign of obscured peaks. They are both majorly contributed by their respective ES2 excited states as listed in Table 3-79 and Table 3-80. The NTO analyses of both excited states reveal the "transfer" from the conjugated core-linker units to the linker units themselves, which are slightly different from both CTBQs and CLBQs.

The main theme that can be seen across all six core and linker combinations is the absence of ES1, the usual major contributor for absorption spectra of **210** oligomers, in any of the excited state lists. Instead, the major contributors of **221** oligomers are their respective ES2 states, and in many cases, these ES2 states involve molecular orbitals other than frontier molecular orbitals (HOMO-1, HOMO, LUMO, and LUMO+1). It is possible that cyclisation has created more complicated electronic structures, and some electronic transitions are not permitted due to symmetries.

Meanwhile, while **210** and **221** oligomers were selected to represent the two extreme cases of strains in the oligomer structures, this set of representations is possibly flawed. There is only one linker unit in one **210** oligomer molecule, but there are two in one **221** oligomer molecule. For the two linker units of the same **221** oligomer molecule, the partial molecular orbitals on both units can be in either the same or the different phase, resulting in multiple molecular orbitals with different structures and energies. These multiple molecular orbitals, however, cannot be observed in the **210** oligomer because there is only one linker unit. Therefore, the **320** oligomer model, with three core units bound together with two linker units, might be the better representation.

Structures of **221** oligomers themselves also possess further complications on their own. Not only are they branched, but they are also cyclic. To the best of my knowledge, there is no reported study on cyclic oligo(aniline)s, either theoretically or experimentally.

Nonetheless, there are some conclusions to be drawn from this comparative study. For the absorption peaks in the visible-near-infrared region of oxidised oligomers, cyclisation has led to shorter wavelengths in general. The relationships between the oligomer structures and absorption peak positions are, however, less straightforward due to more complicated molecular orbital structures.

3.3.3 Comparisons between Theoretical and Experimental Spectra

This section discusses the actual spectra measured from oligomers and polymers obtained from the syntheses of PANI-CMPs using the BH.BXJ method, as explained in detail in Chapter 2. Oligomers and polymers in this case refer to two different products obtained after the end of the reaction. Polymers are the insoluble products which are filtered out, while oligomers are the soluble products remaining in the supernatants. Unreacted monomers are removed by redissolving the evaporated solid from supernatants in tetrahydrofuran and precipitating by adding methanol. This process also removes small oligomers. However, it is the more practical way to remove unreacted monomers from the products that are essentially oligomer mixtures of different sizes.

As noted in previous publications,[68, 69] PANI-CMPs can be readily oxidised in air. The same can also be observed in their oligoaniline counterparts. In the synthesis of a PANI-CMP from **TPA**-Br_3 and **BZN**-$(NH_2)_2$, for example, the initial products are brown solid polymer suspended in yellow solution of oligomers. As the products are left exposed to air, however, both the polymer and the oligomer turn dark blue. While oxidative doping normally occurs from **LEB** to **ES** states (see Scheme 1-10), it is possible that air-oxidation could result in **EB** products instead of **ES**. The most common oxidant in air is triplet oxygen ($^3O_2$), which will produce superoxide ion ($O_2^{\cdot-}$) upon the acceptance of an electron.[73] The sources of electrons in the oxidation of PANI-CMPs are the imino group, represented as $HNAr_2$ in Equation 3-10. Due to its basicity, $O_2^{\cdot-}$ can abstract a proton and eventually disproportionate into oxygen and HO_2^-, the conjugate base of hydrogen peroxide (Equation 3-11).[74] Both are oxidative species. In this case, the most readily available proton source is the newly formed imino radical cation ($HNAr_2^{\cdot+}$). Therefore, both oxidation and

deprotonation occur simultaneously during in-air oxidation process, so it is assumed in this work that the products are in the **EB** state and not the **ES** state.

$$O_2 + HNAr_2 \rightarrow O_2^{\cdot-} + HNAr_2^{\cdot+} \quad 3\text{-}10$$

$$2O_2^{\cdot-} + HNAr_2^{\cdot+} \rightarrow O_2 + HO_2^{-} + NAr_2^{\cdot} \quad 3\text{-}11$$

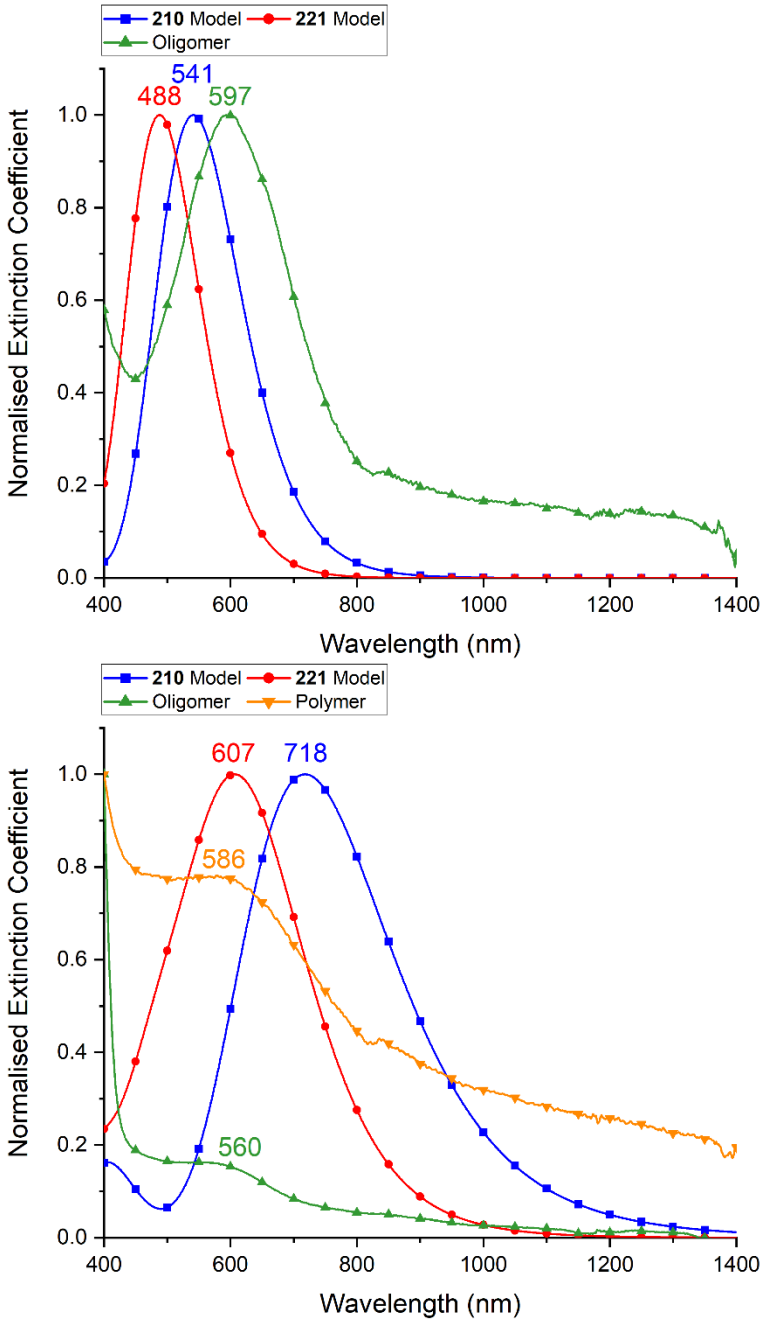

*Figure 3-45 Normalised absorption spectra of **TPA-BZN** (top) and **TPA-FLR** (bottom) from calculations (squares for the **210 EB** model and circles for the **221 EB** model) and from measurements (up triangles for oligomers and down triangles for polymers where applicable)*

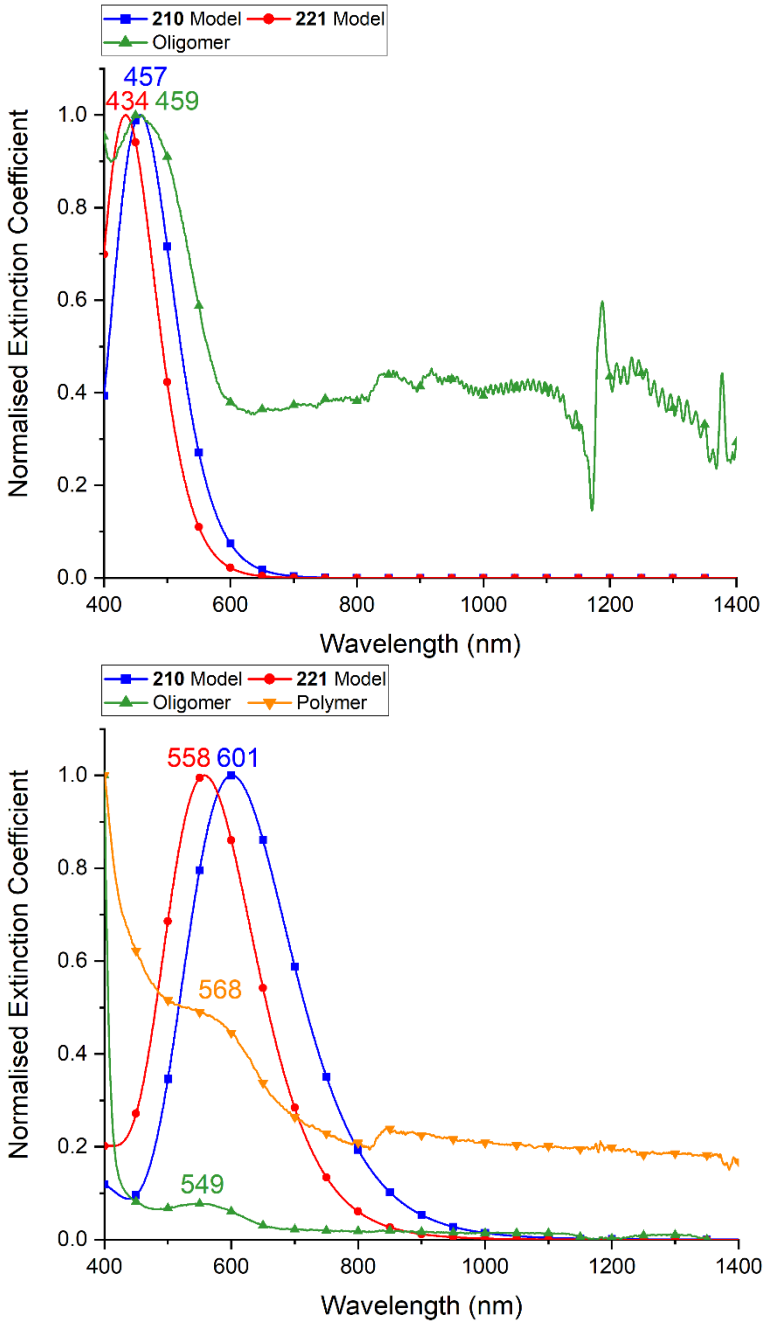

*Figure 3-46 Normalised absorption spectra of **TPB-BZN** (top) and **TPB-FLR** (bottom) from calculations (squares for the **210 EB** model and circles for the **221 EB** model) and from measurements (up triangles for oligomers and down triangles for polymers where applicable)*

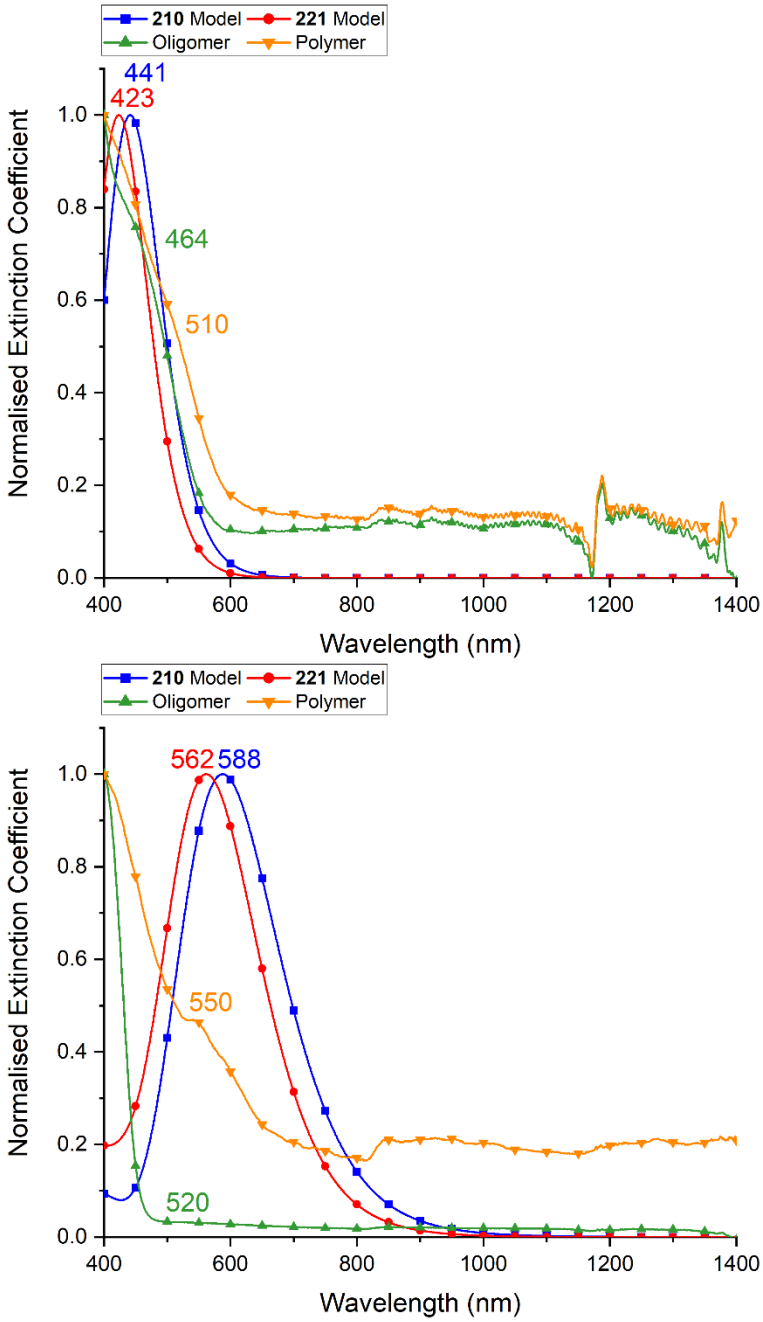

*Figure 3-47 Normalised absorption spectra of **TPT-BZN** (top) and **TPT-FLR** (bottom) from calculations (squares for the **210 EB** model and circles for the **221 EB** model) and from measurements (up triangles for oligomers and down triangles for polymers where applicable)*

Table 3-87 Comparisons between calculated and measured peak positions in the visible region of PANI-CMP models, oligomers, and polymers

Monomer Unit		Calculated Peak Position (nm)		Measured Peak Position (nm)	
Core	**Linker**	**210 Model**	**221 Model**	**Oligomer**	**Polymer**
TPA	**BZN**	541	488	597	-
TPA	**FLR**	718	607	560	586
TPB	**BZN**	457	434	459	-
TPB	**FLR**	601	558	549	568
TPT	**BZN**	441	423	464	510
TPT	**FLR**	588	562	520	550

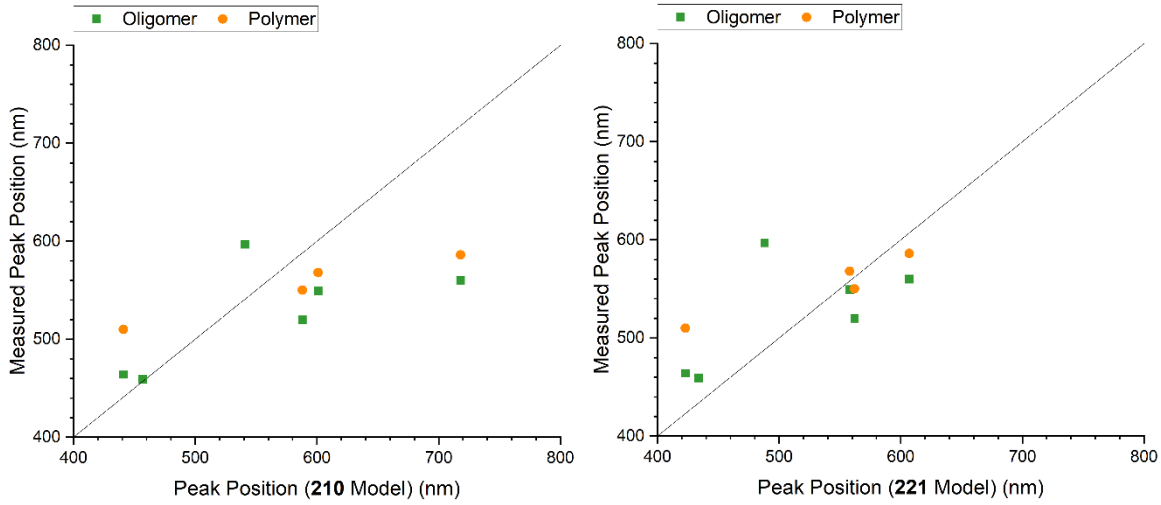

Figure 3-48 Comparions between calculated and measured peak positions in the visible region of PANI-CMP models, oligomers, and polymers

Figure 3-45 compares the spectra obtained from calculations and from measurements for PANI-CMPs prepared from **TPA**-Br_3 and **BZN**-$(NH_2)_2$ (**TPA-BZN**) and from **TPA**-Br_3 and **FLR**-$(NH_2)_2$ (**TPA-FLR**), while those of **TPB** and **TPT** core units can be found in Figure 3-46 and Figure 3-47. Two types of products are collected, soluble oligomeric products from the supernatants and insoluble polymers, and their spectra are shown together. Peak positions are summarised in Table 3-87 and represented graphically in Figure 3-48.

Clearly, there are mismatches between the peak positions obtained from TD-DFT calculations and from products collected after the syntheses of PANI-CMPs. These disagreements imply that the models proposed and analysed are not good candidates for the PANI-CMP materials. It should be pointed out, however, that similar computational methods have been applied for the study of oligo(aniline)s, both unbranched and branched, with good agreement.[12, 13, 47] Therefore, the issue should not be from the poor choices for the computational methods, but instead, it comes from the poor choices for the representations of experimental and computational data in this study.

From the experimental side, as to be discussed in detail in Section 4.3, oligomers in this study are represented by the oligomeric products in the supernatant from the synthesis of PANI-CMPs. They are, actually, mixtures of oligomers with different sizes and structures, which subsequently have different absorption spectra. This fact means that the spectra of "oligomers" are actually mixtures of spectra of subspecies present in the oligomeric products obtained rather than spectra of pure oligomers.

The issue in the case of polymers, unlike the case of oligomers, comes from the computational models not representing the polymers properly. Even assuming that the optoelectronic properties of polymer chains or networks are uniform once these chains or networks have grown to a certain size, these optoelectronic spectra are still the results of bulk polymers (i.e., the quaternary structures, see Scheme 3-1) and may not be represented properly by the oligomeric models that include only the secondary structures. Therefore, a different approach, with larger scale models with hundreds to thousands of repeating units coupled with methods based on classical mechanics, might be required altogether. This issue will be discussed in detail in Section 6.1.1.1.

Another structure-property relationship issue for the optical spectroscopic study of PANI-CMPs and oligomers is that the trend for one group of polymers or oligomers may not apply to another group, even if they are performed on the same set of monomer units with similar chemical properties. This issue arose from the study of PANI-CMPs synthesised using the same monomer units from the previous study on modified tetra(aniline)s[47] (Scheme 3-19), with the syntheses of these polymers being discussed in Section 4.2. The trends found in absorption peak positions from oligomers and from polymers are totally different (Table 3-88), which means that while oligomeric models can be good representations for oligomers, they cannot be applied directly to the study of polymers.

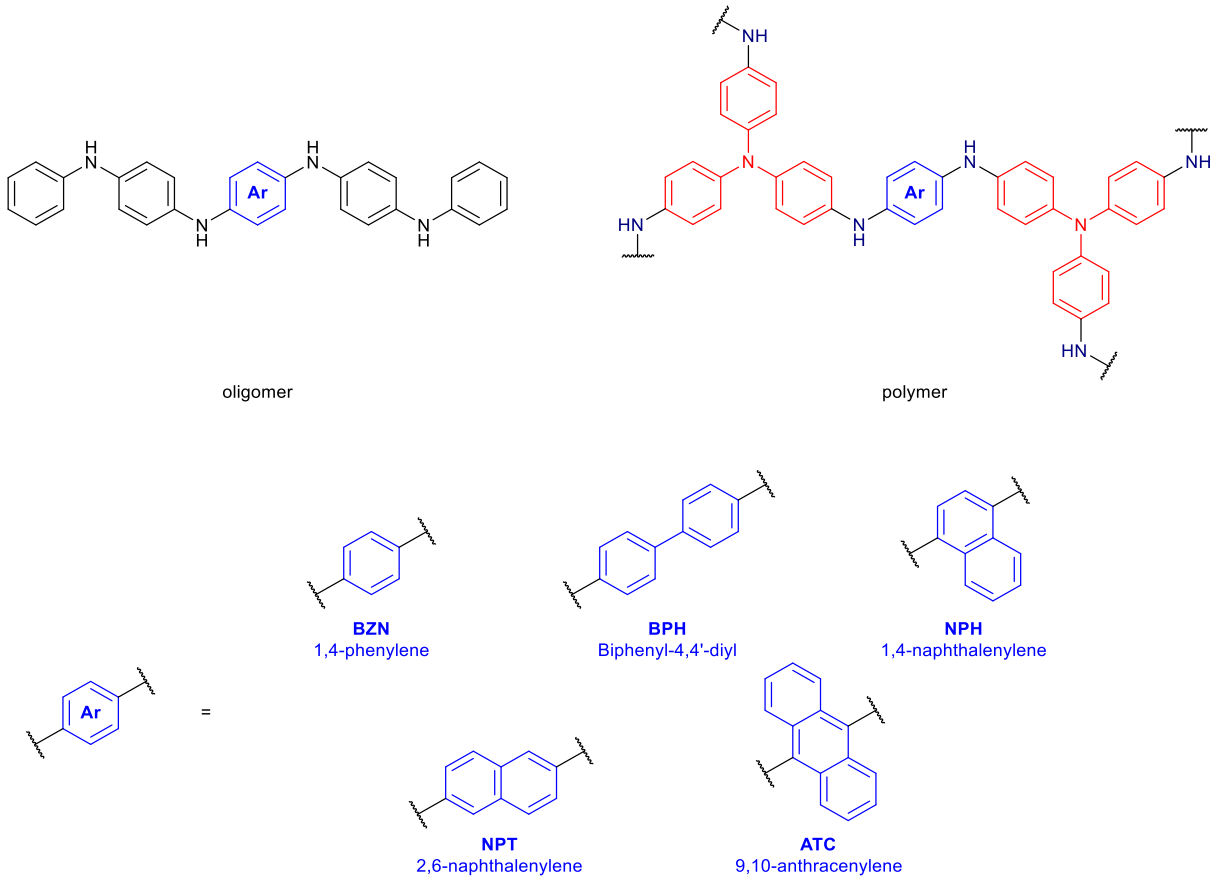

Scheme 3-19 Structures of oligomers and polymers in the comparison between absorption spectra

Table 3-88 Absorption peaks measured from synthesised oligomers (ref [47]) and polymers. In the case of polymers, there can be more than one CTBQ peak. Italicised numbers refer to peaks which positions cannot be clearly determined.

Monomer	Oligomer CTBQ peak (nm)	Polymer CTBQ peak (nm)
BZN	568	662
BPH	506	*850*
NPH	538	607
NPT	558	*510* and *660*
ATC	478	573

3.4 Conclusions and Remarks

Structures of polymers, including PANI-CMPs, can be considered to be in a four-tier hierarchy. This hierarchy ranges from the atomic arrangements within individual repeating units (primary structures), arrangements of repeating units within the polymer networks or chains

(secondary structures), arrangements of interacting polymer fragments within the bulk polymer structure (tertiary structures), to the structures of the bulk polymers themselves (quaternary structures). Modelling attempts in this chapter cover the primary and secondary levels, with different descriptors being selected for the discussions of geometric and electronic structures. Models with different building blocks and chemical (oxidation, doping, and spin) states have been thoroughly described and compared, with some trends between structures and properties being found.

For the primary structures of poly(aniline)s and structurally related PANI-CMPs, the repeating units are the BQ units, which are important for the chemical properties of these materials and can exist in different forms depending on oxidation, doping, and spin states. HOMBQ (harmonic oscillator measure of electron delocalisation in BQ units) indices have been developed based on previously published generalised methods[38-41] derived from harmonic oscillators, with the scale set so that the BQ unit in the **LEB** state has the HOMBQ index of 1, and the BQ unit in the **EB** state has the HOMBQ index of 0. There is no new descriptor created for secondary structures, however. The newly developed HOMBQ index has been found to be a good representation of electron delocalisation between core and linker units in the singlet oligo(aniline) systems.

Geometric and electronic structures of TANI, branched derivatives, and PANI-CMP models have been optimised using DFT calculations and thoroughly analysed in this chapter. For PANI-CMPs, different oligomeric models, namely **210** and **221**, have been selected to represent PANI-CMPs with different topologies. Overall, the introduction of branching leads to better stabilisations of positive charges introduced upon oxidations, and it can affect the relative stability of different spin isomers. Meanwhile, effects of cyclisation in this study are still inconclusive since the **221** models used in this study possess both branches and cycles. Therefore, studies on cyclic oligo(aniline)s are required for better understanding. Nonetheless, these **221** models can still express further complications as oligomer structures become cyclised compared to the **210** models.

TD-DFT methods have been applied for the studies of optoelectronic properties of PANI-CMP models. A structure-property relationship can be found, at least in the simpler **210** models of PANI-CMPs, between the core-linker electron delocalisation effects and the energies of electronic transitions, which have been the case for transitions in the ^{1}**ES** and **EB** states but not in the ^{3}**ES** state. However, for the more complicated **221** models, deeper analyses are still required. Meanwhile, the attempts to use the PANI-CMP models to explain optoelectronic properties have not been successful. These properties, especially of the highly crosslinked PANI-CMPs, are governed by more complicated structures further than the secondary level, which are the limit of **210** and **221** models selected for studies discussed in this section. These models have not captured structural features such as interactions between fragments not covalently bonded, which are in the realm of tertiary structures. Therefore, better models with non-covalent interactions between oligomer fragments should be studied next.

While a definite and clear structure-property relationship for the design of PANI-CMPs might not have been determined yet, theoretical studies discussed in this chapter should lead to more theoretical studies that are better designed and systemised which could potentially lead to clear design rules for these materials.

3.5 References

1. M. A. Zwijnenburg, G. Cheng, T. O. McDonald, K. E. Jelfs, J. X. Jiang, S. Ren, T. Hasell, F. Blanc, A. I. Cooper and D. J. Adams, *Macromolecules*, 2013, **46**, 7696-7704.
2. Z. T. de Oliveira and M. C. dos Santos, *Chem. Phys.*, 2000, **260**, 95-103.

3. A. Varela-Alvarez, J. A. Sordo and G. E. Scuseria, *J. Am. Chem. Soc.*, 2005, **127**, 11318-11327.
4. C. Alemán, C. A. Ferreira, J. Torras, A. Meneguzzi, M. Canales, M. A. S. Rodrigues and J. Casanovas, *Polymer*, 2008, **49**, 5169-5176.
5. G. Yang, W. H. Hou, X. M. Feng, X. F. Jiang and J. Guo, *Int. J. Quantum. Chem.*, 2008, **108**, 1155-1163.
6. J. Romanova, J. Petrova, A. Tadjer and N. Gospodinova, *Synth. Met.*, 2010, **160**, 1050-1054.
7. J. N. Petrova, J. R. Romanova, G. K. Madjarova, A. N. Ivanova and A. V. Tadjer, *J. Phys. Chem. B*, 2011, **115**, 3765-3776.
8. J. Romanova, G. Madjarova, A. Tadjer and N. Gospodinova, *Int. J. Quantum. Chem.*, 2011, **111**, 435-443.
9. J. Petrova, J. Romanova, G. Madjarova, A. Ivanova and A. Tadjer, *J. Phys. Chem. B*, 2012, **116**, 6543-6552.
10. M. Canales, J. Torras, G. Fabregat, A. Meneguzzi and C. Aleman, *J. Phys. Chem. B*, 2014, **118**, 11552-11562.
11. Y. H. Zhang, Q. Xi, J. L. Chen and Y. P. Duan, *J. Clust. Sci.*, 2014, **25**, 1501-1510.
12. B. M. Mills, N. Fey, T. Marszalek, W. Pisula, P. Rannou and C. F. J. Faul, *Chem. - Eur. J.*, 2016, **22**, 16950-16956.
13. B. M. Mills, Z. Shao, S. R. Flynn, P. Rannou, D. M. Lindsay, N. Fey and C. F. J. Faul, *Mol. Syst. Des. Eng.*, 2019, **4**, 103-109.
14. P. Hohenberg and W. Kohn, *Phys. Rev. B: Condens. Matter Mater. Phys.*, 1964, **136**, B864.
15. W. Kohn and L. J. Sham, *Phys. Rev.*, 1965, **140**, 1133-1138.
16. R. G. Parr and Y. Weitao, *Density-Functional Theory of Atoms and Molecules*, Oxford University Press, New York, 1995.
17. D. R. Salahub and M. C. Zerner, *The Challenge of d and f Electrons : Theory and Computation*, American Chemical Society, Washington, 1989.
18. A. D. Becke, *J. Chem. Phys.*, 1993, **98**, 5648-5652.
19. C. Lee, W. Yang and R. G. Parr, *Phys. Rev. B: Condens. Matter Mater. Phys.*, 1988, **37**, 785-789.
20. B. Miehlich, A. Savin, H. Stoll and H. Preuss, *Chem. Phys. Lett.*, 1989, **157**, 200-206.
21. R. Ditchfield, D. P. Miller and J. A. Pople, *J. Chem. Phys.*, 1971, **54**, 4186-4193.
22. W. J. Hehre, R. Ditchfield and J. A. Pople, *J. Chem. Phys.*, 1972, **56**, 2257-2261.
23. P. C. Hariharan and J. A. Pople, *Theor. Chim. Acta*, 1973, **28**, 213-222.
24. P. C. Hariharan and J. A. Pople, *Mol. Phys.*, 1974, **27**, 209-214.
25. M. S. Gordon, *Chem. Phys. Lett.*, 1980, **76**, 163-168.
26. M. M. Francl, W. J. Pietro, W. J. Hehre, J. S. Binkley, M. S. Gordon, D. J. DeFrees and J. A. Pople, *J. Chem. Phys.*, 1982, **77**, 3654-3665.
27. R. C. Binning Jr. and L. A. Curtiss, *J. Comput. Chem.*, 1990, **11**, 1206-1216.
28. J. P. Blaudeau, M. P. McGrath, L. A. Curtiss and L. Radom, *J. Chem. Phys.*, 1997, **107**, 5016-5021.
29. V. A. Rassolov, J. A. Pople, M. A. Ratner and T. L. Windus, *J. Chem. Phys.*, 1998, **109**, 1223-1229.
30. V. A. Rassolov, M. A. Ratner, J. A. Pople, P. C. Redfern and L. A. Curtiss, *J. Comput. Chem.*, 2001, **22**, 976-984.
31. S. Grimme, S. Ehrlich and L. Goerigk, *J. Comput. Chem.*, 2011, **32**, 1456-1465.
32. S. Miertuš, E. Scrocco and J. Tomasi, *Chem. Phys.*, 1981, **55**, 117-129.
33. S. Miertuš and J. Tomasi, *Chem. Phys.*, 1982, **65**, 239-245.
34. J. L. Pascual-ahuir, E. Silla and I. Tuñon, *J. Comput. Chem.*, 1994, **15**, 1127-1138.
35. J. Tomasi, B. Mennucci and R. Cammi, *Chem. Rev.*, 2005, **105**, 2999-3093.
36. T. M. Krygowski, H. Szatylowicz, O. A. Stasyuk, J. Dominikowska and M. Palusiak, *Chem. Rev.*, 2014, **114**, 6383-6422.
37. A. Julg and P. François, *Theor. Chim. Acta*, 1967, **8**, 249-259.
38. J. Kruszewski and T. M. Krygowski, *Tetrahedron Lett.*, 1972, **13**, 3839-3842.
39. C. P. Frizzo and M. A. P. Martins, *Struct. Chem.*, 2012, **23**, 375-380.
40. T. M. Krygowski, *J. Chem. Inf. Comput. Sci.*, 1993, **33**, 70-78.

41. E. D. Raczynska, M. Hallman, K. Kolczynska and T. M. Stepniewski, *Symmetry-Basel*, 2010, **2**, 1485-1509.
42. G. Ćirić-Marjanović, *Synth. Met.*, 2013, **177**, 1-47.
43. S. S. Zade and M. Bendikov, *Org. Lett.*, 2006, **8**, 5243-5246.
44. S. S. Zade, N. Zamoshchik and M. Bendikov, *Acc. Chem. Res.*, 2011, **44**, 14-24.
45. J. G. Masters, Y. Sun, A. G. MacDiarmid and A. J. Epstein, *Synth. Met.*, 1991, **41**, 715-718.
46. C. Cavazzoni, R. Colle, R. Farchioni and G. Grosso, *J. Chem. Phys.*, 2008, **128**, 234903.
47. Z. Shao, P. Rannou, S. Sadki, N. Fey, D. M. Lindsay and C. F. J. Faul, *Chem. - Eur. J.*, 2011, **17**, 12512-12521.
48. C. W. Lin, R. L. Li, S. Robbennolt, M. T. Yeung, G. Akopov and R. B. Kaner, *Macromolecules*, 2017, **50**, 5892-5897.
49. M. J. Frisch, G. W. Trucks, H. B. Schlegel, G. E. Scuseria, M. A. Robb, J. R. Cheeseman, G. Scalmani, V. Barone, G. A. Petersson, H. Nakatsuji, X. Li, M. Caricato, A. V. Marenich, J. Bloino, B. G. Janesko, R. Gomperts, B. Mennucci, H. P. Hratchian, J. V. Ortiz, A. F. Izmaylov, J. L. Sonnenberg, D. Williams-Young, F. Ding, F. Lipparini, F. Egidi, J. Goings, B. Peng, A. Petrone, T. Henderson, D. Ranasinghe, V. G. Zakrzewski, J. Gao, N. Rega, G. Zheng, W. Liang, M. Hada, M. Ehara, K. Toyota, R. Fukuda, J. Hasegawa, M. Ishida, T. Nakajima, Y. Honda, O. Kitao, H. Nakai, T. Vreven, K. Throssell, J. J. A. Montgomery, J. E. Peralta, F. Ogliaro, M. J. Bearpark, J. J. Heyd, E. N. Brothers, K. N. Kudin, V. N. Staroverov, T. A. Keith, R. Kobayashi, J. Normand, K. Raghavachari, A. P. Rendell, J. C. Burant, S. S. Iyengar, J. Tomasi, M. Cossi, J. M. Millam, M. Klene, C. Adamo, R. Cammi, J. W. Ochterski, R. L. Martin, K. Morokuma, O. Farkas, J. B. Foresman and D. J. Fox, Gaussian 16, Revision A.03, Gaussian, Inc., Wallingford, CT, 2016
50. M. J. Frisch, G. W. Trucks, H. B. Schlegel, G. E. Scuseria, M. A. Robb, J. R. Cheeseman, G. Scalmani, V. Barone, B. Mennucci, G. A. Petersson, H. Nakatsuji, M. Caricato, X. Li, H. P. Hratchian, A. F. Izmaylov, J. Bloino, G. Zheng, J. L. Sonnenberg, M. Hada, M. Ehara, K. Toyota, R. Fukuda, J. Hasegawa, M. Ishida, T. Nakajima, Y. Honda, O. Kitao, H. Nakai, T. Vreven, J. J. A. Montgomery, J. E. Peralta, F. Ogliaro, M. Bearpark, J. J. Heyd, E. Brothers, K. N. Kudin, V. N. Staroverov, T. Keith, R. Kobayashi, J. Normand, K. Raghavachari, A. Rendell, J. C. Burant, S. S. Iyengar, J. Tomasi, M. Cossi, N. Rega, J. M. Millam, M. Klene, J. E. Knox, J. B. Cross, V. Bakken, C. Adamo, J. Jaramillo, R. Gomperts, R. E. Stratmann, O. Yazyev, A. J. Austin, R. Cammi, C. Pomelli, J. W. Ochterski, R. L. Martin, K. Morokuma, V. G. Zakrzewski, G. A. Voth, P. Salvador, J. J. Dannenberg, S. Dapprich, A. D. Daniels, O. Farkas, J. B. Foresman, J. V. Ortiz, J. Cioslowski and D. J. Fox, Gaussian 09, Revision D.01, Gaussian, Inc., Wallingford, CT, 2013
51. M. J. Frisch, G. W. Trucks, H. B. Schlegel, G. E. Scuseria, M. A. Robb, J. R. Cheeseman, G. Scalmani, V. Barone, G. A. Petersson, H. Nakatsuji, X. Li, M. Caricato, A. V. Marenich, J. Bloino, B. G. Janesko, R. Gomperts, B. Mennucci, H. P. Hratchian, J. V. Ortiz, A. F. Izmaylov, J. L. Sonnenberg, D. Williams-Young, F. Ding, F. Lipparini, F. Egidi, J. Goings, B. Peng, A. Petrone, T. Henderson, D. Ranasinghe, V. G. Zakrzewski, J. Gao, N. Rega, G. Zheng, W. Liang, M. Hada, M. Ehara, K. Toyota, R. Fukuda, J. Hasegawa, M. Ishida, T. Nakajima, Y. Honda, O. Kitao, H. Nakai, T. Vreven, K. Throssell, J. J. A. Montgomery, J. E. Peralta, F. Ogliaro, M. J. Bearpark, J. J. Heyd, E. N. Brothers, K. N. Kudin, V. N. Staroverov, T. A. Keith, R. Kobayashi, J. Normand, K. Raghavachari, A. P. Rendell, J. C. Burant, S. S. Iyengar, J. Tomasi, M. Cossi, J. M. Millam, M. Klene, C. Adamo, R. Cammi, J. W. Ochterski, R. L. Martin, K. Morokuma, O. Farkas, J. B. Foresman and D. J. Fox, Gaussian 16, Revision C.01, Gaussian, Inc., Wallingford, CT, 2019
52. R. L. Martin, *J. Chem. Phys.*, 2003, **118**, 4775-4777.
53. J. P. Foster and F. Weinhold, *J. Am. Chem. Soc.*, 1980, **102**, 7211-7218.
54. A. E. Reed and F. Weinhold, *J. Chem. Phys.*, 1983, **78**, 4066-4073.
55. A. E. Reed and F. Weinhold, *J. Chem. Phys.*, 1985, **83**, 1736-1740.
56. A. E. Reed, R. B. Weinstock and F. Weinhold, *J. Chem. Phys.*, 1985, **83**, 735-746.
57. J. E. Carpenter, Doctor of Philosophy, University of Wisconsin, Madison, 1987.
58. J. E. Carpenter and F. Weinhold, *J. Mol. Struct.: THEOCHEM*, 1988, **46**, 41-62.

59. A. E. Reed, L. A. Curtiss and F. Weinhold, *Chem. Rev.*, 1988, **88**, 899-926.
60. F. Weinhold and J. E. Carpenter, in *The Structure of Small Molecules and Ions*, eds. R. Naaman and Z. Vager, Springer US, Boston, MA, 1988, ch. Chapter 24, pp. 227-236.
61. R. D. Dennington, II, T. A. Keith and J. M. Millam, GaussView Version 6.1.1, Semichem Inc., Shawnee Mission, KS, 2019
62. O. Bastiansen and A. Skancke, *Acta Chem. Scand.*, 1967, **21**, 587-589.
63. A. Jablonski, *Nature*, 1933, **131**, 839-840.
64. D. R. Dalton, *Foundations of Organic Chemistry : Unity and Diversity of Structures, Pathways, and Reactions*, John Wiley & Sons, Incorporated, Hoboken, UNITED STATES, 2011.
65. G. E. Tranter, in *Encyclopedia of Spectroscopy and Spectrometry*, ed. J. C. Lindon, Elsevier, Oxford, 1999, pp. 2383-2389.
66. A. G. Green and A. E. Woodhead, *J. Chem. Soc. Trans.*, 1910, **97**, 2388-2403.
67. A. G. Green and A. E. Woodhead, *J. Chem. Soc. Trans.*, 1912, **101**, 1117-1123.
68. Y. Liao, J. Weber and C. F. J. Faul, *Chem. Commun.*, 2014, **50**, 8002-8005.
69. Y. Liao, J. Weber, B. M. Mills, Z. Ren and C. F. J. Faul, *Macromolecules*, 2016, **49**, 6322-6333.
70. J. Romanova, J. Petrova, A. Ivanova, A. Tadjer and N. Gospodinova, *J. Mol. Struct.: THEOCHEM*, 2010, **954**, 36-44.
71. T. Yanai, D. P. Tew and N. C. Handy, *Chem. Phys. Lett.*, 2004, **393**, 51-57.
72. Y. Tawada, T. Tsuneda, S. Yanagisawa, T. Yanai and K. Hirao, *J. Chem. Phys.*, 2004, **120**, 8425-8433.
73. H. Taube, *J. Gen. Physiol.*, 1965, **49**, 29-50.
74. M. Hayyan, M. A. Hashim and I. M. AlNashef, *Chem. Rev.*, 2016, **116**, 3029-3085.

Chapter 4 Syntheses of PANI-CMPs and Properties of Prepared Materials

This chapter discusses experimental aspects of the study on PANI-CMPs, which can be separated into the syntheses and the characterisations. Syntheses of PANI-CMPs can be divided into two eras by the publication of the Bristol-Xi'an Jiaotong (BXJ)[1] tuning of solubility parameters in 2019. Prior to the BXJ publication, different synthesis techniques have been applied with varying degrees of success. The BXJ method has later been adopted for the syntheses of materials in this study with greater success than the previous attempts.

Post-BXJ syntheses of PANI-CMPs have been performed using different monomers, different functionality pathways, different functional group ratios, and different solubility tuning. Some synthesis attempts ended up producing mostly oligomers with only limited amounts of polymers to be collected. However, more than half of these attempts created polymers with different degrees of porosities, which will also be compared and discussed in this chapter.

4.1 Tuning Properties of PANI-CMPs

As explained in Chapter 1, tuning properties of resulting materials can be done in two ways, varying the chemical structures of starting materials, or varying external conditions during the synthesis. For the studies of CMPs, both approaches have been attempted.

4.1.1 Effects of Monomer Unit Structures

One of the first reported CMPs was poly(aryleneethynylene).[2] This family of materials has been investigated by Jiang, Cooper, and co-workers. They designed six different materials based on Sonogashira-Hagihara coupling reactions between aromatic terminal alkynes and haloarenes, with structures shown in Scheme 4-1.[3-5] Materials in this series have struts of different lengths, with the shortest in **CMP-0** and sequentially longest in **CMP-5**, with the exception of **CMP-4** being similar to **CMP-1** in structure but synthesised from different pathways. They found that specific surface areas and microporous surface areas of materials in this series also depend on the strut lengths. The longer strut lengths, the lower surface areas. The BET surface area of **CMP-0**, with shortest struts or linkers, was 1018 m^2g^{-1}, compared to 512 m^2g^{-1} in **CMP-5**.[5]

In addition, the effects of core or node sizes have also been studied. Two materials prepared from Suzuki-Miyaura coupling reactions have been studied by Hayashi *et al.*[6] Both materials were prepared from the same linker unit, 2,3,5,6-tetrafluoro-1,4-phenylene, coupled with two different core units, 1,1,2,2-tetrakis(1,4-phenylene)ethylene (**TPE**) and pyrene-1,3,6,8-tetrayl (**PYR**), respectively. Structures of these materials are shown in Scheme 4-2. They found that the material prepared with the larger **TPE** core had a lower surface area (508 m^2g^{-1}) than the **PYR** counterpart (824 m^2g^{-1}), which is in line with the previously mentioned effect from strut lengths.

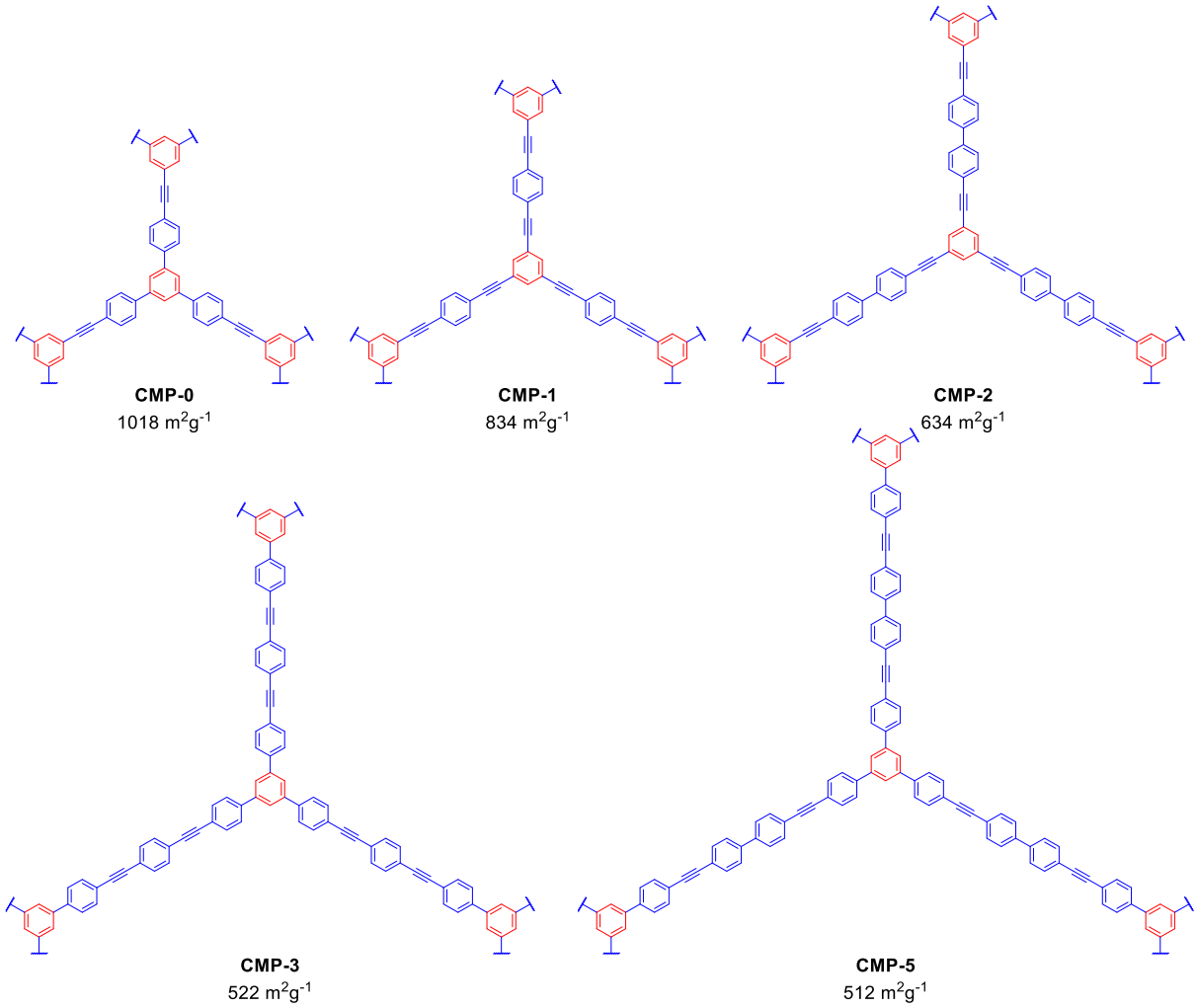

*Scheme 4-1 Structures of poly(aryleneethylnylene) materials (**CMP-0** to **CMP-5**, excluding **CMP-4**) studied by Jiang, Cooper, and co-workers* [5]

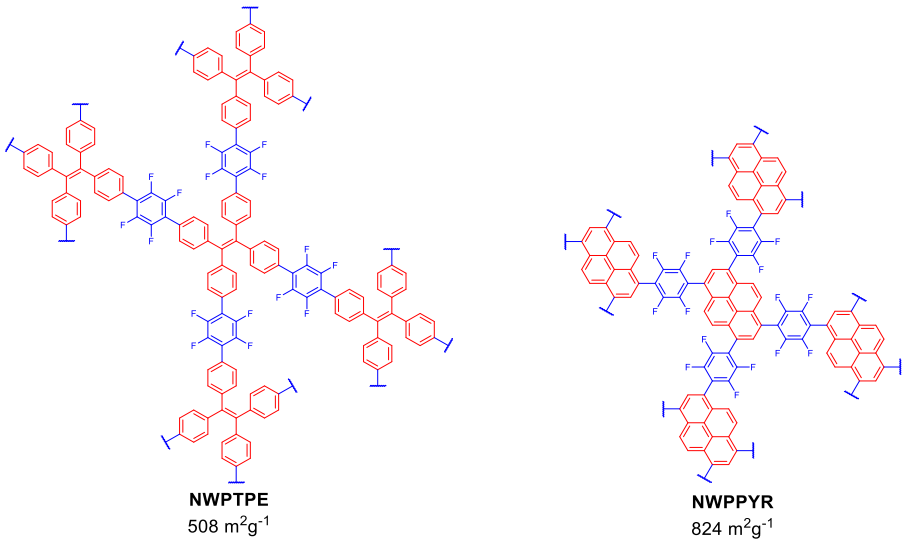

*Scheme 4-2 Structures of two fluorine-containing materials **NWPTPE** and **NWPPYR** studied by Hayashi et al.*[6]

For the development of CMPs for CO_2 adsorption, introduction of polar functional groups was found to be more important than changes in surface area. Dawson, Adams, and Cooper modified **CMP-1** by adding four different functionalities, namely carboxylic acid, hydroxyl, amino,

and methyl groups (Scheme 4-3 and Table 4-1).[7] While the surface areas of these materials varied from 522 m^2g^{-1}, for **CMP-1-COOH**, to 1043 m^2g^{-1}, for **CMP-1-(OH)$_2$**, the amounts of CO_2 adsorbed at 1 bar and 298 K were clustered closely, varying from 0.94 $mmol \cdot g^{-1}$ for **CMP-1-(CH_3)$_2$** to 1.18 $mmol \cdot g^{-1}$ for unfunctionalised **CMP-1**. Materials of this series have shown that the relationship between specific surface areas and the amount of CO_2 uptakes are not straightforward, with the material with highest surface area (**CMP-1-(OH)$_2$**) being second in terms of CO_2 adsorption, coming behind the unfunctionalised **CMP-1** which is the third highest in terms of specific surface areas. Meanwhile, while adding functional groups that can interact with CO_2 molecules may theoretically increase the adsorbed amounts, functional groups themselves may cause the decrease in surface areas or pore volume, ultimately diminishing the uptake of CO_2.

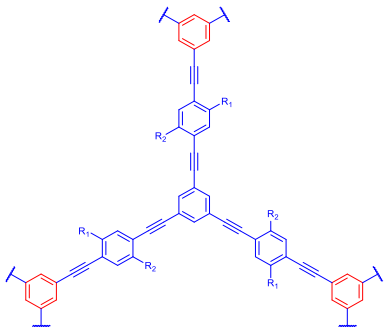

*Scheme 4-3 Structures of functionalised **CMP-1** materials studied by Dawson, Adams, and Cooper[7]*

*Table 4-1 Functional groups R_1 and R_2 of functionalised **CMP-1** materials and their specific surface areas studied by Dawson, Adams, and Cooper taken from reference [7]*

Material	Functional Group		Specific Surface Area ($m^2 \cdot g^{-1}$)	CO_2 Uptake at 298 K and 1 bar ($mmol \cdot g^{-1}$)
	R_1 Group	R_2 Group		
CMP-1	–H	–H	834	1.18
CMP-1-COOH	–COOH	–H	522	*not reported*
CMP-1-NH_2	–NH_2	–H	710	*not reported*
CMP-1-(CH_3)$_2$	–CH_3	–CH_3	899	0.94
CMP-1-(OH)$_2$	–OH	–OH	1043	1.07

Note: Absorption figures for uptakes of **CMP-1-COOH** and **CMP-1-NH_2** are not explicitly reported, but they are shown graphically to be close to that of **CMP-1-(CH_3)$_2$** (0.94 $mmol \cdot g^{-1}$).

4.1.2 Effects from Monomer Functionalities

For coupling reactions between starting materials with different active functionalities, several combinations for skeletal structures and functional groups in the initial set up are possible. For example, the synthesis of *N*-phenyl-2-naphthylamine using Buchwald-Hartwig (BH) cross-coupling reaction (Scheme 4-4) can be performed in two different ways, either from 2-naphthylamine and bromobenzene (the left route) or from 2-bromonaphthalene and aniline (the right route).

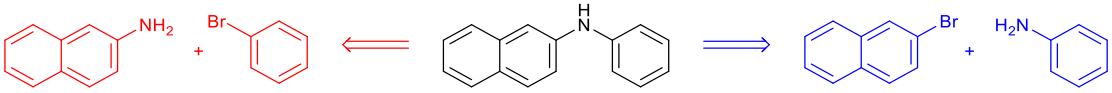

Scheme 4-4 Retrosynthesis analyses for the synthesis of N-phenyl-2-naphthylamine using BH cross-coupling reaction

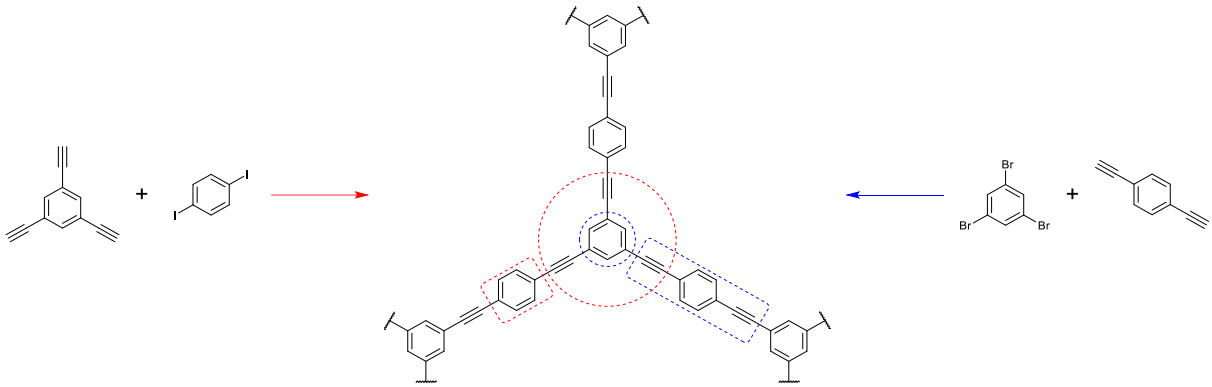

*Scheme 4-5 Monomers used in the syntheses of **CMP-1** (the left pathway) and **CMP-4** (the right pathway)[3]*

A similar principle also applies for the design and synthesis of CMPs via coupling reactions. As mentioned in Section 4.1.1, the names **CMP-1** and **CMP-4** are given to two different materials with the same polymer topologies but synthesised from different pathways.[3] Both materials had similar surface areas (834 $m^2 \cdot g^{-1}$ for **CMP-1**, 744 $m^2 \cdot g^{-1}$ for **CMP-4**) and microporous surface areas (675 $m^2 \cdot g^{-1}$ for **CMP-1**, 596 $m^2 \cdot g^{-1}$ for **CMP-4**). It is suggested that the slightly lower surface areas in **CMP-4** when compared to **CMP-1** are because of the lower reactivity of bromo groups compared to iodo groups upon Sonogashira-Hagihara coupling reactions.[5]

In all previous reports of PANI-CMPs,[1, 8-10] all these materials have been synthesised from brominated cores and aminated linkers. This has left a gap in the study of the effects of functional groups on obtained materials and their properties.

4.1.3 Previous Property Tuning Attempts of PANI-CMPs

Poly(aniline)-based CMPs or PANI-CMPs have been developed in the Faul Research Group, based on the synthesis of poly(aniline)s via BH cross-coupling reactions between haloarenes and aminoarenes.[8, 9, 11] By using monomers with connectivity of more than two, i.e., having more than two reactive points that can propagate the growth of polymer chains, highly crosslinked polymer products can be achieved. The concept of cores or nodes with high connectivities linked together with linkers or struts is not novel, nor is it unique for CMPs. In fact, this concept is inherited from MOFs in which metal ions can coordinate with four or six ligands. This core-linker concept is then borrowed for all-organic COFs, and it is also the basis of the original **CMP-1** in which benzene rings "cores" are linked together by ethyne-1,2-diyl-1,4-phenylene-ethyne-1,2-diyl linkers (Scheme 4-1).

PANI-CMPs developed in this research group are generally copolymers prepared from two monomers, namely cores and linkers. Cores are monomers with multiple connectivities such as tris(4-bromophenyl)amine[8] (connectivity of 3) and hexakis(4-bromophenyl)benzene[9] (connectivity of 6), while linkers are monomers with connectivities of two acting as link between two core units. Structures of these monomers are shown in Scheme 4-6.

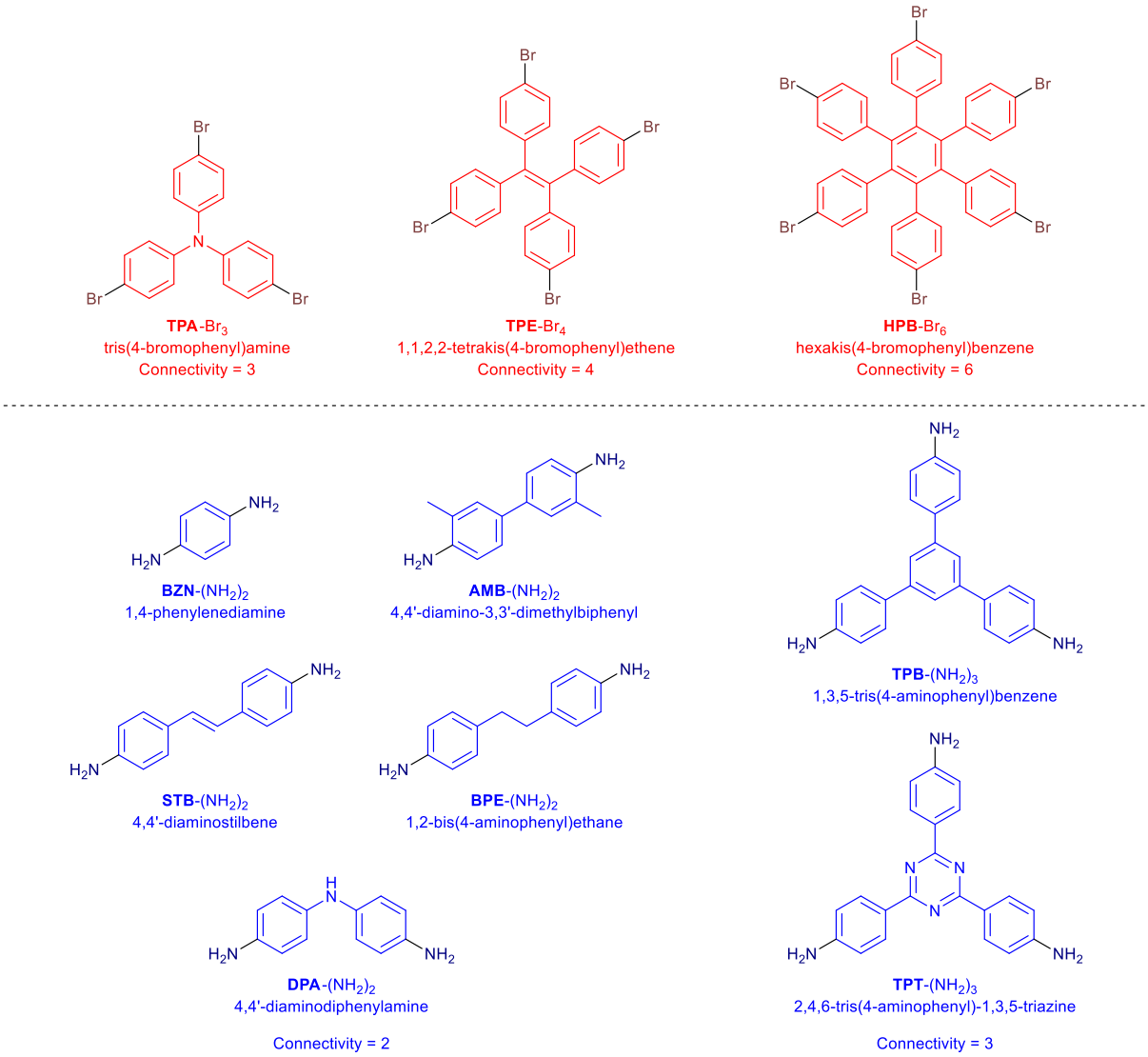

Scheme 4-6 Structures of brominated core (top) and aminated linker (bottom) monomers in the designs of PANI-CMPs in the Faul Research Group[8, 9, 11]

Table 4-2 Previously developed PANI-CMPs in the Faul Research Group from monomers compiled in Scheme 4-6

Material	Monomer		Specific Surface Area ($m^2 \cdot g^{-1}$)	Reference
	Core	Linker		
PTPA-1	**TPA**-Br_3	**BZN**-$(NH_2)_2$	52	Liao *et al.* (2014)[8]
PTPA-2	**TPA**-Br_3	**AMB**-$(NH_2)_2$	62	
PTPA-3	**TPA**-Br_3	**STB**-$(NH_2)_2$	450	
PTPA-4	**TPA**-Br_3	**BPE**-$(NH_2)_2$	22	
HCMP-1	**HPB**-Br_6	**BZN**-$(NH_2)_2$	308	Liao *et al.* (2016)[9]
HCMP-2	**HPB**-Br_6	**DPA**-$(NH_2)_2$	58	
HCMP-3	**HPB**-Br_6	**AMB**-$(NH_2)_2$	50	
HCMP-4	**HPB**-Br_6	**STB**-$(NH_2)_2$	28	
LPCMP-1	**TPA**-Br_3	**TPB**-$(NH_2)_3$	1280	Pan *et al.* (2019)[11]
LPCMP-2	**TPA**-Br_3	**TPT**-$(NH_2)_3$	516	
LPCMP-3	**TPE**-Br_4	**TPB**-$(NH_2)_3$	1340	
LPCMP-4	**TPE**-Br_4	**TPT**-$(NH_2)_3$	570	

The main structural difference of PANI-CMPs from other aforementioned CMPs studied by Jiang *et al.* and Hayashi *et al.* is that linkers in PANI-CMPs possess more complicated structural motifs compared to those in the other two groups of CMPs. Such complications emerge from amino groups linking between core and linker units, with the C–N–C angles involved approximately 120°-130° depending on oxidation states (discussed in detail in Chapter 3), along with other non-linear geometries such as *trans*-alkene in **PTPA-3** and **HCMP-4** and methylene groups in **PTPA-4**. These structural complications can create further complications that can disrupt the trend, as observed in *trans*-stilbene-linked **PTPA-3** and **HCMP-4**. While **PTPA-3** possessed the highest surface area in the **PTPA** series, **HCMP-4** yield the lowest surface area compared with a similar set of linkers in the **HCMP** series.

It is notable that polymers of the **LPCMP** series have clearly greater specific surface areas compared to those in the **PTPA** and **HCMP** series. Arguably, **LPCMP** materials are synthesised with added sodium nitrate, which might aid the formation of highly crosslinked polymer structures. This issue has been investigated in the publication of BXJ method, which will be discussed later.

4.1.4 PANI-CMPs Studied in This Project

This project aims to explore structure-property relationships for the design of PANI-CMPs. Therefore, this chapter will discuss different materials prepared from different monomers. Different series of materials have been prepared to explore different aspects of PANI-CMP properties, with varying degrees of success.

4.2 Studies of PANI-CMPs Prior to the BXJ Publication

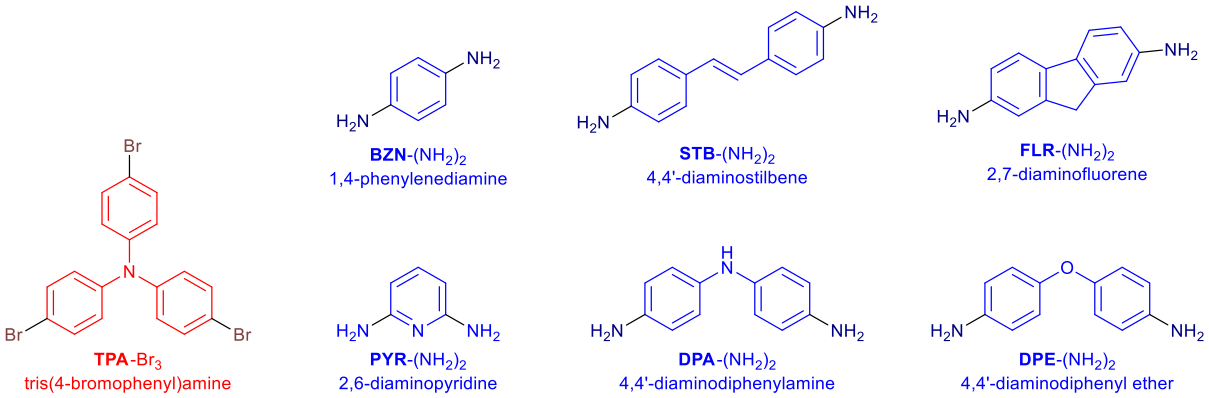

Scheme 4-7 Structures of core and linker monomers used in the studies of PANI-CMPs in the first series

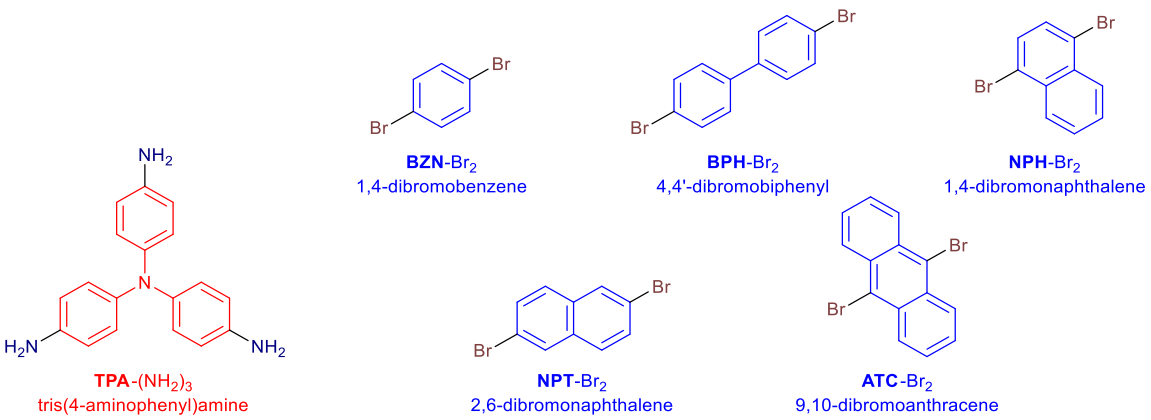

Scheme 4-8 Structures of core and linker monomers used in the studies of PANI-CMPs in the second series

The first attempts to study PANI-CMPs were done using tris(4-bromophenyl)amine (**TPA**-Br_3) as a core monomer coupled with the six linker monomers, respectively, as listed in Scheme 4-7. The second attempts for the studies of PANI-CMPs were done using the different approach from the first series. For this second series, the aminated counterpart, tris(4-aminophenyl)amine or **TPA**-$(NH_2)_3$, was used instead of **TPA**-Br_3. This core monomer was coupled with five linker monomers, listed in Scheme 4-8, which are the same set of monomers that were used in the studies of tetra(aniline) modifications.[12] Materials in both series were synthesised using stoichiometric ratio of core monomers to linker monomers and were performed in toluene at 110 °C under flowing nitrogen atmosphere and ambient pressure.

*Table 4-3 Specific surface areas and microporous surface areas from nitrogen isotherm analyses at 77 K of **TPA**-based PANI-CMPs synthesised in the first two series*

Material	BET Specific Surface Area ($m^2 \cdot g^{-1}$)	Microscopic Surface Area ($m^2 \cdot g^{-1}$)
PTPA-BZN-1	21.1	0.0
PTPA-BZN-2	36.8	0.0
PTPA-STB-1	21.6	0.0
PTPA-FLR-1	43.3	0.0
PTPA-PYR-1	33.8	0.0
PTPA-DPE-1	26.7	0.0
PTPA-DPA-1	549.6	206.6
PTPA-BPH-2	22.5	1.4
PTPA-NPH-2	26.4	0.0
PTPA-NPT-2	40.5	0.0
PTPA-ATC-2	32.9	0.0

Note: Material names are in the format **PCOR-LKR-n** when **COR** and **LKR** are names of core and linker units, respectively, as listed in Scheme 4-7 and Scheme 4-8, while **n** is the series number (**1** for the first series and **2** for the second series).

Table 4-3 lists specific surface areas and microporous surface areas of PANI-CMPs in the first two series. These materials are shown to have low surface areas, except for **PTPA-DPA-1** with 549.6 $m^2 \cdot g^{-1}$ in specific surface area. **PTPA-DPA-1** is also the only material to have significant microporosity (206.6 $m^2 \cdot g^{-1}$). For the majority of materials of both series, with surface areas being under 50 $m^2 \cdot g^{-1}$, it is arguable that the porosities and microporosities of these materials are suppressed by hostile synthesis conditions that do not promote high porosity, and therefore, the conclusions for the effects of monomer structures on porosities of materials cannot be drawn.

The remarkably high surface area can be attributed to the fact that the **DPA**-$(NH_2)_2$ monomer being used is actually its sulfate salt. The presence of sulfate ions aids the formation of intermediates that lead to highly porous materials. This phenomenon, together with another report of the improvement in porosity as a result of the addition of sodium nitrate,[11] has initiated separate studies of tuning porosity of materials by varying solubility parameters of the synthesis matrices, which has ultimately led to the Bristol-Xi'an Jiaotong approach.[1, 10]

Materials in the **PTPA-LKR-2** series were synthesised for the comparative studies of optical spectroscopic spectra compared to the earlier published work on tetra(aniline)s. The discussions can be found in Section 3.3.3.

To improve porosity properties, different synthesis methods were applied for the synthesis of **PTPA-BZN** with different degrees of success. Specific surface areas, as determined from nitrogen isotherm adsorption at 77 K and calculated using the BET method, of **PTPA-BZN** prepared from different methods are given in Table 4-4. All these materials were prepared from

TPA-Br_3 and **BZN**-$(NH_2)_2$, i.e., the normal functionality pathway, which is the same material as in the Series 1.

*Table 4-4 Specific surface areas of **PTPA-BZN** prepared from different synthesis methods. All reactions were carried out in toluene (b.p. 110 °C) unless stated otherwise.*

Synthesis Condition	Specific Surface Area ($m^2 \cdot g^{-1}$)
High pressure (150 °C, 7 bar in an autoclave, 24 hr)	419.5
High pressure (150 °C, 2 bar in an autoclave, 24 hr)	139.0
Build-up pressure (120 °C in a sealed Schlenk flask, 24 hr)	308.2
Build-up pressure (110 °C in a sealed Schlenk flask, 24 hr)	82.1
Build-up pressure (110 °C in a sealed Schlenk flask, 48 hr)	425.0
Ambient pressure (110 °C in an open Schlenk flask, 48 hr)	69.7

From Table 4-4, it is clearly shown that surface areas of PANI-CMPs can be enhanced by increasing the reaction pressure. This can either be achieved by performing the synthesis in a high-pressure steel autoclave or in a sealed Schlenk flask. However, heating up liquid in a container that is not specifically designed to withstand high pressures can be a safety concern, while the use of a specifically made reactor can be costly and may not be practical for upscaled studies. Meanwhile, extending reaction time can improve the results to an extent, but the effectiveness is still limited especially when performing the synthesis at ambient pressure.

4.3 Syntheses of PANI-CMPs by BH.BXJ Method

The BH.BXJ method is based on the BH coupling reaction and BXJ method of solubility tuning.[1, 10] Salt is added to the synthesis matrix to adjust the solubility parameters to matches those of the desired polymers. To exploit this tuning method, however, the first batches have to be prepared in a trial-and-error manner first to obtain the "polymers" so that their solubility parameters can be determined.

4.3.1 Factors to Consider for the Synthesis

For the BH.BXJ series of PANI-CMPs, three core (**TPA**, **TPB**, and **TPT**) and two linker monomers (**BZN** and **FLR**) are selected. Reactions were performed in both normal (**N**) and reversed (**R**) functionality pathways.

Porosity properties of porous materials have also been found to be affected by the ratios between reacting monomers. For example, porous materials **CMP-1** to **CMP-4** synthesised from different monomer ratios were compared, with the optimum ratio between ethynyl and halogen groups for each material found to be either 3:2 or 5:3.[3]

Comparison between materials from different stoichiometric ratios and different synthetic pathways can be challenging, especially for materials synthesised from monomers with different connectivities such as [A_3 + B_2] in this case. Table 4-5 lists the ratios of chemical species, namely core units, linker units, amino groups, and bromo groups, at the initial set-up for the syntheses of PANI-CMPs. From the table, it means that simply swapping functionalities can create two materials with different chemical components, assuming all monomers go into the resulting polymers.

Table 4-5 Ratios of species involved in the synthesis of PANI-CMPs using different functional group ratios and synthetic pathways

Amino:Bromo	Synthesis Pathway	Functional Group		Mole Ratio of Species Involved			
		Core (A_3)	Linker (B_2)	Core Unit	Linker Unit	Amino Group	Bromo Group
3:2 (Amino-Excess; **A**)	Normal	Bromo	Amino	4	9	18	12
	Reversed	Amino	Bromo	6	6	18	12
1:1 (Stoichiometric; **S**)	Normal	Bromo	Amino	4	6	12	12
	Reversed	Amino	Bromo	6	4	12	12
2:3 (Bromo-Excess; **B**)	Normal	Bromo	Amino	6	6	12	18
	Reversed	Amino	Bromo	9	4	12	18

As most of the materials, besides **PTPA-BZN**, have never been studied before, initial reference points are required for further optimisation of solubility parameters. To obtain these points, solubility tuning was carried out in an on-and-off basis using sodium bromide, which is the same chemical species as one of the by-products from Buchwald-Hartwig coupling reactions between bromoarenes and aminoarenes. The "tuning" for the "on" synthesis was done by adding 0.50 mmol of NaBr on top of the initial starting materials in the "off" synthesis.

Nomenclatures of PANI-CMPs are in the **PCOR-LKR-SN(x)** format, with **COR** and **LKR** referring to the abbreviations for core and linker units, similar to materials in Table 4-3. The third part refers to the synthesis approaches, namely functional group ratios, functionality pathways, and the addition of sodium bromide. Full explanations can be found in Section 2.2.1.

With these factors, namely two core units, three linker units, three stoichiometric ratios, two functionality pathways, and two modes of solubility tuning, in theory, 72 materials should be obtained.

4.3.2 Synthesis Outcomes

Table 4-6 lists the outcomes of the syntheses of PANI-CMPs under different initial conditions. The criterion to determine whether a synthesis is a success or a failure is the amount of insoluble polymer obtained compared to the soluble oligomer. Generally, if the synthesis did not yield polymer in high enough amounts for further purification or characterisation processes, that synthesis is a failure. Out of 72 reactions attempted, 47 of these successfully produced polymer in significant amounts, while 25 of these did not produce enough polymer for further studies.

Most of these failures happened in the amino-excess functional group ratio, with 16 reactions out of 24 performed ending in oligomeric products. Meanwhile, nine reactions starting with 1:1 ratio between amino and bromo groups also ended in failures. It is worth noting that all bromo-excess reactions produced polymer in significant amounts. The failures of amino-excess reactions can be attributed to the fact that while one amino group can, in theory, undergo the coupling reaction twice, because the resulting secondary amine can still undergo another coupling reaction (although not expected), a bromo group can be used only once. Starting reactions with lower amount of bromo groups may lead to a premature depletion of bromo groups.

Table 4-6 Summary of synthesis outcomes for PANI-CMP attempts with different monomer units and synthesis initial conditions. Black squares (■) refer to successful syntheses with high amounts of polymers obtained, while white squares (□) refer to unsuccessful syntheses where products obtained are mostly soluble oligomers. "On" refers to the synthesis attempts with additional NaBr, while "off" refers to synthesis attempts without additional NaBr.

Core Unit	Functional Group Ratio	BZN-linked				FLR-linked			
		Normal Functionality		Reversed Functionality		Normal Functionality		Reversed Functionality	
		On	Off	On	Off	On	Off	On	Off
TPA	Amino-Excess	□	□	□	□	■	■	□	□
	Stoichiometric	□	□	□	□	■	■	■	□
	Bromo-Excess	■	■	■	■	■	■	■	■
TPB	Amino-Excess	□	□	□	□	■	■	□	□
	Stoichiometric	□	□	□	□	■	■	■	■
	Bromo-Excess	■	■	■	■	■	■	■	■
TPT	Amino-Excess	□	□	□	■	■	■	□	■
	Stoichiometric	■	■	■	■	■	■	■	■
	Bromo-Excess	■	■	■	■	■	■	■	■

The majority (eight) of nine failed reactions that were started with the equal amount of amino and bromo groups fall between **PTPA-BZN** and **PTPB-BZN** attempts, while the syntheses of **PTPT-BZN** along with all **FLR**-linked PANI-CMPs (except **PTPA-FLR-SRx**) were successful. Thin-layer chromatography (TLC) analyses of the supernatant, where oligomeric products were obtained from, revealed that most of these products are mixtures of oligomers with lower retention factors (R_f) than either of the monomers. Their lower R_f values can be attributed to their higher molecular weights, which cause flowing through the absorbent to be harder. While the TLC analyses shown in Figure 4-1 are taken from the amine-excess syntheses, the trend were observed in almost all cases.

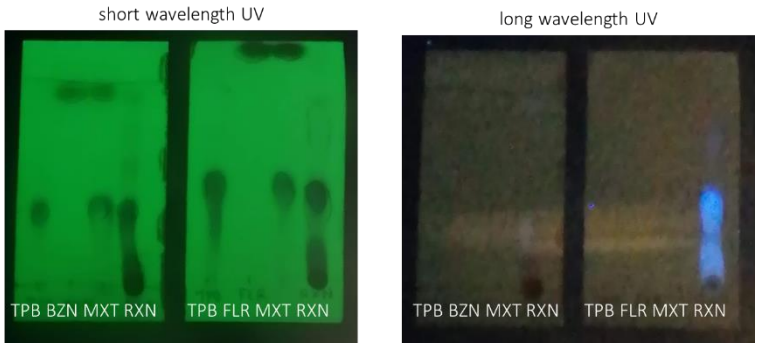

*Figure 4-1 Thin-layer chromatography (TLC) analyses of supernatant obtained (**RXN**) after syntheses compared to monomers, viewed under short wavelength UV (left) and long wavelength UV (right) lamps. These analyses were performed from supernatants of **PTPB-BZN-AR** (left sheet) and **PTPB-FLR-AR** (right sheet), which both failed to produce polymers.*

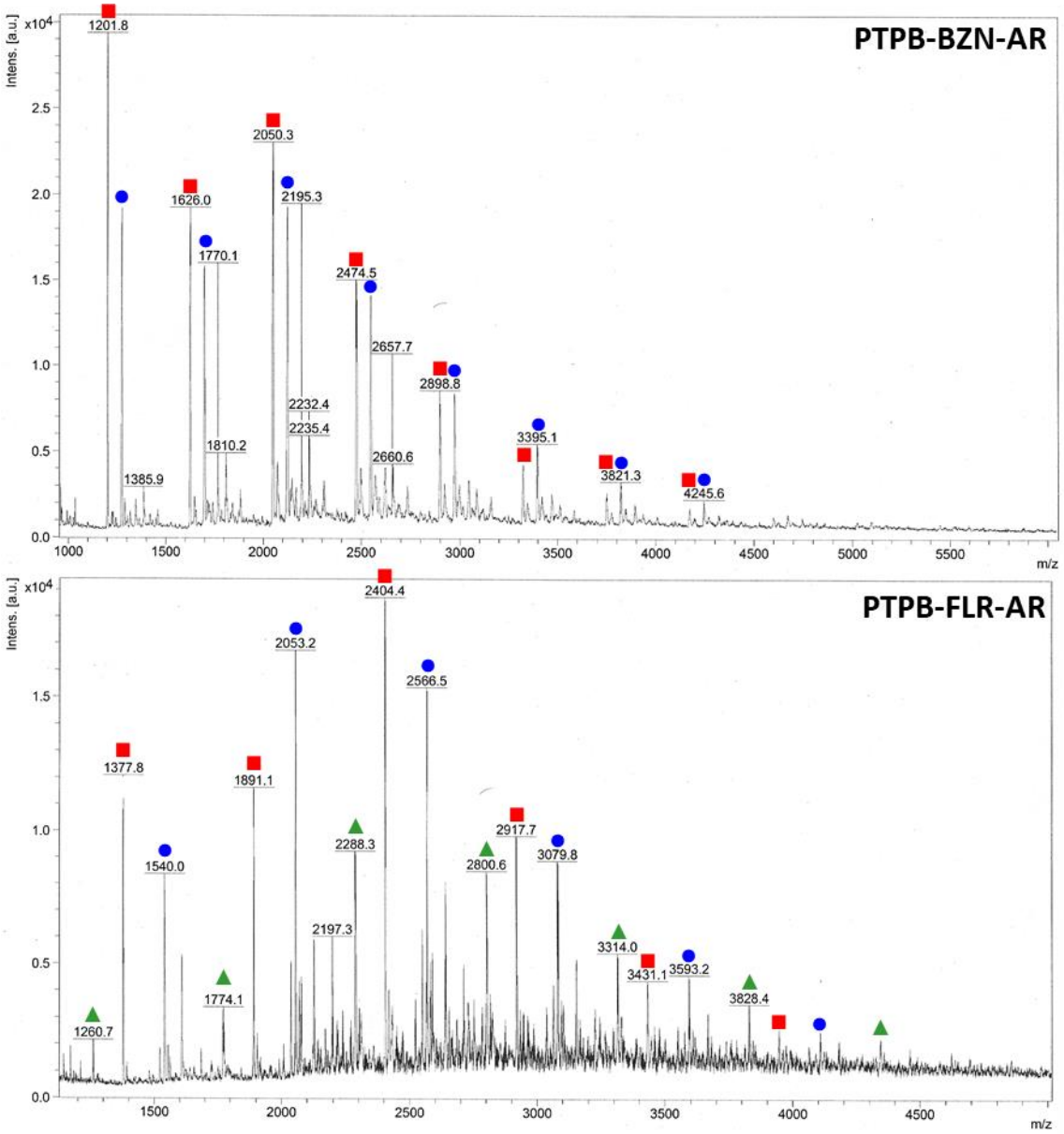

*Figure 4-2 Mass spectrometry analyses of the oligomeric products from the failed syntheses of **PTPB-BZN-AR** (top) and **PTPB-FLR-AR** (bottom). Squares, circles, and triangles denotes peaks with constant distances, see the main text for discussions.*

Mass spectrometry analyses of the oligomeric products from both reactions (Figure 4-2) also confirmed the formations of oligomers. For the **PTPB-BZN-AR** synthesis, the mass spectrum (the top spectrum) appears to be as series of peak groups, with each consecutive group being approximately 424 in mass per charge (m/z). The two series can be delineated, marked with red squares and blue circles. The m/z differences of 424 are roughly close to the mass of a **110** oligomer (one core, one linker, and no cyclisation) as shown in Scheme 4-9. It is worth noting that the m/z differences of **PTPB-BZN-AR** oligomeric products are between 425.19 of the unoxidised form and 423.17 of the oxidised form, implying that the resulting oligomers may have been partially oxidised.

A similar trend can also be observed in the case of **PTPB-FLR-AR**, with the differences being approximately 513 in m/z. However, as the differences are closer to 513.22 of the

unoxidised form than to 511.20 of the oxidised form, the oligomers might not be oxidised, unlike in the previous case.

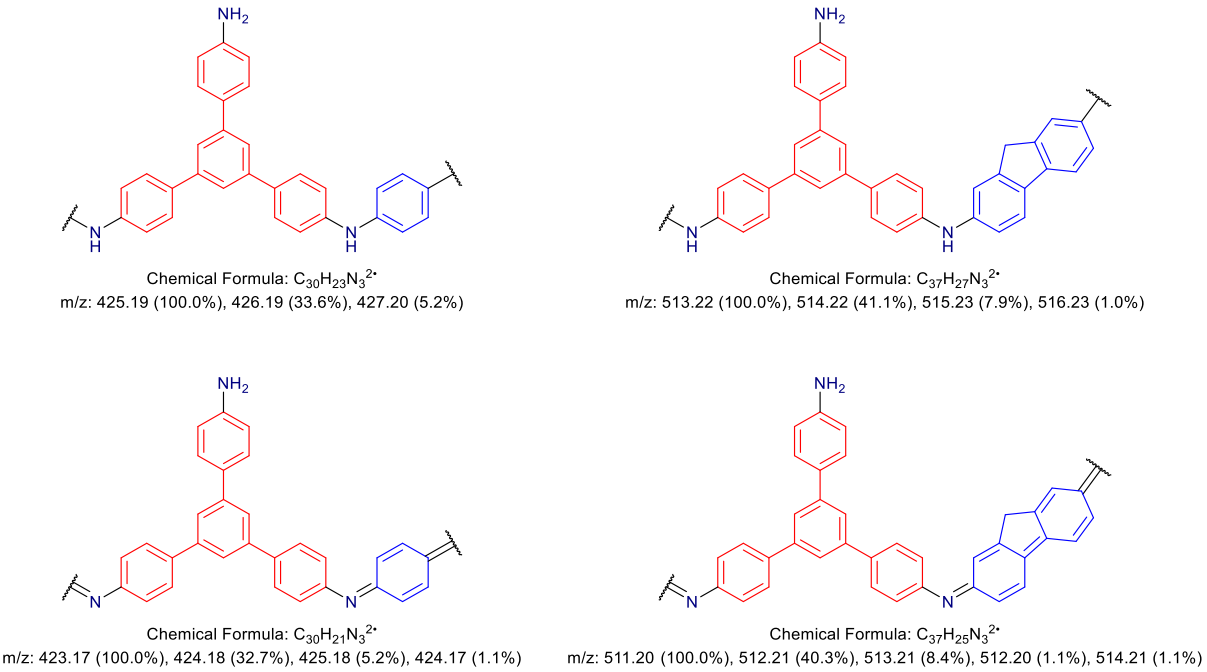

*Scheme 4-9 Structures of **110** oligomeric fragments from **TPB**-$(NH_2)_3$ core monomer and **BZN**-Br_2 (left) or **FLR**-Br_2 (right) linker monomer in unoxidised form (top row) and oxidised form (bottom row)*

*Table 4-7 Theoretical m/z values of different oligomers in the series of mass spectrometry peaks from the analyses of **PTPB-BZN-AR** and **PTPB-FLR-AR***

PTPB-BZN-AR				PTPB-FLR-AR					
Series 1 (■)		Series 2 (●)		Series 1 (■)		Series 2 (●)		Series 3 (▲)	
Olig.	m/z	Olig.	m/z	Olig.	m/z	Olig.	m/z	Olig.	m/z
320	1201.6	**331**	1276.6	**320**	1378.6	**331**	1540.7	**341**	1783.6
430	1627.7	**441**	1701.8	**430**	1891.8	**441**	2053.9	**451**	2297.9
540	2052.9	**551**	2126.9	**540**	2405.1	**551**	2568.1	**561**	2811.1
650	2478.1	**661**	2553.1	**650**	2919.3	**661**	3081.3	**671**	3324.3
760	2904.3	**771**	2978.3	**760**	3432.5	**771**	3594.6	**781**	3838.5
870	3329.5	**881**	3403.5	**870**	3946.7	**881**	4108.8	**891**	4350.7

In the mass spectrum of **PTPB-FLR-AR** oligomeric products, there are the same two series found in the **PTPB-BZN-AR** oligomeric products along with the third series, marked with green triangles. For the common two series, the series marked with squares belong to oligomers with *n* core units, *n*-1 linker units, and zero cycles, while the series marked with circles belong to oligomers with *n* core units, *n* linker units, and one cycle. The theoretical m/z values are listed in Table 4-7. Meanwhile, for the third series (although in the table, they are assigned to oligomers with *n* core units, *n*+1 linker units, and one cycle), the difference between the theoretical and actual m/z values are around 10 (m/z of 1783.6 calculated for the **341** oligomer compared to 1774.1 measured in Figure 4-2, for example). However, this series is the closest series that can practically be theorised.

The presences of high molecular weight oligomers in supernatants from failed attempts to form PANI-CMPs imply the premature terminations of polymerisation. While such behaviour in the case of amino-excess syntheses can be attributed to the lower amounts of bromo groups

compared with amino groups at the initial set up, additional attributing factors may exist in the cases of **PTPA-BZN** and **PTPB-BZN**. The first few steps during the polymerisation process towards the formation of PANI-CMPs from normal and reversed functionality pathways are illustrated in Scheme 4-10 and Scheme 4-11, respectively. In both pathways, processes initiate with one molecule of core coupled with one molecule of linker, forming a **110** oligomer.

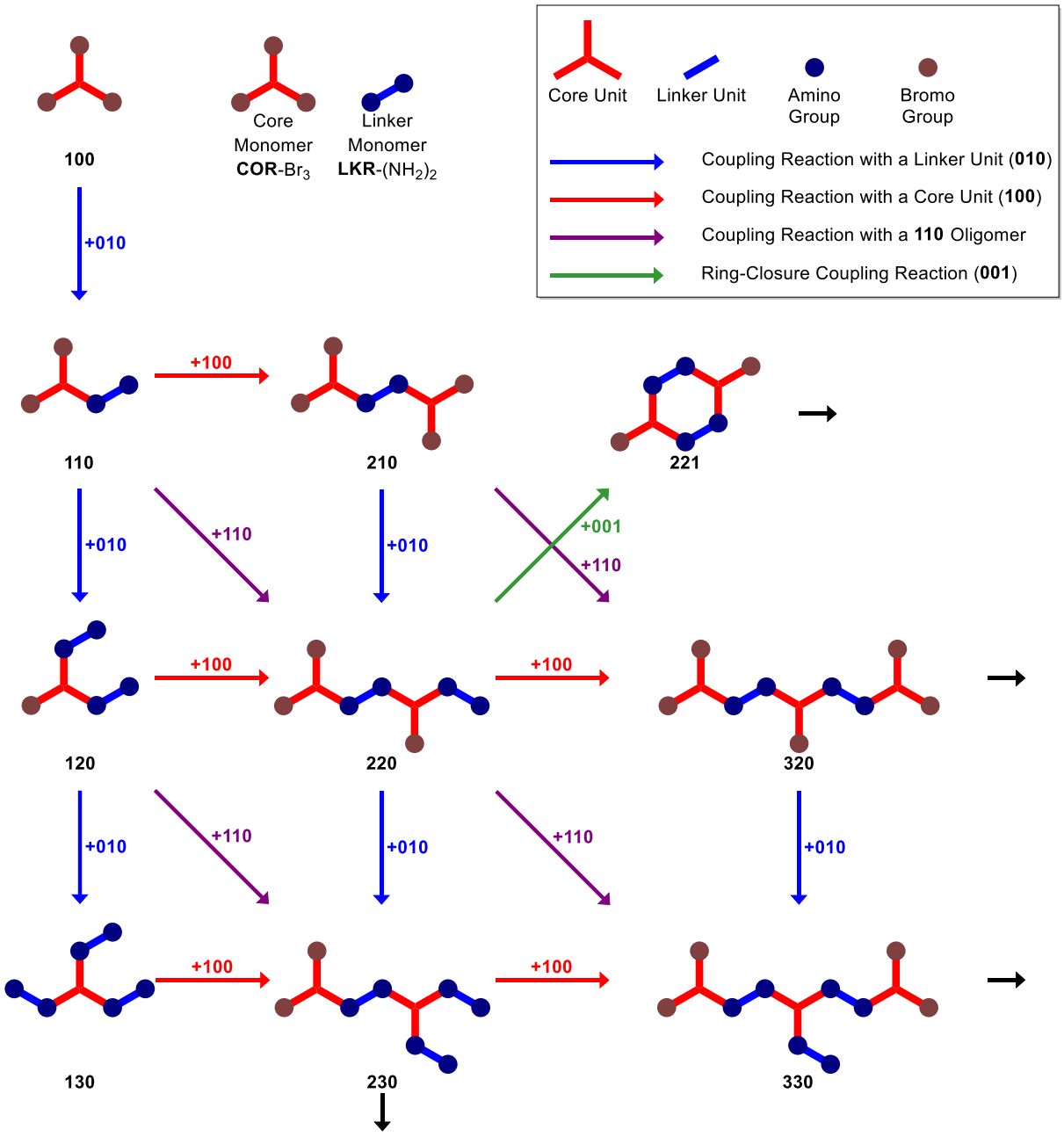

*Scheme 4-10 Reactions taking place in the first few steps of the polymerisation process towards the formation of PANI-CMPs from **normal** functionality pathway. Chemical species shown in these steps are denoted by three-digit codes representing, from the first to the third digit, the number of core units, the number of linker units, and the number of cycles. Not all possible reactions and not all possible isomers, if applicable, are listed.*

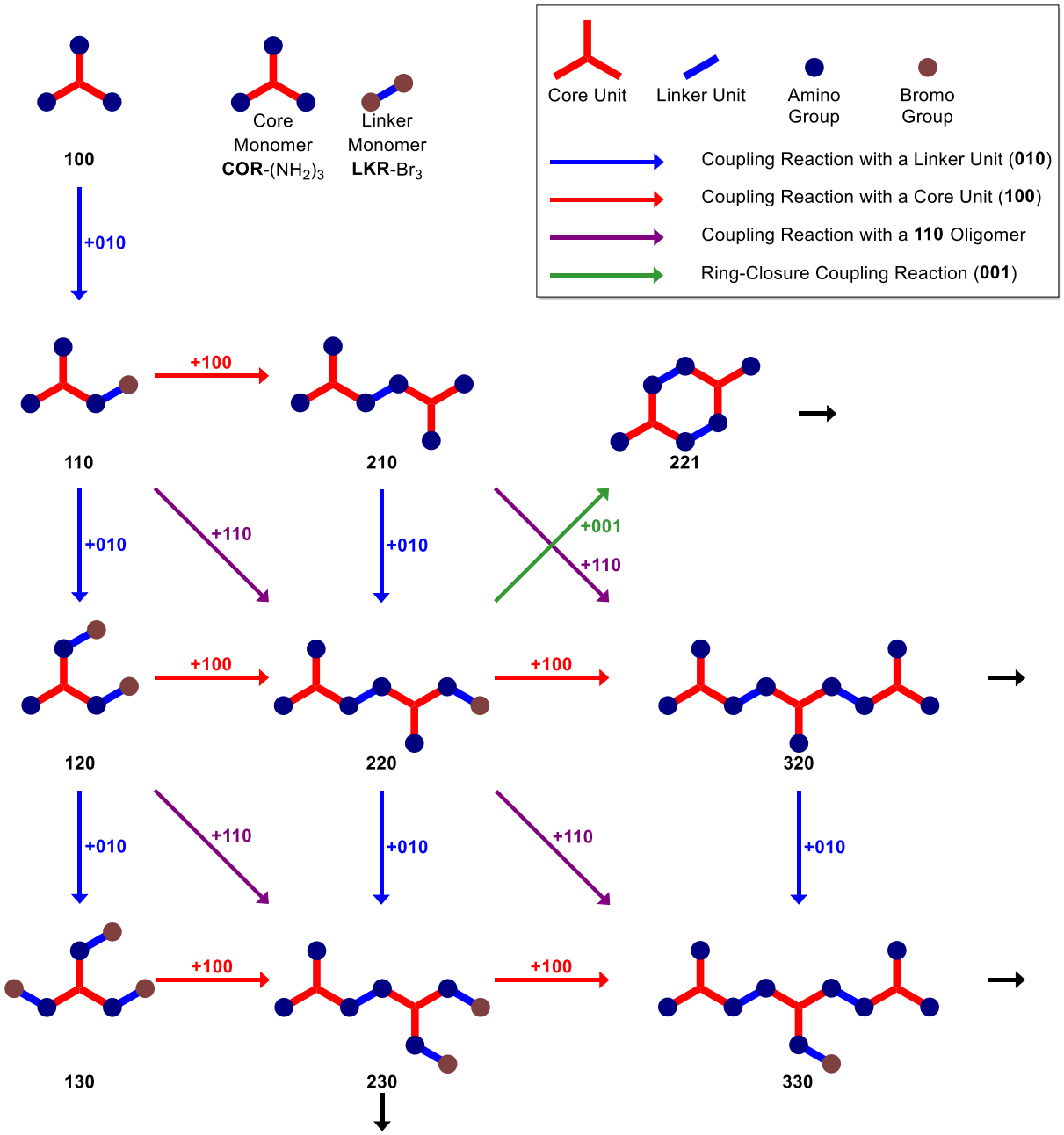

*Scheme 4-11 Reactions taking place in the first few steps of the polymerisation process towards the formation of PANI-CMPs from **reversed** functionality pathway. Chemical species shown in these steps are denoted by three-digit codes representing, from the first to the third digit, the number of core units, the number of linker units, and the number of cycles. Not all possible reactions and not all possible isomers, if applicable, are listed.*

There are three possibilities for the newly formed **110** oligomer molecule to react further. It can react with another molecule of core (red horizontal arrows), another molecule of linker (blue vertical arrows), or another molecule of **110** oligomer (purple diagonal arrows), yielding three possible products which can then react further to form larger and larger oligomer molecules. The probability for each of the three possible "second" reactions depends on the availability of the involved chemical species, which in turn depends on the amount of these species either being added at the initial set up or being generated from the previous step. For example, in the reaction set with excess amount of core monomer, after the first generation of reactions, there might be more **110** oligomer or the leftover core monomer than each other, depending on what the excess amount was in the original set up. Nonetheless, there is probably only trace amount of linker

monomer left. Therefore, the chance of a **110** oligomer to react with another linker monomer to form a **120** oligomer is almost negligible.

The difference between **110** oligomers from normal and reversed functionality pathways is the number of available functional groups. In the normal pathway, as a core monomer with three bromo groups coupled with a linker monomer with two amino groups, the resulting **110** oligomer has two bromo groups and one primary amino group remaining along with the newly formed secondary amino group. Meanwhile, in the reversed pathway, the resulting **110** oligomer instead has one bromo group and two amino groups along with, again, the new secondary amino group. Such difference in functionality of oligomers becomes more pronounced in larger oligomers. For example, **220** and **320** oligomers from the reversed pathway do not have any bromo group remaining at all (Scheme 4-11). If the amount of brominated linker is limited, the whole polymerisation process will then be harder to progress due to the lack of reactive species. It might end prematurely as soon as all remaining bromo groups have been used up, resulting in a mixture of oligomers instead of polymer. Meanwhile, the corresponding oligomers in the normal pathway (Scheme 4-10) have more bromo groups along with the secondary amino groups, which can also undergo BH cross-coupling reactions with bromo groups.[13]

Changing core and linker units can create further complications to the coupling reactions. Gelation is a crucial step for the formation of highly crosslinked polymer networks[14] and can only be achieved when the HSP distance (R_a) between the gelator and the matrix is in the optimum range.[15] For a CMP synthesis, however, both the gelator (the growing oligomer or polymer chain) and the matrix (the rest of the reaction mixture including unreacted monomers) are dynamic. As polymerisation progresses, monomers are taken out of the matrix and added to the gelator. The dynamic nature of this chemical system means that the HSP distance is in fact a function of time. Starting reactions with different monomers, even with the same skeletons, means that reactions will have different starting HSP distances and eventually different trajectories over time. The latter means that different reactions might take different times for the HSP distances to reach the gel-forming range. Gelation can also complicate the kinetics of coupling reactions due to different viscosities between gels and solutions.

On the issue of solubility tuning by adding sodium bromide, out of 36 comparable pairs, only three of these pairs yielded different results in terms of the success of polymer formations, namely **PTPA-FLR-SR**, **PTPT-BZN-AR**, and **PTPT-FLR-AR**. Nonetheless, this result has proved that adding sodium bromide to alter the solubility parameters of the liquid reaction matrix can shift the equilibrium in the way that accommodate the formation of larger oligomer fragments and eventually polymer networks. This phenomenon could be investigated further for the optimisation of polymer yields.

4.4 FT-IR Spectroscopic Analyses of PANI-CMPs

Spectroscopic techniques being used in this study are FT-IR spectroscopy and UV-Vis-NIR spectroscopy. FT-IR spectroscopy or vibrational spectroscopy uses infrared light and is meant for the study of vibrations of molecules, while UV-Vis-NIR spectroscopy uses waves ranging from ultraviolet to near infrared, which probes electronic configurations. UV-Vis-NIR spectroscopy of PANI-CMPs have been mostly discussed in Section 3.3 owing to its connection to electronic structures. Therefore, this section will focus on FT-IR spectroscopic studies.

FT-IR or Fourier-transform infrared spectroscopy is a spectroscopic technique for the analysis of molecular vibrations. Each functional group in organic compounds has its own unique frequency to be absorbed, which means that one can use this technique to identify or detect specific functional groups or the lack there of. The flaw of this technique is that not all functional groups can be detected using FT-IR spectroscopy. Usually, vibrational modes to be detected in

FT-IR spectroscopy, or being "IR active", must cause changes in dipole moments. Some functional groups, such as alkyne, cannot be detected using this technique. However, this technique is able to distinguish functional groups involved in the synthesis of PANI-CMPs, so it is chosen for the studies of these materials.

The chemistry of Buchwald-Hartwig coupling reaction, in the syntheses of PANI-CMPs in this work, involves the formation of a secondary amino group from a bromo group and a primary amino group. Therefore, the three main changes to look for in FT-IR spectra of prepared materials compared to their starting monomers are the disappearance of bromo group signals, the disappearance of primary amino group signals, and the emergence of secondary amino group signals.

*Table 4-8 Expected ranges and positions for FT-IR transmission peaks of functional groups in PANI-CMPs and their monomers. Vibrations related to the functional groups are shown as **bold**, and their corresponding peaks are shown in the last two columns.*

Wavenumber Range (cm^{-1})	**Contributing Vibration**	**Approximated Key Vibration Peak (cm^{-1})**	
		Measured Spectra	**Uncorrected Calculated Spectra**
3500-3100	**N–H stretching**	3400, 3300, and 3200	3650, 3550, 3230, and 3180
3100-2900	C–H stretching		
1700-1100	C–C/C–N in-plane stretching		
1100-950	**C–Br stretching**	1050 and 1000	1090 and 1020
900-400	**NH_2 wagging** C–C/C–N out-of-plane stretching	600 and 500	650

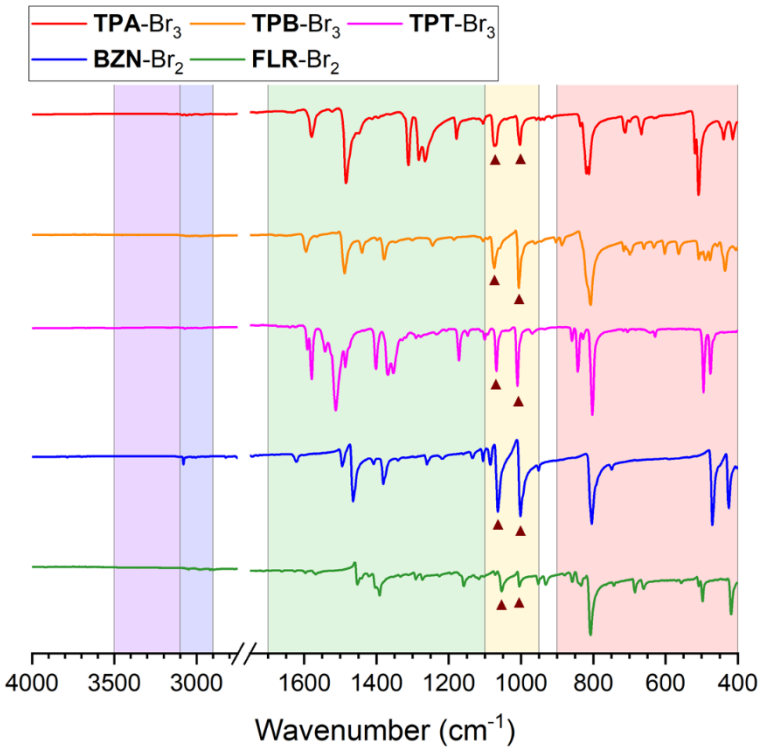

*Figure 4-3 FT-IR transmission spectra of **brominated** core and linker monomers. Reddish brown triangles mark the positions of C–Br stretching absorption peaks.*

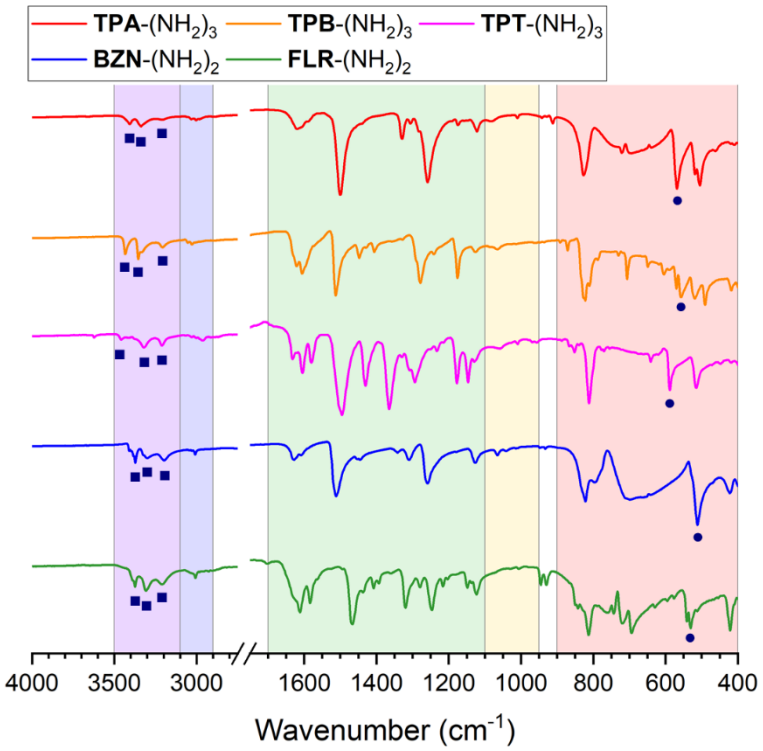

*Figure 4-4 FT-IR transmission spectra of **aminated** core and linker monomers. Blue squares mark the positions of N–H stretching absorption peaks, and blue circles denote the positions of NH_2 wagging absorption peaks.*

FT-IR transmission spectra of core and linker monomers used in this study are shown in Figure 4-3 for brominated monomers and Figure 4-4 for aminated monomers. Overall, these spectra can be divided into five regions, which are also related to types of vibrations contributing to the absorptions (as listed in Table 4-8). The first (3500 to 3100 cm^{-1}) and the fourth (1100 to 950 cm^{-1}) are directly related to the amino and bromo functional groups, which will be discussed in detail later. The second group (3100 to 2900 cm^{-1}) contains C–H bond stretching peaks. Theoretically, both **FLR** monomers should produce two groups of peaks, for aromatic and aliphatic C–H bonds. However, the signals in all cases are too weak to be useful.

Absorption peaks in the third (1700 to 1100 cm^{-1}) and the fifth (900 to 400 cm^{-1}) are more complicated than those in the three aforementioned groups. Both regions are dominated by stretching modes of C–C or C–N bonds in the aromatic rings, with in-plane stretching modes being in the third region and out-of-plane stretching modes being in the fifth region. Peaks of the fifth region are generally considered as complicated and not much useful for structure elucidation, while peaks of the third region are more useful in that regard. To aid the identifications of vibrational modes contributing to the absorptions in the third and the fourth regions, DFT calculations (B3LYP-D3(BJ)/6-31G(d)/1,4-dioxane PCM solvation model) have been applied. Detailed comparisons can be found in Appendix B.

For brominated monomers, the peaks related to C–Br bonds can be found around 1050 and 1000 cm^{-1} (the fourth region), as shown in Figure 4-3 and Table 4-8. These peaks, in fact, emerge from the coupling between the in-plane vibrations of aromatic ring and their substituents (the third region). The peak at 1050 cm^{-1} corresponds to the vibrational mode ν_{18}, while the peak at 1000 cm^{-1} corresponds to the vibrational mode ν_{12} (see Appendix B.1). Both vibrational modes in **BZN**-Br_2 are illustrated as examples in Figure 4-5. These peaks are found only in brominated monomers and are almost undetectable in their aminated counterparts (Figure 4-4). The main difference is that bromine atoms are around six times as heavy as carbon or nitrogen atoms. The

significantly greater mass of bromine atoms means that the vibrations involving C–Br bonds occur in the way that bromine atoms remain almost static, while carbon atoms displace from their original positions further than when with lighter substituents. Some modes, such as the aforementioned ν_{18} and ν_{12} modes, cause significant changes in dipole moments and therefore become IR active. However, for C–NH_2 counterparts, because these amino groups are located at the *para* position against either another amino group (in **BZN**-$(NH_2)_2$) or carbon atoms in aryl fragments (in other monomers), the same modes cause smaller changes in total dipole moments.

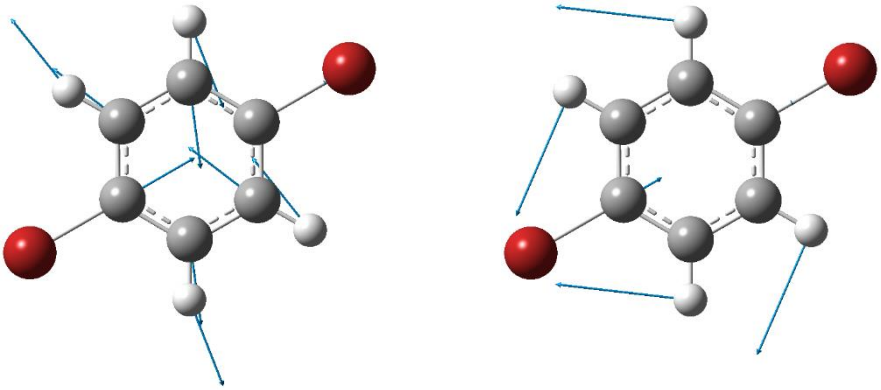

*Figure 4-5 Displacement vectors of atoms involved in vibrational mode ν_{12} (left) and ν_{18} (right) of **BZN**-Br_2, depicted using Gaussview 6.1.1*[16]

While vibrational peaks originating from C–NH_2 are insignificant, some peaks involving N–H bonds themselves in the amino group can be useful. Two main groups of peaks in this case are N–H stretching peaks (between 3400 and 3100 cm^{-1}, the first region in Figure 4-4) and NH_2 wagging (appear between 700 and 500 cm^{-1}, the fifth region). While it is also possible to observe other vibrational modes of NH_2 groups such as rocking and scissoring, these modes appear in the similar region as the out-of-plane bond stretching peaks of aromatic skeletal moieties (the third region). Such similarities in energy cause two problems for the usage of these peaks for identifications. Firstly, these vibrational modes can couple with skeletal vibrational modes of similar wavenumbers or energies, creating newer and more complicated vibrational modes. Secondly, peaks from these vibrational modes themselves can be obscured by the abundant existing peaks of skeletal vibrational modes. Therefore, it is less practical to rely on these rocking and scissoring peaks, and stretching and wagging peaks alone should be suitable for identification.

It should be noted, however, that DFT calculations of vibrational spectra usually have some systematic errors. These errors can be fixed easily by multiplying the wavenumbers obtained from calculations with a scaling factor. There are several published databases for scaling factors for corrections of vibrational spectra based on combinations of functionals and basis sets.[17-21] However, the scaling factor for the PANI-CMPs is determined from comparisons between measured and calculated spectra of monomers, and it is determined to be 0.9650. Details about the scaling factor can be found in Section B.2 in the Appendix.

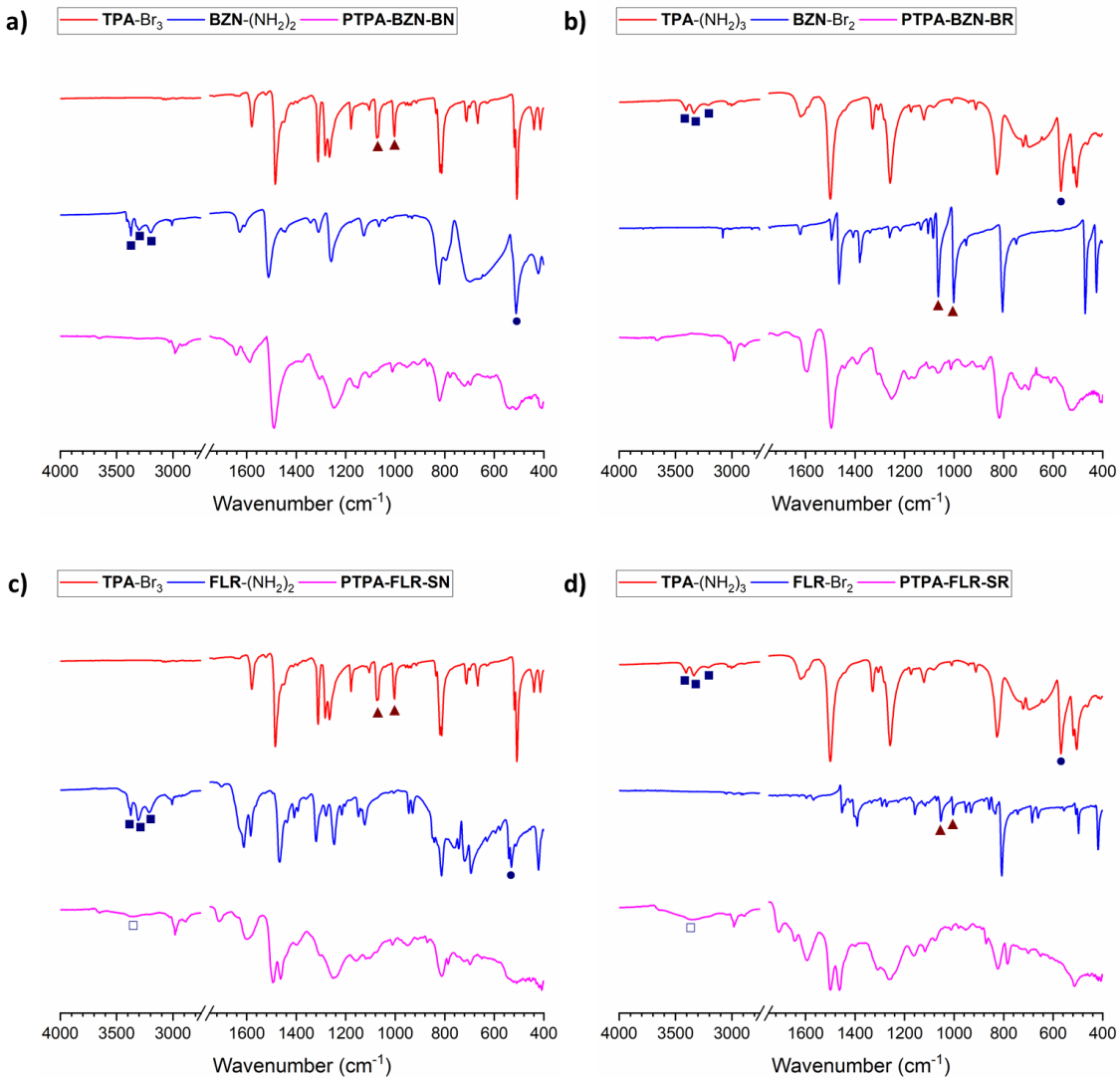

*Figure 4-6 Measured FT-IR transmission spectra of a) **PTPA-BZN-BN**, b) **PTPA-BZN-BR**, c) **PTPA-FLR-SN**, and d) **PTPA-FLR-SR** compared to measured spectra of corresponding monomers. Reddish brown triangles mark the positions of C–Br stretching absorption peaks. Blue squares mark the positions of N–H stretching absorption peaks (filled for NH_2, empty for NH), and blue circles denote the positions of NH_2 wagging absorption peaks.*

FT-IR transmission spectra of PANI-CMPs synthesised in this study are shown in Figure 4-6 (**PTPA** series), Figure 4-7 (**PTPB** series), and Figure 4-8 (**PTPT** series). It should be noted that while FT-IR spectra of materials synthesised from stoichiometric ratio of bromo and amino groups should give the fairer comparison between the two pathways due to smallest differences in amounts of chemical species involved (see Table 4-5), it is not applicable for **PTPA-BZN** due to the failure to produce enough polymers as explained. Therefore, **PTPA-BZN-BN** and **PTPA-BZN-BR** synthesised via the bromo-excess pathways, the only successful polymerisations, are chosen for the comparison instead.

Regardless of core-linker combinations, the same trends are observed across all materials. Absorption spectra exhibit the suppressions of C–Br stretching signals (triangles) as well as NH_2 wagging signals (circles), while the stretching N–H signals (squares) have become less intense as well. The newly formed secondary amino groups do not produce vibrational signals as strong as the parent primary amino groups. In some cases, the signals are totally indistinguishable from the background, see Figure 4-6a, for example. These changes in vibrational spectra imply the

successful formation of secondary amino groups as a result of Buchwald-Hartwig coupling reactions.

While functional group signals imply the successful formation of secondary amino groups as a result of BH coupling reactions, the skeletal vibrational signals (between 1700 and 1100 cm^{-1}) have become more obscured and less reliable for structure elucidations. In all twelve cases, skeletal peaks are broader than those of monomers, and neighbouring peaks are overlapping and become less distinctive. These broadenings are possibly because PANI-CMPs consist of different moieties with slightly different structures, unlike monomers in which all components are the same structurally. Those slightly different structures may have different vibrational modes depending on components, and even with the same (or common) vibrational modes, moieties with slightly different structures still vibrate at slightly different frequencies. These slightly different frequencies have contributed to peak broadenings as seen in FT-IR spectra of all twelve PANI-CMPs.

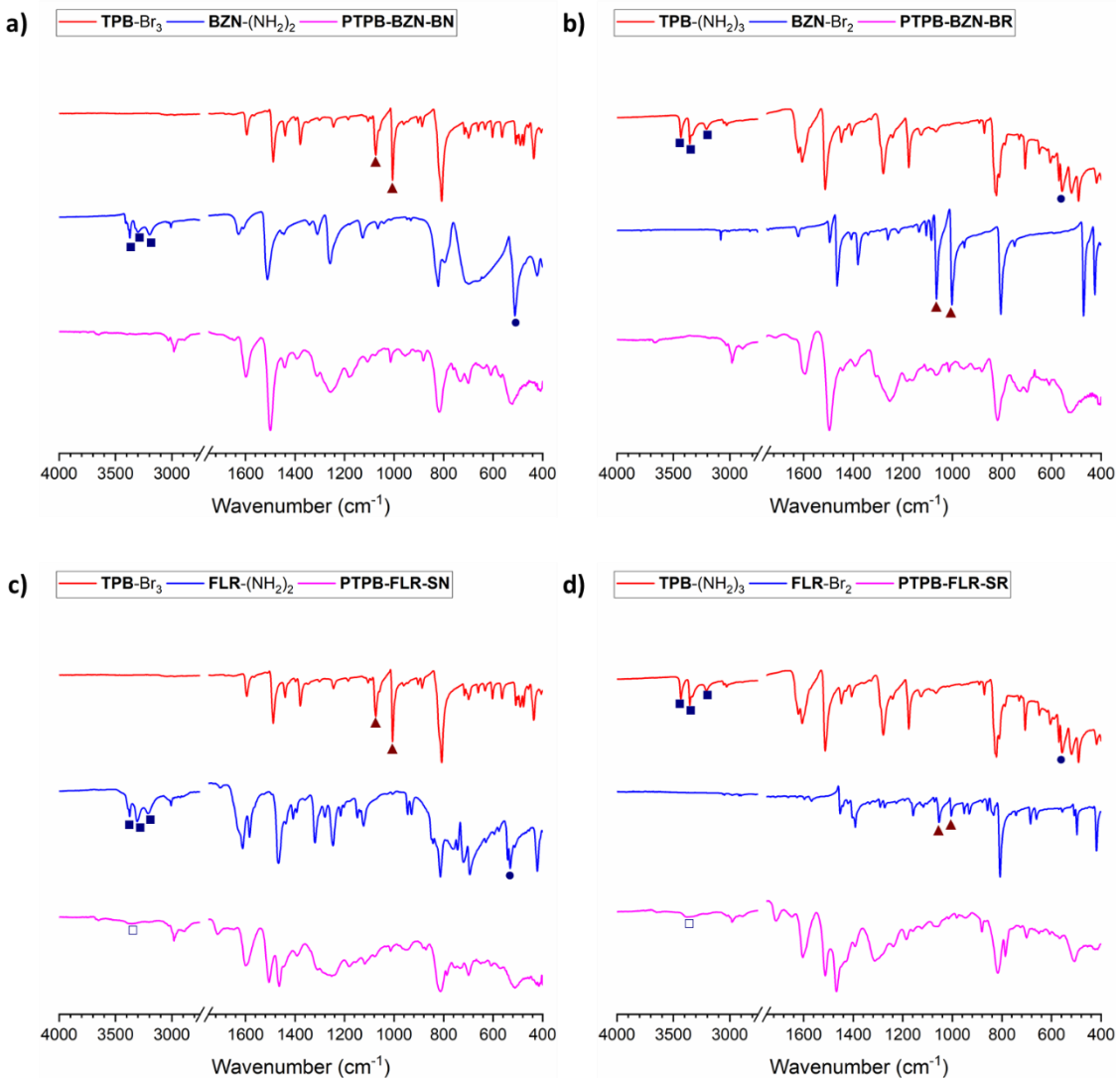

*Figure 4-7 Measured FT-IR transmission spectra of a) **PTPB-BZN-SN**, b) **PTPB-BZN-SR**, c) **PTPB-FLR-SN**, and d) **PTPB-FLR-SR** compared to measured spectra of corresponding monomers. Reddish brown triangles mark the positions of C–Br stretching absorption peaks. Blue squares mark the positions of N–H stretching absorption peaks (filled for NH_2, empty for NH), and blue circles denote the positions of NH_2 wagging absorption peaks.*

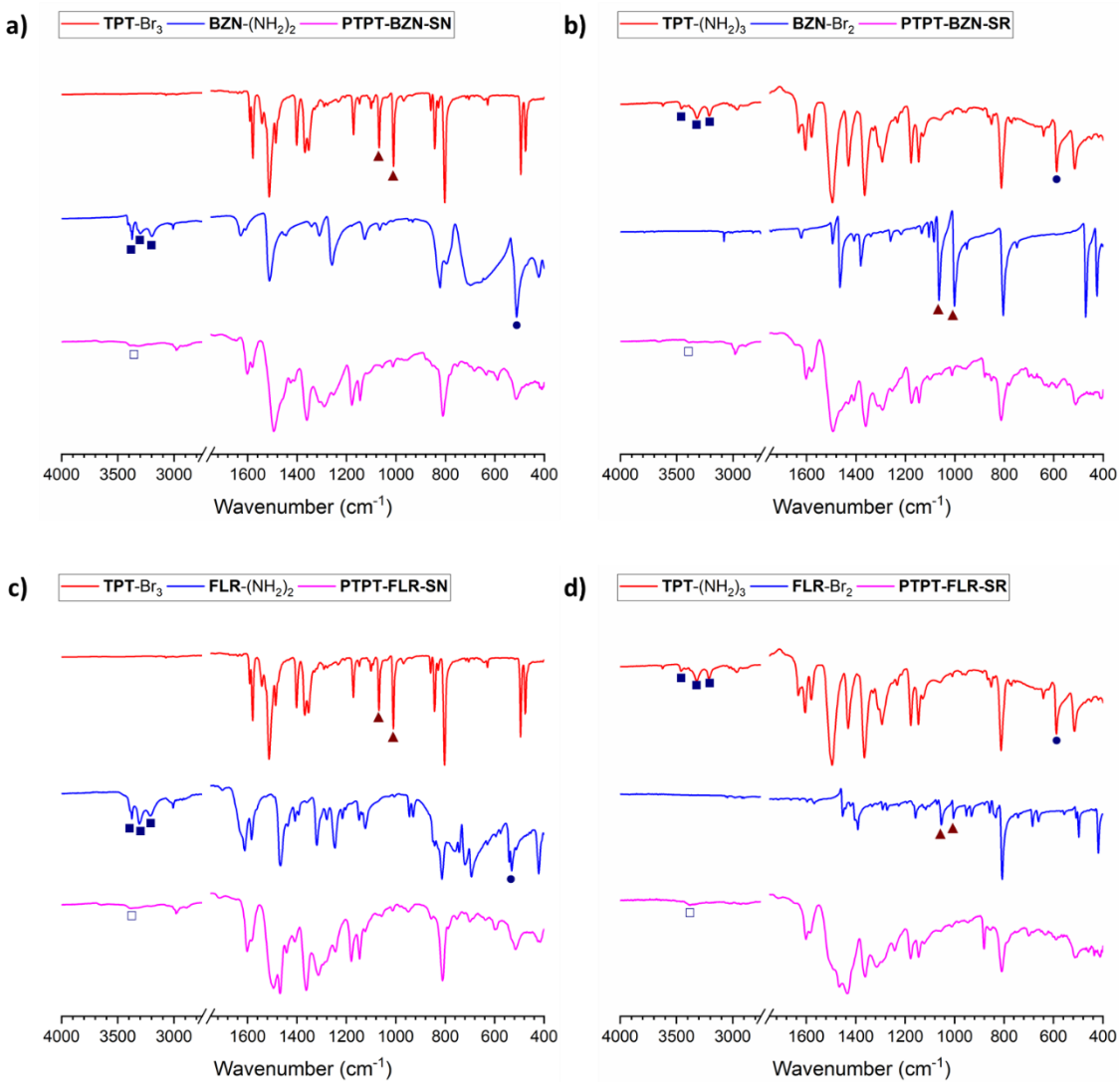

*Figure 4-8 Measured FT-IR transmission spectra of a) **PTPT-BZN-SN**, b) **PTPT-BZN-SR**, c) **PTPT-FLR-SN**, and d) **PTPT-FLR-SR** compared to measured spectra of corresponding monomers. Reddish brown triangles mark the positions of C–Br stretching absorption peaks. Blue squares mark the positions of N–H stretching absorption peaks (filled for NH_2, empty for NH), and blue circles denote the positions of NH_2 wagging absorption peaks.*

Overall, FT-IR spectroscopy can be useful to determine whether coupling reactions have taken place successfully, which have been confirmed for all core-linker combinations and both functionality pathways. However, while the combination of theoretical and experimental studies can identify the skeletal vibrational modes of monomers with satisfactorily agreements, it cannot be translated towards the studies of PANI-CMPs due to more complicated spectra. These complications are results from polymers being mixtures of components with slightly different vibrational frequencies.

4.5 Porosity and Morphology Analyses of PANI-CMPs

Several techniques have been chosen for the analysis of porosity and morphology PANI-CMPs. The main analyses used for materials are adsorption isotherms of nitrogen and CO_2, while selected materials are subjected for SEM imaging and powder X-ray diffraction analysis.

4.5.1 Nitrogen Adsorption Isotherm Analyses at 77 K

As explained in Chapter 1, determination of nitrogen adsorption isotherms at 77 K is the standard technique for the analysis of surface areas, microporosities, and pore size distributions of porous materials. To limit the issues from different monomer unit ratios, only materials

prepared with stoichiometric ratios between amino and bromo groups will be discussed in this section.

Table 4-9 Porosity data of PANI-CMPs prepared from different monomers, approaches, and solubility tunings, obtained from nitrogen adsorption isotherm at 77 K. Grey rows refer to materials that failed to be obtained in suitable amounts for porosity determinations (> 50 mg). Isotherm types marked with a prime (') mark mean that the isotherm plot slightly differ from the IUPAC classifications.

Materials	BET Surface Area ($m^2 \cdot g^{-1}$)	Isotherm Type	Pore Volume ($mL \cdot g^{-1}$)	Microporosity Grading
BZN-linked materials				
PTPA-BZN-SN				
PTPA-BZN-SNx				
PTPA-BZN-SR				
PTPA-BZN-SRx				
PTPB-BZN-SN				
PTPB-BZN-SNx				
PTPB-BZN-SR				
PTPB-BZN-SRx				
PTPT-BZN-SN	274.4	VI	0.238	Yes
PTPT-BZN-SNx	143.3	III'	0.223	No
PTPT-BZN-SR	47.8	III	0.106	No
PTPT-BZN-SRx	24.1	II	0.029	Yes
FLR-linked materials				
PTPA-FLR-SN	570.9	I'	0.308	Yes
PTPA-FLR-SNx	340.7	II	0.241	Yes
PTPA-FLR-SR	396.4	II	0.344	Yes
PTPA-FLR-SRx				
PTPB-FLR-SN	721.0	I'	0.435	Yes
PTPB-FLR-SNx	747.1	I'	0.412	Yes
PTPB-FLR-SR	12.7	VI	0.017	Yes
PTPB-FLR-SRx	26.1	III	0.039	No
PTPT-FLR-SN	20.0	II	0.030	Yes
PTPT-FLR-SNx	324.5	II	0.228	Yes
PTPT-FLR-SR	19.7	II'	0.034	Yes
PTPT-FLR-SRx	57.8	II	0.090	Yes

Table 4-9 lists BET surface areas, isotherm types, and pore volumes of materials obtained from nitrogen adsorption isotherm analysis at 77 K. Overall, there is no trend or general conclusion that can be clearly observed from these data in terms of structure-property relationships. However, while this set of experiments fails to generate general conclusions, there are several points that are worth discussing.

Regarding the solubility tuning, it is clearly shown that the on-and-off basis of sodium bromide addition is not the appropriate way to study. Of the seven comparable pairs synthesised with and without added sodium bromide, two pairs produced materials with high porosity in both conditions, while three pairs yielded materials with low porosity in both conditions. The remaining two pairs showed the opposite trends; **PTPT-BZN** synthesised with added sodium bromide possessed higher porosity, while the opposite is true for **PTPT-FLR**. In the first publication of the BXJ method,[1] the relationships between amounts of salt (sodium sulfate) added and the resulting specific surface areas and the uptakes of CO_2 are not linear, and both relationships peak at the different amounts of sodium sulfate added. Therefore, more

experiments with varied amounts of salt added should be performed to understand the relationship between solubility tuning and properties of materials obtained better.

The effects of normal and reversed approaches, on the other hand, can be more clearly described. In all seven comparable cases, none had produced materials with the same properties, despite the fact that the end products are essentially the same after all functional groups reacted (that is, where the polymerisation proceeded successfully to yield microporous materials). As explained, the gelation process is the crucial step for the formation of microporous networks. To form a gel, the distance between the gelator and the matrix in the solubility parameter space has to be in the appropriate range between solutions and suspensions.[15] Polymerisation reactions for the formation of CMPs can be viewed as a special case of gelation because both gelator and matrix are dynamic. The gelator in these cases is the growing oligomers, and the matrix in these cases is the other non-oligomer components in the reaction mixtures, including solvents, monomers, reagents, and even salts added for solubility tuning. The solubility space distances will change over time as oligomer units grow, and gels or suspensions may be formed if the distances have become far enough. Even if the end products are the same, coming from different approaches, one approach might end up unable to form a gel, which means that a porous network might not be achieved.

Some materials fall into the low surface area categories because their synthesis processes are not optimum and cannot sustain the formation of gels. It is probably impossible to draw any SPR-related conclusions from these data because the effects from failures to form gels are not negligible. To observe the SPR clearly, materials from each core and linker combination should be synthesised at optimised conditions, where solubility parameters of the synthesis media are tuned to allow a sol and a gel to form. This issue can also be observed in the discussion regarding CO_2 adsorption in Section 4.6.

Another issue in regarding surface areas of these materials is that these data were only recorded once for each material. There are several publications discussing the validity and reproducibility of isotherm analysis methods and surface area calculation methods.[22, 23] Besides, results from the analyses of some materials either have poor fitting or have low value of the constant *c* (see Table D-1 in Appendix D.1.2), with the most severe case being **PTPT-BZN-SNx** (R^2 = 0.599, *c* = 1.655). Therefore, repeated measurements of either the same material or materials of different batches with the same methods are still required, which could solve the reproducibility problem and either solve the poor fitting problem or confirm that the BET model is not appropriate for that particular material.

4.5.2 Electron Microscope Imaging of Selected PANI-CMPs

PTPB-FLR-SN and **PTPB-FLR-SR** were subjected to scanning electron microscope (SEM) imaging due to their difference in BET surface area (721.0 $m^2 \cdot g^{-1}$ for the **SN** polymer compared to 12.7 $m^2 \cdot g^{-1}$ for the **SR** polymer) despite being from the same monomer units. These images are shown in Figure 4-9.

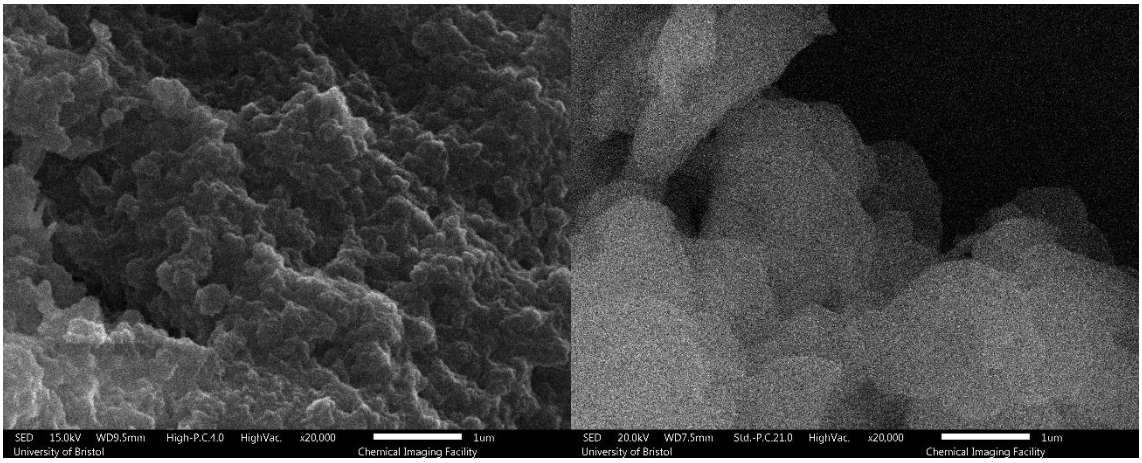

*Figure 4-9 SEM images of **PTPB-FLR-SN** (left, BET surface areas 721.0 $m^2 \cdot g^{-1}$) and **PTPB-FLR-SR** (right, BET surface areas 12.7 $m^2 \cdot g^{-1}$). Scale bars = 1 μm.*

There are clear differences in morphologies of **PTPB-FLR** synthesised from the **SN** and **SR** pathways. Structures of **PTPB-FLR-SN**, with higher levels of microporosity, contain smaller grains and more cavities compared to those of **PTPB-FLR-SR**, which presented a generally smooth surface.

4.5.3 Powder X-Ray Diffraction (XRD) of Selected PANI-CMPs

The same two materials from Section 4.5.2 have also been subjected to the powder XRD analysis to determine crystallinity or amorphousness, with the results shown in Figure 4-10. The results are plotted as graphs of intensities against the doubles of incident angles (2θ) obtained from the instrument. Crystalline materials, regardless of whether being ionic or covalent, produce sharp peaks at certain 2θ values due to the diffractions caused by gaps of certain widths in the structures. Positions of these peaks are related to the distances (d) between atoms in the crystalline substructures in accordance with the Bragg's equation, shown in Equation 4-1. (Please note that θ is used in the Bragg's equation, but the values obtained from the instrument and used in the result plots are 2θ.)

$$n\lambda = 2d \sin \theta \qquad 4\text{-}1$$

The n in Equation 4-1 is the diffraction order, which is generally assumed to be one for the first order, while the λ is the wavelength of the X-ray used to analyse materials, which is 1.5406 Å for the Cu Kα source. Unlike crystalline materials, amorphous materials only produce broad peaks because the distances d between atoms are less certain. In this thesis, significant peak positions will be reported along with their corresponding distances. Also, due to the significant fluctuations, peak positions will be rounded to the nearest half degrees (.0° or .5°), which means that the distances have to be rounded to the nearest tenths of an Angstrom.

For both materials, there are large peaks situated at approximately 12.0°. However, the large broad peaks are actually the results of the sample holder itself rather than the materials. To confirm, two separate analyses have been performed on an empty sample holder and a sample holder with Vaseline used for attaching samples onto the sample holder surfaces (Figure E-13). Indeed, in both instances, there are large peaks at the same position. Therefore, these 12.0° peaks will not be discussed further.

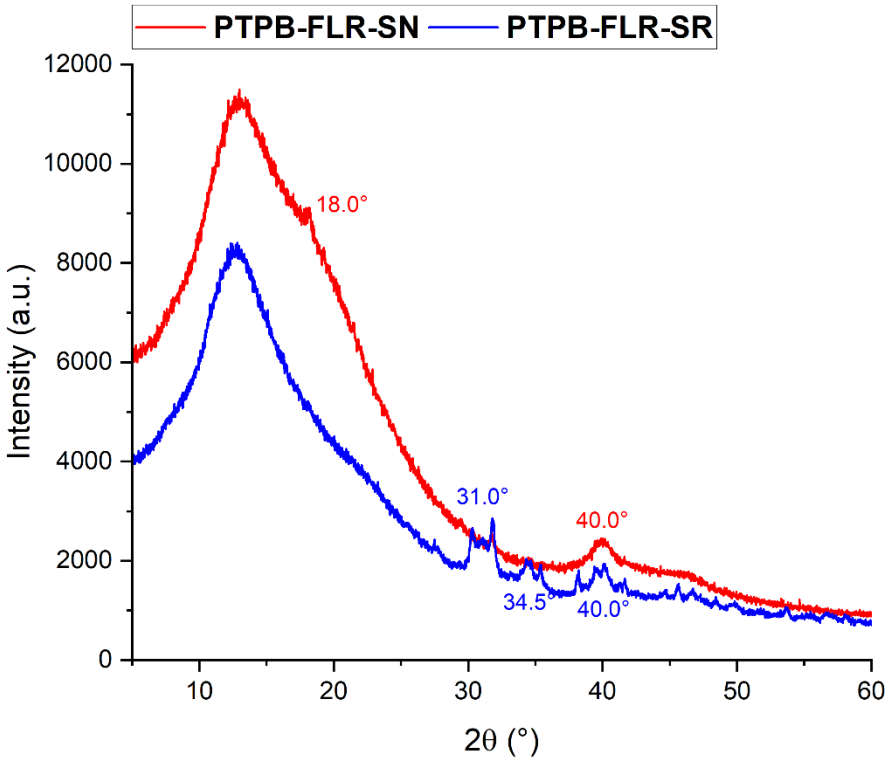

*Figure 4-10 XRD analysis results of **PTPB-FLR-SN** and **PTPB-FLR-SR***

For **PTPB-FLR-SN**, two small peaks are observed at 2θ values of 18.0° (4.9 Å) and 40.0° (2.3 Å). The peak at 18.0° is almost unnoticeable and possibly belongs to some impurities. Meanwhile, the peak at 40.0° might be from the material itself. However, for the **SR** counterpart, several peaks are observed from the 2θ values of 30° onwards. The relatively stronger peaks among these can be grouped into three groups, 31.0° (2.9 Å), 34.5° (2.6 Å), and 40.0° (2.3 Å). Because these **PTPB-FLR-SR** peaks are sharper than those of **PTPB-FLR-SN**, it is plausible to suggest that these sharp peaks, especially around 31.0°, come from the π-π stacking within the polymer structure. The stacking might also explain the low BET surface area (12.7 $m^2 \cdot g^{-1}$) compared to its **SN** counterpart (721.0 $m^2 \cdot g^{-1}$). However, further experiments should be performed on other materials to either confirm or dispute this conclusion.

4.6 Carbon Dioxide Adsorption at Ambient Temperatures

Since CO_2 adsorption is one of potential applications of PANI-CMPs, CO_2 adsorption isotherm analyses have been performed on these materials. Adsorption analyses were performed at two different temperatures, 273 and 298 K, respectively, to study the thermodynamics of CO_2 adsorption onto PANI-CMP surfaces.

4.6.1 CO_2 Uptake Performances at 273 K of PANI-CMPs

Table 4-10 lists data obtained from the CO_2 isotherm analyses at 273 K, namely the uptake of CO_2 at relative pressure of 0.95, surface areas accessible by CO_2, and pore volumes accessible by CO_2. Surface areas and pore volumes of materials as analysed from CO_2 adsorption are different from those analysed from N_2 adsorption due to many factors including different kinetic diameters and adsorption isotherm behaviours as relative pressures increase and decrease. These CO_2 surface area values are from Monte Carlo analyses of adsorption isotherm data of CO_2 adsorption at 273 K.

*Table 4-10 Porosity data of PANI-CMPs prepared from different monomers, approaches, and solubility tunings, obtained from carbon dioxide adsorption isotherm at **273 K**.*

Materials	CO_2 Uptake at $p/p°$ 0.95		CO_2 Surface Area ($m^2 \cdot g^{-1}$)	Pore Volume ($mL \cdot g^{-1}$)
	wt%	$mmol \cdot g^{-1}$		
BZN-linked materials				
PTPA-BZN-SN				
PTPA-BZN-SNx				
PTPA-BZN-SR				
PTPA-BZN-SRx				
PTPB-BZN-SN				
PTPB-BZN-SNx				
PTPB-BZN-SR				
PTPB-BZN-SRx				
PTPT-BZN-SN	10.14	2.33	607.8	0.227
PTPT-BZN-SNx	7.53	1.74	395.6	0.130
PTPT-BZN-SR	3.23	0.74	181.0	0.064
PTPT-BZN-SRx	2.91	0.67	131.8	0.039
FLR-linked materials				
PTPA-FLR-SN	7.55	1.74	392.8	0.132
PTPA-FLR-SNx	7.44	1.71	392.6	0.129
PTPA-FLR-SR	11.90	2.74	627.8	0.223
PTPA-FLR-SRx				
PTPB-FLR-SN	9.50	2.19	484.6	0.155
PTPB-FLR-SNx	7.83	1.80	427.5	0.148
PTPB-FLR-SR	5.55	1.28	293.0	0.093
PTPB-FLR-SRx	4.99	1.15	266.4	0.086
PTPT-FLR-SN	6.65	1.53	338.0	0.105
PTPT-FLR-SNx	6.82	1.57	354.6	0.113
PTPT-FLR-SR	3.41	0.79	186.2	0.063
PTPT-FLR-SRx	4.41	1.02	237.5	0.079

In terms of CO_2 uptake, three materials have higher amounts, namely **PTPA-FLR-SR** (11.90 wt%; 2.74 $mmol \cdot g^{-1}$), **PTPT-BZN-SN** (10.14 wt%; 2.33 $mmol \cdot g^{-1}$), and **PTPB-FLR-SN** (9.50 wt%; 2.19 $mmol \cdot g^{-1}$), compared to the rest of materials (2.91-7.83 wt%; 0.67-1.80 $mmol \cdot g^{-1}$). For a comparison with the previously published work,[1] the uptakes of **PTPA-BZN-BN** materials that were synthesised in THF and tuned with different sodium halide salts are 13.42-15.84 wt% (3.05-3.60 $mmol \cdot g^{-1}$), compared to 7.66-15.32 wt% (1.74-3.48 $mmol \cdot g^{-1}$) for materials tuned with other salts and only 3.08 wt% (0.70 $mmol \cdot g^{-1}$) for the untuned (control) material. While these are not direct comparisons, these data can provide some details regarding performances of PANI-CMPs. The top three materials, namely **PTPA-FLR-SR**, **PTPT-BZN-SN**, and **PTPB-FLR-SN**, might be comparable to **PTPA-BZN-BN** tuned with other salts in the published work. However, their performance is still lacking compared with other CMPs such as **F_{12}CTF-3** (29.0 wt%; 6.58 $mmol \cdot g^{-1}$),[24] **3D-CON** (26.7 wt%; 6.07 $mmol \cdot g^{-1}$),[25] and **P-PCz-3** (25.3 wt%; 5.76 $mmol \cdot g^{-1}$),[26] with uptakes of at least 25 wt%. It is also worth noting that several other porous materials have been reported to have CO_2 adsorptions higher than 30 wt%, such as **ZJNU-40** (33 wt%; 7.6 $mmol \cdot g^{-1}$),[27] **CPM-33b** (34 wt%; 7.8 $mmol \cdot g^{-1}$),[28] and **Mg-MOF-74(S)** (35.0 wt%; 7.95 $mmol \cdot g^{-1}$ at 298 K).[29]

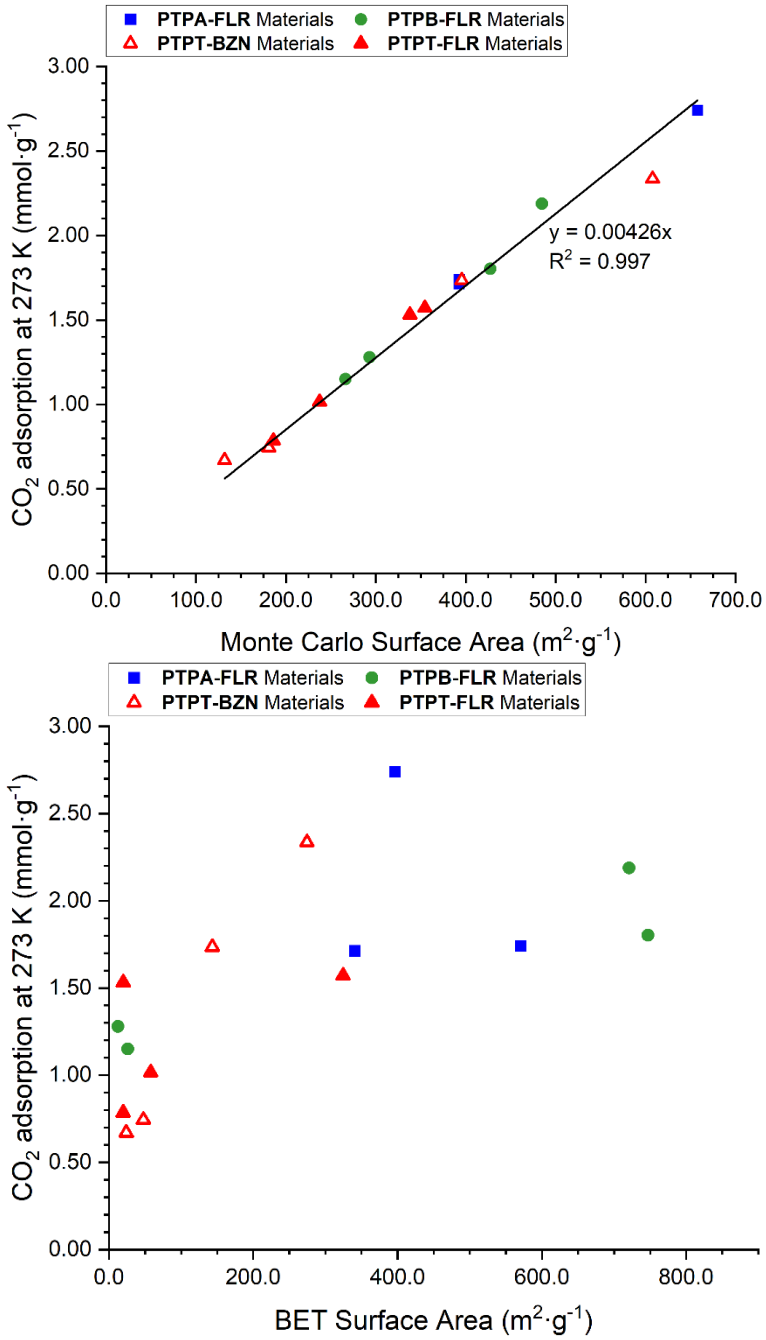

Figure 4-11 Relationships between surface areas, from Monte Carlo analyses of CO_2 adsorption isotherm at 273 K (top) and from BET analyses of N_2 adsorption isotherm at 77 K (bottom), and CO_2 uptake at 273 K of PANI-CMPs

These top three materials also have the highest CO_2 Monte Carlo surface areas, 627.8 $m^2 \cdot g^{-1}$ in **PTPA-FLR-SR**, 607.8 $m^2 \cdot g^{-1}$ in **PTPT-BZN-SN**, and 484.6 $m^2 \cdot g^{-1}$ for **PTPB-FLR-SN**. The material with fourth highest CO_2 uptake, **PTPB-FLR-SNx** (7.83 wt%; 1.80 $mmol \cdot g^{-1}$), is also the next highest in terms of CO_2 surface area with the surface area of 427.5 $m^2 \cdot g^{-1}$. In fact, there is a linear relationship between the Monte Carlo CO_2 surface areas and the uptake of CO_2, which is illustrated in Figure 4-11. However, the linear relationship is not observed in BET surface areas from nitrogen adsorption isotherm at 77 K.

It is arguable that BET surface area analysis is a popular method used for the analyses of porous materials, and the use of the same method for analyses leads to fair comparisons between materials of the same or different groups. However, the stronger correlation between surface

areas from Monte Carlo analyses of CO_2 isotherm data and CO_2 uptake at 273 K compared to those from BET analyses of nitrogen isotherm data has shown that BET surface areas alone are not a good indicator whether materials can absorb CO_2 or other adsorbates. Disagreements between trends of BET surface areas and trends of CO_2 uptakes in porous materials, including PANI-CMPs, have also been observed and discussed in many publications.[1, 7, 10, 30] Therefore, for porous materials proposed for adsorptions, analysing surface areas with the same gas as the intended gas (CO_2 analyses for CO_2 adsorptive materials, for example) may be more appropriate.

While there is no overall observable trend between BET surface areas and CO_2 uptakes, materials can still be divided into two groups by surface areas, above and below 100 $m^2 \cdot g^{-1}$. Materials with surface areas lower than 100 $m^2 \cdot g^{-1}$ clearly have lower CO_2 uptakes (2.91-6.65 wt%; 0.67-1.53 $mmol \cdot g^{-1}$) than those with higher surface areas (6.82-11.90 wt%; 1.57-2.74 $mmol \cdot g^{-1}$). These data mean that having high surface areas is a necessary condition for high uptakes of CO_2 although it is not a sufficient condition for high uptake on its own. Low BET surface areas can hinder CO_2 adsorption simply because there are limited surface areas for CO_2 molecules to interact with. Once the hindrance from low surface areas has been overcome, the interactions between material surfaces and CO_2 can then be explored.

Table 4-11 Summary of CO_2 uptake of PANI-CMPs synthesised from different monomer units, pathways, and solubility tuning

		With Added NaBr			Without Added NaBr		
		TPA	**TPB**	**TPT**	**TPA**	**TPB**	**TPT**
BZN	Normal			●			○
	Reversed			×			×
FLR	Normal	○	●	×	○	○	○
	Reversed	●	×	×		×	×
●	High CO_2 uptakes			×	Low CO_2 uptakes		
○	Moderate CO_2 uptakes				Yield only small amount		

Table 4-11 maps the CO_2 uptakes of PANI-CMPs based on monomer units, functionality pathways, and solubility tuning by adding sodium bromide. There is no clear trend regarding the effects from these factors because, as discussed in the previous section, some of these materials were not formed properly with the optimised solubility tuning to ensure gelation of reaction mixtures. These materials then have low surface areas due to the lack of gelation, which is crucial for the formation of highly crosslinked polymer structures. Such low surface areas can hinder the uptake of CO_2 as shown in Figure 4-11. Once the issue of poor surface areas due to mismatched solubility parameters has been overcome, a fair comparison can then be made.

To summarise, **PTPA-FLR-SR**, **PTPT-BZN-SN**, and **PTPB-FLR-SN** have the highest CO_2 uptakes at 273 K among the synthesised PANI-CMPs in this work. While their performances are comparable to that of the previously published PANI-CMPs, their performances still lag far behind top performers in the field of CO_2 adsorbents. Their CO_2 uptake performances have been found to correlate with surface areas accessible to CO_2 based on Monte Carlo analyses of the adsorption isotherms of CO_2 itself rather than the BET surface areas analysed from nitrogen adsorption isotherms. However, having large surface areas is still a necessary condition for high CO_2 adsorption although there are more factors involved other than BET surface areas. Meanwhile, the effects from monomer units and synthesis pathways are still inconclusive because some materials have low surface areas, which hinder CO_2 adsorption, due to poorly tuned solubilities. To ensure a fair comparison, materials should be prepared in a matrix optimised by solubility parameters.

4.6.2 Thermodynamics of CO_2 Adsorptions of PANI-CMPs

To study the thermodynamics of CO_2 adsorptions, isotherm analyses were performed at 298 K, room temperature, in addition to those performed at 273 K mentioned in the previous section. Performing isotherm analyses at two or more different temperatures can be used to determine the thermodynamic parameters such as isosteric enthalpies of adsorption (ΔH_{ads}), which reflects the strength of binding between materials and CO_2 and, in turn, relates back to the chemical affinities between monomer units and CO_2. These chemical affinities will be explored in detail in the next chapter. Generally, since the adsorption process is exothermic, values of ΔH_{ads} will be negative, and uptake at higher temperatures will be less than uptake at lower temperatures.

Table 4-12 lists thermodynamics-related data from CO_2 isotherm adsorption analyses at 273 K and 298 K of PANI-CMPs. There is a linear relationship between the CO_2 uptakes at two temperatures, which are shown in Figure 4-12.

Calculations for the isosteric enthalpies of adsorption can be done in two different ways, namely using Clausius-Clapeyron equation and using virial analysis.[31] Both methods have been explained in detail in Chapter 1 and will not be discussed in detail here. The difference between the two approaches is in the fitting equations. The Clausius-Clapeyron approach, coupled with the Freundlich-Langmuir model of adsorption for determining pressures as a function of amounts adsorbed, fits data from two different temperatures separately and therefore yields two sets of parameters. Meanwhile, the virial analysis approach can fit data from both set together and yield only one set of parameters because the fitting equation for the virial analysis approach itself is also a function of temperatures, which can be set as constants for each data set, while that for the Freundlich-Langmuir model does not contain any terms related to temperatures. The differences between the two approaches will be discussed, with the data obtained from two analysis methods listed in the last two columns of Table 4-12. Comparative plots between the two methods can also be found in Section D.2.4 in the Appendix.

Table 4-12 CO_2 uptakes of PANI-CMPs at two different temperatures, 273 K and 298 K, the range of calculated ΔH_{ads} from Freundlich-Langmuir adsorption model and Clausius-Clapeyron equation, and the predicted isosteric enthalpies of adsorption at zero coverage ($\Delta H°_{ads}$).

Materials	CO_2 Uptake at $p/p°$ 0.95				Langmuir $-\Delta H_{ads}$ Range ($kJ \cdot mol^{-1}$)	Predicted Virial $\Delta H°_{ads}$ ($kJ \cdot mol^{-1}$)
	at 273 K		at 298 K			
	wt%	$mmol \cdot g^{-1}$	wt%	$mmol \cdot g^{-1}$		
BZN-linked materials						
PTPA-BZN-SN						
PTPA-BZN-SNx						
PTPA-BZN-SR						
PTPA-BZN-SRx						
PTPB-BZN-SN						
PTPB-BZN-SNx						
PTPB-BZN-SR						
PTPB-BZN-SRx						
PTPT-BZN-SN	10.14	2.33	6.89	1.59	19.4-27.3	-25.5
PTPT-BZN-SNx	7.53	1.74	5.91	1.36	15.5-20.9	-21.4
PTPT-BZN-SR	3.23	0.74	2.15	0.50	20.9-29.7	-31.0
PTPT-BZN-SRx	2.91	0.67	2.46	0.57	10.5-21.8	-24.4
FLR-linked materials						
PTPA-FLR-SN	7.55	1.74	4.84	1.12	22.8-27.9	-27.8
PTPA-FLR-SNx	7.44	1.71	5.07	1.17	22.7-28.0	-28.8
PTPA-FLR-SR	11.90	2.74	8.82	2.03	17.6-31.1	-34.6
PTPA-FLR-SRx						
PTPB-FLR-SN	9.50	2.19	7.35	1.69	17.2-20.7	-22.8
PTPB-FLR-SNx	7.83	1.80	5.41	1.25	19.8-23.1	-23.2
PTPB-FLR-SR	5.55	1.28	4.20	0.97	20.4-25.3	-26.3
PTPB-FLR-SRx	4.99	1.15	3.74	0.86	19.1-25.7	-27.1
PTPT-FLR-SN	6.65	1.53	4.65	1.07	19.4-27.3	-29.3
PTPT-FLR-SNx	6.82	1.57	4.95	1.14	21.1-27.2	-28.5
PTPT-FLR-SR	3.41	0.79	2.88	0.66	20.9-29.7	-25.9
PTPT-FLR-SRx	4.41	1.02	3.11	0.72	21.1-27.6	-28.4

One flaw of the Clausius-Clapeyron approach is that the fitted equations tend to deviate from the experimental data, especially at low pressures/uptakes.[31] These deviations consequently cause the calculated ΔH_{ads} to infinitely increase or decrease at pressure extremities, and therefore, it is not recommended for the prediction of ΔH_{ads} beyond the valid range where the adsorption ranges from two temperatures overlapped.[31] This issue can be seen in all comparisons between the $\Delta H_{ads}(n)$ plots in Section 7.7.4. In these plots, while the range of calculated ΔH_{ads} are similar from the two methods, deviations occur at low adsorption. However, for the virial analysis method, fitting is more reliable. This method, as a result, has been used for the determination of $\Delta H°_{ads}$ in various publications.

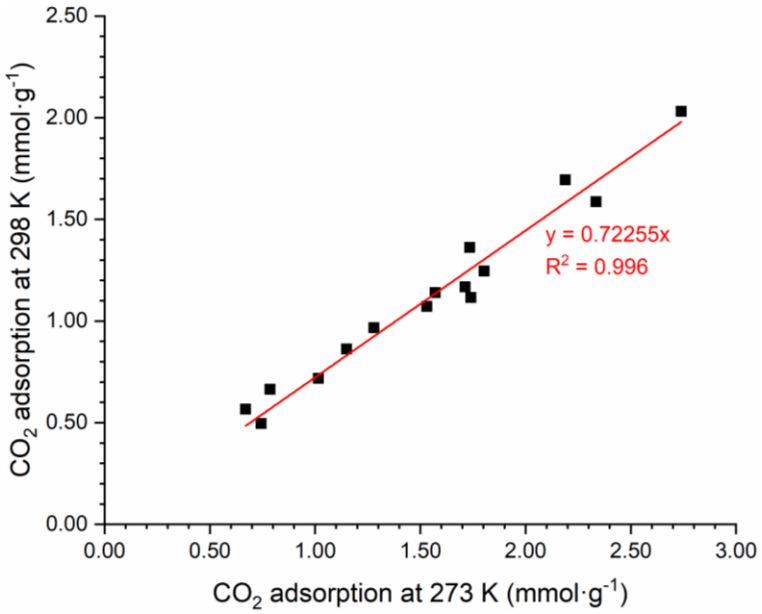

Figure 4-12 A linear plot between CO_2 adsorption at p/p° 0.95 at 273 K and 298 K of PANI-CMPs

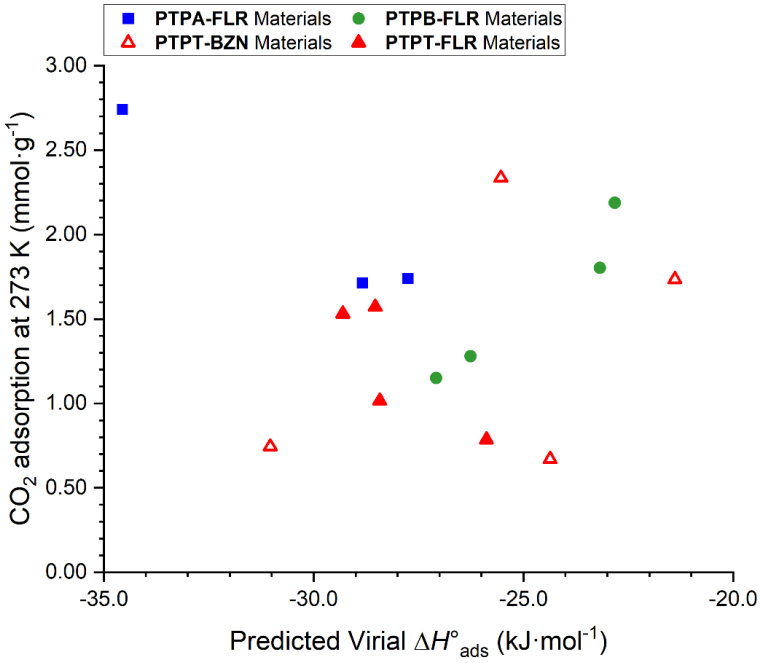

Figure 4-13 The relationship between the predicted $\Delta H°_{ads}$ from virial analyses and the uptakes of CO_2 of PANI-CMPs in this study

In terms of $\Delta H°_{ads}$, **PTPA-FLR-SR** with the highest CO_2 uptake also has the largest value of zero-coverage adsorption isosteric enthalpy (-34.0 kJ·mol^{-1}). However, the relationship between $\Delta H°_{ads}$ and the uptake of CO_2 can be complicated, as shown in Figure 4-13. **PTPT-BZN-SR**, with the second largest value of $\Delta H°_{ads}$ at -31.0 kJ·mol^{-1} but a BET surface area of only 47.8 m^2·g^{-1} (Table 4-9), has poor CO_2 uptake at only 0.74 mmol·g^{-1}. Meanwhile, the second and third best performing materials for CO_2 adsorption, **PTPT-BZN-SN** (-25.5 kJ·mol^{-1}) and **PTPB-FLR-SN** (-22.8 kJ·mol^{-1}), have fairly small $\Delta H°_{ads}$ among PANI-CMPs.

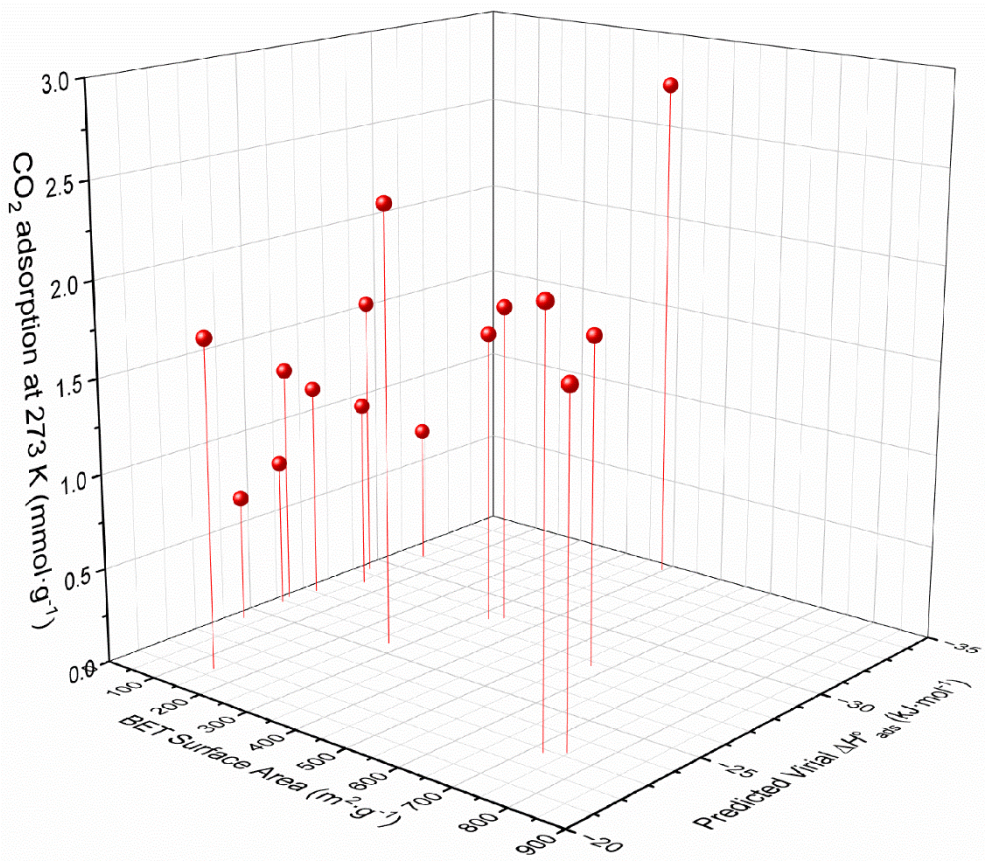

Figure 4-14 A three-dimensional plot for the relationships among BET surface areas, $\Delta H°_{ads}$, and the CO_2 uptakes at 273 K

$\Delta H°_{ads}$ can be a good indicator for strong or weak interactions between material surfaces and gas molecules. As illustrated in Figure 4-13 and Figure 4-14, however, these data on their own may not be able to predict or compare CO_2 uptake. These data might illustrate that some materials can be strong contenders for CO_2 adsorptions if their surface areas have been tuned.

4.7 Conclusions and Remarks

Several synthesis methods have been attempted to tune the properties of PANI-CMPs, including the use of high pressure. However, the most practical solution for property tuning appears to be solubility tuning using salts. Further synthesis attempts are needed, with amounts of salts adding to the reaction mixture being varied more systematically with gradients to optimise the surface areas.

Syntheses of PANI-CMPs from different functionality pathways have been compared. In many cases, syntheses with stoichiometric ratios between amino and bromo groups or with excess amino groups lead to premature terminations of polymerisation reactions, resulting in mixtures of soluble oligomers instead of microporous polymers, as intended. Such premature terminations are the result of the faster consumption of bromo groups compared to amino groups in stoichiometric and amino-excess syntheses. To ensure satisfactory yields of polymers, excess bromo groups should be used for Buchwald-Hartwig coupling reactions.

Structure-property relationships for the syntheses of PANI-CMPs cannot be clearly derived from this study yet. BET surface areas themselves can be affected by solubility parameters, which means that the surface areas can be optimised by varying amounts of salt for tuning. These are external factors that may override or obscure effects from changing the chemical properties of monomer unit themselves. In addition, there are also reproducibility and data fitting issues, which means that repeated experiments are still required. Meanwhile, for CO_2

adsorption, there are also other factors that could influence either positively or negatively, including BET surface areas and $\Delta H°_{ads}$, with the latter factor seen as a result from chemical properties of monomer units themselves. It is proven, nonetheless, that low BET surface areas can hinder the adsorption of CO_2 even in the materials with high $\Delta H°_{ads}$. At the moment, **PTPA-FLR-SR**, with BET surface area of 396.4 $m^2 \cdot g^{-1}$ and the highest $\Delta H°_{ads}$ of -34.0 $kJ \cdot mol^{-1}$, has the highest uptake of CO_2 at 11.90 wt% or 2.74 $mmol \cdot g^{-1}$. However, its performance is still lagging behind many published materials.

Overall, while there is no clear conclusion to be drawn from these investigations so far, data obtained from these experiments should lead towards a more systematic approach to understand relationships among different morphological and thermodynamic factors governing properties of PANI-CMPs.

4.8 References

1. J. Chen, W. Yan, E. J. Townsend, J. Feng, L. Pan, V. Del Angel Hernandez and C. F. J. Faul, *Angew. Chem. Int. Ed.*, 2019, **58**, 11715-11719.
2. U. H. F. Bunz, *Chem. Rev.*, 2000, **100**, 1605-1644.
3. J. Jiang, F. Su, A. Trewin, C. D. Wood, N. L. Campbell, H. Niu, C. Dickinson, A. Y. Ganin, M. J. Rosseinsky, Y. Z. Khimyak and A. I. Cooper, *Angew. Chem. Int. Ed.*, 2007, **46**, 8574-8578.
4. J. Jiang, F. Su, A. Trewin, C. D. Wood, N. L. Campbell, H. Niu, C. Dickinson, A. Y. Ganin, M. J. Rosseinsky, Y. Z. Khimyak and A. I. Cooper, *Angew. Chem. Int. Ed.*, 2008, **47**, 1167-1167.
5. J. Jiang, F. Su, A. Trewin, C. D. Wood, H. Niu, J. T. Jones, Y. Z. Khimyak and A. I. Cooper, *J. Am. Chem. Soc.*, 2008, **130**, 7710-7720.
6. S. Hayashi, Y. Togawa, S. I. Yamamoto, T. Koizumi, K. Nishi and A. Asano, *J. Polym. Sci., Part A: Polym. Chem.*, 2017, **55**, 3862-3867.
7. R. Dawson, D. J. Adams and A. I. Cooper, *Chem. Sci.*, 2011, **2**, 1173-1177.
8. Y. Liao, J. Weber and C. F. J. Faul, *Chem. Commun.*, 2014, **50**, 8002-8005.
9. Y. Liao, J. Weber, B. M. Mills, Z. Ren and C. F. J. Faul, *Macromolecules*, 2016, **49**, 6322-6333.
10. J. Chen, T. Qiu, W. Yan and C. F. J. Faul, *J. Mater. Chem. A*, 2020, **8**, 22657-22665.
11. L. Pan, Z. Liu, M. Tian, B. C. Schroeder, A. E. Aliev and C. F. J. Faul, *ACS Appl. Mater. Interfaces*, 2019, **11**, 48352-48362.
12. Z. Shao, P. Rannou, S. Sadki, N. Fey, D. M. Lindsay and C. F. J. Faul, *Chem. - Eur. J.*, 2011, **17**, 12512-12521.
13. D. S. Surry and S. L. Buchwald, *Chem. Sci.*, 2011, **2**, 27-50.
14. A. Laybourn, R. Dawson, R. Clowes, T. Hasell, A. I. Cooper, Y. Z. Khimyak and D. J. Adams, *Polym. Chem.*, 2014, **5**, 6325-6333.
15. K. K. Diehn, H. Oh, R. Hashemipour, R. G. Weiss and S. R. Raghavan, *Soft Matter*, 2014, **10**, 2632-2640.
16. R. D. Dennington, II, T. A. Keith and J. M. Millam, GaussView Version 6.1.1, Semichem Inc., Shawnee Mission, KS, 2019
17. G. Rauhut and P. Pulay, *J. Phys. Chem.*, 2002, **99**, 3093-3100.
18. A. P. Scott and L. Radom, *J. Phys. Chem.*, 1996, **100**, 16502-16513.
19. T. Sundius, *Vib. Spectrosc.*, 2002, **29**, 89-95.
20. J. P. Merrick, D. Moran and L. Radom, *J. Phys. Chem. A*, 2007, **111**, 11683-11700.
21. NIST Computational Chemistry Comparison and Benchmark Database, http://cccbdb.nist.gov/, (accessed March 2021).
22. J. Park, J. D. Howe and D. S. Sholl, *Chem. Mater.*, 2017, **29**, 10487-10495.
23. J. W. M. Osterrieth, J. Rampersad, D. Madden, N. Rampal, L. Skoric, B. Connolly, M. D. Allendorf, V. Stavila, J. L. Snider, R. Ameloot, J. Marreiros, C. Ania, D. Azevedo, E. Vilarrasa-Garcia, B. F. Santos, X.-H. Bu, Z. Chang, H. Bunzen, N. R. Champness, S. L. Griffin, B. Chen, R.-B. Lin, B. Coasne, S. Cohen, J. C. Moreton, Y. J. Colón, L. Chen, R. Clowes, F.-X. Coudert, Y. Cui, B. Hou, D. M. D'Alessandro, P. W. Doheny, M. Dincă, C. Sun, C. Doonan, M. T. Huxley, J. D. Evans, P. Falcaro, R. Ricco, O. Farha, K. B. Idrees, T. Islamoglu, P. Feng, H. Yang, R. S.

Forgan, D. Bara, S. Furukawa, E. Sanchez, J. Gascon, S. Telalović, S. K. Ghosh, S. Mukherjee, M. R. Hill, M. M. Sadiq, P. Horcajada, P. Salcedo-Abraira, K. Kaneko, R. Kukobat, J. Kenvin, S. Keskin, S. Kitagawa, K.-i. Otake, R. P. Lively, S. J. A. DeWitt, P. Llewellyn, B. V. Lotsch, S. T. Emmerling, A. M. Pütz, C. Martí-Gastaldo, N. M. Padial, J. García-Martínez, N. Linares, D. Maspoch, J. A. Suárez del Pino, P. Moghadam, R. Oktavian, R. E. Morris, P. S. Wheatley, J. Navarro, C. Petit, D. Danaci, M. J. Rosseinsky, A. P. Katsoulidis, M. Schröder, X. Han, S. Yang, C. Serre, G. Mouchaham, D. S. Sholl, R. Thyagarajan, D. Siderius, R. Q. Snurr, R. B. Goncalves, S. Telfer, S. J. Lee, V. P. Ting, J. L. Rowlandson, T. Uemura, T. Iiyuka, M. A. van der Veen, D. Rega, V. Van Speybroeck, S. M. J. Rogge, A. Lamaire, K. S. Walton, L. W. Bingel, S. Wuttke, J. Andreo, O. Yaghi, B. Zhang, C. T. Yavuz, T. S. Nguyen, F. Zamora, C. Montoro, H. Zhou, A. Kirchon and D. Fairen-Jimenez, *Adv. Mater.*, **n/a**, 2201502.

24. Z. Yang, S. Wang, Z. Zhang, W. Guo, K. Jie, M. I. Hashim, O. Š. Miljanić, D. e. Jiang, I. Popovs and S. Dai, *J. Mater. Chem. A*, 2019, **7**, 17277-17282.
25. J. Mahmood, S. J. Kim, H. J. Noh, S. M. Jung, I. Ahmad, F. Li, J. M. Seo and J. B. Baek, *Angew. Chem. Int. Ed.*, 2018, **57**, 3415-3420.
26. F. Jiang, T. Jin, X. Zhu, Z. Q. Tian, C. L. Do-Thanh, J. Hu, D. E. Jiang, H. L. Wang, H. L. Liu and S. Dai, *Macromolecules*, 2016, **49**, 5325-5330.
27. C. Song, Y. He, B. Li, Y. Ling, H. Wang, Y. Feng, R. Krishna and B. Chen, *Chem. Commun.*, 2014, **50**, 12105-12108.
28. X. Zhao, X. Bu, Q.-G. Zhai, H. Tran and P. Feng, *J. Am. Chem. Soc.*, 2015, **137**, 1396-1399.
29. D.-A. Yang, H.-Y. Cho, J. Kim, S.-T. Yang and W.-S. Ahn, *Energy Environ. Sci.*, 2012, **5**, 6465-6473.
30. Y. Liao, Z. Cheng, M. Trunk and A. Thomas, *Polym. Chem.*, 2017, **8**, 7240-7247.
31. A. Nuhnen and C. Janiak, *Dalton Trans.*, 2020, **49**, 10295-10307.

Chapter 5 Computational Studies of Adsorption Performances of PANI-CMPs

Adsorption of molecules onto material surfaces can be divided into two groups based on the strengths of interactions between adsorbent and adsorbate, namely chemisorption and physisorption. Unlike chemisorption, physisorption does not form chemical bonds between adsorbent and adsorbate. Therefore, the interaction between adsorbent and adsorbate can be considered as non-covalent. This topic is one of several important aspects for the design of porous materials for applications requiring adsorbent–adsorbate interactions such as carbon capture and utilisation (CCU) and catalysis.

This chapter will discuss the theoretical study of non-bonding interactions between PANI-CMP fragments and adsorbate molecules. These calculations have been performed at the DFT level of theory to understand these interactions at a molecular level more accurately and to explore the potential of such studies to generate insight in simple and more complicated models of PANI-CMPs.

5.1 Non-Covalent Interactions for the Studies of Adsorptions

Interactions between adsorbents and adsorbates in physisorption involve non-covalent interactions (NCIs). Therefore, a good understanding of non-covalent interactions needs to be established in order to create plausible models for adsorbent-adsorbate interactions.

5.1.1 General Concepts about Non-Covalent Interactions

Non-covalent interactions (NCIs) are interactions between chemical species in which pairings of electrons and types of chemical bonding remain unchanged between reactants and resulting complexes.[1] Similar to chemical bonding, these interactions arise from a balancing act between repulsive and attractive interactions. While the only instances of repulsive interactions are steric hindrance[2] emerging from the Pauli exchange repulsion,[1] attractive interactions can be categorised by their strengths.[1] The weakest interactions are London dispersion interactions, which arise from electron movements that are uncertain and consequently can create electronically more positive or more negative regions in molecules.[3] London dispersion interactions are the major source of NCIs involving at least one chemical species with zero dipole moment and the only source of NCIs in inert gas dimers such as $(He)_2$.[1]

Following London dispersion interactions, stronger attractive NCIs are weak molecular interactions, hydrogen-bonding interactions, charge-transfer interactions, and ionic interactions. Kollman has argued that although these interactions, including London dispersion, vary in strength, they are essentially electrostatic interactions, and simple models should be enough to study these interactions theoretically with acceptable agreements with experimental data.[1] However, there have been attempts to study these interactions using different approaches and adopting a range of perspectives. For example, these NCIs can be considered as the interactions between dipoles or other types of poles in multipole systems, with the most significant ones being dipoles and quadrupoles.[4] Meanwhile, hydrogen bonds as well as bonds involving other groups of nonmetal elements such as halogen bonds or chalcogen bonds can be considered as Lewis acid-base interactions.[5] These different perspectives will be explained further over the next paragraphs.

Weak molecular interactions or van der Waals forces can be subdivided further based on the source of such interactions. London dispersion itself can be considered as a type of van der Waals force. Examples of other weak molecular interactions include induced-dipole–dipole and permanent-dipole–dipole interactions. Dipole interactions emerge from molecules with non-zero

molecular dipole moments, which can interact with other molecules with either non-zero molecular dipole moments (permanent-dipole–dipole) or zero molecular dipole moments (induced-dipole–dipole). In turn, molecular dipole moments are the summations of bond dipole moments. Therefore, it is possible for molecules, especially symmetric molecules such as CO_2, C_6F_6, CF_4, and SF_6, to have all bond dipole moments cancelling each other out and result in zero molecular dipole moments.

The concept of higher-degree polar moments has been introduced to explain weak molecular interactions in symmetric "non-polar" molecules as powers of two such as quadrupoles, octupoles, and hexadecapoles. Multipoles beyond quadrupoles, however, contribute less to intermolecular interactions and therefore become of less interest.[4] Quadrupoles in molecules with D_{nh} (including $D_{\infty h}$) symmetry are usually illustrated to have one type of charge distributed along the C_n rotational axis and the opposite type of charge distributed along the σ_h plane (Figure 5-1). While the two "bars" of charges are of the same length in Figure 5-1 for illustrative purpose of the four poles of the quadrupole system, the distribution of charges along the σ_h plane can be actually more like "belts" depending on the shape of the electrostatic surface potential (ESP) surface of molecules of interests. This is the case for linear molecules such as CO_2 and C_2H_2, shown in Figure 5-2.[5]

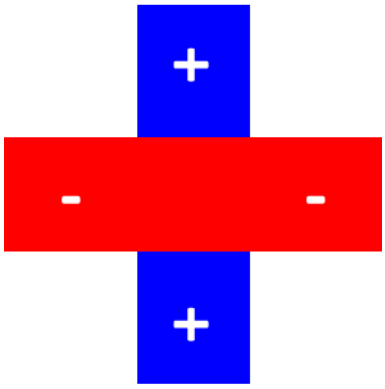

Figure 5-1 An example of quadrupole illustration, with positive charges distributed along the C_n rotational axis (vertical) and negative charges distributed along the σ_h plane (horizontal). Quadrupoles can also be represented in the other way round (negative charges along the plane, positive charges along the axis).

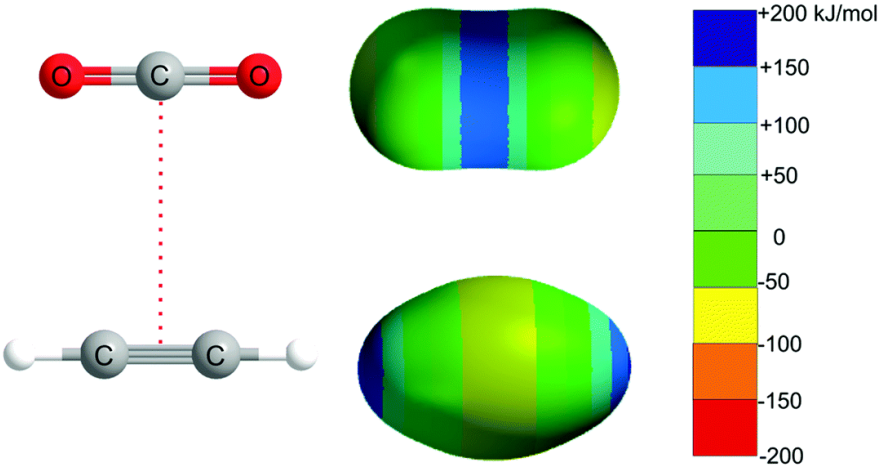

Figure 5-2 Quadrupole-quadrupole interactions between CO_2 and C_2H_2 along with ESP surfaces of both molecules, adapted from Legon[5]

Lewis acid-base interactions, meanwhile, involve donations of electron pairs from one filled orbital of one chemical species (Lewis base) to one empty orbital of another chemical

species (Lewis acid). In some cases, these interactions lead to the formation of new covalent bonds such as those in metal complexes. However, not all donations of electron pairs lead to the formation of covalent bonds. An example of these weaker interactions is hydrogen bond, which is defined by the IUPAC as:[6, 7]

"The hydrogen bond is an attractive interaction between a hydrogen atom from a molecule or a molecular fragment X–H in which X is more electronegative than H, and an atom or a group of atoms in the same or a different molecule, in which there is evidence of bond formation."

Consider the formation of a hydrogen bond between SO_2 and HF,[5] HF is the donor of a hydrogen atom for the hydrogen bond. The size of the S=O···H angle suggests that there is an interaction between the HF hydrogen atom and the lone pair electrons of one of the oxygen atoms in SO_2, which suits the definition of Lewis acid-base interactions. A similar concept of the interaction between other nonmetal atoms, instead of hydrogen, in the electrophilic region of a molecule and the nucleophilic region of a molecule has been applied to other groups of elements. In fact, the halogen bond has been defined in 2013 by the IUPAC as:[8]

"A halogen bond occurs when there is evidence of a net attractive interaction between an electrophilic region associated with a halogen atom in a molecular entity and a nucleophilic region in another, or the same, molecular entity."

A halogen bond analogue of SO_2–HF is SO_2–ClF. In this case, because chlorine is less electronegative than fluorine, the chlorine end of ClF becomes more electrophilic and can interact with the oxygen atom of SO_2 in the same way the hydrogen atom in HF does.

In the Perspective article by Legon,[5] older publications involving similar bonds from different nonmetal elements have been compiled and revisited, with ESPs of chemical entities involved shown in comparison with structures obtained from experiments at low temperatures. Definitions for chalcogen bonds (with Group 16 elements), pnictogen bonds (Group 15 elements), and tetrel bonds (Group 14 elements) have been proposed in the same manner as the halogen bond.

While Kollman[1] might argue that all non-covalent interactions are basically the same, the different perspectives and further categorisations can lead to a better understanding of the origins of these interactions. This improved understanding can then eventually lead to the establishment of structure-property relationships for further development of chemical compounds or materials for desirable applications.

5.1.2 Studies of Non-Covalent Interactions between Aromatic Systems and CO_2

Aromatic rings are prominent in the structures of poly(aniline)s and PANI-CMPs. Therefore, these moieties can play important roles in adsorbent-adsorbate interactions in these materials. In fact, many publications about CO_2-absorbing porous materials, especially those with electronegative heteroatoms such as nitrogen, oxygen, or fluorine, usually attribute their high CO_2 affinities to "quadrupole-dipole interactions".[9-26] Generally, aromatic rings have π-conjugating systems formed from p-orbitals not involved in C–C or C–H bonding. These systems can be extended by further conjugation with p-orbitals of substituents. Aromatic rings can be considered as quadrupoles, with the negative regions lying above and below the ring plane and the positive regions surrounding the ring peripherals.[27]

Interactions between aromatic rings and other chemical species are usually considered to be from the centres of aromatic rings.[27, 28] These interactions can be categorised by types of chemical species interacting with the π-systems, namely π–π, π–XH, π–cation, π–anion, and π–lone-pair.[27] For π–XH interactions, they are similar to hydrogen bonds because such interactions

involve electrophilic hydrogen atoms interacting with nucleophilic π-systems. This similarity means that it is possible for halogen bonds or other nonmetal bonds to take place in the same manner.

Interactions between CO_2 and aromatic systems have been studied both theoretically and experimentally. However, before discussing the interactions between aromatic systems and carbon dioxide, it is worth discussing the interactions arising from a CO_2 molecule itself first. As shown in Figure 5-2, a molecule of CO_2 can be viewed as a quadrupole. Each C=O bond has its dipole moment with the positive end on the carbon atom, creating a quadrupole with negative ends on oxygen atoms and positive area surrounding carbon atom. The nucleophilic region on the carbon atom is capable to form tetrel bonding. Meanwhile, the electrophilic regions on oxygen atoms can be the acceptor for hydrogen or similar bonds.[5]

Studies of NCIs between CO_2 and chemical systems with aromatic rings have been performed on aromatic systems of various sizes, from single molecules[29-33] to large fragments of graphene network[34] or polymer.[35-37] Several spectroscopic techniques such as Fourier transform microwave spectroscopy (FTMW) for molecular rotations have been developed for the study of non-covalent complexes, allowing experimental data to be obtained for comparison with the theoretical results.[30-32] However, since these experiments are conducted on gas or vapour states, it has become less practical to generate reliable experimental data for large chemical systems, especially those of less volatile solid compounds or polymers.

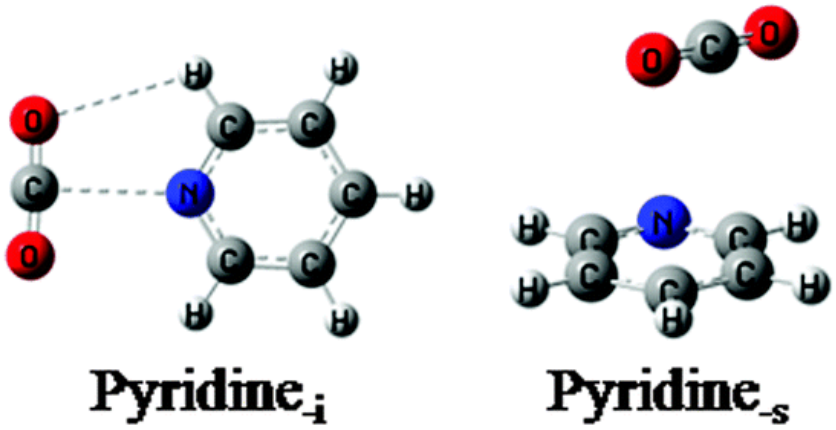

Figure 5-3 Two modes of interactions between pyridine and CO_2, taken from Lee et al.[29]

Lee *et al.* have found that for aromatic compounds with heteroatoms, there are two possible modes to interact with a CO_2 molecule, namely "electrostatic in-plane" and "dispersive π-π stacking" modes.[29] As shown in Figure 5-3, the electrostatic in-plane mode, denoted with the subscript "-i" in the referenced publication, has the CO_2 molecule lying along the same plane as the aromatic ring plane. Meanwhile, the stacking mode, denoted with the subscript "-s" in the publication, has the CO_2 molecule hovering and parallel to the aromatic ring plane. From their calculations (M06-2X/aVDZ), they have found that binding energies are greater in pyridine and other compounds containing oxygen or nitrogen (Table 5-1). However, the opposite is true for thiophene.

Regardless of the binding mode, tetrel and hydrogen bonds are prevalent in the interaction between CO_2 and other aromatic molecules, as illustrated in Figure 5-3. The coexistence of tetrel bond and hydrogen bonds in the interactions between heteroatom-containing aromatic compounds and CO_2 has been investigated and confirmed by combined theoretical and experimental studies on acetophenone[31] and 2-methoxypyridine.[32] For both

compounds, rotational spectroscopic parameters of DFT-generated complex structures are compared to those recorded from the Fourier-transform microwave spectroscopy.

Table 5-1 Binding energies of CO_2 onto different heteroatom-containing aromatic molecules from computational studies (M06-2X/aVDZ) by Lee et al.[29]

Molecule	Binding Energy (kJ·mol^{-1})	
	In-plane Mode	Stacking Mode
Furan	-11.6	-10.1
Thiophene	-6.6	-11.3
Pyridine	-19.3	-11.0
Imidazole	-19.7	-15.1
Pyrazine	-17.0	-9.0

Experimental studies on NCIs between CO_2 and small molecules can also reveal the flaws in the theoretical studies, and it should also be noted that inaccuracies regarding NCIs are among several issues in the development of computational methods, even with the most sophisticated DFT functionals (see the related discussion in Section 1.3.1.2). In the study on acetophenone–CO_2 interactions,[31] the second most stable structure of acetophenone–CO_2 complex is predicted to be only about 1 kJ·mol^{-1} less stable than the most stable structure. However, this mode of interaction cannot be detected in the rotational spectroscopic study, although the 1 kJ·mol^{-1} difference in energy, using Boltzmann distributions, means that the ratio between the more and the less favourable structures should be roughly 2:3. This disagreement means that calculations can overestimate stabilities of some complex structures, and improvements are still needed for accuracies with regards to such studies.

While it is arguable that experimental studies on the interactions between larger chemical systems and CO_2 to validate the experimental data are less practical compared to those on the smaller chemical systems, these studies can still offer insights into non-covalent interactions taking place on the material surfaces. Studies on small molecules, as explained earlier, are done in the vapour or gas phases, which are practical for compounds that are gaseous or volatile. However, adsorbents are generally highly networked solids, which means that the environments at the material surfaces where adsorptions take place will be different from the gaseous phases. For instance, an adsorbate molecule can bind to two different moieties or more, which may not be observed in the studies with smaller fragments. Meanwhile, two or more adsorbate molecules can interact among themselves as well as interacting with the material surfaces. These two examples have been observed in the computational study of CO_2 adsorption onto a per-hydroxylated pillar[6]arene fragment (Figure 5-4).[35]

Figure 5-4 also exhibits a circumstance where the stacking mode can be more stable than the in-plane mode. Structures of pillar[*n*]arenes are *para*-hydroquinone units linked by methylene groups into polygons, with *n* being the number of hydroquinone units. For the aforementioned pillar[6]arene, with six hydroquinone units arranged into a roughly equilateral hexagon, the alignment allows a CO_2 molecule to interact with two adjacent hydroquinone moieties simultaneously while being in the stacking mode respectively to both moieties. Such enhancements cause the stacking mode to become more favourable in larger and more complex systems, which might not be the case for smaller molecules with only one aromatic ring. This issue should then be investigated for translational studies towards larger systems such as solid state adsorbents.

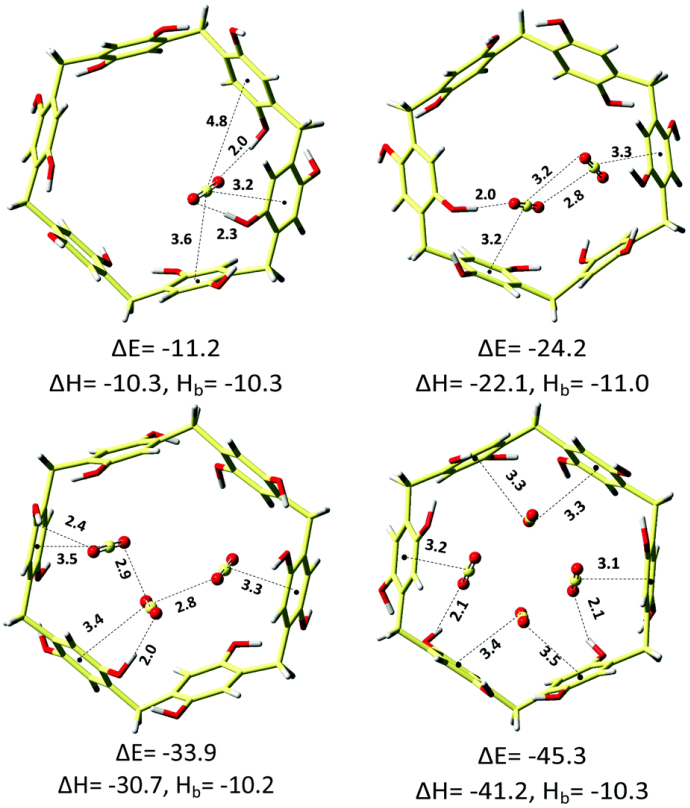

Figure 5-4 DFT-optimised structures of per-hydroxylated pillar[6]arene with one to four CO_2 molecules held inside, taken from Sahu et al.[35]

Many publications on porous materials for the adsorption of CO_2 have attributed the high adsorptions to the quadrupole-dipole interactions. However, these statements are usually speculation, while theoretical studies are few and far between. So far, CO_2 has been known to form tetrel bonds from the carbon atom and to form hydrogen bonds from the oxygen atoms. These NCIs with heteroatom-containing aromatic compounds have been delineated in several studies[30-32] by comparing data from calculations and experiments, which are mostly based on rotational spectroscopy. The analytical techniques are more practical to perform on gaseous or volatile compounds compared to solid or less volatile compounds or polymers. Meanwhile, the computational methods themselves still have flaws especially regarding dispersion, the source of non-covalent interactions, which are arguably stemmed from the flaws in KS-DFT methods themselves (see the relevant discussions in Section 1.3.1.2). The faults in both techniques are the reasons for the still large gap between experimental and theoretical studies on NCIs in adsorption.

DFT calculations have been applied for the studies of NCIs between CO_2 molecules and PANI-CMP fragments due to their previous performances in the studies of oligo(aniline) systems.[38, 39] Grimme's dispersion correction D3 with Becke-Johnson damping (D3(BJ))[40] model of empirical dispersion has been applied to mitigate the flaws of KS-DFT methods regarding NCIs. While DFT methods have their own flaws regarding the NCIs, they are still QM-based methods that use electron densities to represent chemical systems. These facts mean that DFT methods are still be more beneficial compared to other methods for the studies of NCIs in chemical systems where charge distributions are the main foci.

5.2 Studies of CO_2 Interactions on **OTPA-BZN-210** Models

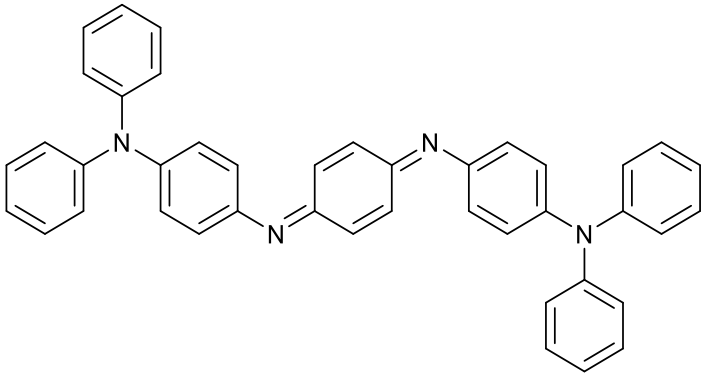

*Figure 5-5 A chemical structure for **OTPA-BZN-210** in the **EB** state*

In this section, computational studies of interactions between PANI-CMPs and CO_2 molecules are discussed. The **210** models (**EB** state shown in Figure 5-5), with two core units, one linker unit, and no cyclisation, were chosen for these theoretical studies. While these small models may not be able to capture electronic properties, these models can offer insights into interactions with CO_2 molecules while not being expensive for calculations. It is worth noting that these theoretical studies are still different from data obtained from measurements. In these studies, binding energies are determined from the interaction with one molecule of CO_2.

5.2.1 Binding Sites on **OTPA-BZN-210** Models

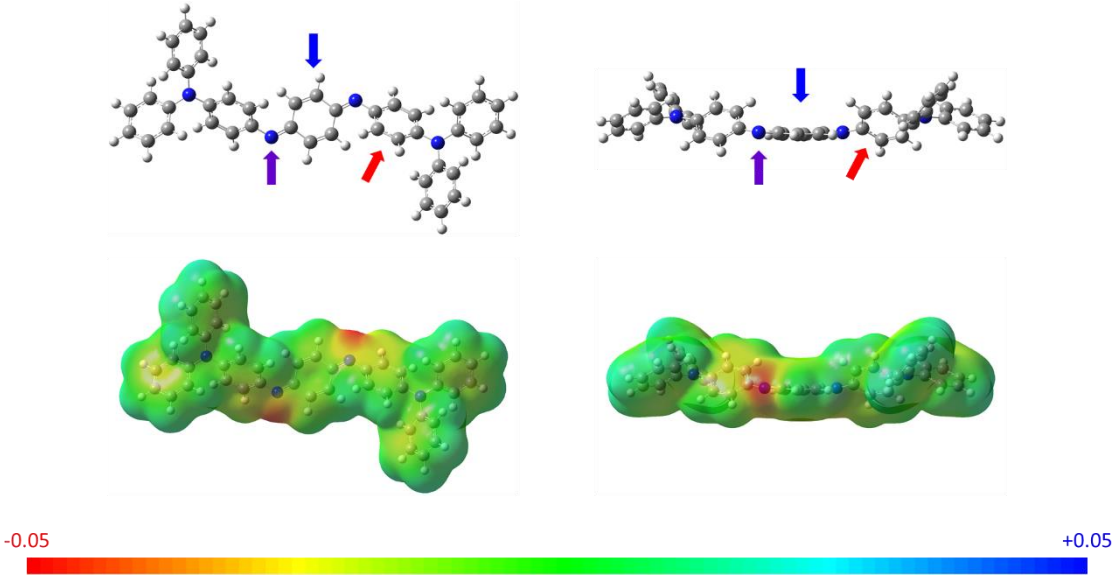

*Figure 5-6 DFT-optimised structures (B3LYP-D3(BJ)/6-31G(d)/THF PCM) of **OTPA-BZN-210** in **EB** state (taken from Chapter 3) and the ESP surfaces. Arrows mark three possible binding sites on the molecule of **EB OTPA-BZN-210**.*

Optimised structures and ESP surfaces of **OTPA-BZN-210** in **EB** state are shown in Figure 5-6. There are three types of possible locations for a CO_2 molecule to interact with. The first type is any of the two imine nitrogen atoms, which are the most electro-negative regions as shown in the ESP mapping. The electrophilic carbon atom of CO_2 can form a tetrel bond to these imine nitrogen atoms. Meanwhile, aromatic systems can be possible candidates. These can be found in either the core or the linker unit in this oligomer, and to keep in line with earlier discussions regarding poly(aniline)-like structures of PANI-CMPs and their oligomers, the term "BQ unit" will be used for the discussions in this chapter as well. The two types of BQ units, core and linker,

make up the second and the third types of potential binding sites in addition to the imine nitrogen atoms.

These studies will be mainly performed on the **EB** state oligomeric fragments because these poly(aniline)-based materials are readily oxidised, and therefore, the **EB** state is likely the most prevalent state in the undoped PANI-CMPs (see Section 3.3.3 for the discussion regarding possible oxidation states). Alignment of CO_2 molecules with these **OTPA-BZN-210** fragments from DFT optimisations are shown in Figure 5-7. For BQ unit binding sites (core and linker), there are two possible placements for CO_2 molecules: near the hydrogen atoms from adjacent BQ units, or away from the aforementioned hydrogen atoms, as shown in Figure 5-7b) and c) for linker unit binding sites and Figure 5-3d) and e) for core unit binding sites.

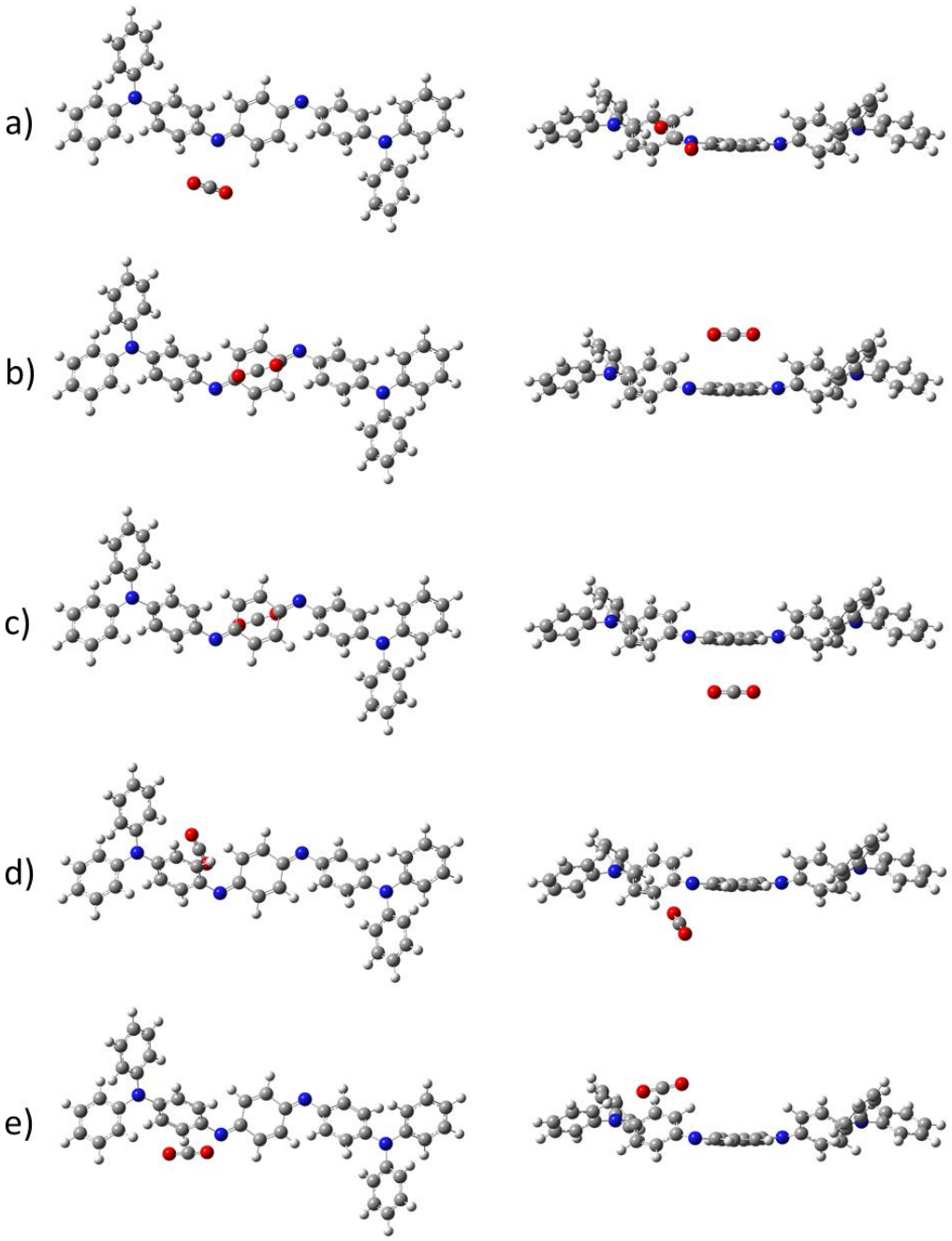

*Figure 5-7 Alignments of CO_2 molecules on three different binding sites; **a)** imine nitrogen atom, **b)** and **c)** linker unit, **d)** and **e)** core unit*

*Table 5-2 Binding energies and distances between CO_2 molecules and **OTPA-BZN-210** fragments from DFT optimisation, with the relative energies compared to the most stable binding sites given in the parentheses. CO_2 distances are measured as either C–N distances (for imine binding site) or the average distances of CO_2 atoms from the BQ unit plane (for other BQ unit binding sites). O···H distances are measured between each oxygen atom and the nearest hydrogen atom.*

Binding Site	**Binding Energy (kJ·mol^{-1})**	**CO_2 Distances (Å)**	**O···H Distances (Å)**	
Imine N atom, **a)**	-22.28 (+2.65)	2.870	2.481	3.018
Linker unit, **b)**	-23.00 (+1.93)	3.229	2.613	2.614
Linker unit, **c)**	-18.42 (+6.51)	3.161	4.396	4.382
Core unit, **d)**	-24.93 (0.00)	3.117	2.843	2.529
Core unit, **e)**	-22.13 (+2.80)	3.122	4.498	2.511

Table 5-2 lists binding energies and distances from CO_2 molecules to the oligomer fragments. Binding energies are determined from Equation 5-1. All three terms on the right-hand side are taken from their respective DFT-optimised structures. It should be noted that this method of binding energy calculation might suffer from the basis set superposition error (BSSE). However, for this discussion, the effects from BSSE are assumed to be small.

$$\Delta E_{\text{binding}} = E_{\text{complex}} - (E_{\text{oligomer}} + E_{CO_2}) \qquad 5\text{-}1$$

Generally, adsorption of gas molecules onto the material surfaces are exothermic, which means that the binding energies will be negative, and the larger magnitudes of binding energies imply stronger interactions. Comparisons between binding sites of the same types, **b)** vs **c)** for linker binding sites and **d)** vs **e)** for core binding sites, suggest that positions of nearby *ortho* hydrogen atoms affect the binding energies greatly. Binding energies from the systems with CO_2 placed near hydrogen atoms are larger than those of the systems with CO_2 placed away from hydrogen atoms by 2.80 kJ·mol^{-1} (core unit) and 4.58 kJ·mol^{-1} (linker unit). The differences in energy might suggest that hydrogen bonds can help stabilising the oligomer–CO_2 complexes. It can also be argued that the larger difference in linker unit binding energies is due to the fact that in the core unit binding mode **e)**, there is still one hydrogen atom in the vicinity of the CO_2 molecule (2.511 Å) comparable to the two hydrogen atoms in the binding mode **d)** (2.843 Å and 2.529 Å). The existence of the one hydrogen atom is possibly enough to stabilise the resulting complex, which is not the case for the linker unit binding mode **c)** with both nearest hydrogen atoms being more than 4 Å from the oxygen atoms. In fact, hydrogen bonds are usually considered to be approximately 1 to 3 Å, and longer distances than that will be considered as van der Waals interactions.[41]

Meanwhile, if the core and linker binding modes with less hydrogen bonding (modes **c)** and **e)**) are excluded, the range of binding energies among modes **a)**, **b)**, and **d)** is only 2.65 kJ·mol^{-1}. The weakest interaction coming from imine nitrogen binding site (-22.28 kJ·mol^{-1}), followed by linker unit (-23.00 kJ·mol^{-1}) and core unit (-24.93 kJ·mol^{-1}) binding sites. It is notable that effects from hydrogen bond formations are stronger than effects from binding sites alone. Therefore, the effects from positions of *ortho* hydrogen atoms from adjacent BQ units forming hydrogen bonds with CO_2 will be investigated further in Section 5.2.2.

To explore the effects of CO_2 binding on structural parameters of binding sites, these parameters, namely bond lengths, bond angles, and dihedral angles, involving atoms near the binding sites before and after CO_2 binding, were compared. Because different sets of atoms are involved in different binding sites, comparisons and discussions will be done separately.

For imine group binding sites, binding of CO_2 consists of two non-covalent interactions. The first interaction, which is presumably the major contributor, is the interaction between the carbon atom of CO_2 and the nitrogen atom of the imine group. This interaction can be considered as a tetrel bond between nucleophilic CO_2 carbon and lone-pair-electron-bearing imine nitrogen.[5] The second interaction arises from the hydrogen bonds from the hydrogen atoms in the *ortho* positions of the two rings bound the imine nitrogen atom to the oxygen atoms of CO_2. While this is possible in theory, as hydrogen atoms on the *ortho* carbon atoms in BQ units are partially positive, the DFT-optimised structure of imine-bound **210**–CO_2 complex suggests otherwise. Viewing through the tetrel bond, the oxygen atoms appear to be pushed away from the *ortho* hydrogen atoms (Figure 5-8).

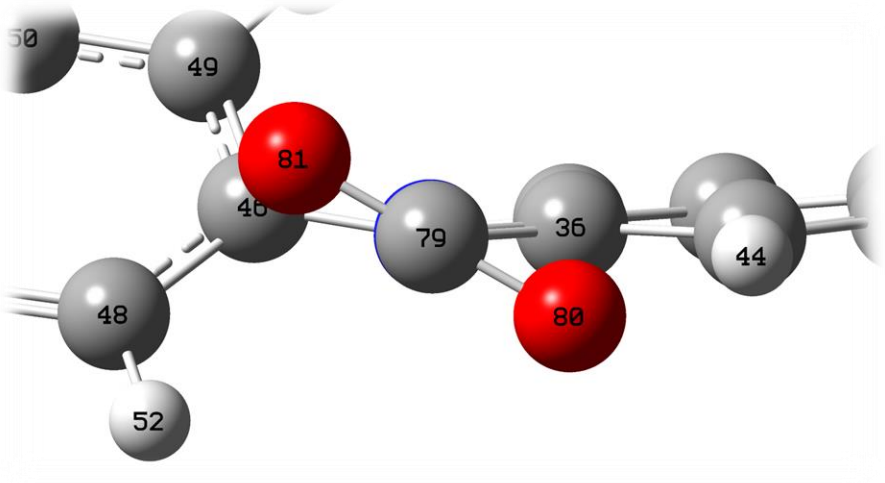

*Figure 5-8 The alignment of the CO_2 molecule bound to the imine nitrogen atom of **OTPA-BZN-210** fragment from DFT optimisation (B3LYP-D3(BJ)/6-31G(d)/aniline PCM, visualised in GaussView 6.1.1), viewed through the tetrel bond between CO_2 carbon atom (number 79) and the imine nitrogen atom (obscured blue atom behind carbon atom number 79)*

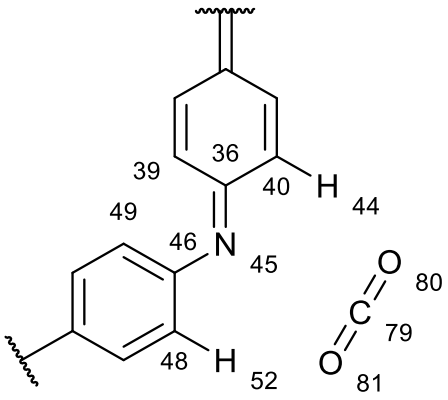

Scheme 5-1 Numbering of atoms involved in the geometries of imine binding site

There is no significant change in bond lengths for both species involved in the interaction (Table 5-3), and the change in dihedral angles are relatively small, approximately 1.5°, upon the interaction with CO_2. These small changes in dihedral angles, however, also suggest the repulsion between hydrogen and oxygen atoms. The more significant change, however, is in the geometry of CO_2, specifically the O–C–O angle. The deviation from a perfect linear structure, together with the slight decrease in C–N–C bond angle between the two aromatic rings and magnitudes of N···C–O angles, suggest that CO_2 carbon atom is possibly being attracted towards the imine group. It can

be concluded that in the case of imine binding site, the tetrel bonding between the electrophilic carbon atom of CO_2 and imine nitrogen atom is the primary interaction.

Table 5-3 Comparisons between structural parameters befor and after a CO_2 molecule is bound to the imine binding site from DFT-optimisesd structures.

Parameter		Before Binding	After Binding
C–H bond length	C^{40}–H^{44}	1.086 Å	1.085 Å
	C^{48}–H^{52}	1.085 Å	1.085 Å
Ring dihedral angle	C^{39}–C^{36}–N^{45}–C^{46}	-12.1°	-12.2°
	C^{36}–N^{45}–C^{46}–C^{49}	-41.3°	-42.8°
C–N–C bond angle	C^{36}–N^{45}–C^{46}	123.1°	122.9°
C–O bond length	C^{79}–O^{80}	1.169 Å	1.170 Å
	C^{79}–O^{81}	1.169 Å	1.169 Å
O–C–O bond angle	O^{80}–C^{79}–O^{81}	180.0°	176.3°
N···C–O angle	N^{45}···C^{79}–O^{80}	-	94.4°
	N^{45}···C^{79}–O^{81}	-	89.2°
O···H distance	H^{44}···O^{80}	-	2.481 Å
	H^{52}···O^{81}	-	3.018 Å
N···C distance	N^{45}···C^{79}	-	2.870 Å

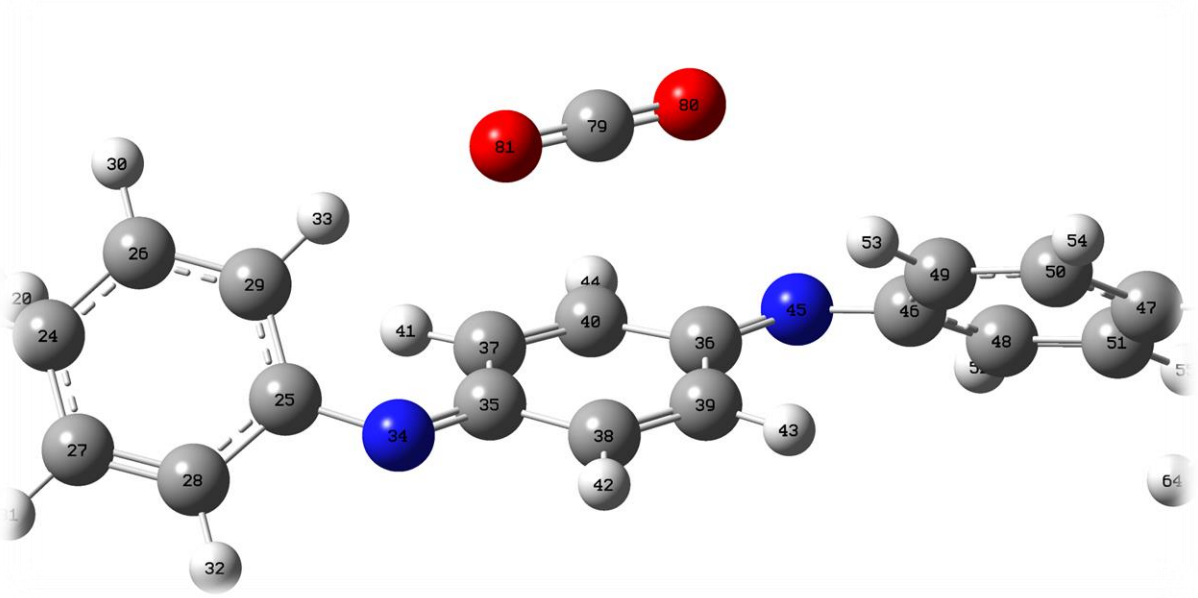

*Figure 5-9 The alignment of the CO_2 molecule bound to the linker unit binding site of **OTPA-BZN-210** oligomer fragment from DFT optimisation (B3LYP-D3(BJ)/6-31G(d)/aniline PCM, visualised in GaussView 6.1.1)*

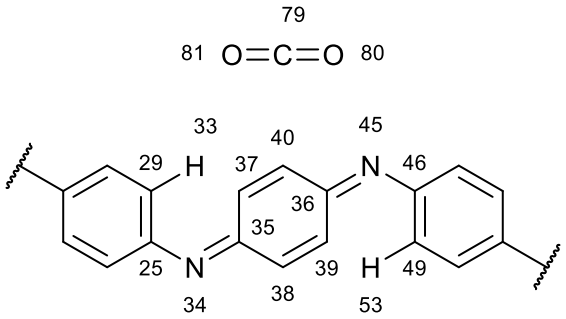

Scheme 5-2 Numbering of atoms involved in the geometries of linker unit binding site, matching Figure 5-9

Table 5-4 Comparison of structural parameters before and after a CO_2 molecule is bound to the linker unit binding site from DFT-optimised structures.

Parameter		Before Binding	After Binding
C–H bond length	C^{29}–H^{33}	1.085 Å	1.084 Å
	C^{49}–H^{53}	1.085 Å	1.084 Å
C–O bond length	C^{79}–O^{81}	1.169 Å	1.169 Å
	C^{79}–O^{80}	1.169 Å	1.169 Å
O–C–O bond angle	O^{81}–C^{79}–O^{80}	180.0°	179.5°
H···O distance	H^{33}···O^{81}	-	2.613 Å
	H^{53}···O^{80}	-	2.614 Å

For the linker unit binding site, structures are more complicated due to the larger number of atoms from the oligomer fragment involved. The CO_2 molecule lies above the BQ unit, along the rough imaginary line passing through imine nitrogen atoms and *ipso* carbon atoms (Figure 5-9), with oxygen atoms pointing towards the *ortho* hydrogen atom from the neighbouring BQ units. Therefore, atoms involved in the linker unit binding site, as well as the core unit binding site where CO_2 molecules can bind in the similar manner, are those of the linker BQ unit itself along with all atoms describing the dihedral angles between the linker BQ unit and neighbouring units and also *ortho* hydrogen atoms interacting with CO_2 oxygen atoms, as illustrated in Figure 5-9.

Structural parameters, namely bond lengths and bond angles, of the BQ unit itself remained unchanged upon the binding (Table 5-4 and Table A-11). This is also the case for inter-unit parameters such as C–N–C angles and ring dihedral angles. The geometry of the bound CO_2 itself also changes less significantly, with the deviation from linearity being only 0.5°, compared to 3.7° in the case of the imine binding site. These insignificant changes, yet resulting in slightly larger binding energies, imply that the structure of the **BZN** linker unit binding site is probably matching the structure of CO_2 molecules. A CO_2 molecule can align itself to both form a tetrel bond with the π-system of the BQ unit and form hydrogen bonds between the oxygen atoms and *ortho* hydrogen atoms without further adjustments.

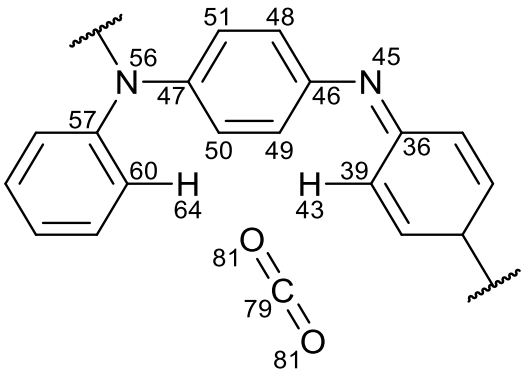

Scheme 5-3 Numbering of atoms involved in the geometries of core unit binding site, matching Figure 5-10

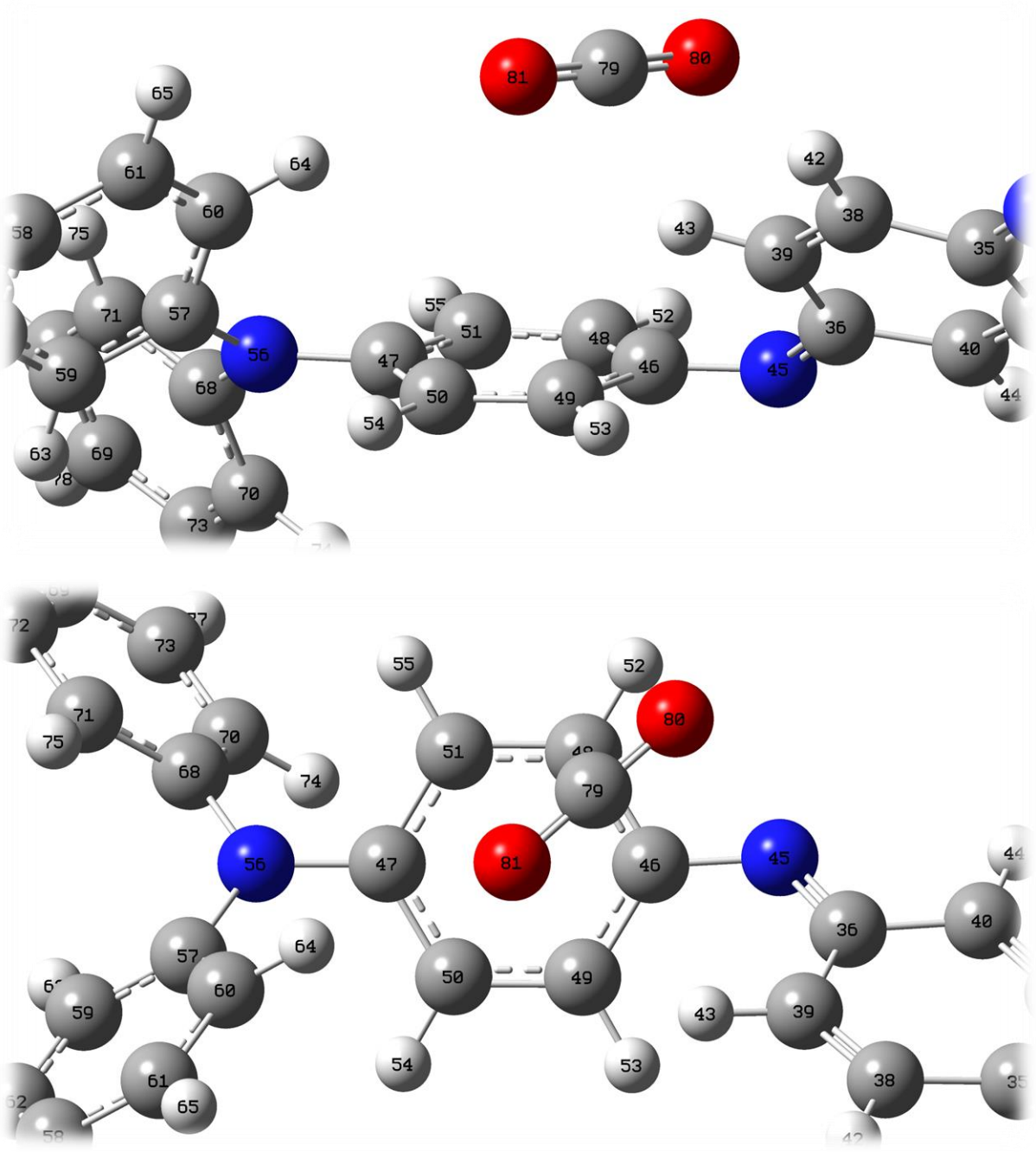

*Figure 5-10 The alignment of the CO_2 molecule bound to the core unit binding site of **OTPA-BZN-210** oligomer fragment from DFT optimisation (B3LYP-D3(BJ)/6-31G(d)/aniline PCM, visualised in GaussView 6.1.1)*

Table 5-5 Comparison of structural parameters before and after a CO_2 molecule is bound to the core unit binding site from DFT-optimised structures.

Parameter		Before Binding	After Binding
C–H bond length	C^{39}–H^{43}	1.083 Å	1.083 Å
	C^{60}–H^{64}	1.085 Å	1.084 Å
C–O bond length	C^{79}–O^{81}	1.169 Å	1.169 Å
	C^{79}–O^{80}	1.169 Å	1.168 Å
O–C–O bond angle	O^{81}–C^{79}–O^{80}	180.0°	179.0°
H···O distance	H^{43}···O^{80}	-	3.309 Å
	H^{43}···O^{81}	-	2.843 Å
	H^{64}···O^{81}	-	2.529 Å

Similar trends in structural parameters are also observed in the case of core unit binding site (Table 5-5 and Table A-18), with structures of the BQ unit themselves remaining almost unchanged. However, there are some differences between the structures of the core and the linker unit binding sites themselves. The two *ortho* hydrogen atoms are on the same side along the rough imaginary line passing imine nitrogen atoms and *ipso* carbon atoms in the core binding sites (Scheme 5-3), while these hydrogen atoms lie on the different side in the linker binding site. Such differences have led to different binding modes on the two BQ-unit-based binding sites. While the CO_2 molecule aligns along the aforementioned imaginary line over the linker unit, in the case of the core unit, the molecule lies so that the oxygen atom (O^{81} in Figure 5-10) interacts with both *ortho* hydrogen atoms (H^{43} and H^{64}). This alignment also allows another oxygen atom (O^{80}) to be in close proximity of *ortho* H^{43}. In this case, as the carbon atom does not directly over the centre of the BQ unit, unlike in linker unit binding site, it is unlikely for the tetrel bond to form. Instead, the CO_2 molecule is balanced with three hydrogen bonds instead of only two. This might explain the larger magnitude of binding energy for the core unit binding site.

Since the alignment of the two adjacent BQ units against the binding BQ unit can affect the geometry of bound structures of oligomer-fragment–CO_2 complex, the effects of conformers will be discussed in detail in the next section.

Three possible binding sites on the structure of **EB OTPA-BZN-210** oligomer have been identified, namely imine group site, linker unit site, and core unit site. From the DFT calculations (B3LYP-D3(BJ)/6-31G(d)/aniline PCM), the core unit site is the most favourable binding site in terms of binding energies, followed by the linker unit site and the imine group site. In terms of molecular geometry, there are only slight changes observed upon the binding of CO_2 onto these binding sites. The most significant changes are observed for imine binding site, with the CO_2 molecule being bent so that the carbon atom become slightly closer that the oxygen atoms. However, the changes are still almost negligible.

5.2.2 Effects of Conformers

Ph/Ph-capped tetra(aniline) in the **EB** state, with structures similar to **OTPA-BZN-210** in the **EB** state but without branching on any nitrogen atoms, has been found to possess four different conformers depending on alignments of Unit B and Unit D against Unit C, the middle BQ unit.[42] These different conformers emerge from two different aspects, *cis-trans* isomerism and *syn-anti* conformers (Scheme 5-4), the latter resulting from twisting the unit plane away to mitigate steric hindrance from *ortho* hydrogen atoms. The concept of *cis-trans* isomerism in this case is similar to the normal *cis-trans* isomerism with respect to a double bond, but the whole BQ unit is considered instead of just one double bond. Meanwhile, the *syn-anti* isomerism refers to how *ortho* hydrogen atoms in the closer position point upwards or downwards.

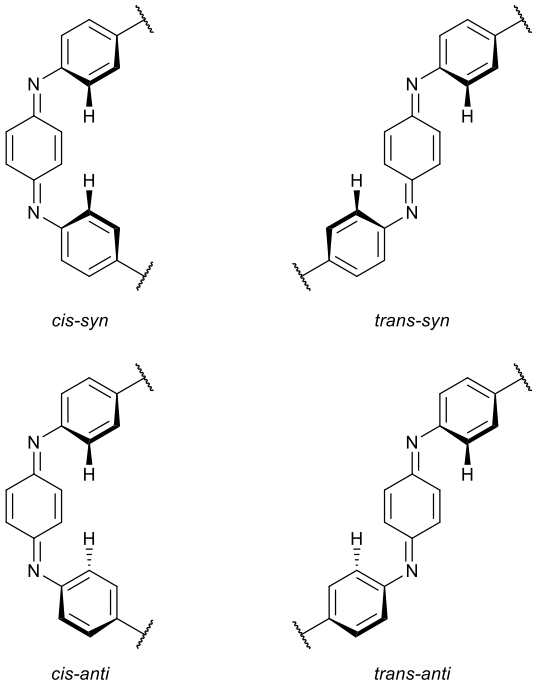

Scheme 5-4 Four different conformers of two adjacent BQ units respective to the middle BQ unit

In the case of core and linker binding sites, the linker unit binding site (Figure 5-9) resembles the *trans-syn* conformer, while the core unit binding site (Figure 5-10) resembles the *cis-syn* conformer. As explained in the previous section, the *cis-syn* conformer of the core unit binding site allows three hydrogen bonds to be formed, while the *trans-syn* conformer of the linker unit allows two hydrogen bonds and one tetrel bond to be formed. The different types of non-covalent interactions may lead to the difference in binding energies. Here, the effects of conformers on binding energies will be discussed, starting from the stabilities of **OTPA-BZN-210** in different conformers and then followed by how these different binding modes affect binding energies.

*Table 5-6 Comparison of DFT-calculated relative energies of tetra(aniline) and **OTPA-BZN-210** in **EB** state respective to the conformer with lowest energy (cis-syn in both cases). Calculated energies of tetra(aniline) are taken from Thomas et al.[42]*

Conformer	DFT-Calculated Relative Energy (kJ·mol^{-1})	
	EB Tetra(aniline)	EB OTPA-BZN-210
cis-syn	0.00	0.00
cis-anti	3.29	3.74
trans-syn	2.13	1.51
trans-anti	2.48	1.87

In the previously published work on theoretical studies of tetra(aniline),[42] *cis-syn* has been found to be the most stable conformer, followed by *trans-syn*, *trans-anti*, and with *cis-anti* being the least stable. The energy difference between energies of the two *trans* conformers is smaller than the two *cis* conformers, and *syn* conformers are more stable than their *anti* counterparts. All these trends are also observed in the branched oligomer derivative **OTPA-BZN-210**. It is also worth noting that the energy range between the most and the least stable conformer is close to the binding energy range (3.74 kJ·mol^{-1} vs 2.65 kJ·mol^{-1}). This means that the effects from one factor can interfere with the effects from another factor. However, as this issue has been raised after most calculations have been performed on *trans-syn* models, all further calculations

beyond the end of this section will be performed on *trans-syn* models, if applicable, although they are not the most stable conformers. There should not be any significant difference as a result of the most stable conformers not being used.

For discussions regarding effects from conformers in this section, core unit binding sites will not be the concern in this section, for clarity, and only linker unit binding sites will be discussed.

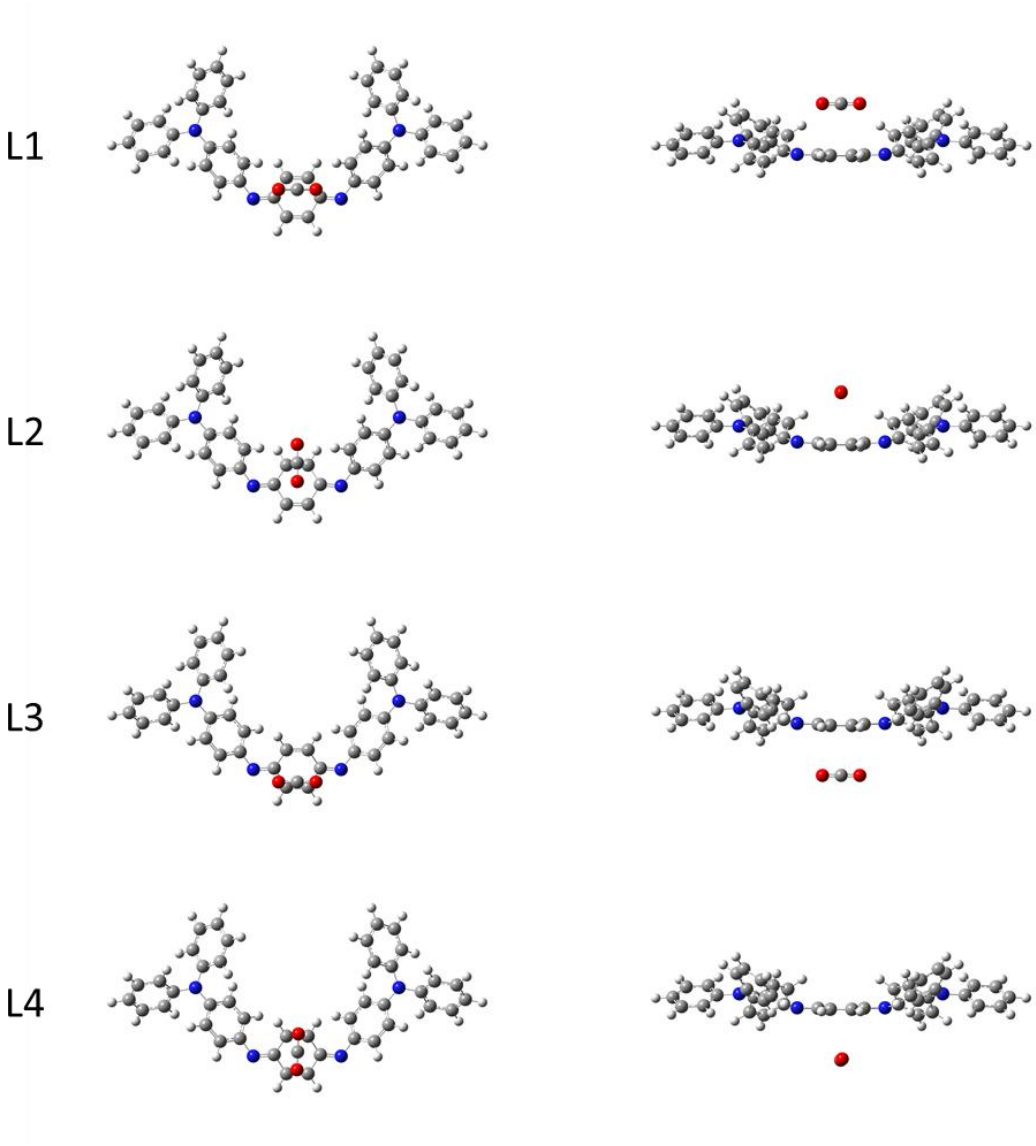

*Figure 5-11 Different positions of CO_2 on the fragment of the **OTPA-BZN-210** oligomer in the cis-syn conformer. These initial set-ups are also applied for the trans-syn conformer, while only L1 and L2 modes are applicable for the anti conformers.*

*Table 5-7 Binding energies of different binding modes on the linker unit binding sites of **OTPA-BZN-210** oligomers in different conformers. Italicised numbers mean that the optimisation process ended in error and failed to restart.*

Binding Mode	Binding Energy (kJ·mol^{-1})			
	cis-syn	***trans-syn***	***cis-anti***	***trans-anti***
L1	-22.85	-22.95	-21.16	-20.88
L2	-21.30	*-22.30*	*-18.64*	-19.12
L3	-18.52	-18.38	-	-
L4	-16.12	-18.38	-	-

Four different binding modes for a CO_2 molecule to bind on the linker unit have been trialled (Figure 5-11). L1 and L2 modes have the CO_2 molecule placed near the *ortho* hydrogen atoms, while L3 and L4 modes have the molecule placed away from these *ortho* atoms. Because there is no difference between L1 and L3 (and between L2 and L4) in *anti* conformers, L3 and L4 were not applied to the two *anti* conformers. The difference between L1 and L2 is that in L1, the CO_2 molecule is placed along the line passing two C–N bonds, while in L2, the molecule is placed perpendicular to this line. L3 and L4, for *syn* conformers, are differentiated in the same manner.

As shown in Figure 5-11, L1 and L2 modes yield different structures of fragment–CO_2 complexes, as do L3 and L4 modes. The different optimised structures imply a relatively high barrier for the rotation of the CO_2 molecule. In almost all cases, the alignments with CO_2 lying parallel to the BQ unit led to greater binding energies (Table 5-7), except *trans-syn* L3 and L4 of which both modes yield the same energy. It is possible that, for the *trans-syn* conformer, the greater distances between oxygen atoms and hydrogen atoms, forming hydrogen bonds, allowing the CO_2 molecule to rotate more freely, and allowing the optimisation of both modes to yield the same structure. For other cases, however, the parallel alignment might lead to better interactions between CO_2 quadrupole moments and C–N dipole moments.

Data in Table 5-7 also show that the closer distances between hydrogen-bond-forming oxygen atoms and hydrogen atoms lead to larger binding energies. This is clearly observed in the *cis-syn* conformer with L1 and L2 yielding greater binding energies than L3 and L4, respectively. These data show the strong influences from hydrogen bonding in the binding of CO_2 molecule onto linker unit binding sites. Meanwhile, the effects from tetrel bonding may not be as strong. This fact is illustrated as none of the optimised structures on the *cis-syn* conformer has the electrophilic carbon atom of CO_2 lying directly above the BQ unit at all.

It should also be noted that there is no significant difference in energy between *cis-syn* and *trans-syn* in modes L1 and L2, while structures of CO_2 binding site themselves obviously differ. Therefore, while it can be argued in the previous section that the core and the linker binding sites have different geometries, the difference in binding energy between the two sites are more likely to be from the additional hydrogen bonding rather than the *cis-trans* geometry alone.

5.2.3 Effects of Oxidation States

In addition to the **EB** state of **OTPA-BZN-210**, the same oligomer in the **LEB** state has also been studied to understand the effects of oxidation states on the interaction with CO_2. For poly(aniline)s and their derivatives, the **EB** state or the emeraldine base state refers to the half-oxidised state. Half of the BQ units have changed from benzenoid to quinoid form upon the oxidation, see Scheme 1-6, with two hydrogen atoms removed from each BQ unit undergoing oxidation. As discussed in the Section 3.2, the main changes to the chemical structures between **LEB** and **EB** state **OTPA-BZN-210** happen around the linker BQ unit. The HOMBQ index of the linker BQ unit decreases from 0.998 to 0.314, compared to a slight decrease from 0.993 to 0.985 for the core BQ unit. Nonetheless, as discussed in the Section 5.2.1, the effects of binding with CO_2

on the structures of BQ units themselves are negligible. Therefore, the BQ unit binding sites, either core or linker, in the **LEB** state should not show different results from those in the **EB** state. However, this should not be the case for the imine binding site. The imine groups in the **EB** state become amine groups, with one additional hydrogen atom, upon the reduction to the **LEB** state. Therefore, the extra hydrogen atom can disrupt the usual binding mode happening in the **EB** state.

*Table 5-8 Binding energies of CO_2 on **OTPA-BZN-210** in **LEB** and **EB** states, as determined from DFT-optimised structures*

Binding Site	Binding Energy (kJ·mol^{-1})	
	LEB State	EB State
Amine/imine group	-21.79	-22.28
Linker unit	-22.52	-23.00
Core unit	-25.77	-24.93

For core and linker unit binding sites, binding energies in the **LEB** state are approximately 0.5 kJ·mol^{-1} smaller than the corresponding energies in the **EB** state, and there is no significant difference between binding of CO_2 onto these binding sites in **LEB** and **EB** states (Section 7.2.2.1). However, the trend goes in the opposite direction for the amine/imine group binding site, with the **LEB** state having a larger binding energy by 0.84 kJ·mol^{-1}. This opposite trend can be explained by considering the structure of the **LEB**–CO_2 complex (Figure 5-12). Since there is a hydrogen atom bound to the nitrogen atom, tetrel bond formation in the case of the **LEB** state cannot be in the same way as in the **EB** state. This new mode of tetrel bonding puts three hydrogen atoms close to oxygen atoms of CO_2 and potentially can form hydrogen bond interactions, namely two *ortho* hydrogen atoms H^{44} and H^{53} and the amino group hydrogen atom H^{82} itself, compared to only two atoms and two hydrogen bonds in the **EB** state (Figure 5-8). This greater number of hydrogen atoms stabilise CO_2 more and increase the magnitude of the binding energy.

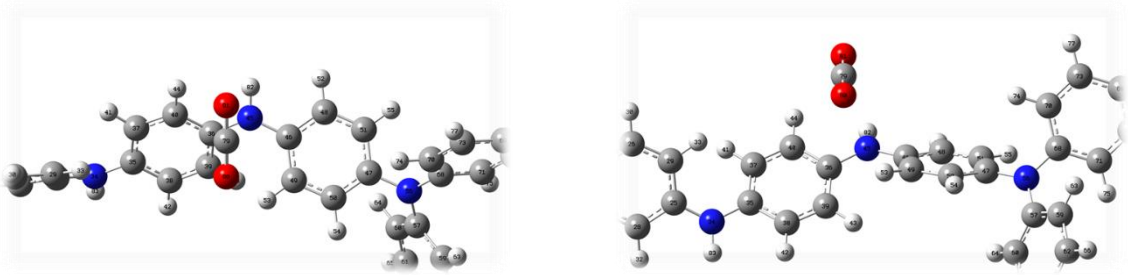

*Figure 5-12 Binding geometries of CO_2 onto the amine group of **OTPA-BZN-210** in the **LEB** state from top and tilt front views*

Overall, there is no significant difference emerging from the change in oxidation state from **EB** to **LEB** state in terms of binding energies, with the same trend being observed. However, the extra hydrogen atoms on the imine (or amine) group alter the geometries of oligomer–CO_2 complex, with the CO_2 being bound parallelly to the plane of the amine group instead of aligned in-plane as in the **EB** state.

5.3 Effects of Monomer Units

To study the effects of core and linker units on binding energies of CO_2 onto the identified binding sites, all combinations of core units (**TPA**, **TPB**, and **TPT**) and linker units (**BZN** and **FLR**) have been attempted. All calculations were performed on **210** models in the **EB** state.

*Table 5-9 Binding energies on different binding sites of **210** oligomers from different core and linker unit combinations*

Binding Site	Binding Energy (kJ·mol^{-1})					
	TPA-BZN	**TPA-FLR**	**TPB-BZN**	**TPB-FLR**	**TPT-BZN**	**TPT-FLR**
Imine Nitrogen	-22.28	-22.60	-21.82	-22.20	-21.40	-20.06
Linker Unit	-23.00	-23.22	-22.90	-23.02	-22.98	-22.93
Core Unit	-24.93	-25.02	-25.18	-23.12	-23.11	-22.30

Overall, CO_2-fragment binding energies are between -20.06 and -25.18 kJ·mol^{-1}, with the range (3.78 kJ·mol^{-1}) comparable to the effects of conformers or different binding sites alone. While the same trend of imine group < linker unit < core unit in binding energies can still be observed, this comparable range implies that the effects from monomer units can be hindered by contributions from other factors. Also, different monomer units yield binding sites of different structures, which will affect the binding energies even further. Therefore, delineating these effects should be done with care.

5.3.1 Geometries of Imine Binding Sites

Table 5-10 lists significant parameters observed upon the binding of CO_2 onto imine binding sites, with data summarised from Section 0 in the Appendix. Dihedral angle differences are calculated from the combined adjacent C–C–N–C and C–N–C–C dihedral angles before and after binding. Positive changes mean that the twisting between the two neighbouring units become further away from the plane, regardless of the sign of the listed dihedral angles, or in mathematical terms, $|D_{\text{C–C–N–C}} + D_{\text{C–N–C–C}}|_{\text{after}} - |D_{\text{C–C–N–C}} + D_{\text{C–N–C–C}}|_{\text{before}}$. For O–C–O angle differences, the positive numbers imply that the CO_2 molecule is bent so that the carbon atom seems pulled towards the oligomer more than the oxygen atoms. The bending of CO_2 molecules will be discussed in Section A.4.7.7 in the Appendix.

*Table 5-10 Key parameters related to binding of CO_2 onto imine binding sites of **210** oligomers from all six core and linker unit combinations. See the main text for meanings of signs for angle differences.*

Parameter	TPA-BZN	TPA-FLR	TPB-BZN	TPB-FLR	TPT-BZN	TPT-FLR
Dihedral angle difference	+1.6°	+2.5°	+0.9°	+1.7°	+1.6°	-0.5°
O–C–O angle difference	+3.7°	+3.6°	+3.4°	+3.2°	+2.9°	+3.0°
O···H distance	2.481 Å	2.584 Å	2.474 Å	2.522 Å	2.472 Å	3.587 Å
	3.018 Å	2.526 Å	3.096 Å	2.574 Å	2.727 Å	2.881 Å
N···C distance	2.870 Å	2.892 Å	2.878 Å	2.907 Å	2.921 Å	2.846 Å
Binding energy (kJ·mol^{-1})	-22.28	-22.60	-21.82	-22.20	-21.40	-20.06

Similar trends have been observed across all six core-linker combinations, and their binding energies do not differ much from each other, except for **TPT-FLR** of which the binding energy is only -20.06 kJ·mol^{-1}. Binding energies of other core-linker combinations are narrowly dispersed between -21.40 and -22.60 kJ·mol^{-1}, with the range of only 1.20 kJ·mol^{-1}. Across all six combinations, the CO_2 molecules bound to the imine sites have been bent by approximately 3°, and the tetrel bonds between CO_2 carbon atom and imine nitrogen atom are approximately 2.9 Å. Changes in dihedral angles are less significant. Bending phenomena of CO_2 molecules due to tetrel bonding have also been observed in infrared spectra of heteroatom-containing aliphatic polymers saturated with CO_2.[43, 44]

Hydrogen bond lengths appear to be the major cause for variances in binding energies. In the case of **TPT-FLR**, a distance between one oxygen atom and the hydrogen-bond-forming hydrogen atom is 3.587 Å, the largest distance among all 12 oxygen-hydrogen pairs which also corresponds to the smallest binding energy of -20.06 kJ·mol^{-1}. However, the effects become more complicated among the remaining five oligomers. Complications aside, their effects on binding energies are still small.

5.3.2 Geometries of Linker Binding Sites

Important structural parameters for linker binding sites of **210** oligomers are listed in Table 5-11, while other parameters can be found in Section 0 (for **BZN**-linked oligomers) and 0 (for **FLR**-linked oligomers) in the Appendix. Unlike in Table 5-10, however, the differences in O–C–O angles of bound CO_2 are not listed with positive or negative signs. Since the changes in these angles are relatively small, less than 1°, and also due to the more complicated geometries of CO_2 binding in the stacking mode (Figure 5-9) compared to the in-plane-like mode for imine binding sites (Figure 5-8), there is no practical point to determine whether the CO_2 molecule is bent towards or away from the BQ plane.

For each complex, the distance between the CO_2 molecule and the BQ unit bound are determined by calculating the distance between each atom and the plane of the BQ unit using analytical geometry. Details regarding calculations are listed in Section A.4.7.7 in the Appendix.

*Table 5-11 Key parameters related to binding of CO_2 onto linker binding sites of **210** oligomers from all six core and linker unit combinations.*

Parameter	TPA-BZN	TPB-BZN	TPT-BZN	TPA-FLR	TPB-FLR	TPT-FLR
O–C–O angle difference	0.5°	0.3°	0.2°	0.9°	0.7°	0.6°
O···H distance	2.613 Å	2.594 Å	2.573 Å	2.805 Å	2.815 Å	2.828 Å
	2.613 Å	2.596 Å	2.579 Å	2.799 Å	2.758 Å	2.738 Å
BQ···C distance	3.226 Å	3.241 Å	3.236 Å	3.161 Å	3.166 Å	3.168 Å
BQ···O distance	3.206 Å	3.202 Å	3.205 Å	3.153 Å	3.156 Å	3.153 Å
	3.257 Å	3.287 Å	3.269 Å	3.187 Å	3.191 Å	3.194 Å
BQ···CO_2 average distance	3.229 Å	3.243 Å	3.237 Å	3.167 Å	3.171 Å	3.172 Å
Binding energy (kJ·mol^{-1})	-23.00	-22.90	-22.98	-23.22	-23.02	-22.93

There is no significant change seen in the geometries of BQ units due to the interaction with CO_2 for both linkers (see the Appendix), nor is there for interaction-related parameters listed in the table among oligomers with the same linker unit but different core units. For binding energies, there is no significant difference between oligomers with **BZN** and **FLR** linker units.

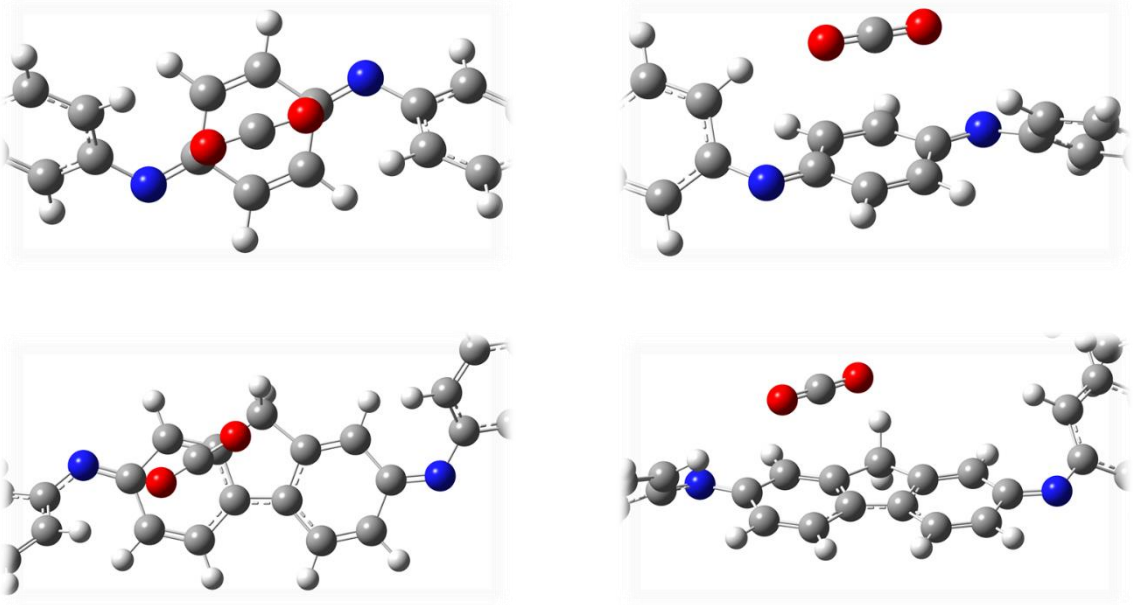

*Figure 5-13 Binding geometries of CO_2 onto **BZN** (top) and **FLR** (bottom) linker units of the respective **210** oligomers with **TPA** core units from top and tilt front views (DFT-optimised, B3LYP-D3(BJ)/6-31G(d)/Aniline PCM, visualised in GaussView 6.1.1)*

Although numbers in Table 5-11 are similar across both linker units, there are differences between the two linker units to a certain extent. Hydrogen bonds in **BZN**-linked oligomers are slightly shorter than those in **FLR**-linked oligomers (2.6 Å for **BZN** vs 2.8 Å for **FLR**), and the average distances between CO_2 and the BQ units in **BZN**-linked oligomers are slightly longer (3.24 Å for **BZN** vs 3.17 Å for **FLR**). In fact, since the geometries of the two linkers are different, it is not surprising that binding modes onto both linker units will be different as well, as illustrated in Figure 5-13. For **BZN** linkers, the CO_2 molecule will lie along the imaginary line passing through both C=N bonds as discussed in Section 5.2.1, with oxygen atoms forming hydrogen bonds with *ortho* hydrogen atoms from neighbouring core units. However, since the structure of a **FLR** linker is longer than that of a **BZN** linker, the binding CO_2 molecule cannot reach both *ortho* hydrogen atoms. Instead, while one oxygen atom forms a hydrogen bond with one *ortho* hydrogen atom, the CO_2 molecule is aligned so that another oxygen atom forms a hydrogen bond with a benzylic hydrogen atom of the fluorene unit.

While **BZN** and **FLR** linker units provide different binding modes, their binding energies remain similar. The overall effects from core or linker units are almost negligible.

5.3.3 Geometries of Core Binding Sites

There are more variations across three core units compared to two linker units in terms of chemical structures. Therefore, it the discussions of CO_2 binding onto core units compared to binding onto linker units become more nuanced. Core unit binding sites are not only the binding sites with largest binding energies, but they are also binding sites with largest fluctuations in binding energies (Table 5-9). It is then more sensible to list and discuss the binding geometries separately.

Key parameters for **210** oligomers with **TPA** core binding with CO_2 are listed in Table 5-12. The general structure of the complex between a CO_2 molecule and the core unit has already been discussed in detail in Section 5.2.1, so it will not be discussed here again. In general, there are three hydrogen atoms forming hydrogen bonds instead of two, with one oxygen atom forming hydrogen bonds with two hydrogen atoms (Figure 5-10). This is the case for both **OTPA-BZN-**

210 and **OTPA-FLR-210**, and therefore, the difference in binding energies from the two oligomers is miniscule.

*Table 5-12 Key parameters related to binding of CO_2 onto **TPA** core binding sites of **210** oligomers linked by **BZN** and **FLR** linkers*

Parameter	TPA-BZN	TPA-FLR
O–C–O angle difference	1.0°	1.1°
O···H distance	2.529 Å	2.544 Å
	2.843 Å	2.818 Å
	3.309 Å	3.344 Å
BQ···C distance	3.110 Å	3.138 Å
BQ···O distance	3.235 Å	3.240 Å
	3.005 Å	3.057 Å
BQ···CO_2 average distance	3.117 Å	3.145 Å
Binding energy (kJ·mol^{-1})	-24.93	-25.02

*Table 5-13 Key parameters related to binding of CO_2 onto **TPB** core binding sites of **210** oligomers linked by **BZN** and **FLR** linkers. For O···H distances, oxygen and hydrogen atoms involved are numbered as in Figure 5-14.*

Parameter	TPB-BZN	TPB-FLR
O–C–O angle difference	1.1°	1.2°
O···H distance	2.555 Å (O^{96}···H^{20})	2.538 Å (O^{107}···H^{20})
	2.795 Å (O^{96}···H^{28})	4.177 Å (O^{107}···H^{28})
	2.633 Å (O^{97}···H^{49})	2.653 Å (O^{108}···H^{49})
BQ···C distance	3.217 Å	3.188 Å
BQ···O distance	3.247 Å	3.196 Å
	3.208 Å	3.202 Å
BQ···CO_2 average distance	3.224 Å	3.195 Å
Binding energy (kJ·mol^{-1})	-25.18	-23.12

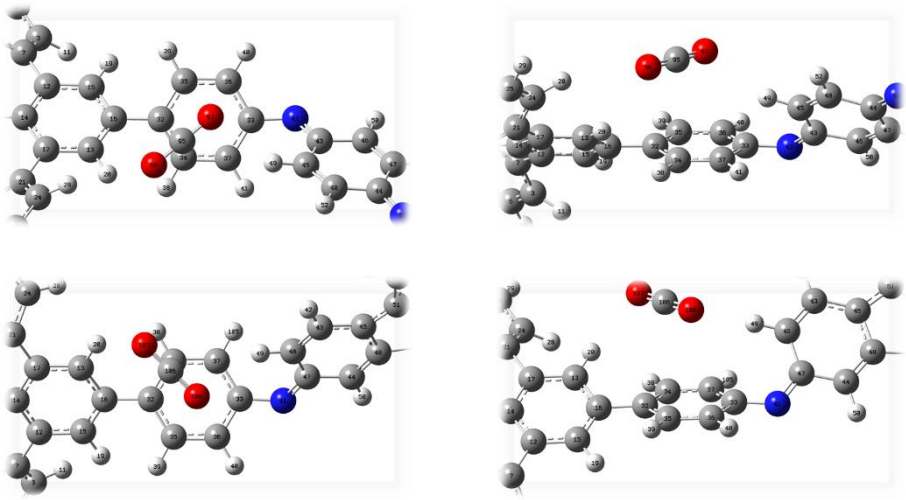

*Figure 5-14 Binding geometries of CO_2 onto **TPB** core units of **OTPB-BZN-210** (top) and **OTPB-FLR-210** (bottom) from top and tilt front views (DFT-optimised, B3LYP-D3(BJ)/6-31G(d)/Aniline PCM, visualised in GaussView 6.1.1)*

In the case of **TPB** core units, there are significant differences between **OTPB-BZN-210** and **OTPB-FLR-210**. The conformer of the triphenylbenzene core in the DFT-optimised structure of the former has the hub ring and the blade rings (see Section 3.2.2.1) twisted in the different ways from those in the latter, resulting in different numbers of hydrogen atoms in the vicinity of

the CO_2 molecules and different numbers of hydrogen bonds formed. For the **BZN**-linked oligomer, three hydrogen atoms are close to CO_2 oxygen atoms, namely H^{20} from the hub ring, H^{28} from the blade ring, and H^{49} from the **FLR** unit (Figure 5-14). In the case of the **FLR**-linked oligomer, however, phenyl rings from the **TPB** were twisted differently, which caused H^{28} to be further away from the CO_2 molecule (2.795 Å in **OTPB-BZN-210**, 4.177 Å in **OTPB-FLR-210**). This difference in hydrogen bonding is the most probable cause for the relatively larger difference in binding energies (2.06 kJ·mol^{-1} in **TPB** cases compared to 0.09 kJ·mol^{-1} in **TPA** cases).

*Table 5-14 Key parameters related to binding of CO_2 onto **TPT** core binding sites of **210** oligomers linked by **BZN** and **FLR** linkers*

Parameter	TPT-BZN	TPT-FLR
O–C–O angle difference	1.0°	0.7°
O···H distance	2.535 Å	2.701 Å
BQ···C distance	3.180 Å	3.238 Å
BQ···O distance	3.213 Å	3.228 Å
	3.168 Å	3.263 Å
BQ···CO_2 average distance	3.187 Å	3.243 Å
Binding energy (kJ·mol^{-1})	-23.11	-22.30

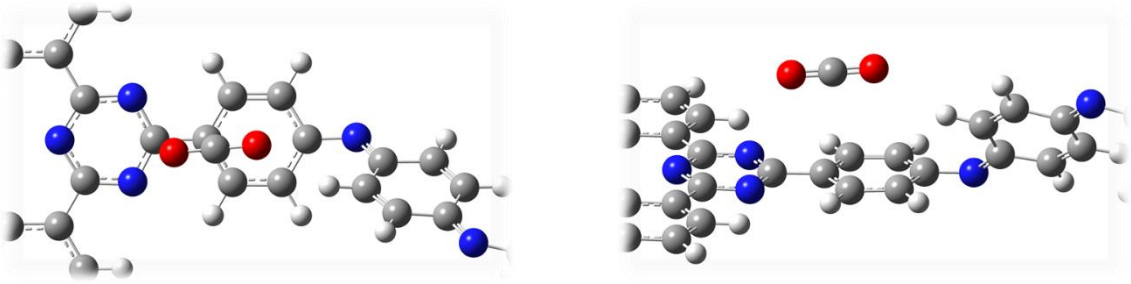

*Figure 5-15 Binding geometries of CO_2 onto the **TPT** core unit of **OTPT-BZN-210** from top and tilt front views (DFT-optimised, B3LYP-D3(BJ)/6-31G(d)/Aniline PCM, visualised in GaussView 6.1.1)*

TPT core units have the most different structures from the rest of core units in this study. Due to the lack of steric hindrances arising from *ortho* hydrogen atoms in blade parts, all three blades can be coplanar (Figure 5-15). This planar structure results in smaller numbers of hydrogen bonds formed because other hydrogen atoms in the core unit structures are too far away, which can explain why binding energies for **TPT**-based oligomers are smaller than the corresponding oligomers with **TPA** or **TPB** core units. It should also be noted that the polarity of C–N bonds in the triazine moieties might have positively contributed to and addressed the lack of hydrogen bonds.

It should also be noted that there is a difference between binding energy of **OTPT-BZN-210** and **OTPT-FLR-210** (0.81 kJ·mol^{-1}, compared to 0.09 kJ·mol^{-1} for **TPA** oligomers). This can be attributed to the difference in hydrogen bond lengths. In the case of **TPT** oligomers, O···H distances in the two oligomers differ by 0.166 Å, while the differences between corresponding pairs of oxygen-hydrogen are only roughly 0.03 Å in **TPA** oligomers.

Effects of core unit structures on the binding energies are more complicated. However, the general trend is that binding modes with more hydrogen bonds tend to be more favourable than those with fewer hydrogen bonds. The complications arise from the differences in chemical structures of the units themselves that create different numbers of hydrogen atoms available for hydrogen bonding.

5.4 Computational Studies on Adsorption of **OTPA-BZN-430** Models

Small fragments are usually chosen to represent porous materials for the theoretical studies of adsorbent-adsorbate interactions. Their smaller sizes mean that they are less demanding in terms of computational resources, allowing DFT calculations, with higher contribution from quantum mechanics, to be performed with more ease. However, one can argue that small models may not properly represent their respective materials. While this issue can be easily overcome in the cases of COFs or MOFs, which are crystalline, by the use of periodic boundary conditions (PBCs), it is more challenging in the case of CMPs or other amorphous materials. In this section, **430** models (four core units, three linker units, and no cyclisation) have been chosen to explore the feasibility of using larger models for DFT studies of interactions.

While there is only one possible arrangement for **210** oligomers, there are two possible arrangements for **430** oligomers. Structures of these oligomers can be viewed in the same way as carbon skeletons, with carbon atom being core units and C–C bonds being linker units. There are two ways for four carbon atoms to be arranged, all in the same chain (butane) or with one carbon atom branched out (isobutane). Structures of **430** oligomers can be considered in a similar way. In one case, four core and three linker units are arranged in the linear manner. In the other case, one core unit is bound to three linker units, and to each linker unit, one additional core unit is bound. The former isomer will be called linear **430** oligomer, and the latter will be called star-shaped **430** oligomer. Structures of linear and star-shaped **430** oligomers are shown in Scheme 5-5.

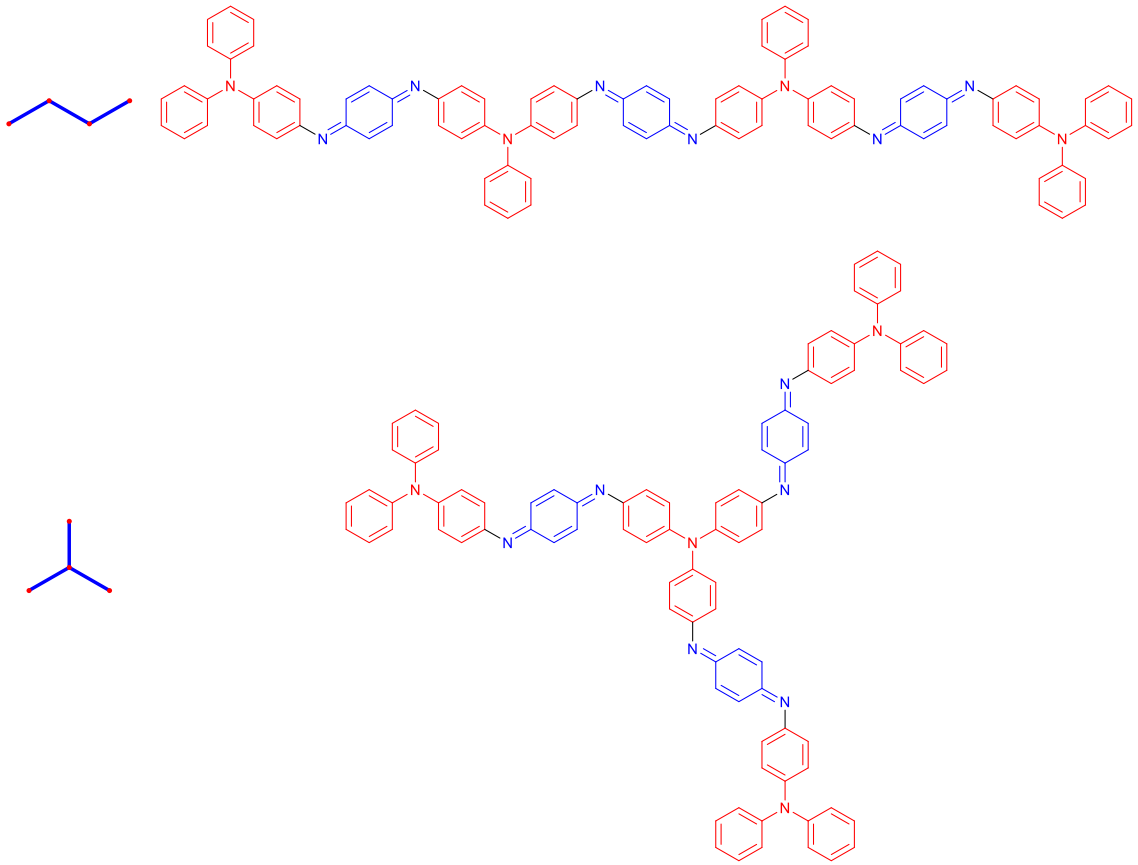

*Scheme 5-5 Structures of linear (top) and star-shaped (bottom) **OTPA-BZN-430** in **EB** state, compared to two corresponding isomers of butane*

Optimised structures of the two **430** oligomers are shown in Figure 5-16. During the conformational search and DFT optimisation processes of these oligomers, however, one

difference between the two isomers emerges. Molecular mechanics calculations used for the screening of possible conformers suggest the coiling of the linear **430** oligomer, while the subsequent DFT calculations suggest that the coiled structure of linear **430** oligomer is less favourable than the star-shaped **430** oligomer by 121.8 kJ·mol^{-1}. It is possible that the use of D3(BJ) model of electron dispersion overestimates non-covalent interactions. It might be worth exploring further whether coiling is possible for the star-shaped counterpart as well as the linear structure. However, this issue will not be discussed further in this section, beyond acknowledging that this may add noise to calculated energies.

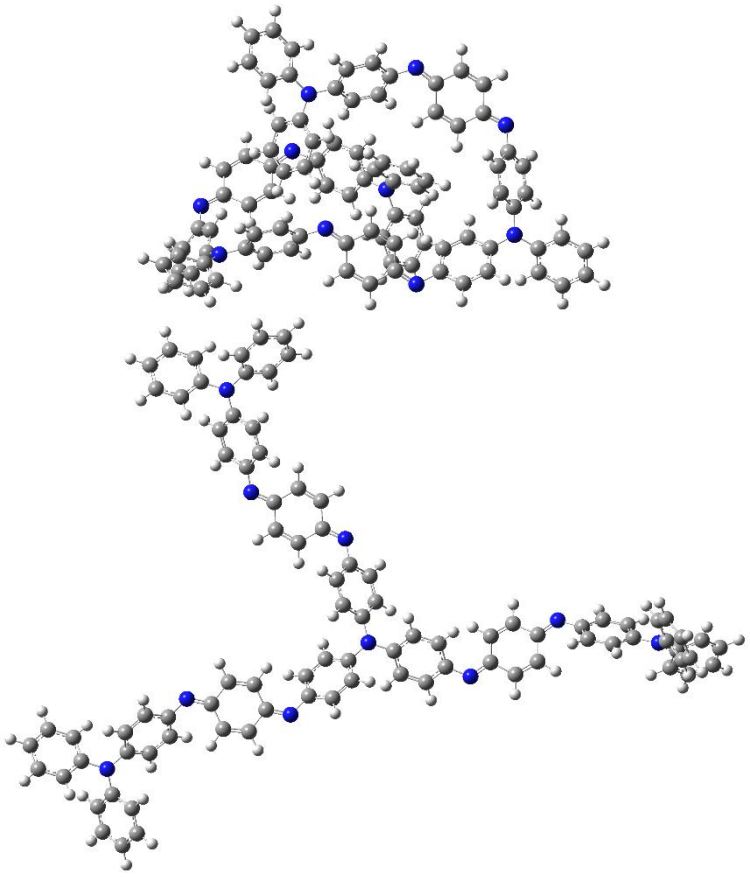

*Figure 5-16 DFT-optimised structures of linear (top) and star-shaped (bottom) **OTPA-BZN-430** oligomers*

The existence of coiling in the case of linear **430** oligomer means that binding sites on this oligomer have become more complicated. These binding modes will be discussed in their respective sections.

5.4.1 Star-Shaped **OTPA-BZN-430** Oligomer

As shown in Figure 5-16, the optimised structure of star-shaped **OTPA-BZN-430** oligomer is more straightforward compared to the coiled structure of linear oligomer. Binding sites are more or less the same as those in **210** oligomers. However, there is another issue emerging because of the asymmetry of the linker units. For each linker unit, one end is connected to a core unit, while another end is connected to a core unit which is further connected to two other branches. The latter end bears less resemblance to that of **210** oligomers. To distinguish between binding sites on the different sides of linker units, these binding site names will be modified by the word “inner” or “outer” regarding their positions towards the core unit binding will all three linkers (Figure 5-17).

Meanwhile, the structure of this star-shaped oligomer is not symmetric. To account for this radial asymmetry, binding energies from each of the corresponding binding sites on different branches will be averaged.

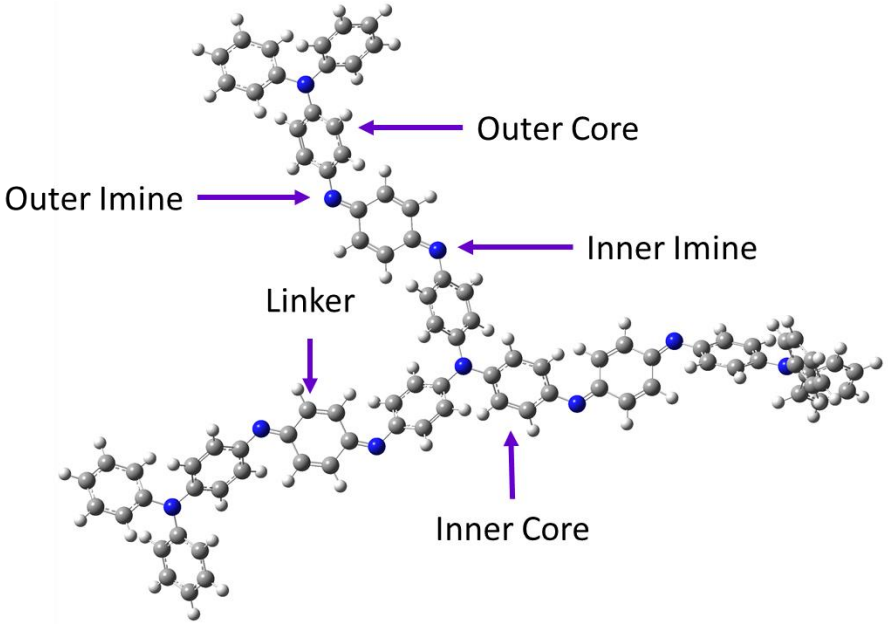

*Figure 5-17 Different binding sites on the structure of star-shaped **OTPA-BZN-430** oligomer*

*Table 5-15 Binding energies of CO_2 on the different binding sites on star-shaped **OTPA-BZN-430** oligomer compared to those binding on corresponding sites on **OTPA-BZN-210***

Star-Shaped OTPA-BZN-430						**OTPA-BZN-210**	
Binding Site	**Binding Energy (kJ·mol^{-1})**					**Binding Site**	**Binding Energy (kJ·mol^{-1})**
	Branch 1	**Branch 2**	**Branch 3**	**Average**	**Range**		
Inner Imine Group	-21.74	-22.45	-22.32	-22.17	0.71	Imine Group	-22.28
Outer Imine Group	-22.09	-22.23	-22.23	-22.18	0.14		
Linker Unit	-23.14	-23.11	-22.39	-22.88	0.75	Linker Unit	-23.00
Inner Core Unit	-24.82	-25.07	-25.24	-25.04	0.42	Core Unit	-24.93
Outer Core Unit	-23.56	-24.75	-24.70	-24.34	1.19		

Table 5-15 listed binding energies of CO_2 on different sites across the structure of star-shaped **OTPA-BZN-430** along with those of corresponding sites on **OTPA-BZN-210**, grouped by types of binding sites and branches these sites are located. Generally, the same trend can be observed, with binding energies on imine sites being lower than those of linker sites and then core sites. Apparently, there is no significant difference between binding energies from inner and outer imine groups and between binding energies from larger and smaller models although the energies from inner sites fluctuate more compared to those from outer sites. Meanwhile, for the core unit binding sites, binding energies of inner sites are slightly greater in magnitude (-25.04

kJ·mol^{-1} for inner sites, -24.34 kJ·mol^{-1} for outer sites). It should also be noted that the difference of 0.70 kJ·mol^{-1} is comparable to that of losing or gaining one weak hydrogen bond as a result of conformational changes, among other factors.

5.4.2 Linear **OTPA-BZN-430** Oligomer

Because the structure of linear **OTPA-BZN-430** oligomer is more complicated due to coiling, it is less practical to either control the conformer or differentiate binding sites. Instead, five different cavities or sites where a molecule of CO_2 can be accommodated were chosen randomly for further optimisation. Details regarding these initial positions and resulting optimised structures will be listed in the appendix.

One major issue emerging from the optimisations of these complexes is the convergence towards the optimised structures. Optimisation processes for linear **430** oligomer complexes with CO_2 took significantly longer, even when performed with 24 processors, and failed to finish in the initially set time frame of one week. For comparison, optimisations for star-shaped counterparts, with the same numbers of atoms and electrons, were performed with 8 processors and usually finished within three days. The convergence issue might emerge not from the numbers of atoms involved alone, but from the numbers of atom pairs of which interactions between them cannot be neglected. For an atom, coiling brings more atoms in the vicinity of that atom and increases the number of interacting atoms significantly. Such increases cause the time to calculate the energy of each step towards the optimised structure to increase. Details of optimisation processes are listed in Section A.4.8.1 in the Appendix.

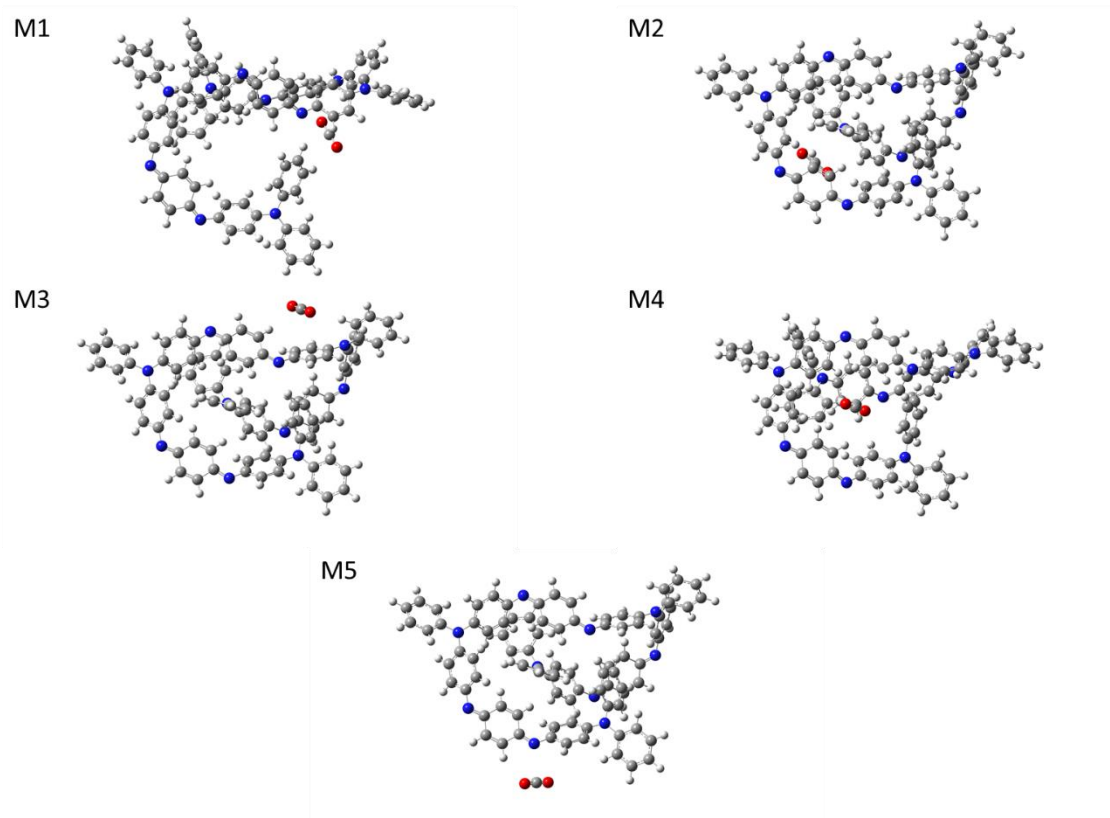

*Figure 5-18 Optimised structures of oligomer–CO_2 from coiled **OTPA-BZN-430** oligomer in five different modes*

*Table 5-16 Binding energies of CO_2 onto coiled **OTPA-BZN-430** oligomer fragment calculated from optimised structures of the oligomer before binding (second column) and from single-point energy (SPE, see main text) of the optimised structures of the oligomer after binding with CO_2 molecule removed (third column) along with differences between binding energies calculated from the two methods*

Binding Mode	Binding Energy ($kJ \cdot mol^{-1}$)	SPE-Corrected Binding Energy ($kJ \cdot mol^{-1}$)	Energy Difference ($kJ \cdot mol^{-1}$)
M1	+17.32	-30.77	+48.09
M2	-161.47	-40.85	-120.61
M3	-145.59	-24.54	-121.04
M4	-132.34	-37.26	-95.08
M5	-143.73	-22.06	-121.67

Table 5-16 lists different binding energies based on two difference calculating methods. The second column shows energies calculated using Equation 5-1, while the third column shows energies calculated using the single-point energies (SPEs) of oligomer fragments after CO_2 binding with the CO_2 molecule removed. This SPE-based correction has become necessary in the case of **OTPA-BZN-430** since the structures of oligomers might change significantly upon binding with the CO_2 molecule. These structure changes are most obvious in the case of binding mode M1 (Figure 5-18), in which the oligomer uncoils, resulting in an increase in energy. The other four cases, however, alter the oligomer structures which cause the energies to be far lower than the optimised structure prior to CO_2 uptake. It is possibly because the insertion of a CO_2 molecule might enable the fragment to overcome local barriers from the previous local minimum to the new minima. Nonetheless, correcting binding energies with SPEs has produced energies within more reasonable and comparable ranges.

After removing effects from the changes in oligomer structures, binding energies can be divided into two groups based on their magnitudes and corresponding binding modes. Modes M3 and M5 produce smaller binding energies than the other three modes, and considering their binding modes, the CO_2 molecule interactions are almost similar to those on the **210** oligomers (linker unit binding site for mode M3 and imine group binding site for mode M5). Meanwhile, the other three modes have the CO_2 molecule interacting with more than one binding site. More interactions mean larger binding energies as a result.

It is reasonable to conclude that in the larger porous material structures, where a CO_2 molecule can interact with more than one binding site or non-covalent bond donor/acceptor simultaneously, binding energies can be larger or even multiplied. This phenomenon has also been observed in other studies.[29, 35] However, using DFT optimisations on these coiled large models might not be a practical method for the study of interactions between oligomer fragments and CO_2, considering the difficulties in convergences during optimisation processes. It would be more sensible to assume that the oligomer structures remain almost unchanged upon the interaction with the CO_2 molecule, which has been the case in **210** oligomers. This way would reduce the problem down to model of PANI-CMP fragments accurately.

5.5 Conclusions and Remarks

Non-covalent interactions, which are the major types of interactions found in physisorptions on porous material surfaces, between PANI-CMP oligomer fragments and CO_2 molecules have been studied using DFT calculations. Three different types of binding sites have been identified, namely imine/amine group, core unit, and linker unit binding sites, and most non-covalent interactions between oligomer fragments and CO_2 molecules are either tetrel bonds, formed between CO_2 carbon atoms and imine/amine nitrogen atoms, or hydrogen bonds, formed

between hydrogen atoms with positive partial charges from the oligomers and CO_2 oxygen atoms. While changing monomer units (core or linker) can yield different binding sites with different geometric structures, these two non-covalent bonds are still the main contributors.

There are, however, several issues that need to be considered for further studies, especially for the validation of theoretical data against experimental data. The first issue is the effects from conformers. Some monomer units may exist in multiple different conformers with similar energies, but these conformers might interact differently with a CO_2 molecule, which is the case for **TPB** core units, for example. Different conformers should be taken into account to accurately predict the binding energies based on monomer units. They can be weighed by their ratios according to Boltzmann distributions, for example.

Systematic errors resulting from computational methods can also be an issue. Some computational methods can overestimate or underestimate the effects from interactions, leading to errors in binding energies. However, as discussed, such misestimations can only be detected directly in the case of smaller molecules, for which experiments can be designed practically.

Another issue is the practicality of using DFT calculations for the optimisation of large oligomer fragments, which has been the case for amorphous porous materials such as CMPs, including PANI-CMPs. Optimisations of these large fragments have been proven to be expensive in terms of resources and calculation time. Since the binding energies corrected by single-point energies are in the more reasonable range than binding energies calculated from optimised structures, DFT optimisations of oligomer fragments may be wasteful. While accurate or reasonably accurate structures of polymers are still required for accurate placements of atoms involving in non-covalent interactions, they can be obtained via other methods that allow large systems to be optimised such as specifically created QM-MM/MD methods, for example. These methods will be discussed in Section 6.1.1.1.

5.6 References

1. P. A. Kollman, *Acc. Chem. Res.*, 1977, **10**, 365-371.
2. E. R. Johnson, S. Keinan, P. Mori-Sánchez, J. Contreras-García, A. J. Cohen and W. Yang, *J. Am. Chem. Soc.*, 2010, **132**, 6498-6506.
3. F. London, *Trans. Faraday Soc.*, 1937, **33**, 8b-26.
4. J. H. Williams, *Acc. Chem. Res.*, 1993, **26**, 593-598.
5. A. C. Legon, *Phys. Chem. Chem. Phys.*, 2017, **19**, 14884-14896.
6. E. Arunan, G. R. Desiraju, R. A. Klein, J. Sadlej, S. Scheiner, I. Alkorta, D. C. Clary, R. H. Crabtree, J. J. Dannenberg, P. Hobza, H. G. Kjaergaard, A. C. Legon, B. Mennucci and D. J. Nesbitt, *Pure Appl. Chem.*, 2011, **83**, 1619-1636.
7. E. Arunan, G. R. Desiraju, R. A. Klein, J. Sadlej, S. Scheiner, I. Alkorta, D. C. Clary, R. H. Crabtree, J. J. Dannenberg, P. Hobza, H. G. Kjaergaard, A. C. Legon, B. Mennucci and D. J. Nesbitt, *Pure Appl. Chem.*, 2011, **83**, 1637-1641.
8. G. R. Desiraju, P. S. Ho, L. Kloo, A. C. Legon, R. Marquardt, P. Metrangolo, P. Politzer, G. Resnati and K. Rissanen, *Pure Appl. Chem.*, 2013, **85**, 1711-1713.
9. R. Dawson, E. Stöckel, J. R. Holst, D. J. Adams and A. I. Cooper, *Energy Environ. Sci.*, 2011, **4**, 4239-4245.
10. W. Lu, D. Yuan, J. Sculley, D. Zhao, R. Krishna and H. C. Zhou, *J. Am. Chem. Soc.*, 2011, **133**, 18126-18129.
11. Q. Chen, M. Luo, P. Hammershoj, D. Zhou, Y. Han, B. W. Laursen, C. G. Yan and B. H. Han, *J. Am. Chem. Soc.*, 2012, **134**, 6084-6087.
12. H. A. Patel, S. Hyun Je, J. Park, D. P. Chen, Y. Jung, C. T. Yavuz and A. Coskun, *Nat. Commun.*, 2013, **4**, 1357.
13. P. Arab, M. G. Rabbani, A. K. Sekizkardes, T. İslamoğlu and H. M. El-Kaderi, *Chem. Mater.*, 2014, **26**, 1385-1392.

14. Q. Chen, D. P. Liu, M. Luo, L. J. Feng, Y. C. Zhao and B. H. Han, *Small*, 2014, **10**, 308-315.
15. B. Ashourirad, A. K. Sekizkardes, S. Altarawneh and H. M. El-Kaderi, *Chem. Mater.*, 2015, **27**, 1349-1358.
16. N. Popp, T. Homburg, N. Stock and J. Senker, *J. Mater. Chem. A*, 2015, **3**, 18492-18504.
17. G. Chang, Z. Shang, T. Yu and L. Yang, *J. Mater. Chem. A*, 2016, **4**, 2517-2523.
18. F. Jiang, T. Jin, X. Zhu, Z. Q. Tian, C. L. Do-Thanh, J. Hu, D. E. Jiang, H. L. Wang, H. L. Liu and S. Dai, *Macromolecules*, 2016, **49**, 5325-5330.
19. S. L. Qiao, H. Wei, T. Wang, W. Huang, C. Y. Gu, R. Q. Yang and X. Y. Li, *New J. Chem.*, 2016, **40**, 3172-3176.
20. G. Deng and Z. Wang, *ACS Appl. Mater. Interfaces*, 2017, **9**, 41618-41627.
21. G. Li, C. Yao, J. Wang and Y. Xu, *Sci. Rep.*, 2017, **7**, 13972.
22. S. S. Hou and B. Tan, *Macromolecules*, 2018, **51**, 2923-2931.
23. S. Xu, J. He, S. Jin and B. Tan, *J. Colloid Interface Sci.*, 2018, **509**, 457-462.
24. A. Comotti, F. Castiglioni, S. Bracco, J. Perego, A. Pedrini, M. Negroni and P. Sozzani, *Chem. Commun.*, 2019, **55**, 8999-9002.
25. X. F. Liu, C. Y. Xu, X. H. Yang, Y. B. He, Z. Y. Guo and D. Yan, *Microporous Mesoporous Mater.*, 2019, **275**, 95-101.
26. Z. Yang, S. Wang, Z. Zhang, W. Guo, K. Jie, M. I. Hashim, O. Š. Miljanić, D. e. Jiang, I. Popovs and S. Dai, *J. Mater. Chem. A*, 2019, **7**, 17277-17282.
27. A. J. Neel, M. J. Hilton, M. S. Sigman and F. D. Toste, *Nature*, 2017, **543**, 637-646.
28. R. K. Raju, J. W. G. Bloom, Y. An and S. E. Wheeler, *ChemPhysChem*, 2011, **12**, 3116-3130.
29. H. M. Lee, I. S. Youn, M. Saleh, J. W. Lee and K. S. Kim, *Phys. Chem. Chem. Phys.*, 2015, **17**, 10925-10933.
30. M. Becucci, F. Mazzoni, G. Pietraperzia, J. Řezáč, D. Natchigallová and P. Hobza, *Phys. Chem. Chem. Phys.*, 2017, **19**, 22749-22758.
31. M. Li, J. Lei, G. Feng, J.-U. Grabow and Q. Gou, *Spectrochim. Acta, Part A*, 2020, **238**, 118424.
32. W. Y. Cheng, Y. Zheng, S. Herbers, H. L. Zheng and Q. Gou, *ChemPhysChem*, 2021, **22**, 154-159.
33. M. Wang, X. Fan, L. Zhang, J. Liu, B. Wang, R. Cheng, M. Li, J. Tian and J. Shi, *Nanoscale*, 2017, **9**, 17593-17600.
34. Y. Zhang, W. Z. Wang and Y. B. Wang, *Comput. Theor. Chem.*, 2019, **1147**, 8-12.
35. D. Sahu, K. Jana and B. Ganguly, *New J. Chem.*, 2017, **41**, 12044-12051.
36. S. Sarfaraz, M. Yar, M. Ans, M. A. Gilani, R. Ludwig, M. A. Hashmi, M. Hussain, S. Muhammad and K. Ayub, *RSC Adv.*, 2022, **12**, 3909-3923.
37. S. T. Kostakoglu, Y. Chumakov, Y. Zorlu, A. E. Sadak, S. Denizalti, A. G. Gurek and M. M. Ayhan, *Mater. Adv.*, 2021, **2**, 3685-3694.
38. B. M. Mills, Z. Shao, S. R. Flynn, P. Rannou, D. M. Lindsay, N. Fey and C. F. J. Faul, *Mol. Syst. Des. Eng.*, 2019, **4**, 103-109.
39. B. M. Mills, N. Fey, T. Marszalek, W. Pisula, P. Rannou and C. F. J. Faul, *Chem. - Eur. J.*, 2016, **22**, 16950-16956.
40. S. Grimme, S. Ehrlich and L. Goerigk, 2011, **32**, 1456-1465.
41. S. J. Grabowski, in *Understanding Hydrogen Bonds: Theoretical and Experimental Views*, The Royal Society of Chemistry, 2021, pp. 1-40.
42. J. O. Thomas, H. D. Andrade, B. M. Mills, N. A. Fox, H. J. Hoerber and C. F. J. Faul, *Small*, 2015, **11**, 3430-3434.
43. S. G. Kazarian, M. F. Vincent, F. V. Bright, C. L. Liotta and C. A. Eckert, *J. Am. Chem. Soc.*, 1996, **118**, 1729-1736.
44. A. A. Gabrienko, A. V. Ewing, A. M. Chibiryaev, A. M. Agafontsev, K. A. Dubkov and S. G. Kazarian, *Phys. Chem. Chem. Phys.*, 2016, **18**, 6465-6475.

Chapter 6 Conclusions and Further Opportunities

This chapter serves to discuss the overall conclusions from the experimental and computational studies of structure-property relationships (SPRs) in PANI-CMPs along with suggestions for further studies. Discussions in this chapter will be divided into two main focus areas, the theoretical studies (Section 6.1) and the experimental studies (Section 6.2). In each dedicated section, there are an overall conclusion related to the SPR in PANI-CMPs and other suggestions for additional experiments required to achieve a better and more complete understanding of PANI-CMPs in terms of structures, properties, and relationships among them.

6.1 Theoretical Studies of PANI-CMPs

The main conclusion from theoretical studies of PANI-CMPs is that some properties of PANI-CMPs are too complicated to be predicted or explained solely based on oligomeric models. Attempts at modelling PANI-CMPs can be categorised into two groups based on the systems to recreate. In Chapter 3, structures of PANI-CMPs were modelled, aiming to build models for geometric and electronic structures of PANI-CMPs. In Chapter 5, discussions were focused on non-covalent interactions (NCIs) between PANI-CMP fragments and CO_2 molecules. While the two subfields of the theoretical studies have led to the same conclusion that models of higher complexities are required to portray the properties of PANI-CMPs more accurately, there are different details that should be explored separately in each own dedicated section.

6.1.1 Modelling Structures of PANI-CMPs

In this study, four hierarchical levels of polymer structures have been established, see Section 3.1 for details of each level. Oligomeric models used in this thesis cover up to the secondary structures of polymers, which concern the arrangements of BQ units in the oligomer structures including alignments of adjacent BQ units and chain topologies. In this work, these oligomeric models can be applied successfully to the detailed studies of primary and secondary structures of branched oligo(aniline)s. However, despite earlier successes for the studies of oligo(aniline)s, these models cannot be translated directly into models for PANI-CMPs yet, especially for the optoelectronic properties (Section 3.3.3). These models do not portray other aspects of the PANI-CMP structures that can affect optoelectronic properties such as π-π NCIs, which are the interactions that can take place between BQ units that are not covalently bound. Arguably, optoelectronic properties of PANI-CMPs would be more related to tertiary structures, which consider NCIs between different BQ units, or even the quaternary or the bulk structures themselves rather than the secondary structures corresponding to the oligomeric models. Opportunities for the modelling of high-level PANI-CMP structures will be discussed in Section 6.1.1.1. Meanwhile, there are some gaps left in the studies of PANI-CMP secondary structures that have not been covered yet in this thesis, which may be topics for further studies of oligo(aniline)s. These gaps will be discussed in Section 6.1.1.2.

6.1.1.1 Modelling Tertiary and Quaternary Structures of PANI-CMPs

Structures of higher levels in the hierarchy of structures are required for simulations of such properties. These high-level structures might not be simulated using the same techniques or levels of theory due to technical limitations. Therefore, different approaches might be needed for the structures of tertiary and quaternary levels, especially for the latter where the number of atoms involved in the system can be thousands or millions. For the simplicity of methodological discussion, the border between tertiary (multiple fragments interacting) and quaternary (bulk) levels will be set where the limitations of quantum methods (DFT or HF) are.

Tertiary structures of PANI-CMPs concern the interactions among fragments of PANI-CMPs that may not be directly bound. Structures of this level have been explored only during the

study of interactions between PANI-CMP fragments and CO_2 molecules in Chapter 5, which is not directly related to the studies of PANI-CMP structures. DFT optimisations with dispersion models of linear **430** oligomers (four core units, three linker units, no cycle, see Section 5.4.2) have resulted in coiled structures. The coiling behaviour implies that it is possible for polymer fragments that are separated by other chemical moieties to interact.

While optimisations of linear **430** oligomers reveal the possibility for NCIs, their structures can still be complicated. Arguably, NCIs between oligomer fragments can be represented more simply by, again, **210** oligomers. Their simple structures mean that it is easier to set initial positions for optimisations and easier to identify different interacting modes. These results can then be applied towards the larger and more complicated models to assist the identifications in such systems.

The more serious challenge for the optimisation of **430** oligomers is the convergence towards the optimised structures. Since there are more atoms in the vicinity in the case of unbranched oligomers compared to the branched ones where chains are too short to interact, optimisation processes of unbranched oligomers usually take longer time and more processors to achieve. These significant increases in optimisation times and resources have shown that the limits for DFT optimisations might have been reached. Therefore, for the bulk structures of PANI-CMPs, QM-heavy methods such as DFT or HF are no longer applicable, and molecular mechanics (MM) have become the main methods of choice.

Bulk structures of microporous polymers, including CMPs, have been simulated by various MM-based approaches. These approaches can be categorised into two types, reconstructive and mimetic.[1] The two approaches are comparable to the classical "top-down" and "bottom-up" approaches. The reconstructive approaches rely on creating large models to match experimental results, which are similar to the "top-down" approaches. Meanwhile, the mimetic approaches rely on simulating the steps in the polymerisation processes from monomers to larger monomers, which are similar to the "bottom-up" approaches discussed in this thesis.

Optimisation of bulk structures and interactions between bulk structures and adsorbate molecules can be performed using two different techniques, Monte Carlo (MC) and molecular dynamics (MD).[1] The two techniques differ in how they generate the next step in the simulation. On the one hand, MC is a statistical method which uses randomness to generate the next step and uses probabilities to decide whether the next step is accepted or rejected. On the other hand, MD is a dynamics method which uses classical mechanics to decide the movements of atoms and molecules and is time-dependent in nature.

For the artificial creations of bulk microporous polymer structures from monomers, several computational codes have been developed and published in literature including *Polymatic*[2] and *Ambuild*.[3] Both examples form the new bonds between monomer units when the two moieties are moved into the vicinity within the cut-off range. However, the difference between the two examples is that *Polymatic* uses only monomers in the structure-building process while *Ambuild* also includes catalysts and solvents, which allows other factors such as concentrations and ratios of catalyst loads to be considered. Nonetheless, after bulk structures have been built, regardless of the computational codes or procedures used, the resulting structures have to undergo compression and relaxation steps, usually until the densities of simulated materials match desired or experimentally obtained values.[1] These bulk structures, after compressions and relaxations, have been found to match morphological properties of synthesised materials and enable local structural features that cannot be determined experimentally in amorphous materials, such as analyses of substructures, to be performed.[3-7]

6.1.1.2 Gaps in Theoretical Studies of PANI-CMP Secondary Structures

This study has used DFT methods to optimise secondary structures of PANI-CMP oligomeric models (Section 3.2.2), with each model consisting of two core units and one or two linker units. Structures of these optimised models have been analysed using various descriptors. Computational studies at the level performed in this thesis have covered only primary and secondary structures of PANI-CMPs due to the sizes of selected models.

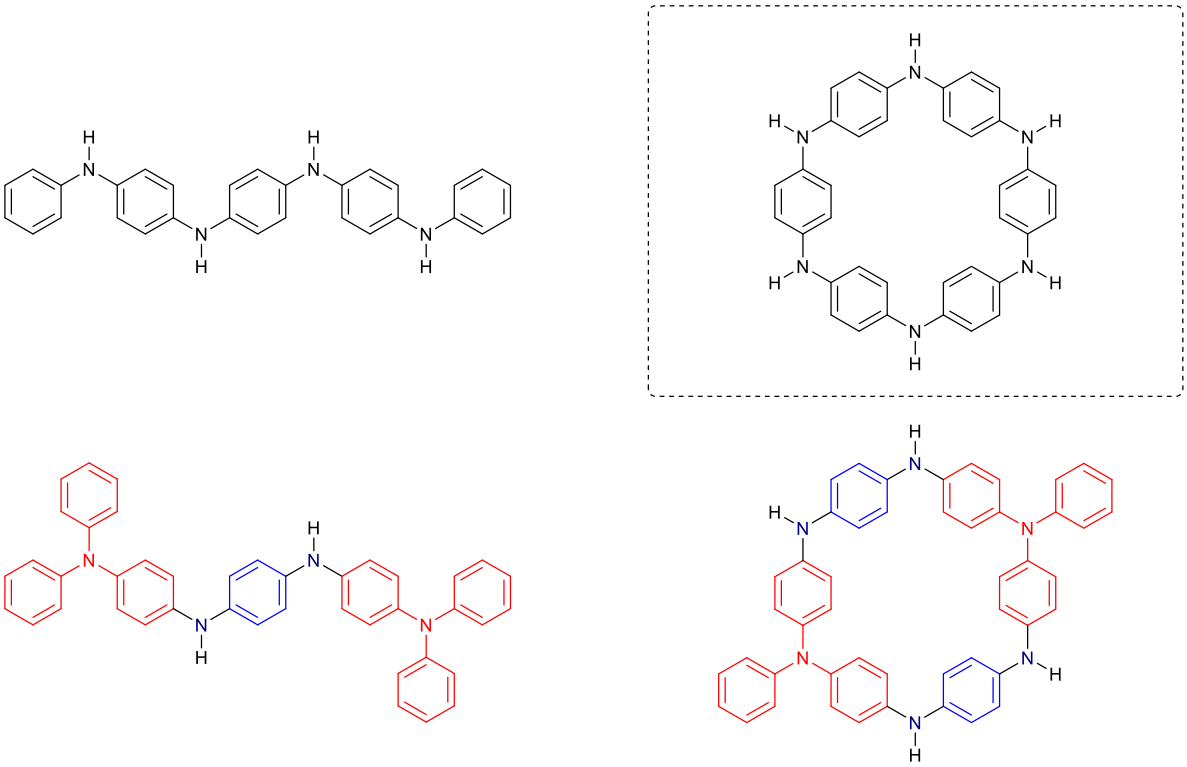

Scheme 6-1 Oligo(aniline)s containing different topological features, namely branches and cycles. Unbranched cyclic oligomers (an example of which encased in a dashed frame) are not discussed in this thesis.

Two different topological features, branch and cycle, have been studied in this study, represented by two types of oligo(aniline)s, **210** (two core units, one linker units, no cycle) and **221** (two core units, two linker units, one cycle) oligomers, see Scheme 6-1. For **210** oligomers, it has been found that branching at nitrogen atoms creates BQ units that can stabilise positive charges, resulted from oxidation, better than those in the unbranched oligomers. While it is also proven that higher steric hindrance, which resulted from branching, affects geometric structures of oligomers, the effects on electronic structures are not significant. Meanwhile, the effects from cyclisation in **221** oligomers can be complicated by the effects of branching, and additional studies on unbranched counterparts are still required.

The **210** oligomeric models are the simplest oligomeric models of PANI-CMPs because of their symmetries and the fact that each of these models has only one linker unit. Their simplicities are helpful for the delineation of contributing electronic transitions. However, these models can be too simple to capture optoelectronic properties of actual PANI-CMPs or their larger oligomers. There are multiple linker units in poly- and oligo(aniline) systems. Even in the symmetric systems such as in the **221** oligomeric models, multiple excited states with similar energies can exist. These excited states are similar in energies because the origin and destination orbitals are similar in energies, only differing by symmetry elements. Therefore, for better comparisons between uncyclised and cyclised oligomers, **320** oligomeric models with two linker units in each model should be used to represent uncyclised oligomers.

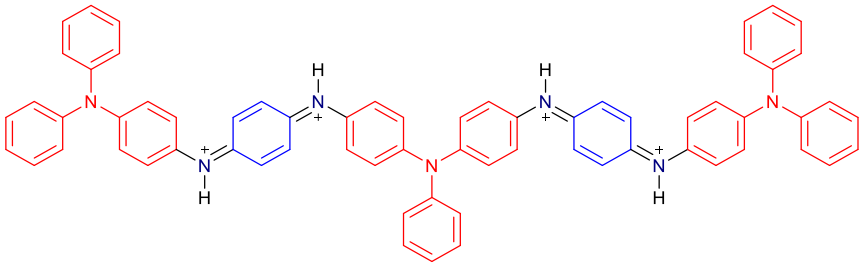

*Scheme 6-2 A structure of **OTPA-BZN-320** in the singlet **ES** state*

Since electronic transitions in oligo(aniline)s are charge transfers in nature, in larger systems of PANI-CMP oligomers with more than two linker units, there are more possibilities for charge transfers to happen. Besides, if the chains are long enough, such as in linear **430** oligomers, it is possible for NCIs to occur, which can create further complications in electronic transitions since it has yet to be determined whether charge transfers in branched oligo(aniline)s can take place between core and linker units that are not covalently bonded directly.

Another issue for theoretical studies of PANI-CMP oligomers in this work is that there is no verification against experimental data for optimised structures. The verification could be achieved by synthesising the actual oligomers and performing analyses on their structures.[8, 9]

6.1.2 Interactions between PANI-CMPs and Adsorbate Molecules

For the study of NCIs between PANI-CMP fragments and CO_2 molecules, the use of secondary level models can help to identify different binding sites on the fragments. The binding energies calculated from these models are of similar magnitudes as the $\Delta H°_{ads}$ values obtained from synthesised PANI-CMPs. However, these models, again, might not be sufficiently accurate models for PANI-CMPs yet. Larger oligomeric models have been attempted in this study (Section 5.4), and larger binding energies are obtained from the studies of larger models. Larger models also provided instances in which the CO_2 molecule can interact with multiple binding sites simultaneously, which have been shown in the literature to increase the binding energies.[10] Therefore, larger models of oligomers are required in future studies.

Another issue for the studies in this thesis is that only one set of functional, basis set, and dispersion model has been used for calculations of binding energies. It is likely that different combinations of initial conditions for calculations will yield different numbers or even different trends entirely. However, it is less practical to experimentally validate calculated data in the case of interactions between CO_2 molecules and PANI-CMP surfaces since related analysis techniques such as Fourier-transform microwave (FTMW) spectroscopy are less practical for non-volatile polymers. Therefore, for large and structurally complicated PANI-CMPs, isosteric enthalpies of adsorption appear to be the only practical descriptors that can be obtained experimentally. However, FTMW spectroscopic analysis of structures of the adducts between PANI-CMP oligomers and CO_2 can be performed using smaller model oligomers instead of polymers, and their results can be compared to those obtained from calculations.

6.2 Experimental Studies of PANI-CMPs

A number of PANI-CMPs have been synthesised in this study from different building blocks using different synthesis pathways and conditions. The syntheses of PANI-CMPs in this thesis involve three core monomers, two linker monomers, two functionality pathways, three functional group ratios, and two options for solubility parameter tuning, which should produce 72 different materials if all planned materials successfully produce polymers. In total, 47 different PANI-CMPs have been successfully produced out of 72 initially planned. While the number of materials appear to be ample, clear conclusions related to SPRs in PANI-CMPs can still not be

drawn. The only conclusion that can be drawn from the experimental studies is that SPRs in PANI-CMPs are less straightforward than initially anticipated, and therefore, more data from more systematic studies are required to create the clearer "big pictures" of SPRs in PANI-CMPs. This issue will be discussed in detail in Section 6.2.1.

Meanwhile, there are some gaps that could not be addressed over the course of this PhD study that can be opportunities for further studies of PANI-CMPs. These opportunities will be discussed in Section 6.2.2.

6.2.1 Systematic Studies of Structure-Property and Property-Property Relationships

Although different materials in this study have different properties, the relationships between monomer structures and morphological properties cannot be clearly observed. In fact, even among materials prepared from the same pair of core and linker monomers, properties of resulting polymers still vary depending on factors other than the monomers themselves. It has been proven in this study that two out of three non-structural factors, namely functionality pathways and solubility parameter tuning options, have affected the porosity properties of resulting PANI-CMPs. Meanwhile, while not investigated during the course of this study due to the impacts of the COVID-19 pandemic, the ratios between different monomers have been proven in the literature to also affect the porosity properties of CMPs.[11] Arguably, for a given pair of core and linker monomers, properties related to porosities of resulting PANI-CMPs can still be affected by other factors totally unrelated to the monomer structures themselves.

Beside the interferences from non-structural factors discussed earlier, complications related to SPRs in PANI-CMPs can also be the result of the complicated relationships among properties of materials themselves. One material property may be dictated by multiple predecessor properties. BET surface areas of different PANI-CMPs are an example of this complication since they are influenced by non-structural factors as well as monomer structures. Another example of this multiple-on-one influence can also be seen between BET surface areas and the uptakes of CO_2. While PANI-CMPs with low surface areas performed worse for CO_2 adsorptions, PANI-CMP with highest BET surface area and PANI-CMP with highest uptake of CO_2 are not the same material. The nonlinear relationship between BET surface areas and CO_2 uptakes proves that there are more governing factors other than BET surface areas for the uptake of CO_2. Indeed, there are additional aspects that need to be considered in further studies such as the non-covalent interactions between CO_2 molecules and PANI-CMP surfaces (discussed in Chapter 5), microporosities, and pore volumes (discussed in Chapter 4).

Further studies of PANI-CMPs should focus not only on the relationships between structures of monomers and the properties of PANI-CMPs synthesised, but also on the relationships among different properties of PANI-CMPs as well. The relationships among different properties can be in two main ways. Firstly, one factor may correlate with another factor. One example in this thesis is the linear relationship between Monte Carlo surface areas from CO_2 adsorption isotherms and CO_2 uptakes of PANI-CMPs, see Section 4.6.1. This linear correlation implies that surface areas accessible to the particular adsorbate molecules might be more relevant to the uptakes of the same adsorbate than the surface area measured from the standard probe adsorbate. Secondly, one factor is influenced by several preceding factors rather than only one. In this case, detailed and systematic studies, in which all or most unrelated factors are controlled, are required. For example, for the study between monomer structures and BET surface areas, the synthesis conditions for a given pair of core and linker monomers should be controlled and optimised, using the BXJ solubility parameter tuning method,[12, 13] so that the highest possible surface area of that monomer pair at a given ratio is achieved. In turn, different materials with different BET surface areas will be produced from the same monomers, which can

then be subjected to CO_2 adsorption analyses, for example, to compare materials with different porosities and microporosities and measure the effects of these factors on the uptakes of CO_2. Data from these series of materials can then be mapped to see the relationships between different pairs or groups of factors.

6.2.2 Further Explorations of PANI-CMP Properties

As mentioned, there are several other aspects of PANI-CMPs other than SPRs to be explored further in future studies. These aspects can be loosely divided by the three stages of PANI-CMP developments, namely syntheses, analyses, and applications. This section is by no mean exhaustive.

6.2.2.1 Different Synthesis Methods of PANI-CMPs

Prior to the publication of the BXJ method, syntheses of PANI-CMPs have been attempted using high-pressure autoclaves (Section 4.2). While PANI-CMPs synthesised at elevated pressures have higher surface areas than those synthesised at ambient pressure, there is an additional cost from the use of specialised autoclaves compared to the BXJ solubility tuning that can be performed at normal pressure. Therefore, this pressurised method has been abandoned in favour of the BXJ tuning instead. However, since properties of CMPs are known to be easily affected by non-structural factors, syntheses of PANI-CMPs at high pressures might be worth exploring.

6.2.2.2 Further Analyses of PANI-CMPs

There are several other properties of poly(aniline)s and their derivatives that have been analysed and reported before but not explored in this thesis. For example, several spectroscopic properties of PANI-CMPs have not been explored yet, although used in prior studies of PANI-CMPs and their oligomeric derivatives, such as solid state ^{13}C NMR spectroscopy,[14] X-ray photoelectron spectroscopy (XPS),[15] and electron paramagnetic resonance (EPR) spectroscopy.[9] The first two techniques can be used to determine the ratio of BQ units in benzenoid (unoxidised) and quinoid (oxidised) forms since BQ units in these different forms have different signals. Meanwhile, the EPR spectroscopy is helpful for the determination of uncoupled electrons or radicals in the doped states.

Besides ^{13}C NMR and XPS spectroscopic techniques, redox reactions of PANI-CMPs can also be observed using electrochemistry-based techniques such as cyclic voltammetry (CV) and differential pulsed voltammetry (DPV).[16] In the previous publication, DPV measurements have been used to trace different redox reactions as oligo(aniline)s being oxidised from the **LEB** state to the fully oxidised state. These electrochemistry techniques can be performed on PANI-CMPs and oligomers to compare the oxidation reactions between the two groups of materials.

6.2.2.3 Explorations of Other Adsorbates

Developments of porous materials for adsorption are not limited to only CO_2. Several publications have mentioned the uses of porous materials for adsorption of CH_4, H_2, N_2, and water vapour among other gases. Even in the carbon capture and utilisation field alone, there is the issue of selectivity towards CO_2 against other gases that can appear in the sources of CO_2 such as exhaust gases. Therefore, it is obvious that there is the need for theoretical studies of interactions between PANI-CMPs and other adsorbate molecules.

Other fields where CMPs, including PANI-CMPs, can be applied are analytical detections and purifications.[15] These fields cover not only gases discussed earlier but other vapours and dissolved substances.

6.3 References

1. G. Kupgan, L. J. Abbott, K. E. Hart and C. M. Colina, *Chem. Rev.*, 2018, **118**, 5488-5538.

2. L. J. Abbott, K. E. Hart and C. M. Colina, *Theor. Chem. Acc.*, 2013, **132**, 1334.
3. J. M. H. Thomas, C. Mollart, L. Turner, P. Heasman, P. Fayon and A. Trewin, *J. Phys. Chem. B*, 2020, **124**, 7318-7326.
4. L. J. Abbott and C. M. Colina, *J. Chem. Eng. Data*, 2014, **59**, 3177-3182.
5. L. J. Abbott and C. M. Colina, *Macromolecules*, 2014, **47**, 5409-5415.
6. V. M. Suresh, S. Bonakala, S. Roy, S. Balasubramanian and T. K. Maji, *J. Phys. Chem. C*, 2014, **118**, 24369-24376.
7. S. Bonakala and S. Balasubramanian, *J. Phys. Chem. B*, 2016, **120**, 557-565.
8. J. O. Thomas, H. D. Andrade, B. M. Mills, N. A. Fox, H. J. Hoerber and C. F. J. Faul, *Small*, 2015, **11**, 3430-3434.
9. B. M. Mills, Z. Shao, S. R. Flynn, P. Rannou, D. M. Lindsay, N. Fey and C. F. J. Faul, *Mol. Syst. Des. Eng.*, 2019, **4**, 103-109.
10. D. Sahu, K. Jana and B. Ganguly, *New J. Chem.*, 2017, **41**, 12044-12051.
11. J. Jiang, F. Su, A. Trewin, C. D. Wood, N. L. Campbell, H. Niu, C. Dickinson, A. Y. Ganin, M. J. Rosseinsky, Y. Z. Khimyak and A. I. Cooper, *Angew. Chem. Int. Ed.*, 2007, **46**, 8574-8578.
12. J. Chen, W. Yan, E. J. Townsend, J. Feng, L. Pan, V. Del Angel Hernandez and C. F. J. Faul, *Angew. Chem. Int. Ed.*, 2019, **58**, 11715-11719.
13. J. Chen, T. Qiu, W. Yan and C. F. J. Faul, *J. Mater. Chem. A*, 2020, **8**, 22657-22665.
14. Y. Liao, J. Weber, B. M. Mills, Z. Ren and C. F. J. Faul, *Macromolecules*, 2016, **49**, 6322-6333.
15. L. Pan, Z. Liu, M. Tian, B. C. Schroeder, A. E. Aliev and C. F. J. Faul, *ACS Appl. Mater. Interfaces*, 2019, **11**, 48352-48362.
16. Z. Shao, P. Rannou, S. Sadki, N. Fey, D. M. Lindsay and C. F. J. Faul, *Chem. - Eur. J.*, 2011, **17**, 12512-12521.

Appendix A Details Related to DFT Optimisations and Microscopic Structures

This appendix section serves to provide additional details regarding DFT optimisations of chemical structures discussed in Chapters 3 and 5. Details in this appendix mostly consist of Cartesian (x, y, and z) coordinates of atoms in the optimised structures. However, for coiled linear **OTPA-BZN-430** oligomer studies, further details regarding optimisation processes of the oligomer structure itself and its interaction with CO_2 molecules are also given.

Cartesian coordinates of atoms in the optimised structures are listed as rows and columns. Each row consists of, from left to right, the element, the x-coordinate, the y-coordinate, and the z-coordinate.

In addition, descriptors related to microscopic structures, namely primary and secondary structures according to the polymer structure hierarchy discussed in Chapter 3, derived from DFT-optimised structures are also listed in this appendix section. Microscopic structures in this section cover both structures of unbound oligomers and bound oligomers with CO_2 molecules, the latter of which may have been stretched slightly beyond the primary and secondary structures.

A.1 Optimised Structures of TANI and Branched Derivatives for Microscopic Structure Analyses

A.1.1 Optimised Structures of TANI

*A.1.1.1 TANI, **LEB** State*

H	0.285924	-2.356344	0.665730
C	0.158205	-1.322761	0.353915
C	-0.159061	1.326715	-0.399976
C	-1.091440	-0.900071	-0.127481
C	1.229503	-0.442146	0.459421
C	1.090761	0.903979	0.081474
C	-1.230102	0.446003	-0.505681
H	2.169729	-0.796845	0.866075
H	-2.170439	0.800459	-0.912411
H	-0.286738	2.360330	-0.711682
H	-2.123228	-1.835538	-0.270644
H	-1.830950	-2.801406	-0.322297
H	2.121835	1.839969	0.223103
H	1.829526	2.805534	0.278864
C	-3.498571	-1.630975	-0.127350
C	-6.308739	-1.330911	0.134809
C	-4.049202	-0.510306	0.516998
C	-4.382092	-2.610261	-0.614911
C	-5.757861	-2.461224	-0.488539
C	-5.427720	-0.368176	0.649539
H	-3.398559	0.240279	0.949907
H	-3.980890	-3.490239	-1.111122
H	-6.418594	-3.226460	-0.887692
H	-5.820421	0.489221	1.185263
C	3.498623	1.633984	0.099193
C	6.311612	1.331140	-0.126736
C	4.056385	0.514218	-0.540656
C	4.376756	2.611132	0.600506
C	5.753901	2.460759	0.491788
C	5.436306	0.370592	-0.655260
H	3.410496	-0.234351	-0.984109
H	3.970113	3.490464	1.093448
H	6.410261	3.224247	0.901381
H	5.834965	-0.486024	-1.187792

H	-7.702467	-1.232098	0.288235
H	-8.200856	-2.111614	0.280205
H	7.707029	1.231195	-0.261689
H	8.206273	2.110089	-0.245098
C	-8.500351	-0.100376	0.126399
C	-10.223018	2.117728	-0.177064
C	-8.014952	1.120585	-0.376563
C	-9.865082	-0.192544	0.464741
C	-10.710973	0.900872	0.309092
C	-8.872364	2.211309	-0.517331
H	-6.976700	1.210224	-0.672549
H	-10.251872	-1.131701	0.853107
H	-11.759688	0.801236	0.576184
H	-8.474335	3.143511	-0.909750
H	-10.882595	2.972657	-0.289486
C	8.501630	0.097810	-0.095875
C	10.218405	-2.123367	0.218325
C	8.009163	-1.124735	0.396294
C	9.870303	0.189927	-0.417933
C	10.713219	-0.905024	-0.257024
C	8.863770	-2.216956	0.542402
H	6.967466	-1.214538	0.679905
H	10.262551	1.130280	-0.797825
H	11.765070	-0.805387	-0.511479
H	8.460253	-3.150370	0.926235
H	10.875761	-2.979456	0.334847

*A.1.1.2 TANI, ^{1}**ES** State*

H	0.310452	-2.346338	0.751819
C	0.191414	-1.326824	0.400218
C	-0.191438	1.326793	-0.400160
C	-1.102183	-0.874668	0.009533
C	1.264030	-0.477598	0.404870
C	1.102160	0.874637	-0.009477
C	-1.264054	0.477567	-0.404812
H	2.216706	-0.824497	0.781217
H	-2.216730	0.824461	-0.781166
H	-0.310474	2.346303	-0.751771
H	-2.121268	-1.773440	0.041092
H	-1.827373	-2.745786	0.091696
H	2.121247	1.773407	-0.041049
H	1.827350	2.745753	-0.091640
C	-3.487499	-1.588884	0.020296
C	-6.290249	-1.326972	-0.086878
C	-4.111570	-0.387737	0.433548
C	-4.296914	-2.684271	-0.369663
C	-5.661971	-2.555832	-0.428008
C	-5.479529	-0.258445	0.381145
H	-3.523914	0.411808	0.866094
H	-3.829734	-3.620942	-0.657242
H	-6.270848	-3.391841	-0.756146
H	-5.942414	0.644756	0.756462
C	3.487480	1.588859	-0.020284
C	6.290235	1.326964	0.086857
C	4.111557	0.387727	-0.433572
C	4.296894	2.684246	0.369680
C	5.661952	2.555815	0.428008
C	5.479516	0.258442	-0.381182
H	3.523902	-0.411812	-0.866128
H	3.829711	3.620909	0.657282
H	6.270826	3.391822	0.756156
H	5.942402	-0.644749	-0.756522

H	-7.647041	-1.245447	-0.162385
H	-8.137472	-2.126344	-0.271630
H	7.647028	1.245448	0.162360
H	8.137447	2.126351	0.271603
C	-8.468790	-0.105451	-0.074321
C	-10.190707	2.091730	0.087458
C	-8.073250	1.134894	-0.598860
C	-9.738792	-0.248543	0.505038
C	-10.592296	0.847601	0.582132
C	-8.932942	2.226550	-0.504865
H	-7.120566	1.234100	-1.105801
H	-10.042159	-1.212672	0.902185
H	-11.571249	0.730575	1.036266
H	-8.622620	3.182595	-0.914794
H	-10.857128	2.945800	0.153068
C	8.468798	0.105465	0.074297
C	10.190765	-2.091676	-0.087483
C	8.073296	-1.134883	0.598857
C	9.738790	0.248583	-0.505079
C	10.592317	-0.847543	-0.582175
C	8.933013	-2.226519	0.504862
H	7.120627	-1.234105	1.105821
H	10.042130	1.212714	-0.902238
H	11.571261	-0.730499	-1.036324
H	8.622722	-3.182566	0.914811
H	10.857206	-2.945731	-0.153093

*A.1.1.3 TANI, ^{3}**ES** State*

H	0.227522	-2.227346	1.066814
C	0.134910	-1.258288	0.587179
C	-0.134909	1.258277	-0.587297
C	-1.067667	-0.903047	-0.042644
C	1.191635	-0.362025	0.639383
C	1.067669	0.903036	0.042523
C	-1.191637	0.362017	-0.639494
H	2.092031	-0.628899	1.178982
H	-2.092037	0.628892	-1.179087
H	-0.227522	2.227337	-1.066929
H	-2.099339	-1.854707	-0.095862
H	-1.797525	-2.821857	-0.147412
H	2.099339	1.854700	0.095744
H	1.797518	2.821847	0.147311
C	-3.447606	-1.653921	-0.071300
C	-6.250077	-1.342685	-0.064308
C	-4.037308	-0.422752	0.323089
C	-4.298838	-2.746083	-0.397901
C	-5.660066	-2.595639	-0.393555
C	-5.401815	-0.271035	0.326824
H	-3.412661	0.386555	0.678193
H	-3.858646	-3.698682	-0.674642
H	-6.299227	-3.428267	-0.669123
H	-5.833414	0.654290	0.685298
C	3.447609	1.653924	0.071199
C	6.250082	1.342697	0.064292
C	4.037330	0.422765	-0.323198
C	4.298827	2.746083	0.397846
C	5.660057	2.595644	0.393542
C	5.401837	0.271052	-0.326890
H	3.412698	-0.386539	-0.678333
H	3.858623	3.698673	0.674600
H	6.299205	3.428266	0.669157
H	5.833451	-0.654269	-0.685356

H	-7.607213	-1.241059	-0.085037
H	-8.114344	-2.119295	-0.133182
H	7.607215	1.241066	0.085090
H	8.114347	2.119298	0.133293
C	-8.410238	-0.088592	-0.032037
C	-10.096760	2.133389	0.077281
C	-8.005127	1.124790	-0.611581
C	-9.673024	-0.195809	0.572539
C	-10.507826	0.914700	0.626131
C	-8.849104	2.229560	-0.544305
H	-7.063178	1.189577	-1.142956
H	-9.981506	-1.140841	1.009116
H	-11.479686	0.829897	1.101549
H	-8.536116	3.164548	-0.997755
H	-10.750524	2.998385	0.121933
C	8.410236	0.088594	0.032118
C	10.096752	-2.133396	-0.077116
C	8.005071	-1.124799	0.611600
C	9.673072	0.195816	-0.572355
C	10.507871	-0.914698	-0.625904
C	8.849044	-2.229574	0.544365
H	7.063077	-1.189592	1.142897
H	9.981599	1.140856	-1.008881
H	11.479771	-0.829891	-1.101240
H	8.536012	-3.164570	0.997768
H	10.750514	-2.998396	-0.121735

A.1.2 Optimised Structures of TANI-2

*A.1.2.1 TANI-2, **LEB** State*

H	0.639851	-3.515126	2.082916
C	0.642993	-2.648957	1.426208
C	0.643106	-0.421374	-0.232293
C	1.828958	-2.298108	0.755635
C	-0.513715	-1.893594	1.280358
C	-0.531883	-0.762351	0.451276
C	1.805949	-1.169763	-0.083531
H	-1.413059	-2.177010	1.817347
H	2.689724	-0.895308	-0.647429
H	0.642204	0.438768	-0.894097
H	2.956291	-3.104957	0.913275
H	2.779057	-4.055210	1.207291
H	-1.708188	0.017645	0.306665
C	4.299014	-2.772434	0.702837
C	7.051038	-2.197787	0.320749
C	4.790976	-1.464400	0.845115
C	5.215418	-3.791489	0.393667
C	6.563278	-3.509214	0.205424
C	6.141408	-1.183805	0.660160
H	4.121184	-0.663383	1.136059
H	4.860971	-4.813400	0.286548
H	7.248872	-4.313745	-0.047708
H	6.495228	-0.170553	0.813668
C	-2.964003	-0.619271	0.159095
C	-5.466263	-1.917363	-0.117334
C	-3.095577	-1.772253	-0.628602
C	-4.108706	-0.116238	0.796117
C	-5.336305	-0.752702	0.657909
C	-4.322716	-2.411932	-0.767289
H	-2.226707	-2.164573	-1.146645
H	-4.031171	0.774967	1.409936
H	-6.207717	-0.354992	1.171691

H	-4.398839	-3.279948	-1.411866
H	8.424488	-1.959395	0.164880
H	9.027372	-2.749774	0.347034
H	-6.730973	-2.499348	-0.262679
H	-7.515180	-1.879492	-0.113934
C	9.052333	-0.844031	-0.385590
C	10.441775	1.354302	-1.487146
C	8.369483	0.135020	-1.130650
C	10.444042	-0.708423	-0.213530
C	11.125329	0.373322	-0.762500
C	9.063486	1.220063	-1.664685
H	7.305103	0.037241	-1.307572
H	10.982740	-1.460348	0.358053
H	12.199174	0.452556	-0.615591
H	8.514418	1.962985	-2.237273
H	10.973534	2.202831	-1.906399
C	-7.055681	-3.842982	-0.445540
C	-7.842758	-6.530121	-0.803832
C	-6.158646	-4.893399	-0.178915
C	-8.356594	-4.162525	-0.880003
C	-8.742258	-5.488684	-1.049767
C	-6.554373	-6.217116	-0.366357
H	-5.164445	-4.676297	0.192876
H	-9.059029	-3.358500	-1.085509
H	-9.752459	-5.707860	-1.384918
H	-5.844455	-7.012020	-0.153601
H	-8.142049	-7.563822	-0.946804
C	-1.621525	1.430954	0.317276
C	-1.459799	4.258205	0.344416
C	-0.755545	2.092400	1.200977
C	-2.392229	2.205981	-0.561816
C	-2.315104	3.594541	-0.551613
C	-0.675501	3.479777	1.212274
H	-0.148127	1.512298	1.887677
H	-3.050362	1.712549	-1.269376
H	-2.896048	4.163903	-1.268021
H	-0.008791	3.973173	1.914860
H	-1.313368	5.650291	0.359451
H	-0.433277	5.991038	0.720991
C	-2.272887	6.629344	0.103436
C	-4.124001	8.706165	-0.374573
C	-1.836025	7.950998	-0.110235
C	-3.654738	6.366674	0.086534
C	-4.560764	7.397981	-0.157695
C	-2.752162	8.972876	-0.339472
H	-0.770160	8.165175	-0.096721
H	-4.019072	5.365820	0.284556
H	-5.623703	7.171616	-0.164960
H	-2.388562	9.984320	-0.499583
H	-4.836930	9.502744	-0.563623

*A.1.2.2 TANI-2, ^{1}**ES** State*

H	0.575855	-3.774076	1.768941
C	0.575763	-2.831667	1.230976
C	0.636133	-0.369099	-0.102420
C	1.784857	-2.369314	0.638025
C	-0.564720	-2.073725	1.180008
C	-0.554779	-0.812664	0.528945
C	1.776164	-1.129253	-0.059007
H	-1.464035	-2.412010	1.680242
H	2.650463	-0.813487	-0.612616
H	0.621369	0.549226	-0.677375

H	2.888969	-3.155028	0.732611
H	2.715012	-4.112541	1.022113
H	-1.696103	-0.028164	0.491667
C	4.225538	-2.848974	0.488195
C	6.950062	-2.338022	-0.032231
C	4.751443	-1.550342	0.637585
C	5.097664	-3.901664	0.141685
C	6.428328	-3.652091	-0.116523
C	6.085111	-1.298046	0.381077
H	4.127390	-0.748983	1.013715
H	4.711013	-4.912072	0.050579
H	7.083692	-4.468492	-0.404583
H	6.476495	-0.303091	0.549036
C	-2.963455	-0.621988	0.417330
C	-5.501051	-1.823446	0.273427
C	-3.168371	-1.763266	-0.387870
C	-4.050764	-0.070339	1.130704
C	-5.290371	-0.660208	1.062062
C	-4.410087	-2.351516	-0.465578
H	-2.352076	-2.145878	-0.990049
H	-3.894085	0.794517	1.764824
H	-6.114533	-0.253734	1.639591
H	-4.563852	-3.189073	-1.133046
H	8.282835	-2.142659	-0.296355
H	8.853889	-2.978589	-0.311866
H	-6.752567	-2.360431	0.229006
H	-7.495206	-1.781130	0.602668
C	8.973982	-0.936986	-0.503943
C	10.455948	1.403094	-0.941664
C	8.378179	0.167787	-1.133231
C	10.322412	-0.869515	-0.118508
C	11.055358	0.292484	-0.341465
C	9.118466	1.330561	-1.336747
H	7.355968	0.106718	-1.487899
H	10.784361	-1.727330	0.361952
H	12.096834	0.331979	-0.036853
H	8.647694	2.178535	-1.825111
H	11.027469	2.310788	-1.107682
C	-7.162840	-3.597745	-0.309797
C	-8.084198	-6.028626	-1.343669
C	-6.376948	-4.753327	-0.189908
C	-8.420429	-3.668483	-0.926311
C	-8.876081	-4.881012	-1.436477
C	-6.838026	-5.957811	-0.717320
H	-5.430524	-4.716532	0.337289
H	-9.027033	-2.771607	-1.011414
H	-9.849614	-4.926317	-1.914784
H	-6.224931	-6.848481	-0.620031
H	-8.439562	-6.971366	-1.747412
C	-1.590588	1.369119	0.515858
C	-1.389691	4.173364	0.562882
C	-0.622611	1.998183	1.330654
C	-2.446790	2.159698	-0.281225
C	-2.347075	3.532168	-0.266814
C	-0.525790	3.368863	1.353792
H	0.014810	1.398106	1.969642
H	-3.151685	1.677206	-0.948475
H	-2.969640	4.119701	-0.928497
H	0.195354	3.848046	2.008018
H	-1.238525	5.526596	0.609242
H	-0.388624	5.860579	1.048543
C	-2.081625	6.528135	0.084010
C	-3.680880	8.594409	-0.915344
C	-1.488998	7.689805	-0.431504

C	-3.478976	6.413442	0.121466	H	-3.942879	5.544112	0.573091
C	-4.268353	7.442096	-0.388826	H	-5.349326	7.347036	-0.356064
C	-2.288902	8.716756	-0.924976	H	-1.821904	9.611392	-1.325100
H	-0.406496	7.775450	-0.452540	H	-4.301969	9.394206	-1.305990

*A.1.2.3 TANI-2, ^{3}**ES** State*

H	0.640068	-3.625009	1.906169	C	-4.079791	0.020844	1.016994
C	0.602077	-2.759342	1.252950	C	-5.328306	-0.558228	0.961171
C	0.533423	-0.507858	-0.400180	C	-4.451567	-2.330711	-0.458712
C	1.713330	-2.433504	0.459230	H	-2.382305	-2.185901	-0.958102
C	-0.528518	-1.956946	1.232474	H	-3.925492	0.915551	1.608884
C	-0.564048	-0.819704	0.413231	H	-6.153171	-0.112488	1.508639
C	1.663503	-1.312559	-0.384935	H	-4.601107	-3.207868	-1.074566
H	-1.375610	-2.193699	1.865641	H	8.234501	-2.212769	-0.105365
H	2.482571	-1.096462	-1.059780	H	8.823531	-3.034168	-0.008949
H	0.485543	0.345986	-1.066028	H	-6.810955	-2.278406	0.195604
H	2.830682	-3.284413	0.496852	H	-7.552155	-1.659383	0.500774
H	2.627535	-4.263338	0.669508	C	8.917401	-1.013516	-0.371757
H	-1.715779	0.012543	0.398812	C	10.370099	1.312887	-0.890631
C	4.149678	-2.967093	0.361167	C	8.351129	0.002365	-1.159112
C	6.899835	-2.422420	0.056716	C	10.223111	-0.876465	0.126678
C	4.635188	-1.633357	0.431332	C	10.940687	0.285706	-0.132467
C	5.085701	-4.027276	0.203504	C	9.079789	1.162363	-1.405113
C	6.421463	-3.763306	0.057928	H	7.373239	-0.132385	-1.605641
C	5.973694	-1.367592	0.281937	H	10.656877	-1.671960	0.724900
H	3.956348	-0.821932	0.658553	H	11.946311	0.391459	0.261451
H	4.728990	-5.051834	0.177953	H	8.642528	1.943471	-2.018609
H	7.123674	-4.578478	-0.084336	H	10.933302	2.218674	-1.090571
H	6.330303	-0.352094	0.394047	C	-7.227091	-3.545444	-0.254432
C	-2.988820	-0.568318	0.341524	C	-8.164097	-6.039857	-1.121000
C	-5.545431	-1.753495	0.231131	C	-6.446619	-4.695907	-0.062231
C	-3.201856	-1.750236	-0.398333	C	-8.488318	-3.655317	-0.859664

C	-8.951517	-4.897258	-1.285110	H	-2.921003	4.224348	-0.903388
C	-6.914774	-5.930928	-0.506432	H	0.418480	3.807171	1.804346
H	-5.497217	-4.628937	0.456398	H	-1.044566	5.561654	0.532664
H	-9.093318	-2.764482	-1.001859	H	-0.144831	5.855339	0.893009
H	-9.928043	-4.969658	-1.754241	C	-1.890938	6.599519	0.100760
H	-6.303708	-6.815256	-0.352927	C	-3.496170	8.746235	-0.715609
H	-8.524571	-7.005907	-1.460036	C	-1.303646	7.767065	-0.410404
C	-1.558567	1.405078	0.426044	C	-3.286888	6.520734	0.222850
C	-1.252405	4.207449	0.484889	C	-4.078593	7.588263	-0.195892
C	-0.517476	1.993953	1.175136	C	-2.104703	8.832790	-0.810880
C	-2.425900	2.238504	-0.310124	H	-0.222704	7.827254	-0.499393
C	-2.278003	3.609939	-0.286695	H	-3.745836	5.646188	0.669133
C	-0.369328	3.363239	1.203480	H	-5.157595	7.518158	-0.096634
H	0.150547	1.366984	1.754125	H	-1.639070	9.730326	-1.206535
H	-3.190721	1.792443	-0.935504	H	-4.119003	9.575856	-1.034894

A.1.3 Optimised Structures of TANI-23

*A.1.3.1 TANI-23, **LEB** State*

H	-1.581549	1.233573	1.452818	C	-1.366485	4.678535	0.852981
C	-0.892568	0.694828	0.810805	C	-2.329758	3.113972	-0.704133
C	0.892573	-0.694837	-0.810814	C	-3.540989	3.794679	-0.648865
C	-0.000004	1.413145	-0.000008	C	-2.575235	5.362131	0.909193
C	-0.892562	-0.694841	0.810808	H	-0.523791	5.024580	1.442365
C	0.000009	-1.413154	-0.000002	H	-2.232187	2.246514	-1.348642
C	0.892567	0.694832	-0.810818	H	-4.364249	3.464645	-1.271591
H	-1.581538	-1.233590	1.452823	H	-2.669007	6.235803	1.549120
H	1.581542	1.233581	-1.452834	C	1.226431	3.536614	-0.050903
H	1.581554	-1.233582	-1.452827	C	3.688412	4.928196	-0.169203
N	0.000015	-2.828170	0.000002	C	2.329731	3.114002	0.704109
N	-0.000011	2.828160	-0.000012	C	1.366444	4.678542	-0.853020
C	-1.226461	3.536601	0.050875	C	2.575187	5.362150	-0.909236
C	-3.688459	4.928155	0.169171	C	3.540954	3.794724	0.648840

H	2.232169	2.246547	1.348623
H	0.523747	5.024572	-1.442409
H	2.668952	6.235816	-1.549172
H	4.364220	3.464701	1.271565
C	-1.226428	-3.536623	0.050884
C	-3.688411	-4.928203	0.169165
C	-2.329722	-3.114011	-0.704138
C	-1.366448	-4.678549	0.853001
C	-2.575192	-5.362156	0.909209
C	-3.540945	-3.794733	-0.648878
H	-2.232154	-2.246557	-1.348653
H	-0.523757	-5.024579	1.442399
H	-2.668963	-6.235821	1.549146
H	-4.364207	-3.464710	-1.271610
C	1.226465	-3.536612	-0.050878
C	3.688461	-4.928169	-0.169156
C	1.366495	-4.678541	-0.852990
C	2.329755	-3.113986	0.704140
C	3.540986	-3.794696	0.648881
C	2.575245	-5.362137	-0.909196
H	0.523806	-5.024582	-1.442384
H	2.232180	-2.246530	1.348651
H	4.364244	-3.464662	1.271611
H	2.669023	-6.235804	-1.549128
N	4.872118	5.671499	-0.225610
H	4.765776	6.639190	-0.496847
N	-4.872118	-5.671504	0.225564
H	-4.765781	-6.639194	0.496806
C	6.187750	5.228627	-0.090317
C	8.892703	4.458344	0.146121
C	6.560183	3.877465	-0.211104
C	7.194054	6.187091	0.136656
C	8.527228	5.803868	0.246540
C	7.898163	3.506107	-0.084863
H	5.810809	3.124775	-0.424581
H	6.917169	7.234475	0.228235
H	9.284427	6.563685	0.420101
H	8.162750	2.456537	-0.182385
H	9.931949	4.159595	0.242372
C	-6.187748	-5.228630	0.090254
C	-8.892694	-4.458338	-0.146219
C	-6.560176	-3.877465	0.211025
C	-7.194052	-6.187092	-0.136723
C	-8.527224	-5.803864	-0.246624
C	-7.898154	-3.506103	0.084767
H	-5.810801	-3.124776	0.424503
H	-6.917170	-7.234477	-0.228290
H	-9.284424	-6.563680	-0.420187
H	-8.162738	-2.456531	0.182278
H	-9.931938	-4.159586	-0.242484
N	-4.872170	5.671452	0.225576
H	-4.765826	6.639151	0.496783
N	4.872175	-5.671460	-0.225554
H	4.765844	-6.639153	-0.496786
C	-6.187806	5.228578	0.090321
C	-8.892771	4.458308	-0.146031
C	-7.194106	6.187039	-0.136681
C	-6.560251	3.877425	0.211185
C	-7.898237	3.506073	0.084986
C	-8.527286	5.803822	-0.246525
H	-6.917214	7.234416	-0.228314
H	-5.810884	3.124739	0.424696
H	-8.162833	2.456511	0.182570
H	-9.284480	6.563638	-0.420111

H	-9.932022	4.159563	-0.242250
C	6.187802	-5.228574	-0.090255
C	8.892746	-4.458264	0.146193
C	7.194114	-6.187027	0.136729
C	6.560223	-3.877409	-0.211048
C	7.898199	-3.506037	-0.084802
C	8.527284	-5.803790	0.246618
H	6.917238	-7.234413	0.228312
H	5.810843	-3.124728	-0.424534
H	8.162776	-2.456465	-0.182330
H	9.284489	-6.563599	0.420188
H	9.931989	-4.159504	0.242448

*A.1.3.2 TANI-23, ^{1}**ES** State*

H	-1.669632	1.226678	1.371754
C	-0.966427	0.685597	0.750417
C	0.966434	-0.685536	-0.750383
C	-0.000064	1.406345	0.000007
C	-0.966361	-0.685619	0.750427
C	0.000072	-1.406284	0.000028
C	0.966368	0.685680	-0.750392
H	-1.669513	-1.226758	1.371772
H	1.669519	1.226819	-1.371740
H	1.669636	-1.226616	-1.371724
N	0.000135	-2.787090	0.000037
N	-0.000133	2.787150	-0.000002
C	-1.209502	3.500106	0.128841
C	-3.634303	4.900719	0.401800
C	-1.269458	4.663450	0.920691
C	-2.364057	3.066896	-0.550350
C	-3.555280	3.751620	-0.421454
C	-2.458096	5.348143	1.054376
H	-0.385929	4.999827	1.450988
H	-2.305406	2.210074	-1.212407
H	-4.418090	3.431389	-0.990650
H	-2.505336	6.227662	1.689074
C	1.209164	3.500226	-0.128853
C	3.633823	4.901080	-0.401822
C	2.363764	3.067134	0.550337
C	1.269003	4.663571	-0.920712
C	2.457573	5.348381	-1.054403
C	3.554919	3.751975	0.421434
H	2.305201	2.210307	1.212396
H	0.385440	4.999856	-1.451009
H	2.504725	6.227900	-1.689109
H	4.417768	3.431829	0.990620
C	-1.209167	-3.500159	0.128886
C	-3.633834	-4.901001	0.401849
C	-2.363765	-3.067056	-0.550302
C	-1.269011	-4.663507	0.920737
C	-2.457584	-5.348313	1.054425
C	-3.554924	-3.751892	-0.421402
H	-2.305197	-2.210227	-1.212357
H	-0.385448	-4.999801	1.451031
H	-2.504740	-6.227835	1.689124
H	-4.417769	-3.431740	-0.990589
C	1.209496	-3.500059	-0.128804
C	3.634282	-4.900712	-0.401754
C	1.269437	-4.663408	-0.920645
C	2.364054	-3.066870	0.550396
C	3.555269	-3.751612	0.421505
C	2.458063	-5.348123	-1.054318

H	0.385903	-4.999777	-1.450938	H	-8.248588	-2.637869	0.082295
H	2.305412	-2.210054	1.212462	H	-9.799061	-4.438052	-0.660066
H	4.418066	-3.431407	0.990731	N	-4.786144	5.624812	0.563694
H	2.505286	-6.227651	-1.689005	H	-4.671420	6.550147	0.958263
N	4.785599	5.625274	-0.563722	N	4.786094	-5.624859	-0.563641
H	4.670802	6.550586	-0.958322	H	4.671300	-6.550221	-0.958124
N	-4.785610	-5.625194	0.563746	C	-6.105191	5.271949	0.220794
H	-4.670811	-6.550513	0.958331	C	-8.769213	4.671329	-0.411329
C	6.104666	5.272524	-0.220788	C	-6.984202	6.290231	-0.178366
C	8.768715	4.672110	0.411405	C	-6.573966	3.953340	0.325403
C	6.573524	3.953939	-0.325314	C	-7.896604	3.660907	-0.001936
C	6.983603	6.290884	0.178334	C	-8.307840	5.988088	-0.486952
C	8.307257	5.988843	0.486953	H	-6.621547	7.311530	-0.252220
C	7.896176	3.661609	0.002059	H	-5.918492	3.169830	0.687531
H	5.918099	3.170366	-0.687396	H	-8.248914	2.637220	0.082362
H	6.620880	7.312163	0.252131	H	-8.977924	6.784648	-0.795993
H	8.977286	6.785462	0.795960	H	-9.799519	4.437269	-0.660047
H	8.248552	2.637939	-0.082174	C	6.105187	-5.272062	-0.220842
H	9.799033	4.438129	0.660150	C	8.769311	-4.671643	0.411059
C	-6.104681	-5.272442	0.220828	C	6.984109	-6.290380	0.178423
C	-8.768740	-4.672031	-0.411333	C	6.574114	-3.953525	-0.325695
C	-6.573549	-3.953863	0.325390	C	7.896800	-3.661190	0.001535
C	-6.983615	-6.290799	-0.178312	C	8.307794	-5.988337	0.486907
C	-8.307273	-5.988759	-0.486915	H	6.621346	-7.311628	0.252447
C	-7.896205	-3.661534	-0.001967	H	5.918729	-3.170002	-0.687952
H	-5.918129	-3.170295	0.687491	H	8.249227	-2.637559	-0.082956
H	-6.620886	-7.312074	-0.252135	H	8.977803	-6.784925	0.796040
H	-8.977298	-6.785376	-0.795937	H	9.799656	-4.437660	0.659691

*A.1.3.3 TANI-23, ³**ES** State*

H	-1.369078	1.239300	1.659825	C	0.785476	-0.693710	-0.927522
C	-0.785480	0.693711	0.927517	C	-0.000003	1.391812	-0.000003

C	-0.785478	-0.693711	0.927518
C	-0.000001	-1.391810	-0.000002
C	0.785475	0.693712	-0.927522
H	-1.369075	-1.239301	1.659826
H	1.369074	1.239301	-1.659830
H	1.369074	-1.239299	-1.659830
N	0.000001	-2.813976	-0.000001
N	-0.000003	2.813978	-0.000003
C	-1.217854	3.498931	0.097857
C	-3.686162	4.844185	0.317576
C	-1.307014	4.717176	0.805321
C	-2.378235	2.976165	-0.510855
C	-3.586608	3.632806	-0.409148
C	-2.513052	5.374979	0.909470
H	-0.429002	5.117851	1.298365
H	-2.311581	2.066535	-1.096460
H	-4.451994	3.237679	-0.925034
H	-2.576650	6.295250	1.481866
C	1.217849	3.498931	-0.097863
C	3.686158	4.844181	-0.317582
C	2.378229	2.976163	0.510849
C	1.307009	4.717175	-0.805327
C	2.513048	5.374976	-0.909476
C	3.586603	3.632803	0.409142
H	2.311575	2.066532	1.096453
H	0.428998	5.117851	-1.298371
H	2.576647	6.295247	-1.481874
H	4.451990	3.237674	0.925026
C	-1.217846	-3.498932	0.097884
C	-3.686145	-4.844191	0.317658
C	-2.378246	-2.976157	-0.510783
C	-1.306980	-4.717189	0.805328
C	-2.513014	-5.374995	0.909504
C	-3.586615	-3.632800	-0.409048
H	-2.311611	-2.066516	-1.096375
H	-0.428951	-5.117872	1.298335
H	-2.576592	-6.295277	1.481886
H	-4.452018	-3.237665	-0.924900
C	1.217851	-3.498928	-0.097886
C	3.686154	-4.844178	-0.317659
C	1.306989	-4.717186	-0.805328
C	2.378249	-2.976147	0.510780
C	3.586621	-3.632786	0.409045
C	2.513025	-5.374988	-0.909503
H	0.428961	-5.117873	-1.298334
H	2.311611	-2.066505	1.096369
H	4.452023	-3.237647	0.924895
H	2.576607	-6.295270	-1.481884
N	4.858721	5.542382	-0.444749
H	4.768269	6.502625	-0.753828
N	-4.858701	-5.542399	0.444853
H	-4.768231	-6.502650	0.753901
C	6.171780	5.113798	-0.175092
C	8.825317	4.363289	0.321142
C	6.585843	3.793629	-0.411457
C	7.099049	6.059963	0.287624
C	8.417408	5.683495	0.529217
C	7.904327	3.425768	-0.151278
H	5.890877	3.070705	-0.822714
H	6.777317	7.082211	0.464705
H	9.125502	6.423580	0.889441
H	8.215285	2.402215	-0.337631
H	9.852085	4.070724	0.516816
C	-6.171775	-5.113817	0.175262

C	-8.825342	-4.363319	-0.320833
C	-6.585844	-3.793662	0.411695
C	-7.099053	-6.059975	-0.287449
C	-8.417426	-5.683513	-0.528974
C	-7.904342	-3.425806	0.151585
H	-5.890870	-3.070746	0.822954
H	-6.777317	-7.082213	-0.464580
H	-9.125526	-6.423593	-0.889195
H	-8.215305	-2.402264	0.337990
H	-9.852120	-4.070759	-0.516454
N	-4.858724	5.542388	0.444743
H	-4.768267	6.502633	0.753815
N	4.858714	-5.542380	-0.444854
H	4.768249	-6.502632	-0.753903
C	-6.171786	5.113810	0.175093
C	-8.825331	4.363314	-0.321124
C	-7.099049	6.059976	-0.287631
C	-6.585859	3.793647	0.411477
C	-7.904346	3.425792	0.151306
C	-8.417412	5.683515	-0.529217
H	-6.777311	7.082219	-0.464725
H	-5.890898	3.070722	0.822743
H	-8.215312	2.402244	0.337672
H	-9.125501	6.423601	-0.889447
H	-9.852101	4.070754	-0.516792
C	6.171785	-5.113791	-0.175262
C	8.825346	-4.363276	0.320836
C	7.099069	-6.059944	0.287447
C	6.585844	-3.793632	-0.411691
C	7.904341	-3.425768	-0.151579
C	8.417440	-5.683474	0.528973
H	6.777341	-7.082185	0.464575
H	5.890865	-3.070719	-0.822946
H	8.215296	-2.402223	-0.337980
H	9.125545	-6.423550	0.889192
H	9.852123	-4.070709	0.516458

A.1.4 Optimised Structures of TANI-14

*A.1.4.1 TANI-14, **LEB** State*

H	1.789204	11.665625	-0.938853
C	1.874095	10.593992	-1.096927
C	2.075416	7.840559	-1.477662
C	0.854823	9.757580	-0.647201
C	3.004074	10.066010	-1.726814
C	3.097263	8.684018	-1.908432
C	0.941158	8.368607	-0.839518
H	-0.011901	10.174145	-0.145385
H	3.799503	10.720990	-2.069096
H	3.966450	8.256296	-2.400524
H	2.148891	6.769157	-1.630165
N	-0.082761	7.507565	-0.381796
C	-1.443840	7.884348	-0.442609
C	-4.163710	8.600579	-0.566113
C	-1.935838	8.635753	-1.522932
C	-2.332322	7.492653	0.572447
C	-3.678906	7.843141	0.502977
C	-3.280674	8.995690	-1.574270
H	-1.260281	8.933120	-2.317643
H	-1.960089	6.912635	1.409981
H	-4.350095	7.530925	1.298369
H	-3.642056	9.576910	-2.418187

H	-5.212555	8.877187	-0.613820
C	0.265839	6.234410	0.153229
C	0.941158	3.706835	1.227312
C	-0.369383	5.071555	-0.296571
C	1.253964	6.118954	1.139680
C	1.589999	4.877751	1.664133
C	-0.044796	3.825770	0.230606
H	-1.123382	5.144898	-1.074057
H	1.757474	7.011479	1.497412
H	2.351526	4.807557	2.436410
H	-0.533683	2.940471	-0.157820
N	1.328975	2.484735	1.771519
H	2.256242	2.458355	2.172558
C	0.648127	1.261025	1.731899
C	-0.648127	-1.261025	1.731899
C	-0.753647	1.172309	1.757390
C	1.385549	0.066012	1.734295
C	0.753647	-1.172309	1.757390
C	-1.385549	-0.066012	1.734295
H	-1.353157	2.074558	1.799015
H	2.471528	0.110601	1.734234
H	1.353157	-2.074558	1.799015
H	-2.471528	-0.110601	1.734234
N	-1.328975	-2.484735	1.771519
H	-2.256242	-2.458355	2.172558
C	-0.941158	-3.706835	1.227312
C	-0.265839	-6.234410	0.153229
C	-1.589999	-4.877751	1.664133
C	0.044796	-3.825770	0.230606
C	0.369383	-5.071555	-0.296571
C	-1.253964	-6.118954	1.139680
H	-2.351526	-4.807557	2.436410
H	0.533683	-2.940471	-0.157820
H	1.123382	-5.144898	-1.074057
H	-1.757474	-7.011479	1.497412
N	0.082761	-7.507565	-0.381796
C	1.443840	-7.884348	-0.442609
C	4.163710	-8.600579	-0.566113
C	1.935838	-8.635753	-1.522932
C	2.332322	-7.492653	0.572447
C	3.678906	-7.843141	0.502977
C	3.280674	-8.995690	-1.574270
H	1.260281	-8.933120	-2.317643
H	1.960089	-6.912635	1.409981
H	4.350095	-7.530925	1.298369
H	3.642056	-9.576910	-2.418187
H	5.212555	-8.877187	-0.613820
C	-0.941158	-8.368607	-0.839518
C	-3.004074	-10.066010	-1.726814
C	-2.075416	-7.840559	-1.477662
C	-0.854823	-9.757580	-0.647201
C	-1.874095	-10.593992	-1.096927
C	-3.097263	-8.684018	-1.908432
H	-2.148891	-6.769157	-1.630165
H	0.011901	-10.174145	-0.145385
H	-1.789204	-11.665625	-0.938853
H	-3.966450	-8.256296	-2.400524
H	-3.799503	-10.720990	-2.069096

*A.1.4.2 TANI-14, ^{1}**ES** State*

H	0.802313	11.893195	1.050604
C	1.068203	10.983927	0.520800
C	1.752529	8.636464	-0.836467
C	0.179437	9.912369	0.508958
C	2.298502	10.887088	-0.135625
C	2.636779	9.712279	-0.812020
C	0.525910	8.736274	-0.167383
H	-0.773576	9.974296	1.022996
H	2.988404	11.724946	-0.123477
H	3.584925	9.636556	-1.334896
H	1.997791	7.729456	-1.378678
N	-0.395452	7.646544	-0.197465
C	-1.752529	7.932308	-0.529441
C	-4.400674	8.528779	-1.167275
C	-2.034796	8.769788	-1.616148
C	-2.792248	7.401618	0.245931
C	-4.113032	7.697882	-0.081423
C	-3.358661	9.064647	-1.929565
H	-1.220378	9.173765	-2.207346
H	-2.560674	6.777271	1.102176
H	-4.917305	7.290473	0.522977
H	-3.576863	9.708091	-2.776046
H	-5.431329	8.761514	-1.415673
C	0.014362	6.359978	0.078653
C	0.826308	3.724228	0.659811
C	-0.690730	5.247142	-0.450630
C	1.163547	6.116064	0.875191
C	1.561089	4.829758	1.151088
C	-0.293786	3.960585	-0.171836
H	-1.520895	5.415388	-1.124954
H	1.713229	6.949048	1.294274
H	2.421072	4.658480	1.790826
H	-0.799829	3.134375	-0.654699
N	1.273394	2.458813	0.974153
H	2.254764	2.408565	1.234925
C	0.614197	1.265629	0.995325
C	-0.614197	-1.265629	0.995325
C	-0.803175	1.157176	1.037730
C	1.395179	0.078304	1.049869
C	0.803175	-1.157176	1.037730
C	-1.395179	-0.078304	1.049869
H	-1.418484	2.043728	1.110211
H	2.476818	0.155585	1.096716
H	1.418484	-2.043728	1.110211
H	-2.476818	-0.155585	1.096716
N	-1.273394	-2.458813	0.974153
H	-2.254764	-2.408565	1.234925
C	-0.826308	-3.724228	0.659811
C	-0.014362	-6.359978	0.078653
C	-1.561089	-4.829758	1.151088
C	0.293786	-3.960585	-0.171836
C	0.690730	-5.247142	-0.450630
C	-1.163547	-6.116064	0.875191
H	-2.421072	-4.658480	1.790826
H	0.799829	-3.134375	-0.654699
H	1.520895	-5.415388	-1.124954
H	-1.713229	-6.949048	1.294274
N	0.395452	-7.646544	-0.197465
C	1.752529	-7.932308	-0.529441
C	4.400674	-8.528779	-1.167275
C	2.034796	-8.769788	-1.616148
C	2.792248	-7.401618	0.245931

C	4.113032	-7.697882	-0.081423
C	3.358661	-9.064647	-1.929565
H	1.220378	-9.173765	-2.207346
H	2.560674	-6.777271	1.102176
H	4.917305	-7.290473	0.522977
H	3.576863	-9.708091	-2.776046
H	5.431329	-8.761514	-1.415673
C	-0.525910	-8.736274	-0.167383
C	-2.298502	-10.887088	-0.135625
C	-1.752529	-8.636464	-0.836467
C	-0.179437	-9.912369	0.508958
C	-1.068203	-10.983927	0.520800
C	-2.636779	-9.712279	-0.812020
H	-1.997791	-7.729456	-1.378678
H	0.773576	-9.974296	1.022996
H	-0.802313	-11.893195	1.050604
H	-3.584925	-9.636556	-1.334896
H	-2.988404	-11.724946	-0.123477

*A.1.4.3 TANI-14, ^{3}**ES** State*

H	1.209564	11.788304	0.090072
C	1.478565	10.780915	-0.210773
C	2.176743	8.180718	-0.973129
C	0.541317	9.758993	-0.097808
C	2.761324	10.511601	-0.697798
C	3.105859	9.211805	-1.077978
C	0.895441	8.456240	-0.475008
H	-0.451529	9.955538	0.290981
H	3.488030	11.313019	-0.784411
H	4.095393	9.001236	-1.470551
H	2.426967	7.174334	-1.290346
N	-0.064861	7.410229	-0.369824
C	-1.392618	7.665144	-0.815499
C	-3.987256	8.191589	-1.679080
C	-1.597419	8.332894	-2.030866
C	-2.481755	7.268242	-0.026515
C	-3.775994	7.531065	-0.465891
C	-2.896230	8.591883	-2.456849
H	-0.745373	8.627533	-2.633121
H	-2.307482	6.781011	0.926475
H	-4.619543	7.232252	0.147917
H	-3.057246	9.100202	-3.402012
H	-4.998189	8.397688	-2.015892
C	0.279544	6.179437	0.156382
C	0.949560	3.666780	1.250498
C	-0.404876	5.004753	-0.249907
C	1.329938	6.062291	1.103951
C	1.654853	4.838681	1.633987
C	-0.076575	3.778684	0.276442
H	-1.161676	5.069898	-1.021829
H	1.851110	6.949930	1.439977
H	2.436013	4.766954	2.383878
H	-0.570379	2.890701	-0.096013
N	1.317519	2.475305	1.806884
H	2.207842	2.470519	2.292743
C	0.637023	1.247808	1.783689
C	-0.637023	-1.247808	1.783689
C	-0.765159	1.171253	1.814509
C	1.392618	0.065289	1.803375
C	0.765159	-1.171253	1.814509
C	-1.392618	-0.065289	1.803375
H	-1.362647	2.072801	1.872122

H	2.476636	0.117789	1.816208	C	2.481755	-7.268242	-0.026515
H	1.362647	-2.072801	1.872122	C	3.775994	-7.531065	-0.465891
H	-2.476636	-0.117789	1.816208	C	2.896230	-8.591883	-2.456849
N	-1.317519	-2.475305	1.806884	H	0.745373	-8.627533	-2.633121
H	-2.207842	-2.470519	2.292743	H	2.307482	-6.781011	0.926475
C	-0.949560	-3.666780	1.250498	H	4.619543	-7.232252	0.147917
C	-0.279544	-6.179437	0.156382	H	3.057246	-9.100202	-3.402012
C	-1.654853	-4.838681	1.633987	H	4.998189	-8.397688	-2.015892
C	0.076575	-3.778684	0.276442	C	-0.895441	-8.456240	-0.475008
C	0.404876	-5.004753	-0.249907	C	-2.761324	-10.511601	-0.697798
C	-1.329938	-6.062291	1.103951	C	-2.176743	-8.180718	-0.973129
H	-2.436013	-4.766954	2.383878	C	-0.541317	-9.758993	-0.097808
H	0.570379	-2.890701	-0.096013	C	-1.478565	-10.780915	-0.210773
H	1.161676	-5.069898	-1.021829	C	-3.105859	-9.211805	-1.077978
H	-1.851110	-6.949930	1.439977	H	-2.426967	-7.174334	-1.290346
N	0.064861	-7.410229	-0.369824	H	0.451529	-9.955538	0.290981
C	1.392618	-7.665144	-0.815499	H	-1.209564	-11.788304	0.090072
C	3.987256	-8.191589	-1.679080	H	-4.095393	-9.001236	-1.470551
C	1.597419	-8.332894	-2.030866	H	-3.488030	-11.313019	-0.784411

A.1.5 Microscopic Structures of TANI and Branched Derivatives

Table A-1 NBO Partial charges of nitrogen atoms in TANI and branched TANI derivatives in the emeraldine salt states compared to the leucoemeraldine state from DFT calculations

Model	State	Nitrogen Partial Charge				Hydrogen Partial Charge			
		N^1	N^2	N^3	N^4	H^1	H^2	H^3	H^4
TANI	LEB	-0.613	-0.612	-0.612	-0.613	+0.427	+0.428	+0.428	+0.427
	^{1}ES	-0.522	-0.454	-0.454	-0.522	+0.451	+0.462	+0.462	+0.451
	^{3}ES	-0.481	-0.504	-0.504	-0.481	+0.455	+0.455	+0.455	+0.455
TANI-2	LEB	-0.607	-0.445	-0.609	-0.610	+0.429		+0.430	+0.428
	^{1}ES	-0.539	-0.285	-0.488	-0.554	+0.448		+0.455	+0.443
	^{3}ES	-0.548	-0.328	-0.507	-0.477	+0.444		+0.456	+0.456
TANI-23	LEB	-0.607	-0.444	-0.444	-0.607	+0.430			+0.430
	^{1}ES	-0.557	-0.310	-0.310	-0.557	+0.444			+0.444
	^{3}ES	-0.548	-0.329	-0.329	-0.548	+0.445			+0.445
TANI-14	LEB	-0.444	-0.608	-0.608	-0.444		+0.430	+0.430	
	^{1}ES	-0.359	-0.464	-0.464	-0.359		+0.460	+0.460	
	^{3}ES	-0.314	-0.517	-0.517	-0.314		+0.453	+0.453	

Table A-2 NBO Partial charges of carbon and hydrogen atoms in TANI and branched TANI derivatives in the emeraldine salt states compared to the leucoemeraldine state from DFT calculations

Model	State	Unit	NBO Partial Charge										
			C_{ipso}		C_{ortho}				H_{ortho}				Ring
			C_{iA}	C_{iB}	C_{oA1}	C_{oA2}	C_{oB1}	C_{oB2}	H_{oA1}	H_{oA1}	H_{oA1}	H_{oA1}	
TANI	LEB	B	+0.124	+0.145	-0.252	-0.259	-0.262	-0.275	+0.244	+0.249	+0.243	+0.249	+0.206
		C	+0.134	+0.135	-0.257	-0.268	-0.268	-0.257	+0.243	+0.249	+0.249	+0.243	+0.203
		D	+0.145	+0.125	-0.274	-0.262	-0.259	-0.252	+0.249	+0.243	+0.249	+0.244	+0.208
	^{1}ES	B	+0.218	+0.151	-0.239	-0.248	-0.208	-0.223	+0.266	+0.270	+0.268	+0.269	+0.524
		C	+0.199	+0.199	-0.207	-0.233	-0.233	-0.207	+0.272	+0.274	+0.274	+0.272	+0.610
		D	+0.151	+0.218	-0.223	-0.208	-0.248	-0.239	+0.269	+0.268	+0.270	+0.266	+0.524
	^{3}ES	B	+0.199	+0.208	-0.228	-0.217	-0.238	-0.225	+0.272	+0.268	+0.270	+0.268	+0.577
		C	+0.144	+0.144	-0.236	-0.219	-0.219	-0.236	+0.267	+0.266	+0.266	+0.267	+0.444
		D	+0.208	+0.199	-0.225	-0.238	-0.217	-0.228	+0.268	+0.270	+0.268	+0.272	+0.577
TANI-2	LEB	B	+0.142	+0.126	-0.259	-0.270	-0.245	-0.243	+0.244	+0.250	+0.251	+0.251	+0.247
		C	+0.116	+0.150	-0.239	-0.240	-0.277	-0.265	+0.250	+0.251	+0.249	+0.243	+0.238
		D	+0.138	+0.131	-0.268	-0.258	-0.262	-0.254	+0.250	+0.244	+0.250	+0.245	+0.216
	^{1}ES	B	+0.222	+0.121	-0.246	-0.261	-0.204	-0.203	+0.264	+0.268	+0.273	+0.272	+0.506
		C	+0.158	+0.212	-0.205	-0.211	-0.247	-0.229	+0.276	+0.276	+0.272	+0.268	+0.570
		D	+0.130	+0.196	-0.232	-0.219	-0.260	-0.247	+0.263	+0.262	+0.264	+0.259	+0.416
	^{3}ES	B	+0.200	+0.133	-0.247	-0.259	-0.219	-0.215	+0.259	+0.264	+0.268	+0.266	+0.450
		C	+0.132	+0.151	-0.213	-0.214	-0.240	-0.224	+0.271	+0.271	+0.268	+0.266	+0.468
		D	+0.211	+0.199	-0.238	-0.226	-0.226	-0.216	+0.270	+0.268	+0.272	+0.268	+0.582
TANI-23	LEB	B	+0.145	+0.123	-0.260	-0.271	-0.242	-0.241	+0.245	+0.250	+0.251	+0.251	+0.251
		C	+0.133	+0.133	-0.248	-0.248	-0.248	-0.248	+0.251	+0.251	+0.251	+0.251	+0.278
		D	+0.123	+0.145	-0.241	-0.242	-0.271	-0.260	+0.251	+0.251	+0.250	+0.245	+0.251
	^{1}ES	B	+0.207	+0.111	-0.251	-0.267	-0.210	-0.209	+0.259	+0.264	+0.269	+0.267	+0.440
		C	+0.181	+0.181	-0.221	-0.221	-0.221	-0.221	+0.275	+0.275	+0.275	+0.275	+0.578
		D	+0.111	+0.207	-0.209	-0.210	-0.267	-0.251	+0.267	+0.269	+0.264	+0.259	+0.440
	^{3}ES	B	+0.200	+0.134	-0.246	-0.259	-0.220	-0.215	+0.260	+0.264	+0.268	+0.266	+0.452
		C	+0.137	+0.137	-0.216	-0.216	-0.216	-0.216	+0.271	+0.271	+0.271	+0.271	+0.494
		D	+0.134	+0.200	-0.215	-0.220	-0.259	-0.246	+0.266	+0.268	+0.264	+0.260	+0.452
TANI-14	LEB	B	+0.105	+0.159	-0.232	-0.229	-0.267	-0.281	+0.252	+0.251	+0.244	+0.250	+0.252
		C	+0.135	+0.135	-0.254	-0.265	-0.265	-0.254	+0.245	+0.250	+0.250	+0.245	+0.222
		D	+0.159	+0.105	-0.281	-0.267	-0.229	-0.232	+0.250	+0.244	+0.251	+0.252	+0.252
	^{1}ES	B	+0.206	+0.158	-0.236	-0.230	-0.211	-0.230	+0.272	+0.272	+0.267	+0.268	+0.536
		C	+0.193	+0.193	-0.210	-0.236	-0.236	-0.210	+0.270	+0.273	+0.273	+0.270	+0.580
		D	+0.158	+0.206	-0.230	-0.211	-0.230	-0.236	+0.268	+0.267	+0.272	+0.272	+0.536
	^{3}ES	B	+0.176	+0.210	-0.216	-0.210	-0.249	-0.231	+0.273	+0.273	+0.269	+0.266	+0.561
		C	+0.144	+0.144	-0.223	-0.239	-0.239	-0.223	+0.264	+0.266	+0.266	+0.264	+0.424
		D	+0.210	+0.176	-0.249	-0.231	-0.210	-0.216	+0.269	+0.266	+0.273	+0.273	+0.561

A.2 Optimised Structures of PANI-CMP Oligomeric Models for Primary and Secondary Structure Analyses

A.2.1 Optimised Structures of **OTPA-BZN-210** Oligomers

*A.2.1.1 **OTPA-BZN-210**, **LEB** State*

H	-1.876186	11.627656	1.001472	C	1.385374	7.882327	0.450002
C	-1.951258	10.553706	1.148670	C	4.097681	8.625310	0.569560
C	-2.127583	7.794944	1.501357	C	1.875762	8.620357	1.540000
C	-0.927907	9.730702	0.684246	C	2.271415	7.517411	-0.576777
C	-3.073009	10.009739	1.779318	C	3.614464	7.881076	-0.509265
C	-3.153735	8.625315	1.946621	C	3.216800	8.993870	1.589373
C	-1.001601	8.339292	0.862534	H	1.201620	8.896755	2.343513
H	-0.067476	10.159140	0.181632	H	1.899638	6.948158	-1.421907
H	-3.871817	10.654395	2.133222	H	4.284107	7.589839	-1.313922
H	-4.016462	8.185289	2.439331	H	3.577216	9.564514	2.440928
H	-2.190411	6.721412	1.643320	H	5.143842	8.912244	0.615762
N	0.027718	7.492630	0.390911	C	-0.310187	6.222132	-0.156133

C	-0.961858	3.699498	-1.255562
C	0.341316	5.061695	0.276100
C	-1.303106	6.106423	-1.137714
C	-1.626876	4.867520	-1.674817
C	0.028313	3.818291	-0.263434
H	1.099378	5.135507	1.049536
H	-1.819537	6.997081	-1.481314
H	-2.391708	4.797358	-2.443972
H	0.529346	2.934244	0.112030
N	-1.338218	2.479605	-1.813598
H	-2.267463	2.448191	-2.209268
C	-0.652844	1.258437	-1.776085
C	0.652844	-1.258437	-1.776085
C	0.749058	1.175221	-1.803249
C	-1.385374	0.060631	-1.779153
C	-0.749058	-1.175221	-1.803249
C	1.385374	-0.060631	-1.779153
H	1.344562	2.079980	-1.846901
H	-2.471629	0.101094	-1.778194
H	-1.344562	-2.079980	-1.846901
H	2.471629	-0.101094	-1.778194
N	1.338218	-2.479605	-1.813598
H	2.267463	-2.448191	-2.209268
C	0.961858	-3.699498	-1.255562
C	0.310187	-6.222132	-0.156133
C	1.626876	-4.867520	-1.674817
C	-0.028313	-3.818291	-0.263434
C	-0.341316	-5.061695	0.276100
C	1.303106	-6.106423	-1.137714
H	2.391708	-4.797358	-2.443972
H	-0.529346	-2.934244	0.112030
H	-1.099378	-5.135507	1.049536
H	1.819537	-6.997081	-1.481314
N	-0.027718	-7.492630	0.390911
C	-1.385374	-7.882327	0.450002
C	-4.097681	-8.625310	0.569560
C	-1.875762	-8.620357	1.540000
C	-2.271415	-7.517411	-0.576777
C	-3.614464	-7.881076	-0.509265
C	-3.216800	-8.993870	1.589373
H	-1.201620	-8.896755	2.343513
H	-1.899638	-6.948158	-1.421907
H	-4.284107	-7.589839	-1.313922
H	-3.577216	-9.564514	2.440928
H	-5.143842	-8.912244	0.615762
C	1.001601	-8.339292	0.862534
C	3.073009	-10.009739	1.779318
C	2.127583	-7.794944	1.501357
C	0.927907	-9.730702	0.684246
C	1.951258	-10.553706	1.148670
C	3.153735	-8.625315	1.946621
H	2.190411	-6.721412	1.643320
H	0.067476	-10.159140	0.181632
H	1.876186	-11.627656	1.001472
H	4.016462	-8.185289	2.439331
H	3.871817	-10.654395	2.133222

*A.2.1.2 **OTPA-BZN-210**, **^{1}ES** State*

H	-1.381496	11.859164	-0.909744
C	-1.597760	10.921748	-0.407347
C	-2.155824	8.502500	0.880465
C	-0.654194	9.898708	-0.428663

C	-2.819176	10.741277	0.247992
C	-3.094266	9.531181	0.890009
C	-0.937871	8.686320	0.212405
H	0.292754	10.025820	-0.941740
H	-3.551235	11.542375	0.262404
H	-4.034865	9.392290	1.413411
H	-2.351363	7.568854	1.397230
N	0.038399	7.645568	0.209487
C	1.382084	7.990900	0.537447
C	4.002774	8.703749	1.165006
C	1.632021	8.825579	1.634526
C	2.439971	7.521298	-0.253388
C	3.747159	7.876153	0.068659
C	2.942557	9.178045	1.942937
H	0.804022	9.181966	2.237223
H	2.231507	6.900905	-1.118482
H	4.565621	7.518773	-0.548123
H	3.136688	9.818964	2.797031
H	5.022839	8.982752	1.408972
C	-0.308234	6.346399	-0.090829
C	-0.994539	3.684315	-0.716110
C	0.447936	5.259294	0.421985
C	-1.442317	6.061679	-0.895882
C	-1.776846	4.762799	-1.194999
C	0.111219	3.960267	0.123001
H	1.267524	5.456678	1.101458
H	-2.028723	6.875431	-1.303127
H	-2.624833	4.562705	-1.842550
H	0.653062	3.150575	0.594988
N	-1.382084	2.404238	-1.048156
H	-2.357295	2.312710	-1.319674
C	-0.669481	1.238203	-1.069649
C	0.669481	-1.238203	-1.069649
C	0.749840	1.191242	-1.112341
C	-1.395896	0.018673	-1.122944
C	-0.749840	-1.191242	-1.112341
C	1.395896	-0.018673	-1.122944
H	1.326743	2.103481	-1.185659
H	-2.480244	0.047438	-1.166619
H	-1.326743	-2.103481	-1.185659
H	2.480244	-0.047438	-1.166619
N	1.382084	-2.404238	-1.048156
H	2.357295	-2.312710	-1.319674
C	0.994539	-3.684315	-0.716110
C	0.308234	-6.346399	-0.090829
C	1.776846	-4.762799	-1.194999
C	-0.111219	-3.960267	0.123001
C	-0.447936	-5.259294	0.421985
C	1.442317	-6.061679	-0.895882
H	2.624833	-4.562705	-1.842550
H	-0.653062	-3.150575	0.594988
H	-1.267524	-5.456678	1.101458
H	2.028723	-6.875431	-1.303127
N	-0.038399	-7.645568	0.209487
C	-1.382084	-7.990900	0.537447
C	-4.002774	-8.703749	1.165006
C	-1.632021	-8.825579	1.634526
C	-2.439971	-7.521298	-0.253388
C	-3.747159	-7.876153	0.068659
C	-2.942557	-9.178045	1.942937
H	-0.804022	-9.181966	2.237223
H	-2.231507	-6.900905	-1.118482
H	-4.565621	-7.518773	-0.548123
H	-3.136688	-9.818964	2.797031

H	-5.022839	-8.982752	1.408972	C	3.094266	-9.531181	0.890009
C	0.937871	-8.686320	0.212405	H	2.351363	-7.568854	1.397230
C	2.819176	-10.741277	0.247992	H	-0.292754	-10.025820	-0.941740
C	2.155824	-8.502500	0.880465	H	1.381496	-11.859164	-0.909744
C	0.654194	-9.898708	-0.428663	H	4.034865	-9.392290	1.413411
C	1.597760	-10.921748	-0.407347	H	3.551235	-11.542375	0.262404

*A.2.1.3 **OTPA-BZN-210**, ^{3}**ES** State*

H	-1.218451	11.797741	-0.092820	C	-0.940249	3.674928	-1.252844
C	-1.485086	10.788924	0.204972	C	0.410472	5.016830	0.248154
C	-2.179267	8.185124	0.959577	C	-1.318918	6.071378	-1.113740
C	-0.544247	9.770415	0.093864	C	-1.642074	4.846349	-1.642409
C	-2.768675	10.514699	0.687095	C	0.083699	3.789356	-0.277373
C	-3.111247	9.213278	1.063817	H	1.165179	5.083939	1.022022
C	-0.896644	8.465746	0.466936	H	-1.838721	6.958469	-1.453419
H	0.449505	9.970599	-0.290824	H	-2.420201	4.774381	-2.395473
H	-3.497640	11.314013	0.773058	H	0.577458	2.902088	0.097034
H	-4.101207	8.999937	1.453652	N	-1.309736	2.480738	-1.805165
H	-2.427050	7.177597	1.275095	H	-2.198717	2.475929	-2.293199
N	0.067295	7.423013	0.364361	C	-0.632594	1.251106	-1.777074
C	1.391617	7.680286	0.817598	C	0.632594	-1.251106	-1.777074
C	3.979626	8.207884	1.698621	C	0.769145	1.168423	-1.806924
C	1.587638	8.351587	2.032809	C	-1.391617	0.070837	-1.794939
C	2.486485	7.280647	0.037436	C	-0.769145	-1.168423	-1.806924
C	3.777282	7.544753	0.485211	C	1.391617	-0.070837	-1.794939
C	2.883253	8.610453	2.467616	H	1.370513	2.067351	-1.865878
H	0.731526	8.648538	2.628099	H	-2.475650	0.126868	-1.807062
H	2.318735	6.792125	-0.916132	H	-1.370513	-2.067351	-1.865878
H	4.625442	7.245754	-0.122064	H	2.475650	-0.126868	-1.807062
H	3.037778	9.121123	3.412500	N	1.309736	-2.480738	-1.805165
H	4.988014	8.415015	2.042094	H	2.198717	-2.475929	-2.293199
C	-0.272952	6.190418	-0.161912	C	0.940249	-3.674928	-1.252844

C	0.272952	-6.190418	-0.161912
C	1.642074	-4.846349	-1.642409
C	-0.083699	-3.789356	-0.277373
C	-0.410472	-5.016830	0.248154
C	1.318918	-6.071378	-1.113740
H	2.420201	-4.774381	-2.395473
H	-0.577458	-2.902088	0.097034
H	-1.165179	-5.083939	1.022022
H	1.838721	-6.958469	-1.453419
N	-0.067295	-7.423013	0.364361
C	-1.391617	-7.680286	0.817598
C	-3.979626	-8.207884	1.698621
C	-1.587638	-8.351587	2.032809
C	-2.486485	-7.280647	0.037436
C	-3.777282	-7.544753	0.485211
C	-2.883253	-8.610453	2.467616
H	-0.731526	-8.648538	2.628099
H	-2.318735	-6.792125	-0.916132
H	-4.625442	-7.245754	-0.122064
H	-3.037778	-9.121123	3.412500
H	-4.988014	-8.415015	2.042094
C	0.896644	-8.465746	0.466936
C	2.768675	-10.514699	0.687095
C	2.179267	-8.185124	0.959577
C	0.544247	-9.770415	0.093864
C	1.485086	-10.788924	0.204972
C	3.111247	-9.213278	1.063817
H	2.427050	-7.177597	1.275095
H	-0.449505	-9.970599	-0.290824
H	1.218451	-11.797741	-0.092820
H	4.101207	-8.999937	1.453652
H	3.497640	-11.314013	0.773058

A.2.1.4 ***OTPA-BZN-210, EB*** *State*

H	1.741435	11.741569	-1.119905
C	1.254494	10.908211	-0.621486
C	0.017129	8.754924	0.649014
C	1.902841	9.676638	-0.558326
C	-0.017129	11.069350	-0.066008
C	-0.631826	9.985029	0.564760
C	1.288896	8.590428	0.081560
H	2.885261	9.548145	-1.000314
H	-0.522673	12.028519	-0.123323
H	-1.616960	10.098777	1.008126
H	-0.454625	7.917319	1.151895
N	1.955252	7.338905	0.159125
C	3.337985	7.305996	0.479232
C	6.072240	7.251570	1.108450
C	3.849803	8.139726	1.483885
C	4.205900	6.446073	-0.209528
C	5.560953	6.415474	0.112832
C	5.209557	8.115775	1.786864
H	3.178117	8.802211	2.019488
H	3.812273	5.807220	-0.993046
H	6.222052	5.744713	-0.428532
H	5.592778	8.767061	2.567244
H	7.130137	7.230473	1.351888
C	1.250495	6.140573	-0.067728
C	-0.148930	3.719859	-0.538106
C	1.556480	4.979351	0.664053
C	0.212291	6.082781	-1.016137
C	-0.491417	4.906829	-1.219127

C	0.882889	3.791254	0.424560
H	2.323330	5.019462	1.429919
H	-0.043234	6.971425	-1.582618
H	-1.298823	4.870416	-1.943620
H	1.110567	2.919198	1.028663
N	-0.919375	2.589876	-0.778310
C	-0.421260	1.380423	-0.815864
C	0.421260	-1.380423	-0.815864
C	0.991955	1.015530	-0.868132
C	-1.375017	0.281357	-0.896927
C	-0.991955	-1.015530	-0.868132
C	1.375017	-0.281357	-0.896927
H	1.731371	1.804882	-0.933208
H	-2.422605	0.558485	-0.965407
H	-1.731371	-1.804882	-0.933208
H	2.422605	-0.558485	-0.965407
N	0.919375	-2.589876	-0.778310
C	0.148930	-3.719859	-0.538106
C	-1.250495	-6.140573	-0.067728
C	0.491417	-4.906829	-1.219127
C	-0.882889	-3.791254	0.424560
C	-1.556480	-4.979351	0.664053
C	-0.212291	-6.082781	-1.016137
H	1.298823	-4.870416	-1.943620
H	-1.110567	-2.919198	1.028663
H	-2.323330	-5.019462	1.429919
H	0.043234	-6.971425	-1.582618
N	-1.955252	-7.338905	0.159125
C	-3.337985	-7.305996	0.479232
C	-6.072240	-7.251570	1.108450
C	-3.849803	-8.139726	1.483885
C	-4.205900	-6.446073	-0.209528
C	-5.560953	-6.415474	0.112832
C	-5.209557	-8.115775	1.786864
H	-3.178117	-8.802211	2.019488
H	-3.812273	-5.807220	-0.993046
H	-6.222052	-5.744713	-0.428532
H	-5.592778	-8.767061	2.567244
H	-7.130137	-7.230473	1.351888
C	-1.288896	-8.590428	0.081560
C	0.017129	-11.069350	-0.066008
C	-0.017129	-8.754924	0.649014
C	-1.902841	-9.676638	-0.558326
C	-1.254494	-10.908211	-0.621486
C	0.631826	-9.985029	0.564760
H	0.454625	-7.917319	1.151895
H	-2.885261	-9.548145	-1.000314
H	-1.741435	-11.741569	-1.119905
H	1.616960	-10.098777	1.008126
H	0.522673	-12.028519	-0.123323

A.2.2 Optimised Structures of **OTPA-BZN-221** Oligomers

A.2.2.1 ***OTPA-BZN-221, LEB*** *State*

H	-0.000000	-0.000000	11.440731
C	-0.000000	-0.000000	10.355016
C	-0.000000	-0.000000	7.533097
C	-0.498991	-1.094121	9.644103
C	0.498991	1.094121	9.644103
C	0.508504	1.097931	8.251505
C	-0.508504	-1.097931	8.251505
H	-0.898079	-1.953362	10.176679

H	0.898079	1.953362	10.176679
H	0.911889	1.947733	7.712092
H	-0.911889	-1.947733	7.712092
N	-0.000000	-0.000000	6.129691
C	-0.000584	1.208580	5.376968
C	-0.119626	3.461555	3.677449
C	0.927832	1.375190	4.341056
C	-0.953374	2.211885	5.592044
C	-1.010903	3.322932	4.754603
C	0.877520	2.484569	3.507922
H	1.687157	0.615612	4.184951
H	-1.672644	2.102965	6.397632
H	-1.782201	4.073060	4.910315
H	1.615010	2.600564	2.721731
C	0.000584	-1.208580	5.376968
C	0.119626	-3.461555	3.677449
C	0.953374	-2.211885	5.592044
C	-0.927832	-1.375190	4.341056
C	-0.877520	-2.484569	3.507922
C	1.010903	-3.322932	4.754603
H	1.672644	-2.102965	6.397632
H	-1.687157	-0.615612	4.184951
H	-1.615010	-2.600564	2.721731
H	1.782201	-4.073060	4.910315
N	0.208660	-4.566468	2.822090
H	0.782881	-5.324936	3.166766
C	0.094780	-4.515128	1.417599
C	-0.094780	-4.515128	-1.417599
C	0.035446	-5.718192	0.694344
C	0.059138	-3.315234	0.693162
C	-0.059138	-3.315234	-0.693162
C	-0.035446	-5.718192	-0.694344
H	0.057799	-6.663823	1.229964
H	0.120422	-2.365417	1.210104
H	-0.120422	-2.365417	-1.210104
H	-0.057799	-6.663823	-1.229964
N	-0.208660	-4.566468	-2.822090
H	-0.782881	-5.324936	-3.166766
C	-0.119626	-3.461555	-3.677449
C	-0.000584	-1.208580	-5.376968
C	-1.010903	-3.322932	-4.754603
C	0.877520	-2.484569	-3.507922
C	0.927832	-1.375190	-4.341056
C	-0.953374	-2.211885	-5.592044
H	-1.782201	-4.073060	-4.910315
H	1.615010	-2.600564	-2.721731
H	1.687157	-0.615612	-4.184951
H	-1.672644	-2.102965	-6.397632
N	-0.000000	0.000000	-6.129691
C	0.000584	1.208580	-5.376968
C	0.119626	3.461555	-3.677449
C	0.953374	2.211885	-5.592044
C	-0.927832	1.375190	-4.341056
C	-0.877520	2.484569	-3.507922
C	1.010903	3.322932	-4.754603
H	1.672644	2.102965	-6.397632
H	-1.687157	0.615612	-4.184951
H	-1.615010	2.600564	-2.721731
H	1.782201	4.073060	-4.910315
C	-0.000000	0.000000	-7.533097
C	-0.000000	0.000000	-10.355016
C	0.508504	-1.097931	-8.251505
C	-0.508504	1.097931	-8.251505
C	-0.498991	1.094121	-9.644103

C	0.498991	-1.094121	-9.644103
H	0.911889	-1.947733	-7.712092
H	-0.911889	1.947733	-7.712092
H	-0.898079	1.953362	-10.176679
H	0.898079	-1.953362	-10.176679
H	-0.000000	0.000000	-11.440731
N	0.208660	4.566468	-2.822090
H	0.782881	5.324936	-3.166766
C	0.094780	4.515128	-1.417599
C	-0.094780	4.515128	1.417599
C	0.035446	5.718192	-0.694344
C	0.059138	3.315234	-0.693162
C	-0.059138	3.315234	0.693162
C	-0.035446	5.718192	0.694344
H	0.057799	6.663823	-1.229964
H	0.120422	2.365417	-1.210104
H	-0.120422	2.365417	1.210104
H	-0.057799	6.663823	1.229964
N	-0.208660	4.566468	2.822090
H	-0.782881	5.324936	3.166766

*A.2.2.2 **OTPA-BZN-221**, **^{1}ES** State*

H	-0.000000	-0.000000	11.434226
C	-0.000000	-0.000000	10.349331
C	-0.000000	-0.000000	7.578950
C	-0.785734	-0.928119	9.655202
C	0.785734	0.928119	9.655202
C	0.793948	0.934129	8.267405
C	-0.793948	-0.934129	8.267405
H	-1.405531	-1.632314	10.198785
H	1.405531	1.632314	10.198785
H	1.432123	1.614272	7.714889
H	-1.432123	-1.614272	7.714889
N	-0.000000	-0.000000	6.165644
C	0.053950	1.177247	5.439901
C	-0.098119	3.358466	3.690422
C	0.831387	1.198643	4.248035
C	-0.669504	2.338498	5.825321
C	-0.748294	3.402531	4.962962
C	0.785282	2.276203	3.410042
H	1.513779	0.379841	4.051045
H	-1.234968	2.341232	6.749692
H	-1.377319	4.251499	5.209986
H	1.445286	2.324526	2.554608
C	-0.053950	-1.177247	5.439901
C	0.098119	-3.358466	3.690422
C	0.669504	-2.338498	5.825321
C	-0.831387	-1.198643	4.248035
C	-0.785282	-2.276203	3.410042
C	0.748294	-3.402531	4.962962
H	1.234968	-2.341232	6.749692
H	-1.513779	-0.379841	4.051045
H	-1.445286	-2.324526	2.554608
H	1.377319	-4.251499	5.209986
N	0.339392	-4.341036	2.788458
H	0.795149	-5.176739	3.143146
C	0.147114	-4.305437	1.396382
C	-0.147114	-4.305437	-1.396382
C	0.068950	-5.518384	0.689973
C	0.092431	-3.095549	0.685440
C	-0.092431	-3.095549	-0.685440
C	-0.068950	-5.518384	-0.689973

H	0.116327	-6.461955	1.223535
H	0.209368	-2.147934	1.191852
H	-0.209368	-2.147934	-1.191852
H	-0.116327	-6.461955	-1.223535
N	-0.339392	-4.341036	-2.788458
H	-0.795149	-5.176739	-3.143146
C	-0.098119	-3.358466	-3.690422
C	0.053950	-1.177247	-5.439901
C	-0.748294	-3.402531	-4.962962
C	0.785282	-2.276203	-3.410042
C	0.831387	-1.198643	-4.248035
C	-0.669504	-2.338498	-5.825321
H	-1.377319	-4.251499	-5.209986
H	1.445286	-2.324526	-2.554608
H	1.513779	-0.379841	-4.051045
H	-1.234968	-2.341232	-6.749692
N	-0.000000	0.000000	-6.165644
C	-0.053950	1.177247	-5.439901
C	0.098119	3.358466	-3.690422
C	0.669504	2.338498	-5.825321
C	-0.831387	1.198643	-4.248035
C	-0.785282	2.276203	-3.410042
C	0.748294	3.402531	-4.962962
H	1.234968	2.341232	-6.749692
H	-1.513779	0.379841	-4.051045
H	-1.445286	2.324526	-2.554608
H	1.377319	4.251499	-5.209986
C	-0.000000	0.000000	-7.578950
C	-0.000000	0.000000	-10.349331
C	0.793948	-0.934129	-8.267405
C	-0.793948	0.934129	-8.267405
C	-0.785734	0.928119	-9.655202
C	0.785734	-0.928119	-9.655202
H	1.432123	-1.614272	-7.714889
H	-1.432123	1.614272	-7.714889
H	-1.405531	1.632314	-10.198785
H	1.405531	-1.632314	-10.198785
H	-0.000000	0.000000	-11.434226
N	0.339392	4.341036	-2.788458
H	0.795149	5.176739	-3.143146
C	0.147114	4.305437	-1.396382
C	-0.147114	4.305437	1.396382
C	0.068950	5.518384	-0.689973
C	0.092431	3.095549	-0.685440
C	-0.092431	3.095549	0.685440
C	-0.068950	5.518384	0.689973
H	0.116327	6.461955	-1.223535
H	0.209368	2.147934	-1.191852
H	-0.209368	2.147934	1.191852
H	-0.116327	6.461955	1.223535
N	-0.339392	4.341036	2.788458
H	-0.795149	5.176739	3.143146

*A.2.2.3 **OTPA-BZN-221**, ^{5}**ES** State*

H	0.000000	-0.000000	11.362732
C	0.000000	-0.000000	10.278053
C	0.000000	-0.000000	7.491061
C	-0.573289	-1.074685	9.579877
C	0.573289	1.074685	9.579877
C	0.578335	1.085339	8.197251
C	-0.578335	-1.085339	8.197251
H	-1.031438	-1.892690	10.124351

H	1.031438	1.892690	10.124351
H	1.056095	1.889833	7.651895
H	-1.056095	-1.889833	7.651895
N	0.000000	-0.000000	6.105348
C	0.047472	1.202737	5.349552
C	-0.014317	3.411826	3.663201
C	0.937444	1.278448	4.266767
C	-0.821850	2.266794	5.633720
C	-0.854039	3.367008	4.786864
C	0.925041	2.390199	3.443313
H	1.650370	0.480496	4.094562
H	-1.507548	2.202888	6.470249
H	-1.565569	4.165974	4.966408
H	1.651210	2.476001	2.644565
C	-0.047472	-1.202737	5.349552
C	0.014317	-3.411826	3.663201
C	0.821850	-2.266794	5.633720
C	-0.937444	-1.278448	4.266767
C	-0.925041	-2.390199	3.443313
C	0.854039	-3.367008	4.786864
H	1.507548	-2.202888	6.470249
H	-1.650370	-0.480496	4.094562
H	-1.651210	-2.476001	2.644565
H	1.565569	-4.165974	4.966408
N	0.122142	-4.495301	2.771080
H	0.348651	-5.395750	3.182956
C	0.054348	-4.451685	1.410405
C	-0.054348	-4.451685	-1.410405
C	0.030831	-5.677857	0.684074
C	0.033564	-3.228024	0.684098
C	-0.033564	-3.228024	-0.684098
C	-0.030831	-5.677857	-0.684074
H	0.051138	-6.617545	1.226059
H	0.082289	-2.283078	1.206790
H	-0.082289	-2.283078	-1.206790
H	-0.051138	-6.617545	-1.226059
N	-0.122142	-4.495301	-2.771080
H	-0.348651	-5.395750	-3.182956
C	-0.014317	-3.411826	-3.663201
C	0.047472	-1.202737	-5.349552
C	-0.854039	-3.367008	-4.786864
C	0.925041	-2.390199	-3.443313
C	0.937444	-1.278448	-4.266767
C	-0.821850	-2.266794	-5.633720
H	-1.565569	-4.165974	-4.966408
H	1.651210	-2.476001	-2.644565
H	1.650370	-0.480496	-4.094562
H	-1.507548	-2.202888	-6.470249
N	-0.000000	0.000000	-6.105348
C	-0.047472	1.202737	-5.349552
C	0.014317	3.411826	-3.663201
C	0.821850	2.266794	-5.633720
C	-0.937444	1.278448	-4.266767
C	-0.925041	2.390199	-3.443313
C	0.854039	3.367008	-4.786864
H	1.507548	2.202888	-6.470249
H	-1.650370	0.480496	-4.094562
H	-1.651210	2.476001	-2.644565
H	1.565569	4.165974	-4.966408
C	-0.000000	0.000000	-7.491061
C	-0.000000	0.000000	-10.278053
C	0.578335	-1.085339	-8.197251
C	-0.578335	1.085339	-8.197251
C	-0.573289	1.074685	-9.579877

C	0.573289	-1.074685	-9.579877
H	1.056095	-1.889833	-7.651895
H	-1.056095	1.889833	-7.651895
H	-1.031438	1.892690	-10.124351
H	1.031438	-1.892690	-10.124351
H	-0.000000	0.000000	-11.362732
N	0.122142	4.495301	-2.771080
H	0.348651	5.395750	-3.182956
C	0.054348	4.451685	-1.410405
C	-0.054348	4.451685	1.410405
C	0.030831	5.677857	-0.684074
C	0.033564	3.228024	-0.684098
C	-0.033564	3.228024	0.684098
C	-0.030831	5.677857	0.684074
H	0.051138	6.617545	-1.226059
H	0.082289	2.283078	-1.206790
H	-0.082289	2.283078	1.206790
H	-0.051138	6.617545	1.226059
N	-0.122142	4.495301	2.771080
H	-0.348651	5.395750	3.182956

A.2.2.4 ***OTPA-BZN-221, EB*** *State*

H	0.000000	-0.000000	11.345617
C	0.000000	-0.000000	10.259987
C	0.000000	-0.000000	7.446019
C	-0.560662	-1.065353	9.551595
C	0.560662	1.065353	9.551595
C	0.571895	1.067439	8.158860
C	-0.571895	-1.067439	8.158860
H	-1.007357	-1.899673	10.085290
H	1.007357	1.899673	10.085290
H	1.025944	1.890339	7.617756
H	-1.025944	-1.890339	7.617756
N	0.000000	-0.000000	6.038158
C	0.022774	1.203191	5.286688
C	-0.047166	3.448060	3.578187
C	0.959564	1.340617	4.251203
C	-0.894467	2.239733	5.516882
C	-0.910255	3.355444	4.688895
C	0.927982	2.441421	3.409784
H	1.704366	0.564767	4.106883
H	-1.603763	2.154071	6.333660
H	-1.634290	4.147707	4.849499
H	1.674463	2.544888	2.629407
C	-0.022774	-1.203191	5.286688
C	0.047166	-3.448060	3.578187
C	0.894467	-2.239733	5.516882
C	-0.959564	-1.340617	4.251203
C	-0.927982	-2.441421	3.409784
C	0.910255	-3.355444	4.688895
H	1.603763	-2.154071	6.333660
H	-1.704366	-0.564767	4.106883
H	-1.674463	-2.544888	2.629407
H	1.634290	-4.147707	4.849499
N	0.158639	-4.560575	2.746030
C	0.086009	-4.459503	1.444724
C	-0.086009	-4.459503	-1.444724
C	0.057197	-5.698118	0.673257
C	0.046436	-3.216791	0.673774
C	-0.046436	-3.216791	-0.673774
C	-0.057197	-5.698118	-0.673257
H	0.101047	-6.622923	1.239739

H	0.102091	-2.274561	1.203731	H	1.634290	4.147707	-4.849499
H	-0.102091	-2.274561	-1.203731	C	-0.000000	-0.000000	-7.446019
H	-0.101047	-6.622923	-1.239739	C	-0.000000	-0.000000	-10.259987
N	-0.158639	-4.560575	-2.746030	C	0.571895	-1.067439	-8.158860
C	-0.047166	-3.448060	-3.578187	C	-0.571895	1.067439	-8.158860
C	0.022774	-1.203191	-5.286688	C	-0.560662	1.065353	-9.551595
C	-0.910255	-3.355444	-4.688895	C	0.560662	-1.065353	-9.551595
C	0.927982	-2.441421	-3.409784	H	1.025944	-1.890339	-7.617756
C	0.959564	-1.340617	-4.251203	H	-1.025944	1.890339	-7.617756
C	-0.894467	-2.239733	-5.516882	H	-1.007357	1.899673	-10.085290
H	-1.634290	-4.147707	-4.849499	H	1.007357	-1.899673	-10.085290
H	1.674463	-2.544888	-2.629407	H	-0.000000	-0.000000	-11.345617
H	1.704366	-0.564767	-4.106883	N	0.158639	4.560575	-2.746030
H	-1.603763	-2.154071	-6.333660	C	0.086009	4.459503	-1.444724
N	-0.000000	-0.000000	-6.038158	C	-0.086009	4.459503	1.444724
C	-0.022774	1.203191	-5.286688	C	0.057197	5.698118	-0.673257
C	0.047166	3.448060	-3.578187	C	0.046436	3.216791	-0.673774
C	0.894467	2.239733	-5.516882	C	-0.046436	3.216791	0.673774
C	-0.959564	1.340617	-4.251203	C	-0.057197	5.698118	0.673257
C	-0.927982	2.441421	-3.409784	H	0.101047	6.622923	-1.239739
C	0.910255	3.355444	-4.688895	H	0.102091	2.274561	-1.203731
H	1.603763	2.154071	-6.333660	H	-0.102091	2.274561	1.203731
H	-1.704366	0.564767	-4.106883	H	-0.101047	6.622923	1.239739
H	-1.674463	2.544888	-2.629407	N	-0.158639	4.560575	2.746030

A.2.3 Optimised Structures of **OTPA-FLR-210** Oligomers

A.2.3.1 ***OTPA-FLR-210, LEB*** *State*

H	-13.471131	2.530738	0.109343	C	-10.507374	3.828943	1.144449
C	-12.417345	2.582622	0.369072	C	-10.258866	1.489854	0.549526
C	-9.708773	2.694696	1.015897	H	-12.054166	0.523876	-0.150875
C	-11.623524	1.447713	0.220130	H	-12.487845	4.666313	0.935384
C	-11.867034	3.782049	0.827751	H	-10.063863	4.752011	1.507611

H	-8.655875	2.733428	1.273849
N	-9.442687	0.344568	0.399593
C	-9.935556	-0.948522	0.691540
C	-10.888656	-3.530011	1.279590
C	-10.807588	-1.157649	1.772465
C	-9.543899	-2.048371	-0.088800
C	-10.012172	-3.325629	0.211287
C	-11.284301	-2.436049	2.053203
H	-11.106680	-0.315317	2.386933
H	-8.871816	-1.893733	-0.926057
H	-9.698155	-4.164227	-0.404165
H	-11.958190	-2.578174	2.893622
H	-11.256624	-4.526000	1.506583
C	-8.102428	0.495788	-0.053241
C	-5.440287	0.773829	-0.962513
C	-7.046337	-0.132355	0.617472
C	-7.810669	1.278443	-1.178054
C	-6.502301	1.418510	-1.622739
C	-5.734881	-0.001040	0.173466
H	-7.256554	-0.724472	1.502471
H	-8.618160	1.773935	-1.707398
H	-6.294563	2.018598	-2.504898
H	-4.934242	-0.471847	0.731137
N	-4.141266	0.971978	-1.431841
H	-3.995368	1.817023	-1.966303
H	-2.021075	-3.040675	-0.658339
C	-1.932953	-1.973442	-0.843675
C	-1.740638	0.786337	-1.353430
C	-0.680384	-1.366727	-0.947037
C	-3.087755	-1.208218	-0.999882
C	-3.007966	0.177188	-1.241833
C	-0.598230	0.017956	-1.213919
H	-4.057870	-1.689022	-0.957737
H	-1.676352	1.855632	-1.542433
C	0.676370	-1.904864	-0.837889
C	3.443401	-2.375271	-0.730114
C	1.148172	-3.197594	-0.599533
C	1.598496	-0.854140	-1.033270
C	2.965664	-1.075150	-0.992928
C	2.520660	-3.423309	-0.539138
H	0.459457	-4.024888	-0.450850
H	3.662076	-0.266056	-1.182564
H	2.896569	-4.422924	-0.336342
C	0.855383	0.442792	-1.290874
H	1.105293	0.872510	-2.269924
H	1.100405	1.209969	-0.544704
N	4.806363	-2.681068	-0.702347
H	5.042545	-3.642543	-0.904166
C	5.886278	-1.839201	-0.434356
C	8.152300	-0.240790	0.113937
C	7.159331	-2.199303	-0.912528
C	5.771490	-0.670003	0.338682
C	6.890213	0.111438	0.606858
C	8.272030	-1.411728	-0.645981
H	7.266661	-3.097349	-1.515407
H	4.813550	-0.391237	0.761123
H	6.787855	1.004804	1.214651
H	9.244178	-1.699566	-1.033056
N	9.288887	0.571841	0.381742
C	9.209160	1.968395	0.173134
C	9.022319	4.746049	-0.236552
C	9.849659	2.862644	1.046399
C	8.471058	2.482219	-0.905357
C	8.375009	3.858408	-1.099291

C	9.762115	4.236456	0.833416
H	10.413048	2.474470	1.888100
H	7.975352	1.797021	-1.584614
H	7.799787	4.237102	-1.939743
H	10.264438	4.912698	1.519696
H	8.950525	5.817868	-0.394556
C	10.479267	-0.030771	0.851140
C	12.839946	-1.254241	1.771717
C	10.420263	-1.112147	1.744900
C	11.734819	0.428259	0.420636
C	12.900719	-0.174597	0.887085
C	11.591650	-1.719624	2.191694
H	9.453665	-1.470198	2.082759
H	11.788957	1.256323	-0.277902
H	13.863023	0.194456	0.543004
H	11.525909	-2.554793	2.883648
H	13.751033	-1.726034	2.127027

*A.2.3.2 **OTPA-FLR-210**, **^{1}ES** State*

H	-13.578300	1.785722	-1.218388
C	-12.651936	2.000683	-0.695090
C	-10.261511	2.551245	0.645713
C	-11.688467	1.003741	-0.569760
C	-12.425398	3.272520	-0.161607
C	-11.229003	3.543195	0.507289
C	-10.489076	1.281293	0.098657
H	-11.852382	0.017036	-0.988923
H	-13.179184	4.046850	-0.262664
H	-11.053282	4.524606	0.936460
H	-9.340854	2.747325	1.184899
N	-9.511174	0.254248	0.243407
C	-9.950121	-1.035061	0.662116
C	-10.844250	-3.552217	1.467417
C	-10.851187	-1.146300	1.729178
C	-9.503447	-2.181952	-0.008845
C	-9.948234	-3.435945	0.401655
C	-11.295220	-2.404598	2.125636
H	-11.189131	-0.251627	2.240544
H	-8.827551	-2.082927	-0.851595
H	-9.606331	-4.322417	-0.123323
H	-11.988885	-2.489397	2.956207
H	-11.193518	-4.531165	1.780083
C	-8.174475	0.499917	-0.013152
C	-5.446320	0.964520	-0.557077
C	-7.164644	-0.252524	0.636855
C	-7.780940	1.521121	-0.913354
C	-6.448427	1.749047	-1.172444
C	-5.831456	-0.023805	0.376669
H	-7.445308	-0.984770	1.383769
H	-8.535306	2.105894	-1.424543
H	-6.164170	2.510675	-1.892203
H	-5.081500	-0.561058	0.943807
N	-4.125675	1.239934	-0.862063
H	-3.956556	2.181450	-1.202948
H	-2.013779	-2.812873	-0.589592
C	-1.944395	-1.730853	-0.630513
C	-1.743293	1.090439	-0.847848
C	-0.686954	-1.091492	-0.645123
C	-3.090453	-0.971639	-0.700890
C	-3.011655	0.448646	-0.784299
C	-0.607283	0.328836	-0.771794

H	-4.055477	-1.458365	-0.746262
H	-1.693871	2.172225	-0.933979
C	0.632663	-1.630041	-0.590582
C	3.377257	-2.146591	-0.554490
C	1.081112	-2.965825	-0.508606
C	1.576670	-0.562554	-0.677914
C	2.927639	-0.802927	-0.664264
C	2.432661	-3.214134	-0.499967
H	0.374117	-3.786924	-0.455765
H	3.635503	0.006466	-0.786315
H	2.799878	-4.233491	-0.430860
C	0.843823	0.755486	-0.804743
H	1.094996	1.275151	-1.737326
H	1.090059	1.441000	0.015021
N	4.701473	-2.492022	-0.539246
H	4.885123	-3.472132	-0.731025
C	5.834301	-1.730526	-0.320774
C	8.225497	-0.286395	0.076437
C	7.066038	-2.223437	-0.810261
C	5.828003	-0.523673	0.414407
C	6.995886	0.181962	0.602887
C	8.233279	-1.518775	-0.623161
H	7.083793	-3.150592	-1.375312
H	4.921103	-0.180501	0.895026
H	6.983432	1.083880	1.202156
H	9.160018	-1.894447	-1.038138
N	9.391481	0.433656	0.261743
C	9.357344	1.845801	0.448478
C	9.324381	4.613297	0.800170
C	10.125403	2.428372	1.465051
C	8.580497	2.647810	-0.398903
C	8.562925	4.027857	-0.214561
C	10.106342	3.809861	1.634882
H	10.722391	1.797119	2.114093
H	8.011476	2.188945	-1.200463
H	7.965764	4.647895	-0.875855
H	10.697730	4.258970	2.426527
H	9.312715	5.689979	0.936747
C	10.661605	-0.213811	0.275509
C	13.161280	-1.450913	0.322364
C	10.851207	-1.374141	1.038051
C	11.723624	0.333637	-0.455643
C	12.969401	-0.286980	-0.427232
C	12.099582	-1.991024	1.052528
H	10.028754	-1.774924	1.620987
H	11.563817	1.231754	-1.042278
H	13.789911	0.135194	-0.998804
H	12.246249	-2.886501	1.648199
H	14.134162	-1.931694	0.340854

*A.2.3.3 **OTPA-FLR-210**, ^{3}**ES** State*

H	-13.456858	1.920256	-0.429976
C	-12.423151	2.158900	-0.201537
C	-9.755707	2.773943	0.376395
C	-11.507177	1.128494	-0.013994
C	-12.014325	3.492479	-0.106443
C	-10.681351	3.795515	0.182955
C	-10.170539	1.439213	0.269505
H	-11.812218	0.091266	-0.096140
H	-12.733352	4.292068	-0.253003
H	-10.363127	4.829118	0.272895

H	-8.724722	2.999270	0.626786
N	-9.233705	0.385309	0.473990
C	-9.620019	-0.709375	1.299358
C	-10.403296	-2.845467	2.906446
C	-10.278618	-0.461512	2.511409
C	-9.361232	-2.023296	0.884320
C	-9.751636	-3.086133	1.694089
C	-10.666331	-1.532904	3.309906
H	-10.469173	0.560069	2.820764
H	-8.878913	-2.201638	-0.070546
H	-9.559738	-4.103770	1.369534
H	-11.168551	-1.342363	4.252853
H	-10.709692	-3.677270	3.532591
C	-7.981473	0.425855	-0.108613
C	-5.422204	0.491799	-1.298502
C	-6.877946	-0.222993	0.503696
C	-7.767373	1.130580	-1.322072
C	-6.522021	1.161864	-1.898273
C	-5.629340	-0.187166	-0.069433
H	-7.012617	-0.709670	1.461898
H	-8.600995	1.616001	-1.814038
H	-6.379323	1.677790	-2.842795
H	-4.791569	-0.634077	0.449691
N	-4.204768	0.568218	-1.911202
H	-4.123707	1.273127	-2.635737
H	-1.943405	-3.258022	-0.727672
C	-1.899846	-2.215032	-1.025068
C	-1.799495	0.482062	-1.860662
C	-0.673486	-1.569527	-1.204737
C	-3.078017	-1.513719	-1.257858
C	-3.033406	-0.163038	-1.653195
C	-0.632055	-0.222734	-1.634487
H	-4.032609	-2.019108	-1.173213
H	-1.778311	1.522164	-2.173562
C	0.695569	-2.047944	-1.040197
C	3.448969	-2.431030	-0.895056
C	1.191956	-3.298584	-0.659087
C	1.583230	-0.996410	-1.362919
C	2.953560	-1.178417	-1.304002
C	2.566756	-3.484787	-0.588285
H	0.521001	-4.116079	-0.414706
H	3.633942	-0.389163	-1.602500
H	2.972068	-4.443422	-0.278715
C	0.803943	0.236148	-1.769505
H	1.037688	0.550676	-2.794479
H	1.023949	1.093349	-1.120891
N	4.827920	-2.691993	-0.833615
H	5.098970	-3.644936	-1.050552
C	5.847320	-1.845228	-0.505058
C	8.030645	-0.182134	0.157448
C	7.181206	-2.251660	-0.776374
C	5.635752	-0.597227	0.137361
C	6.700054	0.212611	0.452954
C	8.244407	-1.444709	-0.455184
H	7.357154	-3.198968	-1.276228
H	4.636683	-0.303530	0.431849
H	6.526756	1.142455	0.980613
H	9.251334	-1.756248	-0.703628
N	9.094519	0.640438	0.474707
C	8.930809	2.054309	0.534256
C	8.637319	4.821993	0.644083
C	9.481689	2.768815	1.606625
C	8.242496	2.721592	-0.488714
C	8.095969	4.104453	-0.425746

C	9.330623	4.151088	1.655989
H	10.008445	2.238573	2.392215
H	7.849042	2.159828	-1.328879
H	7.571264	4.623209	-1.221617
H	9.748961	4.704930	2.490206
H	8.524180	5.900499	0.687130
C	10.380952	0.098490	0.759874
C	12.901939	-0.935122	1.337486
C	10.500041	-1.006543	1.614089
C	11.519996	0.694503	0.202148
C	12.776373	0.172656	0.493889
C	11.762614	-1.520985	1.895239
H	9.612460	-1.438405	2.063538
H	11.412145	1.546880	-0.459346
H	13.658918	0.627565	0.055858
H	11.856724	-2.371312	2.562951
H	13.884591	-1.337038	1.562594

*A.2.3.4 **OTPA-FLR-210**, **EB** State*

H	-13.526029	1.689450	-1.065192
C	-12.569948	1.935803	-0.612116
C	-10.106230	2.551260	0.542252
C	-11.598769	0.945016	-0.485395
C	-12.314624	3.238998	-0.178305
C	-11.076652	3.540025	0.394667
C	-10.358908	1.245406	0.097312
H	-11.792889	-0.063902	-0.833769
H	-13.071221	4.010358	-0.285143
H	-10.867642	4.547289	0.743611
H	-9.150567	2.782448	1.000690
N	-9.373227	0.234107	0.239255
C	-9.758554	-1.059950	0.675973
C	-10.526757	-3.618578	1.536405
C	-10.695406	-1.207913	1.709160
C	-9.210184	-2.203250	0.076037
C	-9.587639	-3.471185	0.512614
C	-11.080257	-2.480061	2.127080
H	-11.116414	-0.324298	2.176967
H	-8.491701	-2.089613	-0.728821
H	-9.155565	-4.347993	0.038682
H	-11.806803	-2.580081	2.928437
H	-10.823989	-4.608406	1.869215
C	-8.019665	0.515254	-0.034482
C	-5.289502	1.060301	-0.597478
C	-6.996857	-0.056698	0.742998
C	-7.660788	1.389828	-1.077484
C	-6.330006	1.678010	-1.328391
C	-5.663892	0.197496	0.461148
H	-7.259348	-0.695375	1.579569
H	-8.437471	1.846764	-1.681025
H	-6.059222	2.360272	-2.128069
H	-4.895711	-0.222264	1.102212
N	-3.989435	1.425101	-0.890958
H	-2.049715	-2.733602	-0.643021
C	-1.952518	-1.652141	-0.676978
C	-1.641245	1.167086	-0.910528
C	-0.657831	-1.053670	-0.687753
C	-3.063053	-0.862456	-0.733713
C	-2.970392	0.590384	-0.821438
C	-0.539749	0.379018	-0.821909
H	-4.046128	-1.316646	-0.764948

H	-1.577210	2.245702	-1.017298
C	0.617005	-1.629028	-0.626435
C	3.384963	-2.262531	-0.552328
C	1.024258	-2.993979	-0.540767
C	1.619497	-0.593223	-0.710533
C	2.947109	-0.881320	-0.673082
C	2.354109	-3.289493	-0.530425
H	0.280279	-3.783921	-0.495974
H	3.689221	-0.097792	-0.773379
H	2.703528	-4.315291	-0.473045
C	0.929777	0.750093	-0.852530
H	1.204112	1.251038	-1.789048
H	1.197883	1.435035	-0.039054
N	4.631132	-2.693100	-0.511406
C	5.715292	-1.858434	-0.313675
C	8.073789	-0.325649	0.081974
C	6.928066	-2.192236	-0.958447
C	5.735877	-0.757937	0.577144
C	6.891476	-0.020317	0.779901
C	8.071007	-1.428317	-0.792683
H	6.933887	-3.047672	-1.626652
H	4.849719	-0.526231	1.158366
H	6.891368	0.797870	1.492135
H	8.976727	-1.683607	-1.331920
N	9.238601	0.444796	0.270828
C	9.141472	1.846026	0.473225
C	8.955849	4.618181	0.870092
C	9.935780	2.477393	1.441461
C	8.254341	2.613749	-0.295756
C	8.158947	3.988121	-0.088935
C	9.846598	3.855093	1.628887
H	10.618675	1.883655	2.039789
H	7.645876	2.127330	-1.050790
H	7.468228	4.570643	-0.691975
H	10.467730	4.331198	2.382247
H	8.884183	5.690638	1.023554
C	10.515974	-0.173855	0.270455
C	13.045495	-1.389084	0.273351
C	10.713928	-1.394949	0.931420
C	11.594549	0.434857	-0.387682
C	12.850634	-0.167653	-0.376093
C	11.969250	-1.999242	0.922135
H	9.882200	-1.862283	1.447904
H	11.440834	1.377127	-0.902885
H	13.677352	0.314755	-0.889771
H	12.108521	-2.945048	1.437964
H	14.024106	-1.859373	0.274319

A.2.4 Optimised Structures of **OTPA-FLR-221** Oligomers

A.2.4.1 ***OTPA-FLR-221**, **LEB** State*

H	-12.501537	-1.904986	0.996514
C	-11.968955	-1.067127	0.554358
C	-10.576375	1.070756	-0.564101
C	-10.576372	-1.070756	0.564115
C	-12.679846	0.000000	0.000012
C	-11.968957	1.067127	-0.554337
C	-9.858537	0.000000	0.000005
H	-10.036788	-1.898365	1.011194
H	-13.765526	0.000000	0.000014
H	-12.501541	1.904987	-0.996491

H	-10.036792	1.898365	-1.011183
N	-8.457278	0.000000	0.000002
C	-7.686819	-1.193970	0.107804
C	-5.841589	-3.322527	0.101944
C	-7.854739	-2.273113	-0.766994
C	-6.641190	-1.236930	1.041527
C	-5.736214	-2.286480	1.045311
C	-6.940491	-3.327077	-0.769117
H	-8.668791	-2.260173	-1.484855
H	-6.526482	-0.417756	1.743857
H	-4.921412	-2.300061	1.761392
H	-7.046784	-4.129658	-1.494340
C	-7.686820	1.193970	-0.107803
C	-5.841590	3.322527	-0.101949
C	-6.641195	1.236931	-1.041530
C	-7.854737	2.273113	0.766996
C	-6.940489	3.327077	0.769116
C	-5.736218	2.286480	-1.045316
H	-6.526489	0.417757	-1.743861
H	-8.668786	2.260173	1.484860
H	-7.046780	4.129659	1.494339
H	-4.921419	2.300062	-1.761400
N	-4.854271	4.321320	-0.048893
H	-5.132197	5.180699	0.408219
H	-1.317193	1.430448	0.563300
C	-1.649728	2.446338	0.365259
C	-2.545081	5.071005	-0.125804
C	-0.730493	3.479785	0.189686
C	-3.012876	2.722628	0.302361
C	-3.476655	4.026230	0.041804
C	-1.188483	4.794620	-0.043821
H	-3.725873	1.922740	0.460324
H	-2.902804	6.077623	-0.329443
C	0.730497	3.479785	0.189685
C	3.476657	4.026233	0.041799
C	1.649732	2.446339	0.365256
C	1.188484	4.794621	-0.043823
C	2.545082	5.071007	-0.125808
C	3.012880	2.722630	0.302356
H	1.317198	1.430449	0.563297
H	2.902804	6.077625	-0.329448
H	3.725878	1.922743	0.460318
C	0.000000	5.728844	-0.197585
H	-0.000001	6.238545	-1.169894
H	0.000001	6.518681	0.565336
N	4.854273	4.321323	-0.048900
H	5.132200	5.180703	0.408209
C	5.841591	3.322529	-0.101955
C	7.686818	1.193970	-0.107806
C	6.940492	3.327081	0.769108
C	5.736215	2.286479	-1.045318
C	6.641191	1.236929	-1.041530
C	7.854738	2.273116	0.766989
H	7.046785	4.129665	1.494328
H	4.921414	2.300058	-1.761400
H	6.526482	0.417752	-1.743858
H	8.668789	2.260177	1.484851
N	8.457276	-0.000000	0.000002
C	7.686816	-1.193970	0.107807
C	5.841589	-3.322530	0.101950
C	7.854739	-2.273116	-0.766988
C	6.641186	-1.236928	1.041527
C	5.736210	-2.286479	1.045313
C	6.940493	-3.327081	-0.769109

H	8.668793	-2.260177	-1.484848
H	6.526475	-0.417752	1.743855
H	4.921407	-2.300058	1.761392
H	7.046788	-4.129664	-1.494329
C	9.858535	-0.000000	0.000005
C	12.679844	-0.000000	0.000012
C	10.576372	1.070756	-0.564101
C	10.576370	-1.070756	0.564116
C	11.968952	-1.067127	0.554358
C	11.968955	1.067127	-0.554337
H	10.036790	1.898364	-1.011183
H	10.036785	-1.898365	1.011194
H	12.501534	-1.904987	0.996514
H	12.501539	1.904986	-0.996491
H	13.765524	-0.000000	0.000015
N	4.854273	-4.321324	0.048894
H	5.132200	-5.180702	-0.408218
H	1.317198	-1.430447	-0.563293
C	1.649731	-2.446338	-0.365256
C	2.545081	-5.071008	0.125798
C	0.730496	-3.479785	-0.189689
C	3.012880	-2.722629	-0.302357
C	3.476656	-4.026234	-0.041805
C	1.188484	-4.794621	0.043814
H	3.725878	-1.922741	-0.460315
H	2.902804	-6.077627	0.329434
C	-0.730494	-3.479784	-0.189690
C	-3.476655	-4.026231	-0.041810
C	-1.649728	-2.446337	-0.365259
C	-1.188483	-4.794620	0.043812
C	-2.545081	-5.071006	0.125794
C	-3.012877	-2.722627	-0.302362
H	-1.317194	-1.430446	-0.563295
H	-2.902805	-6.077625	0.329430
H	-3.725874	-1.922739	-0.460321
C	-0.000000	-5.728845	0.197572
H	0.000000	-6.518679	-0.565352
H	-0.000001	-6.238550	1.169879
N	-4.854272	-4.321321	0.048887
H	-5.132198	-5.180699	-0.408227

*A.2.4.2 **OTPA-FLR-221**, **^{1}ES** State*

H	-12.091875	-1.265853	1.742384
C	-11.549770	-0.720296	0.977716
C	-10.159933	0.726563	-0.983794
C	-10.159826	-0.726524	0.984010
C	-12.244405	0.000024	0.000227
C	-11.549877	0.720341	-0.977340
C	-9.474429	0.000014	0.000066
H	-9.606120	-1.254630	1.751991
H	-13.329388	0.000028	0.000289
H	-12.092066	1.265902	-1.741944
H	-9.606315	1.254667	-1.751840
N	-8.048171	0.000009	-0.000011
C	-7.349953	-1.181951	0.168788
C	-5.706381	-3.456690	0.141694
C	-7.854650	-2.421669	-0.315229
C	-6.074206	-1.157260	0.801622
C	-5.270707	-2.259093	0.781797
C	-7.057210	-3.539092	-0.311300
H	-8.838424	-2.463173	-0.766240
H	-5.760774	-0.265179	1.329247

H	-4.308405	-2.245622	1.277436
H	-7.420415	-4.460340	-0.753906
C	-7.349966	1.181973	-0.168833
C	-5.706397	3.456711	-0.141736
C	-6.074246	1.157302	-0.801723
C	-7.854649	2.421676	0.315236
C	-7.057209	3.539100	0.311311
C	-5.270747	2.259136	-0.781896
H	-5.760832	0.265236	-1.329384
H	-8.838405	2.463164	0.766286
H	-7.420397	4.460333	0.753960
H	-4.308462	2.245681	-1.277569
N	-4.839357	4.481544	0.039002
H	-5.216175	5.403472	0.238193
H	-1.261995	2.102658	1.593766
C	-1.618110	2.964003	1.037811
C	-2.547500	5.256863	-0.355418
C	-0.725935	3.887637	0.489092
C	-2.976304	3.182118	0.882994
C	-3.441547	4.307359	0.171111
C	-1.186653	5.036675	-0.194196
H	-3.690493	2.507481	1.340002
H	-2.925186	6.120718	-0.893410
C	0.725915	3.887634	0.489120
C	3.441543	4.307358	0.171265
C	1.618065	2.963990	1.037863
C	1.186665	5.036678	-0.194137
C	2.547520	5.256871	-0.355288
C	2.976266	3.182104	0.883107
H	1.261925	2.102634	1.593785
H	2.925230	6.120732	-0.893253
H	3.690432	2.507459	1.340137
C	0.000017	5.855643	-0.670217
H	0.000044	5.984944	-1.759469
H	0.000004	6.863115	-0.235979
N	4.839358	4.481545	0.039217
H	5.216169	5.403467	0.238446
C	5.706404	3.456722	-0.141548
C	7.349969	1.181983	-0.168749
C	7.057200	3.539076	0.311552
C	5.270778	2.259196	-0.781816
C	6.074276	1.157364	-0.801695
C	7.854639	2.421651	0.315424
H	7.420374	4.460278	0.754278
H	4.308516	2.245781	-1.277534
H	5.760883	0.265341	-1.329442
H	8.838384	2.463104	0.766504
N	8.048173	0.000006	-0.000006
C	7.349958	-1.181969	0.168710
C	5.706388	-3.456707	0.141499
C	7.854639	-2.421648	-0.315427
C	6.074241	-1.157335	0.801606
C	5.270743	-2.259166	0.781724
C	7.057199	-3.539072	-0.311556
H	8.838398	-2.463113	-0.766474
H	5.760836	-0.265303	1.329330
H	4.308468	-2.245740	1.277414
H	7.420388	-4.460284	-0.754248
C	9.474431	0.000013	0.000070
C	12.244407	0.000032	0.000227
C	10.159931	0.726762	-0.983644
C	10.159830	-0.726719	0.983867
C	11.549775	-0.720488	0.977571
C	11.549875	0.720545	-0.977192

H	9.606309	1.255027	-1.751574
H	9.606127	-1.254989	1.751737
H	12.091882	-1.266201	1.742125
H	12.092061	1.266266	-1.741684
H	13.329390	0.000040	0.000288
N	4.839352	-4.481542	-0.039253
H	5.216175	-5.403482	-0.238381
H	1.261921	-2.102768	-1.594032
C	1.618061	-2.964086	-1.038052
C	2.547519	-5.256872	0.355254
C	0.725912	-3.887698	-0.489253
C	2.976262	-3.182179	-0.883268
C	3.441542	-4.307381	-0.171343
C	1.186665	-5.036697	0.194080
H	3.690426	-2.507560	-1.340339
H	2.925230	-6.120694	0.893279
C	-0.725935	-3.887702	-0.489225
C	-3.441547	-4.307381	-0.171181
C	-1.618110	-2.964101	-1.038001
C	-1.186654	-5.036693	0.194142
C	-2.547501	-5.256862	0.355392
C	-2.976304	-3.182194	-0.883151
H	-1.261996	-2.102796	-1.594018
H	-2.925186	-6.120677	0.893446
H	-3.690492	-2.507584	-1.340200
C	0.000017	-5.855631	0.670214
H	0.000003	-6.863129	0.236037
H	0.000045	-5.984865	1.759474
N	-4.839353	-4.481538	-0.039026
H	-5.216184	-5.403483	-0.238109

*A.2.4.3 **OTPA-FLR-221**, **^{5}ES** State*

H	-12.354024	-1.727696	1.100274
C	-11.791479	-0.974402	0.559598
C	-10.354245	1.004584	-0.816199
C	-10.406533	-0.987979	0.610025
C	-12.463553	0.017393	-0.167516
C	-11.739695	1.002847	-0.852157
C	-9.679329	0.006265	-0.080107
H	-9.881263	-1.729685	1.199869
H	-13.547839	0.021786	-0.200667
H	-12.260976	1.759464	-1.428384
H	-9.786828	1.739145	-1.375065
N	-8.283063	0.000022	-0.037437
C	-7.541246	-1.198489	0.097749
C	-5.784288	-3.359117	0.091057
C	-7.838273	-2.334900	-0.673412
C	-6.421595	-1.194976	0.950248
C	-5.559248	-2.272079	0.955234
C	-6.959601	-3.411451	-0.675602
H	-8.702907	-2.337394	-1.327036
H	-6.245158	-0.348449	1.602958
H	-4.702696	-2.280196	1.618592
H	-7.145320	-4.257239	-1.328887
C	-7.520135	1.184865	-0.136007
C	-5.754787	3.341674	-0.062765
C	-6.334191	1.150699	-0.895547
C	-7.870039	2.350331	0.569661
C	-6.989661	3.423679	0.603415
C	-5.468029	2.222738	-0.867893
H	-6.115735	0.287963	-1.513365
H	-8.784426	2.380356	1.150765

H	-7.224545	4.294700	1.205846
H	-4.563284	2.204440	-1.463830
N	-4.795879	4.354527	0.072888
H	-5.123376	5.313783	0.106310
H	-1.263929	1.648118	1.065616
C	-1.618071	2.616356	0.727780
C	-2.531921	5.194117	-0.058747
C	-0.710998	3.644749	0.403924
C	-2.965812	2.862179	0.629126
C	-3.444300	4.136590	0.201548
C	-1.183278	4.940381	0.033017
H	-3.675994	2.093281	0.904002
H	-2.907836	6.166363	-0.361747
C	0.713229	3.633868	0.363758
C	3.443738	4.101809	0.066420
C	1.621095	2.588277	0.624752
C	1.184213	4.926194	-0.021304
C	2.530174	5.167549	-0.160528
C	2.966896	2.822804	0.483780
H	1.268949	1.614156	0.947511
H	2.904712	6.139139	-0.467385
H	3.676824	2.040907	0.718144
C	0.000424	5.848248	-0.240055
H	-0.019940	6.256880	-1.257201
H	0.020626	6.705695	0.443481
N	4.790466	4.323036	-0.083292
H	5.110100	5.285500	-0.063951
C	5.761645	3.315654	-0.188870
C	7.540438	1.173040	-0.183890
C	6.982399	3.421480	0.498275
C	5.497576	2.180881	-0.978108
C	6.371121	1.113623	-0.965571
C	7.871646	2.354105	0.502340
H	7.198362	4.306650	1.087224
H	4.604042	2.144755	-1.589796
H	6.168869	0.232651	-1.562983
H	8.775866	2.401860	1.098118
N	8.303382	-0.009550	-0.037095
C	7.554470	-1.195748	0.147755
C	5.767311	-3.330700	0.218135
C	7.840250	-2.366645	-0.575736
C	6.434114	-1.146627	0.998983
C	5.557874	-2.210942	1.044431
C	6.946869	-3.429699	-0.538953
H	8.706819	-2.406795	-1.225629
H	6.269153	-0.274321	1.620101
H	4.702643	-2.183954	1.708938
H	7.123238	-4.304441	-1.156010
C	9.698209	-0.005749	-0.082205
C	12.482470	0.004110	-0.172954
C	10.372265	0.972874	-0.845877
C	10.426991	-0.979800	0.635487
C	11.811694	-0.967469	0.582279
C	11.757459	0.970789	-0.883037
H	9.804343	1.692261	-1.423600
H	9.903367	-1.702975	1.249221
H	12.375337	-1.704547	1.143649
H	12.277859	1.711684	-1.480012
H	13.566716	0.008110	-0.207310
N	4.781798	-4.326584	0.139825
H	5.092626	-5.289562	0.070386
H	1.248338	-1.565923	-0.704404
C	1.602581	-2.553953	-0.429843
C	2.519095	-5.164255	0.230094

C	0.696838	-3.609884	-0.207730
C	2.950046	-2.795180	-0.317156
C	3.431952	-4.091923	0.032784
C	1.171337	-4.917101	0.116697
H	3.656421	-2.003453	-0.526473
H	2.896080	-6.149212	0.487504
C	-0.726915	-3.622433	-0.249367
C	-3.461486	-4.136356	-0.104773
C	-1.635996	-2.584983	-0.537586
C	-1.197001	-4.935187	0.061143
C	-2.544640	-5.199010	0.126005
C	-2.983088	-2.841396	-0.469803
H	-1.282576	-1.600811	-0.826501
H	-2.919196	-6.185364	0.381728
H	-3.693832	-2.065688	-0.722354
C	-0.010681	-5.849421	0.301285
H	0.011632	-6.682154	-0.411942
H	-0.030687	-6.293098	1.303797
N	-4.810948	-4.368234	-0.011352
H	-5.128686	-5.330625	-0.059179

*A.2.4.4 **OTPA-FLR-221**, **EB** State*

H	-12.270572	-1.766501	1.226138
C	-11.736612	-0.991395	0.683461
C	-10.343939	0.991941	-0.694757
C	-10.343956	-0.991946	0.694698
C	-12.444651	-0.000003	-0.000056
C	-11.736596	0.991389	-0.683555
C	-9.631435	-0.000002	-0.000021
H	-9.801751	-1.754568	1.243054
H	-13.530290	-0.000004	-0.000069
H	-12.270543	1.766494	-1.226245
H	-9.801722	1.754564	-1.243100
N	-8.223561	-0.000001	-0.000003
C	-7.467398	-1.193852	0.127573
C	-5.674749	-3.376927	0.143437
C	-7.733162	-2.336977	-0.642924
C	-6.360173	-1.202157	0.991454
C	-5.473681	-2.264337	0.991737
C	-6.865524	-3.423657	-0.609779
H	-8.601730	-2.353727	-1.293291
H	-6.183192	-0.344707	1.632233
H	-4.612579	-2.253404	1.652312
H	-7.052655	-4.291335	-1.234465
C	-7.467395	1.193849	-0.127567
C	-5.674754	3.376931	-0.143410
C	-6.360150	1.202150	-0.991420
C	-7.733179	2.336979	0.642917
C	-6.865544	3.423662	0.609782
C	-5.473660	2.264333	-0.991692
H	-6.183150	0.344695	-1.632188
H	-8.601762	2.353731	1.293265
H	-7.052693	4.291344	1.234456
H	-4.612541	2.253395	-1.652245
N	-4.762323	4.424105	-0.071742
H	-1.249699	1.647445	0.895552
C	-1.616102	2.618732	0.575437
C	-2.522640	5.235453	-0.120479
C	-0.696419	3.670819	0.289623
C	-2.950949	2.851017	0.466600
C	-3.480493	4.156583	0.071709
C	-1.189387	4.989091	-0.041627

H	-3.656965	2.068561	0.714810
H	-2.920792	6.213429	-0.373380
C	0.696552	3.670829	0.289429
C	3.480550	4.156643	0.070776
C	1.616329	2.618750	0.574973
C	1.189405	4.989113	-0.041945
C	2.522632	5.235501	-0.121148
C	2.951141	2.851056	0.465766
H	1.250029	1.647452	0.895171
H	2.920702	6.213489	-0.374137
H	3.657249	2.068606	0.713746
C	-0.000029	5.909994	-0.258615
H	-0.000168	6.348762	-1.263378
H	0.000059	6.746681	0.450529
N	4.762339	4.424161	-0.072969
C	5.674735	3.376945	-0.144379
C	7.467311	1.193816	-0.127955
C	6.865682	3.423969	0.608546
C	5.473398	2.263959	-0.992095
C	6.359873	1.201761	-0.991565
C	7.733281	2.337268	0.641985
H	7.052991	4.291920	1.232798
H	4.612110	2.252741	-1.652425
H	6.182702	0.344019	-1.631901
H	8.602001	2.354276	1.292143
N	8.223475	0.000005	-0.000010
C	7.467317	-1.193807	0.127948
C	5.674747	-3.376940	0.144400
C	7.733280	-2.337260	-0.641994
C	6.359892	-1.201754	0.991574
C	5.473419	-2.263955	0.992118
C	6.865684	-3.423964	-0.608540
H	8.601991	-2.354267	-1.292164
H	6.182728	-0.344011	1.631911
H	4.612142	-2.252738	1.652460
H	7.052987	-4.291916	-1.232793
C	9.631347	0.000007	-0.000021
C	12.444561	0.000008	-0.000043
C	10.343852	0.991774	-0.695006
C	10.343864	-0.991760	0.694953
C	11.736520	-0.991212	0.683722
C	11.736508	0.991227	-0.683796
H	9.801634	1.754258	-1.243543
H	9.801655	-1.754245	1.243497
H	12.270478	-1.766180	1.226597
H	12.270458	1.766195	-1.226680
H	13.530200	0.000008	-0.000051
N	4.762352	-4.424159	0.073003
H	1.250044	-1.647499	-0.895287
C	1.616343	-2.618780	-0.575035
C	2.522644	-5.235493	0.121231
C	0.696565	-3.670842	-0.289432
C	2.951155	-2.851081	-0.465816
C	3.480564	-4.156646	-0.070753
C	1.189417	-4.989108	0.042017
H	3.657263	-2.068645	-0.713841
H	2.920713	-6.213467	0.374275
C	-0.696406	-3.670831	-0.289628
C	-3.480481	-4.156580	-0.071688
C	-1.616087	-2.618761	-0.575507
C	-1.189375	-4.989083	0.041699
C	-2.522629	-5.235438	0.120565
C	-2.950934	-2.851039	-0.466661
H	-1.249683	-1.647494	-0.895680

H	-2.920782	-6.213400	0.373524
H	-3.656948	-2.068597	-0.714924
C	-0.000017	-5.909975	0.258741
H	0.000069	-6.746704	-0.450353
H	-0.000157	-6.348682	1.263530
N	-4.762312	-4.424098	0.071775

A.2.5 Optimised Structures of **OTPB-BZN-210** Oligomers

A.2.5.1 ***OTPB-BZN-210, LEB*** *State*

H	-1.680736	6.296952	-12.994639
C	-1.081321	6.243562	-12.090144
C	0.435536	6.091666	-9.758464
C	-0.909251	5.018103	-11.448254
C	-0.496194	7.399123	-11.568301
C	0.262635	7.317738	-10.398851
C	-0.147441	4.921660	-10.272263
H	-1.389493	4.129879	-11.847782
H	-0.630569	8.354089	-12.068024
H	0.728712	8.209136	-9.988399
H	1.047674	6.033533	-8.863338
C	0.039961	3.618216	-9.589287
C	0.372432	1.156186	-8.296268
C	0.175930	2.436616	-10.330193
C	0.065517	3.543460	-8.190439
C	0.233086	2.319781	-7.525518
C	0.340589	1.197812	-9.696400
H	0.153694	2.481841	-11.414024
H	-0.096047	4.445627	-7.609581
H	0.556799	0.209586	-7.799067
C	0.498892	-0.044027	-10.492212
C	0.793674	-2.404873	-12.001806
C	1.208950	-0.039887	-11.704014
C	-0.060056	-1.255053	-10.051903
C	0.086200	-2.423455	-10.797978
C	1.354166	-1.207546	-12.451560
H	1.670515	0.880369	-12.049387
H	-0.632863	-1.273763	-9.129457
H	-0.360666	-3.347739	-10.442595
H	1.913747	-1.183566	-13.382452
H	0.907272	-3.314855	-12.583844
C	0.260994	2.256970	-6.047969
C	0.325571	2.123843	-3.206726
C	-0.262407	1.154930	-5.352528
C	0.807469	3.299915	-5.280063
C	0.846355	3.236956	-3.894510
C	-0.241792	1.082831	-3.964455
H	-0.732312	0.348229	-5.907681
H	1.240920	4.162129	-5.778214
H	1.296563	4.048234	-3.327995
H	-0.694932	0.234030	-3.466545
N	0.362009	2.122775	-1.817088
H	0.462813	3.029527	-1.382641
C	0.166496	1.046925	-0.939405
C	-0.166496	-1.046925	0.939405
C	0.575891	-0.261594	-1.242489
C	-0.408030	1.286885	0.318393
C	-0.575891	0.261594	1.242489
C	0.408030	-1.286885	-0.318393
H	1.056916	-0.473356	-2.190425
H	-0.746371	2.289516	0.566714
H	-1.056916	0.473356	2.190425

H	0.746371	-2.289516	-0.566714
N	-0.362009	-2.122775	1.817088
H	-0.462813	-3.029527	1.382641
C	-0.325571	-2.123843	3.206726
C	-0.260994	-2.256970	6.047969
C	-0.846355	-3.236956	3.894510
C	0.241792	-1.082831	3.964455
C	0.262407	-1.154930	5.352528
C	-0.807469	-3.299915	5.280063
H	-1.296563	-4.048234	3.327995
H	0.694932	-0.234030	3.466545
H	0.732312	-0.348229	5.907681
H	-1.240920	-4.162129	5.778214
C	-0.233086	-2.319781	7.525518
C	-0.175930	-2.436616	10.330193
C	-0.065517	-3.543460	8.190439
C	-0.372432	-1.156186	8.296268
C	-0.340589	-1.197812	9.696400
C	-0.039961	-3.618216	9.589287
H	0.096047	-4.445627	7.609581
H	-0.556799	-0.209586	7.799067
H	-0.153694	-2.481841	11.414024
C	-0.498892	0.044027	10.492212
C	-0.793674	2.404873	12.001806
C	-1.208950	0.039887	11.704014
C	0.060056	1.255053	10.051903
C	-0.086200	2.423455	10.797978
C	-1.354166	1.207546	12.451560
H	-1.670515	-0.880369	12.049387
H	0.632863	1.273763	9.129457
H	0.360666	3.347739	10.442595
H	-1.913747	1.183566	13.382452
H	-0.907272	3.314855	12.583844
C	0.147441	-4.921660	10.272263
C	0.496194	-7.399123	11.568301
C	-0.435536	-6.091666	9.758464
C	0.909251	-5.018103	11.448254
C	1.081321	-6.243562	12.090144
C	-0.262635	-7.317738	10.398851
H	-1.047674	-6.033533	8.863338
H	1.389493	-4.129879	11.847782
H	1.680736	-6.296952	12.994639
H	-0.728712	-8.209136	9.988399
H	0.630569	-8.354089	12.068024

*A.2.5.2 **OTPB-BZN-210**, **^{1}ES** State*

H	-1.529764	6.330378	-13.005876
C	-0.958268	6.263118	-12.084854
C	0.489228	6.078894	-9.709888
C	-0.819489	5.031282	-11.447893
C	-0.374019	7.407076	-11.537209
C	0.350525	7.310333	-10.347296
C	-0.094004	4.921669	-10.250664
H	-1.299022	4.152431	-11.868270
H	-0.481376	8.366402	-12.034549
H	0.816500	8.193194	-9.919528
H	1.076702	6.007215	-8.799368
C	0.053284	3.613813	-9.569541
C	0.291352	1.118622	-8.297099
C	0.196486	2.431105	-10.311858
C	0.039386	3.527190	-8.174684
C	0.153937	2.285526	-7.523532

C	0.320303	1.177105	-9.693023
H	0.211138	2.487548	-11.394916
H	-0.125205	4.427380	-7.593395
H	0.438347	0.163239	-7.806231
C	0.488679	-0.052684	-10.502548
C	0.808392	-2.389397	-12.035811
C	1.240603	-0.035001	-11.688401
C	-0.100755	-1.261796	-10.099082
C	0.057757	-2.419344	-10.858591
C	1.398859	-1.192935	-12.447631
H	1.724581	0.884184	-12.004423
H	-0.708658	-1.288447	-9.199516
H	-0.413397	-3.343158	-10.535787
H	1.990311	-1.161721	-13.357923
H	0.931012	-3.291071	-12.628367
C	0.125884	2.204760	-6.060201
C	0.064008	2.035715	-3.248860
C	-0.383915	1.057739	-5.406588
C	0.575759	3.278893	-5.257205
C	0.537467	3.206747	-3.881155
C	-0.424473	0.966475	-4.030486
H	-0.809722	0.253251	-5.994112
H	0.987259	4.165131	-5.725130
H	0.908833	4.031051	-3.279940
H	-0.902345	0.114338	-3.564582
N	0.049746	2.027662	-1.861546
H	0.040994	2.956158	-1.444165
C	0.040869	1.011462	-0.976964
C	-0.040869	-1.011462	0.976964
C	0.344196	-0.341159	-1.330101
C	-0.285773	1.319847	0.383925
C	-0.344196	0.341159	1.330101
C	0.285773	-1.319847	-0.383925
H	0.680242	-0.581489	-2.329081
H	-0.555293	2.337767	0.645671
H	-0.680242	0.581489	2.329081
H	0.555293	-2.337767	-0.645671
N	-0.049746	-2.027662	1.861546
H	-0.040994	-2.956158	1.444165
C	-0.064008	-2.035715	3.248860
C	-0.125884	-2.204760	6.060201
C	-0.537467	-3.206747	3.881155
C	0.424473	-0.966475	4.030486
C	0.383915	-1.057739	5.406588
C	-0.575759	-3.278893	5.257205
H	-0.908833	-4.031051	3.279940
H	0.902345	-0.114338	3.564582
H	0.809722	-0.253251	5.994112
H	-0.987259	-4.165131	5.725130
C	-0.153937	-2.285526	7.523532
C	-0.196486	-2.431105	10.311858
C	-0.039386	-3.527190	8.174684
C	-0.291352	-1.118622	8.297099
C	-0.320303	-1.177105	9.693023
C	-0.053284	-3.613813	9.569541
H	0.125205	-4.427380	7.593395
H	-0.438347	-0.163239	7.806231
H	-0.211138	-2.487548	11.394916
C	-0.488679	0.052684	10.502548
C	-0.808392	2.389397	12.035811
C	-1.240603	0.035001	11.688401
C	0.100755	1.261796	10.099082
C	-0.057757	2.419344	10.858591
C	-1.398859	1.192935	12.447631

H	-1.724581	-0.884184	12.004423
H	0.708658	1.288447	9.199516
H	0.413397	3.343158	10.535787
H	-1.990311	1.161721	13.357923
H	-0.931012	3.291071	12.628367
C	0.094004	-4.921669	10.250664
C	0.374019	-7.407076	11.537209
C	-0.489228	-6.078894	9.709888
C	0.819489	-5.031282	11.447893
C	0.958268	-6.263118	12.084854
C	-0.350525	-7.310333	10.347296
H	-1.076702	-6.007215	8.799368
H	1.299022	-4.152431	11.868270
H	1.529764	-6.330378	13.005876
H	-0.816500	-8.193194	9.919528
H	0.481376	-8.366402	12.034549

*A.2.5.3 **OTPB-BZN-210**, ^{3}**ES** State*

H	-1.559524	6.288188	-12.989763
C	-0.981135	6.233237	-12.072375
C	0.485112	6.081856	-9.705909
C	-0.838086	5.010369	-11.419785
C	-0.391522	7.384031	-11.545094
C	0.342554	7.303876	-10.359658
C	-0.103743	4.917982	-10.226269
H	-1.322001	4.126683	-11.824620
H	-0.501522	8.336182	-12.055333
H	0.812996	8.192131	-9.948565
H	1.080467	6.022766	-8.799794
C	0.047250	3.620862	-9.527757
C	0.297621	1.133302	-8.232835
C	0.173597	2.425168	-10.257703
C	0.059968	3.551300	-8.135003
C	0.180188	2.313501	-7.466455
C	0.304779	1.175014	-9.626500
H	0.170410	2.468416	-11.341256
H	-0.090245	4.459086	-7.563112
H	0.451935	0.183123	-7.735767
C	0.458897	-0.061464	-10.426929
C	0.760508	-2.412078	-11.939582
C	1.189211	-0.052656	-11.626517
C	-0.118867	-1.267948	-9.999021
C	0.030663	-2.432548	-10.749000
C	1.339013	-1.218211	-12.375312
H	1.664799	0.864327	-11.961071
H	-0.710549	-1.287459	-9.088565
H	-0.431023	-3.354618	-10.408447
H	1.914278	-1.194979	-13.296032
H	0.876090	-3.319648	-12.524389
C	0.184270	2.252407	-6.012301
C	0.205474	2.113654	-3.184283
C	-0.233239	1.078851	-5.325408
C	0.585508	3.367366	-5.225237
C	0.596340	3.307081	-3.854962
C	-0.236875	1.003099	-3.954119
H	-0.616027	0.238463	-5.891251
H	0.929892	4.272225	-5.710929
H	0.932534	4.158834	-3.272072
H	-0.628143	0.121386	-3.464269
N	0.233681	2.108560	-1.823172
H	0.346674	3.017902	-1.384761
C	0.113255	1.031728	-0.934110

C	-0.113255	-1.031728	0.934110
C	0.598342	-0.251088	-1.243510
C	-0.473424	1.274815	0.319498
C	-0.598342	0.251088	1.243510
C	0.473424	-1.274815	-0.319498
H	1.114355	-0.435014	-2.177279
H	-0.868001	2.258461	0.552110
H	-1.114355	0.435014	2.177279
H	0.868001	-2.258461	-0.552110
N	-0.233681	-2.108560	1.823172
H	-0.346674	-3.017902	1.384761
C	-0.205474	-2.113654	3.184283
C	-0.184270	-2.252407	6.012301
C	-0.596340	-3.307081	3.854962
C	0.236875	-1.003099	3.954119
C	0.233239	-1.078851	5.325408
C	-0.585508	-3.367366	5.225237
H	-0.932534	-4.158834	3.272072
H	0.628143	-0.121386	3.464269
H	0.616027	-0.238463	5.891251
H	-0.929892	-4.272225	5.710929
C	-0.180188	-2.313501	7.466455
C	-0.173597	-2.425168	10.257703
C	-0.059968	-3.551300	8.135003
C	-0.297621	-1.133302	8.232835
C	-0.304779	-1.175014	9.626500
C	-0.047250	-3.620862	9.527757
H	0.090245	-4.459086	7.563112
H	-0.451935	-0.183123	7.735767
H	-0.170410	-2.468416	11.341256
C	-0.458897	0.061464	10.426929
C	-0.760508	2.412078	11.939582
C	-1.189211	0.052656	11.626517
C	0.118867	1.267948	9.999021
C	-0.030663	2.432548	10.749000
C	-1.339013	1.218211	12.375312
H	-1.664799	-0.864327	11.961071
H	0.710549	1.287459	9.088565
H	0.431023	3.354618	10.408447
H	-1.914278	1.194979	13.296032
H	-0.876090	3.319648	12.524389
C	0.103743	-4.917982	10.226269
C	0.391522	-7.384031	11.545094
C	-0.485112	-6.081856	9.705909
C	0.838086	-5.010369	11.419785
C	0.981135	-6.233237	12.072375
C	-0.342554	-7.303876	10.359658
H	-1.080467	-6.022766	8.799794
H	1.322001	-4.126683	11.824620
H	1.559524	-6.288188	12.989763
H	-0.812996	-8.192131	9.948565
H	0.501522	-8.336182	12.055333

*A.2.5.4 **OTPB-BZN-210**, **EB** State*

H	-1.290551	6.302320	-12.991108
C	-0.782930	6.233701	-12.033101
C	0.497109	6.043446	-9.565831
C	-0.705613	5.004423	-11.380278
C	-0.221409	7.373769	-11.454387
C	0.418838	7.273216	-10.217454
C	-0.063918	4.889153	-10.136361
H	-1.168055	4.129009	-11.826406

H	-0.282202	8.331731	-11.962601
H	0.865939	8.152306	-9.761958
H	1.018405	5.970225	-8.615941
C	0.021415	3.581929	-9.440692
C	0.157145	1.110382	-8.126962
C	0.197034	2.395811	-10.165792
C	-0.089164	3.507580	-8.045936
C	-0.021572	2.279224	-7.373710
C	0.265207	1.152471	-9.523165
H	0.281968	2.440961	-11.246507
H	-0.279271	4.413854	-7.480660
H	0.262653	0.159324	-7.615590
C	0.466257	-0.093169	-10.302893
C	0.843739	-2.461336	-11.780899
C	1.295797	-0.109603	-11.436007
C	-0.170318	-1.286713	-9.924969
C	0.016678	-2.458946	-10.655722
C	1.482162	-1.281274	-12.167970
H	1.816924	0.796558	-11.730155
H	-0.834773	-1.288481	-9.065958
H	-0.491152	-3.369493	-10.350440
H	2.134165	-1.274014	-13.036883
H	0.989316	-3.374367	-12.350853
C	-0.134730	2.215598	-5.899103
C	-0.337169	2.084789	-3.072518
C	-0.774146	1.135997	-5.267259
C	0.380802	3.240717	-5.084968
C	0.261340	3.191729	-3.703378
C	-0.870845	1.062470	-3.882889
H	-1.226422	0.354640	-5.870323
H	0.891682	4.081728	-5.543566
H	0.655566	3.991789	-3.084824
H	-1.402894	0.237573	-3.420033
N	-0.468778	2.112399	-1.684654
C	-0.223561	1.076946	-0.932785
C	0.223561	-1.076946	0.932785
C	0.396000	-0.179622	-1.355357
C	-0.585781	1.188083	0.478508
C	-0.396000	0.179622	1.355357
C	0.585781	-1.188083	-0.478508
H	0.728598	-0.274393	-2.382195
H	-1.063630	2.115639	0.777954
H	-0.728598	0.274393	2.382195
H	1.063630	-2.115639	-0.777954
N	0.468778	-2.112399	1.684654
C	0.337169	-2.084789	3.072518
C	0.134730	-2.215598	5.899103
C	-0.261340	-3.191729	3.703378
C	0.870845	-1.062470	3.882889
C	0.774146	-1.135997	5.267259
C	-0.380802	-3.240717	5.084968
H	-0.655566	-3.991789	3.084824
H	1.402894	-0.237573	3.420033
H	1.226422	-0.354640	5.870323
H	-0.891682	-4.081728	5.543566
C	0.021572	-2.279224	7.373710
C	-0.197034	-2.395811	10.165792
C	0.089164	-3.507580	8.045936
C	-0.157145	-1.110382	8.126962
C	-0.265207	-1.152471	9.523165
C	-0.021415	-3.581929	9.440692
H	0.279271	-4.413854	7.480660
H	-0.262653	-0.159324	7.615590
H	-0.281968	-2.440961	11.246507

C	-0.466257	0.093169	10.302893	C	0.063918	-4.889153	10.136361
C	-0.843739	2.461336	11.780899	C	0.221409	-7.373769	11.454387
C	-1.295797	0.109603	11.436007	C	-0.497109	-6.043446	9.565831
C	0.170318	1.286713	9.924969	C	0.705613	-5.004423	11.380278
C	-0.016678	2.458946	10.655722	C	0.782930	-6.233701	12.033101
C	-1.482162	1.281274	12.167970	C	-0.418838	-7.273216	10.217454
H	-1.816924	-0.796558	11.730155	H	-1.018405	-5.970225	8.615941
H	0.834773	1.288481	9.065958	H	1.168055	-4.129009	11.826406
H	0.491152	3.369493	10.350440	H	1.290551	-6.302320	12.991108
H	-2.134165	1.274014	13.036883	H	-0.865939	-8.152306	9.761958
H	-0.989316	3.374367	12.350853	H	0.282202	-8.331731	11.962601

A.2.6 Optimised Structures of **OTPB-BZN-221** Oligomers

A.2.6.1 ***OTPB-BZN-221, LEB*** *State*

H	1.719269	-12.215097	-1.421357	H	-2.148272	-7.967261	0.035133
C	0.968687	-11.699948	-0.828404	H	-0.003044	-4.256974	0.095273
C	-0.960549	-10.361898	0.671709	C	2.485352	-5.245843	0.118224
C	0.965131	-10.306811	-0.778972	C	4.819003	-3.627258	0.011210
C	0.006046	-12.430605	-0.128744	C	3.623701	-5.655849	-0.593814
C	-0.958902	-11.755098	0.621275	C	2.567666	-4.029976	0.820093
C	0.000817	-9.614414	-0.028154	C	3.706395	-3.240302	0.781640
H	1.702441	-9.746099	-1.345822	C	4.767390	-4.864173	-0.653754
H	0.007948	-13.516099	-0.167442	H	3.598257	-6.585377	-1.155413
H	-1.707193	-12.313962	1.176309	H	1.727897	-3.707607	1.428312
H	-1.699179	-9.846528	1.278350	H	3.743141	-2.317132	1.349149
C	-0.000817	-8.131334	0.020952	H	5.617771	-5.186279	-1.249439
C	-0.002125	-5.340895	0.124665	C	-2.489410	-5.247719	0.119589
C	1.208078	-7.420279	0.051399	C	-4.822040	-3.627981	0.008121
C	-1.210200	-7.421704	0.056042	C	-2.573280	-4.032788	0.822942
C	-1.227385	-6.021237	0.111464	C	-3.625506	-5.656087	-0.596779
C	1.223888	-6.019561	0.103954	C	-4.768678	-4.863606	-0.658886
H	2.145590	-7.966384	0.079284	C	-3.711651	-3.242694	0.782570

H	-1.734894	-3.711571	1.433706
H	-3.599102	-6.584252	-1.160492
H	-5.617250	-5.184341	-1.257894
H	-3.749683	-2.320306	1.351271
N	-5.961217	-2.826258	-0.064857
H	-6.790808	-3.268169	-0.438321
C	-5.947689	-1.415655	-0.096164
C	-5.946175	1.415556	-0.093747
C	-4.823832	-0.694554	-0.526823
C	-7.087961	-0.696333	0.290748
C	-7.087195	0.696773	0.291973
C	-4.823054	0.694024	-0.525663
H	-3.946866	-1.224716	-0.880152
H	-7.972676	-1.235227	0.618964
H	-7.971268	1.236126	0.621067
H	-3.945587	1.223798	-0.878294
N	-5.958472	2.825940	-0.060280
H	-6.789858	3.269108	-0.428213
C	-4.819003	3.627258	0.011210
C	-2.485352	5.245843	0.118224
C	-4.767390	4.864173	-0.653754
C	-3.706395	3.240302	0.781640
C	-2.567666	4.029976	0.820093
C	-3.623701	5.655849	-0.593814
H	-5.617771	5.186279	-1.249439
H	-3.743141	2.317132	1.349149
H	-1.727897	3.707607	1.428312
H	-3.598257	6.585377	-1.155413
C	-1.223888	6.019561	0.103954
C	1.210200	7.421704	0.056042
C	-1.208078	7.420279	0.051399
C	0.002125	5.340895	0.124665
C	1.227385	6.021237	0.111464
C	0.000817	8.131334	0.020952
H	-2.145590	7.966384	0.079284
H	0.003044	4.256974	0.095273
H	2.148272	7.967261	0.035133
C	2.489410	5.247719	0.119589
C	4.822040	3.627981	0.008121
C	3.625506	5.656087	-0.596779
C	2.573280	4.032788	0.822942
C	3.711651	3.242694	0.782570
C	4.768678	4.863606	-0.658886
H	3.599102	6.584252	-1.160492
H	1.734894	3.711571	1.433706
H	3.749683	2.320306	1.351271
H	5.617250	5.184341	-1.257894
C	-0.000817	9.614414	-0.028154
C	-0.006046	12.430605	-0.128744
C	-0.965131	10.306811	-0.778972
C	0.960549	10.361898	0.671709
C	0.958902	11.755098	0.621275
C	-0.968687	11.699948	-0.828404
H	-1.702441	9.746099	-1.345822
H	1.699179	9.846528	1.278350
H	1.707193	12.313962	1.176309
H	-1.719269	12.215097	-1.421357
H	-0.007948	13.516099	-0.167442
N	5.961217	2.826258	-0.064857
H	6.790808	3.268169	-0.438321
C	5.947689	1.415655	-0.096164
C	5.946175	-1.415556	-0.093747
C	4.823832	0.694554	-0.526823
C	7.087961	0.696333	0.290748

C	7.087195	-0.696773	0.291973	H	7.971268	-1.236126	0.621067
C	4.823054	-0.694024	-0.525663	H	3.945587	-1.223798	-0.878294
H	3.946866	1.224716	-0.880152	N	5.958472	-2.825940	-0.060280
H	7.972676	1.235227	0.618964	H	6.789858	-3.269108	-0.428213

*A.2.6.2 **OTPB-BZN-221**, ^{1}**ES** State*

H	1.753721	-12.106684	-1.222247	H	3.591411	-6.566565	-0.986185
C	0.987051	-11.584932	-0.657357	H	1.723194	-3.536230	1.446502
C	-0.988836	-10.232518	0.772172	H	3.747844	-2.168346	1.304618
C	0.985180	-10.192105	-0.620279	H	5.626402	-5.200524	-1.129864
C	0.002385	-12.306518	0.020775	C	-2.482753	-5.130131	0.162487
C	-0.985179	-11.625478	0.735395	C	-4.794961	-3.550281	-0.033754
C	-0.003091	-9.496621	0.095188	C	-2.566459	-3.884913	0.822448
H	1.740431	-9.640037	-1.172086	C	-3.621879	-5.596777	-0.530449
H	0.004540	-13.391889	-0.007572	C	-4.770260	-4.829879	-0.620362
H	-1.749906	-12.179208	1.271713	C	-3.698679	-3.101756	0.732386
H	-1.746500	-9.713721	1.351808	H	-1.745211	-3.548439	1.444024
C	-0.004795	-8.015574	0.130891	H	-3.587618	-6.551133	-1.043167
C	-0.005851	-5.208085	0.230082	H	-5.619546	-5.180984	-1.195888
C	1.200327	-7.299169	0.156791	H	-3.766895	-2.176065	1.291764
C	-1.210496	-7.299456	0.140152	N	-5.917007	-2.735433	-0.206144
C	-1.226077	-5.896597	0.192292	H	-6.819272	-3.208048	-0.263357
C	1.215214	-5.895719	0.200889	C	-5.922321	-1.399678	-0.305144
H	2.136035	-7.845803	0.187907	C	-5.919282	1.406906	-0.288422
H	-2.147160	-7.844743	0.111727	C	-4.718965	-0.673858	-0.606529
H	-0.006762	-4.125107	0.203539	C	-7.157786	-0.676336	-0.168617
C	2.472304	-5.130449	0.186936	C	-7.156383	0.684705	-0.160136
C	4.788236	-3.554211	0.000492	C	-4.717846	0.681826	-0.599225
C	3.620574	-5.606293	-0.484654	H	-3.837093	-1.217461	-0.920159
C	2.550425	-3.879428	0.836792	H	-8.080805	-1.225213	-0.015882
C	3.684445	-3.098391	0.751843	H	-8.078712	1.232564	-0.000410
C	4.770260	-4.841496	-0.569733	H	-3.835106	1.227197	-0.907172

N	-5.910912	2.741656	-0.174260	H	1.745211	3.548439	1.444024
H	-6.812320	3.216529	-0.226876	H	3.766895	2.176065	1.291764
C	-4.788236	3.554211	0.000492	H	5.619546	5.180984	-1.195888
C	-2.472304	5.130449	0.186936	C	0.003091	9.496621	0.095188
C	-4.770260	4.841496	-0.569733	C	-0.002385	12.306518	0.020775
C	-3.684445	3.098391	0.751843	C	-0.985180	10.192105	-0.620279
C	-2.550425	3.879428	0.836792	C	0.988836	10.232518	0.772172
C	-3.620574	5.606293	-0.484654	C	0.985179	11.625478	0.735395
H	-5.626402	5.200524	-1.129864	C	-0.987051	11.584932	-0.657357
H	-3.747844	2.168346	1.304618	H	-1.740431	9.640037	-1.172086
H	-1.723194	3.536230	1.446502	H	1.746500	9.713721	1.351808
H	-3.591411	6.566565	-0.986185	H	1.749906	12.179208	1.271713
C	-1.215214	5.895719	0.200889	H	-1.753721	12.106684	-1.222247
C	1.210496	7.299456	0.140152	H	-0.004540	13.391889	-0.007572
C	-1.200327	7.299169	0.156791	N	5.917007	2.735433	-0.206144
C	0.005851	5.208085	0.230082	H	6.819272	3.208048	-0.263357
C	1.226077	5.896597	0.192292	C	5.922321	1.399678	-0.305144
C	0.004795	8.015574	0.130891	C	5.919282	-1.406906	-0.288422
H	-2.136035	7.845803	0.187907	C	4.718965	0.673858	-0.606529
H	0.006762	4.125107	0.203539	C	7.157786	0.676336	-0.168617
H	2.147160	7.844743	0.111727	C	7.156383	-0.684705	-0.160136
C	2.482753	5.130131	0.162487	C	4.717846	-0.681826	-0.599225
C	4.794961	3.550281	-0.033754	H	3.837093	1.217461	-0.920159
C	3.621879	5.596777	-0.530449	H	8.080805	1.225213	-0.015882
C	2.566459	3.884913	0.822448	H	8.078712	-1.232564	-0.000410
C	3.698679	3.101756	0.732386	H	3.835106	-1.227197	-0.907172
C	4.770260	4.829879	-0.620362	N	5.910912	-2.741656	-0.174260
H	3.587618	6.551133	-1.043167	H	6.812320	-3.216529	-0.226876

*A.2.6.3 **OTPB-BZN-221**, ^{5}**ES** State*

H	1.729396	-12.202874	-0.690374	C	-1.004149	-10.142798	1.126804
C	0.966280	-11.628034	-0.174800	C	0.972499	-10.238149	-0.263056

C	-0.022479	-12.279879	0.565585
C	-1.006257	-11.532690	1.217010
C	-0.014455	-9.476599	0.384989
H	1.731146	-9.743664	-0.862202
H	-0.026071	-13.363289	0.634552
H	-1.771968	-12.031981	1.802701
H	-1.757684	-9.571475	1.660274
C	-0.011401	-8.000269	0.284989
C	-0.007002	-5.193240	0.136651
C	1.196043	-7.288062	0.238060
C	-1.216352	-7.283505	0.240944
C	-1.234990	-5.876553	0.169622
C	1.218912	-5.881226	0.162058
H	2.127306	-7.836335	0.313623
H	-2.150181	-7.831965	0.270670
H	-0.005203	-4.118968	0.013210
C	2.466840	-5.124321	0.094045
C	4.807904	-3.564196	-0.192213
C	3.670783	-5.694675	-0.403819
C	2.505919	-3.768623	0.522434
C	3.634734	-3.004512	0.391126
C	4.816724	-4.946532	-0.536089
H	3.681945	-6.725890	-0.735870
H	1.643848	-3.334282	1.011978
H	3.653465	-1.991695	0.771069
H	5.714416	-5.388591	-0.955567
C	-2.480774	-5.115821	0.093769
C	-4.816724	-3.548478	-0.196374
C	-2.515940	-3.759473	0.520351
C	-3.685237	-5.682264	-0.407082
C	-4.828730	-4.930528	-0.541082
C	-3.642412	-2.992047	0.387899
H	-1.653043	-3.327493	1.010576
H	-3.699789	-6.713139	-0.740023
H	-5.726762	-5.369994	-0.962544
H	-3.658615	-1.979286	0.768126
N	-5.922074	-2.787940	-0.411192
H	-6.797554	-3.274920	-0.588425
C	-5.950578	-1.381288	-0.453725
C	-5.946826	1.399751	-0.451515
C	-4.889562	-0.683082	-1.054833
C	-7.051248	-0.683878	0.068617
C	-7.049218	0.704413	0.069925
C	-4.887748	0.699633	-1.053807
H	-4.096371	-1.225239	-1.555016
H	-7.880664	-1.225455	0.509796
H	-7.877136	1.247521	0.512049
H	-4.092984	1.240291	-1.553069
N	-5.915060	2.806413	-0.407347
H	-6.789226	3.295608	-0.584654
C	-4.807904	3.564196	-0.192213
C	-2.466840	5.124321	0.094045
C	-4.816724	4.946532	-0.536089
C	-3.634734	3.004512	0.391126
C	-2.505919	3.768623	0.522434
C	-3.670783	5.694675	-0.403819
H	-5.714416	5.388591	-0.955567
H	-3.653465	1.991695	0.771069
H	-1.643848	3.334282	1.011978
H	-3.681945	6.725890	-0.735870
C	-1.218912	5.881226	0.162058
C	1.216352	7.283505	0.240944
C	-1.196043	7.288062	0.238060
C	0.007002	5.193240	0.136651

C	1.234990	5.876553	0.169622
C	0.011401	8.000269	0.284989
H	-2.127306	7.836335	0.313623
H	0.005203	4.118968	0.013210
H	2.150181	7.831965	0.270670
C	2.480774	5.115821	0.093769
C	4.816724	3.548478	-0.196374
C	3.685237	5.682264	-0.407082
C	2.515940	3.759473	0.520351
C	3.642412	2.992047	0.387899
C	4.828730	4.930528	-0.541082
H	3.699789	6.713139	-0.740023
H	1.653043	3.327493	1.010576
H	3.658615	1.979286	0.768126
H	5.726762	5.369994	-0.962544
C	0.014455	9.476599	0.384989
C	0.022479	12.279879	0.565585
C	-0.972499	10.238149	-0.263056
C	1.004149	10.142798	1.126804
C	1.006257	11.532690	1.217010
C	-0.966280	11.628034	-0.174800
H	-1.731146	9.743664	-0.862202
H	1.757684	9.571475	1.660274
H	1.771968	12.031981	1.802701
H	-1.729396	12.202874	-0.690374
H	0.026071	13.363289	0.634552
N	5.922074	2.787940	-0.411192
H	6.797554	3.274920	-0.588425
C	5.950578	1.381288	-0.453725
C	5.946826	-1.399751	-0.451515
C	4.889562	0.683082	-1.054833
C	7.051248	0.683878	0.068617
C	7.049218	-0.704413	0.069925
C	4.887748	-0.699633	-1.053807
H	4.096371	1.225239	-1.555016
H	7.880664	1.225455	0.509796
H	7.877136	-1.247521	0.512049
H	4.092984	-1.240291	-1.553069
N	5.915060	-2.806413	-0.407347
H	6.789226	-3.295608	-0.584654

A.2.6.4 ***OTPB-BZN-221, EB*** *State*

H	1.718973	-11.895928	-2.012961
C	0.969685	-11.440583	-1.371591
C	-0.956760	-10.253840	0.254657
C	0.967235	-10.058889	-1.187195
C	0.007777	-12.235089	-0.744293
C	-0.955668	-11.635518	0.069458
C	0.004227	-9.443116	-0.371117
H	1.703962	-9.446710	-1.698839
H	0.009130	-13.311629	-0.888156
H	-1.703338	-12.245191	0.568865
H	-1.694235	-9.799962	0.909902
C	0.002962	-7.972373	-0.177420
C	0.000936	-5.202806	0.210526
C	1.210496	-7.265422	-0.080693
C	-1.205423	-7.267982	-0.074950
C	-1.221793	-5.880862	0.121784
C	1.224676	-5.877665	0.112949
H	2.149044	-7.809245	-0.113144
H	-2.143746	-7.807451	-0.153759
H	-0.000156	-4.121956	0.299520

C	2.488239	-5.110308	0.191406
C	4.825259	-3.506916	0.219110
C	3.607251	-5.444975	-0.592178
C	2.589385	-3.992089	1.036065
C	3.729174	-3.200304	1.050365
C	4.763762	-4.674657	-0.563075
H	3.557771	-6.303374	-1.255374
H	1.765026	-3.745256	1.697884
H	3.793384	-2.350266	1.722092
H	5.616136	-4.933045	-1.183431
C	-2.486356	-5.114108	0.195393
C	-4.824075	-3.511661	0.220903
C	-2.589013	-3.996202	1.040289
C	-3.603933	-5.448628	-0.590181
C	-4.760803	-4.678673	-0.562116
C	-3.729174	-3.204913	1.053618
H	-1.765346	-3.749080	1.702898
H	-3.553559	-6.306082	-1.254445
H	-5.612034	-4.936978	-1.184075
H	-3.794502	-2.355090	1.725521
N	-5.989728	-2.742076	0.203587
C	-5.924397	-1.443806	0.102419
C	-5.924728	1.438445	0.101678
C	-4.726640	-0.676977	-0.247895
C	-7.155020	-0.677918	0.287246
C	-7.155159	0.672354	0.286942
C	-4.726825	0.671714	-0.248354
H	-3.843863	-1.222288	-0.560952
H	-8.060530	-1.248051	0.468413
H	-8.060781	1.242382	0.467875
H	-3.844187	1.217017	-0.561807
N	-5.990464	2.736755	0.202337
C	-4.825259	3.506916	0.219110
C	-2.488239	5.110308	0.191406
C	-4.763762	4.674657	-0.563075
C	-3.729174	3.200304	1.050365
C	-2.589385	3.992089	1.036065
C	-3.607251	5.444975	-0.592178
H	-5.616136	4.933045	-1.183431
H	-3.793384	2.350266	1.722092
H	-1.765026	3.745256	1.697884
H	-3.557771	6.303374	-1.255374
C	-1.224676	5.877665	0.112949
C	1.205423	7.267982	-0.074950
C	-1.210496	7.265422	-0.080693
C	-0.000936	5.202806	0.210526
C	1.221793	5.880862	0.121784
C	-0.002962	7.972373	-0.177420
H	-2.149044	7.809245	-0.113144
H	0.000156	4.121956	0.299520
H	2.143746	7.807451	-0.153759
C	2.486356	5.114108	0.195393
C	4.824075	3.511661	0.220903
C	3.603933	5.448628	-0.590181
C	2.589013	3.996202	1.040289
C	3.729174	3.204913	1.053618
C	4.760803	4.678673	-0.562116
H	3.553559	6.306082	-1.254445
H	1.765346	3.749080	1.702898
H	3.794502	2.355090	1.725521
H	5.612034	4.936978	-1.184075
C	-0.004227	9.443116	-0.371117
C	-0.007777	12.235089	-0.744293
C	-0.967235	10.058889	-1.187195

C	0.956760	10.253840	0.254657
C	0.955668	11.635518	0.069458
C	-0.969685	11.440583	-1.371591
H	-1.703962	9.446710	-1.698839
H	1.694235	9.799962	0.909902
H	1.703338	12.245191	0.568865
H	-1.718973	11.895928	-2.012961
H	-0.009130	13.311629	-0.888156
N	5.989728	2.742076	0.203587
C	5.924397	1.443806	0.102419
C	5.924728	-1.438445	0.101678
C	4.726640	0.676977	-0.247895
C	7.155020	0.677918	0.287246
C	7.155159	-0.672354	0.286942
C	4.726825	-0.671714	-0.248354
H	3.843863	1.222288	-0.560952
H	8.060530	1.248051	0.468413
H	8.060781	-1.242382	0.467875
H	3.844187	-1.217017	-0.561807
N	5.990464	-2.736755	0.202337

A.2.7 Optimised Structures of **OTPB-FLR-210** Oligomers

A.2.7.1 ***OTPB-FLR-210, LEB*** *State*

H	-15.789100	3.716544	-0.364791
C	-14.802928	3.706942	0.090875
C	-12.263391	3.673422	1.236457
C	-13.965310	2.609231	-0.100503
C	-14.373574	4.794045	0.855031
C	-13.099789	4.772310	1.426826
C	-12.681805	2.574122	0.468914
H	-14.298368	1.779248	-0.716613
H	-15.025654	5.649840	1.003857
H	-12.758993	5.608870	2.030395
H	-11.284839	3.654951	1.706851
C	-11.792499	1.404990	0.261779
C	-10.111102	-0.804474	-0.108178
C	-12.318586	0.106480	0.226188
C	-10.409690	1.575809	0.116428
C	-9.552497	0.481506	-0.069235
C	-11.489190	-1.007935	0.041777
H	-13.380442	-0.041956	0.392340
H	-9.993428	2.577302	0.148729
H	-9.468701	-1.655982	-0.306908
C	-12.059512	-2.376468	0.002551
C	-13.142479	-4.976520	-0.072724
C	-13.309904	-2.618944	-0.589490
C	-11.362752	-3.463106	0.556175
C	-11.897689	-4.749798	0.518200
C	-13.846533	-3.904964	-0.626045
H	-13.853080	-1.796199	-1.044857
H	-10.405729	-3.292305	1.040156
H	-11.345146	-5.574915	0.958805
H	-14.812072	-4.071428	-1.095391
H	-13.559922	-5.978831	-0.101775
C	-8.095623	0.678359	-0.236755
C	-5.293954	1.039566	-0.565225
C	-7.172171	-0.256344	0.258921
C	-7.577333	1.809106	-0.891154
C	-6.211106	1.986466	-1.058833
C	-5.800649	-0.085365	0.110417
H	-7.531666	-1.121496	0.808437

H	-8.256681	2.546724	-1.307887
H	-5.839793	2.858630	-1.590861
H	-5.121226	-0.807495	0.546776
N	-3.933193	1.282883	-0.728148
H	-3.679727	2.249910	-0.877140
H	-2.015339	-2.882795	-1.129536
C	-1.892656	-1.833425	-0.875253
C	-1.602360	0.894721	-0.250327
C	-0.648239	-1.331099	-0.491914
C	-2.988988	-0.976083	-0.954729
C	-2.861816	0.388466	-0.630731
C	-0.513402	0.042411	-0.191743
H	-3.944785	-1.358543	-1.292865
H	-1.502432	1.948612	-0.000787
C	0.653892	-1.978036	-0.323294
C	3.332459	-2.673460	0.145527
C	1.058048	-3.306319	-0.473639
C	1.595487	-1.004993	0.075434
C	2.917703	-1.338090	0.321580
C	2.389980	-3.643647	-0.248410
H	0.350512	-4.075117	-0.771961
H	3.621436	-0.589487	0.667781
H	2.718189	-4.671460	-0.380358
C	0.921848	0.349025	0.188559
H	1.374921	1.088403	-0.484898
H	0.999899	0.764511	1.201800
N	4.642670	-3.089279	0.403628
H	4.750688	-4.064328	0.646634
C	5.823053	-2.355360	0.331432
C	8.303206	-0.970226	0.203346
C	6.958825	-2.836111	1.009748
C	5.952022	-1.177955	-0.427547
C	7.166718	-0.504103	-0.477414
C	8.168810	-2.159973	0.939530
H	6.877385	-3.740068	1.607971
H	5.112023	-0.809869	-1.004228
H	7.242007	0.387206	-1.093471
H	9.017980	-2.544801	1.496451
C	9.589103	-0.241311	0.143709
C	12.027639	1.144324	0.028815
C	10.809418	-0.932330	0.165749
C	9.616706	1.158654	0.063449
C	10.825691	1.863932	-0.000150
C	12.034466	-0.254340	0.114287
H	10.805292	-2.017326	0.174215
H	8.683235	1.710494	0.099521
H	12.970276	1.679697	-0.015498
C	10.832049	3.345403	-0.075917
C	10.840652	6.159055	-0.225768
C	11.812850	4.098860	0.589649
C	9.855590	4.030195	-0.817844
C	9.858912	5.422231	-0.891574
C	11.817879	5.490920	0.514929
H	12.561793	3.590160	1.189253
H	9.103025	3.464522	-1.359139
H	9.098557	5.931364	-1.477165
H	12.581387	6.054657	1.043612
H	10.844099	7.243671	-0.283452
C	13.313991	-1.004702	0.130810
C	15.743934	-2.430381	0.170961
C	13.457447	-2.161593	0.914267
C	14.412423	-0.576905	-0.632792
C	15.615088	-1.281550	-0.612358
C	14.659144	-2.867774	0.933834

H	12.627315	-2.494929	1.529993	H	14.750806	-3.755897	1.552790
H	14.314218	0.300534	-1.264985	H	16.680770	-2.979775	0.186522
H	16.449933	-0.937292	-1.216317				

*A.2.7.2 **OTPB-FLR-210**, **^{1}ES** State*

H	-15.770408	3.559453	-0.831678	H	-10.393487	-3.278234	1.269784
C	-14.818722	3.589543	-0.309129	H	-11.296434	-5.575976	1.219203
C	-12.365184	3.658920	1.011034	H	-14.617263	-4.217626	-1.152883
C	-13.951372	2.501694	-0.392670	H	-13.418801	-6.059066	0.014534
C	-14.462704	4.716609	0.434457	C	-8.066686	0.681941	-0.030902
C	-13.232497	4.746860	1.094363	C	-5.283783	1.081442	-0.179323
C	-12.711191	2.520291	0.265682	C	-7.166668	-0.241007	0.541900
H	-14.226709	1.639719	-0.993042	C	-7.530080	1.827468	-0.655620
H	-15.138891	5.563862	0.500055	C	-6.164522	2.033964	-0.723622
H	-12.950850	5.615079	1.683169	C	-5.797219	-0.050317	0.480453
H	-11.422770	3.680838	1.550244	H	-7.550957	-1.093755	1.089819
C	-11.788404	1.363319	0.172928	H	-8.193599	2.547239	-1.120659
C	-10.048249	-0.836013	0.035411	H	-5.768384	2.909758	-1.228762
C	-12.283636	0.051187	0.161854	H	-5.133639	-0.733974	0.996090
C	-10.404143	1.555525	0.109684	N	-3.912217	1.341798	-0.265042
C	-9.521742	0.465516	0.045058	H	-3.672378	2.329882	-0.287318
C	-11.428624	-1.058370	0.088316	H	-2.068467	-2.786711	-0.856277
H	-13.351930	-0.111031	0.256709	C	-1.943484	-1.735960	-0.619397
H	-10.010823	2.565842	0.121035	C	-1.556964	1.048678	-0.127165
H	-9.380319	-1.683470	-0.071989	C	-0.648331	-1.198077	-0.377227
C	-11.976502	-2.435599	0.069668	C	-3.028275	-0.905712	-0.593485
C	-13.016920	-5.050299	0.029455	C	-2.864990	0.496126	-0.316868
C	-13.176302	-2.720830	-0.601981	C	-0.482319	0.213662	-0.142490
C	-11.308102	-3.484545	0.721662	H	-4.011255	-1.287850	-0.833460
C	-11.823118	-4.779499	0.701447	H	-1.448748	2.112422	0.060951
C	-13.691689	-4.015618	-0.621708	C	0.609699	-1.823831	-0.346358
H	-13.695260	-1.927477	-1.131483	C	3.296946	-2.554038	-0.152066

C	0.965687	-3.194650	-0.485369
C	1.624778	-0.834696	-0.086831
C	2.940039	-1.178475	0.011476
C	2.279080	-3.547880	-0.374910
H	0.208327	-3.948034	-0.669918
H	3.694509	-0.443842	0.258828
H	2.579855	-4.585400	-0.480954
C	0.980749	0.522716	0.067152
H	1.357151	1.240661	-0.670780
H	1.169898	0.954213	1.056959
N	4.569349	-2.989118	-0.073122
H	4.680321	-3.996636	0.011097
C	5.772106	-2.274981	-0.067092
C	8.257946	-0.953218	-0.015158
C	6.865324	-2.849706	0.606547
C	5.935473	-1.057781	-0.754007
C	7.160202	-0.413982	-0.717910
C	8.080827	-2.191445	0.636958
H	6.740401	-3.791154	1.132482
H	5.134805	-0.657186	-1.363490
H	7.287082	0.499731	-1.286976
H	8.899714	-2.625499	1.199009
C	9.554018	-0.254931	0.018388
C	12.013422	1.070845	0.093252
C	10.753298	-0.980852	0.097375
C	9.609030	1.147517	-0.025580
C	10.833242	1.824207	0.013927
C	11.991621	-0.330728	0.134158
H	10.726942	-2.064606	0.073171
H	8.688362	1.720973	-0.032338
H	12.967882	1.585338	0.123230
C	10.882299	3.305652	-0.012356
C	10.973250	6.117795	-0.067016
C	11.831873	4.007891	0.747214
C	9.979698	4.038035	-0.800148
C	10.024505	5.430845	-0.827339
C	11.876707	5.400736	0.720044
H	12.523169	3.460340	1.380757
H	9.256970	3.510268	-1.415330
H	9.324503	5.979694	-1.450691
H	12.613696	5.926324	1.320217
H	11.009188	7.202964	-0.088768
C	13.253473	-1.106127	0.199820
C	15.646729	-2.581197	0.325340
C	13.331032	-2.285611	0.957975
C	14.397232	-0.678572	-0.493573
C	15.582508	-1.409308	-0.431239
C	14.516247	-3.016348	1.020053
H	12.464552	-2.617872	1.522195
H	14.350207	0.217900	-1.104527
H	16.454428	-1.066836	-0.980888
H	14.559275	-3.921648	1.618691
H	16.570505	-3.150060	0.374062

*A.2.7.3 **OTPB-FLR-210**, ^{3}**ES** State*

H	-15.804912	3.538153	-0.681400
C	-14.848031	3.557790	-0.168153
C	-12.380575	3.602360	1.128250
C	-13.970549	2.483568	-0.303896
C	-14.495422	4.658074	0.616029
C	-13.258701	4.676038	1.264177

C	-12.723379	2.491289	0.341234
H	-14.243917	1.643445	-0.935347
H	-15.179795	5.494471	0.722432
H	-12.980414	5.523012	1.884472
H	-11.433009	3.613016	1.658614
C	-11.788732	1.350738	0.190747
C	-10.032151	-0.831635	-0.051334
C	-12.270817	0.033013	0.132076
C	-10.409852	1.558387	0.118176
C	-9.514227	0.477273	0.002739
C	-11.407426	-1.067517	0.004106
H	-13.336447	-0.142885	0.231051
H	-10.029004	2.571582	0.167041
H	-9.361002	-1.669156	-0.201357
C	-11.947140	-2.445562	-0.065178
C	-12.971818	-5.061195	-0.200850
C	-13.149938	-2.710225	-0.739800
C	-11.267262	-3.514208	0.541106
C	-11.775132	-4.810180	0.473826
C	-13.657268	-4.006444	-0.807141
H	-13.677393	-1.900219	-1.234614
H	-10.350850	-3.323426	1.091711
H	-11.240875	-5.623053	0.956889
H	-14.584974	-4.193513	-1.339838
H	-13.368133	-6.070910	-0.252154
C	-8.072685	0.707409	-0.083979
C	-5.281807	1.125981	-0.279961
C	-7.147365	-0.278862	0.345990
C	-7.548635	1.927791	-0.583285
C	-6.193685	2.139813	-0.674757
C	-5.787582	-0.084382	0.261826
H	-7.513522	-1.189755	0.804421
H	-8.222783	2.697727	-0.938524
H	-5.811590	3.067031	-1.089458
H	-5.110041	-0.827033	0.662741
N	-3.944563	1.385327	-0.401642
H	-3.701344	2.365364	-0.519993
H	-1.998867	-2.705574	-1.133765
C	-1.895496	-1.679860	-0.795872
C	-1.610288	1.022098	0.007682
C	-0.657621	-1.179744	-0.372612
C	-2.995081	-0.836006	-0.810840
C	-2.864046	0.506324	-0.387762
C	-0.521528	0.175699	0.020077
H	-3.942075	-1.190152	-1.197560
H	-1.523292	2.059440	0.316761
C	0.640690	-1.826013	-0.265349
C	3.292492	-2.553297	0.118215
C	1.023764	-3.152095	-0.506968
C	1.584605	-0.872934	0.190413
C	2.905080	-1.223820	0.391802
C	2.345596	-3.512509	-0.307210
H	0.304568	-3.890682	-0.844186
H	3.615751	-0.514804	0.799203
H	2.669384	-4.530507	-0.500107
C	0.909750	0.462097	0.415200
H	1.353784	1.255680	-0.197997
H	0.988121	0.789493	1.459134
N	4.601696	-2.992335	0.307725
H	4.694807	-3.980912	0.523946
C	5.776105	-2.298062	0.232354
C	8.269473	-0.963911	0.128837
C	6.942593	-2.903144	0.771526
C	5.885717	-1.033223	-0.402336

C	7.102381	-0.391993	-0.441702
C	8.148898	-2.246462	0.724514
H	6.866745	-3.872593	1.254146
H	5.031666	-0.602373	-0.908214
H	7.174603	0.549032	-0.973852
H	9.013066	-2.708685	1.186212
C	9.552348	-0.264805	0.083618
C	12.003175	1.077643	-0.003959
C	10.764442	-0.982035	0.123281
C	9.597802	1.140957	-0.000320
C	10.814504	1.824731	-0.043552
C	11.995428	-0.324303	0.078785
H	10.749646	-2.065498	0.126299
H	8.676680	1.710953	0.029552
H	12.954400	1.597537	-0.038976
C	10.852832	3.304113	-0.120370
C	10.920788	6.111924	-0.271996
C	11.843558	4.034670	0.555289
C	9.897702	4.005037	-0.874471
C	9.931417	5.396149	-0.949468
C	11.876496	5.425955	0.480280
H	12.576981	3.512573	1.162332
H	9.141486	3.454965	-1.426886
H	9.190453	5.920768	-1.545567
H	12.645573	5.974752	1.015742
H	10.948062	7.195862	-0.331362
C	13.266006	-1.086200	0.105699
C	15.675453	-2.535242	0.160364
C	13.390879	-2.239801	0.896509
C	14.369562	-0.670303	-0.656409
C	15.563241	-1.389141	-0.629475
C	14.584938	-2.957783	0.923533
H	12.556726	-2.559880	1.513962
H	14.283948	0.205661	-1.292415
H	16.403937	-1.057569	-1.231691
H	14.666810	-3.842371	1.548291
H	16.606292	-3.094051	0.182206

*A.2.7.4 **OTPB-FLR-210, EB** State*

H	-15.687878	3.335544	-1.074622
C	-14.760980	3.413685	-0.513416
C	-12.370126	3.604724	0.904773
C	-13.853646	2.355594	-0.529418
C	-14.476115	4.572999	0.211100
C	-13.276411	4.663854	0.919915
C	-12.643501	2.433744	0.179171
H	-14.072513	1.467955	-1.115551
H	-15.182589	5.397887	0.223337
H	-13.048679	5.557728	1.493757
H	-11.451886	3.674860	1.480199
C	-11.679462	1.306564	0.158158
C	-9.860095	-0.824102	0.141179
C	-12.132379	-0.019706	0.162068
C	-10.299313	1.546355	0.150464
C	-9.375325	0.491813	0.142971
C	-11.234359	-1.095552	0.152519
H	-13.197588	-0.217106	0.221310
H	-9.939300	2.569775	0.151401
H	-9.157635	-1.648696	0.080623
C	-11.728944	-2.493701	0.153254
C	-12.668035	-5.149702	0.154039

C	-12.890530	-2.846720	-0.552956
C	-11.047385	-3.498015	0.859996
C	-11.511199	-4.812535	0.859823
C	-13.356000	-4.160667	-0.552059
H	-13.417980	-2.089565	-1.125525
H	-10.161312	-3.240314	1.432527
H	-10.973086	-5.572570	1.419273
H	-14.252527	-4.413736	-1.110973
H	-13.030145	-6.173697	0.154424
C	-7.919691	0.757951	0.118098
C	-5.120523	1.254709	0.061513
C	-7.018347	-0.085742	0.789660
C	-7.390896	1.870349	-0.562882
C	-6.027978	2.127862	-0.572876
C	-5.649498	0.148229	0.761843
H	-7.399078	-0.922580	1.367540
H	-8.059080	2.533668	-1.103602
H	-5.632239	2.991679	-1.097848
H	-4.979603	-0.495452	1.322961
N	-3.773836	1.592376	0.056932
H	-2.122517	-2.526780	-1.108946
C	-1.959876	-1.518973	-0.738214
C	-1.453956	1.154109	0.119246
C	-0.633837	-1.073371	-0.443369
C	-3.007775	-0.665571	-0.579988
C	-2.818605	0.708710	-0.116733
C	-0.417266	0.292492	-0.017385
H	-4.010563	-0.983919	-0.838201
H	-1.319345	2.183512	0.436535
C	0.586592	-1.744013	-0.515918
C	3.285555	-2.621267	-0.487630
C	0.888855	-3.099775	-0.855735
C	1.657153	-0.846381	-0.137258
C	2.951623	-1.251355	-0.120544
C	2.182147	-3.517038	-0.819369
H	0.091392	-3.784757	-1.127567
H	3.744142	-0.582091	0.193666
H	2.454255	-4.538763	-1.062974
C	1.065418	0.505015	0.212636
H	1.468740	1.303657	-0.421299
H	1.280802	0.786520	1.250469
N	4.486239	-3.151894	-0.506828
C	5.645013	-2.394744	-0.390694
C	8.126937	-1.023583	-0.180447
C	6.699820	-2.913469	0.387854
C	5.874260	-1.192923	-1.095766
C	7.091372	-0.531619	-0.993650
C	7.901189	-2.230505	0.507076
H	6.539001	-3.846899	0.918127
H	5.106447	-0.811278	-1.760914
H	7.253111	0.369407	-1.577750
H	8.676143	-2.630082	1.154128
C	9.414795	-0.304386	-0.063809
C	11.852864	1.062642	0.163097
C	10.618201	-1.006896	0.093209
C	9.457458	1.096641	-0.106144
C	10.667991	1.793310	0.002661
C	11.843431	-0.337804	0.211316
H	10.607231	-2.091537	0.074543
H	8.529570	1.654606	-0.175870
H	12.796035	1.591627	0.251361
C	10.691870	3.275986	-0.033528
C	10.735271	6.091651	-0.109615
C	11.580523	4.004003	0.774333

C	9.825202	3.986681	-0.879924
C	9.845879	5.379997	-0.917426
C	11.602699	5.397371	0.736264
H	12.241175	3.474250	1.454124
H	9.147758	3.440728	-1.529808
H	9.172334	5.909933	-1.585038
H	12.292787	5.941473	1.374935
H	10.752213	7.177256	-0.138991
C	13.107437	-1.098490	0.366102
C	15.506099	-2.545139	0.665920
C	13.146837	-2.276968	1.129220
C	14.293733	-0.659489	-0.244195
C	15.481008	-1.374662	-0.095192
C	14.333346	-2.993473	1.277190
H	12.245533	-2.619896	1.628635
H	14.278961	0.235137	-0.859520
H	16.385712	-1.021609	-0.582075
H	14.343323	-3.898623	1.877849
H	16.430922	-3.102850	0.781457

A.2.8 Optimised Structures of **OTPB-FLR-221** Oligomers

*A.2.8.1 **OTPB-FLR-221**, **LEB** State*

H	1.701034	14.223279	-2.200919
C	0.953426	13.738719	-1.579132
C	-0.968579	12.477407	-0.006084
C	0.956724	12.350399	-1.452361
C	-0.012202	14.502878	-0.920670
C	-0.973884	13.865559	-0.133850
C	-0.003425	11.696314	-0.662958
H	1.695762	11.763475	-1.989473
H	-0.015496	15.584496	-1.019995
H	-1.725300	14.450658	0.389010
H	-1.705433	11.992425	0.627326
C	-0.000209	10.219013	-0.523571
C	0.003425	7.442500	-0.265219
C	1.211125	9.512398	-0.470311
C	-1.209909	9.509562	-0.465371
C	-1.224333	8.113844	-0.338595
C	1.229213	8.116531	-0.346601
H	2.148436	10.057420	-0.522436
H	-2.147276	10.047507	-0.566054
H	0.005266	6.372611	-0.091881
C	2.484312	7.334643	-0.272559
C	4.780317	5.688022	0.028029
C	3.641382	7.809035	0.364035
C	2.531410	6.034987	-0.810495
C	3.650108	5.230884	-0.675463
C	4.769633	7.003772	0.518028
H	3.644836	8.804759	0.798528
H	1.678134	5.655451	-1.364089
H	3.658425	4.235937	-1.106916
H	5.633719	7.382113	1.058366
C	-2.477528	7.328980	-0.270001
C	-4.772337	5.679938	0.026724
C	-2.520941	6.027923	-0.804826
C	-3.637756	7.803352	0.361073
C	-4.765471	6.997163	0.513059
C	-3.638890	5.222514	-0.671366
H	-1.665587	5.648264	-1.355064
H	-3.643826	8.800562	0.792228

H	-5.632273	7.375754	1.048839
H	-3.644341	4.226536	-1.100451
N	-5.873560	4.836485	0.193499
H	-6.735484	5.273069	0.494032
H	-3.552413	1.294896	1.982306
C	-4.427231	1.635302	1.435101
C	-6.692844	2.540947	0.016856
C	-5.363862	0.725926	0.942481
C	-4.621510	2.993903	1.212105
C	-5.731327	3.456709	0.481247
C	-6.506302	1.184690	0.253420
H	-3.900945	3.712221	1.586789
H	-7.543707	2.904081	-0.553635
C	-5.365231	-0.734784	0.943071
C	-5.737581	-3.465107	0.483778
C	-4.430267	-1.645454	1.436485
C	-6.508506	-1.191930	0.254305
C	-6.697387	-2.548048	0.018645
C	-4.627027	-3.003868	1.214368
H	-3.554861	-1.306184	1.983451
H	-7.548729	-2.910202	-0.551737
H	-3.907664	-3.723286	1.589293
C	-7.342232	-0.003013	-0.193728
H	-8.334811	-0.001912	0.276811
H	-7.513815	-0.003245	-1.277575
N	-5.882045	-4.845231	0.196254
H	-6.740313	-5.281992	0.507074
C	-4.780317	-5.688022	0.028029
C	-2.484312	-7.334643	-0.272559
C	-3.650108	-5.230884	-0.675463
C	-4.769633	-7.003772	0.518028
C	-3.641382	-7.809035	0.364035
C	-2.531410	-6.034987	-0.810495
H	-3.658425	-4.235937	-1.106916
H	-5.633719	-7.382113	1.058366
H	-3.644836	-8.804759	0.798528
H	-1.678134	-5.655451	-1.364089
C	-1.229213	-8.116531	-0.346601
C	1.209909	-9.509562	-0.465371
C	-0.003425	-7.442500	-0.265219
C	-1.211125	-9.512398	-0.470311
C	0.000209	-10.219013	-0.523571
C	1.224333	-8.113844	-0.338595
H	-0.005266	-6.372611	-0.091881
H	-2.148436	-10.057420	-0.522436
H	2.147276	-10.047507	-0.566054
C	2.477528	-7.328980	-0.270001
C	4.772337	-5.679938	0.026724
C	2.520941	-6.027923	-0.804826
C	3.637756	-7.803352	0.361073
C	4.765471	-6.997163	0.513059
C	3.638890	-5.222514	-0.671366
H	1.665587	-5.648264	-1.355064
H	3.643826	-8.800562	0.792228
H	5.632273	-7.375754	1.048839
H	3.644341	-4.226536	-1.100451
C	0.003425	-11.696314	-0.662958
C	0.012202	-14.502878	-0.920670
C	0.968579	-12.477407	-0.006084
C	-0.956724	-12.350399	-1.452361
C	-0.953426	-13.738719	-1.579132
C	0.973884	-13.865559	-0.133850
H	1.705433	-11.992425	0.627326
H	-1.695762	-11.763475	-1.989473

H	-1.701034	-14.223279	-2.200919
H	1.725300	-14.450658	0.389010
H	0.015496	-15.584496	-1.019995
N	5.873560	-4.836485	0.193499
H	6.735484	-5.273069	0.494032
H	3.552413	-1.294896	1.982306
C	4.427231	-1.635302	1.435101
C	6.692844	-2.540947	0.016856
C	5.363862	-0.725926	0.942481
C	4.621510	-2.993903	1.212105
C	5.731327	-3.456709	0.481247
C	6.506302	-1.184690	0.253420
H	3.900945	-3.712221	1.586789
H	7.543707	-2.904081	-0.553635
C	5.365231	0.734784	0.943071
C	5.737581	3.465107	0.483778
C	4.430267	1.645454	1.436485
C	6.508506	1.191930	0.254305
C	6.697387	2.548048	0.018645
C	4.627027	3.003868	1.214368
H	3.554861	1.306184	1.983451
H	7.548729	2.910202	-0.551737
H	3.907664	3.723286	1.589293
C	7.342232	0.003013	-0.193728
H	8.334811	0.001912	0.276811
H	7.513815	0.003245	-1.277575
N	5.882045	4.845231	0.196254
H	6.740313	5.281992	0.507074

*A.2.8.2 **OTPB-FLR-221**, **^{1}ES** State*

H	-1.749216	14.405807	1.289425
C	-0.981524	13.845302	0.764164
C	0.995028	12.394074	-0.561302
C	-0.981868	12.452862	0.823505
C	0.006665	14.517419	0.042075
C	0.994740	13.786419	-0.620665
C	0.006665	11.706811	0.161804
H	-1.739985	11.941217	1.408908
H	0.006918	15.602308	-0.003493
H	1.762480	14.300298	-1.191597
H	1.753206	11.834274	-1.100983
C	0.007778	10.225444	0.222204
C	0.009994	7.428993	0.357457
C	-1.199303	9.509974	0.230654
C	1.216491	9.514375	0.279780
C	1.230924	8.114668	0.348063
C	-1.212649	8.110197	0.302092
H	-2.136705	10.053365	0.181694
H	2.151763	10.062494	0.315930
H	0.014348	6.345555	0.340121
C	-2.462590	7.322901	0.277255
C	-4.709708	5.655890	0.053097
C	-3.595169	7.730229	-0.455571
C	-2.524091	6.097101	0.968194
C	-3.626251	5.269984	0.860602
C	-4.714599	6.913554	-0.565597
H	-3.578756	8.672545	-0.992237
H	-1.705280	5.800649	1.613442
H	-3.670406	4.338767	1.414629
H	-5.556824	7.217616	-1.178134
C	2.481443	7.328520	0.382725
C	4.719248	5.644046	0.236097

C	2.520362	6.117375	1.100254
C	3.633159	7.718371	-0.328251
C	4.748992	6.892134	-0.400327
C	3.619028	5.280563	1.030049
H	1.684900	5.839306	1.732532
H	3.633894	8.651614	-0.881018
H	5.606454	7.179430	-0.999970
H	3.644858	4.356501	1.597440
N	5.778965	4.721430	0.072039
H	6.729279	5.069899	0.180282
H	3.171703	1.245344	-1.205511
C	4.125733	1.601593	-0.834239
C	6.715254	2.503237	0.003358
C	5.185939	0.690954	-0.563812
C	4.337475	2.930976	-0.645124
C	5.617177	3.412557	-0.177866
C	6.488590	1.169693	-0.163558
H	3.563575	3.649364	-0.876831
H	7.679268	2.887649	0.319911
C	5.193045	-0.702662	-0.613409
C	5.631491	-3.435259	-0.348735
C	4.145051	-1.603084	-0.956677
C	6.497415	-1.195312	-0.233946
C	6.729273	-2.534493	-0.128805
C	4.359396	-2.938470	-0.820803
H	3.200677	-1.233954	-1.339834
H	7.691244	-2.929347	0.182420
H	3.595977	-3.651116	-1.101274
C	7.411576	-0.016015	0.032929
H	8.253750	0.007352	-0.668977
H	7.838095	-0.044418	1.041748
N	5.780512	-4.751287	-0.127920
H	6.726461	-5.115051	-0.033476
C	4.709708	-5.655890	0.053097
C	2.462590	-7.322901	0.277255
C	3.626251	-5.269984	0.860602
C	4.714599	-6.913554	-0.565597
C	3.595169	-7.730229	-0.455571
C	2.524091	-6.097101	0.968194
H	3.670406	-4.338767	1.414629
H	5.556824	-7.217616	-1.178134
H	3.578756	-8.672545	-0.992237
H	1.705280	-5.800649	1.613442
C	1.212649	-8.110197	0.302092
C	-1.216491	-9.514375	0.279780
C	-0.009994	-7.428993	0.357457
C	1.199303	-9.509974	0.230654
C	-0.007778	-10.225444	0.222204
C	-1.230924	-8.114668	0.348063
H	-0.014348	-6.345555	0.340121
H	2.136705	-10.053365	0.181694
H	-2.151763	-10.062494	0.315930
C	-2.481443	-7.328520	0.382725
C	-4.719248	-5.644046	0.236097
C	-2.520362	-6.117375	1.100254
C	-3.633159	-7.718371	-0.328251
C	-4.748992	-6.892134	-0.400327
C	-3.619028	-5.280563	1.030049
H	-1.684900	-5.839306	1.732532
H	-3.633894	-8.651614	-0.881018
H	-5.606454	-7.179430	-0.999970
H	-3.644858	-4.356501	1.597440
C	-0.006665	-11.706811	0.161804
C	-0.006665	-14.517419	0.042075

C	-0.995028	-12.394074	-0.561302
C	0.981868	-12.452862	0.823505
C	0.981524	-13.845302	0.764164
C	-0.994740	-13.786419	-0.620665
H	-1.753206	-11.834274	-1.100983
H	1.739985	-11.941217	1.408908
H	1.749216	-14.405807	1.289425
H	-1.762480	-14.300298	-1.191597
H	-0.006918	-15.602308	-0.003493
N	-5.778965	-4.721430	0.072039
H	-6.729279	-5.069899	0.180282
H	-3.171703	-1.245344	-1.205511
C	-4.125733	-1.601593	-0.834239
C	-6.715254	-2.503237	0.003358
C	-5.185939	-0.690954	-0.563812
C	-4.337475	-2.930976	-0.645124
C	-5.617177	-3.412557	-0.177866
C	-6.488590	-1.169693	-0.163558
H	-3.563575	-3.649364	-0.876831
H	-7.679268	-2.887649	0.319911
C	-5.193045	0.702662	-0.613409
C	-5.631491	3.435259	-0.348735
C	-4.145051	1.603084	-0.956677
C	-6.497415	1.195312	-0.233946
C	-6.729273	2.534493	-0.128805
C	-4.359396	2.938470	-0.820803
H	-3.200677	1.233954	-1.339834
H	-7.691244	2.929347	0.182420
H	-3.595977	3.651116	-1.101274
C	-7.411576	0.016015	0.032929
H	-8.253750	-0.007352	-0.668977
H	-7.838095	0.044418	1.041748
N	-5.780512	4.751287	-0.127920
H	-6.726461	5.115051	-0.033476

*A.2.8.3 **OTPB-FLR-221**, ^{5}**ES** State*

H	1.672014	13.308803	-3.576128
C	0.931806	12.980555	-2.852699
C	-0.980648	12.119208	-1.014563
C	0.941244	11.660547	-2.406429
C	-0.031669	13.874266	-2.380531
C	-0.987408	13.439427	-1.459939
C	-0.015024	11.212774	-1.480901
H	1.676777	10.965907	-2.801332
H	-0.037998	14.902901	-2.727937
H	-1.734443	14.130813	-1.081938
H	-1.711898	11.796105	-0.279642
C	-0.008394	9.809892	-1.004983
C	0.002832	7.148655	-0.129091
C	1.201992	9.134500	-0.791576
C	-1.213568	9.125512	-0.787831
C	-1.226488	7.786876	-0.354058
C	1.226488	7.794048	-0.363341
H	2.131467	9.660554	-0.975684
H	-2.146458	9.627618	-1.016706
H	0.007520	6.150202	0.284945
C	2.474627	7.047511	-0.172320
C	4.822304	5.529840	0.258624
C	3.719053	7.680479	0.080958
C	2.463342	5.632130	-0.266316
C	3.594863	4.885943	-0.055664
C	4.871035	6.949090	0.279946

H	3.768860	8.760104	0.159540
H	1.556982	5.118990	-0.562637
H	3.568758	3.811796	-0.185534
H	5.806835	7.450626	0.504080
C	-2.468654	7.029338	-0.168954
C	-4.806014	5.493327	0.248453
C	-2.447786	5.615161	-0.273738
C	-3.716744	7.652370	0.089598
C	-4.864052	6.911816	0.281898
C	-3.574610	4.859800	-0.069733
H	-1.537478	5.111445	-0.573470
H	-3.772177	8.730981	0.177811
H	-5.803569	7.405015	0.509345
H	-3.542232	3.786944	-0.208008
N	-5.926642	4.746651	0.485363
H	-6.829765	5.197174	0.359960
H	-4.060688	1.252023	2.749174
C	-4.822363	1.598595	2.058924
C	-6.865529	2.510541	0.302868
C	-5.703116	0.703961	1.440825
C	-4.930720	2.945472	1.762006
C	-5.917327	3.395946	0.854813
C	-6.736094	1.162079	0.584718
H	-4.273656	3.667078	2.232959
H	-7.620842	2.880471	-0.382928
C	-5.711454	-0.747870	1.448855
C	-5.939399	-3.440375	0.874479
C	-4.846153	-1.645829	2.083499
C	-6.744430	-1.203466	0.591605
C	-6.879797	-2.552429	0.314086
C	-4.959716	-2.993225	1.790308
H	-4.094353	-1.301489	2.785503
H	-7.632224	-2.920642	-0.375837
H	-4.310713	-3.717129	2.268983
C	-7.510636	-0.019580	0.036125
H	-8.553323	-0.015667	0.378626
H	-7.538909	-0.022211	-1.059469
N	-5.946220	-4.791329	0.502615
H	-6.848048	-5.245659	0.380937
C	-4.822304	-5.529840	0.258624
C	-2.474627	-7.047511	-0.172320
C	-3.594863	-4.885943	-0.055664
C	-4.871035	-6.949090	0.279946
C	-3.719053	-7.680479	0.080958
C	-2.463342	-5.632130	-0.266316
H	-3.568758	-3.811796	-0.185534
H	-5.806835	-7.450626	0.504080
H	-3.768860	-8.760104	0.159540
H	-1.556982	-5.118990	-0.562637
C	-1.226488	-7.794048	-0.363341
C	1.213568	-9.125512	-0.787831
C	-0.002832	-7.148655	-0.129091
C	-1.201992	-9.134500	-0.791576
C	0.008394	-9.809892	-1.004983
C	1.226488	-7.786876	-0.354058
H	-0.007520	-6.150202	0.284945
H	-2.131467	-9.660554	-0.975684
H	2.146458	-9.627618	-1.016706
C	2.468654	-7.029338	-0.168954
C	4.806014	-5.493327	0.248453
C	2.447786	-5.615161	-0.273738
C	3.716744	-7.652370	0.089598
C	4.864052	-6.911816	0.281898
C	3.574610	-4.859800	-0.069733

H	1.537478	-5.111445	-0.573470
H	3.772177	-8.730981	0.177811
H	5.803569	-7.405015	0.509345
H	3.542232	-3.786944	-0.208008
C	0.015024	-11.212774	-1.480901
C	0.031669	-13.874266	-2.380531
C	0.980648	-12.119208	-1.014563
C	-0.941244	-11.660547	-2.406429
C	-0.931806	-12.980555	-2.852699
C	0.987408	-13.439427	-1.459939
H	1.711898	-11.796105	-0.279642
H	-1.676777	-10.965907	-2.801332
H	-1.672014	-13.308803	-3.576128
H	1.734443	-14.130813	-1.081938
H	0.037998	-14.902901	-2.727937
N	5.926642	-4.746651	0.485363
H	6.829765	-5.197174	0.359960
H	4.060688	-1.252023	2.749174
C	4.822363	-1.598595	2.058924
C	6.865529	-2.510541	0.302868
C	5.703116	-0.703961	1.440825
C	4.930720	-2.945472	1.762006
C	5.917327	-3.395946	0.854813
C	6.736094	-1.162079	0.584718
H	4.273656	-3.667078	2.232959
H	7.620842	-2.880471	-0.382928
C	5.711454	0.747870	1.448855
C	5.939399	3.440375	0.874479
C	4.846153	1.645829	2.083499
C	6.744430	1.203466	0.591605
C	6.879797	2.552429	0.314086
C	4.959716	2.993225	1.790308
H	4.094353	1.301489	2.785503
H	7.632224	2.920642	-0.375837
H	4.310713	3.717129	2.268983
C	7.510636	0.019580	0.036125
H	8.553323	0.015667	0.378626
H	7.538909	0.022211	-1.059469
N	5.946220	4.791329	0.502615
H	6.848048	5.245659	0.380937

*A.2.8.4 **OTPB-FLR-221**, **EB** State*

H	1.695094	14.534018	-0.795486
C	0.948107	13.928261	-0.290263
C	-0.972732	12.361366	0.981318
C	0.949091	12.545124	-0.464468
C	-0.014350	14.534270	0.519872
C	-0.975269	13.744506	1.154653
C	-0.010801	11.738916	0.168918
H	1.685819	12.086009	-1.116894
H	-0.015726	15.611944	0.655135
H	-1.723861	14.204805	1.793345
H	-1.708700	11.753162	1.498750
C	-0.009111	10.266438	-0.013029
C	-0.005711	7.499178	-0.373255
C	1.202016	9.563401	-0.108575
C	-1.218655	9.559677	-0.102414
C	-1.231726	8.170435	-0.283211
C	1.218655	8.174796	-0.292509
H	2.139753	10.104411	-0.029885
H	-2.157346	10.103730	-0.070211
H	-0.004065	6.417431	-0.443651

C	2.468942	7.382938	-0.344368
C	4.702749	5.636156	-0.234143
C	3.580265	7.675793	0.465677
C	2.542016	6.245792	-1.167653
C	3.628690	5.386971	-1.114639
C	4.687931	6.833491	0.505214
H	3.556265	8.549960	1.109979
H	1.729163	6.029956	-1.854283
H	3.664106	4.510614	-1.754186
H	5.523898	7.053246	1.162036
C	-2.480215	7.376640	-0.339396
C	-4.711607	5.626726	-0.230090
C	-2.550813	6.238860	-1.162028
C	-3.593109	7.668650	0.468931
C	-4.699606	6.824926	0.508046
C	-3.636246	5.378482	-1.109327
H	-1.737265	6.023938	-1.848082
H	-3.570714	8.543903	1.111895
H	-5.536806	7.044092	1.163492
H	-3.669841	4.501683	-1.748356
N	-5.785458	4.741676	-0.127005
H	-3.066204	1.240644	1.004902
C	-4.030195	1.608076	0.665521
C	-6.635830	2.515115	-0.084300
C	-5.086631	0.689720	0.383496
C	-4.249085	2.939372	0.516648
C	-5.545472	3.467611	0.084582
C	-6.400720	1.183482	0.029996
H	-3.464218	3.648059	0.748752
H	-7.606044	2.915294	-0.362185
C	-5.085411	-0.699951	0.382529
C	-5.539769	-3.478333	0.081081
C	-4.027261	-1.616832	0.662966
C	-6.398710	-1.195513	0.028609
C	-6.631662	-2.527408	-0.086894
C	-4.243972	-2.948337	0.512802
H	-3.063664	-1.248123	1.002085
H	-7.601303	-2.928909	-0.364870
H	-3.457769	-3.655944	0.743680
C	-7.322550	-0.006672	-0.180283
H	-8.150993	-0.007785	0.538726
H	-7.772166	-0.006477	-1.179818
N	-5.777947	-4.752645	-0.130849
C	-4.702749	-5.636156	-0.234143
C	-2.468942	-7.382938	-0.344368
C	-3.628690	-5.386971	-1.114639
C	-4.687931	-6.833491	0.505214
C	-3.580265	-7.675793	0.465677
C	-2.542016	-6.245792	-1.167653
H	-3.664106	-4.510614	-1.754186
H	-5.523898	-7.053246	1.162036
H	-3.556265	-8.549960	1.109979
H	-1.729163	-6.029956	-1.854283
C	-1.218655	-8.174796	-0.292509
C	1.218655	-9.559677	-0.102414
C	0.005711	-7.499178	-0.373255
C	-1.202016	-9.563401	-0.108575
C	0.009111	-10.266438	-0.013029
C	1.231726	-8.170435	-0.283211
H	0.004065	-6.417431	-0.443651
H	-2.139753	-10.104411	-0.029885
H	2.157346	-10.103730	-0.070211
C	2.480215	-7.376640	-0.339396
C	4.711607	-5.626726	-0.230090

C	2.550813	-6.238860	-1.162028
C	3.593109	-7.668650	0.468931
C	4.699606	-6.824926	0.508046
C	3.636246	-5.378482	-1.109327
H	1.737265	-6.023938	-1.848082
H	3.570714	-8.543903	1.111895
H	5.536806	-7.044092	1.163492
H	3.669841	-4.501683	-1.748356
C	0.010801	-11.738916	0.168918
C	0.014350	-14.534270	0.519872
C	0.972732	-12.361366	0.981318
C	-0.949091	-12.545124	-0.464468
C	-0.948107	-13.928261	-0.290263
C	0.975269	-13.744506	1.154653
H	1.708700	-11.753162	1.498750
H	-1.685819	-12.086009	-1.116894
H	-1.695094	-14.534018	-0.795486
H	1.723861	-14.204805	1.793345
H	0.015726	-15.611944	0.655135
N	5.785458	-4.741676	-0.127005
H	3.066204	-1.240644	1.004902
C	4.030195	-1.608076	0.665521
C	6.635830	-2.515115	-0.084300
C	5.086631	-0.689720	0.383496
C	4.249085	-2.939372	0.516648
C	5.545472	-3.467611	0.084582
C	6.400720	-1.183482	0.029996
H	3.464218	-3.648059	0.748752
H	7.606044	-2.915294	-0.362185
C	5.085411	0.699951	0.382529
C	5.539769	3.478333	0.081081
C	4.027261	1.616832	0.662966
C	6.398710	1.195513	0.028609
C	6.631662	2.527408	-0.086894
C	4.243972	2.948337	0.512802
H	3.063664	1.248123	1.002085
H	7.601303	2.928909	-0.364870
H	3.457769	3.655944	0.743680
C	7.322550	0.006672	-0.180283
H	8.150993	0.007785	0.538726
H	7.772166	0.006477	-1.179818
N	5.777947	4.752645	-0.130849

A.2.9 Optimised Structures of **OTPT-BZN-210** Oligomers

A.2.9.1 ***OTPT-BZN-210, LEB*** *State*

H	1.387367	5.842332	-13.315496
C	1.371693	5.817155	-12.229805
C	1.331121	5.749350	-9.438519
C	1.003038	4.647369	-11.570224
C	1.720429	6.955095	-11.497701
C	1.699015	6.917637	-10.100912
C	0.979435	4.603212	-10.167887
H	0.730766	3.758435	-12.127063
H	2.007725	7.867021	-12.013299
H	1.969475	7.800135	-9.528481
H	1.310880	5.707873	-8.355753
C	0.587819	3.359683	-9.464857
N	-0.116380	1.104218	-8.196042
N	0.254930	2.295620	-10.213716
N	0.588893	3.370517	-8.125494
C	0.230355	2.219461	-7.525918

C	-0.091025	1.191018	-9.532413
C	-0.468661	-0.010371	-10.312222
C	-1.182896	-2.282418	-11.787596
C	-0.468946	0.026391	-11.714992
C	-0.830080	-1.197033	-9.656150
C	-1.184663	-2.325550	-10.390815
C	-0.824346	-1.103780	-12.446957
H	-0.189233	0.946278	-12.215024
H	-0.827625	-1.218168	-8.572640
H	-1.462815	-3.239869	-9.874779
H	-0.822017	-1.066298	-13.532403
H	-1.459791	-3.163378	-12.359629
C	0.216329	2.179040	-6.060253
C	0.201632	2.092963	-3.231004
C	-0.164407	1.014327	-5.372031
C	0.575984	3.308770	-5.302266
C	0.571270	3.269324	-3.920000
C	-0.177864	0.963892	-3.987204
H	-0.464553	0.144149	-5.944563
H	0.866092	4.216326	-5.818981
H	0.861134	4.148158	-3.349794
H	-0.506184	0.061370	-3.486902
N	0.194303	2.115491	-1.849250
H	0.210478	3.034367	-1.427791
C	0.086913	1.038696	-0.953387
C	-0.086913	-1.038696	0.953387
C	0.679830	-0.209137	-1.200103
C	-0.588372	1.230087	0.261057
C	-0.679830	0.209137	1.200103
C	0.588372	-1.230087	-0.261057
H	1.242838	-0.372440	-2.111637
H	-1.067595	2.184619	0.460523
H	-1.242838	0.372440	2.111637
H	1.067595	-2.184619	-0.460523
N	-0.194303	-2.115491	1.849250
H	-0.210478	-3.034367	1.427791
C	-0.201632	-2.092963	3.231004
C	-0.216329	-2.179040	6.060253
C	-0.571270	-3.269324	3.920000
C	0.177864	-0.963892	3.987204
C	0.164407	-1.014327	5.372031
C	-0.575984	-3.308770	5.302266
H	-0.861134	-4.148158	3.349794
H	0.506184	-0.061370	3.486902
H	0.464553	-0.144149	5.944563
H	-0.866092	-4.216326	5.818981
C	-0.230355	-2.219461	7.525918
N	-0.254930	-2.295620	10.213716
N	-0.588893	-3.370517	8.125494
N	0.116380	-1.104218	8.196042
C	0.091025	-1.191018	9.532413
C	-0.587819	-3.359683	9.464857
C	0.468661	0.010371	10.312222
C	1.182896	2.282418	11.787596
C	0.468946	-0.026391	11.714992
C	0.830080	1.197033	9.656150
C	1.184663	2.325550	10.390815
C	0.824346	1.103780	12.446957
H	0.189233	-0.946278	12.215024
H	0.827625	1.218168	8.572640
H	1.462815	3.239869	9.874779
H	0.822017	1.066298	13.532403
H	1.459791	3.163378	12.359629
C	-0.979435	-4.603212	10.167887

C	-1.720429	-6.955095	11.497701	H	-1.310880	-5.707873	8.355753
C	-1.331121	-5.749350	9.438519	H	-0.730766	-3.758435	12.127063
C	-1.003038	-4.647369	11.570224	H	-1.387367	-5.842332	13.315496
C	-1.371693	-5.817155	12.229805	H	-1.969475	-7.800135	9.528481
C	-1.699015	-6.917637	10.100912	H	-2.007725	-7.867021	12.013299

*A.2.9.2 **OTPT-BZN-210**, **^{1}ES** State*

H	1.554603	5.826215	-13.189336	H	-1.511212	-3.257621	-9.974238
C	1.495896	5.790021	-12.105826	H	-0.670799	-1.053279	-13.572660
C	1.344503	5.698676	-9.317076	H	-1.381627	-3.155056	-12.453464
C	1.093338	4.617248	-11.473740	C	0.039122	2.107818	-6.028434
C	1.822994	6.917999	-11.348234	C	-0.109206	1.998635	-3.249943
C	1.746267	6.869391	-9.953630	C	-0.471272	0.962537	-5.391952
C	1.014544	4.562153	-10.072848	C	0.445826	3.211362	-5.257348
H	0.836434	3.736618	-12.050520	C	0.361831	3.168667	-3.878393
H	2.136501	7.832407	-11.843229	C	-0.554751	0.900383	-4.012582
H	1.999284	7.745228	-9.363883	H	-0.825044	0.139223	-5.999614
H	1.280355	5.650813	-8.236353	H	0.824579	4.092346	-5.759639
C	0.584923	3.320607	-9.402514	H	0.688355	4.012995	-3.279509
N	-0.219278	1.060554	-8.182949	H	-1.023382	0.048593	-3.535162
N	0.268197	2.263505	-10.165328	N	-0.167817	2.007841	-1.853220
N	0.530522	3.311233	-8.056551	H	-0.301112	2.933749	-1.447513
C	0.121154	2.163106	-7.508484	C	-0.070897	1.009983	-0.973508
C	-0.124924	1.153151	-9.523669	C	0.070897	-1.009983	0.973508
C	-0.473033	-0.032557	-10.329119	C	0.381474	-0.307662	-1.334547
C	-1.127809	-2.282027	-11.859483	C	-0.433182	1.284232	0.394863
C	-0.401432	0.019611	-11.730440	C	-0.381474	0.307662	1.334547
C	-0.875908	-1.222398	-9.701933	C	0.433182	-1.284232	-0.394863
C	-1.200786	-2.340139	-10.465045	H	0.738806	-0.500297	-2.336817
C	-0.727877	-1.100377	-12.489491	H	-0.814703	2.266830	0.652773
H	-0.089569	0.941024	-12.207786	H	-0.738806	0.500297	2.336817
H	-0.928130	-1.256463	-8.620057	H	0.814703	-2.266830	-0.652773

N	0.167817	-2.007841	1.853220
H	0.301112	-2.933749	1.447513
C	0.109206	-1.998635	3.249943
C	-0.039122	-2.107818	6.028434
C	-0.361831	-3.168667	3.878393
C	0.554751	-0.900383	4.012582
C	0.471272	-0.962537	5.391952
C	-0.445826	-3.211362	5.257348
H	-0.688355	-4.012995	3.279509
H	1.023382	-0.048593	3.535162
H	0.825044	-0.139223	5.999614
H	-0.824579	-4.092346	5.759639
C	-0.121154	-2.163106	7.508484
N	-0.268197	-2.263505	10.165328
N	-0.530522	-3.311233	8.056551
N	0.219278	-1.060554	8.182949
C	0.124924	-1.153151	9.523669
C	-0.584923	-3.320607	9.402514
C	0.473033	0.032557	10.329119
C	1.127809	2.282027	11.859483
C	0.401432	-0.019611	11.730440
C	0.875908	1.222398	9.701933
C	1.200786	2.340139	10.465045
C	0.727877	1.100377	12.489491
H	0.089569	-0.941024	12.207786
H	0.928130	1.256463	8.620057
H	1.511212	3.257621	9.974238
H	0.670799	1.053279	13.572660
H	1.381627	3.155056	12.453464
C	-1.014544	-4.562153	10.072848
C	-1.822994	-6.917999	11.348234
C	-1.344503	-5.698676	9.317076
C	-1.093338	-4.617248	11.473740
C	-1.495896	-5.790021	12.105826
C	-1.746267	-6.869391	9.953630
H	-1.280355	-5.650813	8.236353
H	-0.836434	-3.736618	12.050520
H	-1.554603	-5.826215	13.189336
H	-1.999284	-7.745228	9.363883
H	-2.136501	-7.832407	11.843229

A.2.9.3 ***OTPT-BZN-210****, ³****ES*** *State*

H	1.299470	5.834787	-13.255034
C	1.305693	5.808193	-12.169720
C	1.320893	5.742252	-9.375899
C	0.951931	4.638015	-11.504707
C	1.667866	6.945622	-11.442811
C	1.674430	6.909849	-10.045680
C	0.957254	4.595857	-10.100930
H	0.668570	3.750426	-12.058029
H	1.944013	7.857621	-11.963754
H	1.955194	7.792970	-9.479945
H	1.321835	5.704939	-8.292874
C	0.581751	3.357363	-9.395997
N	-0.130754	1.096185	-8.115207
N	0.250825	2.283212	-10.129462
N	0.589486	3.363014	-8.048478
C	0.223836	2.213462	-7.471356
C	-0.094798	1.172656	-9.460153
C	-0.452560	-0.027994	-10.236534
C	-1.123774	-2.307065	-11.713915
C	-0.419073	0.003577	-11.640026

C	-0.825258	-1.212098	-9.580227
C	-1.158971	-2.344488	-10.317253
C	-0.753336	-1.131459	-12.372663
H	-0.129336	0.920391	-12.139489
H	-0.848357	-1.230894	-8.497031
H	-1.446654	-3.257229	-9.804394
H	-0.725219	-1.100925	-13.457515
H	-1.384052	-3.191741	-12.287448
C	0.215850	2.172384	-5.994599
C	0.230314	2.074787	-3.196195
C	-0.244745	1.016982	-5.317422
C	0.652195	3.293874	-5.249227
C	0.653853	3.256763	-3.877571
C	-0.249290	0.959186	-3.945009
H	-0.615683	0.186365	-5.904194
H	0.988184	4.174719	-5.781040
H	1.000512	4.108171	-3.300741
H	-0.658742	0.096471	-3.436505
N	0.271019	2.084370	-1.840606
H	0.425444	2.994259	-1.411880
C	0.131782	1.017688	-0.937831
C	-0.131782	-1.017688	0.937831
C	0.605125	-0.271307	-1.238604
C	-0.459382	1.286573	0.308020
C	-0.605125	0.271307	1.238604
C	0.459382	-1.286573	-0.308020
H	1.126656	-0.466698	-2.166922
H	-0.841714	2.277398	0.529017
H	-1.126656	0.466698	2.166922
H	0.841714	-2.277398	-0.529017
N	-0.271019	-2.084370	1.840606
H	-0.425444	-2.994259	1.411880
C	-0.230314	-2.074787	3.196195
C	-0.215850	-2.172384	5.994599
C	-0.653853	-3.256763	3.877571
C	0.249290	-0.959186	3.945009
C	0.244745	-1.016982	5.317422
C	-0.652195	-3.293874	5.249227
H	-1.000512	-4.108171	3.300741
H	0.658742	-0.096471	3.436505
H	0.615683	-0.186365	5.904194
H	-0.988184	-4.174719	5.781040
C	-0.223836	-2.213462	7.471356
N	-0.250825	-2.283212	10.129462
N	-0.589486	-3.363014	8.048478
N	0.130754	-1.096185	8.115207
C	0.094798	-1.172656	9.460153
C	-0.581751	-3.357363	9.395997
C	0.452560	0.027994	10.236534
C	1.123774	2.307065	11.713915
C	0.419073	-0.003577	11.640026
C	0.825258	1.212098	9.580227
C	1.158971	2.344488	10.317253
C	0.753336	1.131459	12.372663
H	0.129336	-0.920391	12.139489
H	0.848357	1.230894	8.497031
H	1.446654	3.257229	9.804394
H	0.725219	1.100925	13.457515
H	1.384052	3.191741	12.287448
C	-0.957254	-4.595857	10.100930
C	-1.667866	-6.945622	11.442811
C	-1.320893	-5.742252	9.375899
C	-0.951931	-4.638015	11.504707
C	-1.305693	-5.808193	12.169720

C	-1.674430	-6.909849	10.045680	H	-1.299470	-5.834787	13.255034
H	-1.321835	-5.704939	8.292874	H	-1.955194	-7.792970	9.479945
H	-0.668570	-3.750426	12.058029	H	-1.944013	-7.857621	11.963754

A.2.9.4 ***OTPT-BZN-210, EB*** *State*

H	1.914749	5.730141	-12.935278	H	-1.426102	-3.149294	-12.476977
C	1.770265	5.690814	-11.859631	C	-0.264973	2.031051	-5.931700
C	1.398623	5.587763	-9.093497	C	-0.605062	1.910435	-3.136305
C	1.274761	4.530728	-11.270210	C	-0.755440	0.865258	-5.322716
C	2.080719	6.801195	-11.070048	C	0.033795	3.143743	-5.125831
C	1.893582	6.746331	-9.686278	C	-0.154204	3.093752	-3.753765
C	1.084585	4.469360	-9.881077	C	-0.919740	0.799384	-3.946368
H	1.030444	3.663288	-11.872086	H	-1.003699	0.012830	-5.944221
H	2.466938	7.705647	-11.531234	H	0.402394	4.047710	-5.596301
H	2.133806	7.607568	-9.069824	H	0.060529	3.956255	-3.131313
H	1.249455	5.532984	-8.021472	H	-1.321951	-0.097411	-3.486412
C	0.558032	3.237568	-9.252678	N	-0.825578	1.926824	-1.761540
N	-0.397500	1.004052	-8.114206	C	-0.404447	0.984921	-0.968959
N	0.266162	2.199296	-10.051769	C	0.404447	-0.984921	0.968959
N	0.402801	3.229166	-7.920036	C	0.499309	-0.109036	-1.329884
C	-0.078194	2.091325	-7.393519	C	-0.860772	1.036016	0.419145
C	-0.208593	1.103581	-9.438627	C	-0.499309	0.109036	1.329884
C	-0.544868	-0.068771	-10.276569	C	0.860772	-1.036016	-0.419145
C	-1.179905	-2.288384	-11.862071	H	0.892880	-0.144234	-2.338847
C	-0.358185	-0.023141	-11.666769	H	-1.543599	1.841522	0.669897
C	-1.053339	-1.237339	-9.688651	H	-0.892880	0.144234	2.338847
C	-1.368625	-2.339859	-10.478386	H	1.543599	-1.841522	-0.669897
C	-0.674213	-1.127679	-12.453482	N	0.825578	-1.926824	1.761540
H	0.034419	0.882544	-12.113994	C	0.605062	-1.910435	3.136305
H	-1.195648	-1.265195	-8.614659	C	0.264973	-2.031051	5.931700
H	-1.761850	-3.240257	-10.015659	C	0.154204	-3.093752	3.753765
H	-0.526464	-1.084347	-13.528530	C	0.919740	-0.799384	3.946368

C	0.755440	-0.865258	5.322716
C	-0.033795	-3.143743	5.125831
H	-0.060529	-3.956255	3.131313
H	1.321951	0.097411	3.486412
H	1.003699	-0.012830	5.944221
H	-0.402394	-4.047710	5.596301
C	0.078194	-2.091325	7.393519
N	-0.266162	-2.199296	10.051769
N	-0.402801	-3.229166	7.920036
N	0.397500	-1.004052	8.114206
C	0.208593	-1.103581	9.438627
C	-0.558032	-3.237568	9.252678
C	0.544868	0.068771	10.276569
C	1.179905	2.288384	11.862071
C	0.358185	0.023141	11.666769
C	1.053339	1.237339	9.688651
C	1.368625	2.339859	10.478386
C	0.674213	1.127679	12.453482
H	-0.034419	-0.882544	12.113994
H	1.195648	1.265195	8.614659
H	1.761850	3.240257	10.015659
H	0.526464	1.084347	13.528530
H	1.426102	3.149294	12.476977
C	-1.084585	-4.469360	9.881077
C	-2.080719	-6.801195	11.070048
C	-1.398623	-5.587763	9.093497
C	-1.274761	-4.530728	11.270210
C	-1.770265	-5.690814	11.859631
C	-1.893582	-6.746331	9.686278
H	-1.249455	-5.532984	8.021472
H	-1.030444	-3.663288	11.872086
H	-1.914749	-5.730141	12.935278
H	-2.133806	-7.607568	9.069824
H	-2.466938	-7.705647	11.531234

A.2.10 Optimised Structures of **OTPT-BZN-221** Oligomers

*A.2.10.1 **OTPT-BZN-221**, **LEB** State*

H	0.043668	11.902743	-2.151277
C	0.038597	11.362252	-1.209137
C	0.025414	9.969632	1.210567
C	0.025414	9.969632	-1.210567
C	0.045349	12.062601	-0.000000
C	0.038597	11.362252	1.209137
C	0.018923	9.260184	-0.000000
H	0.019990	9.414931	-2.141501
H	0.055736	13.148867	-0.000000
H	0.043668	11.902743	2.151277
H	0.019990	9.414931	2.141501
C	0.005660	7.777601	-0.000000
N	-0.010806	5.103921	-0.000000
N	-0.000342	7.155460	-1.189778
N	-0.000342	7.155460	1.189778
C	-0.009306	5.809704	1.141332
C	-0.009306	5.809704	-1.141332
C	-0.017923	5.051123	-2.399612
C	-0.018616	3.533156	-4.791108
C	-0.000450	5.684172	-3.654967
C	-0.050754	3.646800	-2.369777
C	-0.055298	2.897931	-3.533036
C	0.001182	4.943972	-4.827896
H	0.018459	6.767616	-3.697776

H	-0.085509	3.147630	-1.408672
H	-0.103684	1.818148	-3.472309
H	0.025393	5.450086	-5.789483
C	-0.017923	5.051123	2.399612
C	-0.018616	3.533156	4.791108
C	-0.050754	3.646800	2.369777
C	-0.000450	5.684172	3.654967
C	0.001182	4.943972	4.827896
C	-0.055298	2.897931	3.533036
H	-0.085509	3.147630	1.408672
H	0.018459	6.767616	3.697776
H	0.025393	5.450086	5.789483
H	-0.103684	1.818148	3.472309
N	-0.014125	2.816205	5.982059
H	-0.380877	3.302172	6.789886
C	0.025163	1.407829	6.061830
C	0.025163	-1.407829	6.061830
C	1.039824	0.693793	5.406032
C	-0.935564	0.697369	6.791059
C	-0.935564	-0.697369	6.791059
C	1.039824	-0.693793	5.406032
H	1.826766	1.235555	4.892339
H	-1.716397	1.237072	7.319524
H	-1.716397	-1.237072	7.319524
H	1.826766	-1.235555	4.892339
N	-0.014125	-2.816205	5.982059
H	-0.380877	-3.302172	6.789886
C	-0.018616	-3.533156	4.791108
C	-0.017923	-5.051123	2.399612
C	0.001182	-4.943972	4.827896
C	-0.055298	-2.897931	3.533036
C	-0.050754	-3.646800	2.369777
C	-0.000450	-5.684172	3.654967
H	0.025393	-5.450086	5.789483
H	-0.103684	-1.818148	3.472309
H	-0.085509	-3.147630	1.408672
H	0.018459	-6.767616	3.697776
C	-0.009306	-5.809704	1.141332
N	-0.000342	-7.155460	-1.189778
N	-0.000342	-7.155460	1.189778
N	-0.010806	-5.103921	0.000000
C	-0.009306	-5.809704	-1.141332
C	0.005660	-7.777601	0.000000
C	-0.017923	-5.051123	-2.399612
C	-0.018616	-3.533156	-4.791108
C	-0.000450	-5.684172	-3.654967
C	-0.050754	-3.646800	-2.369777
C	-0.055298	-2.897931	-3.533036
C	0.001182	-4.943972	-4.827896
H	0.018459	-6.767616	-3.697776
H	-0.085509	-3.147630	-1.408672
H	-0.103684	-1.818148	-3.472309
H	0.025393	-5.450086	-5.789483
C	0.018923	-9.260184	0.000000
C	0.045349	-12.062601	0.000000
C	0.025414	-9.969632	1.210567
C	0.025414	-9.969632	-1.210567
C	0.038597	-11.362252	-1.209137
C	0.038597	-11.362252	1.209137
H	0.019990	-9.414931	2.141501
H	0.019990	-9.414931	-2.141501
H	0.043668	-11.902743	-2.151277
H	0.043668	-11.902743	2.151277
H	0.055736	-13.148867	0.000000

N	-0.014125	-2.816205	-5.982059
H	-0.380877	-3.302172	-6.789886
C	0.025163	-1.407829	-6.061830
C	0.025163	1.407829	-6.061830
C	1.039824	-0.693793	-5.406032
C	-0.935564	-0.697369	-6.791059
C	-0.935564	0.697369	-6.791059
C	1.039824	0.693793	-5.406032
H	1.826766	-1.235555	-4.892339
H	-1.716397	-1.237072	-7.319524
H	-1.716397	1.237072	-7.319524
H	1.826766	1.235555	-4.892339
N	-0.014125	2.816205	-5.982059
H	-0.380877	3.302172	-6.789886

A.2.10.2 ***OTPT-BZN-221****, ¹****ES*** State*

H	1.903416	11.508468	-2.151705
C	1.722071	10.997543	-1.211322
C	1.255783	9.686985	1.214559
C	1.255783	9.686985	-1.214559
C	1.956145	11.654890	0.000000
C	1.722071	10.997543	1.211322
C	1.018859	9.021086	0.000000
H	1.070603	9.167268	-2.147244
H	2.320127	12.677883	0.000000
H	1.903416	11.508468	2.151705
H	1.070603	9.167268	2.147244
C	0.526183	7.637016	0.000000
N	-0.422471	5.120110	0.000000
N	0.316839	7.031613	-1.187722
N	0.316839	7.031613	1.187722
C	-0.151044	5.783886	1.131346
C	-0.151044	5.783886	-1.131346
C	-0.352823	5.036503	-2.395423
C	-0.573844	3.513940	-4.711806
C	0.043485	5.574889	-3.632810
C	-0.925580	3.755120	-2.342345
C	-1.048312	2.996662	-3.490176
C	-0.072689	4.825501	-4.793944
H	0.462925	6.573180	-3.664562
H	-1.273932	3.372664	-1.390817
H	-1.546659	2.035031	-3.461016
H	0.263715	5.226836	-5.744299
C	-0.352823	5.036503	2.395423
C	-0.573844	3.513940	4.711806
C	-0.925580	3.755120	2.342345
C	0.043485	5.574889	3.632810
C	-0.072689	4.825501	4.793944
C	-1.048312	2.996662	3.490176
H	-1.273932	3.372664	1.390817
H	0.462925	6.573180	3.664562
H	0.263715	5.226836	5.744299
H	-1.546659	2.035031	3.461016
N	-0.623291	2.718205	5.867348
H	-0.830373	3.200483	6.742395
C	-0.455668	1.398978	5.924160
C	-0.455668	-1.398978	5.924161
C	0.153181	0.676262	4.832905
C	-0.851356	0.678404	7.111653
C	-0.851356	-0.678404	7.111653
C	0.153181	-0.676262	4.832905
H	0.669108	1.226907	4.056007

H	-1.217868	1.230468	7.970475
H	-1.217868	-1.230468	7.970475
H	0.669107	-1.226908	4.056007
N	-0.623291	-2.718206	5.867348
H	-0.830374	-3.200483	6.742396
C	-0.573843	-3.513940	4.711806
C	-0.352820	-5.036502	2.395423
C	-0.072689	-4.825502	4.793944
C	-1.048309	-2.996661	3.490176
C	-0.925576	-3.755118	2.342345
C	0.043485	-5.574889	3.632811
H	0.263713	-5.226838	5.744299
H	-1.546654	-2.035029	3.461016
H	-1.273927	-3.372661	1.390817
H	0.462924	-6.573180	3.664563
C	-0.151041	-5.783885	1.131346
N	0.316840	-7.031613	-1.187722
N	0.316840	-7.031613	1.187722
N	-0.422467	-5.120108	-0.000000
C	-0.151041	-5.783885	-1.131346
C	0.526184	-7.637016	-0.000000
C	-0.352820	-5.036502	-2.395423
C	-0.573843	-3.513940	-4.711806
C	0.043485	-5.574889	-3.632811
C	-0.925576	-3.755118	-2.342345
C	-1.048309	-2.996661	-3.490176
C	-0.072689	-4.825502	-4.793944
H	0.462924	-6.573180	-3.664563
H	-1.273927	-3.372661	-1.390817
H	-1.546654	-2.035029	-3.461016
H	0.263713	-5.226838	-5.744299
C	1.018858	-9.021087	-0.000000
C	1.956141	-11.654892	-0.000000
C	1.255781	-9.686986	1.214559
C	1.255781	-9.686986	-1.214559
C	1.722068	-10.997544	-1.211322
C	1.722068	-10.997544	1.211322
H	1.070602	-9.167268	2.147244
H	1.070602	-9.167268	-2.147244
H	1.903412	-11.508469	-2.151705
H	1.903412	-11.508469	2.151705
H	2.320123	-12.677884	-0.000000
N	-0.623291	-2.718206	-5.867348
H	-0.830374	-3.200483	-6.742396
C	-0.455668	-1.398978	-5.924161
C	-0.455668	1.398978	-5.924160
C	0.153181	-0.676262	-4.832905
C	-0.851356	-0.678404	-7.111653
C	-0.851356	0.678404	-7.111653
C	0.153181	0.676262	-4.832905
H	0.669107	-1.226908	-4.056007
H	-1.217868	-1.230468	-7.970475
H	-1.217868	1.230468	-7.970475
H	0.669108	1.226907	-4.056007
N	-0.623291	2.718205	-5.867348
H	-0.830373	3.200483	-6.742395

A.2.10.3 ***OTPT-BZN-221****,* ^{5}***ES*** *State*

H	0.821963	11.822869	-2.151678
C	0.744139	11.285883	-1.211701
C	0.542974	9.909724	1.215361
C	0.542974	9.909724	-1.215361

C	0.844504	11.975890	0.000000
C	0.744139	11.285883	1.211701
C	0.440841	9.210721	0.000000
H	0.463258	9.365079	-2.148760
H	1.001205	13.050230	0.000000
H	0.821963	11.822869	2.151678
H	0.463258	9.365079	2.148760
C	0.224789	7.760153	0.000000
N	-0.211927	5.099545	0.000000
N	0.131823	7.123343	-1.187685
N	0.131823	7.123343	1.187685
C	-0.083566	5.807057	1.131166
C	-0.083566	5.807057	-1.131166
C	-0.169944	5.044436	-2.391685
C	-0.242846	3.522558	-4.741854
C	0.015130	5.671995	-3.646509
C	-0.443593	3.656656	-2.333550
C	-0.487511	2.903257	-3.477324
C	-0.031573	4.934597	-4.807102
H	0.205325	6.737822	-3.677672
H	-0.634367	3.204696	-1.368459
H	-0.749809	1.854991	-3.431042
H	0.131528	5.408724	-5.769034
C	-0.169944	5.044436	2.391685
C	-0.242846	3.522558	4.741854
C	-0.443593	3.656656	2.333550
C	0.015130	5.671995	3.646509
C	-0.031573	4.934597	4.807102
C	-0.487511	2.903257	3.477324
H	-0.634367	3.204696	1.368459
H	0.205325	6.737822	3.677672
H	0.131528	5.408724	5.769034
H	-0.749809	1.854991	3.431042
N	-0.233835	2.792319	5.884347
H	-0.291926	3.297668	6.767324
C	-0.160185	1.385528	5.957827
C	-0.160185	-1.385528	5.957827
C	0.717888	0.691939	5.109177
C	-0.954796	0.694190	6.885866
C	-0.954796	-0.694190	6.885866
C	0.717888	-0.691939	5.109177
H	1.410383	1.234069	4.477499
H	-1.608235	1.237834	7.559112
H	-1.608235	-1.237834	7.559112
H	1.410383	-1.234068	4.477499
N	-0.233835	-2.792319	5.884347
H	-0.291926	-3.297668	6.767324
C	-0.242846	-3.522558	4.741854
C	-0.169945	-5.044436	2.391685
C	-0.031573	-4.934597	4.807102
C	-0.487511	-2.903257	3.477324
C	-0.443594	-3.656656	2.333549
C	0.015130	-5.671995	3.646509
H	0.131529	-5.408724	5.769034
H	-0.749810	-1.854992	3.431042
H	-0.634368	-3.204696	1.368459
H	0.205325	-6.737822	3.677672
C	-0.083567	-5.807057	1.131166
N	0.131823	-7.123343	-1.187685
N	0.131823	-7.123343	1.187685
N	-0.211928	-5.099545	-0.000000
C	-0.083567	-5.807057	-1.131166
C	0.224789	-7.760153	-0.000000
C	-0.169945	-5.044436	-2.391685

C	-0.242846	-3.522558	-4.741854
C	0.015130	-5.671995	-3.646509
C	-0.443594	-3.656656	-2.333549
C	-0.487511	-2.903257	-3.477324
C	-0.031573	-4.934597	-4.807102
H	0.205325	-6.737822	-3.677672
H	-0.634368	-3.204696	-1.368459
H	-0.749810	-1.854992	-3.431042
H	0.131529	-5.408724	-5.769034
C	0.440841	-9.210721	-0.000000
C	0.844506	-11.975890	-0.000000
C	0.542975	-9.909724	1.215361
C	0.542975	-9.909724	-1.215361
C	0.744141	-11.285883	-1.211701
C	0.744141	-11.285883	1.211701
H	0.463259	-9.365079	2.148760
H	0.463259	-9.365079	-2.148760
H	0.821965	-11.822869	-2.151678
H	0.821965	-11.822869	2.151678
H	1.001208	-13.050230	-0.000000
N	-0.233835	-2.792319	-5.884347
H	-0.291926	-3.297668	-6.767324
C	-0.160185	-1.385528	-5.957827
C	-0.160185	1.385528	-5.957827
C	0.717888	-0.691939	-5.109177
C	-0.954796	-0.694190	-6.885866
C	-0.954796	0.694190	-6.885866
C	0.717888	0.691939	-5.109177
H	1.410383	-1.234068	-4.477499
H	-1.608235	-1.237834	-7.559112
H	-1.608235	1.237834	-7.559112
H	1.410383	1.234069	-4.477499
N	-0.233835	2.792319	-5.884347
H	-0.291926	3.297668	-6.767324

A.2.10.4 ***OTPT-BZN-221, EB*** *State*

H	2.676860	11.080621	-2.151444
C	2.429176	10.599869	-1.209668
C	1.790376	9.362721	1.211554
C	1.790376	9.362721	-1.211554
C	2.750414	11.221439	-0.000000
C	2.429176	10.599869	1.209668
C	1.465744	8.732942	-0.000000
H	1.535454	8.871042	-2.143005
H	3.248793	12.186579	-0.000000
H	2.676860	11.080621	2.151444
H	1.535454	8.871042	2.143005
C	0.786817	7.418497	-0.000000
N	-0.504607	5.072379	-0.000000
N	0.502777	6.859003	-1.188397
N	0.502777	6.859003	1.188397
C	-0.140112	5.681536	1.138139
C	-0.140112	5.681536	-1.138139
C	-0.428367	4.972425	-2.399732
C	-0.812291	3.463944	-4.749356
C	0.106998	5.408122	-3.624234
C	-1.209713	3.806291	-2.378789
C	-1.406165	3.065826	-3.532586
C	-0.095310	4.675618	-4.786563
H	0.696469	6.317720	-3.646150
H	-1.645015	3.482425	-1.441114
H	-2.023988	2.174236	-3.511092

H	0.331546	5.001759	-5.729422
C	-0.428367	4.972425	2.399732
C	-0.812291	3.463944	4.749356
C	-1.209713	3.806291	2.378789
C	0.106998	5.408122	3.624234
C	-0.095310	4.675618	4.786563
C	-1.406165	3.065826	3.532586
H	-1.645015	3.482425	1.441114
H	0.696469	6.317720	3.646150
H	0.331546	5.001759	5.729422
H	-2.023988	2.174236	3.511092
N	-0.981391	2.727794	5.921852
C	-0.805111	1.436591	5.916524
C	-0.805112	-1.436606	5.916539
C	-0.175298	0.673794	4.835503
C	-1.224648	0.675204	7.091871
C	-1.224648	-0.675207	7.091879
C	-0.175304	-0.673822	4.835506
H	0.327845	1.221732	4.047329
H	-1.594406	1.245914	7.937501
H	-1.594406	-1.245909	7.937515
H	0.327829	-1.221771	4.047334
N	-0.981396	-2.727804	5.921867
C	-0.812248	-3.463936	4.749369
C	-0.428258	-4.972378	2.399732
C	-0.095316	-4.675639	4.786588
C	-1.406027	-3.065756	3.532574
C	-1.209548	-3.806206	2.378773
C	0.107025	-5.408124	3.624252
H	0.331470	-5.001822	5.729464
H	-2.023804	-2.174134	3.511066
H	-1.644785	-3.482300	1.441081
H	0.696452	-6.317750	3.646181
C	-0.139984	-5.681480	1.138139
N	0.502837	-6.858984	-1.188398
N	0.502837	-6.858984	1.188398
N	-0.504452	-5.072307	0.000000
C	-0.139984	-5.681480	-1.138139
C	0.786852	-7.418491	0.000000
C	-0.428258	-4.972378	-2.399732
C	-0.812248	-3.463936	-4.749369
C	0.107025	-5.408124	-3.624252
C	-1.209548	-3.806206	-2.378773
C	-1.406027	-3.065756	-3.532574
C	-0.095316	-4.675639	-4.786588
H	0.696452	-6.317750	-3.646181
H	-1.644785	-3.482300	-1.441081
H	-2.023804	-2.174134	-3.511066
H	0.331470	-5.001822	-5.729464
C	1.465696	-8.732978	0.000000
C	2.750209	-11.221556	0.000000
C	1.790288	-9.362778	1.211553
C	1.790288	-9.362778	-1.211553
C	2.429010	-10.599966	-1.209668
C	2.429010	-10.599966	1.209668
H	1.535398	-8.871083	2.143005
H	1.535398	-8.871083	-2.143005
H	2.676664	-11.080734	-2.151444
H	2.676664	-11.080734	2.151444
H	3.248527	-12.186728	0.000000
N	-0.981396	-2.727804	-5.921867
C	-0.805112	-1.436606	-5.916539
C	-0.805111	1.436591	-5.916524
C	-0.175304	-0.673822	-4.835506

C	-1.224648	-0.675207	-7.091879	H	-1.594406	-1.245909	-7.937515
C	-1.224648	0.675204	-7.091871	H	-1.594406	1.245914	-7.937501
C	-0.175298	0.673794	-4.835503	H	0.327845	1.221732	-4.047329
H	0.327829	-1.221771	-4.047334	N	-0.981391	2.727794	-5.921852

A.2.11 Optimised Structures of **OTPT-FLR-210** Oligomers

*A.2.11.1 **OTPT-FLR-210**, **LEB** State*

H	15.978738	2.955148	-0.562408	H	10.620071	-5.631132	-0.331092
C	14.912952	3.154152	-0.498329	H	14.664135	-4.186494	-0.599616
C	12.172304	3.662990	-0.332819	H	13.058424	-6.082017	-0.508592
C	14.012560	2.092766	-0.452621	C	8.093290	0.711802	-0.087128
C	14.447305	4.471113	-0.461841	C	5.315511	1.214110	0.119573
C	13.075074	4.722159	-0.379106	C	7.164673	-0.342949	-0.071148
C	12.633476	2.338154	-0.369355	C	7.602099	2.028270	-0.013350
H	14.361479	1.067125	-0.480061	C	6.245459	2.276630	0.089648
H	15.150628	5.298183	-0.497737	C	5.802632	-0.106524	0.025687
H	12.709434	5.744478	-0.350699	H	7.529278	-1.360707	-0.150208
H	11.105757	3.844492	-0.268719	H	8.305586	2.852668	-0.029992
C	11.674357	1.210579	-0.320407	H	5.883688	3.299337	0.156931
N	9.941478	-0.834027	-0.229019	H	5.110791	-0.939101	0.002620
N	12.171200	-0.036250	-0.369395	N	3.969609	1.521719	0.200057
N	10.369843	1.501437	-0.230773	H	3.726518	2.473277	-0.041187
C	9.532490	0.448010	-0.186609	H	1.980694	-2.038363	2.336471
C	11.263872	-1.025450	-0.321532	C	1.881833	-1.211588	1.638640
C	11.759306	-2.420286	-0.373295	C	1.648055	0.957872	-0.141325
C	12.695416	-5.058890	-0.470817	C	0.658958	-0.933701	1.025831
C	13.134364	-2.681300	-0.473521	C	2.984944	-0.403225	1.370099
C	10.857915	-3.494621	-0.322513	C	2.884363	0.672793	0.468990
C	11.324729	-4.805606	-0.371038	C	0.550133	0.164148	0.144255
C	13.598139	-3.993534	-0.521959	H	3.923684	-0.589278	1.878532
H	13.824612	-1.846776	-0.512554	H	1.572418	1.791668	-0.835075
H	9.797419	-3.285039	-0.245106	C	-0.644425	-1.594002	1.114845

C	-3.307185	-2.438005	0.908225
C	-1.065329	-2.721956	1.822312
C	-1.559701	-0.900898	0.293566
C	-2.875681	-1.317333	0.173151
C	-2.392553	-3.131349	1.722478
H	-0.375848	-3.275453	2.453544
H	-3.560118	-0.806202	-0.494716
H	-2.737407	-3.995782	2.283487
C	-0.867144	0.265577	-0.382969
H	-1.333314	1.224745	-0.122279
H	-0.906216	0.189249	-1.477394
N	-4.617189	-2.932141	0.809524
H	-4.718248	-3.928834	0.947341
C	-5.795618	-2.236744	0.609952
C	-8.274940	-0.928576	0.219508
C	-6.952522	-2.964387	0.254370
C	-5.908269	-0.841384	0.785230
C	-7.125431	-0.208854	0.588024
C	-8.163091	-2.322698	0.065799
H	-6.880962	-4.040615	0.120648
H	-5.048585	-0.263619	1.100805
H	-7.203895	0.862735	0.731636
H	-9.042465	-2.892135	-0.212057
C	-9.556655	-0.247489	0.009103
N	-11.906500	1.000899	-0.377741
N	-10.624646	-0.994704	-0.328176
N	-9.598595	1.089244	0.163962
C	-10.790500	1.666257	-0.037491
C	-11.772315	-0.328733	-0.511604
C	-10.884816	3.135504	0.124829
C	-11.062363	5.914456	0.432764
C	-12.106737	3.794702	-0.078771
C	-9.752729	3.882832	0.484267
C	-9.842549	5.263958	0.637093
C	-12.193332	5.176145	0.074566
H	-12.977098	3.211622	-0.356064
H	-8.812452	3.366930	0.639938
H	-8.961357	5.834445	0.915796
H	-13.143108	5.678169	-0.085135
H	-11.131228	6.991934	0.552238
C	-12.973786	-1.109468	-0.886689
C	-15.245988	-2.586334	-1.596938
C	-12.896584	-2.503048	-1.032300
C	-14.200958	-0.463394	-1.100406
C	-15.329517	-1.198897	-1.453586
C	-14.026861	-3.235784	-1.385236
H	-11.945488	-2.995049	-0.865393
H	-14.253323	0.613009	-0.986313
H	-16.275259	-0.690610	-1.617366
H	-13.958157	-4.314083	-1.495554
H	-16.126997	-3.159005	-1.872362

A.2.11.2 ***OTPT-FLR-210****,* ***¹ES*** *State*

H	15.783249	3.126487	0.303497
C	14.710816	3.285263	0.243169
C	11.951438	3.694617	0.088105
C	13.858108	2.196337	0.085977
C	14.188509	4.579099	0.322957
C	12.807782	4.780729	0.245055
C	12.470180	2.392536	0.007309
H	14.251269	1.188443	0.022897

H	14.855283	5.427611	0.445516
H	12.400043	5.785274	0.306563
H	10.879087	3.838920	0.026432
C	11.564285	1.238732	-0.158300
N	9.914485	-0.862753	-0.455286
N	12.105579	0.013696	-0.235195
N	10.241379	1.476883	-0.222615
C	9.467872	0.395450	-0.369614
C	11.250318	-1.008944	-0.384086
C	11.805443	-2.374033	-0.474528
C	12.860530	-4.960830	-0.644708
C	13.192358	-2.579014	-0.401579
C	10.952178	-3.477386	-0.634038
C	11.479000	-4.763087	-0.718363
C	13.714976	-3.866355	-0.486287
H	13.844502	-1.722317	-0.278897
H	9.882551	-3.312050	-0.690379
H	10.813680	-5.612371	-0.841964
H	14.788659	-4.017625	-0.429074
H	13.270001	-5.964602	-0.710668
C	8.002013	0.607810	-0.438941
C	5.243668	1.004246	-0.547623
C	7.135528	-0.484867	-0.597864
C	7.471148	1.905922	-0.364323
C	6.102350	2.109078	-0.428387
C	5.763187	-0.296210	-0.659177
H	7.555607	-1.478567	-0.692594
H	8.146641	2.745015	-0.253112
H	5.690429	3.110876	-0.359121
H	5.106110	-1.137825	-0.844760
N	3.859693	1.256542	-0.615245
H	3.608858	2.121661	-1.089312
H	2.109833	-2.099553	1.914842
C	1.961519	-1.287238	1.212278
C	1.508009	0.921462	-0.548714
C	0.647340	-0.930600	0.782611
C	3.027877	-0.568782	0.761670
C	2.832204	0.535658	-0.146948
C	0.451079	0.192788	-0.106038
H	4.024520	-0.788269	1.119641
H	1.379297	1.765070	-1.219202
C	-0.593870	-1.483967	1.108641
C	-3.273994	-2.195723	1.420448
C	-0.921721	-2.604304	1.930755
C	-1.637677	-0.747284	0.430964
C	-2.947004	-1.086198	0.572276
C	-2.229067	-2.956262	2.067506
H	-0.144639	-3.164874	2.437496
H	-3.726419	-0.564997	0.032881
H	-2.512476	-3.798658	2.690019
C	-1.021422	0.355850	-0.394969
H	-1.391684	1.343829	-0.098073
H	-1.242798	0.238946	-1.462131
N	-4.535750	-2.592570	1.630766
H	-4.644821	-3.489524	2.099002
C	-5.745987	-1.963446	1.279703
C	-8.194900	-0.816552	0.597200
C	-6.826957	-2.786961	0.926281
C	-5.898934	-0.568258	1.336646
C	-7.118799	-0.006336	0.991986
C	-8.037991	-2.211917	0.576912
H	-6.702092	-3.864869	0.901805
H	-5.092818	0.060232	1.696503
H	-7.259957	1.066191	1.042180

H	-8.875867	-2.831510	0.282592
C	-9.492846	-0.205432	0.222034
N	-11.827975	0.892542	-0.458110
N	-10.476603	-1.030165	-0.154091
N	-9.589003	1.127727	0.283067
C	-10.784144	1.638247	-0.066356
C	-11.635605	-0.434700	-0.490113
C	-10.955995	3.103821	-0.015058
C	-11.286159	5.881544	0.083547
C	-12.180939	3.684505	-0.380132
C	-9.898144	3.928138	0.399976
C	-10.064453	5.309321	0.448412
C	-12.342865	5.066128	-0.330597
H	-12.993021	3.041742	-0.699089
H	-8.955581	3.473475	0.681672
H	-9.242531	5.941212	0.771447
H	-13.293003	5.508465	-0.614354
H	-11.414509	6.959308	0.122444
C	-12.758433	-1.291795	-0.919061
C	-14.888082	-2.914264	-1.735064
C	-12.604558	-2.686131	-0.976352
C	-13.989599	-0.718096	-1.274360
C	-15.047393	-1.526928	-1.679775
C	-13.664944	-3.491202	-1.382657
H	-11.651746	-3.122943	-0.700899
H	-14.101017	0.358826	-1.227291
H	-15.996956	-1.076760	-1.952982
H	-13.539213	-4.568931	-1.425194
H	-15.714509	-3.543752	-2.051793

*A.2.11.3 **OTPT-FLR-210**, ^{3}**ES** State*

H	15.865249	3.124870	-0.191983
C	14.792684	3.293008	-0.179280
C	12.032708	3.727165	-0.147555
C	13.922246	2.207299	-0.206811
C	14.288043	4.595582	-0.135477
C	12.907085	4.809712	-0.119618
C	12.533743	2.416249	-0.191017
H	14.302686	1.193097	-0.241124
H	14.969000	5.441340	-0.113667
H	12.513357	5.821047	-0.085443
H	10.960079	3.881429	-0.135176
C	11.609439	1.267019	-0.219083
N	9.927055	-0.832882	-0.267401
N	12.132859	0.031909	-0.243685
N	10.285952	1.515972	-0.218276
C	9.499472	0.434390	-0.243002
C	11.264228	-0.990261	-0.267102
C	11.803974	-2.362608	-0.294968
C	12.835181	-4.962714	-0.350507
C	13.191922	-2.573402	-0.282587
C	10.937140	-3.466290	-0.334813
C	11.452543	-4.758953	-0.362709
C	13.702780	-3.867733	-0.310038
H	13.852358	-1.714786	-0.250981
H	9.866774	-3.296531	-0.344163
H	10.777511	-5.608885	-0.394360
H	14.777103	-4.024394	-0.300074
H	13.235416	-5.972079	-0.372425
C	8.036661	0.657575	-0.241308
C	5.269095	1.071982	-0.218550

C	7.151609	-0.440303	-0.272731
C	7.517957	1.969436	-0.231146
C	6.156913	2.180014	-0.232924
C	5.786311	-0.248624	-0.265256
H	7.564265	-1.440007	-0.325985
H	8.206637	2.804805	-0.220682
H	5.754247	3.187906	-0.213815
H	5.118072	-1.095205	-0.353076
N	3.924656	1.339425	-0.209467
H	3.669746	2.283546	-0.491410
H	2.001006	-2.165743	2.038079
C	1.895277	-1.343279	1.339100
C	1.593176	0.862201	-0.419247
C	0.650575	-1.028050	0.776330
C	2.995271	-0.565619	1.019425
C	2.854396	0.522968	0.124298
C	0.505596	0.079291	-0.099011
H	3.946906	-0.752816	1.499459
H	1.505733	1.706683	-1.095914
C	-0.650889	-1.653458	0.949820
C	-3.310681	-2.435493	0.937237
C	-1.028105	-2.783458	1.690534
C	-1.602680	-0.934162	0.182712
C	-2.927646	-1.316514	0.161699
C	-2.353658	-3.176699	1.673456
H	-0.301807	-3.343767	2.268691
H	-3.645800	-0.811505	-0.472029
H	-2.677632	-4.038809	2.247312
C	-0.931074	0.204090	-0.550769
H	-1.363247	1.176306	-0.285536
H	-1.027802	0.101864	-1.638513
N	-4.620913	-2.887626	0.970989
H	-4.730154	-3.876194	1.187977
C	-5.789513	-2.200693	0.763139
C	-8.234900	-0.909228	0.332368
C	-6.956470	-2.958045	0.480878
C	-5.873063	-0.788388	0.871912
C	-7.082768	-0.163089	0.656300
C	-8.153958	-2.315479	0.255934
H	-6.889427	-4.039184	0.414039
H	-5.010508	-0.212599	1.181311
H	-7.169339	0.911639	0.755237
H	-9.047170	-2.879307	0.018439
C	-9.525043	-0.222993	0.098794
N	-11.846795	1.012690	-0.325827
N	-10.572032	-0.982866	-0.240616
N	-9.548533	1.106767	0.242838
C	-10.742305	1.689592	0.022952
C	-11.724201	-0.317789	-0.449359
C	-10.840420	3.153562	0.177136
C	-11.030565	5.929448	0.476331
C	-12.061257	3.807985	-0.052356
C	-9.715889	3.903060	0.557883
C	-9.812746	5.283576	0.706425
C	-12.153277	5.188768	0.096736
H	-12.925261	3.223255	-0.345323
H	-8.776971	3.391719	0.735046
H	-8.939709	5.857340	1.002536
H	-13.100294	5.688714	-0.082200
H	-11.104708	7.006641	0.593039
C	-12.916597	-1.095746	-0.835081
C	-15.179407	-2.568420	-1.570789
C	-12.837045	-2.490045	-0.980349
C	-14.140771	-0.446275	-1.061274

C	-15.264873	-1.180868	-1.427127	H	-16.208525	-0.672675	-1.600576
C	-13.963825	-3.220523	-1.346522	H	-13.895854	-4.298493	-1.457489
H	-11.889623	-2.985628	-0.804001	H	-16.057635	-3.139834	-1.856578
H	-14.194820	0.629905	-0.946719				

A.2.11.4 ***OTPT-FLR-210, EB*** *State*

H	15.697277	3.029060	0.286430	H	14.609755	-4.119882	-0.359464
C	14.627428	3.201344	0.214082	H	13.066160	-6.047421	-0.643857
C	11.876070	3.642289	0.027121	C	7.893353	0.605484	-0.551114
C	13.762031	2.121815	0.057147	C	5.107200	1.045109	-0.734100
C	14.121500	4.502366	0.278119	C	7.009226	-0.472007	-0.726540
C	12.744229	4.719493	0.184233	C	7.367155	1.908947	-0.490521
C	12.377902	2.333262	-0.037616	C	6.004285	2.127343	-0.600852
H	14.142639	1.108425	0.005695	C	5.641475	-0.261793	-0.813318
H	14.797701	5.343608	0.400523	H	7.413295	-1.475382	-0.796085
H	12.347625	5.729335	0.233364	H	8.047954	2.743053	-0.366447
H	10.806176	3.797999	-0.047388	H	5.598172	3.133212	-0.567781
C	11.456425	1.187177	-0.205095	H	4.971547	-1.099321	-0.978672
N	9.788592	-0.891278	-0.512611	N	3.760735	1.326858	-0.894670
N	11.989034	-0.043978	-0.259021	H	2.138892	-1.624304	2.216999
N	10.143381	1.444981	-0.293660	C	1.968978	-0.945149	1.386807
C	9.344252	0.375559	-0.447997	C	1.442889	0.910546	-0.717967
C	11.116027	-1.052251	-0.412917	C	0.638802	-0.714135	0.914344
C	11.653861	-2.429768	-0.476672	C	3.010680	-0.289936	0.807901
C	12.671466	-5.036510	-0.597090	C	2.809790	0.653654	-0.292049
C	13.035221	-2.656515	-0.377144	C	0.411979	0.239466	-0.151029
C	10.787421	-3.522067	-0.637178	H	4.017627	-0.431395	1.181750
C	11.294930	-4.817307	-0.696820	H	1.301740	1.630740	-1.517626
C	13.539415	-3.953104	-0.437204	C	-0.576632	-1.254834	1.328999
H	13.698397	-1.808361	-0.253415	C	-3.267989	-2.023330	1.779533
H	9.721894	-3.339379	-0.713495	C	-0.868210	-2.242973	2.321543
H	10.617574	-5.657069	-0.821342	C	-1.654493	-0.679516	0.551339

C	-2.946192	-1.036799	0.756780
C	-2.158823	-2.619956	2.517841
H	-0.064723	-2.688221	2.900044
H	-3.746513	-0.623085	0.154132
H	-2.424377	-3.369877	3.255458
C	-1.072518	0.301608	-0.446516
H	-1.476357	1.311611	-0.308953
H	-1.295164	0.010106	-1.479940
N	-4.466686	-2.466437	2.075042
C	-5.626074	-1.876051	1.597133
C	-8.093983	-0.798083	0.740517
C	-6.668018	-2.717496	1.151173
C	-5.861762	-0.482717	1.640489
C	-7.076081	0.040919	1.223930
C	-7.869191	-2.186433	0.711678
H	-6.498150	-3.789326	1.143034
H	-5.093003	0.173222	2.035659
H	-7.254361	1.109182	1.267181
H	-8.656756	-2.837019	0.349562
C	-9.376289	-0.235118	0.285081
N	-11.711986	0.791191	-0.550085
N	-10.311756	-1.085091	-0.171515
N	-9.538865	1.097557	0.349025
C	-10.720738	1.564501	-0.079127
C	-11.461890	-0.527528	-0.577332
C	-10.947604	3.026296	-0.029751
C	-11.376695	5.792511	0.063067
C	-12.163920	3.569862	-0.470801
C	-9.948455	3.882392	0.458348
C	-10.163384	5.257345	0.503888
C	-12.375539	4.945349	-0.424094
H	-12.930875	2.902643	-0.846374
H	-9.011964	3.455270	0.797514
H	-9.385086	5.912893	0.883376
H	-13.319649	5.357966	-0.767459
H	-11.543142	6.865311	0.099135
C	-12.523587	-1.423045	-1.088654
C	-14.532332	-3.118239	-2.056042
C	-12.316185	-2.810065	-1.140465
C	-13.747375	-0.893747	-1.526454
C	-14.744945	-1.737973	-2.007125
C	-13.315828	-3.651416	-1.621686
H	-11.368578	-3.211491	-0.800823
H	-13.900593	0.178233	-1.483701
H	-15.689176	-1.320271	-2.343956
H	-13.147246	-4.723664	-1.658362
H	-15.311415	-3.775674	-2.431165

A.2.12 Optimised Structures of **OTPT-FLR-221** Oligomers

A.2.12.1 ***OTPT-FLR-221****, **LEB** State*

H	-2.151276	13.571365	1.693836
C	-1.209133	13.048079	1.558528
C	1.210557	11.699661	1.210167
C	-1.210557	11.699661	1.210167
C	0.000000	13.726227	1.733630
C	1.209133	13.048079	1.558528
C	0.000000	11.012763	1.032517
H	-2.141751	11.162892	1.071719
H	0.000000	14.778018	2.005289
H	2.151276	13.571365	1.693836

H	2.141751	11.162892	1.071719
C	0.000000	9.577335	0.661511
N	0.000000	6.985216	-0.013263
N	-1.187968	8.973803	0.506210
N	1.187968	8.973803	0.506210
C	1.140459	7.670881	0.168009
C	-1.140459	7.670881	0.168009
C	-2.406928	6.947352	-0.004677
C	-4.830482	5.511071	-0.287690
C	-3.646134	7.573349	0.219508
C	-2.409725	5.598149	-0.397094
C	-3.590546	4.889912	-0.544922
C	-4.833271	6.872831	0.084592
H	-3.661731	8.616566	0.514100
H	-1.462039	5.111668	-0.596558
H	-3.559347	3.860366	-0.878496
H	-5.781645	7.367722	0.277445
C	2.406928	6.947352	-0.004677
C	4.830482	5.511071	-0.287690
C	2.409725	5.598149	-0.397094
C	3.646134	7.573349	0.219508
C	4.833271	6.872831	0.084592
C	3.590546	4.889912	-0.544922
H	1.462039	5.111668	-0.596558
H	3.661731	8.616566	0.514100
H	5.781645	7.367722	0.277445
H	3.559347	3.860366	-0.878496
N	6.041300	4.851466	-0.417639
H	6.854414	5.441853	-0.529752
H	8.395199	1.341830	-2.159886
C	7.579710	1.663558	-1.518211
C	5.479143	2.533356	0.151699
C	6.773312	0.732632	-0.859657
C	7.314195	3.023571	-1.367914
C	6.260822	3.470615	-0.549942
C	5.729381	1.182809	-0.022053
H	7.915192	3.755798	-1.900406
H	4.697743	2.871014	0.823565
C	6.773312	-0.732632	-0.859657
C	6.260822	-3.470615	-0.549942
C	7.579710	-1.663558	-1.518211
C	5.729381	-1.182809	-0.022053
C	5.479143	-2.533356	0.151699
C	7.314195	-3.023571	-1.367914
H	8.395199	-1.341830	-2.159886
H	4.697743	-2.871014	0.823565
H	7.915192	-3.755798	-1.900406
C	5.007411	-0.000000	0.589527
H	5.073343	-0.000000	1.685657
H	3.937770	-0.000000	0.343516
N	6.041300	-4.851466	-0.417639
H	6.854414	-5.441853	-0.529752
C	4.830482	-5.511071	-0.287690
C	2.406928	-6.947352	-0.004677
C	3.590546	-4.889912	-0.544922
C	4.833271	-6.872831	0.084592
C	3.646134	-7.573349	0.219508
C	2.409725	-5.598149	-0.397094
H	3.559347	-3.860366	-0.878496
H	5.781645	-7.367722	0.277445
H	3.661731	-8.616566	0.514100
H	1.462039	-5.111668	-0.596558
C	1.140459	-7.670881	0.168009
N	-1.187968	-8.973803	0.506210

N	-0.000000	-6.985216	-0.013263
N	1.187968	-8.973803	0.506210
C	-0.000000	-9.577335	0.661511
C	-1.140459	-7.670881	0.168009
C	-2.406928	-6.947352	-0.004677
C	-4.830482	-5.511071	-0.287690
C	-2.409725	-5.598149	-0.397094
C	-3.646134	-7.573349	0.219508
C	-4.833271	-6.872831	0.084592
C	-3.590546	-4.889912	-0.544922
H	-1.462039	-5.111668	-0.596558
H	-3.661731	-8.616566	0.514100
H	-5.781645	-7.367722	0.277445
H	-3.559347	-3.860366	-0.878496
C	-0.000000	-11.012763	1.032517
C	-0.000000	-13.726227	1.733630
C	-1.210557	-11.699661	1.210167
C	1.210557	-11.699661	1.210167
C	1.209133	-13.048079	1.558528
C	-1.209133	-13.048079	1.558528
H	-2.141751	-11.162892	1.071719
H	2.141751	-11.162892	1.071719
H	2.151276	-13.571365	1.693836
H	-2.151276	-13.571365	1.693836
H	-0.000000	-14.778018	2.005289
N	-6.041300	-4.851466	-0.417639
H	-6.854414	-5.441853	-0.529752
H	-8.395199	-1.341830	-2.159886
C	-7.579710	-1.663558	-1.518211
C	-5.479143	-2.533356	0.151699
C	-6.773312	-0.732632	-0.859657
C	-7.314195	-3.023571	-1.367914
C	-6.260822	-3.470615	-0.549942
C	-5.729381	-1.182809	-0.022053
H	-7.915192	-3.755798	-1.900406
H	-4.697743	-2.871014	0.823565
C	-6.773312	0.732632	-0.859657
C	-6.260822	3.470615	-0.549942
C	-7.579710	1.663558	-1.518211
C	-5.729381	1.182809	-0.022053
C	-5.479143	2.533356	0.151699
C	-7.314195	3.023571	-1.367914
H	-8.395199	1.341830	-2.159886
H	-4.697743	2.871014	0.823565
H	-7.915192	3.755798	-1.900406
C	-5.007411	0.000000	0.589527
H	-5.073343	0.000000	1.685657
H	-3.937770	0.000000	0.343516
N	-6.041300	4.851466	-0.417639
H	-6.854414	5.441853	-0.529752

A.2.12.2 ***OTPT-FLR-221****,* ***¹ES*** *State*

H	-2.151605	13.014170	2.683280
C	-1.210770	12.520436	2.460461
C	1.213522	11.252474	1.887355
C	-1.213522	11.252474	1.887355
C	0.000000	13.156770	2.748231
C	1.210770	12.520436	2.460461
C	0.000000	10.608009	1.596127
H	-2.145869	10.749564	1.658970
H	0.000000	14.146361	3.195292
H	2.151605	13.014170	2.683280

H	2.145869	10.749564	1.658970
C	0.000000	9.266684	0.988874
N	0.000000	6.829957	-0.154039
N	-1.185610	8.685145	0.727225
N	1.185610	8.685145	0.727225
C	1.132677	7.476040	0.160640
C	-1.132677	7.476040	0.160640
C	-2.411477	6.783885	-0.123003
C	-4.801388	5.420204	-0.582970
C	-3.634743	7.346705	0.276071
C	-2.405642	5.551125	-0.793678
C	-3.588960	4.873003	-1.035091
C	-4.826569	6.675137	0.044883
H	-3.635483	8.306380	0.778242
H	-1.463946	5.141122	-1.135745
H	-3.580344	3.950542	-1.603574
H	-5.769136	7.099742	0.374347
C	2.411477	6.783885	-0.123003
C	4.801388	5.420204	-0.582970
C	2.405642	5.551125	-0.793678
C	3.634743	7.346705	0.276071
C	4.826569	6.675137	0.044883
C	3.588960	4.873003	-1.035091
H	1.463946	5.141122	-1.135745
H	3.635483	8.306380	0.778242
H	5.769136	7.099742	0.374347
H	3.580344	3.950542	-1.603574
N	6.022755	4.749371	-0.797422
H	6.819119	5.346663	-1.009277
H	8.710765	1.280427	-1.834812
C	7.780751	1.629887	-1.401064
C	5.307645	2.501915	-0.234563
C	6.804531	0.698844	-0.930069
C	7.517898	2.962737	-1.306834
C	6.258323	3.430851	-0.774953
C	5.582891	1.174535	-0.319075
H	8.230375	3.695372	-1.671911
H	4.414351	2.865408	0.256226
C	6.804531	-0.698844	-0.930069
C	6.258323	-3.430851	-0.774953
C	7.780751	-1.629887	-1.401064
C	5.582891	-1.174535	-0.319075
C	5.307645	-2.501915	-0.234563
C	7.517898	-2.962737	-1.306834
H	8.710765	-1.280427	-1.834812
H	4.414351	-2.865408	0.256226
H	8.230375	-3.695372	-1.671911
C	4.765597	-0.000000	0.158348
H	4.659596	-0.000000	1.250021
H	3.754605	-0.000000	-0.262538
N	6.022755	-4.749371	-0.797422
H	6.819119	-5.346663	-1.009277
C	4.801388	-5.420204	-0.582970
C	2.411477	-6.783885	-0.123003
C	3.588960	-4.873003	-1.035091
C	4.826569	-6.675137	0.044883
C	3.634743	-7.346705	0.276071
C	2.405642	-5.551125	-0.793678
H	3.580344	-3.950542	-1.603574
H	5.769136	-7.099742	0.374347
H	3.635483	-8.306380	0.778242
H	1.463946	-5.141122	-1.135745
C	1.132677	-7.476040	0.160640
N	-1.185610	-8.685145	0.727225

N	-0.000000	-6.829957	-0.154039
N	1.185610	-8.685145	0.727225
C	-0.000000	-9.266684	0.988874
C	-1.132677	-7.476040	0.160640
C	-2.411477	-6.783885	-0.123003
C	-4.801388	-5.420204	-0.582970
C	-2.405642	-5.551125	-0.793678
C	-3.634743	-7.346705	0.276071
C	-4.826569	-6.675137	0.044883
C	-3.588960	-4.873003	-1.035091
H	-1.463946	-5.141122	-1.135745
H	-3.635483	-8.306380	0.778242
H	-5.769136	-7.099742	0.374347
H	-3.580344	-3.950542	-1.603574
C	-0.000000	-10.608009	1.596127
C	-0.000000	-13.156770	2.748231
C	-1.213522	-11.252474	1.887355
C	1.213522	-11.252474	1.887355
C	1.210770	-12.520436	2.460461
C	-1.210770	-12.520436	2.460461
H	-2.145869	-10.749564	1.658970
H	2.145869	-10.749564	1.658970
H	2.151605	-13.014170	2.683280
H	-2.151605	-13.014170	2.683280
H	-0.000000	-14.146361	3.195292
N	-6.022755	-4.749371	-0.797422
H	-6.819119	-5.346663	-1.009277
H	-8.710765	-1.280427	-1.834812
C	-7.780751	-1.629887	-1.401064
C	-5.307645	-2.501915	-0.234563
C	-6.804531	-0.698844	-0.930069
C	-7.517898	-2.962737	-1.306834
C	-6.258323	-3.430851	-0.774953
C	-5.582891	-1.174535	-0.319075
H	-8.230375	-3.695372	-1.671911
H	-4.414351	-2.865408	0.256226
C	-6.804531	0.698844	-0.930069
C	-6.258323	3.430851	-0.774953
C	-7.780751	1.629887	-1.401064
C	-5.582891	1.174535	-0.319075
C	-5.307645	2.501915	-0.234563
C	-7.517898	2.962737	-1.306834
H	-8.710765	1.280427	-1.834812
H	-4.414351	2.865408	0.256226
H	-8.230375	3.695372	-1.671911
C	-4.765597	0.000000	0.158348
H	-4.659596	0.000000	1.250021
H	-3.754605	0.000000	-0.262538
N	-6.022755	4.749371	-0.797422
H	-6.819119	5.346663	-1.009277

A.2.12.3 ***OTPT-FLR-221****,* ***^{5}ES*** *State*

H	-2.151640	13.328549	2.084319
C	-1.211070	12.816003	1.908402
C	1.214126	11.500465	1.455925
C	-1.214126	11.500465	1.455925
C	0.000000	13.476002	2.135586
C	1.211070	12.816003	1.908402
C	0.000000	10.831851	1.225949
H	-2.147111	10.979464	1.276561
H	0.000000	14.502812	2.488722
H	2.151640	13.328549	2.084319

H	2.147111	10.979464	1.276561
C	0.000000	9.441331	0.748476
N	0.000000	6.896469	-0.145641
N	-1.184938	8.834218	0.542911
N	1.184938	8.834218	0.542911
C	1.131545	7.574027	0.101554
C	-1.131545	7.574027	0.101554
C	-2.409533	6.862202	-0.112167
C	-4.812261	5.464108	-0.428199
C	-3.636124	7.483234	0.202393
C	-2.407525	5.553513	-0.635624
C	-3.585793	4.857810	-0.801603
C	-4.825009	6.803660	0.036950
H	-3.629754	8.495240	0.587315
H	-1.465853	5.105625	-0.925435
H	-3.579751	3.878360	-1.261395
H	-5.768848	7.268809	0.301882
C	2.409533	6.862202	-0.112167
C	4.812261	5.464108	-0.428199
C	2.407525	5.553513	-0.635624
C	3.636124	7.483234	0.202393
C	4.825009	6.803660	0.036950
C	3.585793	4.857810	-0.801603
H	1.465853	5.105625	-0.925435
H	3.629754	8.495240	0.587315
H	5.768848	7.268809	0.301882
H	3.579751	3.878360	-1.261395
N	6.013832	4.806777	-0.537070
H	6.837470	5.402650	-0.589453
H	8.651087	1.327520	-1.768190
C	7.734421	1.652412	-1.289362
C	5.343928	2.519079	-0.017195
C	6.803625	0.728778	-0.785411
C	7.462773	3.004358	-1.177367
C	6.253947	3.444282	-0.581496
C	5.623239	1.175618	-0.135621
H	8.156508	3.736741	-1.577308
H	4.478459	2.864672	0.534514
C	6.803625	-0.728778	-0.785411
C	6.253947	-3.444282	-0.581496
C	7.734421	-1.652412	-1.289362
C	5.623239	-1.175618	-0.135621
C	5.343928	-2.519079	-0.017195
C	7.462773	-3.004358	-1.177367
H	8.651087	-1.327520	-1.768190
H	4.478459	-2.864672	0.534514
H	8.156508	-3.736741	-1.577308
C	4.816500	-0.000000	0.359716
H	4.727651	-0.000000	1.453217
H	3.796920	-0.000000	-0.042377
N	6.013832	-4.806777	-0.537070
H	6.837470	-5.402650	-0.589453
C	4.812261	-5.464108	-0.428199
C	2.409533	-6.862202	-0.112167
C	3.585793	-4.857810	-0.801603
C	4.825009	-6.803660	0.036950
C	3.636124	-7.483234	0.202393
C	2.407525	-5.553513	-0.635624
H	3.579751	-3.878360	-1.261395
H	5.768848	-7.268809	0.301882
H	3.629754	-8.495240	0.587315
H	1.465853	-5.105625	-0.925435
C	1.131545	-7.574027	0.101554
N	-1.184938	-8.834218	0.542911

N	-0.000000	-6.896469	-0.145641
N	1.184938	-8.834218	0.542911
C	-0.000000	-9.441331	0.748476
C	-1.131545	-7.574027	0.101554
C	-2.409533	-6.862202	-0.112167
C	-4.812261	-5.464108	-0.428199
C	-2.407525	-5.553513	-0.635624
C	-3.636124	-7.483234	0.202393
C	-4.825009	-6.803660	0.036950
C	-3.585793	-4.857810	-0.801603
H	-1.465853	-5.105625	-0.925435
H	-3.629754	-8.495240	0.587315
H	-5.768848	-7.268809	0.301882
H	-3.579751	-3.878360	-1.261395
C	-0.000000	-10.831851	1.225949
C	-0.000000	-13.476002	2.135586
C	-1.214126	-11.500465	1.455925
C	1.214126	-11.500465	1.455925
C	1.211070	-12.816003	1.908402
C	-1.211070	-12.816003	1.908402
H	-2.147111	-10.979464	1.276561
H	2.147111	-10.979464	1.276561
H	2.151640	-13.328549	2.084319
H	-2.151640	-13.328549	2.084319
H	-0.000000	-14.502812	2.488722
N	-6.013832	-4.806777	-0.537070
H	-6.837470	-5.402650	-0.589453
H	-8.651087	-1.327520	-1.768190
C	-7.734421	-1.652412	-1.289362
C	-5.343928	-2.519079	-0.017195
C	-6.803625	-0.728778	-0.785411
C	-7.462773	-3.004358	-1.177367
C	-6.253947	-3.444282	-0.581496
C	-5.623239	-1.175618	-0.135621
H	-8.156508	-3.736741	-1.577308
H	-4.478459	-2.864672	0.534514
C	-6.803625	0.728778	-0.785411
C	-6.253947	3.444282	-0.581496
C	-7.734421	1.652412	-1.289362
C	-5.623239	1.175618	-0.135621
C	-5.343928	2.519079	-0.017195
C	-7.462773	3.004358	-1.177367
H	-8.651087	1.327520	-1.768190
H	-4.478459	2.864672	0.534514
H	-8.156508	3.736741	-1.577308
C	-4.816500	0.000000	0.359716
H	-4.727651	0.000000	1.453217
H	-3.796920	0.000000	-0.042377
N	-6.013832	4.806777	-0.537070
H	-6.837470	5.402650	-0.589453

A.2.12.4 ***OTPT-FLR-221, EB*** *State*

H	-2.151406	12.356660	3.680196
C	-1.209509	11.909101	3.376797
C	1.211245	10.756836	2.595013
C	-1.211245	10.756836	2.595013
C	0.000000	12.488258	3.769730
C	1.209509	11.909101	3.376797
C	0.000000	10.170348	2.197112
H	-2.142586	10.298510	2.283705
H	0.000000	13.387248	4.379457
H	2.151406	12.356660	3.680196

H	2.142586	10.298510	2.283705
C	0.000000	8.945717	1.365287
N	0.000000	6.749331	-0.171678
N	-1.187142	8.426050	1.015104
N	1.187142	8.426050	1.015104
C	1.138615	7.324049	0.247217
C	-1.138615	7.324049	0.247217
C	-2.408752	6.685311	-0.139696
C	-4.823749	5.370044	-0.792076
C	-3.637730	7.155566	0.356499
C	-2.409227	5.575730	-1.001462
C	-3.590680	4.929018	-1.325446
C	-4.825041	6.522400	0.022675
H	-3.642367	8.021133	1.009110
H	-1.466551	5.227132	-1.406809
H	-3.580331	4.087329	-2.010067
H	-5.773808	6.883456	0.406604
C	2.408752	6.685311	-0.139696
C	4.823749	5.370044	-0.792076
C	2.409227	5.575730	-1.001462
C	3.637730	7.155566	0.356499
C	4.825041	6.522400	0.022675
C	3.590680	4.929018	-1.325446
H	1.466551	5.227132	-1.406809
H	3.642367	8.021133	1.009110
H	5.773808	6.883456	0.406604
H	3.580331	4.087329	-2.010067
N	6.037448	4.779821	-1.113473
H	8.612993	1.283750	-2.254231
C	7.696547	1.635739	-1.790594
C	5.268565	2.506503	-0.544713
C	6.740201	0.697232	-1.287346
C	7.439305	2.966458	-1.681654
C	6.198303	3.476996	-1.106766
C	5.539164	1.182357	-0.640146
H	8.135306	3.709591	-2.056407
H	4.377931	2.861708	-0.039798
C	6.740201	-0.697232	-1.287346
C	6.198303	-3.476996	-1.106766
C	7.696547	-1.635739	-1.790594
C	5.539164	-1.182357	-0.640146
C	5.268565	-2.506503	-0.544713
C	7.439305	-2.966458	-1.681654
H	8.612993	-1.283750	-2.254231
H	4.377931	-2.861708	-0.039798
H	8.135306	-3.709591	-2.056407
C	4.732549	-0.000000	-0.146452
H	4.644795	-0.000000	0.947100
H	3.711928	-0.000000	-0.545948
N	6.037448	-4.779821	-1.113473
C	4.823749	-5.370044	-0.792076
C	2.408752	-6.685311	-0.139696
C	3.590680	-4.929018	-1.325446
C	4.825041	-6.522400	0.022675
C	3.637730	-7.155566	0.356499
C	2.409227	-5.575730	-1.001462
H	3.580331	-4.087329	-2.010067
H	5.773808	-6.883456	0.406604
H	3.642367	-8.021133	1.009110
H	1.466551	-5.227132	-1.406809
C	1.138615	-7.324049	0.247217
N	-1.187142	-8.426050	1.015104
N	-0.000000	-6.749331	-0.171678
N	1.187142	-8.426050	1.015104

C	-0.000000	-8.945717	1.365287	N	-6.037448	-4.779821	-1.113473
C	-1.138615	-7.324049	0.247217	H	-8.612993	-1.283750	-2.254231
C	-2.408752	-6.685311	-0.139696	C	-7.696547	-1.635739	-1.790594
C	-4.823749	-5.370044	-0.792076	C	-5.268565	-2.506503	-0.544713
C	-2.409227	-5.575730	-1.001462	C	-6.740201	-0.697232	-1.287346
C	-3.637730	-7.155566	0.356499	C	-7.439305	-2.966458	-1.681654
C	-4.825041	-6.522400	0.022675	C	-6.198303	-3.476996	-1.106766
C	-3.590680	-4.929018	-1.325446	C	-5.539164	-1.182357	-0.640146
H	-1.466551	-5.227132	-1.406809	H	-8.135306	-3.709591	-2.056407
H	-3.642367	-8.021133	1.009110	H	-4.377931	-2.861708	-0.039798
H	-5.773808	-6.883456	0.406604	C	-6.740201	0.697232	-1.287346
H	-3.580331	-4.087329	-2.010067	C	-6.198303	3.476996	-1.106766
C	-0.000000	-10.170348	2.197112	C	-7.696547	1.635739	-1.790594
C	-0.000000	-12.488258	3.769730	C	-5.539164	1.182357	-0.640146
C	-1.211245	-10.756836	2.595013	C	-5.268565	2.506503	-0.544713
C	1.211245	-10.756836	2.595013	C	-7.439305	2.966458	-1.681654
C	1.209509	-11.909101	3.376797	H	-8.612993	1.283750	-2.254231
C	-1.209509	-11.909101	3.376797	H	-4.377931	2.861708	-0.039798
H	-2.142586	-10.298510	2.283705	H	-8.135306	3.709591	-2.056407
H	2.142586	-10.298510	2.283705	C	-4.732549	0.000000	-0.146452
H	2.151406	-12.356660	3.680196	H	-4.644795	0.000000	0.947100
H	-2.151406	-12.356660	3.680196	H	-3.711928	0.000000	-0.545948
H	-0.000000	-13.387248	4.379457	N	-6.037448	4.779821	-1.113473

A.3 Optimised Structures of PANI-CMP Oligomeric Models for Non-Covalent Interactions with CO_2

A.3.1 Optimised Structures of **OTPA-BZN-210** Oligomers

*A.3.1.1 **OTPA-BZN-210**, **EB** State, trans-syn Conformer (Default Conformer)*

H	-0.636485	11.852748	-1.120851	C	-2.612108	9.657797	0.562816
C	-0.947493	10.938959	-0.622560	C	-0.451360	8.674793	0.080873
C	-1.730666	8.582059	0.647607	H	0.922211	9.931879	-1.000319
C	-0.066337	9.861664	-0.558891	H	-2.912821	11.681887	-0.125501
C	-2.225961	10.842982	-0.067769	H	-3.600379	9.572551	1.005606

H	-2.025943	7.667091	1.150274
N	0.451360	7.581499	0.158930
C	1.812777	7.825257	0.479190
C	4.502791	8.317551	1.108775
C	2.147813	8.744920	1.483348
C	2.834911	7.155244	-0.208864
C	4.168751	7.395669	0.113682
C	3.484942	8.992790	1.786483
H	1.357354	9.260508	2.018383
H	2.576734	6.450220	-0.991978
H	4.950477	6.869858	-0.427141
H	3.730401	9.707923	2.566464
H	5.543588	8.507995	1.352352
C	-0.000048	6.266545	-0.067647
C	-0.888359	3.615197	-0.537319
C	0.531331	5.189965	0.664548
C	-1.005694	6.002504	-1.016104
C	-1.460674	4.709747	-1.218718
C	0.108341	3.891296	0.425369
H	1.274697	5.382534	1.430427
H	-1.433297	6.822186	-1.582831
H	-2.244533	4.512716	-1.943181
H	0.505285	3.082337	1.029776
N	-1.417824	2.354201	-0.777233
C	-0.688345	1.268554	-0.814749
C	0.688345	-1.268554	-0.814749
C	0.769269	1.193068	-0.867050
C	-1.403516	0.001233	-0.895829
C	-0.769269	-1.193068	-0.867050
C	1.403516	-0.001233	-0.895829
H	1.336153	2.114198	-0.932180
H	-2.485331	0.063775	-0.964329
H	-1.336153	-2.114198	-0.932180
H	2.485331	-0.063775	-0.964329
N	1.417824	-2.354201	-0.777233
C	0.888359	-3.615197	-0.537319
C	0.000048	-6.266545	-0.067647
C	1.460674	-4.709747	-1.218718
C	-0.108341	-3.891296	0.425369
C	-0.531331	-5.189965	0.664548
C	1.005694	-6.002504	-1.016104
H	2.244533	-4.512716	-1.943181
H	-0.505285	-3.082337	1.029776
H	-1.274697	-5.382534	1.430427
H	1.433297	-6.822186	-1.582831
N	-0.451360	-7.581499	0.158930
C	-1.812777	-7.825257	0.479190
C	-4.502791	-8.317551	1.108775
C	-2.147813	-8.744920	1.483348
C	-2.834911	-7.155244	-0.208864
C	-4.168751	-7.395669	0.113682
C	-3.484942	-8.992790	1.786483
H	-1.357354	-9.260508	2.018383
H	-2.576734	-6.450220	-0.991978
H	-4.950477	-6.869858	-0.427141
H	-3.730401	-9.707923	2.566464
H	-5.543588	-8.507995	1.352352
C	0.451360	-8.674793	0.080873
C	2.225961	-10.842982	-0.067769
C	1.730666	-8.582059	0.647607
C	0.066337	-9.861664	-0.558891
C	0.947493	-10.938959	-0.622560
C	2.612108	-9.657797	0.562816
H	2.025943	-7.667091	1.150274

H	-0.922211	-9.931879	-1.000319	H	3.600379	-9.572551	1.005606
H	0.636485	-11.852748	-1.120851	H	2.912821	-11.681887	-0.125501

*A.3.1.2 **OTPA-BZN-210**, **EB** State, trans-anti Conformer*

H	11.652398	1.642957	-1.554975	C	4.032716	-0.029544	0.780166
C	10.799369	1.778857	-0.896256	H	5.710418	-1.234337	1.353232
C	8.598139	2.113798	0.784317	H	6.573164	2.090115	-1.232954
C	9.793766	0.814859	-0.872895	H	4.193879	2.762378	-1.146403
C	10.706884	2.919383	-0.094894	H	3.337022	-0.595110	1.391218
C	9.599354	3.081802	0.740813	N	2.262800	1.560894	0.089414
C	8.685858	0.974383	-0.028346	C	1.223962	0.767026	0.034766
H	9.859497	-0.065043	-1.504150	C	-1.223919	-0.766737	-0.034055
H	11.488825	3.672228	-0.120812	C	1.226392	-0.658910	-0.278542
H	9.518929	3.959936	1.375187	C	-0.077062	1.372249	0.291048
H	7.745356	2.233460	1.444230	C	-1.226351	0.659192	0.279294
N	7.667217	-0.014337	0.006349	C	0.077103	-1.371964	-0.290289
C	8.030024	-1.386614	0.024160	H	2.164693	-1.132770	-0.541519
C	8.757636	-4.096862	0.054521	H	-0.071791	2.426940	0.548804
C	9.097119	-1.824183	0.821868	H	-2.164642	1.133055	0.542279
C	7.331040	-2.316186	-0.759787	H	0.071839	-2.426661	-0.548032
C	7.689627	-3.662177	-0.734199	N	-2.262758	-1.560612	-0.088854
C	9.460527	-3.169234	0.827005	C	-3.572666	-1.100988	-0.068201
H	9.635533	-1.106218	1.431410	C	-6.309916	-0.361802	-0.032816
H	6.511015	-1.977223	-1.383986	C	-4.531215	-1.877311	0.616492
H	7.139770	-4.371397	-1.346346	C	-4.032647	0.029929	-0.779497
H	10.289311	-3.494457	1.449410	C	-5.374084	0.381536	-0.773545
H	9.039108	-5.145426	0.066256	C	-5.863289	-1.500099	0.664032
C	6.309897	0.361819	0.033011	H	-4.193942	-2.762674	1.146062
C	3.572710	1.101164	0.068582	H	-3.336914	0.595721	-1.390293
C	5.374138	-0.381218	0.774144	H	-5.710333	1.234836	-1.352387
C	5.863210	1.499856	-0.664211	H	-6.573316	-2.090631	1.232404
C	4.531159	1.877187	-0.616554	N	-7.667253	0.014287	-0.006153

C	-8.030102	1.386557	-0.023479
C	-8.757711	4.096821	-0.052811
C	-9.097022	1.824472	-0.821228
C	-7.331297	2.315792	0.761036
C	-7.689881	3.661789	0.735965
C	-9.460422	3.169530	-0.825858
H	-9.635308	1.106784	-1.431208
H	-6.511417	1.976550	1.385274
H	-7.140163	4.370740	1.348547
H	-10.289070	3.495024	-1.448303
H	-9.039184	5.145389	-0.064152
C	-8.685844	-0.974520	0.027467
C	-10.706797	-2.919666	0.091920
C	-8.597709	-2.113424	-0.785866
C	-9.794124	-0.815586	0.871641
C	-10.799684	-1.779651	0.893966
C	-9.598899	-3.081502	-0.743409
H	-7.744638	-2.232629	-1.445490
H	-9.860171	0.063915	1.503422
H	-11.653004	-1.644209	1.552400
H	-9.518152	-3.959234	-1.378297
H	-11.488712	-3.672566	0.117026

*A.3.1.3 **OTPA-BZN-210**, **EB** State, cis-syn Conformer*

H	10.644868	-1.544186	-1.427660
C	9.992583	-0.955787	-0.788649
C	8.301182	0.549119	0.841128
C	8.620386	-1.196251	-0.806603
C	10.526702	0.043367	0.028648
C	9.672564	0.795473	0.838649
C	7.764064	-0.446243	0.012175
H	8.204173	-1.963981	-1.450317
H	11.595731	0.233090	0.034807
H	10.075539	1.569838	1.485148
H	7.640248	1.123613	1.481536
N	6.367027	-0.700582	0.005090
C	5.904404	-2.042829	0.006848
C	4.998971	-4.698852	0.005684
C	6.521096	-3.001065	0.823979
C	4.832086	-2.424773	-0.812516
C	4.379739	-3.742432	-0.802691
C	6.073926	-4.320622	0.813604
H	7.348040	-2.705067	1.460733
H	4.360427	-1.685793	-1.451625
H	3.548403	-4.024867	-1.442371
H	6.560795	-5.052900	1.451362
H	4.648677	-5.726546	0.005219
C	5.447672	0.366336	0.012058
C	3.583265	2.502756	0.008571
C	4.236481	0.264266	0.719110
C	5.728391	1.564902	-0.670831
C	4.829801	2.618508	-0.642474
C	3.317900	1.302824	0.706584
H	4.026109	-0.635191	1.287380
H	6.662014	1.663728	-1.213469
H	5.055204	3.544387	-1.162084
H	2.408617	1.216721	1.292356
N	2.747460	3.610538	0.008771
C	1.443608	3.515809	-0.057406
C	-1.442961	3.515787	-0.056948
C	0.676965	2.323027	-0.408483
C	0.676243	4.735852	0.153580

C	-0.675526	4.735838	0.153787
C	-0.676455	2.323020	-0.408268
H	1.218788	1.444079	-0.739767
H	1.245461	5.640022	0.344891
H	-1.244709	5.639990	0.345284
H	-1.218340	1.444052	-0.739393
N	-2.746789	3.610662	0.009622
C	-3.582761	2.503038	0.009475
C	-5.447562	0.366782	0.013260
C	-4.829495	2.619007	-0.641134
C	-3.317421	1.302968	0.707284
C	-4.236130	0.264563	0.719989
C	-5.728251	1.565536	-0.669382
H	-5.054996	3.544961	-1.160576
H	-2.408001	1.216679	1.292827
H	-4.025702	-0.634898	1.288221
H	-6.661940	1.664666	-1.211835
N	-6.366897	-0.699986	0.006485
C	-5.904537	-2.042410	0.010065
C	-5.000192	-4.698700	0.012445
C	-6.521470	-2.999193	0.828671
C	-4.832575	-2.425866	-0.809013
C	-4.380737	-3.743696	-0.797431
C	-6.074830	-4.318947	0.820076
H	-7.348184	-2.701894	1.465125
H	-4.360795	-1.687929	-1.449240
H	-3.549669	-4.027399	-1.436894
H	-6.561830	-5.050159	1.458952
H	-4.650306	-5.726534	0.013348
C	-7.764036	-0.445906	0.011006
C	-10.526808	0.042781	0.022673
C	-8.302834	0.549604	0.838681
C	-8.618702	-1.196538	-0.808894
C	-9.991017	-0.956522	-0.793335
C	-9.674290	0.795506	0.833815
H	-7.643128	1.124539	1.479960
H	-8.201133	-1.964402	-1.451570
H	-10.642052	-1.545393	-1.433182
H	-10.078626	1.569971	1.479342
H	-11.595911	0.232147	0.026982

*A.3.1.4 **OTPA-BZN-210, EB** State, cis-anti Conformer*

H	-10.522188	-1.816516	1.811265
C	-9.957204	-1.091016	1.232909
C	-8.488399	0.763200	-0.245467
C	-8.616801	-1.340584	0.946310
C	-10.567877	0.087693	0.797877
C	-9.824227	1.013200	0.061821
C	-7.872565	-0.415153	0.200516
H	-8.139405	-2.250364	1.294735
H	-11.610706	0.282362	1.029142
H	-10.288736	1.930132	-0.289591
H	-7.915697	1.475805	-0.829586
N	-6.510340	-0.674517	-0.103877
C	-6.123237	-1.975996	-0.516750
C	-5.364789	-4.553539	-1.328699
C	-6.922563	-2.699926	-1.413293
C	-4.941800	-2.553486	-0.028621
C	-4.564401	-3.829317	-0.441864
C	-6.546723	-3.982603	-1.806623
H	-7.834293	-2.252476	-1.794619
H	-4.327105	-1.997946	0.671730

H	-3.646982	-4.264415	-0.055653
H	-7.175578	-4.532005	-2.501425
H	-5.071496	-5.550634	-1.642779
C	-5.551510	0.354307	-0.010287
C	-3.607811	2.407967	0.189053
C	-4.493917	0.434580	-0.933004
C	-5.642050	1.334786	0.994737
C	-4.709458	2.357000	1.068132
C	-3.533870	1.429865	-0.827457
H	-4.435881	-0.287356	-1.740338
H	-6.457274	1.293398	1.708678
H	-4.790986	3.117749	1.837961
H	-2.749047	1.494607	-1.574062
N	-2.730773	3.478825	0.306393
C	-1.436306	3.366989	0.156090
C	1.436289	3.366956	-0.155979
C	-0.673539	2.123829	0.067004
C	-0.668659	4.604164	0.096254
C	0.668629	4.604139	-0.096185
C	0.673519	2.123804	-0.066785
H	-1.206919	1.183351	0.136290
H	-1.232941	5.528103	0.173924
H	1.232955	5.528051	-0.173888
H	1.206863	1.183298	-0.135961
N	2.730744	3.478791	-0.306343
C	3.607800	2.407962	-0.189031
C	5.551530	0.354315	0.010283
C	4.709389	2.356942	-1.068189
C	3.533946	1.429911	0.827537
C	4.494006	0.434634	0.933070
C	5.641988	1.334738	-0.994804
H	4.790851	3.117651	-1.838067
H	2.749183	1.494689	1.574203
H	4.436027	-0.287261	1.740446
H	6.457157	1.293317	-1.708807
N	6.510360	-0.674513	0.103850
C	6.123259	-1.975974	0.516770
C	5.364790	-4.553481	1.328819
C	6.922627	-2.699913	1.413269
C	4.941766	-2.553435	0.028741
C	4.564358	-3.829248	0.442033
C	6.546776	-3.982572	1.806647
H	7.834397	-2.252485	1.794523
H	4.327034	-1.997886	-0.671570
H	3.646897	-4.264323	0.055898
H	7.175664	-4.531981	2.501414
H	5.071491	-5.550562	1.642937
C	7.872573	-0.415155	-0.200603
C	10.567861	0.087682	-0.798088
C	8.488418	0.763219	0.245310
C	8.616787	-1.340612	-0.946388
C	9.957177	-1.091048	-1.233049
C	9.824233	1.013214	-0.062039
H	7.915735	1.475844	0.829421
H	8.139382	-2.250408	-1.294760
H	10.522143	-1.816567	-1.811399
H	10.288751	1.930162	0.289318
H	11.610679	0.282348	-1.029400

*A.3.1.5 **OTPA-BZN-210**, **LEB** State, trans-syn Conformer*

H	-1.874706	11.627682	1.001745
C	-1.950425	10.553708	1.148461

C	-2.128361	7.794916	1.499946
C	-0.927194	9.730386	0.684381
C	-3.072854	10.010064	1.778147
C	-3.154371	8.625628	1.944853
C	-1.001707	8.338951	0.862057
H	-0.066187	10.158558	0.182521
H	-3.871571	10.654977	2.131792
H	-4.017635	8.185844	2.436848
H	-2.191782	6.721361	1.641462
N	0.027578	7.492055	0.390829
C	1.385349	7.881192	0.451156
C	4.097777	8.623114	0.573057
C	1.875176	8.618500	1.541871
C	2.271974	7.516462	-0.575156
C	3.615092	7.879595	-0.506480
C	3.216302	8.991498	1.592400
H	1.200494	8.894743	2.344986
H	1.900551	6.947758	-1.420817
H	4.285223	7.588525	-1.310794
H	3.576314	9.561594	2.444496
H	5.144008	8.909652	0.620165
C	-0.310291	6.221695	-0.156488
C	-0.961893	3.699368	-1.256520
C	0.340923	5.061117	0.275778
C	-1.302863	6.106281	-1.138454
C	-1.626573	4.867506	-1.675873
C	0.027919	3.817841	-0.264043
H	1.098736	5.134745	1.049473
H	-1.819022	6.997091	-1.482059
H	-2.391044	4.797580	-2.445424
H	0.528638	2.933624	0.111449
N	-1.338204	2.479548	-1.814857
C	-0.652879	1.258396	-1.777381
C	0.652879	-1.258396	-1.777381
C	0.749008	1.175243	-1.804568
C	-1.385349	0.060585	-1.780421
C	-0.749008	-1.175243	-1.804568
C	1.385349	-0.060585	-1.780421
H	1.344434	2.080055	-1.848211
H	-2.471616	0.100994	-1.779357
H	-1.344434	-2.080055	-1.848211
H	2.471616	-0.100994	-1.779357
N	1.338204	-2.479548	-1.814857
C	0.961893	-3.699368	-1.256520
C	0.310291	-6.221695	-0.156488
C	1.626573	-4.867506	-1.675873
C	-0.027919	-3.817841	-0.264043
C	-0.340923	-5.061117	0.275778
C	1.302863	-6.106281	-1.138454
H	2.391044	-4.797580	-2.445424
H	-0.528638	-2.933624	0.111449
H	-1.098736	-5.134745	1.049473
H	1.819022	-6.997091	-1.482059
N	-0.027578	-7.492055	0.390829
C	-1.385349	-7.881192	0.451156
C	-4.097777	-8.623114	0.573057
C	-1.875176	-8.618500	1.541871
C	-2.271974	-7.516462	-0.575156
C	-3.615092	-7.879595	-0.506480
C	-3.216302	-8.991498	1.592400
H	-1.200494	-8.894743	2.344986
H	-1.900551	-6.947758	-1.420817
H	-4.285223	-7.588525	-1.310794
H	-3.576314	-9.561594	2.444496

H	-5.144008	-8.909652	0.620165	H	2.191782	-6.721361	1.641462
C	1.001707	-8.338951	0.862057	H	0.066187	-10.158558	0.182521
C	3.072854	-10.010064	1.778147	H	1.874706	-11.627682	1.001745
C	2.128361	-7.794916	1.499946	H	4.017635	-8.185844	2.436848
C	0.927194	-9.730386	0.684381	H	3.871571	-10.654977	2.131792
C	1.950425	-10.553708	1.148461	H	-2.267477	2.448173	-2.210415
C	3.154371	-8.625628	1.944853	H	2.267477	-2.448173	-2.210415

A.3.2 Optimised Structures of Other **210** Oligomers

Structures of all oligomers in this section are in the *trans-syn* conformer.

A.3.2.1 ***OTPA-FLR-210, EB*** *State*

H	-13.526053	1.690729	-1.064473	H	-11.807819	-2.580383	2.927039
C	-12.569832	1.936777	-0.611516	H	-10.825209	-4.608544	1.867351
C	-10.105804	2.551450	0.542525	C	-8.019754	0.515146	-0.034580
C	-11.598888	0.945740	-0.485120	C	-5.289504	1.059945	-0.597239
C	-12.314127	3.239831	-0.177561	C	-6.997116	-0.057004	0.742942
C	-11.076001	3.540459	0.395247	C	-7.660679	1.389758	-1.077477
C	-10.358861	1.245730	0.097424	C	-6.329858	1.677834	-1.328206
H	-11.793294	-0.063091	-0.833587	C	-5.664092	0.197072	0.461249
H	-13.070552	4.011395	-0.284168	H	-7.259821	-0.695696	1.579440
H	-10.866681	4.547625	0.744299	H	-8.437287	1.846849	-1.681001
H	-9.149984	2.782311	1.000798	H	-6.058807	2.360199	-2.127694
N	-9.373399	0.234192	0.239073	H	-4.895993	-0.222747	1.102376
C	-9.758990	-1.059911	0.675350	N	-3.989431	1.424664	-0.890562
C	-10.527756	-3.618663	1.534887	H	-2.049489	-2.733936	-0.642575
C	-10.696015	-1.208041	1.708350	C	-1.952386	-1.652454	-0.676500
C	-9.210728	-2.203126	0.075166	C	-1.641301	1.166747	-0.910034
C	-9.588467	-3.471114	0.511298	C	-0.657735	-1.053936	-0.687159
C	-11.081133	-2.480241	2.125817	C	-3.062979	-0.862860	-0.733329
H	-11.116946	-0.324478	2.176321	C	-2.970425	0.589985	-0.821020
H	-8.492106	-2.089320	-0.729543	C	-0.539775	0.378759	-0.821326
H	-9.156484	-4.347861	0.037156	H	-4.046046	-1.317067	-0.764709

H	-1.577472	2.245364	-1.016838
C	0.617127	-1.629222	-0.625773
C	3.385167	-2.262589	-0.551762
C	1.024502	-2.994130	-0.540068
C	1.619572	-0.593382	-0.709871
C	2.947192	-0.881405	-0.672468
C	2.354353	-3.289596	-0.529769
H	0.280557	-3.784117	-0.495239
H	3.689300	-0.097870	-0.772819
H	2.703950	-4.315325	-0.472399
C	0.929750	0.749900	-0.851873
H	1.204098	1.250899	-1.788370
H	1.197752	1.434823	-0.038330
N	4.631298	-2.693100	-0.510920
C	5.715421	-1.858413	-0.313330
C	8.073870	-0.325539	0.081890
C	6.928066	-2.192135	-0.958371
C	5.736111	-0.757958	0.577502
C	6.891720	-0.020279	0.780063
C	8.070976	-1.428151	-0.792826
H	6.933693	-3.047606	-1.626518
H	4.850049	-0.526397	1.158933
H	6.891775	0.797882	1.492335
H	8.976641	-1.683348	-1.332203
N	9.238739	0.444931	0.270586
C	9.141640	1.846175	0.472669
C	8.956037	4.618428	0.868901
C	9.936211	2.477831	1.440498
C	8.254244	2.613688	-0.296210
C	8.158872	3.988094	-0.089703
C	9.847032	3.855560	1.627597
H	10.619322	1.884252	2.038737
H	7.645576	2.127022	-1.050922
H	7.467954	4.570448	-0.692688
H	10.468385	4.331876	2.380647
H	8.884383	5.690925	1.022110
C	10.516051	-0.173809	0.270375
C	13.045432	-1.389302	0.273544
C	10.713800	-1.394949	0.931305
C	11.594779	0.434809	-0.387587
C	12.850782	-0.167831	-0.375851
C	11.969047	-1.999364	0.922148
H	9.881921	-1.862218	1.447605
H	11.441207	1.377125	-0.902748
H	13.677622	0.314512	-0.889404
H	12.108143	-2.945222	1.437936
H	14.023993	-1.859701	0.274608

*A.3.2.2 **OTPB-BZN-210, EB** State*

H	-14.227944	-2.309348	-1.484045
C	-13.275525	-2.597498	-1.048086
C	-10.819628	-3.322227	0.050195
C	-12.292637	-1.631429	-0.838515
C	-13.034363	-3.930722	-0.710101
C	-11.801754	-4.288880	-0.160274
C	-11.048989	-1.978048	-0.285779
H	-12.480313	-0.601736	-1.127918
H	-13.799887	-4.683647	-0.873727
H	-11.606581	-5.321820	0.113813
H	-9.873730	-3.606260	0.501703
C	-10.003473	-0.949500	-0.062292

C	-8.029067	0.993188	0.361272
C	-10.349433	0.340715	0.360987
C	-8.650873	-1.249178	-0.270014
C	-7.651383	-0.288495	-0.062605
C	-9.373377	1.322636	0.577027
H	-11.393948	0.584164	0.525094
H	-8.372559	-2.245619	-0.596690
H	-7.265239	1.746130	0.524926
C	-9.755875	2.684053	1.025528
C	-10.481549	5.268835	1.878415
C	-10.806959	2.872167	1.937772
C	-9.075746	3.816524	0.548789
C	-9.434199	5.095734	0.971209
C	-11.166612	4.151240	2.359571
H	-11.329202	2.007771	2.336934
H	-8.276681	3.693994	-0.176312
H	-8.899957	5.958882	0.584225
H	-11.977724	4.273977	3.071757
H	-10.761272	6.265463	2.207339
C	-6.225347	-0.618423	-0.287538
C	-3.492460	-1.238297	-0.727536
C	-5.218779	-0.077326	0.529598
C	-5.835389	-1.495439	-1.316072
C	-4.501341	-1.819791	-1.518200
C	-3.877675	-0.371994	0.315388
H	-5.491995	0.562615	1.362999
H	-6.589295	-1.919089	-1.972324
H	-4.211580	-2.503817	-2.309586
H	-3.121767	0.028348	0.983378
N	-2.174486	-1.637132	-0.947739
C	-1.178850	-0.797085	-0.964338
C	1.183763	0.852710	-0.923507
C	-1.271164	0.663673	-0.976247
C	0.163354	-1.368504	-1.048994
C	1.276128	-0.605777	-1.005989
C	-0.158383	1.427599	-0.981458
H	-2.252709	1.120486	-1.019588
H	0.220071	-2.449266	-1.133541
H	2.257692	-1.060038	-1.070629
H	-0.215022	2.511189	-1.013649
N	2.179487	1.690849	-0.865401
C	3.496941	1.280890	-0.663170
C	6.228339	0.636495	-0.250493
C	4.507461	1.898018	-1.424229
C	3.879672	0.365483	0.337933
C	5.219994	0.059067	0.539248
C	5.840710	1.562087	-1.236501
H	4.219509	2.619245	-2.182552
H	3.122222	-0.064955	0.985113
H	5.491814	-0.620282	1.341360
H	6.596320	2.014968	-1.870963
C	7.652874	0.293178	-0.040305
C	10.348851	-0.362461	0.357692
C	8.656503	1.256318	-0.214736
C	8.025656	-1.004576	0.336914
C	9.368614	-1.346624	0.542305
C	10.008372	0.942675	-0.022030
H	8.378710	2.277033	-0.455700
H	7.263750	-1.771957	0.424602
H	11.392492	-0.615912	0.512016
C	9.745437	-2.727853	0.929982
C	10.458086	-5.350349	1.671545
C	10.915585	-3.323641	0.431842
C	8.939273	-3.472208	1.806703

C	9.291185	-4.770207	2.173321	C	10.948419	2.942390	-1.213376
C	11.268873	-4.621110	0.799352	C	12.181206	2.015645	0.641296
H	11.539086	-2.774387	-0.267258	C	13.166551	2.987067	0.472004
H	8.043140	-3.020291	2.221547	C	11.932790	3.914804	-1.382357
H	8.657316	-5.325771	2.858693	H	10.098047	2.914583	-1.888282
H	12.174402	-5.066010	0.396554	H	12.270715	1.293943	1.447733
H	10.732897	-6.361501	1.957447	H	14.024781	3.003757	1.137840
C	11.056567	1.977132	-0.198944	H	11.833500	4.647641	-2.178140
C	13.046614	3.941163	-0.540519	H	13.813998	4.698430	-0.672275

*A.3.2.3 **OTPB-FLR-210**, **EB** State*

H	-15.796385	2.790095	-1.498826	C	-12.456138	-4.796273	2.236118
C	-14.824628	3.047323	-1.086844	C	-12.801067	-2.870075	0.813598
C	-12.320487	3.691159	-0.048287	C	-10.823161	-3.011957	2.186680
C	-13.895201	2.040381	-0.831337	C	-11.250416	-4.245538	2.675382
C	-14.505377	4.381337	-0.825197	C	-13.229949	-4.102690	1.303306
C	-13.248948	4.698769	-0.305052	H	-13.396964	-2.349979	0.069489
C	-12.628143	2.345692	-0.307959	H	-9.896920	-2.579510	2.553326
H	-14.143056	1.008306	-1.061035	H	-10.644881	-4.772836	3.407154
H	-15.229078	5.166287	-1.024708	H	-14.165679	-4.525839	0.948971
H	-12.993385	5.732506	-0.089959	H	-12.789741	-5.756996	2.617459
H	-11.355837	3.945728	0.380486	C	-7.887425	0.720254	-0.243677
C	-11.641060	1.271791	-0.038403	C	-5.119362	1.157526	-0.724699
C	-9.775418	-0.749467	0.495104	C	-6.906936	0.151550	0.587160
C	-12.056894	0.028166	0.456198	C	-7.452355	1.532131	-1.307761
C	-10.274081	1.486169	-0.256662	C	-6.103444	1.765742	-1.530814
C	-9.327223	0.486065	0.006065	C	-5.552956	0.356826	0.354734
C	-11.135458	-0.992512	0.726758	H	-7.211541	-0.437213	1.447269
H	-13.106811	-0.130831	0.678987	H	-8.184164	1.974363	-1.976918
H	-9.942180	2.447048	-0.635528	H	-5.779973	2.398125	-2.351702
H	-9.059931	-1.549945	0.651547	H	-4.818216	-0.060322	1.035988
C	-11.591018	-2.304291	1.247435	N	-3.788387	1.469968	-0.967234

H	-2.126991	-2.805043	-0.832399
C	-1.961598	-1.731624	-0.840519
C	-1.460636	1.072596	-0.985609
C	-0.628235	-1.215573	-0.835655
C	-3.016069	-0.872437	-0.876386
C	-2.827057	0.577261	-0.922694
C	-0.415223	0.213169	-0.922308
H	-4.028288	-1.256799	-0.912258
H	-1.328697	2.147811	-1.056177
C	0.600241	-1.873712	-0.790820
C	3.316229	-2.695577	-0.728976
C	0.912038	-3.268576	-0.742938
C	1.673187	-0.903081	-0.838645
C	2.975445	-1.281083	-0.807286
C	2.215623	-3.653932	-0.735217
H	0.114723	-4.005350	-0.723070
H	3.772915	-0.549960	-0.872218
H	2.496222	-4.701562	-0.705689
C	1.075221	0.486642	-0.936650
H	1.386770	0.998989	-1.854913
H	1.383785	1.123840	-0.099332
N	4.525737	-3.205038	-0.697374
C	5.662348	-2.429398	-0.505786
C	8.100429	-1.020499	-0.112391
C	6.812877	-2.740901	-1.258588
C	5.770361	-1.422720	0.478447
C	6.966153	-0.742520	0.669677
C	7.994620	-2.036459	-1.080176
H	6.744590	-3.526804	-2.004305
H	4.922146	-1.214983	1.122660
H	7.030631	-0.001156	1.460465
H	8.848826	-2.266465	-1.709735
C	9.366636	-0.280364	0.087721
C	11.762760	1.125859	0.466416
C	10.604629	-0.919423	-0.069809
C	9.352926	1.077145	0.438506
C	10.541476	1.792754	0.631349
C	11.809869	-0.229996	0.115629
H	10.630982	-1.969936	-0.339508
H	8.402171	1.584934	0.562447
H	12.689943	1.669913	0.613096
C	10.507753	3.228769	1.002463
C	10.443224	5.955312	1.707777
C	11.445684	3.761851	1.901610
C	9.537053	4.088763	0.463482
C	9.504485	5.437927	0.812781
C	11.414248	5.111180	2.250432
H	12.189126	3.108153	2.347982
H	8.818601	3.701148	-0.252678
H	8.749915	6.087565	0.378256
H	12.144385	5.501533	2.953796
H	10.418385	7.006558	1.979735
C	13.111102	-0.921828	-0.055517
C	15.582006	-2.234967	-0.380971
C	13.277180	-2.254734	0.354532
C	14.207494	-0.259788	-0.631759
C	15.430484	-0.909210	-0.792466
C	14.499640	-2.904988	0.193013
H	12.448864	-2.776176	0.824905
H	14.092402	0.763082	-0.977843
H	16.263619	-0.381099	-1.247648
H	14.608830	-3.933897	0.524093
H	16.534685	-2.741285	-0.506474

A.3.2.4 ***OTPT-BZN-210, EB*** *State*

H	14.200195	-2.084038	-1.057154
C	13.152401	-2.246976	-1.291786
C	10.457495	-2.664063	-1.894792
C	12.186883	-1.383030	-0.781808
C	12.774888	-3.320294	-2.103090
C	11.425624	-3.526188	-2.402819
C	10.830180	-1.584431	-1.079207
H	12.467381	-0.547019	-0.151848
H	13.529139	-3.993584	-2.500187
H	11.128886	-4.359427	-3.032989
H	9.408106	-2.813648	-2.120283
C	9.802797	-0.667201	-0.538209
N	7.941447	0.997669	0.442765
N	10.212100	0.343278	0.244741
N	8.521214	-0.898048	-0.861153
C	7.624288	-0.040325	-0.348202
C	9.246766	1.150275	0.712368
C	9.648418	2.279903	1.579650
C	10.409335	4.417483	3.221337
C	10.998942	2.475937	1.907107
C	8.682939	3.165691	2.082453
C	9.063014	4.227981	2.898389
C	11.375441	3.539003	2.723714
H	11.738842	1.787991	1.515025
H	7.642134	3.008823	1.824462
H	8.309791	4.909290	3.283019
H	12.422604	3.683470	2.972798
H	10.704421	5.246533	3.858126
C	6.201244	-0.252501	-0.672958
C	3.481089	-0.664986	-1.285262
C	5.216265	0.603890	-0.156261
C	5.809513	-1.307432	-1.515788
C	4.474796	-1.497975	-1.836042
C	3.875369	0.401787	-0.450781
H	5.518236	1.427777	0.479772
H	6.570244	-1.963055	-1.922898
H	4.171207	-2.301048	-2.499671
H	3.123063	1.083055	-0.066639
N	2.160636	-0.865057	-1.679428
C	1.171080	-0.896934	-0.835536
C	-1.171080	-0.896704	0.835701
C	1.280548	-0.939013	0.624151
C	-0.176677	-0.960236	-1.398865
C	-1.280550	-0.938925	-0.623982
C	0.176674	-0.960068	1.399039
H	2.268016	-0.985498	1.067875
H	-0.243250	-1.011289	-2.480964
H	-2.268021	-0.985297	-1.067707
H	0.243242	-1.011008	2.481142
N	-2.160628	-0.864680	1.679595
C	-3.481083	-0.664656	1.285398
C	-6.201242	-0.252338	0.673010
C	-4.474759	-1.497651	1.836208
C	-3.875392	0.402052	0.450845
C	-5.216287	0.604069	0.156281
C	-5.809487	-1.307187	1.515920
H	-4.171155	-2.300666	2.499901
H	-3.123107	1.083325	0.066669
H	-5.518286	1.427892	-0.479821
H	-6.570197	-1.962816	1.923059

C	-7.624289	-0.040247	0.348196
N	-10.212105	0.343236	-0.244799
N	-8.521187	-0.897986	0.861162
N	-7.941479	0.997732	-0.442779
C	-9.246801	1.150278	-0.712405
C	-9.802776	-0.667197	0.538197
C	-9.648482	2.279853	-1.579742
C	-10.409461	4.417342	-3.221518
C	-10.999007	2.475810	-1.907240
C	-8.683033	3.165669	-2.082551
C	-9.063139	4.227914	-2.898531
C	-11.375537	3.538832	-2.723890
H	-11.738884	1.787840	-1.515156
H	-7.642226	3.008860	-1.824530
H	-8.309938	4.909246	-3.283166
H	-12.422701	3.683242	-2.973005
H	-10.704571	5.246359	-3.858339
C	-10.830122	-1.584477	1.079176
C	-12.774757	-3.320438	2.103031
C	-10.457384	-2.664161	1.894668
C	-12.186843	-1.383075	0.781853
C	-13.152324	-2.247067	1.291821
C	-11.425477	-3.526335	2.402680
H	-9.407981	-2.813743	2.120100
H	-12.467382	-0.547023	0.151966
H	-14.200132	-2.084125	1.057256
H	-11.128697	-4.359616	3.032775
H	-13.528980	-3.993766	2.500116

*A.3.2.5 **OTPT-FLR-210**, **EB** State*

H	15.846363	-1.405062	-2.175563
C	14.788567	-1.514649	-2.395946
C	12.067917	-1.795307	-2.960910
C	13.845513	-0.871868	-1.598255
C	14.375674	-2.298252	-3.476769
C	13.013577	-2.436566	-3.756661
C	12.476191	-1.006775	-1.874131
H	14.153109	-0.261472	-0.757295
H	15.112333	-2.799055	-4.098428
H	12.689278	-3.044727	-4.595986
H	11.008863	-1.894877	-3.168115
C	11.472673	-0.323914	-1.027199
N	9.655795	0.915369	0.508883
N	11.918181	0.421967	-0.003662
N	10.177120	-0.489966	-1.330964
C	9.301276	0.148566	-0.536455
C	10.972851	1.022346	0.736846
C	11.413074	1.855610	1.878244
C	12.245866	3.431983	4.038427
C	12.779417	2.004404	2.161703
C	10.468122	2.504683	2.687713
C	10.883809	3.287929	3.761248
C	13.191723	2.788437	3.236055
H	13.503507	1.500766	1.532044
H	9.414737	2.385328	2.462674
H	10.146041	3.786908	4.382734
H	14.251098	2.898416	3.448499
H	12.568821	4.043399	4.876159
C	7.865713	-0.003046	-0.827654
C	5.110412	-0.308222	-1.376943
C	6.902837	0.645656	-0.036881
C	7.432819	-0.789324	-1.911053

C	6.083840	-0.922915	-2.193836
C	5.549720	0.496040	-0.300213
H	7.233866	1.269732	0.785205
H	8.174306	-1.282218	-2.529016
H	5.749049	-1.518246	-3.037192
H	4.816324	1.024683	0.300072
N	3.778446	-0.430867	-1.738042
H	2.146966	-1.655278	2.367556
C	1.974668	-1.323906	1.347826
C	1.451979	-0.564506	-1.354214
C	0.637596	-1.151340	0.869292
C	3.022304	-1.089404	0.513191
C	2.821277	-0.669781	-0.874205
C	0.413412	-0.777245	-0.511361
H	4.037809	-1.244860	0.857211
H	1.313140	-0.286561	-2.394221
C	-0.584820	-1.312379	1.518066
C	-3.291048	-1.504586	2.341734
C	-0.884358	-1.702377	2.861619
C	-1.665421	-1.046456	0.590899
C	-2.963898	-1.133447	0.971227
C	-2.183957	-1.810657	3.242928
H	-0.080748	-1.915439	3.559708
H	-3.768911	-0.959217	0.266646
H	-2.456254	-2.108933	4.249847
C	-1.078508	-0.698844	-0.762470
H	-1.386651	0.298923	-1.096719
H	-1.398910	-1.405010	-1.537838
N	-4.497184	-1.634784	2.840201
C	-5.637270	-1.212336	2.174537
C	-8.068096	-0.397136	0.985672
C	-6.771846	-2.051795	2.197340
C	-5.758643	0.062362	1.575243
C	-6.954771	0.459687	0.997489
C	-7.956080	-1.659609	1.595870
H	-6.688278	-3.019580	2.681272
H	-4.914334	0.743441	1.601449
H	-7.044392	1.441506	0.547080
H	-8.816814	-2.318179	1.597917
C	-9.332194	0.024317	0.358580
N	-11.635269	0.791212	-0.787845
N	-10.365240	-0.834941	0.381500
N	-9.381972	1.244213	-0.203272
C	-10.551720	1.583512	-0.764113
C	-11.494809	-0.408701	-0.202255
C	-10.655046	2.917113	-1.397869
C	-10.849679	5.440386	-2.597800
C	-11.852371	3.320971	-2.008304
C	-9.556188	3.790045	-1.394514
C	-9.654656	5.044150	-1.991369
C	-11.947371	4.575716	-2.604544
H	-12.696710	2.641612	-2.007250
H	-8.635021	3.471167	-0.920904
H	-8.799697	5.713869	-1.984065
H	-12.877569	4.880480	-3.075025
H	-10.925195	6.419003	-3.063135
C	-12.661804	-1.319126	-0.201031
C	-14.870292	-3.041760	-0.198073
C	-12.571861	-2.585653	0.396766
C	-13.869292	-0.924273	-0.797295
C	-14.966242	-1.781930	-0.794965
C	-13.670700	-3.440793	0.397353
H	-11.636398	-2.883807	0.855493
H	-13.931639	0.055254	-1.256733

H	-15.897044	-1.468560	-1.258559	H	-15.726818	-3.709812	-0.196871
H	-13.592682	-4.419188	0.862285				

A.3.3 Optimised Structures of **OTPA-BZN-430** Oligomers

*A.3.3.1 Star-Shaped **OTPA-BZN-430**, **EB** State*

H	-0.489143	-0.110642	1.103620	H	2.270625	-3.765089	-1.326419
C	0.024534	0.469055	0.344235	H	3.444460	-0.224326	0.809327
C	1.422901	1.980494	-1.531177	H	5.796354	-0.951509	0.732769
C	1.031168	-0.138797	-0.423947	H	4.629730	-4.521735	-1.352191
C	-0.308947	1.800628	0.146076	N	6.689408	-3.274658	-0.396009
C	0.372655	2.585818	-0.810211	N	-2.720796	-5.272618	0.721263
C	1.725810	0.638174	-1.367458	N	0.146827	3.942780	-1.003977
H	-1.064856	2.261495	0.773338	C	-3.999504	-5.015003	0.815371
H	2.509673	0.181514	-1.961874	C	-6.866185	-4.708931	0.938705
H	1.967638	2.581372	-2.252268	C	-4.896043	-6.161805	0.895830
N	1.349014	-1.503406	-0.238034	C	-4.620107	-3.697744	0.931331
C	0.315123	-2.438950	-0.003115	C	-5.963474	-3.567363	1.017370
C	-1.767601	-4.291058	0.480943	C	-6.241521	-6.029050	0.926293
C	0.484654	-3.477531	0.928594	H	-4.424779	-7.139727	0.916638
C	-0.894891	-2.354289	-0.711044	H	-3.980825	-2.825072	0.993732
C	-1.922067	-3.253202	-0.464962	H	-6.429588	-2.593276	1.130723
C	-0.525523	-4.402494	1.139688	H	-6.875079	-6.905516	0.992556
H	1.417700	-3.556913	1.475854	C	7.740724	-2.533695	-0.631169
H	-1.019624	-1.581088	-1.461596	C	10.209389	-1.087689	-1.005018
H	-2.835775	-3.193581	-1.047009	C	9.041865	-3.167184	-0.452346
H	-0.389091	-5.210716	1.850975	C	7.750338	-1.161614	-1.132559
C	2.696140	-1.928930	-0.277058	C	8.914339	-0.502609	-1.330779
C	5.396103	-2.768408	-0.371511	C	10.203352	-2.490736	-0.598246
C	3.044623	-3.149690	-0.880872	H	9.030662	-4.217821	-0.178761
C	3.708059	-1.147464	0.304395	H	6.806826	-0.694210	-1.388371
C	5.033864	-1.550779	0.246330	H	8.930279	0.507284	-1.729179
C	4.363752	-3.573417	-0.896456	H	11.151561	-2.996924	-0.461553

C	-1.051520	4.465990	-1.032776
C	-3.579310	5.856880	-1.006775
C	-1.132605	5.921178	-1.064146
C	-2.318398	3.744103	-1.119516
C	-3.496677	4.407680	-1.136576
C	-2.311751	6.582195	-1.023449
H	-0.187712	6.454209	-1.107121
H	-2.296727	2.665137	-1.217047
H	-4.440723	3.879388	-1.228595
H	-2.331996	7.665116	-1.053356
N	-8.147864	-4.446166	0.959313
N	11.257898	-0.325272	-1.175432
N	-4.780215	6.374369	-0.959837
C	-9.124489	-5.404057	0.726850
C	-11.263807	-7.212482	0.287722
C	-9.037590	-6.411696	-0.260371
C	-10.332534	-5.297314	1.448032
C	-11.366273	-6.199629	1.260083
C	-10.089800	-7.286023	-0.483777
H	-8.159774	-6.462550	-0.895984
H	-10.420557	-4.511426	2.191420
H	-12.268028	-6.121986	1.857196
H	-10.014618	-8.030664	-1.268593
C	12.535274	-0.685183	-0.761785
C	15.209985	-1.231835	-0.002582
C	12.829798	-1.307369	0.470769
C	13.618884	-0.299646	-1.577816
C	14.926491	-0.583156	-1.219147
C	14.140352	-1.574534	0.841724
H	12.023329	-1.553302	1.153411
H	13.405408	0.220092	-2.506662
H	15.743220	-0.289544	-1.869327
H	14.343263	-2.049349	1.795317
C	-5.021219	7.709717	-0.669503
C	-5.719173	10.398358	-0.099870
C	-4.333341	8.448681	0.319502
C	-6.099447	8.340392	-1.325651
C	-6.421198	9.663846	-1.074353
C	-4.685143	9.758260	0.607220
H	-3.560085	7.964423	0.906681
H	-6.651107	7.775033	-2.069996
H	-7.227325	10.138472	-1.622629
H	-4.165817	10.295702	1.393038
N	-6.056109	11.736484	0.176986
N	16.540854	-1.511077	0.368817
N	-12.319305	-8.119090	0.076075
C	17.492203	-1.893188	-0.612851
C	19.379210	-2.654784	-2.545680
C	18.794825	-1.375203	-0.573171
C	17.142226	-2.797087	-1.626611
C	18.079405	-3.164656	-2.589751
C	19.730826	-1.763048	-1.529514
H	19.065196	-0.673155	0.208451
H	16.137517	-3.205575	-1.653058
H	17.794613	-3.865361	-3.369479
H	20.736373	-1.354262	-1.486665
H	20.109207	-2.949305	-3.293487
C	16.941624	-1.413732	1.727642
C	17.744072	-1.219840	4.409265
C	16.521979	-0.332052	2.515306
C	17.767662	-2.396326	2.291727
C	18.171005	-2.291339	3.621264
C	16.914873	-0.244964	3.849184
H	15.889903	0.432950	2.076690

H	18.089410	-3.234878	1.683187
H	18.811312	-3.059312	4.045846
H	16.582444	0.597990	4.448304
H	18.054451	-1.144892	5.447010
C	-7.407105	12.169017	0.105804
C	-10.071394	13.037110	-0.026611
C	-7.721330	13.399142	-0.489119
C	-8.435862	11.377554	0.636272
C	-9.758746	11.808178	0.559384
C	-9.044966	13.830402	-0.544888
H	-6.925151	14.009553	-0.902057
H	-8.192030	10.430012	1.105029
H	-10.546417	11.185422	0.973760
H	-9.274991	14.785615	-1.008192
H	-11.102626	13.372929	-0.078020
C	-5.048523	12.666966	0.545659
C	-3.065304	14.514452	1.269689
C	-3.824380	12.695013	-0.137974
C	-5.273413	13.571983	1.592639
C	-4.288968	14.493609	1.943103
C	-2.838746	13.607783	0.231299
H	-3.653866	12.001048	-0.954294
H	-6.219206	13.547707	2.123511
H	-4.475903	15.189450	2.756029
H	-1.894932	13.619134	-0.306371
H	-2.297751	15.229439	1.549871
C	-12.046137	-9.462926	-0.292864
C	-11.518059	-12.121646	-1.016401
C	-11.021149	-10.178805	0.342511
C	-12.806184	-10.088489	-1.291321
C	-12.546084	-11.411812	-1.641376
C	-10.756121	-11.495773	-0.026767
H	-10.439129	-9.698018	1.121689
H	-13.596791	-9.533400	-1.785038
H	-13.142399	-11.884782	-2.416413
H	-9.959434	-12.039119	0.473298
H	-11.313702	-13.150570	-1.296391
C	-13.668765	-7.698641	0.216282
C	-16.338736	-6.881287	0.485289
C	-14.596501	-8.518812	0.873860
C	-14.087522	-6.467378	-0.307860
C	-15.412443	-6.061069	-0.163250
C	-15.923548	-8.112844	0.997543
H	-14.270985	-9.469898	1.281904
H	-13.371858	-5.836808	-0.824811
H	-15.723956	-5.104733	-0.573548
H	-16.632502	-8.757680	1.508952
H	-17.372089	-6.564799	0.589562

*A.3.3.2 Linear/Coiled **OTPA-BZN-430**, **EB** State*

H	9.140045	-0.685705	-1.507890
C	8.603136	-0.136370	-0.741357
C	7.197644	1.262069	1.221293
C	8.016385	-0.835158	0.323717
C	8.483940	1.245829	-0.825541
C	7.728015	1.967697	0.119199
C	7.348993	-0.113259	1.323795
H	8.927616	1.784599	-1.656629
H	6.935931	-0.646684	2.174065
H	6.689038	1.810093	2.007771
N	8.046364	-2.255308	0.384933
C	9.261366	-2.949440	0.183128

C	11.692421	-4.299802	-0.218783
C	9.290981	-4.163419	-0.520946
C	10.461192	-2.415956	0.679877
C	11.664537	-3.085167	0.470804
C	10.498077	-4.833282	-0.708482
H	8.370073	-4.573512	-0.920827
H	10.441395	-1.480012	1.227994
H	12.584080	-2.658778	0.861667
H	10.504122	-5.771953	-1.255375
C	6.812870	-2.927835	0.519151
C	4.279653	-4.143069	0.872816
C	6.685398	-4.117757	1.260234
C	5.665845	-2.390875	-0.088273
C	4.425360	-2.971194	0.100689
C	5.446809	-4.730671	1.402668
H	7.562665	-4.555571	1.724311
H	5.761250	-1.509001	-0.711630
H	3.557524	-2.552714	-0.388510
H	5.355517	-5.647399	1.976789
N	3.049195	-4.774551	1.031556
N	7.613543	3.349823	-0.024037
C	1.970323	-4.076623	1.283342
C	-0.527056	-2.678721	1.661551
C	0.681785	-4.750446	1.158665
C	1.933171	-2.689354	1.732688
C	0.759891	-2.052140	1.933781
C	-0.495352	-4.093088	1.290873
H	0.710747	-5.808132	0.914012
H	2.866447	-2.184201	1.945501
H	0.734044	-1.032121	2.296633
H	-1.434179	-4.621691	1.171349
C	6.470135	3.962925	0.142731
C	4.047854	5.478086	0.588914
C	5.168280	3.317166	0.286842
C	6.476074	5.419722	0.184435
C	5.348165	6.122389	0.433051
C	4.032623	4.021175	0.496202
H	5.116134	2.240088	0.215921
H	7.435591	5.910154	0.053646
H	5.359134	7.205573	0.503159
H	3.100101	3.489298	0.635340
N	-1.583499	-1.937000	1.862501
N	3.029184	6.265134	0.825168
C	-2.893330	-2.319286	1.592881
C	-5.635827	-2.913827	1.198931
C	-3.332444	-2.964017	0.417561
C	-3.870900	-1.915268	2.525919
C	-5.208524	-2.222604	2.346896
C	-4.681425	-3.250228	0.223284
H	-2.614154	-3.223303	-0.353837
H	-3.547036	-1.364505	3.403120
H	-5.939423	-1.924238	3.090426
H	-4.999665	-3.759662	-0.680500
C	1.704912	5.852357	0.848906
C	-1.066819	5.242365	0.960800
C	1.128970	4.902875	-0.025826
C	0.839301	6.516995	1.746025
C	-0.507112	6.201238	1.826458
C	-0.224972	4.614688	0.026179
H	1.740328	4.441571	-0.793819
H	1.264588	7.265554	2.406910
H	-1.139414	6.704258	2.549632
H	-0.655185	3.902718	-0.665437
N	-2.436507	4.926142	1.003255

N	-6.995908	-3.261263	1.045751
C	-7.748175	-3.714272	2.159561
C	-9.251110	-4.619823	4.351556
C	-9.085488	-3.319897	2.313459
C	-7.169927	-4.567689	3.111351
C	-7.916937	-5.006312	4.202334
C	-9.829845	-3.779123	3.397981
H	-9.533051	-2.655963	1.581573
H	-6.138883	-4.882327	2.990239
H	-7.455806	-5.666670	4.931325
H	-10.864470	-3.465340	3.503716
H	-9.832078	-4.969812	5.199365
C	-7.621776	-3.171372	-0.225344
C	-8.863825	-2.968861	-2.726907
C	-7.455739	-2.019436	-0.997766
C	-8.407373	-4.228345	-0.706061
C	-9.030285	-4.111356	-1.948266
C	-8.041184	-1.921937	-2.273130
H	-6.886532	-1.188636	-0.596188
H	-8.533086	-5.120358	-0.102278
H	-9.646689	-4.926614	-2.315640
H	-9.342299	-2.874867	-3.696078
C	-3.405931	5.919396	1.297421
C	-5.342376	7.868246	1.869975
C	-4.503826	5.608421	2.112857
C	-3.287047	7.212491	0.767299
C	-4.245727	8.179373	1.062594
C	-5.466945	6.576719	2.387584
H	-4.595282	4.608747	2.524129
H	-2.445517	7.451427	0.125802
H	-4.141259	9.176823	0.645210
H	-6.312396	6.322036	3.020341
H	-6.091412	8.622351	2.091583
C	-2.866183	3.600546	0.714250
C	-3.705141	0.981612	0.168385
C	-2.223802	2.510507	1.315415
C	-3.936550	3.372232	-0.160355
C	-4.358488	2.068517	-0.417786
C	-2.630901	1.207901	1.033830
H	-1.409923	2.697685	2.007401
H	-4.433646	4.215462	-0.628379
H	-5.193028	1.903378	-1.091333
H	-2.117936	0.370509	1.497735
H	-4.031049	-0.032373	-0.038827
H	12.631467	-4.822319	-0.373241
N	-7.922936	-0.782004	-3.075604
C	-6.769354	-0.209288	-3.280192
C	-4.326380	1.262665	-3.754775
C	-5.469530	-0.717359	-2.845659
C	-6.761478	1.060767	-4.002030
C	-5.622688	1.760756	-4.200552
C	-4.331911	-0.024404	-3.056682
H	-5.426735	-1.666051	-2.326342
H	-7.723739	1.431218	-4.340955
H	-5.625603	2.718429	-4.711459
H	-3.399815	-0.408886	-2.666932
N	-3.278615	2.016049	-3.964561
C	-2.009023	1.551567	-3.627439
C	0.417540	0.587992	-2.543638
C	-1.534575	0.264946	-3.944437
C	-1.139652	2.414563	-2.934598
C	0.048344	1.940458	-2.399823
C	-0.344136	-0.211144	-3.416081
H	-2.121406	-0.374909	-4.595435

H	-1.447843	3.442047	-2.770373
H	0.689242	2.603212	-1.832556
H	-0.030162	-1.220165	-3.648782
N	1.523662	0.062216	-1.855061
C	1.977595	-1.250531	-2.236233
C	2.821939	-3.797027	-2.996767
C	3.029755	-1.390104	-3.141318
C	1.340096	-2.381378	-1.714351
C	1.758041	-3.653361	-2.102649
C	3.457822	-2.666641	-3.513062
H	3.506092	-0.500336	-3.540725
H	0.522291	-2.252569	-1.013953
H	1.262606	-4.528493	-1.695590
H	4.287265	-2.775813	-4.205115
H	3.156561	-4.788418	-3.286334
C	1.868339	0.480496	-0.539128
C	2.616092	1.129951	2.099450
C	3.165270	0.217024	-0.073930
C	0.950175	1.086581	0.332477
C	1.335478	1.425590	1.628504
C	3.523855	0.510178	1.238700
H	3.886500	-0.234104	-0.742937
H	-0.066834	1.273920	0.014938
H	0.613806	1.899719	2.285969
H	4.525712	0.266548	1.576475
H	2.902013	1.380754	3.115926

A.4 Optimised Structures of Adducts between PANI-CMP Oligomers and CO_2

A.4.1 Optimised Structures of Adducts between **OTPA-BZN-210** Oligomers and CO_2

*A.4.1.1 **OTPA-BZN-210**, **EB** State, with CO_2 Binding on Imine Nitrogen Atom*

H	11.955705	1.395318	-1.135377
C	11.026013	1.687467	-0.655454
C	8.629089	2.421438	0.568576
C	9.990211	0.761480	-0.551872
C	10.868293	2.985514	-0.163818
C	9.663452	3.346596	0.443946
C	8.783715	1.121925	0.064958
H	10.108046	-0.243078	-0.944311
H	11.674943	3.706844	-0.252558
H	9.530602	4.350127	0.837978
H	7.699090	2.698008	1.053999
N	7.733264	0.173686	0.184411
C	8.039726	-1.156373	0.576020
C	8.656207	-3.783102	1.345907
C	8.964422	-1.394070	1.602912
C	7.427447	-2.243608	-0.064263
C	7.729356	-3.545935	0.327888
C	9.274086	-2.700287	1.976029
H	9.435318	-0.552940	2.100591
H	6.718721	-2.060440	-0.865001
H	7.247966	-4.379031	-0.176320
H	9.992317	-2.870495	2.773017
H	8.894671	-4.799568	1.643890
C	6.400139	0.549952	-0.067675
C	3.711917	1.287054	-0.587183
C	5.345585	-0.000794	0.682578
C	6.093694	1.499471	-1.060628
C	4.782009	1.882053	-1.288152
C	4.029795	0.347625	0.419507
H	5.568981	-0.699103	1.481686

H	6.895176	1.941154	-1.642293
H	4.551840	2.623223	-2.046950
H	3.237323	-0.060720	1.037937
N	2.429028	1.743759	-0.855530
C	1.378394	0.963582	-0.858053
C	-1.090142	-0.527954	-0.785714
C	1.370195	-0.496446	-0.841610
C	0.079807	1.614666	-0.971686
C	-1.083273	0.927300	-0.908994
C	0.208001	-1.188640	-0.837552
H	2.316835	-1.022109	-0.883837
H	0.091697	2.693698	-1.091875
H	-2.030335	1.446175	-0.997044
H	0.199048	-2.273010	-0.858683
N	-2.147006	-1.296421	-0.706317
C	-3.426000	-0.799183	-0.483706
C	-6.097540	0.027906	-0.028062
C	-4.504198	-1.414846	-1.151426
C	-3.725779	0.212015	0.454873
C	-5.034842	0.606143	0.687876
C	-5.808030	-0.990193	-0.955342
H	-4.290379	-2.208130	-1.859998
H	-2.925126	0.645416	1.045264
H	-5.245615	1.362382	1.436104
H	-6.616972	-1.452023	-1.510487
N	-7.424654	0.446373	0.192814
C	-7.705915	1.808245	0.477995
C	-8.270621	4.499576	1.037645
C	-8.627723	2.144558	1.479779
C	-7.070047	2.829773	-0.242683
C	-7.346331	4.164599	0.045080
C	-8.911645	3.481958	1.748173
H	-9.116632	1.354815	2.040296
H	-6.363150	2.570199	-1.023669
H	-6.846795	4.945782	-0.520865
H	-9.627989	3.728397	2.526736
H	-8.489105	5.540868	1.254103
C	-8.489811	-0.491305	0.149828
C	-10.603151	-2.335568	0.070176
C	-8.350317	-1.753465	0.745023
C	-9.695747	-0.158886	-0.483965
C	-10.745599	-1.074293	-0.513282
C	-9.398925	-2.669514	0.694458
H	-7.420663	-2.008693	1.242599
H	-9.802230	0.816095	-0.947732
H	-11.674487	-0.803693	-1.007252
H	-9.277316	-3.643837	1.159135
H	-11.420774	-3.049309	0.039217
C	-2.176435	-4.147724	-0.376276
O	-1.195683	-4.320383	-0.991054
O	-3.159568	-4.049161	0.247689

*A.4.1.2 **OTPA-BZN-210**, **EB** State, with CO_2 Binding on Core Unit, near Hydrogen Atoms*

H	11.985839	-1.407591	1.194627
C	11.073379	-1.633910	0.650389
C	8.720698	-2.199629	-0.737912
C	10.064862	-0.675324	0.578702
C	10.909592	-2.881816	0.044220
C	9.726830	-3.159059	-0.645465
C	8.880965	-0.951188	-0.119962
H	10.186681	0.289670	1.059314

H	11.694646	-3.629145	0.107906
H	9.590091	-4.122422	-1.128380
H	7.808458	-2.409897	-1.286237
N	7.858736	0.031068	-0.206276
C	8.212809	1.379827	-0.473851
C	8.924931	4.042834	-0.997424
C	9.189427	1.675039	-1.435729
C	7.596643	2.427718	0.225606
C	7.946495	3.748925	-0.044551
C	9.546189	2.998386	-1.686229
H	9.663440	0.864659	-1.979347
H	6.847615	2.199421	0.976496
H	7.461633	4.551096	0.504496
H	10.304486	3.213215	-2.433785
H	9.200498	5.073326	-1.199950
C	6.507945	-0.329337	-0.040612
C	3.783881	-1.035250	0.307457
C	5.499208	0.306813	-0.786361
C	6.137898	-1.347210	0.858495
C	4.809326	-1.712174	1.000824
C	4.165801	-0.027240	-0.606412
H	5.772390	1.060694	-1.516548
H	6.903569	-1.854912	1.434502
H	4.530454	-2.505245	1.687353
H	3.410212	0.449453	-1.222084
N	2.480688	-1.478179	0.486804
C	1.448396	-0.674450	0.508819
C	-0.986664	0.876785	0.468966
C	1.471997	0.782609	0.603827
C	0.132664	-1.300969	0.518154
C	-1.013103	-0.584202	0.467140
C	0.324391	1.498019	0.610143
H	2.426826	1.281292	0.720643
H	0.117693	-2.386259	0.545846
H	-1.969854	-1.092615	0.463597
H	0.333798	2.578782	0.713653
N	-2.017535	1.681101	0.435298
C	-3.308787	1.237663	0.177598
C	-6.000633	0.472345	-0.264559
C	-4.363762	1.824631	0.907553
C	-3.645186	0.304917	-0.827846
C	-4.964282	-0.056816	-1.053332
C	-5.677425	1.424783	0.719252
H	-4.118140	2.560900	1.665834
H	-2.864262	-0.097109	-1.464978
H	-5.203732	-0.757921	-1.845286
H	-6.465964	1.852891	1.328111
N	-7.333116	0.062739	-0.463828
C	-7.619684	-1.285103	-0.807774
C	-8.196283	-3.945649	-1.484332
C	-8.585833	-1.573466	-1.782104
C	-6.944247	-2.337618	-0.172541
C	-7.227949	-3.656868	-0.519560
C	-8.875563	-2.896699	-2.108507
H	-9.104522	-0.758370	-2.275677
H	-6.201938	-2.115455	0.586167
H	-6.697925	-4.463489	-0.020901
H	-9.626640	-3.106704	-2.864730
H	-8.419380	-4.975569	-1.746011
C	-8.400035	0.985579	-0.306510
C	-10.514287	2.805171	-0.000332
C	-8.294952	2.285938	-0.821159
C	-9.572415	0.602537	0.360815
C	-10.623104	1.506450	0.502607

C	-9.343277	3.189068	-0.658210
H	-7.391765	2.580237	-1.345329
H	-9.652512	-0.402105	0.762301
H	-11.525771	1.196528	1.021457
H	-9.248390	4.193284	-1.061418
H	-11.332314	3.509195	0.118205
C	-3.678110	-0.726729	2.722216
O	-3.086830	0.052883	3.360294
O	-4.259312	-1.522749	2.093093

*A.4.1.3 **OTPA-BZN-210**, **EB** State, with CO_2 Binding on Core Unit, away from Hydrogen Atoms*

H	12.113942	1.363581	-0.919320
C	11.179428	1.589097	-0.413493
C	8.769972	2.153650	0.874026
C	10.131206	0.673334	-0.474664
C	11.028304	2.794738	0.275803
C	9.817133	3.071890	0.914310
C	8.918213	0.948289	0.172859
H	10.244360	-0.257602	-1.020146
H	11.844746	3.509380	0.315511
H	9.689018	4.001947	1.460744
H	7.834730	2.363004	1.382469
N	7.854301	0.009248	0.123500
C	8.136000	-1.371470	0.295829
C	8.703040	-4.099074	0.632712
C	9.045322	-1.789238	1.278178
C	7.513987	-2.329626	-0.517923
C	7.791230	-3.683373	-0.340655
C	9.330530	-3.143876	1.435934
H	9.523595	-1.048731	1.910497
H	6.817045	-2.006520	-1.283983
H	7.302433	-4.414886	-0.977850
H	10.037110	-3.453750	2.200626
H	8.922405	-5.154406	0.763113
C	6.530376	0.442268	-0.086115
C	3.861718	1.292430	-0.526194
C	5.456446	-0.198547	0.557039
C	6.253772	1.536259	-0.927126
C	4.951202	1.969687	-1.113177
C	4.149889	0.206902	0.331281
H	5.657151	-1.014025	1.243300
H	7.070998	2.048122	-1.423147
H	4.743859	2.820726	-1.754171
H	3.341575	-0.277951	0.868673
N	2.589252	1.803967	-0.742192
C	1.530077	1.048761	-0.884257
C	-0.958063	-0.398306	-1.091503
C	1.504993	-0.396757	-1.090742
C	0.241673	1.728868	-0.922950
C	-0.930974	1.058131	-0.990329
C	0.333540	-1.061231	-1.215746
H	2.445792	-0.924795	-1.191123
H	0.269611	2.813300	-0.877324
H	-1.868806	1.600022	-1.020719
H	0.308202	-2.131384	-1.397296
N	-2.018525	-1.162025	-1.155518
C	-3.301154	-0.708371	-0.881880
C	-5.995105	-0.020539	-0.324415
C	-4.367076	-1.268448	-1.617202

C	-3.626158	0.179604	0.169760
C	-4.944970	0.501558	0.451584
C	-5.681132	-0.908488	-1.369674
H	-4.131354	-1.969273	-2.411738
H	-2.837771	0.556113	0.812458
H	-5.173768	1.152689	1.288109
H	-6.479998	-1.327248	-1.971484
N	-7.332500	0.315005	-0.041723
C	-7.660790	1.613940	0.426980
C	-8.315834	4.182060	1.349244
C	-8.580819	1.777020	1.472635
C	-7.072837	2.746603	-0.155016
C	-7.393675	4.019118	0.312543
C	-8.909645	3.054477	1.921314
H	-9.032967	0.901164	1.925699
H	-6.367964	2.621475	-0.970222
H	-6.930874	4.887733	-0.147203
H	-9.623951	3.166579	2.732016
H	-8.569298	5.175679	1.706086
C	-8.360259	-0.655329	-0.185250
C	-10.398910	-2.561241	-0.459946
C	-8.159622	-1.971455	0.255369
C	-9.587241	-0.299298	-0.762580
C	-10.600639	-1.247130	-0.888848
C	-9.172781	-2.916652	0.107406
H	-7.213133	-2.244753	0.708537
H	-9.738792	0.718547	-1.106347
H	-11.547166	-0.958843	-1.337223
H	-9.005849	-3.933350	0.451827
H	-11.188174	-3.299331	-0.566113
C	-3.775573	-2.602693	1.691081
O	-2.664888	-2.369439	1.969610
O	-4.886756	-2.854541	1.430397

*A.4.1.4 **OTPA-BZN-210**, **EB** State, with CO_2 Binding on Linker Unit, near Hydrogen Atoms*

H	-11.794802	-1.246580	-1.402726
C	-10.874950	-1.521048	-0.894219
C	-8.503088	-2.209631	0.402680
C	-9.846105	-0.587202	-0.791953
C	-10.722469	-2.804814	-0.364859
C	-9.530028	-3.143180	0.279360
C	-8.652147	-0.924587	-0.138553
H	-9.959776	0.405908	-1.213665
H	-11.523495	-3.532508	-0.452627
H	-9.401378	-4.135224	0.702809
H	-7.583018	-2.468454	0.915996
N	-7.608779	0.031320	-0.021299
C	-7.928208	1.370853	0.323616
C	-8.569785	4.017402	1.001297
C	-8.881702	1.635832	1.317103
C	-7.299581	2.441140	-0.329470
C	-7.614250	3.753354	0.016946
C	-9.203555	2.951398	1.644163
H	-9.365247	0.808222	1.825192
H	-6.568217	2.236976	-1.104343
H	-7.119948	4.572882	-0.496963
H	-9.944147	3.142443	2.415575
H	-8.818003	5.041375	1.263486
C	-6.268012	-0.347163	-0.230082
C	-3.566401	-1.087215	-0.663428
C	-5.234817	0.222365	0.535092

C	-5.934147	-1.317164	-1.193569
C	-4.615916	-1.700888	-1.378719
C	-3.911262	-0.126935	0.314133
H	-5.480957	0.936872	1.313039
H	-6.719463	-1.773754	-1.785773
H	-4.364624	-2.457997	-2.114779
H	-3.136276	0.290509	0.947018
N	-2.274886	-1.544422	-0.888399
C	-1.230642	-0.757352	-0.900150
C	1.230706	0.757859	-0.899978
C	-1.233592	0.702871	-0.933446
C	0.075289	-1.401167	-0.964433
C	1.233657	-0.702356	-0.933594
C	-0.075225	1.401690	-0.964116
H	-2.184106	1.219958	-0.987910
H	0.072595	-2.485167	-1.025525
H	2.184174	-1.219428	-0.988147
H	-0.072531	2.485703	-1.024969
N	2.274956	1.544915	-0.888033
C	3.566461	1.087590	-0.663219
C	6.268034	0.347253	-0.230141
C	4.615993	1.701399	-1.378363
C	3.911281	0.127010	0.314060
C	5.234821	-0.222430	0.534895
C	5.934206	1.317543	-1.193348
H	4.364733	2.458726	-2.114209
H	3.136281	-0.290589	0.946828
H	5.480935	-0.937178	1.312629
H	6.719535	1.774251	-1.785444
N	7.608782	-0.031374	-0.021498
C	7.928138	-1.371018	0.323050
C	8.569577	-4.017785	1.000008
C	8.881662	-1.636318	1.316422
C	7.299408	-2.441094	-0.330284
C	7.614010	-3.753418	0.015774
C	9.203447	-2.951990	1.643123
H	9.365284	-0.808871	1.824704
H	6.568019	-2.236679	-1.105067
H	7.119630	-4.572780	-0.498325
H	9.944063	-3.143285	2.414449
H	8.817741	-5.041843	1.261918
C	8.652213	0.924489	-0.138566
C	10.722651	2.804630	-0.364512
C	8.503277	2.209402	0.403012
C	9.846104	0.587191	-0.792130
C	10.875008	1.520992	-0.894218
C	9.530274	3.142911	0.279870
H	7.583256	2.468155	0.916452
H	9.959678	-0.405817	-1.214109
H	11.794809	1.246593	-1.402856
H	9.401720	4.134854	0.703586
H	11.523722	3.532291	-0.452142
C	-0.000102	-0.000277	2.293734
O	1.049382	0.514003	2.298900
O	-1.049645	-0.514437	2.298921

*A.4.1.5 **OTPA-BZN-210**, **EB** State, with CO_2 Binding on Linker Unit, away from Hydrogen Atoms*

H	-11.792244	1.287287	0.893344	H	-6.721514	1.813337	1.316506
C	-10.866580	1.548467	0.388401	H	-4.368318	2.497820	1.658656
C	-8.479939	2.203129	-0.898888	H	-3.111978	-0.331521	-1.318243
C	-9.838957	0.610390	0.317398	N	-2.267414	1.551095	0.479708
C	-10.705650	2.819865	-0.167620	C	-1.227020	0.760857	0.520318
C	-9.505875	3.141370	-0.806830	C	1.226241	-0.762511	0.517245
C	-8.637550	0.930743	-0.330856	C	-1.236145	-0.699035	0.579175
H	-9.959240	-0.372880	0.759807	C	0.079993	1.400517	0.607388
H	-11.505804	3.551035	-0.104220	C	1.235420	0.697225	0.579939
H	-9.370577	4.123530	-1.250750	C	-0.080707	-1.402410	0.603566
H	-7.554027	2.448616	-1.408244	H	-2.188637	-1.210219	0.652227
N	-7.595236	-0.029761	-0.416086	H	0.080089	2.483581	0.683104
C	-7.914755	-1.376314	-0.732911	H	2.187977	1.208221	0.653421
C	-8.557131	-4.036067	-1.355177	H	-0.080729	-2.485669	0.676416
C	-8.856359	-1.661796	-1.731989	N	2.266614	-1.552617	0.474306
C	-7.298400	-2.432572	-0.046242	C	3.556700	-1.093434	0.244179
C	-7.613359	-3.751685	-0.365166	C	6.255152	-0.348849	-0.202101
C	-9.178754	-2.983752	-2.031587	C	4.612767	-1.727352	0.931409
H	-9.330349	-0.844924	-2.265829	C	3.893217	-0.109322	-0.711855
H	-6.576400	-2.212217	0.732975	C	5.214733	0.243282	-0.939952
H	-7.128709	-4.560303	0.174560	C	5.929687	-1.342135	0.740380
H	-9.910084	-3.190853	-2.807669	H	4.367492	-2.501110	1.651939
H	-8.805663	-5.065217	-1.595923	H	3.111111	0.333752	-1.319666
C	-6.256070	0.349690	-0.200061	H	5.453234	0.978102	-1.701096
C	-3.557530	1.092632	0.248407	H	6.720552	-1.815247	1.311832
C	-5.215626	-0.241325	-0.938763	N	7.594270	0.031398	-0.416986
C	-5.930601	1.341078	0.744412	C	7.913523	1.378485	-0.731826
C	-4.613620	1.725509	0.936586	C	8.555479	4.039236	-1.350234
C	-3.894084	0.110499	-0.709673	C	8.855484	1.665556	-1.730110
H	-5.454155	-0.974588	-1.701400	C	7.296606	2.433654	-0.043993

C	7.611360	3.753276	-0.361009
C	9.177669	2.987995	-2.027793
H	9.329913	0.849520	-2.264840
H	6.574325	2.212062	0.734613
H	7.126269	4.561044	0.179594
H	9.909279	3.196329	-2.803280
H	8.803841	5.068774	-1.589493
C	8.636962	-0.928762	-0.332333
C	10.705804	-2.817147	-0.170123
C	8.480425	-2.200379	-0.902372
C	9.837671	-0.608795	0.317398
C	10.865676	-1.546492	0.387898
C	9.506723	-3.138276	-0.810823
H	7.555047	-2.445550	-1.412852
H	9.957109	0.373884	0.761349
H	11.790790	-1.285624	0.894008
H	9.372261	-4.119850	-1.256289
H	11.506242	-3.548041	-0.107108
C	0.005887	-0.007921	3.728791
O	1.046353	-0.540506	3.731691
O	-1.034547	0.524676	3.737102

*A.4.1.6 **OTPA-BZN-210**, **LEB** State, with CO_2 Binding on Imine Nitrogen Atom*

H	-11.810289	-2.123433	0.689304
C	-10.742835	-2.176180	0.885365
C	-7.999992	-2.295272	1.363579
C	-9.919403	-1.141344	0.447997
C	-10.206612	-3.281165	1.551237
C	-8.829894	-3.333246	1.781449
C	-8.536313	-1.186198	0.689392
H	-10.341016	-0.294108	-0.082063
H	-10.851227	-4.089073	1.883930
H	-8.396164	-4.182550	2.302268
H	-6.932989	-2.335795	1.554405
N	-7.689293	-0.144785	0.245851
C	-8.107151	1.205545	0.274649
C	-8.905570	3.903914	0.335087
C	-8.902240	1.691049	1.325961
C	-7.713588	2.089355	-0.743379
C	-8.105057	3.425690	-0.704974
C	-9.302687	3.025066	1.345863
H	-9.201531	1.018689	2.122744
H	-7.100228	1.721117	-1.558678
H	-7.790872	4.093767	-1.502265
H	-9.917456	3.381877	2.167706
H	-9.213864	4.944745	0.358489
C	-6.387651	-0.461776	-0.236463
C	-3.803002	-1.073300	-1.206190
C	-5.262667	0.218323	0.242891
C	-6.205253	-1.462357	-1.200041
C	-4.935769	-1.766232	-1.673741
C	-3.988832	-0.075020	-0.232961
H	-5.388730	0.982817	1.003116
H	-7.067997	-2.000363	-1.579834
H	-4.813311	-2.537060	-2.430385
H	-3.133762	0.448011	0.178103
N	-2.549901	-1.429567	-1.702128
C	-1.345946	-0.720760	-1.601133
C	1.138367	0.636783	-1.466809
C	-1.289414	0.682185	-1.650008
C	-0.136182	-1.426576	-1.515674

C	1.086672	-0.764875	-1.470998
C	-0.071290	1.344814	-1.561882
H	-2.201520	1.257134	-1.762723
H	-0.154105	-2.513341	-1.496551
H	2.002515	-1.343040	-1.438025
H	-0.052110	2.431156	-1.581979
N	2.337484	1.366552	-1.400112
C	3.597408	0.908891	-1.006749
C	6.183407	0.124135	-0.184441
C	4.743781	1.483608	-1.582160
C	3.767910	-0.057937	0.000218
C	5.043096	-0.438719	0.402237
C	6.015916	1.095175	-1.179697
H	4.630613	2.230077	-2.364228
H	2.902527	-0.479642	0.496440
H	5.160276	-1.177450	1.188628
H	6.890138	1.541570	-1.642462
N	7.484274	-0.280150	0.225383
C	7.784169	-1.658959	0.322449
C	8.351378	-4.407753	0.521038
C	8.604115	-2.144986	1.353870
C	7.249075	-2.566445	-0.605950
C	7.526285	-3.927435	-0.498631
C	8.889699	-3.505527	1.441879
H	9.012956	-1.452038	2.081355
H	6.616429	-2.197250	-1.406014
H	7.103362	-4.614349	-1.226591
H	9.526020	-3.862981	2.246821
H	8.570470	-5.468420	0.597817
C	8.454306	0.702980	0.530130
C	10.371101	2.676781	1.119037
C	8.077529	1.894263	1.170882
C	9.802197	0.513486	0.184194
C	10.748787	1.489523	0.486931
C	9.028952	2.871913	1.453193
H	7.038409	2.045811	1.442730
H	10.099907	-0.399471	-0.320241
H	11.786993	1.325106	0.211762
H	8.718449	3.786960	1.950091
H	11.111002	3.438181	1.346487
C	1.442189	2.599872	1.152120
O	1.458597	1.587751	1.735524
O	1.416319	3.625924	0.591243
H	2.340841	2.232100	-1.922674
H	-2.474934	-2.370251	-2.063187

*A.4.1.7 **OTPA-BZN-210**, **LEB** State, with CO_2 Binding on Core Unit*

H	11.968258	-2.186282	-0.255884
C	10.917509	-2.222755	-0.530273
C	8.216333	-2.297871	-1.211129
C	10.102540	-1.129333	-0.246561
C	10.392437	-3.363758	-1.142064
C	9.036127	-3.392928	-1.474726
C	8.740953	-1.152067	-0.591280
H	10.514186	-0.253231	0.242825
H	11.029784	-4.216730	-1.354577
H	8.611672	-4.270047	-1.955562
H	7.166001	-2.321905	-1.480899
N	7.901785	-0.051414	-0.302992
C	8.370328	1.278096	-0.409497
C	9.271366	3.935772	-0.628672

C	9.260690	1.647892	-1.431174
C	7.933699	2.257045	0.497966
C	8.376675	3.572554	0.380687
C	9.711027	2.962361	-1.529200
H	9.594401	0.901362	-2.143790
H	7.246638	1.978650	1.289770
H	8.027843	4.315346	1.092933
H	10.399419	3.228850	-2.326573
H	9.619180	4.960855	-0.713316
C	6.557536	-0.287341	0.103484
C	3.888040	-0.739135	0.920050
C	5.495669	0.382337	-0.514419
C	6.269214	-1.196911	1.129375
C	4.958387	-1.422933	1.527712
C	4.180631	0.167963	-0.114469
H	5.704330	1.075875	-1.322988
H	7.082005	-1.726030	1.616683
H	4.752973	-2.124095	2.332596
H	3.377311	0.680091	-0.630300
N	2.590825	-1.014892	1.347032
C	1.420746	-0.288038	1.086244
C	-1.005031	1.116879	0.649043
C	1.402900	1.115623	1.019580
C	0.202176	-0.967878	0.951300
C	-0.993536	-0.282586	0.754926
C	0.216521	1.798080	0.783464
H	2.320422	1.675596	1.161233
H	0.188197	-2.053113	1.011615
H	-1.915212	-0.846831	0.680288
H	0.228249	2.883250	0.720782
N	-2.171756	1.875371	0.450728
C	-3.448772	1.375972	0.176279
C	-6.054685	0.428002	-0.359821
C	-4.568013	1.944386	0.808685
C	-3.660784	0.345421	-0.756196
C	-4.944131	-0.118828	-1.016114
C	-5.850445	1.473983	0.548283
H	-4.423069	2.739576	1.534981
H	-2.818761	-0.074808	-1.294517
H	-5.093423	-0.914029	-1.739197
H	-6.701319	1.910850	1.060660
N	-7.359780	-0.076053	-0.608255
C	-7.578574	-1.474395	-0.583871
C	-7.989833	-4.256035	-0.545711
C	-8.474470	-2.073956	-1.483503
C	-6.887690	-2.282911	0.332918
C	-7.089475	-3.661469	0.341449
C	-8.682059	-3.451140	-1.453857
H	-9.003496	-1.455934	-2.201077
H	-6.192899	-1.827454	1.029662
H	-6.545948	-4.272107	1.057293
H	-9.379373	-3.898113	-2.157113
H	-8.148825	-5.330053	-0.530949
C	-8.424936	0.826276	-0.836889
C	-10.527985	2.641445	-1.280088
C	-8.210514	1.998052	-1.580168
C	-9.704413	0.575278	-0.315650
C	-10.744729	1.472600	-0.546336
C	-9.252944	2.898021	-1.789768
H	-7.224982	2.195714	-1.988158
H	-9.875929	-0.323018	0.267578
H	-11.728203	1.261711	-0.135378
H	-9.068141	3.799330	-2.367747
H	-11.339934	3.341657	-1.451375

C	-3.655755	-0.255928	2.911580	H	-2.163824	2.773349	0.916573
O	-4.143173	-1.183885	2.393352	H	2.458496	-1.914285	1.788192
O	-3.160567	0.656366	3.447971				

*A.4.1.8 **OTPA-BZN-210, LEB** State, with CO_2 Binding on Linker Unit*

H	-11.767305	-1.852858	0.561226	C	-4.847404	-1.647052	-1.684332
C	-10.705050	-1.936316	0.774129	C	-3.879981	-0.004318	-0.201001
C	-7.974648	-2.134046	1.295791	H	-5.272312	1.071967	1.027317
C	-9.847492	-0.918153	0.364031	H	-6.986905	-1.824131	-1.630354
C	-10.209251	-3.063452	1.434160	H	-4.732537	-2.409916	-2.450193
C	-8.838429	-3.154900	1.686265	H	-3.017429	0.478358	0.240601
C	-8.470328	-1.002685	0.627574	N	-2.452842	-1.379887	-1.659344
H	-10.237770	-0.053397	-0.161715	C	-1.248168	-0.669249	-1.623041
H	-10.880362	-3.858188	1.745517	C	1.247366	0.681744	-1.615172
H	-8.435940	-4.021975	2.202860	C	-1.189147	0.733929	-1.643986
H	-6.912396	-2.205286	1.503399	C	-0.036569	-1.379068	-1.620426
N	-7.588775	0.021445	0.211771	C	1.188465	-0.721369	-1.639088
C	-7.970574	1.381979	0.252222	C	0.035669	1.391605	-1.617401
C	-8.697277	4.100041	0.335936	H	-2.103421	1.314509	-1.685116
C	-8.771533	1.874714	1.295730	H	-0.057515	-2.465841	-1.617138
C	-7.534704	2.268548	-0.746051	H	2.102897	-1.301934	-1.676420
C	-7.890854	3.614340	-0.696078	H	0.056690	2.478359	-1.611883
C	-9.136305	3.218701	1.327015	N	2.451776	1.393188	-1.643337
H	-9.103421	1.200090	2.077535	C	3.704133	1.001139	-1.175575
H	-6.916638	1.894802	-1.555266	C	6.287639	0.323648	-0.249584
H	-7.544285	4.284328	-1.478210	C	4.847255	1.652992	-1.674951
H	-9.756319	3.580899	2.142540	C	3.878706	0.010809	-0.191780
H	-8.977998	5.148408	0.368253	C	5.152255	-0.315163	0.261916
C	-6.288158	-0.324193	-0.253337	C	6.116574	1.317282	-1.221961
C	-3.704932	-0.992632	-1.186722	H	4.732758	2.417442	-2.439287
C	-5.153411	0.317124	0.256348	H	3.015702	-0.469629	0.251376
C	-6.116566	-1.315782	-1.227726	H	5.270821	-1.071515	1.031449

H	6.987410	1.823706	-1.625932
N	7.588331	-0.026486	0.211861
C	7.966002	-1.388249	0.250062
C	8.684612	-4.108564	0.329354
C	8.767722	-1.884493	1.291312
C	7.525293	-2.272413	-0.748210
C	7.877446	-3.619338	-0.700412
C	9.128474	-3.229613	1.320402
H	9.103357	-1.211679	2.073079
H	6.906639	-1.895923	-1.555706
H	7.527160	-4.287449	-1.482493
H	9.749155	-3.594557	2.134193
H	8.962212	-5.157812	0.359968
C	8.474159	0.994406	0.626577
C	10.221725	3.048601	1.431203
C	7.983786	2.126598	1.297296
C	9.850388	0.905692	0.359579
C	10.712251	1.920604	0.768710
C	8.851830	3.144208	1.686781
H	6.922288	2.201044	1.507616
H	10.236571	0.040248	-0.168057
H	11.773706	1.833933	0.553125
H	8.453427	4.011999	2.205337
H	10.896174	3.840805	1.741800
C	0.003089	0.013963	1.644231
O	0.982511	0.651746	1.658557
O	-0.976249	-0.624027	1.651978
H	2.406444	2.315422	-2.053296
H	-2.404731	-2.303518	-2.065809

A.4.2 Optimised Structures of Adducts between **OTPA-FLR-210** Oligomers and CO_2

*A.4.2.1 **OTPA-FLR-210**, **EB** State, with CO_2 Binding on Imine Nitrogen Atom*

H	13.353568	1.199378	0.750149
C	12.400327	1.447535	0.292079
C	9.943459	2.068338	-0.873802
C	11.395207	0.484175	0.242501
C	12.182739	2.727006	-0.224865
C	10.948038	3.031091	-0.803236
C	10.158260	0.787128	-0.345085
H	11.560292	-0.505307	0.655554
H	12.965829	3.477630	-0.178027
H	10.768027	4.019475	-1.216443
H	8.989984	2.301066	-1.335992
N	9.137275	-0.196744	-0.406933
C	9.472966	-1.530589	-0.755831
C	10.143569	-4.167905	-1.443216
C	10.391395	-1.782359	-1.785481
C	8.893823	-2.609884	-0.072087
C	9.222715	-3.917348	-0.422909
C	10.727896	-3.092954	-2.117361
H	10.836177	-0.948376	-2.317927
H	8.189737	-2.415970	0.730153
H	8.767131	-4.743644	0.115401
H	11.440730	-3.273404	-2.916973
H	10.403040	-5.188126	-1.709094
C	7.797736	0.149345	-0.137441
C	5.097699	0.830809	0.417066
C	6.745164	-0.439307	-0.860362
C	7.483278	1.104724	0.846967
C	6.167341	1.458287	1.094630

C	5.426292	-0.117561	-0.581127
H	6.972814	-1.144422	-1.652591
H	8.283738	1.572525	1.409851
H	5.934750	2.200327	1.850192
H	4.633480	-0.554069	-1.179829
N	3.808190	1.255933	0.684724
H	1.824525	-2.878749	0.895424
C	1.735742	-1.799609	0.807856
C	1.450034	1.032213	0.720492
C	0.446646	-1.192376	0.753975
C	2.852691	-1.017824	0.772238
C	2.773249	0.436598	0.700888
C	0.342712	0.246956	0.722876
H	3.832403	-1.473424	0.851083
H	1.388681	2.114874	0.692026
C	-0.833871	-1.758539	0.758842
C	-3.607537	-2.369286	0.759068
C	-1.254226	-3.120229	0.831337
C	-1.826065	-0.710099	0.721966
C	-3.156369	-0.987727	0.717652
C	-2.586906	-3.401949	0.856263
H	-0.517993	-3.917232	0.878059
H	-3.890795	-0.190710	0.726261
H	-2.946319	-4.423966	0.918944
C	-1.122955	0.633631	0.707471
H	-1.392806	1.243361	1.578483
H	-1.383227	1.221488	-0.181060
N	-4.857953	-2.789297	0.770215
C	-5.934230	-1.973476	0.476822
C	-8.278153	-0.472488	-0.091602
C	-7.149241	-2.218264	1.156639
C	-5.945767	-0.983673	-0.535824
C	-7.094104	-0.262818	-0.821771
C	-8.284481	-1.466786	0.904946
H	-7.162450	-2.990301	1.919532
H	-5.058866	-0.830794	-1.141455
H	-7.087144	0.466336	-1.624796
H	-9.191255	-1.648612	1.471363
N	-9.434922	0.282476	-0.366893
C	-9.325065	1.645346	-0.747744
C	-9.117077	4.341617	-1.497547
C	-10.121115	2.155486	-1.783532
C	-8.425128	2.496033	-0.088983
C	-8.318629	3.831557	-0.470854
C	-10.020685	3.496822	-2.146553
H	-10.814152	1.496948	-2.296266
H	-7.815533	2.104187	0.718330
H	-7.617982	4.479518	0.048090
H	-10.643261	3.878851	-2.950584
H	-9.036672	5.384805	-1.787596
C	-10.720240	-0.313718	-0.276978
C	-13.265035	-1.482709	-0.104256
C	-10.942780	-1.602290	-0.783739
C	-11.781614	0.385985	0.315022
C	-13.045626	-0.194903	0.390767
C	-12.205788	-2.182501	-0.687172
H	-10.124051	-2.140497	-1.249522
H	-11.608311	1.381231	0.710519
H	-13.859154	0.357972	0.851759
H	-12.364517	-3.181351	-1.083521
H	-14.249722	-1.935194	-0.037172
C	3.505467	4.060425	1.323751
O	2.831020	4.236157	0.384729
O	4.169057	3.954589	2.280690

*A.4.2.2 **OTPA-FLR-210**, **EB** State, with CO_2 Binding on Core Unit*

H	-13.185957	1.587955	-1.025716
C	-12.260339	1.883202	-0.539741
C	-9.873879	2.623764	0.699522
C	-11.260699	0.933425	-0.340928
C	-12.071763	3.207241	-0.136054
C	-10.871771	3.570807	0.479857
C	-10.059130	1.296595	0.284970
H	-11.403129	-0.091608	-0.666300
H	-12.850274	3.946304	-0.299057
H	-10.714559	4.595013	0.805978
H	-8.948213	2.903905	1.191102
N	-9.042977	0.330138	0.498951
C	-9.394508	-0.975696	0.930104
C	-10.093882	-3.556196	1.781323
C	-10.375968	-1.153916	1.915890
C	-8.765558	-2.098797	0.372053
C	-9.110317	-3.377254	0.805354
C	-10.726520	-2.437567	2.328922
H	-10.858395	-0.284995	2.350884
H	-8.011112	-1.962375	-0.394918
H	-8.615908	-4.238890	0.365543
H	-11.488564	-2.561564	3.093149
H	-10.364454	-4.554868	2.110595
C	-7.690796	0.656080	0.271586
C	-4.959704	1.247058	-0.223704
C	-6.682106	0.146219	1.107402
C	-7.320536	1.504257	-0.788092
C	-5.989044	1.819568	-1.005227
C	-5.347123	0.422417	0.858964
H	-6.957408	-0.470707	1.956053
H	-8.087449	1.916903	-1.434488
H	-5.706945	2.473652	-1.823818
H	-4.588295	0.040791	1.534211
N	-3.654893	1.602168	-0.513902
H	-1.773732	-2.579741	-0.210540
C	-1.660113	-1.501350	-0.276188
C	-1.312261	1.307463	-0.574577
C	-0.357194	-0.924802	-0.342664
C	-2.759433	-0.695407	-0.314319
C	-2.648070	0.754255	-0.441854
C	-0.221366	0.503334	-0.506683
H	-3.747472	-1.138581	-0.288840
H	-1.234878	2.382432	-0.705853
C	0.909309	-1.519724	-0.311543
C	3.667507	-2.196914	-0.316781
C	1.297470	-2.889503	-0.213045
C	1.924798	-0.501880	-0.448222
C	3.247982	-0.811067	-0.449650
C	2.622011	-3.206363	-0.240960
H	0.543130	-3.666160	-0.128451
H	3.998482	-0.041989	-0.590705
H	2.957241	-4.236357	-0.175294
C	1.251955	0.849667	-0.592529
H	1.502681	1.328925	-1.546808
H	1.557684	1.544710	0.198793
N	4.907035	-2.647654	-0.309000
C	6.011310	-1.829337	-0.164879
C	8.407727	-0.330035	0.113228
C	7.196558	-2.202312	-0.838994
C	6.080478	-0.707325	0.696376

C	7.254484	0.014186	0.841637	H	10.962943	4.329521	2.226421
C	8.357208	-1.455393	-0.730984	H	9.354689	5.689555	0.897812
H	7.165074	-3.074498	-1.484326	C	10.857348	-0.215058	0.206236
H	5.218768	-0.445523	1.301046	C	13.366246	-1.469318	0.138448
H	7.292263	0.849748	1.532297	C	11.063581	-1.422253	0.889577
H	9.239918	-1.740989	-1.292590	C	11.916975	0.360405	-0.509772
N	9.590280	0.424107	0.242766	C	13.163459	-0.261385	-0.533408
C	9.524150	1.830789	0.419594	C	12.308425	-2.046349	0.845202
C	9.401864	4.613064	0.764461	H	10.246562	-1.863214	1.450810
C	10.364460	2.466915	1.344801	H	11.756222	1.292070	-1.041850
C	8.623059	2.598572	-0.332811	H	13.975824	0.195008	-1.091781
C	8.559344	3.978365	-0.151529	H	12.454633	-2.981142	1.378847
C	10.306328	3.849535	1.506367	H	14.337062	-1.954777	0.112063
H	11.058389	1.873000	1.930117	C	-5.400982	-0.884155	-2.611668
H	7.979186	2.108074	-1.055137	O	-4.790658	-0.182380	-3.318321
H	7.857399	4.561054	-0.741278	O	-6.002263	-1.604981	-1.914189

*A.4.2.3 **OTPA-FLR-210**, **EB** State, with CO_2 Binding on Linker Unit*

H	-13.464112	1.589624	-1.008043	C	-10.489387	-1.196293	1.728825
C	-12.492421	1.857910	-0.603184	C	-9.063857	-2.228421	0.065684
C	-9.988766	2.529619	0.427357	C	-9.409508	-3.485507	0.556517
C	-11.506498	0.880269	-0.489118	C	-10.843158	-2.458246	2.201452
C	-12.232632	3.175547	-0.218453	H	-10.899398	-0.302407	2.186763
C	-10.974835	3.504624	0.292562	H	-8.380932	-2.133374	-0.771863
C	-10.246388	1.209000	0.031546	H	-8.988607	-4.372679	0.091899
H	-11.704533	-0.140231	-0.799500	H	-11.534293	-2.539831	3.035561
H	-13.001063	3.936463	-0.315333	H	-10.575980	-4.591173	1.998446
H	-10.761849	4.523593	0.603009	C	-7.907511	0.496212	-0.179293
H	-9.017065	2.782847	0.837942	C	-5.211953	1.048095	-0.876291
N	-9.245261	0.211300	0.160821	C	-6.846500	-0.043169	0.569986
C	-9.598336	-1.071968	0.652861	C	-7.603381	1.342616	-1.262304
C	-10.303277	-3.609528	1.623105	C	-6.287789	1.635399	-1.579677

C	-5.529620	0.213850	0.223283
H	-7.066618	-0.658062	1.436120
H	-8.410392	1.773822	-1.844617
H	-6.058826	2.295620	-2.410334
H	-4.727533	-0.173540	0.842743
N	-3.926113	1.411854	-1.227607
H	-2.008354	-2.753543	-0.962385
C	-1.905228	-1.673217	-1.010245
C	-1.578843	1.141926	-1.281375
C	-0.607590	-1.081247	-1.017426
C	-3.010660	-0.877753	-1.078231
C	-2.909793	0.573357	-1.175492
C	-0.481288	0.348965	-1.178752
H	-3.997441	-1.324465	-1.101426
H	-1.508638	2.219025	-1.398681
C	0.664167	-1.657266	-0.910769
C	3.426159	-2.291486	-0.730389
C	1.065258	-3.019859	-0.775835
C	1.670556	-0.625321	-0.992171
C	2.995481	-0.913817	-0.903703
C	2.393563	-3.316573	-0.715156
H	0.318500	-3.807297	-0.732795
H	3.741951	-0.134029	-1.000309
H	2.739080	-4.340724	-0.618516
C	0.989216	0.714631	-1.190485
H	1.284390	1.185351	-2.136244
H	1.239115	1.420116	-0.390133
N	4.669501	-2.721901	-0.634861
C	5.746956	-1.883280	-0.420451
C	8.091618	-0.340737	0.017026
C	6.982019	-2.235974	-1.010720
C	5.736818	-0.758352	0.439729
C	6.885224	-0.015817	0.663345
C	8.119067	-1.467980	-0.825537
H	7.010805	-3.109955	-1.653818
H	4.830700	-0.510614	0.982261
H	6.860510	0.821674	1.352291
H	9.043273	-1.738688	-1.324321
N	9.249553	0.434371	0.225438
C	9.147598	1.840127	0.390896
C	8.953979	4.621164	0.714923
C	9.913188	2.494199	1.367148
C	8.285298	2.589634	-0.422983
C	8.185605	3.968644	-0.252301
C	9.820339	3.876061	1.518464
H	10.576863	1.914647	2.000000
H	7.699276	2.085659	-1.184214
H	7.514239	4.536863	-0.889856
H	10.419118	4.369784	2.278551
H	8.879163	5.697057	0.840227
C	10.526241	-0.183761	0.280839
C	13.053647	-1.397349	0.393998
C	10.703503	-1.385447	0.981847
C	11.624174	0.406588	-0.361615
C	12.879054	-0.194884	-0.295360
C	11.958240	-1.989305	1.027372
H	9.856296	-1.838094	1.486135
H	11.486223	1.333867	-0.907574
H	13.721075	0.273015	-0.797469
H	12.081608	-2.920019	1.573780
H	14.031568	-1.867064	0.437638
C	-1.054427	0.307178	1.998993
O	-2.211589	0.147187	2.025784
O	0.103861	0.466443	1.991078

A.4.3 Optimised Structures of Adducts between **OTPB-BZN-210** Oligomers and CO_2

*A.4.3.1 **OTPB-BZN-210**, **EB** State, with CO_2 Binding on Imine Nitrogen Atom*

H	14.137382	-1.950062	1.367885	H	11.787979	4.716561	-3.013346
C	13.187343	-2.239246	0.927434	H	10.549076	6.669839	-2.095277
C	10.737368	-2.967299	-0.181933	C	6.109623	-0.334502	0.233642
C	12.191279	-1.281005	0.745978	C	3.388788	-1.008245	0.657198
C	12.962417	-3.566276	0.555558	C	5.094969	0.211015	-0.569987
C	11.732702	-3.926134	0.000379	C	5.733631	-1.241158	1.241432
C	10.950452	-1.629368	0.188042	C	4.405162	-1.591364	1.435468
H	12.366606	-0.256779	1.061354	C	3.758766	-0.110835	-0.363303
H	13.738228	-4.313109	0.697196	H	5.357801	0.875581	-1.387263
H	11.550008	-4.954076	-0.299850	H	6.494224	-1.668459	1.887452
H	9.793744	-3.251896	-0.637818	H	4.127968	-2.298854	2.210067
C	9.891118	-0.609077	-0.006294	H	2.995601	0.293752	-1.020431
C	7.890330	1.317607	-0.376267	N	2.074563	-1.432260	0.861487
C	10.219072	0.695947	-0.397298	C	1.070060	-0.603528	0.915396
C	8.543074	-0.931699	0.196561	C	-1.297949	1.036370	0.939989
C	7.530663	0.020699	0.015554	C	1.157059	0.855800	0.986572
C	9.229700	1.670072	-0.586363	C	-0.268779	-1.185612	0.978944
H	11.259859	0.957336	-0.557472	C	-1.383456	-0.424349	0.966594
H	8.278405	-1.939773	0.497891	C	0.041380	1.614504	1.021797
H	7.116198	2.064195	-0.519385	H	2.136890	1.314105	1.047239
C	9.593274	3.047190	-1.001407	H	-0.322843	-2.267853	1.023412
C	10.283135	5.661726	-1.790832	H	-2.363119	-0.884733	1.015570
C	10.638917	3.271697	-1.911669	H	0.093761	2.696197	1.096373
C	8.900229	4.158427	-0.494292	N	-2.297002	1.872132	0.912163
C	9.241002	5.452382	-0.885262	C	-3.612235	1.465676	0.690814
C	10.980827	4.565507	-2.302097	C	-6.340225	0.827579	0.248528
H	11.170856	2.424356	-2.333947	C	-4.626947	2.055329	1.468043
H	8.105042	4.007364	0.229703	C	-3.989076	0.582620	-0.341218
H	8.697033	6.298568	-0.475067	C	-5.327829	0.279349	-0.556747

C	-5.958528	1.721776	1.265394
H	-4.343239	2.752396	2.250161
H	-3.228580	0.176167	-1.000185
H	-5.595277	-0.373837	-1.381705
H	-6.717502	2.151585	1.911745
C	-7.763002	0.486755	0.023146
C	-10.455579	-0.164590	-0.402816
C	-8.770180	1.440738	0.225173
C	-8.130387	-0.799647	-0.395913
C	-9.471667	-1.139354	-0.615541
C	-10.120484	1.129031	0.018811
H	-8.496359	2.454110	0.499419
H	-7.365772	-1.561506	-0.505531
H	-11.497957	-0.416474	-0.567842
C	-9.842977	-2.509045	-1.046951
C	-10.544985	-5.109680	-1.870864
C	-11.012185	-3.123842	-0.570174
C	-9.032311	-3.223176	-1.944410
C	-9.378993	-4.510385	-2.351818
C	-11.360232	-4.410489	-0.978462
H	-11.639055	-2.598611	0.144207
H	-8.136803	-2.755617	-2.342985
H	-8.741728	-5.042381	-3.052567
H	-12.265108	-4.870672	-0.591686
H	-10.815689	-6.112423	-2.188541
C	-11.172705	2.153750	0.225903
C	-13.171052	4.098187	0.626035
C	-11.070277	3.086503	1.270874
C	-12.295740	2.214938	-0.615146
C	-13.285219	3.176626	-0.416833
C	-12.058773	4.049200	1.468892
H	-10.221184	3.040309	1.946372
H	-12.380902	1.519109	-1.444475
H	-14.142184	3.211372	-1.083599
H	-11.963905	4.756540	2.287944
H	-13.941705	4.847818	0.780424
C	1.984713	-4.294902	0.581893
O	3.037254	-4.258461	0.075863
O	0.931202	-4.399341	1.080650

*A.4.3.2 **OTPB-BZN-210**, **EB** State, with CO_2 Binding on Core Unit*

H	13.931045	2.420065	-1.452933
C	12.981441	2.731967	-1.027289
C	10.532625	3.516536	0.045365
C	11.998920	1.779486	-0.761395
C	12.743426	4.081472	-0.758810
C	11.514357	4.469569	-0.221507
C	10.758736	2.156246	-0.220680
H	12.183998	0.735750	-0.997310
H	13.508619	4.823816	-0.966415
H	11.321701	5.515769	-0.001196
H	9.589574	3.825071	0.486674
C	9.713141	1.142310	0.061659
C	7.738182	-0.769964	0.599422
C	10.059912	-0.124925	0.549262
C	8.360250	1.432343	-0.157892
C	7.360294	0.485093	0.103311
C	9.082916	-1.091423	0.822153
H	11.105279	-0.361576	0.717895
H	8.083518	2.409878	-0.538271
H	6.976849	-1.512545	0.805290

C	9.460470	-2.433681	1.328435
C	10.174944	-4.985088	2.283897
C	10.529063	-2.592537	2.225564
C	8.755925	-3.578116	0.918942
C	9.109537	-4.840537	1.392712
C	10.883238	-3.855295	2.698253
H	11.070023	-1.717464	2.573283
H	7.940395	-3.478977	0.208966
H	8.556579	-5.713861	1.058293
H	11.708368	-3.955370	3.397803
H	10.450355	-5.968986	2.652493
C	5.934453	0.797564	-0.148768
C	3.203380	1.389136	-0.643113
C	4.918567	0.276107	0.671587
C	5.551497	1.636322	-1.211553
C	4.219226	1.949312	-1.439084
C	3.578363	0.554340	0.428387
H	5.182964	-0.335735	1.528304
H	6.310391	2.040313	-1.874190
H	3.937012	2.605630	-2.256136
H	2.814842	0.167662	1.095819
N	1.886322	1.777409	-0.884848
C	0.897552	0.930133	-0.907212
C	-1.448864	-0.740987	-0.866904
C	1.004141	-0.529596	-0.912658
C	-0.449098	1.489193	-1.003752
C	-1.554625	0.716100	-0.960713
C	-0.101331	-1.303782	-0.918922
H	1.989891	-0.974664	-0.961707
H	-0.515558	2.568765	-1.095872
H	-2.540162	1.160455	-1.033176
H	-0.034732	-2.386909	-0.948124
N	-2.436873	-1.587819	-0.804280
C	-3.758520	-1.189296	-0.606955
C	-6.496906	-0.569421	-0.203712
C	-4.761836	-1.825933	-1.361542
C	-4.151838	-0.266635	0.383379
C	-5.495507	0.027985	0.579943
C	-6.098751	-1.502315	-1.178560
H	-4.465503	-2.552668	-2.111314
H	-3.399718	0.178965	1.026478
H	-5.775451	0.713725	1.373778
H	-6.849101	-1.970713	-1.807986
C	-7.925184	-0.239106	0.001670
C	-10.628257	0.391639	0.390412
C	-8.917693	-1.216169	-0.158123
C	-8.312514	1.059801	0.359698
C	-9.659324	1.389645	0.559852
C	-10.273006	-0.915179	0.030526
H	-8.628150	-2.237093	-0.383911
H	-7.559193	1.836836	0.435981
H	-11.674709	0.635524	0.541109
C	-10.052044	2.772279	0.926161
C	-10.795009	5.397581	1.626862
C	-11.228661	3.346879	0.418461
C	-9.254891	3.539245	1.791546
C	-9.621818	4.838638	2.137952
C	-11.596924	4.645757	0.765716
H	-11.845478	2.779754	-0.272251
H	-8.353833	3.104102	2.213589
H	-8.994690	5.411952	2.814852
H	-12.507240	5.074010	0.355730
H	-11.081520	6.409827	1.896959
C	-11.309156	-1.964427	-0.129337

C	-13.275536	-3.957675	-0.437074
C	-11.190221	-2.944508	-1.128232
C	-12.432619	-2.002875	0.712478
C	-13.406230	-2.988786	0.559955
C	-12.162839	-3.931412	-1.280411
H	-10.340782	-2.917367	-1.804340
H	-12.530167	-1.269405	1.507278
H	-14.263647	-3.005082	1.226848
H	-12.055318	-4.675782	-2.064330
H	-14.033726	-4.726289	-0.555690
C	4.839643	-2.060279	-1.603344
O	5.481240	-2.717098	-0.879354
O	4.190154	-1.423013	-2.336206

*A.4.3.3 **OTPB-BZN-210**, **EB** State, with CO_2 Binding on Linker Unit*

H	14.209852	2.206114	-1.890397
C	13.272655	2.518240	-1.438250
C	10.855086	3.303674	-0.297396
C	12.291411	1.568123	-1.159516
C	13.048968	3.865793	-1.148531
C	11.835549	4.254330	-0.577054
C	11.066873	1.945370	-0.584568
H	12.464708	0.526199	-1.411805
H	13.813156	4.606315	-1.366105
H	11.654332	5.298923	-0.340057
H	9.924857	3.612292	0.170249
C	10.022832	0.933765	-0.288633
C	8.051376	-0.977690	0.269192
C	10.374215	-0.340799	0.175603
C	8.666302	1.233848	-0.468229
C	7.668105	0.288770	-0.193765
C	9.399644	-1.306960	0.458802
H	11.421794	-0.584337	0.318739
H	8.383819	2.218371	-0.825862
H	7.288845	-1.718809	0.484654
C	9.787845	-2.652020	0.949730
C	10.524611	-5.205712	1.882900
C	10.862385	-2.810387	1.840017
C	9.089835	-3.798303	0.536046
C	9.453852	-5.062145	0.998137
C	11.227505	-4.074107	2.301554
H	11.399055	-1.934002	2.190985
H	8.271901	-3.699445	-0.171426
H	8.905467	-5.936695	0.659561
H	12.057021	-4.173646	2.995941
H	10.808653	-6.190356	2.242766
C	6.237774	0.618947	-0.389441
C	3.496966	1.236938	-0.772940
C	5.252663	0.113857	0.475473
C	5.822370	1.460628	-1.437383
C	4.484434	1.784883	-1.612671
C	3.906885	0.406735	0.289605
H	5.547209	-0.495990	1.324077
H	6.558766	1.856289	-2.130012
H	4.175028	2.441479	-2.419717
H	3.168732	0.041469	0.995164
N	2.173925	1.632626	-0.969083
C	1.179017	0.793409	-0.947405
C	-1.185459	-0.861306	-0.899381
C	1.271345	-0.667617	-0.930660
C	-0.165571	1.362476	-1.011242

C	-1.277866	0.598396	-0.963233
C	0.159002	-1.433166	-0.934268
H	2.253174	-1.124655	-0.960124
H	-0.224537	2.443491	-1.089843
H	-2.259829	1.053017	-1.016203
H	0.217869	-2.516878	-0.953136
N	-2.180682	-1.700033	-0.872907
C	-3.502893	-1.292493	-0.696340
C	-6.241539	-0.647648	-0.343588
C	-4.492554	-1.881509	-1.505121
C	-3.909387	-0.406597	0.321647
C	-5.254144	-0.101079	0.493183
C	-5.829276	-1.544310	-1.346226
H	-4.185593	-2.580387	-2.276819
H	-3.169196	-0.006222	1.005768
H	-5.546572	0.553460	1.308613
H	-6.567714	-1.973052	-2.016645
C	-7.670024	-0.302391	-0.165483
C	-10.373678	0.357671	0.170242
C	-8.673460	-1.251319	-0.406445
C	-8.047139	0.983438	0.246806
C	-9.393895	1.327236	0.422013
C	-10.028949	-0.935196	-0.245902
H	-8.394341	-2.264582	-0.675584
H	-7.284085	1.741940	0.386462
H	-11.420163	0.613071	0.300173
C	-9.774601	2.695972	0.848271
C	-10.494785	5.294338	1.663608
C	-10.923083	3.319168	0.333565
C	-8.993958	3.400520	1.779286
C	-9.349608	4.686609	2.182478
C	-11.280118	4.604726	0.737548
H	-11.525954	2.801327	-0.406419
H	-8.115700	2.926093	2.207037
H	-8.735966	5.211052	2.909521
H	-12.168405	5.071544	0.321381
H	-10.772541	6.296186	1.978014
C	-11.077201	-1.954609	-0.495072
C	-13.068139	-3.888402	-0.976011
C	-10.941431	-2.882829	-1.540293
C	-12.229773	-2.015063	0.305086
C	-13.215550	-2.971452	0.066754
C	-11.926244	-3.840217	-1.778330
H	-10.068494	-2.837164	-2.184712
H	-12.341591	-1.322919	1.134329
H	-14.095908	-3.005714	0.702340
H	-11.805098	-4.544019	-2.596968
H	-13.835957	-4.633865	-1.161572
C	0.004804	0.062695	2.269871
O	0.993454	0.685702	2.253101
O	-0.983854	-0.560133	2.292814

A.4.4 Optimised Structures of Adducts between **OTPB-FLR-210** Oligomers and CO_2

*A.4.4.1 **OTPB-FLR-210**, **EB** State, with CO_2 Binding on Imine Nitrogen Atom*

H	-15.694522	2.441005	-1.114281
C	-14.722130	2.696029	-0.702427
C	-12.216319	3.335542	0.334681
C	-13.767908	1.696923	-0.517068
C	-14.426966	4.020042	-0.371008
C	-13.169594	4.335402	0.148122

C	-12.499632	2.000231	0.004467
H	-13.997475	0.674109	-0.800764
H	-15.170030	4.798877	-0.515807
H	-12.932512	5.360871	0.417182
H	-11.250656	3.586739	0.763158
C	-11.485912	0.935057	0.199469
C	-9.569110	-1.070229	0.593869
C	-11.867113	-0.342809	0.630656
C	-10.127465	1.191450	-0.026782
C	-9.155465	0.199813	0.166932
C	-10.919845	-1.356026	0.831132
H	-12.909776	-0.537358	0.859307
H	-9.822219	2.178625	-0.357510
H	-8.833999	-1.861691	0.695600
C	-11.338906	-2.704342	1.284817
C	-12.134793	-5.265718	2.146176
C	-12.543275	-3.272102	0.837950
C	-10.541290	-3.445551	2.171962
C	-10.934317	-4.713397	2.597652
C	-12.937917	-4.539086	1.264716
H	-13.161879	-2.725113	0.132671
H	-9.618784	-3.013609	2.548489
H	-10.306128	-5.266701	3.290067
H	-13.869874	-4.962731	0.901156
H	-12.441690	-6.253209	2.478412
C	-7.725185	0.479144	-0.090807
C	-4.976467	1.003716	-0.590030
C	-6.719761	-0.107855	0.696139
C	-7.324388	1.351494	-1.119539
C	-5.984842	1.626809	-1.353130
C	-5.374879	0.141094	0.454471
H	-6.997423	-0.745779	1.529921
H	-8.076476	1.808134	-1.755782
H	-5.690925	2.302645	-2.148490
N	-3.651328	1.352149	-0.825160
H	-1.968574	-2.909023	-1.006287
C	-1.806037	-1.837786	-0.931571
C	-1.315291	0.972300	-0.859485
C	-0.474822	-1.319187	-0.886008
C	-2.863040	-0.981446	-0.901219
C	-2.679400	0.468177	-0.840438
C	-0.268006	0.112453	-0.860738
H	-3.873959	-1.364933	-0.967407
H	-1.181098	2.048352	-0.835730
C	0.756502	-1.973708	-0.888725
C	3.475432	-2.786477	-0.884084
C	1.073933	-3.366822	-0.948085
C	1.825203	-0.997643	-0.857231
C	3.128974	-1.371531	-0.851801
C	2.379126	-3.746182	-0.967386
H	0.279677	-4.106080	-0.987278
H	3.923470	-0.634339	-0.856924
H	2.664183	-4.791762	-1.018904
C	1.221114	0.392765	-0.847031
H	1.533803	0.978194	-1.720104
H	1.523122	0.962559	0.039817
N	4.686905	-3.291949	-0.890462
C	5.820486	-2.530143	-0.636796
C	8.253968	-1.150272	-0.129584
C	6.973364	-2.779584	-1.408932
C	5.923524	-1.602330	0.422608
C	7.117274	-0.936410	0.668998
C	8.152630	-2.087880	-1.174030
H	6.908699	-3.505505	-2.213439

H	5.073476	-1.447501	1.079165
H	7.178139	-0.258877	1.515362
H	9.008537	-2.266024	-1.817873
C	9.518423	-0.426170	0.131175
C	11.911653	0.948279	0.626678
C	10.757748	-1.048262	-0.076022
C	9.501877	0.898280	0.591165
C	10.688998	1.597590	0.843572
C	11.961602	-0.374385	0.166589
H	10.786290	-2.073298	-0.430106
H	8.550139	1.392910	0.754399
H	12.837700	1.480106	0.818469
C	10.652430	2.998387	1.330818
C	10.582403	5.657883	2.256892
C	11.587765	3.457276	2.272587
C	9.681470	3.898288	0.862048
C	9.646183	5.214260	1.320602
C	11.553611	4.773461	2.730667
H	12.331155	2.770180	2.665725
H	8.965001	3.569629	0.115076
H	8.891465	5.896278	0.939196
H	12.281746	5.105860	3.465190
H	10.555417	6.683288	2.613982
C	13.264069	-1.048107	-0.058774
C	15.737075	-2.327159	-0.487932
C	13.430794	-2.410548	0.238496
C	14.360942	-0.339128	-0.575126
C	15.584989	-0.971680	-0.787049
C	14.654259	-3.043878	0.025586
H	12.602158	-2.970453	0.661721
H	14.245372	0.709020	-0.834573
H	16.418493	-0.406525	-1.194563
H	14.763861	-4.096845	0.269386
H	16.690539	-2.820319	-0.653462
H	-4.619591	-0.291787	1.102701
C	-3.127913	4.041010	-1.798021
O	-3.791363	3.852428	-2.742133
O	-2.448999	4.288166	-0.878682

*A.4.4.2 **OTPB-FLR-210**, **EB** State, with CO_2 Binding on Core Unit*

H	-15.421831	3.001011	-1.459368
C	-14.441838	3.262428	-1.070154
C	-11.917048	3.915724	-0.089092
C	-13.528208	2.254018	-0.767786
C	-14.096361	4.602634	-0.884470
C	-12.829682	4.924738	-0.392828
C	-12.251007	2.563975	-0.272498
H	-13.796694	1.215713	-0.938697
H	-14.807719	5.388722	-1.120537
H	-12.553685	5.963778	-0.236576
H	-10.944073	4.175541	0.317130
C	-11.280672	1.488266	0.046219
C	-9.445446	-0.534979	0.672602
C	-11.713900	0.280170	0.609170
C	-9.912241	1.665867	-0.194417
C	-8.980597	0.664066	0.113407
C	-10.807780	-0.740789	0.925837
H	-12.764570	0.152136	0.847743
H	-9.567655	2.599388	-0.626471
H	-8.745415	-1.340268	0.861940
C	-11.280286	-2.017029	1.515147
C	-12.176183	-4.443424	2.631832

C	-12.507297	-2.578974	1.126261
C	-10.510997	-2.695461	2.474602
C	-10.953451	-3.896489	3.026585
C	-12.951471	-3.778942	1.679303
H	-13.104963	-2.082959	0.367289
H	-9.570530	-2.265436	2.806004
H	-10.346007	-4.401249	3.772531
H	-13.900372	-4.199856	1.358922
H	-12.521541	-5.378870	3.062399
C	-7.539474	0.862031	-0.162014
C	-4.770696	1.257307	-0.679884
C	-6.556290	0.317089	0.683169
C	-7.104245	1.622183	-1.263778
C	-5.755764	1.837801	-1.504108
C	-5.201831	0.498758	0.430260
H	-6.858840	-0.234703	1.567866
H	-7.836882	2.040863	-1.946843
H	-5.433866	2.433631	-2.352406
N	-3.439703	1.557618	-0.935000
H	-1.802918	-2.722380	-0.738489
C	-1.631242	-1.650090	-0.759764
C	-1.113259	1.149111	-0.946233
C	-0.294838	-1.141760	-0.760022
C	-2.680297	-0.785239	-0.809427
C	-2.482345	0.662183	-0.877150
C	-0.073258	0.284386	-0.868412
H	-3.694164	-1.161794	-0.852566
H	-0.974805	2.222290	-1.033225
C	0.929670	-1.806255	-0.704899
C	3.640765	-2.643451	-0.634229
C	1.233172	-3.202158	-0.636336
C	2.008418	-0.842827	-0.767493
C	3.308357	-1.228144	-0.732265
C	2.534381	-3.595201	-0.624303
H	0.431467	-3.933734	-0.604686
H	4.110091	-0.502866	-0.808969
H	2.808696	-4.643967	-0.579638
C	1.418737	0.548833	-0.885423
H	1.733873	1.046650	-1.810402
H	1.730399	1.195690	-0.056690
N	4.847240	-3.159514	-0.598208
C	5.988850	-2.387495	-0.422143
C	8.435236	-0.984849	-0.059947
C	7.134392	-2.715351	-1.175571
C	6.106157	-1.367713	0.547350
C	7.306058	-0.690666	0.723535
C	8.320160	-2.013934	-1.012723
H	7.058874	-3.511305	-1.909833
H	5.261830	-1.146784	1.192299
H	7.377714	0.061409	1.503503
H	9.170206	-2.256696	-1.643104
C	9.705507	-0.247219	0.123086
C	12.109099	1.154690	0.468802
C	10.940120	-0.893189	-0.032817
C	9.698996	1.114954	0.455519
C	10.891355	1.828464	0.631882
C	12.149027	-0.205941	0.136095
H	10.960962	-1.947369	-0.288298
H	8.750933	1.628106	0.577972
H	13.039175	1.697101	0.602705
C	10.865289	3.269407	0.984007
C	10.815247	6.005279	1.653517
C	11.810285	3.810636	1.870800
C	9.894935	4.126031	0.439058

C	9.869550	5.479811	0.770636
C	11.786016	5.164569	2.201907
H	12.553662	3.159969	2.321694
H	9.170993	3.731858	-0.267932
H	9.115085	6.126617	0.331725
H	12.521578	5.561294	2.895989
H	10.795982	7.060117	1.911662
C	13.446610	-0.904881	-0.033730
C	15.910584	-2.231459	-0.357148
C	13.610527	-2.232674	0.393417
C	14.541618	-0.254824	-0.626016
C	15.761183	-0.910890	-0.785728
C	14.829561	-2.889581	0.232926
H	12.783398	-2.744587	0.876188
H	14.427954	0.763632	-0.985338
H	16.593232	-0.392118	-1.253462
H	14.937182	-3.914281	0.577303
H	16.860586	-2.742973	-0.481874
H	-4.464773	0.099883	1.119972
C	-6.557467	-2.138089	-1.396467
O	-7.176105	-2.711649	-0.586958
O	-5.931605	-1.585923	-2.214409

*A.4.4.3 **OTPB-FLR-210**, **EB** State, with CO_2 Binding on Linker Unit*

H	-15.766272	2.724158	-1.325734
C	-14.778861	2.991886	-0.960283
C	-12.235280	3.662593	-0.041536
C	-13.831630	1.993753	-0.737670
C	-14.457829	4.330477	-0.725560
C	-13.181595	4.661385	-0.265490
C	-12.544546	2.312649	-0.274698
H	-14.082024	0.957884	-0.946685
H	-15.195422	5.108550	-0.899502
H	-12.924098	5.698837	-0.071634
H	-11.254193	3.927774	0.341014
C	-11.538555	1.248100	-0.040219
C	-9.636288	-0.755546	0.425913
C	-11.922736	0.006226	0.483467
C	-10.184392	1.469814	-0.321730
C	-9.219348	0.478599	-0.093474
C	-10.982717	-1.005754	0.720750
H	-12.960370	-0.157783	0.754840
H	-9.877039	2.429553	-0.723478
H	-8.908788	-1.549747	0.556871
C	-11.405165	-2.316117	1.272019
C	-12.207721	-4.805643	2.318029
C	-12.629374	-2.893529	0.897237
C	-10.591145	-3.010891	2.181557
C	-10.987499	-4.243259	2.698580
C	-13.027323	-4.124903	1.415350
H	-13.261485	-2.383491	0.176409
H	-9.652533	-2.569294	2.503074
H	-10.346217	-4.760507	3.406693
H	-13.974953	-4.557166	1.106562
H	-12.517170	-5.765432	2.721462
C	-7.793982	0.720279	-0.410013
C	-5.055623	1.172309	-1.019569
C	-6.772793	0.163259	0.378993
C	-7.413774	1.528260	-1.497932
C	-6.078144	1.769680	-1.784131
C	-5.432221	0.375288	0.084073
H	-7.034214	-0.421209	1.256085

H	-8.178589	1.960890	-2.135660
H	-5.796931	2.398909	-2.622851
N	-3.736562	1.488849	-1.315730
H	-2.096501	-2.793907	-1.231104
C	-1.925749	-1.721350	-1.236314
C	-1.410798	1.081498	-1.376825
C	-0.590088	-1.211667	-1.217915
C	-2.975178	-0.856300	-1.271087
C	-2.778703	0.592274	-1.304227
C	-0.369344	0.216582	-1.310663
H	-3.990093	-1.233517	-1.306453
H	-1.273228	2.156337	-1.441600
C	0.635005	-1.872220	-1.133043
C	3.344043	-2.698852	-0.964918
C	0.940544	-3.266829	-1.053347
C	1.711276	-0.904749	-1.161088
C	3.010397	-1.285190	-1.078831
C	2.242007	-3.655055	-0.995135
H	0.140697	-4.001077	-1.048460
H	3.811548	-0.556898	-1.126968
H	2.518516	-4.702675	-0.939010
C	1.121472	0.484669	-1.298250
H	1.454443	0.978855	-2.218866
H	1.410460	1.132720	-0.463442
N	4.550190	-3.210195	-0.880194
C	5.680563	-2.433870	-0.658001
C	8.104779	-1.022328	-0.196199
C	6.858740	-2.761677	-1.359439
C	5.752674	-1.409656	0.311415
C	6.941841	-0.728241	0.536368
C	8.034243	-2.055881	-1.148509
H	6.817371	-3.561028	-2.092736
H	4.880731	-1.188832	0.918528
H	6.977539	0.027226	1.315513
H	8.911583	-2.298691	-1.740281
C	9.363793	-0.280144	0.038639
C	11.746029	1.130344	0.482425
C	10.605724	-0.923490	-0.059163
C	9.338992	1.083724	0.363116
C	10.520556	1.801647	0.587727
C	11.804182	-0.232000	0.159578
H	10.640480	-1.978956	-0.307756
H	8.385034	1.594655	0.440945
H	12.667921	1.676002	0.654304
C	10.475319	3.244546	0.929764
C	10.389314	5.984357	1.579469
C	11.380565	3.794193	1.852139
C	9.526228	4.094793	0.339259
C	9.482998	5.450481	0.661043
C	11.338576	5.150057	2.173394
H	12.106104	3.148660	2.338069
H	8.833734	3.694079	-0.395021
H	8.745715	6.092182	0.186859
H	12.043203	5.553305	2.895255
H	10.356226	7.040703	1.829925
C	13.109814	-0.928312	0.052119
C	15.589234	-2.249897	-0.152013
C	13.257410	-2.253500	0.493116
C	14.229064	-0.278310	-0.493035
C	15.456248	-0.931883	-0.593683
C	14.484077	-2.907939	0.391587
H	12.410510	-2.765182	0.940563
H	14.129444	0.738071	-0.862258
H	16.307476	-0.413195	-1.025636

H	14.578410	-3.930604	0.745773	C	-0.987575	0.072420	1.865086
H	16.545184	-2.759469	-0.230737	O	-2.154008	0.004193	1.880088
H	-4.661738	-0.027287	0.733675	O	0.179727	0.138185	1.864361

A.4.5 Optimised Structures of Adducts between **OTPT-BZN-210** Oligomers and CO_2

*A.4.5.1 **OTPT-BZN-210**, **EB** State, with CO_2 Binding on Imine Nitrogen Atom*

H	14.296871	-1.713253	-1.725105	H	12.529914	2.909748	3.585903
C	13.250798	-1.795961	-2.005006	H	10.807580	4.167052	4.863368
C	10.560106	-2.008291	-2.722998	C	6.302854	-0.006154	-0.909424
C	12.285948	-1.089246	-1.292065	C	3.580963	-0.258940	-1.595241
C	12.874751	-2.609257	-3.077343	C	5.321102	0.710138	-0.206856
C	11.527635	-2.713181	-3.434067	C	5.907330	-0.835247	-1.973731
C	10.931428	-1.189608	-1.645254	C	4.571589	-0.943507	-2.326472
H	12.565011	-0.455419	-0.458505	C	3.979340	0.585661	-0.537996
H	13.628516	-3.159850	-3.632853	H	5.626374	1.363874	0.601785
H	11.232140	-3.344156	-4.267135	H	6.665739	-1.380475	-2.523138
H	9.512345	-2.080613	-2.990238	H	4.264702	-1.570650	-3.157102
C	9.904806	-0.439287	-0.888732	H	3.229697	1.162360	-0.005996
N	8.044670	0.924385	0.481854	N	2.259379	-0.361755	-2.021612
N	10.314964	0.340854	0.123597	C	1.270679	-0.580316	-1.204807
N	8.622773	-0.581971	-1.257789	C	-1.069692	-0.952657	0.426759
C	7.726614	0.118935	-0.544549	C	1.380006	-0.948698	0.208036
C	9.350132	1.003398	0.780864	C	-0.077460	-0.511695	-1.766094
C	9.751942	1.875980	1.906313	C	-1.180288	-0.663208	-1.004609
C	10.512579	3.526771	4.036986	C	0.278012	-1.140852	0.961930
C	11.104605	1.998836	2.259531	H	2.367535	-1.094359	0.629621
C	8.784120	2.588414	2.631176	H	-0.145557	-0.317177	-2.831679
C	9.164038	3.408625	3.690205	H	-2.168151	-0.605489	-1.445828
C	11.481006	2.820065	3.319073	H	0.348838	-1.427415	2.005153
H	11.846442	1.445950	1.695259	N	-2.065228	-1.113077	1.249891
H	7.741479	2.488668	2.352937	C	-3.383309	-0.827707	0.893856
H	8.408910	3.956497	4.246158	C	-6.090049	-0.275401	0.343259

C	-4.381364	-1.774947	1.191761
C	-3.764718	0.414884	0.347715
C	-5.099826	0.684408	0.081915
C	-5.710080	-1.508463	0.901123
H	-4.088520	-2.717455	1.639862
H	-3.007223	1.170111	0.164441
H	-5.392646	1.642081	-0.332247
H	-6.475427	-2.246058	1.111960
C	-7.506863	0.010134	0.047949
N	-10.082965	0.528678	-0.491002
N	-8.411814	-0.942179	0.325865
N	-7.810281	1.205447	-0.483692
C	-9.109973	1.419835	-0.737880
C	-9.687310	-0.638177	0.041475
C	-9.495361	2.720859	-1.328073
C	-10.224722	5.182826	-2.446115
C	-10.841096	2.998588	-1.613299
C	-8.518591	3.688720	-1.608756
C	-8.882967	4.912200	-2.164600
C	-11.201969	4.223202	-2.169011
H	-11.589758	2.246341	-1.394158
H	-7.481373	3.467124	-1.386138
H	-8.121018	5.655844	-2.378830
H	-12.245625	4.430325	-2.386604
H	-10.507601	6.137737	-2.879739
C	-10.723316	-1.653345	0.333712
C	-12.683976	-3.574376	0.888771
C	-10.365040	-2.891216	0.889526
C	-12.073587	-1.387368	0.058760
C	-13.047084	-2.343621	0.335444
C	-11.341129	-3.845177	1.164822
H	-9.320445	-3.089211	1.099444
H	-12.342813	-0.429179	-0.370024
H	-14.089875	-2.130042	0.119939
H	-11.055653	-4.800605	1.595079
H	-13.444503	-4.319427	1.104174
C	-1.899211	-1.735594	4.098457
O	-0.814741	-1.304904	4.183182
O	-2.979858	-2.179026	4.072043

*A.4.5.2 **OTPT-BZN-210, EB** State, with CO_2 Binding on Core Unit*

H	-14.438151	-2.222001	0.963426
C	-13.384770	-2.389614	1.167781
C	-10.675442	-2.819350	1.692335
C	-12.438411	-1.472637	0.718004
C	-12.980911	-3.522147	1.879847
C	-11.624523	-3.734115	2.140741
C	-11.074706	-1.680054	0.976602
H	-12.739289	-0.590609	0.164848
H	-13.720292	-4.236645	2.230150
H	-11.307403	-4.613116	2.694140
H	-9.620697	-2.972613	1.888652
C	-10.067414	-0.707031	0.499241
N	-8.242006	1.058881	-0.365356
N	-10.502826	0.369529	-0.173833
N	-8.776544	-0.956929	0.766211
C	-7.898351	-0.046570	0.315443
C	-9.554576	1.224810	-0.587595
C	-9.984522	2.426649	-1.336167
C	-10.798633	4.700936	-2.753417
C	-11.345622	2.651131	-1.594249

C	-9.035325	3.352869	-1.795318
C	-9.441821	4.483003	-2.499747
C	-11.748594	3.782398	-2.298934
H	-12.072985	1.931720	-1.236749
H	-7.985999	3.173034	-1.592732
H	-8.700975	5.194908	-2.851612
H	-12.803858	3.948793	-2.494361
H	-11.114382	5.583037	-3.303054
C	-6.466170	-0.276110	0.583251
C	-3.728389	-0.720800	1.084573
C	-5.502041	0.644615	0.143649
C	-6.044482	-1.413385	1.294221
C	-4.700692	-1.622297	1.560662
C	-4.152743	0.427823	0.384276
H	-5.827047	1.530706	-0.388999
H	-6.788953	-2.119774	1.642198
H	-4.373603	-2.490928	2.122778
H	-3.416546	1.157399	0.062781
N	-2.397146	-0.947820	1.424092
C	-1.426931	-0.869680	0.561042
C	0.874161	-0.641109	-1.148836
C	-1.570313	-0.745521	-0.891370
C	-0.065738	-0.979836	1.083469
C	1.019984	-0.851902	0.293472
C	-0.485038	-0.660633	-1.687613
H	-2.567403	-0.755020	-1.315493
H	0.026409	-1.157584	2.150233
H	2.018082	-0.944439	0.704349
H	-0.576330	-0.587481	-2.766643
N	1.845150	-0.491995	-2.001157
C	3.166460	-0.312162	-1.599400
C	5.877793	0.067258	-0.936783
C	4.168344	-1.088138	-2.212882
C	3.546578	0.687260	-0.680372
C	4.883430	0.874701	-0.360918
C	5.499591	-0.915883	-1.868239
H	3.874881	-1.838698	-2.939429
H	2.784334	1.323273	-0.242070
H	5.175917	1.642170	0.346163
H	6.267768	-1.533560	-2.318434
C	7.292866	0.237055	-0.556366
N	9.856360	0.508258	0.179533
N	8.195160	-0.588984	-1.108167
N	7.592942	1.197334	0.331966
C	8.886600	1.294188	0.673095
C	9.465147	-0.416368	-0.711113
C	9.268527	2.331313	1.656684
C	9.991547	4.293143	3.519796
C	10.607572	2.473936	2.051673
C	8.295189	3.181004	2.204544
C	8.656453	4.156023	3.130521
C	10.965285	3.449812	2.978191
H	11.353331	1.813667	1.624655
H	7.263123	3.064630	1.895114
H	7.897273	4.809784	3.549720
H	12.003700	3.553633	3.278814
H	10.271974	5.054081	4.242454
C	10.498809	-1.303016	-1.289481
C	12.455105	-2.982262	-2.383178
C	10.143561	-2.294171	-2.217402
C	11.843914	-1.161408	-0.915039
C	12.815227	-1.997113	-1.459849
C	11.117437	-3.128208	-2.760124
H	9.102980	-2.397998	-2.501697

H	12.110900	-0.393734	-0.198221	C	5.279889	-1.926340	1.466017
H	13.853969	-1.880978	-1.164908	O	4.181474	-2.184509	1.159929
H	10.834224	-3.892889	-3.477422	O	6.376485	-1.681671	1.787220
H	13.213872	-3.633648	-2.807293				

*A.4.5.3 **OTPT-BZN-210**, **EB** State, with CO_2 Binding on Linker Unit*

H	-14.139104	-2.490559	0.954470	H	-12.560865	3.490848	-2.845651
C	-13.087657	-2.619179	1.194012	H	-10.894846	5.137040	-3.678441
C	-10.383366	-2.948245	1.809449	C	-6.214463	-0.341540	0.693541
C	-12.153158	-1.701786	0.720902	C	-3.484083	-0.676956	1.301810
C	-12.674397	-3.702050	1.974631	C	-5.259691	0.568849	0.213803
C	-11.320536	-3.863830	2.280671	C	-5.787392	-1.411391	1.499537
C	-10.792087	-1.858680	1.024943	C	-4.447562	-1.564904	1.818609
H	-12.461405	-0.857949	0.114782	C	-3.912766	0.405409	0.505646
H	-13.404511	-4.417005	2.342979	H	-5.589719	1.404580	-0.392216
H	-10.996100	-4.704364	2.887062	H	-6.524841	-2.108977	1.878737
H	-9.330689	-3.063049	2.040027	H	-4.116918	-2.380367	2.453596
C	-9.797456	-0.884976	0.522880	H	-3.184264	1.128510	0.155780
N	-7.994970	0.880287	-0.389647	N	-2.156880	-0.844061	1.690730
N	-10.240605	0.135917	-0.227486	C	-1.170308	-0.839152	0.844655
N	-8.509822	-1.078753	0.845935	C	1.169634	-0.842176	-0.837566
C	-7.642948	-0.171259	0.367980	C	-1.283376	-0.858421	-0.615700
C	-9.303706	0.993414	-0.661886	C	0.181258	-0.877815	1.402050
C	-9.742487	2.135924	-1.493660	C	1.282681	-0.857262	0.622822
C	-10.572818	4.298312	-3.067916	C	-0.181954	-0.881908	-1.394847
C	-11.098571	2.297493	-1.816938	H	-2.272292	-0.891872	-1.057114
C	-8.806544	3.068528	-1.966841	H	0.252697	-0.916554	2.484279
C	-9.221094	4.143019	-2.749319	H	2.271556	-0.890077	1.064371
C	-11.509596	3.373085	-2.599835	H	-0.253389	-0.923700	-2.476962
H	-11.815753	1.573497	-1.448222	N	2.156113	-0.849663	-1.683753
H	-7.761196	2.937722	-1.712655	C	3.483412	-0.681404	-1.295828
H	-8.490531	4.860501	-3.111228	C	6.214236	-0.344202	-0.690255

C	4.446897	-1.569437	-1.812547
C	3.912378	0.401927	-0.501098
C	5.259473	0.566193	-0.210528
C	5.786937	-1.415026	-1.494847
H	4.116028	-2.385647	-2.446456
H	3.184055	1.125205	-0.151243
H	5.589656	1.402662	0.394384
H	6.524369	-2.112626	-1.874053
C	7.642947	-0.172845	-0.366226
N	10.240989	0.136308	0.226469
N	8.510097	-1.079198	-0.845830
N	7.994864	0.878506	0.391712
C	9.303803	0.992626	0.662569
C	9.797934	-0.884429	-0.524163
C	9.742471	2.134869	1.494766
C	10.572577	4.296687	3.069918
C	11.098763	2.297391	1.816690
C	8.806207	3.066235	1.969746
C	9.220646	4.140447	2.752667
C	11.509676	3.372698	2.600039
H	11.816191	1.574345	1.446592
H	7.760699	2.934691	1.716604
H	8.489834	4.856965	3.115980
H	12.561106	3.491201	2.844806
H	10.894517	5.135189	3.680802
C	10.792921	-1.856745	-1.028197
C	12.675952	-3.697411	-1.981691
C	10.384317	-2.946263	-1.812828
C	12.154240	-1.698532	-0.725955
C	13.089098	-2.614579	-1.200959
C	11.321846	-3.860505	-2.285940
H	9.331451	-3.062096	-2.042021
H	12.462391	-0.854730	-0.119737
H	14.140737	-2.484933	-0.962814
H	10.997497	-4.701013	-2.892414
H	13.406345	-4.411316	-2.351522
C	-0.000687	2.357240	-0.011018
O	0.974800	2.357313	-0.654608
O	-0.976151	2.360669	0.632619

A.4.6 Optimised Structures of Adducts between **OTPT-FLR-210** Oligomers and CO_2

*A.4.6.1 **OTPT-FLR-210**, **EB** State, with CO_2 Binding on Imine Nitrogen Atom*

H	-16.177002	-1.052616	-2.295191
C	-15.123959	-1.182483	-2.527008
C	-12.415589	-1.516202	-3.121080
C	-14.162358	-0.890456	-1.563221
C	-14.735816	-1.641269	-3.788572
C	-13.379770	-1.807156	-4.082539
C	-12.798968	-1.054974	-1.852292
H	-14.451013	-0.534138	-0.581288
H	-15.486996	-1.868772	-4.539500
H	-13.074656	-2.163702	-5.061971
H	-11.360963	-1.641164	-3.336954
C	-11.775542	-0.745792	-0.828819
N	-9.922855	-0.187206	1.029085
N	-12.197171	-0.307453	0.368019
N	-10.486892	-0.921465	-1.156019
C	-9.592778	-0.630817	-0.195846
C	-11.234684	-0.040595	1.265083
C	-11.648564	0.446104	2.600204

C	-12.431834	1.366600	5.126806
C	-13.008068	0.623392	2.899612
C	-10.685354	0.734392	3.579315
C	-11.076447	1.191816	4.834906
C	-13.395736	1.081267	4.156187
H	-13.746221	0.398308	2.138753
H	-9.637430	0.594452	3.341035
H	-10.324736	1.412260	5.587138
H	-14.449967	1.215849	4.379750
H	-12.735626	1.723565	6.106714
C	-8.163813	-0.808013	-0.505032
C	-5.421385	-1.138165	-1.101793
C	-7.182829	-0.520818	0.458503
C	-7.755969	-1.282607	-1.765125
C	-6.413573	-1.465096	-2.051586
C	-5.835895	-0.677256	0.169111
H	-7.494963	-0.175421	1.437346
H	-8.511771	-1.515032	-2.506310
H	-6.098095	-1.844921	-3.018000
H	-5.088887	-0.480703	0.931330
N	-4.098095	-1.393393	-1.421577
H	-2.373972	2.665267	-0.168245
C	-2.225163	1.630168	-0.460953
C	-1.763619	-1.047356	-1.338278
C	-0.899584	1.108302	-0.591697
C	-3.291434	0.827903	-0.723012
C	-3.121662	-0.561964	-1.147798
C	-0.706391	-0.251038	-1.051371
H	-4.298582	1.221276	-0.654534
H	-1.648255	-2.068691	-1.686956
C	0.337235	1.709984	-0.368665
C	3.059786	2.438427	-0.070588
C	0.667596	3.035716	0.055156
C	1.396213	0.768305	-0.667842
C	2.702781	1.103027	-0.529233
C	1.975501	3.383428	0.176448
H	-0.119368	3.752611	0.267659
H	3.492360	0.403633	-0.778755
H	2.267195	4.380867	0.487880
C	0.779293	-0.535270	-1.133149
H	1.072237	-1.376541	-0.494005
H	1.089814	-0.790122	-2.153540
N	4.277553	2.892520	0.102998
C	5.402874	2.082700	0.084754
C	7.810048	0.605405	0.117143
C	6.552641	2.558939	-0.581360
C	5.495182	0.867223	0.799193
C	6.680406	0.147922	0.815776
C	7.726215	1.823371	-0.581072
H	6.490509	3.505535	-1.108181
H	4.638737	0.518573	1.366749
H	6.749443	-0.778873	1.373446
H	8.599680	2.184005	-1.111701
C	9.062673	-0.169575	0.127943
N	11.344088	-1.583419	0.145138
N	10.111393	0.317244	-0.556652
N	9.085915	-1.321087	0.820268
C	10.246127	-1.993271	0.799977
C	11.229520	-0.422351	-0.519073
C	10.321136	-3.268743	1.547039
C	10.462783	-5.682229	2.961068
C	11.508515	-4.016732	1.554852
C	9.205350	-3.742081	2.254540
C	9.277507	-4.942033	2.957087

C	11.577172	-5.216408	2.258370	C	14.723792	-0.191135	-1.940978
H	12.366030	-3.645305	1.006039	C	13.462367	1.740281	-2.669456
H	8.291876	-3.159007	2.244097	H	11.419297	1.835181	-1.979778
H	8.409585	-5.301100	3.502345	H	13.653752	-1.586705	-0.689269
H	12.499881	-5.789207	2.259383	H	15.647436	-0.762258	-1.926871
H	10.517772	-6.618197	3.509575	H	13.403726	2.672925	-3.222834
C	12.412900	0.072442	-1.257403	H	15.521440	1.371433	-3.195942
C	14.652713	1.008407	-2.654223	C	5.331636	5.328788	1.128656
C	12.347917	1.276489	-1.975481	O	5.383988	4.859994	2.197965
C	13.611119	-0.657997	-1.246149	O	5.305625	5.847637	0.080731

*A.4.6.2 **OTPT-FLR-210**, **EB** State, with CO_2 Binding on Core Unit*

H	15.980321	1.576753	-2.323670	C	10.804010	-1.431695	3.334494
C	14.914753	1.703855	-2.490743	C	11.263003	-2.089344	4.472729
C	12.174216	2.030112	-2.918210	C	13.546296	-1.771023	3.739768
C	14.004844	1.210834	-1.559148	H	13.787851	-0.728351	1.865192
C	14.458776	2.360243	-3.637006	H	9.742889	-1.292465	3.163794
C	13.086827	2.521824	-3.847785	H	10.551652	-2.468624	5.200501
C	12.625805	1.369778	-1.765124	H	14.612867	-1.902647	3.896614
H	14.346210	0.700360	-0.666196	H	12.991228	-2.774137	5.566953
H	15.169642	2.744396	-4.362972	C	8.062637	0.710697	-0.315524
H	12.729039	3.031643	-4.737488	C	5.287828	1.027916	-0.749087
H	11.107935	2.149511	-3.070751	C	7.132534	0.219792	0.615722
C	11.657394	0.846243	-0.775786	C	7.586903	1.382584	-1.456441
N	9.904165	-0.102479	1.019402	C	6.228332	1.557157	-1.659412
N	12.143379	0.220099	0.307775	C	5.770175	0.369459	0.405529
N	10.351163	1.027508	-1.019036	H	7.496494	-0.278893	1.506615
C	9.508178	0.537605	-0.094163	H	8.302773	1.772220	-2.170828
C	11.228811	-0.237940	1.177366	H	5.860286	2.087197	-2.531991
C	11.714641	-0.937304	2.388016	H	5.062441	0.011075	1.146037
C	12.634507	-2.260882	4.678558	N	3.944292	1.278888	-0.974620
C	13.090672	-1.112673	2.600516	H	2.424601	-3.012384	-0.435598

C	2.225053	-1.949289	-0.532198
C	1.628983	0.819575	-0.891830
C	0.875956	-1.473447	-0.535997
C	3.249403	-1.065480	-0.668658
C	3.010900	0.369278	-0.829154
C	0.613925	-0.062752	-0.732135
H	4.273140	-1.418892	-0.696198
H	1.461848	1.881169	-1.044320
C	-0.327666	-2.162019	-0.403256
C	-3.009281	-3.057948	-0.195767
C	-0.590736	-3.557466	-0.225883
C	-1.432894	-1.230954	-0.501367
C	-2.720060	-1.644095	-0.403401
C	-1.879143	-3.981145	-0.145564
H	0.231402	-4.263878	-0.165104
H	-3.541709	-0.944145	-0.501878
H	-2.123965	-5.030145	-0.016500
C	-0.884062	0.163523	-0.726995
H	-1.192623	0.856061	0.064984
H	-1.235614	0.590474	-1.673912
N	-4.203212	-3.590767	-0.091826
C	-5.343747	-2.812410	0.044577
C	-7.726740	-1.319025	0.282646
C	-6.472619	-3.124991	-0.741893
C	-5.455648	-1.779163	1.000715
C	-6.627825	-1.048091	1.114489
C	-7.635567	-2.379333	-0.636611
H	-6.397175	-3.939477	-1.455096
H	-4.616049	-1.568954	1.654954
H	-6.703828	-0.247248	1.840869
H	-8.487695	-2.598001	-1.269731
C	-8.938736	-0.486069	0.353455
N	-11.119083	1.074621	0.437046
N	-10.016451	-0.873780	-0.346775
N	-8.886381	0.630468	1.099199
C	-9.997325	1.380705	1.108102
C	-11.083280	-0.063469	-0.273990
C	-9.982473	2.629294	1.902233
C	-9.950412	4.995323	3.400270
C	-11.126238	3.439249	1.971651
C	-8.822233	3.016533	2.590364
C	-8.807862	4.193338	3.334329
C	-11.108766	4.615014	2.717472
H	-12.018274	3.133837	1.437361
H	-7.942310	2.386648	2.530458
H	-7.905738	4.486459	3.863266
H	-11.998460	5.235888	2.766832
H	-9.937965	5.913051	3.981245
C	-12.297975	-0.448947	-1.025946
C	-14.597204	-1.179809	-2.447969
C	-12.321721	-1.637539	-1.771788
C	-13.437378	0.369895	-0.999622
C	-14.579600	0.005139	-1.707486
C	-13.465853	-1.999550	-2.477913
H	-11.438208	-2.265003	-1.786332
H	-13.411281	1.286312	-0.421698
H	-15.457161	0.644474	-1.682338
H	-13.476468	-2.921300	-3.052155
H	-15.489066	-1.463369	-2.999434
C	-6.100366	1.257060	-1.132059
O	-7.130259	1.238365	-1.682715
O	-5.064216	1.285318	-0.590056

*A.4.6.3 **OTPT-FLR-210**, **EB** State, with CO_2 Binding on Linker Unit*

H	-15.825946	-1.168059	2.116113
C	-14.777549	-1.320492	2.355167
C	-12.081057	-1.710813	2.968504
C	-13.794745	-0.736582	1.560182
C	-14.416511	-2.100103	3.457232
C	-13.066349	-2.293370	3.761313
C	-12.437127	-0.926983	1.860187
H	-14.062079	-0.129767	0.703013
H	-15.184145	-2.555101	4.076622
H	-12.782255	-2.898564	4.617196
H	-11.030801	-1.853416	3.194443
C	-11.391265	-0.307322	1.015823
N	-9.497596	0.816841	-0.516020
N	-11.787279	0.430727	-0.033414
N	-10.109350	-0.519259	1.347416
C	-9.193651	0.062558	0.554123
C	-10.804823	0.972459	-0.770840
C	-11.189836	1.794185	-1.940264
C	-11.918147	3.349651	-4.152794
C	-12.543608	1.994003	-2.251273
C	-10.204556	2.381261	-2.749003
C	-10.568328	3.154196	-3.848551
C	-12.903964	2.767616	-3.351548
H	-13.299090	1.537628	-1.622498
H	-9.161177	2.222405	-2.502865
H	-9.799551	3.605098	-4.469193
H	-13.953979	2.917469	-3.585055
H	-12.200593	3.953055	-5.010734
C	-7.771062	-0.140399	0.876043
C	-5.042649	-0.543868	1.485611
C	-6.767837	0.449859	0.089274
C	-7.391205	-0.917310	1.985917
C	-6.054435	-1.098728	2.298394
C	-5.427003	0.251995	0.381520
H	-7.057864	1.067641	-0.752808
H	-8.163811	-1.364537	2.600421
H	-5.760076	-1.686695	3.161797
H	-4.659474	0.738708	-0.211227
N	-3.721936	-0.705571	1.870626
H	-2.107787	-2.086830	-2.190113
C	-1.931043	-1.726002	-1.181272
C	-1.396932	-0.890103	1.496590
C	-0.592281	-1.530620	-0.716942
C	-2.974514	-1.465713	-0.349242
C	-2.767390	-0.997986	1.021158
C	-0.361551	-1.124740	0.654646
H	-3.992149	-1.627522	-0.683774
H	-1.253368	-0.578343	2.526291
C	0.626965	-1.671383	-1.376484
C	3.325927	-1.782952	-2.234525
C	0.920847	-2.067136	-2.719436
C	1.709926	-1.361734	-0.466070
C	3.005187	-1.409752	-0.863177
C	2.218163	-2.136693	-3.117242
H	0.115254	-2.313668	-3.404085
H	3.813128	-1.200497	-0.171692
H	2.487055	-2.436428	-4.124633
C	1.130330	-1.015490	0.890307
H	1.418362	-0.007907	1.209800
H	1.471988	-1.709308	1.667695
N	4.528873	-1.875313	-2.748788
C	5.661796	-1.405949	-2.102618

C	8.075625	-0.494994	-0.950022
C	6.826061	-2.203317	-2.135877
C	5.743796	-0.123599	-1.513022
C	6.931808	0.320750	-0.953042
C	8.002536	-1.764347	-1.551801
H	6.771788	-3.176576	-2.612950
H	4.874750	0.525857	-1.532310
H	6.991068	1.307985	-0.509572
H	8.886694	-2.391025	-1.560983
C	9.330742	-0.024648	-0.339587
N	11.616646	0.829681	0.778772
N	10.393301	-0.846871	-0.368856
N	9.342817	1.199328	0.215347
C	10.505473	1.582919	0.762332
C	11.512990	-0.377632	0.200809
C	10.567882	2.922374	1.388933
C	10.685494	5.456631	2.575504
C	11.754438	3.368454	1.990965
C	9.440773	3.758499	1.387369
C	9.501020	5.018211	1.977461
C	11.811096	4.628591	2.580647
H	12.620562	2.717061	1.988807
H	8.528157	3.407122	0.920219
H	8.624451	5.659388	1.971434
H	12.733121	4.966100	3.044832
H	10.731141	6.439545	3.035635
C	12.711393	-1.246210	0.192305
C	14.979193	-2.889882	0.176213
C	12.659320	-2.519913	-0.394643
C	13.911052	-0.804186	0.770996
C	15.037548	-1.622596	0.762077
C	13.787589	-3.335791	-0.401739
H	11.729687	-2.854552	-0.839860
H	13.944015	0.180641	1.222039
H	15.962085	-1.272844	1.211989
H	13.738755	-4.320104	-0.858072
H	15.858723	-3.527307	0.169939
C	-1.000187	1.802620	-0.583525
O	0.168359	1.817952	-0.550816
O	-2.168004	1.797226	-0.622912

A.4.7 Microscopic Structures of the Adducts between **210** Oligomers and CO_2

This section summarises the microscopic structures of the adducts between **210** oligomers and CO_2 molecules.

*Table A-3 Structural parameters related to the interactions between a CO_2 molecule and a **210** PANI-CMP fragment in the **EB** state with different core and linker combinations on different binding sites. CO_2 distances are measured as C···N distances for imine nitrogen binding sites and measured as the average distances of CO_2 atoms from the BQ unit plane for core and linker unit binding sites. Only one N···H distance can be found for **TPT**-based oligomer fragments due to their flat D_{3h} geometry.*

Core-Linker Combination	Binding Site	Structural Parameters					
		PANI-CMP–CO_2 Interactions			CO_2 Geometries		
		CO_2 Distance (Å)	N···H Distance (Å)		C–O Distance (Å)		O–C–O Angle (°)
OTPA-BZN	Imine Nitrogen	2.870	2.481	3.018	1.170	1.169	176.3
	Linker Unit	3.229	2.613	2.614	1.169	1.169	179.5
	Core Unit	3.117	2.843	2.529	1.168	1.169	179.0
OTPA-FLR	Imine Nitrogen	2.892	2.526	2.584	1.169	1.169	176.4
	Linker Unit	3.167	2.805	2.799	1.169	1.168	179.1
	Core Unit	3.145	2.544	2.818	1.169	1.168	178.9
OTPB-BZN	Imine Nitrogen	2.878	3.096	2.474	1.168	1.170	176.6
	Linker Unit	3.243	2.594	2.596	1.169	1.169	179.7
	Core Unit	3.224	2.555	2.633	1.169	1.168	178.9
OTPB-FLR	Imine Nitrogen	2.907	2.522	2.574	1.169	1.169	176.8
	Linker Unit	3.171	2.815	2.758	1.169	1.169	179.3
	Core Unit	3.195	2.538	2.653	1.169	1.169	178.8
OTPT-BZN	Imine Nitrogen	2.921	2.472	2.727	1.170	1.168	177.1
	Linker Unit	3.237	2.573	2.579	1.169	1.169	179.8
	Core Unit	3.187	2.535	-	1.169	1.169	179.0
OTPT-FLR	Imine Nitrogen	2.846	3.398	2.881	1.170	1.169	177.0
	Linker Unit	3.172	2.828	2.738	1.169	1.168	179.4
	Core Unit	3.243	2.701	-	1.170	1.168	179.3

A.4.7.1 Microscopic Structures of Imine/Amine Binding Sites

This section lists microscopic structures for both imine and amine binding sites, the latter of which is an equivalent of the former for the reduced **LEB** state.

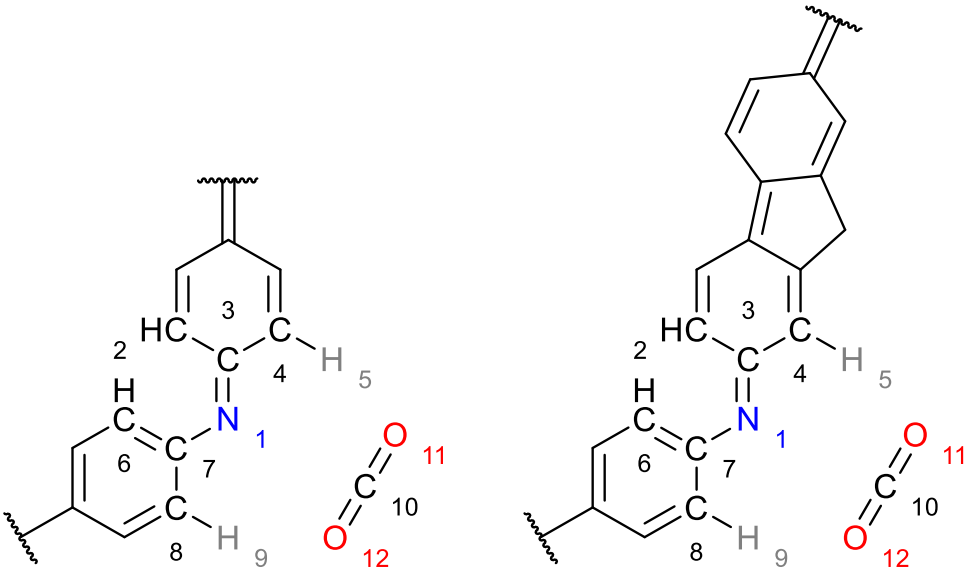

Scheme A-1 General numbering of atoms involved in the geometries of imine binding site

*Table A-4 Comparisons between structural parameters before and after a CO_2 molecule is bound to the imine binding site from DFT-optimisesd structures of **EB OTPA-BZN-210**–CO_2 complex.*

Parameter		Before Binding	After Binding
Oligomer fragment structure parameters			
C_{ipso}–C_{ortho} bond length	C^2–C^3	1.460 Å	1.460 Å
	C^3–C^4	1.457 Å	1.458 Å
	C^6–C^7	1.413 Å	1.412 Å
	C^7–C^8	1.411 Å	1.410 Å
C_{ortho}–H bond length	C^4–H^5	1.086 Å	1.085 Å
	C^8–H^9	1.085 Å	1.085 Å
C_{ipso}–N bond length	C^3–N^1	1.308 Å	1.309 Å
	C^7–N^1	1.389 Å	1.390 Å
C_{ortho}–C_{ipso}–C_{ortho} bond angle	C^2–C^3–C^4	116.3°	116.4°
	C^6–C^7–C^8	117.6°	117.7°
C_{ipso}–C_{ortho}–H bond angle	C^3–C^4–H^5	116.3°	116.5°
	C^7–C^8–H^9	118.3°	118.5°
C_{ortho}–C_{ipso}–N bond angle	C^2–C^3–N^1	126.9°	126.4°
	C^4–C^3–N^1	116.7°	117.1°
	C^6–C^7–N^1	124.3°	123.9°
	C^8–C^7–N^1	117.8°	118.1°
C_{ipso}–N–C_{ipso} bond angle	C^3–N^1–C^7	123.1°	122.9°
Dihedral angle	C^2–C^3–N^1–C^7	-12.1°	-12.1°
	C^3–N^1–C^7–C^6	-41.3°	-42.8°
CO_2 structural parameters			
C–O bond length	C^{10}–O^{11}	1.169 Å	1.170 Å
	C^{10}–O^{12}	1.169 Å	1.169 Å
O–C–O bond angle	O^{11}–C^{10}–O^{12}	180.0°	176.3°

Parameter		Before Binding	After Binding
Interaction-related parameters			
N···C–O angle	$N^{1}\cdots C^{10}–O^{11}$	-	94.4°
	$N^{1}\cdots C^{10}–O^{12}$	-	89.2°
O···H distance	$H^{5}\cdots O^{11}$	-	2.481 Å
	$H^{9}\cdots O^{12}$	-	3.018 Å
N···C distance	$N^{1}\cdots C^{10}$	-	2.870 Å

*Table A-5 Comparisons between structural parameters before and after a CO_2 molecule is bound to the imine binding site from DFT-optimisesd structures of **EB OTPA-FLR-210**–CO_2 complex.*

Parameter		Before Binding	After Binding
Oligomer fragment structure parameters			
C_{ipso}–C_{ortho} bond length	$C^{2}–C^{3}$	1.458 Å	1.458 Å
	$C^{3}–C^{4}$	1.452 Å	1.451 Å
	$C^{6}–C^{7}$	1.416 Å	1.415 Å
	$C^{7}–C^{8}$	1.414 Å	1.413 Å
C_{ortho}–H bond length	$C^{4}–H^{5}$	1.086 Å	1.085 Å
	$C^{8}–H^{9}$	1.085 Å	1.084 Å
C_{ipso}–N bond length	$C^{3}–N^{1}$	1.319 Å	1.320 Å
	$C^{7}–N^{1}$	1.382 Å	1.384 Å
C_{ortho}–C_{ipso}–C_{ortho} bond angle	$C^{2}–C^{3}–C^{4}$	117.2°	117.3°
	$C^{6}–C^{7}–C^{8}$	117.3°	117.4°
C_{ipso}–C_{ortho}–H bond angle	$C^{3}–C^{4}–H^{5}$	117.0°	117.4°
	$C^{7}–C^{8}–H^{9}$	118.2°	118.4°
C_{ortho}–C_{ipso}–N bond angle	$C^{2}–C^{3}–N^{1}$	125.8°	125.2°
	$C^{4}–C^{3}–N^{1}$	116.9°	117.4°
	$C^{6}–C^{7}–N^{1}$	124.6°	124.0°
	$C^{8}–C^{7}–N^{1}$	117.9°	118.4°
C_{ipso}–N–C_{ipso} bond angle	$C^{3}–N^{1}–C^{7}$	123.3°	122.8°
Dihedral angle	$C^{2}–C^{3}–N^{1}–C^{7}$	14.7°	15.8°
	$C^{3}–N^{1}–C^{7}–C^{6}$	39.3°	40.7°
CO_2 structural parameters			
C–O bond length	$C^{10}–O^{11}$	1.169 Å	1.169 Å
	$C^{10}–O^{12}$	1.169 Å	1.169 Å
O–C–O bond angle	$O^{11}–C^{10}–O^{12}$	180.0°	176.4°
Interaction-related parameters			
N···C–O angle	$N^{1}\cdots C^{10}–O^{11}$	-	91.6°
	$N^{1}\cdots C^{10}–O^{12}$	-	91.9°
O···H distance	$H^{5}\cdots O^{11}$	-	2.584 Å
	$H^{9}\cdots O^{12}$	-	2.526 Å
N···C distance	$N^{1}\cdots C^{10}$	-	2.892 Å

*Table A-6 Comparisons between structural parameters before and after a CO_2 molecule is bound to the imine binding site from DFT-optimisesd structures of **EB OTPB-BZN-210**–CO_2 complex.*

Parameter		Before Binding	After Binding
Oligomer fragment structure parameters			
C_{ipso}–C_{ortho} bond length	C^2–C^3	1.464 Å	1.464 Å
	C^3–C^4	1.461 Å	1.461 Å
	C^6–C^7	1.409 Å	1.408 Å
	C^7–C^8	1.407 Å	1.407 Å
C_{ortho}–H bond length	C^4–H^5	1.085 Å	1.085 Å
	C^8–H^9	1.085 Å	1.085 Å
C_{ipso}–N bond length	C^3–N^1	1.303 Å	1.303 Å
	C^7–N^1	1.395 Å	1.396 Å
C_{ortho}–C_{ipso}–C_{ortho} bond angle	C^2–C^3–C^4	116.6°	116.7°
	C^6–C^7–C^8	118.3°	118.4°
C_{ipso}–C_{ortho}–H bond angle	C^3–C^4–H^5	116.2°	116.4°
	C^7–C^8–H^9	118.6°	118.7°
C_{ortho}–C_{ipso}–N bond angle	C^2–C^3–N^1	126.5°	126.2°
	C^4–C^3–N^1	116.8°	117.0°
	C^6–C^7–N^1	123.4°	123.2°
	C^8–C^7–N^1	118.1°	118.3°
C_{ipso}–N–C_{ipso} bond angle	C^3–N^1–C^7	122.7°	122.6°
Dihedral angle	C^2–C^3–N^1–C^7	-10.4°	-10.2°
	C^3–N^1–C^7–C^6	-47.4°	-48.5°
CO_2 structural parameters			
C–O bond length	C^{10}–O^{11}	1.169 Å	1.170 Å
	C^{10}–O^{12}	1.169 Å	1.168 Å
O–C–O bond angle	O^{11}–C^{10}–O^{12}	180.0°	176.6°
Interaction-related parameters			
N···C–O angle	N^1···C^{10}–O^{11}	-	94.3°
	N^1···C^{10}–O^{12}	-	89.0°
O···H distance	H^5···O^{11}	-	2.474 Å
	H^9···O^{12}	-	3.096 Å
N···C distance	N^1···C^{10}	-	2.878 Å

*Table A-7 Comparisons between structural parameters befor and after a CO_2 molecule is bound to the imine binding site from DFT-optimisesd structures of **EB OTPB-FLR-210**–CO_2 complex.*

Parameter		Before Binding	After Binding
Oligomer fragment structure parameters			
C_{ipso}–C_{ortho} bond length	C^2–C^3	1.412 Å	1.412 Å
	C^3–C^4	1.410 Å	1.410 Å
	C^6–C^7	1.463 Å	1.462 Å
	C^7–C^8	1.455 Å	1.454 Å
C_{ortho}–H bond length	C^4–H^5	1.085 Å	1.084 Å
	C^8–H^9	1.086 Å	1.085 Å
C_{ipso}–N bond length	C^3–N^1	1.389 Å	1.390 Å
	C^7–N^1	1.313 Å	1.314 Å
C_{ortho}–C_{ipso}–C_{ortho} bond angle	C^2–C^3–C^4	117.9°	117.9°
	C^6–C^7–C^8	117.4°	117.4°
C_{ipso}–C_{ortho}–H bond angle	C^3–C^4–H^5	118.4°	118.6°
	C^7–C^8–H^9	117.0°	117.4°
C_{ortho}–C_{ipso}–N bond angle	C^2–C^3–N^1	123.7°	123.2°
	C^4–C^3–N^1	118.2°	118.1°
	C^6–C^7–N^1	125.5°	125.1°
	C^8–C^7–N^1	117.1°	117.4°
C_{ipso}–N–C_{ipso} bond angle	C^3–N^1–C^7	122.9°	122.6°
Dihedral angle	C^2–C^3–N^1–C^7	45.6°	46.2°
	C^3–N^1–C^7–C^6	12.5°	13.6°
CO_2 structural parameters			
C–O bond length	C^{10}–O^{11}	1.169 Å	1.169 Å
	C^{10}–O^{12}	1.169 Å	1.169 Å
O–C–O bond angle	O^{11}–C^{10}–O^{12}	180.0°	176.8°
Interaction-related parameters			
N···C–O angle	N^1···C^{10}–O^{11}	-	91.1°
	N^1···C^{10}–O^{12}	-	92.1°
O···H distance	H^5···O^{11}	-	2.522 Å
	H^9···O^{12}	-	2.574 Å
N···C distance	N^1···C^{10}	-	2.907 Å

*Table A-8 Comparisons between structural parameters before and after a CO_2 molecule is bound to the imine binding site from DFT-optimisesd structures of **EB OTPT-BZN-210**–CO_2 complex.*

Parameter		Before Binding	After Binding
Oligomer fragment structure parameters			
C_{ipso}–C_{ortho} bond length	C^2–C^3	1.464 Å	1.464 Å
	C^3–C^4	1.462 Å	1.462 Å
	C^6–C^7	1.411 Å	1.410 Å
	C^7–C^8	1.409 Å	1.408 Å
C_{ortho}–H bond length	C^4–H^5	1.085 Å	1.084 Å
	C^8–H^9	1.085 Å	1.084 Å
C_{ipso}–N bond length	C^3–N^1	1.301 Å	1.302 Å
	C^7–N^1	1.393 Å	1.395 Å
C_{ortho}–C_{ipso}–C_{ortho} bond angle	C^2–C^3–C^4	116.9°	116.9°
	C^6–C^7–C^8	118.8°	118.9°
C_{ipso}–C_{ortho}–H bond angle	C^3–C^4–H^5	116.3°	116.5°
	C^7–C^8–H^9	118.6°	118.7°
C_{ortho}–C_{ipso}–N bond angle	C^2–C^3–N^1	126.2°	125.8°
	C^4–C^3–N^1	116.9°	117.2°
	C^6–C^7–N^1	122.8°	122.3°
	C^8–C^7–N^1	118.2°	118.6°
C_{ipso}–N–C_{ipso} bond angle	C^3–N^1–C^7	122.8°	122.4°
Dihedral angle	C^2–C^3–N^1–C^7	-9.9°	-9.9°
	C^3–N^1–C^7–C^6	-51.0°	-52.6°
CO_2 structural parameters			
C–O bond length	C^{10}–O^{11}	1.169 Å	1.170 Å
	C^{10}–O^{12}	1.169 Å	1.168 Å
O–C–O bond angle	O^{11}–C^{10}–O^{12}	180.0°	177.1°
Interaction-related parameters			
N···C–O angle	N^1···C^{10}–O^{11}	-	92.6°
	N^1···C^{10}–O^{12}	-	90.4°
O···H distance	H^5···O^{11}	-	2.472 Å
	H^9···O^{12}	-	2.727 Å
N···C distance	N^1···C^{10}	-	2.921 Å

*Table A-9 Comparisons between structural parameters before and after a CO_2 molecule is bound to the imine binding site from DFT-optimisesd structures of **EB OTPT-FLR-210**–CO_2 complex.*

Parameter		Before Binding	After Binding
Oligomer fragment structure parameters			
C_{ipso}–C_{ortho} bond length	C^2–C^3	1.457 Å	1.456 Å
	C^3–C^4	1.460 Å	1.459 Å
	C^6–C^7	1.414 Å	1.413 Å
	C^7–C^8	1.412 Å	1.412 Å
C_{ortho}–H bond length	C^4–H^5	1.085 Å	1.085 Å
	C^8–H^9	1.085 Å	1.085 Å
C_{ipso}–N bond length	C^3–N^1	1.312 Å	1.311 Å
	C^7–N^1	1.386 Å	1.387 Å
C_{ortho}–C_{ipso}–C_{ortho} bond angle	C^2–C^3–C^4	117.6°	117.7°
	C^6–C^7–C^8	118.3°	118.4°
C_{ipso}–C_{ortho}–H bond angle	C^3–C^4–H^5	116.1°	116.4°
	C^7–C^8–H^9	118.4°	118.5°
C_{ortho}–C_{ipso}–N bond angle	C^2–C^3–N^1	126.1°	125.9°
	C^4–C^3–N^1	116.2°	116.3°
	C^6–C^7–N^1	123.3°	123.3°
	C^8–C^7–N^1	118.2°	118.0°
C_{ipso}–N–C_{ipso} bond angle	C^3–N^1–C^7	122.9°	123.3°
Dihedral angle	C^2–C^3–N^1–C^7	-11.3°	-11.2°
	C^3–N^1–C^7–C^6	-47.9°	-47.5°
CO_2 structural parameters			
C–O bond length	C^{10}–O^{11}	1.169 Å	1.169 Å
	C^{10}–O^{12}	1.169 Å	1.170 Å
O–C–O bond angle	O^{11}–C^{10}–O^{12}	180.0°	177.0°
Interaction-related parameters			
N···C–O angle	N^1···C^{10}–O^{11}	-	90.2°
	N^1···C^{10}–O^{12}	-	92.8°
O···H distance	H^5···O^{11}	-	3.587 Å
	H^9···O^{12}	-	2.881 Å
N···C distance	N^1···C^{10}	-	2.846 Å

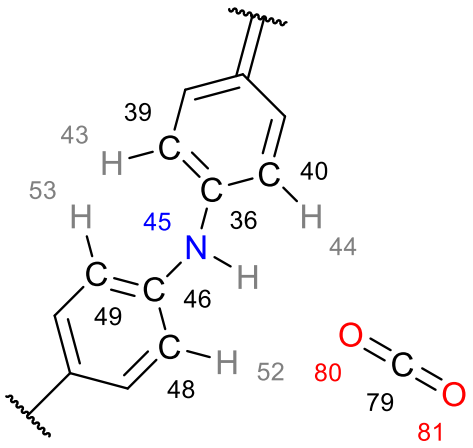

Scheme A-2 Numbering of atoms involved in the geometries of amine binding site. The unnumbered hydrogen atom has different numberings in the optimised structures before and after binding and thus will only be referred to simply as H.

*Table A-10 Comparisons between structural parameters before and after a CO_2 molecule is bound to the amine binding site from DFT-optimisesd structures of **LEB OTPA-BZN-210**–CO_2 complex.*

Parameter		Before Binding	After Binding
Oligomer fragment structure parameters			
C_{ipso}–C_{ortho} bond length	C^{36}–C^{39}	1.405 Å	1.403 Å
	C^{36}–C^{40}	1.404 Å	1.405 Å
	C^{46}–C^{48}	1.408 Å	1.405 Å
	C^{46}–C^{49}	1.407 Å	1.406 Å
C_{ortho}–H bond length	C^{39}–H^{43}	1.084 Å	1.084 Å
	C^{40}–H^{44}	1.087 Å	1.087 Å
	C^{48}–H^{52}	1.087 Å	1.087 Å
	C^{49}–H^{53}	1.083 Å	1.083 Å
C_{ipso}–N bond length	C^{36}–N^{45}	1.401 Å	1.405 Å
	C^{46}–N^{45}	1.393 Å	1.397 Å
N–H bond length	N^{45}–H	1.010 Å	1.011 Å
C_{ortho}–C_{ipso}–C_{ortho} bond angle	C^{39}–C^{36}–C^{40}	118.0°	118.1°
	C^{48}–C^{46}–C^{49}	118.2°	118.4°
C_{ipso}–C_{ortho}–H bond angle	C^{36}–C^{39}–H^{43}	120.0°	120.1°
	C^{36}–C^{40}–H^{44}	119.3°	119.3°
	C^{46}–C^{48}–H^{52}	119.3°	119.4°
	C^{46}–C^{49}–H^{53}	120.1°	119.9°
C_{ortho}–C_{ipso}–N bond angle	C^{39}–C^{36}–N^{45}	122.6°	123.4°
	C^{40}–C^{36}–N^{45}	119.2°	118.4°
	C^{48}–C^{46}–N^{45}	118.7°	119.1°
	C^{49}–C^{46}–N^{45}	123.1°	122.4°
C_{ipso}–N–C_{ipso} bond angle	C^{36}–N^{45}–C^{46}	128.3°	127.8°
C_{ipso}–N–H bond angle	C^{36}–N^{45}–H	115.7°	115.0°
	C^{46}–N^{45}–H	115.7°	115.0°
Dihedral angle	C^{40}–C^{36}–N^{45}–C^{46}	-34.5°	-17.1°
	C^{36}–N^{45}–C^{46}–C^{48}	-16.8°	-34.7°
CO_2 structural parameters			
C–O bond length	C^{79}–O^{80}	1.169 Å	1.168 Å
	C^{79}–O^{81}	1.169 Å	1.170 Å
O–C–O bond angle	O^{80}–C^{79}–O^{81}	180.0°	178.6°
Interaction-related parameters			
N···C–O angle	N^{45}···C^{79}–O^{80}	-	93.7°
	N^{45}···C^{79}–O^{81}	-	87.6°
O···H distance	H^{44}···O^{81}	-	2.882 Å
	H^{53}···O^{80}	-	2.812 Å
	H···O^{81}	-	3.019 Å
N···C distance	N^{45}···C^{79}	-	2.973 Å

*A.4.7.2 Microscopic Structures of **BZN** Linker Binding Sites*

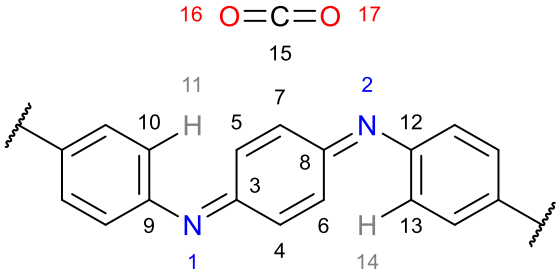

*Scheme A-3 Numbering of atoms involved in the geometries of **BZN** linker unit binding site*

*Table A-11 Comparisons between structural parameters before and after a CO_2 molecule is bound to the **BZN** linker unit binding site from DFT-optimisesd structures of **EB OTPA-BZN-210**–CO_2 complex.*

Parameter		Before Binding	After Binding
BQ unit structure parameters			
C_{ipso}–C_{ortho} bond length	C^3–C^4	1.457 Å	1.457 Å
	C^3–C^5	1.460 Å	1.461 Å
	C^8–C^6	1.460 Å	1.461 Å
	C^8–C^7	1.457 Å	1.457 Å
C_{ortho}–C_{ortho} bond length	C^4–C^6	1.353 Å	1.353 Å
	C^5–C^7	1.353 Å	1.353 Å
C_{ipso}–N bond length	C^3–N^1	1.308 Å	1.308 Å
	C^8–N^2	1.308 Å	1.308 Å
C_{ortho}–C_{ipso}–C_{ortho} bond angle	C^4–C^3–C^5	116.3°	116.3°
	C^6–C^8–C^7	116.3°	116.3°
C_{ipso}–C_{ortho}–C_{ortho} bond angle	C^3–C^4–C^6	122.4°	122.5°
	C^3–C^5–C^7	121.0°	121.0°
	C^8–C^6–C^4	121.0°	121.0°
	C^8–C^7–C^5	122.4°	122.5°
C_{ortho}–C_{ipso}–N bond angle	C^4–C^3–N^1	116.7°	116.7°
	C^5–C^3–N^1	126.9°	126.9°
	C^6–C^8–N^2	126.9°	126.9°
	C^7–C^8–N^2	116.7°	116.7°
Adjacent unit structure parameters			
N–C_{ipso} bond length	N^1–C^9	1.389 Å	1.388 Å
	N^2–C^{12}	1.389 Å	1.388 Å
C_{ipso}–C_{ortho} bond length	C^9–C^{10}	1.413 Å	1.413 Å
	C^{12}–C^{13}	1.413 Å	1.413 Å
C_{ortho}–H bond length	C^{10}–H^{11}	1.085 Å	1.084 Å
	C^{13}–H^{14}	1.085 Å	1.084 Å
C_{ipso}–N–C_{ipso} bond angle	C^3–N^1–C^9	123.1°	123.1°
	C^8–N^2–C^{12}	123.1°	123.1°
N–C_{ipso}–C_{ortho} bond angle	N^1–C^9–C^{10}	124.3°	124.3°
	N^2–C^{12}–C^{13}	124.3°	124.3°
C_{ipso}–C_{ortho}–H bond angle	C^9–C^{10}–H^{11}	119.5°	119.4°
	C^{12}–C^{13}–H^{14}	119.5°	119.4°
Dihedral angle	C^5–C^3–N^1–C^9	-12.1°	-12.1°
	C^3–N^1–C^9–C^{10}	-41.3°	-41.9°
	C^6–C^8–N^2–C^{12}	-12.1°	-12.1°
	C^8–N^2–C^{12}–C^{13}	-41.3°	-41.9°
CO_2 structural parameters			

Parameter		Before Binding	After Binding
C–O bond length	C^{15}–O^{16}	1.169 Å	1.169 Å
	C^{15}–O^{17}	1.169 Å	1.169 Å
O–C–O bond angle	O^{16}–C^{15}–O^{17}	180.0°	179.5°
Interaction-related parameters			
O···H distance	H^{11}···O^{16}	-	2.613 Å
	H^{14}···O^{17}	-	2.613 Å
BQ···CO_2 distance	BQ···C^{15}	-	3.226 Å
	BQ···O^{16}	-	3.206 Å
	BQ···O^{17}	-	3.257 Å
	Average	-	3.229 Å

*Table A-12 Comparisons between structural parameters before and after a CO_2 molecule is bound to the **BZN** linker unit binding site from DFT-optimisesd structures of **LEB OTPA-BZN-210**–CO_2 complex.*

Parameter		Before Binding	After Binding
BQ unit structure parameters			
C_{ipso}–C_{ortho} bond length	C^3–C^4	1.404 Å	1.404 Å
	C^3–C^5	1.405 Å	1.405 Å
	C^8–C^6	1.405 Å	1.405 Å
	C^8–C^7	1.404 Å	1.404 Å
C_{ortho}–C_{ortho} bond length	C^4–C^6	1.390 Å	1.391 Å
	C^5–C^7	1.390 Å	1.391 Å
C_{ipso}–N bond length	C^3–N^1	1.401 Å	1.399 Å
	C^8–N^2	1.401 Å	1.399 Å
C_{ortho}–C_{ipso}–C_{ortho} bond angle	C^4–C^3–C^5	118.0°	118.0°
	C^6–C^8–C^7	118.0°	118.0°
C_{ipso}–C_{ortho}–C_{ortho} bond angle	C^3–C^4–C^6	121.3°	121.4°
	C^3–C^5–C^7	120.6°	120.6°
	C^8–C^6–C^4	120.6°	120.6°
	C^8–C^7–C^5	121.3°	121.4°
C_{ortho}–C_{ipso}–N bond angle	C^4–C^3–N^1	119.2°	119.1°
	C^5–C^3–N^1	122.6°	122.9°
	C^6–C^8–N^2	122.6°	122.9°
	C^7–C^8–N^2	119.2°	119.1°
Adjacent unit structure parameters			
N–C_{ipso} bond length	N^1–C^9	1.393 Å	1.393 Å
	N^2–C^{12}	1.393 Å	1.393 Å
C_{ipso}–C_{ortho} bond length	C^9–C^{10}	1.407 Å	1.407 Å
	C^{12}–C^{13}	1.407 Å	1.407 Å
C_{ortho}–H bond length	C^{10}–H^{11}	1.083 Å	1.083 Å
	C^{13}–H^{14}	1.083 Å	1.083 Å
C_{ipso}–N–C_{ipso} bond angle	C^3–N^1–C^9	128.3°	128.6°
	C^8–N^2–C^{12}	128.3°	128.6°
N–C_{ipso}–C_{ortho} bond angle	N^1–C^9–C^{10}	123.1°	123.0°
	N^2–C^{12}–C^{13}	123.1°	123.0°
C_{ipso}–C_{ortho}–H bond angle	C^9–C^{10}–H^{11}	120.1°	120.0°
	C^{12}–C^{13}–H^{14}	120.1°	120.0°
Dihedral angle	C^5–C^3–N^1–C^9	-34.5°	-29.0°
	C^3–N^1–C^9–C^{10}	-16.8°	-22.0°
	C^6–C^8–N^2–C^{12}	-34.5°	-28.4°
	C^8–N^2–C^{12}–C^{13}	-16.8°	-22.6°
CO_2 structural parameters			
C–O bond length	C^{15}–O^{16}	1.169 Å	1.169 Å
	C^{15}–O^{17}	1.169 Å	1.169 Å
O–C–O bond angle	O^{16}–C^{15}–O^{17}	180.0°	178.9°

Parameter		Before Binding	After Binding
Interaction-related parameters			
O···H distance	$H^{11}\cdots O^{16}$	-	2.715 Å
	$H^{14}\cdots O^{17}$	-	2.715 Å
BQ···CO_2 distance	BQ···C^{15}	-	3.263 Å
	BQ···O^{16}	-	3.274 Å
	BQ···O^{17}	-	3.274 Å
	Average	-	3.270 Å

*Table A-13 Comparisons between structural parameters before and after a CO_2 molecule is bound to the **BZN** linker unit binding site from DFT-optimisesd structures of **EB OTPB-BZN-210**–CO_2 complex.*

Parameter		Before Binding	After Binding
BQ unit structure parameters			
C_{ipso}–C_{ortho} bond length	C^3–C^4	1.461 Å	1.461 Å
	C^3–C^5	1.464 Å	1.464 Å
	C^8–C^6	1.464 Å	1.464 Å
	C^8–C^7	1.461 Å	1.461 Å
C_{ortho}–C_{ortho} bond length	C^4–C^6	1.350 Å	1.350 Å
	C^5–C^7	1.350 Å	1.350 Å
C_{ipso}–N bond length	C^3–N^1	1.303 Å	1.302 Å
	C^8–N^2	1.303 Å	1.302 Å
C_{ortho}–C_{ipso}–C_{ortho} bond angle	C^4–C^3–C^5	116.6°	116.6°
	C^6–C^8–C^7	116.6°	116.6°
C_{ipso}–C_{ortho}–C_{ortho} bond angle	C^3–C^4–C^6	122.3°	122.4°
	C^3–C^5–C^7	120.9°	120.9°
	C^8–C^6–C^4	120.9°	120.9°
	C^8–C^7–C^5	122.3°	122.4°
C_{ortho}–C_{ipso}–N bond angle	C^4–C^3–N^1	116.8°	116.8°
	C^5–C^3–N^1	126.5°	126.5°
	C^6–C^8–N^2	126.5°	126.5°
	C^7–C^8–N^2	116.8°	116.9°
Adjacent unit structure parameters			
N–C_{ipso} bond length	N^1–C^9	1.395 Å	1.395 Å
	N^2–C^{12}	1.395 Å	1.395 Å
C_{ipso}–C_{ortho} bond length	C^9–C^{10}	1.409 Å	1.409 Å
	C^{12}–C^{13}	1.409 Å	1.409 Å
C_{ortho}–H bond length	C^{10}–H^{11}	1.085 Å	1.085 Å
	C^{13}–H^{14}	1.085 Å	1.085 Å
C_{ipso}–N–C_{ipso} bond angle	C^3–N^1–C^9	122.7°	122.7°
	C^8–N^2–C^{12}	122.6°	122.6°
N–C_{ipso}–C_{ortho} bond angle	N^1–C^9–C^{10}	123.4°	123.3°
	N^2–C^{12}–C^{13}	123.4°	123.3°
C_{ipso}–C_{ortho}–H bond angle	C^9–C^{10}–H^{11}	119.5°	119.4°
	C^{12}–C^{13}–H^{14}	119.4°	119.4°
Dihedral angle	C^5–C^3–N^1–C^9	-10.4°	-10.4°
	C^3–N^1–C^9–C^{10}	-47.4°	-48.5°
	C^6–C^8–N^2–C^{12}	-10.4°	-10.4°
	C^8–N^2–C^{12}–C^{13}	-47.4°	-48.5°
CO_2 structural parameters			
C–O bond length	C^{15}–O^{16}	1.169 Å	1.169 Å
	C^{15}–O^{17}	1.169 Å	1.169 Å
O–C–O bond angle	O^{16}–C^{15}–O^{17}	180.0°	179.7°
Interaction-related parameters			
O···H distance	H^{11}···O^{16}	-	2.594 Å
	H^{14}···O^{17}	-	2.596 Å
BQ···CO_2 distance	BQ···C^{15}	-	3.241 Å
	BQ···O^{16}	-	3.202 Å
	BQ···O^{17}	-	3.287 Å
	Average	-	3.243 Å

*Table A-14 Comparisons between structural parameters before and after a CO_2 molecule is bound to the **BZN** linker unit binding site from DFT-optimisesd structures of **EB OTPT-BZN-210**–CO_2 complex.*

Parameter		Before Binding	After Binding
BQ unit structure parameters			
C_{ipso}–C_{ortho} bond length	C^3–C^4	1.462 Å	1.462 Å
	C^3–C^5	1.464 Å	1.465 Å
	C^8–C^6	1.464 Å	1.464 Å
	C^8–C^7	1.462 Å	1.462 Å
C_{ortho}–C_{ortho} bond length	C^4–C^6	1.349 Å	1.349 Å
	C^5–C^7	1.349 Å	1.349 Å
C_{ipso}–N bond length	C^3–N^1	1.301 Å	1.300 Å
	C^8–N^2	1.301 Å	1.300 Å
C_{ortho}–C_{ipso}–C_{ortho} bond angle	C^4–C^3–C^5	116.9°	116.8°
	C^6–C^8–C^7	116.9°	116.8°
C_{ipso}–C_{ortho}–C_{ortho} bond angle	C^3–C^4–C^6	122.2°	122.3°
	C^3–C^5–C^7	120.8°	120.9°
	C^8–C^6–C^4	120.8°	120.9°
	C^8–C^7–C^5	122.2°	122.3°
C_{ortho}–C_{ipso}–N bond angle	C^4–C^3–N^1	116.9°	117.0°
	C^5–C^3–N^1	126.2°	126.2°
	C^6–C^8–N^2	126.2°	126.2°
	C^7–C^8–N^2	116.9°	116.9°
Adjacent unit structure parameters			
N–C_{ipso} bond length	N^1–C^9	1.393 Å	1.393 Å
	N^2–C^{12}	1.393 Å	1.393 Å
C_{ipso}–C_{ortho} bond length	C^9–C^{10}	1.411 Å	1.410 Å
	C^{12}–C^{13}	1.411 Å	1.410 Å
C_{ortho}–H bond length	C^{10}–H^{11}	1.085 Å	1.084 Å
	C^{13}–H^{14}	1.085 Å	1.084 Å
C_{ipso}–N–C_{ipso} bond angle	C^3–N^1–C^9	122.8°	122.8°
	C^8–N^2–C^{12}	122.8°	122.8°
N–C_{ipso}–C_{ortho} bond angle	N^1–C^9–C^{10}	122.8°	122.6°
	N^2–C^{12}–C^{13}	122.8°	122.6°
C_{ipso}–C_{ortho}–H bond angle	C^9–C^{10}–H^{11}	119.4°	119.3°
	C^{12}–C^{13}–H^{14}	119.4°	119.3°
Dihedral angle	C^5–C^3–N^1–C^9	-9.9°	-9.4°
	C^3–N^1–C^9–C^{10}	-50.9°	-52.5°
	C^6–C^8–N^2–C^{12}	-9.9°	-9.4°
	C^8–N^2–C^{12}–C^{13}	-51.0°	-52.4°
CO_2 structural parameters			
C–O bond length	C^{15}–O^{16}	1.169 Å	1.169 Å
	C^{15}–O^{17}	1.169 Å	1.169 Å
O–C–O bond angle	O^{16}–C^{15}–O^{17}	180.0°	179.8°
Interaction-related parameters			
O···H distance	H^{11}···O^{16}	-	2.573 Å
	H^{14}···O^{17}	-	2.579 Å
BQ···CO_2 distance	BQ···C^{15}	-	3.236 Å
	BQ···O^{16}	-	3.205 Å
	BQ···O^{17}	-	3.269 Å
	Average	-	3.237 Å

*A.4.7.3 Microscopic Structures of **FLR** Linker Binding Sites*

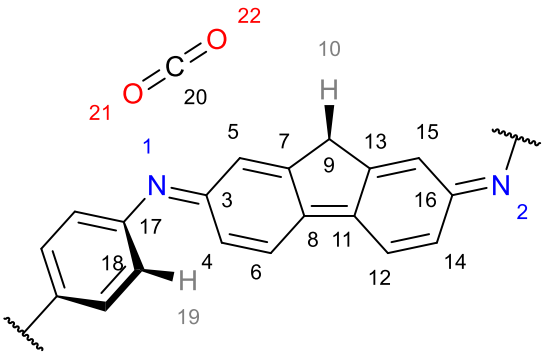

*Scheme A-4 Numbering of atoms involved in the geometries of **FLR** linker unit binding site*

*Table A-15 Comparisons between structural parameters before and after a CO_2 molecule is bound to the **FLR** linker unit binding site from DFT-optimisesd structures of **EB OTPA-FLR-210**–CO_2 complex.*

Parameter		Before Binding	After Binding
BQ unit structure parameters			
C_{ipso}–C_{ortho} bond length	C^3–C^4	1.458 Å	1.458 Å
	C^3–C^5	1.452 Å	1.451 Å
	C^{16}–C^{14}	1.455 Å	1.455 Å
	C^{16}–C^{15}	1.454 Å	1.454 Å
C_{ortho}–C_{meta} bond length	C^4–C^6	1.364 Å	1.364 Å
	C^5–C^7	1.357 Å	1.358 Å
	C^{14}–C^{12}	1.362 Å	1.362 Å
	C^{15}–C^{13}	1.359 Å	1.359 Å
C_{meta}–C_{para} bond length	C^6–C^8	1.426 Å	1.426 Å
	C^7–C^8	1.444 Å	1.445 Å
	C^{12}–C^{11}	1.427 Å	1.427 Å
	C^{13}–C^{11}	1.444 Å	1.444 Å
C_{para}–C_{para} bond length	C^8–C^{11}	1.400 Å	1.400 Å
C_{meta}–C_{meso} bond length	C^7–C^9	1.516 Å	1.515 Å
	C^{13}–C^9	1.517 Å	1.516 Å
C_{ipso}–N bond length	C^3–N^1	1.319 Å	1.319 Å
	C^{16}–N^2	1.319 Å	1.319 Å
C_{ortho}–C_{ipso}–C_{ortho} bond angle	C^4–C^3–C^5	117.2°	117.3°
	C^{14}–C^{16}–C^{15}	117.3°	117.3°
C_{ipso}–C_{ortho}–C_{meta} bond angle	C^3–C^4–C^6	121.8°	121.9°
	C^3–C^5–C^7	120.6°	120.5°
	C^{16}–C^{14}–C^{12}	122.6°	122.5°
	C^{16}–C^{15}–C^{13}	119.9°	119.9°
C_{ortho}–C_{meta}–C_{para} bond angle	C^4–C^3–C^1	119.7°	119.7°
	C^5–C^3–C^1	121.1°	121.1°
	C^{14}–C^{16}–C^2	119.1°	119.1°
	C^{15}–C^{16}–C^2	121.6°	121.6°
C_{meta}–C_{para}–C_{meta} bond angle	C^6–C^8–C^7	119.4°	119.4°
	C^{12}–C^{11}–C^{13}	119.4°	119.5°
C_{meta}–C_{para}–C_{para} bond angle	C^6–C^8–C^{11}	130.8°	130.9°
	C^7–C^8–C^{11}	109.7°	109.7°
	C^{12}–C^{11}–C^8	131.0°	131.0°
	C^{13}–C^{11}–C^8	109.6°	109.6°
C_{para}–C_{meta}–C_{meso} bond angle	C^8–C^7–C^9	108.9°	108.9°
	C^{11}–C^{13}–C^9	109.0°	109.0°

Parameter		Before Binding	After Binding
C_{meta}–C_{meso}–C_{meta} bond angle	C^7–C^9–C^{13}	102.8°	102.8°
C_{ortho}–C_{ipso}–N bond angle	C^4–C^3–N^1	125.8°	125.6°
	C^5–C^3–N^1	116.9°	117.1°
	C^{14}–C^{16}–N^2	116.0°	116.0°
	C^{15}–C^{16}–N^2	126.7°	126.7°
Adjacent unit and interacting hydrogen atom structure parameters			
N–C_{ipso} bond length	N^1–C^{17}	1.382 Å	1.382 Å
C_{ipso}–C_{ortho} bond length	C^{17}–C^{18}	1.416 Å	1.416 Å
C_{ortho}–H bond length	C^{18}–H^{19}	1.085 Å	1.085 Å
C_{meso}–H bond length	C^9–H^{10}	1.097 Å	1.096 Å
C_{ipso}–N–C_{ipso} bond angle	C^3–N^1–C^{17}	123.3°	123.7°
N–C_{ipso}–C_{ortho} bond angle	N^1–C^{17}–C^{18}	124.6°	124.1°
C_{ipso}–C_{ortho}–H bond angle	C^{17}–C^{18}–H^{19}	119.4°	119.2°
C_{meta}–C_{meso}–H bond angle	C^7–C^9–H^{10}	112.0°	111.8°
	C^{13}–C^9–H^{10}	111.9°	111.8°
Unit dihedral angle	C^4–C^3–N^1–C^{17}	14.7°	16.0°
	C^3–N^1–C^{17}–C^{18}	39.3°	39.8°
Fluorene proton dihedral angle	C^5–C^7–C^9–H^{10}	59.8°	58.2°
	C^{15}–C^{13}–C^9–H^{10}	-59.6°	-59.1°
CO_2 structural parameters			
C–O bond length	C^{20}–O^{21}	1.169 Å	1.169 Å
	C^{20}–O^{22}	1.169 Å	1.169 Å
O–C–O bond angle	O^{21}–C^{20}–O^{22}	180.0°	179.1°
Interaction-related parameters			
O···H distance	H^{19}···O^{21}	-	2.805 Å
	H^{10}···O^{22}	-	2.799 Å
BQ···CO_2 distance	BQ···C^{20}	-	3.161 Å
	BQ···O^{21}	-	3.153 Å
	BQ···O^{22}	-	3.187 Å
	Average	-	3.167 Å

*Table A-16 Comparisons between structural parameters before and after a CO_2 molecule is bound to the **FLR** linker unit binding site from DFT-optimisesd structures of **EB OTPB-FLR-210**–CO_2 complex.*

Parameter		Before Binding	After Binding
BQ unit structure parameters			
C_{ipso}–C_{ortho} bond length	C^3–C^4	1.463 Å	1.462 Å
	C^3–C^5	1.455 Å	1.455 Å
	C^{16}–C^{14}	1.459 Å	1.459 Å
	C^{16}–C^{15}	1.457 Å	1.457 Å
C_{ortho}–C_{meta} bond length	C^4–C^6	1.361 Å	1.360 Å
	C^5–C^7	1.355 Å	1.355 Å
	C^{14}–C^{12}	1.359 Å	1.359 Å
	C^{15}–C^{13}	1.356 Å	1.356 Å
C_{meta}–C_{para} bond length	C^6–C^8	1.430 Å	1.430 Å
	C^7–C^8	1.447 Å	1.448 Å
	C^{12}–C^{11}	1.430 Å	1.430 Å
	C^{13}–C^{11}	1.448 Å	1.448 Å
C_{para}–C_{para} bond length	C^8–C^{11}	1.394 Å	1.394 Å
C_{meta}–C_{meso} bond length	C^7–C^9	1.515 Å	1.515 Å
	C^{13}–C^9	1.516 Å	1.516 Å
C_{ipso}–N bond length	C^3–N^1	1.313 Å	1.312 Å
	C^{16}–N^2	1.312 Å	1.312 Å
C_{ortho}–C_{ipso}–C_{ortho} bond angle	C^4–C^3–C^5	117.4°	117.4°
	C^{14}–C^{16}–C^{15}	117.4°	117.5°

Parameter		Before Binding	After Binding
C_{ipso}–C_{ortho}–C_{meta} bond angle	C^3–C^4–C^6	121.8°	121.8°
	C^3–C^5–C^7	120.4°	120.4°
	C^{16}–C^{14}–C^{12}	122.5°	122.5°
	C^{16}–C^{15}–C^{13}	119.8°	119.8°
C_{ortho}–C_{meta}–C_{para} bond angle	C^4–C^3–C^1	119.7°	119.6°
	C^5–C^3–C^1	121.0°	121.0°
	C^{14}–C^{16}–C^2	119.1°	119.0°
	C^{15}–C^{16}–C^2	121.6°	121.6°
C_{meta}–C_{para}–C_{meta} bond angle	C^6–C^8–C^7	119.6°	119.5°
	C^{12}–C^{11}–C^{13}	119.6°	119.6°
C_{meta}–C_{para}–C_{para} bond angle	C^6–C^8–C^{11}	130.6°	130.7°
	C^7–C^8–C^{11}	109.8°	109.7°
	C^{12}–C^{11}–C^8	130.8°	130.8°
	C^{13}–C^{11}–C^8	109.6°	109.6°
C_{para}–C_{meta}–C_{meso} bond angle	C^8–C^7–C^9	108.9°	108.9°
	C^{11}–C^{13}–C^9	108.9°	109.0°
C_{meta}–C_{meso}–C_{meta} bond angle	C^7–C^9–C^{13}	102.8°	102.8°
C_{ortho}–C_{ipso}–N bond angle	C^4–C^3–N^1	125.5°	125.4°
	C^5–C^3–N^1	117.1°	117.1°
	C^{14}–C^{16}–N^2	116.1°	116.1°
	C^{15}–C^{16}–N^2	126.4°	126.4°
Adjacent unit and interacting hydrogen atom structure parameters			
N–C_{ipso} bond length	N^1–C^{17}	1.389 Å	1.389 Å
C_{ipso}–C_{ortho} bond length	C^{17}–C^{18}	1.412 Å	1.413 Å
C_{ortho}–H bond length	C^{18}–H^{19}	1.085 Å	1.085 Å
C_{meso}–H bond length	C^9–H^{10}	1.097 Å	1.096 Å
C_{ipso}–N–C_{ipso} bond angle	C^3–N^1–C^{17}	122.9°	122.4°
N–C_{ipso}–C_{ortho} bond angle	N^1–C^{17}–C^{18}	123.7°	123.3°
C_{ipso}–C_{ortho}–H bond angle	C^{17}–C^{18}–H^{19}	119.3°	119.2°
C_{meta}–C_{meso}–H bond angle	C^7–C^9–H^{10}	112.0°	111.7°
	C^{13}–C^9–H^{10}	111.9°	111.8°
Unit dihedral angle	C^4–C^3–N^1–C^{17}	12.5°	13.7°
	C^3–N^1–C^{17}–C^{18}	45.6°	45.8°
Fluorene proton dihedral angle	C^5–C^7–C^9–H^{10}	59.8°	58.1°
	C^{15}–C^{13}–C^9–H^{10}	-59.6°	-59.1°
CO_2 structural parameters			
C–O bond length	C^{20}–O^{21}	1.169 Å	1.169 Å
	C^{20}–O^{22}	1.169 Å	1.169 Å
O–C–O bond angle	O^{21}–C^{20}–O^{22}	180.0°	179.3°
Interaction-related parameters			
O···H distance	H^{19}···O^{21}	-	2.815 Å
	H^{10}···O^{22}	-	2.758 Å
BQ···CO_2 distance	BQ···C^{20}	-	3.166 Å
	BQ···O^{21}	-	3.156 Å
	BQ···O^{22}	-	3.191 Å
	Average	-	3.171 Å

*Table A-17 Comparisons between structural parameters before and after a CO_2 molecule is bound to the **FLR** linker unit binding site from DFT-optimisesd structures of **EB OTPT-FLR-210**–CO_2 complex.*

Parameter		Before Binding	After Binding
BQ unit structure parameters			
C_{ipso}–C_{ortho} bond length	C^3–C^4	1.463 Å	1.463 Å
	C^3–C^5	1.455 Å	1.455 Å
	C^{16}–C^{14}	1.460 Å	1.460 Å

Parameter		Before Binding	After Binding
	C^{16}–C^{15}	1.457 Å	1.457 Å
C_{ortho}–C_{meta} bond length	C^{4}–C^{6}	1.360 Å	1.360 Å
	C^{5}–C^{7}	1.354 Å	1.355 Å
	C^{14}–C^{12}	1.359 Å	1.359 Å
	C^{15}–C^{13}	1.356 Å	1.356 Å
C_{meta}–C_{para} bond length	C^{6}–C^{8}	1.431 Å	1.430 Å
	C^{7}–C^{8}	1.448 Å	1.449 Å
	C^{12}–C^{11}	1.431 Å	1.431 Å
	C^{13}–C^{11}	1.448 Å	1.448 Å
C_{para}–C_{para} bond length	C^{8}–C^{11}	1.393 Å	1.393 Å
C_{meta}–C_{meso} bond length	C^{7}–C^{9}	1.515 Å	1.514 Å
	C^{13}–C^{9}	1.516 Å	1.515 Å
C_{ipso}–N bond length	C^{3}–N^{1}	1.311 Å	1.311 Å
	C^{16}–N^{2}	1.312 Å	1.312 Å
C_{ortho}–C_{ipso}–C_{ortho} bond angle	C^{4}–C^{3}–C^{5}	117.6°	117.6°
	C^{14}–C^{16}–C^{15}	117.6°	117.7°
C_{ipso}–C_{ortho}–C_{meta} bond angle	C^{3}–C^{4}–C^{6}	121.7°	121.7°
	C^{3}–C^{5}–C^{7}	120.3°	120.3°
	C^{16}–C^{14}–C^{12}	122.4°	122.3°
	C^{16}–C^{15}–C^{13}	119.7°	119.7°
C_{ortho}–C_{meta}–C_{para} bond angle	C^{4}–C^{3}–C^{1}	119.6°	119.6°
	C^{5}–C^{3}–C^{1}	121.0°	121.0°
	C^{14}–C^{16}–C^{2}	119.0°	119.0°
	C^{15}–C^{16}–C^{2}	121.5°	121.5°
C_{meta}–C_{para}–C_{meta} bond angle	C^{6}–C^{8}–C^{7}	119.7°	119.6°
	C^{12}–C^{11}–C^{13}	119.7°	119.7°
C_{meta}–C_{para}–C_{para} bond angle	C^{6}–C^{8}–C^{11}	130.6°	130.7°
	C^{7}–C^{8}–C^{11}	109.8°	109.7°
	C^{12}–C^{11}–C^{8}	130.7°	130.7°
	C^{13}–C^{11}–C^{8}	109.6°	109.6°
C_{para}–C_{meta}–C_{meso} bond angle	C^{8}–C^{7}–C^{9}	108.9°	108.9°
	C^{11}–C^{13}–C^{9}	109.0°	109.0°
C_{meta}–C_{meso}–C_{meta} bond angle	C^{7}–C^{9}–C^{13}	102.8°	102.8°
C_{ortho}–C_{ipso}–N bond angle	C^{4}–C^{3}–N^{1}	125.2°	125.1°
	C^{5}–C^{3}–N^{1}	117.2°	117.2°
	C^{14}–C^{16}–N^{2}	116.2°	116.2°
	C^{15}–C^{16}–N^{2}	126.1°	126.1°
Adjacent unit and interacting hydrogen atom structure parameters			
N–C_{ipso} bond length	N^{1}–C^{17}	1.385 Å	1.385 Å
C_{ipso}–C_{ortho} bond length	C^{17}–C^{18}	1.414 Å	1.414 Å
C_{ortho}–H bond length	C^{18}–H^{19}	1.085 Å	1.085 Å
C_{meso}–H bond length	C^{9}–H^{10}	1.097 Å	1.096 Å
C_{ipso}–N–C_{ipso} bond angle	C^{3}–N^{1}–C^{17}	123.1°	122.7°
N–C_{ipso}–C_{ortho} bond angle	N^{1}–C^{17}–C^{18}	123.2°	122.8°
C_{ipso}–C_{ortho}–H bond angle	C^{17}–C^{18}–H^{19}	119.2°	119.1°
C_{meta}–C_{meso}–H bond angle	C^{7}–C^{9}–H^{10}	112.0°	111.8°
	C^{13}–C^{9}–H^{10}	111.8°	111.8°
Unit dihedral angle	C^{4}–C^{3}–N^{1}–C^{17}	-12.3°	-13.6°
	C^{3}–N^{1}–C^{17}–C^{18}	-47.9°	-47.8°
Fluorene proton dihedral angle	C^{5}–C^{7}–C^{9}–H^{10}	-59.7°	-57.9°
	C^{15}–C^{13}–C^{9}–H^{10}	59.6°	59.0°
CO_2 structural parameters			
C–O bond length	C^{20}–O^{21}	1.169 Å	1.169 Å
	C^{20}–O^{22}	1.169 Å	1.169 Å
O–C–O bond angle	O^{21}–C^{20}–O^{22}	180.0°	179.4°
Interaction-related parameters			

Parameter		Before Binding	After Binding
O···H distance	$H^{19}\cdots O^{21}$	-	2.828 Å
	$H^{10}\cdots O^{22}$	-	2.738 Å
BQ···CO_2 distance	BQ···C^{20}	-	3.168 Å
	BQ···O^{21}	-	3.153 Å
	BQ···O^{22}	-	3.194 Å
	Average	-	3.172 Å

*A.4.7.4 Microscopic Structures of **TPA** Core Binding Sites*

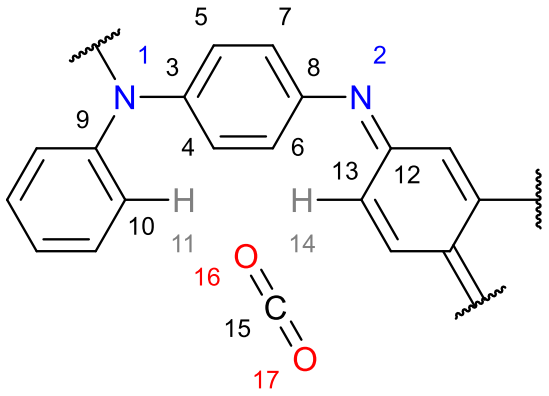

*Scheme A-5 Numbering of atoms involved in the geometries of **TPA** core unit binding site*

*Table A-18 Comparisons between structural parameters before and after a CO_2 molecule is bound to the **TPA** core unit binding site from DFT-optimisesd structures of **EB OTPA-BZN-210**–CO_2 complex.*

Parameter		Before Binding	After Binding
BQ unit structure parameters			
C_{ipso}–C_{ortho} bond length	C^3–C^4	1.406 Å	1.406 Å
	C^3–C^5	1.407 Å	1.407 Å
	C^8–C^6	1.413 Å	1.412 Å
	C^8–C^7	1.411 Å	1.411 Å
C_{ortho}–C_{ortho} bond length	C^4–C^6	1.387 Å	1.386 Å
	C^5–C^7	1.385 Å	1.386 Å
C_{ipso}–N bond length	C^3–N^1	1.409 Å	1.408 Å
	C^8–N^2	1.389 Å	1.389 Å
C_{ortho}–C_{ipso}–C_{ortho} bond angle	C^4–C^3–C^5	118.5°	118.5°
	C^6–C^8–C^7	117.6°	117.7°
C_{ipso}–C_{ortho}–C_{ortho} bond angle	C^3–C^4–C^6	120.8°	120.8°
	C^3–C^5–C^7	120.6°	120.5°
	C^8–C^6–C^4	121.0°	121.0°
	C^8–C^7–C^5	121.3°	121.2°
C_{ortho}–C_{ipso}–N bond angle	C^4–C^3–N^1	120.7°	120.6°
	C^5–C^3–N^1	120.8°	120.9°
	C^6–C^8–N^2	124.3°	124.4°
	C^7–C^8–N^2	117.8°	117.8°
Adjacent unit structure parameters			
N–C_{ipso} bond length	N^1–C^9	1.420 Å	1.420 Å
	N^2–C^{12}	1.308 Å	1.308 Å
C_{ipso}–C_{ortho} bond length	C^9–C^{10}	1.403 Å	1.403 Å
	C^{12}–C^{13}	1.460 Å	1.461 Å
C_{ortho}–H bond length	C^{10}–H^{11}	1.085 Å	1.084 Å

Parameter		Before Binding	After Binding
	C^{13}–H^{14}	1.083 Å	1.083 Å
C_{ipso}–N–C_{ipso} bond angle	C^{3}–N^{1}–C^{9}	120.3°	120.1°
	C^{8}–N^{2}–C^{12}	123.1°	122.8°
N–C_{ipso}–C_{ortho} bond angle	N^{1}–C^{9}–C^{10}	120.4°	120.3°
	N^{2}–C^{12}–C^{13}	126.9°	126.9°
C_{ipso}–C_{ortho}–H bond angle	C^{9}–C^{10}–H^{11}	119.4°	119.5°
	C^{12}–C^{13}–H^{14}	118.7°	119.0°
Dihedral angle	C^{5}–C^{3}–N^{1}–C^{9}	35.5°	36.4°
	C^{3}–N^{1}–C^{9}–C^{10}	42.8°	42.0°
	C^{6}–C^{8}–N^{2}–C^{12}	-41.3°	-43.3°
	C^{8}–N^{2}–C^{12}–C^{13}	-12.1°	-10.6°
CO_2 structural parameters			
C–O bond length	C^{15}–O^{16}	1.169 Å	1.169 Å
	C^{15}–O^{17}	1.169 Å	1.168 Å
O–C–O bond angle	O^{16}–C^{15}–O^{17}	180.0°	179.0°
Interaction-related parameters			
O···H distance	H^{11}···O^{16}	-	2.529 Å
	H^{14}···O^{16}	-	2.843 Å
	H^{14}···O^{17}	-	3.309 Å
BQ···CO_2 distance	BQ···C^{15}	-	3.110 Å
	BQ···O^{16}	-	3.235 Å
	BQ···O^{17}	-	3.005 Å
	Average	-	3.117 Å

*Table A-19 Comparisons between structural parameters before and after a CO_2 molecule is bound to the **TPA** core unit binding site from DFT-optimisesd structures of **LEB OTPA-BZN-210**–CO_2 complex.*

Parameter		Before Binding	After Binding
BQ unit structure parameters			
C_{ipso}–C_{ortho} bond length	C^{3}–C^{4}	1.399 Å	1.401 Å
	C^{3}–C^{5}	1.401 Å	1.400 Å
	C^{8}–C^{6}	1.407 Å	1.406 Å
	C^{8}–C^{7}	1.408 Å	1.406 Å
C_{ortho}–C_{ortho} bond length	C^{4}–C^{6}	1.391 Å	1.389 Å
	C^{5}–C^{7}	1.389 Å	1.391 Å
C_{ipso}–N bond length	C^{3}–N^{1}	1.424 Å	1.421 Å
	C^{8}–N^{2}	1.393 Å	1.398 Å
C_{ortho}–C_{ipso}–C_{ortho} bond angle	C^{4}–C^{3}–C^{5}	118.6°	118.7°
	C^{6}–C^{8}–C^{7}	118.2°	118.3°
C_{ipso}–C_{ortho}–C_{ortho} bond angle	C^{3}–C^{4}–C^{6}	121.1°	120.9°
	C^{3}–C^{5}–C^{7}	120.7°	120.6°
	C^{8}–C^{6}–C^{4}	120.5°	120.6°
	C^{8}–C^{7}–C^{5}	121.0°	120.9°
C_{ortho}–C_{ipso}–N bond angle	C^{4}–C^{3}–N^{1}	120.7°	120.5°
	C^{5}–C^{3}–N^{1}	120.7°	120.8°
	C^{6}–C^{8}–N^{2}	123.1°	122.0°
	C^{7}–C^{8}–N^{2}	118.7°	119.6°
Adjacent unit structure parameters			
N–C_{ipso} bond length	N^{1}–C^{9}	1.414 Å	1.416 Å
	N^{2}–C^{12}	1.401 Å	1.406 Å
C_{ipso}–C_{ortho} bond length	C^{9}–C^{10}	1.404 Å	1.404 Å
	C^{12}–C^{13}	1.405 Å	1.403 Å
C_{ortho}–H bond length	C^{10}–H^{11}	1.085 Å	1.084 Å
	C^{13}–H^{14}	1.084 Å	1.083 Å
C_{ipso}–N–C_{ipso} bond angle	C^{3}–N^{1}–C^{9}	119.3°	119.3°

Parameter		Before Binding	After Binding
	$C^8–N^2–C^{12}$	128.3°	126.4°
N–C_{ipso}–C_{ortho} bond angle	$N^1–C^9–C^{10}$	120.2°	120.3°
	$N^2–C^{12}–C^{13}$	122.6°	123.7°
C_{ipso}–C_{ortho}–H bond angle	$C^9–C^{10}–H^{11}$	119.3°	119.5°
	$C^{12}–C^{13}–H^{14}$	120.0°	120.5°
Dihedral angle	$C^5–C^3–N^1–C^9$	50.0°	47.9°
	$C^3–N^1–C^9–C^{10}$	36.0°	36.1°
	$C^6–C^8–N^2–C^{12}$	-16.8°	-44.1°
	$C^8–N^2–C^{12}–C^{13}$	-34.5°	-7.9°
CO_2 structural parameters			
C–O bond length	$C^{15}–O^{16}$	1.169 Å	1.169 Å
	$C^{15}–O^{17}$	1.169 Å	1.168 Å
O–C–O bond angle	$O^{16}–C^{15}–O^{17}$	180.0°	178.8°
Interaction-related parameters			
O···H distance	$H^{11}\cdots O^{16}$	-	2.545 Å
	$H^{14}\cdots O^{16}$	-	2.831 Å
	$H^{14}\cdots O^{17}$	-	3.387 Å
BQ···CO_2 distance	BQ···C^{15}	-	3.086 Å
	BQ···O^{16}	-	3.295 Å
	BQ···O^{17}	-	2.901 Å
	Average	-	3.094 Å

*Table A-20 Comparisons between structural parameters before and after a CO_2 molecule is bound to the **TPA** core unit binding site from DFT-optimisesd structures of **EB OTPA-FLR-210**–CO_2 complex.*

Parameter		Before Binding	After Binding
BQ unit structure parameters			
C_{ipso}–C_{ortho} bond length	$C^3–C^4$	1.406 Å	1.406 Å
	$C^3–C^5$	1.408 Å	1.407 Å
	$C^8–C^6$	1.416 Å	1.415 Å
	$C^8–C^7$	1.414 Å	1.413 Å
C_{ortho}–C_{ortho} bond length	$C^4–C^6$	1.386 Å	1.386 Å
	$C^5–C^7$	1.385 Å	1.385 Å
C_{ipso}–N bond length	$C^3–N^1$	1.409 Å	1.409 Å
	$C^8–N^2$	1.382 Å	1.383 Å
C_{ortho}–C_{ipso}–C_{ortho} bond angle	$C^4–C^3–C^5$	118.5°	118.5°
	$C^6–C^8–C^7$	117.3°	117.4°
C_{ipso}–C_{ortho}–C_{ortho} bond angle	$C^3–C^4–C^6$	120.8°	120.8°
	$C^3–C^5–C^7$	120.6°	120.5°
	$C^8–C^6–C^4$	121.2°	121.1°
	$C^8–C^7–C^5$	121.5°	121.4°
C_{ortho}–C_{ipso}–N bond angle	$C^4–C^3–N^1$	120.7°	120.6°
	$C^5–C^3–N^1$	120.8°	120.9°
	$C^6–C^8–N^2$	124.6°	124.6°
	$C^7–C^8–N^2$	117.9°	117.8°
Adjacent unit structure parameters			
N–C_{ipso} bond length	$N^1–C^9$	1.419 Å	1.419 Å
	$N^2–C^{12}$	1.319 Å	1.318 Å
C_{ipso}–C_{ortho} bond length	$C^9–C^{10}$	1.403 Å	1.403 Å
	$C^{12}–C^{13}$	1.458 Å	1.460 Å
C_{ortho}–H bond length	$C^{10}–H^{11}$	1.085 Å	1.085 Å
	$C^{13}–H^{14}$	1.083 Å	1.083 Å
C_{ipso}–N–C_{ipso} bond angle	$C^3–N^1–C^9$	120.2°	120.0°
	$C^8–N^2–C^{12}$	123.3°	123.0°
N–C_{ipso}–C_{ortho} bond angle	$N^1–C^9–C^{10}$	120.4°	120.3°

Parameter		Before Binding	After Binding
	$N^2–C^{12}–C^{13}$	125.8°	125.8°
$C_{ipso}–C_{ortho}–H$ bond angle	$C^9–C^{10}–H^{11}$	119.4°	119.5°
	$C^{12}–C^{13}–H^{14}$	118.3°	118.6°
Dihedral angle	$C^5–C^3–N^1–C^9$	-36.3°	-37.6°
	$C^3–N^1–C^9–C^{10}$	-42.5°	-41.4°
	$C^6–C^8–N^2–C^{12}$	39.3°	41.5°
	$C^8–N^2–C^{12}–C^{13}$	14.7°	12.7°
CO_2 structural parameters			
C–O bond length	$C^{15}–O^{16}$	1.169 Å	1.169 Å
	$C^{15}–O^{17}$	1.169 Å	1.168 Å
O–C–O bond angle	$O^{16}–C^{15}–O^{17}$	180.0°	178.9°
Interaction-related parameters			
O···H distance	$H^{11}\cdots O^{16}$	-	2.544 Å
	$H^{14}\cdots O^{16}$	-	2.818 Å
	$H^{14}\cdots O^{17}$	-	3.344 Å
BQ···CO_2 distance	BQ···C^{15}	-	3.138 Å
	BQ···O^{16}	-	3.240 Å
	BQ···O^{17}	-	3.057 Å
	Average	-	3.145 Å

*A.4.7.5 Microscopic Structures of **TPB** Linker Binding Sites*

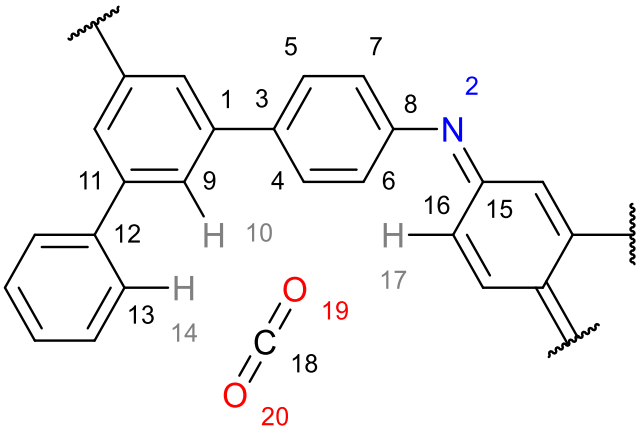

*Scheme A-6 Numbering of atoms involved in the geometries of **TPB** core unit binding site*

*Table A-21 Comparisons between structural parameters before and after a CO_2 molecule is bound to the **TPB** core unit binding site from DFT-optimisesd structures of **EB OTPB-BZN-210**–CO_2 complex.*

Parameter		Before Binding	After Binding
BQ unit structure parameters			
$C_{ipso}–C_{ortho}$ bond length	$C^3–C^4$	1.405 Å	1.406 Å
	$C^3–C^5$	1.407 Å	1.407 Å
	$C^8–C^6$	1.409 Å	1.409 Å
	$C^8–C^7$	1.407 Å	1.407 Å
$C_{ortho}–C_{ortho}$ bond length	$C^4–C^6$	1.390 Å	1.390 Å
	$C^5–C^7$	1.388 Å	1.387 Å
$C_{ipso}–C/N$ bond length	$C^3–C^1$	1.481 Å	1.481 Å
	$C^8–N^2$	1.395 Å	1.394 Å
$C_{ortho}–C_{ipso}–C_{ortho}$ bond angle	$C^4–C^3–C^5$	117.8°	117.7°
	$C^6–C^8–C^7$	118.3°	118.3°
$C_{ipso}–C_{ortho}–C_{ortho}$ bond angle	$C^3–C^4–C^6$	121.3°	121.3°

Parameter		Before Binding	After Binding
	$C^3–C^5–C^7$	121.2°	121.3°
	$C^8–C^6–C^4$	120.5°	120.5°
	$C^8–C^7–C^5$	120.7°	120.7°
$C_{ortho}–C_{ipso}–C/N$ bond angle	$C^4–C^3–C^1$	121.1°	121.2°
	$C^5–C^3–C^1$	121.1°	121.1°
	$C^6–C^8–N^2$	123.4°	123.2°
	$C^7–C^8–N^2$	118.1°	118.2°
Adjacent unit structure parameters			
$N–C_{ipso}$ bond length	$N^2–C^{15}$	1.303 Å	1.302 Å
$C_{ipso}–C_{ortho}$ bond length	$C^{15}–C^{16}$	1.464 Å	1.464 Å
$C_{ortho}–H$ bond length	$C^{16}–H^{17}$	1.083 Å	1.083 Å
Core unit C–C bond length	$C^1–C^9$	1.402 Å	1.401 Å
	$C^9–C^{11}$	1.401 Å	1.400 Å
	$C^{11}–C^{12}$	1.484 Å	1.483 Å
	$C^{12}–C^{13}$	1.404 Å	1.405 Å
Core unit C–H bond length	$C^9–H^{10}$	1.085 Å	1.083 Å
	$C^{13}–H^{14}$	1.086 Å	1.086 Å
$C_{ipso}–N–C_{ipso}$ bond angle	$C^8–N^2–C^{15}$	122.7°	122.6°
$N–C_{ipso}–C_{ortho}$ bond angle	$N^2–C^{15}–C^{16}$	126.5°	126.4°
$C_{ipso}–C_{ortho}–H$ bond angle	$C^{15}–C^{16}–H^{17}$	118.6°	118.5°
Core unit C–C–C bond angle	$C^3–C^1–C^9$	120.6°	120.6°
	$C^1–C^9–C^{11}$	121.3°	121.4°
	$C^9–C^{11}–C^{12}$	120.7°	120.4°
	$C^{11}–C^{12}–C^{13}$	120.8°	120.7°
Core unit C–C–H bond angle	$C^1–C^9–H^{10}$	119.4°	119.5°
	$C^{11}–C^9–H^{10}$	119.3°	119.2°
	$C^{12}–C^{13}–H^{14}$	119.5°	119.5°
Unit dihedral angle	$C^6–C^8–N^2–C^{15}$	-47.4°	-48.6°
	$C^8–N^2–C^{15}–C^{16}$	-10.4°	-10.8°
Core dihedral angle	$C^4–C^3–C^1–C^9$	35.9°	34.4°
	$C^9–C^{11}–C^{12}–C^{13}$	37.2°	36.1°
CO_2 structural parameters			
C–O bond length	$C^{18}–O^{19}$	1.169 Å	1.169 Å
	$C^{18}–O^{20}$	1.169 Å	1.168 Å
O–C–O bond angle	$O^{19}–C^{18}–O^{20}$	180.0°	178.9°
Interaction-related parameters			
O···H distance	$H^{10}\cdots O^{19}$	-	2.555 Å
	$H^{14}\cdots O^{19}$	-	2.795 Å
	$H^{17}\cdots O^{20}$	-	2.633 Å
$BQ\cdots CO_2$ distance	$BQ\cdots C^{18}$	-	3.217 Å
	$BQ\cdots O^{19}$	-	3.247 Å
	$BQ\cdots O^{20}$	-	3.208 Å
	Average	-	3.224 Å

*Table A-22 Comparisons between structural parameters before and after a CO_2 molecule is bound to the **TPB** core unit binding site from DFT-optimisesd structures of **EB OTPB-FLR-210**–CO_2 complex.*

Parameter		Before Binding	After Binding
BQ unit structure parameters			
$C_{ipso}–C_{ortho}$ bond length	$C^3–C^4$	1.405 Å	1.406 Å
	$C^3–C^5$	1.407 Å	1.407 Å
	$C^8–C^6$	1.412 Å	1.412 Å
	$C^8–C^7$	1.410 Å	1.409 Å
$C_{ortho}–C_{ortho}$ bond length	$C^4–C^6$	1.389 Å	1.390 Å
	$C^5–C^7$	1.387 Å	1.387 Å

Parameter		Before Binding	After Binding
C_{ipso}–C/N bond length	C^3–C^1	1.480 Å	1.480 Å
	C^8–N^2	1.389 Å	1.388 Å
C_{ortho}–C_{ipso}–C_{ortho} bond angle	C^4–C^3–C^5	117.7°	117.6°
	C^6–C^8–C^7	117.9°	117.9°
C_{ipso}–C_{ortho}–C_{ortho} bond angle	C^3–C^4–C^6	121.4°	121.4°
	C^3–C^5–C^7	121.3°	121.4°
	C^8–C^6–C^4	120.7°	120.7°
	C^8–C^7–C^5	120.9°	120.9°
C_{ortho}–C_{ipso}–C/N bond angle	C^4–C^3–C^1	121.0°	121.1°
	C^5–C^3–C^1	121.3°	121.3°
	C^6–C^8–N^2	123.7°	123.6°
	C^7–C^8–N^2	118.2°	118.2°
Adjacent unit structure parameters			
N–C_{ipso} bond length	N^2–C^{15}	1.313 Å	1.312 Å
C_{ipso}–C_{ortho} bond length	C^{15}–C^{16}	1.463 Å	1.462 Å
C_{ortho}–H bond length	C^{16}–H^{17}	1.083 Å	1.082 Å
Core unit C–C bond length	C^1–C^9	1.402 Å	1.402 Å
	C^9–C^{11}	1.401 Å	1.401 Å
	C^{11}–C^{12}	1.483 Å	1.483 Å
	C^{12}–C^{13}	1.405 Å	1.405 Å
Core unit C–H bond length	C^9–H^{10}	1.085 Å	1.084 Å
	C^{13}–H^{14}	1.086 Å	1.086 Å
C_{ipso}–N–C_{ipso} bond angle	C^8–N^2–C^{15}	122.9°	122.9°
N–C_{ipso}–C_{ortho} bond angle	N^2–C^{15}–C^{16}	125.5°	125.4°
C_{ipso}–C_{ortho}–H bond angle	C^{15}–C^{16}–H^{17}	118.1°	118.0°
Core unit C–C–C bond angle	C^3–C^1–C^9	120.6°	120.7°
	C^1–C^9–C^{11}	121.4°	121.3°
	C^9–C^{11}–C^{12}	120.6°	120.5°
	C^{11}–C^{12}–C^{13}	120.8°	120.8°
Core unit C–C–H bond angle	C^1–C^9–H^{10}	119.3°	119.4°
	C^{11}–C^9–H^{10}	119.2°	119.2°
	C^{12}–C^{13}–H^{14}	119.4°	119.4°
Unit dihedral angle	C^6–C^8–N^2–C^{15}	45.6°	46.7°
	C^8–N^2–C^{15}–C^{16}	12.5°	12.9°
Core dihedral angle	C^4–C^3–C^1–C^9	-35.3°	-34.9°
	C^9–C^{11}–C^{12}–C^{13}	36.5°	35.9°
CO_2 structural parameters			
C–O bond length	C^{18}–O^{19}	1.169 Å	1.169 Å
	C^{18}–O^{20}	1.169 Å	1.169 Å
O–C–O bond angle	O^{19}–C^{18}–O^{20}	180.0°	178.8°
Interaction-related parameters			
O···H distance	H^{10}···O^{19}	-	2.538 Å
	H^{14}···O^{19}	-	4.177 Å
	H^{17}···O^{20}	-	2.653 Å
BQ···CO_2 distance	BQ···C^{18}	-	3.188 Å
	BQ···O^{19}	-	3.196 Å
	BQ···O^{20}	-	3.202 Å
	Average	-	3.195 Å

*A.4.7.6 Microscopic Structures of **TPT** Core Binding Sites*

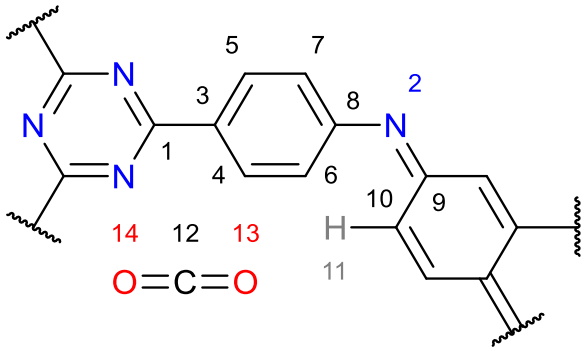

*Scheme A-7 Numbering of atoms involved in the geometries of **TPT** core unit binding site*

*Table A-23 Comparisons between structural parameters before and after a CO_2 molecule is bound to the **TPT** core unit binding site from DFT-optimisesd structures of **EB OTPT-BZN-210**–CO_2 complex.*

Parameter		Before Binding	After Binding
BQ unit structure parameters			
C_{ipso}–C_{ortho} bond length	C^3–C^4	1.404 Å	1.404 Å
	C^3–C^5	1.406 Å	1.406 Å
	C^8–C^6	1.411 Å	1.410 Å
	C^8–C^7	1.409 Å	1.409 Å
C_{ortho}–C_{ortho} bond length	C^4–C^6	1.388 Å	1.388 Å
	C^5–C^7	1.386 Å	1.386 Å
C_{ipso}–C/N bond length	C^3–C^1	1.475 Å	1.475 Å
	C^8–N^2	1.393 Å	1.393 Å
C_{ortho}–C_{ipso}–C_{ortho} bond angle	C^4–C^3–C^5	118.9°	118.9°
	C^6–C^8–C^7	118.8°	118.9°
C_{ipso}–C_{ortho}–C_{ortho} bond angle	C^3–C^4–C^6	120.7°	120.8°
	C^3–C^5–C^7	120.7°	120.7°
	C^8–C^6–C^4	120.4°	120.3°
	C^8–C^7–C^5	120.5°	120.5°
C_{ortho}–C_{ipso}–C/N bond angle	C^4–C^3–C^1	120.5°	120.6°
	C^5–C^3–C^1	120.6°	120.6°
	C^6–C^8–N^2	122.8°	122.6°
	C^7–C^8–N^2	118.2°	118.3°
Adjacent unit structure parameters			
N–C_{ipso} bond length	N^2–C^9	1.301 Å	1.300 Å
C_{ipso}–C_{ortho} bond length	C^9–C^{10}	1.464 Å	1.465 Å
C_{ortho}–H bond length	C^{10}–H^{11}	1.084 Å	1.083 Å
C_{ipso}–N–C_{ipso} bond angle	C^8–N^2–C^9	122.8°	122.8°
N–C_{ipso}–C_{ortho} bond angle	N^2–C^9–C^{10}	126.2°	126.2°
C_{ipso}–C_{ortho}–H bond angle	C^9–C^{10}–H^{11}	118.5°	118.5°
Unit dihedral angle	C^6–C^8–N^2–C^9	-51.0°	-52.4°
	C^8–N^2–C^9–C^{10}	-9.9°	-9.4°
CO_2 structural parameters			
C–O bond length	C^{12}–O^{13}	1.169 Å	1.169 Å
	C^{12}–O^{14}	1.169 Å	1.169 Å
O–C–O bond angle	O^{13}–C^{12}–O^{14}	180.0°	179.0°
Interaction-related parameters			
O···H distance	H^{11}···O^{13}	-	2.535 Å
BQ···CO_2 distance	BQ···C^{12}	-	3.180 Å

Parameter		Before Binding	After Binding
	BQ···O^{13}	-	3.213 Å
	BQ···O^{14}	-	3.168 Å
	Average	-	3.187 Å

*Table A-24 Comparisons between structural parameters before and after a CO_2 molecule is bound to the **TPT** core unit binding site from DFT-optimisesd structures of **EB OTPT-FLR-210**–CO_2 complex.*

Parameter		Before Binding	After Binding
BQ unit structure parameters			
C_{ipso}–C_{ortho} bond length	C^3–C^4	1.405 Å	1.405 Å
	C^3–C^5	1.407 Å	1.407 Å
	C^8–C^6	1.414 Å	1.414 Å
	C^8–C^7	1.412 Å	1.411 Å
C_{ortho}–C_{ortho} bond length	C^4–C^6	1.387 Å	1.387 Å
	C^5–C^7	1.385 Å	1.385 Å
C_{ipso}–C/N bond length	C^3–C^1	1.473 Å	1.473 Å
	C^8–N^2	1.386 Å	1.386 Å
C_{ortho}–C_{ipso}–C_{ortho} bond angle	C^4–C^3–C^5	118.7°	118.7°
	C^6–C^8–C^7	118.3°	118.3°
C_{ipso}–C_{ortho}–C_{ortho} bond angle	C^3–C^4–C^6	120.8°	120.8°
	C^3–C^5–C^7	120.7°	120.7°
	C^8–C^6–C^4	120.6°	120.6°
	C^8–C^7–C^5	120.8°	120.8°
C_{ortho}–C_{ipso}–C/N bond angle	C^4–C^3–C^1	120.6°	120.6°
	C^5–C^3–C^1	120.7°	120.6°
	C^6–C^8–N^2	123.3°	123.3°
	C^7–C^8–N^2	118.2°	118.2°
Adjacent unit structure parameters			
N–C_{ipso} bond length	N^2–C^9	1.312 Å	1.312 Å
C_{ipso}–C_{ortho} bond length	C^9–C^{10}	1.457 Å	1.457 Å
C_{ortho}–H bond length	C^{10}–H^{11}	1.084 Å	1.084 Å
C_{ipso}–N–C_{ipso} bond angle	C^8–N^2–C^9	122.9°	122.9°
N–C_{ipso}–C_{ortho} bond angle	N^2–C^9–C^{10}	126.1°	126.1°
C_{ipso}–C_{ortho}–H bond angle	C^9–C^{10}–H^{11}	119.1°	119.1°
Unit dihedral angle	C^6–C^8–N^2–C^9	-47.9°	-47.7°
	C^8–N^2–C^9–C^{10}	-11.3°	-11.3°
CO_2 structural parameters			
C–O bond length	C^{12}–O^{13}	1.169 Å	1.169 Å
	C^{12}–O^{14}	1.169 Å	1.169 Å
O–C–O bond angle	O^{13}–C^{12}–O^{14}	180.0°	179.3°
Interaction-related parameters			
O···H distance	H^{11}···O^{13}	-	2.701 Å
BQ···CO_2 distance	BQ···C^{12}	-	3.238 Å
	BQ···O^{13}	-	3.228 Å
	BQ···O^{14}	-	3.263 Å
	Average	-	3.243 Å

A.4.7.7 Detailed Discussions of Geometries in PANI-CMPs–CO_2 Non-Covalent Interactions

This section is intended to provide additional details for the analyses of geometries involved in non-covalent interactions between PANI-CMP fragments and CO_2 molecules. Detailed discussions are different for imine/amine binding sites and core/linker unit binding sites due to differences in nature of binding.

For imine and amine unit binding sites, distances between CO_2 molecules and their binding sites can be measured directly from the data visualisation software which has already been discussed in the main part of this thesis. The binding of CO_2 molecules onto these sites, however, causes them to bend slightly from linearity by approximately 3° for imine binding sites. A CO_2 molecule can bend in two different ways respective to the oligomer it is bound onto, either towards the imine/amine group or away from the imine/amine group. Both bending modes are illustrated in Scheme A-8.

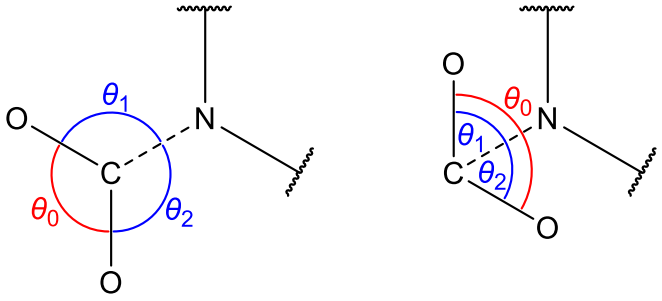

Scheme A-8 Two possible ways for a CO_2 molecule to bend upon binding onto an imine binding site. Solid lines represent covalent bonds (regardless of being single or double), and dashed lines represent non-covalent interactions.

Generally, a CO_2 is described to bend towards the oligomer if the vertex of the O–C–O angle points *towards* the nitrogen atom (the left structure in Scheme A-8), and it is described to bend away from the oligomer if the vertex points *away from* the nitrogen atom (the right structure). However, bond angles are typically measured and reported in the range between 0° and 180°. Therefore, the magnitudes of O–C–O, θ_0, on their own cannot be used to determine whether the CO_2 molecules bend towards or away from the imine/amine groups. To distinguish the two bending modes, two N···C–O angles, namely θ_1 and θ_2, are required.

Assuming that the CO_2 molecule bends in the manner that all four atoms, three CO_2 atoms and the nitrogen atom, remain coplanar, if the CO_2 molecule bends towards the oligomer, on the one hand, the sum of the three aforementioned angles should be approximately 360°. On the other hand, if the CO_2 molecule bends away from the oligomer, the sum of θ_1 and θ_2 should equal to θ_0. However, if neither of the two criteria is satisfied, it is possible that the four atoms involved are not coplanar.

Table A-25 Angles involved in the discussion of geometries involved in the binding of CO_2 onto imine and amine group binding sites (θ_0, θ_1, and θ_2) and their linear combinations

Oligomer	State	O–C–O Angle (θ_0)	N···C–O Angle		$\theta_1+\theta_2$	$\theta_0+\theta_1+\theta_2$
			θ_1	θ_2		
OTPA-BZN-210	**EB**	176.3°	94.4°	89.2°	183.6°	359.9°
OTPA-FLR-210	**EB**	176.4°	91.6°	91.9°	183.5°	359.9°
OTPB-BZN-210	**EB**	176.6°	94.3°	89.0°	183.3°	359.9°
OTPB-FLR-210	**EB**	176.8°	91.1°	92.1°	183.2°	360.0°
OTPT-BZN-210	**EB**	177.1°	92.6°	90.4°	183.0°	360.1°
OTPT-FLR-210	**EB**	177.0°	90.2°	92.8°	183.0°	360.0°
OTPA-BZN-210	**LEB**	178.6°	93.7°	87.6°	181.3°	359.9°

As shown in Table A-25, the sums of all three angles in all seven cases of imine and amine binding sites are approximately 360°, which confirm that CO_2 molecules indeed bend towards the imine or amine groups. Arguably, the small deviations of 0.1° can be attributed to rounding of decimal points.

For core and linker unit binding sites, distances between CO_2 molecules and their binding sites are determined from the average distances of each atom from the aromatic planes of binding sites they are bound onto.

Mathematically, there is always one plane passing through three non-collinear points in the three-dimensional space. Meanwhile, there are six non-hydrogen atoms in a six-membered aromatic ring, and all atom positions can be obtained from the log file of the optimisation calculation. However, not all six positions can be practically used to define the plane passing through them. Typically, calculations involve rounding decimal points up or down which can cause miniscule errors in further calculation steps, which means that different selections of three atoms out of six can produce slightly different equations. Nonetheless, these differences are negligible. For generalisation, three atoms in the positions 1, 3, and 5 are chosen, with Cartesian coordinates being (x_1, y_1, z_1) for atom 1, (x_3, y_3, z_3) for atom 3, and (x_5, y_5, z_5) for atom 5.

The plane equation describing the aromatic system is defined by Equation A-1.

$$Ax + By + Cz + D = 0 \quad \text{A-1}$$

Parameters A, B, C, and D need to satisfy the following criteria.

For atom 1: $$Ax_1 + By_1 + Cz_1 + D = 0 \quad \text{A-2}$$

For atom 3: $$Ax_3 + By_3 + Cz_3 + D = 0 \quad \text{A-3}$$

For atom 5: $$Ax_5 + By_5 + Cz_5 + D = 0 \quad \text{A-4}$$

$$A^2 + B^2 + C^2 = 1 \quad \text{A-5}$$

Equation A-5 is required for convenience. Generally, the distance d between the point (x_0, y_0, z_0) from the plane defined in Equation A-1 is calculated from Equation A-6.

$$d = \frac{Ax_0+By_0+Cz_0+D}{\sqrt{A^2+B^2+C^2}} \quad \text{A-6}$$

By fulfilling the normalisation criterion in Equation A-5, the denominator in Equation A-6 can simply be removed, and the distance d can be obtained simply by substituting x, y, and z coordinates into the expression in Equation A-1.

In the system containing a CO_2 molecule binding onto core or linker unit binding sites, this system can be described geometrically as three points situated over a plane. The three points refer to the three CO_2 atoms, with coordinates of the molecule being (x_C, y_C, z_C) for carbon atom C, (x_{O1}, y_{O1}, z_{O1}) for oxygen atom O1, and (x_{O2}, y_{O2}, z_{O2}) for oxygen atom O2. Meanwhile, the plane refers to the aromatic ring plane which is the part of the BQ elementary unit of poly(aniline)s and mathematically defined using atoms 1, 3, and 5 as in Equation A-1 which satisfies the criteria given in Equations A-2 to A-5. Therefore, the distances between the CO_2 molecule and the aromatic ring of the binding site in this system can be calculated from the following equations.

For atom C: $d_C = Ax_C + By_C + Cz_C + D$ *A-7*

For atom O1: $d_{O1} = Ax_{O1} + By_{O1} + Cz_{O1} + D$ *A-8*

For atom O2: $d_{O2} = Ax_{O2} + By_{O2} + Cz_{O2} + D$ *A-9*

For the CO_2 molecule: $d_{CO_2} = \frac{d_C + d_{O1} + d_{O2}}{3}$ *A-10*

While the bending of CO_2 molecules in the case of imine and amine binding sites are significant, they are far less significant in the case of core and linker unit binding sites, with the magnitudes being about 1°. Meanwhile, to determine directions of bending in this case, a projection of the CO_2 carbon atom is needed because there is no atom that is situated directly under the CO_2 carbon atom, nor is there any atom that can be assumed to be coplanar with the three CO_2 atoms. The complications in this case simply are not worth the significance of the bends themselves.

A.4.8 Optimised Structures of Adducts between **OTPA-BZN-430** Oligomers and CO_2

*A.4.8.1 Optimisation Processes of Adducts between Linear/Coiled **OTPA-BZN-430** Studies and CO_2*

Positions of other atoms in the linear/coiled **OTPA-BZN-430** are taken from the optimised structure listed in Section A.3.3.2. Here, only positions of three atoms in CO_2 molecules will be given for each mode.

Mode 1

C	-4.87557357	-1.11851285	-0.94238205
O	-5.01789627	0.13153504	-0.91601739
O	-4.73325087	-2.36856074	-0.96874671

Mode 2

C	5.02685386	4.52242473	-2.62923355
O	3.94950132	5.17258873	-2.64222781
O	6.10420641	3.87226074	-2.61623928

Mode 3

C	-3.82473009	-5.21023867	2.78965198
O	-3.55147618	-5.32654876	1.56679678
O	-4.09798399	-5.09392859	4.01250718

Mode 4

C	-0.33664175	1.95425560	1.46401024

O	-0.71882088	0.76153150	1.58615321
O	0.04553739	3.14697970	1.34186727
Mode 5			
C	3.59739087	9.16333689	1.35200852
O	2.34998911	9.18654920	1.51638796
O	4.84479264	9.14012459	1.18762909

Table A-26 compared numbers of steps and optimisation times for the optimisation processes of the adducts between star-shaped and linear/coiled **OTPA-BZN-430** of different binding modes. For each calculation job submission to the supercomputer cluster system, an estimated time limit is set for administrative purposes to classify the job priority. Once the time limit has been reached, the calculation job will be terminated even if the optimisation is yet to be finalised, and a continuation job is then submitted starting from the most recent geometry from the previous job. Time limits were set at 3 days for simpler star-shaped oligomers and 7 days for more complicated linear/coiled oligomers.

*Table A-26 Numbers of steps and optimisation times for the optimisation processes of **OTPA-BZN-430**–CO_2 complexes. Numbers of optimisation steps are broken down by the initial submission and the successive submissions from unfinished optimisations, if applicable, and optimisation times are given in the form of day:hour:minute:second.*

Star-Shaped OTPA-BZN-430			**Linear/Coiled OTPA-BZN-430**		
Binding Mode	**Number of Steps**	**Optimisation Time**	**Binding Mode**	**Number of Steps**	**Optimisation Time**
Inner Core 1	45	3:00:35:41.8	Mode 1	89 (76+13)	8:02:11:01.0
Inner Core 2	44	2:07:50.04.0	Mode 2	85 (61+24)	9:18:40:50.1
Inner Core 3	78 (51+27)	4:04:48:56.2	Mode 3	106 (63+43)	12:08:53:58.3
Outer Core 1	89 (58+31)	4:11:04:26.9	Mode 4	92 (62+30)	10:01:50:28.0
Outer Core 2	53	2:08:07:59.5	Mode 5	101 (60+41)	11:04:40:44.6
Outer Core 3	46	2:10:13:34.4			
Linker 1	80 (56+24)	4:01:43:01.4			
Linker 2	30	1:11:53:58.6			
Linker 3	80 (57+23)	4:06:04:30.7			
Inner Imine 1	106 (57+47+2)	6:02:21:21.5			
Inner Imine 2	39	1:19:38:32.0			
Inner Imine 3	30	1:08:48:46.0			
Outer Imine 1	82 (59+23)	4:00:06:17.9			
Outer Imine 2	37	1:16:13:05.2			
Outer Imine 3	36	1:16:32:55.2			
Average	**58**	**3:00:24:12.8**	**Average**	**95**	**10:07:15:24.4**
Median	**46**	**2:10:13:34.4**	**Median**	**92**	**10:01:50:28.0**

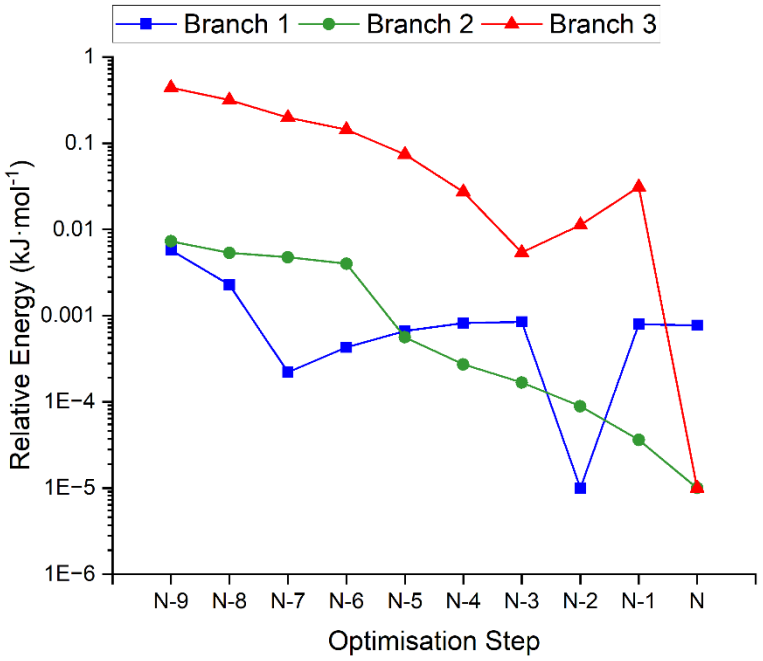

*Figure A-1 Relative energies of the last 10 optimisation steps for the binding of CO_2 onto the inner core units of the **EB** state star-shaped **OTPA-BZN-430**, with N being the number of steps taken in the **first** optimisation submission regardless whether the optimisation process has finalised within the time limit or not. The lowest energy for each mode is set to be 10^{-5} kJ·mol^{-1}*

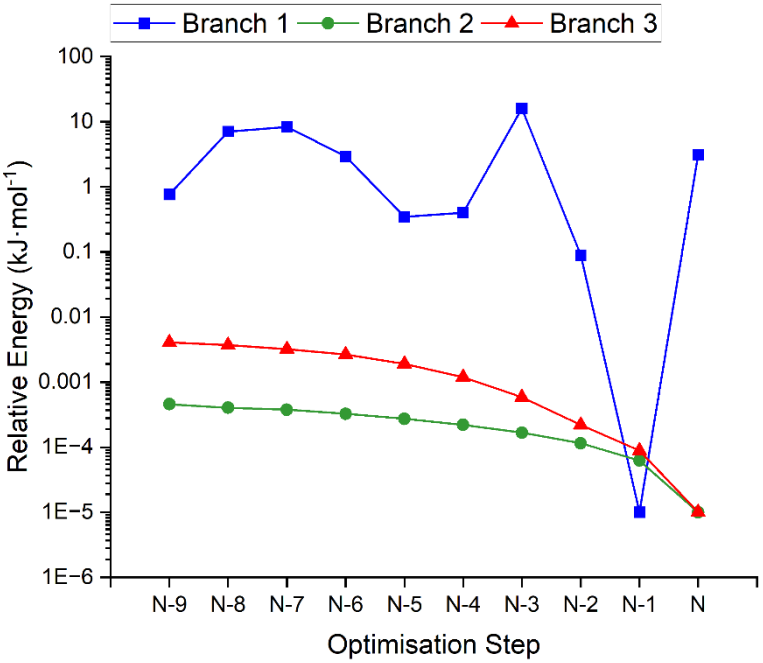

*Figure A-2 Relative energies of the last 10 optimisation steps for the binding of CO_2 onto the outer core units of the **EB** state star-shaped **OTPA-BZN-430**, with N being the number of steps taken in the **first** optimisation submission regardless whether the optimisation process has finalised within the time limit or not. The lowest energy for each mode is set to be 10^{-5} kJ·mol^{-1}*

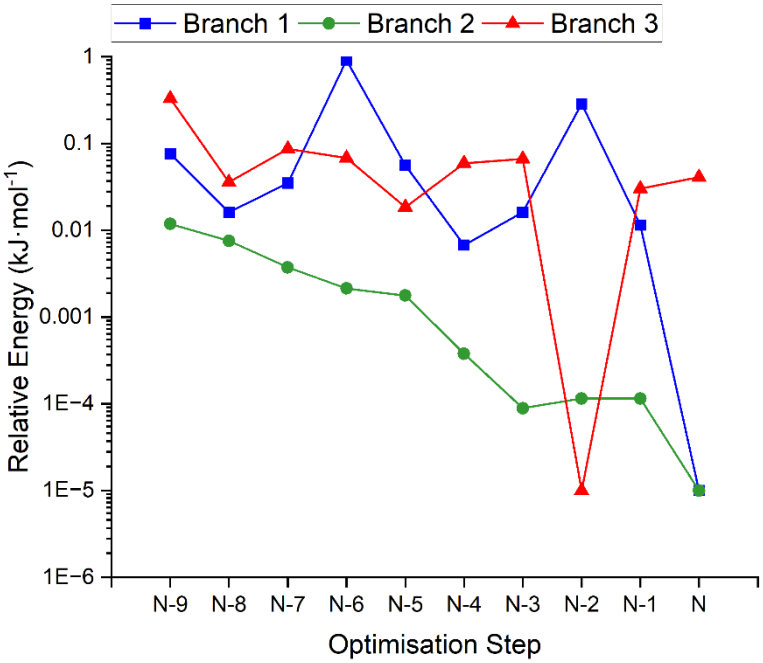

*Figure A-3 Relative energies of the last 10 optimisation steps for the binding of CO_2 onto the linker units of the **EB** state star-shaped **OTPA-BZN-430**, with N being the number of steps taken in the **first** optimisation submission regardless whether the optimisation process has finalised within the time limit or not. The lowest energy for each mode is set to be 10^{-5} kJ·mol^{-1}*

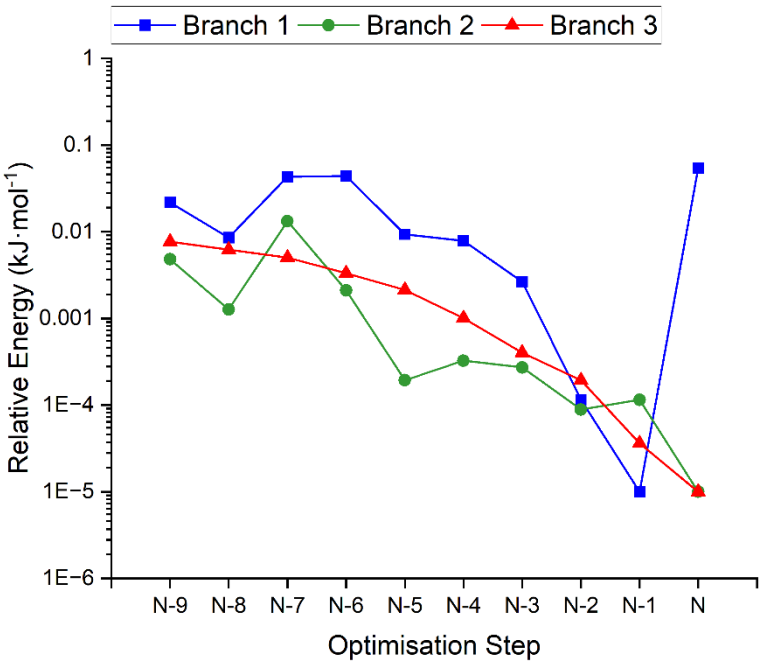

*Figure A-4 Relative energies of the last 10 optimisation steps for the binding of CO_2 onto the inner imine groups of the **EB** state star-shaped **OTPA-BZN-430**, with N being the number of steps taken in the **first** optimisation submission regardless whether the optimisation process has finalised within the time limit or not. The lowest energy for each mode is set to be 10^{-5} kJ·mol^{-1}*

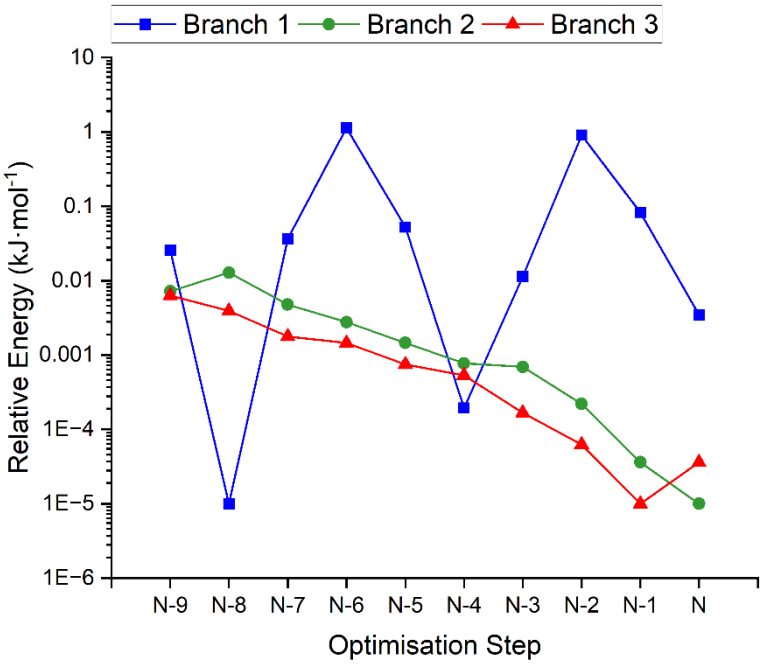

*Figure A-5 Relative energies of the last 10 optimisation steps for the binding of CO_2 onto the outer imine groups of the **EB** state star-shaped **OTPA-BZN-430**, with N being the number of steps taken in the **first** optimisation submission regardless whether the optimisation process has finalised within the time limit or not. The lowest energy for each mode is set to be 10^{-5} kJ·mol^{-1}*

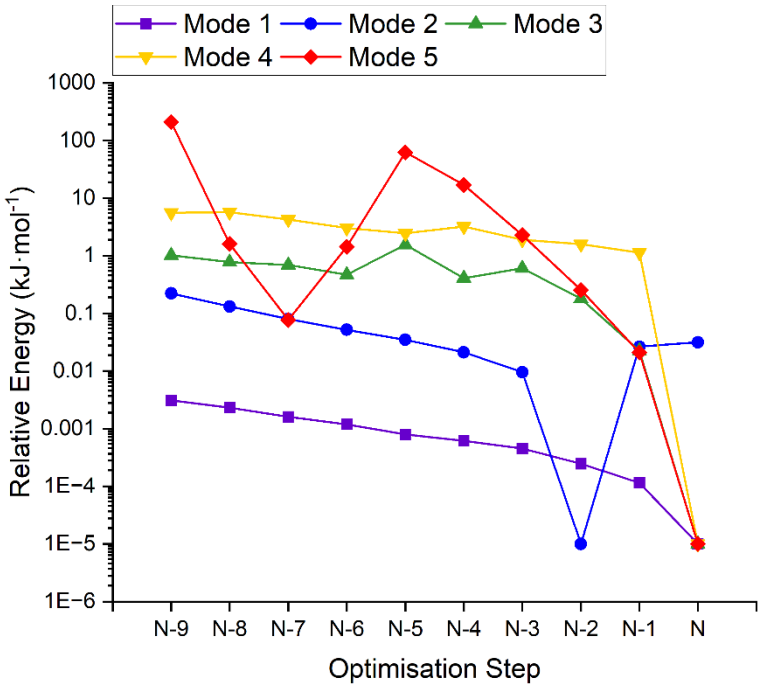

*Figure A-6 Relative energies of the last 10 optimisation steps for the binding of CO_2 onto the **EB** state linear/coiled **OTPA-BZN-430**, with N being the number of steps taken in the **first** optimisation submission regardless whether the optimisation process has finalised within the time limit or not. The lowest energy for each mode is set to be 10^{-5} kJ·mol^{-1}*

*A.4.8.2 Star-Shaped **OTPA-BZN-430**, **EB** State, with CO_2 Binding on Inner Imine Nitrogen Atom, Branch 1*

H	-0.708019	0.011001	1.112274	C	0.820144	-0.009938	-0.407616
C	-0.192129	0.593593	0.356616	C	-0.528334	1.924647	0.159449
C	1.211639	2.112815	-1.508399	C	0.156002	2.713775	-0.791646

C	1.517413	0.771037	-1.345925
H	-1.288628	2.382086	0.783913
H	2.305691	0.317846	-1.937142
H	1.758479	2.716740	-2.225343
N	1.141905	-1.373653	-0.222648
C	0.111594	-2.314193	0.006233
C	-1.964375	-4.177223	0.478762
C	0.284838	-3.358014	0.931523
C	-1.098633	-2.230172	-0.701593
C	-2.122432	-3.134358	-0.461037
C	-0.721851	-4.288028	1.136783
H	1.218119	-3.437426	1.478344
H	-1.226188	-1.453268	-1.447811
H	-3.036117	-3.074804	-1.043127
H	-0.582370	-5.100124	1.843054
C	2.491412	-1.793454	-0.257662
C	5.193223	-2.621685	-0.344729
C	2.848491	-3.006915	-0.870242
C	3.496614	-1.011887	0.334483
C	4.824097	-1.410369	0.279900
C	4.169370	-3.426627	-0.884430
H	2.079327	-3.620953	-1.326056
H	3.227148	-0.093052	0.844131
H	5.583660	-0.811556	0.771718
H	4.439606	-4.369292	-1.345977
N	6.495503	-3.111967	-0.357498
N	-2.914041	-5.163519	0.713381
N	-0.072172	4.070521	-0.983958
C	-4.193786	-4.911065	0.807902
C	-7.061689	-4.616059	0.930833
C	-5.086225	-6.061510	0.881339
C	-4.819270	-3.596748	0.930677
C	-6.163160	-3.471702	1.016468
C	-6.432218	-5.933812	0.911469
H	-4.611440	-7.037832	0.896943
H	-4.183208	-2.722135	0.998546
H	-6.632886	-2.499971	1.135020
H	-7.062643	-6.812935	0.972215
C	7.530469	-2.354419	-0.615183
C	9.950816	-0.846058	-1.053604
C	8.850994	-2.940530	-0.417522
C	7.495624	-1.000291	-1.162337
C	8.637190	-0.313094	-1.392039
C	9.988942	-2.232216	-0.595217
H	8.880490	-3.976141	-0.096943
H	6.536377	-0.571608	-1.426993
H	8.618945	0.681919	-1.826085
H	10.952765	-2.703304	-0.443166
C	-1.271421	4.591397	-1.017214
C	-3.801841	5.977726	-1.001226
C	-1.355026	6.046472	-1.046920
C	-2.536576	3.867333	-1.110598
C	-3.715971	4.528810	-1.132228
C	-2.535525	6.705328	-1.010961
H	-0.410900	6.581253	-1.084792
H	-2.512538	2.788538	-1.209440
H	-4.658617	3.998912	-1.229282
H	-2.557569	7.788246	-1.039592
N	-8.344308	-4.358011	0.952122
N	10.974706	-0.058508	-1.257160
N	-5.003846	6.493108	-0.959658
C	-9.317393	-5.318132	0.713891
C	-11.450164	-7.131435	0.263332
C	-9.226540	-6.319703	-0.279109

C	-10.526033	-5.219893	1.435258
C	-11.556539	-6.124714	1.241589
C	-10.275611	-7.196401	-0.508058
H	-8.348252	-6.363817	-0.914575
H	-10.617106	-4.438664	2.183184
H	-12.458818	-6.053740	1.838749
H	-10.197482	-7.936232	-1.297131
C	12.264072	-0.360940	-0.836608
C	14.958671	-0.790977	-0.072148
C	12.583929	-0.934704	0.413258
C	13.331321	0.037631	-1.668119
C	14.648916	-0.189871	-1.306899
C	13.903943	-1.144413	0.786798
H	11.789035	-1.186941	1.107017
H	13.096865	0.521721	-2.611060
H	15.452794	0.112262	-1.969008
H	14.125961	-1.582048	1.753774
C	-5.248300	7.827904	-0.669474
C	-5.952466	10.515313	-0.101704
C	-4.566844	8.566856	0.323958
C	-6.323596	8.457817	-1.331098
C	-6.648227	9.780735	-1.080605
C	-4.921749	9.875819	0.610729
H	-3.796247	8.083029	0.914982
H	-6.870446	7.892430	-2.078964
H	-7.451790	10.254873	-1.633052
H	-4.407395	10.413257	1.399816
N	-6.292335	11.852943	0.174110
N	16.299016	-1.011943	0.302044
N	-12.502554	-8.040388	0.045893
C	17.262661	-1.381588	-0.672759
C	19.174168	-2.118578	-2.590444
C	18.543086	-0.810221	-0.651572
C	16.947144	-2.326513	-1.659960
C	17.896161	-2.682023	-2.616019
C	19.491774	-1.185733	-1.600322
H	18.786398	-0.076706	0.109788
H	15.959853	-2.776126	-1.671418
H	17.638380	-3.414932	-3.375250
H	20.479974	-0.735502	-1.572238
H	19.913749	-2.403640	-3.332471
C	16.699660	-0.866700	1.656849
C	17.503098	-0.577617	4.329315
C	16.244610	0.219010	2.418789
C	17.561678	-1.805151	2.241685
C	17.965165	-1.652826	3.566595
C	16.638278	0.353191	3.748532
H	15.584763	0.950189	1.963691
H	17.910960	-2.646739	1.652836
H	18.633520	-2.386873	4.007611
H	16.278251	1.198664	4.327808
H	17.813841	-0.465854	5.363628
C	-7.643352	12.284109	0.095375
C	-10.307754	13.149425	-0.052016
C	-7.955492	13.513986	-0.501152
C	-8.674262	11.491492	0.619900
C	-9.997142	11.920738	0.535574
C	-9.279242	13.943866	-0.564368
H	-7.157624	14.125284	-0.909497
H	-8.432085	10.544125	1.089869
H	-10.786496	11.297096	0.945389
H	-9.507641	14.898898	-1.028849
H	-11.339030	13.484169	-0.109224
C	-5.287815	12.784351	0.548694

C	-3.310713	14.633824	1.284402
C	-4.059723	12.813704	-0.127779
C	-5.519703	13.689071	1.594413
C	-4.538262	14.611676	1.950666
C	-3.077189	13.727450	0.247298
H	-3.883725	12.119981	-0.943136
H	-6.468547	13.663798	2.119767
H	-4.730648	15.307263	2.762537
H	-2.130269	13.739793	-0.284864
H	-2.545533	15.349570	1.569100
C	-12.224704	-9.381384	-0.329659
C	-11.687322	-12.034696	-1.066285
C	-11.197296	-10.096871	0.302272
C	-12.982447	-10.004662	-1.331313
C	-12.717732	-11.325332	-1.687855
C	-10.927661	-11.411061	-0.073494
H	-10.617021	-9.617953	1.083896
H	-13.774908	-9.449901	-1.822413
H	-13.312327	-11.796518	-2.465300
H	-10.129132	-11.954093	0.423972
H	-11.479369	-13.061507	-1.351336
C	-13.853429	-7.624835	0.186952
C	-16.526117	-6.816905	0.457631
C	-14.779310	-8.451165	0.839423
C	-14.275418	-6.392144	-0.331220
C	-15.601691	-5.990572	-0.185790
C	-16.107690	-8.049829	0.963930
H	-14.451314	-9.403358	1.242876
H	-13.561160	-5.756762	-0.844208
H	-15.915695	-5.033070	-0.591449
H	-16.815175	-8.699415	1.471350
H	-17.560519	-6.504077	0.562556
C	6.650898	-5.877203	0.530129
O	7.472771	-5.602218	1.315433
O	5.835045	-6.215105	-0.235764

*A.4.8.3 Star-Shaped **OTPA-BZN-430**, **EB** State, with CO_2 Binding on Outer Imine Nitrogen Atom, Branch 1*

H	-0.842684	-0.195593	1.124978
C	-0.318943	0.383811	0.372270
C	1.105020	1.892543	-1.486128
C	0.680529	-0.231036	-0.399545
C	-0.633032	1.721855	0.185709
C	0.061901	2.505936	-0.761756
C	1.388260	0.544548	-1.334367
H	-1.384049	2.187617	0.815236
H	2.166619	0.082234	-1.931634
H	1.659841	2.492252	-2.200465
N	0.978549	-1.602017	-0.226589
C	-0.068860	-2.525434	-0.003417
C	-2.179042	-4.351045	0.460857
C	0.084755	-3.575827	0.917687
C	-1.276718	-2.415904	-0.711516
C	-2.317307	-3.301937	-0.475017
C	-0.939168	-4.487815	1.118880
H	1.015983	-3.674311	1.464960
H	-1.389506	-1.633295	-1.454155
H	-3.229789	-3.222820	-1.056669
H	-0.815309	-5.304956	1.822211
C	2.319362	-2.045396	-0.267698

C	5.008840	-2.916836	-0.370338
C	2.653104	-3.263254	-0.885815
C	3.340165	-1.284519	0.325856
C	4.660626	-1.703620	0.264663
C	3.966861	-3.702703	-0.905820
H	1.871930	-3.863227	-1.339777
H	3.087052	-0.365170	0.842895
H	5.429205	-1.121205	0.761710
H	4.221940	-4.648019	-1.373807
N	6.295356	-3.438171	-0.404683
N	-3.147638	-5.319746	0.692137
N	-0.144411	3.867686	-0.943974
C	-4.421711	-5.042205	0.791766
C	-7.282692	-4.690366	0.927536
C	-5.336804	-6.174879	0.863869
C	-5.020305	-3.716079	0.921904
C	-6.361064	-3.564525	1.013441
C	-6.679793	-6.020365	0.900452
H	-4.881723	-7.160600	0.873877
H	-4.366666	-2.854564	0.990226
H	-6.810699	-2.583988	1.137246
H	-7.327332	-6.886971	0.960887
C	7.357301	-2.704864	-0.616136
C	9.844345	-1.278488	-0.926603
C	8.648846	-3.359970	-0.447990
C	7.388231	-1.320547	-1.080788
C	8.560423	-0.667600	-1.249286
C	9.819302	-2.693597	-0.565422
H	8.623190	-4.417818	-0.205063
H	6.452897	-0.835930	-1.334697
H	8.589194	0.350995	-1.621168
H	10.760572	-3.214333	-0.436175
C	-1.335212	4.407509	-0.974787
C	-3.843663	5.833340	-0.956543
C	-1.395976	5.863923	-0.996304
C	-2.611460	3.703791	-1.073327
C	-3.780252	4.383809	-1.093675
C	-2.566045	6.541011	-0.959634
H	-0.443517	6.384013	-1.029479
H	-2.604223	2.625202	-1.176985
H	-4.730932	3.869244	-1.194692
H	-2.570966	7.624264	-0.982893
N	-8.559764	-4.406711	0.955529
N	10.907340	-0.527452	-1.056108
N	-5.037531	6.367327	-0.916180
C	-9.553221	-5.346017	0.718828
C	-11.724161	-7.115024	0.274358
C	-9.486990	-6.347288	-0.276468
C	-10.756719	-5.224454	1.445301
C	-11.806112	-6.107888	1.254576
C	-10.554500	-7.202185	-0.502343
H	-8.612660	-6.407879	-0.916005
H	-10.828756	-4.442921	2.194963
H	-12.704212	-6.019703	1.855715
H	-10.494803	-7.941980	-1.293050
C	12.174507	-0.923306	-0.640031
C	14.826653	-1.538052	0.139053
C	12.440163	-1.576543	0.581696
C	13.273998	-0.543590	-1.435887
C	14.571024	-0.860229	-1.067709
C	13.740561	-1.877823	0.962783
H	11.619892	-1.820431	1.248479
H	13.083642	-0.001271	-2.356579
H	15.401312	-0.569358	-1.701675

H	13.922379	-2.376254	1.908527
C	-5.261865	7.704827	-0.622312
C	-5.924474	10.401719	-0.049623
C	-4.571700	8.430083	0.375182
C	-6.325054	8.353547	-1.285308
C	-6.629139	9.680856	-1.032375
C	-4.906422	9.743816	0.664334
H	-3.810765	7.932414	0.967236
H	-6.878629	7.798868	-2.036244
H	-7.423316	10.169226	-1.585984
H	-4.385900	10.270847	1.456386
N	-6.243280	11.743996	0.228364
N	16.147454	-1.848573	0.521773
N	-12.795231	-8.002523	0.060218
C	17.103736	-2.230527	-0.454938
C	18.999646	-2.992155	-2.379153
C	18.414906	-1.737057	-0.391027
C	16.749676	-3.109825	-1.488759
C	17.691462	-3.477352	-2.447399
C	19.355076	-2.124998	-1.343228
H	18.688508	-1.053702	0.405871
H	15.738134	-3.499373	-1.534137
H	17.403380	-4.158845	-3.242797
H	20.367203	-1.735302	-1.281489
H	19.733090	-3.286697	-3.123569
C	16.533279	-1.777484	1.886481
C	17.305757	-1.635742	4.580137
C	16.120545	-0.701197	2.685153
C	17.337262	-2.780986	2.445630
C	17.725899	-2.701918	3.781334
C	16.498415	-0.640019	4.024793
H	15.505595	0.079875	2.250542
H	17.653579	-3.615323	1.828501
H	18.349186	-3.485891	4.201994
H	16.171559	0.199028	4.632403
H	17.604540	-1.580963	5.622542
C	-7.586614	12.197818	0.145057
C	-10.235550	13.107753	-0.011338
C	-7.875782	13.433663	-0.450673
C	-8.632650	11.421711	0.664266
C	-9.947836	11.873134	0.575474
C	-9.191911	13.885698	-0.518377
H	-7.066207	14.032157	-0.854922
H	-8.408163	10.469691	1.133625
H	-10.749107	11.262135	0.981181
H	-9.402492	14.845130	-0.982204
H	-11.260857	13.459773	-0.072046
C	-5.224969	12.657946	0.608752
C	-3.220571	14.473057	1.355981
C	-3.994103	12.668728	-0.063208
C	-5.445884	13.563965	1.655711
C	-4.450774	14.469541	2.017699
C	-2.998109	13.565372	0.317597
H	-3.826489	11.974127	-0.879584
H	-6.396954	13.553053	2.177526
H	-4.634729	15.166354	2.830471
H	-2.049175	13.563429	-0.211102
H	-2.444823	15.175511	1.645147
C	-12.545589	-9.348162	-0.318700
C	-12.064124	-12.010326	-1.061754
C	-11.529938	-10.084907	0.307754
C	-13.319800	-9.954565	-1.318092
C	-13.082865	-11.279637	-1.677837
C	-11.288026	-11.403563	-0.071222

H	-10.937034	-9.618884	1.087692	C	-16.394842	-7.943894	0.997931
H	-14.103131	-9.383346	-1.804963	H	-14.763537	-9.329822	1.265304
H	-13.689958	-11.737662	-2.453481	H	-13.814149	-5.697123	-0.819918
H	-10.498364	-11.963174	0.421996	H	-16.152806	-4.928383	-0.552892
H	-11.877808	-13.040593	-1.349289	H	-17.112036	-8.580631	1.507997
C	-14.137033	-7.561149	0.209433	H	-17.819531	-6.369450	0.607376
C	-16.791986	-6.702091	0.496219	C	10.948716	2.320290	-1.370217
C	-15.075192	-8.370667	0.865412	O	10.033685	2.349455	-2.099220
C	-14.537805	-6.319511	-0.304177	O	11.865817	2.362937	-0.647225
C	-15.855225	-5.892581	-0.150740				

*A.4.8.4 Star-Shaped **OTPA-BZN-430**, **EB** State, with CO_2 Binding on Inner Core Unit, Branch 1*

H	-0.650980	-0.093759	1.383989	H	-2.979848	-3.165525	-0.810788
C	-0.109640	0.471147	0.632698	H	-0.653280	-5.180911	2.185688
C	1.358200	1.944152	-1.219133	C	2.541627	-1.973611	0.097739
C	0.909763	-0.157195	-0.101380	C	5.230957	-2.846632	0.032372
C	-0.421524	1.804248	0.410903	C	2.878472	-3.208790	-0.482381
C	0.295633	2.570136	-0.534890	C	3.559059	-1.198750	0.678456
C	1.640818	0.600143	-1.033410	C	4.879683	-1.617968	0.632941
H	-1.188612	2.281135	1.012080	C	4.193239	-3.651292	-0.479901
H	2.436965	0.130359	-1.599771	H	2.101481	-3.821053	-0.926759
H	1.930878	2.530567	-1.930515	H	3.304497	-0.262991	1.164180
N	1.202252	-1.524571	0.107714	H	5.649860	-1.016974	1.105126
C	0.147403	-2.441993	0.322117	H	4.449740	-4.607664	-0.923448
C	-1.975119	-4.259127	0.762215	N	6.525409	-3.352703	0.006181
C	0.273132	-3.471104	1.270917	N	-2.949130	-5.224876	0.982833
C	-1.038558	-2.348981	-0.424100	N	0.091297	3.927235	-0.750738
C	-2.085518	-3.230715	-0.199946	C	-4.226260	-4.948295	1.034227
C	-0.756064	-4.379568	1.461118	C	-7.090583	-4.600048	1.063844
H	1.187644	-3.556533	1.847874	C	-5.141533	-6.081351	1.097524
H	-1.128883	-1.582877	-1.186777	C	-4.830930	-3.621146	1.117640

C	-6.174269	-3.470723	1.160054
C	-6.485199	-5.929040	1.083951
H	-4.685597	-7.065689	1.142795
H	-4.181244	-2.757072	1.191411
H	-6.629431	-2.488971	1.249151
H	-7.133325	-6.795617	1.138451
C	7.561239	-2.614250	-0.294617
C	9.997130	-1.159882	-0.814281
C	8.875253	-3.222352	-0.120594
C	7.536446	-1.269579	-0.866477
C	8.685565	-0.608954	-1.133650
C	10.022306	-2.540058	-0.335599
H	8.886288	-4.257612	0.206414
H	6.579996	-0.829528	-1.121841
H	8.676365	0.378477	-1.585095
H	10.981072	-3.026630	-0.201284
C	-1.099389	4.463874	-0.819864
C	-3.609882	5.884836	-0.887921
C	-1.161946	5.919383	-0.872228
C	-2.372029	3.755839	-0.933233
C	-3.541098	4.432960	-0.994205
C	-2.333584	6.594784	-0.875772
H	-0.209787	6.440606	-0.893818
H	-2.360778	2.675395	-1.014873
H	-4.488425	3.914544	-1.106476
H	-2.339642	7.677360	-0.920546
N	-8.368307	-4.318932	1.041180
N	11.029741	-0.394024	-1.052213
N	-4.805068	6.417408	-0.886131
C	-9.350652	-5.265242	0.786495
C	-11.500269	-7.048087	0.295711
C	-9.246884	-6.282945	-0.188690
C	-10.579139	-5.135345	1.468247
C	-11.618894	-6.025178	1.255702
C	-10.303751	-7.144565	-0.437837
H	-8.350193	-6.351680	-0.795650
H	-10.679514	-4.341609	2.201664
H	-12.537633	-5.929847	1.823625
H	-10.214326	-7.897124	-1.213539
C	12.322539	-0.713619	-0.654440
C	15.024574	-1.181353	0.059945
C	12.658623	-1.271653	0.598147
C	13.378658	-0.349963	-1.515439
C	14.699410	-0.595720	-1.178162
C	13.982366	-1.500162	0.947071
H	11.874208	-1.497008	1.312813
H	13.132967	0.122081	-2.461621
H	15.494261	-0.320229	-1.862436
H	14.217118	-1.925525	1.916532
C	-5.037289	7.760255	-0.623857
C	-5.714822	10.466954	-0.118686
C	-4.373036	8.504467	0.377224
C	-6.083122	8.395791	-1.325923
C	-6.393721	9.727451	-1.105686
C	-4.715404	9.823128	0.633344
H	-3.627172	8.018395	0.997456
H	-6.617283	7.826943	-2.080314
H	-7.173414	10.204908	-1.688618
H	-4.215426	10.365120	1.428531
N	-6.041311	11.814004	0.125779
N	16.368611	-1.421425	0.409268
N	-12.561132	-7.942003	0.058905
C	17.303126	-1.827988	-0.579005
C	19.157095	-2.637259	-2.524037

C	18.594962	-1.282681	-0.595700
C	16.947236	-2.783332	-1.542197
C	17.867765	-3.174747	-2.511985
C	19.514942	-1.694021	-1.557768
H	18.869572	-0.541051	0.146912
H	15.951084	-3.212727	-1.524462
H	17.578693	-3.915308	-3.252291
H	20.512351	-1.263657	-1.559028
H	19.874378	-2.950254	-3.276628
C	16.801346	-1.259121	1.752130
C	17.668009	-0.936778	4.401081
C	16.382819	-0.151589	2.503591
C	17.658685	-2.202701	2.335683
C	18.093690	-2.033980	3.648572
C	16.807776	-0.000749	3.821870
H	15.726540	0.583363	2.049409
H	17.979733	-3.061137	1.755141
H	18.758055	-2.772236	4.088605
H	16.475873	0.861597	4.393025
H	18.003240	-0.812109	5.426234
C	-7.382277	12.264605	-0.002423
C	-10.026655	13.167688	-0.248483
C	-7.656354	13.486759	-0.632480
C	-8.441102	11.498813	0.505994
C	-9.753790	11.946585	0.372707
C	-8.970519	13.935623	-0.744787
H	-6.836717	14.077163	-1.028284
H	-8.228385	10.557509	1.001722
H	-10.565119	11.343682	0.770457
H	-9.169421	14.884391	-1.234954
H	-11.050226	13.517056	-0.343933
C	-5.034282	12.736374	0.515368
C	-3.052470	14.568984	1.280612
C	-3.784474	12.733655	-0.120849
C	-5.285311	13.664723	1.535709
C	-4.301239	14.578733	1.906506
C	-2.800042	13.639113	0.269061
H	-3.593086	12.021746	-0.916816
H	-6.250989	13.664401	2.030073
H	-4.508727	15.292814	2.698358
H	-1.836256	13.626412	-0.231904
H	-2.285494	15.278137	1.576740
C	-12.295908	-9.292338	-0.291714
C	-11.784562	-11.963887	-0.979299
C	-11.299240	-10.016929	0.377937
C	-13.036166	-9.915684	-1.306303
C	-12.784703	-11.245252	-1.638529
C	-11.042158	-11.340341	0.026503
H	-10.732760	-9.537877	1.169529
H	-13.804875	-9.353969	-1.826391
H	-13.365538	-11.716373	-2.426341
H	-10.267427	-11.890357	0.553068
H	-11.586653	-12.997747	-1.245385
C	-13.908421	-7.502794	0.157215
C	-16.573684	-6.648369	0.344073
C	-14.864902	-8.304777	0.795705
C	-14.295957	-6.271107	-0.389404
C	-15.618899	-5.846284	-0.285562
C	-16.189395	-7.880500	0.878576
H	-14.563478	-9.256194	1.221107
H	-13.557790	-5.654726	-0.891621
H	-15.906184	-4.889795	-0.712820
H	-16.920844	-8.511306	1.375597
H	-17.605241	-6.317477	0.416534

C	4.326504	-1.971343	-3.202677	O	4.449707	-0.917397	-2.709979
O	4.207796	-3.014691	-3.713604				

*A.4.8.5 Star-Shaped **OTPA-BZN-430**, **EB** State, with CO_2 Binding on Outer Core Unit, Branch 1*

H	-0.947660	-0.013940	1.045285	H	1.940647	-3.540911	-1.438320
C	-0.448993	0.587884	0.293170	H	2.986001	-0.013733	0.783773
C	0.910766	2.158837	-1.561466	H	5.362493	-0.659019	0.700229
C	0.578465	0.017774	-0.476647	H	4.325007	-4.216176	-1.472997
C	-0.821586	1.910699	0.106424	N	6.338403	-2.921673	-0.477315
C	-0.160129	2.725518	-0.839277	N	-2.997930	-5.249428	0.638885
C	1.253165	0.824779	-1.409561	N	-0.424466	4.076918	-1.021342
H	-1.592928	2.342482	0.735581	C	-4.282951	-5.033447	0.750773
H	2.053082	0.397843	-2.004643	C	-7.155991	-4.819754	0.917137
H	1.440350	2.782989	-2.274048	C	-5.142122	-6.208908	0.824386
N	0.939069	-1.337288	-0.301900	C	-4.942967	-3.738173	0.893556
C	-0.061552	-2.308750	-0.072189	C	-6.288432	-3.651514	0.999560
C	-2.078787	-4.234800	0.403451	C	-6.490557	-6.119173	0.874898
C	0.150482	-3.355447	0.841830	H	-4.640159	-7.171660	0.823421
C	-1.280516	-2.253793	-0.768012	H	-4.330643	-2.846696	0.960306
C	-2.275707	-3.188855	-0.525503	H	-6.783299	-2.694393	1.133657
C	-0.827108	-4.315735	1.048285	H	-7.095398	-7.016091	0.935549
H	1.090829	-3.412783	1.379187	C	7.361511	-2.138072	-0.698626
H	-1.437641	-1.474698	-1.506251	C	9.771090	-0.589188	-1.038010
H	-3.196433	-3.150480	-1.098225	C	8.686408	-2.722970	-0.529059
H	-0.657488	-5.129482	1.746033	C	7.318162	-0.758654	-1.178130
C	2.300723	-1.717170	-0.344505	C	8.455738	-0.050957	-1.361741
C	5.027496	-2.461872	-0.447328	C	9.821118	-1.998921	-0.658236
C	2.692131	-2.910516	-0.975351	H	8.717306	-3.778743	-0.277313
C	3.282904	-0.915780	0.259457	H	6.357382	-0.324683	-1.428655
C	4.622001	-1.272534	0.197802	H	8.432475	0.965436	-1.742996
C	4.025273	-3.288649	-0.995900	H	10.786833	-2.473203	-0.533033

C	-1.636658	4.567587	-1.045882
C	-4.200790	5.890151	-1.009181
C	-1.756694	6.020254	-1.065263
C	-2.883721	3.812830	-1.138844
C	-4.079413	4.444732	-1.150560
C	-2.953097	6.649182	-1.019585
H	-0.826414	6.578802	-1.103673
H	-2.833237	2.735709	-1.245669
H	-5.008955	3.892013	-1.247263
H	-3.002250	7.731387	-1.040710
N	-8.444749	-4.597991	0.961962
N	10.788950	0.219152	-1.185019
N	-5.415061	6.375113	-0.958800
C	-9.394363	-5.583270	0.731304
C	-11.482239	-7.452519	0.299864
C	-9.293307	-6.571214	-0.274198
C	-10.591500	-5.527699	1.475941
C	-11.599080	-6.459831	1.291145
C	-10.320991	-7.475306	-0.493703
H	-8.425973	-6.583289	-0.925936
H	-10.690942	-4.757391	2.234089
H	-12.491690	-6.421334	1.905566
H	-10.236337	-8.204205	-1.292227
C	12.072964	-0.095836	-0.757941
C	14.761087	-0.566448	0.026348
C	12.375116	-0.732680	0.464271
C	13.154624	0.353834	-1.543753
C	14.466534	0.107741	-1.175937
C	13.688992	-0.958700	0.850037
H	11.570236	-1.025537	1.129839
H	12.936119	0.890416	-2.461855
H	15.277518	0.449580	-1.808755
H	13.891778	-1.440728	1.799455
C	-5.691671	7.701424	-0.658753
C	-6.461363	10.366186	-0.069672
C	-5.024301	8.451086	0.336219
C	-6.785888	8.308060	-1.311078
C	-7.142956	9.620566	-1.050140
C	-5.411030	9.748689	0.633382
H	-4.238658	7.983268	0.920263
H	-7.321878	7.733829	-2.060075
H	-7.961128	10.077665	-1.595472
H	-4.906585	10.294002	1.423468
N	-6.834273	11.692793	0.216912
N	16.088894	-0.818591	0.404142
N	-12.512052	-8.389188	0.091735
C	17.103193	-1.038896	-0.565550
C	19.138455	-1.481239	-2.446573
C	18.376730	-0.483909	-0.375161
C	16.857275	-1.820986	-1.703156
C	17.868079	-2.029345	-2.639062
C	19.386884	-0.712788	-1.306960
H	18.566328	0.121817	0.504736
H	15.878983	-2.264990	-1.845280
H	17.663942	-2.637646	-3.515634
H	20.368789	-0.276920	-1.146100
H	19.925344	-1.652523	-3.174815
C	16.434300	-0.930972	1.780885
C	17.132935	-1.149038	4.483692
C	16.057624	0.068069	2.687741
C	17.162939	-2.038740	2.231597
C	17.516183	-2.139380	3.575958
C	16.398803	-0.048687	4.033929
H	15.498558	0.927130	2.331004

H	17.442879	-2.812133	1.524553
H	18.081456	-3.002032	3.916820
H	16.102221	0.730619	4.730015
H	17.404135	-1.233488	5.531705
C	-8.196684	12.088545	0.149688
C	-10.884037	12.883687	0.025174
C	-8.545258	13.313613	-0.436492
C	-9.202764	11.265366	0.675382
C	-10.537093	11.659834	0.602428
C	-9.880344	13.708553	-0.488336
H	-7.766581	13.948582	-0.845756
H	-8.932449	10.321688	1.137358
H	-11.306913	11.012736	1.013039
H	-10.137079	14.660218	-0.944860
H	-11.924180	13.191289	-0.023193
C	-5.852154	12.647613	0.591754
C	-3.919384	14.543205	1.328095
C	-4.628903	12.712643	-0.091004
C	-6.101546	13.539894	1.644137
C	-5.142288	14.485408	2.000725
C	-3.668233	13.649241	0.284353
H	-4.439505	12.028461	-0.911402
H	-7.046508	13.487039	2.174402
H	-5.348116	15.170985	2.817800
H	-2.724857	13.689148	-0.252733
H	-3.171377	15.276791	1.613021
C	-12.202935	-9.717459	-0.303968
C	-11.603380	-12.345942	-1.080615
C	-11.143588	-10.409658	0.300574
C	-12.961203	-10.351589	-1.298402
C	-12.665402	-11.660100	-1.674766
C	-10.843383	-11.711332	-0.095060
H	-10.562662	-9.922592	1.076655
H	-13.778396	-9.814731	-1.768410
H	-13.260779	-12.139887	-2.446333
H	-10.020295	-12.236342	0.381276
H	-11.371379	-13.363145	-1.381146
C	-13.871407	-8.014212	0.261857
C	-16.560731	-7.286620	0.589714
C	-14.761128	-8.873797	0.921653
C	-14.337962	-6.788720	-0.234747
C	-15.672299	-6.427130	-0.060928
C	-16.097944	-8.512283	1.074587
H	-14.398632	-9.820379	1.308457
H	-13.651723	-6.127556	-0.753380
H	-16.020996	-5.474810	-0.450114
H	-16.777109	-9.187358	1.587410
H	-17.601578	-7.004922	0.716756
C	13.831043	-3.981735	-0.021312
O	12.689656	-4.070303	-0.257962
O	14.974157	-3.912294	0.211650

*A.4.8.6 Star-Shaped **OTPA-BZN-430**, **EB** State, with CO_2 Binding on Linker Unit, Branch 1*

H	-0.783563	-0.086867	1.063317
C	-0.268626	0.497188	0.308157
C	1.132859	2.020444	-1.555274
C	0.744323	-0.104181	-0.456967
C	-0.606690	1.827958	0.112488
C	0.076311	2.619106	-0.837905
C	1.440547	0.678928	-1.394343
H	-1.367557	2.283633	0.737547

H	2.229343	0.227495	-1.986198
H	1.678716	2.625901	-2.271681
N	1.067486	-1.467696	-0.274094
C	0.038481	-2.408994	-0.041739
C	-2.034080	-4.273775	0.437828
C	0.214642	-3.450542	0.885509
C	-1.172935	-2.327911	-0.747803
C	-2.195165	-3.233006	-0.503774
C	-0.790444	-4.381505	1.094254
H	1.148822	-3.527299	1.431177
H	-1.302724	-1.552548	-1.495256
H	-3.109955	-3.175804	-1.084370
H	-0.648836	-5.191850	1.802110
C	2.417046	-1.886822	-0.311578
C	5.120039	-2.712655	-0.402442
C	2.772913	-3.100847	-0.924329
C	3.422897	-1.106024	0.280855
C	4.751110	-1.501819	0.224962
C	4.094061	-3.518409	-0.938312
H	2.003201	-3.715764	-1.377954
H	3.152359	-0.189115	0.793547
H	5.508302	-0.909219	0.725825
H	4.366275	-4.461650	-1.400861
N	6.416095	-3.211803	-0.425980
N	-2.981878	-5.261022	0.676044
N	-0.154287	3.975574	-1.029080
C	-4.261725	-5.010395	0.773518
C	-7.129697	-4.719983	0.905923
C	-5.152004	-6.162188	0.852077
C	-4.889003	-3.696835	0.895284
C	-6.232803	-3.573884	0.985426
C	-6.498072	-6.036710	0.886874
H	-4.675487	-7.137656	0.868051
H	-4.254206	-2.820982	0.958852
H	-6.703769	-2.602669	1.103290
H	-7.126759	-6.916774	0.951778
C	7.462682	-2.465697	-0.661255
C	9.927240	-1.018479	-1.083524
C	8.767938	-3.088956	-0.476555
C	7.464752	-1.093632	-1.163140
C	8.625618	-0.435702	-1.386025
C	9.926751	-2.411465	-0.643243
H	8.762742	-4.134247	-0.183255
H	6.517254	-0.626343	-1.403511
H	8.633760	0.571906	-1.790244
H	10.876992	-2.912358	-0.502171
C	-1.354600	4.494139	-1.061618
C	-3.887885	5.875234	-1.043831
C	-1.441207	5.949050	-1.089996
C	-2.618272	3.767587	-1.155472
C	-3.799041	4.426644	-1.176264
C	-2.623074	6.605444	-1.053158
H	-0.498209	6.485844	-1.127585
H	-2.592038	2.688943	-1.255389
H	-4.740602	3.894885	-1.273700
H	-2.647347	7.688343	-1.080792
N	-8.412666	-4.464148	0.932004
N	10.972983	-0.264254	-1.296366
N	-5.090989	6.388011	-1.001528
C	-9.384968	-5.426711	0.700439
C	-11.515890	-7.245716	0.264460
C	-9.296729	-6.430359	-0.290688
C	-10.590340	-5.329358	1.427357
C	-11.619788	-6.236879	1.240799

C	-10.344966	-7.309887	-0.512499
H	-8.421417	-6.474045	-0.930280
H	-10.679498	-4.546597	2.173909
H	-12.519321	-6.166467	1.842153
H	-10.269031	-8.051410	-1.300197
C	12.258579	-0.617865	-0.904295
C	14.948233	-1.156545	-0.196916
C	12.580013	-1.205470	0.338659
C	13.322757	-0.261419	-1.758159
C	14.637569	-0.541763	-1.424453
C	13.898477	-1.468136	0.683682
H	11.790266	-1.418707	1.049982
H	13.088329	0.232646	-2.695933
H	15.439100	-0.271499	-2.103031
H	14.123425	-1.914687	1.645978
C	-5.338502	7.721919	-0.709990
C	-6.049422	10.406919	-0.139150
C	-4.658323	8.461741	0.283684
C	-6.415856	8.349672	-1.370345
C	-6.743841	9.671468	-1.118349
C	-5.016498	9.769487	0.571940
H	-3.886104	7.979386	0.873790
H	-6.961706	7.783558	-2.118392
H	-7.549032	10.144008	-1.669794
H	-4.503066	10.307522	1.361220
N	-6.392816	11.743300	0.138317
N	16.286664	-1.432083	0.149073
N	-12.567196	-8.157623	0.054346
C	17.211755	-1.845094	-0.845162
C	19.046553	-2.667090	-2.803261
C	18.516170	-1.330251	-0.853614
C	16.833657	-2.776360	-1.823420
C	17.744860	-3.174038	-2.799435
C	19.426335	-1.747949	-1.822247
H	18.808137	-0.607077	-0.099514
H	15.827578	-3.182181	-1.812419
H	17.438447	-3.895705	-3.551348
H	20.433601	-1.341202	-1.816919
H	19.756375	-2.984966	-3.560869
C	16.722196	-1.298071	1.493998
C	17.593791	-1.032033	4.147759
C	16.325234	-0.193729	2.261770
C	17.560396	-2.266942	2.063896
C	17.998016	-2.126222	3.379207
C	16.752504	-0.070781	3.582177
H	15.683537	0.560520	1.818558
H	17.864696	-3.122964	1.470907
H	18.647426	-2.883919	3.808415
H	16.437295	0.789413	4.165903
H	17.930919	-0.929143	5.174711
C	-7.745114	12.170724	0.061037
C	-10.412066	13.028619	-0.083428
C	-8.061200	13.400291	-0.534045
C	-8.773360	11.374674	0.585593
C	-10.097517	11.800245	0.502720
C	-9.386215	13.826475	-0.595809
H	-7.265384	14.014246	-0.942408
H	-8.528124	10.427540	1.054446
H	-10.884781	11.173971	0.912541
H	-9.617692	14.781307	-1.059176
H	-11.444332	13.360492	-0.139505
C	-5.390667	12.677125	0.513205
C	-3.418295	14.531408	1.249500
C	-4.163097	12.710600	-0.164022

C	-5.624420	13.580139	1.559986
C	-4.645345	14.505138	1.916535
C	-3.182894	13.626730	0.211340
H	-3.985684	12.018191	-0.980190
H	-6.572850	13.551674	2.085921
H	-4.839161	15.199369	2.729227
H	-2.236357	13.642273	-0.321421
H	-2.654950	15.249023	1.534417
C	-12.287965	-9.498853	-0.319398
C	-11.747735	-12.152541	-1.052491
C	-11.256131	-10.210552	0.309576
C	-13.048713	-10.126099	-1.316277
C	-12.782536	-11.446951	-1.671055
C	-10.985137	-11.524964	-0.064445
H	-10.673512	-9.728540	1.087548
H	-13.844619	-9.574246	-1.805081
H	-13.379477	-11.921246	-2.444802
H	-10.183176	-12.065057	0.430691
H	-11.538680	-13.179508	-1.336174
C	-13.918352	-7.744984	0.201055
C	-16.591648	-6.942874	0.482871
C	-14.839114	-8.572158	0.859677
C	-14.345777	-6.514386	-0.317639
C	-15.672294	-6.115676	-0.166676
C	-16.167839	-8.173732	0.989717
H	-14.506912	-9.522721	1.263532
H	-13.635517	-5.878370	-0.835372
H	-15.990528	-5.159775	-0.572812
H	-16.871324	-8.823949	1.501868
H	-17.626284	-6.632307	0.592109
C	8.615901	-0.710824	2.146527
O	7.567655	-1.206935	2.291737
O	9.663962	-0.211937	2.010398

*A.4.8.7 Star-Shaped **OTPA-BZN-430**, **EB** State, with CO_2 Binding on Inner Imine Nitrogen Atom, Branch 2*

H	-0.557895	-0.275769	1.116124
C	-0.039251	0.299560	0.356832
C	1.370430	1.798518	-1.520815
C	0.957361	-0.317739	-0.416023
C	-0.355495	1.636406	0.163784
C	0.333764	2.414485	-0.791036
C	1.656308	0.452157	-1.361980
H	-1.103885	2.105979	0.793678
H	2.431402	-0.013115	-1.961148
H	1.920295	2.392604	-2.243173
N	1.262952	-1.685847	-0.232562
C	0.220674	-2.611940	0.001380
C	-1.880674	-4.443506	0.483929
C	0.380032	-3.653537	0.931578
C	-0.988810	-2.514150	-0.705874
C	-2.024927	-3.402903	-0.460587
C	-0.639413	-4.568470	1.141809
H	1.312320	-3.743085	1.478540
H	-1.106025	-1.738638	-1.455256
H	-2.938208	-3.333201	-1.042185
H	-0.510906	-5.378917	1.852036
C	2.606990	-2.120806	-0.267508
C	5.301941	-2.977109	-0.356265
C	2.948573	-3.346046	-0.866282

C	3.623202	-1.343410	0.312205
C	4.946466	-1.755106	0.256918
C	4.265110	-3.777858	-0.878945
H	2.171360	-3.958357	-1.310483
H	3.365095	-0.416452	0.812921
H	5.712019	-1.158576	0.741894
H	4.525715	-4.729432	-1.330995
N	6.592216	-3.491008	-0.378612
N	-2.843797	-5.415398	0.723857
N	0.123874	3.777412	-0.971116
C	-4.119834	-5.144812	0.818208
C	-6.983336	-4.809657	0.941397
C	-5.028008	-6.282446	0.898211
C	-4.727060	-3.821389	0.934851
C	-6.069048	-3.677384	1.020770
C	-6.372080	-6.136035	0.928600
H	-4.566790	-7.265153	0.918692
H	-4.078990	-2.955269	0.997887
H	-6.525170	-2.698636	1.134624
H	-7.014497	-7.006059	0.994481
C	7.648125	-2.756688	-0.614295
C	10.125782	-1.326113	-0.988375
C	8.945280	-3.397518	-0.432887
C	7.666453	-1.385722	-1.118473
C	8.834569	-0.734022	-1.316668
C	10.110947	-2.728293	-0.578851
H	8.927544	-4.447498	-0.157155
H	6.726064	-0.913180	-1.376303
H	8.856910	0.274974	-1.717029
H	11.055973	-3.239832	-0.440034
C	-1.070325	4.310350	-1.014503
C	-3.596479	5.701549	-1.009533
C	-1.147707	5.766014	-1.030809
C	-2.335697	3.590104	-1.129917
C	-3.513366	4.254344	-1.156369
C	-2.328355	6.425235	-1.000149
H	-0.204425	6.300770	-1.056830
H	-2.312507	2.512324	-1.238681
H	-4.456104	3.727538	-1.268013
H	-2.347618	7.508464	-1.020000
N	-8.262294	-4.533902	0.961767
N	11.179014	-0.570321	-1.159205
N	-4.797832	6.219316	-0.972136
C	-9.248514	-5.481808	0.728755
C	-11.405829	-7.268521	0.288651
C	-9.171572	-6.489968	-0.258755
C	-10.455603	-5.363110	1.449667
C	-11.498323	-6.254947	1.261246
C	-10.232475	-7.353609	-0.482637
H	-8.294159	-6.549508	-0.894170
H	-10.535896	-4.576609	2.193277
H	-12.399376	-6.168412	1.858199
H	-10.164609	-8.098782	-1.267617
C	12.453804	-0.937311	-0.743633
C	15.124360	-1.498948	0.019277
C	12.743323	-1.558419	0.490634
C	13.540530	-0.560585	-1.559606
C	14.846035	-0.851370	-1.199038
C	14.051860	-1.832993	0.863374
H	11.934701	-1.797710	1.173093
H	13.331172	-0.041778	-2.489910
H	15.665173	-0.564431	-1.849171
H	14.250938	-2.306891	1.818235
C	-5.042850	7.549697	-0.665783

C	-5.748465	10.230673	-0.068980
C	-4.363150	8.277696	0.337253
C	-6.117839	8.186802	-1.321476
C	-6.443033	9.506583	-1.056950
C	-4.718611	9.583049	0.638026
H	-3.594258	7.787218	0.924932
H	-6.663351	7.629617	-2.076420
H	-7.245794	9.986560	-1.605403
H	-4.206080	10.111249	1.434432
N	-6.088643	11.564344	0.221102
N	16.453190	-1.785665	0.392526
N	-12.470287	-8.164533	0.076582
C	17.402761	-2.176507	-0.587404
C	19.286153	-2.955262	-2.516957
C	18.708639	-1.666729	-0.548253
C	17.047706	-3.080862	-1.598998
C	17.983150	-3.456953	-2.560533
C	19.642777	-2.063083	-1.502928
H	18.982969	-0.964319	0.231662
H	16.040424	-3.482989	-1.625042
H	17.694398	-4.157901	-3.338586
H	20.650877	-1.660587	-1.460499
H	20.014744	-3.256416	-3.263493
C	16.853533	-1.687010	1.751354
C	17.655127	-1.490681	4.433101
C	16.439499	-0.600901	2.535904
C	17.673543	-2.672814	2.318654
C	18.076512	-2.566648	3.648208
C	16.831908	-0.512576	3.869843
H	15.812099	0.166542	2.094852
H	17.990949	-3.514786	1.712562
H	18.712109	-3.337160	4.075265
H	16.503831	0.333820	4.466509
H	17.965158	-1.414792	5.470882
C	-7.438138	11.999880	0.135097
C	-10.098177	12.874873	-0.025128
C	-7.741462	13.236001	-0.452732
C	-8.475285	11.205849	0.644727
C	-9.796139	11.640047	0.553995
C	-9.063341	13.670639	-0.522473
H	-6.938356	13.848263	-0.849210
H	-8.239575	10.253682	1.108264
H	-10.590643	11.015447	0.952194
H	-9.285215	14.630486	-0.980101
H	-11.127922	13.213413	-0.087322
C	-5.086952	12.489591	0.618914
C	-3.117002	14.327386	1.400028
C	-3.853889	12.530466	-0.047675
C	-5.327760	13.376845	1.677365
C	-4.349616	14.293875	2.056386
C	-2.874803	13.438377	0.349959
H	-3.671339	11.850355	-0.873003
H	-6.280752	13.342452	2.194643
H	-4.548630	14.976035	2.877976
H	-1.923818	13.459991	-0.174568
H	-2.354467	15.038715	1.702339
C	-12.210377	-9.511072	-0.292066
C	-11.708483	-12.175023	-1.015035
C	-11.192663	-10.236960	0.343652
C	-12.976352	-10.129255	-1.290594
C	-12.729291	-11.455149	-1.640359
C	-10.940598	-11.556546	-0.025347
H	-10.606084	-9.761822	1.122875
H	-13.761302	-9.566451	-1.784604

H	-13.330080	-11.922328	-2.415454
H	-10.149431	-12.107660	0.474981
H	-11.514256	-13.205967	-1.294804
C	-13.815514	-7.730721	0.216647
C	-16.477245	-6.886828	0.485487
C	-14.751490	-8.541740	0.873908
C	-14.221900	-6.495218	-0.307268
C	-15.542721	-6.075748	-0.162738
C	-16.074441	-8.122590	0.997501
H	-14.435539	-9.496114	1.281790
H	-13.499906	-5.871698	-0.823966
H	-15.844624	-5.116252	-0.572842
H	-16.789861	-8.760442	1.508665
H	-17.507400	-6.560059	0.589689
C	2.612635	5.135657	-0.534023
O	3.007644	4.190376	0.028212
O	2.281881	6.114155	-1.084158

*A.4.8.8 Star-Shaped **OTPA-BZN-430**, **EB** State, with CO_2 Binding on Outer Imine Nitrogen Atom, Branch 2*

H	-0.283409	-0.281166	1.099083
C	0.227709	0.315629	0.351408
C	1.619690	1.873637	-1.490324
C	1.257318	-0.264242	-0.408576
C	-0.131454	1.641298	0.160346
C	0.546361	2.449778	-0.779266
C	1.948300	0.536572	-1.335204
H	-0.905010	2.080297	0.781729
H	2.749510	0.102457	-1.923224
H	2.161549	2.492631	-2.198133
N	1.601280	-1.622716	-0.230952
C	0.586800	-2.580748	0.000101
C	-1.455777	-4.478061	0.477735
C	0.777967	-3.617630	0.929317
C	-0.623686	-2.520619	-0.709315
C	-1.631703	-3.441842	-0.466089
C	-0.212302	-4.564625	1.137378
H	1.712100	-3.678120	1.477153
H	-0.764322	-1.748518	-1.458196
H	-2.546214	-3.400390	-1.048466
H	-0.059196	-5.371406	1.846908
C	2.956498	-2.023125	-0.272719
C	5.670648	-2.813089	-0.372824
C	3.327337	-3.229614	-0.891325
C	3.953011	-1.231509	0.321088
C	5.285973	-1.610374	0.260289
C	4.653876	-3.629625	-0.910030
H	2.564898	-3.852758	-1.345990
H	3.672072	-0.319775	0.837302
H	6.037083	-1.003976	0.755520
H	4.937516	-4.567081	-1.377413
N	6.973199	-3.295258	-0.401832
N	-2.388654	-5.479871	0.715152
N	0.294079	3.802686	-0.965171
C	-3.671746	-5.247737	0.814341
C	-6.543174	-4.998208	0.954210
C	-4.545444	-6.412198	0.893455
C	-4.317362	-3.943187	0.937795
C	-5.662499	-3.839440	1.031442
C	-5.893018	-6.305855	0.931909

H	-4.055029	-7.380780	0.907324
H	-3.694920	-3.058383	0.999535
H	-6.147038	-2.875075	1.150518
H	-6.508993	-7.194798	0.997616
C	8.010166	-2.532450	-0.630261
C	10.450586	-1.036642	-0.993553
C	9.323344	-3.143027	-0.459222
C	7.993146	-1.155413	-1.117820
C	9.144185	-0.472744	-1.311310
C	10.471615	-2.443442	-0.600379
H	9.332447	-4.196368	-0.196107
H	7.040532	-0.703214	-1.367154
H	9.140410	0.541201	-1.699584
H	11.429411	-2.933048	-0.470261
C	-0.914564	4.301414	-1.001263
C	-3.470282	5.637923	-0.989262
C	-1.025113	5.754590	-1.020257
C	-2.165266	3.555055	-1.107984
C	-3.358316	4.191735	-1.131660
C	-2.218294	6.390006	-0.985929
H	-0.091381	6.307933	-1.047718
H	-2.119764	2.477875	-1.217061
H	-4.287103	3.642679	-1.242485
H	-2.261786	7.472425	-1.004342
N	-7.829512	-4.760647	0.985095
N	11.484208	-0.253027	-1.158413
N	-4.678747	6.139365	-0.948919
C	-8.788945	-5.736636	0.756304
C	-10.895615	-7.585137	0.326683
C	-8.690235	-6.738113	-0.236033
C	-9.992802	-5.656917	1.487866
C	-11.010021	-6.578695	1.304378
C	-9.726799	-7.632103	-0.454746
H	-7.816870	-6.768790	-0.879032
H	-10.090161	-4.876104	2.235446
H	-11.908155	-6.521498	1.909199
H	-9.643393	-8.371687	-1.243500
C	12.769024	-0.592310	-0.750716
C	15.455368	-1.094753	-0.002215
C	13.078058	-1.221701	0.474619
C	13.843284	-0.176849	-1.564465
C	15.156851	-0.438762	-1.211292
C	14.394282	-1.467124	0.840367
H	12.277941	-1.490456	1.156122
H	13.617791	0.348666	-2.487208
H	15.966404	-0.122326	-1.859732
H	14.608306	-1.947897	1.788523
C	-4.935358	7.471415	-0.648781
C	-5.657179	10.145375	-0.049476
C	-4.282022	8.190368	0.376014
C	-5.988901	8.113359	-1.331394
C	-6.321509	9.430753	-1.064207
C	-4.645769	9.493691	0.678553
H	-3.526555	7.694836	0.976931
H	-6.513433	7.565212	-2.106965
H	-7.108553	9.915601	-1.630899
H	-4.154011	10.015756	1.491945
N	-6.010693	11.475859	0.244544
N	16.792053	-1.351856	0.363898
N	-11.934723	-8.511447	0.119675
C	17.749310	-1.703553	-0.623398
C	19.648277	-2.405130	-2.567186
C	19.041404	-1.160196	-0.579354
C	17.415931	-2.602580	-1.647032

C	18.358834	-2.940309	-2.615497
C	19.983533	-1.518278	-1.541268
H	19.298887	-0.461936	0.209976
H	16.419548	-3.030746	-1.676933
H	18.086935	-3.637574	-3.402872
H	20.980795	-1.090041	-1.494947
H	20.382901	-2.676444	-3.319227
C	17.193262	-1.261774	1.723147
C	17.996690	-1.081862	4.405378
C	16.754647	-0.196841	2.523168
C	18.038723	-2.234644	2.275131
C	18.442385	-2.136488	3.605095
C	17.148202	-0.116816	3.857295
H	16.107453	0.560780	2.093880
H	18.375176	-3.060280	1.656953
H	19.097870	-2.896751	4.020279
H	16.800991	0.713142	4.466091
H	18.307474	-1.012333	5.443379
C	-7.362200	11.900351	0.142191
C	-10.028048	12.752017	-0.052348
C	-7.667685	13.142554	-0.431861
C	-8.400619	11.088369	0.620395
C	-9.723865	11.511154	0.512579
C	-8.992374	13.565409	-0.518498
H	-6.863987	13.768831	-0.804538
H	-8.164124	10.130905	1.072432
H	-10.518962	10.872350	0.886353
H	-9.215511	14.530147	-0.965156
H	-11.059859	13.081466	-0.127858
C	-5.021941	12.402627	0.668627
C	-3.074718	14.242491	1.502259
C	-3.774795	12.451477	0.029047
C	-5.287738	13.283039	1.727002
C	-4.320948	14.201037	2.131895
C	-2.807412	13.360162	0.452634
H	-3.572259	11.776554	-0.795877
H	-6.251173	13.242595	2.224061
H	-4.539727	14.877630	2.953088
H	-1.845505	13.387681	-0.051351
H	-2.321154	14.954489	1.824827
C	-11.638382	-9.847845	-0.258324
C	-11.064537	-12.492086	-0.999716
C	-10.594198	-10.546549	0.364780
C	-12.394544	-10.483307	-1.253465
C	-12.111598	-11.799550	-1.612369
C	-10.306597	-11.856244	-0.013373
H	-10.015105	-10.058244	1.141460
H	-13.200046	-9.941416	-1.737670
H	-12.705139	-12.280355	-2.384709
H	-9.495200	-12.386307	0.477207
H	-10.842478	-13.515424	-1.286613
C	-13.291002	-8.118389	0.273186
C	-15.974232	-7.355356	0.568127
C	-14.196642	-8.959553	0.935011
C	-13.738500	-6.893532	-0.242121
C	-15.069938	-6.514207	-0.084632
C	-15.530374	-8.580518	1.071606
H	-13.848854	-9.905674	1.336175
H	-13.039885	-6.246772	-0.762387
H	-15.403835	-5.562578	-0.488215
H	-16.222050	-9.241397	1.586186
H	-17.012746	-7.059931	0.682442
C	-7.147674	4.666310	-0.793570
O	-7.597536	5.524036	-0.139782

O	-6.760193	3.772890	-1.442571

*A.4.8.9 Star-Shaped **OTPA-BZN-430**, **EB** State, with CO_2 Binding on Inner Core Unit, Branch 2*

H	-0.392623	-0.134860	1.291950	H	3.543112	-0.222655	0.989091
C	0.114481	0.469509	0.547680	H	5.900486	-0.927291	0.870171
C	1.490542	2.042503	-1.293632	H	4.748763	-4.422780	-1.345585
C	1.124029	-0.109030	-0.238954	N	6.804649	-3.197005	-0.352698
C	-0.237452	1.799793	0.379423	N	-2.580567	-5.307389	0.770974
C	0.428984	2.613665	-0.562544	N	0.166770	3.967320	-0.738128
C	1.808694	0.698621	-1.163388	C	-3.859935	-5.063669	0.889671
H	-1.004234	2.235918	1.011209	C	-6.727226	-4.786835	1.061745
H	2.596135	0.266472	-1.771113	C	-4.746184	-6.220204	0.939383
H	2.023634	2.665146	-2.004420	C	-4.489613	-3.756723	1.060894
N	1.451618	-1.475839	-0.094615	C	-5.832722	-3.641076	1.169052
C	0.425905	-2.426174	0.116965	C	-6.092124	-6.100255	0.992437
C	-1.637355	-4.310410	0.555907	H	-4.266761	-7.194158	0.917973
C	0.614661	-3.498155	1.006230	H	-3.856802	-2.881307	1.146375
C	-0.793556	-2.322240	-0.572292	H	-6.305115	-2.675721	1.323594
C	-1.810652	-3.238101	-0.347256	H	-6.717619	-6.983966	1.034672
C	-0.386272	-4.438006	1.194312	C	7.847923	-2.438310	-0.565869
H	1.555019	-3.591632	1.538538	C	10.300866	-0.955704	-0.896262
H	-0.936804	-1.520712	-1.288305	C	9.155814	-3.065760	-0.417297
H	-2.732324	-3.162232	-0.914754	C	7.842166	-1.048515	-1.016033
H	-0.235229	-5.271782	1.872397	C	8.998915	-0.371511	-1.194969
C	2.801766	-1.889821	-0.158143	C	10.310101	-2.373074	-0.542599
C	5.507310	-2.702890	-0.301624	H	9.155843	-4.126017	-0.183511
C	3.155779	-3.083088	-0.811320	H	6.892999	-0.580966	-1.249744
C	3.810980	-1.123370	0.447173	H	9.003430	0.652594	-1.555601
C	5.139553	-1.513303	0.365509	H	11.263763	-2.874788	-0.429216
C	4.478187	-3.495150	-0.851596	C	-1.049246	4.444469	-0.798326
H	2.383625	-3.686971	-1.275489	C	-3.629260	5.733746	-0.851142

C	-1.186694	5.895774	-0.814787
C	-2.282455	3.672859	-0.936213
C	-3.484379	4.290384	-0.991474
C	-2.391940	6.508888	-0.811585
H	-0.262878	6.466198	-0.817831
H	-2.215241	2.597113	-1.045060
H	-4.402658	3.726120	-1.123202
H	-2.454338	7.590446	-0.831156
N	-8.010547	-4.536406	1.110463
N	11.341200	-0.177035	-1.041252
N	-4.850538	6.203321	-0.846065
C	-8.981995	-5.494979	0.858753
C	-11.109848	-7.308754	0.388443
C	-8.902184	-6.463455	-0.167367
C	-10.178023	-5.428595	1.604226
C	-11.205632	-6.334496	1.399980
C	-9.949176	-7.340235	-0.405583
H	-8.034953	-6.480825	-0.819118
H	-10.260935	-4.672357	2.378350
H	-12.097529	-6.289394	2.015005
H	-9.880092	-8.054179	-1.218995
C	12.623196	-0.538790	-0.644097
C	15.305125	-1.084408	0.089973
C	12.926844	-1.203481	0.563827
C	13.700961	-0.111259	-1.446857
C	15.012236	-0.393911	-1.101140
C	14.240871	-1.470075	0.922506
H	12.124417	-1.483245	1.238142
H	13.480062	0.440660	-2.355185
H	15.824475	-0.067295	-1.741120
H	14.450740	-1.977859	1.857415
C	-5.155787	7.524248	-0.551383
C	-5.981398	10.176792	0.017464
C	-4.535092	8.278995	0.469741
C	-6.233803	8.118725	-1.240919
C	-6.617173	9.425480	-0.989419
C	-4.949385	9.570211	0.756706
H	-3.765701	7.819098	1.081062
H	-6.734747	7.540183	-2.010546
H	-7.420796	9.873638	-1.562966
H	-4.481672	10.118774	1.566826
N	-6.381875	11.496844	0.293982
N	16.639524	-1.362322	0.449200
N	-12.159490	-8.218807	0.161234
C	17.594528	-1.694718	-0.546875
C	19.489217	-2.358212	-2.508193
C	18.891051	-1.163510	-0.487179
C	17.254560	-2.562420	-1.595091
C	18.195419	-2.881128	-2.571957
C	19.830962	-1.502761	-1.458036
H	19.153658	-0.489338	0.321172
H	16.254706	-2.981352	-1.637362
H	17.918378	-3.554154	-3.378403
H	20.831687	-1.084224	-1.399359
H	20.222167	-2.614795	-3.267007
C	17.040836	-1.311879	1.810507
C	17.844227	-1.210505	4.496846
C	16.611282	-0.264695	2.638371
C	17.877281	-2.306569	2.336715
C	18.280995	-2.247423	3.668972
C	17.004743	-0.223665	3.974291
H	15.971078	0.509764	2.229120
H	18.206733	-3.118438	1.696900
H	18.929430	-3.024270	4.064040

H	16.664578	0.592896	4.604793
H	18.154982	-1.171369	5.536447
C	-7.744432	11.878367	0.166996
C	-10.431272	12.646147	-0.075036
C	-8.079197	13.099477	-0.434990
C	-8.763788	11.045378	0.649622
C	-10.097612	11.426281	0.518263
C	-9.414673	13.480882	-0.545408
H	-7.289684	13.741907	-0.810499
H	-8.504119	10.104836	1.123970
H	-10.878072	10.771833	0.895765
H	-9.660967	14.429587	-1.013664
H	-11.471377	12.943161	-0.168952
C	-5.429708	12.461622	0.718040
C	-3.558131	14.378227	1.550782
C	-4.178781	12.548112	0.090102
C	-5.737736	13.342943	1.764028
C	-4.808442	14.299004	2.168600
C	-3.248744	13.495154	0.513419
H	-3.944051	11.872496	-0.725662
H	-6.704358	13.273384	2.251613
H	-5.059541	14.976027	2.980108
H	-2.283356	13.551892	0.018655
H	-2.833722	15.120008	1.873018
C	-11.878214	-9.546167	-0.257358
C	-11.333481	-12.173006	-1.079090
C	-10.833666	-10.270686	0.335015
C	-12.649257	-10.147205	-1.262501
C	-12.380768	-11.454975	-1.661251
C	-10.560590	-11.571338	-0.082959
H	-10.242875	-9.809311	1.119296
H	-13.454901	-9.585472	-1.723282
H	-12.985859	-11.908892	-2.440876
H	-9.748719	-12.121463	0.384199
H	-11.122705	-13.189529	-1.397053
C	-13.510509	-7.817485	0.337123
C	-16.183462	-7.036650	0.676669
C	-14.419984	-8.669584	0.979503
C	-13.949131	-6.572610	-0.136197
C	-15.275315	-6.184822	0.043397
C	-15.748632	-8.281417	1.138193
H	-14.079172	-9.631257	1.348371
H	-13.247680	-5.917024	-0.641377
H	-15.602222	-5.217650	-0.327665
H	-16.443282	-8.950952	1.637357
H	-17.217944	-6.734347	0.808269
C	-0.700624	1.007773	-3.379957
O	-1.455251	0.566901	-2.602173
O	0.038360	1.445245	-4.171240

*A.4.8.10 Star-Shaped **OTPA-BZN-430**, **EB** State, with CO_2 Binding on Outer Core Unit, Branch 2*

H	-0.399356	-0.465892	1.238477
C	0.103581	0.145555	0.497061
C	1.475283	1.738051	-1.330276
C	1.119197	-0.421410	-0.290617
C	-0.252105	1.476921	0.340995
C	0.415377	2.302781	-0.590679
C	1.800320	0.396509	-1.209282
H	-1.014415	1.905318	0.983331

H	2.591064	-0.028035	-1.818143
H	2.009388	2.370395	-2.032155
N	1.459275	-1.785454	-0.148348
C	0.442128	-2.744776	0.063556
C	-1.605355	-4.646845	0.501028
C	0.634735	-3.807961	0.962373
C	-0.772926	-2.659704	-0.635516
C	-1.783071	-3.583521	-0.411862
C	-0.358110	-4.756422	1.150202
H	1.572141	-3.887650	1.502098
H	-0.915109	-1.866416	-1.361609
H	-2.700792	-3.522345	-0.987392
H	-0.203785	-5.583480	1.835713
C	2.812561	-2.189044	-0.210462
C	5.523707	-2.983829	-0.351271
C	3.174859	-3.382377	-0.859076
C	3.816457	-1.413497	0.392211
C	5.147733	-1.794498	0.311694
C	4.500036	-3.785382	-0.897907
H	2.406995	-3.993212	-1.321226
H	3.542543	-0.512743	0.930971
H	5.904634	-1.201316	0.814054
H	4.777020	-4.712914	-1.388514
N	6.824454	-3.468936	-0.402026
N	-2.539808	-5.652294	0.714993
N	0.166687	3.660775	-0.743951
C	-3.822202	-5.420574	0.824209
C	-6.692914	-5.169870	0.975003
C	-4.697842	-6.585209	0.872746
C	-4.465169	-4.118905	0.985775
C	-5.810003	-4.015407	1.084355
C	-6.045190	-6.477561	0.915733
H	-4.209190	-7.554689	0.858913
H	-3.840973	-3.237378	1.072021
H	-6.292590	-3.053982	1.231739
H	-6.662738	-7.366872	0.957371
C	7.862120	-2.704104	-0.620481
C	10.304720	-1.207764	-0.966479
C	9.174481	-3.322634	-0.473753
C	7.846065	-1.315974	-1.075511
C	8.997912	-0.632543	-1.261455
C	10.324001	-2.623501	-0.606731
H	9.181988	-4.381905	-0.235639
H	6.893161	-0.855077	-1.307189
H	8.994663	0.390223	-1.625890
H	11.281115	-3.118994	-0.495174
C	-1.039425	4.165957	-0.755152
C	-3.587409	5.516442	-0.692019
C	-1.142575	5.620219	-0.746621
C	-2.295363	3.426804	-0.859142
C	-3.483657	4.071952	-0.857359
C	-2.331001	6.262575	-0.687290
H	-0.205809	6.168398	-0.775898
H	-2.257074	2.351336	-0.985716
H	-4.419617	3.532003	-0.963380
H	-2.368079	7.345293	-0.692032
N	-7.978827	-4.930957	1.012890
N	11.339725	-0.423709	-1.120218
N	-4.794279	6.017868	-0.638283
C	-8.939774	-5.898570	0.756411
C	-11.048716	-7.731361	0.274127
C	-8.842464	-6.871148	-0.264398
C	-10.143456	-5.838348	1.490105
C	-11.161815	-6.753265	1.280297

C	-9.880124	-7.757214	-0.508589
H	-7.969123	-6.884433	-0.908025
H	-10.239771	-5.079239	2.259858
H	-12.059831	-6.712425	1.886623
H	-9.797666	-8.474001	-1.318224
C	12.626110	-0.776676	-0.729331
C	15.315446	-1.305543	-0.010506
C	12.940945	-1.434677	0.479369
C	13.696420	-0.346799	-1.540758
C	15.011341	-0.621334	-1.202420
C	14.258638	-1.693075	0.830583
H	12.144327	-1.715827	1.159971
H	13.466755	0.200218	-2.449881
H	15.817759	-0.293266	-1.848989
H	14.477188	-2.195945	1.766160
C	-5.037025	7.348755	-0.323402
C	-5.685813	10.045300	0.257105
C	-4.380413	8.049868	0.712266
C	-6.070941	8.014117	-1.013233
C	-6.364624	9.345058	-0.757483
C	-4.710060	9.363125	1.006034
H	-3.641759	7.535570	1.318320
H	-6.599684	7.478208	-1.794681
H	-7.128267	9.850678	-1.337769
H	-4.210498	9.875390	1.820855
N	-5.983802	11.394099	0.526238
N	16.653591	-1.575562	0.340855
N	-12.088924	-8.650289	0.040910
C	17.603107	-1.908461	-0.660284
C	19.486960	-2.572881	-2.631719
C	18.897735	-1.371498	-0.612029
C	17.259596	-2.782391	-1.702156
C	18.195004	-3.101576	-2.684087
C	19.832322	-1.711196	-1.587860
H	19.163085	-0.692561	0.191424
H	16.261279	-3.205761	-1.735564
H	17.915247	-3.779461	-3.485511
H	20.831635	-1.288158	-1.538050
H	20.215718	-2.829815	-3.394443
C	17.063874	-1.517318	1.699144
C	17.884911	-1.400410	4.379534
C	16.634613	-0.468800	2.525481
C	17.908893	-2.505522	2.223891
C	18.321314	-2.438634	3.553108
C	17.036891	-0.420081	3.858513
H	15.987730	0.300669	2.117322
H	18.238138	-3.318455	1.585325
H	18.976347	-3.210507	3.947044
H	16.696845	0.397434	4.487841
H	18.202497	-1.355267	5.416824
C	-7.311546	11.878425	0.385264
C	-9.931408	12.843067	0.111946
C	-7.549201	13.113435	-0.234357
C	-8.394458	11.130717	0.869258
C	-9.694820	11.609100	0.722516
C	-8.851364	13.592789	-0.360138
H	-6.711040	13.689924	-0.611412
H	-8.209719	10.179169	1.356676
H	-10.525052	11.019904	1.101345
H	-9.022058	14.551275	-0.841958
H	-10.945456	13.216348	0.006004
C	-4.956805	12.287350	0.931916
C	-2.938095	14.064625	1.729989
C	-3.699187	12.252883	0.311724

C	-5.196740	13.218077	1.952846
C	-4.194193	14.104865	2.339818
C	-2.697265	13.131453	0.718692
H	-3.513018	11.537590	-0.481920
H	-6.168333	13.241278	2.434949
H	-4.393337	14.821299	3.131721
H	-1.727272	13.094169	0.230964
H	-2.156732	14.752437	2.038692
C	-11.794107	-9.976187	-0.373260
C	-11.223347	-12.600151	-1.186031
C	-10.749372	-10.692053	0.229156
C	-12.552288	-10.584359	-1.383841
C	-12.270897	-11.890746	-1.778205
C	-10.463294	-11.991333	-0.184385
H	-10.168668	-10.225150	1.017690
H	-13.358140	-10.029223	-1.852192
H	-12.866064	-12.350330	-2.562130
H	-9.651439	-12.534815	0.290503
H	-11.002490	-13.615606	-1.500541
C	-13.444670	-8.259832	0.205492
C	-16.126642	-7.501194	0.522210
C	-14.351294	-9.117404	0.844518
C	-13.890549	-7.020747	-0.276072
C	-15.221371	-6.643901	-0.107800
C	-15.684421	-8.740281	0.991918
H	-14.004758	-10.074608	1.219632
H	-13.191122	-6.361085	-0.778755
H	-15.554020	-5.681136	-0.485150
H	-16.376889	-9.413900	1.488603
H	-17.164675	-7.207471	0.644969
C	-3.823671	9.312419	-2.900429
O	-3.047398	9.556059	-2.059845
O	-4.582924	9.074258	-3.755281

*A.4.8.11 Star-Shaped **OTPA-BZN-430**, **EB** State, with CO_2 Binding on Linker Unit, Branch 2*

H	-0.399258	-0.294726	1.088118
C	0.108931	0.302869	0.338948
C	1.495507	1.860409	-1.506746
C	1.124377	-0.281149	-0.436080
C	-0.240540	1.633323	0.161633
C	0.435888	2.441031	-0.779472
C	1.812980	0.518983	-1.364594
H	-0.997560	2.078013	0.797680
H	2.603651	0.081173	-1.964134
H	2.035774	2.479353	-2.215845
N	1.457542	-1.644871	-0.271461
C	0.435161	-2.595392	-0.046974
C	-1.625155	-4.477202	0.418378
C	0.619499	-3.644949	0.869533
C	-0.778068	-2.514800	-0.749927
C	-1.794377	-3.428365	-0.512770
C	-0.379547	-4.583988	1.071147
H	1.555197	-3.721368	1.412654
H	-0.914010	-1.732766	-1.489292
H	-2.710727	-3.371013	-1.090893
H	-0.231672	-5.400325	1.770791
C	2.809360	-2.054794	-0.317820
C	5.518130	-2.863110	-0.427357
C	3.170740	-3.261295	-0.942295
C	3.812933	-1.272394	0.276646
C	5.143028	-1.660237	0.211329

C	4.494380	-3.670358	-0.965504
H	2.403175	-3.877366	-1.397955
H	3.539514	-0.360849	0.797171
H	5.899246	-1.061075	0.707588
H	4.770470	-4.607841	-1.437354
N	6.816933	-3.354606	-0.461258
N	-2.566832	-5.472087	0.649157
N	0.193975	3.798136	-0.951863
C	-3.847651	-5.229317	0.753339
C	-6.716620	-4.955582	0.900019
C	-4.731546	-6.386572	0.823326
C	-4.481432	-3.920397	0.890562
C	-5.825489	-3.805562	0.987238
C	-6.078105	-6.268647	0.864817
H	-4.249804	-7.359595	0.827392
H	-3.851031	-3.041847	0.960374
H	-6.301189	-2.838133	1.116688
H	-6.701817	-7.152690	0.923241
C	7.859670	-2.598332	-0.685533
C	10.311740	-1.119680	-1.040757
C	9.168006	-3.220309	-0.519065
C	7.853343	-1.218192	-1.164394
C	9.009690	-0.543454	-1.354220
C	10.321763	-2.528992	-0.656279
H	9.168813	-4.275275	-0.262399
H	6.904272	-0.756920	-1.410596
H	9.013777	0.472864	-1.736247
H	11.275702	-3.026921	-0.529447
C	-1.010157	4.305014	-0.991441
C	-3.559414	5.664194	-1.048565
C	-1.112285	5.759247	-0.997257
C	-2.265442	3.567281	-1.109236
C	-3.451566	4.215699	-1.166899
C	-2.301528	6.404517	-0.994062
H	-0.174272	6.305897	-0.994080
H	-2.227608	2.488495	-1.202312
H	-4.384594	3.674165	-1.289089
H	-2.334058	7.487351	-1.006538
N	-8.000783	-4.706827	0.934466
N	11.351619	-0.343516	-1.201547
N	-4.766448	6.167159	-1.070380
C	-8.969107	-5.672155	0.697858
C	-11.092408	-7.498178	0.254179
C	-8.880302	-6.665543	-0.303504
C	-10.171498	-5.588331	1.431372
C	-11.197007	-6.499459	1.240798
C	-9.924902	-7.548457	-0.528947
H	-8.007872	-6.698265	-0.947670
H	-10.261212	-4.813389	2.185980
H	-12.094020	-6.439735	1.847048
H	-9.848801	-8.281821	-1.324231
C	12.633781	-0.696337	-0.796678
C	15.315838	-1.226908	-0.052414
C	12.937837	-1.333826	0.425677
C	13.711201	-0.287459	-1.609520
C	15.022570	-0.562997	-1.258393
C	14.252017	-1.593075	0.789351
H	12.135658	-1.598187	1.106487
H	13.489965	0.243960	-2.529910
H	15.834588	-0.251388	-1.906105
H	14.462297	-2.079987	1.735219
C	-5.039236	7.499910	-0.797711
C	-5.795136	10.182624	-0.280468
C	-4.423455	8.244973	0.233525

C	-6.077857	8.119793	-1.524066
C	-6.426163	9.440896	-1.297222
C	-4.805218	9.551682	0.494760
H	-3.693251	7.764367	0.874764
H	-6.574985	7.548703	-2.301711
H	-7.198383	9.908068	-1.898139
H	-4.344362	10.094163	1.312961
N	-6.160158	11.518488	-0.029847
N	16.650458	-1.498082	0.311556
N	-12.139806	-8.413635	0.040208
C	17.602987	-1.856630	-0.677762
C	19.492541	-2.571784	-2.625872
C	18.900861	-1.327210	-0.633222
C	17.259092	-2.748544	-1.704160
C	18.197410	-3.092993	-2.674705
C	19.838195	-1.692052	-1.597275
H	19.166550	-0.634390	0.158177
H	16.258174	-3.165961	-1.734545
H	17.917311	-3.784623	-3.464178
H	20.840004	-1.274604	-1.550497
H	20.223509	-2.848339	-3.379567
C	17.053676	-1.415932	1.670670
C	17.860694	-1.251843	4.352894
C	16.625660	-0.349412	2.474328
C	17.890342	-2.398406	2.219073
C	18.295871	-2.308135	3.549028
C	17.020920	-0.277192	3.808393
H	15.985255	0.415539	2.047870
H	18.218549	-3.225294	1.598143
H	18.944459	-3.075821	3.961383
H	16.681931	0.554106	4.419991
H	18.172856	-1.188437	5.390875
C	-7.506366	11.940411	-0.195921
C	-10.161282	12.787115	-0.516140
C	-7.787904	13.163420	-0.820943
C	-8.563023	11.145288	0.270162
C	-9.880651	11.565246	0.100058
C	-9.107687	13.584148	-0.970222
H	-6.969665	13.776475	-1.183861
H	-8.344724	10.203243	0.762044
H	-10.690296	10.939853	0.465167
H	-9.312479	14.533883	-1.456066
H	-11.188973	13.114680	-0.640323
C	-5.188428	12.457856	0.405880
C	-3.276713	14.324414	1.261907
C	-3.918434	12.492947	-0.188032
C	-5.494939	13.365475	1.429711
C	-4.545445	14.296459	1.845666
C	-2.969029	13.415150	0.246895
H	-3.684169	11.797047	-0.986677
H	-6.476205	13.335754	1.891394
H	-4.795792	14.994155	2.639726
H	-1.989105	13.431904	-0.221596
H	-2.536863	15.046743	1.593134
C	-11.855296	-9.749691	-0.347782
C	-11.304674	-12.393329	-1.108910
C	-10.816363	-10.461726	0.269012
C	-12.617882	-10.371555	-1.346631
C	-12.346494	-11.687525	-1.715326
C	-10.540270	-11.771030	-0.118924
H	-10.232296	-9.983987	1.048529
H	-13.419275	-9.819409	-1.826046
H	-12.944940	-12.157691	-2.490429
H	-9.732834	-12.311445	0.366874

H	-11.091605	-13.416411	-1.403439
C	-13.492418	-8.009679	0.197509
C	-16.168472	-7.224613	0.500022
C	-14.405408	-8.847860	0.853009
C	-13.928985	-6.776664	-0.307634
C	-15.256835	-6.386503	-0.146402
C	-15.735570	-8.457800	0.993343
H	-14.066102	-9.800318	1.246364
H	-13.224717	-6.132102	-0.822981
H	-15.582209	-5.428624	-0.542089
H	-16.433007	-9.116480	1.502942
H	-17.204194	-6.920657	0.617277
C	-2.418859	4.860420	2.171752
O	-3.391580	5.508065	2.159547
O	-1.446440	4.212391	2.194043

*A.4.8.12 Star-Shaped **OTPA-BZN-430**, **EB** State, with CO_2 Binding on Inner Imine Nitrogen Atom, Branch 3*

H	-0.435331	0.120404	1.100206
C	0.079462	0.699103	0.340812
C	1.480519	2.207916	-1.534592
C	1.087779	0.090297	-0.424474
C	-0.254072	2.030210	0.140029
C	0.428948	2.814167	-0.816291
C	1.783646	0.865959	-1.368208
H	-1.011102	2.491824	0.765381
H	2.568589	0.408638	-1.960676
H	2.026233	2.807764	-2.255807
N	1.404750	-1.273896	-0.235267
C	0.368784	-2.207752	-0.000187
C	-1.712418	-4.059484	0.479656
C	0.531937	-3.237730	0.941848
C	-0.835488	-2.129090	-0.717588
C	-1.862515	-3.029118	-0.473409
C	-0.477958	-4.162914	1.151926
H	1.460499	-3.310877	1.497504
H	-0.955960	-1.360909	-1.473943
H	-2.772835	-2.975472	-1.061408
H	-0.344227	-4.964049	1.871025
C	2.750548	-1.702685	-0.272600
C	5.448389	-2.550192	-0.363408
C	3.094878	-2.930612	-0.864542
C	3.765669	-0.918309	0.299563
C	5.090276	-1.325610	0.243056
C	4.412858	-3.357801	-0.878074
H	2.318675	-3.548988	-1.302011
H	3.505569	0.010261	0.796246
H	5.855063	-0.723598	0.722460
H	4.675361	-4.311486	-1.324527
N	6.740324	-3.059862	-0.385786
N	-2.669693	-5.041417	0.711738
N	0.203243	4.170819	-1.012096
C	-3.946768	-4.775887	0.814589
C	-6.807343	-4.430583	0.945334
C	-4.857272	-5.912233	0.885852
C	-4.548078	-3.451339	0.946840
C	-5.889284	-3.302660	1.035984
C	-6.200583	-5.758418	0.920014
H	-4.402634	-6.896835	0.899308
H	-3.896091	-2.588777	1.016406

H	-6.341197	-2.323180	1.159661
H	-6.846175	-6.626532	0.980689
C	7.793183	-2.323536	-0.628766
C	10.264999	-0.886767	-1.017586
C	9.092966	-2.958753	-0.446460
C	7.805620	-0.955803	-1.141785
C	8.970999	-0.301301	-1.346786
C	10.255969	-2.286419	-0.599356
H	9.079517	-4.007049	-0.164132
H	6.862996	-0.488326	-1.400703
H	8.988932	0.705130	-1.753774
H	11.203090	-2.793806	-0.459590
C	-0.995131	4.694010	-1.041590
C	-3.523001	6.084616	-1.014212
C	-1.076323	6.149165	-1.073153
C	-2.261953	3.972063	-1.128494
C	-3.440311	4.635526	-1.145053
C	-2.255527	6.810057	-1.031540
H	-0.131507	6.682305	-1.116461
H	-2.240170	2.893144	-1.226559
H	-4.384325	4.107187	-1.237152
H	-2.275936	7.892993	-1.061064
N	-8.085443	-4.150039	0.967617
N	11.315136	-0.128264	-1.195335
N	-4.723914	6.601956	-0.965665
C	-9.075136	-5.090292	0.722306
C	-11.239631	-6.863157	0.261034
C	-8.998256	-6.093761	-0.270335
C	-10.286142	-4.968237	1.436479
C	-11.332388	-5.853364	1.237924
C	-10.062252	-6.950378	-0.504446
H	-8.118235	-6.154177	-0.901977
H	-10.366259	-4.185071	2.183590
H	-12.236187	-5.764898	1.830335
H	-9.994195	-7.691365	-1.293301
C	12.592225	-0.487955	-0.780481
C	15.266737	-1.034462	-0.020392
C	12.886993	-1.101035	0.456560
C	13.675629	-0.111402	-1.600955
C	14.983099	-0.394837	-1.241675
C	14.197462	-1.368215	0.827900
H	12.080883	-1.339862	1.142146
H	13.462092	0.401393	-2.533639
H	15.799626	-0.108164	-1.895200
H	14.400578	-1.835989	1.784930
C	-4.964739	7.936906	-0.673336
C	-5.662931	10.624367	-0.098380
C	-4.275927	8.674481	0.316055
C	-6.043821	8.568384	-1.327308
C	-6.365729	9.891307	-1.073392
C	-4.627823	9.983466	0.606375
H	-3.501836	8.189500	0.901532
H	-6.596148	8.004102	-2.071979
H	-7.172640	10.366604	-1.619938
H	-4.107763	10.519757	1.392495
N	-6.000219	11.961839	0.181332
N	16.597557	-1.313615	0.351539
N	-12.306739	-7.752411	0.038903
C	17.546612	-1.705907	-0.628314
C	19.428977	-2.487384	-2.557770
C	18.850396	-1.190392	-0.594941
C	17.193147	-2.617375	-1.634064
C	18.128028	-2.994836	-2.595607
C	19.784071	-1.588076	-1.549517

H	19.123486	-0.482501	0.180439
H	16.187524	-3.023898	-1.655607
H	17.840517	-3.701312	-3.369106
H	20.790541	-1.181075	-1.511603
H	20.157168	-2.789584	-3.304273
C	17.000483	-1.205575	1.708879
C	17.807217	-0.990688	4.387673
C	16.583529	-0.116850	2.488246
C	17.826001	-2.184631	2.279874
C	18.231476	-2.069242	3.607894
C	16.978537	-0.019321	3.820777
H	15.951858	0.645407	2.044304
H	18.145693	-3.028629	1.677817
H	18.871342	-2.834597	4.037841
H	16.648163	0.829017	4.413406
H	18.119242	-0.907613	5.424305
C	-7.351600	12.393629	0.113241
C	-10.016661	13.260336	-0.012942
C	-7.667568	13.624887	-0.478416
C	-8.379017	11.600331	0.643581
C	-9.702292	12.030290	0.569784
C	-8.991563	14.055434	-0.531085
H	-6.872440	14.236735	-0.891254
H	-8.133845	10.651902	1.109832
H	-10.488901	11.406108	0.984033
H	-9.222931	15.011541	-0.991869
H	-11.048185	13.595620	-0.061934
C	-4.992647	12.892106	0.550553
C	-3.009340	14.739054	1.275752
C	-3.769426	12.922152	-0.134645
C	-5.216569	13.794862	1.599694
C	-4.232098	14.716235	1.950746
C	-2.783736	13.834631	0.235196
H	-3.599664	12.229934	-0.952604
H	-6.161635	13.769035	2.131790
H	-4.418282	15.410303	2.765359
H	-1.840640	13.847534	-0.303698
H	-2.241753	15.453826	1.556389
C	-12.052322	-9.096568	-0.342974
C	-11.562761	-11.755418	-1.091366
C	-11.040608	-9.834239	0.288601
C	-12.818705	-9.700173	-1.349955
C	-12.577745	-11.023767	-1.712488
C	-10.794546	-11.151355	-0.093073
H	-10.454047	-9.370293	1.074550
H	-13.599091	-9.128014	-1.840444
H	-13.178677	-11.479846	-2.494038
H	-10.007994	-11.711878	0.404030
H	-11.373279	-12.784516	-1.381007
C	-13.650912	-7.315733	0.182831
C	-16.310089	-6.467209	0.458137
C	-14.588272	-8.128662	0.835527
C	-14.054338	-6.076172	-0.333506
C	-15.374074	-5.654389	-0.185743
C	-15.910138	-7.707054	0.962451
H	-14.274270	-9.086295	1.237235
H	-13.331051	-5.451447	-0.846947
H	-15.673966	-4.691759	-0.589897
H	-16.626898	-8.346237	1.470032
H	-17.339399	-6.138606	0.564857
C	-1.460950	-7.617994	0.305961
O	-0.592785	-7.097620	-0.278012
O	-2.296988	-8.203038	0.878947

*A.4.8.13 Star-Shaped **OTPA-BZN-430**, **EB** State, with CO_2 Binding on Outer Imine Nitrogen Atom, Branch 3*

H	-0.190229	-0.050652	1.101087
C	0.326879	0.521215	0.338083
C	1.734531	2.011572	-1.547372
C	1.323002	-0.099974	-0.432907
C	0.007771	1.856005	0.137707
C	0.694199	2.630550	-0.823720
C	2.022810	0.666266	-1.381152
H	-0.740353	2.327227	0.766605
H	2.799007	0.198927	-1.977359
H	2.283105	2.604330	-2.272266
N	1.625816	-1.468103	-0.244892
C	0.581891	-2.391532	-0.010501
C	-1.523518	-4.217846	0.474352
C	0.741514	-3.436858	0.915767
C	-0.629820	-2.288276	-0.713597
C	-1.667682	-3.174309	-0.467168
C	-0.279894	-4.349164	1.126819
H	1.675442	-3.531025	1.459085
H	-0.747094	-1.510819	-1.460884
H	-2.582292	-3.100678	-1.046127
H	-0.151513	-5.162083	1.834209
C	2.968848	-1.907062	-0.282294
C	5.660690	-2.771725	-0.374683
C	3.306342	-3.130513	-0.886766
C	3.987356	-1.135364	0.300497
C	5.309389	-1.551111	0.243492
C	4.621465	-3.566671	-0.901300
H	2.527076	-3.738170	-1.333777
H	3.731889	-0.209943	0.805436
H	6.077113	-0.959189	0.730699
H	4.878974	-4.517092	-1.357509
N	6.949387	-3.289871	-0.397924
N	-2.488960	-5.186213	0.716744
N	0.482281	3.989456	-1.020279
C	-3.764426	-4.912017	0.809778
C	-6.625726	-4.567794	0.923621
C	-4.675492	-6.047052	0.889558
C	-4.368478	-3.587326	0.925158
C	-5.710091	-3.436773	1.006622
C	-6.019050	-5.896248	0.915943
H	-4.217531	-7.031210	0.911888
H	-3.717786	-2.723418	0.992224
H	-6.160558	-2.456849	1.122609
H	-6.664999	-6.763720	0.979667
C	8.007365	-2.558642	-0.633399
C	10.488927	-1.135080	-1.007646
C	9.302754	-3.203574	-0.453478
C	8.029370	-1.187149	-1.136072
C	9.199274	-0.538769	-1.334476
C	10.470261	-2.537658	-0.599607
H	9.282071	-4.253813	-0.178979
H	7.090122	-0.711564	-1.392497
H	9.224413	0.470615	-1.733683
H	11.413865	-3.052185	-0.462177
C	-0.710739	4.524579	-1.048510
C	-3.224575	5.940557	-1.023554
C	-0.777412	5.980447	-1.083811
C	-1.984881	3.815005	-1.131052

C	-3.156513	4.490183	-1.148632
C	-1.949888	6.653211	-1.043733
H	0.172649	6.503954	-1.129453
H	-1.974079	2.735537	-1.224753
H	-4.105888	3.970976	-1.237355
H	-1.959417	7.736185	-1.076839
N	-7.906130	-4.296491	0.935004
N	11.544192	-0.382100	-1.178225
N	-4.420217	6.470112	-0.977219
C	-8.886831	-5.251442	0.698762
C	-11.027530	-7.049880	0.237987
C	-8.803070	-6.242172	-0.304004
C	-10.089497	-5.157150	1.428939
C	-11.124258	-6.055403	1.229581
C	-9.856587	-7.112557	-0.538287
H	-7.926470	-6.282922	-0.942106
H	-10.175198	-4.386228	2.187671
H	-12.023250	-5.987922	1.832022
H	-9.784558	-7.844274	-1.335421
C	12.818136	-0.752743	-0.763555
C	15.487652	-1.321960	-0.002558
C	13.106607	-1.376952	0.469421
C	13.905503	-0.376765	-1.579061
C	15.210411	-0.671334	-1.219553
C	14.414598	-1.655150	0.841257
H	12.297696	-1.615614	1.151748
H	13.697037	0.144447	-2.508216
H	16.029979	-0.384933	-1.869363
H	14.612855	-2.131281	1.795166
C	-4.647624	7.808679	-0.690919
C	-5.317775	10.506133	-0.129737
C	-3.951419	8.543909	0.295047
C	-5.720087	8.447986	-1.348159
C	-6.028165	9.775464	-1.101074
C	-4.289680	9.857918	0.578668
H	-3.182651	8.053772	0.883238
H	-6.278120	7.885715	-2.090090
H	-6.829944	10.256379	-1.650239
H	-3.764273	10.392661	1.362277
N	-5.640713	11.848527	0.142790
N	16.815810	-1.612399	0.369712
N	-12.087110	-7.949057	0.013402
C	17.764819	-2.001718	-0.611443
C	19.647106	-2.777618	-2.543117
C	19.071335	-1.493743	-0.570879
C	17.408531	-2.902847	-1.625458
C	18.343460	-3.277517	-2.588049
C	20.004937	-1.888686	-1.526666
H	19.346569	-0.793846	0.210975
H	16.400730	-3.303611	-1.652535
H	18.053801	-3.975965	-3.368007
H	21.013565	-1.487637	-1.483166
H	20.375289	-3.077674	-3.290491
C	17.216525	-1.518889	1.728844
C	18.019130	-1.332689	4.410941
C	16.805458	-0.434054	2.516683
C	18.034099	-2.508509	2.292963
C	18.437593	-2.407388	3.622753
C	17.198349	-0.350750	3.850805
H	16.180012	0.336353	2.078026
H	18.349221	-3.349443	1.684242
H	19.071295	-3.180798	4.047372
H	16.872614	0.494707	4.450073
H	18.329568	-1.260714	5.448879

C	-6.987141	12.294947	0.070387
C	-9.642181	13.190461	-0.064485
C	-7.288603	13.526080	-0.529012
C	-8.023952	11.516311	0.604127
C	-9.342268	11.960513	0.526018
C	-8.607658	13.971003	-0.586010
H	-6.486190	14.126553	-0.944450
H	-7.789907	10.568034	1.076376
H	-10.136298	11.347624	0.942959
H	-8.827792	14.926846	-1.052802
H	-10.669846	13.536899	-0.116844
C	-4.623395	12.769814	0.507883
C	-2.620919	14.599172	1.224811
C	-3.399401	12.783010	-0.176455
C	-4.838453	13.680574	1.551935
C	-3.844397	14.593179	1.898862
C	-2.404232	13.686799	0.189319
H	-3.236457	12.084663	-0.990581
H	-5.784181	13.667798	2.083328
H	-4.023747	15.293614	2.709547
H	-1.460633	13.686663	-0.348844
H	-1.845905	15.307142	1.502260
C	-11.819469	-9.287682	-0.377178
C	-11.300850	-11.936533	-1.143202
C	-10.795822	-10.016817	0.245261
C	-12.582797	-9.895124	-1.384342
C	-12.327433	-11.213631	-1.755433
C	-10.535482	-11.328622	-0.145047
H	-10.211133	-9.550159	1.031008
H	-13.372186	-9.329882	-1.868366
H	-12.926316	-11.672425	-2.536994
H	-9.739767	-11.882226	0.345232
H	-11.100203	-12.961585	-1.439604
C	-13.434252	-7.522877	0.157395
C	-16.099604	-6.692952	0.434878
C	-14.369300	-8.349186	0.796786
C	-13.843410	-6.278971	-0.344205
C	-15.166012	-5.866738	-0.195337
C	-15.693979	-7.936810	0.924587
H	-14.051314	-9.310002	1.187610
H	-13.122174	-5.643028	-0.846600
H	-15.469864	-4.900568	-0.587964
H	-16.408583	-8.586557	1.421741
H	-17.131125	-6.371609	0.542458
C	-9.106846	-1.698729	0.703177
O	-9.951723	-2.169631	0.047401
O	-8.293100	-1.163388	1.351841

*A.4.8.14 Star-Shaped **OTPA-BZN-430**, **EB** State, with CO_2 Binding on Inner Core Unit, Branch 3*

H	-0.403990	-0.179352	0.760618
C	0.120287	0.436182	0.038331
C	1.541476	2.040009	-1.743431
C	1.147870	-0.127548	-0.735883
C	-0.221033	1.772315	-0.110209
C	0.471208	2.603969	-1.018396
C	1.853892	0.694495	-1.631224
H	-0.993564	2.199121	0.520973
H	2.653697	0.270430	-2.228640
H	2.094383	2.676342	-2.426942

N	1.475717	-1.496632	-0.602824
C	0.446230	-2.447508	-0.420384
C	-1.646700	-4.303854	-0.009954
C	0.604989	-3.514455	0.480177
C	-0.753011	-2.343494	-1.143359
C	-1.785717	-3.244723	-0.933194
C	-0.409188	-4.443970	0.652473
H	1.530749	-3.611127	1.036818
H	-0.868260	-1.547348	-1.870947
H	-2.696158	-3.163186	-1.517741
H	-0.285876	-5.269011	1.346117
C	2.827638	-1.907370	-0.621082
C	5.537498	-2.718355	-0.673022
C	3.204459	-3.101546	-1.260039
C	3.815622	-1.139125	0.016422
C	5.146409	-1.528207	-0.020171
C	4.527750	-3.512417	-1.255543
H	2.448809	-3.706722	-1.749099
H	3.529229	-0.237978	0.547932
H	5.889359	-0.940932	0.509201
H	4.815475	-4.440561	-1.738760
N	6.836015	-3.211568	-0.681010
N	-2.619701	-5.268771	0.222570
N	0.235638	3.965819	-1.159630
C	-3.885311	-4.974435	0.367982
C	-6.732490	-4.588361	0.652156
C	-4.811111	-6.095344	0.477842
C	-4.462611	-3.640582	0.520282
C	-5.794528	-3.473581	0.684729
C	-6.148071	-5.925005	0.587416
H	-4.367938	-7.086337	0.463690
H	-3.803236	-2.781118	0.536525
H	-6.225360	-2.486941	0.825493
H	-6.801361	-6.784267	0.681227
C	7.885862	-2.452121	-0.856676
C	10.348445	-0.968035	-1.097033
C	9.187953	-3.079691	-0.664533
C	7.895511	-1.061454	-1.303845
C	9.057648	-0.383664	-1.440178
C	10.345776	-2.386454	-0.747758
H	9.180255	-4.140586	-0.433740
H	6.955099	-0.593619	-1.570083
H	9.074483	0.641338	-1.797890
H	11.295006	-2.888468	-0.602894
C	-0.966850	4.479322	-1.189054
C	-3.507294	5.847042	-1.154452
C	-1.060653	5.933907	-1.163243
C	-2.225419	3.750961	-1.327944
C	-3.409153	4.404844	-1.340047
C	-2.246238	6.582966	-1.118247
H	-0.119999	6.476131	-1.167229
H	-2.192341	2.676982	-1.467925
H	-4.346539	3.872713	-1.470464
H	-2.275699	7.666019	-1.105066
N	-8.002191	-4.288387	0.753180
N	11.392707	-0.188072	-1.202272
N	-4.713429	6.352312	-1.109993
C	-9.019954	-5.212942	0.570798
C	-11.236805	-6.951287	0.247661
C	-9.021942	-6.216181	-0.424966
C	-10.180960	-5.072969	1.360628
C	-11.251395	-5.941439	1.228783
C	-10.111978	-7.055847	-0.591201
H	-8.185123	-6.289300	-1.111610

H	-10.201219	-4.289609	2.111527
H	-12.114215	-5.839549	1.877442
H	-10.105795	-7.796730	-1.383048
C	12.660048	-0.549460	-0.760552
C	15.315460	-1.093055	0.066957
C	12.921735	-1.221505	0.453213
C	13.765259	-0.113636	-1.520456
C	15.063911	-0.395003	-1.129234
C	14.222603	-1.487264	0.857514
H	12.096412	-1.507701	1.096469
H	13.576042	0.444090	-2.432358
H	15.897781	-0.061510	-1.737005
H	14.399653	-2.000892	1.796005
C	-4.971981	7.673386	-0.772920
C	-5.704846	10.332145	-0.113856
C	-4.309940	8.379119	0.257070
C	-6.042955	8.320100	-1.425243
C	-6.381369	9.630155	-1.129443
C	-4.678951	9.673683	0.588140
H	-3.543696	7.878889	0.840028
H	-6.575104	7.779380	-2.201433
H	-7.181086	10.118967	-1.674654
H	-4.179569	10.184571	1.404030
N	-6.059299	11.655769	0.207658
N	16.636633	-1.369874	0.472391
N	-12.329842	-7.823154	0.093578
C	17.629660	-1.686540	-0.491278
C	19.599122	-2.318330	-2.388169
C	18.919101	-1.146663	-0.379649
C	17.334400	-2.547004	-1.558784
C	18.312450	-2.849936	-2.503625
C	19.896164	-1.470179	-1.318672
H	19.147006	-0.477998	0.443671
H	16.339850	-2.972574	-1.641092
H	18.069931	-3.517483	-3.325584
H	20.890928	-1.045022	-1.219947
H	20.361022	-2.562637	-3.122116
C	16.988047	-1.331946	1.847846
C	17.694016	-1.255544	4.562230
C	16.524265	-0.295351	2.670555
C	17.809683	-2.328552	2.393408
C	18.165047	-2.281782	3.739852
C	16.869316	-0.266790	4.020117
H	15.895679	0.480744	2.246660
H	18.165658	-3.132164	1.757387
H	18.802493	-3.059973	4.149873
H	16.502999	0.541625	4.646448
H	17.967045	-1.226060	5.612686
C	-7.412845	12.078738	0.127742
C	-10.082392	12.927788	-0.020954
C	-7.727894	13.327609	-0.426261
C	-8.443474	11.258811	0.609053
C	-9.768773	11.680398	0.524082
C	-9.054332	13.749035	-0.490167
H	-6.930155	13.960098	-0.801231
H	-8.199164	10.296404	1.046218
H	-10.557876	11.035557	0.900185
H	-9.284999	14.718977	-0.921444
H	-11.115656	13.256252	-0.078684
C	-5.067869	12.579786	0.631982
C	-3.116524	14.414687	1.466445
C	-3.830618	12.644488	-0.025089
C	-5.321851	13.441851	1.708171
C	-4.353111	14.357539	2.113632

C	-2.860976	13.550614	0.398864
H	-3.637461	11.983898	-0.863742
H	-6.277737	13.389102	2.218499
H	-4.562602	15.019882	2.948739
H	-1.906765	13.590624	-0.118716
H	-2.361315	15.124785	1.789350
C	-12.122206	-9.170215	-0.306009
C	-11.725195	-11.834593	-1.088635
C	-11.084453	-9.925926	0.258369
C	-12.961151	-9.758502	-1.262933
C	-12.765675	-11.084854	-1.642322
C	-10.884940	-11.245835	-0.140487
H	-10.441411	-9.473686	1.006034
H	-13.761728	-9.172332	-1.701591
H	-13.422740	-11.528951	-2.384607
H	-10.077573	-11.820467	0.304390
H	-11.571537	-12.865849	-1.391507
C	-13.654918	-7.365912	0.324835
C	-16.276861	-6.476558	0.773334
C	-14.560364	-8.165315	1.036565
C	-14.071693	-6.119444	-0.163463
C	-15.372231	-5.677374	0.070255
C	-15.864384	-7.723345	1.249670
H	-14.235843	-9.128411	1.416272
H	-13.373654	-5.505241	-0.722526
H	-15.682719	-4.709547	-0.312940
H	-16.556513	-8.352099	1.802446
H	-17.291755	-6.132148	0.947199
C	-2.021475	-2.623878	2.735685
O	-1.864098	-1.603290	2.186867
O	-2.193697	-3.635668	3.293079

*A.4.8.15 Star-Shaped **OTPA-BZN-430**, **EB** State, with CO_2 Binding on Outer Core Unit, Branch 3*

H	-0.230304	0.135399	0.971402
C	0.316400	0.702094	0.225346
C	1.800577	2.174448	-1.614977
C	1.295951	0.058393	-0.548405
C	0.051618	2.052222	0.049825
C	0.777905	2.818969	-0.888331
C	2.034599	0.815876	-1.473998
H	-0.683744	2.539387	0.681588
H	2.798387	0.330841	-2.072093
H	2.379472	2.760092	-2.321872
N	1.545115	-1.323554	-0.384971
C	0.465330	-2.212091	-0.179120
C	-1.709033	-3.971211	0.246450
C	0.577212	-3.280923	0.727023
C	-0.734615	-2.050329	-0.891132
C	-1.806186	-2.903406	-0.673375
C	-0.478279	-4.160261	0.908742
H	1.501298	-3.419927	1.277511
H	-0.816349	-1.253670	-1.622766
H	-2.711871	-2.784555	-1.258885
H	-0.386111	-4.991705	1.600063
C	2.871471	-1.811191	-0.416056
C	5.530455	-2.773492	-0.493789
C	3.171202	-3.033959	-1.041428
C	3.910365	-1.089611	0.194278
C	5.216714	-1.553066	0.144598

C	4.469402	-3.518438	-1.049161
H	2.375701	-3.603177	-1.509943
H	3.682928	-0.165514	0.714804
H	5.999637	-0.999914	0.652750
H	4.697297	-4.468406	-1.521749
N	6.799546	-3.338359	-0.510815
N	-2.711084	-4.910092	0.456249
N	0.622886	4.189009	-1.058113
C	-3.975977	-4.592077	0.549231
C	-6.823353	-4.146222	0.665443
C	-4.929019	-5.694639	0.592915
C	-4.530612	-3.248480	0.697315
C	-5.865980	-3.052932	0.779839
C	-6.266370	-5.496384	0.617694
H	-4.507064	-6.695063	0.589765
H	-3.848633	-2.411244	0.787341
H	-6.283743	-2.060370	0.918518
H	-6.943538	-6.341051	0.659174
C	7.886135	-2.641653	-0.719182
C	10.421220	-1.300351	-1.033187
C	9.155321	-3.335211	-0.533346
C	7.963570	-1.263319	-1.197040
C	9.158249	-0.653429	-1.367772
C	10.347459	-2.708386	-0.650921
H	9.094020	-4.388729	-0.278196
H	7.045351	-0.750573	-1.457951
H	9.224740	0.361071	-1.748832
H	11.270343	-3.258227	-0.509461
C	-0.546459	4.774210	-1.083205
C	-2.998555	6.294654	-1.045790
C	-0.551463	6.232014	-1.089292
C	-1.848792	4.121071	-1.188567
C	-2.990816	4.845422	-1.199852
C	-1.694774	6.952847	-1.043278
H	0.420027	6.715921	-1.118116
H	-1.882969	3.044250	-1.304582
H	-3.960441	4.368430	-1.305628
H	-1.658263	8.035693	-1.054494
N	-8.090931	-3.824673	0.690626
N	11.504497	-0.581937	-1.174684
N	-4.170961	6.873625	-0.996644
C	-9.099500	-4.742902	0.427968
C	-11.264398	-6.510239	-0.039689
C	-9.055604	-5.687926	-0.620960
C	-10.282419	-4.663713	1.190768
C	-11.327937	-5.552223	0.989255
C	-10.121531	-6.540346	-0.859027
H	-8.193824	-5.712158	-1.279884
H	-10.338170	-3.925169	1.983781
H	-12.205846	-5.505895	1.623802
H	-10.077006	-7.242292	-1.684384
C	12.758201	-1.004117	-0.747740
C	15.394180	-1.678709	0.043350
C	13.005546	-1.659081	0.478209
C	13.870548	-0.652416	-1.540042
C	15.158700	-0.998324	-1.166121
C	14.297160	-1.988937	0.864788
H	12.178283	-1.880971	1.144003
H	13.694825	-0.108431	-2.462895
H	15.997795	-0.729563	-1.798302
H	14.463895	-2.487911	1.813041
C	-4.343397	8.215012	-0.685993
C	-4.901815	10.927857	-0.078576
C	-3.624017	8.901201	0.318495

C	-5.382517	8.911848	-1.338269
C	-5.635512	10.246466	-1.068204
C	-3.907899	10.223052	0.624536
H	-2.881403	8.367703	0.902528
H	-5.958417	8.387845	-2.094428
H	-6.411907	10.771438	-1.613479
H	-3.366045	10.720075	1.421672
N	-5.169169	12.277642	0.216814
N	16.705655	-2.021019	0.430496
N	-12.324510	-7.410709	-0.253843
C	17.655834	-2.425460	-0.543466
C	19.539610	-3.231414	-2.461207
C	18.977172	-1.960467	-0.476815
C	17.285308	-3.298656	-1.576602
C	18.221387	-3.688244	-2.532133
C	19.911215	-2.370381	-1.425854
H	19.263380	-1.281909	0.319774
H	16.265611	-3.666090	-1.623952
H	17.920680	-4.364704	-3.327143
H	20.931427	-2.002727	-1.362139
H	20.268404	-3.543121	-3.203198
C	17.089007	-1.962545	1.796501
C	17.858072	-1.845837	4.492444
C	16.700323	-0.878629	2.596911
C	17.867380	-2.986323	2.355164
C	18.254480	-2.919830	3.691983
C	17.076185	-0.829741	3.937622
H	16.105512	-0.081868	2.162783
H	18.165238	-3.826459	1.736738
H	18.857788	-3.719526	4.112162
H	16.768054	0.015443	4.546513
H	18.155510	-1.800756	5.535691
C	-6.494986	12.782049	0.143653
C	-9.108791	13.791234	0.007409
C	-6.740093	14.034180	-0.437586
C	-7.567275	12.039611	0.658485
C	-8.865094	12.540462	0.579759
C	-8.038773	14.535431	-0.495299
H	-5.910239	14.606576	-0.838504
H	-7.376610	11.074822	1.116598
H	-9.687086	11.955221	0.981968
H	-8.215239	15.507003	-0.947939
H	-10.120523	14.181689	-0.045520
C	-4.116465	13.148164	0.605094
C	-2.043718	14.878163	1.367894
C	-2.887217	13.120060	-0.069377
C	-4.301166	14.050192	1.662504
C	-3.272004	14.913607	2.032222
C	-1.857473	13.974273	0.319129
H	-2.747292	12.428821	-0.893777
H	-5.250985	14.069326	2.186357
H	-3.428137	15.607784	2.853031
H	-0.910234	13.942449	-0.211647
H	-1.241543	15.547665	1.663065
C	-12.060808	-8.736774	-0.689033
C	-11.555495	-11.360505	-1.544248
C	-10.998682	-9.467803	-0.136900
C	-12.868280	-9.328637	-1.670732
C	-12.619270	-10.635118	-2.085974
C	-10.746373	-10.767098	-0.572256
H	-10.376239	-9.014084	0.626527
H	-13.686909	-8.761067	-2.100472
H	-13.252731	-11.082002	-2.846929
H	-9.920233	-11.322488	-0.137316

H	-11.359834	-12.375982	-1.875052
C	-13.667320	-7.007128	-0.027497
C	-16.322781	-6.218163	0.414429
C	-14.557676	-7.862173	0.637246
C	-14.116299	-5.755246	-0.471636
C	-15.433389	-5.363431	-0.241181
C	-15.878059	-7.469854	0.846824
H	-14.208786	-8.829406	0.983303
H	-13.429655	-5.097355	-0.993976
H	-15.768480	-4.390763	-0.589880
H	-16.557991	-8.141711	1.362850
H	-17.350521	-5.912728	0.585624
C	-9.164095	-7.076402	2.988215
O	-9.589791	-6.448449	3.876140
O	-8.727247	-7.719122	2.113768

*A.4.8.16 Star-Shaped **OTPA-BZN-430**, **EB** State, with CO_2 Binding on Linker Unit, Branch 3*

H	-0.308759	0.044262	1.213652
C	0.206820	0.609969	0.445082
C	1.610562	2.085346	-1.454732
C	1.201702	-0.017548	-0.322728
C	-0.113104	1.942835	0.234468
C	0.571105	2.709966	-0.734583
C	1.899582	0.741550	-1.278306
H	-0.860143	2.418818	0.861071
H	2.674661	0.269904	-1.872535
H	2.157610	2.672312	-2.185486
N	1.503674	-1.384010	-0.124854
C	0.459060	-2.303500	0.125526
C	-1.646561	-4.120613	0.641185
C	0.620676	-3.335548	1.065831
C	-0.754188	-2.209474	-0.575496
C	-1.793217	-3.090372	-0.314475
C	-0.401183	-4.243790	1.292172
H	1.556280	-3.423179	1.607462
H	-0.873139	-1.442309	-1.333191
H	-2.705946	-3.021106	-0.895591
H	-0.271643	-5.047162	2.010208
C	2.844585	-1.827911	-0.169543
C	5.532099	-2.704817	-0.275804
C	3.171843	-3.059893	-0.762325
C	3.871502	-1.053832	0.395247
C	5.191264	-1.475710	0.331240
C	4.485021	-3.501623	-0.783555
H	2.386129	-3.669637	-1.194959
H	3.624457	-0.121678	0.891915
H	5.965724	-0.881381	0.804685
H	4.734430	-4.458462	-1.230771
N	6.818661	-3.228296	-0.304500
N	-2.610212	-5.086021	0.903163
N	0.358020	4.066763	-0.942589
C	-3.885805	-4.815527	1.005657
C	-6.748263	-4.480864	1.149409
C	-4.791791	-5.951683	1.120549
C	-4.493986	-3.490382	1.100591
C	-5.835780	-3.346113	1.201695
C	-6.135376	-5.805908	1.161881
H	-4.328976	-6.933127	1.156684
H	-3.847221	-2.621728	1.130962
H	-6.291407	-2.365189	1.297477
H	-6.777295	-6.674443	1.248857

C	7.877049	-2.503896	-0.558295
C	10.360381	-1.093857	-0.970673
C	9.171709	-3.151670	-0.383019
C	7.899568	-1.138235	-1.076717
C	9.069971	-0.496444	-1.292674
C	10.340263	-2.491877	-0.547223
H	9.149604	-4.198685	-0.096553
H	6.959792	-0.662104	-1.330162
H	9.095227	0.508330	-1.703344
H	11.283202	-3.008368	-0.412668
C	-0.835316	4.601495	-0.970161
C	-3.349204	6.017350	-0.945186
C	-0.902343	6.056929	-1.017283
C	-2.109656	3.891167	-1.041523
C	-3.281486	4.566072	-1.059240
C	-2.074728	6.729916	-0.977077
H	0.047414	6.580173	-1.071499
H	-2.099193	2.811028	-1.127256
H	-4.231107	4.046009	-1.139961
H	-2.084525	7.812594	-1.018774
N	-8.027487	-4.207279	1.156004
N	11.416690	-0.346552	-1.158451
N	-4.544680	6.547254	-0.897455
C	-9.002495	-5.163674	0.911932
C	-11.132573	-6.970387	0.433398
C	-8.899005	-6.166030	-0.079442
C	-10.220353	-5.059945	1.616510
C	-11.250281	-5.962287	1.409228
C	-9.947736	-7.039345	-0.321848
H	-8.013358	-6.207389	-0.703990
H	-10.319698	-4.277690	2.362336
H	-12.160642	-5.888919	1.993685
H	-9.861384	-7.779579	-1.109718
C	12.693107	-0.717506	-0.751375
C	15.367350	-1.288276	-0.008811
C	12.990600	-1.329505	0.485532
C	13.774203	-0.354281	-1.580833
C	15.081330	-0.649657	-1.230077
C	14.300999	-1.608582	0.848285
H	12.187136	-1.558002	1.177707
H	13.559015	0.157727	-2.513565
H	15.895947	-0.373206	-1.890346
H	14.506397	-2.075263	1.805358
C	-4.770840	7.887961	-0.620421
C	-5.438659	10.589627	-0.077092
C	-4.070581	8.630699	0.357038
C	-5.845970	8.522336	-1.278121
C	-6.153039	9.851696	-1.039868
C	-4.407701	9.946855	0.632000
H	-3.299319	8.145060	0.945700
H	-6.407025	7.954423	-2.013443
H	-6.957096	10.328487	-1.589312
H	-3.879021	10.487706	1.409213
N	-5.760440	11.934251	0.186658
N	16.697967	-1.579457	0.354536
N	-12.184667	-7.876269	0.202251
C	17.636134	-1.984379	-0.630577
C	19.497115	-2.790727	-2.570616
C	18.945573	-1.482774	-0.607263
C	17.266276	-2.894565	-1.631607
C	18.190613	-3.284358	-2.598405
C	19.868515	-1.892770	-1.567042
H	19.231435	-0.775890	0.164415
H	16.256296	-3.290474	-1.645405

H	17.890363	-3.989668	-3.368120
H	20.879491	-1.496434	-1.536878
H	20.217015	-3.102531	-3.321200
C	17.111385	-1.470879	1.708727
C	17.938704	-1.255033	4.381097
C	16.711269	-0.375054	2.486942
C	17.930413	-2.456588	2.277580
C	18.346201	-2.340789	3.602371
C	17.116435	-0.276974	3.816384
H	16.084615	0.392232	2.044554
H	18.237060	-3.306018	1.676373
H	18.980890	-3.111331	4.030718
H	16.799100	0.576892	4.408194
H	18.258704	-1.171581	5.415265
C	-7.107612	12.379082	0.118572
C	-9.764412	13.270633	-0.008219
C	-7.414043	13.604460	-0.490028
C	-8.140362	11.604231	0.665573
C	-9.459597	12.046345	0.591497
C	-8.733911	14.047501	-0.542992
H	-6.614838	14.202016	-0.915725
H	-7.902375	10.660473	1.144852
H	-10.250442	11.436416	1.018708
H	-8.957904	14.998873	-1.017034
H	-10.792752	13.615528	-0.057457
C	-4.741086	12.859096	0.536116
C	-2.734184	14.695608	1.222557
C	-3.520394	12.864085	-0.154281
C	-4.950469	13.781728	1.570951
C	-3.954356	14.697720	1.902621
C	-2.523076	13.771478	0.196399
H	-3.361620	12.156645	-0.961336
H	-5.893483	13.775430	2.107244
H	-4.129455	15.407313	2.706247
H	-1.582159	13.764758	-0.346408
H	-1.957514	15.406283	1.488199
C	-11.906807	-9.218414	-0.168767
C	-11.370629	-11.874540	-0.896773
C	-10.887562	-9.936247	0.473682
C	-12.657040	-9.840950	-1.176625
C	-12.393004	-11.162852	-1.528909
C	-10.618463	-11.251774	0.102209
H	-10.313028	-9.458225	1.260054
H	-13.443169	-9.284512	-1.675921
H	-12.981742	-11.633265	-2.311266
H	-9.826230	-11.796438	0.607890
H	-11.163122	-12.902355	-1.178510
C	-13.535898	-7.456638	0.327888
C	-16.208576	-6.639815	0.568342
C	-14.470912	-8.278208	0.973185
C	-13.948565	-6.224231	-0.198327
C	-15.275029	-5.818172	-0.067923
C	-15.799298	-7.872478	1.082681
H	-14.149952	-9.230149	1.382851
H	-13.226867	-5.592688	-0.705634
H	-15.581937	-4.860960	-0.479639
H	-16.514026	-8.518334	1.584674
H	-17.243049	-6.323520	0.661524
C	-5.513895	-3.790722	-2.117917
O	-4.814695	-2.861408	-2.238368
O	-6.211763	-4.720949	-2.008968

H	8.642376	-1.996395	-0.228427	N	1.512150	-3.098853	3.223837
C	8.304772	-1.111809	0.299359	N	8.483161	2.540044	-0.123026
C	7.416582	1.167356	1.639767	C	0.515260	-2.254365	3.115639
C	7.440481	-1.244571	1.398768	C	-1.883224	-0.733532	2.605902
C	8.686566	0.147170	-0.143072	C	-0.813234	-2.805047	3.347742
C	8.175868	1.314260	0.457819	C	0.568542	-0.823654	2.831482
C	7.067506	-0.088208	2.106056	C	-0.563389	-0.118302	2.600078
H	9.320966	0.250152	-1.017545	C	-1.944769	-2.107201	3.093812
H	6.472120	-0.185268	3.007419	H	-0.852266	-3.828343	3.708544
H	7.119239	2.049677	2.196768	H	1.525859	-0.318326	2.837943
N	6.919751	-2.495680	1.786051	H	-0.525906	0.941919	2.373225
C	7.641624	-3.688307	1.494782	H	-2.912936	-2.554623	3.282293
C	9.055914	-6.029270	0.909563	C	7.582607	3.481721	-0.253719
C	7.043949	-4.697125	0.729389	C	5.755185	5.693639	-0.633235
C	8.952754	-3.847452	1.958118	C	6.152374	3.359092	0.027345
C	9.656557	-5.012791	1.657398	C	8.031776	4.775089	-0.752862
C	7.746671	-5.866758	0.449369	C	7.183223	5.817065	-0.899956
H	6.036624	-4.557792	0.354887	C	5.299443	4.394205	-0.145445
H	9.408306	-3.059297	2.549244	H	5.769100	2.408419	0.375021
H	10.673236	-5.131860	2.020432	H	9.090207	4.868290	-0.974700
H	7.270466	-6.643766	-0.142028	H	7.527560	6.784912	-1.250663
C	5.560961	-2.597033	2.157507	H	4.252865	4.268245	0.101566
C	2.822599	-2.835368	2.867144	N	-2.885861	0.024372	2.236564
C	5.149051	-3.555561	3.100628	N	5.017338	6.756559	-0.827206
C	4.588150	-1.782777	1.553629	C	-4.179058	-0.440173	2.044642
C	3.252601	-1.898196	1.896593	C	-6.893784	-1.156429	1.606404
C	3.809289	-3.678339	3.431585	C	-4.527457	-1.710031	1.530677
H	5.887078	-4.206358	3.557502	C	-5.228509	0.472184	2.285516
H	4.880274	-1.090244	0.775839	C	-6.555240	0.123733	2.084910
H	2.529304	-1.324452	1.332236	C	-5.852932	-2.062728	1.331951
H	3.488397	-4.424145	4.151582	H	-3.750356	-2.413741	1.255165

H	-4.974412	1.466720	2.638446
H	-7.338474	0.847641	2.278557
H	-6.091304	-3.048800	0.950284
C	3.630176	6.740714	-0.741032
C	0.814540	6.862934	-0.475031
C	2.804879	5.718741	-1.262339
C	2.999713	7.862595	-0.163532
C	1.623238	7.912283	-0.005059
C	1.426064	5.783884	-1.136118
H	3.252308	4.896348	-1.810543
H	3.623649	8.669333	0.207614
H	1.162654	8.761627	0.487847
H	0.804857	4.996961	-1.550733
N	-0.584050	6.875325	-0.291504
N	-8.235102	-1.509613	1.375647
C	-9.276205	-0.979452	2.184037
C	-11.346665	0.049991	3.769652
C	-10.467512	-0.539383	1.591092
C	-9.128735	-0.904500	3.576129
C	-10.156420	-0.382824	4.359137
C	-11.497200	-0.036385	2.383598
H	-10.578298	-0.596104	0.513300
H	-8.210519	-1.255286	4.035432
H	-10.030418	-0.329208	5.436685
H	-12.415878	0.301335	1.912642
H	-12.148207	0.449078	4.383703
C	-8.563669	-2.416766	0.331818
C	-9.176898	-4.213512	-1.725043
C	-7.955173	-2.281866	-0.919734
C	-9.481802	-3.450817	0.556341
C	-9.788078	-4.332917	-0.480451
C	-8.222455	-3.202338	-1.946525
H	-7.277453	-1.456528	-1.100586
H	-9.950399	-3.552132	1.528943
H	-10.506599	-5.129052	-0.308617
H	-9.407202	-4.900356	-2.532680
C	-1.324870	8.072613	-0.434255
C	-2.796545	10.448476	-0.727156
C	-2.402624	8.350332	0.420811
C	-0.992309	8.995414	-1.438477
C	-1.718768	10.176171	-1.573200
C	-3.134420	9.525561	0.265364
H	-2.660592	7.643308	1.201752
H	-0.166844	8.780107	-2.108598
H	-1.448237	10.879787	-2.355501
H	-3.966170	9.725357	0.935106
H	-3.365503	11.366216	-0.840485
C	-1.231457	5.676755	0.115670
C	-2.489990	3.298079	0.918623
C	-0.671797	4.888784	1.131176
C	-2.429250	5.272230	-0.488868
C	-3.054283	4.094443	-0.081895
C	-1.297393	3.706758	1.520918
H	0.248063	5.210946	1.608187
H	-2.862102	5.884468	-1.273450
H	-3.983254	3.794647	-0.556095
H	-0.860837	3.112640	2.318725
H	-2.953821	2.366202	1.227499
H	9.605349	-6.938702	0.685800
N	-7.664210	-3.096784	-3.222478
C	-6.388798	-2.908773	-3.423414
C	-3.608944	-2.539475	-4.120167
C	-5.332493	-2.911166	-2.409068
C	-5.963938	-2.684022	-4.800727

C	-4.668849	-2.476177	-5.119361
C	-4.031709	-2.737451	-2.735669
H	-5.608874	-3.048959	-1.372074
H	-6.746593	-2.671784	-5.552498
H	-4.355465	-2.294798	-6.142545
H	-3.283183	-2.707716	-1.952875
N	-2.387885	-2.389768	-4.561595
C	-1.238622	-2.591748	-3.812284
C	1.263952	-2.939261	-2.515954
C	-1.058263	-3.590486	-2.828507
C	-0.115661	-1.809963	-4.158567
C	1.101244	-1.962509	-3.518035
C	0.164623	-3.756934	-2.194497
H	-1.869273	-4.270614	-2.593220
H	-0.228785	-1.075698	-4.949962
H	1.943043	-1.345008	-3.808202
H	0.280903	-4.536607	-1.449921
N	2.502101	-3.135566	-1.877043
C	2.907221	-4.463207	-1.536544
C	3.737912	-7.052210	-0.870036
C	2.862603	-5.483402	-2.494827
C	3.364827	-4.742736	-0.244630
C	3.782623	-6.032059	0.083059
C	3.271214	-6.773020	-2.157392
H	2.509833	-5.259012	-3.496321
H	3.389368	-3.951176	0.492269
H	4.134415	-6.234954	1.090240
H	3.236348	-7.558255	-2.906957
H	4.058657	-8.056857	-0.611330
C	3.445696	-2.083752	-1.762941
C	5.319403	0.004202	-1.570615
C	4.809056	-2.329310	-1.983606
C	3.031272	-0.784510	-1.426549
C	3.962410	0.249659	-1.343820
C	5.733218	-1.292290	-1.882613
H	5.137716	-3.330351	-2.239909
H	1.980786	-0.590928	-1.237086
H	3.625440	1.250376	-1.087117
H	6.783817	-1.497538	-2.055643
H	6.046312	0.805605	-1.497869
C	-5.704829	1.254087	-0.798733
O	-6.023311	2.309201	-0.407912
O	-5.386302	0.208379	-1.211574

*A.4.8.18 Linear/Coiled **OTPA-BZN-430**, **EB** State, with CO_2 Binding, Mode 2*

H	8.837496	-0.890203	-1.457057
C	8.357642	-0.342753	-0.652211
C	7.099001	1.048947	1.413868
C	7.836358	-1.045499	0.442886
C	8.244346	1.040622	-0.715705
C	7.563527	1.760050	0.286281
C	7.239506	-0.329949	1.490038
H	8.634418	1.585054	-1.569493
H	6.875249	-0.869958	2.358397
H	6.651940	1.592334	2.239885
N	7.857614	-2.468298	0.487306
C	9.064071	-3.165162	0.251711
C	11.483324	-4.517009	-0.216825
C	9.074762	-4.376978	-0.457043
C	10.277437	-2.634418	0.718427
C	11.474172	-3.304325	0.476718

C	10.276106	-5.047234	-0.677466
H	8.144186	-4.784934	-0.835958
H	10.273076	-1.699827	1.269142
H	12.403869	-2.879616	0.844795
H	10.266922	-5.983939	-1.227738
C	6.617089	-3.127818	0.611936
C	4.068028	-4.315479	0.945291
C	6.475045	-4.333178	1.325635
C	5.475890	-2.559466	0.022601
C	4.228649	-3.127325	0.201739
C	5.228366	-4.931686	1.457973
H	7.347564	-4.794384	1.775831
H	5.582554	-1.665960	-0.582034
H	3.365973	-2.686224	-0.275852
H	5.125993	-5.860687	2.010126
N	2.829048	-4.933502	1.087641
N	7.461995	3.144248	0.153576
C	1.758055	-4.224036	1.342345
C	-0.719782	-2.788870	1.706872
C	0.460548	-4.873973	1.190268
C	1.737782	-2.844923	1.816882
C	0.573097	-2.189983	2.010532
C	-0.706853	-4.197894	1.315062
H	0.474867	-5.927917	0.928766
H	2.676362	-2.361154	2.054283
H	0.559395	-1.176134	2.391013
H	-1.652839	-4.707850	1.173065
C	6.347308	3.784192	0.393349
C	3.971183	5.369401	0.847998
C	5.048572	3.172861	0.661795
C	6.382144	5.241494	0.377427
C	5.277796	5.979636	0.630027
C	3.932769	3.910636	0.863036
H	4.978910	2.095444	0.682205
H	7.343724	5.705204	0.181127
H	5.311312	7.064597	0.640400
H	2.997832	3.408706	1.079816
N	-1.766531	-2.031634	1.901199
N	2.962400	6.181410	1.039076
C	-3.076730	-2.388044	1.599710
C	-5.818910	-2.931326	1.137676
C	-3.501131	-3.001912	0.402728
C	-4.066844	-1.988714	2.521349
C	-5.405132	-2.271087	2.308453
C	-4.849836	-3.263264	0.175132
H	-2.770852	-3.256598	-0.358895
H	-3.752953	-1.461769	3.416622
H	-6.146735	-1.976900	3.043013
H	-5.157033	-3.749331	-0.745214
C	1.636564	5.775563	1.063980
C	-1.138138	5.175743	1.134371
C	1.078899	4.794949	0.211855
C	0.754504	6.473631	1.918363
C	-0.593861	6.162302	1.980044
C	-0.276605	4.512908	0.242254
H	1.707752	4.308607	-0.525293
H	1.166090	7.244637	2.561953
H	-1.240065	6.691176	2.671664
H	-0.692334	3.780052	-0.436140
N	-2.509522	4.869426	1.154508
N	-7.180838	-3.253091	0.948558
C	-7.963197	-3.719253	2.035901
C	-9.524897	-4.649375	4.175813
C	-9.297103	-3.307073	2.171466

C	-7.417979	-4.602759	2.979677
C	-8.194078	-5.053671	4.045048
C	-10.070738	-3.778459	3.229982
H	-9.719032	-2.619812	1.445900
H	-6.389595	-4.930879	2.872490
H	-7.758424	-5.737373	4.768161
H	-11.102326	-3.450627	3.321827
H	-10.128604	-5.008842	5.003531
C	-7.776419	-3.126260	-0.333569
C	-8.956239	-2.850609	-2.858132
C	-7.570934	-1.962560	-1.078628
C	-8.570149	-4.158308	-0.853406
C	-9.161694	-4.004995	-2.106981
C	-8.125078	-1.828660	-2.364428
H	-6.996330	-1.150739	-0.647009
H	-8.726460	-5.059543	-0.270857
H	-9.784468	-4.800924	-2.504723
H	-9.410474	-2.728027	-3.835700
C	-3.478657	5.872969	1.418144
C	-5.416938	7.835249	1.929477
C	-4.586167	5.579396	2.226406
C	-3.350684	7.154451	0.863404
C	-4.310786	8.128803	1.128525
C	-5.550537	6.554506	2.471161
H	-4.683762	4.587597	2.655194
H	-2.501244	7.378552	0.226972
H	-4.199984	9.117610	0.692700
H	-6.403909	6.314114	3.098802
H	-6.166862	8.594988	2.127649
C	-2.949580	3.551780	0.843888
C	-3.805450	0.949758	0.245938
C	-2.337813	2.447294	1.450715
C	-4.000052	3.346556	-0.060002
C	-4.430817	2.051200	-0.343460
C	-2.752368	1.152907	1.142810
H	-1.540631	2.616871	2.166297
H	-4.473994	4.200962	-0.531702
H	-5.249567	1.904056	-1.040099
H	-2.261020	0.303583	1.608528
H	-4.136463	-0.057796	0.016294
H	12.417492	-5.040067	-0.396902
N	-7.969495	-0.675226	-3.140565
C	-6.803894	-0.115441	-3.307638
C	-4.331776	1.328757	-3.708461
C	-5.520494	-0.648882	-2.853755
C	-6.763753	1.166695	-4.006966
C	-5.611809	1.853292	-4.171311
C	-4.369135	0.030748	-3.031121
H	-5.502043	-1.606257	-2.349038
H	-7.713834	1.555892	-4.358902
H	-5.590567	2.819072	-4.666277
H	-3.449564	-0.373094	-2.630971
N	-3.269897	2.069133	-3.887643
C	-2.012824	1.582515	-3.532759
C	0.385859	0.572015	-2.429654
C	-1.544794	0.299730	-3.871099
C	-1.150347	2.419696	-2.801409
C	0.023320	1.922142	-2.256992
C	-0.367226	-0.199288	-3.332800
H	-2.125580	-0.319797	-4.546763
H	-1.452158	3.445344	-2.615331
H	0.660357	2.565957	-1.667331
H	-0.058722	-1.204933	-3.585662
N	1.482856	0.022749	-1.735015

C	1.899265	-1.303893	-2.119400
C	2.658496	-3.872830	-2.895114
C	2.974099	-1.474850	-2.991146
C	1.198981	-2.414714	-1.635161
C	1.574210	-3.697259	-2.031415
C	3.358907	-2.763141	-3.370305
H	3.507569	-0.603521	-3.355723
H	0.365458	-2.262122	-0.958163
H	1.029673	-4.556289	-1.653827
H	4.206467	-2.896792	-4.035520
H	2.959724	-4.873083	-3.190726
C	1.777230	0.387339	-0.387704
C	2.445933	0.958651	2.290549
C	3.046935	0.073937	0.119916
C	0.842356	0.993250	0.465280
C	1.189443	1.293219	1.781682
C	3.367390	0.331922	1.449565
H	3.778974	-0.384290	-0.530036
H	-0.158041	1.213276	0.117744
H	0.455752	1.768907	2.424258
H	4.350141	0.052479	1.816228
H	2.700946	1.181593	3.321611
C	3.967274	2.294515	-2.211042
O	3.099864	3.076005	-2.251101
O	4.839007	1.515891	-2.183268

*A.4.8.19 Linear/Coiled **OTPA-BZN-430**, **EB** State, with CO_2 Binding, Mode 3*

H	9.303746	-0.670142	-1.433565
C	8.760791	-0.139003	-0.658495
C	7.339075	1.213070	1.325062
C	8.138307	-0.864987	0.367316
C	8.668352	1.247338	-0.694030
C	7.904959	1.948174	0.260591
C	7.463310	-0.167812	1.379649
H	9.139212	1.807837	-1.495249
H	7.022143	-0.724394	2.200458
H	6.823648	1.741541	2.120442
N	8.139013	-2.286994	0.374582
C	9.345877	-2.996406	0.176854
C	11.762197	-4.376028	-0.214446
C	9.372865	-4.181210	-0.575363
C	10.541054	-2.506616	0.726967
C	11.737388	-3.189841	0.523113
C	10.572358	-4.866058	-0.757603
H	8.456117	-4.556965	-1.016397
H	10.523021	-1.593306	1.312097
H	12.653394	-2.797417	0.955641
H	10.576485	-5.781781	-1.342131
C	6.889025	-2.938368	0.445312
C	4.322887	-4.114877	0.674198
C	6.717170	-4.158650	1.125792
C	5.769673	-2.349112	-0.165403
C	4.513235	-2.911071	-0.036399
C	5.463136	-4.751367	1.206095
H	7.572299	-4.636472	1.591721
H	5.899093	-1.440963	-0.743225
H	3.667193	-2.451534	-0.526697
H	5.338154	-5.691962	1.733419
N	3.075370	-4.725472	0.767995
N	7.817272	3.336219	0.163622
C	2.005974	-4.016786	1.031984

C	-0.474019	-2.595252	1.460627
C	0.706802	-4.650054	0.833815
C	1.987125	-2.657092	1.558182
C	0.821971	-2.011543	1.781132
C	-0.460061	-3.977709	0.985120
H	0.718010	-5.688199	0.515186
H	2.925771	-2.182375	1.813204
H	0.809614	-1.015424	2.205793
H	-1.399295	-4.481333	0.795331
C	6.681553	3.964233	0.326691
C	4.276873	5.508364	0.768994
C	5.365772	3.337968	0.423444
C	6.712031	5.418713	0.414480
C	5.591295	6.133666	0.660321
C	4.238298	4.055428	0.631072
H	5.296464	2.264760	0.317730
H	7.682545	5.895479	0.319103
H	5.619290	7.213877	0.763742
H	3.293932	3.536246	0.734121
N	-1.515133	-1.848442	1.720197
N	3.267501	6.306212	1.008155
C	-2.839745	-2.160789	1.443851
C	-5.621712	-2.578530	1.053239
C	-3.323730	-2.767655	0.265438
C	-3.792324	-1.708951	2.383153
C	-5.146386	-1.926882	2.206774
C	-4.689029	-2.968421	0.074088
H	-2.630112	-3.061593	-0.515326
H	-3.432590	-1.187019	3.263881
H	-5.852274	-1.585755	2.955443
H	-5.038167	-3.447617	-0.834446
C	1.935744	5.917703	0.993410
C	-0.848309	5.357882	1.033080
C	1.359987	5.005545	0.079649
C	1.064969	6.571979	1.893037
C	-0.288367	6.279768	1.937716
C	0.000057	4.741921	0.096501
H	1.977999	4.555672	-0.689765
H	1.490797	7.292466	2.584070
H	-0.925649	6.773233	2.663088
H	-0.429174	4.058883	-0.624486
N	-2.224717	5.068144	1.039993
N	-6.997861	-2.825188	0.884803
C	-7.833127	-3.116507	1.994976
C	-9.509322	-3.708919	4.167391
C	-9.125960	-2.576523	2.060084
C	-7.386130	-3.957850	3.024771
C	-8.218819	-4.240391	4.105218
C	-9.957398	-2.880517	3.136193
H	-9.471789	-1.922119	1.267124
H	-6.391531	-4.385216	2.973843
H	-7.859247	-4.893111	4.895724
H	-10.956463	-2.455539	3.172769
H	-10.157416	-3.938449	5.007717
C	-7.588118	-2.729417	-0.406346
C	-8.772763	-2.510019	-2.930609
C	-7.370276	-1.589730	-1.182394
C	-8.395517	-3.765975	-0.891601
C	-8.988692	-3.641558	-2.148078
C	-7.929911	-1.482752	-2.468697
H	-6.783493	-0.774297	-0.774476
H	-8.561378	-4.646362	-0.280177
H	-9.622296	-4.440270	-2.522252
H	-9.230417	-2.409334	-3.909163

C	-3.178655	6.073216	1.345488
C	-5.083051	8.046879	1.939201
C	-4.293150	5.765453	2.139195
C	-3.026624	7.375721	0.848041
C	-3.969593	8.354697	1.153819
C	-5.240351	6.746375	2.424392
H	-4.410013	4.758463	2.525440
H	-2.171671	7.612435	0.223661
H	-3.839551	9.359424	0.761857
H	-6.099066	6.494134	3.040031
H	-5.819775	8.810616	2.168946
C	-2.675363	3.759608	0.710740
C	-3.557450	1.172311	0.084905
C	-2.055859	2.641153	1.283285
C	-3.744773	3.575306	-0.175611
C	-4.187845	2.287341	-0.473046
C	-2.484473	1.354779	0.962125
H	-1.242564	2.793301	1.984392
H	-4.224410	4.440135	-0.621856
H	-5.020669	2.156632	-1.156255
H	-1.988918	0.496103	1.405497
H	-3.900598	0.170820	-0.152904
H	12.695480	-4.909949	-0.364809
N	-7.769161	-0.346910	-3.268885
C	-6.597952	0.196756	-3.451453
C	-4.112253	1.614114	-3.860342
C	-5.318916	-0.351630	-3.004292
C	-6.546236	1.475263	-4.156086
C	-5.387757	2.151087	-4.320943
C	-4.160645	0.314829	-3.186719
H	-5.309790	-1.309214	-2.499400
H	-7.492986	1.874159	-4.506142
H	-5.358105	3.116945	-4.815374
H	-3.244209	-0.099277	-2.790086
N	-3.043298	2.345668	-4.037055
C	-1.790692	1.841982	-3.692208
C	0.601184	0.793236	-2.611859
C	-1.343396	0.553411	-4.038977
C	-0.911742	2.664434	-2.962990
C	0.258762	2.147868	-2.429035
C	-0.169350	0.035848	-3.512820
H	-1.938320	-0.054422	-4.712945
H	-1.198635	3.693540	-2.772111
H	0.907405	2.778088	-1.833900
H	0.124570	-0.973260	-3.770256
N	1.691794	0.226015	-1.931217
C	2.142735	-1.070886	-2.365351
C	2.985119	-3.584685	-3.229854
C	3.203338	-1.174710	-3.265531
C	1.496096	-2.221039	-1.900150
C	1.912941	-3.476246	-2.340876
C	3.630471	-2.435168	-3.689143
H	3.687032	-0.270055	-3.620154
H	0.673039	-2.121064	-1.201197
H	1.410685	-4.366566	-1.977540
H	4.466388	-2.517066	-4.377191
H	3.318746	-4.563654	-3.560014
C	2.022265	0.586659	-0.595382
C	2.737542	1.121607	2.077575
C	3.308652	0.288271	-0.121966
C	1.098673	1.170714	0.285577
C	1.468368	1.453080	1.599516
C	3.650415	0.524063	1.206582
H	4.034432	-0.144681	-0.798076

H	0.089441	1.385136	-0.039993
H	0.742637	1.909728	2.264833
H	4.643346	0.252947	1.549767
H	3.010763	1.327733	3.107500
C	-3.756587	-5.612734	1.840102
O	-3.427137	-6.078615	0.819452
O	-4.078265	-5.159368	2.867763

*A.4.8.20 Linear/Coiled **OTPA-BZN-430**, **EB** State, with CO_2 Binding, Mode 4*

H	8.756029	-0.368144	-0.212156
C	8.238718	0.153985	0.584366
C	6.884538	1.513957	2.609016
C	7.433179	-0.563335	1.482824
C	8.323807	1.537702	0.672912
C	7.562611	2.250956	1.617026
C	6.836803	0.130743	2.550760
H	8.901501	2.096133	-0.056684
H	6.286405	-0.421733	3.304255
H	6.390801	2.036776	3.421900
N	7.168939	-1.938877	1.314065
C	8.074206	-2.761747	0.587554
C	9.853279	-4.376833	-0.848458
C	7.624142	-3.491681	-0.520883
C	9.419042	-2.835987	0.970033
C	10.303358	-3.634966	0.246968
C	8.510160	-4.302999	-1.226175
H	6.586363	-3.417091	-0.825815
H	9.759788	-2.267708	1.829736
H	11.345022	-3.688128	0.549951
H	8.148801	-4.866805	-2.081579
C	5.861047	-2.420272	1.554289
C	3.248471	-3.390781	2.052629
C	5.664063	-3.724507	2.040987
C	4.737562	-1.625867	1.270805
C	3.461415	-2.099958	1.516037
C	4.382595	-4.205002	2.263293
H	6.525071	-4.354999	2.236468
H	4.869962	-0.647873	0.827868
H	2.611635	-1.504369	1.205642
H	4.230720	-5.212066	2.638005
N	1.999283	-3.948620	2.271579
N	7.519074	3.641085	1.500211
C	0.964106	-3.233290	2.636183
C	-1.484649	-1.773760	3.023827
C	-0.333819	-3.891851	2.602107
C	0.971989	-1.857458	3.126842
C	-0.185973	-1.185390	3.321526
C	-1.491752	-3.209647	2.762918
H	-0.329965	-4.958993	2.402250
H	1.921352	-1.393740	3.365962
H	-0.195367	-0.165501	3.694677
H	-2.439538	-3.732515	2.728467
C	6.376823	4.279097	1.488378
C	3.983226	5.833833	1.040791
C	5.042737	3.677071	1.554255
C	6.417301	5.729255	1.332064
C	5.295021	6.459876	1.145147
C	3.925858	4.408538	1.345218
H	4.952026	2.619385	1.758173
H	7.399796	6.190577	1.343590
H	5.334026	7.534435	0.996987

H	2.950488	3.942611	1.419324
N	-2.511289	-0.962762	3.078224
N	2.975988	6.593668	0.695482
C	-3.799254	-1.288759	2.684593
C	-6.520837	-1.728094	1.993652
C	-4.157028	-2.197562	1.661884
C	-4.842478	-0.559454	3.295230
C	-6.169828	-0.778492	2.973334
C	-5.486160	-2.419137	1.334044
H	-3.387811	-2.712335	1.098211
H	-4.575283	0.184157	4.039313
H	-6.947727	-0.207553	3.467006
H	-5.731798	-3.139466	0.562483
C	1.729483	6.088791	0.350969
C	-0.888042	5.258328	-0.360497
C	1.512301	4.899599	-0.385928
C	0.600761	6.874549	0.667221
C	-0.680041	6.457915	0.346423
C	0.233058	4.496131	-0.736016
H	2.362086	4.328853	-0.745023
H	0.755655	7.802537	1.208260
H	-1.534072	7.061588	0.632774
H	0.090934	3.592422	-1.319033
N	-2.187609	4.846701	-0.709917
N	-7.867731	-1.962877	1.675163
C	-8.883186	-1.812104	2.660296
C	-10.906067	-1.532592	4.579023
C	-10.073986	-1.148157	2.337529
C	-8.711374	-2.339300	3.947381
C	-9.715929	-2.189303	4.901350
C	-11.080827	-1.018428	3.292032
H	-10.202216	-0.740386	1.340268
H	-7.792838	-2.862376	4.191985
H	-9.572392	-2.601335	5.896039
H	-12.000030	-0.502033	3.030997
H	-11.689592	-1.423982	5.322753
C	-8.241942	-2.396101	0.374580
C	-8.989972	-3.239705	-2.187049
C	-7.693168	-1.776821	-0.752732
C	-9.160159	-3.443132	0.221615
C	-9.532722	-3.848678	-1.059951
C	-8.034478	-2.216008	-2.042813
H	-7.013605	-0.941059	-0.628514
H	-9.580029	-3.921083	1.099632
H	-10.251493	-4.654372	-1.177278
H	-9.275465	-3.550086	-3.186618
C	-3.165673	5.817843	-1.055453
C	-5.088955	7.738713	-1.747569
C	-4.459635	5.746788	-0.520429
C	-2.841579	6.856561	-1.939817
C	-3.797010	7.814036	-2.273668
C	-5.414223	6.698203	-0.874014
H	-4.709146	4.945021	0.166287
H	-1.842066	6.905608	-2.359233
H	-3.533300	8.613594	-2.960081
H	-6.413511	6.631930	-0.453223
H	-5.833883	8.481625	-2.016068
C	-2.564773	3.480707	-0.617337
C	-3.406011	0.815014	-0.381503
C	-2.107722	2.685053	0.442978
C	-3.430075	2.924704	-1.571288
C	-3.853698	1.603673	-1.444440
C	-2.521799	1.359357	0.553297
H	-1.437487	3.110742	1.181624

H	-3.776901	3.536111	-2.397644
H	-4.533129	1.189873	-2.182673
H	-2.178264	0.761715	1.391669
H	-3.749590	-0.207977	-0.275720
H	10.543846	-5.004991	-1.402977
N	-7.553491	-1.602321	-3.201446
C	-6.286810	-1.366871	-3.401108
C	-3.539332	-0.777079	-4.076705
C	-5.173374	-1.807543	-2.557835
C	-5.935586	-0.600438	-4.591000
C	-4.653134	-0.303137	-4.889402
C	-3.887186	-1.533148	-2.875533
H	-5.396365	-2.366921	-1.658083
H	-6.759824	-0.265890	-5.212576
H	-4.392633	0.281518	-5.765835
H	-3.094458	-1.842492	-2.206498
N	-2.346713	-0.445169	-4.492873
C	-1.146197	-0.872835	-3.950927
C	1.441498	-1.527724	-2.988314
C	-0.875946	-2.142495	-3.391010
C	-0.064836	0.025896	-4.077957
C	1.194485	-0.283025	-3.599468
C	0.389751	-2.458829	-2.916347
H	-1.650138	-2.900675	-3.363650
H	-0.250172	0.979687	-4.561319
H	2.001607	0.431768	-3.706824
H	0.573592	-3.438234	-2.488556
N	2.718106	-1.845236	-2.483512
C	3.232114	-3.167346	-2.632309
C	4.285329	-5.747769	-2.927567
C	3.115013	-3.839486	-3.855574
C	3.876491	-3.793147	-1.557876
C	4.406466	-5.072797	-1.710308
C	3.632161	-5.126946	-3.995072
H	2.622523	-3.350177	-4.689497
H	3.959385	-3.273901	-0.612721
H	4.902653	-5.542886	-0.866262
H	3.536630	-5.639224	-4.948074
H	4.692538	-6.747733	-3.042545
C	3.560707	-0.823414	-1.980062
C	5.215522	1.249654	-1.043150
C	4.943666	-0.855530	-2.214015
C	3.017194	0.247285	-1.250957
C	3.839124	1.281665	-0.810560
C	5.759653	0.167704	-1.737216
H	5.374106	-1.678451	-2.773190
H	1.951680	0.277694	-1.054112
H	3.401851	2.122711	-0.283053
H	6.827748	0.123892	-1.921027
H	5.854097	2.048993	-0.685726
C	1.889785	1.287886	1.892574
O	2.812246	1.096387	2.585784
O	0.973643	1.484622	1.194673

*A.4.8.21 Linear/Coiled **OTPA-BZN-430**, **EB** State, with CO_2 Binding, Mode 5*

H	8.974077	-1.515232	-1.524519
C	8.469286	-0.923545	-0.767803
C	7.145397	0.585530	1.169694
C	7.841437	-1.570003	0.307088
C	8.430859	0.461563	-0.874173
C	7.716630	1.241234	0.057089

C	7.216579	-0.794268	1.294529
H	8.905732	0.960171	-1.712982
H	6.773024	-1.288920	2.152787
H	6.670078	1.174835	1.947094
N	7.788327	-2.987835	0.391047
C	8.958741	-3.756009	0.193207
C	11.302503	-5.254495	-0.201087
C	8.911916	-4.978864	-0.494295
C	10.190798	-3.288774	0.677579
C	11.350917	-4.031395	0.472240
C	10.075867	-5.722096	-0.678129
H	7.965996	-5.338423	-0.884324
H	10.229772	-2.346278	1.213315
H	12.296290	-3.655684	0.853338
H	10.022999	-6.666633	-1.212239
C	6.517887	-3.584795	0.540652
C	3.919629	-4.643916	0.921129
C	6.323858	-4.751236	1.304044
C	5.402445	-2.993498	-0.074744
C	4.130855	-3.496968	0.127130
C	5.052091	-5.288410	1.460062
H	7.175658	-5.230660	1.774430
H	5.547137	-2.130748	-0.715005
H	3.287618	-3.037860	-0.368551
H	4.909392	-6.187734	2.051004
N	2.655121	-5.200587	1.092095
N	7.682631	2.624733	-0.109186
C	1.618292	-4.438065	1.332439
C	-0.795663	-2.895414	1.689468
C	0.293478	-5.040028	1.220211
C	1.660346	-3.043310	1.757798
C	0.525208	-2.337695	1.949437
C	-0.844425	-4.315202	1.342088
H	0.262466	-6.101707	0.993858
H	2.620965	-2.587815	1.960849
H	0.557859	-1.311901	2.295026
H	-1.811846	-4.791795	1.232152
C	6.578628	3.307334	0.052644
C	4.255960	4.971820	0.487123
C	5.240986	2.743036	0.209876
C	6.672157	4.761336	0.073653
C	5.591413	5.536249	0.316824
C	4.151333	3.517437	0.414275
H	5.122993	1.670412	0.151456
H	7.659361	5.190583	-0.066080
H	5.672339	6.616068	0.375707
H	3.188051	3.045934	0.561432
N	-1.808565	-2.092792	1.879903
N	3.282309	5.815933	0.716869
C	-3.138036	-2.405579	1.616828
C	-5.909210	-2.854181	1.232635
C	-3.613439	-3.039035	0.449570
C	-4.090473	-1.937512	2.545945
C	-5.443108	-2.173877	2.371952
C	-4.976350	-3.253463	0.259953
H	-2.911416	-3.346059	-0.319267
H	-3.735450	-1.395152	3.416298
H	-6.155506	-1.827662	3.112696
H	-5.323570	-3.755319	-0.637387
C	1.936804	5.473893	0.757175
C	-0.862008	5.021307	0.884184
C	1.303937	4.566103	-0.120412
C	1.118897	6.174527	1.670181
C	-0.242261	5.934796	1.757523

C	-0.064374	4.354436	-0.061197
H	1.883970	4.078354	-0.896489
H	1.589093	6.888415	2.338636
H	-0.839988	6.464490	2.490966
H	-0.539541	3.674869	-0.756080
N	-2.248776	4.788639	0.931074
N	-7.286554	-3.129407	1.085535
C	-8.057908	-3.531475	2.205910
C	-9.597810	-4.335217	4.411825
C	-9.370562	-3.062459	2.362526
C	-7.523119	-4.408133	3.161967
C	-8.287846	-4.796180	4.259820
C	-10.133832	-3.471253	3.454061
H	-9.784280	-2.380474	1.627326
H	-6.511671	-4.780318	3.038729
H	-7.860398	-5.475349	4.992052
H	-11.148965	-3.099830	3.561927
H	-10.193107	-4.645828	5.265018
C	-7.910481	-3.017299	-0.184513
C	-9.147656	-2.770629	-2.684766
C	-7.678717	-1.886643	-0.971516
C	-8.759550	-4.031088	-0.650294
C	-9.379001	-3.891824	-1.891910
C	-8.262131	-1.769573	-2.246100
H	-7.059126	-1.086741	-0.582009
H	-8.936060	-4.906913	-0.035647
H	-10.044314	-4.673167	-2.247489
H	-9.623240	-2.659593	-3.653544
C	-3.153876	5.839909	1.226514
C	-4.962603	7.907316	1.803197
C	-4.272644	5.596705	2.036887
C	-2.949721	7.125618	0.703930
C	-3.844966	8.150839	1.001373
C	-5.172146	6.623869	2.313396
H	-4.430132	4.603255	2.443174
H	-2.091900	7.313523	0.067067
H	-3.674356	9.141592	0.589843
H	-6.034507	6.421048	2.942115
H	-5.662140	8.707140	2.026294
C	-2.756914	3.489371	0.651487
C	-3.752236	0.921070	0.129489
C	-2.176591	2.367463	1.256987
C	-3.843071	3.318658	-0.216871
C	-4.342643	2.040363	-0.462599
C	-2.661657	1.089279	0.987577
H	-1.349783	2.511277	1.943978
H	-4.291907	4.186596	-0.688488
H	-5.188610	1.919707	-1.131424
H	-2.197138	0.226613	1.456272
H	-4.139158	-0.073188	-0.068206
H	12.207823	-5.834224	-0.352716
N	-8.079088	-0.648591	-3.063022
C	-6.894264	-0.148594	-3.279023
C	-4.369657	1.167939	-3.781901
C	-5.625307	-0.727725	-2.841991
C	-6.813527	1.108762	-4.018359
C	-5.635717	1.736324	-4.230683
C	-4.449082	-0.107192	-3.066620
H	-5.637581	-1.670200	-2.309782
H	-7.753370	1.531481	-4.358993
H	-5.583296	2.685448	-4.754784
H	-3.539879	-0.541813	-2.675454
N	-3.280165	1.855598	-4.004317
C	-2.038556	1.323754	-3.662810

C	0.331788	0.240751	-2.567522
C	-1.638849	0.007593	-3.960594
C	-1.119879	2.146245	-2.984512
C	0.040139	1.613923	-2.443368
C	-0.475928	-0.526920	-3.426883
H	-2.262415	-0.607698	-4.601016
H	-1.368754	3.192170	-2.836532
H	0.718017	2.247671	-1.885921
H	-0.219969	-1.555405	-3.644891
N	1.408006	-0.336758	-1.873238
C	1.783744	-1.679722	-2.233749
C	2.476485	-4.283232	-2.953809
C	2.823750	-1.895163	-3.138040
C	1.082411	-2.762899	-1.692928
C	1.424722	-4.063214	-2.060861
C	3.175830	-3.200348	-3.489498
H	3.350220	-1.041363	-3.552734
H	0.274751	-2.575481	-0.993995
H	0.880105	-4.901218	-1.638797
H	3.995865	-3.368870	-4.180863
H	2.752171	-5.297002	-3.227544
C	1.783341	0.083642	-0.566395
C	2.581117	0.730725	2.058074
C	3.065528	-0.246273	-0.102737
C	0.906510	0.756361	0.298978
C	1.317609	1.093163	1.587627
C	3.447073	0.045944	1.203603
H	3.756212	-0.748129	-0.767813
H	-0.099598	0.997241	-0.016999
H	0.628313	1.619144	2.240410
H	4.434665	-0.250372	1.540986
H	2.886093	0.980295	3.069312
C	3.425046	8.671204	0.391888
O	2.375399	8.643571	-0.120942
O	4.476669	8.766640	0.896170

Appendix B Detailed Theoretical Study of Vibrational Spectra

B.1 Vibrational Modes of Six-Membered Rings

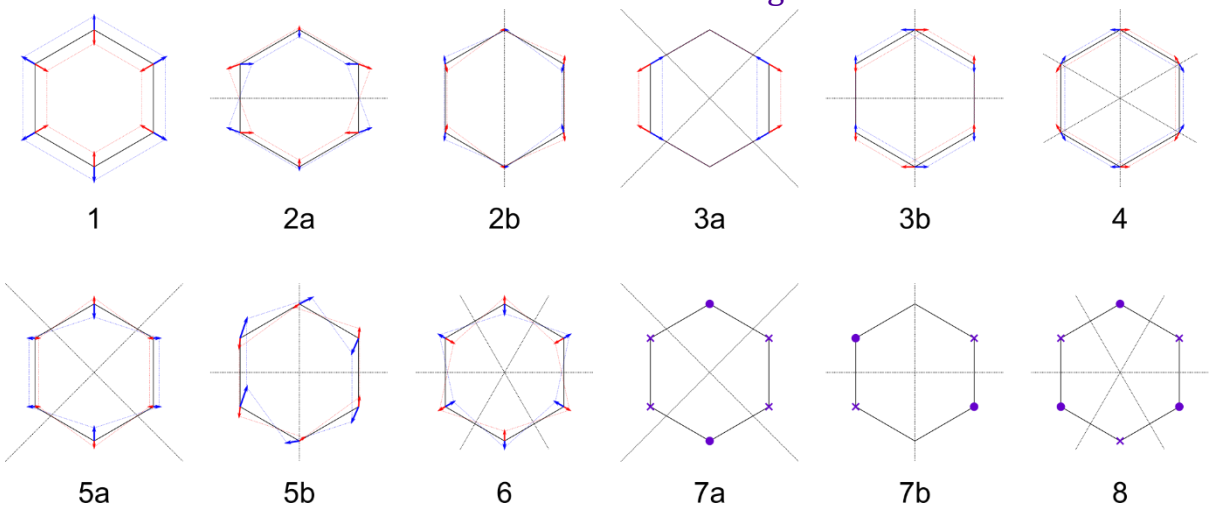

Scheme B-1 Elementary vibrational modes of six-membered aromatic systems

In general, vibrational modes of six-membered aromatic systems can be considered based on elementary vibrational modes (Scheme B-1).[1] Each mode differs from others by either manners of movements or numbers of radial nodes. These movements can be categorised into three groups by their manners: in-plane bond stretching/contracting (modes 1 to 4), in-plane angle widening/narrowing (modes 5 and 6), and out-of-plane (modes 7 and 8). Meanwhile, aromatic rings can be divided by radial nodes into semicircles, quadrants, or sextants depending on the number of nodes. Movements in adjacent regions divided by these nodes are in alternative manner. Double degenerations exist in modes 2, 3, 5, and 7 because their radial nodes can align in two different ways yielding two different vibrations. For planar modes 1 to 6, two opposite ends of vibrations are depicted in Scheme B-1 as blue and red dotted hexagons for each mode, with vectors representing displacements of atoms from the original positions. Out-of-plane vibrational modes 7 and 8 are represented by dots for upwards movements and crosses for downwards movements.

Vibrational modes of these six-membered aromatic units are shown in Scheme B-2 (for benzene)[2-4] and Scheme B-3 (for triazine).[1] These modes can be categorised into three main groups: out-of-plane vibrations, in-plane vibrations, and C–H stretching. The first two groups are corresponding to elementary vibrational modes involving ring deformations shown in Scheme B-1. It should be noted that irreducible representations such as A_{2g} or E' will only be applicable for unsubstituted rings because these representations depend on the symmetry of the system. When one or more hydrogen atoms are substituted, as in all units in this study, the symmetry is then broken. Vibrational modes remain the same, but their corresponding irreducible representations are not applicable any longer.

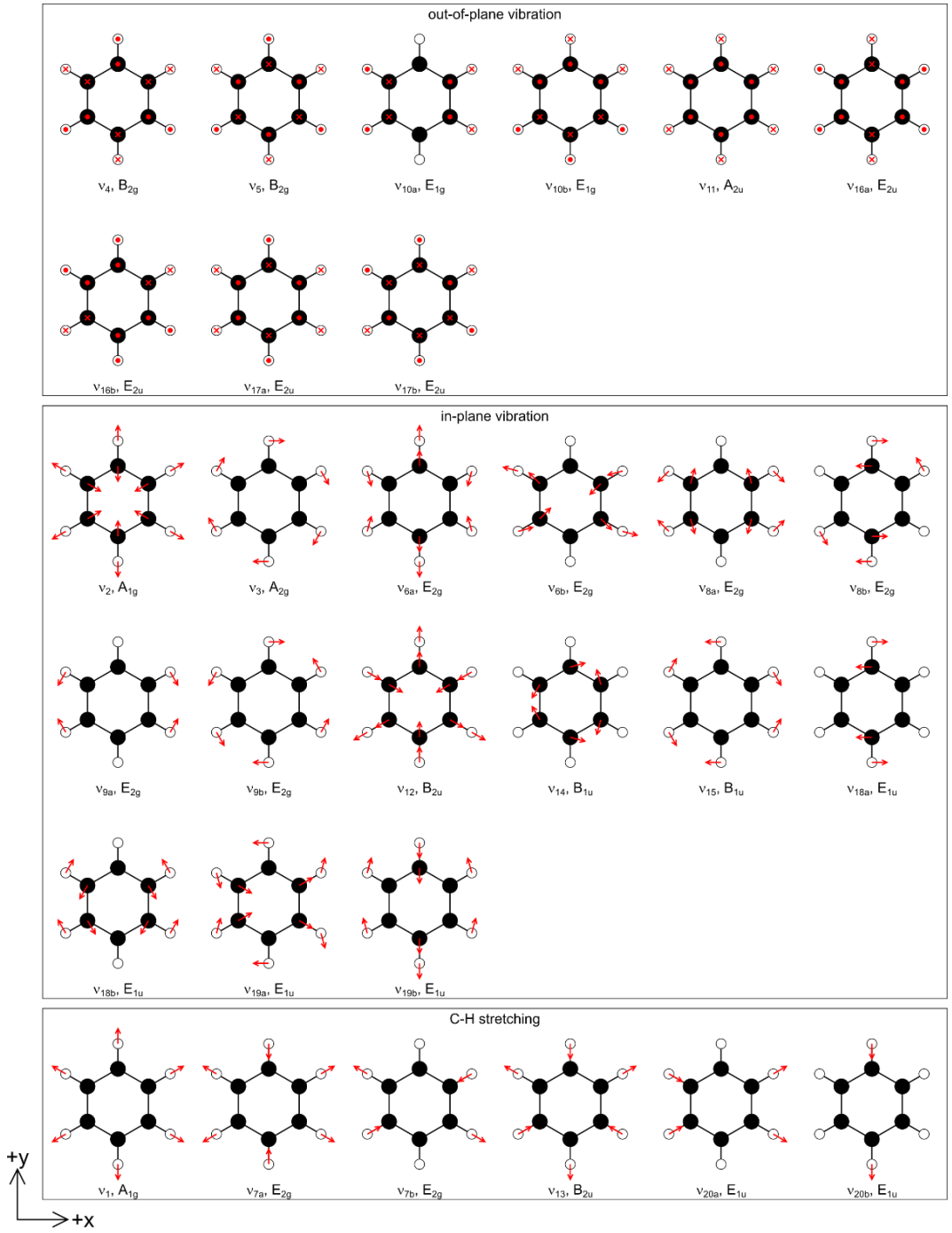

Scheme B-2 Graphic representation of vibrational modes of benzene, showing directions of movements without magnitudes, reproduced from Wilson,[3] Preuss and Bechstedt,[4] and Wang[2]

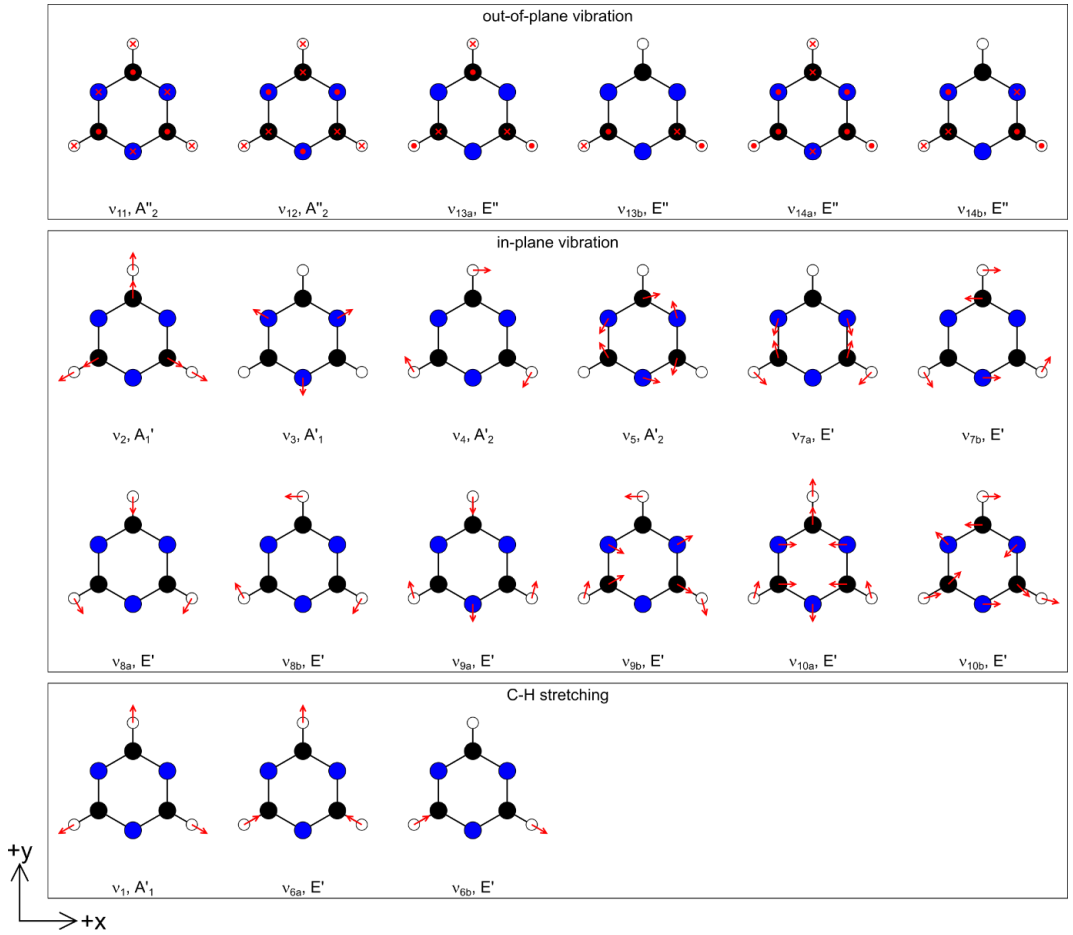

Scheme B-3 Graphic representation of vibrational modes of triazine, showing directions of movements without magnitudes, reproduced from Larkin et al.[1]

B.2 Identification of Monomer Vibrational Peaks

Comparisons between FT-IR transmission spectra of monomers from calculations and from measurements are shown in Figure B-1 to Figure B-5. As explained earlier, however, in order to obtain accurate predictions, calculated energy of vibrations (and therefore wavenumbers) have to be multiplied by scaling factors. Scaling factors reported are varied and depend on the chemical systems considered in each publication.[5] However, the factors can be obtained easily from a comparison between calculated and actual peak positions.[6] Herein, peak positions in the region between 1700 and 1000 cm^{-1} have been used for the determination of the scaling factor (Figure B-6). Several peaks, however, are omitted because their appearances in actual measured spectra are obscuring, rendering determination of actual positions impractical. The factor of 0.9650 obtained in this work is in line with reported values in publications and the database published by the US National Institute of Standards and Technology (NIST)[7] as listed in Table B-1. The major outliers in Figure B-6 are peaks related to NH_2 scissoring between 1700 and 1650 cm^{-1}.

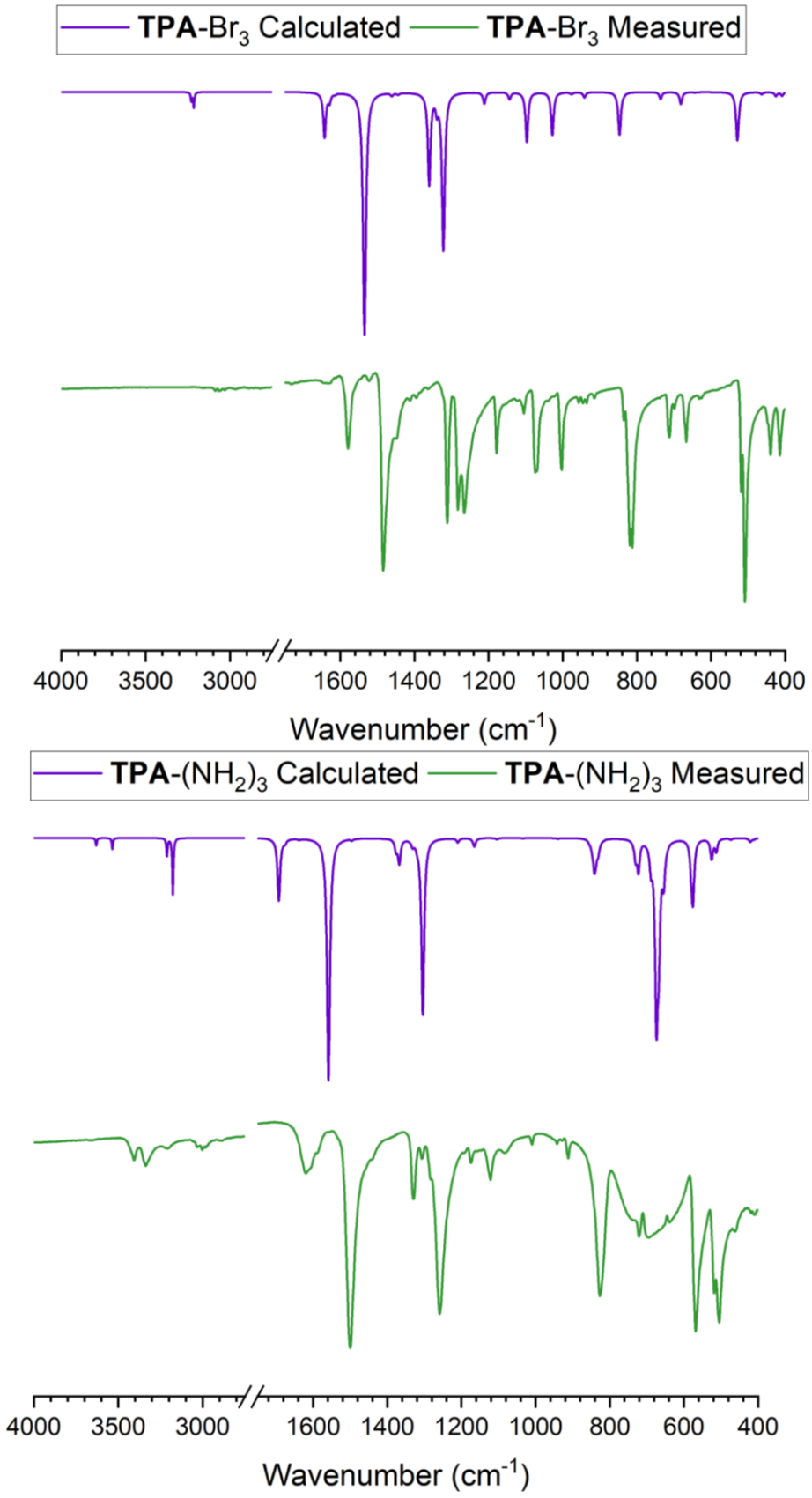

*Figure B-1 Comparison between calculated and measured FT-IR spectra of **TPA**-Br_3 (top) and **TPA**-$(NH_2)_3$ (bottom)*

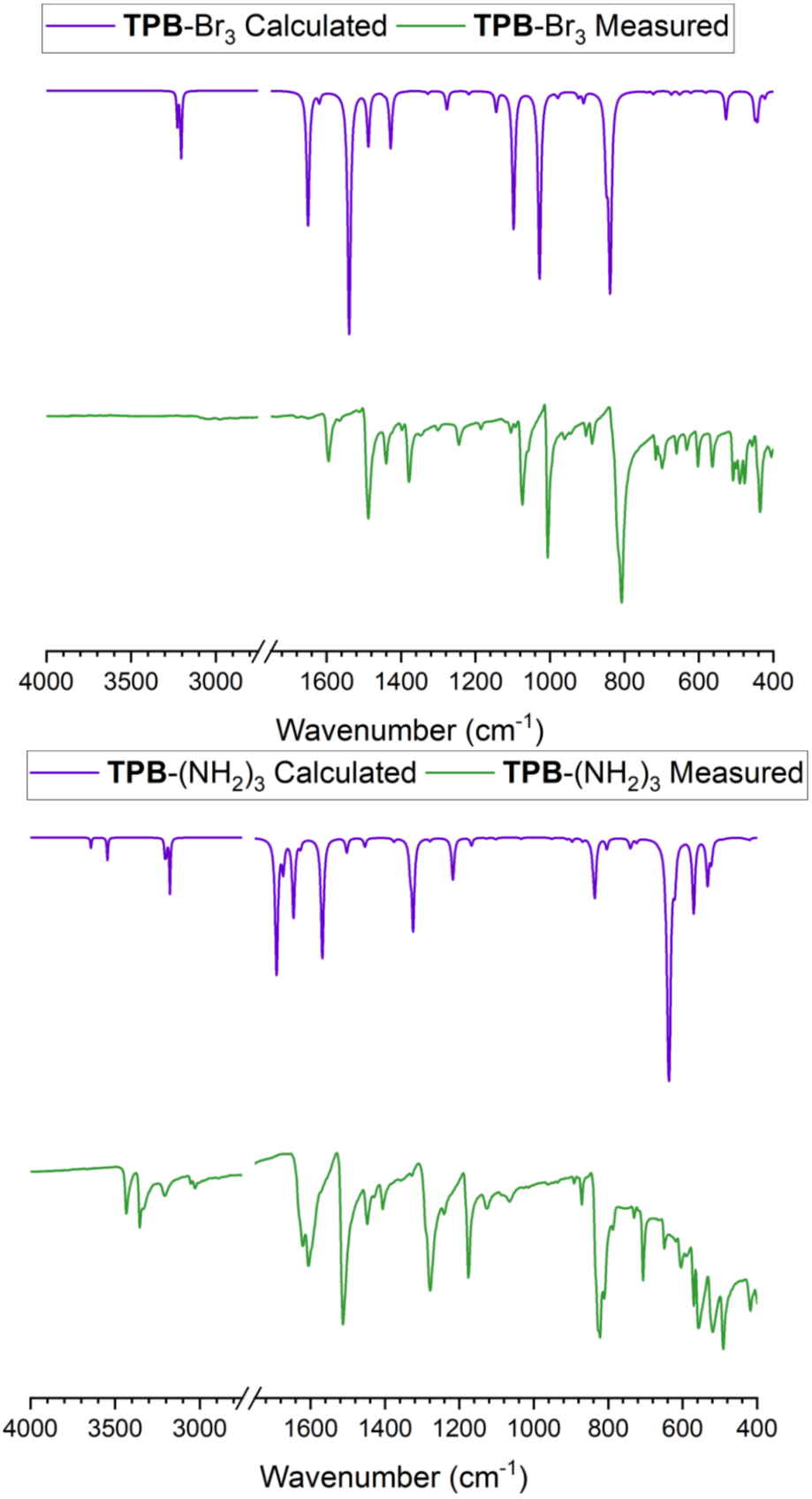

*Figure B-2 Comparison between calculated and measured FT-IR spectra of **TPB**-Br_3 (top) and **TPB**-$(NH_2)_3$ (bottom)*

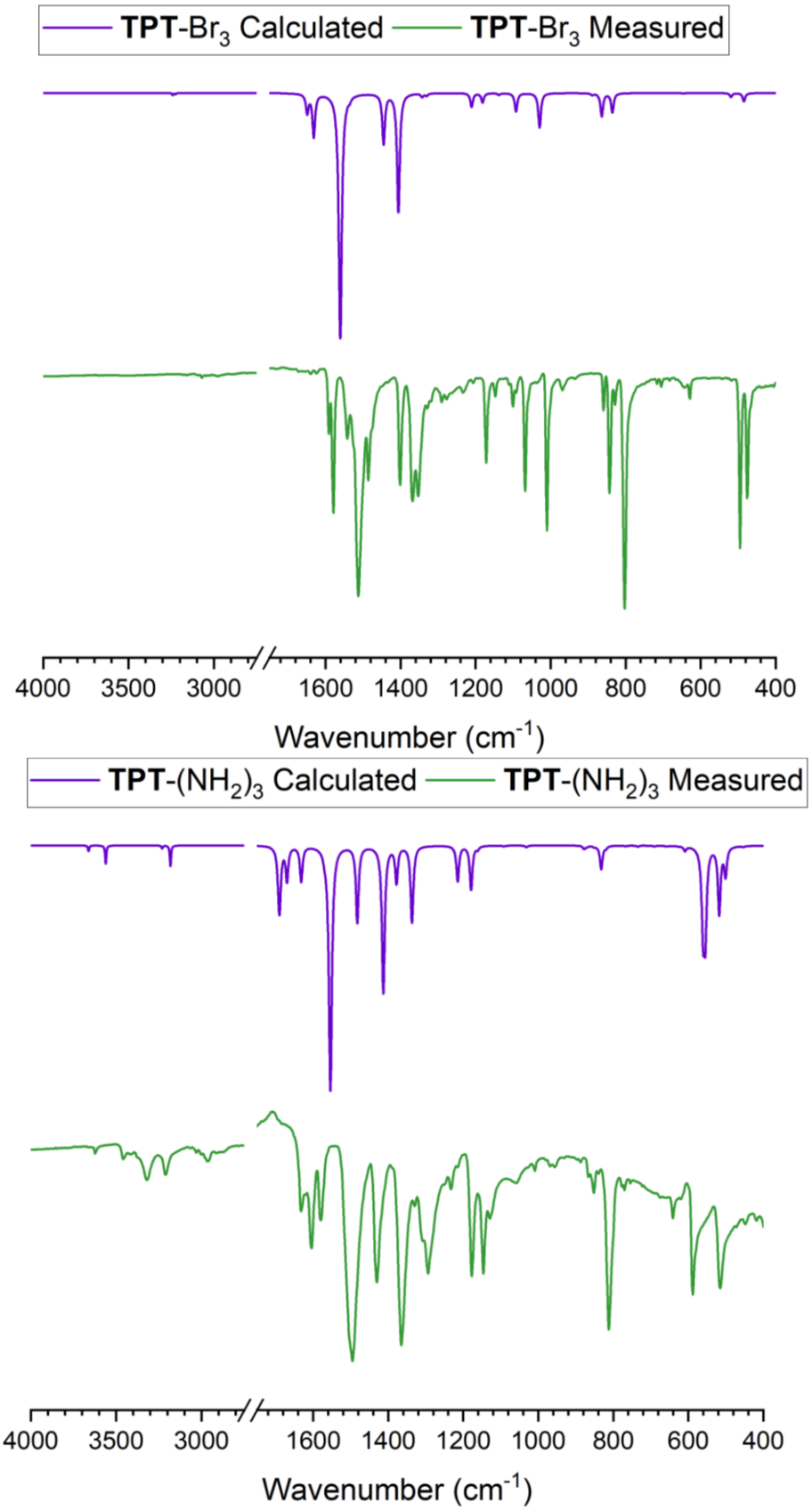

*Figure B-3 Comparison between calculated and measured FT-IR spectra of **TPT**-Br_3 (top) and **TPT**-$(NH_2)_3$ (bottom)*

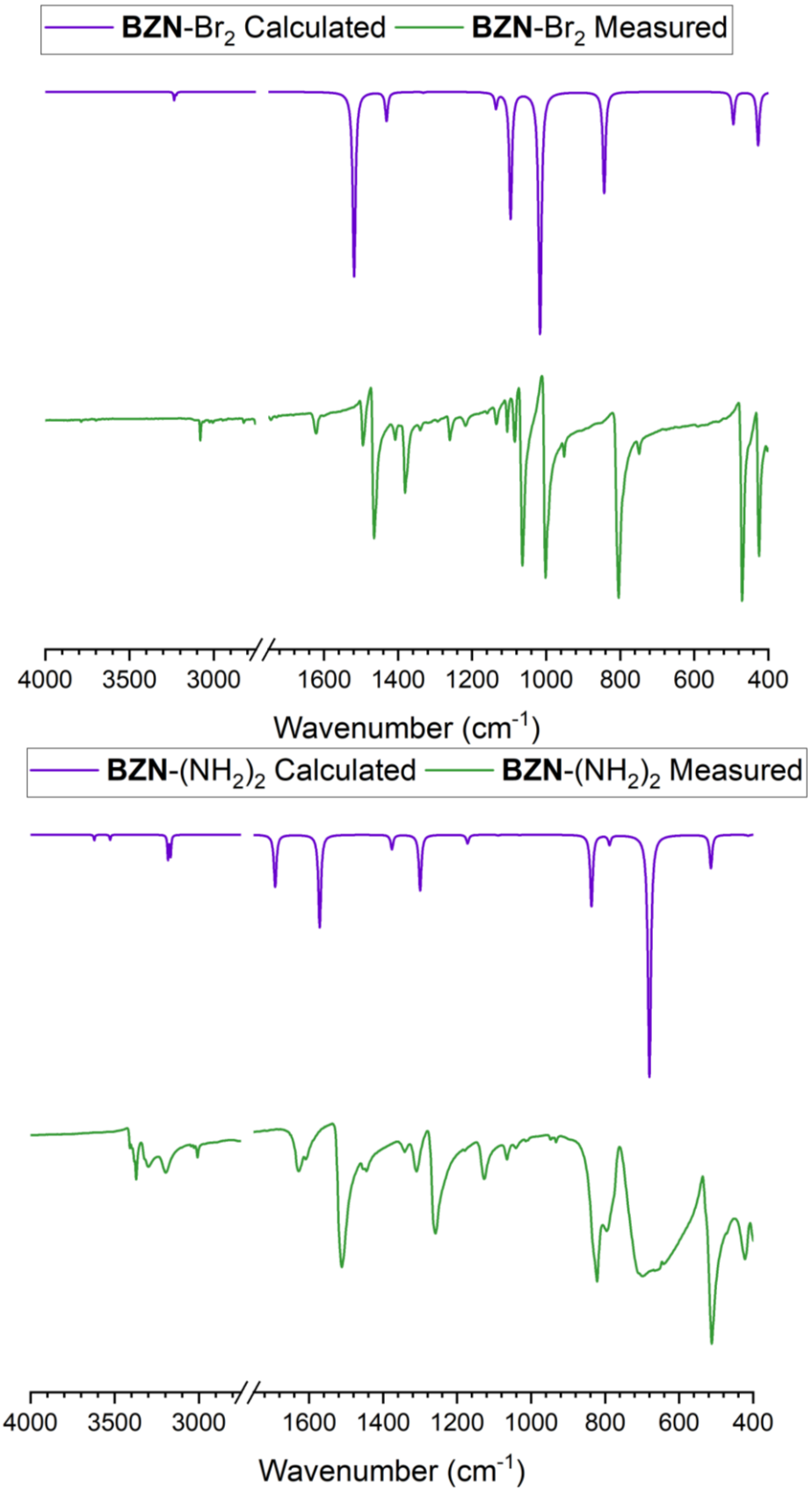

*Figure B-4 Comparison between calculated and measured FT-IR spectra of **BZN**-Br_2 (top) and **FLR**-$(NH_2)_2$ (bottom)*

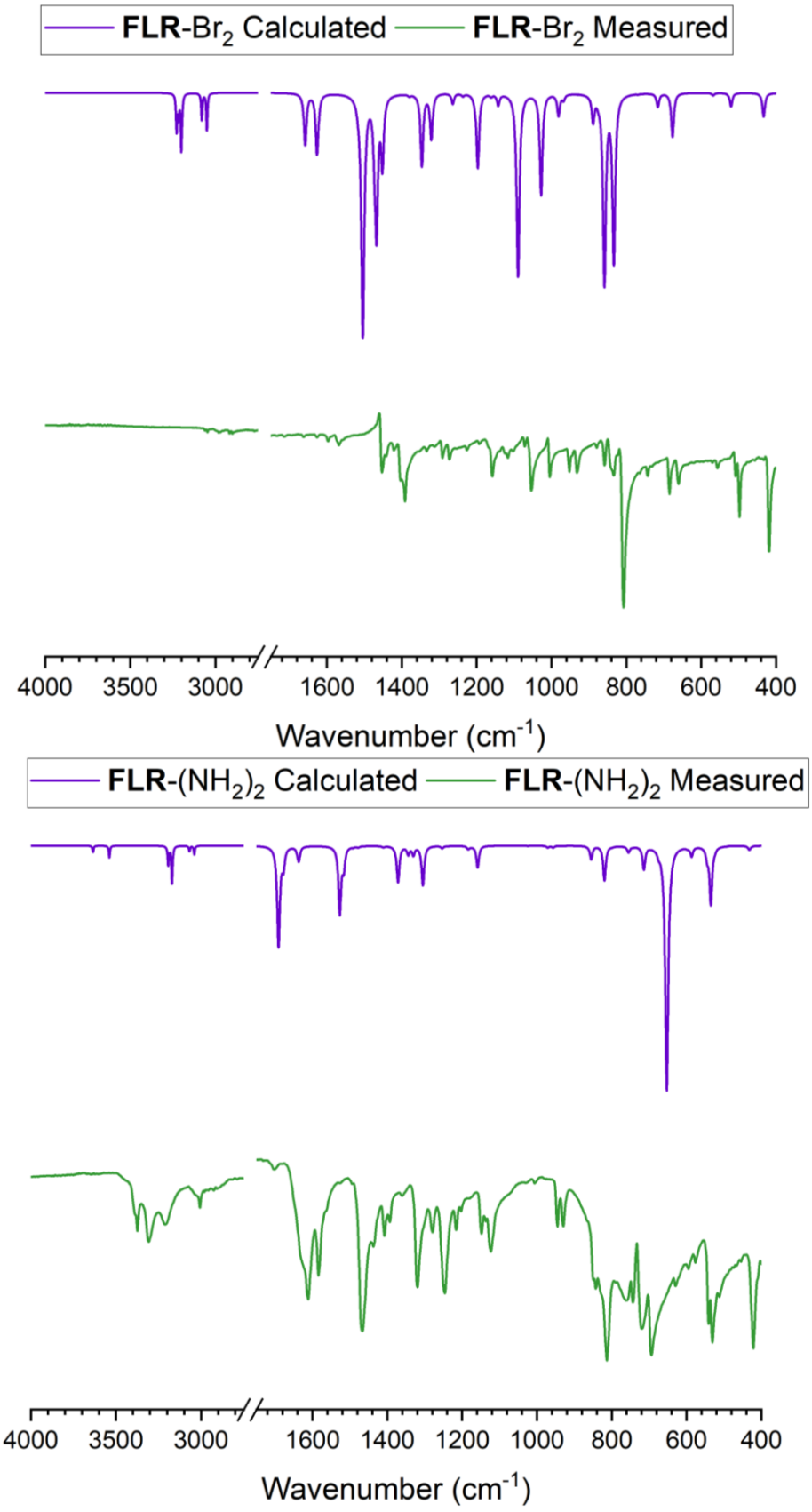

*Figure B-5 Comparison between calculated and measured FT-IR spectra of **FLR**-Br_2 (top) and **FLR**-$(NH_2)_2$ (bottom)*

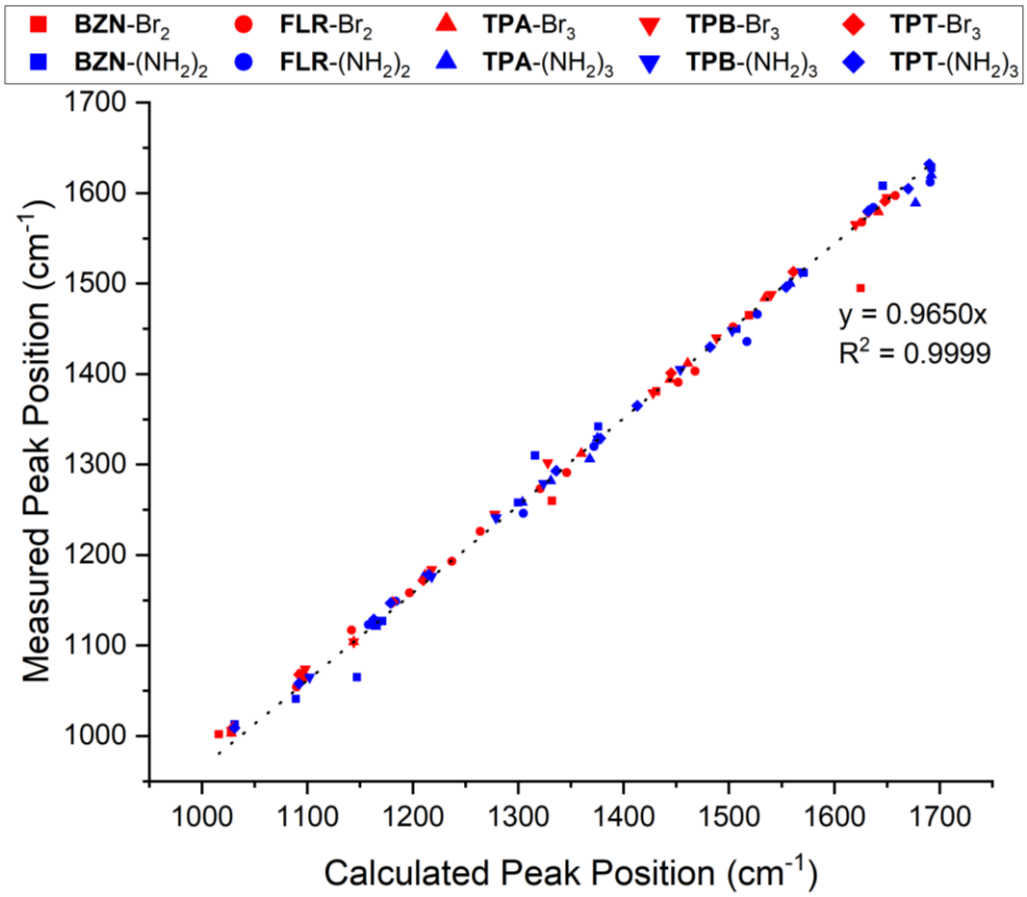

Figure B-6 Linear plot between calculated and measured FT-IR transmission spectra of monomers in the 1700-1000 cm-1

Table B-1 Comparison of scaling factor in this work for PANI-CMPs systems with other reported values for B3LYP functional and 6-31G(d) basis set

Source	System of Interest	Scaling Factor
this work	monomers for PANI-CMPs	0.9650
Rauhut and Pulay (1995)[6]	20 small organic compounds of C, H, O, and N with various functional groups	0.928
	same system, with different modes reported separately	0.806-0.990
Sundius (2002)[8]	ethylene, different modes reported separately	0.905-1.019
Scott and Radom (1996)[9]	122 small polyatomic molecules with up to 4 heavy atoms in the first and second rows of the periodic table and up to 10 atoms in total	0.9614
Merrick *et al.* (2007)[10]		0.9613
NIST Computational Chemistry Comparison and Benchmark Database (2020)[7]		0.960 ± 0.022

Even after scaling, there still be small differences between calculated spectra and their measured counterparts. Generally, absorptions of infrared radiation relate to vibrations of molecules. However, only vibrational modes that result in changes of dipole moments appear in FT-IR transmission spectra, or so-called "IR active". This, in turn, relates to how symmetric the vibrational modes and the molecules themselves are. Meanwhile, calculations in this work are based on structures optimised by DFT calculations which do not take symmetries of molecules into account and may not cover all possible conformations. One example is the amino groups. All DFT-optimised structures of aminated monomers yield $-NH_2$ groups in trigonal pyramidal geometry. However, it is possible that these amino groups can align themselves in trigonal planar geometry as well. The two different geometries can have different symmetries, such as in the case

of **FLR**-$(NH_2)_2$. Amino-pyramidal **FLR**-$(NH_2)_2$ is in either C_2 or C_s symmetry depending on how the two amino groups align themselves relative to each other, while amino-planar **FLR**-$(NH_2)_2$, with 2 σ_v planes compared to none either of those in the amino-pyramidal conformation, is in C_{2v} symmetry. Different symmetries can affect FT-IR transmission spectra in two ways. First, two apparently symmetric modes can appear to be only one peak since their frequencies are too close together to be distinguished. However, if these two modes are not actually symmetric, their frequencies can be different enough to appear split in twain. An example of this phenomenon in this work can be seen in the calculated peak of 1406 cm^{-1} in **TPT**-Br_3 (Figure B-3). On the other hand, symmetries can affect intensities as well as frequencies because different symmetries lead to different dipole moment changes, which in turn lead to different in IR activities. This can explain why some peaks appear negligible in the calculated spectra while the same peaks appear intensely in the measured spectra, or vice versa.

The following tables list the assignments for absorption maxima in the range between 1700 and 1100 cm^{-1}, which are peaks used to calculate the scaling factor. For each peak position, the corresponding vibrational modes are assigned. Many of these peaks are contributed by multiple vibrational modes coupling with each other. Full lists of peak positions from DFT calculations can be found in the following subsection.

*Table B-2 Assignments for absorption maxima in the 1700-1100 cm^{-1} of the FT-IR spectrum of **TPA**-Br_3 core monomer*

Calculated Wavenumber (cm^{-1})		**Measured Wavenumber (cm^{-1})**	**Corresponding Vibration**
Uncorrected	**Corrected (Rounded)**		
1642	1585	1579	bl *as* ν_{8a} × hbl str.
1629	1572	n/a	bl *as* ν_{8b} × hbl str.
1534	1480	1484	bl *as* ν_{18a} × hbl str.
1461	1410	1412	bl *as* ν_{19a} × hbl str.
1444	1393	1394	bl *s* ν_{19a}
1360	1312	1312	bl *as* ν_{19b} × bl *as* ν_{14} × hbl str.
1340	1293	n/a	bl *as* ν_{9b} × bl *as* ν_{14}
1322	1276	*1284*, *1266*	bl *as* ν_{9b} × bl *as* ν_{18b} × hbl str.
1212	1170	1178	bl *s* ν_{9a}
1144	1104	1104	bl *s* ν_{9b}

Note:
Moieties: bl = blade, hbl = hub-blade bond
Vibrational modes: *as* = asymmetric stretching, *s* = symmetric stretching, str. = stretching
Corrected wavenumbers are rounded to nearest integers.
Measured wavenumbers: n/a = cannot be observed in actual spectra, *italic* = obscured or cannot be matched one-to-one with calculated wavenumbers for the determination of scaling factor

*Table B-3 Assignments for absorption maxima in the 1700-1100 cm^{-1} of the FT-IR spectrum of **TPA**-$(NH_2)_3$ core monomer*

Calculated Wavenumber (cm^{-1})		Measured Wavenumber (cm^{-1})	Corresponding Vibration
Uncorrected	**Corrected (Rounded)**		
1692	1633	1620	bl *as* ν_{8a} × NH_2 δ
1677	1618	1589	bl *as* ν_{8a} × hbl str. × NH_2 δ
1638	1581	*1585*	bl *as* ν_{8b} × hbl str. × NH_2 τ
1558	1503	1500	bl *as* ν_{18b} × hbl str.
1495	1443	*1437*	bl *as* ν_{19b} × hbl str. × NH_2 τ
1375	1327	1329	bl *as* ν_{9a} × bl *as* ν_{14} × NH_2 τ
1368	1320	1306	bl *as* ν_{9a} × bl *as* ν_{14} × hbl str.
1331	1284	1282	bl *as* ν_{9a} × hbl str. × C–NH_2 str.
1304	1258	1258	bl *as* ν_{19b} × hbl str. × C–NH_2 str.
1210	1168	1175	bl *as* ν_{9a}
1165	1124	1121	bl *s* ν_{18a} × NH_2 τ

Note:
Moieties: bl = blade, hbl = hub-blade bond, NH_2 = amino group
Vibrational modes: *as* = asymmetric stretching, *s* = symmetric stretching, str. = stretching, δ = bending, τ = twisting
Corrected wavenumbers are rounded to nearest integers.
Measured wavenumbers: n/a = cannot be observed in actual spectra, *italic* = obscured or cannot be matched one-to-one with calculated wavenumbers for the determination of scaling factor

*Table B-4 Assignments for absorption maxima in the 1700-1100 cm^{-1} of the FT-IR spectrum of **TPB**-Br_3 core monomer*

Calculated Wavenumber (cm^{-1})		Measured Wavenumber (cm^{-1})	Corresponding Vibration
Uncorrected	**Corrected (Rounded)**		
1650	1592	1595	bl *as* ν_{8a} × h ν_8
1620	1563	1565	bl *as* ν_{8b} × h ν_{18}
1540	1486	1488	bl *as* ν_{18b}
1488	1436	1440	bl *as* ν_{19a} × h ν_{18}
1428	1378	1379	bl *as* ν_{19a} × h ν_{18}
1328	1282	1302	bl *as* ν_{9b} × bl *as* ν_{14} × h ν_9
1278	1233	1245	bl *as* ν_{19b} × h ν_9 × hbl str.
1218	1175	1184	bl *s* ν_{9a}
1144	1104	1104	bl *as* ν_{9b}

Note:
Moieties: h = hub, bl = blade, hbl = hub-blade bond
Vibrational modes: *as* = asymmetric stretching, *s* = symmetric stretching, str. = stretching
Corrected wavenumbers are rounded to nearest integers.
Measured wavenumbers: n/a = cannot be observed in actual spectra, *italic* = obscured or cannot be matched one-to-one with calculated wavenumbers for the determination of scaling factor

*Table B-5 Assignments for absorption maxima in the 1700-1100 cm^{-1} of the FT-IR spectrum of **TPB**-$(NH_2)_3$ core monomer*

Calculated Wavenumber (cm^{-1})		Measured Wavenumber (cm^{-1})	Corresponding Vibration
Uncorrected	**Corrected (Rounded)**		
1692	1633	n/a	bl *as* ν_{8a} × NH_2 δ
1674	1615	*1620*, *1604*	bl *as* ν_{8a} × NH_2 δ
1646	1588	n/a	bl *as* ν_{8b} × h ν_8 × NH_2 τ
1627	1570	n/a	bl *as* ν_{8b} × h ν_8 × NH_2 τ
1568	1513	1513	bl *as* ν_{18b} × hbl str. × C–NH_2 str.
1503	1450	1448	bl *as* ν_{19b} × h ν_{19} × NH_2 τ
1454	1403	1405	bl *as* ν_{19b} × h ν_{19} × NH_2 τ
1376	1328	1328	bl *as* ν_{9b} × bl *as* ν_{14} × NH_2 τ
1332	1285	n/a	bl *as* ν_{9b} × bl *as* ν_{14} × NH_2 τ
1324	1278	1279	bl *as* ν_{19b} × C–NH_2 str.
1279	1234	1241	bl *as* ν_{19b} × h ν_9 × C–NH_2 str.
1218	1175	1176	bl *s* ν_{9a}
1169	1128	1127	bl *s* ν_{19a} × NH_2 τ

Note:
Moieties: bl = blade, hbl = hub-blade, NH_2 = amino group
Vibrational modes: *as* = asymmetric stretching, *s* = symmetric stretching, str. = stretching, δ = bending, τ = twisting
Corrected wavenumbers are rounded to nearest integers.
Measured wavenumbers: n/a = cannot be observed in actual spectra, *italic* = obscured or cannot be matched one-to-one with calculated wavenumbers for the determination of scaling factor

*Table B-6 Assignments for absorption maxima in the 1700-1100 cm^{-1} of the FT-IR spectrum of **TPT**-Br_3 core monomer*

Calculated Wavenumber (cm^{-1})		Measured Wavenumber (cm^{-1})	Corresponding Vibration
Uncorrected	**Corrected (Rounded)**		
1648	1590	1591	bl *as* ν_{8a} × h ν_{TZ7}
1632	1575	1579	bl *as* ν_{8b} × h ν_{TZ7}
1561	1506	1513	bl *as* ν_{8a} × h ν_{TZ7} × hbl str.
1445	1394	1401	bl *as* ν_{19b} × h $\nu_{TZ8/9}$ × hbl str.
1405	1356	*1370*, *1355*	bl *as* ν_{19a} × h $\nu_{TZ8/9}$ × hbl str.
1342	1295	*1292*	bl *as* ν_{9b} × bl *as* ν_{14} × h $\nu_{TZ8/9}$ × hbl str.
1331	1284	*1277*	bl *as* ν_{14}
1210	1168	1172	bl *as* ν_{9a}
1181	1140	1148	bl *as* ν_{19a} × h $\nu_{TZ8/9}$ × hbl str.

Note:
Moieties: h = hub, bl = blade, hbl = hub-blade bond
Vibrational modes: *as* = asymmetric stretching, *s* = symmetric stretching, str. = stretching
Corrected wavenumbers are rounded to nearest integers.
Measured wavenumbers: n/a = cannot be observed in actual spectra, *italic* = obscured or cannot be matched one-to-one with calculated wavenumbers for the determination of scaling factor

*Table B-7 Assignments for absorption maxima in the 1700-1100 cm^{-1} of the FT-IR spectrum of **TPT**-$(NH_2)_3$ core monomer*

Calculated Wavenumber (cm^{-1})		Measured Wavenumber (cm^{-1})	Corresponding Vibration
Uncorrected	Corrected (Rounded)		
1690	1631	1632	bl *as* ν_{8a} × NH_2 δ
1670	1612	1605	bl *as* ν_{8a} × hbl str. × NH_2 δ
1632	1575	1580	bl *as* ν_{8b} × h ν_{TZ7} × NH_2 τ
1554	1500	1496	bl *as* ν_{19a} × h ν_{TZ7} × NH_2 τ
1482	1430	1430	bl *as* ν_{19a} × h ν_{TZ7} × NH_2 τ
1413	1364	1365	bl *as* ν_{19b} × h $\nu_{TZ8/9}$ × NH_2 τ
1378	1330	1329	bl *as* ν_{19b} × bl *as* ν_{14} × h $\nu_{TZ8/9}$ × NH_2 τ
1336	1289	1293	bl *as* ν_{9b} × hbl str. × C–NH_2 str.
1215	1172	1178	bl *as* ν_{8a} × h $\nu_{TZ8/9}$
1179	1138	1147	bl *as* ν_{8a} × h $\nu_{TZ8/9}$ × hbl str.
1163	1122	1129	bl *as* ν_{19a} × NH_2 τ

Note:
Moieties: bl = blade, hbl = hub-blade, NH_2 = amino group
Vibrational modes: *as* = asymmetric stretching, *s* = symmetric stretching, str. = stretching, δ = bending, τ = twisting
Corrected wavenumbers are rounded to nearest integers.
Measured wavenumbers: n/a = cannot be observed in actual spectra, *italic* = obscured or cannot be matched one-to-one with calculated wavenumbers for the determination of scaling factor

*Table B-8 Assignments for absorption maxima in the 1700-1100 cm^{-1} of the FT-IR spectrum of **BZN**-Br_2 linker monomer*

Calculated Wavenumber (cm^{-1})		Measured Wavenumber (cm^{-1})	Corresponding Vibration
Uncorrected	Corrected (Rounded)		
1625	1568	1495	ν_{8a}
1519	1466	1465	ν_{19b}
1431	1381	1381	ν_{18a}
1332	1285	1260	ν_{14}

Note: Corrected wavenumbers are rounded to nearest integers.

*Table B-9 Assignments for absorption maxima in the 1700-1100 cm^{-1} of the FT-IR spectrum of **BZN**-$(NH_2)_2$ linker monomer*

Calculated Wavenumber (cm^{-1})		Measured Wavenumber (cm^{-1})	Corresponding Vibration
Uncorrected	Corrected (Rounded)		
1692	1633	1628	NH_2 δ × C–NH_2 str.
1646	1588	1608	ν_{8b} × NH_2 τ
1571	1516	1512	ν_{19b} × C–NH_2 str.
1507	1454	1450	ν_{19a} × NH_2 τ
1376	1328	1342	ν_{14} × NH_2 τ
1316	1270	1310	ν_{8a} × C–NH_2 str.
1300	1254	1258	ν_{18b} × C–NH_2 str.
1214	1172	1178	ν_{9a}
1171	1130	1127	ν_{15} × NH_2 τ

Note:
Moieties: bl = blade, hbl = hub-blade, NH_2 = amino group
Vibrational modes: *as* = asymmetric stretching, *s* = symmetric stretching, str. = stretching, δ = bending, τ = twisting
Corrected wavenumbers are rounded to nearest integers.
Measured wavenumbers: n/a = cannot be observed in actual spectra, *italic* = obscured or cannot be matched one-to-one with calculated wavenumbers for the determination of scaling factor

*Table B-10 Assignments for absorption maxima in the 1700-1100 cm^{-1} of the FT-IR spectrum of **FLR**-Br_2 linker monomer*

Calculated Wavenumber (cm^{-1})		Measured Wavenumber (cm^{-1})	Corresponding Vibration
Uncorrected	Corrected (Rounded)		
1658	1600	1597	*as* ν_{8a}
1626	1569	1568	*as* ν_{8b} × CH_2 ω
1504	1451	1452	*as* ν_{19b}
1468	1417	1403	*as* ν_{19a} × CH_2 ω
1452	1401	1391	*s* ν_{19a} × CH_2 δ
1346	1299	1291	*as* ν_{14} × CH_2 ω
1321	1275	1273	*as* ν_3 × CH_2 ω
1264	1220	1226	*s* ν_{15}
1197	1155	1158	*as* ν_{15} × CH_2 ω
1142	1102	1117	*s* ν_{9a}

Note:
Vibrational modes: *as* = asymmetric stretching, *s* = symmetric stretching, str. = stretching, δ = bending, ω = wagging
Corrected wavenumbers are rounded to nearest integers.

*Table B-11 Assignments for absorption maxima in the 1700-1100 cm^{-1} of the FT-IR spectrum of **FLR**-$(NH_2)_2$ linker monomer*

Calculated Wavenumber (cm^{-1})		Measured Wavenumber (cm^{-1})	Corresponding Vibration
Uncorrected	Corrected (Rounded)		
1691	1632	1612	*as* $\nu_{8a} \times NH_2\ \delta$
1678	1619	n/a	*as* $\nu_{8a} \times NH_2\ \delta$
1637	1580	1584	*as* $\nu_{8b} \times CH_2\ \omega$
1527	1474	1466	*as* $\nu_{18a} \times CH_2\ \omega$
1517	1464	1436	*as* $\nu_{19a} \times CH_2\ \omega \times NH_2\ \tau$
1372	1324	1320	*as* $\nu_{14} \times CH_2\ \omega \times NH_2\ \tau$
1344	1297	n/a	*as* $\nu_3 \times CH_2\ \omega$
1330	1283	*1281*	*s* $\nu_3 \times NH_2\ \tau$
1305	1259	1246	*as* $\nu_{9a} \times CH_2\ \omega \times$ C–NH_2 str.
1253	1209	*1214*	*s* ν_{9a}
1184	1143	1149	*s* ν_{15}
1158	1117	1123	*s* $\nu_{19a} \times CH_2\ \omega$

Note:
Moieties: bl = blade, hbl = hub-blade, NH_2 = amino group
Vibrational modes: *as* = asymmetric stretching, *s* = symmetric stretching, str. = stretching, δ = bending, τ = twisting, ω = wagging
Corrected wavenumbers are rounded to nearest integers.
Measured wavenumbers: n/a = cannot be observed in actual spectra, *italic* = obscured or cannot be matched one-to-one with calculated wavenumbers for the determination of scaling factor

B.2.1 Full Lists of DFT-Calculated Vibrational Peak Positions

*Table B-12 All vibrational peak positions (raw data and corrected data with scaling factor of 0.9650) from DFT calculations of **TPA**-Br_3 core monomer*

Calculated Peak Pos. (cm^{-1})	Corrected Peak Pos. (cm^{-1})	Extinction Coeff. (M^{-1}·cm^{-1})
3230.68	3117.61	0.02
3230.08	3117.02	0.06
3229.88	3116.84	0.13
3229.21	3116.19	8.50
3228.87	3115.86	7.70
3228.78	3115.77	10.65
3216.58	3104.00	0.32
3216.56	3103.98	0.43
3216.08	3103.52	0.76
3215.19	3102.66	0.07
3214.82	3102.30	23.43
3214.82	3102.30	23.42
1656.69	1598.71	0.00
1642.60	1585.11	140.86
1642.53	1585.04	141.49
1629.04	1572.02	26.35
1629.03	1572.02	26.65
1614.63	1558.12	6.68
1538.14	1484.30	1.36
1534.82	1481.11	1076.07
1534.75	1481.03	1077.03

Calculated Peak Pos. (cm^{-1})	Corrected Peak Pos. (cm^{-1})	Extinction Coeff. ($M^{-1} \cdot cm^{-1}$)
1461.01	1409.87	9.44
1460.90	1409.77	9.49
1444.40	1393.85	12.85
1360.31	1312.69	365.37
1360.29	1312.68	369.97
1339.64	1292.75	53.88
1339.58	1292.69	58.37
1337.11	1290.31	1.30
1322.08	1275.80	710.35
1321.93	1275.66	702.96
1314.69	1268.67	1.32
1226.41	1183.49	0.00
1211.61	1169.20	46.23
1211.46	1169.06	47.06
1207.21	1164.96	0.00
1146.05	1105.94	2.76
1145.94	1105.83	3.02
1143.13	1103.12	56.68
1096.97	1058.57	234.82
1096.91	1058.52	199.32
1096.63	1058.25	35.62
1028.04	992.06	215.74
1027.87	991.90	199.38
1027.73	991.75	15.60
976.97	942.77	8.10
976.84	942.65	8.46
975.14	941.01	0.01
973.39	939.32	1.58
973.32	939.25	0.99
973.23	939.17	2.18
941.40	908.45	27.77
941.40	908.45	27.71
847.89	818.21	43.51
847.85	818.17	45.94
846.58	816.95	439.13
841.62	812.16	0.11
835.93	806.67	6.76
835.74	806.49	6.41
756.97	730.47	0.00
735.80	710.05	46.59
735.80	710.05	46.29
724.93	699.55	0.54
681.43	657.58	88.48
681.42	657.57	88.51
650.30	627.54	0.00
643.34	620.82	4.10
643.27	620.75	4.09
529.13	510.61	444.64
529.12	510.60	444.41
525.52	507.12	104.85
463.29	447.07	46.28

Calculated Peak Pos. (cm^{-1})	Corrected Peak Pos. (cm^{-1})	Extinction Coeff. ($M^{-1}·cm^{-1}$)
446.66	431.02	0.00
430.77	415.69	0.00
424.88	410.00	45.81
424.87	410.00	47.11
408.11	393.83	43.09
407.99	393.71	43.78
333.73	322.05	46.80
333.73	322.05	47.55
305.35	294.67	7.50
280.68	270.86	23.97
280.64	270.82	24.06
219.60	211.92	4.92
194.26	187.46	36.19
194.21	187.41	35.96
155.48	150.04	0.00
122.83	118.53	29.21
122.74	118.44	29.11
109.80	105.96	0.61
83.49	80.57	0.00
39.73	38.34	235.32
39.64	38.26	234.48
23.85	23.01	42.37
23.58	22.76	44.43
22.32	21.54	50.58

*Table B-13 All vibrational peak positions (raw data and corrected data with scaling factor of 0.9650) from DFT calculations of **TPA**-$(NH_2)_3$ core monomer*

Calculated Peak Pos. (cm^{-1})	Corrected Peak Pos. (cm^{-1})	Extinction Coeff. ($M^{-1}·cm^{-1}$)
3631.00	3503.91	9.67
3630.79	3503.71	9.90
3630.03	3502.98	10.17
3535.46	3411.72	14.16
3535.18	3411.45	14.86
3534.48	3410.77	15.86
3212.80	3100.35	5.07
3212.49	3100.06	3.39
3212.35	3099.92	6.73
3211.68	3099.27	17.97
3211.53	3099.13	17.45
3211.12	3098.73	27.64
3177.77	3066.55	26.35
3177.15	3065.95	50.69
3176.82	3065.63	78.07
3176.33	3065.16	37.95
3176.13	3064.97	31.89
3175.91	3064.75	41.64
1692.94	1633.69	100.45
1692.57	1633.33	169.76
1692.14	1632.92	279.01
1677.86	1619.13	8.18

Calculated Peak Pos. (cm^{-1})	Corrected Peak Pos. (cm^{-1})	Extinction Coeff. ($M^{-1} \cdot cm^{-1}$)
1675.38	1616.74	4.97
1674.85	1616.23	18.55
1637.65	1580.33	4.31
1637.58	1580.26	4.13
1626.56	1569.63	0.93
1569.18	1514.26	0.54
1558.50	1503.95	1486.88
1558.26	1503.72	1490.40
1495.60	1443.25	6.81
1495.32	1442.99	7.88
1480.60	1428.78	0.44
1376.61	1328.43	58.82
1376.18	1328.02	53.12
1369.84	1321.90	24.75
1367.42	1319.56	112.44
1367.22	1319.36	121.66
1331.94	1285.32	33.70
1331.31	1284.71	26.71
1319.14	1272.97	43.51
1315.48	1269.43	0.32
1304.17	1258.52	1177.05
1304.08	1258.44	1143.84
1231.26	1188.16	0.10
1209.91	1167.56	23.60
1209.48	1167.15	25.22
1202.61	1160.51	0.01
1166.83	1125.99	16.51
1166.63	1125.79	16.81
1164.49	1123.73	76.05
1107.12	1068.37	0.64
1106.52	1067.79	1.03
1104.13	1065.49	17.64
1034.31	998.11	3.66
1033.96	997.77	2.89
1032.04	995.92	0.62
952.19	918.87	0.26
951.24	917.94	1.47
941.77	908.81	0.30
940.62	907.70	2.45
940.28	907.37	3.13
939.98	907.08	5.78
931.15	898.56	0.51
930.39	897.83	3.26
854.77	824.85	38.07
847.56	817.89	102.76
841.75	812.29	415.06
837.84	808.52	246.91
831.34	802.24	198.59
825.84	796.94	29.23
822.23	793.45	0.62
818.11	789.48	9.71

Calculated Peak Pos. (cm^{-1})	Corrected Peak Pos. (cm^{-1})	Extinction Coeff. ($M^{-1} \cdot cm^{-1}$)
816.96	788.37	3.40
736.49	710.72	23.59
730.20	704.64	336.02
722.71	697.42	593.69
688.95	664.84	486.34
673.99	650.40	4590.83
667.80	644.43	2246.43
662.39	639.21	23.08
656.36	633.38	161.34
654.22	631.32	698.57
645.02	622.45	30.17
580.02	559.72	535.04
575.67	555.52	1503.62
525.34	506.96	546.79
512.85	494.90	282.01
512.30	494.37	64.72
473.36	456.79	44.28
426.91	411.97	2.54
421.08	406.34	78.73
420.56	405.84	45.65
412.87	398.42	23.46
410.73	396.36	22.27
375.60	362.45	36.30
362.70	350.00	76.68
362.31	349.63	18.01
302.51	291.92	65.67
278.52	268.77	30.78
278.29	268.55	22.85
270.64	261.17	414.40
266.44	257.11	424.43
262.79	253.59	428.46
250.26	241.50	0.22
162.82	157.12	161.73
161.74	156.08	35.29
142.33	137.35	65.19
78.16	75.42	34.80
54.91	52.99	51.08
54.49	52.58	18.13
36.57	35.29	355.56
34.42	33.22	625.19
27.81	26.83	395.45

*Table B-14 All vibrational peak positions (raw data and corrected data with scaling factor of 0.9650) from DFT calculations of **TPB**-Br_3 core monomer*

Calculated Peak Pos. (cm^{-1})	Corrected Peak Pos. (cm^{-1})	Extinction Coeff. ($M^{-1} \cdot cm^{-1}$)
3228.90	3115.89	0.15
3228.76	3115.75	1.60
3228.71	3115.71	2.26
3227.49	3114.53	11.83
3227.45	3114.49	17.10

Calculated Peak Pos. (cm^{-1})	Corrected Peak Pos. (cm^{-1})	Extinction Coeff. ($M^{-1} \cdot cm^{-1}$)
3227.39	3114.43	1.34
3211.72	3099.31	0.12
3210.85	3098.47	7.03
3210.76	3098.38	5.74
3205.36	3093.17	19.92
3204.59	3092.43	16.33
3204.09	3091.95	20.13
3202.47	3090.38	2.54
3201.79	3089.73	4.66
3201.07	3089.03	8.33
1650.91	1593.13	0.96
1650.51	1592.75	82.96
1650.32	1592.56	64.40
1649.59	1591.85	66.33
1649.47	1591.74	82.80
1619.86	1563.17	9.04
1619.49	1562.81	9.38
1619.00	1562.33	0.17
1541.97	1488.00	0.13
1539.58	1485.70	336.73
1539.38	1485.50	336.33
1488.17	1436.09	56.75
1487.79	1435.72	62.16
1445.92	1395.31	3.36
1428.06	1378.08	77.04
1427.92	1377.94	54.16
1386.77	1338.23	0.00
1366.25	1318.43	0.01
1343.03	1296.02	0.07
1340.50	1293.58	0.42
1340.35	1293.44	0.92
1336.08	1289.32	0.06
1327.94	1281.46	3.70
1327.75	1281.28	3.32
1304.43	1258.78	0.52
1277.43	1232.72	24.72
1276.29	1231.62	22.67
1218.61	1175.95	0.35
1218.03	1175.40	3.72
1217.56	1174.95	4.57
1144.56	1104.50	35.77
1144.06	1104.02	18.82
1142.75	1102.75	1.37
1127.76	1088.29	0.35
1127.05	1087.60	0.22
1099.96	1061.46	0.00
1097.78	1059.35	228.86
1097.50	1059.09	226.08
1051.90	1015.08	0.00
1028.05	992.07	355.72
1027.95	991.97	353.26

Calculated Peak Pos. (cm^{-1})	Corrected Peak Pos. (cm^{-1})	Extinction Coeff. ($M^{-1} \cdot cm^{-1}$)
1025.12	989.24	0.56
1017.93	982.30	0.08
982.56	948.17	0.78
981.09	946.75	0.62
980.73	946.41	1.72
979.23	944.96	4.74
977.82	943.60	4.23
977.76	943.54	6.53
924.09	891.74	13.44
922.14	889.87	7.40
909.60	877.77	36.48
856.15	826.19	0.27
854.98	825.05	4.02
851.25	821.45	22.77
849.88	820.13	63.99
849.32	819.59	8.83
847.93	818.25	213.85
839.55	810.17	360.70
837.75	808.43	601.85
744.32	718.27	0.13
742.87	716.86	1.14
739.54	713.65	3.46
722.04	696.77	13.46
720.75	695.52	0.03
673.82	650.24	7.55
673.54	649.97	10.46
653.47	630.59	1.01
652.22	629.39	14.10
647.31	624.65	6.39
623.42	601.60	0.28
621.50	599.74	11.14
581.56	561.20	10.06
527.02	508.57	171.69
513.76	495.78	10.65
463.07	446.87	4.94
449.31	433.58	162.71
442.51	427.02	179.96
424.06	409.21	1.14
422.75	407.96	19.72
422.32	407.54	26.48
402.64	388.55	0.09
375.08	361.95	69.09
362.97	350.27	51.85
335.74	323.99	10.53
323.91	312.57	2.36
316.63	305.54	0.59
260.16	251.06	0.17
246.71	238.07	18.80
246.28	237.66	20.94
205.23	198.04	13.92
196.19	189.32	11.18

Calculated Peak Pos. (cm^{-1})	Corrected Peak Pos. (cm^{-1})	Extinction Coeff. ($M^{-1}{\cdot}cm^{-1}$)
191.60	184.89	14.25
149.02	143.81	9.60
137.81	132.99	0.19
128.47	123.97	7.45
104.28	100.63	0.77
76.20	73.54	0.01
62.11	59.93	0.07
50.17	48.42	0.02
42.30	40.82	0.50
40.60	39.18	0.10
27.52	26.56	18.60
23.19	22.38	13.06
19.45	18.77	32.41

*Table B-15 All vibrational peak positions (raw data and corrected data with scaling factor of 0.9650) from DFT calculations of **TPB**-$(NH_2)_3$ core monomer*

Calculated Peak Pos. (cm^{-1})	Corrected Peak Pos. (cm^{-1})	Extinction Coeff. ($M^{-1}{\cdot}cm^{-1}$)
3643.03	3515.52	13.18
3642.61	3515.12	13.50
3642.38	3514.90	12.45
3545.88	3421.77	27.96
3545.57	3421.47	29.82
3545.27	3421.18	29.56
3208.20	3095.91	0.02
3206.49	3094.26	28.96
3206.37	3094.15	33.87
3201.90	3089.83	21.22
3201.04	3089.00	12.92
3199.32	3087.35	3.45
3198.78	3086.82	0.43
3196.75	3084.86	8.73
3196.60	3084.72	41.70
3177.38	3066.17	33.13
3176.80	3065.62	14.86
3176.73	3065.55	45.79
3176.63	3065.45	42.52
3176.30	3065.13	53.15
3176.13	3064.97	60.45
1691.78	1632.57	284.49
1691.72	1632.51	513.73
1690.74	1631.57	468.09
1673.79	1615.21	113.02
1673.51	1614.94	85.31
1673.14	1614.58	44.00
1645.93	1588.32	349.57
1645.66	1588.06	342.73
1627.78	1570.81	5.04
1627.32	1570.36	26.89
1626.86	1569.92	31.66
1572.50	1517.46	0.25

Calculated Peak Pos. (cm^{-1})	Corrected Peak Pos. (cm^{-1})	Extinction Coeff. ($M^{-1} \cdot cm^{-1}$)
1568.48	1513.58	591.30
1568.16	1513.27	581.83
1502.90	1450.30	65.45
1502.44	1449.86	66.08
1483.89	1431.96	0.24
1453.85	1402.97	40.66
1453.76	1402.88	42.22
1389.55	1340.92	0.02
1382.52	1334.13	0.92
1376.16	1327.99	13.90
1375.53	1327.39	20.95
1355.65	1308.20	1.23
1345.94	1298.84	1.37
1332.12	1285.50	143.12
1331.86	1285.25	111.08
1325.24	1278.86	6.13
1324.39	1278.03	489.85
1324.28	1277.93	494.34
1303.88	1258.25	1.79
1279.26	1234.49	14.77
1278.45	1233.70	14.62
1219.21	1176.53	7.27
1217.99	1175.36	243.67
1216.84	1174.25	239.75
1167.54	1126.67	54.49
1167.30	1126.44	34.17
1166.29	1125.47	1.80
1127.28	1087.82	5.86
1126.79	1087.35	4.72
1102.35	1063.76	8.48
1102.09	1063.52	7.38
1100.22	1061.71	5.43
1060.39	1023.28	0.01
1033.94	997.75	7.92
1033.63	997.45	8.76
1023.19	987.38	0.15
1019.29	983.62	0.06
956.75	923.26	0.19
955.91	922.45	0.84
955.79	922.34	1.03
952.20	918.87	1.73
951.83	918.52	7.98
951.11	917.82	6.58
911.12	879.23	11.72
910.64	878.77	7.81
896.67	865.28	55.52
869.11	838.69	16.91
868.64	838.24	29.83
850.38	820.62	21.84
840.75	811.32	201.31
838.49	809.14	58.02

Calculated Peak Pos. (cm^{-1})	Corrected Peak Pos. (cm^{-1})	Extinction Coeff. ($M^{-1} \cdot cm^{-1}$)
835.81	806.56	898.60
828.34	799.35	2.21
827.72	798.75	3.89
826.68	797.75	2.95
803.79	775.66	99.59
803.67	775.54	81.71
744.01	717.97	6.31
741.03	715.09	113.14
738.62	712.77	76.13
723.62	698.29	75.97
664.57	641.31	3.99
664.40	641.15	19.52
659.04	635.97	5.56
645.27	622.69	230.42
638.88	616.52	3246.74
635.54	613.30	4771.69
624.05	602.21	150.65
620.72	598.99	788.17
600.11	579.11	14.16
577.67	557.45	35.67
570.51	550.54	917.54
569.96	550.01	953.63
532.95	514.29	1167.06
522.89	504.59	550.88
491.45	474.25	18.35
435.49	420.25	13.30
428.88	413.87	28.11
421.02	406.28	2.84
420.47	405.75	25.29
419.92	405.22	42.98
394.86	381.04	10.13
376.50	363.32	76.32
371.99	358.97	26.00
341.00	329.06	62.77
324.22	312.87	48.13
315.69	304.64	20.34
306.48	295.75	350.05
304.23	293.59	372.76
300.83	290.30	312.23
261.58	252.43	9.31
260.65	251.52	18.93
228.61	220.60	4.65
210.87	203.49	0.49
184.21	177.76	46.94
164.13	158.39	108.08
131.78	127.17	15.74
98.49	95.04	25.23
83.73	80.80	8.59
49.37	47.64	92.65
45.92	44.31	50.22
44.06	42.52	50.19

Calculated Peak Pos. (cm^{-1})	Corrected Peak Pos. (cm^{-1})	Extinction Coeff. ($M^{-1}{\cdot}cm^{-1}$)
43.05	41.54	58.10
39.96	38.56	87.31
32.62	31.48	307.62

*Table B-16 All vibrational peak positions (raw data and corrected data with scaling factor of 0.9650) from DFT calculations of **TPT**-Br_3 core monomer*

Calculated Peak Pos. (cm^{-1})	Corrected Peak Pos. (cm^{-1})	Extinction Coeff. ($M^{-1}{\cdot}cm^{-1}$)
3242.40	3128.91	0.07
3241.86	3128.39	7.90
3241.79	3128.32	9.44
3240.86	3127.43	2.36
3240.86	3127.43	1.42
3240.29	3126.88	0.07
3225.53	3112.64	2.79
3225.51	3112.62	3.10
3225.39	3112.50	0.00
3224.96	3112.08	0.00
3224.76	3111.89	3.03
3224.74	3111.88	3.05
1649.31	1591.58	0.45
1648.98	1591.26	182.99
1648.92	1591.21	186.28
1631.59	1574.49	432.95
1631.47	1574.37	436.77
1622.51	1565.72	0.01
1560.92	1506.28	3403.94
1560.88	1506.24	3414.11
1545.11	1491.03	0.02
1535.75	1482.00	32.55
1535.62	1481.88	31.45
1456.05	1405.08	0.02
1445.35	1394.76	581.11
1445.26	1394.68	536.46
1444.99	1394.41	36.63
1405.83	1356.63	1517.58
1405.83	1356.63	1515.92
1352.43	1305.10	0.00
1342.42	1295.43	40.89
1342.39	1295.41	41.93
1332.21	1285.58	1.04
1330.86	1284.28	29.40
1330.49	1283.93	25.78
1233.03	1189.87	0.00
1210.87	1168.49	65.03
1210.59	1168.22	181.56
1210.53	1168.16	118.98
1181.67	1140.31	125.21
1181.34	1139.99	126.30
1138.05	1098.21	23.83
1137.55	1097.74	23.47

Calculated Peak Pos. (cm^{-1})	Corrected Peak Pos. (cm^{-1})	Extinction Coeff. ($M^{-1} \cdot cm^{-1}$)
1134.41	1094.70	0.00
1094.77	1056.45	0.46
1092.30	1054.07	273.27
1092.14	1053.91	271.30
1081.77	1043.91	0.00
1029.58	993.55	9.39
1029.46	993.43	537.40
1029.38	993.35	547.52
1015.66	980.11	0.00
1003.92	968.78	0.00
1002.23	967.15	0.00
1001.74	966.68	0.00
994.67	959.86	0.00
994.29	959.49	0.00
992.46	957.72	0.00
889.24	858.11	57.78
872.16	841.64	0.02
871.86	841.35	0.00
863.64	833.41	433.58
863.58	833.35	435.03
857.28	827.27	0.00
856.80	826.81	0.03
855.12	825.19	0.00
835.32	806.08	737.18
769.54	742.61	0.01
769.06	742.14	0.00
737.23	711.42	0.11
730.50	704.93	0.00
695.34	671.00	0.46
695.20	670.87	0.45
687.11	663.06	0.00
687.04	662.99	0.00
646.16	623.55	0.82
646.03	623.42	11.85
645.99	623.38	12.86
613.82	592.34	0.00
519.00	500.83	232.68
487.60	470.53	0.02
487.13	470.08	0.00
484.61	467.65	277.08
484.51	467.55	273.29
422.70	407.90	0.00
422.16	407.38	0.00
421.20	406.46	0.00
414.45	399.95	0.00
382.50	369.11	106.30
382.48	369.09	108.08
323.38	312.07	20.86
290.79	280.61	0.00
282.39	272.51	0.00
282.31	272.43	0.00

Calculated Peak Pos. (cm^{-1})	Corrected Peak Pos. (cm^{-1})	Extinction Coeff. ($M^{-1} \cdot cm^{-1}$)
253.92	245.03	9.31
253.85	244.96	10.30
184.18	177.74	49.75
184.03	177.59	48.68
156.20	150.74	0.00
155.30	149.87	0.00
142.92	137.92	0.00
129.91	125.36	29.18
128.17	123.69	0.03
58.81	56.75	0.00
58.30	56.25	0.00
33.53	32.36	0.06
33.35	32.18	0.05
32.53	31.39	0.00
28.70	27.70	0.07
25.95	25.04	0.00
20.64	19.92	11.04

*Table B-17 All vibrational peak positions (raw data and corrected data with scaling factor of 0.9650) from DFT calculations of **TPT**-$(NH_2)_3$ core monomer*

Calculated Peak Pos. (cm^{-1})	Corrected Peak Pos. (cm^{-1})	Extinction Coeff. ($M^{-1} \cdot cm^{-1}$)
3662.02	3533.85	18.53
3661.59	3533.43	18.76
3661.22	3533.08	18.60
3561.69	3437.03	54.56
3561.16	3436.52	61.95
3560.80	3436.17	71.88
3232.44	3119.30	0.18
3231.70	3118.59	2.06
3231.46	3118.36	4.13
3230.93	3117.84	1.54
3230.56	3117.49	10.40
3229.74	3116.70	14.18
3183.00	3071.59	30.51
3182.70	3071.30	60.31
3182.17	3070.80	61.34
3181.52	3070.17	29.64
3181.34	3070.00	48.94
3181.32	3069.97	10.14
1692.00	1632.78	470.92
1689.67	1630.54	399.32
1689.43	1630.30	778.11
1670.10	1611.64	336.87
1669.79	1611.35	320.30
1669.67	1611.23	95.18
1631.98	1574.86	394.91
1631.90	1574.78	398.41
1625.30	1568.42	0.02
1578.94	1523.68	0.03
1569.43	1514.50	63.07

Calculated Peak Pos. (cm^{-1})	Corrected Peak Pos. (cm^{-1})	Extinction Coeff. ($M^{-1} \cdot cm^{-1}$)
1569.34	1514.42	55.91
1554.29	1499.89	3857.69
1554.16	1499.76	3870.33
1490.75	1438.57	0.64
1482.51	1430.62	993.22
1482.35	1430.47	992.95
1466.90	1415.56	0.26
1413.09	1363.63	2186.71
1412.87	1363.42	2199.76
1386.41	1337.88	0.58
1378.12	1329.89	476.62
1377.76	1329.53	492.89
1342.13	1295.15	1.08
1337.38	1290.57	30.09
1336.80	1290.01	1066.77
1336.65	1289.86	1071.27
1332.80	1286.15	64.82
1332.26	1285.63	19.73
1237.94	1194.62	0.02
1214.77	1172.25	538.94
1214.61	1172.09	544.97
1211.44	1169.04	0.89
1179.43	1138.15	694.55
1178.71	1137.45	695.97
1161.58	1120.92	49.17
1161.06	1120.42	50.36
1159.82	1119.22	1.07
1093.26	1054.99	7.28
1091.30	1053.11	7.72
1090.90	1052.72	13.60
1084.59	1046.63	0.12
1031.65	995.54	28.23
1031.46	995.36	31.73
1029.64	993.60	1.30
1009.94	974.59	0.02
983.09	948.69	3.72
980.05	945.74	0.72
979.18	944.91	0.18
972.59	938.55	0.01
970.69	936.72	0.01
968.65	934.75	0.01
877.72	847.00	68.54
877.67	846.95	67.15
870.34	839.88	44.39
853.31	823.44	4.59
850.89	821.11	36.01
846.10	816.48	9.71
832.11	802.99	1021.11
830.41	801.34	8.08
829.29	800.26	1.47
828.48	799.48	4.65

Calculated Peak Pos. (cm^{-1})	Corrected Peak Pos. (cm^{-1})	Extinction Coeff. ($M^{-1} \cdot cm^{-1}$)
819.36	790.68	37.39
818.65	790.00	59.68
767.41	740.55	18.04
767.15	740.30	16.85
734.60	708.89	56.37
690.33	666.17	27.69
690.11	665.95	12.18
658.30	635.26	16.39
658.07	635.03	16.92
657.69	634.67	0.21
625.15	603.27	12.28
614.92	593.39	0.27
608.66	587.36	246.70
607.98	586.70	27.56
564.88	545.11	337.74
560.32	540.71	5638.35
554.55	535.14	5995.76
517.51	499.39	4969.14
502.66	485.07	246.07
500.56	483.05	1904.08
453.42	437.55	39.44
452.94	437.08	34.22
422.38	407.60	0.09
421.08	406.34	0.29
419.02	404.36	0.12
393.13	379.37	1.45
372.22	359.19	2.75
371.22	358.23	4.44
351.27	338.97	173.64
349.26	337.03	52.20
348.76	336.56	456.89
348.31	336.12	380.84
307.40	296.64	71.63
306.54	295.81	18.66
256.35	247.38	1.17
256.11	247.14	1.11
220.74	213.01	0.05
171.14	165.15	2.49
170.35	164.39	25.65
169.32	163.40	0.25
162.03	156.35	99.18
80.89	78.06	32.45
80.38	77.57	0.79
56.70	54.72	97.19
55.40	53.46	96.28
38.35	37.01	57.55
37.93	36.61	119.03
34.61	33.40	423.75
32.84	31.70	173.51

*Table B-18 All vibrational peak positions (raw data and corrected data with scaling factor of 0.9650) from DFT calculations of **BZN**-Br_2 linker monomer*

Calculated Peak Pos. (cm^{-1})	Corrected Peak Pos. (cm^{-1})	Extinction Coeff. ($M^{-1}{\cdot}cm^{-1}$)
3236.42	3123.15	0.00
3234.92	3121.70	4.48
3223.41	3110.59	0.00
3222.31	3109.53	1.42
1626.29	1569.37	0.00
1624.09	1567.25	0.00
1518.73	1465.58	268.22
1431.15	1381.06	36.24
1333.56	1286.89	0.00
1331.60	1284.99	1.15
1211.41	1169.01	0.00
1135.44	1095.70	24.28
1095.95	1057.59	233.85
1089.42	1051.29	0.00
1016.48	980.91	576.74
986.88	952.34	0.00
985.00	950.53	0.00
844.28	814.73	0.00
843.22	813.71	236.76
721.37	696.12	0.00
718.53	693.38	0.00
640.56	618.14	0.00
494.35	477.05	119.12
427.41	412.45	231.81
424.90	410.02	0.00
316.96	305.87	0.00
275.08	265.45	0.00
214.70	207.19	0.00
167.57	161.70	13.70
79.76	76.97	16.27

*Table B-19 All vibrational peak positions (raw data and corrected data with scaling factor of 0.9650) from DFT calculations of **BZN**-$(NH_2)_2$ linker monomer*

Calculated Peak Pos. (cm^{-1})	Corrected Peak Pos. (cm^{-1})	Extinction Coeff. ($M^{-1}{\cdot}cm^{-1}$)
3621.40	3494.65	0.00
3621.21	3494.46	14.55
3527.73	3404.26	0.00
3527.20	3403.75	14.03
3187.32	3075.76	0.00
3183.86	3072.43	72.62
3168.55	3057.66	0.00
3167.84	3056.97	62.92
1699.56	1640.07	0.00
1691.73	1632.52	300.46
1683.56	1624.64	0.00
1646.86	1589.22	0.00
1571.36	1516.36	602.28

Calculated Peak Pos. (cm^{-1})	Corrected Peak Pos. (cm^{-1})	Extinction Coeff. ($M^{-1} \cdot cm^{-1}$)
1506.70	1453.96	0.25
1376.15	1327.98	98.46
1375.20	1327.07	0.00
1316.47	1270.40	0.00
1299.87	1254.38	421.26
1214.26	1171.76	0.00
1171.68	1130.67	69.79
1146.60	1106.46	0.00
1089.27	1051.14	6.17
1030.92	994.83	3.61
919.10	886.94	0.00
917.22	885.12	0.00
865.64	835.34	0.00
836.84	807.55	849.66
812.42	783.98	0.00
788.17	760.58	113.20
755.85	729.39	0.00
690.05	665.90	0.00
680.26	656.45	4545.78
662.92	639.71	0.00
514.05	496.06	624.25
475.15	458.52	0.00
427.94	412.97	0.00
413.73	399.25	23.58
352.36	340.03	0.00
319.22	308.05	22.11
238.22	229.88	0.00
236.76	228.47	1052.66
149.05	143.84	250.92

*Table B-20 All vibrational peak positions (raw data and corrected data with scaling factor of 0.9650) from DFT calculations of **FLR**-Br_2 linker monomer*

Calculated Peak Pos. (cm^{-1})	Corrected Peak Pos. (cm^{-1})	Extinction Coeff. ($M^{-1} \cdot cm^{-1}$)
3228.51	3115.52	9.55
3228.06	3115.08	4.91
3216.93	3104.34	5.29
3216.75	3104.16	2.88
3201.07	3089.03	21.26
3195.80	3083.95	3.98
3080.84	2973.01	10.74
3050.73	2943.96	15.18
1657.96	1599.93	38.81
1656.03	1598.07	0.29
1626.54	1569.61	46.43
1621.46	1564.71	3.50
1516.44	1463.36	3.40
1504.14	1451.49	265.73
1472.68	1421.14	34.55
1467.39	1416.04	128.72
1451.73	1400.92	61.82

Calculated Peak Pos. (cm^{-1})	Corrected Peak Pos. (cm^{-1})	Extinction Coeff. ($M^{-1} \cdot cm^{-1}$)
1379.78	1331.49	1.62
1346.38	1299.26	69.50
1321.21	1274.97	42.23
1316.96	1270.87	1.73
1263.72	1219.49	10.02
1236.50	1193.22	2.33
1204.78	1162.62	3.17
1196.94	1155.05	80.06
1172.51	1131.47	0.00
1161.17	1120.53	2.64
1142.33	1102.35	11.88
1089.59	1051.45	20.59
1089.23	1051.11	231.39
1027.60	991.63	132.28
981.10	946.76	27.21
967.55	933.69	7.16
963.23	929.51	0.00
911.19	879.30	0.00
888.77	857.66	36.01
874.83	844.21	4.88
858.49	828.45	335.14
853.78	823.90	0.00
833.50	804.32	294.35
773.37	746.30	0.00
769.12	742.20	0.73
715.94	690.88	22.84
682.10	658.23	0.53
676.51	652.84	81.16
590.59	569.92	0.00
567.75	547.88	5.20
523.99	505.65	0.13
520.58	502.36	12.18
519.72	501.53	19.31
443.79	428.26	0.00
432.98	417.82	67.19
358.74	346.18	0.00
330.66	319.09	6.53
314.17	303.18	230.97
246.00	237.39	97.05
218.41	210.77	8.54
209.44	202.11	4.66
176.68	170.50	1.27
153.39	148.03	0.00
94.07	90.78	12.50
90.76	87.58	0.00
35.14	33.91	32.65

*Table B-21 All vibrational peak positions (raw data and corrected data with scaling factor of 0.9650) from DFT calculations of **FLR**-$(NH_2)_2$ linker monomer*

Calculated Peak Pos. (cm^{-1})	Corrected Peak Pos. (cm^{-1})	Extinction Coeff. ($M^{-1} \cdot cm^{-1}$)
3635.17	3507.93	1.06
3635.16	3507.93	19.62
3538.97	3415.11	0.48
3538.89	3415.03	38.72
3193.56	3081.78	62.31
3191.07	3079.38	11.09
3173.20	3062.14	0.08
3172.25	3061.22	68.48
3170.16	3059.20	51.90
3169.76	3058.82	32.30
3068.24	2960.86	21.00
3040.19	2933.78	33.54
1690.89	1631.71	747.98
1690.04	1630.89	16.41
1677.87	1619.15	135.25
1674.69	1616.08	0.76
1640.35	1582.94	21.10
1636.55	1579.27	97.93
1543.47	1489.45	0.04
1527.00	1473.55	546.73
1516.56	1463.48	162.47
1491.69	1439.48	7.02
1477.77	1426.04	10.19
1410.63	1361.25	10.28
1371.33	1323.34	317.83
1344.18	1297.13	2.06
1344.07	1297.03	68.92
1330.21	1283.65	76.12
1304.93	1259.26	362.85
1253.27	1209.40	20.82
1239.35	1195.97	3.61
1183.85	1142.42	29.58
1175.78	1134.63	7.11
1168.50	1127.60	0.01
1158.60	1118.05	220.89
1147.24	1107.09	0.00
1122.16	1082.89	0.02
1109.80	1070.95	0.01
1024.37	988.51	2.70
970.82	936.84	21.77
956.92	923.43	19.44
953.75	920.36	3.03
928.29	895.80	3.38
927.19	894.74	0.02
865.63	835.33	2.05
854.98	825.06	184.43
829.66	800.62	0.19
819.46	790.78	506.07

Calculated Peak Pos. (cm^{-1})	Corrected Peak Pos. (cm^{-1})	Extinction Coeff. ($M^{-1} \cdot cm^{-1}$)
798.51	770.56	5.88
761.58	734.93	1.71
755.04	728.61	95.15
742.87	716.87	6.98
714.14	689.15	377.45
674.81	651.19	72.49
652.94	630.09	5968.59
641.96	619.49	20.06
597.50	576.59	21.77
586.43	565.90	188.25
545.05	525.97	218.16
535.07	516.35	1326.49
523.61	505.28	44.11
436.66	421.38	6.41
431.73	416.62	108.28
424.39	409.53	3.83
391.14	377.45	6.83
334.50	322.79	0.06
327.10	315.65	3.95
280.01	270.21	761.80
279.44	269.66	16.99
263.40	254.18	156.48
237.25	228.95	134.93
179.28	173.00	13.83
164.20	158.45	48.05
122.05	117.78	39.07
61.16	59.02	203.11

B.3 References

1. P. J. Larkin, M. P. Makowski and N. B. Colthup, *Spectrochim. Acta, Part A*, 1999, **55**, 1011-1020.
2. S. Wang, *Sci. Rep.*, 2020, **10**, 17875.
3. E. B. Wilson, *Phys. Rev.*, 1934, **45**, 0706-0714.
4. M. Preuss and F. Bechstedt, *Phys. Rev. B: Condens. Matter Mater. Phys.*, 2006, **73**, 155413.
5. C. J. Cramer, *Essentials of Computational Chemistry: Theories and Models*, John Wiley & Sons Ltd., United Kingdom, 2 edn., 2004.
6. G. Rauhut and P. Pulay, *J. Phys. Chem.*, 2002, **99**, 3093-3100.
7. NIST Computational Chemistry Comparison and Benchmark Database, http://cccbdb.nist.gov/, (accessed March 2021).
8. T. Sundius, *Vib. Spectrosc.*, 2002, **29**, 89-95.
9. A. P. Scott and L. Radom, *J. Phys. Chem.*, 1996, **100**, 16502-16513.
10. J. P. Merrick, D. Moran and L. Radom, *J. Phys. Chem. A*, 2007, **111**, 11683-11700.

Appendix C TD-DFT Calculated Electronic Transitions in Oligo(aniline) Models

This section compiles the excited states obtained from TD-DFT calculations of oligomeric models. Significant excited states with oscillator strengths of at least 0.2 along with contributing electronic transitions are marked in **bold**. The number of excited states were first set at 50 states and then expanded to 100 or 200 states if the initial numbers of states do not cover the visible and near ultraviolet regions. Excited states listed in this section are limited to those corresponding to the wavelength of 250 nm or longer.

C.1 Electronic Transitions in TANI and Branched Derivatives

C.1.1 Electronic Transitions in TANI

*Table C-1 Attributes of TANI in **LEB** and **ES** (singlet and triplet) states related to electronic structures*

Attribute	LEB State	^{1}ES State	^{3}ES State
Molecular Formula	$C_{30}H_{26}N_4$	$C_{30}H_{26}N_4^{2+}$	$C_{30}H_{26}N_4^{2+}$
Number of Atoms	60	60	60
Number of Electrons	234	232	232
HOMO	MO 117	MO 116	MOs 117A and 115B
LUMO	MO 118	MO 117	MOs 118A and 116B

*C.1.1.1 TANI, **LEB** State*

Excited State 1:	**Singlet-A**	**4.0146 eV**	**308.84 nm**	**f=1.8710**	**<S**2>=0.000**
115→125	-0.12165	116→122	0.10076	117→125	-0.10517
116→121	-0.19775	**117→118**	**0.61768**		
Excited State 2:	**Singlet-A**	**4.2361 eV**	**292.69 nm**	**f=0.3853**	**<S**2>=0.000**
115→119	0.11316	116→120	0.19976	117→122	0.17553
115→122	0.13420	**117→119**	**0.58769**		
Excited State 3:	Singlet-A	4.3064 eV	287.91 nm	f=0.0025	<S**2>=0.000
116→118	0.13939	116→121	-0.15956	117→120	0.53522
116→119	0.26590	116→122	-0.15809		
Excited State 4:	Singlet-A	4.3748 eV	283.40 nm	f=0.0929	<S**2>=0.000
115→119	0.11919	117→121	0.31569	117→123	0.13132
116→120	-0.30968	117→122	0.43985	117→124	0.10869
Excited State 5:	Singlet-A	4.5212 eV	274.23 nm	f=0.0357	<S**2>=0.000
115→121	0.13718	116→118	0.42219	116→119	-0.11751

117→121	-0.36409	117→122	0.27151	117→126	-0.10846

Excited State 6:	Singlet-A	4.7562 eV	260.68 nm	f=0.0776	<S**2>=0.000
114→123	-0.10712	116→121	-0.12596	116→124	0.22413
115→122	0.10565	116→122	0.11257	117→123	0.35534
115→123	-0.25354	116→123	-0.29663	117→124	0.13150

Excited State 7:	Singlet-A	4.7724 eV	259.79 nm	f=0.0081	<S**2>=0.000
114→124	0.11658	116→121	-0.12284	117→123	-0.14528
115→123	0.10670	116→123	0.23899	117→124	0.34801
115→124	-0.24974	116→124	0.31866		

C.1.1.2 TANI, ¹ES State

Excited State 1:	**Singlet-A**	**1.2697 eV**	**976.48 nm**	**f=2.1480**	**<S**2>=0.000**
116→117	**0.71635**	116←117	-0.13842		

Excited State 2:	Singlet-A	2.1226 eV	584.12 nm	f=0.0000	<S**2>=0.000
115→117	0.69984				

Excited State 3:	Singlet-A	3.0113 eV	411.73 nm	f=0.1120	<S**2>=0.000
114→117	0.69719				

Excited State 4:	Singlet-A	3.2050 eV	386.85 nm	f=0.0000	<S**2>=0.000
108→117	-0.47212	110→117	0.49194	113→117	0.16580

Excited State 5:	Singlet-A	3.2301 eV	383.84 nm	f=0.0019	<S**2>=0.000
109→117	0.64142	112→117	0.28405		

Excited State 6:	Singlet-A	3.2462 eV	381.93 nm	f=0.0000	<S**2>=0.000
108→117	0.50848	110→117	0.41088	113→117	0.24415

Excited State 7:	Singlet-A	3.3122 eV	374.33 nm	f=0.0040	<S**2>=0.000
109→117	-0.28516	112→117	0.64019		

Excited State 8:	Singlet-A	3.3126 eV	374.28 nm	f=0.0000	<S**2>=0.000
110→117	-0.28586	113→117	0.63742		
Excited State 9:	Singlet-A	3.3914 eV	365.59 nm	f=0.0000	<S**2>=0.000
111→117	0.68285				
Excited State 10:	Singlet-A	4.1818 eV	296.48 nm	f=0.0000	<S**2>=0.000
115→122	-0.14197	116→118	0.67361		
Excited State 11:	Singlet-A	4.5146 eV	274.63 nm	f=0.0142	<S**2>=0.000
107→117	0.65734	116→122	-0.13719		
Excited State 12:	Singlet-A	4.5572 eV	272.06 nm	f=0.0000	<S**2>=0.000
114→119	0.14546	116→119	0.66321	116→121	-0.14564
Excited State 13:	Singlet-A	4.6261 eV	268.01 nm	f=0.0796	<S**2>=0.000
111→121	-0.10039	116→120	0.59510		
115→121	0.26657	116→122	0.18398		
Excited State 14:	Singlet-A	4.6437 eV	266.99 nm	f=0.0000	<S**2>=0.000
115→120	0.24244	116→119	0.16709	116→121	0.60454
Excited State 15:	**Singlet-A**	**4.8646 eV**	**254.87 nm**	**f=0.7092**	**<S**2>=0.000**
107→117	0.16951	115→125	0.18391	**116→122**	**0.54144**
115→118	-0.29419	116→120	-0.15180		

*C.1.1.3 TANI, ^{3}**ES** State*

Excited State 1:	**3.072-A**	**1.5615 eV**	**794.00 nm**	**f=1.2104**	**<S**2>=2.110**
107B→117B	-0.13857	**114B→117B**	**0.39377**		
111B→118B	0.10666	**115B→116B**	**0.88590**		

Excited State 2:	3.059-A	1.9853 eV	624.53 nm	f=0.0000	<S**2>=2.090						
107B→116B	-0.14179		114B→116B	0.61288		115B→117B	0.72452				
Excited State 3:	3.083-A	2.6644 eV	465.34 nm	f=0.0006	<S**2>=2.126						
108B→116B	0.73870		109B→117B	0.61964		110B→116B	-0.12204				
Excited State 4:	3.083-A	2.6658 eV	465.10 nm	f=0.0000	<S**2>=2.126						
108B→117B	0.61532		109B→116B	0.74683							
Excited State 5:	3.297-A	2.7966 eV	443.33 nm	f=0.0823	<S**2>=2.468						
111A→122A	-0.10913		106B→116B	0.10714		114B→117B	0.49868				
115A→118A	0.16557		107B→117B	0.12134		115B→116B	-0.15827				
117A→118A	0.11881		111B→116B	0.67081		115B→118B	0.20391				
117A→125A	-0.15410		113B→116B	0.13186							
Excited State 6:	3.089-A	2.9040 eV	426.94 nm	f=0.0000	<S**2>=2.135						
107B→116B	0.18005		113B→117B	0.10760		115B→117B	-0.53272				
111B→117B	0.52590		114B→116B	0.56963							
Excited State 7:	3.099-A	3.1911 eV	388.54 nm	f=0.0001	<S**2>=2.151						
111B→117B	-0.11200		112B→118B	0.11777		113B→117B	0.55498				
112B→116B	0.77169		113B→116B	0.10693							
Excited State 8:	3.099-A	3.1911 eV	388.53 nm	f=0.0041	<S**2>=2.151						
111B→116B	-0.15106		112B→117B	0.56635		113B→118B	0.11705				
112B→116B	-0.10907		113B→116B	0.75659							
Excited State 9:	**3.644-A**	**3.3617 eV**	**368.82 nm**	**f=0.5521**	**<S**2>=3.069**						
108A→120A	-0.11680		112A→123A	0.10982		115A→125A	-0.26170				
109A→119A	-0.10256		113A→124A	0.11208		116A→119A	-0.16897				
110A→127A	0.13216		114A→126A	-0.12929		116A→121A	0.21432				
111A→122A	-0.22512		115A→118A	0.10091		**117A→118A**	**0.58706**				

117A→125A	-0.11540	110B→119B	-0.18678	113B→124B	0.11832
117A→127A	-0.11940	110B→121B	0.14216	115B→118B	0.10271
106B→116B	0.14443	111B→116B	-0.15423	115B→125B	-0.17237
107B→117B	-0.17556	111B→118B	-0.13329		
110B→116B	0.11501	112B→123B	0.12035		

Excited State 10: 3.175-A 3.4938 eV 354.87 nm f=0.0241 <S**2>=2.271

115A→122A	0.10735	117A→122A	0.18159	110B→116B	0.91537
117A→118A	-0.11596	108B→116B	0.12112	110B→118B	-0.20568

Excited State 11: 3.737-A 3.5105 eV 353.18 nm f=0.0000 <S**2>=3.241

109A→120A	0.10302	116A→125A	-0.17886	113B→123B	-0.23516
112A→124A	-0.23113	116A→127A	0.11731	114B→116B	-0.30013
113A→123A	-0.23759	117A→126A	0.13884	114B→118B	0.17521
114A→118A	-0.10848	106B→117B	-0.19952	114B→125B	0.17216
114A→125A	-0.17211	107B→116B	0.36541	115B→117B	0.22343
115A→119A	-0.13748	111B→117B	0.11697	115B→120B	-0.13137
115A→121A	0.13609	111B→120B	-0.12423	115B→122B	0.13297
115A→126A	-0.18440	111B→122B	0.10402		
116A→118A	-0.11432	112B→124B	-0.23523		

Excited State 12: 3.572-A 3.6609 eV 338.67 nm f=0.0567 <S**2>=2.940

110A→125A	-0.11112	115A→127A	0.11950	112B→123B	0.20747
111A→122A	0.13797	116A→126A	-0.21685	113B→124B	0.20780
112A→123A	0.21096	117A→118A	-0.28086	114B→117B	0.40686
113A→124A	0.21432	117A→125A	0.13244	114B→120B	0.15097
114A→119A	-0.11202	117A→127A	-0.11662	114B→122B	-0.14883
114A→121A	0.14991	106B→116B	0.25196	115B→116B	-0.24876
115A→118A	-0.13625	107B→117B	-0.26798	115B→118B	-0.12137
115A→125A	-0.10596	111B→125B	-0.13749	115B→125B	-0.10261

Excited State 13:	3.406-A	3.7673 eV	329.11 nm	f=0.1771	<S**2>=2.649	
110A→118A	0.10369	117A→118A	0.22314	111B→125B	-0.12191	
111A→122A	0.13749	117A→120A	-0.14336	112B→123B	0.15300	
112A→123A	0.16941	117A→125A	0.18087	113B→124B	0.15330	
113A→124A	0.17138	117A→127A	0.15853	114B→117B	-0.11588	
114A→126A	-0.12589	106B→116B	-0.22166	115B→116B	0.17727	
115A→118A	-0.15506	107B→117B	0.35955	115B→118B	-0.20416	
116A→119A	-0.25395	110B→119B	0.11231			
116A→121A	0.21203	111B→116B	0.42880			

Excited State 14:	3.171-A	3.7957 eV	326.65 nm	f=0.0000	<S**2>=2.264	
109A→120A	-0.10936	117A→119A	-0.33836	107B→116B	0.36355	
114A→118A	-0.12194	117A→121A	0.38408	111B→117B	0.25119	
116A→118A	0.46792	117A→126A	0.14576	115B→117B	0.25652	
116A→127A	0.12182	106B→117B	-0.13635			

Excited State 15:	3.550-A	3.8822 eV	319.37 nm	f=0.1566	<S**2>=2.900	
108A→120A	-0.19491	116A→121A	0.18614	111B→116B	-0.24702	
109A→119A	-0.15199	116A→126A	0.14686	111B→118B	0.18417	
109A→121A	-0.12770	117A→118A	0.29340	112B→123B	-0.11237	
110A→118A	0.16642	117A→127A	0.18505	113B→124B	-0.11086	
111A→122A	0.26830	108B→119B	0.11180	114B→117B	0.39763	
112A→123A	-0.11566	109B→120B	-0.10350	115B→116B	-0.28752	
113A→124A	-0.11766	110B→119B	0.17982	115B→125B	0.12063	
116A→119A	-0.15817	110B→121B	-0.17506			

Excited State 16:	3.225-A	3.9639 eV	312.78 nm	f=0.0000	<S**2>=2.350	
108A→119A	-0.12321	112A→124A	-0.10543	116A→118A	0.13540	
109A→120A	-0.15015	113A→123A	-0.10759	117A→121A	0.13958	

107B→116B	-0.17243	110B→117B	0.84902		

Excited State 17:	3.520-A	3.9887 eV	310.84 nm	f=0.0000	<S**2>=2.848
108A→119A	0.20973	117A→121A	-0.21010	109B→121B	-0.12805
108A→121A	0.15688	117A→126A	-0.10753	110B→117B	0.47627
109A→120A	0.25217	106B→117B	-0.14730	111B→117B	0.21185
112A→124A	0.18577	107B→116B	0.34285	112B→124B	0.17015
113A→123A	0.18924	108B→120B	0.13319	113B→123B	0.16884
114A→118A	0.11323	108B→122B	0.12811	115B→117B	0.16657
116A→118A	-0.18590	109B→119B	-0.11884		

Excited State 18:	3.131-A	4.0243 eV	308.09 nm	f=0.0503	<S**2>=2.201
110A→120A	0.14605	115A→122A	-0.10567	117A→120A	0.72371
114A→119A	-0.15292	116A→119A	0.43251	117A→125A	0.10357
114A→121A	-0.10955	116A→121A	0.33392		

Excited State 19:	3.097-A	4.0359 eV	307.20 nm	f=0.0000	<S**2>=2.148
110A→119A	0.14919	116A→120A	0.54982	117A→119A	0.58091
114A→120A	-0.19233	116A→122A	0.12733	117A→121A	0.42938

Excited State 20:	3.619-A	4.1984 eV	295.32 nm	f=0.0257	<S**2>=3.024
110A→120A	0.11346	116A→119A	0.12652	111B→119B	-0.16567
110A→122A	-0.18898	116A→121A	0.13364	111B→121B	0.11161
115A→120A	-0.12340	117A→122A	0.73165	115B→119B	0.27002
115A→122A	0.34070	110B→116B	-0.22324	115B→121B	-0.20624

Excited State 21:	3.547-A	4.3299 eV	286.35 nm	f=0.0482	<S**2>=2.895
108A→120A	0.32065	96B→117B	0.12011	108B→121B	-0.16911
109A→119A	0.26435	106B→116B	-0.38205	109B→120B	0.18347
109A→121A	0.21019	107B→117B	0.16977	109B→122B	0.17442
117A→118A	0.11033	108B→119B	-0.17012	111B→116B	-0.33635

114B→117B	0.44938				

Excited State 22:	3.193-A	4.3562 eV	284.62 nm	f=0.0000	<S**2>=2.298
108A→119A	-0.13340	103B→116B	0.12006	111B→117B	0.60214
108A→121A	-0.10663	105B→116B	0.13798	113B→117B	0.13156
109A→120A	-0.16293	106B→117B	0.36402	114B→116B	-0.43297
116A→118A	-0.16227	107B→116B	-0.16062	115B→117B	0.11966
117A→121A	-0.11959	108B→120B	-0.10440		
96B→116B	-0.12856	109B→121B	0.10029		

Excited State 23:	3.912-A	4.5603 eV	271.88 nm	f=0.0596	<S**2>=3.575
108A→120A	0.16314	117A→118A	0.27109	110B→119B	0.39944
109A→119A	0.14790	117A→125A	-0.18940	110B→121B	-0.30349
109A→121A	0.11497	117A→127A	-0.18102	111B→116B	0.10197
110A→118A	-0.10967	106B→116B	0.14801	111B→118B	-0.11249
111A→120A	-0.16619	107B→117B	-0.18917	114B→117B	-0.15580
111A→122A	0.46010	108B→121B	-0.13724	115B→118B	0.10034
115A→118A	0.14705	109B→120B	0.10963		
115A→125A	-0.10785	109B→122B	0.10747		

Excited State 24:	3.840-A	4.6651 eV	265.77 nm	f=0.0000	<S**2>=3.437
109A→120A	-0.11164	115A→126A	-0.10396	112B→116B	0.17289
110A→123A	-0.13257	116A→124A	0.35819	112B→124B	0.17316
112A→124A	0.13188	116A→125A	-0.13588	113B→123B	0.20027
113A→123A	0.16646	117A→123A	0.29426	114B→124B	0.24513
114A→124A	0.27885	117A→126A	0.10175	115B→120B	-0.11352
115A→119A	-0.11368	107B→116B	0.10536	115B→123B	0.21410
115A→123A	-0.32638	111B→123B	0.14258		

Excited State 25:	3.856-A	4.6655 eV	265.75 nm	f=0.0144	<S**2>=3.468				
110A→124A	-0.13476	116A→126A	0.11315	113B→116B	0.17204				
112A→123A	0.12642	117A→124A	0.29900	113B→124B	0.20632				
113A→124A	0.16494	117A→125A	-0.14528	114B→120B	-0.13784				
114A→123A	0.28984	107B→123B	0.10032	114B→123B	0.26167				
115A→124A	-0.33427	111B→124B	0.14125	115B→118B	0.11736				
116A→123A	0.37536	112B→123B	0.16300	115B→124B	0.21950				

Excited State 26:	3.859-A	4.6881 eV	264.46 nm	f=0.0000	<S**2>=3.472				
108A→119A	-0.14133	116A→125A	-0.13665	109B→121B	0.11249				
108A→121A	-0.11911	117A→119A	0.10171	111B→117B	-0.11263				
109A→120A	-0.17553	117A→121A	-0.14050	111B→123B	-0.17343				
112A→124A	0.27122	117A→123A	-0.21150	112B→116B	-0.12524				
113A→123A	0.25054	117A→126A	0.10364	112B→124B	0.23737				
114A→124A	-0.15177	106B→117B	-0.13207	113B→120B	-0.12183				
115A→123A	0.22868	107B→116B	0.14955	113B→123B	0.21225				
115A→126A	-0.12465	108B→120B	-0.11772	114B→124B	-0.18313				
116A→118A	-0.15613	108B→122B	-0.11176	115B→123B	-0.15335				
116A→124A	-0.26545	109B→119B	0.10800						

Excited State 27:	3.905-A	4.6904 eV	264.34 nm	f=0.0809	<S**2>=3.563				
108A→120A	-0.12319	116A→121A	-0.16015	112B→120B	-0.11310				
111A→122A	0.13139	116A→123A	-0.24231	112B→123B	0.26625				
112A→123A	0.29231	116A→126A	0.13414	113B→116B	-0.11969				
113A→124A	0.27035	117A→124A	-0.20467	113B→124B	0.22674				
114A→123A	-0.13276	117A→125A	-0.18699	114B→122B	0.11412				
114A→126A	0.10277	106B→116B	-0.13745	114B→123B	-0.16001				
115A→118A	0.14558	110B→119B	0.10333	115B→118B	0.19308				
115A→124A	0.21555	110B→121B	-0.10238	115B→124B	-0.14188				
116A→119A	0.10453	111B→124B	-0.17638						

Excited State 28:	3.119-A	4.8514 eV	255.57 nm	f=0.0000	<S**2>=2.182			
111B→117B	-0.13582	112B→116B	-0.57548	113B→117B	0.75422			
Excited State 29:	3.114-A	4.8518 eV	255.54 nm	f=0.0024	<S**2>=2.174			
116A→123A	0.10117	112B→117B	0.76967					
111B→116B	0.11582	113B→116B	-0.56542					
Excited State 30:	3.673-A	4.9295 eV	251.52 nm	f=0.0000	<S**2>=3.122			
108A→119A	-0.19101	117A→121A	-0.10971	111B→117B	-0.17639			
108A→121A	-0.15230	117A→126A	-0.12831	112B→124B	-0.16900			
109A→120A	-0.23393	103B→116B	0.11112	113B→123B	-0.16504			
112A→124A	-0.16220	106B→117B	-0.12733	114B→118B	-0.13732			
113A→123A	-0.16084	107B→116B	0.48393	114B→125B	-0.15688			
114A→118A	0.14341	108B→120B	-0.18169	115B→120B	0.18345			
116A→118A	-0.19213	108B→122B	-0.16486	115B→122B	-0.10751			
116A→125A	0.11066	109B→119B	0.16550					
117A→119A	0.10513	109B→121B	0.17215					

C.1.2 Electronic Transitions in TANI-2

*Table C-2 Attributes of TANI-2 in **LEB** and **ES** (singlet and triplet) states related to electronic structures*

Attribute	LEB State	^{1}ES State	^{3}ES State
Molecular Formula	$C_{42}H_{35}N_5$	$C_{42}H_{35}N_5^{2+}$	$C_{42}H_{35}N_5^{2+}$
Number of Atoms	82	82	82
Number of Electrons	322	320	320
HOMO	MO 161	MO 160	MOs 161A and 159B
LUMO	MO 162	MO 161	MOs 162A and 160B

*C.1.2.1 TANI-2, **LEB** State*

Excited State 1:	**Singlet-A**	**3.8715 eV**	**320.25 nm**	**f=0.4960**	**<S**2>=0.000**			
160→163	-0.10587	**161→162**	**0.53807**	161→164	-0.23577			
160→166	-0.12641	161→163	0.23968					

Excited State 2:	**Singlet-A**	**3.8891 eV**	**318.80 nm**	**f=0.8797**	**<S**2>=0.000**
160→162	-0.12915	161→162	-0.29101	161→164	-0.27108
160→166	0.12277	**161→163**	**0.48185**	161→172	-0.10458
Excited State 3:	**Singlet-A**	**3.9486 eV**	**314.00 nm**	**f=1.0450**	**<S**2>=0.000**
159→166	0.13480	160→164	-0.17969	**161→164**	**0.50911**
160→163	-0.13952	**161→163**	**0.32431**	161→173	0.12396
Excited State 4:	Singlet-A	4.2765 eV	289.92 nm	f=0.0359	<S**2>=0.000
160→164	-0.11324	161→165	0.43732	161→171	-0.15704
160→165	0.41820	161→166	-0.11311		
Excited State 5:	Singlet-A	4.3880 eV	282.55 nm	f=0.0434	<S**2>=0.000
159→164	0.10242	160→170	-0.12379	161→168	0.10877
160→162	-0.16114	161→166	0.11674	161→170	0.33176
160→165	0.17053	161→167	0.13816	161→171	0.39431
Excited State 6:	Singlet-A	4.3982 eV	281.90 nm	f=0.0651	<S**2>=0.000
159→163	-0.12636	160→170	-0.14906	161→171	-0.36916
159→164	0.12137	161→167	0.16485		
160→165	-0.13765	161→170	0.38421		
Excited State 7:	**Singlet-A**	**4.4904 eV**	**276.11 nm**	**f=0.2649**	**<S**2>=0.000**
158→166	-0.10736	**160→162**	**0.40429**	**161→166**	**-0.36234**
159→163	-0.15911	160→163	-0.16569	161→170	0.12792
159→164	-0.11696	160→166	-0.11404	161→174	0.10970
Excited State 8:	Singlet-A	4.7428 eV	261.41 nm	f=0.0635	<S**2>=0.000
158→168	0.16507	160→166	0.13241	161→169	0.15358
158→169	0.14897	160→169	0.32090	161→171	-0.10652
159→167	-0.27694	161→168	0.29360		

Excited State 9:	Singlet-A	4.7556 eV	260.71 nm	f=0.0205	<S**2>=0.000						
157→167	0.12562		159→168	0.32687		161→169	0.12736				
158→167	-0.17581		160→167	0.19604		161→170	0.18605				
158→169	0.10558		160→169	0.18126							
159→167	0.12303		161→167	-0.32459							
Excited State 10:	Singlet-A	4.7577 eV	260.60 nm	f=0.1050	<S**2>=0.000						
157→168	0.10064		159→168	-0.18821		161→167	0.12503				
158→169	0.19026		160→168	0.19561		161→168	-0.22148				
159→167	0.21275		160→169	0.29505		161→169	0.23885				
Excited State 11:	**Singlet-A**	**4.9177 eV**	**252.12 nm**	**f=0.2337**	**<S**2>=0.000**						
158→162	-0.19975		159→167	0.10403		160→169	-0.10228				
159→163	-0.22494		160→162	-0.10626		161→168	-0.11176				
159→164	-0.30057		160→166	0.24203		**161→172**	**0.32861**				

*C.1.2.2 TANI-2, ^{1}**ES** State*

Excited State 1:	**Singlet-A**	**1.2655 eV**	**979.70 nm**	**f=1.3673**	**<S**2>=0.000**						
160→161	**0.70476**										
Excited State 2:	**Singlet-A**	**1.7460 eV**	**710.09 nm**	**f=0.9193**	**<S**2>=0.000**						
159→161	**0.70058**										
Excited State 3:	Singlet-A	2.2342 eV	554.95 nm	f=0.1351	<S**2>=0.000						
153→161	0.12580		158→161	0.68657							
Excited State 4:	Singlet-A	3.0467 eV	406.95 nm	f=0.0157	<S**2>=0.000						
150→161	0.11719		153→161	-0.17452		157→161	0.66343				
Excited State 5:	Singlet-A	3.1443 eV	394.32 nm	f=0.0015	<S**2>=0.000						
148→161	-0.20049		149→161	0.52311		150→161	-0.35086				

152→161	0.18673							
Excited State 6:	Singlet-A	3.1555 eV	392.91 nm	f=0.0064	<S**2>=0.000			
148→161	-0.14783	150→161	0.55297	153→161	-0.14488			
149→161	0.32185	152→161	0.11781	157→161	-0.13815			
Excited State 7:	Singlet-A	3.4099 eV	363.60 nm	f=0.0007	<S**2>=0.000			
148→161	0.27188	151→161	0.56168	155→161	0.14407			
149→161	0.13375	154→161	0.18475	156→161	0.13031			
Excited State 8:	Singlet-A	3.4275 eV	361.74 nm	f=0.0007	<S**2>=0.000			
148→161	0.28819	154→161	0.36643					
151→161	-0.34175	155→161	0.38344					
Excited State 9:	Singlet-A	3.4410 eV	360.32 nm	f=0.0012	<S**2>=0.000			
154→161	-0.43994	155→161	0.52730					
Excited State 10:	Singlet-A	3.4641 eV	357.91 nm	f=0.0006	<S**2>=0.000			
148→161	0.51624	151→161	-0.13245	154→161	-0.34784			
149→161	0.18740	152→161	0.11573	155→161	-0.19260			
Excited State 11:	Singlet-A	3.5104 eV	353.19 nm	f=0.0075	<S**2>=0.000			
149→161	-0.24716	152→161	0.62948					
Excited State 12:	Singlet-A	3.5462 eV	349.62 nm	f=0.0014	<S**2>=0.000			
146→161	-0.10780	153→161	0.61150	158→161	-0.12830			
150→161	0.20207	156→161	-0.10910					
152→161	-0.10805	157→161	0.12118					
Excited State 13:	Singlet-A	3.5539 eV	348.87 nm	f=0.0007	<S**2>=0.000			
151→161	-0.17244	156→161	0.67506					

Excited State 14:	**Singlet-A**	**4.1600 eV**	**298.04 nm**	**f=0.3500**	**<S**2>=0.000**	
160→162	**0.63339**	160→166	-0.11877	160→167	0.14394	
Excited State 15:	Singlet-A	4.3849 eV	282.76 nm	f=0.0603	<S**2>=0.000	
158→163	-0.18837	160→163	0.58060	160→165	0.18995	
159→166	0.11248	160→164	-0.10878			
Excited State 16:	Singlet-A	4.4731 eV	277.18 nm	f=0.0722	<S**2>=0.000	
146→161	-0.13708	147→161	0.62343	159→164	0.10932	
Excited State 17:	Singlet-A	4.5334 eV	273.49 nm	f=0.0434	<S**2>=0.000	
158→168	0.11128	160→166	0.13953	160→168	0.55177	
160→163	-0.11049	160→167	-0.28095			
Excited State 18:	**Singlet-A**	**4.6308 eV**	**267.74 nm**	**f=0.4075**	**<S**2>=0.000**	
158→164	-0.24368	159→164	0.15637	**160→164**	**0.46435**	
159→162	0.27889	159→167	-0.16633			
159→163	-0.15219	159→168	-0.10081			
Excited State 19:	Singlet-A	4.7247 eV	262.42 nm	f=0.1759	<S**2>=0.000	
158→166	-0.12896	159→163	0.36790	160→164	0.18920	
158→167	-0.10525	159→164	-0.33657	160→166	0.22103	
159→162	0.11760	159→165	-0.21366	160→167	0.10191	
Excited State 20:	**Singlet-A**	**4.8132 eV**	**257.59 nm**	**f=0.2311**	**<S**2>=0.000**	
147→161	-0.15383	**159→163**	**0.31184**	160→166	0.14146	
158→162	-0.14118	**159→164**	**0.44459**	160→167	-0.13851	
158→171	-0.10402	160→165	0.10140	160→168	-0.16384	
Excited State 21:	Singlet-A	4.9153 eV	252.24 nm	f=0.0953	<S**2>=0.000	
158→163	0.14610	159→162	-0.14374	159→167	-0.14243	
158→165	-0.16820	159→166	-0.29882	160→164	0.11919	

160→165	0.43877		160→167	0.13862	

*C.1.2.3 TANI-2, ³**ES** State*

Excited State 1:	**3.035-A**	**1.1630 eV**	**1066.11 nm**	**f=0.5619**	**<S**2>=2.053**
154B→160B	-0.12289	**159B→160B**	**0.79975**		
154B→161B	0.10006	**159B→161B**	**-0.56418**		
Excited State 2:	**3.073-A**	**1.7117 eV**	**724.32 nm**	**f=0.7826**	**<S**2>=2.111**
147B→161B	-0.10436	**157B→161B**	**-0.38237**		
157B→160B	**-0.42741**	**158B→160B**	**0.76348**		
Excited State 3:	3.082-A	2.2039 eV	562.58 nm	f=0.0912	<S**2>=2.124
147B→160B	-0.13419	157B→160B	-0.51651	158B→160B	-0.39853
152B→160B	0.20387	157B→161B	-0.10097	158B→161B	0.64547
Excited State 4:	3.048-A	2.4204 eV	512.24 nm	f=0.0207	<S**2>=2.073
159B→160B	0.58601	159B→161B	0.79571		
Excited State 5:	3.084-A	2.6372 eV	470.14 nm	f=0.0005	<S**2>=2.127
148B→160B	0.76198	148B→161B	0.58793		
Excited State 6:	3.136-A	2.8115 eV	440.99 nm	f=0.0049	<S**2>=2.209
150B→160B	0.24031	151B→161B	0.36347	157B→160B	0.20746
150B→161B	-0.22707	152B→160B	0.54927	157B→161B	-0.30491
151B→160B	-0.37222	152B→161B	-0.24634		
Excited State 7:	3.272-A	2.9292 eV	423.26 nm	f=0.0143	<S**2>=2.427
158A→162A	0.13551	151B→160B	0.42550	157B→161B	-0.27086
161A→162A	0.13181	151B→161B	-0.10208	158B→161B	-0.31532
147B→160B	0.19594	152B→160B	0.35557	158B→162B	0.15600
150B→160B	-0.25946	152B→161B	0.36257		

Excited State 8:	3.097-A	2.9932 eV	414.22 nm	f=0.0009	<S**2>=2.148			
149B→160B	-0.36862	150B→161B	-0.38060	154B→160B	0.25382			
149B→161B	0.34610	151B→160B	0.31743	154B→161B	-0.17053			
150B→160B	0.54034	151B→161B	-0.19011					
Excited State 9:	3.099-A	3.0410 eV	407.71 nm	f=0.0024	<S**2>=2.151			
146B→160B	-0.12617	151B→161B	-0.33549	157B→161B	-0.29945			
150B→161B	0.11835	152B→161B	-0.26270	158B→160B	0.13848			
151B→160B	0.28014	157B→160B	0.53536	158B→161B	0.45022			
Excited State 10:	3.097-A	3.1199 eV	397.40 nm	f=0.0023	<S**2>=2.148			
152B→160B	-0.10572	153B→161B	0.53536	153B→166B	0.10706			
153B→160B	0.79596	153B→162B	0.12677					
Excited State 11:	3.580-A	3.1879 eV	388.92 nm	f=0.0264	<S**2>=2.954			
156A→171A	0.15938	161A→165A	-0.24147	156B→170B	0.14240			
157A→172A	-0.16262	149B→160B	0.20043	157B→164B	0.10765			
158A→174A	-0.13100	149B→161B	-0.13004	158B→164B	0.15567			
159A→170A	0.11884	150B→161B	0.10360	159B→162B	0.10323			
160A→166A	0.12909	154B→160B	0.49696	159B→166B	-0.12931			
160A→170A	-0.17037	154B→161B	-0.33538	159B→172B	0.15030			
161A→164A	0.17185	155B→171B	-0.11885					
Excited State 12:	**3.790-A**	**3.2816 eV**	**377.82 nm**	**f=0.2362**	**<S**2>=3.341**			
149A→167A	0.11103	158A→170A	0.17352	160A→165A	-0.22871			
151A→163A	0.11830	159A→162A	0.16345	160A→174A	0.10461			
152A→168A	0.10741	159A→164A	-0.12026	**161A→162A**	**0.40565**			
153A→174A	-0.13222	159A→165A	0.13874	161A→166A	0.28623			
156A→171A	0.14882	160A→162A	0.11652	161A→170A	-0.13086			
157A→172A	0.14962	160A→164A	0.14118	150B→163B	-0.10439			

154B→173B	-0.14026	156B→171B	0.12400	158B→172B	-0.15608
155B→170B	-0.14038	158B→160B	0.10218	**159B→164B**	**-0.32630**

Excited State 13:	3.296-A	3.3700 eV	367.91 nm	f=0.1074	<S**2>=2.465

160A→170A	0.11112	149B→160B	0.57261	151B→160B	0.17491
161A→163A	-0.17305	149B→161B	-0.23754	154B→160B	0.28568
161A→164A	-0.23910	150B→160B	0.33044	154B→161B	-0.11046
161A→165A	0.23995	150B→162B	-0.10999		

Excited State 14:	3.671-A	3.4164 eV	362.91 nm	f=0.1445	<S**2>=3.120

148A→164A	-0.10536	161A→165A	0.18108	154B→160B	0.14700
154A→169A	-0.16575	161A→170A	0.13319	154B→161B	-0.12251
155A→170A	-0.13989	146B→160B	-0.13011	155B→170B	0.10778
156A→171A	-0.12061	146B→161B	-0.12685	157B→160B	-0.21462
157A→172A	-0.11473	147B→160B	-0.20551	157B→172B	0.12728
158A→166A	0.17354	149B→160B	-0.10880	158B→161B	-0.11996
159A→162A	0.24673	151B→160B	-0.14728	158B→166B	-0.13768
160A→162A	0.12556	152B→160B	-0.11035	159B→164B	0.18653
161A→162A	0.20874	153B→167B	-0.10887		
161A→164A	-0.13299	153B→168B	0.13401		

Excited State 15:	**3.357-A**	**3.4233 eV**	**362.18 nm**	**f=0.2717**	**<S**2>=2.567**

160A→162A	-0.14733	**149B→160B**	**-0.35153**	154B→160B	0.25322
161A→162A	-0.12042	149B→161B	0.12879	154B→161B	-0.24457
161A→164A	-0.24156	**150B→160B**	**-0.34414**	159B→161B	-0.11821
161A→165A	**0.37138**	151B→160B	-0.13739		

Excited State 16:	3.346-A	3.6062 eV	343.81 nm	f=0.0391	<S**2>=2.548

154A→169A	0.14824	159A→162A	0.12851	161A→162A	0.18947
155A→166A	0.10099	159A→173A	0.12658	146B→160B	0.21841

147B→161B	0.26152	157B→161B	0.52118	158B→161B	0.27511
153B→168B	-0.11537	157B→166B	-0.11691		
155B→160B	-0.10316	158B→160B	0.34290		

Excited State 17:	3.138-A	3.6389 eV	340.71 nm	f=0.0060	<S**2>=2.212
154B→160B	0.17376	155B→160B	-0.20764	156B→160B	0.77678
154B→161B	-0.10235	155B→161B	0.11879	156B→161B	-0.43401

Excited State 18:	3.098-A	3.6434 eV	340.29 nm	f=0.0007	<S**2>=2.149
155B→160B	0.80327	156B→160B	0.22946		
155B→161B	-0.45007	156B→161B	-0.12725		

Excited State 19:	3.774-A	3.6740 eV	337.46 nm	f=0.0123	<S**2>=3.310
149A→163A	-0.12692	160A→162A	-0.13239	149B→163B	0.12788
151A→167A	-0.11718	160A→164A	0.10685	152B→161B	-0.12687
152A→168A	0.14991	160A→165A	-0.13505	154B→164B	0.21967
153A→164A	0.11140	160A→174A	-0.15044	156B→160B	0.10076
153A→165A	-0.16659	161A→166A	0.20552	156B→170B	0.10838
155A→162A	0.10774	161A→170A	-0.12079	156B→171B	-0.13575
157A→172A	-0.17430	161A→175A	0.25620	158B→161B	-0.20010
158A→170A	-0.10391	147B→160B	-0.20190	159B→164B	-0.25151
159A→162A	-0.18457	147B→161B	0.11334	159B→173B	0.20614

Excited State 20:	3.667-A	3.6893 eV	336.07 nm	f=0.0151	<S**2>=3.112
153A→170A	-0.12292	161A→163A	0.16560	154B→160B	0.33043
156A→171A	-0.25029	161A→164A	0.20063	154B→161B	-0.17064
157A→172A	0.18986	161A→165A	-0.15279	154B→172B	-0.13750
158A→174A	0.10023	161A→174A	-0.20553	155B→160B	0.12288
159A→175A	-0.11187	145B→160B	-0.10619	155B→169B	-0.10979
160A→175A	0.13595	150B→160B	-0.12611	155B→170B	0.15496

155B→171B	0.16475	156B→170B	-0.16142	159B→175B	0.12768
156B→160B	-0.22224	158B→173B	-0.14058		
156B→161B	0.11775	159B→172B	-0.12076		

Excited State 21: 3.606-A 3.7429 eV 331.25 nm f=0.0310 <S**2>=3.000

154A→169A	-0.34453	161A→163A	0.11877	153B→168B	0.24902
155A→173A	-0.13442	161A→166A	-0.10310	157B→161B	0.14596
158A→162A	-0.14347	147B→161B	0.20927	157B→166B	0.12038
158A→173A	0.10892	151B→160B	0.20895	158B→160B	0.22451
159A→164A	-0.10686	152B→160B	0.44481	158B→162B	-0.12575
159A→166A	-0.11698	153B→167B	-0.19957		

Excited State 22: 3.350-A 3.7854 eV 327.53 nm f=0.0348 <S**2>=2.556

153A→168A	0.14380	159A→168A	-0.15704	161A→165A	0.31068
158A→163A	0.12141	160A→168A	0.24140	161A→167A	-0.26836
159A→166A	0.10317	161A→163A	0.64011	150B→160B	0.10897
159A→167A	0.10919	161A→164A	0.20051	159B→169B	-0.16881

Excited State 23: 3.376-A 3.8283 eV 323.86 nm f=0.1769 <S**2>=2.599

148A→164A	-0.13311	159A→173A	0.18157	147B→160B	0.16946
149A→163A	-0.11282	160A→162A	0.24632	148B→165B	0.11568
150A→162A	0.17425	160A→166A	-0.15687	149B→163B	0.11673
151A→167A	-0.11850	160A→173A	0.12366	152B→160B	-0.12852
158A→162A	-0.10668	161A→162A	0.14772	152B→161B	0.13074
159A→162A	0.36574	161A→163A	0.15195	152B→162B	0.16082
159A→164A	-0.11218	161A→166A	-0.13361	157B→161B	-0.29033
159A→166A	-0.19766	146B→160B	0.20833	158B→160B	-0.17830

Excited State 24: 3.102-A 3.9338 eV 315.18 nm f=0.0009 <S**2>=2.155

160A→163A	-0.10013	161A→168A	-0.10641	149B→161B	0.53795

150B→160B	0.16923	151B→161B	0.32132	154B→161B	0.22898
150B→161B	0.62617	154B→160B	0.14129		

Excited State 25: 3.719-A 3.9455 eV 314.24 nm f=0.0028 <S**2>=3.207

153A→163A	0.13423	160A→163A	0.23996	154B→163B	0.11125
153A→167A	-0.12862	160A→164A	0.12102	159B→163B	-0.38597
159A→163A	-0.20566	160A→165A	0.10458	159B→167B	-0.21310
159A→167A	0.14607	160A→167A	-0.20700	159B→168B	-0.15085
159A→168A	-0.10235	161A→168A	0.56932		

Excited State 26: 3.438-A 4.0213 eV 308.32 nm f=0.0158 <S**2>=2.705

148A→163A	-0.11372	157A→172A	-0.10630	152B→160B	-0.21020
148A→164A	0.18283	159A→162A	-0.13658	152B→161B	0.29118
148A→165A	0.11020	147B→160B	0.48964	153B→168B	0.12070
152A→168A	0.12982	147B→161B	-0.18623	158B→161B	0.24966
154A→169A	-0.17167	148B→165B	-0.14921		
156A→171A	-0.11130	151B→161B	0.14835		

Excited State 27: 3.125-A 4.0379 eV 307.05 nm f=0.0252 <S**2>=2.191

150A→164A	0.14856	159A→165A	0.28253	160A→165A	0.19264
155A→164A	-0.10594	159A→166A	-0.12889	161A→163A	-0.17215
159A→163A	-0.34150	160A→163A	-0.24504	161A→164A	0.28252
159A→164A	0.48700	160A→164A	0.33680	161A→165A	0.16401

Excited State 28: 3.518-A 4.2352 eV 292.75 nm f=0.0213 <S**2>=2.845

148A→164A	-0.15264	159A→164A	0.14751	160A→165A	0.10800
150A→163A	-0.16575	159A→165A	0.14903	160A→168A	-0.11549
158A→163A	0.20508	159A→167A	0.11504	161A→163A	0.20616
158A→167A	0.17898	160A→163A	0.10516	161A→165A	0.12557
159A→163A	0.15486	160A→164A	0.10099	161A→167A	0.50432

146B→160B	-0.15050	150B→160B	0.10775	158B→163B	-0.19894
146B→161B	-0.14598	152B→161B	0.17757	159B→169B	0.13668
148B→165B	0.13561	152B→163B	0.12927		
149B→160B	0.11755	157B→160B	0.10819		

Excited State 29: 3.461-A 4.2551 eV 291.38 nm f=0.0836 <S**2>=2.745

148A→163A	0.16079	146B→160B	-0.30997	157B→160B	0.19724
148A→164A	-0.25508	146B→161B	-0.26863	157B→161B	0.19979
148A→165A	-0.15361	147B→161B	-0.11496	158B→161B	0.10940
161A→162A	-0.15579	148B→165B	0.23016	158B→163B	0.10337
161A→163A	-0.11843	148B→166B	-0.10018	159B→164B	-0.14135
161A→167A	-0.26381	152B→161B	0.36261		

Excited State 30: 3.415-A 4.3319 eV 286.21 nm f=0.0271 <S**2>=2.666

149A→167A	-0.13499	146B→161B	-0.24652	151B→161B	0.10877
151A→163A	-0.15269	147B→160B	-0.27294	151B→169B	-0.15120
152A→168A	-0.23180	147B→161B	0.19894	152B→160B	-0.10664
161A→162A	0.18546	149B→167B	-0.11148	152B→161B	0.41078
161A→166A	0.17868	150B→163B	0.13984	157B→160B	0.26977
146B→160B	0.18103	151B→160B	-0.10892	157B→161B	-0.22765

Excited State 31: 3.882-A 4.3730 eV 283.52 nm f=0.1175 <S**2>=3.517

149A→168A	-0.24926	132B→160B	-0.11419	151B→163B	0.24320
151A→168A	0.26749	132B→161B	0.10477	151B→167B	0.16716
152A→163A	0.30523	145B→160B	0.18056	151B→168B	0.12490
152A→164A	0.12621	145B→161B	-0.16340	151B→169B	-0.11834
152A→165A	0.11620	149B→169B	0.21840	152B→163B	-0.14547
152A→167A	-0.27312	149B→171B	0.12092	154B→160B	0.15934
161A→164A	-0.18682	150B→163B	-0.12952		
161A→165A	0.26952	150B→169B	-0.15616		

Excited State 32:	3.998-A	4.4077 eV	281.29 nm	f=0.0121	<S**2>=3.747				
153A→172A	-0.17723	161A→171A	-0.14385	157B→171B	0.12557				
155A→172A	0.13942	161A→172A	-0.36410	158B→170B	-0.21078				
158A→172A	0.24200	154B→170B	-0.13585	158B→171B	0.18115				
159A→172A	-0.12188	154B→171B	0.15798	159B→169B	-0.13888				
160A→171A	0.11804	156B→160B	0.17116	159B→170B	-0.24566				
160A→172A	0.43865	157B→170B	-0.14796	159B→171B	0.28283				

Excited State 33:	3.978-A	4.4171 eV	280.69 nm	f=0.0075	<S**2>=3.707				
153A→171A	0.18157	161A→171A	-0.34051	158B→169B	0.11904				
155A→171A	0.13472	161A→172A	0.14458	158B→170B	-0.18278				
158A→171A	0.23446	154B→170B	0.18253	158B→171B	-0.17289				
159A→171A	0.36076	154B→171B	0.10802	159B→169B	-0.14908				
159A→172A	-0.10001	155B→160B	0.17429	159B→170B	0.30217				
160A→171A	-0.26935	157B→170B	-0.13299	159B→171B	0.17900				
161A→162A	-0.10629	157B→171B	-0.12215						

Excited State 34:	3.721-A	4.4297 eV	279.89 nm	f=0.0350	<S**2>=3.212				
149A→163A	-0.21462	161A→171A	-0.12054	150B→167B	-0.14112				
149A→167A	-0.21288	146B→160B	-0.19386	150B→168B	-0.11211				
151A→163A	-0.21608	147B→160B	0.12485	151B→163B	0.13793				
151A→167A	-0.19438	147B→161B	-0.20606	152B→160B	0.15775				
158A→162A	0.11081	149B→163B	0.20125	157B→161B	0.21477				
159A→171A	0.10228	149B→167B	-0.14714	159B→163B	-0.10027				
161A→162A	0.33506	149B→168B	-0.11472	159B→164B	0.21300				
161A→166A	0.17809	150B→163B	0.26155						

Excited State 35:	3.500-A	4.5456 eV	272.76 nm	f=0.0706	<S**2>=2.813				
149A→163A	-0.12098	151A→167A	-0.13231	152A→168A	0.19581				

156A→171A	0.13496	151B→161B	0.12627	158B→169B	-0.10410
161A→168A	0.29276	151B→169B	0.12345	159B→163B	0.42132
147B→160B	-0.16893	152B→161B	0.13674	159B→164B	0.41321
147B→161B	0.10179	155B→170B	-0.10509	159B→167B	0.15796
149B→163B	0.13249	156B→161B	-0.12252	159B→168B	0.11834

Excited State 36: 3.317-A 4.5779 eV 270.83 nm f=0.0000 <S**2>=2.500

152A→168A	0.11639	154B→160B	-0.27073	156B→170B	-0.10923
157A→172A	0.17256	154B→161B	-0.38455	156B→171B	0.11938
149B→161B	0.11787	155B→160B	-0.12073	159B→163B	-0.13142
150B→160B	0.11827	155B→161B	-0.20793	159B→164B	0.18248
150B→161B	0.14711	156B→160B	0.28364		
151B→160B	-0.12423	156B→161B	0.49449		

Excited State 37: 3.363-A 4.5890 eV 270.17 nm f=0.0117 <S**2>=2.578

152A→168A	0.12807	152B→161B	0.12051	159B→163B	-0.34065
156A→171A	0.14161	154B→160B	0.33492	159B→164B	0.17851
161A→168A	-0.22530	154B→161B	0.50560	159B→167B	-0.15145
151B→160B	-0.16796	155B→170B	-0.12134	159B→168B	-0.11494
151B→161B	-0.13016	159B→162B	0.13637		

Excited State 38: 3.118-A 4.6006 eV 269.49 nm f=0.0017 <S**2>=2.180

154B→161B	0.13146	155B→161B	0.62204	156B→161B	0.52406
155B→160B	0.35685	156B→160B	0.29397	159B→163B	0.11732

Excited State 39: 3.208-A 4.6089 eV 269.01 nm f=0.0035 <S**2>=2.323

157A→172A	0.14233	154B→161B	-0.34316	156B→160B	-0.22360
161A→168A	-0.13814	155B→160B	0.29620	156B→161B	-0.40470
154B→160B	-0.24651	155B→161B	0.52600	159B→163B	-0.20279

Excited State 40:	3.933-A	4.6546 eV	266.37 nm	f=0.0791	<S**2>=3.617	
156A→171A	-0.35158	155B→170B	0.22461	158B→164B	0.23180	
157A→172A	0.25600	155B→171B	0.23137	158B→173B	0.10018	
161A→174A	0.16855	156B→170B	-0.22313	159B→162B	0.32986	
154B→161B	0.15323	156B→171B	0.12795	159B→166B	-0.24914	
155B→169B	-0.17238	157B→164B	0.12537	159B→172B	0.20937	

Excited State 41:	3.824-A	4.6644 eV	265.81 nm	f=0.0312	<S**2>=3.406	
148A→163A	-0.12608	159A→169A	-0.16984	151B→161B	-0.11063	
148A→164A	0.20611	159A→173A	-0.12659	152B→161B	0.10534	
148A→165A	0.12545	160A→162A	0.12703	153B→160B	-0.12281	
154A→169A	0.34888	160A→169A	-0.11622	153B→161B	0.11933	
155A→169A	-0.15793	161A→166A	-0.11276	153B→167B	0.21943	
158A→169A	0.13544	146B→160B	-0.13452	153B→168B	-0.27587	
159A→162A	0.17060	147B→160B	-0.11151	157B→165B	0.10837	
159A→166A	-0.12355	148B→165B	-0.22582			

Excited State 42:	3.694-A	4.6878 eV	264.48 nm	f=0.0203	<S**2>=3.162	
148A→164A	0.10499	148B→165B	-0.10789	153B→162B	-0.10780	
150A→169A	-0.14916	151B→160B	-0.10755	153B→165B	-0.12581	
154A→169A	0.15650	151B→161B	-0.12395	153B→166B	-0.10590	
155A→169A	0.30788	152B→161B	0.11450	157B→167B	0.16435	
158A→169A	-0.28168	152B→167B	-0.11595	157B→168B	-0.20444	
159A→169A	0.35615	152B→168B	0.14465	158B→168B	0.13080	
160A→169A	0.24683	153B→160B	0.30710			
161A→169A	0.12089	153B→161B	-0.25772			

Excited State 43:	3.539-A	4.7020 eV	263.69 nm	f=0.0335	<S**2>=2.882	
156A→171A	0.15566	159A→174A	0.10505	160A→174A	-0.17822	
157A→172A	0.22350	160A→165A	0.10867	161A→170A	0.19085	

149B→161B	-0.10959	152B→161B	-0.15954	156B→171B	0.18919
150B→161B	-0.15586	155B→170B	-0.17166	159B→164B	-0.20294
151B→160B	0.31454	156B→161B	0.10591	159B→173B	0.17426
151B→161B	0.40254	156B→169B	-0.10107		
152B→160B	-0.16176	156B→170B	-0.14147		

Excited State 44: 3.468-A 4.7151 eV 262.95 nm f=0.0426 <S**2>=2.757

154A→169A	0.12750	145B→160B	-0.12187	156B→170B	0.16130
157A→172A	-0.20600	150B→160B	-0.10029	156B→171B	-0.15909
160A→165A	-0.12704	150B→161B	-0.12398	159B→162B	0.19131
160A→174A	0.14141	151B→160B	0.27784	159B→163B	-0.17820
161A→165A	0.10719	151B→161B	0.38724	159B→164B	0.23836
161A→170A	-0.17222	152B→160B	-0.13356	159B→173B	-0.11952
161A→174A	-0.11392	152B→161B	-0.12848		

Excited State 45: 3.581-A 4.7379 eV 261.69 nm f=0.2233 <S2>=2.956**

156A→171A	0.19346	145B→161B	0.13298	159B→164B	-0.13707
159A→174A	0.12295	151B→161B	-0.13290	159B→166B	-0.27199
161A→164A	-0.10065	154B→160B	-0.11487	159B→169B	0.17022
161A→165A	0.18407	155B→170B	-0.16196	159B→171B	0.10418
161A→167A	-0.10904	155B→171B	-0.11933	159B→173B	0.11034
161A→170A	0.12098	158B→164B	0.14322	159B→175B	0.14542
161A→174A	-0.12696	**159B→162B**	**0.45293**		
145B→160B	-0.17032	159B→163B	0.14570		

Excited State 46: 3.477-A 4.7850 eV 259.11 nm f=0.0120 <S**2>=2.773

149A→163A	-0.10769	159A→162A	0.12790	147B→160B	-0.22220
155A→162A	-0.10690	159A→166A	0.10971	149B→163B	0.14530
155A→169A	0.10101	159A→169A	0.11410	153B→160B	-0.30148
157A→172A	-0.10003	160A→165A	0.11340	153B→161B	0.45877

157B→162B	-0.10374	159B→164B	-0.23207		
159B→162B	0.10167	159B→169B	-0.16148		

Excited State 47: 3.392-A 4.7918 eV 258.74 nm f=0.0240 <S**2>=2.627

154A→169A	0.10047	147B→160B	0.16103	158B→167B	-0.10008
155A→169A	0.14148	149B→163B	-0.11139	159B→164B	0.17284
158A→169A	-0.13218	153B→160B	-0.36559	159B→169B	0.13567
159A→169A	0.16850	153B→161B	0.57631		
160A→169A	0.11694	157B→168B	-0.12644		

Excited State 48: 3.455-A 4.8441 eV 255.95 nm f=0.0377 <S**2>=2.734

161A→163A	0.10252	150B→160B	-0.27278	159B→164B	-0.11068
161A→167A	-0.14850	150B→161B	-0.25022	159B→169B	0.46118
147B→160B	-0.10933	158B→163B	-0.20402	159B→171B	0.22809
149B→160B	0.29252	158B→167B	-0.10963		
149B→161B	0.25824	159B→162B	-0.11536		

Excited State 49: 3.245-A 4.9281 eV 251.58 nm f=0.0056 <S**2>=2.382

152A→165A	-0.10132	149B→161B	0.54290	158B→163B	0.15069
161A→167A	0.14732	150B→160B	-0.26047	159B→169B	-0.36928
149B→160B	0.38077	150B→161B	-0.34869	159B→171B	-0.14494

C.1.3 Electronic Transitions in TANI-23

*Table C-3 Attributes of TANI-23 in **LEB** and **ES** (singlet and triplet) states related to electronic structures*

Attribute	LEB State	^{1}ES State	^{3}ES State
Molecular Formula	$C_{54}H_{44}N_6$	$C_{54}H_{44}N_6^{2+}$	$C_{54}H_{44}N_6^{2+}$
Number of Atoms	104	104	104
Number of Electrons	410	408	408
HOMO	MO 205	MO 204	MOs 205A and 203B
LUMO	MO 206	MO 205	MOs 206A and 204B

*C.1.3.1 TANI-23, **LEB** State*

Excited State 1: Singlet-A 3.7482 eV 330.78 nm f=0.7829 <S2>=0.000**

201→207	-0.10674	203→208	0.10044	204→211	-0.12354

205→207	**0.63559**	205→219	-0.12655		

Excited State 2:	Singlet-A	3.8067 eV	325.70 nm	f=0.0484	<S**2>=0.000
201→206	-0.10793	204→210	0.21489	205→206	0.62971

Excited State 3:	Singlet-A	3.9535 eV	313.61 nm	f=0.0000	<S**2>=0.000
202→211	0.12349	204→209	-0.33835	205→220	-0.10951
203→207	0.12464	205→208	0.54664		

Excited State 4:	**Singlet-A**	**3.9964 eV**	**310.24 nm**	**f=2.4914**	**<S**2>=0.000**
202→207	0.12205	**204→208**	**-0.35585**	205→221	0.11289
203→211	0.12224	**205→209**	**0.54163**		

Excited State 5:	Singlet-A	4.0590 eV	305.46 nm	f=0.0000	<S**2>=0.000
204→206	0.36589	204→218	-0.10571	205→210	0.53140

Excited State 6:	Singlet-A	4.4078 eV	281.28 nm	f=0.0439	<S**2>=0.000
202→206	0.18535	204→211	-0.13389	205→212	0.22644
203→210	-0.18820	204→217	0.29587	205→216	0.45134

Excited State 7:	Singlet-A	4.4123 eV	281.00 nm	f=0.0000	<S**2>=0.000
202→210	0.18655	204→216	0.29747	205→217	0.45888
203→206	-0.18573	205→211	-0.15682		
204→212	0.15855	205→214	0.15296		

Excited State 8:	**Singlet-A**	**4.4620 eV**	**277.87 nm**	**f=0.2369**	**<S**2>=0.000**
201→206	-0.12680	**204→210**	**-0.30862**		
201→218	-0.11325	**205→218**	**0.54073**		

Excited State 9:	Singlet-A	4.4878 eV	276.27 nm	f=0.0000	<S**2>=0.000
202→208	-0.20675	204→207	0.48496	205→214	-0.14431
203→209	-0.20361	205→211	-0.30445	205→222	0.11764

Excited State 10:	Singlet-A	4.7538 eV	260.81 nm	f=0.1707	<S**2>=0.000
201→212	0.17935	203→215	-0.26635	205→212	0.27919
202→209	0.12101	204→211	-0.20072	205→216	-0.19254
202→213	-0.26181	204→214	0.17936		
203→208	0.12193	204→217	-0.15280		

Excited State 11:	Singlet-A	4.7617 eV	260.38 nm	f=0.0000	<S**2>=0.000
200→213	0.13584	202→214	0.22814	205→215	0.34923
201→215	0.19276	203→212	-0.27658		
202→211	-0.15624	204→213	-0.30962		

Excited State 12:	Singlet-A	4.7652 eV	260.19 nm	f=0.0355	<S**2>=0.000
200→215	0.13277	203→211	-0.15527	205→213	0.34241
201→213	0.19526	203→214	0.22787		
202→212	-0.27050	204→215	-0.31016		

Excited State 13:	Singlet-A	4.7743 eV	259.69 nm	f=0.0000	<S**2>=0.000
200→212	-0.13026	203→213	0.28347	205→211	-0.11492
201→214	0.15884	204→212	0.27421	205→214	0.27830
202→215	0.28126	204→216	-0.14427	205→217	-0.18030

Excited State 14:	Singlet-A	4.8879 eV	253.66 nm	f=0.0000	<S**2>=0.000
201→207	0.19086	203→208	0.30084	204→214	-0.23289
202→209	0.29764	203→215	0.11251	205→212	-0.10033
202→213	0.11611	204→211	-0.16617	205→219	0.30528

C.1.3.2 TANI-23, ¹ES State

Excited State 1:	**Singlet-A**	**1.1272 eV**	**1099.94 nm**	**f=1.2241**	**<S**2>=0.000**
204→205	**0.71071**	204←205	-0.10827		

Excited State 2:	Singlet-A	1.7500 eV	708.50 nm	f=0.0002	<S**2>=0.000
202→205	0.69925				

Excited State 3:	**Singlet-A**	**1.7505 eV**	**708.28 nm**	**f=1.3513**	**<S**2>=0.000**
203→205	**0.70016**				

Excited State 4:	Singlet-A	2.3042 eV	538.08 nm	f=0.0000	<S**2>=0.000
193→205	0.13291	201→205	0.68641		

Excited State 5:	Singlet-A	3.0133 eV	411.45 nm	f=0.0256	<S**2>=0.000
200→205	0.69606				

Excited State 6:	Singlet-A	3.1112 eV	398.51 nm	f=0.0000	<S**2>=0.000		
188→205	0.38580	190→205	0.53216	194→205	0.24875		

Excited State 7:	Singlet-A	3.2171 eV	385.39 nm	f=0.0000	<S**2>=0.000
191→205	-0.42077	193→205	0.54937		

Excited State 8:	Singlet-A	3.2417 eV	382.47 nm	f=0.0030	<S**2>=0.000
192→205	0.69473				

Excited State 9:	Singlet-A	3.4094 eV	363.66 nm	f=0.0006	<S**2>=0.000		
189→205	0.62619	195→205	0.27225	198→205	-0.15798		

Excited State 10:	Singlet-A	3.5122 eV	353.01 nm	f=0.0000	<S**2>=0.000		
188→205	0.28901	190→205	-0.16539	197→205	0.61804		

Excited State 11:	Singlet-A	3.5188 eV	352.35 nm	f=0.0000	<S**2>=0.000
193→205	-0.18089	199→205	0.67167		

Excited State 12:	Singlet-A	3.5236 eV	351.87 nm	f=0.0022	<S**2>=0.000
196→205	0.69502				

Excited State 13:	Singlet-A	3.5259 eV	351.64 nm	f=0.0006	<S**2>=0.000
189→205	0.10011	195→205	0.15702	198→205	0.67779
Excited State 14:	Singlet-A	3.5570 eV	348.56 nm	f=0.0000	<S**2>=0.000
188→205	0.50289	190→205	-0.35386	197→205	-0.32925
Excited State 15:	Singlet-A	3.5786 eV	346.46 nm	f=0.0074	<S**2>=0.000
189→205	-0.30099	195→205	0.61425	198→205	-0.10315
Excited State 16:	Singlet-A	3.5793 eV	346.40 nm	f=0.0000	<S**2>=0.000
186→205	0.13173	193→205	0.36043	201→205	-0.12887
191→205	0.53729	199→205	0.18695		
Excited State 17:	Singlet-A	3.5936 eV	345.02 nm	f=0.0000	<S**2>=0.000
190→205	-0.23886	194→205	0.63927		
Excited State 18:	Singlet-A	3.9885 eV	310.85 nm	f=0.0000	<S**2>=0.000
200→206	0.10793	204→206	0.66882		
Excited State 19:	Singlet-A	4.1014 eV	302.29 nm	f=0.0000	<S**2>=0.000
200→207	0.11443	204→207	0.66921		
Excited State 20:	**Singlet-A**	**4.4277 eV**	**280.02 nm**	**f=1.9276**	**<S**2>=0.000**
201→209	-0.16337	203→211	-0.19494		
202→206	0.26363	**204→208**	**0.57101**		
Excited State 21:	Singlet-A	4.4411 eV	279.17 nm	f=0.0000	<S**2>=0.000
201→208	-0.17201	203→206	0.26673		
202→211	-0.20975	204→209	0.55819		
Excited State 22:	Singlet-A	4.4517 eV	278.51 nm	f=0.0061	<S**2>=0.000
183→205	-0.11671	187→205	0.65577		

Excited State 23:	**Singlet-A**	**4.5866 eV**	**270.32 nm**	**f=0.2786**	**<S**2>=0.000**	
201→207	-0.14268	203→213	-0.20104			
202→212	-0.18741	**204→210**	**0.57873**			

Excited State 24:	Singlet-A	4.6413 eV	267.13 nm	f=0.0626	<S**2>=0.000	
201→212	-0.14682	202→214	0.14190	204→211	-0.12598	
202→207	-0.30380	203→208	0.19986	204→213	0.36315	
202→209	0.21551	203→210	-0.28560			

Excited State 25:	Singlet-A	4.6480 eV	266.74 nm	f=0.0000	<S**2>=0.000	
201→213	-0.13472	203→207	-0.31343	204→212	0.38106	
202→208	0.18278	203→209	0.19937			
202→210	-0.29440	203→214	0.14364			

Excited State 26:	Singlet-A	4.8109 eV	257.72 nm	f=0.0059	<S**2>=0.000	
187→205	-0.15660	202→207	0.19869	203→210	0.16125	
201→206	-0.12882	202→209	0.30925	204→211	-0.31126	
201→219	-0.13783	203→208	0.32917	204→213	-0.14117	

Excited State 27:	Singlet-A	4.8675 eV	254.72 nm	f=0.0000	<S**2>=0.000	
201→210	0.15723	203→206	-0.22662	204→214	0.51469	
202→213	0.22005	203→212	0.18738			

Excited State 28:	Singlet-A	4.9157 eV	252.22 nm	f=0.0000	<S**2>=0.000	
186→205	-0.15049	202→208	0.35594	203→209	0.34259	
200→206	-0.10837	202→210	0.15512	204→219	0.24634	
201→211	0.15877	203→207	0.22880			

*C.1.3.3 TANI-23, ^{3}**ES** State*

Excited State 1:	3.034-A	1.0400 eV	1192.14 nm	f=0.0000	<S**2>=2.052	
194B→204B	0.12465	202B→204B	0.83270	203B→205B	-0.52179	

Excited State 2:	**3.034-A**	**1.1012 eV**	**1125.95 nm**	**f=1.2319**	**<S**2>=2.052**	
195B→204B	-0.12256	**202B→205B**	**-0.50595**	**203B→204B**	**0.83960**	
Excited State 3:	3.083-A	1.9265 eV	643.58 nm	f=0.3233	<S**2>=2.127	
187B→205B	0.14873	193B→204B	0.23740	201B→204B	0.86348	
190B→204B	0.13808	200B→205B	0.33569			
Excited State 4:	3.047-A	2.2633 eV	547.80 nm	f=0.0000	<S**2>=2.071	
202B→204B	0.54101	203B→205B	0.82741			
Excited State 5:	3.049-A	2.2679 eV	546.68 nm	f=0.0814	<S**2>=2.074	
202B→205B	0.83493	203B→204B	0.52696			
Excited State 6:	3.088-A	2.3019 eV	538.61 nm	f=0.0000	<S**2>=2.134	
187B→204B	0.19933	200B→204B	0.73714	201B→205B	0.57744	
Excited State 7:	3.113-A	2.7664 eV	448.18 nm	f=0.0032	<S**2>=2.173	
190B→204B	-0.44957	193B→204B	0.63816			
192B→205B	0.50939	200B→205B	-0.21126			
Excited State 8:	3.081-A	2.7957 eV	443.47 nm	f=0.0000	<S**2>=2.123	
190B→205B	-0.38382	193B→205B	0.42944			
192B→204B	0.76869	201B→205B	0.13652			
Excited State 9:	3.096-A	2.9003 eV	427.48 nm	f=0.0057	<S**2>=2.146	
188B→204B	-0.21113	191B→204B	0.73628	195B→204B	0.35351	
189B→205B	0.47162	194B→205B	0.10283			
Excited State 10:	3.087-A	2.9628 eV	418.47 nm	f=0.0000	<S**2>=2.132	
188B→205B	-0.31990	191B→205B	0.46207	195B→205B	0.16653	
189B→204B	0.76610	194B→204B	0.13267			

Excited State 11:	3.389-A	3.0233 eV	410.09 nm	f=0.0006	<S**2>=2.622				
188A→214A	-0.10481	205A→215A	-0.12657	192B→205B	-0.24451				
189A→206A	-0.14957	186B→204B	0.25627	193B→204B	0.22956				
191A→207A	0.10021	186B→206B	0.10967	193B→206B	0.12775				
201A→206A	-0.22707	190B→204B	0.48909	200B→205B	-0.39737				
205A→206A	-0.33609	191B→207B	-0.11993	201B→206B	0.16106				

Excited State 12:	3.065-A	3.1082 eV	398.90 nm	f=0.0000	<S**2>=2.099				
186B→205B	0.10540	192B→204B	-0.18410	200B→204B	-0.59056				
190B→205B	0.27368	193B→205B	0.25928	201B→205B	0.64789				

Excited State 13:	3.424-A	3.1401 eV	394.85 nm	f=0.0103	<S**2>=2.680				
202A→215A	-0.12983	188B→204B	0.33030	196B→215B	-0.10073				
203A→211A	0.14639	189B→205B	-0.22329	200B→208B	-0.11878				
204A→208A	0.16249	191B→204B	-0.13678	201B→209B	0.11245				
205A→209A	0.16412	194B→205B	0.31861	202B→211B	-0.12603				
184B→204B	0.10057	195B→204B	0.57707	203B→206B	-0.10385				

Excited State 14:	3.519-A	3.1521 eV	393.33 nm	f=0.0000	<S**2>=2.846				
196A→217A	-0.10859	203A→215A	0.15263	196B→216B	-0.10626				
197A→219A	-0.10921	204A→209A	-0.18875	199B→215B	0.11579				
198A→218A	0.10923	205A→208A	-0.19227	200B→209B	0.13061				
199A→216A	0.11030	185B→204B	-0.11534	201B→208B	-0.13023				
200A→221A	-0.10502	189B→204B	-0.12531	202B→206B	0.11379				
201A→220A	-0.10635	191B→205B	-0.10636	202B→219B	0.10523				
202A→211A	-0.17113	194B→204B	0.59518	203B→211B	0.13829				
203A→206A	-0.10528	195B→205B	0.35619						

Excited State 15:	3.760-A	3.2356 eV	383.19 nm	f=0.1681	<S**2>=3.285				
194A→220A	-0.10169	196A→218A	-0.11059	197A→216A	0.11428				

198A→217A	0.11356	205A→206A	0.48130	200B→205B	-0.15964
199A→219A	-0.11177	205A→215A	-0.10186	200B→211B	-0.11411
200A→222A	0.11096	190B→204B	0.14453	201B→204B	0.13015
201A→215A	0.15672	194B→220B	-0.10356	201B→219B	0.11954
202A→209A	0.25038	196B→218B	0.10534	202B→208B	-0.23770
203A→208A	0.24916	197B→215B	-0.10941	203B→209B	-0.24291
204A→211A	0.26281	199B→217B	-0.10651		

Excited State 16: 3.335-A 3.2906 eV 376.78 nm f=0.0576 <S**2>=2.531

202A→215A	0.10715	205A→209A	-0.13910	191B→204B	0.35717
203A→211A	-0.11831	188B→204B	0.70047	191B→206B	0.12809
204A→208A	-0.16053	188B→206B	0.10890	194B→205B	-0.12369
205A→207A	0.17210	189B→205B	-0.23796		

Excited State 17: 3.984-A 3.3346 eV 371.81 nm f=0.0000 <S**2>=3.717

194A→221A	-0.11790	202A→220A	0.13916	195B→220B	-0.12816
195A→220A	0.10813	203A→209A	-0.23423	196B→217B	0.14400
196A→219A	0.15535	203A→221A	-0.13630	197B→216B	-0.13482
197A→217A	0.15897	204A→206A	-0.18880	198B→215B	0.14791
198A→216A	0.15985	204A→215A	0.18183	199B→218B	-0.14291
199A→218A	0.15652	205A→211A	-0.22165	200B→219B	0.14790
200A→215A	0.12755	187B→204B	0.16516	201B→211B	-0.17197
201A→211A	0.13242	190B→205B	0.11034	202B→209B	0.28027
201A→222A	0.10139	193B→205B	0.10278	203B→208B	0.28292
202A→208A	-0.23490	194B→221B	-0.13146		

Excited State 18: 3.414-A 3.3876 eV 365.99 nm f=0.0000 <S**2>=2.664

190A→213A	-0.10953	202A→211A	0.19052	204A→209A	0.39596
192A→207A	-0.10107	203A→206A	0.15820	205A→208A	0.47626
193A→210A	-0.10969	203A→215A	-0.13542	194B→204B	0.41335

195B→205B	0.24627	202B→206B	-0.11770	203B→205B	0.13349

Excited State 19:	**3.375-A**	**3.4102 eV**	**363.57 nm**	**f=0.7764**	**<S**2>=2.598**
190A→212A	0.10722	203A→211A	0.17233	192B→210B	-0.10185
192A→210A	0.12541	**204A→208A**	**0.38057**	194B→205B	-0.27739
193A→207A	0.10553	**205A→209A**	**0.45626**	**195B→204B**	**-0.35860**
202A→206A	0.14925	188B→204B	0.19490	202B→205B	0.14971
202A→215A	-0.11600	191B→204B	0.23464	203B→206B	-0.11837

Excited State 20:	3.257-A	3.5146 eV	352.77 nm	f=0.0080	<S**2>=2.402
205A→206A	-0.13323	190B→204B	0.13206	200B→205B	0.70061
187B→205B	0.23884	193B→204B	0.17507	201B→204B	-0.41192

Excited State 21:	3.087-A	3.5504 eV	349.21 nm	f=0.0126	<S**2>=2.132
193B→204B	0.14605	196B→205B	-0.39380	199B→204B	0.87463

Excited State 22:	3.084-A	3.5520 eV	349.06 nm	f=0.0000	<S**2>=2.128
196B→204B	0.88906	199B→205B	-0.39798		

Excited State 23:	3.088-A	3.5538 eV	348.88 nm	f=0.0000	<S**2>=2.133
194B→204B	-0.11816	197B→205B	-0.15900	198B→205B	-0.36149
197B→204B	0.82081	198B→204B	-0.31748		

Excited State 24:	3.087-A	3.5539 eV	348.87 nm	f=0.0013	<S**2>=2.132
195B→204B	0.10314	197B→205B	-0.36126	198B→205B	0.15893
197B→204B	0.31779	198B→204B	0.82157		

Excited State 25:	3.713-A	3.6401 eV	340.61 nm	f=0.0000	<S**2>=3.196
192A→213A	0.11146	195A→208A	-0.13353	198A→216A	0.10372
193A→212A	0.10940	196A→219A	0.10188	199A→218A	0.10269
194A→209A	-0.16085	197A→217A	0.10331	200A→206A	-0.12799

202A→208A	0.14770	205A→211A	0.21432	195B→208B	0.15908
202A→220A	0.13089	205A→222A	-0.20595	201B→205B	-0.26018
203A→209A	0.15743	187B→204B	0.26067	202B→209B	-0.17299
203A→221A	-0.13318	190B→205B	0.13703	202B→221B	0.15712
204A→206A	0.29255	193B→205B	0.18200	203B→208B	-0.17062
204A→223A	-0.17413	194B→209B	-0.17435	203B→220B	-0.15537

Excited State 26: 3.421-A 3.6493 eV 339.75 nm f=0.1768 <S**2>=2.675

196A→218A	0.12127	186B→204B	0.11242	199B→217B	0.10368
197A→216A	-0.12351	187B→205B	0.14087	200B→211B	0.10825
198A→217A	-0.12281	190B→204B	0.39189	201B→204B	-0.23228
199A→219A	0.12188	193B→204B	0.46819	202B→208B	0.12580
201A→206A	0.17182	196B→218B	-0.10397	203B→209B	0.11624
205A→206A	0.34328	197B→215B	0.10618		
205A→215A	0.10950	199B→204B	-0.14722		

Excited State 27: 3.775-A 3.6636 eV 338.42 nm f=0.0000 <S**2>=3.314

194A→215A	-0.11579	204A→209A	-0.18612	197B→217B	-0.15060
195A→211A	0.13000	204A→221A	0.18135	198B→218B	0.14704
196A→217A	0.17874	205A→208A	-0.23902	199B→215B	-0.17507
197A→219A	0.17872	205A→220A	-0.17856	200B→209B	-0.11703
198A→218A	-0.17876	185B→204B	-0.10937	200B→221B	-0.13619
199A→216A	-0.18088	194B→204B	0.34553	201B→220B	-0.13838
200A→209A	0.15640	194B→219B	0.11794	202B→223B	-0.10431
201A→208A	-0.11784	195B→205B	0.12414	203B→211B	-0.10418
201A→220A	0.10162	195B→211B	-0.12480	203B→222B	-0.12980
202A→222A	0.15750	196B→216B	0.16167		
203A→223A	0.13938	197B→204B	0.10775		

Excited State 28:	3.750-A	3.6779 eV	337.10 nm	f=0.0859	<S**2>=3.265				
194A→211A	-0.13340	204A→220A	0.17436	197B→218B	-0.14393				
195A→215A	0.10984	205A→209A	0.24885	198B→204B	-0.10362				
196A→216A	0.17607	205A→221A	-0.17522	198B→217B	0.14752				
197A→218A	-0.17542	184B→204B	0.11213	199B→216B	-0.15857				
198A→219A	0.17543	188B→204B	-0.11879	200B→208B	0.11337				
199A→217A	-0.17658	191B→204B	-0.17873	200B→220B	-0.13362				
200A→208A	-0.15131	194B→205B	0.12547	201B→221B	-0.13310				
201A→209A	0.11388	194B→211B	-0.12570	202B→211B	0.10148				
202A→223A	-0.13652	195B→204B	0.33274	202B→222B	0.12800				
203A→222A	-0.15369	195B→219B	0.11689	203B→223B	0.10352				
204A→208A	0.17618	196B→215B	0.17126						

Excited State 29:	3.877-A	3.7033 eV	334.79 nm	f=0.0045	<S**2>=3.507				
188A→207A	0.16933	204A→211A	0.14596	193B→206B	0.15995				
189A→206A	-0.17042	204A→222A	-0.17560	194B→208B	-0.15867				
191A→214A	-0.12111	205A→215A	-0.12606	195B→209B	0.14871				
194A→208A	-0.14867	205A→223A	-0.21936	200B→205B	0.18439				
195A→209A	-0.12719	186B→204B	0.17240	201B→206B	0.10298				
200A→211A	-0.11024	187B→205B	-0.18430	202B→208B	-0.21158				
201A→215A	-0.11767	188B→207B	-0.15845	202B→220B	-0.15205				
202A→209A	0.15726	190B→204B	-0.11623	203B→209B	-0.20737				
202A→221A	-0.12916	190B→206B	0.11208	203B→221B	0.15491				
203A→208A	0.15678	191B→214B	0.11835						
203A→220A	0.12695	193B→204B	-0.13712						

Excited State 30:	3.286-A	3.7479 eV	330.81 nm	f=0.0247	<S**2>=2.449				
194A→212A	-0.10650	202A→213A	-0.19437	204A→210A	-0.41052				
200A→210A	0.10948	203A→212A	0.19364	205A→207A	0.73107				
201A→207A	0.15311	204A→208A	-0.11554	205A→214A	0.13306				

188B→204B	-0.10203	202B→213B	-0.11797	203B→212B	0.10381

Excited State 31:	3.089-A	3.8213 eV	324.46 nm	f=0.0000	<S**2>=2.135
204A→207A	-0.22051	189B→204B	-0.17033	195B→205B	0.28936
205A→210A	0.20747	191B→205B	0.59564		
188B→205B	0.58083	194B→204B	-0.18589		

Excited State 32:	3.337-A	3.8402 eV	322.86 nm	f=0.0000	<S**2>=2.534
194A→213A	-0.11747	204A→207A	-0.46026	191B→205B	-0.26911
195A→212A	0.10988	204A→214A	-0.24968	195B→205B	-0.13000
200A→207A	0.11367	205A→208A	0.14819	202B→212B	-0.13049
202A→212A	-0.21942	205A→210A	0.55087	203B→213B	0.13716
203A→213A	0.22404	188B→205B	-0.19995		

Excited State 33:	3.661-A	3.9354 eV	315.05 nm	f=0.0000	<S**2>=3.101
194A→207A	-0.11836	204A→213A	-0.36639	201B→205B	0.14617
195A→210A	0.13684	205A→211A	0.12053	202B→207B	-0.30398
202A→210A	-0.27956	205A→212A	0.41820	202B→214B	-0.15918
203A→207A	0.26057	187B→204B	-0.23209	203B→210B	0.29572
203A→214A	0.16615	193B→205B	-0.20657		

Excited State 34:	3.746-A	3.9488 eV	313.98 nm	f=0.0249	<S**2>=3.258
194A→210A	-0.14154	204A→211A	-0.11477	202B→210B	-0.32467
195A→207A	0.11265	204A→212A	-0.38247	203B→207B	0.32584
202A→207A	-0.27231	205A→213A	0.44462	203B→214B	0.17644
202A→214A	-0.17892	205A→215A	0.12257		
203A→210A	0.29710	194B→210B	-0.10169		

Excited State 35:	3.460-A	3.9890 eV	310.82 nm	f=0.0000	<S**2>=2.743
193A→212A	-0.10850	197A→217A	-0.12446	199A→218A	-0.12343
196A→219A	-0.12182	198A→216A	-0.12488	204A→213A	-0.13649

205A→212A	0.15161	193B→205B	0.34684	201B→205B	-0.30068
179B→204B	-0.10083	196B→217B	-0.10649	202B→207B	-0.13497
183B→204B	-0.12296	197B→216B	0.10097	203B→210B	0.11880
187B→204B	0.49237	198B→215B	-0.10831		
190B→205B	0.29271	199B→218B	0.10741		

Excited State 36: 3.203-A 4.2038 eV 294.93 nm f=0.0000 <S**2>=2.315

192A→213A	0.11152	187B→204B	-0.42498	193B→205B	0.55517
193A→212A	0.10122	190B→205B	0.14326	200B→204B	0.27985
186B→205B	0.43026	192B→204B	-0.19354		

Excited State 37: 3.595-A 4.2244 eV 293.49 nm f=0.0880 <S**2>=2.980

188A→214A	-0.17191	205A→206A	0.41014	191B→207B	-0.23007
190A→210A	0.20262	186B→204B	0.39454	192B→213B	-0.13379
191A→207A	0.21690	187B→205B	-0.25463	200B→205B	0.21881
192A→212A	0.18716	188B→214B	0.15582	202B→208B	0.15925
193A→213A	0.17709	189B→210B	-0.17617	203B→209B	0.17034
195A→207A	0.11115	190B→212B	0.10918		

Excited State 38: 3.479-A 4.2540 eV 291.45 nm f=0.0086 <S**2>=2.775

189A→207A	-0.21521	204A→210A	-0.28267	190B→207B	0.10512
201A→207A	-0.26332	205A→207A	-0.35298	193B→207B	0.11313
201A→214A	0.18424	205A→209A	-0.13373	201B→207B	0.17031
202A→213A	-0.16314	205A→214A	0.56021	202B→213B	-0.15228
203A→212A	0.15667	188B→204B	0.12645	203B→212B	0.15220

Excited State 39: 3.760-A 4.3551 eV 284.68 nm f=0.2611 <S2>=3.285**

188A→213A	-0.14149	192A→210A	0.28582	204A→208A	-0.18399
190A→212A	0.23922	193A→207A	0.23492	204A→210A	0.10268
191A→213A	0.18980	193A→214A	0.16299	205A→209A	-0.23275

167B→204B	-0.12064	189B→211B	0.11257	192B→210B	-0.25545
168B→205B	-0.10668	189B→213B	-0.17514	193B→207B	-0.16281
184B→204B	-0.20760	190B→207B	0.14810	194B→205B	-0.23939
185B→205B	0.19192	190B→214B	0.12405	195B→204B	0.25808
188B→212B	0.12543	191B→212B	-0.14893		

Excited State 40: 3.834-A 4.3598 eV 284.38 nm f=0.0000 <S**2>=3.424

188A→212A	0.14905	205A→208A	-0.24690	190B→210B	-0.20696
189A→210A	0.11370	167B→205B	0.10651	191B→205B	-0.11849
190A→213A	-0.25856	168B→204B	0.12318	191B→213B	0.14252
191A→212A	-0.19619	184B→205B	0.17620	192B→207B	0.22787
192A→207A	-0.25421	185B→204B	-0.21329	192B→214B	0.16640
192A→214A	-0.19634	188B→213B	-0.12135	193B→210B	0.17737
193A→210A	-0.28613	189B→212B	0.20686	194B→204B	-0.19396
204A→209A	-0.20353	189B→219B	-0.10980		

Excited State 41: 3.711-A 4.3662 eV 283.96 nm f=0.0034 <S**2>=3.193

188A→207A	-0.30060	186B→204B	0.31967	193B→204B	0.16464
188A→214A	0.19569	187B→205B	-0.27428	195B→207B	0.12372
191A→207A	-0.16795	188B→207B	0.27430	196B→205B	-0.11777
191A→214A	0.19419	188B→214B	-0.15770	200B→205B	0.23298
195A→207A	-0.12650	191B→207B	0.23643	203B→207B	-0.12270
195A→214A	0.12666	191B→214B	-0.20500	203B→209B	-0.10027
205A→206A	-0.25608	192B→205B	-0.16446		

Excited State 42: 3.800-A 4.3971 eV 281.97 nm f=0.0000 <S**2>=3.360

194A→219A	-0.12136	202A→218A	-0.27876	194B→217B	-0.12692
195A→218A	-0.11271	203A→219A	-0.27940	195B→218B	-0.12427
200A→217A	0.18298	204A→217A	0.26396	197B→204B	0.27511
201A→216A	0.20919	205A→216A	-0.25076	197B→205B	0.15772

198B→204B	-0.11406	201B→215B	-0.21338	203B→218B	-0.21451
198B→205B	0.38319	202B→212B	0.11224		
200B→216B	-0.19674	202B→217B	0.21487		

Excited State 43: 3.792-A 4.3975 eV 281.94 nm f=0.0000 <S**2>=3.345

194A→217A	0.12179	204A→219A	-0.26246	200B→217B	0.19489
195A→216A	-0.11484	205A→218A	-0.24842	201B→218B	0.19488
200A→219A	-0.17983	194B→216B	0.12808	202B→216B	-0.22675
201A→218A	0.20529	195B→215B	0.13753	203B→215B	0.24040
202A→216A	-0.28138	196B→204B	0.30415		
203A→217A	0.28115	199B→205B	0.42569		

Excited State 44: 3.793-A 4.3980 eV 281.91 nm f=0.0029 <S**2>=3.347

194A→218A	-0.12017	204A→216A	-0.26500	198B→204B	0.27590
195A→219A	-0.11209	205A→217A	0.25370	198B→205B	-0.15908
200A→216A	-0.18292	194B→218B	0.12574	200B→215B	0.21464
201A→217A	-0.20577	195B→217B	0.12276	201B→216B	0.19351
202A→219A	-0.27954	197B→204B	0.11436	202B→218B	-0.22093
203A→218A	-0.28005	197B→205B	0.38634	203B→217B	0.21851

Excited State 45: 3.793-A 4.4002 eV 281.77 nm f=0.0004 <S**2>=3.346

194A→216A	-0.11925	204A→218A	-0.25592	199B→204B	0.28991
195A→217A	0.10793	205A→219A	-0.24341	200B→218B	-0.18887
200A→218A	-0.17557	186B→204B	0.10672	201B→217B	-0.18888
201A→219A	0.19935	194B→215B	-0.13718	202B→215B	0.23367
202A→217A	0.27366	195B→216B	-0.11490	203B→216B	-0.22043
203A→216A	-0.27452	196B→205B	0.40637		

Excited State 46: 3.296-A 4.4693 eV 277.41 nm f=0.0081 <S**2>=2.466

190A→212A	0.11330	192A→210A	0.13938	193A→207A	0.10461

188B→204B	0.11240	194B→205B	0.71952	203B→206B	0.13784
191B→204B	0.10982	195B→204B	-0.37538		
192B→210B	-0.12088	197B→205B	0.23406		

Excited State 47: 3.366-A 4.4725 eV 277.22 nm f=0.0342 <S**2>=2.583

202A→217A	-0.11562	190B→204B	0.22191	202B→210B	-0.16256
203A→216A	0.11503	192B→205B	0.24015	202B→215B	-0.12397
204A→212A	0.13184	196B→205B	0.56360	203B→207B	0.23975
204A→218A	0.12151	199B→204B	0.22938	203B→209B	-0.16783
205A→213A	-0.16960	201B→212B	0.11791	203B→214B	0.13569
205A→219A	0.12057	202B→208B	-0.23228		

Excited State 48: 3.284-A 4.4757 eV 277.02 nm f=0.0000 <S**2>=2.445

202A→218A	-0.10829	194B→204B	-0.32741	201B→215B	-0.10114
203A→219A	-0.10881	195B→205B	0.56388	202B→206B	-0.14322
204A→217A	0.10259	197B→204B	-0.18018	203B→218B	-0.10135
188B→205B	-0.13569	197B→205B	-0.18832		
191B→205B	-0.21230	198B→205B	-0.45568		

Excited State 49: 3.364-A 4.4819 eV 276.64 nm f=0.0000 <S**2>=2.578

200A→219A	0.10162	205A→218A	0.15005	199B→205B	0.75335
201A→218A	-0.11652	190B→205B	0.12158	200B→217B	-0.13719
202A→216A	0.16301	192B→204B	0.10909	201B→218B	-0.13239
203A→217A	-0.16331	195B→215B	-0.10293	202B→216B	0.15282
204A→219A	0.15586	196B→204B	0.30546	203B→215B	-0.17254

Excited State 50: 3.304-A 4.4865 eV 276.35 nm f=0.0016 <S**2>=2.480

201A→217A	0.10433	204A→216A	0.13602	195B→204B	0.15387
202A→219A	0.14178	205A→217A	-0.13046	197B→204B	0.11573
203A→218A	0.14225	194B→205B	-0.28924	197B→205B	0.68649

198B→204B	0.28062	200B→215B	-0.13913	202B→218B	0.13498
198B→205B	-0.28407	201B→216B	-0.12327	203B→217B	-0.13825

C.1.4 Electronic Transitions in TANI-14

*Table C-4 Attributes of TANI-14 in **LEB** and **ES** (singlet and triplet) states related to electronic structures*

Attribute	LEB State	^{1}ES State	^{3}ES State
Molecular Formula	$C_{42}H_{34}N_4$	$C_{42}H_{34}N_4^{2+}$	$C_{42}H_{34}N_4^{2+}$
Number of Atoms	80	80	80
Number of Electrons	314	312	312
HOMO	MO 157	MO 156	MOs 157A and 155B
LUMO	MO 158	MO 157	MOs 158A and 156B

*C.1.4.1 TANI-14, **LEB** State*

Excited State 1:	**Singlet-B**	**3.9414 eV**	**314.57 nm**	**f=1.6564**	**<S**2>=0.000**	
155→169	0.11870	156→164	0.25739	**157→158**	**0.61839**	
Excited State 2:	Singlet-B	4.1765 eV	296.86 nm	f=0.1850	<S**2>=0.000	
155→163	0.11064	157→159	0.48152	157→163	0.13862	
156→160	0.37091	157→161	0.12838	157→166	-0.12930	
Excited State 3:	Singlet-A	4.1942 eV	295.61 nm	f=0.0446	<S**2>=0.000	
155→160	-0.12434	156→159	0.39490	157→162	-0.11810	
156→158	0.10469	157→160	0.47234	157→165	-0.15587	
Excited State 4:	Singlet-B	4.3472 eV	285.21 nm	f=0.1626	<S**2>=0.000	
149→158	-0.11259	155→163	0.24184	157→161	0.15673	
155→159	0.13014	156→160	-0.18382	157→163	0.55183	
Excited State 5:	Singlet-A	4.4010 eV	281.72 nm	f=0.1089	<S**2>=0.000	
155→164	-0.13139	156→169	-0.10958			
156→158	0.45468	157→164	0.44927			
Excited State 6:	Singlet-A	4.4060 eV	281.40 nm	f=0.0441	<S**2>=0.000	
155→160	0.11812	156→159	-0.13235	157→160	-0.10009	
155→162	0.23103	156→161	0.43147	157→162	-0.40871	

Excited State 7:	**Singlet-B**	**4.4114 eV**	**281.05 nm**	**f=0.5632**	**<S**2>=0.000**	
155→161	0.24974	**156→162**	**0.43166**	157→163	0.17615	
156→160	0.10810	**157→161**	**-0.39021**	157→166	0.10461	
Excited State 8:	Singlet-A	4.6871 eV	264.52 nm	f=0.0088	<S**2>=0.000	
154→159	0.14630	156→159	0.12770	156→166	0.34033	
155→160	-0.21737	156→161	0.10833	157→165	0.42136	
155→162	0.12232	156→163	-0.11486			
Excited State 9:	Singlet-B	4.6897 eV	264.38 nm	f=0.1017	<S**2>=0.000	
154→160	0.14467	156→160	0.12823	157→166	0.42732	
155→159	-0.19966	156→162	-0.12463			
155→163	0.10284	156→165	0.34377			
Excited State 10:	Singlet-B	4.8652 eV	254.84 nm	f=0.0636	<S**2>=0.000	
155→158	-0.23110	156→164	0.23099	157→167	-0.34474	
155→167	0.22030	156→168	0.34503	157→169	-0.14187	
Excited State 11:	Singlet-A	4.9053 eV	252.75 nm	f=0.0160	<S**2>=0.000	
147→161	0.10416	154→167	0.10429	156→167	0.42355	
148→162	0.10791	155→168	0.26106	157→168	-0.38435	

*C.1.4.2 TANI-14, ^{1}**ES** State*

Excited State 1:	**Singlet-B**	**1.0881 eV**	**1139.41 nm**	**f=2.2527**	**<S**2>=0.000**	
156→157	**0.71610**	156←157	-0.13518			
Excited State 2:	Singlet-A	1.8837 eV	658.18 nm	f=0.0337	<S**2>=0.000	
155→157	0.70422					
Excited State 3:	Singlet-B	2.8002 eV	442.77 nm	f=0.0377	<S**2>=0.000	
152→157	-0.13425	154→157	0.68610			

Excited State 4:	Singlet-B	3.0664 eV	404.33 nm	f=0.0071	<S**2>=0.000
146→157	-0.47323	151→157	0.50347	152→157	0.10390
Excited State 5:	Singlet-A	3.0684 eV	404.07 nm	f=0.0005	<S**2>=0.000
145→157	-0.46364	150→157	0.48931	153→157	-0.18189
Excited State 6:	Singlet-A	3.1007 eV	399.86 nm	f=0.0004	<S**2>=0.000
145→157	-0.15555	150→157	0.10428		
147→157	-0.15634	153→157	0.65648		
Excited State 7:	Singlet-A	3.1749 eV	390.51 nm	f=0.0000	<S**2>=0.000
144→157	0.69267				
Excited State 8:	Singlet-B	3.1877 eV	388.95 nm	f=0.0036	<S**2>=0.000
146→157	0.13282	152→157	0.67704	154→157	0.12742
Excited State 9:	Singlet-A	3.3582 eV	369.19 nm	f=0.0001	<S**2>=0.000
145→157	0.49469	147→157	-0.11489	150→157	0.46868
Excited State 10:	Singlet-B	3.3584 eV	369.18 nm	f=0.0450	<S**2>=0.000
146→157	0.49430	151→157	0.48720		
Excited State 11:	Singlet-A	3.4052 eV	364.11 nm	f=0.0003	<S**2>=0.000
142→157	0.10130	150→157	0.11359		
147→157	0.66124	153→157	0.15921		
Excited State 12:	Singlet-B	3.4979 eV	354.46 nm	f=0.0528	<S**2>=0.000
149→157	0.69736				
Excited State 13:	Singlet-A	3.4985 eV	354.39 nm	f=0.0050	<S**2>=0.000
148→157	0.69585				

Excited State 14:	Singlet-A	4.0075 eV	309.38 nm	f=0.0369	<S**2>=0.000
155→162	-0.18214	156→158	0.66915		
Excited State 15:	Singlet-B	4.4098 eV	281.16 nm	f=0.0087	<S**2>=0.000
141→157	0.11330	155→161	-0.11614	156→162	-0.13399
143→157	0.59503	156→160	0.25183		
Excited State 16:	Singlet-A	4.4197 eV	280.52 nm	f=0.0150	<S**2>=0.000
155→160	-0.28626	156→159	-0.27607	156→161	0.55232
Excited State 17:	Singlet-B	4.4338 eV	279.63 nm	f=0.0239	<S**2>=0.000
143→157	-0.26314	155→161	-0.26242	156→160	0.55785
Excited State 18:	Singlet-A	4.5829 eV	270.54 nm	f=0.0018	<S**2>=0.000
154→159	-0.15072	156→159	0.61894	156→161	0.27207
Excited State 19:	**Singlet-B**	**4.6041 eV**	**269.29 nm**	**f=0.2909**	**<S**2>=0.000**
143→157	0.18614	155→167	0.15239		
155→158	**-0.33210**	**156→162**	**0.54576**		
Excited State 20:	Singlet-A	4.8789 eV	254.12 nm	f=0.0194	<S**2>=0.000
155→163	0.33531	156→164	0.59148		
Excited State 21:	**Singlet-B**	**4.8798 eV**	**254.08 nm**	**f=0.4298**	**<S**2>=0.000**
155→164	**0.33547**	**156→163**	**0.59206**		
Excited State 22:	Singlet-A	4.9183 eV	252.09 nm	f=0.0010	<S**2>=0.000
128→157	0.10717	142→157	0.67049	147→157	-0.10741

*C.1.4.3 TANI-14, ^{3}**ES** State*

Excited State 1:	**3.061-B**	**1.3411 eV**	**924.51 nm**	**f=1.1505**	**<S**2>=2.092**
154B→157B	**-0.43173**	**155B→156B**	**0.88289**		

Excited State 2:	3.046-A	1.7420 eV	711.72 nm	f=0.1104	<S**2>=2.070
154B→156B	-0.59635	155B→157B	0.75745		
Excited State 3:	3.086-B	2.6454 eV	468.69 nm	f=0.0138	<S**2>=2.132
144B→156B	0.61739	150B→156B	0.40376		
145B→157B	0.53584	151B→157B	-0.33310		
Excited State 4:	3.085-A	2.6456 eV	468.64 nm	f=0.0003	<S**2>=2.129
144B→157B	0.53145	150B→157B	0.33338		
145B→156B	0.62197	151B→156B	-0.40473		
Excited State 5:	3.247-B	2.7365 eV	453.08 nm	f=0.0153	<S**2>=2.386
155A→158A	0.14249	149B→156B	0.41153	155B→156B	0.25175
157A→158A	-0.12617	152B→157B	-0.12221	155B→158B	-0.18277
157A→167A	-0.12267	153B→156B	0.48286		
143B→157B	-0.10949	154B→157B	0.55345		
Excited State 6:	3.061-A	2.7425 eV	452.08 nm	f=0.0003	<S**2>=2.093
143B→156B	-0.11767	152B→156B	-0.13415	154B→156B	0.62935
149B→157B	0.31265	153B→157B	0.35515	155B→157B	0.54747
Excited State 7:	3.293-A	3.0147 eV	411.27 nm	f=0.0012	<S**2>=2.461
155A→163A	0.12887	145B→156B	0.29878	151B→156B	0.46955
156A→162A	-0.15025	147B→156B	0.37415	154B→161B	0.10919
157A→163A	0.11522	148B→157B	0.30068		
144B→157B	0.24865	150B→157B	-0.37670		
Excited State 8:	3.294-B	3.0149 eV	411.23 nm	f=0.1078	<S**2>=2.463
155A→162A	-0.13005	144B→156B	-0.29347	148B→156B	-0.36673
156A→163A	0.15024	145B→157B	-0.25012	150B→156B	0.47084
157A→162A	-0.11592	147B→157B	-0.30969	151B→157B	-0.37646

154B→162B	-0.10830				

Excited State 9:	3.089-A	3.0489 eV	406.65 nm	f=0.0002	<S**2>=2.135
149B→157B	0.32667	153B→157B	-0.47390	155B→157B	0.16046
152B→156B	0.75438	154B→156B	0.13437		

Excited State 10:	3.127-B	3.0538 eV	406.00 nm	f=0.0103	<S**2>=2.195
149B→156B	-0.43775	153B→156B	0.58628		
152B→157B	-0.58584	154B→157B	-0.13776		

Excited State 11:	3.183-B	3.2344 eV	383.33 nm	f=0.0008	<S**2>=2.282
144B→156B	-0.26194	147B→157B	0.42846	151B→157B	-0.32114
145B→157B	-0.22039	148B→156B	0.47083	152B→162B	-0.10043
146B→156B	0.25630	150B→156B	0.42054	153B→161B	0.11380

Excited State 12:	3.183-A	3.2345 eV	383.32 nm	f=0.0038	<S**2>=2.283
144B→157B	-0.21782	147B→156B	0.53655	151B→156B	-0.42208
145B→156B	-0.26595	148B→157B	0.37649	152B→161B	-0.10012
146B→157B	0.20320	150B→157B	0.31976	153B→162B	0.11374

Excited State 13:	**3.557-B**	**3.3191 eV**	**373.55 nm**	**f=0.5570**	**<S**2>=2.912**
146A→171A	-0.11185	**157A→158A**	**0.63833**	155B→156B	0.15313
149A→164A	0.21776	157A→167A	0.12064	155B→158B	0.14457
155A→158A	-0.12900	146B→164B	0.19065	155B→169B	0.13726
155A→167A	-0.20933	149B→156B	0.14783		
156A→161A	0.29911	154B→157B	0.16726		

Excited State 14:	3.754-A	3.5122 eV	353.01 nm	f=0.0105	<S**2>=3.274
147A→163A	-0.18114	150A→166A	0.11768	152A→167A	0.10695
148A→162A	0.18843	151A→159A	0.14128	152A→169A	-0.10533
150A→160A	0.13919	151A→165A	-0.11477	153A→168A	0.16512

154A→169A	-0.12259	142B→157B	0.19316	152B→167B	0.16416
155A→161A	0.15554	143B→156B	0.37343	153B→168B	0.15469
155A→170A	-0.13391	147B→161B	-0.17383	154B→156B	0.24439
156A→158A	0.12453	148B→162B	-0.15926	154B→158B	-0.13706
156A→167A	-0.13725	149B→157B	-0.22713	154B→169B	0.10927
156A→171A	0.11187	150B→160B	0.16704	155B→157B	0.13602
157A→170A	-0.12451	151B→159B	-0.16080	155B→163B	-0.14966

Excited State 15: 3.512-B 3.5480 eV 349.45 nm f=0.0035 <S**2>=2.833

147A→162A	-0.13292	156A→170A	0.13743	151B→160B	-0.12761
148A→163A	0.13825	142B→156B	0.21161	152B→168B	-0.12296
149A→164A	0.12590	143B→157B	0.32804	154B→157B	0.49291
150A→159A	0.10997	146B→156B	-0.11134	154B→163B	0.12690
151A→160A	0.10956	147B→162B	-0.12867	155B→156B	0.28962
152A→168A	-0.10167	148B→161B	-0.11505	155B→158B	0.12493
153A→169A	0.11473	149B→156B	-0.24239		
155A→158A	-0.12378	150B→159B	0.12187		

Excited State 16: 3.194-B 3.5812 eV 346.21 nm f=0.0077 <S**2>=2.300

155A→164A	0.13048	146B→156B	0.80807	149B→156B	-0.16863
157A→164A	-0.20031	146B→158B	-0.17609		
144B→156B	0.10396	148B→156B	-0.39013		

Excited State 17: 3.247-A 3.6766 eV 337.23 nm f=0.0598 <S**2>=2.385

144A→160A	-0.11091	156A→171A	-0.10693	149B→157B	0.25884
145A→159A	-0.11454	157A→160A	0.18507	153B→157B	0.11179
146A→161A	0.11921	157A→161A	0.50285	154B→158B	0.12135
154A→158A	-0.15653	157A→170A	0.13608	155B→157B	-0.16018
156A→158A	0.48385	143B→156B	-0.26608		

Excited State 18:	3.706-B	3.6912 eV	335.89 nm	f=0.1356	<S**2>=3.183				
147A→169A	0.10698	155A→162A	-0.21468	150B→156B	-0.17013				
148A→170A	0.10449	156A→160A	0.15237	150B→167B	-0.15182				
150A→167A	-0.12118	156A→163A	0.24422	151B→157B	0.10669				
150A→169A	0.12504	157A→159A	-0.15079	151B→168B	-0.13202				
151A→168A	0.15975	157A→162A	-0.18567	152B→160B	-0.13771				
152A→160A	-0.11443	146B→156B	0.18341	152B→166B	0.12932				
152A→166A	-0.15626	147B→157B	0.28363	153B→161B	-0.11017				
153A→159A	0.11959	147B→168B	0.10699	153B→165B	0.10692				
153A→165A	-0.16652	148B→156B	0.35289	154B→162B	-0.15754				
154A→163A	0.15632	149B→159B	-0.10599	155B→161B	0.14524				

Excited State 19:	3.699-A	3.6913 eV	335.88 nm	f=0.0003	<S**2>=3.171				
148A→169A	-0.10849	156A→159A	0.13695	150B→157B	-0.10392				
150A→168A	0.15816	156A→162A	0.24732	150B→168B	0.13060				
151A→167A	-0.11980	157A→160A	-0.11023	151B→156B	0.16701				
151A→169A	0.12358	157A→161A	0.11942	151B→167B	0.14929				
152A→159A	-0.11757	157A→163A	-0.18425	152B→159B	-0.13146				
152A→165A	0.15296	146B→157B	0.10794	152B→165B	-0.12485				
153A→160A	0.11629	147B→156B	0.39660	153B→162B	-0.11140				
153A→166A	0.16800	147B→169B	0.10556	153B→166B	-0.10864				
154A→162A	0.15356	148B→157B	0.26284	154B→161B	-0.15789				
155A→163A	-0.21258	149B→160B	-0.11068	155B→162B	0.14108				

Excited State 20:	3.497-B	3.7395 eV	331.56 nm	f=0.1138	<S**2>=2.808				
146A→158A	-0.11954	156A→160A	-0.10609	142B→156B	-0.19390				
149A→164A	0.18506	156A→161A	-0.28518	143B→157B	-0.33122				
153A→169A	0.11455	157A→158A	-0.19793	146B→164B	0.15151				
155A→158A	-0.15967	157A→167A	0.20492	149B→156B	0.41077				
155A→171A	-0.10183	157A→171A	0.14311	152B→168B	-0.10545				

153B→156B	0.17110	155B→158B	0.22660		

Excited State 21:	3.654-B	3.7668 eV	329.15 nm	f=0.1286	<S**2>=3.089

144A→159A	0.13540	154A→161A	-0.14402	149B→156B	0.24215
145A→160A	0.12950	156A→161A	0.21060	149B→158B	-0.16758
146A→158A	0.17673	156A→170A	0.17293	152B→168B	-0.12941
147A→162A	-0.11256	157A→158A	0.30213	153B→156B	0.17615
148A→163A	0.11770	157A→171A	-0.19223	153B→158B	-0.10134
149A→164A	-0.18469	142B→156B	0.15335	153B→167B	-0.11244
150A→165A	-0.12162	146B→156B	0.10327	154B→157B	-0.26024
151A→166A	0.12394	146B→164B	-0.16346	154B→163B	0.14687
152A→168A	-0.11195	147B→162B	-0.12728	155B→156B	-0.18231
153A→169A	0.12406	148B→161B	-0.12035	155B→169B	-0.14500

Excited State 22:	3.579-A	3.9300 eV	315.48 nm	f=0.0054	<S**2>=2.952

144A→160A	0.20257	142B→157B	-0.11699	150B→166B	-0.10731
145A→159A	0.20961	143B→156B	-0.36532	151B→165B	-0.10246
150A→166A	0.14844	144B→160B	-0.13451	152B→167B	0.13261
151A→165A	-0.14449	145B→159B	-0.13531	153B→157B	0.14903
152A→169A	-0.11101	146B→157B	0.38603	153B→168B	0.12734
153A→168A	0.15138	147B→161B	-0.11356	154B→156B	-0.11146
156A→158A	-0.15072	148B→157B	-0.16544	155B→157B	-0.16696
157A→161A	-0.13607	149B→157B	0.21290		

Excited State 23:	3.147-A	3.9494 eV	313.93 nm	f=0.0002	<S**2>=2.226

143B→156B	0.14922	148B→157B	-0.36861		
146B→157B	0.78031	149B→157B	-0.30387		

Excited State 24:	3.192-B	4.0041 eV	309.64 nm	f=0.0221	<S**2>=2.298

146A→159A	0.12827	154A→160A	0.13524	154A→166A	-0.12302

155A→164A	-0.11867	156A→166A	0.15034	157A→165A	0.18641
156A→160A	-0.47840	157A→159A	0.66385	146B→156B	0.11386
156A→161A	0.12948	157A→162A	-0.14523		
156A→163A	0.12679	157A→164A	0.13484		

Excited State 25: 3.139-A 4.0194 eV 308.46 nm f=0.0256 <S**2>=2.214

146A→160A	0.13867	156A→162A	0.12710	157A→163A	-0.15498
154A→159A	0.14613	156A→165A	-0.14807	157A→166A	-0.22666
154A→165A	0.12541	157A→160A	0.63597		
156A→159A	-0.52314	157A→161A	-0.19857		

Excited State 26: 3.708-B 4.1595 eV 298.08 nm f=0.0148 <S**2>=3.188

146A→164A	-0.18523	157A→165A	-0.12402	153B→164B	0.11456
155A→164A	-0.36767	146B→156B	0.20463	155B→164B	0.37864
156A→160A	0.15423	148B→156B	-0.11239		
157A→164A	0.66958	149B→164B	0.17677		

Excited State 27: 3.181-A 4.2710 eV 290.29 nm f=0.0070 <S**2>=2.279

144A→160A	-0.13265	126B→156B	0.10857	149B→157B	0.42445
145A→159A	-0.13693	141B→156B	-0.21048	153B→157B	0.37738
156A→158A	-0.14315	142B→157B	0.43715	154B→156B	-0.36386
157A→161A	-0.12534	143B→156B	0.30972		

Excited State 28: 3.542-B 4.2877 eV 289.16 nm f=0.0371 <S**2>=2.886

144A→159A	-0.27159	141B→157B	-0.13589	145B→166B	0.15147
144A→165A	-0.12393	142B→156B	0.44621	146B→164B	0.10319
145A→160A	-0.26441	143B→157B	0.26338	149B→156B	0.25919
145A→166A	0.13172	144B→159B	0.17688	153B→156B	0.22705
149A→164A	0.12819	144B→165B	-0.14018	154B→157B	-0.33761
151A→166A	-0.10221	145B→160B	0.17703		

Excited State 29:	3.887-B	4.5180 eV	274.42 nm	f=0.1127	<S**2>=3.528	
144A→159A	-0.21159	151A→160A	0.11485	144B→159B	0.14704	
144A→165A	-0.13534	155A→158A	-0.11112	144B→165B	-0.15724	
145A→160A	-0.21155	157A→158A	0.29254	145B→160B	0.15606	
145A→166A	0.13943	157A→167A	0.10329	145B→166B	0.16330	
147A→164A	-0.10315	157A→171A	0.11194	146B→164B	-0.34699	
149A→164A	-0.36888	142B→156B	-0.24226	148B→164B	0.15130	
150A→159A	0.12044	143B→157B	-0.20686			

Excited State 30:	3.770-A	4.5741 eV	271.06 nm	f=0.0212	<S**2>=3.303	
144A→160A	-0.23807	156A→167A	0.10479	144B→166B	0.20002	
144A→166A	0.16665	157A→161A	-0.23467	145B→159B	0.18558	
145A→159A	-0.24649	124B→156B	0.12380	145B→165B	-0.18993	
145A→165A	-0.16124	133B→157B	-0.10467	150B→160B	0.13294	
150A→160A	0.14170	136B→157B	0.12161	151B→159B	-0.12870	
151A→159A	0.14524	141B→156B	0.24028	152B→167B	0.13249	
152A→169A	-0.11873	142B→157B	-0.21863	153B→168B	0.11177	
153A→168A	0.13773	143B→156B	-0.23495			
156A→158A	-0.20479	144B→160B	0.18523			

Excited State 31:	3.867-B	4.6026 eV	269.38 nm	f=0.0733	<S**2>=3.488	
147A→169A	-0.11825	154A→160A	0.16863	156A→166A	0.16311	
148A→168A	0.14753	154A→166A	0.13577	157A→162A	-0.26196	
149A→164A	-0.12174	155A→159A	-0.16602	157A→165A	0.17539	
150A→169A	-0.12809	155A→162A	-0.14674	142B→156B	0.10781	
151A→168A	-0.12272	155A→165A	0.10194	146B→164B	-0.10611	
152A→166A	0.13046	156A→160A	0.11243	147B→168B	-0.16599	
153A→159A	-0.12351	156A→161A	-0.13932	148B→167B	0.15021	
153A→165A	0.17673	156A→163A	0.26258	151B→168B	0.10550	

152B→160B	0.13135	153B→159B	-0.16414	155B→158B	0.12690
152B→162B	-0.12271	153B→165B	-0.15265	155B→159B	0.19134
152B→166B	-0.14527	154B→160B	-0.19650		

Excited State 32: 3.868-A 4.6036 eV 269.32 nm f=0.0001 <S**2>=3.491

147A→168A	-0.15322	155A→160A	-0.17466	150B→168B	-0.12252
148A→167A	-0.11268	155A→163A	-0.16464	151B→167B	-0.10493
148A→169A	0.12436	155A→166A	-0.10736	152B→159B	0.14421
150A→168A	-0.14444	156A→159A	0.14116	152B→161B	-0.12963
151A→169A	-0.14703	156A→162A	0.30602	152B→165B	0.15819
152A→165A	-0.14477	156A→165A	-0.16593	153B→160B	-0.19272
153A→160A	-0.13764	157A→163A	-0.28945	153B→162B	0.10765
153A→166A	-0.19610	157A→166A	-0.16157	153B→166B	0.16076
154A→159A	0.18840	147B→167B	0.18169	154B→159B	-0.20131
154A→165A	-0.14489	148B→168B	-0.16097	155B→160B	0.20736

Excited State 33: 3.872-B 4.6109 eV 268.89 nm f=0.0389 <S**2>=3.498

149A→164A	-0.30827	157A→162A	0.14176	148B→164B	0.15344
152A→168A	0.11322	157A→167A	0.21850	152B→168B	0.13212
153A→169A	-0.11473	136B→156B	-0.10518	153B→167B	0.13322
155A→158A	-0.16875	141B→157B	-0.19223	155B→158B	0.24542
156A→161A	-0.18029	142B→156B	0.19455		
156A→163A	-0.16875	146B→164B	-0.27041		

Excited State 34: 3.769-A 4.6460 eV 266.86 nm f=0.0049 <S**2>=3.302

147A→168A	0.12645	152A→165A	-0.12692	156A→159A	-0.11475
148A→169A	-0.13648	154A→162A	0.12236	156A→162A	0.24034
150A→168A	-0.17368	155A→160A	0.17027	156A→165A	0.34952
151A→169A	-0.15243	155A→163A	-0.18551	157A→163A	-0.20369
152A→159A	0.14338	155A→166A	0.20863	157A→166A	0.33029

147B→156B	0.10828	152B→159B	0.15400	155B→160B	-0.20475
149B→160B	0.13823	153B→162B	-0.10031	155B→162B	0.14894
150B→168B	-0.16958	154B→159B	0.15896		
151B→167B	-0.17706	154B→161B	-0.14584		

Excited State 35: 3.769-B 4.6472 eV 266.79 nm f=0.0054 <S**2>=3.301

147A→169A	-0.12969	155A→162A	0.17667	150B→167B	-0.17128
148A→168A	0.13440	155A→165A	0.20682	151B→168B	-0.16527
150A→169A	0.14738	156A→160A	0.12323	152B→160B	-0.15448
151A→168A	0.16824	156A→163A	-0.23380	153B→161B	0.10406
152A→160A	-0.14006	156A→166A	0.35559	154B→160B	-0.16560
152A→166A	-0.12486	157A→162A	0.19464	154B→162B	0.14752
154A→163A	-0.12238	157A→165A	0.31943	155B→159B	0.20177
155A→159A	-0.17226	149B→159B	-0.13679	155B→161B	-0.14254

Excited State 36: 3.184-A 4.7126 eV 263.09 nm f=0.0006 <S**2>=2.285

156A→169A	0.10459	149B→157B	-0.27985	152B→156B	0.55015
141B→156B	0.13095	150B→157B	-0.31836	153B→157B	0.52722
142B→157B	-0.10633	151B→156B	-0.23528		

Excited State 37: 3.192-B 4.7181 eV 262.79 nm f=0.0062 <S**2>=2.298

156A→168A	-0.10027	151B→157B	-0.31162	155B→158B	0.10888
149B→156B	-0.25381	152B→157B	0.61601		
150B→156B	-0.27288	153B→156B	0.46464		

Excited State 38: 3.215-A 4.7775 eV 259.51 nm f=0.0002 <S**2>=2.334

144B→157B	0.11586	150B→157B	0.64990	153B→157B	0.17189
145B→156B	-0.11727	151B→156B	0.54346		
149B→157B	-0.10560	152B→156B	0.19248		

Excited State 39:	3.162-B	4.7783 eV	259.47 nm	f=0.0045	<S**2>=2.250	
144B→156B	0.12216	150B→156B	0.53531	153B→156B	0.20739	
145B→157B	-0.11173	151B→157B	0.65913	155B→158B	0.14007	
149B→156B	-0.12196	152B→157B	0.21361			

Excited State 40:	3.703-B	4.8052 eV	258.02 nm	f=0.0138	<S**2>=3.178	
147A→165A	0.11689	157A→171A	-0.15427	149B→156B	0.11804	
148A→166A	0.12323	124B→157B	0.10590	152B→168B	0.10349	
153A→169A	-0.11721	125B→156B	-0.13193	153B→167B	0.12226	
154A→161A	-0.10133	133B→156B	-0.12304	154B→163B	0.29025	
154A→168A	0.14108	136B→156B	0.17328	154B→168B	-0.11854	
155A→167A	0.16699	141B→157B	0.26155	155B→158B	0.43749	
156A→168A	0.16319	142B→156B	-0.18350	155B→167B	-0.14155	
157A→167A	-0.10379	147B→160B	-0.11031			
157A→169A	-0.17447	148B→159B	-0.10158			

Excited State 41:	3.873-A	4.8171 eV	257.38 nm	f=0.0019	<S**2>=3.500	
144A→160A	-0.10668	154A→167A	-0.11155	150B→157B	-0.15643	
145A→159A	-0.11008	154A→169A	0.11542	150B→162B	0.13726	
147A→160A	-0.11825	155A→161A	0.18293	151B→156B	-0.13607	
147A→166A	-0.12253	155A→168A	-0.10191	151B→161B	-0.13730	
148A→159A	0.12033	156A→167A	-0.14270	152B→156B	-0.14422	
148A→165A	-0.12452	157A→170A	-0.13246	152B→167B	-0.15890	
150A→163A	0.10079	143B→156B	-0.18607	153B→157B	-0.14190	
150A→166A	-0.10521	147B→159B	-0.15886	153B→168B	-0.18385	
151A→165A	0.10473	147B→165B	-0.11601	154B→158B	-0.23579	
152A→169A	0.11945	148B→160B	-0.14701	154B→167B	0.13949	
153A→168A	-0.17084	148B→166B	0.11059	155B→163B	-0.29460	
154A→158A	0.13425	149B→157B	0.19607			

Excited State 42:	3.647-B	4.8389 eV	256.22 nm	f=0.0142	<S**2>=3.076	
147A→165A	0.13117	157A→169A	-0.21467	151B→160B	-0.12930	
148A→166A	0.13809	147B→162B	0.14688	151B→166B	0.10676	
150A→165A	-0.11663	148B→161B	0.13124	152B→157B	0.38845	
151A→166A	0.11989	149B→156B	-0.14067	153B→156B	0.13548	
154A→168A	0.13230	149B→167B	0.10103	154B→163B	-0.12870	
155A→169A	-0.24259	150B→159B	0.12597	154B→168B	-0.16416	
156A→168A	0.32260	150B→165B	0.10024	155B→158B	-0.22904	
157A→167A	0.19378	151B→157B	0.13550	155B→167B	-0.13835	

Excited State 43:	3.771-A	4.8393 eV	256.20 nm	f=0.0008	<S**2>=3.305	
147A→163A	-0.12815	156A→169A	-0.32414	151B→159B	0.14880	
147A→166A	0.12592	157A→168A	0.27971	151B→165B	0.12449	
148A→162A	0.13066	141B→156B	0.12537	152B→156B	0.11681	
148A→165A	0.13056	142B→157B	-0.11044	153B→157B	0.30064	
150A→160A	-0.10568	147B→161B	-0.17110	153B→163B	0.11044	
150A→166A	-0.14733	148B→162B	-0.15559	154B→158B	-0.13299	
151A→159A	-0.10638	149B→157B	-0.11308	154B→167B	-0.13667	
151A→165A	0.14421	149B→168B	0.12063	154B→169B	0.10314	
154A→169A	-0.13732	150B→160B	-0.15414	155B→163B	-0.14421	
155A→168A	0.25387	150B→166B	0.12976	155B→168B	-0.16871	

Excited State 44:	3.543-B	4.9287 eV	251.56 nm	f=0.0160	<S**2>=2.888	
147A→162A	0.10652	157A→158A	-0.12618	152B→168B	-0.11385	
148A→163A	-0.11082	157A→164A	-0.21963	154B→160B	-0.13366	
149A→158A	0.11635	142B→156B	0.20930	155B→158B	0.37060	
154A→161A	0.10790	143B→157B	0.12867	155B→159B	0.27467	
155A→158A	0.15260	147B→160B	0.10323	155B→164B	0.31895	
156A→161A	0.11266	149B→158B	0.10007	155B→165B	-0.12350	
156A→170A	-0.11534	149B→164B	0.13187	155B→169B	0.16592	

C.2 Electronic Transitions in PANI-CMP Oligomeric Models

C.2.1 Electronic Transitions in **OTPA-BZN-210** Oligomers

*Table C-5 Attributes of **OTPA-BZN-210** in **LEB**, **ES** (singlet and triplet), and **EB** states related to electronic structures*

Attribute	LEB State	^{1}ES State	^{3}ES State	EB State
Molecular Formula	$C_{42}H_{34}N_4$	$C_{42}H_{34}N_4^{2+}$	$C_{42}H_{34}N_4^{2+}$	$C_{42}H_{32}N_4$
Number of Atoms	80	80	80	78
Number of Electrons	314	312	312	312
HOMO	MO 157	MO 156	MOs 157A, 155B	MO 156
LUMO	MO 158	MO 157	MOs 158A, 156B	MO 157

*C.2.1.1 **OTPA-BZN-210**, **LEB** State*

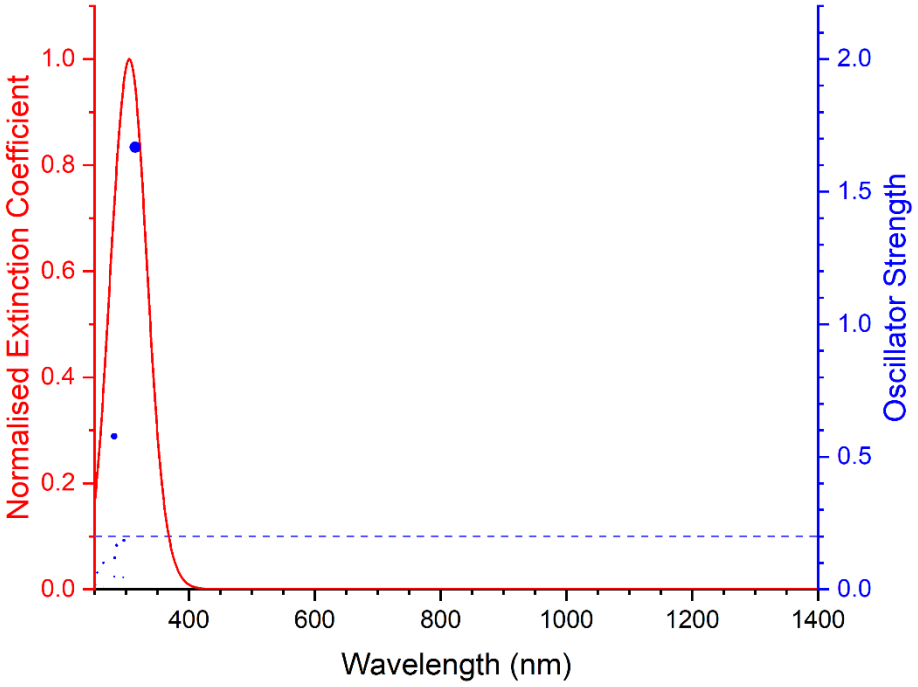

*Figure C-1 Excited states and normalised absorption spectra from TD-DFT calculations of **OTPA-BZN-210** in **LEB** state. The areas of excited state dots are proportional to their oscillator strengths.*

Excited State 1:	**Singlet-B**	**3.9412 eV**	**314.59 nm**	**f=1.6679**	**<S**2>=0.000**	
155→169	0.11992	156→164	0.25914	**157→158**	**0.61732**	
Excited State 2:	Singlet-B	4.1751 eV	296.96 nm	f=0.1843	<S**2>=0.000	
155→163	0.11133	157→159	0.48542	157→163	0.12668	
156→160	-0.37566	157→161	0.12063	157→165	-0.12785	

Excited State 3:	Singlet-A	4.1922 eV	295.75 nm	f=0.0452	<S**2>=0.000	
155→160	-0.12149	156→159	-0.39811	157→162	0.10922	
156→158	-0.10571	157→160	0.47521	157→166	-0.15091	
Excited State 4:	Singlet-B	4.3438 eV	285.43 nm	f=0.1662	<S**2>=0.000	
149→158	-0.11106	155→163	0.24853	157→161	0.17208	
155→159	0.13030	156→160	0.18083	157→163	0.54806	
Excited State 5:	Singlet-A	4.3915 eV	282.33 nm	f=0.1186	<S**2>=0.000	
155→164	-0.12776	156→169	-0.11304			
156→158	0.45618	157→164	0.44907			
Excited State 6:	Singlet-A	4.4014 eV	281.69 nm	f=0.0481	<S**2>=0.000	
155→160	-0.11086	156→159	-0.12128	157→162	-0.41258	
155→162	0.23125	156→161	0.43568			
Excited State 7:	**Singlet-B**	**4.4067 eV**	**281.36 nm**	**f=0.5778**	**<S**2>=0.000**	
155→161	0.24989	**157→161**	**-0.38872**			
156→162	**0.43501**	157→163	0.18696			
Excited State 8:	Singlet-A	4.6868 eV	264.54 nm	f=0.0090	<S**2>=0.000	
154→159	-0.14714	156→159	-0.12621	157→166	0.42261	
155→160	-0.21710	156→163	0.11220			
155→162	-0.11555	156→165	-0.34651			
Excited State 9:	Singlet-B	4.6890 eV	264.42 nm	f=0.1004	<S**2>=0.000	
154→160	-0.14554	156→160	-0.12746	157→165	0.42847	
155→159	-0.19835	156→162	-0.11836			
155→163	0.10361	156→166	-0.34753			
Excited State 10:	Singlet-B	4.8657 eV	254.81 nm	f=0.0637	<S**2>=0.000	
155→158	-0.24108	155→167	-0.21302	156→164	0.23752	

156→168	-0.33884	157→167	0.34096	157→169	-0.15209

Excited State 11:	Singlet-A	4.9067 eV	252.68 nm	f=0.0166	<S**2>=0.000
147→161	-0.10283	154→167	0.10391	156→167	0.42454
148→162	-0.10750	155→168	0.25784	157→168	-0.38601

*C.2.1.2 **OTPA-BZN-210**, **^{1}ES** State*

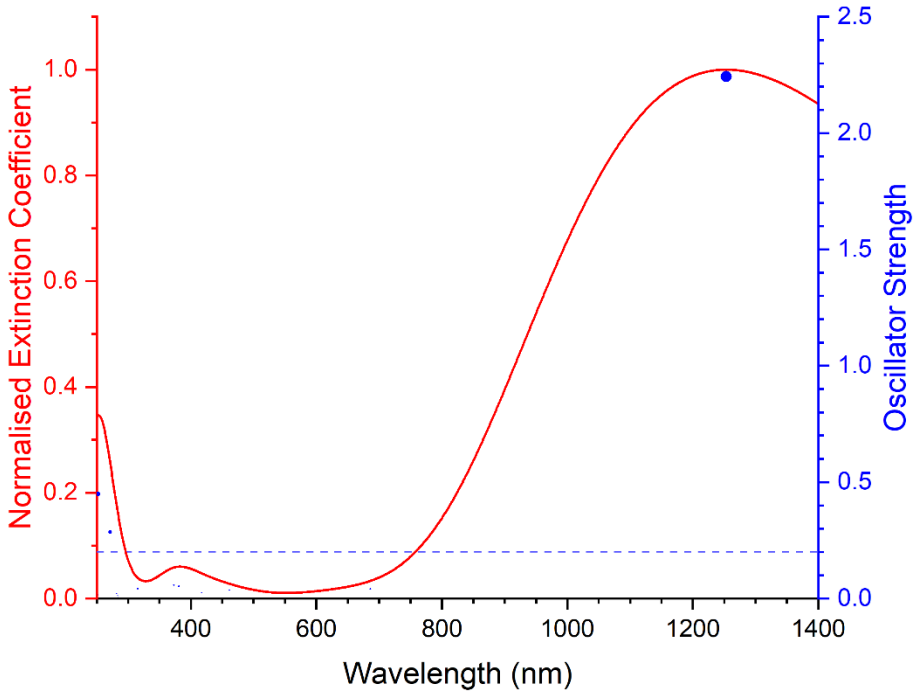

*Figure C-2 Excited states and normalised absorption spectra from TD-DFT calculations of **OTPA-BZN-210** in **^{1}ES** state. The areas of excited state dots are proportional to their oscillator strengths.*

Excited State 1:	**Singlet-B**	**0.9891 eV**	**1253.51 nm**	**f=2.2435**	**<S**2>=0.000**
156→157	**0.71795**	156←157	-0.14147		

Excited State 2:	Singlet-A	1.8073 eV	686.01 nm	f=0.0403	<S**2>=0.000
155→157	0.70484				

Excited State 3:	Singlet-B	2.6878 eV	461.29 nm	f=0.0353	<S**2>=0.000
152→157	0.13100	154→157	0.68710		

Excited State 4:	Singlet-A	2.9349 eV	422.45 nm	f=0.0001	<S**2>=0.000
151→157	0.16765	153→157	0.67375		

Excited State 5:	Singlet-B	2.9693 eV	417.55 nm	f=0.0238	<S**2>=0.000				
146→157	0.32399		150→157	0.61169					
Excited State 6:	Singlet-A	2.9802 eV	416.03 nm	f=0.0006	<S**2>=0.000				
145→157	0.34903		151→157	0.58367		153→157	-0.16692		
Excited State 7:	Singlet-B	3.0257 eV	409.77 nm	f=0.0004	<S**2>=0.000				
146→157	-0.14282		152→157	0.67560		154→157	-0.12328		
Excited State 8:	Singlet-A	3.1990 eV	387.57 nm	f=0.0001	<S**2>=0.000				
144→157	0.65125		145→157	-0.20669		151→157	0.12926		
Excited State 9:	Singlet-B	3.2547 eV	380.94 nm	f=0.0514	<S**2>=0.000				
146→157	0.59072		149→157	0.14286		150→157	-0.33779		
Excited State 10:	Singlet-A	3.2618 eV	380.11 nm	f=0.0003	<S**2>=0.000				
144→157	0.24422		148→157	0.12372					
145→157	0.55267		151→157	-0.32648					
Excited State 11:	Singlet-A	3.3137 eV	374.15 nm	f=0.0006	<S**2>=0.000				
144→157	-0.10311		148→157	-0.40500					
147→157	0.54691		153→157	0.10139					
Excited State 12:	Singlet-B	3.3219 eV	373.23 nm	f=0.0578	<S**2>=0.000				
146→157	-0.13701		149→157	0.68744					
Excited State 13:	Singlet-A	3.3269 eV	372.67 nm	f=0.0045	<S**2>=0.000				
145→157	-0.14034		147→157	0.39721		148→157	0.55535		
Excited State 14:	Singlet-A	3.9300 eV	315.48 nm	f=0.0419	<S**2>=0.000				
155→162	-0.16830		156→158	0.67320					

Excited State 15:	Singlet-B	4.3546 eV	284.72 nm	f=0.0060	<S**2>=0.000			
143→157	0.64811		156→161	0.12744		156→162	-0.13290	
Excited State 16:	Singlet-A	4.3777 eV	283.22 nm	f=0.0133	<S**2>=0.000			
155→161	0.25554		156→159	0.33297		156→160	0.54005	
Excited State 17:	Singlet-B	4.3954 eV	282.08 nm	f=0.0211	<S**2>=0.000			
143→157	-0.13270		155→160	0.26442		156→161	0.61248	
Excited State 18:	Singlet-A	4.4874 eV	276.29 nm	f=0.0036	<S**2>=0.000			
154→159	-0.13791		156→159	0.59286		156→160	-0.31960	
Excited State 19:	**Singlet-B**	**4.5649 eV**	**271.61 nm**	**f=0.2861**	**<S**2>=0.000**			
143→157	0.16276		155→167	0.13428				
155→158	**-0.32099**		**156→162**	**0.56400**				
Excited State 20:	Singlet-A	4.8356 eV	256.40 nm	f=0.0009	<S**2>=0.000			
128→157	-0.10497		142→157	0.67500		147→157	-0.10385	
Excited State 21:	Singlet-A	4.9099 eV	252.52 nm	f=0.0156	<S**2>=0.000			
155→163	0.32165		156→164	0.60200				
Excited State 22:	**Singlet-B**	**4.9104 eV**	**252.49 nm**	**f=0.4484**	**<S**2>=0.000**			
155→164	**0.32120**		**156→163**	**0.60196**				

*C.2.1.3 **OTPA-BZN-210**, ^{3}**ES** State*

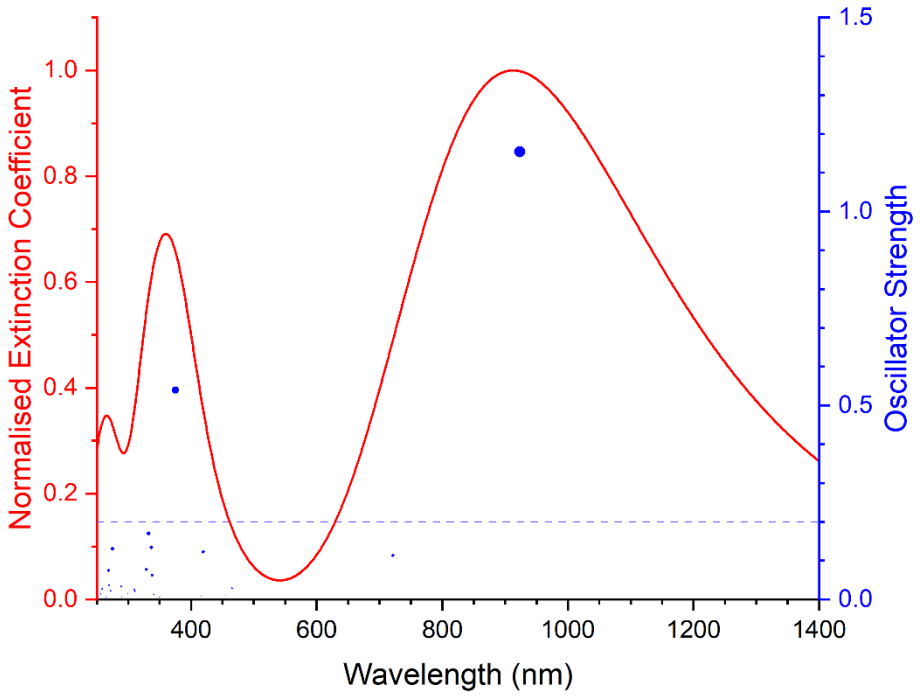

*Figure C-3 Excited states and normalised absorption spectra from TD-DFT calculations of **OTPA-BZN-210** in ^{3}**ES** state. The areas of excited state dots are proportional to their oscillator strengths.*

Excited State 1:	**3.061-B**	**1.3425 eV**	**923.52 nm**	**f=1.1538**	**<S**2>=2.093**
154B→157B	**-0.44034**	**155B→156B**	**0.87919**		
Excited State 2:	3.047-A	1.7181 eV	721.64 nm	f=0.1130	<S**2>=2.071
154B→156B	-0.59415	155B→157B	0.76103		
Excited State 3:	3.092-B	2.6629 eV	465.60 nm	f=0.0283	<S**2>=2.140
144B→156B	0.57374	150B→156B	-0.45086		
145B→157B	0.50379	151B→157B	-0.37663		
Excited State 4:	3.089-A	2.6630 eV	465.58 nm	f=0.0005	<S**2>=2.136
144B→157B	0.49993	150B→157B	-0.37664		
145B→156B	0.57859	151B→156B	-0.45437		
Excited State 5:	3.234-B	2.7262 eV	454.79 nm	f=0.0107	<S**2>=2.365
155A→158A	0.13380	143B→157B	-0.11391	152B→157B	-0.17189
157A→158A	-0.12284	146B→164B	-0.10121	153B→156B	0.50213
157A→167A	-0.12160	149B→156B	0.39200	154B→157B	0.53955

155B→156B	0.25589	155B→158B	-0.17816		

Excited State 6:	3.066-A	2.7386 eV	452.73 nm	f=0.0002	<S**2>=2.100
143B→156B	-0.12343	152B→156B	-0.19660	154B→156B	0.61162
149B→157B	0.30195	153B→157B	0.38135	155B→157B	0.52812

Excited State 7:	3.242-A	2.9556 eV	419.49 nm	f=0.0015	<S**2>=2.378
155A→163A	0.11404	144B→157B	0.30325	148B→157B	0.31559
156A→162A	-0.13289	145B→156B	0.35769	150B→157B	0.36883
157A→163A	0.10196	147B→156B	0.37482	151B→156B	0.45304

Excited State 8:	3.243-B	2.9558 eV	419.46 nm	f=0.1228	<S**2>=2.380
155A→162A	0.11482	144B→156B	0.35209	148B→156B	0.37882
156A→163A	-0.13321	145B→157B	0.30485	150B→156B	0.45303
157A→162A	0.10246	147B→157B	0.31411	151B→157B	0.36853

Excited State 9:	3.083-A	2.9747 eV	416.79 nm	f=0.0003	<S**2>=2.127
149B→157B	0.34031	153B→157B	-0.46453	155B→157B	0.20394
152B→156B	0.73587	154B→156B	0.18676		

Excited State 10:	3.134-B	2.9807 eV	415.96 nm	f=0.0092	<S**2>=2.206
149B→156B	0.44722	153B→156B	-0.56197	155B→156B	0.11932
152B→157B	0.58291	154B→157B	0.18060		

Excited State 11:	3.159-B	3.1614 eV	392.19 nm	f=0.0013	<S**2>=2.244
144B→156B	-0.27314	148B→156B	0.55789	153B→162B	0.10513
145B→157B	-0.23385	150B→156B	-0.37365		
147B→157B	0.46259	151B→157B	-0.28985		

Excited State 12:	3.159-A	3.1614 eV	392.18 nm	f=0.0046	<S**2>=2.244
144B→157B	-0.23152	145B→156B	-0.27667	147B→156B	0.56959

148B→157B	0.45293	150B→157B	-0.29049	151B→156B	-0.37274

Excited State 13:	**3.577-B**	**3.3061 eV**	**375.01 nm**	**f=0.5400**	**<S**2>=2.948**
146A→171A	-0.10958	**157A→158A**	**0.63623**	155B→156B	0.15701
147A→164A	0.22532	157A→167A	0.13193	155B→158B	0.16233
155A→158A	-0.13946	146B→164B	0.21111	155B→169B	0.13139
155A→167A	-0.21713	149B→156B	0.14558		
156A→161A	0.28952	154B→157B	0.17176		

Excited State 14:	3.721-A	3.5153 eV	352.70 nm	f=0.0094	<S**2>=3.211
148A→162A	0.18475	155A→170A	0.13316	150B→160B	-0.15339
149A→163A	0.18257	156A→158A	0.10510	150B→166B	0.10063
150A→159A	-0.12914	156A→167A	-0.13757	151B→159B	-0.14685
150A→165A	0.11485	156A→171A	0.11948	152B→167B	-0.15242
151A→160A	-0.12743	157A→170A	0.12884	153B→168B	0.15419
151A→166A	0.11882	142B→157B	0.20619	154B→156B	0.25949
152A→169A	-0.11063	143B→156B	0.39229	154B→158B	-0.13791
153A→168A	0.15948	147B→162B	-0.16567	154B→169B	0.10542
154A→169A	-0.11560	148B→161B	-0.15631	155B→157B	0.14945
155A→161A	0.15021	149B→157B	-0.24167	155B→163B	-0.13628

Excited State 15:	3.495-B	3.5464 eV	349.60 nm	f=0.0057	<S**2>=2.804
147A→164A	0.12098	156A→170A	-0.13670	151B→160B	-0.11891
148A→163A	0.13771	142B→156B	0.22129	152B→168B	-0.12007
149A→162A	0.13556	143B→157B	0.34072	154B→157B	0.49447
150A→160A	-0.10344	147B→161B	-0.11567	154B→163B	0.11261
151A→159A	-0.10336	148B→162B	-0.12142	155B→156B	0.29025
153A→169A	0.11660	149B→156B	-0.26334	155B→158B	0.11923
155A→158A	-0.11721	150B→159B	-0.11309		

Excited State 16:	3.217-B	3.6366 eV	340.93 nm	f=0.0132	<S**2>=2.337	
155A→164A	0.14314	146B→156B	0.88005	148B→156B	-0.13296	
157A→164A	-0.22545	146B→158B	-0.19587			

Excited State 17:	3.275-A	3.6652 eV	338.27 nm	f=0.0618	<S**2>=2.431	
144A→160A	-0.11862	156A→167A	-0.10473	143B→156B	-0.24954	
145A→159A	-0.12219	156A→171A	-0.10077	149B→157B	0.25315	
146A→161A	0.12087	157A→160A	0.18686	154B→158B	0.12274	
154A→158A	-0.15611	157A→161A	0.51064	155B→157B	-0.14659	
156A→158A	0.48975	157A→170A	-0.12875			

Excited State 18:	3.762-A	3.6782 eV	337.08 nm	f=0.0005	<S**2>=3.288	
148A→169A	0.10652	156A→159A	-0.13274	150B→168B	0.13251	
149A→170A	0.11071	156A→162A	-0.26468	151B→156B	-0.16930	
150A→167A	-0.10346	157A→160A	0.11022	151B→167B	0.15881	
150A→169A	0.14448	157A→161A	-0.10006	152B→159B	0.13144	
151A→168A	0.16441	157A→163A	0.19863	152B→165B	-0.14254	
152A→159A	0.11213	147B→156B	-0.33890	153B→160B	-0.10023	
152A→165A	-0.16049	147B→169B	-0.12191	153B→166B	0.12566	
153A→160A	-0.11545	148B→157B	-0.24434	154B→162B	0.16861	
153A→166A	0.18203	148B→168B	-0.11619	155B→161B	-0.14040	
154A→162A	-0.15944	149B→160B	0.10245			
155A→163A	0.22879	150B→157B	-0.10847			

Excited State 19:	3.762-B	3.6786 eV	337.05 nm	f=0.1338	<S**2>=3.289	
148A→170A	-0.11230	152A→160A	-0.10687	155A→162A	-0.22954	
149A→169A	-0.10332	152A→166A	0.16064	156A→160A	0.14158	
150A→168A	-0.16405	153A→159A	0.11760	156A→163A	0.26152	
151A→167A	0.10363	153A→165A	-0.18088	157A→159A	-0.14459	
151A→169A	-0.14726	154A→163A	0.16112	157A→162A	-0.19874	

147B→157B	0.24342	150B→167B	-0.15999	153B→162B	-0.10559
147B→168B	0.11886	151B→157B	0.10942	153B→165B	-0.12483
148B→156B	0.32733	151B→168B	-0.13314	154B→161B	-0.15684
148B→169B	0.12028	152B→160B	-0.13809	155B→162B	0.15455
150B→156B	0.17188	152B→166B	0.14298		

Excited State 20: 3.474-B 3.7322 eV 332.20 nm f=0.1698 <S**2>=2.767

146A→158A	-0.14987	157A→158A	-0.25502	146B→164B	0.19218
147A→164A	0.20865	157A→167A	0.21890	149B→156B	0.35608
155A→158A	-0.15576	157A→171A	0.16526	149B→158B	0.10943
156A→160A	-0.12979	142B→156B	-0.22244	153B→156B	0.11623
156A→161A	-0.31856	143B→157B	-0.32370	155B→158B	0.22450

Excited State 21: 3.707-B 3.7669 eV 329.14 nm f=0.0770 <S**2>=3.185

144A→159A	0.13995	156A→170A	-0.16878	150B→165B	0.10652
145A→160A	0.13449	157A→158A	0.24967	151B→160B	-0.10354
146A→158A	0.15435	157A→171A	-0.16529	151B→166B	0.11032
147A→164A	-0.15447	142B→156B	0.11166	152B→168B	-0.14870
148A→163A	0.13532	144B→159B	-0.10346	153B→156B	0.18072
149A→162A	0.13249	145B→160B	-0.10383	153B→167B	0.12139
150A→166A	0.14144	146B→156B	0.11175	154B→157B	-0.25589
151A→165A	0.13963	146B→164B	-0.14355	154B→163B	0.14335
152A→168A	-0.12507	147B→161B	-0.13157	155B→156B	-0.18674
153A→169A	0.15270	148B→162B	-0.14244	155B→169B	-0.12558
154A→161A	-0.13408	149B→156B	0.31685		
156A→161A	0.14996	149B→158B	-0.15797		

Excited State 22: 3.670-A 3.9188 eV 316.38 nm f=0.0047 <S**2>=3.118

144A→160A	-0.21651	148A→162A	-0.10887	150A→165A	-0.15643
145A→159A	-0.22360	149A→163A	-0.10672	151A→166A	-0.16176

152A→169A	0.12616	143B→156B	0.38626	151B→165B	-0.11229
153A→168A	-0.16673	144B→160B	0.14936	152B→167B	0.13747
154A→158A	-0.10235	145B→159B	0.14876	153B→157B	-0.15142
154A→169A	0.10667	146B→157B	-0.14035	153B→168B	-0.14363
156A→158A	0.14880	147B→162B	0.12208	154B→156B	0.12836
157A→161A	0.13590	148B→161B	0.11435	155B→157B	0.17825
157A→170A	-0.10183	149B→157B	-0.30144		
142B→157B	0.13791	150B→166B	-0.11734		

Excited State 23: 3.067-A 3.9898 eV 310.76 nm f=0.0002 <S**2>=2.101

146B→157B	0.94923	148B→157B	-0.12252	149B→157B	-0.18175

Excited State 24: 3.215-B 3.9915 eV 310.62 nm f=0.0214 <S**2>=2.334

146A→159A	0.13269	156A→160A	-0.47801	157A→162A	-0.13185
152A→160A	-0.10078	156A→161A	0.13594	157A→164A	0.12177
154A→160A	0.14227	156A→163A	0.11562	157A→165A	0.17190
154A→166A	0.11590	156A→166A	-0.13475	146B→156B	0.12223
155A→164A	-0.11451	157A→159A	0.67050		

Excited State 25: 3.161-A 4.0064 eV 309.46 nm f=0.0255 <S**2>=2.248

146A→160A	0.14385	156A→159A	-0.52340	157A→161A	-0.20719
152A→159A	-0.10825	156A→162A	0.11659	157A→163A	-0.14085
154A→159A	0.15421	156A→165A	-0.13145	157A→166A	0.20640
154A→165A	0.11762	157A→160A	0.64222		

Excited State 26: 3.721-B 4.1383 eV 299.60 nm f=0.0147 <S**2>=3.211

146A→164A	-0.18374	157A→164A	0.66188	153B→164B	0.10408
155A→164A	-0.36116	146B→156B	0.25760	155B→164B	0.38587
156A→160A	0.15622	149B→164B	0.18237		

Excited State 27:	3.166-A	4.2737 eV	290.11 nm	f=0.0059	<S**2>=2.257	
144A→160A	-0.12581	126B→156B	-0.10557	149B→157B	0.44727	
145A→159A	-0.12985	141B→156B	-0.21894	153B→157B	0.36668	
156A→158A	-0.13421	142B→157B	0.44417	154B→156B	-0.36030	
157A→161A	-0.11371	143B→156B	0.31069			

Excited State 28:	3.513-B	4.2883 eV	289.12 nm	f=0.0337	<S**2>=2.834	
144A→159A	-0.26552	142B→156B	0.45170	146B→164B	0.11779	
144A→165A	-0.10817	143B→157B	0.26678	149B→156B	0.28953	
145A→160A	-0.25865	144B→159B	0.17859	153B→156B	0.23268	
145A→166A	-0.11566	144B→165B	0.12672	154B→157B	-0.33605	
147A→164A	0.13957	145B→160B	0.17948			
141B→157B	-0.14677	145B→166B	0.13615			

Excited State 29:	3.879-B	4.5058 eV	275.17 nm	f=0.1307	<S**2>=3.513	
144A→159A	-0.23486	155A→158A	-0.10262	144B→159B	0.16957	
144A→165A	-0.13252	157A→158A	0.30240	144B→165B	0.15820	
145A→160A	-0.23424	157A→171A	0.10222	145B→160B	0.18031	
145A→166A	-0.13828	124B→157B	0.10097	145B→166B	0.16467	
147A→164A	-0.34848	141B→157B	0.10852	146B→159B	-0.10127	
150A→160A	-0.11751	142B→156B	-0.24411	146B→164B	-0.34835	
151A→159A	-0.12229	143B→157B	-0.19911			

Excited State 30:	3.775-A	4.5599 eV	271.90 nm	f=0.0221	<S**2>=3.313	
144A→160A	0.25707	152A→169A	0.11398	134B→157B	-0.12396	
144A→166A	0.15907	153A→168A	-0.13266	136B→157B	-0.11026	
145A→159A	0.26590	156A→158A	0.21157	141B→156B	-0.24056	
145A→165A	0.15323	156A→167A	-0.10695	142B→157B	0.21042	
150A→159A	0.14051	157A→161A	0.24497	143B→156B	0.21893	
151A→160A	0.13785	124B→156B	-0.12907	144B→160B	-0.20821	

144B→166B	-0.19407	150B→160B	0.12932	153B→168B	-0.11021
145B→159B	-0.20697	151B→159B	0.12501		
145B→165B	-0.18541	152B→167B	0.12110		

Excited State 31: 3.872-B 4.5992 eV 269.58 nm f=0.0369 <S**2>=3.499

147A→164A	-0.34640	157A→165A	0.10131	146B→164B	-0.34405
152A→168A	0.11885	157A→167A	0.22513	152B→168B	0.13610
153A→169A	-0.13507	134B→156B	-0.10812	153B→167B	-0.12897
155A→158A	-0.18084	141B→157B	-0.20698	155B→158B	0.28450
156A→161A	-0.22489	142B→156B	0.20925		

Excited State 32: 3.869-A 4.6113 eV 268.87 nm f=0.0002 <S**2>=3.492

148A→169A	0.13429	155A→160A	-0.16625	148B→168B	-0.17672
149A→168A	0.14670	155A→163A	-0.17972	150B→168B	0.12395
150A→169A	0.15287	155A→166A	0.10362	152B→159B	0.14347
151A→168A	0.15137	156A→159A	0.13340	152B→162B	-0.11512
152A→165A	-0.14593	156A→162A	0.31578	152B→165B	-0.17126
153A→160A	-0.13334	156A→165A	-0.14848	153B→160B	-0.19053
153A→166A	0.20548	157A→163A	-0.29475	153B→166B	0.17530
154A→159A	0.18090	157A→166A	0.14161	154B→159B	-0.19589
154A→165A	-0.15647	147B→167B	-0.18028	155B→160B	0.20386

Excited State 33: 3.868-B 4.6123 eV 268.81 nm f=0.0749 <S**2>=3.491

148A→168A	0.14341	154A→160A	0.17379	157A→162A	-0.29175
149A→169A	0.12298	154A→166A	-0.15092	157A→165A	0.11473
150A→168A	0.15405	155A→159A	-0.16249	147B→168B	-0.17438
151A→169A	0.15705	155A→162A	-0.18147	148B→167B	-0.17492
152A→166A	-0.14504	156A→160A	0.13286	151B→168B	0.12742
153A→159A	-0.13280	156A→163A	0.31400	152B→160B	0.15059
153A→165A	0.19833	156A→166A	-0.14017	152B→161B	-0.10483

152B→166B	-0.16979	153B→165B	0.16425	155B→159B	0.19000
153B→159B	-0.17909	154B→160B	-0.19373		

Excited State 34: 3.700-A 4.6637 eV 265.85 nm f=0.0042 <S**2>=3.173

148A→169A	-0.13345	156A→159A	-0.10998	151B→167B	0.16525
149A→168A	-0.12835	156A→162A	0.21251	152B→156B	0.15488
150A→169A	0.14869	156A→165A	0.33021	152B→159B	0.14196
151A→168A	0.15947	157A→163A	-0.17742	153B→157B	0.16364
152A→159A	0.13191	157A→166A	-0.30638	154B→159B	0.15321
152A→165A	-0.12132	147B→156B	0.11886	154B→162B	-0.12875
154A→162A	0.11785	149B→160B	0.12094	155B→160B	-0.20182
155A→160A	0.16126	150B→157B	0.15049	155B→161B	0.12170
155A→163A	-0.16610	150B→168B	0.15633		
155A→166A	-0.20356	151B→156B	-0.18991		

Excited State 35: 3.707-B 4.6644 eV 265.81 nm f=0.0040 <S**2>=3.185

148A→168A	-0.13040	156A→160A	-0.11223	151B→168B	0.15574
149A→169A	-0.13325	156A→163A	0.21337	152B→157B	-0.17084
150A→168A	0.15756	156A→166A	0.33646	152B→160B	0.14518
151A→169A	0.14865	157A→162A	-0.17563	153B→156B	-0.12853
152A→160A	0.13087	157A→165A	-0.30173	153B→162B	-0.11115
152A→166A	-0.12326	148B→156B	0.12101	154B→160B	0.16037
154A→163A	0.11954	149B→159B	0.11933	154B→161B	-0.11840
155A→159A	0.15986	150B→156B	-0.18485	155B→159B	-0.19919
155A→162A	-0.16367	150B→167B	0.16400	155B→162B	0.12490
155A→165A	-0.20385	151B→157B	0.14982		

Excited State 36: 3.208-A 4.6789 eV 264.99 nm f=0.0022 <S**2>=2.323

156A→165A	-0.12855	141B→156B	0.11911	149B→157B	-0.27583
157A→166A	0.11677	142B→157B	-0.10931	150B→157B	0.28970

151B→156B	-0.22782	152B→156B	0.52975	153B→157B	0.53185

Excited State 37:	3.233-B	4.6833 eV	264.74 nm	f=0.0067	<S**2>=2.364
147A→164A	-0.10136	149B→156B	-0.24282	153B→156B	0.46476
156A→166A	0.12348	150B→156B	0.22901	155B→158B	0.10743
157A→165A	-0.10526	151B→157B	-0.31055		
146B→164B	-0.10206	152B→157B	0.59978		

Excited State 38:	3.104-B	4.7362 eV	261.78 nm	f=0.0036	<S**2>=2.159
144B→156B	0.10474	151B→157B	0.66006	155B→158B	0.11029
149B→156B	-0.11723	152B→157B	0.30639		
150B→156B	-0.55003	153B→156B	0.23657		

Excited State 39:	3.111-A	4.7368 eV	261.75 nm	f=0.0000	<S**2>=2.169
145B→156B	0.10060	150B→157B	0.67118	152B→156B	-0.26858
149B→157B	0.13454	151B→156B	-0.55006	153B→157B	-0.24936

Excited State 40:	3.627-B	4.7933 eV	258.66 nm	f=0.0272	<S**2>=3.039
146A→158A	0.10081	124B→157B	0.11517	152B→168B	0.10024
153A→169A	-0.10922	125B→156B	-0.13921	153B→167B	-0.10362
154A→161A	-0.10854	134B→156B	0.14665	154B→161B	-0.12139
155A→167A	0.14403	136B→156B	0.15934	154B→163B	0.29510
157A→158A	-0.10724	141B→157B	0.26194	155B→158B	0.51091
157A→167A	-0.18231	142B→156B	-0.16540	155B→167B	0.10498
157A→171A	-0.15671	149B→156B	0.14712		

Excited State 41:	3.949-A	4.8107 eV	257.73 nm	f=0.0008	<S**2>=3.648
144A→160A	-0.10895	149A→160A	0.10694	151A→163A	-0.10458
145A→159A	-0.11307	149A→166A	-0.12227	151A→166A	-0.12193
148A→159A	0.11295	150A→162A	-0.10278	152A→169A	0.12821
148A→165A	-0.12281	150A→165A	-0.12108	153A→168A	-0.18143

154A→158A	0.14132	143B→156B	-0.16804	152B→167B	0.15852
154A→169A	0.13118	147B→159B	-0.15405	153B→168B	-0.19267
155A→161A	0.20510	147B→165B	0.12596	154B→158B	-0.25962
156A→167A	-0.13233	148B→160B	-0.15803	154B→167B	-0.14474
157A→170A	0.13655	148B→166B	0.12780	155B→161B	0.12624
125B→157B	-0.10772	149B→157B	0.15581	155B→163B	-0.29860
141B→156B	0.10630	150B→161B	-0.13704		
142B→157B	-0.11059	151B→162B	-0.14724		

Excited State 42: 3.806-B 4.8439 eV 255.96 nm f=0.0136 <S**2>=3.371

148A→160A	0.10545	156A→168A	0.36259	151B→160B	-0.15127
148A→166A	-0.18140	157A→167A	0.13031	151B→166B	0.11114
149A→159A	0.10592	157A→169A	-0.27617	152B→157B	0.27267
149A→165A	-0.17819	147B→161B	0.15529	153B→169B	-0.12502
150A→166A	0.11047	148B→162B	0.16241	154B→168B	-0.19235
151A→165A	0.10910	149B→167B	-0.10791	155B→158B	-0.14744
154A→168A	0.16975	150B→159B	-0.14517	155B→167B	0.16639
155A→169A	-0.27789	150B→165B	0.10747		

Excited State 43: 3.844-A 4.8475 eV 255.77 nm f=0.0012 <S**2>=3.444

148A→162A	0.13150	154A→169A	-0.15407	151B→159B	0.15775
148A→165A	0.16004	155A→168A	0.27711	151B→165B	-0.13060
149A→163A	0.12985	156A→169A	-0.35376	153B→157B	0.23013
149A→166A	0.15882	157A→168A	0.29473	153B→163B	0.11275
150A→159A	0.10853	147B→162B	-0.18551	153B→170B	0.10006
150A→165A	-0.13900	148B→161B	-0.16939	154B→167B	0.13977
151A→160A	0.10803	149B→168B	0.11941	154B→169B	0.11836
151A→166A	-0.14308	150B→160B	0.16503	155B→168B	-0.18017
152A→169A	0.10148	150B→166B	-0.13592		

Excited State 44:	3.557-B	4.9105 eV	252.49 nm	f=0.0094	<S**2>=2.913

147A→158A	0.12730	156A→170A	0.11331	153B→167B	0.10274
147A→167A	0.10202	157A→158A	-0.11374	154B→160B	-0.12818
148A→163A	-0.11790	157A→164A	-0.23641	155B→158B	0.31401
149A→162A	-0.11769	142B→156B	0.19772	155B→159B	0.28985
150A→166A	0.10010	143B→157B	0.11880	155B→164B	0.33207
154A→161A	0.11368	149B→158B	0.10255	155B→165B	0.11887
155A→158A	0.15664	149B→164B	0.14142	155B→169B	0.15539
156A→161A	0.10833	152B→168B	-0.11821		

*C.2.1.4 **OTPA-BZN-210**, **EB** State*

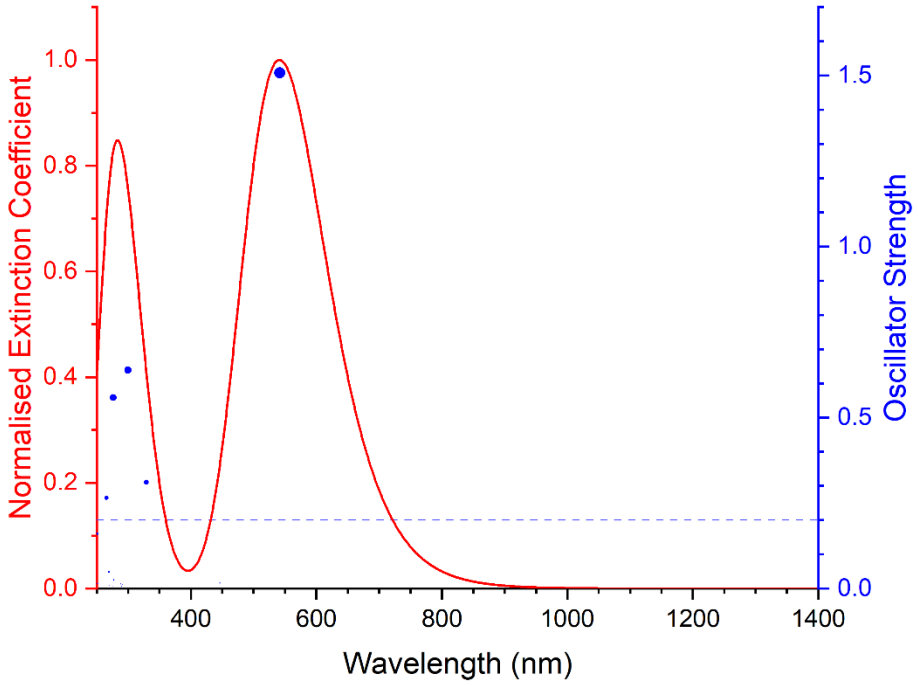

*Figure C-4 Excited states and normalised absorption spectra from TD-DFT calculations of **OTPA-BZN-210** in **EB** state. The areas of excited state dots are proportional to their oscillator strengths.*

Excited State 1:	**Singlet-B**	**2.2896 eV**	**541.50 nm**	**f=1.5080**	**<S**2>=0.000**

154→157	-0.17171	**156→157**	**0.66058**		

Excited State 2:	Singlet-A	2.7782 eV	446.28 nm	f=0.0159	<S**2>=0.000

142→157	0.10754	153→157	0.26902	155→157	0.62521

Excited State 3:	**Singlet-B**	**3.7692 eV**	**328.94 nm**	**f=0.3103**	**<S**2>=0.000**			
141→157	0.25912		146→157	0.22396		**154→157**	**-0.35435**	
144→157	**0.39577**		148→157	0.13165		156→157	-0.18973	
Excited State 4:	Singlet-A	3.8458 eV	322.39 nm	f=0.0006	<S**2>=0.000			
142→157	0.33088		153→157	0.47475				
149→157	-0.17638		155→157	-0.29732				
Excited State 5:	**Singlet-B**	**4.1352 eV**	**299.83 nm**	**f=0.6387**	**<S**2>=0.000**			
144→157	**0.31657**		148→157	0.10038				
146→157	0.19718		**154→157**	**0.55301**				
Excited State 6:	Singlet-A	4.2530 eV	291.52 nm	f=0.0125	<S**2>=0.000			
143→157	0.37025		155→160	-0.28287		156→168	-0.10212	
145→157	-0.23333		156→158	0.13117				
151→157	0.21640		156→159	0.32634				
Excited State 7:	Singlet-B	4.2772 eV	289.87 nm	f=0.0057	<S**2>=0.000			
146→157	0.19123		155→159	-0.35100		156→165	-0.13320	
150→157	-0.24391		156→160	0.43099				
Excited State 8:	Singlet-A	4.3032 eV	288.12 nm	f=0.0130	<S**2>=0.000			
143→157	0.57853		156→158	-0.14424				
155→160	0.22432		156→159	-0.24809				
Excited State 9:	Singlet-A	4.4700 eV	277.37 nm	f=0.0257	<S**2>=0.000			
155→161	-0.15949		156→158	0.51077		156→162	-0.15538	
155→163	-0.31369		156→159	-0.20348				
Excited State 10:	**Singlet-B**	**4.4824 eV**	**276.60 nm**	**f=0.5580**	**<S**2>=0.000**			
154→161	0.14622		**155→162**	**0.44216**		**156→161**	**0.48246**	

Excited State 11:	Singlet-A	4.4834 eV	276.54 nm	f=0.0074	<S**2>=0.000						
154→162	0.13685		155→163	-0.12511		156→162	0.45849				
155→161	0.41509		156→158	0.19900							
Excited State 12:	Singlet-B	4.5938 eV	269.90 nm	f=0.0081	<S**2>=0.000						
144→157	0.19175		154→160	0.11182		156→160	0.24476				
146→157	-0.30835		155→159	-0.23060		156→161	0.10157				
150→157	0.37324		155→168	-0.10349		156→165	0.14363				
Excited State 13:	Singlet-A	4.6029 eV	269.36 nm	f=0.0480	<S**2>=0.000						
143→157	0.12415		154→159	0.10927		156→164	-0.11455				
145→157	0.35941		155→160	-0.23181		156→168	0.12140				
149→157	0.12745		155→165	-0.13399							
151→157	-0.35005		156→159	0.21881							
Excited State 14:	**Singlet-B**	**4.6677 eV**	**265.62 nm**	**f=0.2657**	**<S**2>=0.000**						
144→157	-0.10496		155→159	-0.10120		**156→163**	**-0.44195**				
155→158	**0.44618**		156→157	0.11500							
Excited State 15:	Singlet-A	4.9328 eV	251.35 nm	f=0.0140	<S**2>=0.000						
145→157	0.13310		154→159	-0.12135		156→164	0.37598				
151→157	-0.24822		155→165	0.32062		156→168	-0.26650				
Excited State 16:	Singlet-B	4.9535 eV	250.29 nm	f=0.1604	<S**2>=0.000						
146→157	0.10242		154→160	0.12019		156→165	0.43413				
150→157	-0.26587		155→164	0.18751							
153→159	0.10956		155→168	-0.30692							

C.2.2 Electronic Transitions in **OTPA-BZN-221** Oligomers

*Table C-6 Attributes of **OTPA-BZN-221** in **LEB**, **ES** (singlet and quintet), and **EB** states related to electronic structures*

Attribute	LEB State	^{1}ES State	^{5}ES State	EB State
Molecular Formula	$C_{48}H_{38}N_6$	$C_{48}H_{38}N_6^{4+}$	$C_{48}H_{38}N_6^{4+}$	$C_{48}H_{36}N_6$
Number of Atoms	92	88	88	88
Number of Electrons	368	364	364	364
HOMO	MO 184	MO 182	MOs 184A, 180B	MO 182
LUMO	MO 185	MO 183	MOs 185A, 181B	MO 183

*C.2.2.1 **OTPA-BZN-221**, **LEB** State*

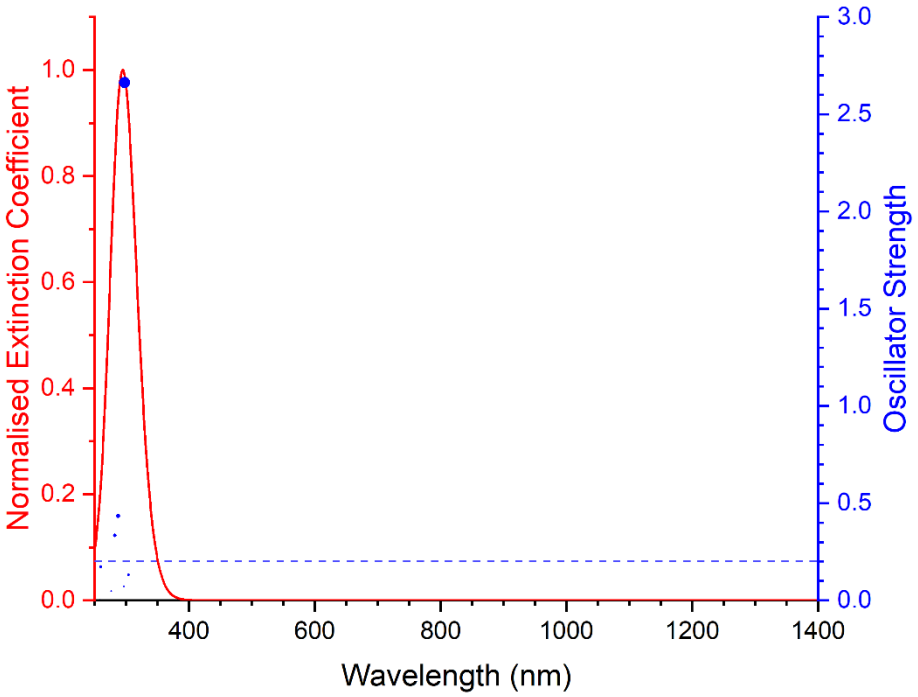

*Figure C-5 Excited states and normalised absorption spectra from TD-DFT calculations of **OTPA-BZN-221** in **LEB** state. The areas of excited state dots are proportional to their oscillator strengths.*

Excited State 1:	Singlet-B3	3.8436 eV	322.57 nm	f=0.0036	<S**2>=0.000
182→187	-0.21997	183→186	-0.19956	183→192	-0.13321
182→197	0.11829	183→190	-0.17819	184→185	0.56001
Excited State 2:	**Singlet-B2**	**4.0784 eV**	**304.00 nm**	**f=0.1317**	**<S**2>=0.000**
182→189	-0.13414	183→185	-0.31175	**184→186**	**0.50937**
182→191	0.12677	183→188	-0.23564		

Excited State 3:	**Singlet-B1**	**4.1605 eV**	**298.00 nm**	**f=2.6625**	**<S**2>=0.000**	
181→197	0.12689	183→189	-0.23124	**184→187**	**0.50226**	
182→185	**-0.31915**	183→191	-0.16000			
Excited State 4:	Singlet-B3	4.1804 eV	296.59 nm	f=0.0709	<S**2>=0.000	
182→193	-0.11909	183→190	0.23262			
183→186	-0.33308	184→188	0.49832			
Excited State 5:	Singlet-A	4.2945 eV	288.70 nm	f=0.0000	<S**2>=0.000	
181→191	0.11481	182→192	0.25737	184→191	-0.28013	
182→186	-0.28869	183→193	-0.13747			
182→190	-0.14690	184→189	0.39153			
Excited State 6:	**Singlet-B2**	**4.3125 eV**	**287.50 nm**	**f=0.4344**	**<S**2>=0.000**	
182→189	-0.12441	**183→188**	**0.33609**			
183→185	-0.25875	**184→190**	**0.47307**			
Excited State 7:	**Singlet-B2**	**4.3921 eV**	**282.29 nm**	**f=0.3343**	**<S**2>=0.000**	
181→186	0.15802	182→189	0.27264	183→185	-0.22776	
181→190	0.10035	182→191	-0.24228	**184→192**	**0.43279**	
181→192	-0.10351	182→194	0.15309			
Excited State 8:	Singlet-A	4.4371 eV	279.43 nm	f=0.0000	<S**2>=0.000	
181→189	-0.13223	183→193	-0.11201	184→189	-0.28079	
183→187	0.41114	183→197	0.11166	184→191	-0.37543	
Excited State 9:	Singlet-B1	4.4803 eV	276.73 nm	f=0.0473	<S**2>=0.000	
180→186	0.14546	182→188	-0.21882	183→194	0.25852	
182→185	-0.14914	183→191	0.23986	184→193	0.46171	
Excited State 10:	Singlet-A	4.5601 eV	271.89 nm	f=0.0000	<S**2>=0.000	
180→188	-0.11253	181→189	-0.14165	182→190	-0.16867	

182→192	0.19507	183→187	0.13137	184→194	0.45098
182→196	0.11811	183→193	0.30632		

Excited State 11:	Singlet-B3	4.7404 eV	261.55 nm	f=0.0000	<S**2>=0.000
179→186	-0.12939	181→195	0.19506	183→192	-0.16279
181→185	0.16684	182→193	0.12889	183→196	0.35108
181→188	0.11299	183→186	-0.11008	184→195	0.38945

Excited State 12:	Singlet-B2	4.7683 eV	260.02 nm	f=0.1721	<S**2>=0.000
179→188	0.10735	181→192	-0.10043	183→188	0.10300
179→195	0.10347	181→196	0.18866	183→195	0.39100
181→186	-0.12052	182→194	0.12355	184→196	0.40341

Excited State 13:	Singlet-B1	4.7913 eV	258.77 nm	f=0.0077	<S**2>=0.000
181→187	0.27505	183→189	-0.27579	184→197	0.28552
182→185	0.37057	183→191	-0.14902		
182→188	-0.14030	183→194	0.15580		

Excited State 14:	Singlet-B3	4.9554 eV	250.20 nm	f=0.0005	<S**2>=0.000
181→185	0.33090	182→197	-0.14166	183→196	-0.13768
181→188	-0.13377	183→186	-0.13589	184→195	-0.10916
182→187	0.32032	183→190	-0.30025	184→198	-0.20790

*C.2.2.2 **OTPA-BZN-221**, **^{1}ES** State*

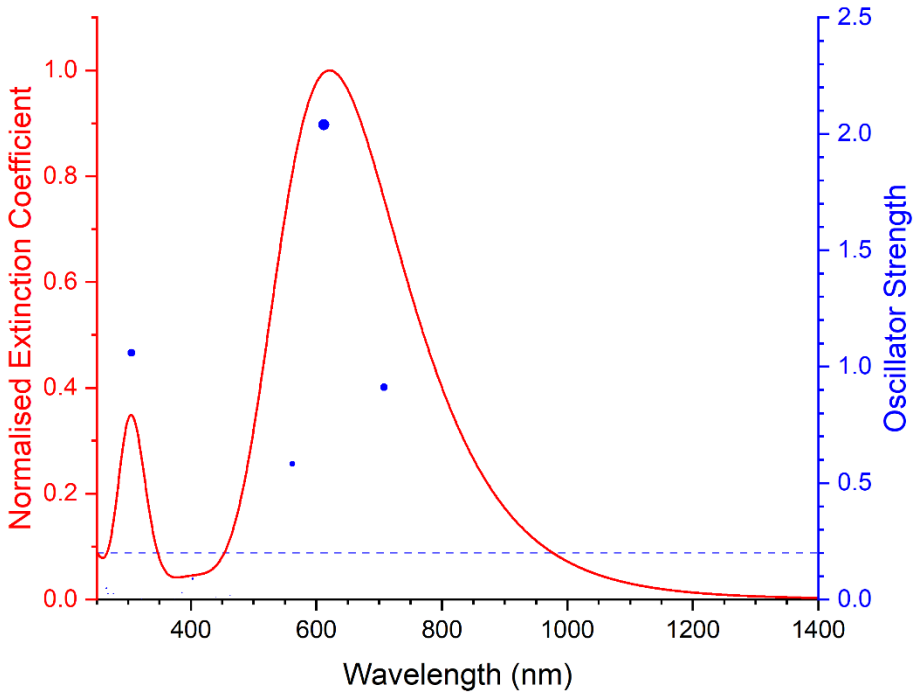

*Figure C-6 Excited states and normalised absorption spectra from TD-DFT calculations of **OTPA-BZN-221** in **^{1}ES** state. The areas of excited state dots are proportional to their oscillator strengths.*

Excited State 1:	Singlet-B3	0.8125 eV	1526.01 nm	f=0.0001	<S**2>=0.000	
180→184	0.12260	182→183	0.69203			
Excited State 2:	**Singlet-B2**	**1.7511 eV**	**708.04 nm**	**f=0.9118**	**<S**2>=0.000**	
182→184	**0.70951**					
Excited State 3:	**Singlet-B1**	**2.0257 eV**	**612.05 nm**	**f=2.0394**	**<S**2>=0.000**	
179→184	0.19041	**181→183**	**0.67712**			
Excited State 4:	**Singlet-B2**	**2.2075 eV**	**561.64 nm**	**f=0.5832**	**<S**2>=0.000**	
173→184	0.12554	**180→183**	**0.68791**			
Excited State 5:	Singlet-A	2.4512 eV	505.82 nm	f=0.0000	<S**2>=0.000	
174→184	0.10464	179→183	0.37153	181→184	0.58801	
Excited State 6:	Singlet-B3	2.6041 eV	476.12 nm	f=0.0005	<S**2>=0.000	
177→184	-0.25365	178→183	-0.40097	180→184	0.49879	

Excited State 7:	Singlet-B2	2.6789 eV	462.82 nm	f=0.0169	<S**2>=0.000
177→183	0.57003	178→184	0.39816		
Excited State 8:	Singlet-B3	2.7184 eV	456.10 nm	f=0.0036	<S**2>=0.000
173→183	0.15156	178→183	0.40826		
177→184	0.31482	180→184	0.44484		
Excited State 9:	Singlet-A	2.8020 eV	442.48 nm	f=0.0000	<S**2>=0.000
171→184	-0.25978	174→184	-0.27962	179→183	-0.32306
172→183	0.39307	176→183	-0.12300	181→184	0.27440
Excited State 10:	Singlet-B1	2.8156 eV	440.34 nm	f=0.0104	<S**2>=0.000
171→183	0.42400	174→183	0.37231		
172→184	-0.35680	179→184	0.19642		
Excited State 11:	Singlet-A	2.9438 eV	421.16 nm	f=0.0000	<S**2>=0.000
171→184	-0.30062	174→184	0.13942	179→183	0.39881
172→183	0.37091	176→183	-0.13664	181→184	-0.25518
Excited State 12:	Singlet-B1	3.0763 eV	403.04 nm	f=0.0881	<S**2>=0.000
171→183	-0.35412	174→183	0.38253	181→183	-0.13639
172→184	0.20754	179→184	0.37838		
Excited State 13:	Singlet-B2	3.2111 eV	386.11 nm	f=0.0280	<S**2>=0.000
169→184	0.36740	170→183	0.48354	175→183	-0.34355
Excited State 14:	Singlet-B3	3.2271 eV	384.20 nm	f=0.0029	<S**2>=0.000
169→183	0.54034	170→184	0.40911	173→183	-0.14663
Excited State 15:	Singlet-A	3.2998 eV	375.74 nm	f=0.0000	<S**2>=0.000
172→183	0.16669	176→183	0.67233		

Excited State 16:	Singlet-B2	3.3103 eV	374.54 nm	f=0.0014	<S**2>=0.000	
169→184	0.18824	170→183	0.28107	175→183	0.60585	
Excited State 17:	Singlet-B3	3.6162 eV	342.86 nm	f=0.0000	<S**2>=0.000	
166→184	-0.11018	175→184	-0.41117			
173→183	0.52217	180→184	-0.12174			
Excited State 18:	Singlet-B1	3.6648 eV	338.31 nm	f=0.0001	<S**2>=0.000	
176→184	0.68866					
Excited State 19:	Singlet-B3	3.7004 eV	335.06 nm	f=0.0000	<S**2>=0.000	
169→183	0.12387	175→184	0.56439			
173→183	0.36733	180→184	-0.10127			
Excited State 20:	Singlet-B1	3.8557 eV	321.56 nm	f=0.0031	<S**2>=0.000	
168→184	-0.15638	179→184	0.51507			
174→183	-0.40862	181→183	-0.12833			
Excited State 21:	Singlet-A	3.9640 eV	312.77 nm	f=0.0000	<S**2>=0.000	
168→183	0.34324	174→184	0.50583			
171→184	-0.11573	179→183	-0.27748			
Excited State 22:	Singlet-B2	4.0091 eV	309.26 nm	f=0.0001	<S**2>=0.000	
166→183	-0.15111	177→183	0.13398	180→183	-0.13506	
173→184	0.58605	178→184	-0.28177			
Excited State 23:	**Singlet-B1**	**4.0610 eV**	**305.30 nm**	**f=1.0592**	**<S**2>=0.000**	
180→186	-0.15845	181→187	-0.12157	**182→185**	**0.65197**	
Excited State 24:	Singlet-B3	4.2257 eV	293.41 nm	f=0.0006	<S**2>=0.000	
173→183	-0.12450	177→184	0.56979	178→183	-0.39421	

Excited State 25:	Singlet-B2	4.2428 eV	292.22 nm	f=0.0008	<S**2>=0.000			
173→184	0.29345		177→183	-0.38848		178→184	0.50050	
Excited State 26:	Singlet-A	4.3571 eV	284.56 nm	f=0.0000	<S**2>=0.000			
167→184	0.19698		172→183	-0.25199		182→186	-0.14334	
168→183	0.42620		174→184	-0.33597				
171→184	-0.22361		179→183	0.12639				
Excited State 27:	Singlet-B1	4.4787 eV	276.83 nm	f=0.0242	<S**2>=0.000			
167→183	-0.17635		171→183	0.34323		174→183	0.12106	
168→184	-0.20451		172→184	0.49866		182→188	-0.14064	
Excited State 28:	Singlet-A	4.5448 eV	272.81 nm	f=0.0000	<S**2>=0.000			
171→184	-0.37307		180→185	-0.14490		182→186	0.42540	
172→183	-0.24438		180→188	-0.16636		182→189	-0.17128	
Excited State 29:	Singlet-B3	4.5664 eV	271.51 nm	f=0.0004	<S**2>=0.000			
180→190	0.15287		182→187	0.57125				
181→185	-0.30965		182→195	0.13218				
Excited State 30:	Singlet-B1	4.6225 eV	268.22 nm	f=0.0248	<S**2>=0.000			
167→183	0.21862		172→184	0.22508		182→188	0.49716	
168→184	0.15367		180→186	-0.14287				
171→183	0.19141		180→189	0.18458				
Excited State 31:	Singlet-A	4.6340 eV	267.55 nm	f=0.0000	<S**2>=0.000			
167→184	0.15732		172→183	0.22884		182→189	-0.27339	
168→183	0.27453		180→188	-0.16450				
171→184	0.34333		182→186	0.29661				
Excited State 32:	Singlet-B1	4.6635 eV	265.86 nm	f=0.0480	<S**2>=0.000			
165→184	0.10938		167→183	0.40634		168→184	0.33653	

171→183	0.12178	180→189	-0.13037		
172→184	0.13137	182→188	-0.32323		

Excited State 33:	Singlet-A	4.6665 eV	265.69 nm	f=0.0000	<S**2>=0.000
168→183	0.15263	181→191	0.10502	182→192	-0.15165
180→185	-0.25747	182→186	0.26236		
180→188	0.13593	182→189	0.49063		

Excited State 34:	Singlet-B2	4.8736 eV	254.40 nm	f=0.0053	<S**2>=0.000
169→184	0.14272	180→187	0.12041	182→190	0.34951
170→183	-0.11435	181→189	0.14838	182→191	0.41058
176→185	-0.10169	181→192	-0.21042	182→194	0.13629

Excited State 35:	Singlet-B3	4.9026 eV	252.89 nm	f=0.0002	<S**2>=0.000
169→183	-0.41423	170→184	0.56069		

Excited State 36:	Singlet-B2	4.9042 eV	252.81 nm	f=0.0004	<S**2>=0.000
169→184	0.53421	170→183	-0.40214	182→190	-0.10050

*C.2.2.3 **OTPA-BZN-221**, **^{5}ES** State*

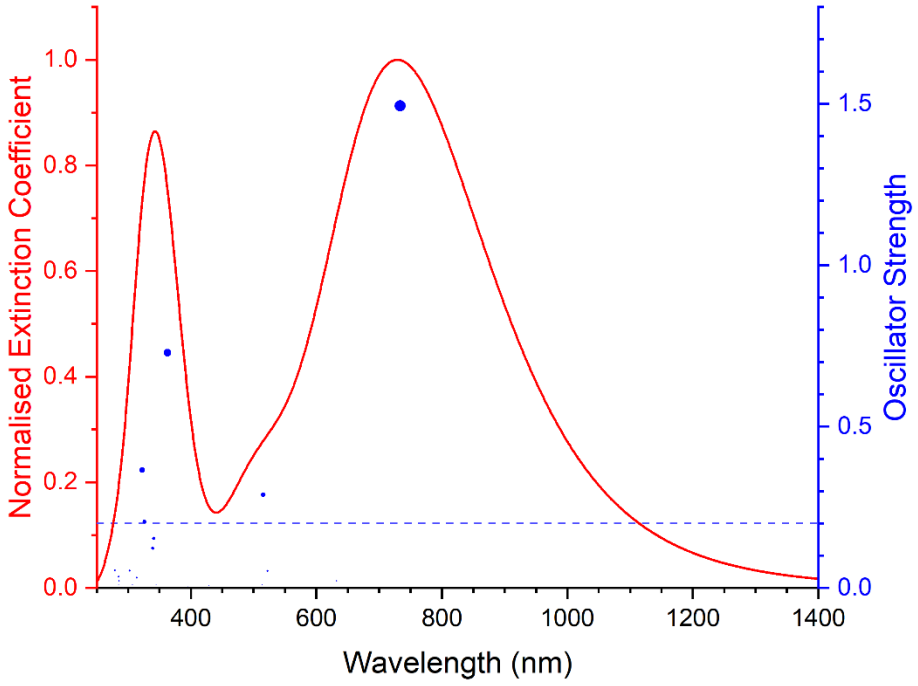

*Figure C-7 Excited states and normalised absorption spectra from TD-DFT calculations of **OTPA-BZN-221** in **^{5}ES** state. The areas of excited state dots are proportional to their oscillator strengths.*

Excited State 1:	5.065-B3	1.6575 eV	748.00 nm	f=0.0001	<S**2>=6.164			
167B→184B	0.11945	177B→182B	0.18025	180B→183B	0.41750			
168B→183B	0.15707	179B→181B	0.80064					
173B→182B	-0.17180	179B→184B	0.18442					
Excited State 2:	**5.062-B1**	**1.6898 eV**	**733.73 nm**	**f=1.4934**	**<S**2>=6.155**			
168B→184B	0.16535	**179B→183B**	**0.35452**					
178B→182B	**-0.40426**	**180B→181B**	**0.79416**					
Excited State 3:	5.048-B2	1.9603 eV	632.47 nm	f=0.0213	<S**2>=6.122			
172B→182B	0.11089	176B→182B	0.62426	177B→184B	-0.27305			
173B→181B	0.16059	177B→181B	0.65709	179B→182B	0.15966			
Excited State 4:	5.049-B3	1.9771 eV	627.09 nm	f=0.0006	<S**2>=6.123			
172B→181B	0.11411	176B→181B	0.66546	177B→182B	0.59247			
173B→182B	0.24122	176B→184B	-0.27232	180B→183B	-0.10657			

Excited State 5:	5.061-A	1.9989 eV	620.25 nm	f=0.0000	<S**2>=6.153
168B→182B	-0.22171	178B→184B	0.20798		
178B→181B	-0.63661	180B→182B	0.65470		
Excited State 6:	5.049-B1	2.3749 eV	522.06 nm	f=0.0519	<S**2>=6.122
167B→183B	0.11350	170B→181B	-0.22271	178B→182B	0.39320
168B→181B	0.25748	170B→184B	-0.12021	179B→183B	0.59252
169B→183B	0.15146	175B→181B	-0.15477	180B→184B	0.46963
Excited State 7:	**5.106-B2**	**2.4057 eV**	**515.39 nm**	**f=0.2888**	**<S**2>=6.267**
182A→185A	-0.10832	172B→182B	-0.10803	176B→182B	-0.12851
167B→182B	-0.18848	**173B→181B**	**-0.54335**	**179B→182B**	**0.69861**
171B→181B	0.13729	173B→184B	0.13238		
Excited State 8:	5.065-B3	2.4109 eV	514.27 nm	f=0.0000	<S**2>=6.163
168B→183B	0.11056	170B→183B	0.63593	175B→183B	-0.12280
169B→181B	-0.52682	172B→181B	-0.22840		
169B→184B	-0.42059	172B→184B	-0.14150		
Excited State 9:	5.064-B1	2.4132 eV	513.77 nm	f=0.0100	<S**2>=6.160
168B→181B	-0.15562	170B→184B	-0.41267	178B→182B	-0.10115
169B→183B	0.59498	172B→183B	0.22094	179B→183B	-0.15041
170B→181B	-0.50845	175B→181B	0.20827	180B→184B	-0.10350
Excited State 10:	5.055-B3	2.6710 eV	464.19 nm	f=0.0008	<S**2>=6.138
167B→181B	0.21948	173B→182B	0.38782	179B→184B	0.50242
168B→183B	0.16987	177B→182B	-0.10239	180B→183B	0.52008
172B→181B	0.20636	179B→181B	-0.33314		
Excited State 11:	5.076-A	2.7002 eV	459.17 nm	f=0.0000	<S**2>=6.192
168B→182B	-0.13454	174B→181B	0.72667	174B→184B	-0.17140

175B→182B	-0.57930	178B→181B	0.17980		

Excited State 12:	5.075-B1	2.7076 eV	457.91 nm	f=0.0052	<S**2>=6.190
168B→181B	0.19262	175B→181B	0.70538	179B→183B	0.10070
174B→182B	-0.58042	175B→184B	-0.17866	180B→184B	0.10450

Excited State 13:	5.094-B2	2.8754 eV	431.19 nm	f=0.0004	<S**2>=6.238
169B→182B	-0.15978	172B→182B	0.54473	176B→182B	-0.10351
171B→181B	0.68454	173B→181B	0.22872	177B→181B	-0.16030
171B→184B	-0.14226	174B→183B	-0.10986	178B→183B	-0.11190

Excited State 14:	5.087-B3	2.8902 eV	428.99 nm	f=0.0074	<S**2>=6.220
167B→181B	-0.10469	172B→184B	-0.16197	179B→181B	0.10261
169B→181B	-0.22913	173B→182B	0.12800	179B→184B	-0.15923
171B→182B	0.54776	175B→183B	0.13591	180B→183B	-0.11754
172B→181B	0.65499	176B→181B	-0.16040		

Excited State 15:	5.139-A	3.1132 eV	398.26 nm	f=0.0000	<S**2>=6.351
180A→185A	-0.10322	173B→183B	0.37297	178B→184B	0.31466
166B→184B	-0.13806	174B→181B	-0.12510	180B→182B	0.53264
168B→182B	0.10607	177B→183B	-0.15715		
171B→183B	-0.19824	178B→181B	0.46402		

Excited State 16:	5.166-B2	3.1355 eV	395.42 nm	f=0.0030	<S**2>=6.421
182A→185A	0.16207	171B→184B	-0.14957	177B→181B	-0.16622
184A→187A	0.13403	173B→181B	0.33254	177B→184B	-0.10868
166B→183B	-0.16674	173B→184B	0.26168	178B→183B	0.48729
171B→181B	-0.10592	174B→183B	-0.11103	179B→182B	0.50937

Excited State 17:	5.078-B1	3.2391 eV	382.77 nm	f=0.0024	<S**2>=6.196
165B→181B	0.10675	166B→182B	0.24214	168B→181B	0.41074

168B→184B	-0.13554	179B→183B	-0.46016		
178B→182B	0.38483	180B→181B	0.51680		

Excited State 18: 5.375-B3 3.2544 eV 380.97 nm f=0.0000 <S**2>=6.973

172A→185A	0.10393	180A→199A	-0.12670	173B→182B	-0.12258
173A→195A	-0.10594	182A→187A	0.26998	174B→188B	-0.12709
174A→194A	-0.11333	182A→190A	0.17603	175B→186B	-0.11523
175A→187A	0.10723	183A→186A	0.25042	178B→185B	-0.12992
176A→189A	-0.13888	184A→185A	0.48357	179B→181B	-0.23278
179A→190A	-0.12436	167B→181B	-0.17231	180B→183B	0.27757
180A→188A	0.13613	171B→193B	0.11421	180B→189B	0.12414

Excited State 19: 5.225-A 3.3538 eV 369.68 nm f=0.0000 <S**2>=6.575

180A→185A	0.16477	165B→182B	0.24195	178B→184B	-0.14455
182A→186A	-0.12495	166B→181B	0.41592	179B→185B	0.16735
182A→200A	0.13431	166B→184B	-0.12330	180B→182B	0.33068
183A→187A	-0.13605	168B→182B	0.39918	180B→187B	-0.13114
184A→188A	0.12419	173B→183B	-0.19983		
184A→199A	-0.15703	178B→181B	0.24827		

Excited State 20: 5.424-B1 3.4171 eV 362.83 nm f=0.7286 <S2>=7.104**

169A→185A	0.13008	**183A→185A**	**0.34132**	173B→185B	-0.14145
170A→192A	-0.10564	**184A→186A**	**0.37937**	174B→193B	-0.12874
173A→190A	-0.11149	184A→200A	-0.13704	175B→191B	0.10029
174A→189A	-0.11851	165B→181B	0.23315	178B→187B	0.10498
175A→195A	-0.11055	166B→182B	0.21221	179B→186B	0.11130
176A→194A	-0.12104	167B→183B	-0.17497	179B→189B	0.12992
180A→187A	-0.21298	168B→184B	-0.16369	180B→190B	-0.11022
182A→188A	-0.21143	171B→188B	0.13035		
182A→199A	0.17291	172B→186B	-0.11047		

Excited State 21:	5.066-B3	3.5111 eV	353.12 nm	f=0.0004	<S**2>=6.165	
182A→187A	-0.10067	167B→181B	-0.14374	177B→182B	0.18358	
183A→186A	-0.22974	172B→184B	0.18005	179B→181B	-0.27428	
183A→193A	-0.14519	173B→182B	-0.33286	179B→184B	-0.31605	
184A→185A	-0.33486	175B→183B	0.30571	180B→183B	0.49494	

Excited State 22:	5.069-B1	3.5970 eV	344.69 nm	f=0.0092	<S**2>=6.174	
165B→181B	-0.14022	170B→181B	0.13258	176B→183B	-0.14179	
165B→184B	0.10807	172B→183B	0.32978	178B→182B	0.25830	
166B→182B	-0.24830	174B→182B	0.27758	179B→183B	-0.16148	
168B→181B	-0.29758	175B→181B	0.32161	180B→181B	0.11980	
169B→183B	-0.12259	175B→184B	0.35442	180B→184B	0.39022	

Excited State 23:	5.221-B2	3.6385 eV	340.76 nm	f=0.1531	<S**2>=6.564	
176A→190A	-0.12644	171B→184B	0.19481	177B→181B	-0.24684	
180A→186A	0.10522	172B→182B	-0.22929	177B→184B	-0.14601	
182A→185A	-0.24260	173B→181B	0.42373	178B→183B	-0.16964	
183A→188A	0.11618	173B→184B	0.14599	178B→189B	-0.10681	
184A→187A	-0.23925	174B→183B	-0.35591	179B→182B	0.15195	
184A→190A	-0.17320	175B→188B	0.10667	180B→185B	0.12103	
171B→181B	-0.14171	176B→182B	0.11794			

Excited State 24:	5.199-B2	3.6534 eV	339.37 nm	f=0.1223	<S**2>=6.507	
175A→189A	-0.10512	171B→181B	-0.19600	174B→186B	0.10140	
182A→185A	-0.23028	171B→184B	-0.29949	177B→184B	0.10675	
183A→188A	0.11193	172B→182B	0.22503	178B→183B	0.45953	
184A→187A	-0.27417	174B→183B	0.44976			

Excited State 25:	5.077-A	3.6571 eV	339.03 nm	f=0.0000	<S**2>=6.195	
166B→181B	-0.11192	168B→182B	-0.10124	171B→183B	-0.39360	

173B→183B	-0.27317	175B→182B	0.45433	178B→184B	0.25256
174B→181B	0.28392	177B→183B	0.27843		
174B→184B	0.43113	178B→181B	0.21955		

Excited State 26:	5.087-B3	3.7330 eV	332.13 nm	f=0.0011	<S**2>=6.220
183A→186A	0.16241	169B→184B	-0.11568	176B→181B	-0.12056
183A→193A	0.10053	171B→182B	-0.36100	176B→184B	-0.14434
184A→185A	0.18170	172B→181B	0.14284	179B→181B	0.17317
184A→198A	0.11027	172B→184B	0.33631	180B→183B	-0.14526
167B→181B	0.16264	174B→185B	-0.10162		
169B→181B	-0.10645	175B→183B	0.62588		

Excited State 27:	5.305-A	3.7765 eV	328.31 nm	f=0.0000	<S**2>=6.787
173A→189A	-0.13480	182A→193A	0.14601	174B→181B	-0.18741
174A→190A	-0.10376	183A→187A	-0.14603	174B→184B	-0.18376
175A→194A	-0.10552	184A→188A	0.29332	175B→193B	0.12882
176A→195A	-0.15183	165B→182B	-0.13957	177B→183B	-0.13238
179A→194A	-0.12442	166B→181B	-0.29170	178B→181B	0.25873
180A→185A	0.13899	168B→182B	-0.21572	178B→184B	0.12873
181A→188A	-0.16041	171B→189B	0.12180	179B→185B	0.12060
181A→191A	0.10666	172B→188B	0.11514		
182A→186A	-0.27716	173B→183B	0.17621		

Excited State 28:	**5.089-B1**	**3.8038 eV**	**325.95 nm**	**f=0.2054**	**<S**2>=6.224**
181A→193A	-0.11924	165B→184B	-0.11237	175B→181B	0.19337
183A→185A	-0.22096	166B→182B	0.28712	**175B→184B**	**0.34715**
183A→198A	-0.12718	168B→181B	0.20895	176B→183B	-0.15363
184A→186A	-0.20883	169B→183B	-0.13794	178B→182B	-0.10987
184A→193A	-0.10535	172B→183B	0.31447	179B→183B	0.24022
165B→181B	0.20187	**174B→182B**	**0.31895**	180B→181B	-0.16153

180B→184B	-0.26028				

Excited State 29:	**5.177-B1**	**3.8467 eV**	**322.31 nm**	**f=0.3653**	**<S**2>=6.449**
172A→186A	-0.10763	184A→200A	0.13960	174B→182B	0.11002
177A→197A	-0.11352	165B→181B	-0.14668	176B→183B	-0.12649
178A→196A	-0.11600	165B→184B	-0.11428	176B→196B	-0.11309
181A→193A	0.19269	167B→183B	0.26984	177B→195B	-0.11269
183A→185A	0.30478	168B→181B	0.29988	178B→182B	-0.15254
183A→198A	0.22472	168B→184B	0.18857	178B→187B	-0.12141
184A→186A	**0.33434**	172B→183B	0.20691	180B→181B	-0.13375
184A→193A	0.14320	173B→185B	0.10458	180B→184B	-0.21285

Excited State 30:	5.141-B3	3.9126 eV	316.88 nm	f=0.0001	<S**2>=6.358
176A→189A	-0.11847	184A→198A	-0.20476	175B→183B	0.25571
181A→185A	-0.14724	165B→183B	0.16326	177B→182B	-0.11454
183A→186A	-0.24416	167B→181B	-0.20279	179B→181B	0.12360
183A→193A	-0.21360	167B→184B	-0.22224	179B→184B	0.42862
183A→200A	-0.12039	168B→183B	-0.25126	180B→183B	-0.14001
184A→185A	-0.27354	171B→182B	-0.13918		
184A→196A	0.10908	173B→182B	0.18564		

Excited State 31:	5.079-B2	3.9497 eV	313.91 nm	f=0.0309	<S**2>=6.198
162B→181B	-0.12067	172B→182B	-0.10906	177B→184B	-0.16873
166B→183B	-0.11185	173B→181B	-0.28748	178B→183B	0.49936
167B→182B	-0.23488	173B→184B	0.30847	179B→182B	-0.38802
171B→181B	0.27044	174B→183B	-0.37370		

Excited State 32:	5.218-B3	4.0194 eV	308.47 nm	f=0.0001	<S**2>=6.556
170A→191A	-0.18894	171A→192A	0.19413	167B→184B	-0.22059
171A→187A	-0.10656	165B→183B	0.14590	168B→183B	-0.29508

169B→191B	0.11483	176B→181B	0.17796	179B→184B	-0.34131
170B→192B	-0.14620	176B→184B	0.10835	180B→183B	0.37879
172B→181B	-0.11562	177B→182B	-0.28913		
173B→182B	0.34328	179B→181B	0.21182		

Excited State 33: 5.210-B1 4.0272 eV 307.87 nm f=0.0001 <S**2>=6.535

170A→192A	0.11932	168B→184B	0.15688	179B→183B	-0.39219
171A→191A	-0.13585	172B→183B	0.10018	180B→181B	-0.17147
167B→183B	0.19117	175B→181B	-0.17834	180B→184B	0.45975
168B→181B	0.14052	178B→182B	-0.45009		

Excited State 34: 5.474-B1 4.0378 eV 307.06 nm f=0.0103 <S**2>=7.242

170A→192A	-0.15022	179A→188A	0.12350	173B→195B	0.10503
171A→191A	0.15711	181A→186A	0.26526	176B→186B	-0.10643
172A→193A	-0.11583	182A→188A	0.24126	176B→196B	0.22951
173A→197A	-0.10052	182A→191A	-0.11534	177B→188B	0.11556
174A→196A	-0.10368	183A→185A	0.20962	177B→195B	0.22396
177A→197A	0.25993	183A→198A	0.13976	178B→197B	-0.10331
178A→189A	0.14721	184A→193A	0.24751	179B→183B	0.10732
178A→196A	0.25585	169B→192B	0.10927	180B→184B	-0.15304

Excited State 35: 5.361-A 4.0400 eV 306.89 nm f=0.0000 <S**2>=6.936

177A→189A	-0.10842	165B→182B	0.24920	176B→195B	-0.24240
177A→196A	-0.26224	166B→181B	0.29572	177B→196B	-0.22404
178A→197A	-0.28225	166B→184B	-0.15707	178B→181B	-0.24324
181A→188A	-0.12334	168B→182B	0.15510	178B→184B	0.17490
182A→186A	-0.12121	171B→183B	-0.21044	180B→182B	-0.26892
184A→188A	0.10825	173B→183B	0.20781	180B→187B	0.10676

Excited State 36:	5.307-A	4.0480 eV	306.28 nm	f=0.0000	<S**2>=6.790	
173A→189A	-0.10632	182A→200A	0.10624	174B→181B	0.12054	
175A→194A	-0.10438	183A→187A	-0.13284	176B→195B	0.17983	
177A→196A	0.18644	183A→192A	0.10178	177B→183B	-0.18129	
178A→197A	0.20268	184A→191A	0.16202	177B→196B	0.17047	
179A→186A	0.10526	161B→181B	-0.11186	178B→181B	-0.17681	
179A→193A	-0.12507	165B→182B	0.14884	178B→184B	0.25884	
181A→188A	0.16734	166B→184B	-0.15337	178B→190B	0.12151	
181A→199A	0.11287	171B→183B	-0.25602	180B→182B	-0.22022	
182A→193A	-0.11775	173B→183B	0.37864			

Excited State 37:	5.082-B2	4.0973 eV	302.60 nm	f=0.0529	<S**2>=6.206	
181A→187A	-0.13170	183A→188A	0.30370	184A→190A	0.19794	
181A→192A	0.22035	183A→191A	0.52955	184A→192A	0.48127	
182A→189A	-0.10552	184A→187A	-0.37527	169B→182B	-0.14038	

Excited State 38:	5.088-A	4.1080 eV	301.81 nm	f=0.0000	<S**2>=6.222	
169A→192A	-0.10253	183A→187A	-0.33458	184A→188A	0.30226	
181A→188A	0.12074	183A→190A	0.12044	184A→191A	0.53015	
181A→191A	0.21758	183A→192A	0.50190	170B→182B	0.15603	

Excited State 39:	5.275-B3	4.1905 eV	295.87 nm	f=0.0000	<S**2>=6.706	
170A→188A	-0.11466	182A→187A	-0.11309	170B→192B	-0.17138	
170A→191A	-0.22181	184A→198A	0.14578	171B→182B	0.15564	
171A→187A	-0.12364	162B→182B	-0.11147	173B→182B	-0.30812	
171A→192A	0.23100	167B→181B	-0.41997	177B→182B	0.14509	
181A→185A	0.10927	169B→191B	0.13469	179B→184B	0.45947	

Excited State 40:	5.069-B2	4.2367 eV	292.64 nm	f=0.0019	<S**2>=6.173	
171B→181B	-0.11072	173B→181B	0.22356	173B→184B	0.12480	

174B→183B	-0.25944	177B→181B	0.64445		
176B→182B	-0.56267	177B→184B	0.25373		

Excited State 41: 5.336-B1 4.2430 eV 292.21 nm f=0.0007 <S**2>=6.869

170A→187A	0.10694	178A→196A	-0.17836	169B→192B	0.13393
170A→192A	-0.16541	161B→182B	-0.11080	170B→191B	-0.11057
171A→191A	0.18614	165B→181B	0.36959	176B→196B	-0.15220
173A→192A	-0.10507	166B→182B	0.24895	177B→195B	-0.14742
174A→189A	0.12253	167B→183B	-0.15521	178B→182B	-0.27512
177A→197A	-0.17994	168B→181B	-0.13831	180B→184B	0.43913

Excited State 42: 5.081-B3 4.2550 eV 291.39 nm f=0.0001 <S**2>=6.205

167B→184B	0.11487	173B→182B	-0.29441	176B→184B	0.26520
168B→183B	0.12761	175B→183B	0.20618	177B→182B	-0.46418
171B→182B	0.11922	176B→181B	0.66926		

Excited State 43: 5.264-B3 4.3394 eV 285.71 nm f=0.0215 <S**2>=6.677

169A→194A	0.12887	182A→190A	-0.36571	172B→181B	0.21896
180A→195A	0.19025	182A→192A	0.13382	178B→188B	0.11677
181A→189A	-0.12843	183A→194A	0.24249	180B→186B	0.10402
182A→187A	0.27454	184A→189A	0.59604		

Excited State 44: 5.256-B2 4.3500 eV 285.02 nm f=0.0345 <S**2>=6.656

169A→195A	-0.12500	182A→189A	0.44748	169B→182B	-0.11655
179A→189A	-0.12038	183A→195A	-0.26312	171B→181B	-0.18603
180A→194A	-0.17879	184A→187A	0.26456	179B→193B	0.11074
181A→187A	-0.12195	184A→190A	-0.41924	180B→188B	0.13082
181A→190A	0.10496	184A→192A	0.33442		
182A→185A	0.13986	184A→197A	0.11428		

Excited State 45:	5.126-B1	4.3520 eV	284.89 nm	f=0.0093	<S**2>=6.319	
182A→195A	-0.11587	169B→183B	-0.13689	172B→183B	-0.42262	
183A→189A	0.11170	170B→181B	-0.39278	174B→182B	0.36579	
184A→194A	0.13490	170B→184B	0.13583	175B→181B	0.43762	
167B→183B	0.14305	171B→185B	-0.10297	176B→183B	0.28871	

Excited State 46:	5.112-A	4.3543 eV	284.74 nm	f=0.0000	<S**2>=6.283	
182A→194A	0.12084	171B→183B	0.43593	175B→182B	0.46546	
183A→192A	0.10513	172B→185B	0.11223	177B→183B	-0.41788	
184A→195A	-0.16690	174B→181B	0.48098	178B→181B	0.13647	

Excited State 47:	5.076-B3	4.4043 eV	281.51 nm	f=0.0005	<S**2>=6.191	
169B→181B	0.63498	170B→183B	0.40566	172B→181B	0.42333	
169B→184B	-0.26542	171B→182B	-0.24197	175B→183B	-0.21645	

Excited State 48:	5.099-B1	4.4397 eV	279.26 nm	f=0.0008	<S**2>=6.250	
182A→195A	-0.11125	169B→183B	0.43400	175B→181B	0.16024	
183A→189A	0.12139	170B→181B	0.67527	176B→183B	0.21862	
184A→194A	0.14304	170B→184B	-0.23423			
168B→181B	0.17717	174B→182B	0.19719			

Excited State 49:	5.274-B2	4.4478 eV	278.75 nm	f=0.0539	<S**2>=6.704	
173A→194A	0.12304	184A→187A	-0.19915	173B→181B	-0.28756	
174A→195A	0.13240	184A→190A	-0.15550	174B→183B	-0.28840	
175A→189A	0.14551	171B→181B	-0.36393	174B→186B	-0.16275	
176A→187A	-0.12697	171B→184B	-0.19625	175B→185B	0.10935	
176A→190A	0.10847	172B→182B	0.42624	175B→188B	-0.17053	
182A→185A	-0.19714	172B→193B	-0.14137	177B→184B	-0.10740	

Excited State 50:	5.261-A	4.4581 eV	278.11 nm	f=0.0000	<S**2>=6.671	
175A→194A	0.11547	176A→195A	0.11298	177A→196A	0.10978	

178A→197A	0.11137	154B→181B	0.10894	172B→188B	-0.11325
181A→188A	-0.14174	163B→182B	-0.18016	173B→183B	0.18653
182A→186A	-0.25690	164B→181B	-0.20031	174B→181B	0.11666
182A→193A	0.10423	165B→182B	-0.17286	174B→184B	0.12276
183A→187A	-0.10453	166B→181B	-0.12589	175B→193B	-0.13513
183A→192A	-0.11006	168B→182B	0.27095	176B→195B	0.10395
184A→188A	0.24307	170B→182B	-0.10334	177B→183B	-0.13647
184A→191A	-0.16613	171B→183B	-0.17932	178B→181B	-0.15710
152B→182B	0.14442	171B→186B	0.10057	178B→184B	-0.23024

*C.2.2.4 **OTPA-BZN-221**, **EB** State*

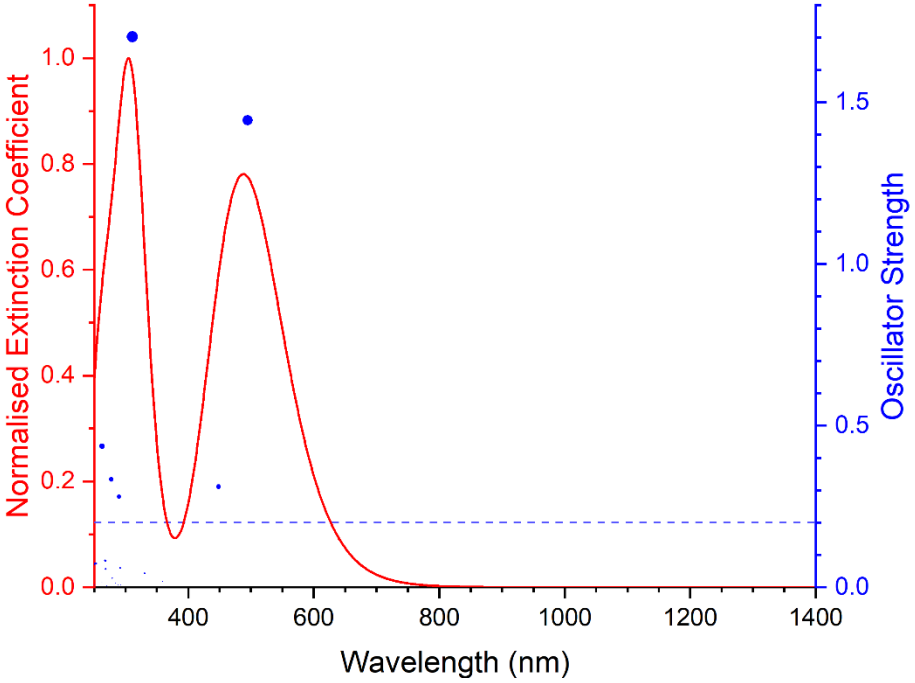

*Figure C-8 Excited states and normalised absorption spectra from TD-DFT calculations of **OTPA-BZN-221** in **EB** state. The areas of excited state dots are proportional to their oscillator strengths.*

Excited State 1:	Singlet-B3	2.1459 eV	577.78 nm	f=0.0001	<S**2>=0.000
179→183	-0.11332	180→184	-0.23482	182→183	0.63459

Excited State 2:	**Singlet-B1**	**2.5051 eV**	**494.93 nm**	**f=1.4442**	**<S**2>=0.000**
171→184	0.10284	180→183	-0.28023		
179→184	-0.10510	**182→184**	**0.60493**		

Excited State 3:	**Singlet-B2**	**2.7662 eV**	**448.21 nm**	**f=0.3111**	**<S**2>=0.000**	
177→183	0.15867	178→184	-0.21897	**181→183**	**0.62928**	
Excited State 4:	Singlet-A	2.9454 eV	420.94 nm	f=0.0000	<S**2>=0.000	
177→184	0.17641	178→183	-0.27388	181→184	0.59555	
Excited State 5:	Singlet-B1	3.4515 eV	359.22 nm	f=0.0180	<S**2>=0.000	
166→184	0.13604	172→183	-0.13936	180→183	0.51718	
171→184	-0.12639	179→184	0.16098	182→184	0.34918	
Excited State 6:	Singlet-B3	3.5107 eV	353.16 nm	f=0.0015	<S**2>=0.000	
163→184	0.10870	171→183	-0.22332	180→184	0.45577	
166→183	0.17913	172→184	-0.19166	182→183	0.26912	
169→184	0.13172	179→183	0.21818			
Excited State 7:	Singlet-B2	3.7525 eV	330.41 nm	f=0.0425	<S**2>=0.000	
164→184	0.18756	177→183	-0.32763	181→183	0.28173	
165→183	0.26316	178→184	0.39136			
Excited State 8:	Singlet-A	3.7763 eV	328.32 nm	f=0.0000	<S**2>=0.000	
164→183	0.18282	177→184	-0.24777	181→184	0.35838	
165→184	0.23013	178→183	0.42218			
Excited State 9:	Singlet-B3	3.9515 eV	313.76 nm	f=0.0021	<S**2>=0.000	
166→183	-0.10828	172→184	0.30130	181→185	0.10097	
169→184	-0.18551	179→183	0.22780	182→186	-0.10062	
171→183	0.37342	180→184	0.30164			
Excited State 10:	**Singlet-B1**	**3.9850 eV**	**311.13 nm**	**f=1.7025**	**<S**2>=0.000**	
163→183	-0.11512	169→183	-0.22721	180→183	0.29015	
166→184	-0.13281	**171→184**	**0.37488**			
168→183	0.10517	**172→183**	**0.35778**			

Excited State 11:	Singlet-B3	4.2379 eV	292.56 nm	f=0.0070	<S**2>=0.000			
167→183	0.20390		174→183	0.29884		181→188	0.22761	
168→184	0.19418		179→183	0.22631		182→186	-0.25657	
169→184	0.19935		180→184	-0.19677		182→190	0.14247	
Excited State 12:	Singlet-B2	4.2510 eV	291.66 nm	f=0.0595	<S**2>=0.000			
170→184	-0.17184		177→183	0.14488		182→185	-0.32565	
173→183	-0.25015		181→186	0.33053		182→188	-0.31454	
Excited State 13:	**Singlet-B1**	**4.2780 eV**	**289.82 nm**	**f=0.2794**	**<S**2>=0.000**			
167→184	**0.39978**		169→183	0.17876		179→184	0.13716	
168→183	**0.44741**		174→184	0.16765		180→183	-0.11867	
Excited State 14:	Singlet-B3	4.2969 eV	288.55 nm	f=0.0075	<S**2>=0.000			
167→183	0.43052		181→185	-0.15694		182→186	0.28181	
168→184	0.39034		181→188	-0.16109				
Excited State 15:	Singlet-B3	4.3696 eV	283.74 nm	f=0.0131	<S**2>=0.000			
167→183	-0.14361		179→183	0.52710		181→185	-0.20547	
168→184	-0.11327		180→184	-0.24495		182→186	0.21335	
Excited State 16:	Singlet-A	4.4456 eV	278.89 nm	f=0.0000	<S**2>=0.000			
170→183	0.39646		177→184	-0.21501		182→192	0.21696	
173→184	0.34629		178→183	-0.14394				
175→183	0.15515		181→191	-0.13306				
Excited State 17:	Singlet-B1	4.4465 eV	278.84 nm	f=0.0273	<S**2>=0.000			
167→184	-0.21648		172→183	0.20404		179→184	0.29859	
168→183	-0.23555		174→184	0.28150		181→192	0.14529	
169→183	0.22679		176→183	0.14459		182→191	-0.16118	

182→194	-0.11022				

Excited State 18:	**Singlet-B2**	**4.4693 eV**	**277.41 nm**	**f=0.3336**	**<S**2>=0.000**
170→184	-0.15206	178→184	0.10588	181→193	-0.17081
173→183	-0.23292	181→183	0.11174	**182→185**	**0.46951**
177→183	0.16241	181→190	-0.18917	182→188	-0.17705

Excited State 19:	Singlet-B1	4.5817 eV	270.61 nm	f=0.0042	<S**2>=0.000
169→183	-0.18680	180→183	-0.15864	182→189	0.15421
174→184	-0.22202	181→187	-0.12971	182→194	0.11058
179→184	0.53713	181→192	-0.11074		

Excited State 20:	Singlet-A	4.6173 eV	268.52 nm	f=0.0000	<S**2>=0.000
180→185	-0.12029	181→191	0.22093	182→187	0.52806
181→189	-0.28639	181→194	-0.14698		

Excited State 21:	Singlet-B3	4.6208 eV	268.32 nm	f=0.0566	<S**2>=0.000
167→183	-0.11072	174→183	0.45879	181→188	-0.12777
168→184	-0.10447	179→183	-0.12251	182→186	0.23653
169→184	0.19553	180→184	0.14728	182→193	0.10415
172→184	0.15943	181→185	-0.15595		

Excited State 22:	Singlet-B2	4.6253 eV	268.06 nm	f=0.0821	<S**2>=0.000
170→184	-0.22739	178→184	0.11392	182→185	-0.11415
173→183	-0.30614	181→186	-0.19555	182→188	0.37609
177→183	0.22340	181→190	0.22183		

Excited State 23:	**Singlet-B1**	**4.7162 eV**	**262.89 nm**	**f=0.4366**	**<S**2>=0.000**
179→184	0.17847	**181→187**	**0.39508**	**182→189**	**-0.36191**
180→183	-0.13055	181→197	0.11570	182→191	0.27574

Excited State 24:	Singlet-B3	4.7274 eV	262.26 nm	f=0.0137	<S**2>=0.000	
169→184	-0.11458	181→185	-0.32443	182→193	0.17001	
174→183	-0.12453	181→188	0.28074			
180→184	0.12038	182→190	0.40431			

Excited State 25:	Singlet-A	4.8866 eV	253.72 nm	f=0.0000	<S**2>=0.000	
164→183	-0.12175	177→184	0.23816	181→191	-0.23781	
170→183	-0.12080	178→183	0.22753	181→194	-0.20228	
173→184	-0.12789	180→188	-0.10014	182→192	0.40986	

Excited State 26:	Singlet-B1	4.8977 eV	253.15 nm	f=0.0732	<S**2>=0.000	
169→183	0.17132	180→186	-0.13565	182→191	0.35195	
174→184	0.30421	181→192	-0.30584	182→194	0.20098	
176→183	0.10891	182→189	0.19494			

Excited State 27:	Singlet-B3	4.9357 eV	251.20 nm	f=0.0073	<S**2>=0.000	
174→183	0.13481	179→186	-0.11059	182→186	0.14092	
175→187	-0.10207	179→196	0.13498	182→193	-0.27022	
176→184	0.13913	181→195	0.37015	182→196	0.31322	

Excited State 28:	Singlet-B2	4.9410 eV	250.93 nm	f=0.0722	<S**2>=0.000	
175→184	0.12715	178→184	-0.14219	181→196	0.31756	
176→187	-0.10336	179→195	0.14909	182→195	0.41704	
177→183	-0.14271	181→193	-0.20347			

C.2.3 Electronic Transitions in **OTPA-FLR-210** Oligomers

*Table C-7 Attributes of **OTPA-FLR-210** in **LEB**, **ES** (singlet and triplet), and **EB** states related to electronic structures*

Attribute	LEB State	^{1}ES State	^{3}ES State	EB State
Molecular Formula	$C_{49}H_{38}N_4$	$C_{49}H_{38}N_4^{2+}$	$C_{49}H_{38}N_4^{2+}$	$C_{49}H_{36}N_4$
Number of Atoms	91	91	91	89
Number of Electrons	360	358	358	358
HOMO	MO 180	MO 179	MOs 180A, 178B	MO 179
LUMO	MO 181	MO 180	MOs 181A, 179B	MO 180

*C.2.3.1 **OTPA-FLR-210**, **LEB** State*

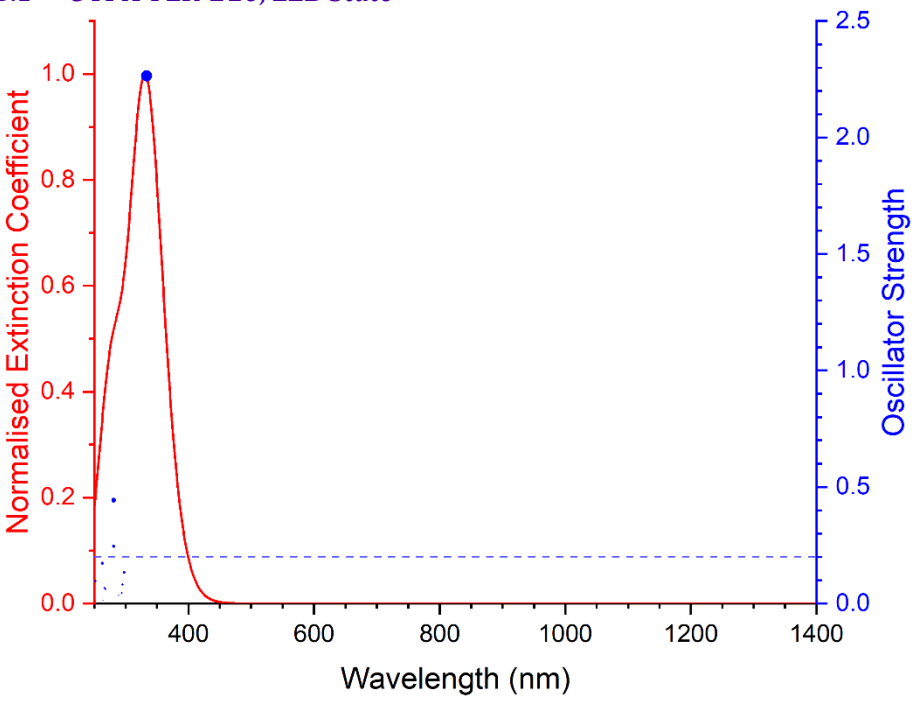

*Figure C-9 Excited states and normalised absorption spectra from TD-DFT calculations of **OTPA-FLR-210** in **LEB** state. The areas of excited state dots are proportional to their oscillator strengths.*

Excited State 1:	**Singlet-A**	**3.7204 eV**	**333.25 nm**	**f=2.2636**	**<S**2>=0.000**
178→181	-0.15493	179→187	0.19245		
178→188	0.10809	**180→181**	**0.61800**		
Excited State 2:	Singlet-A	4.1648 eV	297.69 nm	f=0.1338	<S**2>=0.000
178→187	-0.11865	179→188	-0.11593	180→184	0.25321
179→181	-0.29530	180→182	0.33157	180→187	-0.14924
179→183	0.26626	180→183	0.13298		

Excited State 3:	Singlet-A	4.1965 eV	295.45 nm	f=0.0806	<S**2>=0.000			
178→183	0.17123		179→183	0.11873		180→183	0.41502	
179→182	0.40848		180→182	-0.14118		180→189	-0.12845	
Excited State 4:	Singlet-A	4.2146 eV	294.17 nm	f=0.0450	<S**2>=0.000			
178→182	0.11852		179→183	0.29173		180→184	-0.14824	
179→181	0.29894		179→188	0.16406		180→186	0.17628	
179→182	-0.11801		180→182	0.26938		180→187	0.24218	
Excited State 5:	Singlet-A	4.2947 eV	288.69 nm	f=0.0343	<S**2>=0.000			
170→181	-0.11237		179→181	0.12776		180→186	-0.12988	
178→182	-0.12290		179→183	-0.12482		180→187	0.36003	
178→184	-0.18795		180→184	0.40271				
Excited State 6:	**Singlet-A**	**4.4070 eV**	**281.33 nm**	**f=0.4428**	**<S**2>=0.000**			
178→185	-0.16934		179→185	-0.14472		180→186	0.30104	
178→186	0.20910		**179→186**	**0.37452**				
179→184	0.18850		180→185	-0.22270				
Excited State 7:	**Singlet-A**	**4.4075 eV**	**281.30 nm**	**f=0.2448**	**<S**2>=0.000**			
177→185	0.10477		178→186	-0.11562		180→184	-0.14015	
178→184	-0.15009		179→184	0.16190		180→185	-0.29903	
178→185	-0.21873		**179→185**	**0.40787**		180→186	-0.17550	
Excited State 8:	Singlet-A	4.6283 eV	267.88 nm	f=0.0609	<S**2>=0.000			
175→181	-0.11050		179→184	-0.21946		180→189	0.15477	
177→187	0.11180		179→186	0.16198		180→193	-0.13524	
178→181	0.30146		179→187	0.20568				
178→193	0.10955		180→188	0.35119				

Excited State 9:	Singlet-A	4.6519 eV	266.53 nm	f=0.0670	<S**2>=0.000	
175→181	0.15893	178→188	0.11575	180→189	-0.26690	
177→182	-0.12319	178→193	-0.14678	180→192	-0.10437	
177→184	-0.13083	179→187	0.25586	180→193	0.27824	
178→181	0.16854	179→190	-0.17819			
178→183	-0.12773	180→188	0.13771			

Excited State 10:	Singlet-A	4.6989 eV	263.86 nm	f=0.0133	<S**2>=0.000	
177→183	0.16383	179→188	-0.12799	180→190	0.37425	
178→182	0.18526	179→189	0.33475			
178→190	0.14783	180→189	-0.11055			

Excited State 11:	Singlet-A	4.7188 eV	262.75 nm	f=0.1718	<S**2>=0.000	
175→181	0.11573	178→189	0.16710	180→189	0.22500	
177→182	0.11292	179→187	0.10020	180→192	-0.12886	
178→183	0.14736	179→190	0.31853	180→193	0.31212	

Excited State 12:	Singlet-A	4.9063 eV	252.70 nm	f=0.0097	<S**2>=0.000	
177→192	0.12065	179→191	-0.11712	180→192	0.11568	
178→191	0.26918	179→192	0.36137			
179→188	-0.14428	180→191	0.32072			

Excited State 13:	Singlet-A	4.9254 eV	251.72 nm	f=0.0955	<S**2>=0.000	
177→191	0.13378	179→192	0.11604	180→193	0.12371	
178→192	0.25822	180→191	-0.11274			
179→191	0.39624	180→192	0.30390			

*C.2.3.2 **OTPA-FLR-210**, **¹ES** State*

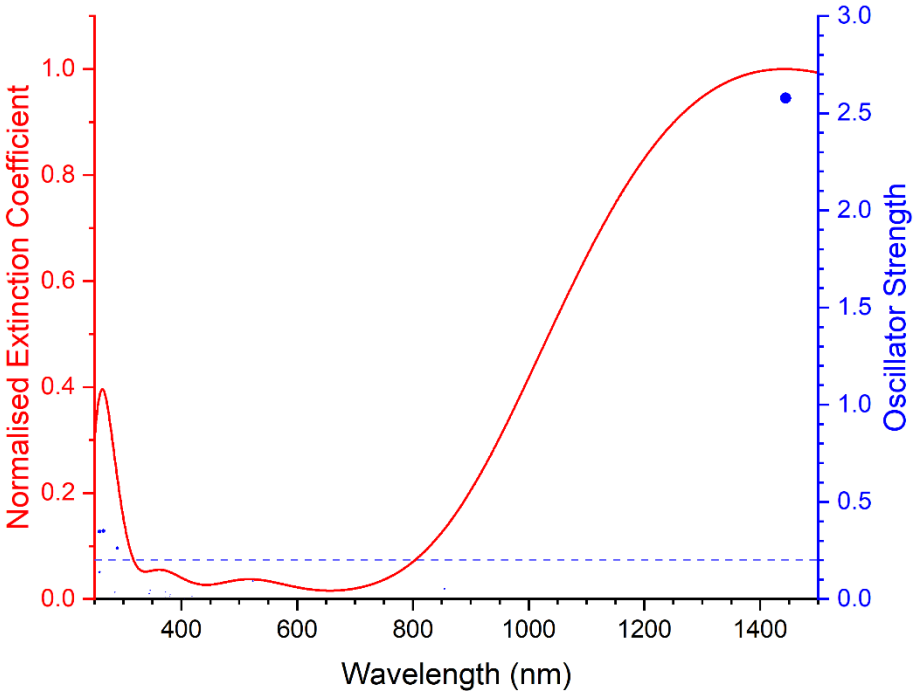

*Figure C-10 Excited states and normalised absorption spectra from TD-DFT calculations of **OTPA-FLR-210** in **¹ES** state. The areas of excited state dots are proportional to their oscillator strengths.*

Excited State 1:	**Singlet-A**	**0.8586 eV**	**1444.07 nm**	**f=2.5784**	**<S**2>=0.000**	
179→180	**0.71877**		179←180	-0.14455		
Excited State 2:	Singlet-A	1.4507 eV	854.63 nm	f=0.0527	<S**2>=0.000	
178→180	0.70467					
Excited State 3:	Singlet-A	2.3679 eV	523.61 nm	f=0.0917	<S**2>=0.000	
177→180	0.69801					
Excited State 4:	Singlet-A	2.7727 eV	447.17 nm	f=0.0059	<S**2>=0.000	
167→180	0.63458		168→180	0.13921	169→180	-0.24312
Excited State 5:	Singlet-A	2.8570 eV	433.96 nm	f=0.0009	<S**2>=0.000	
172→180	-0.27864		176→180	0.62742		
Excited State 6:	Singlet-A	2.9638 eV	418.32 nm	f=0.0139	<S**2>=0.000	
168→180	0.17574		173→180	0.32631	175→180	0.39963
169→180	0.19709		174→180	-0.38884		

Excited State 7:	Singlet-A	2.9762 eV	416.58 nm	f=0.0010	<S**2>=0.000			
167→180	-0.14689		169→180	-0.23070		173→180	0.43196	
168→180	0.20643		172→180	-0.13982		174→180	0.40412	
Excited State 8:	Singlet-A	2.9958 eV	413.85 nm	f=0.0009	<S**2>=0.000			
168→180	-0.21031		173→180	-0.25375		175→180	0.56289	
169→180	-0.13674		174→180	0.20322				
Excited State 9:	Singlet-A	3.0553 eV	405.80 nm	f=0.0012	<S**2>=0.000			
165→180	0.59448		173→180	0.10799				
172→180	0.28808		176→180	0.19781				
Excited State 10:	Singlet-A	3.1098 eV	398.69 nm	f=0.0001	<S**2>=0.000			
165→180	-0.35150		172→180	0.54716		176→180	0.22325	
Excited State 11:	Singlet-A	3.2554 eV	380.86 nm	f=0.0237	<S**2>=0.000			
167→180	0.16204		169→180	0.53886		174→180	0.35152	
168→180	0.15560		171→180	0.13016				
Excited State 12:	Singlet-A	3.2587 eV	380.47 nm	f=0.0156	<S**2>=0.000			
167→180	-0.16799		169→180	-0.11449		173→180	-0.34149	
168→180	0.55352		170→180	0.14371				
Excited State 13:	Singlet-A	3.3246 eV	372.93 nm	f=0.0362	<S**2>=0.000			
169→180	-0.10166		170→180	0.31974		171→180	0.61048	
Excited State 14:	Singlet-A	3.3251 eV	372.87 nm	f=0.0074	<S**2>=0.000			
168→180	-0.11386		170→180	0.60702		171→180	-0.32112	
Excited State 15:	Singlet-A	3.5781 eV	346.51 nm	f=0.0439	<S**2>=0.000			
177→181	-0.11415		178→183	-0.13846		179→181	0.66442	

Excited State 16:	Singlet-A	3.5982 eV	344.57 nm	f=0.0275	<S**2>=0.000
163→180	-0.13625	166→180	0.67462		
Excited State 17:	Singlet-A	4.2804 eV	289.66 nm	f=0.2615	<S**2>=0.000
178→181	0.41417	179→182	0.29053		
178→189	0.11875	179→183	-0.40661		
Excited State 18:	Singlet-A	4.3387 eV	285.76 nm	f=0.0342	<S**2>=0.000
178→184	0.26881	179→184	0.49832		
178→185	0.19099	179→185	-0.29389		
Excited State 19:	Singlet-A	4.3414 eV	285.58 nm	f=0.0253	<S**2>=0.000
178→184	0.20172	179→184	0.30721		
178→185	-0.26058	179→185	0.49892		
Excited State 20:	Singlet-A	4.4529 eV	278.44 nm	f=0.0247	<S**2>=0.000
164→180	0.11144	178→181	-0.22501	179→183	0.15547
177→182	-0.17883	179→182	0.58420		
Excited State 21:	Singlet-A	4.5040 eV	275.27 nm	f=0.0019	<S**2>=0.000
164→180	0.65761				
Excited State 22:	Singlet-A	4.6707 eV	265.45 nm	f=0.3501	<S**2>=0.000
163→180	0.13059	178→188	-0.10082	179→183	0.43684
178→181	0.45514	178→189	-0.12521		
Excited State 23:	Singlet-A	4.7580 eV	260.58 nm	f=0.0105	<S**2>=0.000
177→181	0.17608	178→183	-0.26932	179→188	0.26266
178→182	0.16626	179→186	0.38184	179→189	0.23380

Excited State 24:	**Singlet-A**	**4.7875 eV**	**258.97 nm**	**f=0.3472**	**<S**2>=0.000**	
178→188	-0.27775	179→187	-0.17236	**179→189**	**-0.33789**	
178→189	0.20888	**179→188**	**0.42084**			
Excited State 25:	Singlet-A	4.7898 eV	258.85 nm	f=0.1374	<S**2>=0.000	
177→187	0.12284	179→187	0.53204			
178→187	0.34831	179→189	-0.17023			
Excited State 26:	Singlet-A	4.8092 eV	257.81 nm	f=0.0061	<S**2>=0.000	
155→180	0.17280	166→180	0.12523			
163→180	0.62220	178→181	-0.11809			

*C.2.3.3 **OTPA-FLR-210**, **^{3}ES** State*

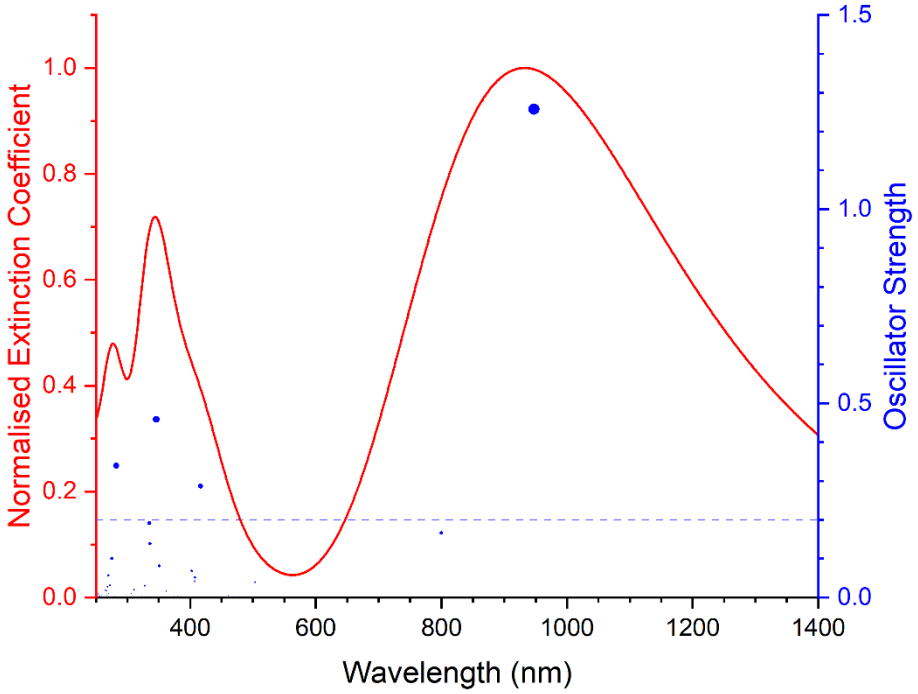

*Figure C-11 Excited states and normalised absorption spectra from TD-DFT calculations of **OTPA-FLR-210** in **^{3}ES** state. The areas of excited state dots are proportional to their oscillator strengths.*

Excited State 1:	**3.071-A**	**1.3081 eV**	**947.78 nm**	**f=1.2576**	**<S**2>=2.107**	
176B→179B	0.11826	**177B→180B**	**-0.50089**	**178B→179B**	**0.83210**	
Excited State 2:	3.048-A	1.5503 eV	799.76 nm	f=0.1659	<S**2>=2.072	
176B→180B	0.18544	177B→179B	-0.60767	178B→180B	0.73725	

Excited State 3:	3.356-A	2.4621 eV	503.57 nm	f=0.0395	<S**2>=2.566	
178A→181A	0.17727	167B→180B	-0.19434	178B→179B	-0.31776	
180A→181A	0.22868	176B→179B	0.59513	178B→181B	0.25528	
180A→188A	-0.13404	177B→180B	-0.46591			
Excited State 4:	3.064-A	2.5890 eV	478.90 nm	f=0.0041	<S**2>=2.097	
167B→179B	0.23376	176B→180B	-0.54686	178B→180B	0.56413	
174B→179B	-0.12256	177B→179B	0.51446			
Excited State 5:	3.090-A	2.6889 eV	461.10 nm	f=0.0059	<S**2>=2.136	
165B→179B	0.61396	166B→180B	-0.14699	171B→180B	-0.33256	
165B→180B	0.53400	171B→179B	-0.38061			
Excited State 6:	3.090-A	2.6893 eV	461.03 nm	f=0.0043	<S**2>=2.137	
165B→180B	-0.14809	166B→180B	-0.55316	172B→180B	-0.34696	
166B→179B	0.59583	172B→179B	0.37285			
Excited State 7:	**3.620-A**	**2.9771 eV**	**416.47 nm**	**f=0.2871**	**<S**2>=3.026**	
176A→191A	-0.14136	167B→180B	0.11594	176B→181B	-0.14164	
178A→181A	0.20118	170B→187B	-0.11884	177B→180B	0.16345	
178A→188A	-0.15794	173B→179B	0.24846	178B→179B	0.20118	
179A→182A	0.13263	174B→180B	-0.30264	178B→181B	0.28161	
180A→181A	**0.48754**	175B→191B	0.12541	178B→188B	-0.14584	
180A→188A	-0.14425	176B→179B	-0.30529			
Excited State 8:	3.318-A	3.0410 eV	407.71 nm	f=0.0415	<S**2>=2.503	
178A→186A	0.10537	169B→179B	0.35296	172B→180B	-0.39523	
166B→179B	-0.27208	169B→180B	-0.33095			
166B→180B	0.25076	172B→179B	0.43065			

Excited State 9:	3.320-A	3.0428 eV	407.46 nm	f=0.0519	<S**2>=2.506
172A→192A	-0.10205	165B→179B	0.27728	171B→179B	0.43709
178A→185A	-0.10915	165B→180B	0.23966	171B→180B	0.37373
179A→185A	-0.10390	168B→179B	0.36412	177B→185B	0.10178
179A→186A	0.10371	168B→180B	0.31990		
Excited State 10:	3.102-A	3.0567 eV	405.61 nm	f=0.0012	<S**2>=2.156
173B→180B	-0.58722	176B→180B	0.16515	178B→180B	0.15300
174B→179B	0.70836	177B→179B	0.13166		
Excited State 11:	3.179-A	3.0795 eV	402.61 nm	f=0.0679	<S**2>=2.276
179A→182A	-0.10076	174B→180B	-0.55924	178B→181B	-0.11241
180A→181A	-0.24333	177B→180B	-0.19991		
173B→179B	0.63783	178B→179B	-0.21038		
Excited State 12:	3.191-A	3.2586 eV	380.48 nm	f=0.0024	<S**2>=2.296
166B→179B	0.24039	169B→179B	0.48920	172B→179B	-0.41211
166B→180B	-0.22826	169B→180B	-0.45028	172B→180B	0.37065
Excited State 13:	3.193-A	3.2600 eV	380.32 nm	f=0.0025	<S**2>=2.300
165B→179B	-0.24588	168B→179B	0.50283	171B→179B	-0.42263
165B→180B	-0.21934	168B→180B	0.43364	171B→180B	-0.35575
Excited State 14:	3.136-A	3.3084 eV	374.75 nm	f=0.0042	<S**2>=2.209
167B→179B	-0.10962	170B→180B	-0.45566	175B→181B	-0.16372
170B→179B	-0.10135	175B→179B	0.81609		
Excited State 15:	3.396-A	3.3539 eV	369.67 nm	f=0.0012	<S**2>=2.633
177A→181A	-0.12030	167B→179B	0.48418	175B→179B	0.14156
180A→194A	-0.11248	170B→179B	0.13191	175B→180B	-0.16398
164B→180B	-0.20343	173B→180B	-0.22925	176B→180B	-0.27085

177B→179B	-0.36394	178B→180B	-0.26615		
177B→181B	0.16301	178B→184B	-0.13073		

Excited State 16: 3.152-A 3.3768 eV 367.16 nm f=0.0044 <S**2>=2.234

167B→180B	-0.10105	170B→181B	0.11605		
170B→179B	-0.62663	175B→180B	0.66331		

Excited State 17: 3.330-A 3.4264 eV 361.85 nm f=0.0165 <S**2>=2.522

163B→180B	0.10784	173B→179B	0.20441	177B→180B	0.49676
164B→179B	0.26649	175B→180B	-0.12911	177B→184B	-0.10101
167B→180B	-0.39673	176B→179B	0.28519	178B→179B	0.30731

Excited State 18: 3.662-A 3.5326 eV 350.97 nm f=0.0815 <S**2>=3.103

166A→183A	0.11994	178A→182A	-0.16806	168B→185B	-0.11435
167A→184A	-0.11742	178A→194A	-0.13691	169B→186B	-0.10757
168A→185A	0.10149	179A→181A	0.40225	171B→182B	-0.10597
169A→186A	0.10259	179A→185A	0.11126	172B→183B	0.10666
172A→183A	0.12247	179A→187A	0.10711	173B→192B	-0.10874
173A→184A	0.12123	179A→188A	0.15421	174B→193B	-0.10489
177A→181A	-0.11466	180A→182A	0.42889	176B→180B	-0.10201
177A→195A	0.11244	163B→179B	0.11529	178B→194B	0.10620

Excited State 19: 3.451-A 3.5804 eV 346.28 nm f=0.4589 <S2>=2.728**

177A→194A	0.10960	180A→187A	0.12386	176B→179B	0.26950
178A→181A	-0.18601	180A→188A	0.19916	177B→180B	0.10313
179A→182A	**0.43441**	164B→179B	0.10269	178B→181B	-0.26063
180A→181A	0.31513	167B→180B	-0.24592		
180A→185A	0.13127	173B→179B	0.11326		

Excited State 20: 3.693-A 3.6873 eV 336.24 nm f=0.0115 <S**2>=3.159

172A→192A	0.15571	173A→193A	-0.15075	174A→184A	0.10345

174A→189A	0.12254	179A→187A	-0.14335	171B→192B	0.12999
174A→190A	-0.11809	180A→183A	0.10655	172B→179B	0.10908
175A→189A	0.10342	180A→186A	0.14681	172B→193B	-0.11399
175A→190A	0.11075	168B→179B	0.28392	173B→182B	0.13063
177A→185A	0.12764	168B→180B	0.23071	173B→190B	0.12559
177A→187A	-0.10880	169B→179B	0.27350	174B→183B	0.12097
178A→186A	-0.20215	169B→180B	-0.24114	174B→189B	0.12017
179A→184A	-0.12779	169B→193B	0.10068	177B→186B	-0.12936
179A→185A	0.18379	171B→179B	0.10496		

Excited State 21: 3.692-A 3.6876 eV 336.22 nm f=0.1385 <S**2>=3.158

172A→192A	-0.15417	179A→183A	0.12655	171B→192B	-0.12821
173A→193A	-0.14989	179A→186A	0.21795	172B→179B	0.10386
174A→183A	-0.10474	180A→184A	-0.10394	172B→193B	-0.11253
174A→189A	-0.12303	180A→185A	0.13043	173B→183B	0.13176
174A→190A	-0.11883	168B→179B	-0.28203	173B→189B	0.12180
175A→189A	-0.10267	168B→180B	-0.23182	174B→182B	0.11520
175A→190A	0.10934	169B→179B	0.27560	174B→190B	0.12943
177A→186A	0.15997	169B→180B	-0.23859	176B→186B	-0.11219
178A→185A	-0.16966	169B→193B	0.10047	177B→185B	0.11952
178A→187A	0.13306	171B→179B	-0.11085	178B→186B	-0.10313

Excited State 22: 3.579-A 3.7016 eV 334.95 nm f=0.1908 <S**2>=2.952

170A→181A	0.12490	179A→182A	-0.24154	167B→184B	0.10541
172A→189A	-0.12771	179A→194A	0.16831	168B→185B	0.13089
173A→190A	-0.11895	180A→181A	-0.29750	169B→186B	-0.11598
174A→192A	-0.11470	180A→195A	0.15734	174B→192B	-0.11866
177A→182A	0.15456	163B→180B	-0.15791	176B→179B	0.31991
178A→195A	-0.11356	164B→179B	-0.18466	176B→181B	-0.15499

177B→180B	0.27753	178B→179B	0.15015		
177B→184B	0.12968	178B→188B	-0.12180		

Excited State 23: 3.549-A 3.7783 eV 328.14 nm f=0.0305 <S**2>=2.898

166A→183A	0.11958	179A→181A	0.29031	169B→186B	0.11907
167A→184A	-0.12831	179A→195A	-0.18751	173B→192B	0.11174
170A→182A	-0.15325	180A→182A	0.32824	174B→193B	0.11608
172A→189A	-0.12528	180A→194A	-0.13366	176B→180B	0.31925
173A→190A	0.13345	163B→179B	-0.16437	176B→184B	-0.14792
174A→193A	0.10474	164B→180B	-0.10821	177B→179B	0.22762
177A→181A	-0.12404	167B→179B	-0.15143	177B→188B	0.12405
178A→194A	0.10042	168B→185B	0.11565	178B→180B	0.10854

Excited State 24: 3.762-A 3.8378 eV 323.06 nm f=0.0049 <S**2>=3.288

165A→181A	0.16042	180A→196A	-0.20007	175B→187B	-0.24581
171A→191A	0.23857	163B→179B	0.21413	176B→180B	0.20282
176A→185A	0.14528	164B→180B	0.24662	177B→179B	0.10076
176A→187A	0.20237	167B→179B	-0.22402	177B→181B	0.12762
176A→188A	-0.17858	167B→181B	-0.16724	178B→180B	0.10323
178A→182A	0.15316	170B→191B	0.22023	178B→184B	-0.11375
179A→188A	-0.14345	175B→185B	-0.11355	178B→194B	0.10297
180A→182A	-0.12814	175B→186B	0.11656	178B→196B	-0.13283

Excited State 25: 3.265-A 3.9854 eV 311.09 nm f=0.0185 <S**2>=2.414

170A→183A	-0.12616	180A→183A	0.54014	180A→189A	-0.11500
178A→183A	-0.14728	180A→184A	-0.21337	175B→180B	0.12077
179A→183A	-0.28006	180A→185A	0.12899	178B→187B	0.12467
179A→184A	-0.43070	180A→187A	0.15166		
179A→189A	0.10991	180A→188A	-0.12952		

Excited State 26:	3.131-A	3.9932 eV	310.49 nm	f=0.0209	<S**2>=2.201	
170A→184A	-0.14409	179A→184A	0.30900	180A→184A	0.56424	
177A→183A	0.10782	179A→186A	0.12467	180A→189A	-0.11392	
178A→184A	-0.18329	179A→190A	0.11587	180A→190A	0.13948	
179A→183A	-0.48758	180A→183A	0.21841			

Excited State 27:	3.461-A	4.0319 eV	307.51 nm	f=0.0009	<S**2>=2.745	
166A→183A	0.19736	164B→180B	0.40304	175B→187B	0.10970	
167A→184A	-0.19633	165B→182B	0.11745	176B→180B	-0.38623	
171A→191A	-0.11497	166B→183B	0.11571	177B→179B	-0.34602	
176A→187A	-0.10003	167B→179B	-0.28086			
163B→179B	0.28976	170B→191B	-0.10257			

Excited State 28:	3.665-A	4.0457 eV	306.46 nm	f=0.0103	<S**2>=3.108	
177A→191A	0.10179	180A→183A	-0.17392	175B→180B	0.32401	
178A→183A	0.12934	180A→185A	0.24230	176B→187B	-0.10828	
178A→185A	0.13030	180A→186A	0.18006	178B→185B	0.12885	
178A→187A	0.17614	180A→187A	0.34677	178B→186B	-0.12459	
178A→188A	-0.16542	180A→188A	-0.28481	178B→187B	0.25172	
179A→183A	0.14111	170B→179B	0.17954			
179A→184A	0.20448	170B→181B	-0.13096			

Excited State 29:	3.513-A	4.0724 eV	304.45 nm	f=0.0017	<S**2>=2.835	
166A→183A	0.18762	173A→190A	-0.12073	166B→183B	-0.11771	
166A→184A	0.10918	163B→180B	0.29574	167B→180B	-0.24059	
167A→183A	-0.11303	164B→179B	0.45722	176B→179B	-0.26474	
167A→184A	0.21602	165B→182B	0.10117	177B→180B	-0.32683	
172A→189A	-0.11010	166B→182B	-0.10624			

Excited State 30:	3.357-A	4.1669 eV	297.55 nm	f=0.0069	<S**2>=2.568	
180A→181A	0.12163	164B→179B	0.11809	175B→179B	0.10363	
180A→185A	-0.10181	170B→179B	0.58130	175B→180B	0.54491	
180A→187A	-0.13886	170B→180B	0.18243	178B→187B	-0.14888	
163B→180B	0.11925	170B→181B	-0.18072			

Excited State 31:	3.212-A	4.2219 eV	293.67 nm	f=0.0012	<S**2>=2.329	
180A→191A	-0.12880	170B→180B	0.79846	175B→180B	-0.13311	
170B→179B	-0.12152	175B→179B	0.38347	175B→181B	-0.21300	

Excited State 32:	**3.544-A**	**4.3914 eV**	**282.33 nm**	**f=0.3393**	**<S**2>=2.891**	
166A→183A	-0.16650	164B→179B	0.12082	176B→179B	-0.10895	
167A→184A	-0.16058	167B→180B	-0.14098	177B→184B	-0.14246	
176A→191A	-0.14369	170B→179B	0.15591	**178B→181B**	**0.42999**	
178A→181A	-0.19243	170B→187B	-0.17166	178B→187B	-0.11137	
180A→181A	**-0.37254**	175B→180B	0.10626			
180A→188A	0.27022	175B→191B	0.16734			

Excited State 33:	3.862-A	4.4294 eV	279.91 nm	f=0.0048	<S**2>=3.479	
165A→187A	-0.11624	180A→193A	-0.11371	177B→187B	-0.10742	
177A→187A	0.12630	167B→187B	0.11633	178B→189B	-0.13032	
178A→191A	0.29420	170B→180B	0.10040	178B→191B	0.34389	
179A→185A	-0.10729	175B→179B	0.19278	178B→193B	-0.13122	
179A→187A	-0.14038	176B→180B	0.12908			
180A→191A	0.54206	176B→191B	-0.14684			

Excited State 34:	3.850-A	4.5039 eV	275.28 nm	f=0.1007	<S**2>=3.456	
171A→185A	0.15170	176A→191A	0.31343	170B→179B	-0.19514	
171A→187A	0.21109	180A→187A	0.10731	170B→185B	0.11809	
171A→188A	-0.17516	180A→188A	-0.10223	170B→186B	-0.11810	

170B→187B	0.25108	175B→191B	-0.26006	177B→184B	-0.11606
175B→180B	-0.11458	175B→193B	0.10277	178B→181B	0.53363

Excited State 35: 3.852-A 4.5491 eV 272.54 nm f=0.0312 <S**2>=3.460

166A→183A	0.30659	180A→182A	-0.21899	166B→183B	0.20813
166A→189A	-0.16282	180A→196A	0.10130	166B→189B	-0.11975
167A→184A	-0.30630	163B→179B	-0.10234	166B→190B	-0.15156
167A→190A	-0.16145	164B→180B	-0.16310	167B→179B	0.22688
172A→183A	0.12631	165B→182B	0.20889	176B→180B	0.12278
173A→184A	0.12857	165B→189B	0.15231		
179A→181A	-0.24064	165B→190B	-0.13594		

Excited State 36: 3.883-A 4.5977 eV 269.67 nm f=0.0099 <S**2>=3.520

168A→192A	0.10145	178A→186A	0.15110	172B→193B	-0.11009
169A→193A	-0.20786	178A→190A	0.13370	173B→190B	0.12876
173A→193A	-0.13966	179A→184A	0.11572	174B→183B	0.13573
174A→190A	-0.14090	179A→185A	-0.18759	174B→186B	0.10763
175A→183A	0.10574	179A→186A	-0.10202	174B→189B	0.12376
175A→184A	-0.11352	179A→187A	0.15245	176B→182B	-0.14965
175A→190A	0.17039	179A→190A	-0.18201	177B→183B	-0.23465
177A→184A	0.18185	180A→186A	-0.20036	178B→182B	-0.19664
177A→190A	-0.11039	180A→190A	-0.15897	178B→183B	-0.11632
178A→183A	0.11694	168B→192B	-0.10747		
178A→184A	-0.12334	169B→193B	0.20807		

Excited State 37: 3.887-A 4.5982 eV 269.63 nm f=0.0563 <S**2>=3.527

168A→192A	0.21586	175A→183A	0.11190	177A→189A	0.10893
169A→193A	0.10266	175A→184A	0.11160	178A→183A	0.12408
172A→192A	0.14710	175A→189A	0.16672	178A→184A	0.12030
174A→189A	0.15565	177A→183A	0.18381	178A→185A	-0.16134

178A→189A	0.13837	180A→187A	-0.13090	174B→182B	-0.13342
179A→183A	0.11785	180A→189A	-0.15258	174B→190B	-0.13675
179A→185A	-0.13653	168B→192B	-0.23082	176B→183B	0.16176
179A→186A	0.23361	169B→193B	-0.10330	177B→182B	0.23570
179A→189A	0.18791	171B→192B	0.11918	178B→182B	-0.11424
180A→185A	0.16814	173B→189B	-0.13875	178B→183B	0.19200

Excited State 38: 3.589-A 4.6120 eV 268.83 nm f=0.0274 <S**2>=2.970

166A→183A	-0.12695	155B→180B	0.13725	166B→190B	-0.11820
167A→184A	-0.15598	160B→179B	-0.13769	167B→179B	0.15662
167A→190A	-0.10425	161B→179B	0.19957	170B→180B	-0.10512
178A→181A	0.11639	163B→179B	0.13010	174B→179B	-0.12837
179A→182A	-0.17734	163B→180B	0.23227	176B→180B	0.18309
180A→185A	-0.13139	164B→179B	0.19015	178B→181B	-0.22117
180A→187A	-0.11469	165B→189B	-0.10044	178B→184B	-0.10753
180A→188A	-0.12837	166B→183B	0.10404		

Excited State 39: 3.594-A 4.6167 eV 268.55 nm f=0.0052 <S**2>=2.980

166A→183A	0.11715	163B→179B	0.21241	174B→179B	-0.22610
171A→191A	-0.15067	163B→180B	-0.11990	175B→187B	0.17343
176A→185A	-0.11016	164B→179B	-0.10426	176B→180B	0.32325
176A→187A	-0.15072	167B→179B	0.27629	177B→181B	0.16287
176A→188A	0.10207	167B→181B	-0.11042	178B→181B	0.14857
178A→182A	0.10402	170B→180B	-0.14221	178B→184B	-0.15615
179A→182A	0.12063	170B→191B	-0.15167		
180A→188A	0.12725	173B→180B	-0.11596		

Excited State 40: 3.789-A 4.6404 eV 267.18 nm f=0.0069 <S**2>=3.339

168A→192A	0.10213	172A→192A	-0.20570	174A→189A	-0.10514
170A→183A	-0.10432	173A→193A	0.16572	177A→185A	0.10186

178A→183A	0.11075	179A→190A	-0.18400	173B→190B	-0.10555
178A→186A	-0.21176	180A→186A	0.18565	174B→183B	-0.15229
178A→189A	0.16720	180A→189A	-0.18590	177B→183B	-0.14669
178A→190A	0.13744	180A→190A	-0.15592	177B→186B	-0.11756
179A→185A	0.16973	171B→192B	-0.20046	178B→182B	-0.17013
179A→187A	-0.19959	172B→193B	0.14903	178B→187B	-0.10101
179A→189A	0.22729	173B→182B	-0.17001		

Excited State 41: 3.807-A 4.6429 eV 267.04 nm f=0.0174 <S**2>=3.374

169A→193A	-0.11638	178A→189A	-0.15081	172B→193B	0.17921
170A→184A	0.11133	178A→190A	0.17951	173B→183B	-0.17450
172A→192A	0.17091	179A→186A	0.25216	173B→189B	-0.10245
173A→193A	0.19937	179A→189A	-0.20811	174B→182B	-0.14480
174A→183A	0.10024	179A→190A	-0.24831	176B→186B	-0.10051
174A→190A	0.10199	180A→185A	0.13049	177B→182B	-0.15442
177A→186A	0.14138	180A→187A	-0.14032	177B→187B	-0.11331
178A→184A	-0.11844	180A→189A	0.16113	178B→183B	-0.17678
178A→185A	-0.14804	180A→190A	-0.19475	178B→186B	-0.11643
178A→187A	0.14847	171B→192B	0.16449		

Excited State 42: 3.714-A 4.6688 eV 265.56 nm f=0.0014 <S**2>=3.198

172A→189A	-0.12040	180A→194A	0.15195	174B→179B	-0.14695
173A→190A	0.12967	180A→196A	0.13211	174B→193B	0.12405
174A→193A	0.11648	155B→179B	0.15284	175B→187B	-0.10453
175A→192A	-0.10027	160B→180B	-0.13863	176B→180B	0.15169
177A→181A	0.15981	161B→180B	0.18525	177B→181B	-0.17722
178A→182A	-0.14220	163B→179B	0.23843	178B→184B	0.16694
179A→185A	0.11559	167B→179B	0.21430	178B→196B	0.10479
179A→188A	0.13710	173B→192B	0.12507		

Excited State 43:	3.244-A	4.6802 eV	264.91 nm	f=0.0193	<S**2>=2.381	
178A→181A	-0.20676	163B→180B	0.28278	174B→180B	-0.40264	
179A→182A	0.18287	164B→179B	0.10092	176B→179B	0.37460	
160B→179B	-0.12654	167B→180B	0.40708			
161B→179B	0.16154	173B→179B	-0.19831			

Excited State 44:	3.563-A	4.7840 eV	259.16 nm	f=0.0054	<S**2>=2.924	
168A→183A	0.10412	179A→192A	0.18045	173B→180B	-0.10774	
168A→189A	0.16203	179A→193A	0.10264	174B→180B	0.26384	
169A→190A	0.10811	180A→187A	0.13037	177B→184B	0.14359	
170A→181A	0.10789	180A→188A	-0.16261	177B→192B	-0.12551	
171A→181A	0.11483	180A→192A	-0.11709	178B→182B	0.11935	
177A→192A	0.13337	171B→179B	0.10678	178B→185B	-0.13650	
178A→188A	-0.11252	171B→180B	-0.11672	178B→186B	0.12748	
178A→192A	0.14190	171B→185B	0.11185	178B→187B	-0.27662	
178A→193A	-0.10124	173B→179B	0.32503			

Excited State 45:	3.517-A	4.7945 eV	258.60 nm	f=0.0034	<S**2>=2.842	
169A→184A	-0.11330	180A→193A	0.15481	177B→191B	-0.10391	
169A→190A	0.18158	169B→186B	0.11075	178B→182B	-0.15836	
171A→181A	-0.21406	172B→183B	0.10110	178B→184B	-0.11786	
177A→193A	0.14634	172B→186B	-0.10354	178B→185B	0.16200	
178A→193A	-0.19030	173B→179B	0.15034	178B→186B	-0.16949	
179A→193A	0.20142	173B→180B	0.12623	178B→187B	0.33392	
180A→185A	-0.10735	174B→179B	0.18132	178B→188B	-0.14885	
180A→187A	-0.16191	176B→187B	-0.12730			
180A→188A	0.23092	176B→193B	-0.11141			

Excited State 46:	3.729-A	4.8012 eV	258.23 nm	f=0.0019	<S**2>=3.226	
168A→183A	-0.11247	168A→189A	-0.18960	169A→190A	0.14633	

171A→181A	0.12468	180A→188A	-0.13670	173B→180B	0.12844
177A→192A	-0.13319	180A→192A	0.17854	174B→179B	0.22004
177A→193A	0.11799	180A→193A	0.11865	176B→192B	-0.13063
178A→192A	-0.22001	167B→179B	0.14644	177B→192B	0.11030
178A→193A	-0.13718	168B→185B	0.12486	177B→193B	-0.13466
179A→192A	-0.22217	171B→182B	-0.11541	178B→187B	-0.20287
179A→193A	0.19947	171B→185B	-0.10419	178B→192B	-0.13399

Excited State 47: 3.342-A 4.8277 eV 256.82 nm f=0.0001 <S**2>=2.542

168A→189A	0.10495	161B→180B	0.16099	173B→180B	0.45143
178A→192A	0.10173	163B→179B	0.16596	174B→179B	0.34365
179A→181A	-0.11755	167B→179B	0.10428	177B→188B	0.13624
179A→192A	0.10587	171B→179B	-0.27280	178B→184B	-0.13636
155B→179B	0.12163	171B→180B	0.32398		
160B→180B	-0.12222	172B→179B	-0.11359		

Excited State 48: 3.776-A 4.8331 eV 256.53 nm f=0.0037 <S**2>=3.315

168A→185A	-0.10317	179A→193A	-0.14647	172B→190B	-0.10724
172A→189A	0.18308	180A→192A	0.10376	173B→179B	0.14076
173A→190A	0.14063	180A→193A	-0.12045	174B→180B	0.29254
174A→192A	0.11127	163B→180B	0.13538	176B→181B	-0.13659
177A→182A	0.13780	164B→179B	0.13758	177B→184B	0.17644
178A→192A	-0.11784	168B→185B	0.15034	178B→188B	-0.20064
178A→193A	0.14034	169B→186B	-0.12303		
179A→192A	-0.16988	171B→189B	0.13086		

Excited State 49: 3.592-A 4.8461 eV 255.84 nm f=0.0093 <S**2>=2.975

167A→184A	-0.12416	176A→181A	0.10280	163B→179B	-0.10526
173A→190A	0.15241	180A→196A	-0.10739	167B→179B	0.10733
174A→193A	0.10644	161B→180B	-0.11874	167B→180B	-0.21478

169B→183B	0.10700	173B→179B	-0.16667	177B→184B	0.11629
171B→179B	-0.32625	174B→180B	-0.13735	177B→188B	-0.15977
171B→180B	0.36013	174B→193B	0.10538	178B→184B	0.15111
172B→190B	-0.10178	176B→184B	0.12718	178B→188B	-0.10563

Excited State 50: 3.437-A 4.8519 eV 255.54 nm f=0.0051 <S**2>=2.702

166A→183A	-0.10630	171B→179B	-0.10460	174B→179B	-0.21094
172A→189A	0.11790	172B→179B	0.33122	174B→180B	-0.24482
179A→193A	0.10724	172B→180B	0.36025	176B→184B	-0.10028
167B→179B	-0.14334	173B→179B	-0.23392	177B→188B	0.12593
167B→180B	-0.20150	173B→180B	-0.27579	178B→184B	-0.10779

Excited State 51: 3.119-A 4.8786 eV 254.14 nm f=0.0020 <S**2>=2.182

167B→179B	0.11303	172B→179B	0.55867	173B→180B	0.30403
171B→179B	0.15006	172B→180B	0.57506	174B→179B	0.25294
171B→180B	-0.18483	173B→179B	0.11328	174B→180B	0.14157

Excited State 52: 3.152-A 4.8877 eV 253.66 nm f=0.0090 <S**2>=2.235

167B→180B	0.22236	172B→179B	0.11764	173B→180B	-0.25243
171B→179B	-0.43966	172B→180B	0.14503	174B→179B	-0.14364
171B→180B	0.48831	173B→179B	0.36887	174B→180B	0.33629

Excited State 53: 3.759-A 4.9349 eV 251.24 nm f=0.0044 <S**2>=3.282

171A→182A	-0.10052	179A→188A	0.12923	177B→182B	-0.11249
171A→196A	0.18304	180A→191A	0.28035	178B→183B	-0.13894
176A→181A	0.61018	175B→179B	-0.12314	178B→189B	0.12242
176A→188A	-0.33365	175B→181B	-0.23236	178B→191B	-0.14182
178A→191A	0.12130	175B→188B	0.12543		

*C.2.3.4 **OTPA-FLR-210, EB** State*

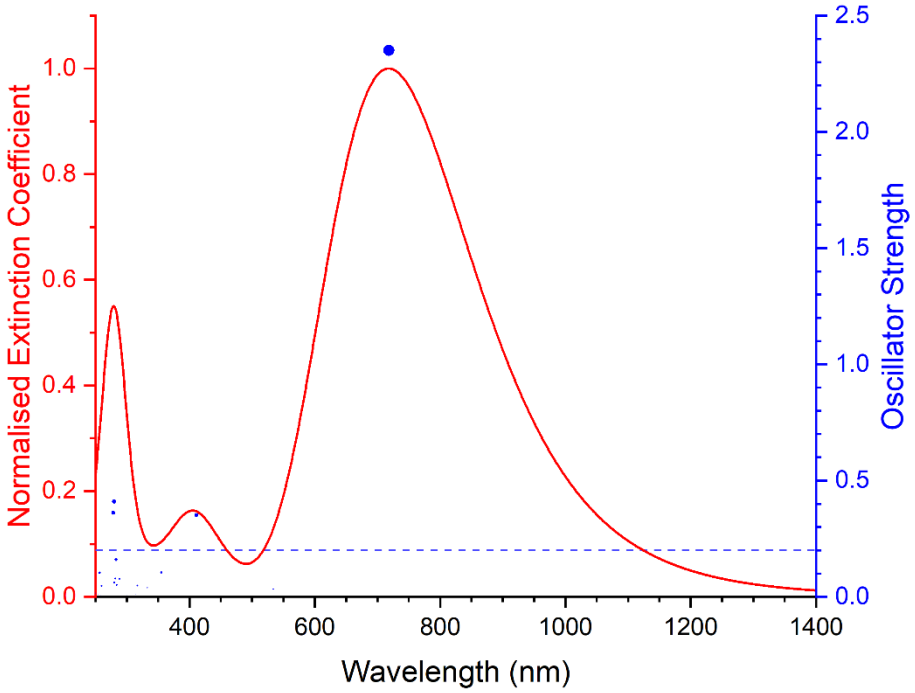

*Figure C-12 Excited states and normalised absorption spectra from TD-DFT calculations of **OTPA-FLR-210** in **EB** state. The areas of excited state dots are proportional to their oscillator strengths.*

Excited State 1:	**Singlet-A**	**1.7261 eV**	**718.28 nm**	**f=2.3499**	**<S**2>=0.000**
178→181	-0.10292	**179→180**	**0.69023**		
Excited State 2:	Singlet-A	2.3230 eV	533.72 nm	f=0.0326	<S**2>=0.000
176→180	0.21654	178→180	0.65638		
Excited State 3:	**Singlet-A**	**3.0164 eV**	**411.03 nm**	**f=0.3514**	**<S**2>=0.000**
175→180	0.29713	**177→180**	**0.62157**		
Excited State 4:	Singlet-A	3.4919 eV	355.06 nm	f=0.1050	<S**2>=0.000
163→180	-0.25245	175→180	0.50044	177→180	-0.31165
171→180	0.19039	176→181	-0.11418	179→180	-0.10659
Excited State 5:	Singlet-A	3.5171 eV	352.52 nm	f=0.0003	<S**2>=0.000
162→180	-0.10075	172→180	-0.11030	176→180	0.53428
164→180	0.27316	175→181	-0.11519	178→180	-0.23762

Excited State 6:	Singlet-A	3.7230 eV	333.03 nm	f=0.0392	<S**2>=0.000
166→180	0.64753	170→180	0.22393		
Excited State 7:	Singlet-A	3.9112 eV	317.00 nm	f=0.0482	<S**2>=0.000
176→180	0.14002	178→187	-0.17571	179→181	0.62319
Excited State 8:	Singlet-A	3.9491 eV	313.96 nm	f=0.0107	<S**2>=0.000
164→180	0.11130	165→180	0.65721	167→180	0.12058
Excited State 9:	Singlet-A	4.1213 eV	300.84 nm	f=0.0080	<S**2>=0.000
165→180	-0.12187	174→180	0.22884	179→191	-0.11706
167→180	0.27243	178→183	-0.22162		
173→180	0.30401	179→182	0.33886		
Excited State 10:	Singlet-A	4.1344 eV	299.88 nm	f=0.0031	<S**2>=0.000
166→180	0.15150	174→180	0.32504	179→183	-0.29458
170→180	-0.24993	178→182	0.17172		
173→180	-0.24794	178→184	-0.14493		
Excited State 11:	Singlet-A	4.3018 eV	288.22 nm	f=0.0772	<S**2>=0.000
164→180	0.12163	177→182	-0.11470	179→182	0.41978
167→180	-0.13237	177→184	-0.10473	179→184	0.35392
173→180	-0.14172	177→187	-0.12751		
174→180	-0.14635	178→181	0.15642		
Excited State 12:	Singlet-A	4.3679 eV	283.85 nm	f=0.0503	<S**2>=0.000
164→180	-0.26247	174→180	0.11617	178→184	0.17323
166→180	0.10572	176→180	0.13391	179→182	0.11431
170→180	-0.17921	177→183	0.12797	179→183	0.29578
173→180	-0.25883	178→182	-0.23418		

Excited State 13:	Singlet-A	4.3823 eV	282.92 nm	f=0.1597	<S**2>=0.000	
167→180	0.17655	178→183	0.31950	179→184	0.33724	
174→180	0.24815	178→186	-0.14168	179→186	-0.12974	
177→182	-0.11856	179→182	-0.13168			
177→184	0.10716	179→183	0.15703			

Excited State 14:	Singlet-A	4.4020 eV	281.65 nm	f=0.0787	<S**2>=0.000	
164→180	0.40559	178→184	0.17287	179→184	-0.12260	
176→180	-0.23179	178→185	0.16944	179→185	-0.18889	
177→185	-0.10798	178→186	-0.10149	179→186	-0.10071	
178→181	-0.12642	179→183	0.12899	179→187	0.13023	

Excited State 15:	**Singlet-A**	**4.4283 eV**	**279.98 nm**	**f=0.4097**	**<S**2>=0.000**	
167→180	0.10086	177→186	0.19566	**178→186**	**0.33160**	
174→180	0.11299	178→183	0.10632	179→185	-0.24584	
177→185	-0.13126	178→185	0.24339	**179→186**	**0.36264**	

Excited State 16:	Singlet-A	4.4312 eV	279.80 nm	f=0.0618	<S**2>=0.000	
164→180	0.15413	178→185	-0.30413	179→186	0.21857	
173→180	-0.11261	178→186	0.22749	179→187	0.11776	
177→185	0.18137	179→183	0.12724			
177→186	0.11541	179→185	0.32135			

Excited State 17:	**Singlet-A**	**4.4523 eV**	**278.47 nm**	**f=0.3610**	**<S**2>=0.000**	
164→180	-0.17448	**178→181**	**-0.32848**	**179→187**	**0.44518**	
176→180	0.11116	178→189	0.10415			
177→182	-0.15821	179→184	0.12891			

Excited State 18:	Singlet-A	4.7737 eV	259.72 nm	f=0.0464	<S**2>=0.000	
161→180	0.13527	171→180	0.43479			
163→180	-0.32087	175→180	-0.32338			

Excited State 19:	Singlet-A	4.7888 eV	258.90 nm	f=0.0053	<S**2>=0.000			
172→180	0.31182		178→184	0.17310		178→191	-0.14357	
177→181	0.13645		178→190	0.13645		179→188	0.39822	
Excited State 20:	Singlet-A	4.8159 eV	257.45 nm	f=0.0021	<S**2>=0.000			
172→180	-0.17262		177→181	-0.18816		178→187	0.19847	
173→180	0.14369		177→183	0.11223		178→191	-0.26114	
174→180	-0.12278		177→189	0.13351		179→189	0.38816	
Excited State 21:	Singlet-A	4.8320 eV	256.59 nm	f=0.1035	<S**2>=0.000			
173→180	0.15201		177→191	0.12258		178→193	-0.12405	
174→180	0.19589		178→188	-0.14773		179→191	0.42053	
176→183	0.12334		178→189	-0.24529				
177→184	-0.11648		178→192	0.10661				
Excited State 22:	Singlet-A	4.8792 eV	254.11 nm	f=0.0123	<S**2>=0.000			
164→180	0.16812		178→184	-0.11424		179→193	0.19001	
172→180	0.45174		179→188	-0.24087				
177→181	-0.13978		179→192	-0.18867				
Excited State 23:	Singlet-A	4.9274 eV	251.62 nm	f=0.0033	<S**2>=0.000			
161→180	-0.14410		177→190	-0.16806		179→190	-0.26988	
163→180	0.33672		178→189	0.16026		179→193	0.11459	
171→180	0.22549		178→192	0.21887				
Excited State 24:	Singlet-A	4.9552 eV	250.21 nm	f=0.0147	<S**2>=0.000			
163→180	-0.12286		177→188	0.16722		179→192	-0.14945	
172→180	-0.21912		178→187	-0.17094		179→193	0.40495	
173→180	0.13444		178→190	0.11838				
177→181	0.15656		178→191	-0.12398				

C.2.4 Electronic Transitions in **OTPA-FLR-221** Oligomers

*Table C-8 Attributes of **OTPA-FLR-221** in **LEB**, **ES** (singlet and quintet), and **EB** states related to electronic structures*

Attribute	LEB State	^{1}ES State	^{5}ES State	EB State
Molecular Formula	$C_{62}H_{46}N_6$	$C_{62}H_{46}N_6^{4+}$	$C_{62}H_{46}N_6^{4+}$	$C_{62}H_{42}N_6$
Number of Atoms	114	114	114	110
Number of Electrons	460	456	456	456
HOMO	MO 230	MO 228	MOs 230A, 226B	MO 228
LUMO	MO 231	MO 229	MOs 231A, 227B	MO 229

*C.2.4.1 **OTPA-FLR-221**, **LEB** State*

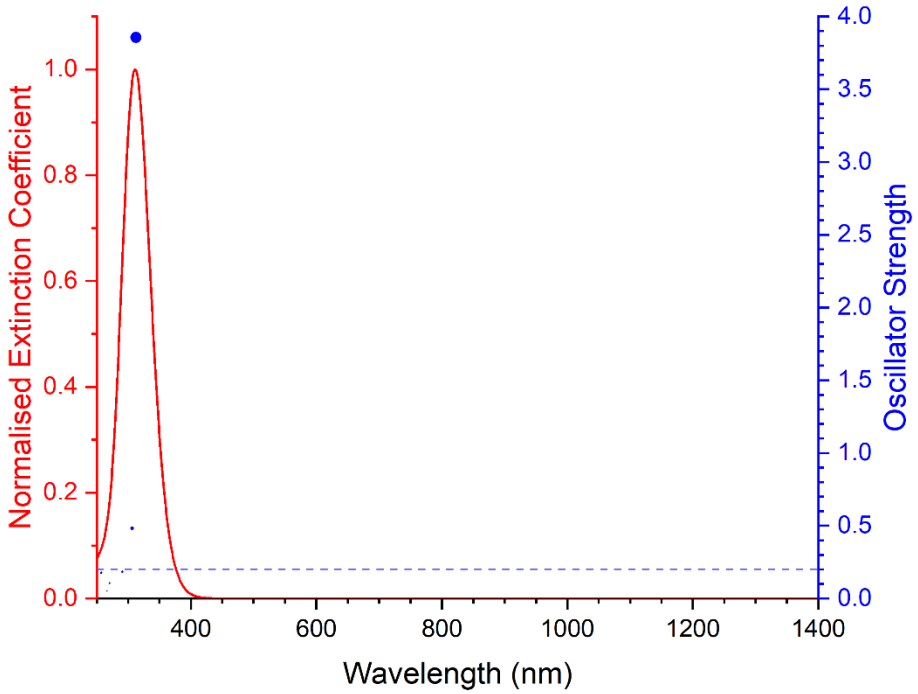

*Figure C-13 Excited states and normalised absorption spectra from TD-DFT calculations of **OTPA-FLR-221** in **LEB** state. The areas of excited state dots are proportional to their oscillator strengths.*

Excited State 1:	Singlet-A	3.7271 eV	332.65 nm	f=0.0000	<S**2>=0.000
227→241	0.10136	229→234	-0.22678	230→231	0.51238
228→232	0.32065	229→236	-0.16290		
Excited State 2:	**Singlet-A**	**3.9657 eV**	**312.64 nm**	**f=3.8553**	**<S**2>=0.000**
227→232	0.12735	**228→231**	**0.41607**	**230→232**	**0.46472**
227→239	-0.10364	229→237	-0.19323		

Excited State 3:	**Singlet-A**	**4.0446 eV**	**306.54 nm**	**f=0.4806**	**<S**2>=0.000**	
227→234	-0.13334	229→233	-0.25477	**230→234**	**0.44319**	
229→231	**-0.35261**	229→241	0.15177	230→236	0.12021	
Excited State 4:	Singlet-A	4.1531 eV	298.53 nm	f=0.0000	<S**2>=0.000	
226→240	0.11057	228→235	-0.20527	230→233	0.46436	
227→238	0.14192	229→234	-0.31362			
228→232	-0.14549	229→236	0.19435			
Excited State 5:	Singlet-A	4.2619 eV	290.91 nm	f=0.1818	<S**2>=0.000	
227→236	-0.14074	229→238	-0.23461	230→236	0.42277	
229→231	-0.21358	229→241	0.15191			
229→233	0.28469	230→234	-0.13947			
Excited State 6:	Singlet-A	4.2991 eV	288.39 nm	f=0.0003	<S**2>=0.000	
226→234	-0.10974	228→233	-0.34559	229→240	0.16487	
227→235	0.16511	228→238	-0.21941	230→235	0.42807	
Excited State 7:	Singlet-A	4.3898 eV	282.44 nm	f=0.0000	<S**2>=0.000	
227→233	0.22104	228→243	0.12701	229→236	-0.22137	
228→235	-0.33756	229→234	0.12769	230→238	0.40573	
Excited State 8:	Singlet-A	4.3973 eV	281.96 nm	f=0.0000	<S**2>=0.000	
226→231	0.15270	229→232	-0.32597	230→237	0.40838	
227→237	-0.16510	229→235	0.16122			
228→234	0.15019	229→239	-0.24797			
Excited State 9:	Singlet-A	4.4932 eV	275.93 nm	f=0.0000	<S**2>=0.000	
226→233	0.18979	228→242	-0.10942	229→239	0.17519	
228→234	0.22081	229→232	0.10893	229→243	0.22708	
228→236	-0.12558	229→235	0.17856	230→240	0.41236	

Excited State 10:	Singlet-A	4.5557 eV	272.15 nm	f=0.0000	<S**2>=0.000
227→231	0.30471	228→239	-0.10962	230→241	0.33070
228→232	0.27345	229→234	0.20179		
228→235	-0.13681	229→236	0.27933		
Excited State 11:	Singlet-A	4.5831 eV	270.53 nm	f=0.1043	<S**2>=0.000
227→232	-0.17213	228→238	0.15794	230→239	0.34281
227→239	-0.12228	229→237	-0.31033	230→243	0.19815
228→231	-0.18606	229→240	0.21499		
Excited State 12:	Singlet-A	4.6581 eV	266.17 nm	f=0.0496	<S**2>=0.000
227→232	0.14731	228→238	0.18442	229→246	0.16398
227→235	-0.18415	229→237	0.26214	230→239	-0.13618
228→231	0.16914	229→240	0.23802	230→243	0.34635
Excited State 13:	Singlet-A	4.6950 eV	264.08 nm	f=0.0068	<S**2>=0.000
222→232	0.12802	227→234	-0.18660	229→238	0.19972
223→231	-0.12643	227→245	0.14966	229→244	0.17289
225→233	-0.14698	228→240	-0.22123	230→242	0.29857
226→235	0.15112	228→246	0.20526	230→245	0.18217
Excited State 14:	Singlet-A	4.7953 eV	258.55 nm	f=0.0000	<S**2>=0.000
222→231	0.14745	226→238	-0.15188	228→245	0.29144
223→232	-0.14903	227→240	-0.17530	229→243	0.24917
225→235	0.10975	228→242	0.11214	230→246	0.35442
Excited State 15:	Singlet-A	4.7973 eV	258.45 nm	f=0.0000	<S**2>=0.000
225→242	0.13454	227→244	-0.22471	229→245	-0.14689
227→238	-0.14819	229→242	0.37263	230→244	0.36173

Excited State 16:	Singlet-A	4.8205 eV	257.20 nm	f=0.1755	<S**2>=0.000
222→232	-0.10266	228→246	-0.19602	230→245	-0.29751
225→238	0.12408	229→244	0.34413		
227→242	-0.24621	230→242	0.20052		

*C.2.4.2 **OTPA-FLR-221**, **¹ES** State*

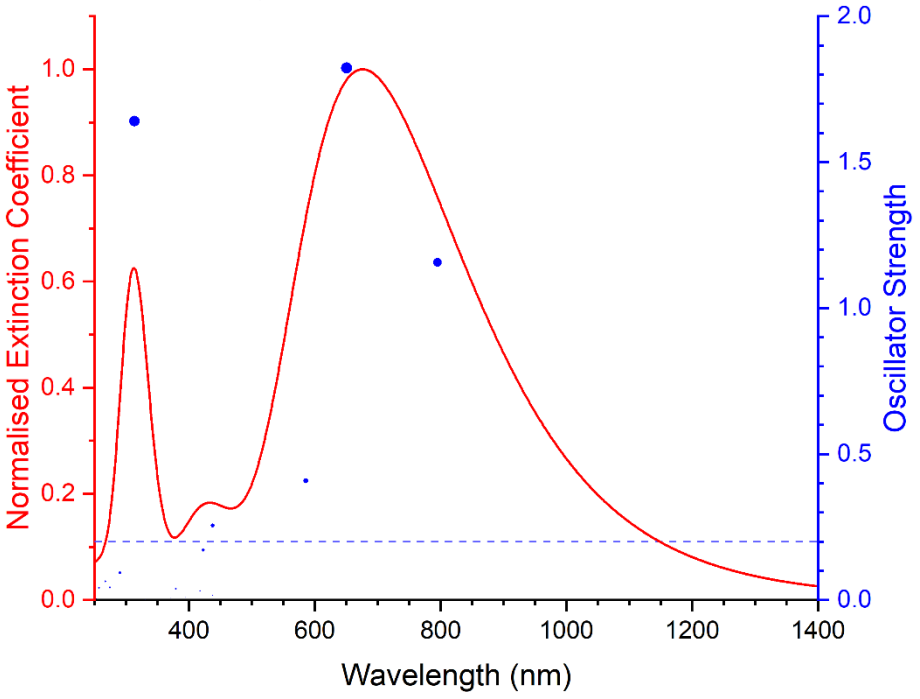

*Figure C-14 Excited states and normalised absorption spectra from TD-DFT calculations of **OTPA-FLR-221** in **¹ES** state. The areas of excited state dots are proportional to their oscillator strengths.*

Excited State 1:	Singlet-A	1.0477 eV	1183.36 nm	f=0.0000	<S**2>=0.000
226→230	0.18984	228→229	0.67583		

Excited State 2:	**Singlet-A**	**1.5592 eV**	**795.20 nm**	**f=1.1562**	**<S**2>=0.000**
226→229	0.23834	**228→230**	**0.67161**		

Excited State 3:	**Singlet-A**	**1.9058 eV**	**650.56 nm**	**f=1.8230**	**<S**2>=0.000**
225→230	0.13991	**227→229**	**0.68185**		

Excited State 4:	**Singlet-A**	**2.1162 eV**	**585.88 nm**	**f=0.4086**	**<S**2>=0.000**
224→230	0.19318	**226→229**	**0.63893**	228→230	-0.22602

Excited State 5:	Singlet-A	2.1641 eV	572.91 nm	f=0.0000	<S**2>=0.000				
225→229	0.15850		227→230	0.67626					
Excited State 6:	Singlet-A	2.3412 eV	529.59 nm	f=0.0000	<S**2>=0.000				
224→229	0.24613		226→230	0.63099		228→229	-0.18278		
Excited State 7:	Singlet-A	2.8098 eV	441.26 nm	f=0.0000	<S**2>=0.000				
214→229	0.12949		219→230	0.35251		225→229	0.22230		
215→230	-0.19004		221→230	0.15278					
216→229	0.28029		222→229	0.39430					
Excited State 8:	Singlet-A	2.8268 eV	438.61 nm	f=0.0000	<S**2>=0.000				
217→229	0.49292		224→229	-0.17817					
218→230	0.43930		226→230	0.10775					
Excited State 9:	Singlet-A	2.8297 eV	438.16 nm	f=0.0156	<S**2>=0.000				
217→230	0.42748		218→229	0.52409		224→230	-0.11928		
Excited State 10:	**Singlet-A**	**2.8308 eV**	**437.98 nm**	**f=0.2546**	**<S**2>=0.000**				
214→230	0.17505		216→230	0.28889		221→229	0.23213		
215→229	-0.29955		**219→229**	**0.36102**		222→230	0.31022		
Excited State 11:	Singlet-A	2.8639 eV	432.93 nm	f=0.0000	<S**2>=0.000				
214→229	-0.24102		221→230	-0.21533		227→230	-0.12938		
215→230	0.23787		222→229	-0.13455					
219→230	0.17717		225→229	0.50756					
Excited State 12:	Singlet-A	2.9329 eV	422.73 nm	f=0.1701	<S**2>=0.000				
214→230	-0.22395		219→229	0.34464		225→230	0.44498		
215→229	0.24521		221→229	-0.22373		227→229	-0.12143		

Excited State 13:	Singlet-A	2.9676 eV	417.80 nm	f=0.0305	<S**2>=0.000
220→230	-0.30082	223→229	0.61081		
Excited State 14:	Singlet-A	3.0295 eV	409.26 nm	f=0.0000	<S**2>=0.000
211→229	-0.11168	223→230	0.49115		
220→229	-0.41743	224→229	-0.21131		
Excited State 15:	Singlet-A	3.0870 eV	401.63 nm	f=0.0000	<S**2>=0.000
214→229	-0.31296	216→229	-0.21451	222→229	0.42026
215→230	0.33073	221→230	0.17038	225→229	-0.17715
Excited State 16:	Singlet-A	3.0952 eV	400.57 nm	f=0.0000	<S**2>=0.000
213→230	-0.16356	220→229	-0.14149	224→229	0.56689
217→229	0.20856	223→230	0.14607	226→230	-0.21451
Excited State 17:	Singlet-A	3.1398 eV	394.88 nm	f=0.0077	<S**2>=0.000
214→230	-0.25538	216→230	-0.14979	222→230	0.38199
215→229	0.34768	221→229	0.32100	225→230	-0.18178
Excited State 18:	Singlet-A	3.2669 eV	379.52 nm	f=0.0377	<S**2>=0.000
213→229	-0.21382	224→230	0.62150		
217→230	0.13396	226→229	-0.18484		
Excited State 19:	Singlet-A	3.3369 eV	371.56 nm	f=0.0071	<S**2>=0.000
211→230	0.45081	212→229	0.51403	223→229	0.14014
Excited State 20:	Singlet-A	3.3444 eV	370.72 nm	f=0.0000	<S**2>=0.000
211→229	0.50993	212→230	0.44621	223→230	0.15452
Excited State 21:	Singlet-A	3.6232 eV	342.19 nm	f=0.0016	<S**2>=0.000
216→230	-0.11085	221→229	0.48078	225→230	0.40716
219→229	-0.18122	222→230	-0.19699		

Excited State 22:	Singlet-A	3.6380 eV	340.80 nm	f=0.0000	<S**2>=0.000					
210→230	0.13272		219→230	0.30701		225→229	-0.31561			
214→229	-0.26619		221→230	-0.24715						
216→229	0.34399		222→229	-0.11399						
Excited State 23:	Singlet-A	3.6524 eV	339.46 nm	f=0.0000	<S**2>=0.000					
220→229	0.53160		223→230	0.45548						
Excited State 24:	Singlet-A	3.7310 eV	332.31 nm	f=0.0008	<S**2>=0.000					
220→230	0.62861		223→229	0.30598						
Excited State 25:	Singlet-A	3.7387 eV	331.62 nm	f=0.0000	<S**2>=0.000					
214→229	-0.14761		221→230	0.57546						
216→229	0.14357		222→229	-0.31210						
Excited State 26:	Singlet-A	3.7451 eV	331.05 nm	f=0.0018	<S**2>=0.000					
210→229	-0.13739		219→229	-0.24210		225→230	0.21823			
214→230	0.19341		221→229	-0.22478		227→229	-0.10571			
216→230	-0.25648		222→230	0.42992						
Excited State 27:	**Singlet-A**	**3.9548 eV**	**313.50 nm**	**f=1.6407**	**<S**2>=0.000**					
219→229	0.10530		227→233	0.19078						
226→232	0.21902		**228→231**	**0.61328**						
Excited State 28:	Singlet-A	4.2372 eV	292.61 nm	f=0.0000	<S**2>=0.000					
209→229	-0.17078		216→229	-0.23755		225→229	-0.14940			
210→230	-0.25941		219→230	0.40576		226→231	0.18189			
214→229	0.12434		222→229	-0.14150		228→232	0.26342			
Excited State 29:	Singlet-A	4.2654 eV	290.67 nm	f=0.0934	<S**2>=0.000					
209→230	0.18442		210→229	0.40045		214→230	-0.17110			

216→230	0.31704	222→230	0.13802		
219→229	-0.31374	225→230	0.14600		

Excited State 30: Singlet-A 4.2821 eV 289.54 nm f=0.0000 <S**2>=0.000

226→236	-0.11870	227→238	0.11948		
227→231	0.34126	228→233	0.54466		

Excited State 31: Singlet-A 4.2977 eV 288.49 nm f=0.0025 <S**2>=0.000

204→230	-0.10719	213→229	0.55485	218→229	0.23773
208→230	0.10761	217→230	-0.21073	224→230	0.22793

Excited State 32: Singlet-A 4.3733 eV 283.50 nm f=0.0000 <S**2>=0.000

214→229	-0.11808	219→230	-0.23084	228→232	0.45358
216→229	0.25965	226→231	0.32767		

Excited State 33: Singlet-A 4.3803 eV 283.05 nm f=0.0000 <S**2>=0.000

213→230	0.22175	218→230	0.50884		
217→229	-0.40464	224→229	0.12823		

Excited State 34: Singlet-A 4.4298 eV 279.89 nm f=0.0015 <S**2>=0.000

213→229	0.29989	217→230	0.49162	218→229	-0.39150

Excited State 35: Singlet-A 4.5196 eV 274.32 nm f=0.0000 <S**2>=0.000

204→229	-0.14338	213→230	0.57722	218→230	-0.17413
208→229	0.15897	217→229	0.20756	224→229	0.15341

Excited State 36: Singlet-A 4.5201 eV 274.30 nm f=0.0432 <S**2>=0.000

216→230	0.11705	227→239	0.12286	228→241	0.11577
226→235	0.30329	228→234	0.53990		

Excited State 37: Singlet-A 4.5735 eV 271.09 nm f=0.0000 <S**2>=0.000

224→235	0.10541	226→234	0.34713	228→235	0.54559

Excited State 38:	Singlet-A	4.6356 eV	267.46 nm	f=0.0632	<S**2>=0.000			
209→230	-0.27005		215→229	0.21000		219→229	-0.18537	
210→229	-0.34175		216→230	0.42344				
Excited State 39:	Singlet-A	4.6809 eV	264.87 nm	f=0.0000	<S**2>=0.000			
209→229	0.38641		215→230	-0.22663		219→230	0.14015	
210→230	0.35949		216→229	-0.27766		228→232	0.12576	
Excited State 40:	Singlet-A	4.7416 eV	261.48 nm	f=0.0000	<S**2>=0.000			
220→233	0.11749		227→234	-0.19956		228→239	-0.34324	
221→231	0.11882		227→238	-0.11997		228→243	0.10678	
226→236	-0.11889		227→241	-0.20996				
226→240	-0.13306		228→237	0.37376				
Excited State 41:	Singlet-A	4.8197 eV	257.24 nm	f=0.0415	<S**2>=0.000			
222→231	-0.12133		227→232	-0.13061		228→240	0.16100	
226→233	-0.27981		227→235	0.15714		228→245	0.15589	
226→237	-0.18843		228→236	0.46304				
Excited State 42:	Singlet-A	4.8559 eV	255.33 nm	f=0.0053	<S**2>=0.000			
214→230	0.36445		227→237	-0.13972		228→238	0.26429	
215→229	0.28853		227→239	0.11142		228→241	0.20778	
226→232	-0.13761		227→243	-0.11880				
Excited State 43:	Singlet-A	4.8638 eV	254.91 nm	f=0.0000	<S**2>=0.000			
209→229	0.22188		214→229	0.42375				
210→230	0.12228		215→230	0.47549				
Excited State 44:	Singlet-A	4.8947 eV	253.30 nm	f=0.0047	<S**2>=0.000			
209→230	0.15290		210→229	0.14812		214→230	0.35040	

215→229	0.29792	227→239	-0.11774	228→241	-0.21341
226→232	0.12009	227→243	0.11364		
227→237	0.10939	228→238	-0.21394		

*C.2.4.3 **OTPA-FLR-221**, **^{5}ES** State*

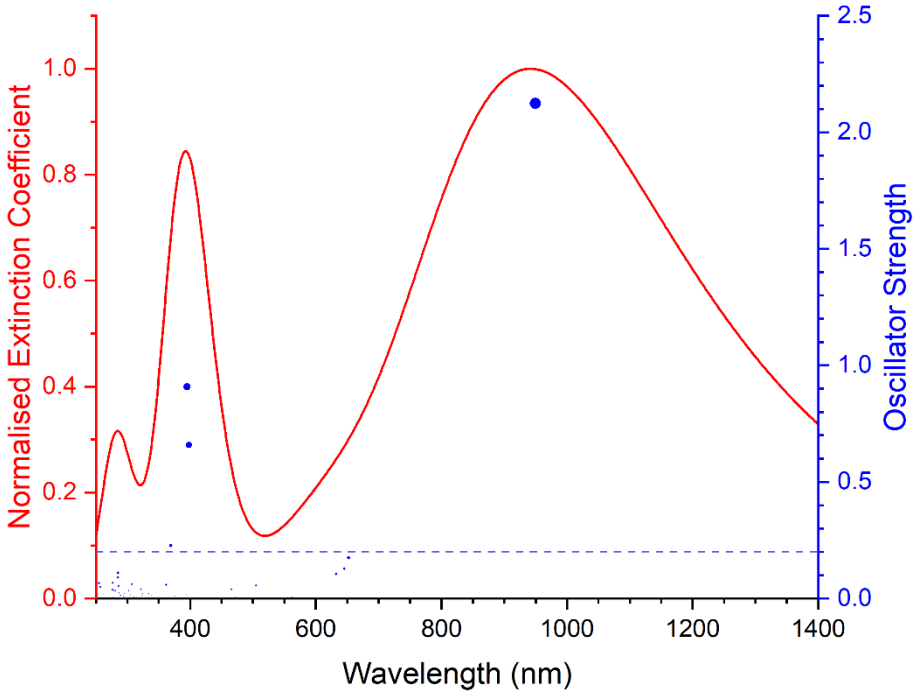

*Figure C-15 Excited states and normalised absorption spectra from TD-DFT calculations of **OTPA-FLR-221** in **^{5}ES** state. The areas of excited state dots are proportional to their oscillator strengths.*

Excited State 1:	5.051-A	0.9944 eV	1246.81 nm	f=0.0075	<S**2>=6.129
223B→228B	-0.19010	226B→227B	0.83808	226B←227B	0.11535
225B→228B	-0.10821	226B→230B	-0.18953		
225B→229B	-0.43373	225B←229B	-0.10873		
Excited State 2:	**5.050-A**	**1.3054 eV**	**949.81 nm**	**f=2.1238**	**<S**2>=6.124**
222B→230B	-0.13238	**225B→227B**	**0.73170**	226B→228B	-0.13607
224B→228B	-0.20981	225B→230B	-0.17593	**226B→229B**	**-0.55186**
Excited State 3:	5.064-A	1.9007 eV	652.32 nm	f=0.1738	<S**2>=6.162
213B→228B	0.11155	222B→228B	0.21474	224B→227B	0.45132
218B→228B	-0.10192	223B→227B	-0.29406	224B→230B	0.21254
221B→228B	-0.10822	223B→230B	-0.11439	225B→228B	-0.42966

225B→229B	0.13392	226B→228B	0.48300	226B→229B	-0.21333

Excited State 4:	5.061-A	1.9208 eV	645.49 nm	f=0.1273	<S**2>=6.153
218B→228B	0.10671	224B→227B	-0.35210	225B→229B	-0.11942
222B→227B	0.12308	224B→228B	0.20408	225B→230B	-0.20365
222B→228B	-0.21291	224B→230B	-0.16913	226B→228B	0.37784
223B→227B	-0.32990	225B→227B	-0.17984	226B→229B	-0.35492
223B→230B	-0.13591	225B→228B	0.39766		

Excited State 5:	5.054-A	1.9612 eV	632.20 nm	f=0.1057	<S**2>=6.136
218B→227B	0.10676	224B→228B	-0.36001	226B→228B	0.43889
222B→227B	-0.25985	225B→227B	0.34508	226B→229B	0.39899
223B→227B	-0.23648	225B→228B	0.12984		
223B→230B	-0.10456	225B→230B	0.34496		

Excited State 6:	5.052-A	2.0718 eV	598.45 nm	f=0.0006	<S**2>=6.131
211B→227B	0.12475	221B→230B	-0.11826	225B→229B	0.51097
213B→227B	0.15312	222B→229B	0.10246	226B→227B	0.32714
220B→228B	-0.14758	223B→228B	-0.34336	226B→230B	0.50819
221B→227B	-0.26381	225B→228B	0.15583		

Excited State 7:	5.073-A	2.1888 eV	566.46 nm	f=0.0005	<S**2>=6.185
215B→229B	-0.10447	218B→230B	-0.32006	221B→227B	0.18166
218B→227B	0.54471	219B→227B	-0.20335	222B→227B	0.21603
218B→228B	0.11386	219B→229B	-0.21115	222B→229B	0.17572
218B→229B	0.49616	219B→230B	0.13986		

Excited State 8:	5.063-A	2.2032 eV	562.74 nm	f=0.0060	<S**2>=6.159
213B→228B	0.10741	220B→228B	-0.41596	221B→228B	0.40632
218B→227B	0.14477	220B→230B	0.28480	221B→230B	-0.14778
220B→227B	0.52566	221B→227B	-0.26540	225B→229B	-0.14367

226B→227B	-0.10990	226B→228B	0.16930	226B→230B	-0.11165

Excited State 9:	5.066-A	2.2139 eV	560.03 nm	f=0.0035	<S**2>=6.166
213B→227B	0.10163	220B→227B	0.30564	221B→230B	0.20003
218B→227B	-0.14716	220B→228B	0.32685	222B→229B	0.10550
219B→227B	-0.15611	220B→230B	0.16780	225B→229B	0.13793
219B→228B	0.13487	221B→227B	0.47281	226B→227B	0.11918
219B→229B	0.27283	221B→228B	0.36511	226B→228B	0.11520
219B→230B	0.20170	221B→229B	-0.15774	226B→230B	0.11053

Excited State 10:	5.071-A	2.2185 eV	558.87 nm	f=0.0009	<S**2>=6.178
218B→229B	-0.19343	220B→227B	0.13295	221B→230B	0.21421
219B→227B	0.52829	220B→228B	0.22542	222B→227B	0.18350
219B→229B	-0.48740	221B→227B	0.16162	222B→229B	-0.17455
219B→230B	-0.26800	221B→228B	0.19327	225B→229B	0.10619

Excited State 11:	5.081-A	2.4212 eV	512.08 nm	f=0.0007	<S**2>=6.203
212B→227B	0.12130	215B→227B	-0.16304	217B→227B	0.29620
212B→229B	0.14642	215B→229B	-0.13961	217B→229B	0.16509
214B→227B	0.40325	216B→227B	0.34754	224B→227B	-0.10249
214B→229B	0.36304	216B→229B	0.36276		
214B→230B	-0.27170	216B→230B	-0.18859		

Excited State 12:	5.082-A	2.4486 eV	506.35 nm	f=0.0009	<S**2>=6.206
212B→227B	0.11832	214B→230B	0.20688	216B→230B	-0.27088
212B→229B	-0.11654	215B→227B	-0.12134	217B→227B	-0.25656
214B→227B	-0.25397	216B→227B	0.43010	217B→229B	0.24333
214B→229B	0.39429	216B→229B	-0.39841		

Excited State 13:	5.066-A	2.4548 eV	505.07 nm	f=0.0553	<S**2>=6.166
210B→228B	0.11964	214B→228B	0.11451	217B→228B	-0.20811

218B→227B	-0.17898	224B→228B	0.36239	226B→229B	0.41001
222B→227B	0.49302	225B→227B	0.44744		
222B→230B	0.19521	225B→230B	-0.10568		

Excited State 14: 5.076-A 2.5787 eV 480.79 nm f=0.0003 <S**2>=6.191

214B→227B	0.33929	216B→229B	0.12196	223B→229B	-0.12059
215B→228B	0.29301	217B→227B	-0.36057	224B→227B	0.31867
215B→229B	-0.11174	217B→230B	-0.26780	225B→228B	0.44264
216B→228B	0.13247	222B→228B	0.38477		

Excited State 15: 5.091-A 2.6265 eV 472.05 nm f=0.0062 <S**2>=6.229

208B→230B	0.11040	217B→227B	-0.19452	224B→227B	-0.14977
210B→229B	0.18179	217B→229B	-0.10251	224B→229B	-0.30465
213B→228B	-0.15240	220B→227B	-0.16660	226B→228B	0.42768
215B→228B	0.14592	223B→227B	0.58230	226B→229B	-0.10618
216B→227B	-0.11757	223B→230B	-0.18837		

Excited State 16: 5.079-A 2.6610 eV 465.94 nm f=0.0394 <S**2>=6.200

210B→228B	-0.11408	217B→228B	-0.50484	225B→227B	-0.18308
214B→228B	0.20003	217B→229B	0.11166	225B→230B	0.20421
215B→227B	0.56599	222B→227B	0.13393	226B→229B	-0.20325
215B→230B	0.22496	222B→230B	0.10443		
216B→227B	0.20453	224B→228B	-0.10250		

Excited State 17: 5.090-A 2.6924 eV 460.51 nm f=0.0015 <S**2>=6.228

210B→230B	0.18079	223B→227B	0.22378	225B→228B	0.41149
214B→227B	-0.13071	223B→228B	-0.10531	225B→229B	-0.10803
215B→228B	-0.31710	223B→229B	-0.37842	226B→228B	0.14564
216B→228B	-0.10296	224B→227B	0.32969		
217B→227B	0.39355	224B→230B	-0.12924		

Excited State 18:	5.069-A	2.7085 eV	457.77 nm	f=0.0004	<S**2>=6.173	
211B→227B	-0.11059	220B→228B	-0.12479	225B→229B	0.57466	
213B→227B	-0.27855	223B→228B	0.37365	226B→227B	0.34956	
213B→230B	-0.15060	225B→228B	0.11253	226B→230B	-0.41826	

Excited State 19:	5.086-A	2.8784 eV	430.74 nm	f=0.0026	<S**2>=6.216	
211B→227B	0.28558	212B→230B	0.19812	216B→228B	-0.17081	
211B→228B	0.27007	213B→227B	-0.28638	216B→230B	-0.12052	
211B→230B	0.13270	213B→228B	-0.27729	226B→230B	0.12091	
212B→227B	0.49300	213B→230B	-0.11363			
212B→228B	0.38730	216B→227B	-0.17774			

Excited State 20:	5.086-A	2.8841 eV	429.89 nm	f=0.0021	<S**2>=6.217	
211B→227B	-0.35855	212B→228B	-0.36006	213B→230B	0.14048	
211B→228B	0.30461	212B→230B	0.15159	216B→227B	-0.13726	
211B→230B	-0.15941	213B→227B	0.36174	216B→228B	0.15818	
212B→227B	0.39277	213B→228B	-0.31001	226B→230B	-0.14230	

Excited State 21:	5.216-A	3.0028 eV	412.89 nm	f=0.0070	<S**2>=6.551	
226A→236A	-0.10367	227A→238A	-0.14402	229A→232A	-0.48969	
226A→247A	-0.10881	228A→233A	0.29228	230A→231A	0.63080	

Excited State 22:	5.132-A	3.0264 eV	409.67 nm	f=0.0001	<S**2>=6.333	
226A→231A	-0.12307	216B→228B	-0.10921	223B→229B	0.48263	
208B→229B	-0.11907	217B→230B	0.12619	224B→230B	0.30639	
209B→228B	0.13537	218B→228B	-0.16266	225B→228B	0.31865	
210B→227B	0.40528	220B→229B	-0.10882	225B→232B	-0.11258	
215B→228B	-0.24273	222B→228B	0.23978	226B→231B	0.13853	

Excited State 23:	**5.140-A**	**3.1138 eV**	**398.18 nm**	**f=0.6587**	**<S**2>=6.354**
226A→233A	-0.13750	209B→227B	0.12110	222B→227B	0.14722
229A→231A	**0.36194**	210B→228B	0.18687	**225B→230B**	**0.60946**
230A→232A	**-0.35849**	215B→227B	-0.13627	226B→229B	-0.20128

Excited State 24:	**5.132-A**	**3.1390 eV**	**394.97 nm**	**f=0.9074**	**<S**2>=6.334**
226A→233A	0.11909	**230A→232A**	**0.44755**	222B→227B	0.17587
227A→232A	0.10349	210B→228B	0.17226	**225B→230B**	**0.48057**
228A→236A	-0.10355	215B→227B	-0.12244	226B→229B	-0.24335
229A→231A	**-0.43220**	218B→227B	-0.14299		

Excited State 25:	5.129-A	3.1412 eV	394.70 nm	f=0.0185	<S**2>=6.327
227A→231A	0.11924	208B→228B	0.13668	223B→228B	0.23606
229A→232A	-0.16906	211B→227B	-0.38320	225B→229B	-0.17155
230A→231A	0.10029	213B→227B	-0.30228	226B→227B	0.12127
230A→238A	-0.11772	222B→229B	-0.14620	226B→230B	0.61307

Excited State 26:	5.146-A	3.2978 eV	375.96 nm	f=0.0088	<S**2>=6.369
227A→233A	0.11221	210B→229B	-0.21975	223B→230B	0.42168
228A→238A	-0.14042	211B→228B	-0.28449	224B→229B	0.39935
230A→233A	-0.15097	213B→228B	-0.23026	226B→228B	0.31349
208B→227B	0.29533	220B→230B	-0.11522		

Excited State 27:	**5.361-A**	**3.3568 eV**	**369.35 nm**	**f=0.2266**	**<S**2>=6.936**
214A→242A	0.10630	228A→238A	0.19700	223B→227B	0.28148
226A→232A	0.18012	229A→235A	-0.10747	223B→230B	0.10737
226A→248A	-0.10253	229A→236A	0.12622	224B→229B	0.26087
227A→233A	-0.15736	**230A→233A**	**0.40646**	225B→231B	0.13262
228A→231A	**0.35950**	211B→228B	-0.14486	226B→232B	-0.12661

Excited State 28:	5.273-A	3.4253 eV	361.96 nm	f=0.0584	<S**2>=6.702				
218A→231A	-0.12517	209B→227B	-0.23667	223B→231B	0.16642				
226A→233A	0.12351	210B→228B	-0.11461	224B→228B	-0.26707				
227A→232A	-0.13049	211B→229B	0.30202	224B→232B	-0.13683				
229A→231A	0.12811	213B→229B	0.25840	225B→227B	-0.14892				
229A→238A	-0.16615	218B→227B	-0.11228	225B→230B	0.11263				
230A→232A	-0.13099	218B→230B	0.12512	226B→233B	-0.12004				
230A→237A	0.10567	222B→227B	0.26109						
230A→248A	-0.12383	222B→230B	-0.27212						

Excited State 29:	5.483-A	3.4958 eV	354.67 nm	f=0.0006	<S**2>=7.265				
213A→235A	-0.10482	228A→232A	0.21176	208B→229B	-0.14734				
214A→234A	-0.11823	228A→237A	0.16072	210B→227B	0.15473				
218A→233A	-0.15956	228A→239A	0.15723	212B→235B	-0.11910				
219A→242A	-0.14151	228A→248A	-0.13673	217B→241B	-0.11711				
220A→241A	0.11083	229A→233A	-0.24857	223B→233B	0.19070				
226A→231A	0.20594	230A→235A	0.19690	224B→227B	-0.22118				
226A→238A	0.11965	230A→236A	-0.22254	224B→230B	0.11086				
227A→235A	-0.10099	230A→247A	-0.10675	226B→231B	-0.18887				
227A→236A	0.11504	207B→227B	-0.10847						

Excited State 30:	5.141-A	3.5386 eV	350.38 nm	f=0.0003	<S**2>=6.358				
227A→231A	-0.12978	213B→230B	-0.19952	223B→229B	-0.11520				
228A→233A	0.12778	218B→229B	-0.15064	224B→231B	-0.10150				
229A→232A	0.16577	220B→228B	-0.11753	225B→229B	-0.21662				
230A→238A	0.17041	222B→228B	0.10971	226B→227B	0.14436				
209B→229B	-0.13172	222B→229B	0.43240	226B→230B	0.17636				
211B→230B	-0.26599	223B→228B	0.45104						

Excited State 31:	5.106-A	3.6160 eV	342.88 nm	f=0.0007	<S**2>=6.268				
207B→227B	-0.12824	214B→230B	-0.12467	223B→229B	0.47455				
209B→228B	-0.17422	217B→227B	-0.11965	224B→227B	0.47481				
210B→227B	-0.16602	217B→230B	0.18958	224B→230B	-0.19832				
210B→230B	-0.14949	222B→228B	-0.31264	225B→228B	0.13020				
212B→229B	0.16991	223B→228B	0.14425						

Excited State 32:	5.201-A	3.6660 eV	338.20 nm	f=0.0129	<S**2>=6.513				
226A→233A	-0.12234	209B→230B	0.13932	223B→231B	-0.11434				
228A→236A	0.11255	210B→228B	0.17947	224B→228B	-0.39393				
229A→238A	0.10257	211B→229B	0.16773	225B→227B	-0.15699				
230A→237A	-0.10685	217B→228B	0.10685	225B→230B	-0.19088				
230A→248A	0.10427	218B→227B	-0.16785	226B→233B	0.10419				
207B→228B	0.13578	222B→227B	0.42499						
209B→227B	0.12753	222B→230B	-0.25566						

Excited State 33:	5.109-A	3.7061 eV	334.54 nm	f=0.0193	<S**2>=6.275				
228A→231A	-0.11753	213B→228B	0.24840	221B→228B	-0.12496				
230A→233A	-0.14680	214B→229B	0.21658	223B→227B	0.19261				
212B→227B	0.18521	217B→228B	-0.11170	223B→230B	-0.24451				
212B→230B	-0.21006	217B→229B	-0.40816	224B→229B	0.54754				

Excited State 34:	5.190-A	3.7383 eV	331.66 nm	f=0.0004	<S**2>=6.484				
227A→231A	0.16197	213B→227B	0.42822	219B→229B	-0.14346				
228A→233A	-0.22381	213B→230B	-0.20410	221B→227B	-0.12077				
229A→232A	-0.14147	215B→229B	-0.22400	221B→230B	0.11843				
230A→238A	-0.21462	216B→228B	-0.12776	223B→228B	0.15631				
209B→229B	-0.14930	218B→229B	-0.19070						
211B→227B	0.25132	219B→227B	-0.22748						

Excited State 35:	5.142-A	3.7563 eV	330.07 nm	f=0.0015	<S**2>=6.361	
227A→231A	0.12081	230A→240A	0.10019	216B→228B	0.16911	
228A→233A	-0.18415	211B→227B	0.24524	219B→227B	0.35638	
229A→232A	-0.10919	211B→230B	-0.11578	219B→229B	0.12048	
230A→234A	-0.12905	213B→230B	0.12997	222B→228B	0.12775	
230A→238A	-0.12309	215B→229B	0.25374	222B→229B	0.53524	

Excited State 36:	5.101-A	3.7855 eV	327.53 nm	f=0.0004	<S**2>=6.255	
207B→227B	0.15086	215B→227B	-0.14476	219B→230B	0.10326	
209B→228B	0.20906	215B→228B	-0.13424	220B→229B	0.11529	
210B→227B	0.20526	216B→229B	-0.12282	221B→227B	-0.10379	
210B→230B	0.10546	217B→227B	-0.25781	222B→227B	0.14514	
212B→228B	0.12713	217B→230B	0.22603	222B→228B	-0.18291	
212B→229B	0.19679	218B→227B	0.18459	223B→229B	-0.10542	
214B→227B	0.21385	219B→227B	0.33973	224B→230B	-0.19787	
214B→228B	-0.13664	219B→229B	0.29689	225B→228B	-0.10814	

Excited State 37:	5.106-A	3.7953 eV	326.68 nm	f=0.0047	<S**2>=6.267	
207B→227B	-0.10818	215B→229B	-0.18243	219B→229B	0.31379	
209B→228B	-0.15273	215B→230B	0.11610	221B→227B	-0.10046	
210B→227B	-0.14846	217B→227B	0.21246	221B→229B	-0.19531	
212B→229B	-0.18166	217B→228B	-0.16593	222B→227B	0.11273	
213B→229B	0.17988	217B→230B	-0.15469	222B→228B	0.11587	
214B→227B	-0.19280	218B→227B	0.24585	222B→229B	-0.16883	
214B→228B	-0.10566	218B→230B	0.12003	222B→230B	0.12979	
215B→227B	-0.29875	219B→227B	0.25225	224B→230B	0.14528	

Excited State 38:	5.093-A	3.8152 eV	324.97 nm	f=0.0209	<S**2>=6.236	
209B→230B	0.10576	214B→228B	0.20637	215B→229B	0.16473	
213B→229B	0.42393	215B→227B	-0.26797	215B→230B	0.33666	

216B→230B	0.12695	218B→229B	0.16419	222B→227B	-0.22320
217B→228B	-0.23897	219B→229B	-0.18692	222B→229B	0.16142
218B→227B	-0.29408	221B→229B	-0.15574	222B→230B	0.13469

Excited State 39: 5.169-A 3.8386 eV 322.99 nm f=0.0131 <S**2>=6.429

222A→244A	-0.10674	213B→230B	-0.12945	219B→227B	0.33087
227A→239A	-0.11724	214B→228B	0.11162	219B→230B	0.10527
228A→235A	0.14597	215B→227B	0.13386	220B→244B	0.10094
229A→237A	-0.10255	215B→229B	-0.25528	221B→227B	-0.17865
230A→234A	0.13275	216B→229B	-0.12049	221B→243B	0.10453
209B→227B	0.12394	218B→227B	-0.29928	222B→227B	-0.10318
211B→230B	0.11276	218B→229B	0.39330	224B→228B	-0.12292
212B→228B	0.18775	218B→230B	-0.13605		

Excited State 40: 5.311-A 3.8528 eV 321.80 nm f=0.0397 <S**2>=6.803

221A→243A	0.12822	227A→248A	-0.10607	215B→229B	0.14187
221A→246A	0.11537	228A→235A	0.11278	217B→228B	-0.13752
222A→244A	-0.17583	228A→236A	-0.18522	218B→227B	0.31566
225A→235A	0.11736	230A→239A	0.14533	218B→229B	-0.24807
225A→236A	-0.11800	207B→228B	0.13471	220B→244B	0.16344
225A→247A	0.10399	209B→227B	0.15962	221B→229B	-0.10448
227A→232A	-0.10911	209B→230B	0.10522	221B→243B	0.17323
227A→237A	-0.12346	210B→228B	0.14510	224B→228B	-0.20070
227A→239A	-0.15942	213B→229B	0.11153	224B→239B	0.10508

Excited State 41: 5.504-A 3.9100 eV 317.09 nm f=0.0006 <S**2>=7.322

221A→244A	-0.27117	225A→237A	-0.10140	228A→232A	-0.13025
222A→243A	0.22274	225A→239A	-0.16637	228A→237A	-0.11583
222A→246A	0.18098	227A→235A	0.13648	228A→239A	-0.15404
223A→244A	-0.10983	227A→236A	-0.15436	230A→235A	-0.10260

230A→236A	0.11211	210B→227B	0.30170	223B→229B	-0.19262
208B→229B	-0.11370	220B→243B	-0.25646	224B→236B	-0.14467
209B→228B	0.11677	221B→244B	-0.24281		

Excited State 42: 5.083-A 3.9336 eV 315.20 nm f=0.0068 <S**2>=6.209

212B→227B	0.25765	215B→227B	-0.11415	217B→227B	-0.16015
213B→228B	-0.13081	215B→228B	-0.11872	217B→229B	-0.36372
214B→227B	-0.18942	216B→227B	0.35556	219B→228B	0.54496
214B→229B	-0.12321	216B→229B	0.14639	223B→227B	-0.13785
214B→230B	-0.10014	216B→230B	0.17233	224B→229B	-0.18978

Excited State 43: 5.088-A 3.9568 eV 313.34 nm f=0.0029 <S**2>=6.222

212B→227B	-0.12860	215B→228B	-0.24633	218B→228B	0.58033
212B→229B	0.14451	216B→229B	0.27627	222B→228B	0.17329
214B→227B	-0.36214	217B→227B	-0.24146	224B→229B	0.12683
214B→230B	-0.24045	217B→229B	0.20551		

Excited State 44: 5.230-A 3.9849 eV 311.14 nm f=0.0061 <S**2>=6.589

229A→249A	-0.10368	212B→230B	-0.19432	223B→227B	-0.17722
230A→235A	-0.11939	214B→229B	0.27056	223B→229B	-0.13142
230A→250A	0.10219	215B→228B	-0.12489	224B→227B	-0.11721
207B→227B	-0.11889	216B→227B	-0.20705	224B→229B	-0.20438
209B→228B	-0.16687	217B→227B	-0.12039	224B→230B	0.10830
210B→227B	-0.11044	217B→229B	-0.24167	225B→232B	-0.11810
211B→228B	-0.22936	217B→230B	0.12944	226B→231B	0.10096
212B→229B	0.12211	219B→228B	-0.26761		

Excited State 45: 5.291-A 3.9938 eV 310.44 nm f=0.0027 <S**2>=6.750

226A→231A	-0.13870	230A→250A	0.12308	209B→228B	-0.18906
229A→249A	-0.14251	207B→227B	-0.14637	210B→227B	-0.11117

211B→228B	0.17697	217B→227B	-0.12692	223B→229B	-0.14143
212B→229B	0.11888	217B→229B	0.24345	224B→227B	-0.15322
212B→230B	0.15237	217B→230B	0.17300	224B→229B	0.19310
214B→227B	0.10090	218B→228B	-0.23151	224B→230B	0.12949
214B→229B	-0.22734	219B→228B	0.10506	225B→232B	-0.14883
216B→227B	0.11384	223B→227B	0.11997	226B→231B	0.14051

Excited State 46: 5.153-A 4.0339 eV 307.36 nm f=0.0091 <S**2>=6.389

226A→241A	0.14832	229A→239A	0.26149	218B→229B	-0.13381
227A→240A	0.14187	230A→234A	0.48341	219B→227B	-0.13219
228A→235A	0.15971	230A→237A	-0.11740	221B→227B	0.13669
228A→236A	0.13894	230A→240A	0.29480		
229A→237A	-0.42025	209B→227B	-0.13913		

Excited State 47: 5.321-A 4.0374 eV 307.09 nm f=0.0608 <S**2>=6.828

221A→243A	-0.14117	230A→234A	0.18976	213B→229B	-0.11076
221A→246A	-0.12334	230A→237A	0.18333	218B→227B	0.14195
222A→244A	0.19680	207B→228B	0.20068	218B→229B	-0.11393
229A→234A	-0.19014	209B→227B	0.38833	220B→244B	-0.15901
229A→237A	-0.14969	210B→228B	0.25369	221B→243B	-0.16381
229A→239A	0.10323	211B→229B	-0.10140	225B→230B	-0.14351

Excited State 48: 5.176-A 4.0583 eV 305.50 nm f=0.0188 <S**2>=6.446

227A→237A	0.14006	230A→237A	0.44979	217B→228B	0.11485
228A→241A	0.14645	230A→239A	-0.30528	219B→229B	0.11330
229A→234A	-0.40446	209B→227B	-0.16396	222B→227B	0.12301
229A→240A	-0.35400	210B→228B	-0.12989		

Excited State 49: 5.236-A 4.0751 eV 304.25 nm f=0.0120 <S**2>=6.605

228A→231A	0.11049	207B→229B	0.16721	208B→227B	0.20189

208B→229B	0.11621	220B→227B	0.28416	224B→227B	-0.13908
208B→230B	-0.17244	220B→230B	-0.13167	224B→229B	-0.20802
210B→227B	-0.12015	221B→228B	-0.25956	224B→230B	0.10150
210B→229B	-0.24536	222B→228B	0.12541	226B→231B	-0.10406
212B→229B	0.11638	223B→227B	0.21535		
213B→228B	0.15019	223B→230B	-0.19681		

Excited State 50: 5.255-A 4.0891 eV 303.21 nm f=0.0022 <S**2>=6.653

225A→232A	-0.11273	210B→227B	-0.21095	223B→227B	-0.13035
226A→231A	0.13061	210B→229B	0.14334	223B→229B	0.23362
228A→232A	0.11673	210B→230B	0.15989	223B→230B	0.16395
229A→249A	0.11347	212B→229B	0.20259	224B→227B	-0.19030
230A→250A	-0.10316	215B→228B	-0.13170	224B→230B	0.14675
207B→227B	0.12098	220B→227B	-0.14913	225B→232B	0.16738
207B→230B	-0.12040	220B→229B	0.13632	226B→231B	-0.17799
208B→229B	0.25147	221B→228B	0.13860		
208B→230B	0.10654	222B→228B	0.21452		

Excited State 51: 5.477-A 4.1057 eV 301.98 nm f=0.0329 <S**2>=7.250

219A→234A	-0.13056	228A→238A	-0.19496	216B→245B	0.11513
223A→237A	-0.11478	229A→241A	-0.15899	218B→238B	-0.10895
224A→237A	-0.10992	229A→250A	0.14320	219B→237B	-0.14206
224A→240A	0.15430	230A→235A	0.18911	223B→230B	-0.20247
225A→231A	-0.10815	230A→236A	0.16909	224B→229B	0.24480
226A→232A	0.12475	230A→243A	0.10508	225B→231B	0.15347
227A→233A	0.10728	230A→249A	-0.15987	226B→232B	-0.12831
228A→234A	0.13746	214B→246B	-0.11080		

Excited State 52: 5.370-A 4.1871 eV 296.11 nm f=0.0007 <S**2>=6.959

214A→234A	0.10910	215A→241A	0.12661	216A→243A	-0.10057

224A→237A	0.13754	216B→246B	-0.11574	221B→227B	0.16249
207B→227B	-0.19989	217B→227B	-0.15238	223B→228B	-0.11663
209B→228B	-0.19529	217B→230B	0.15881	223B→229B	-0.26460
210B→227B	-0.11272	218B→237B	0.11192	224B→230B	0.28839
210B→230B	-0.10326	219B→238B	0.12978	225B→228B	0.12871
215B→228B	-0.14220	220B→228B	-0.11209		

Excited State 53: 5.095-A 4.1903 eV 295.89 nm f=0.0002 <S**2>=6.239

213B→230B	-0.12432	219B→227B	0.16987	221B→230B	-0.30266
215B→229B	-0.25911	220B→228B	-0.43862	223B→228B	-0.12360
216B→229B	-0.10524	221B→227B	0.63035	223B→229B	0.10616

Excited State 54: 5.261-A 4.1992 eV 295.26 nm f=0.0196 <S**2>=6.670

226A→237A	0.14031	230A→233A	0.14562	216B→227B	-0.21200
226A→242A	-0.11594	230A→235A	0.33227	217B→229B	-0.11867
227A→235A	-0.11901	230A→236A	0.28927	223B→230B	0.12651
228A→234A	0.38656	211B→228B	-0.13144	225B→231B	-0.14971
229A→241A	-0.21889	214B→229B	0.23989	226B→232B	0.13483

Excited State 55: 5.166-A 4.2148 eV 294.16 nm f=0.0088 <S**2>=6.422

207B→229B	-0.11288	214B→227B	0.11752	220B→227B	0.53273
208B→227B	-0.13145	216B→229B	-0.13492	220B→230B	-0.27401
208B→230B	0.11149	217B→227B	0.12859	221B→228B	-0.37467
210B→229B	0.11851	217B→229B	0.22338	223B→230B	0.10466
213B→228B	-0.13344	219B→228B	0.14403		

Excited State 56: 5.136-A 4.2310 eV 293.04 nm f=0.0004 <S**2>=6.345

230A→241A	0.15615	216B→228B	0.16756	218B→228B	-0.21490
214B→227B	-0.27366	216B→229B	0.34711	219B→228B	-0.34684
216B→227B	0.16881	217B→227B	-0.28661	220B→227B	0.29453

220B→230B	-0.16318	221B→228B	-0.15544	222B→228B	-0.22773

Excited State 57:	5.165-A	4.2397 eV	292.44 nm	f=0.0022	<S**2>=6.418
227A→234A	-0.13663	208B→228B	0.10091	219B→230B	-0.10617
228A→235A	0.18275	211B→227B	-0.28717	220B→228B	0.13696
228A→236A	0.14114	211B→229B	-0.11933	221B→230B	0.10775
229A→242A	0.12866	213B→227B	-0.16286	222B→229B	0.39068
230A→234A	0.13641	215B→229B	-0.23856	223B→228B	-0.28144
230A→238A	-0.13175	216B→228B	-0.22062		
230A→240A	-0.20619	219B→228B	-0.10021		

Excited State 58:	5.103-A	4.2722 eV	290.21 nm	f=0.0022	<S**2>=6.261
214B→227B	-0.13594	216B→227B	-0.43604	218B→228B	-0.31981
214B→228B	0.13512	216B→229B	0.14552	219B→228B	0.45719
214B→229B	0.33804	217B→227B	-0.12700	220B→227B	-0.10234
215B→227B	0.18405	217B→229B	0.27620	220B→229B	-0.10581

Excited State 59:	5.165-A	4.2810 eV	289.62 nm	f=0.0143	<S**2>=6.420
226A→245A	0.10288	230A→240A	-0.24319	215B→229B	0.13837
227A→234A	-0.17797	203B→227B	-0.10862	218B→227B	0.11789
228A→235A	0.23301	207B→228B	0.10374	218B→229B	0.10435
228A→236A	0.23183	209B→230B	0.11141	221B→229B	-0.11053
229A→237A	0.12084	211B→227B	0.20228	222B→227B	-0.16933
229A→242A	0.17512	211B→229B	0.32072	223B→228B	0.16233
230A→234A	0.18767	213B→229B	0.15939	224B→228B	0.22802
230A→238A	-0.23582	215B→227B	0.15273		

Excited State 60:	5.157-A	4.2920 eV	288.87 nm	f=0.0119	<S**2>=6.399
227A→234A	0.10670	228A→236A	-0.12463	230A→234A	-0.10164
228A→235A	-0.16893	229A→242A	-0.11293	230A→238A	0.17790

230A→240A	0.12864	213B→229B	0.18987	222B→227B	-0.17579
203B→227B	-0.13946	213B→230B	-0.10340	222B→229B	0.13135
207B→228B	0.13853	215B→227B	0.17101	223B→228B	-0.18841
209B→230B	0.12667	215B→229B	-0.19490	224B→228B	0.29464
211B→227B	-0.23062	218B→227B	0.14702		
211B→229B	0.35360	221B→229B	-0.16142		

Excited State 61: 5.527-A 4.3113 eV 287.58 nm f=0.0036 <S**2>=7.386

213A→242A	-0.12079	224A→246A	0.10202	216B→228B	0.27771
215A→238A	-0.10035	228A→233A	0.11475	216B→237B	0.18317
215A→240A	-0.14845	230A→231A	0.26066	217B→234B	0.16581
216A→237A	0.19423	203B→229B	-0.11152	218B→245B	0.10985
216A→239A	-0.10825	204B→227B	0.11941	218B→246B	-0.12970
217A→234A	-0.13216	205B→227B	0.12080	219B→230B	0.11508
220A→234A	-0.14473	211B→227B	0.10273	219B→245B	-0.11476
223A→241A	0.13215	212B→242B	0.12175	222B→235B	0.11531
224A→243A	-0.11706	214B→238B	-0.18310		

Excited State 62: 5.262-A 4.3303 eV 286.32 nm f=0.0230 <S**2>=6.673

226A→234A	0.22916	229A→246A	0.11987	218B→228B	0.25169
228A→237A	0.16152	230A→241A	0.36915	219B→228B	0.11357
228A→239A	-0.10189	211B→229B	0.11780	221B→229B	0.23340
228A→242A	-0.16915	214B→227B	0.17186	222B→228B	0.14921
229A→233A	-0.11844	214B→228B	-0.18368	225B→237B	0.10799
229A→235A	-0.19280	215B→228B	-0.11118	226B→234B	-0.14150
229A→236A	-0.18845	216B→229B	-0.11574		
229A→243A	-0.18489	217B→228B	-0.15196		

Excited State 63: 5.174-A 4.3344 eV 286.05 nm f=0.0532 <S**2>=6.443

226A→234A	-0.11010	230A→241A	-0.17575	211B→229B	0.19663

213B→229B	-0.10153	216B→227B	-0.11690	218B→230B	0.18488
214B→227B	-0.13495	216B→228B	0.12450	219B→230B	0.13737
214B→228B	-0.30539	217B→228B	-0.33025	221B→229B	0.45370
214B→229B	0.13440	217B→229B	0.11105	222B→227B	-0.10789
215B→227B	-0.14676	218B→228B	-0.15657		

Excited State 64: 5.444-A 4.3488 eV 285.10 nm f=0.1099 <S**2>=7.161

214A→242A	-0.12360	230A→233A	0.18764	215B→234B	-0.14463
216A→234A	0.11250	203B→227B	-0.10835	216B→238B	-0.13698
217A→237A	-0.11700	211B→229B	0.10602	217B→235B	-0.14253
219A→234A	-0.10904	212B→227B	-0.10307	218B→245B	0.10174
228A→231A	0.13111	212B→241B	-0.10511	219B→246B	0.13009
228A→238A	0.12257	214B→228B	0.13951	221B→229B	0.32156
229A→231A	-0.11236	214B→237B	0.11651	222B→234B	-0.10306
230A→232A	0.12982	215B→227B	-0.15092	223B→230B	-0.12865

Excited State 65: 5.455-A 4.3540 eV 284.76 nm f=0.0902 <S**2>=7.190

213A→241A	-0.10500	230A→233A	-0.22429	216B→234B	0.11762
214A→242A	0.14398	212B→227B	0.12030	217B→235B	0.16932
219A→234A	0.13450	212B→241B	0.12200	219B→246B	0.10773
220A→235A	0.10358	213B→242B	0.10243	221B→229B	0.27413
228A→231A	-0.15403	214B→228B	0.11588	222B→234B	0.11796
228A→238A	-0.15765	214B→237B	0.11026	223B→230B	0.13702
230A→232A	0.11496	215B→234B	0.11266	226B→232B	-0.11031

Excited State 66: 5.154-A 4.3812 eV 282.99 nm f=0.0008 <S**2>=6.392

229A→237A	0.11524	213B→227B	-0.24958	216B→229B	-0.15505
230A→231A	-0.10389	215B→228B	-0.18270	218B→229B	-0.26327
230A→238A	-0.11648	215B→229B	-0.16151	218B→230B	-0.12507
212B→228B	0.12501	216B→228B	0.50829	219B→227B	-0.10772

219B→229B	-0.16431	219B→230B	0.28997	220B→229B	0.28054

Excited State 67: 5.113-A 4.3892 eV 282.48 nm f=0.0009 <S**2>=6.286

212B→229B	0.21390	216B→229B	0.21263	221B→229B	0.12554
213B→227B	0.10549	218B→228B	-0.14507	223B→229B	0.11812
214B→227B	-0.26586	218B→229B	0.13304	224B→230B	-0.10014
215B→228B	0.21605	219B→230B	-0.11865		
216B→228B	-0.10334	220B→229B	0.67620		

Excited State 68: 5.256-A 4.4083 eV 281.25 nm f=0.0328 <S**2>=6.657

216A→240A	-0.10067	214B→237B	-0.10240	218B→230B	-0.22855
228A→241A	-0.14053	215B→227B	-0.14980	218B→245B	-0.10103
229A→234A	0.13213	215B→230B	0.14835	219B→229B	0.27969
230A→242A	0.16412	217B→228B	0.12305	221B→229B	0.21844
214B→228B	0.50872	218B→227B	0.10578		
214B→229B	-0.12089	218B→229B	-0.16948		

Excited State 69: 5.280-A 4.4553 eV 278.28 nm f=0.0336 <S**2>=6.720

218A→234A	-0.10412	229A→240A	0.14949	219B→229B	0.12215
226A→235A	0.14873	230A→242A	-0.29096	220B→229B	-0.11926
226A→236A	0.12495	213B→229B	0.26856	221B→229B	0.38656
228A→241A	0.20019	215B→227B	0.15277	223B→234B	0.10208
228A→245A	0.14221	217B→228B	0.10678	226B→235B	0.12637
229A→238A	0.18124	218B→229B	-0.10315		

Excited State 70: 5.441-A 4.4605 eV 277.96 nm f=0.0047 <S**2>=7.152

214A→234A	0.13131	228A→232A	0.11103	229A→233A	-0.17375
219A→242A	0.13786	228A→237A	0.11060	229A→235A	0.10154
221A→244A	-0.10555	228A→239A	0.14094	230A→235A	0.17145
226A→238A	0.15846	228A→242A	0.11282	230A→236A	-0.16619

230A→242A	0.11786	213B→234B	0.13509	221B→234B	-0.10537
230A→245A	-0.15173	215B→242B	0.11671	223B→235B	0.10684
212B→229B	0.11504	217B→241B	0.14507	224B→230B	0.15460
212B→235B	0.12674	220B→243B	-0.10567	226B→238B	0.10083
213B→229B	-0.11161	221B→229B	-0.14831		

Excited State 71: 5.429-A 4.4685 eV 277.46 nm f=0.0080 <S**2>=7.120

213A→242A	0.11803	229A→239A	0.10941	213B→241B	-0.10101
214A→241A	-0.12682	230A→238A	-0.16673	214B→234B	0.13672
215A→234A	-0.14640	230A→240A	0.16803	215B→229B	-0.20086
219A→235A	0.13221	203B→229B	-0.11209	215B→235B	-0.14591
219A→236A	0.11958	209B→229B	-0.10709	216B→228B	-0.10629
220A→234A	0.11108	211B→241B	0.10830	217B→234B	-0.12798
227A→231A	0.13369	212B→237B	0.10613	217B→238B	-0.12258
228A→233A	-0.22257	212B→242B	-0.11302	222B→229B	0.10464
229A→232A	-0.16744	213B→227B	-0.17252	222B→235B	-0.12250

Excited State 72: 5.262-A 4.4745 eV 277.09 nm f=0.0671 <S**2>=6.673

226A→237A	-0.14663	228A→240A	-0.21982	230A→246A	0.32460
226A→242A	-0.11857	229A→241A	0.24438	219B→228B	0.12679
227A→233A	-0.12173	229A→245A	-0.32307	225B→238B	0.12162
227A→236A	-0.11119	229A→247A	0.16647	226B→237B	0.12168
228A→238A	-0.11703	230A→243A	-0.31721		

Excited State 73: 5.156-A 4.4855 eV 276.41 nm f=0.0014 <S**2>=6.395

228A→242A	-0.11141	212B→228B	-0.11816	214B→229B	0.10617
229A→243A	0.12981	212B→229B	-0.33661	217B→227B	-0.12306
229A→246A	-0.14463	212B→230B	0.10395	217B→229B	-0.12298
230A→245A	0.18716	213B→228B	-0.13039	220B→229B	0.46968
212B→227B	-0.20854	214B→227B	0.17164	222B→228B	-0.23225

224B→230B	0.29949	226B→231B	-0.10541		

Excited State 74: 5.427-A 4.4919 eV 276.02 nm f=0.0372 <S**2>=7.113

213A→234A	-0.14969	229A→238A	0.16395	211B→235B	-0.11316
214A→235A	-0.13405	230A→237A	-0.11540	212B→234B	0.17148
214A→236A	-0.11487	230A→239A	-0.20669	213B→235B	0.14233
219A→241A	0.15613	190B→228B	0.12825	215B→241B	0.13678
220A→242A	-0.12963	203B→230B	0.11964	217B→242B	0.16335
226A→233A	-0.11052	207B→228B	-0.11851	221B→229B	-0.18440
227A→232A	0.11291	209B→227B	-0.10845	222B→230B	0.13515
228A→235A	-0.15951	210B→228B	0.12816	225B→230B	-0.10158
228A→236A	0.17161	211B→229B	0.18623		

Excited State 75: 5.161-A 4.5139 eV 274.67 nm f=0.0017 <S**2>=6.409

230A→242A	-0.10170	212B→229B	0.13520	217B→229B	-0.11978
211B→227B	0.33693	213B→227B	-0.29992	218B→229B	0.11787
211B→228B	0.12086	213B→228B	-0.13466	220B→229B	-0.10994
211B→230B	-0.28330	213B→230B	0.11393	222B→229B	-0.19215
212B→227B	-0.17877	215B→229B	-0.23047	224B→230B	-0.14720
212B→228B	-0.33243	216B→228B	-0.13727		

Excited State 76: 5.125-A 4.5241 eV 274.05 nm f=0.0033 <S**2>=6.317

211B→227B	0.15904	213B→227B	-0.16738	222B→228B	-0.11093
211B→228B	-0.16843	213B→228B	0.27800	223B→230B	0.10829
211B→230B	-0.16305	214B→229B	-0.23188	224B→230B	0.10841
212B→227B	0.48692	215B→229B	-0.14357	225B→231B	-0.10243
212B→228B	-0.26830	216B→230B	0.13240		
212B→230B	-0.26063	217B→229B	0.26054		

Excited State 77:	5.138-A	4.5752 eV	270.99 nm	f=0.0218	<S**2>=6.349	
228A→231A	0.14107	213B→228B	0.24976	222B→228B	0.15694	
208B→227B	-0.25247	213B→229B	-0.10957	223B→227B	0.14070	
208B→230B	-0.11818	215B→228B	-0.12058	223B→230B	0.43761	
211B→228B	0.28571	218B→228B	-0.11276	224B→230B	-0.30742	
212B→229B	-0.19104	221B→228B	-0.12483	225B→231B	-0.13597	

Excited State 78:	5.112-A	4.5764 eV	270.92 nm	f=0.0015	<S**2>=6.282	
204B→227B	0.37571	205B→229B	-0.36804	207B→227B	-0.10031	
204B→229B	0.35643	205B→230B	0.20485	210B→227B	0.16896	
204B→230B	-0.21138	206B→227B	0.22189	213B→229B	0.12914	
205B→227B	-0.35067	206B→230B	-0.13177	224B→230B	-0.19300	

Excited State 79:	5.144-A	4.5825 eV	270.56 nm	f=0.0010	<S**2>=6.365	
228A→241A	-0.10444	208B→227B	0.11268	217B→228B	0.12240	
229A→240A	-0.10764	211B→228B	-0.11317	221B→229B	0.17932	
230A→242A	0.17299	211B→229B	-0.27999	222B→228B	0.12922	
204B→227B	-0.11151	212B→229B	-0.13825	222B→230B	0.10752	
204B→229B	-0.14202	213B→229B	0.44647	223B→230B	-0.17704	
205B→227B	0.17585	214B→228B	-0.20294	224B→230B	-0.20857	
205B→229B	0.12479	215B→227B	0.20153			

Excited State 80:	5.172-A	4.5894 eV	270.15 nm	f=0.0063	<S**2>=6.438	
228A→232A	-0.11199	211B→229B	-0.24742	217B→229B	-0.11554	
229A→243A	-0.10427	212B→227B	-0.10399	218B→228B	0.14940	
229A→246A	0.12212	213B→228B	0.13840	221B→229B	0.12606	
230A→245A	-0.15066	213B→229B	0.25606	222B→228B	-0.22140	
208B→227B	-0.15394	214B→228B	-0.10780	223B→230B	0.30147	
211B→228B	0.14231	215B→227B	0.11548	224B→230B	0.32717	

Excited State 81:	5.168-A	4.6005 eV	269.50 nm	f=0.0027	<S**2>=6.426
226A→240A	-0.10125	205B→227B	0.14947	214B→227B	-0.13778
228A→242A	-0.18581	206B→227B	0.28568	215B→228B	0.18082
229A→243A	0.11524	206B→229B	-0.36371	216B→229B	-0.14545
229A→246A	-0.14963	206B→230B	-0.19147	217B→227B	0.11301
230A→245A	0.22947	212B→229B	0.43962	217B→229B	-0.10059

Excited State 82:	5.159-A	4.6039 eV	269.31 nm	f=0.0018	<S**2>=6.405
228A→242A	-0.13809	205B→227B	-0.14442	206B→230B	0.26769
229A→246A	-0.10973	206B→227B	-0.41541	210B→227B	-0.13813
230A→245A	0.17359	206B→228B	0.10130	212B→229B	0.26075
204B→227B	0.12169	206B→229B	0.49419		

Excited State 83:	5.126-A	4.6685 eV	265.58 nm	f=0.0002	<S**2>=6.318
199B→227B	0.13105	209B→229B	-0.14056	218B→229B	0.11212
199B→229B	0.11189	211B→230B	-0.21386	219B→230B	0.12495
199B→230B	-0.10389	212B→228B	0.10551	222B→229B	-0.17957
203B→229B	-0.19966	213B→227B	0.10383	223B→228B	-0.22179
204B→227B	0.24273	213B→230B	-0.34258	223B→232B	0.10327
205B→227B	0.25085	215B→229B	0.35992	225B→233B	0.11633
208B→228B	0.25999	216B→229B	0.14049	226B→236B	-0.10456

Excited State 84:	5.129-A	4.6895 eV	264.39 nm	f=0.0002	<S**2>=6.327
207B→228B	-0.12552	215B→230B	-0.12703	219B→229B	-0.19347
209B→227B	-0.12839	217B→228B	0.26661	222B→230B	0.63109
211B→229B	0.20329	218B→227B	0.12111	224B→228B	-0.23117
214B→228B	0.19931	218B→230B	0.20486		

Excited State 85:	5.432-A	4.6975 eV	263.93 nm	f=0.0000	<S**2>=7.127
214A→234A	-0.10165	219A→242A	-0.11156	221A→244A	-0.15364

222A→243A	0.12255	206B→227B	0.17603	223B→233B	-0.13068
222A→246A	0.10500	206B→229B	-0.12057	224B→236B	0.13364
200B→227B	0.10834	210B→227B	-0.26756	225B→232B	-0.19589
204B→227B	0.11637	212B→229B	-0.17011	226B→231B	0.34364
204B→229B	0.10334	220B→243B	-0.15498		
205B→229B	-0.12295	221B→244B	-0.14492		

Excited State 86: 5.163-A 4.7210 eV 262.62 nm f=0.0183 <S**2>=6.413

229A→231A	0.13696	201B→227B	-0.11286	209B→227B	-0.12281
199B→227B	0.41067	202B→227B	0.12202	211B→229B	-0.13602
199B→229B	0.38790	202B→230B	-0.14311	214B→228B	-0.12083
199B→230B	-0.19174	203B→227B	-0.21011	218B→230B	-0.12635
200B→228B	0.11153	203B→230B	0.15233	219B→230B	-0.15597
200B→229B	0.13076	205B→229B	0.14118	222B→230B	-0.15351

Excited State 87: 5.241-A 4.7345 eV 261.87 nm f=0.0103 <S**2>=6.616

222A→244A	-0.12850	200B→227B	0.23823	209B→227B	0.11095
226A→233A	0.11166	200B→228B	-0.11752	218B→230B	0.16113
227A→239A	0.12569	201B→227B	0.13189	219B→230B	-0.11100
229A→231A	-0.20044	201B→228B	0.11929	220B→244B	0.13277
230A→232A	-0.14259	202B→227B	0.10150	221B→243B	0.13508
199B→227B	0.29353	202B→229B	0.12188	226B→233B	-0.12109
199B→229B	0.30335	203B→227B	-0.11036		
199B→230B	-0.24279	203B→229B	-0.11982		

Excited State 88: 5.096-A 4.7463 eV 261.22 nm f=0.0003 <S**2>=6.242

200B→229B	0.15641	201B→230B	0.13000	203B→227B	-0.15433
200B→230B	0.10856	202B→227B	0.32669	203B→229B	0.11485
201B→227B	-0.12974	202B→229B	-0.31675	215B→228B	0.11949
201B→229B	0.17462	202B→230B	-0.17765	216B→228B	-0.28632

218B→229B	-0.17621	219B→227B	0.10630	221B→230B	-0.15291
218B→230B	-0.22527	219B→230B	0.45119		

Excited State 89: 5.081-A 4.7558 eV 260.70 nm f=0.0000 <S**2>=6.203

199B→227B	0.18852	202B→227B	-0.27792	218B→229B	-0.22111
200B→227B	0.11586	202B→229B	0.33256	218B→230B	-0.16589
200B→229B	-0.11218	202B→230B	0.16015	219B→227B	0.10616
200B→230B	-0.11483	203B→229B	-0.14780	219B→229B	-0.11807
201B→227B	0.15161	208B→228B	-0.10476	219B→230B	0.44549
201B→229B	-0.17425	211B→230B	0.11584	221B→230B	-0.21948
201B→230B	-0.11312	216B→228B	-0.28706		

Excited State 90: 5.111-A 4.7914 eV 258.76 nm f=0.0012 <S**2>=6.279

203B→227B	-0.14477	214B→228B	0.26104	219B→229B	-0.17669
207B→228B	0.15478	217B→228B	0.14381	219B→230B	0.27021
210B→228B	-0.15441	218B→229B	0.10127	222B→230B	-0.17592
211B→229B	-0.26319	218B→230B	0.62188	224B→228B	0.20432

Excited State 91: 5.153-A 4.7990 eV 258.35 nm f=0.0006 <S**2>=6.389

225A→232A	-0.11680	200B→228B	0.18474	217B→230B	-0.14236
226A→231A	0.19630	200B→230B	-0.11119	222B→228B	-0.17239
228A→232A	0.17689	201B→227B	0.18026	223B→233B	-0.17274
229A→233A	-0.20564	201B→228B	0.11753	224B→230B	0.12842
230A→247A	-0.13527	201B→230B	0.11033	225B→232B	-0.19576
190B→227B	0.10551	202B→228B	0.16380	226B→231B	0.47970
200B→227B	-0.19700	210B→227B	0.21346		

Excited State 92: 5.341-A 4.8235 eV 257.04 nm f=0.0492 <S**2>=6.882

228A→231A	-0.12210	208B→227B	-0.27968	210B→229B	0.24067
207B→229B	-0.12508	208B→230B	0.10845	223B→230B	0.13298

223B→236B	0.11371	225B→231B	0.49482		
224B→233B	-0.16165	226B→232B	-0.46328		

Excited State 93: 5.184-A 4.8358 eV 256.39 nm f=0.0016 <S**2>=6.469

228A→232A	0.12638	201B→227B	-0.24729	207B→227B	-0.29822
199B→228B	0.15835	201B→228B	-0.17621	209B→228B	-0.12254
200B→227B	0.31266	201B→230B	-0.13438	210B→227B	0.36276
200B→228B	-0.29383	202B→228B	-0.12718	226B→240B	-0.11936
200B→230B	0.16380	203B→228B	0.17955		

Excited State 94: 5.093-A 4.8668 eV 254.76 nm f=0.0650 <S**2>=6.235

229A→231A	0.29619	200B→228B	-0.33216	201B→230B	0.16945
230A→232A	0.25774	200B→230B	0.16660	202B→227B	0.27168
199B→227B	-0.15651	201B→227B	0.31617	202B→230B	0.15719
200B→227B	0.30923	201B→228B	0.39024	218B→230B	0.11718

Excited State 95: 5.278-A 4.9123 eV 252.40 nm f=0.0155 <S**2>=6.715

225A→243A	0.11983	228A→243A	0.14286	208B→227B	-0.20697
225A→244A	0.16200	228A→244A	0.20428	210B→229B	0.10028
225A→246A	0.10945	228A→246A	0.15046	220B→228B	0.12295
227A→243A	-0.17365	230A→243A	0.10228	220B→230B	-0.19988
227A→244A	-0.16480	230A→244A	0.12493	221B→228B	0.25495
227A→246A	-0.14448	230A→246A	0.14939	221B→230B	-0.17193

Excited State 96: 5.188-A 4.9133 eV 252.34 nm f=0.0016 <S**2>=6.478

225A→239A	0.11303	200B→227B	-0.20193	201B→230B	0.13931
227A→235A	-0.12611	200B→228B	0.17929	202B→228B	0.19806
227A→236A	0.11375	200B→230B	-0.10822	207B→227B	-0.17431
228A→232A	0.12639	201B→227B	0.25877	210B→227B	0.10950
229A→233A	0.29569	201B→228B	0.17965	214B→230B	0.18287

215B→228B	0.11190	221B→244B	-0.10068	226B→240B	-0.11359
216B→229B	0.12453	225B→239B	-0.11420		
217B→230B	0.21967	226B→231B	-0.18845		

Excited State 97: 5.298-A 4.9177 eV 252.12 nm f=0.0081 <S**2>=6.768

220A→244A	-0.12354	228A→243A	-0.22785	220B→230B	-0.14799
225A→243A	-0.18790	228A→244A	0.15564	220B→239B	0.11480
225A→244A	0.12310	228A→246A	-0.17011	221B→228B	0.11203
225A→246A	-0.12434	230A→244A	-0.21065	221B→230B	0.17612
227A→240A	0.11473	208B→227B	-0.17687	221B→236B	0.11013
227A→243A	-0.11941	210B→229B	0.10495	224B→234B	0.10677
227A→244A	0.27264	220B→228B	-0.22838		

Excited State 98: 5.235-A 4.9258 eV 251.70 nm f=0.0077 <S**2>=6.602

225A→244A	0.12855	212B→230B	0.11253	217B→230B	-0.18765
227A→243A	-0.14698	213B→228B	0.10447	220B→230B	-0.14929
228A→244A	0.17323	214B→229B	0.21931	221B→228B	0.11625
230A→246A	0.10824	214B→230B	-0.13018	224B→233B	-0.12390
208B→227B	0.17038	215B→230B	-0.11688	225B→234B	0.15796
210B→229B	-0.20241	216B→229B	-0.11447	226B→237B	-0.16384
211B→228B	0.15246	216B→230B	0.40000		

Excited State 99: 5.107-A 4.9310 eV 251.44 nm f=0.0016 <S**2>=6.271

229A→233A	-0.11475	215B→229B	-0.13804	217B→230B	0.51938
212B→229B	0.10455	216B→228B	0.12061	218B→228B	0.15717
214B→230B	0.47130	216B→229B	0.25595	226B→231B	0.13869
215B→228B	0.14020	217B→227B	0.12112		

Excited State 100: 5.190-A 4.9455 eV 250.70 nm f=0.0073 <S**2>=6.485

225A→244A	-0.12620	227A→243A	0.13261	227A→246A	0.10810

228A→244A	-0.17219	213B→228B	-0.14980	217B→229B	0.15253
229A→231A	-0.21629	214B→229B	0.21518	219B→228B	-0.10399
230A→232A	-0.19683	215B→230B	-0.18890	220B→230B	-0.18491
208B→227B	-0.20149	216B→227B	0.11649	221B→228B	0.10138
212B→230B	0.11112	216B→230B	0.51807		

*C.2.4.4 **OTPA-FLR-221**, **EB** State*

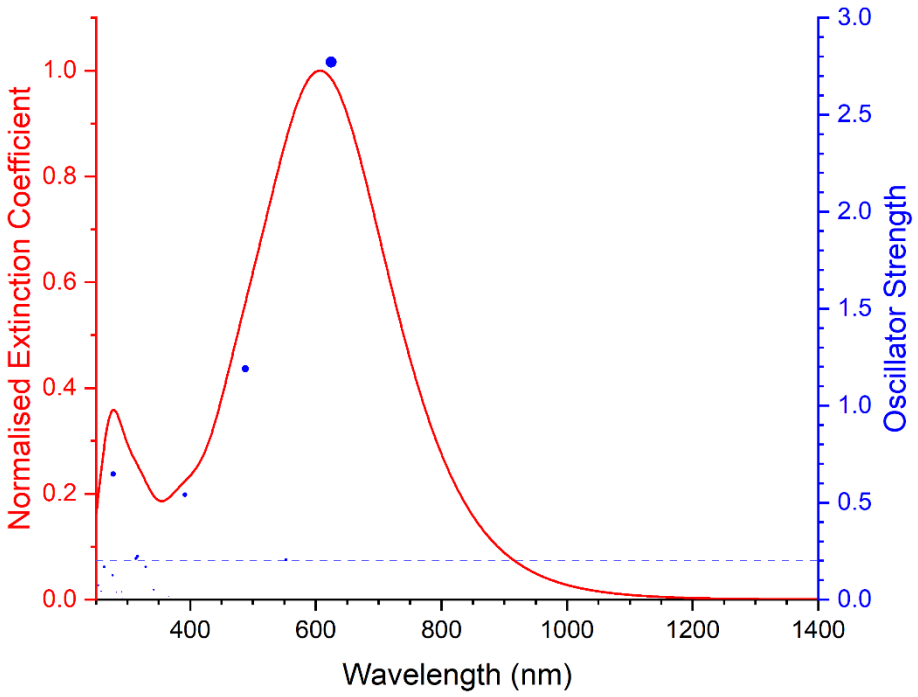

*Figure C-16 Excited states and normalised absorption spectra from TD-DFT calculations of **OTPA-FLR-221** in **EB** state. The areas of excited state dots are proportional to their oscillator strengths.*

Excited State 1:	Singlet-A	1.6054 eV	772.30 nm	f=0.0000	<S**2>=0.000
226→230	-0.21560	228→229	0.65463		
Excited State 2:	**Singlet-A**	**1.9849 eV**	**624.63 nm**	**f=2.7706**	**<S**2>=0.000**
226→229	-0.19790	**228→230**	**0.66270**		
Excited State 3:	**Singlet-A**	**2.2435 eV**	**552.65 nm**	**f=0.2051**	**<S**2>=0.000**
223→229	0.12235	224→230	0.19338	**227→229**	**0.65249**
Excited State 4:	Singlet-A	2.4005 eV	516.49 nm	f=0.0000	<S**2>=0.000
223→230	0.12701	224→229	0.21807	227→230	0.64290

Excited State 5:	**Singlet-A**	**2.5402 eV**	**488.09 nm**	**f=1.1905**	**<S**2>=0.000**	
225→230	0.10928	**226→229**	**0.66487**	228→230	0.20334	
Excited State 6:	Singlet-A	2.6414 eV	469.39 nm	f=0.0000	<S**2>=0.000	
225→229	0.14922	226→230	0.64704	228→229	0.22889	
Excited State 7:	Singlet-A	3.0685 eV	404.06 nm	f=0.0000	<S**2>=0.000	
221→229	0.19723	225→229	0.57061			
222→230	0.28042	226→230	-0.12477			
Excited State 8:	**Singlet-A**	**3.1664 eV**	**391.56 nm**	**f=0.5401**	**<S**2>=0.000**	
217→230	0.11103	**222→229**	**0.33914**			
221→230	0.21237	**225→230**	**0.52815**			
Excited State 9:	Singlet-A	3.3384 eV	371.39 nm	f=0.0000	<S**2>=0.000	
210→230	-0.15514	224→229	0.54141			
223→230	0.21549	227→230	-0.27695			
Excited State 10:	Singlet-A	3.3912 eV	365.61 nm	f=0.0170	<S**2>=0.000	
208→230	-0.10101	218→229	-0.10251	224→230	0.50844	
210→229	-0.18018	223→229	0.27700	227→229	-0.24983	
Excited State 11:	Singlet-A	3.5915 eV	345.22 nm	f=0.0000	<S**2>=0.000	
206→230	-0.12153	217→229	0.16974	222→230	0.38960	
209→229	0.18756	221→229	0.26913	225→229	-0.37424	
Excited State 12:	Singlet-A	3.6216 eV	342.35 nm	f=0.0512	<S**2>=0.000	
206→229	0.11187	221→230	-0.19503	226→229	-0.10339	
209→230	-0.15689	222→229	-0.39291			
217→230	-0.13983	225→230	0.44716			

Excited State 13:	Singlet-A	3.7550 eV	330.19 nm	f=0.0000	<S**2>=0.000			
213→230	0.38162		216→230	-0.25004		221→229	-0.13418	
214→229	0.45723		217→229	0.19696				
Excited State 14:	Singlet-A	3.7657 eV	329.24 nm	f=0.1683	<S**2>=0.000			
213→229	0.42374		216→229	-0.27363		221→230	-0.11777	
214→230	0.42060		217→230	0.16420				
Excited State 15:	**Singlet-A**	**3.9222 eV**	**316.11 nm**	**f=0.2233**	**<S**2>=0.000**			
211→230	-0.22165		218→229	0.18777		**228→231**	**0.43001**	
212→229	-0.24935		226→232	0.16342		228→233	0.10638	
215→230	0.14655		227→234	0.18408				
Excited State 16:	Singlet-A	3.9497 eV	313.91 nm	f=0.0000	<S**2>=0.000			
208→229	0.11777		212→230	0.41362		218→230	-0.18259	
211→229	0.44218		215→229	-0.20803				
Excited State 17:	**Singlet-A**	**3.9502 eV**	**313.87 nm**	**f=0.2118**	**<S**2>=0.000**			
211→230	0.30956		218→229	-0.15545		227→236	0.13059	
212→229	**0.34492**		223→229	-0.12667		**228→231**	**0.37879**	
215→230	-0.13722		226→232	0.14399				
Excited State 18:	Singlet-A	4.0896 eV	303.17 nm	f=0.0000	<S**2>=0.000			
213→230	0.16322		217→229	-0.27353		227→233	0.22586	
214→229	0.16139		221→229	0.23360		227→238	0.16313	
216→230	0.13428		227→231	0.10603		228→234	0.36090	
Excited State 19:	Singlet-A	4.0939 eV	302.85 nm	f=0.0135	<S**2>=0.000			
211→230	0.20096		218→229	0.24485		226→235	-0.10515	
212→229	0.21879		223→229	0.26758		227→234	0.16668	
215→230	0.12884		224→230	-0.13368		227→236	-0.16840	

228→231	-0.11131	228→233	0.30057	228→238	0.12119

Excited State 20: Singlet-A 4.1500 eV 298.76 nm f=0.0000 <S**2>=0.000

208→229	0.13788	215→229	-0.11293	226→231	0.28965
210→230	0.11339	218→230	-0.11447	227→237	-0.16873
211→229	-0.11595	223→230	-0.10553	228→232	0.43604
212→230	-0.10386	224→229	0.17809	228→235	-0.12443

Excited State 21: Singlet-A 4.2111 eV 294.42 nm f=0.0000 <S**2>=0.000

211→229	0.16700	218→230	0.26935	224→229	-0.11713
212→230	0.14204	220→229	-0.13027	226→231	0.15012
215→229	0.24558	223→230	0.36069	228→232	0.24733

Excited State 22: Singlet-A 4.2283 eV 293.23 nm f=0.0080 <S**2>=0.000

213→229	-0.24693	217→230	0.34088	222→229	0.13083
214→230	-0.17742	219→229	0.15353	228→240	0.10886
216→229	-0.27731	221→230	-0.31836		

Excited State 23: Singlet-A 4.2614 eV 290.95 nm f=0.0394 <S**2>=0.000

210→229	-0.10829	224→230	-0.31436	227→234	-0.21262
223→229	0.38071	226→235	0.10992	228→233	-0.32579

Excited State 24: Singlet-A 4.2865 eV 289.24 nm f=0.0000 <S**2>=0.000

213→230	-0.12466	221→229	-0.23446	227→244	0.12496
214→229	-0.12326	222→230	0.11930	228→234	0.32783
216→230	-0.10451	227→231	0.31160	228→236	0.20146
217→229	0.23279	227→233	0.11800		

Excited State 25: Singlet-A 4.3571 eV 284.56 nm f=0.0000 <S**2>=0.000

208→229	0.18186	218→230	0.17502	224→229	0.25766
210→230	0.16513	223→230	-0.27635	226→233	-0.22798

227→237	0.14158	228→235	0.34210		

Excited State 26:	Singlet-A	4.3884 eV	282.53 nm	f=0.0372	<S**2>=0.000
208→230	0.21291	218→229	0.39664	227→236	0.11096
210→229	0.23076	224→230	0.23307	228→233	-0.24244
215→230	0.14247	226→235	0.16073		

Excited State 27:	Singlet-A	4.3889 eV	282.50 nm	f=0.0002	<S**2>=0.000
216→230	0.10496	227→231	0.26436	228→234	-0.12650
217→229	-0.17786	227→233	-0.20036	228→236	0.40371
221→229	0.20222	227→238	-0.19860		
225→236	0.12379	227→244	0.12527		

Excited State 28:	Singlet-A	4.4333 eV	279.67 nm	f=0.0000	<S**2>=0.000
208→229	-0.18968	224→229	-0.13765	228→232	0.14742
210→230	-0.17307	225→235	-0.15642	228→235	0.34536
215→229	-0.13452	226→233	-0.25545	228→239	0.10047
218→230	-0.27439	226→238	0.15782		

Excited State 29:	**Singlet-A**	**4.4658 eV**	**277.63 nm**	**f=0.6476**	**<S**2>=0.000**
221→230	-0.12211	227→232	-0.29916	**228→237**	**0.46174**
225→237	0.15144	227→235	0.13708		
226→234	-0.10977	227→239	-0.26510		

Excited State 30:	Singlet-A	4.4809 eV	276.69 nm	f=0.1253	<S**2>=0.000
207→229	0.16433	212→229	-0.10119	225→233	0.11883
208→230	0.23871	215→230	-0.13706	226→235	0.15723
210→229	0.22137	218→229	-0.27287	227→234	0.15732
211→230	-0.10319	223→229	0.29554	228→238	0.20001

Excited State 31:	Singlet-A	4.5020 eV	275.40 nm	f=0.0119	<S**2>=0.000	
208→230	-0.16476	225→233	0.19322	227→236	-0.18314	
210→229	-0.16413	226→235	0.29809	228→233	-0.15189	
223→229	-0.19037	227→234	0.12061	228→238	0.37684	

Excited State 32:	Singlet-A	4.5574 eV	272.05 nm	f=0.0000	<S**2>=0.000	
207→230	0.13880	215→229	-0.13362	227→237	0.21761	
208→229	0.23273	218→230	-0.17070	228→232	-0.12326	
210→230	0.17644	223→230	0.39147	228→239	-0.20663	
211→229	-0.10140	226→231	0.11537			

Excited State 33:	Singlet-A	4.6322 eV	267.66 nm	f=0.0000	<S**2>=0.000	
216→230	0.10493	221→229	-0.36522			
217→229	-0.35706	222→230	0.43773			

Excited State 34:	Singlet-A	4.6478 eV	266.76 nm	f=0.0026	<S**2>=0.000	
216→229	-0.12867	222→229	-0.36461	228→240	0.16743	
217→230	0.21502	227→232	-0.10916			
221→230	0.43453	227→243	-0.10091			

Excited State 35:	Singlet-A	4.7117 eV	263.14 nm	f=0.1682	<S**2>=0.000	
206→229	0.12114	226→234	0.17175	227→243	-0.20166	
209→230	-0.12521	227→232	-0.13286	228→240	0.36675	
217→230	-0.32639	227→235	-0.12598			
222→229	0.18724	227→239	-0.10078			

Excited State 36:	Singlet-A	4.7551 eV	260.74 nm	f=0.0000	<S**2>=0.000	
205→229	-0.10935	218→230	0.23938	225→235	-0.11945	
208→229	0.13205	220→229	0.17258	226→231	-0.22297	
210→230	0.15511	223→230	0.15477	226→238	0.12697	
215→229	-0.12205	225→232	0.11324	227→237	-0.20365	

227→240	0.10918	228→239	0.19272		
227→246	0.13710	228→243	-0.23529		

Excited State 37: Singlet-A 4.7892 eV 258.89 nm f=0.0000 <S**2>=0.000

219→230	-0.19647	225→241	0.15199	227→238	0.15796
220→239	0.10043	225→245	-0.10300	227→242	-0.31692
225→234	0.12270	226→240	-0.11612	228→241	0.40060

Excited State 38: Singlet-A 4.7974 eV 258.44 nm f=0.0428 <S**2>=0.000

210→229	0.10316	225→242	0.15148	227→245	0.11328
215→230	-0.10062	226→232	0.17663	228→242	0.35435
220→230	0.24403	227→236	-0.13308		
225→231	-0.16881	227→241	-0.28634		

Excited State 39: Singlet-A 4.8284 eV 256.78 nm f=0.0028 <S**2>=0.000

206→229	0.12541	217→230	-0.16321	222→229	0.10539
209→230	-0.12960	219→229	0.49730	228→240	-0.17535
216→229	-0.21789	221→230	0.22319		

Excited State 40: Singlet-A 4.8352 eV 256.42 nm f=0.0000 <S**2>=0.000

208→229	0.17325	226→231	-0.26577	227→246	-0.12443
210→230	0.12850	226→238	-0.12948	228→239	0.17982
218→230	-0.19312	227→237	-0.12865	228→243	0.31531
225→232	0.15017	227→240	-0.24156		

Excited State 41: Singlet-A 4.8478 eV 255.75 nm f=0.0000 <S**2>=0.000

204→229	-0.13146	213→230	-0.10764	219→230	0.33652
206→230	0.20796	216→230	-0.31346	221→229	0.24785
209→229	-0.27414	217→229	-0.12211	222→230	0.15542

Excited State 42: Singlet-A 4.8789 eV 254.12 nm f=0.0000 <S**2>=0.000

208→229	-0.12813	220→229	0.58377		
218→230	0.21533	228→243	0.14428		

Excited State 43: Singlet-A 4.8833 eV 253.90 nm f=0.0740 <S**2>=0.000

203→229	-0.10029	225→231	0.21441	227→245	0.10584
205→230	0.13485	226→232	-0.22780	228→242	0.17037
210→229	-0.16387	227→234	0.12121	228→244	0.24722
215→230	0.17514	227→236	0.19629		
218→229	-0.10792	227→241	-0.19935		

Excited State 44: Singlet-A 4.9385 eV 251.06 nm f=0.0006 <S**2>=0.000

207→229	-0.11048	215→230	-0.31237	225→231	0.12291
208→230	-0.12012	218→229	0.26371	226→232	-0.11931
210→229	-0.10048	220→230	0.46510		

C.2.5 Electronic Transitions in **OTPB-BZN-210** Oligomers

*Table C-9 Attributes of **OTPB-BZN-210** in **LEB**, **ES** (singlet and triplet), and **EB** states related to electronic structures*

Attribute	**LEB State**	**^{1}ES State**	**^{3}ES State**	**EB State**
Molecular Formula	$C_{54}H_{40}N_2$	$C_{54}H_{40}N_2^{2+}$	$C_{54}H_{40}N_2^{2+}$	$C_{54}H_{40}N_2$
Number of Atoms	96	96	96	94
Number of Electrons	378	376	376	376
HOMO	MO 189	MO 188	MOs 189A, 187B	MO 188
LUMO	MO 190	MO 189	MOs 190A, 188B	MO 189

*C.2.5.1 **OTPB-BZN-210, LEB** State*

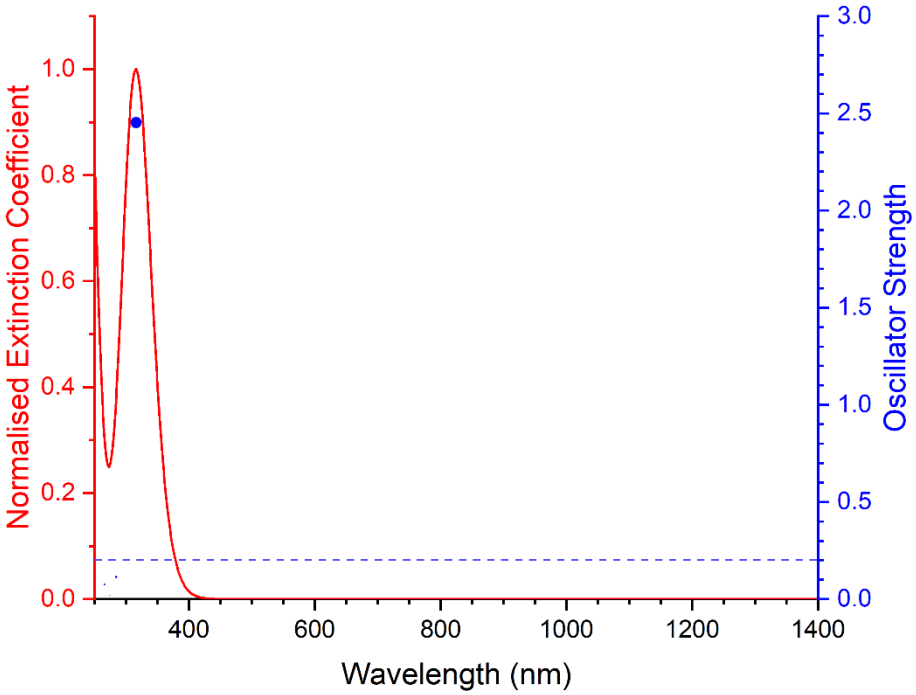

*Figure C-17 Excited states and normalised absorption spectra from TD-DFT calculations of **OTPB-BZN-210** in **LEB** state. The areas of excited state dots are proportional to their oscillator strengths.*

Excited State 1:	**Singlet-AU**	**3.9192 eV**	**316.35 nm**	**f=2.4526**	**<S**2>=0.000**
188→193	0.20654		189→194	-0.29602	
189→190	**0.56245**		189→203	-0.12302	
Excited State 2:	Singlet-AU	4.3555 eV	284.66 nm	f=0.1135	<S**2>=0.000
185→195	-0.11386		189→195	0.62267	
189→194	0.10132		189→200	0.11329	
Excited State 3:	Singlet-AG	4.4416 eV	279.14 nm	f=0.0000	<S**2>=0.000
188→190	0.38782		189→196	-0.16241	
189→193	0.50285		189→197	-0.12870	
Excited State 4:	Singlet-AG	4.5034 eV	275.31 nm	f=0.0000	<S**2>=0.000
185→191	0.20206		188→192	-0.31346	189→196 -0.14829
186→190	-0.14558		188→200	-0.10607	189→197 0.21359
187→193	0.14684		189→191	0.39700	

Excited State 5:	Singlet-AU	4.5131 eV	274.72 nm	f=0.0191	<S**2>=0.000			
184→191	-0.10053		188→191	-0.32017		189→200	0.18453	
185→192	0.21013		188→197	-0.11006		189→201	0.12648	
186→193	0.15503		189→192	0.39999				
187→190	-0.15341		189→198	-0.11091				
Excited State 6:	Singlet-AG	4.6497 eV	266.65 nm	f=0.0000	<S**2>=0.000			
177→190	0.11648		188→192	0.15004		188→201	-0.12986	
185→191	-0.12735		188→195	0.15530		189→191	-0.15964	
186→190	0.12702		188→198	0.10730		189→196	-0.25382	
187→193	-0.12954		188→200	-0.18769		189→197	0.39943	
Excited State 7:	Singlet-AU	4.6615 eV	265.97 nm	f=0.0748	<S**2>=0.000			
185→192	-0.11106		188→196	0.16872		189→200	0.35800	
186→193	-0.11898		188→197	-0.24559		189→201	0.24630	
187→190	0.11689		189→192	-0.13647				
188→191	0.12812		189→198	-0.20941				

*C.2.5.2 **OTPB-BZN-210**, **¹ES** State*

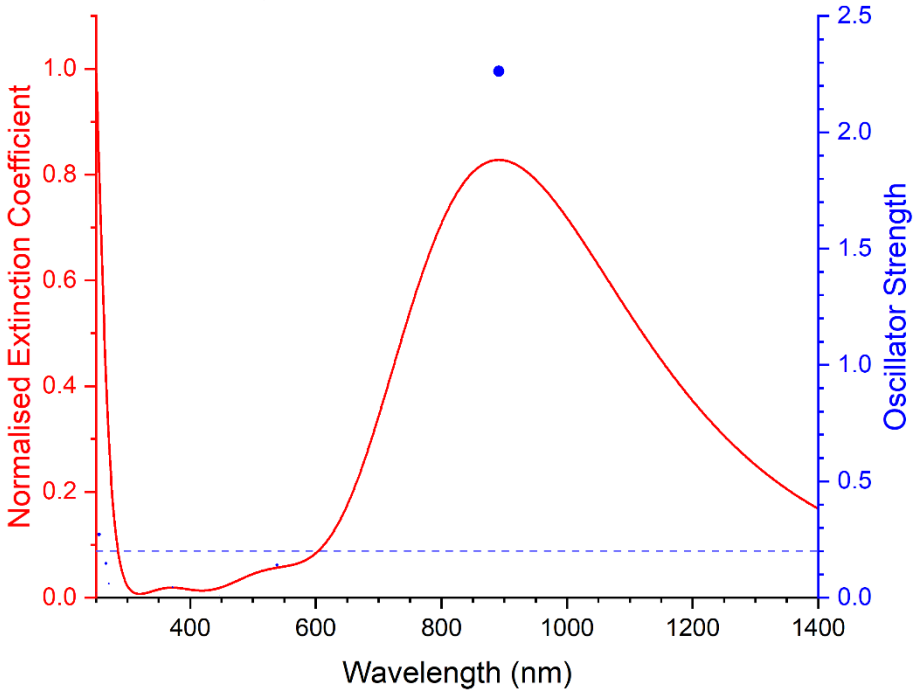

*Figure C-18 Excited states and normalised absorption spectra from TD-DFT calculations of **OTPB-BZN-210** in **¹ES** state. The areas of excited state dots are proportional to their oscillator strengths.*

Excited State 1:	**Singlet-AU**	**1.3905 eV**	**891.66 nm**	**f=2.2626**	**<S**2>=0.000**	
184→189	0.18266	**188→189**	**0.67965**			
Excited State 2:	Singlet-AG	1.7049 eV	727.21 nm	f=0.0000	<S**2>=0.000	
187→189	0.70098					
Excited State 3:	Singlet-AU	1.7050 eV	727.19 nm	f=0.0001	<S**2>=0.000	
186→189	0.70134					
Excited State 4:	Singlet-AG	1.9190 eV	646.07 nm	f=0.0000	<S**2>=0.000	
179→189	-0.19064	185→189	0.67760			
Excited State 5:	Singlet-AU	2.3024 eV	538.51 nm	f=0.1402	<S**2>=0.000	
176→189	0.10397	184→189	0.67050	188→189	-0.18815	
Excited State 6:	Singlet-AG	2.5945 eV	477.87 nm	f=0.0000	<S**2>=0.000	
173→189	0.14890	179→189	0.65764	185→189	0.19530	

Excited State 7:	Singlet-AU	2.6433 eV	469.05 nm	f=0.0000	<S**2>=0.000
180→189	0.70103				
Excited State 8:	Singlet-AG	2.6434 eV	469.02 nm	f=0.0000	<S**2>=0.000
181→189	0.69938				
Excited State 9:	Singlet-AU	2.6760 eV	463.31 nm	f=0.0000	<S**2>=0.000
182→189	0.70092				
Excited State 10:	Singlet-AG	2.6761 eV	463.30 nm	f=0.0000	<S**2>=0.000
183→189	0.70031				
Excited State 11:	Singlet-AG	2.7704 eV	447.53 nm	f=0.0000	<S**2>=0.000
175→189	0.69618				
Excited State 12:	Singlet-AU	2.7756 eV	446.69 nm	f=0.0094	<S**2>=0.000
174→189	0.68963	176→189	0.11122		
Excited State 13:	Singlet-AG	3.0820 eV	402.28 nm	f=0.0000	<S**2>=0.000
172→189	0.69363				
Excited State 14:	Singlet-AU	3.3302 eV	372.31 nm	f=0.0449	<S**2>=0.000
174→189	-0.10006	176→189	0.67740	184→189	-0.11463
Excited State 15:	Singlet-AG	3.6081 eV	343.62 nm	f=0.0000	<S**2>=0.000
177→189	0.69381				
Excited State 16:	Singlet-AU	3.6083 eV	343.61 nm	f=0.0089	<S**2>=0.000
178→189	0.69177				
Excited State 17:	Singlet-AG	3.7007 eV	335.03 nm	f=0.0000	<S**2>=0.000
173→189	0.66988	179→189	-0.15388		

Excited State 18:	Singlet-AG	4.4478 eV	278.76 nm	f=0.0000	<S**2>=0.000				
179→192	0.14481		185→192	-0.17669					
184→190	0.21996		188→190	0.61536					
Excited State 19:	Singlet-AG	4.5782 eV	270.81 nm	f=0.0000	<S**2>=0.000				
185→193	-0.13917		186→195	-0.18973		187→192	0.37114		
186→190	0.41032		186→197	0.12886		188→194	-0.17505		
Excited State 20:	Singlet-AU	4.5783 eV	270.81 nm	f=0.0600	<S**2>=0.000				
185→194	0.13746		187→190	0.41015		187→197	0.12811		
186→192	0.37109		187→195	-0.19042		188→193	0.17906		
Excited State 21:	Singlet-AU	4.6627 eV	265.91 nm	f=0.1464	<S**2>=0.000				
152→189	-0.13804		167→189	0.25204		188→192	0.17484		
161→189	0.31967		171→189	0.28374					
163→189	0.38071		185→190	-0.12723					
Excited State 22:	Singlet-AG	4.8316 eV	256.61 nm	f=0.0000	<S**2>=0.000				
153→189	-0.14314		160→189	0.31971		170→189	0.54852		
154→189	-0.13371		166→189	0.13376					
Excited State 23:	**Singlet-AU**	**4.8622 eV**	**255.00 nm**	**f=0.2717**	**<S**2>=0.000**				
161→189	-0.11510		179→190	0.19125		185→195	0.11674		
171→189	-0.24501		**185→190**	**-0.37277**		**188→192**	**0.41781**		
Excited State 24:	Singlet-AU	4.9511 eV	250.42 nm	f=0.0196	<S**2>=0.000				
157→189	0.20581		167→189	-0.12395		171→189	0.51327		
163→189	-0.29949		169→189	0.14653		185→190	-0.11472		

*C.2.5.3 **OTPB-BZN-210**, ^{3}**ES** State*

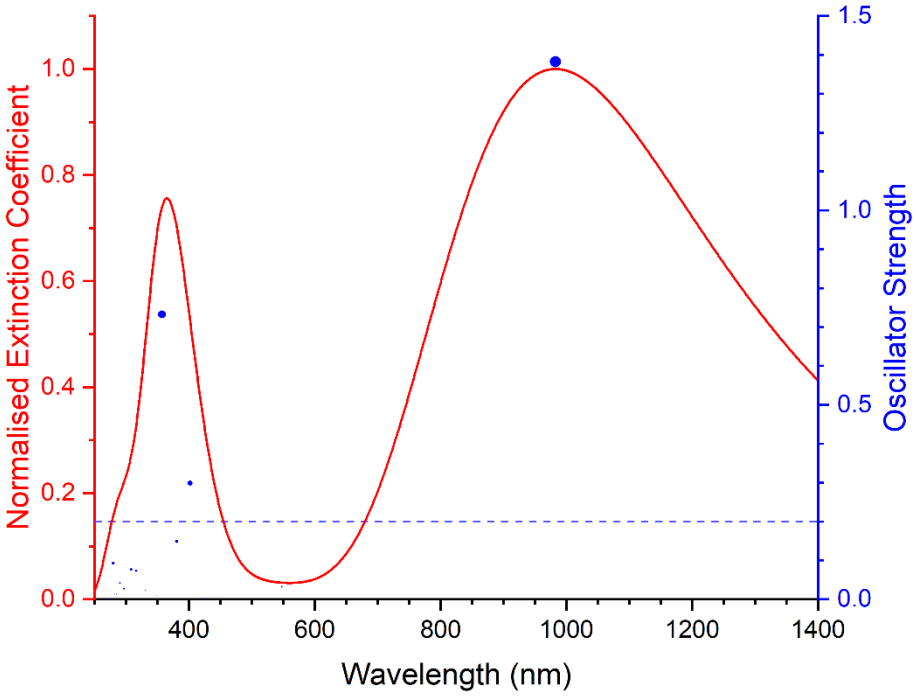

*Figure C-19 Excited states and normalised absorption spectra from TD-DFT calculations of **OTPB-BZN-210** in ^{5}**ES** state. The areas of excited state dots are proportional to their oscillator strengths.*

Excited State 1:	**3.080-AU**	**1.2618 eV**	**982.62 nm**	**f=1.3821**	**<S**2>=2.122**
178B→189B	-0.25471	184B→189B	0.26938		
179B→188B	**0.48508**	**185B→188B**	**0.77053**		
Excited State 2:	3.079-AG	1.4653 eV	846.11 nm	f=0.0000	<S**2>=2.120
176B→188B	0.17373	186B→188B	0.83185	187B→189B	-0.47960
177B→189B	0.13229	186B→190B	-0.10011		
Excited State 3:	3.079-AU	1.4654 eV	846.10 nm	f=0.0002	<S**2>=2.120
176B→189B	-0.13268	186B→189B	-0.47987	187B→190B	-0.10003
177B→188B	-0.17324	187B→188B	0.83079		
Excited State 4:	3.074-AG	1.7186 eV	721.41 nm	f=0.0000	<S**2>=2.113
189A→191A	-0.11067	178B→188B	-0.36853	184B→188B	0.67532
174B→189B	-0.10900	179B→189B	0.19523	185B→189B	0.54430
Excited State 5:	3.078-AU	2.0973 eV	591.17 nm	f=0.0022	<S**2>=2.118
172B→188B	0.68993	173B→189B	-0.57957	174B→188B	0.28467

175B→188B	-0.22450	177B→188B	0.13317		

Excited State 6:	3.078-AG	2.0992 eV	590.62 nm	f=0.0000	<S**2>=2.118
172B→189B	-0.52058	174B→189B	-0.20096	176B→188B	-0.11553
173B→188B	0.78075	175B→189B	0.15658		

Excited State 7:	3.124-AU	2.2630 eV	547.87 nm	f=0.0324	<S**2>=2.190
169B→189B	-0.10481	179B→188B	0.71639	185B→190B	0.10505
172B→188B	-0.13826	184B→189B	-0.39909		
174B→188B	0.31825	185B→188B	-0.35855		

Excited State 8:	3.070-AG	2.3939 eV	517.92 nm	f=0.0000	<S**2>=2.106
169B→188B	-0.12916	178B→188B	-0.23915	184B→188B	-0.60449
174B→189B	0.15573	179B→189B	0.61323	185B→189B	0.32566

Excited State 9:	3.065-AU	2.7532 eV	450.33 nm	f=0.0002	<S**2>=2.098
180B→188B	0.90647	181B→189B	0.36483	183B→188B	-0.16011

Excited State 10:	3.061-AG	2.7534 eV	450.30 nm	f=0.0000	<S**2>=2.093
180B→189B	0.36185	181B→188B	0.89923	182B→188B	-0.21126

Excited State 11:	3.066-AU	2.7565 eV	449.79 nm	f=0.0002	<S**2>=2.100
180B→188B	0.15012	182B→189B	0.38109	183B→188B	0.89978

Excited State 12:	3.061-AG	2.7568 eV	449.75 nm	f=0.0000	<S**2>=2.093
181B→188B	0.20911	182B→188B	0.89224	183B→189B	0.37812

Excited State 13:	3.377-AU	2.7965 eV	443.36 nm	f=0.0071	<S**2>=2.602
179A→190A	0.11487	188A→196A	0.10174	174B→188B	0.42622
186A→191A	0.15152	189A→197A	0.12055	178B→189B	0.41475
187A→192A	0.11216	162B→188B	0.11664	179B→188B	-0.24230
188A→193A	-0.12943	172B→188B	-0.15128	179B→190B	0.10874

184B→189B	-0.24467	185B→190B	0.12962	187B→192B	-0.13398
185B→188B	0.39903	186B→193B	-0.14737		

Excited State 14: 3.234-AG 2.8875 eV 429.39 nm f=0.0000 <S**2>=2.364

187A→193A	0.11425	178B→188B	0.64501	187B→193B	0.12936
172B→189B	-0.12472	185B→189B	0.49846		
174B→189B	0.34125	186B→192B	0.11755		

Excited State 15: 3.156-AU 2.9024 eV 427.18 nm f=0.0044 <S**2>=2.240

172B→188B	0.27415	175B→190B	0.16393		
175B→188B	0.91453	186B→189B	0.10308		

Excited State 16: 3.089-AG 2.9171 eV 425.02 nm f=0.0000 <S**2>=2.135

176B→188B	-0.12613	186B→188B	0.54008		
177B→189B	-0.11976	187B→189B	0.80389		

Excited State 17: 3.092-AU 2.9177 eV 424.94 nm f=0.0014 <S**2>=2.141

175B→188B	-0.10517	177B→188B	0.13429	187B→188B	0.53472
176B→189B	0.11828	186B→189B	0.79819		

Excited State 18: 3.907-AG 3.0696 eV 403.90 nm f=0.0000 <S**2>=3.567

179A→191A	0.10665	188A→195A	-0.15657	185B→189B	-0.19537
185A→198A	-0.13498	189A→191A	0.16686	185B→191B	-0.17893
186A→190A	0.16961	189A→198A	0.11499	185B→198B	0.14622
186A→197A	0.13227	169B→188B	-0.10840	186B→192B	0.25308
186A→199A	-0.11432	178B→188B	-0.34764	186B→194B	0.11733
187A→193A	0.22669	179B→189B	0.14750	187B→193B	0.27693
187A→196A	-0.16962	184B→190B	0.12395	187B→196B	0.10768
188A→192A	-0.19789	184B→197B	-0.12809		
188A→194A	0.11004	184B→199B	0.11103		

Excited State 19:	**3.817-AU**	**3.0858 eV**	**401.79 nm**	**f=0.2989**	**<S**2>=3.391**	
185A→197A	0.12238	189A→190A	-0.27529	185B→195B	-0.10079	
186A→191A	-0.19436	174B→188B	0.18372	185B→197B	0.12635	
186A→198A	-0.13411	178B→189B	0.19908	186B→193B	0.26812	
187A→192A	-0.18835	179B→188B	-0.15537	186B→196B	0.10497	
187A→194A	0.10498	184B→189B	-0.29216	187B→192B	0.24455	
187A→195A	-0.15106	184B→191B	0.11319	187B→194B	0.11322	
188A→193A	0.21615	184B→198B	-0.15932			
188A→196A	-0.16067	185B→188B	0.18038			

Excited State 20:	3.211-AU	3.2556 eV	380.84 nm	f=0.1489	<S**2>=2.327	
176A→194A	0.14098	174B→188B	0.38098	184B→189B	0.72495	
185A→190A	-0.10803	175B→194B	-0.13760	185B→188B	-0.28469	
189A→190A	-0.21395	178B→189B	0.11580			
172B→188B	-0.14188	179B→190B	0.10162			

Excited State 21:	3.142-AG	3.3230 eV	373.11 nm	f=0.0000	<S**2>=2.218	
165B→188B	-0.11040	174B→189B	-0.35694	184B→188B	-0.39697	
169B→188B	0.17599	178B→188B	-0.18265	185B→189B	0.50658	
172B→189B	0.14150	179B→189B	-0.50480			

Excited State 22:	4.094-AU	3.3563 eV	369.41 nm	f=0.0001	<S**2>=3.940	
180A→193A	-0.10060	186A→193A	0.17504	179B→192B	-0.10100	
181A→201A	0.18518	186A→196A	-0.13882	180B→201B	0.18407	
182A→200A	0.18511	187A→197A	0.13064	181B→200B	0.18616	
183A→203A	-0.18638	187A→199A	-0.18068	182B→202B	0.18738	
184A→202A	-0.18644	188A→191A	-0.12017	183B→203B	0.18523	
185A→192A	-0.14110	188A→198A	-0.21482	184B→193B	-0.21875	
185A→195A	-0.12739	176B→189B	-0.10688	184B→206B	-0.11253	
185A→206A	0.10982	177B→188B	-0.18293	185B→192B	0.18034	

186B→189B	0.10607	186B→198B	0.21311	187B→199B	-0.16794
186B→191B	-0.12250	187B→197B	0.14050		

Excited State 23: 4.092-AG 3.3563 eV 369.40 nm f=0.0000 <S**2>=3.936

181A→200A	-0.18381	187A→198A	-0.21470	183B→202B	-0.18857
182A→201A	-0.18305	188A→197A	0.13233	184B→192B	-0.19826
183A→202A	0.18786	188A→199A	-0.18025	184B→205B	0.11218
184A→203A	0.18756	189A→193A	-0.11398	185B→193B	0.19852
185A→193A	0.16340	176B→188B	0.18384	186B→197B	0.13983
185A→196A	-0.13559	177B→189B	0.10452	186B→199B	-0.16798
185A→207A	0.10969	179B→193B	-0.11131	187B→189B	0.10792
186A→192A	-0.15057	180B→200B	-0.18453	187B→191B	-0.12201
186A→195A	-0.13232	181B→201B	-0.18248	187B→198B	0.21283
187A→191A	-0.11998	182B→203B	-0.18639		

Excited State 24: 3.522-AU 3.4718 eV 357.11 nm f=0.7324 <S2>=2.852**

176A→194A	-0.12118	186A→191A	0.23835	175B→194B	0.12204
179A→197A	0.14831	186A→198A	-0.10028	178B→189B	0.12488
180A→191A	0.25522	188A→193A	0.10841	182B→202B	-0.10061
185A→190A	0.22424	**189A→190A**	**0.53688**	184B→189B	0.21274
185A→199A	-0.10754	174B→188B	0.23397		

Excited State 25: 3.075-AG 3.4771 eV 356.58 nm f=0.0000 <S**2>=2.113

172B→189B	0.23845	175B→189B	0.94584	175B→191B	-0.11659

Excited State 26: 3.186-AU 3.5465 eV 349.59 nm f=0.0098 <S**2>=2.288

172B→188B	-0.10443	177B→188B	0.76698	187B→188B	0.10145
176B→189B	0.41440	186B→189B	-0.27996		

Excited State 27: 3.185-AG 3.5469 eV 349.56 nm f=0.0000 <S**2>=2.286

173B→188B	0.11707	176B→188B	0.76964	177B→189B	0.41709

186B→188B	-0.10095	187B→189B	0.27941		

Excited State 28:	3.735-AG	3.6355 eV	341.04 nm	f=0.0000	<S**2>=3.237
173A→196A	-0.11644	184A→203A	0.12497	179B→191B	-0.12289
174A→195A	-0.10437	185A→204A	-0.11035	180B→200B	0.13168
175A→197A	0.10421	186A→190A	0.34571	181B→201B	0.12899
179A→191A	0.19670	186A→199A	0.10759	182B→203B	-0.12833
180A→190A	0.29793	186A→205A	0.10049	183B→202B	-0.13116
181A→200A	0.12551	187A→207A	-0.10422	185B→189B	0.10461
182A→201A	0.12520	188A→206A	-0.10414	186B→205B	0.10015
183A→202A	0.12520	189A→191A	0.42697	187B→206B	-0.10025

Excited State 29:	3.791-AU	3.7450 eV	331.07 nm	f=0.0233	<S**2>=3.342
176A→192A	-0.10018	186A→191A	-0.18345	174B→188B	0.32845
176A→194A	-0.28318	189A→195A	0.15011	174B→197B	-0.10912
179A→190A	-0.23464	189A→197A	-0.18286	175B→192B	-0.10223
179A→199A	0.10120	189A→199A	-0.15262	175B→194B	0.25613
180A→191A	-0.16295	169B→189B	-0.15031	179B→190B	-0.20104
185A→197A	-0.12267	172B→188B	-0.11877	185B→190B	-0.18706

Excited State 30:	3.061-AG	3.7720 eV	328.69 nm	f=0.0000	<S**2>=2.092
180B→189B	0.91495	181B→188B	-0.37364	183B→189B	-0.12437

Excited State 31:	3.065-AU	3.7722 eV	328.68 nm	f=0.0002	<S**2>=2.099
180B→188B	-0.37221	181B→189B	0.91209	182B→189B	-0.12668

Excited State 32:	3.061-AG	3.8155 eV	324.95 nm	f=0.0000	<S**2>=2.093
180B→189B	0.12303	182B→188B	-0.39019	183B→189B	0.90815

Excited State 33:	3.061-AU	3.8156 eV	324.94 nm	f=0.0001	<S**2>=2.093
181B→189B	0.12396	182B→189B	0.90772	183B→188B	-0.38994

Excited State 34:	3.218-AG	3.9090 eV	317.18 nm	f=0.0000	<S**2>=2.339	
172A→191A	0.11124	149B→189B	-0.12144	174B→189B	-0.18876	
175A→190A	-0.13808	156B→189B	0.17056	174B→191B	-0.10216	
180A→190A	0.20043	160B→189B	0.10761	178B→188B	0.10617	
185A→191A	0.16215	161B→188B	-0.17384	178B→190B	0.14703	
186A→190A	0.13745	162B→189B	0.11925	179B→189B	0.43694	
189A→191A	0.26797	165B→188B	-0.23382	185B→189B	-0.10664	
189A→198A	-0.11670	169B→188B	0.42465			

Excited State 35:	3.420-AU	3.9180 eV	316.45 nm	f=0.0730	<S**2>=2.674	
172A→190A	0.12881	189A→205A	-0.11637	174B→188B	-0.15140	
175A→191A	-0.15659	149B→188B	-0.13591	174B→190B	0.10960	
180A→191A	0.12634	156B→188B	0.23302	178B→189B	0.33406	
180A→198A	-0.11308	160B→188B	0.11932	178B→191B	-0.14636	
185A→190A	0.15657	162B→188B	0.23871	179B→188B	0.26333	
189A→190A	0.18358	165B→189B	-0.19243	184B→191B	0.12515	
189A→199A	0.10527	169B→189B	0.32975	185B→190B	-0.10221	

Excited State 36:	3.828-AU	4.0202 eV	308.40 nm	f=0.0769	<S**2>=3.413	
173A→192A	0.14349	183A→203A	0.11569	174B→188B	-0.17641	
174A→193A	-0.11230	184A→202A	0.11607	175B→194B	0.18749	
174A→196A	-0.10449	186A→191A	-0.12241	176B→193B	-0.13481	
176A→194A	-0.20609	187A→192A	0.12640	177B→192B	0.12593	
177A→192A	0.10568	187A→206A	0.12077	178B→189B	0.30700	
177A→195A	0.10544	188A→193A	-0.14485	179B→188B	0.25325	
178A→193A	0.12309	188A→207A	0.12074	180B→201B	0.11290	
178A→196A	-0.11324	189A→190A	-0.19859	181B→200B	0.11519	
181A→201A	0.11698	169B→189B	0.12069	182B→202B	-0.11389	
182A→200A	0.11743	173B→196B	0.10573	183B→203B	-0.11157	

186B→193B	-0.14538	187B→192B	-0.13311		
186B→206B	0.12435	187B→205B	-0.12396		

Excited State 37: 3.897-AG 4.0532 eV 305.89 nm f=0.0000 <S**2>=3.546

173A→193A	0.14277	187A→193A	0.17976	177B→193B	-0.15326
173A→196A	0.13564	187A→196A	-0.12279	179B→189B	0.14153
174A→192A	-0.13650	187A→207A	-0.13630	180B→200B	0.12589
177A→193A	0.14141	188A→192A	-0.15644	181B→201B	0.12340
177A→196A	-0.13050	188A→195A	-0.11799	182B→203B	-0.12389
178A→192A	0.12096	188A→206A	-0.13615	183B→202B	-0.12643
178A→195A	0.12036	189A→191A	-0.17044	186B→192B	0.16612
181A→200A	0.12697	162B→189B	0.11403	186B→205B	0.13600
182A→201A	0.12655	165B→188B	-0.14100	187B→193B	0.18124
183A→202A	0.12741	169B→188B	0.28840	187B→206B	-0.13626
184A→203A	0.12707	172B→196B	-0.11222		
186A→190A	-0.15383	176B→192B	0.14055		

Excited State 38: 4.013-AG 4.1717 eV 297.20 nm f=0.0000 <S**2>=3.775

177A→191A	0.18622	188A→195A	0.11926	186B→197B	-0.10118
178A→190A	0.16896	188A→197A	-0.18432	187B→189B	-0.10356
187A→191A	0.48003	188A→205A	-0.12330	187B→191B	0.27295
187A→198A	0.10196	176B→188B	0.24073	187B→204B	0.10612
187A→204A	0.13175	177B→191B	-0.11412		
188A→190A	-0.47619	186B→190B	0.25602		

Excited State 39: 4.013-AU 4.1717 eV 297.20 nm f=0.0272 <S**2>=3.775

177A→190A	-0.16893	187A→197A	-0.18498	188A→204A	0.13166
178A→191A	-0.18619	187A→205A	-0.12335	176B→191B	0.11486
187A→190A	-0.47642	188A→191A	0.47956	177B→188B	-0.23885
187A→195A	0.11769	188A→198A	0.10180	186B→189B	-0.10355

186B→191B	0.27325	187B→190B	0.25583		
186B→204B	0.10621	187B→197B	-0.10148		

Excited State 40: 3.654-AU 4.2687 eV 290.45 nm f=0.0417 <S**2>=3.089

175A→191A	0.11632	189A→197A	0.13262	178B→191B	0.12890
176A→194A	-0.11721	156B→188B	-0.14016	179B→188B	0.12846
179A→190A	0.10486	162B→188B	-0.19919	184B→189B	0.15035
185A→190A	-0.21612	172B→188B	0.10097	184B→191B	-0.17092
186A→191A	0.13599	174B→188B	-0.21437	185B→190B	0.20516
186A→198A	0.12582	174B→190B	-0.11215	186B→193B	0.16631
187A→192A	-0.12611	175B→194B	0.11941	187B→192B	0.15164
188A→193A	0.14392	178B→189B	0.46307		

Excited State 41: 3.588-AG 4.3346 eV 286.03 nm f=0.0000 <S**2>=2.968

173A→193A	0.11837	189A→198A	0.12993	172B→196B	-0.13022
173A→196A	0.14219	151B→188B	-0.20242	173B→195B	0.10888
174A→192A	-0.11133	153B→189B	-0.12616	174B→189B	0.11067
175A→190A	0.10663	159B→188B	0.32232	178B→188B	-0.12077
185A→191A	-0.15072	160B→189B	0.28910	178B→190B	-0.10452
186A→190A	0.12782	161B→188B	-0.19919	184B→190B	0.15869
186A→197A	0.12036	169B→188B	0.19811	185B→191B	-0.18028
187A→193A	-0.11459	170B→189B	0.18469	186B→192B	-0.12609
188A→192A	0.10032	171B→188B	0.25306	187B→193B	-0.13708

Excited State 42: 3.184-AU 4.3510 eV 284.96 nm f=0.0130 <S**2>=2.284

179A→194A	-0.11120	153B→188B	-0.21859	169B→189B	0.12884
185A→194A	0.12399	159B→189B	0.32483	170B→188B	0.36253
189A→194A	0.18072	160B→188B	0.50811	171B→189B	0.21190
151B→189B	-0.20649	161B→189B	-0.15449	174B→188B	0.14856
152B→188B	-0.16087	166B→188B	0.17178	178B→189B	-0.22296

Excited State 43:	3.388-AG	4.3511 eV	284.95 nm	f=0.0000	<S**2>=2.619				
173A→193A	-0.16430	151B→188B	-0.22691	171B→188B	0.23438				
173A→196A	-0.18891	153B→189B	-0.14623	172B→189B	0.13572				
174A→192A	0.15854	156B→189B	-0.16825	172B→196B	0.17791				
174A→195A	-0.14117	159B→188B	0.29853	173B→195B	-0.14868				
174A→197A	-0.10096	160B→189B	0.20185	173B→197B	-0.12061				
186A→190A	-0.10669	161B→188B	-0.14778	174B→189B	-0.30655				
189A→191A	-0.15788	162B→189B	-0.17736	178B→188B	0.33507				
146B→188B	-0.13849	170B→189B	0.15501	179B→189B	0.14124				

Excited State 44:	3.550-AU	4.3962 eV	282.03 nm	f=0.0126	<S**2>=2.900				
172A→194A	-0.15107	189A→192A	0.33194	175B→188B	0.11897				
179A→192A	-0.11233	189A→194A	0.51962	179B→194B	0.20238				
179A→194A	-0.33669	160B→188B	-0.14250	185B→194B	0.15713				
185A→192A	0.18122	170B→188B	-0.12152						
185A→194A	0.37121	174B→194B	0.13329						

Excited State 45:	3.854-AU	4.4316 eV	279.77 nm	f=0.0919	<S**2>=3.464				
173A→192A	-0.22832	186A→198A	-0.10418	170B→188B	0.14347				
173A→195A	0.20846	189A→190A	-0.16116	172B→192B	0.11495				
173A→197A	0.15595	146B→189B	-0.11030	172B→195B	0.17888				
174A→193A	0.21679	149B→188B	0.10054	172B→197B	0.16311				
174A→196A	0.24721	151B→189B	-0.11002	173B→193B	0.12845				
175A→193A	-0.10739	153B→188B	-0.11482	173B→196B	-0.27292				
175A→196A	-0.12838	156B→188B	-0.13381	178B→189B	0.22894				
176A→192A	-0.10032	159B→189B	0.14581	184B→191B	0.15110				
186A→191A	-0.16021	160B→188B	0.17853	185B→190B	-0.12571				

Excited State 46:	3.306-AG	4.4879 eV	276.26 nm	f=0.0000	<S**2>=2.482				
172A→196A	0.10686	186A→194A	-0.13147	173B→188B	-0.29075				
175A→195A	0.11148	187A→191A	-0.13867	173B→190B	-0.11639				
179A→193A	0.14081	188A→190A	0.14575	177B→189B	-0.10329				
180A→192A	0.21907	189A→193A	0.47605	186B→190B	0.11192				
185A→196A	0.15513	189A→196A	0.10861	187B→191B	0.11406				
186A→192A	0.36114	172B→189B	-0.35529						

Excited State 47:	3.336-AU	4.4914 eV	276.05 nm	f=0.0029	<S**2>=2.532				
175A→196A	-0.10436	187A→190A	-0.14635	173B→189B	0.35486				
179A→192A	0.15491	188A→191A	0.13898	174B→188B	0.12528				
180A→193A	0.21319	189A→192A	0.40137	176B→189B	-0.10072				
180A→196A	0.12160	189A→194A	-0.25261	177B→188B	0.11003				
185A→195A	-0.14389	172B→188B	0.24507	186B→191B	-0.11765				
186A→193A	0.38564	172B→190B	0.11173	187B→190B	-0.11398				

Excited State 48:	3.465-AG	4.5068 eV	275.11 nm	f=0.0000	<S**2>=2.752				
172A→191A	0.11562	150B→188B	0.16396	172B→189B	-0.18059				
175A→190A	-0.11673	159B→188B	0.26078	174B→189B	0.44345				
180A→190A	0.14120	160B→189B	0.18474	174B→191B	-0.11908				
185A→191A	0.17980	162B→189B	0.13447	178B→188B	-0.22021				
186A→192A	-0.10741	165B→188B	0.10634	179B→189B	-0.17385				
186A→197A	-0.11682	166B→189B	0.10028	184B→190B	-0.18359				
189A→193A	-0.10451	170B→189B	0.11530	184B→197B	0.10219				
189A→198A	-0.14879	171B→188B	0.19992	185B→191B	0.19978				

Excited State 49:	3.434-AU	4.5517 eV	272.39 nm	f=0.0010	<S**2>=2.699				
181A→201A	0.12383	184A→202A	-0.12344	186A→196A	0.20546				
182A→200A	0.12386	185A→192A	0.11853	187A→190A	0.14899				
183A→203A	-0.12331	186A→193A	-0.19530	188A→191A	-0.13754				

189A→192A	-0.11300	174B→188B	0.16103	183B→203B	0.12248
189A→195A	-0.19944	176B→189B	-0.10359	184B→193B	0.10108
172B→188B	0.38275	180B→201B	0.12395	186B→191B	0.14163
172B→190B	0.11356	181B→200B	0.12537	187B→190B	0.12767
173B→189B	0.53811	182B→202B	0.12415		

Excited State 50: 3.437-AG 4.5535 eV 272.28 nm f=0.0000 <S**2>=2.703

181A→200A	-0.12901	188A→190A	0.14463	180B→200B	-0.13009
182A→201A	-0.12853	189A→193A	0.13077	181B→201B	-0.12835
183A→202A	0.11878	189A→196A	-0.22637	182B→203B	-0.11842
184A→203A	0.11857	172B→189B	0.46556	183B→202B	-0.11968
185A→193A	-0.13300	173B→188B	0.42487	185B→193B	-0.10842
186A→192A	0.15571	173B→190B	0.12642	186B→190B	0.12345
186A→194A	-0.10634	174B→189B	0.25382	187B→191B	0.13723
186A→195A	0.19535	175B→189B	-0.10406		
187A→191A	-0.13336	177B→189B	0.11188		

*C.2.5.4 **OTPB-BZN-210, EB** State*

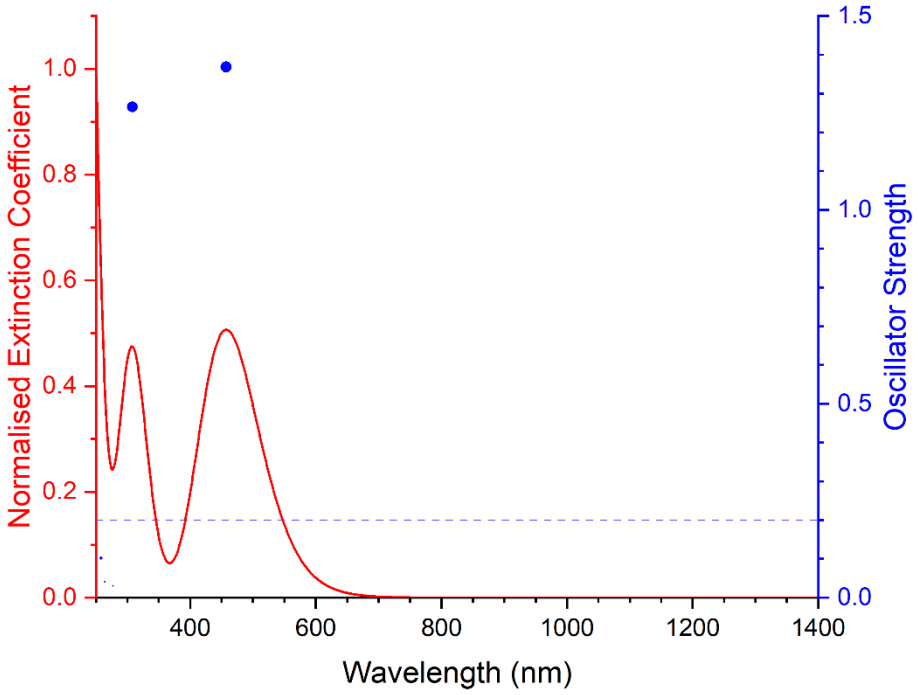

*Figure C-20 Excited states and normalised absorption spectra from TD-DFT calculations of **OTPB-BZN-210** in **EB** state. The areas of excited state dots are proportional to their oscillator strengths.*

Excited State 1:	**Singlet-AU**	**2.7109 eV**	**457.35 nm**	**f=1.3686**	**<S**2>=0.000**	
174→189	-0.16412	184→189	-0.11860	**188→189**	**0.65475**	
Excited State 2:	Singlet-AG	3.0262 eV	409.70 nm	f=0.0000	<S**2>=0.000	
170→189	-0.14052	183→189	0.28825			
175→189	0.23637	187→189	0.56353			
Excited State 3:	**Singlet-AU**	**4.0261 eV**	**307.95 nm**	**f=1.2657**	**<S**2>=0.000**	
169→189	-0.19057	176→189	-0.27081	188→189	0.15603	
174→189	**0.43500**	**178→189**	**-0.34337**	188→193	0.10048	
Excited State 4:	Singlet-AG	4.2763 eV	289.94 nm	f=0.0000	<S**2>=0.000	
173→189	0.61688	175→189	-0.11655	177→189	-0.27980	
Excited State 5:	Singlet-AG	4.4152 eV	280.81 nm	f=0.0000	<S**2>=0.000	
170→189	-0.10042	185→193	0.14721	187→191	-0.12075	
175→189	0.10062	186→190	-0.18206	188→192	0.11656	
185→189	0.58375	187→189	-0.10834			

Excited State 6:	Singlet-AU	4.4170 eV	280.70 nm	f=0.0070	<S**2>=0.000			
176→189	0.11541		186→189	0.59263		188→191	0.12109	
178→189	-0.11026		186→193	0.15110				
185→190	-0.18688		187→192	-0.12525				
Excited State 7:	Singlet-AG	4.4436 eV	279.02 nm	f=0.0000	<S**2>=0.000			
170→189	0.31439		177→189	-0.18131		187→189	0.33028	
173→189	-0.24208		183→189	-0.20954				
175→189	-0.30395		185→189	0.12925				
Excited State 8:	Singlet-AU	4.4698 eV	277.38 nm	f=0.0305	<S**2>=0.000			
176→189	-0.39602		178→189	0.47022		188→196	-0.15744	
177→190	-0.11929		186→189	0.16506				
Excited State 9:	Singlet-AG	4.4836 eV	276.53 nm	f=0.0000	<S**2>=0.000			
170→189	0.10915		177→189	0.54463		187→189	0.12363	
173→189	0.21271		183→189	-0.10016		187→196	0.11091	
175→189	-0.13063		185→189	0.14831		188→195	-0.10524	
Excited State 10:	Singlet-AU	4.6866 eV	264.55 nm	f=0.0413	<S**2>=0.000			
169→189	-0.17271		176→189	0.17305		184→189	0.58295	
174→189	0.17728		178→189	0.13857		188→189	0.15632	
Excited State 11:	Singlet-AG	4.8036 eV	258.11 nm	f=0.0000	<S**2>=0.000			
184→192	-0.19022		185→193	-0.18194		187→191	0.33769	
185→189	0.31299		186→190	0.17006		188→192	-0.33513	
Excited State 12:	Singlet-AU	4.8040 eV	258.08 nm	f=0.1019	<S**2>=0.000			
184→191	-0.19062		186→189	0.31368		187→192	0.33737	
185→190	0.17075		186→193	-0.18309		188→191	-0.33624	

Excited State 13:	Singlet-AG	4.8678 eV	254.70 nm	f=0.0000	<S**2>=0.000
187→193	0.31114	188→190	0.55618		
187→197	0.11136	188→194	0.15183		

C.2.6 Electronic Transitions in **OTPB-BZN-221** Oligomers

*Table C-10 Attributes of **OTPB-BZN-221** in **LEB**, **ES** (singlet and quintet), and **EB** states related to electronic structures*

Attribute	LEB State	^{1}ES State	^{5}ES State	EB State
Molecular Formula	$C_{60}H_{44}N_4$	$C_{60}H_{44}N_4^{4+}$	$C_{60}H_{44}N_4^{4+}$	$C_{60}H_{40}N_4$
Number of Atoms	108	108	108	104
Number of Electrons	432	428	428	428
HOMO	MO 216	MO 214	MOs 216A, 212B	MO 214
LUMO	MO 217	MO 215	MOs 217A, 213B	MO 215

*C.2.6.1 **OTPB-BZN-221**, **LEB** State*

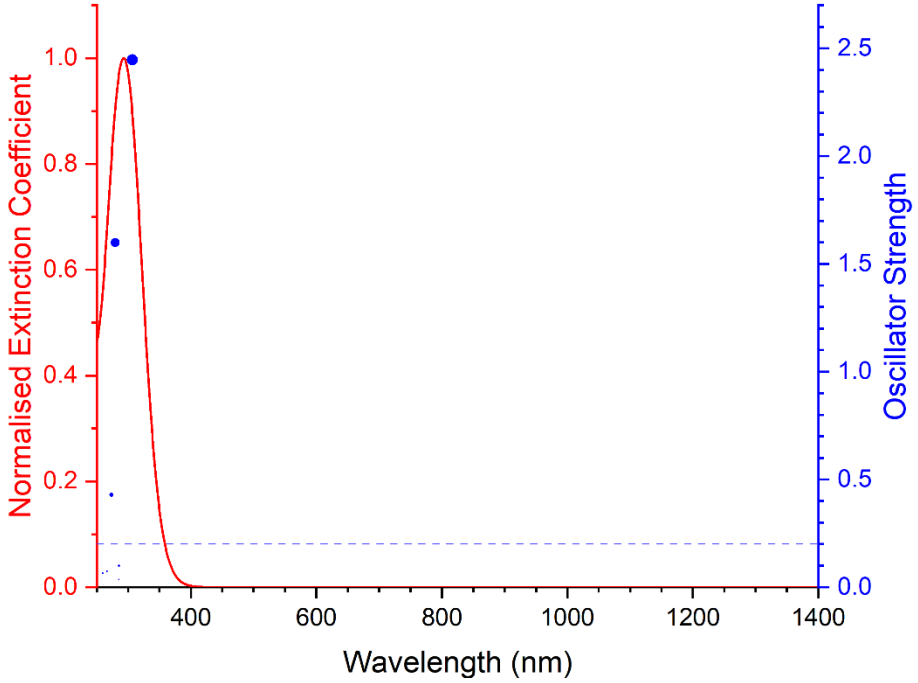

*Figure C-21 Excited states and normalised absorption spectra from TD-DFT calculations of **OTPB-BZN-221** in **LEB** state. The areas of excited state dots are proportional to their oscillator strengths.*

Excited State 1:	Singlet-A	3.8911 eV	318.64 nm	f=0.0000	<S**2>=0.000	
213→220	-0.18194	215→217	0.44040	216→221	-0.29528	
214→219	-0.12792	215→231	-0.15465			
214→228	0.11396	216→218	-0.32137			

Excited State 2:	**Singlet-B**	**4.0436 eV**	**306.62 nm**	**f=2.4468**	**<S**2>=0.000**
214→220	-0.19659	215→221	-0.29852	216→231	-0.15493
215→218	-0.26642	**216→217**	**0.48022**		
Excited State 3:	Singlet-B	4.3417 eV	285.57 nm	f=0.0982	<S**2>=0.000
213→217	0.12635	215→223	0.39648	216→222	0.42794
215→220	-0.20844	215→229	0.11555		
Excited State 4:	Singlet-A	4.3445 eV	285.39 nm	f=0.0349	<S**2>=0.000
214→217	0.11176	215→230	-0.10365	216→223	0.41358
215→222	0.42628	216→220	-0.19238	216→229	0.10912
Excited State 5:	**Singlet-B**	**4.4394 eV**	**279.28 nm**	**f=1.5983**	**<S**2>=0.000**
210→219	-0.14172	215→220	0.24920	216→228	-0.18816
213→217	-0.15465	215→223	0.13574		
214→218	**0.33239**	**216→219**	**0.40324**		
Excited State 6:	Singlet-A	4.4887 eV	276.21 nm	f=0.0001	<S**2>=0.000
210→218	-0.18411	213→220	-0.19644	216→218	0.35720
211→220	-0.11005	214→219	0.29006		
212→217	0.17234	215→217	0.21732		
Excited State 7:	Singlet-A	4.5237 eV	274.08 nm	f=0.0003	<S**2>=0.000
210→220	-0.10926	215→219	0.19560	216→220	0.43560
213→218	0.14770	215→222	0.10197	216→223	0.15780
214→217	-0.31586	215→228	-0.16462		
Excited State 8:	**Singlet-B**	**4.5371 eV**	**273.26 nm**	**f=0.4294**	**<S**2>=0.000**
210→219	0.15162	214→218	-0.17381	215→223	0.12951
212→220	0.20978	214→221	0.10669	216→219	-0.20277
213→217	**-0.31963**	**215→220**	**0.34816**	216→230	-0.10767

Excited State 9:	Singlet-B	4.6530 eV	266.46 nm	f=0.0738	<S**2>=0.000			
203→217	-0.10943		214→229	-0.15937		216→225	0.20344	
213→222	0.17906		215→218	0.15642		216→226	0.32123	
213→230	0.13534		215→224	0.29354				
214→223	0.20036		215→227	-0.20254				
Excited State 10:	Singlet-A	4.6827 eV	264.77 nm	f=0.0000	<S**2>=0.000			
204→217	0.10910		214→222	0.19508		215→226	0.29533	
213→223	0.18510		214→230	0.14686		216→224	0.30375	
213→229	-0.13895		215→225	0.19577		216→227	-0.20979	
Excited State 11:	Singlet-A	4.7487 eV	261.09 nm	f=0.0117	<S**2>=0.000			
213→224	-0.16681		214→226	-0.19078		216→229	0.37541	
213→227	0.11512		215→219	-0.16457				
214→225	-0.12130		215→230	-0.34792				
Excited State 12:	Singlet-B	4.7736 eV	259.73 nm	f=0.0653	<S**2>=0.000			
213→225	0.11842		214→224	0.19214		215→229	-0.36871	
213→226	0.17831		214→227	-0.13262		216→230	0.37373	

*C.2.6.2 **OTPB-BZN-221**, **¹ES** State*

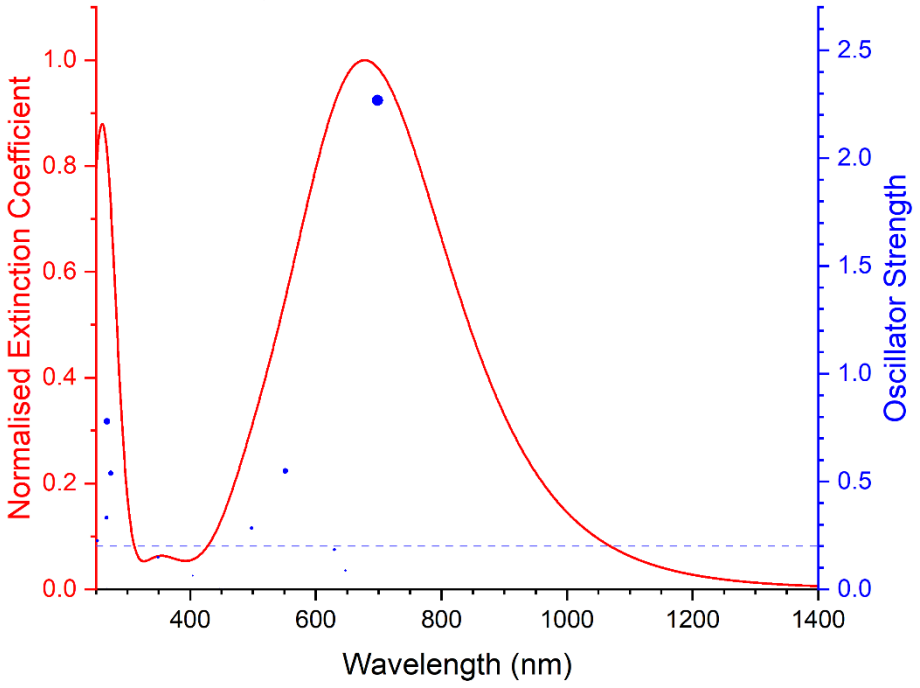

*Figure C-22 Excited states and normalised absorption spectra from TD-DFT calculations of **OTPB-BZN-221** in **¹ES** state. The areas of excited state dots are proportional to their oscillator strengths.*

Excited State 1:	Singlet-A	1.4257 eV	869.63 nm	f=0.0000	<S**2>=0.000
208→216	-0.26335	213→215	0.14390		
212→215	0.56586	214→216	-0.27436		
Excited State 2:	**Singlet-B**	**1.7755 eV**	**698.32 nm**	**f=2.2673**	**<S**2>=0.000**
208→215	-0.25231	213→216	0.15122		
212→216	**0.51432**	**214→215**	**-0.38040**		
Excited State 3:	Singlet-A	1.9034 eV	651.40 nm	f=0.0000	<S**2>=0.000
212→215	0.29901	214→216	0.62588		
Excited State 4:	Singlet-B	1.9150 eV	647.45 nm	f=0.0865	<S**2>=0.000
212→216	0.37856	213→216	0.13426	214→215	0.57702
Excited State 5:	Singlet-B	1.9686 eV	629.80 nm	f=0.1841	<S**2>=0.000
207→216	0.13034	212→216	-0.20028		
209→215	0.10360	213→216	0.65315		

Excited State 6:	Singlet-A	1.9741 eV	628.05 nm	f=0.0005	<S**2>=0.000
207→215	0.10216	212→215	-0.17677	213→215	0.67386
Excited State 7:	**Singlet-B**	**2.2472 eV**	**551.72 nm**	**f=0.5484**	**<S**2>=0.000**
200→216	0.10420	**209→215**	**0.64657**	213→216	-0.12602
207→216	0.16140	211→215	-0.12640		
Excited State 8:	Singlet-A	2.3570 eV	526.02 nm	f=0.0055	<S**2>=0.000
200→215	0.10946	209→216	0.65162		
207→215	0.17944	211→216	-0.13004		
Excited State 9:	**Singlet-B**	**2.4901 eV**	**497.91 nm**	**f=0.2833**	**<S**2>=0.000**
201→216	0.10692	212→216	0.21966		
208→215	**0.63969**	214→215	-0.13462		
Excited State 10:	Singlet-A	2.5195 eV	492.10 nm	f=0.0000	<S**2>=0.000
201→215	0.10633	212→215	0.22718		
208→216	0.63281	214→216	-0.15793		
Excited State 11:	Singlet-A	2.7160 eV	456.49 nm	f=0.0000	<S**2>=0.000
210→215	0.70344				
Excited State 12:	Singlet-B	2.7161 eV	456.47 nm	f=0.0001	<S**2>=0.000
209→215	0.13027	211→215	0.69100		
Excited State 13:	Singlet-B	2.7327 eV	453.70 nm	f=0.0000	<S**2>=0.000
210→216	0.70203				
Excited State 14:	Singlet-A	2.7328 eV	453.68 nm	f=0.0000	<S**2>=0.000
209→216	0.13294	211→216	0.68822		

Excited State 15:	Singlet-B	2.7414 eV	452.26 nm	f=0.0026	<S**2>=0.000
198→215	-0.10337	205→216	-0.45601		
202→215	-0.19488	206→215	0.45845		
Excited State 16:	Singlet-A	2.7416 eV	452.24 nm	f=0.0000	<S**2>=0.000
197→215	0.10338	205→215	0.47788		
202→216	0.18562	206→216	-0.43627		
Excited State 17:	Singlet-B	2.7764 eV	446.56 nm	f=0.0057	<S**2>=0.000
202→215	-0.13145	203→215	0.48520	204→216	0.47471
Excited State 18:	Singlet-A	2.7767 eV	446.52 nm	f=0.0053	<S**2>=0.000
202→216	-0.12512	203→216	0.46186	204→215	0.49793
Excited State 19:	Singlet-A	3.0577 eV	405.48 nm	f=0.0024	<S**2>=0.000
199→216	-0.14144	207→215	0.63549		
200→215	0.13037	209→216	-0.21107		
Excited State 20:	Singlet-B	3.0655 eV	404.44 nm	f=0.0627	<S**2>=0.000
199→215	-0.14316	207→216	0.63796		
200→216	0.11015	209→215	-0.20115		
Excited State 21:	Singlet-A	3.1072 eV	399.02 nm	f=0.0000	<S**2>=0.000
197→215	0.49364	198→216	0.47305	205→215	-0.10140
Excited State 22:	Singlet-B	3.1072 eV	399.02 nm	f=0.0001	<S**2>=0.000
197→216	0.47578	198→215	0.49068		
Excited State 23:	Singlet-A	3.5273 eV	351.50 nm	f=0.0001	<S**2>=0.000
201→215	0.55321	203→216	0.10458	206→216	0.14872
202→216	0.33318	205→215	0.10458	208→216	-0.13067

Excited State 24:	Singlet-B	3.5520 eV	349.05 nm	f=0.1479	<S**2>=0.000			
201→216	0.50366		203→215	0.12134		206→215	0.17746	
202→215	0.38446		205→216	0.10345		208→215	-0.13951	
Excited State 25:	Singlet-A	3.8212 eV	324.46 nm	f=0.0020	<S**2>=0.000			
199→216	-0.34106		200→215	0.54635		207→215	-0.21151	
Excited State 26:	Singlet-B	3.8279 eV	323.89 nm	f=0.0015	<S**2>=0.000			
199→215	-0.38145		200→216	0.52953		207→216	-0.19561	
Excited State 27:	Singlet-A	3.8429 eV	322.63 nm	f=0.0000	<S**2>=0.000			
201→215	-0.38292		203→216	0.15620				
202→216	0.46518		206→216	0.29007				
Excited State 28:	Singlet-B	3.8681 eV	320.53 nm	f=0.0009	<S**2>=0.000			
201→216	0.45476		203→215	-0.12956				
202→215	-0.41949		206→215	-0.29902				
Excited State 29:	Singlet-A	3.9061 eV	317.41 nm	f=0.0000	<S**2>=0.000			
202→216	-0.25640		205→215	0.48394				
203→216	-0.12964		206→216	0.42473				
Excited State 30:	Singlet-B	3.9068 eV	317.35 nm	f=0.0003	<S**2>=0.000			
202→215	-0.27440		205→216	0.50650				
203→215	-0.13827		206→215	0.38343				
Excited State 31:	Singlet-B	3.9194 eV	316.33 nm	f=0.0000	<S**2>=0.000			
202→215	0.17124		203→215	-0.45039		204→216	0.50855	
Excited State 32:	Singlet-A	3.9197 eV	316.31 nm	f=0.0000	<S**2>=0.000			
202→216	0.17746		203→216	-0.47437		204→215	0.48483	

Excited State 33:	Singlet-B	4.3775 eV	283.23 nm	f=0.0001	<S**2>=0.000	
199→215	0.52113	200→216	0.39648	214→217	-0.12394	
Excited State 34:	Singlet-A	4.4230 eV	280.32 nm	f=0.0001	<S**2>=0.000	
199→216	0.57123	200→215	0.39208			
Excited State 35:	**Singlet-B**	**4.5269 eV**	**273.89 nm**	**f=0.5383**	**<S**2>=0.000**	
199→215	0.13797	208→217	0.16484	213→221	-0.19632	
200→216	0.12818	212→218	-0.12289	**214→217**	**0.46532**	
207→219	-0.10239	213→219	-0.25038	214→224	-0.16611	
Excited State 36:	Singlet-A	4.5574 eV	272.05 nm	f=0.0000	<S**2>=0.000	
207→217	0.10358	213→217	0.41300	214→221	-0.23891	
209→223	-0.12166	213→224	-0.18882			
212→222	0.14866	214→219	-0.31005			
Excited State 37:	Singlet-A	4.6227 eV	268.21 nm	f=0.0077	<S**2>=0.000	
208→218	-0.24881	209→221	0.12415	214→218	-0.21066	
209→219	0.17800	212→217	0.54472			
Excited State 38:	**Singlet-B**	**4.6331 eV**	**267.60 nm**	**f=0.7791**	**<S**2>=0.000**	
208→217	-0.23605	**212→218**	**0.51245**	213→218	0.13685	
209→222	-0.22300	212→223	0.10786			
Excited State 39:	**Singlet-B**	**4.6434 eV**	**267.01 nm**	**f=0.3321**	**<S**2>=0.000**	
182→215	-0.10947	**191→216**	**0.38152**	209→217	-0.11030	
188→215	0.10665	**192→215**	**0.38140**	212→218	0.10734	
189→215	-0.10964	194→215	-0.22360	212→219	-0.13722	
Excited State 40:	Singlet-A	4.6537 eV	266.42 nm	f=0.0000	<S**2>=0.000	
182→216	-0.11533	188→216	0.10929	191→215	0.42050	
186→215	0.10047	189→216	-0.11380	192→216	0.36958	

194→216	-0.22049	212→222	0.11172		

Excited State 41:	**Singlet-B**	**4.9127 eV**	**252.38 nm**	**f=0.2249**	**<S**2>=0.000**
209→217	0.20674	**213→218**	**0.32779**	214→229	0.11576
212→219	0.19026	213→223	0.23483		
212→221	0.11875	**214→222**	**0.33890**		

Excited State 42:	Singlet-A	4.9486 eV	250.55 nm	f=0.0004	<S**2>=0.000
212→217	0.14302	213→229	0.18008	214→223	0.31430
213→222	0.37428	214→218	0.36976	214→228	0.12234

*C.2.6.3 **OTPB-BZN-221**, **^{5}ES** State*

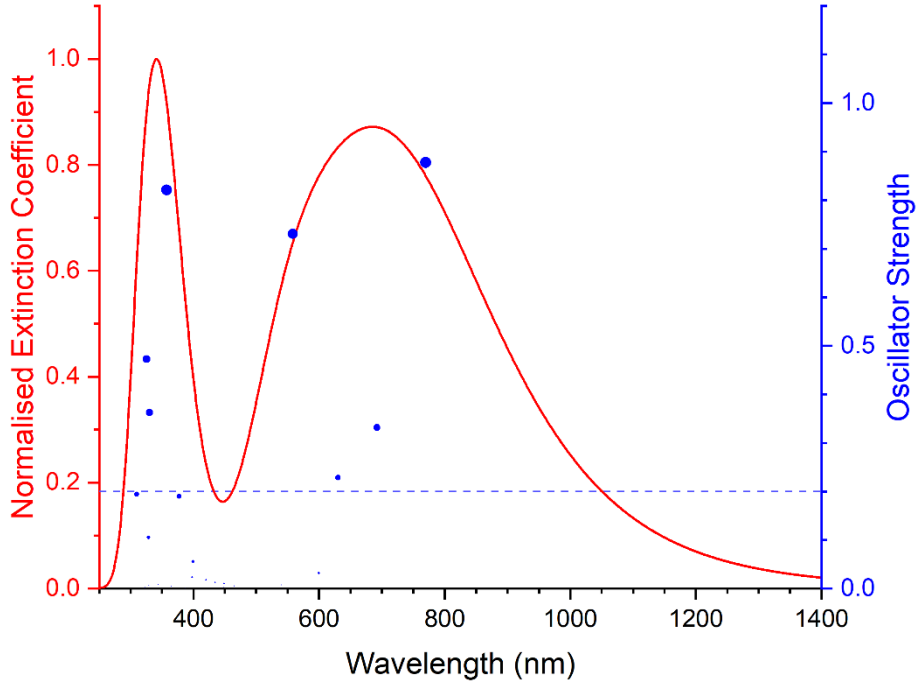

*Figure C-23 Excited states and normalised absorption spectra from TD-DFT calculations of **OTPB-BZN-221** in **^{5}ES** state. The areas of excited state dots are proportional to their oscillator strengths.*

Excited State 1:	5.099-A	1.3630 eV	909.63 nm	f=0.0000	<S**2>=6.249
205B→216B	-0.15374	207B→214B	-0.42801	211B→216B	0.20067
206B→215B	-0.24056	208B→213B	0.67638	212B→214B	0.44624

Excited State 2:	**5.097-B**	**1.6103 eV**	**769.94 nm**	**f=0.8778**	**<S**2>=6.244**
205B→215B	-0.15127	**207B→213B**	**-0.43829**	211B→215B	0.24305
206B→216B	-0.17246	**208B→214B**	**0.49136**	**212B→213B**	**0.62057**

Excited State 3:	**5.093-B**	**1.7916 eV**	**692.03 nm**	**f=0.3315**	**<S**2>=6.234**	
205B→214B	-0.21547	208B→215B	0.12871	**212B→216B**	**0.48024**	
206B→213B	-0.14322	**211B→214B**	**0.78508**			
207B→216B	-0.10868	211B→217B	0.10917			
Excited State 4:	5.085-A	1.8260 eV	678.99 nm	f=0.0018	<S**2>=6.214	
205B→213B	-0.21444	207B→215B	-0.10387	212B→215B	0.42545	
206B→214B	-0.10434	211B→213B	0.83160			
Excited State 5:	5.097-A	1.8852 eV	657.66 nm	f=0.0000	<S**2>=6.245	
200B→214B	0.10457	207B→214B	0.13947	212B→214B	0.71479	
201B→214B	-0.15388	208B→213B	-0.44503	212B→217B	0.10900	
206B→215B	0.13516	211B→216B	0.40000			
Excited State 6:	**5.094-B**	**1.9662 eV**	**630.57 nm**	**f=0.2285**	**<S**2>=6.237**	
200B→213B	0.13375	207B→213B	0.28523	**212B→213B**	**0.62682**	
201B→213B	-0.16491	**208B→214B**	**-0.55421**			
206B→216B	0.17652	211B→215B	0.29755			
Excited State 7:	5.092-B	2.0672 eV	599.77 nm	f=0.0319	<S**2>=6.231	
197B→215B	0.10456	200B→216B	0.36666	203B→214B	0.26369	
198B→213B	0.50385	201B→216B	0.13036	204B→213B	0.29647	
199B→214B	0.45508	202B→215B	-0.40617	206B→213B	0.13475	
Excited State 8:	5.092-A	2.0688 eV	599.30 nm	f=0.0008	<S**2>=6.232	
197B→216B	0.10038	200B→215B	0.39447	203B→213B	0.29896	
198B→214B	0.45185	201B→215B	0.14727	204B→214B	0.26413	
199B→213B	0.51208	202B→216B	-0.37670			

Excited State 9:	5.092-A	2.0771 eV	596.90 nm	f=0.0000	<S**2>=6.231
197B→213B	-0.15355	200B→214B	-0.48808	203B→216B	-0.17562
198B→215B	-0.37971	201B→214B	-0.19055	204B→215B	-0.19122
199B→216B	-0.35342	202B→213B	0.56956		
Excited State 10:	5.092-B	2.0773 eV	596.85 nm	f=0.0045	<S**2>=6.231
197B→214B	0.13575	200B→213B	0.54444	203B→215B	0.19001
198B→216B	0.35070	201B→213B	0.21925	204B→216B	0.17573
199B→215B	0.38005	202B→214B	-0.50480		
Excited State 11:	**5.079-B**	**2.2209 eV**	**558.26 nm**	**f=0.7303**	**<S**2>=6.199**
196B→214B	0.16941	**206B→213B**	**-0.55270**	**208B→215B**	**0.62229**
205B→214B	-0.13751	207B→216B	-0.30519	211B→214B	-0.28117
Excited State 12:	5.099-A	2.2966 eV	539.85 nm	f=0.0076	<S**2>=6.249
212A→217A	0.13609	205B→213B	-0.15029	208B→216B	0.59215
216A→219A	-0.14852	206B→214B	-0.49081	211B→213B	-0.31006
196B→213B	0.16794	207B→215B	-0.34050		
Excited State 13:	5.185-B	2.6668 eV	464.92 nm	f=0.0053	<S**2>=6.470
208A→217A	0.12306	201B→213B	-0.20290	208B→214B	0.31363
212A→219A	0.14969	202B→214B	0.10522	208B→217B	0.14936
197B→214B	0.40683	206B→216B	-0.35286	211B→215B	0.26523
200B→213B	0.11329	207B→213B	0.49269	212B→213B	-0.10924
Excited State 14:	5.083-A	2.7311 eV	453.98 nm	f=0.0000	<S**2>=6.210
209B→215B	-0.31381	210B→213B	0.94072		
Excited State 15:	5.083-B	2.7312 eV	453.96 nm	f=0.0000	<S**2>=6.208
209B→213B	0.94607	210B→215B	-0.31075		
Excited State 16:	5.141-A	2.7625 eV	448.81 nm	f=0.0030	<S**2>=6.357

198B→214B	-0.27842	203B→218B	0.10451	205B→213B	-0.11946
199B→213B	-0.32389	204B→214B	0.56288		
203B→213B	0.64296	204B→217B	-0.11024		

Excited State 17: 5.141-B 2.7625 eV 448.80 nm f=0.0105 <S**2>=6.357

198B→213B	-0.32003	203B→217B	-0.10768	205B→214B	-0.10057
199B→214B	-0.28410	204B→213B	0.65602		
203B→214B	0.55176	204B→218B	0.10751		

Excited State 18: 5.085-A 2.7706 eV 447.50 nm f=0.0000 <S**2>=6.215

209B→214B	0.90017	210B→216B	-0.38817		

Excited State 19: 5.085-B 2.7717 eV 447.32 nm f=0.0001 <S**2>=6.215

208B→214B	-0.10748	209B→216B	-0.39522	210B→214B	0.90266

Excited State 20: 5.159-A 2.7747 eV 446.83 nm f=0.0000 <S**2>=6.405

190B→214B	-0.10547	202B→213B	0.13055	208B→218B	-0.11727
197B→213B	0.48701	206B→215B	-0.34912	211B→216B	0.23040
200B→214B	0.10246	207B→214B	0.51548	212B→214B	-0.11095
201B→214B	-0.19471	208B→213B	0.28459		

Excited State 21: 5.090-A 2.8145 eV 440.52 nm f=0.0002 <S**2>=6.227

197B→216B	-0.26548	207B→215B	-0.37641	211B→213B	-0.28263
206B→214B	0.47961	209B→214B	-0.13487	212B→215B	0.62497

Excited State 22: 5.087-B 2.8508 eV 434.91 nm f=0.0125 <S**2>=6.219

197B→215B	-0.32236	207B→216B	-0.40523	212B→216B	0.45516
201B→216B	0.10445	208B→215B	0.24289		
206B→213B	0.56717	211B→214B	-0.25239		

Excited State 23:	5.128-B	2.9492 eV	420.40 nm	f=0.0178	<S**2>=6.324	
201B→213B	-0.10456	207B→213B	-0.38417	211B→215B	0.66789	
205B→215B	-0.21142	208B→214B	-0.28058	212B→213B	-0.42731	

Excited State 24:	5.237-A	3.0417 eV	407.61 nm	f=0.0019	<S**2>=6.605	
214A→221A	0.10139	201B→215B	-0.24200	211B→213B	-0.31579	
215A→220A	0.11610	205B→213B	-0.14113	211B→218B	-0.11691	
215A→229A	0.10745	206B→214B	-0.20784	211B→223B	-0.10646	
191B→214B	-0.10777	207B→215B	0.33650	212B→215B	0.45971	
197B→216B	0.23919	208B→216B	-0.34066	212B→220B	-0.15746	

Excited State 25:	5.098-A	3.0788 eV	402.70 nm	f=0.0000	<S**2>=6.248	
201B→214B	-0.12072	207B→214B	-0.34923	211B→216B	0.69154	
205B→216B	-0.23160	208B→213B	-0.18481	212B→214B	-0.50722	

Excited State 26:	5.334-B	3.1051 eV	399.29 nm	f=0.0553	<S**2>=6.863	
211A→232A	0.10854	205B→214B	-0.10042	211B→215B	0.45860	
212A→219A	-0.14571	205B→215B	0.10388	211B→220B	0.15649	
214A→220A	-0.17724	206B→213B	-0.10721	211B→229B	0.14798	
214A→229A	-0.14581	207B→213B	0.24152	212B→216B	0.29214	
215A→218A	-0.15034	208B→214B	0.24597	212B→218B	0.10551	
215A→221A	-0.12776	208B→215B	-0.15798	212B→223B	0.13865	
215A→226A	-0.11449	209B→231B	-0.10865	212B→226B	-0.12074	
216A→217A	0.13021	210B→232B	0.10842			
201B→213B	0.13570	211B→214B	-0.22114			

Excited State 27:	5.172-B	3.1153 eV	397.98 nm	f=0.0232	<S**2>=6.437	
197B→215B	0.16753	206B→213B	-0.23698	208B→214B	-0.12647	
201B→216B	-0.18600	207B→213B	-0.10845	208B→215B	-0.31875	
205B→214B	-0.15809	207B→216B	0.13356	211B→214B	-0.41849	

211B→215B	-0.22885	212B→216B	0.55493		

Excited State 28:	5.163-A	3.1948 eV	388.08 nm	f=0.0000	<S**2>=6.413
216A→218A	0.11210	202B→213B	-0.11064	208B→213B	0.33256
190B→214B	0.15871	205B→216B	0.25793	211B→216B	0.40071
197B→213B	-0.24833	206B→215B	0.26067		
201B→214B	0.24992	207B→214B	0.46932		

Excited State 29:	5.562-A	3.2021 eV	387.20 nm	f=0.0008	<S**2>=7.483
210A→232A	0.17616	214A→230A	-0.12930	211B→218B	0.13447
211A→231A	0.11724	215A→220A	-0.21923	211B→223B	0.20051
211A→233A	-0.14373	215A→229A	-0.18653	211B→226B	-0.17281
212A→217A	-0.10425	197B→216B	0.11258	211B→230B	0.12019
213A→229A	-0.10689	206B→214B	-0.32601	212B→215B	0.33192
214A→218A	-0.17037	207B→215B	0.19073	212B→220B	0.23053
214A→221A	-0.18332	209B→232B	-0.17923	212B→229B	0.21205
214A→226A	-0.16807	210B→231B	0.17820		

Excited State 30:	5.399-B	3.2876 eV	377.13 nm	f=0.1898	<S**2>=7.037
208A→225A	0.11943	190B→213B	0.16338	207B→213B	0.30282
210A→233A	0.10541	197B→214B	-0.20717	208B→214B	0.14339
211A→232A	-0.13009	201B→213B	0.23185	209B→231B	0.12649
213A→221A	0.13891	202B→214B	-0.10735	210B→232B	-0.12592
214A→220A	0.10666	203B→215B	-0.20190	211B→215B	0.16033
214A→229A	0.12557	204B→216B	-0.21951	211B→220B	-0.14733
215A→218A	0.13308	204B→221B	-0.10807	211B→229B	-0.14468
215A→230A	0.11911	205B→215B	0.23988	212B→223B	-0.14558
216A→217A	-0.15128	206B→216B	0.21431	212B→226B	0.11249

Excited State 31:	5.103-A	3.3348 eV	371.79 nm	f=0.0000	<S**2>=6.260
197B→213B	-0.10538	199B→216B	-0.22162	204B→215B	0.65446
198B→215B	-0.24286	203B→216B	0.57845	205B→213B	-0.15670
Excited State 32:	5.146-B	3.3408 eV	371.12 nm	f=0.0019	<S**2>=6.371
197B→214B	-0.13585	200B→213B	-0.10556	204B→216B	0.55765
198B→216B	-0.21012	201B→213B	0.11350	207B→213B	0.11730
199B→215B	-0.23365	203B→215B	0.63237		
Excited State 33:	5.132-A	3.3510 eV	369.99 nm	f=0.0004	<S**2>=6.334
190B→215B	0.10883	203B→213B	0.13494	207B→215B	0.25743
191B→214B	-0.13698	203B→216B	0.13236	208B→216B	0.34944
196B→213B	-0.16529	204B→215B	0.14657	212B→215B	0.22850
201B→215B	0.19071	205B→213B	0.69340		
Excited State 34:	5.090-B	3.3954 eV	365.16 nm	f=0.0043	<S**2>=6.226
191B→213B	-0.13589	203B→214B	0.12933	207B→216B	0.38878
196B→214B	-0.10024	205B→214B	0.69340	208B→215B	0.29962
201B→216B	0.20985	206B→213B	-0.12073	212B→216B	0.32692
Excited State 35:	**5.442-B**	**3.4710 eV**	**357.20 nm**	**f=0.8209**	**<S**2>=7.152**
205A→223A	0.10873	213A→218A	0.30572	203B→222B	0.10307
206A→222A	-0.10800	214A→229A	0.13382	204B→221B	0.10170
207A→221A	-0.10081	214A→235A	0.11223	208B→214B	0.15487
208A→225A	-0.16390	215A→218A	-0.13896	209B→231B	0.16443
209A→220A	-0.17835	215A→221A	0.12752	210B→232B	-0.16471
210A→233A	0.11695	215A→226A	0.10366	211B→229B	-0.10096
211A→232A	-0.14982	**216A→217A**	**0.46132**		
212A→219A	-0.31038	203B→215B	-0.11157		

Excited State 36:	5.222-A	3.5062 eV	353.61 nm	f=0.0000	<S**2>=6.567	
205A→222A	0.10820	213A→217A	0.35542	201B→214B	-0.10549	
206A→223A	-0.11033	213A→225A	-0.13502	203B→221B	-0.10889	
207A→225A	-0.10577	214A→219A	-0.12718	204B→215B	0.12266	
208A→221A	-0.11475	215A→217A	-0.30777	204B→222B	-0.11318	
209A→219A	-0.24550	216A→218A	0.47292	205B→216B	-0.10743	
212A→220A	-0.26289	197B→213B	0.17441	206B→215B	-0.23808	

Excited State 37:	5.539-A	3.6051 eV	343.91 nm	f=0.0081	<S**2>=7.419	
207A→220A	0.14735	212A→225A	0.10265	207B→220B	0.10729	
208A→219A	0.18952	213A→220A	-0.13542	208B→219B	0.16090	
209A→218A	0.19328	214A→236A	-0.14465	209B→232B	-0.19833	
210A→232A	0.18189	215A→235A	-0.12975	210B→231B	0.19704	
211A→231A	0.11902	216A→219A	-0.33487	211B→236B	-0.12576	
211A→233A	-0.14698	206B→214B	0.22440	212B→234B	0.10591	
212A→217A	0.36051	206B→217B	-0.12666			

Excited State 38:	5.082-B	3.6578 eV	338.96 nm	f=0.0003	<S**2>=6.206	
209B→213B	0.31625	210B→215B	0.94416			

Excited State 39:	5.082-A	3.6578 eV	338.96 nm	f=0.0000	<S**2>=6.207	
209B→215B	0.94643	210B→213B	0.31571			

Excited State 40:	5.194-A	3.7406 eV	331.46 nm	f=0.0000	<S**2>=6.494	
214A→219A	0.14755	201B→214B	0.53757	208B→213B	-0.29760	
215A→217A	0.14244	205B→216B	0.22894	211B→216B	0.19357	
196B→216B	0.19732	205B→219B	0.11940	211B→219B	-0.10107	
200B→214B	-0.16593	206B→215B	-0.48064	212B→217B	-0.11008	

Excited State 41:	**5.162-B**	**3.7572 eV**	**329.99 nm**	**f=0.3624**	**<S**2>=6.411**	
209A→217A	0.21457	212A→218A	0.23233	213A→219A	-0.20590	

215A→219A	0.12533	197B→215B	0.15763	206B→213B	0.20894
216A→220A	-0.24804	201B→213B	0.20655	207B→216B	0.11741
191B→213B	-0.23959	201B→216B	-0.20696	**208B→215B**	**0.37138**
196B→214B	-0.22760	205B→214B	-0.23674		

Excited State 42: 5.100-B 3.7671 eV 329.12 nm f=0.0057 <S**2>=6.252

209B→216B	0.89424	210B→214B	0.39917		

Excited State 43: 5.086-A 3.7676 eV 329.08 nm f=0.0000 <S**2>=6.218

209B→214B	0.40405	210B→216B	0.90705		

Excited State 44: 5.360-B 3.7723 eV 328.67 nm f=0.1052 <S**2>=6.931

205A→223A	0.10511	212A→219A	0.17654	203B→222B	0.11790
205A→228A	-0.13551	213A→219A	0.11091	204B→221B	0.11999
206A→222A	-0.10010	213A→230A	0.10774	204B→227B	-0.10026
206A→227A	-0.12905	216A→220A	0.12927	205B→215B	0.20120
207A→218A	0.10439	216A→225A	-0.16751	207B→218B	0.11770
208A→217A	0.17771	197B→214B	-0.12894	208B→215B	-0.13643
209A→217A	-0.11499	200B→213B	-0.16049	208B→217B	0.17388
212A→218A	-0.13039	201B→213B	0.45682	209B→216B	-0.14233

Excited State 45: 5.405-A 3.8049 eV 325.86 nm f=0.0000 <S**2>=7.052

197A→218A	0.10713	208A→218A	0.14384	216A→230A	0.19116
198A→217A	0.12045	209A→219A	0.20691	187B→213B	0.15609
200A→223A	0.10827	212A→220A	0.22521	191B→215B	-0.19968
205A→222A	0.12858	213A→224A	-0.10370	196B→216B	-0.15265
205A→227A	0.15150	213A→225A	-0.14268	197B→213B	0.20316
206A→223A	-0.12976	215A→217A	0.11781	197B→218B	-0.10958
206A→228A	0.15869	216A→218A	-0.16168	201B→214B	-0.16632
207A→217A	0.13448	216A→221A	-0.11027	202B→213B	0.10166

203B→221B	-0.14343	204B→228B	-0.11544	208B→218B	0.15477
203B→227B	0.12030	207B→217B	0.15203		
204B→222B	-0.14970	207B→225B	-0.11364		

Excited State 46: 5.318-B 3.8129 eV 325.17 nm f=0.4725 <S2>=6.821**

207A→219A	0.16073	216A→220A	-0.27479	207B→216B	-0.24726
208A→220A	0.10820	191B→213B	0.11993	208B→215B	-0.27416
209A→217A	0.25418	196B→214B	0.18984	211B→217B	-0.10435
212A→218A	0.28558	197B→215B	-0.12470	212B→216B	0.10436
213A→219A	-0.11240	201B→216B	0.18970	212B→219B	-0.12600
214A→217A	0.26738	205B→214B	0.13676		
215A→219A	**0.32586**	206B→213B	-0.13954		

Excited State 47: 5.288-B 3.8343 eV 323.36 nm f=0.0023 <S**2>=6.740

205A→228A	-0.10208	197B→214B	-0.17872	206B→216B	0.52300
207A→218A	0.10597	200B→213B	0.11022	208B→214B	0.32273
211A→232A	0.10393	201B→213B	-0.39835	209B→231B	-0.10871
196B→215B	-0.17903	205B→220B	0.11082	210B→232B	0.10851

Excited State 48: 5.117-A 3.8367 eV 323.16 nm f=0.0010 <S**2>=6.295

209A→218A	-0.13584	194B→213B	0.11862	206B→214B	0.28670
212A→217A	-0.18703	196B→213B	-0.27676	207B→215B	0.18458
213A→220A	0.13308	197B→216B	0.12211	208B→216B	0.51072
216A→219A	0.21653	201B→215B	-0.23321		
191B→214B	-0.20688	205B→213B	-0.33828		

Excited State 49: 5.221-B 4.0066 eV 309.45 nm f=0.1938 <S**2>=6.565

197A→217A	0.11954	209A→220A	0.14938	215A→218A	0.10610
199A→219A	0.14745	213A→218A	-0.20845	216A→217A	-0.18880
204A→220A	0.10413	213A→230A	0.10380	216A→234A	0.12560

183B→214B	-0.12216	196B→215B	0.22807	205B→215B	-0.23800
187B→214B	-0.22499	197B→214B	-0.21940	206B→216B	0.15468
188B→213B	0.10201	197B→217B	-0.13315	206B→219B	0.16764
190B→213B	-0.22168	201B→213B	-0.17741	207B→213B	0.24578
191B→216B	0.27104	202B→214B	-0.17339		

Excited State 50: 5.155-A 4.0504 eV 306.11 nm f=0.0015 <S**2>=6.394

209A→218A	0.10233	190B→215B	-0.11190	206B→214B	0.30629
212A→217A	0.15919	191B→214B	0.24816	207B→215B	0.55491
213A→220A	-0.13726	194B→213B	-0.10761	208B→216B	0.28018
216A→219A	-0.20485	196B→213B	0.25711		
187B→216B	-0.13321	205B→213B	-0.18383		

*C.2.6.4 **OTPB-BZN-221**, **EB** State*

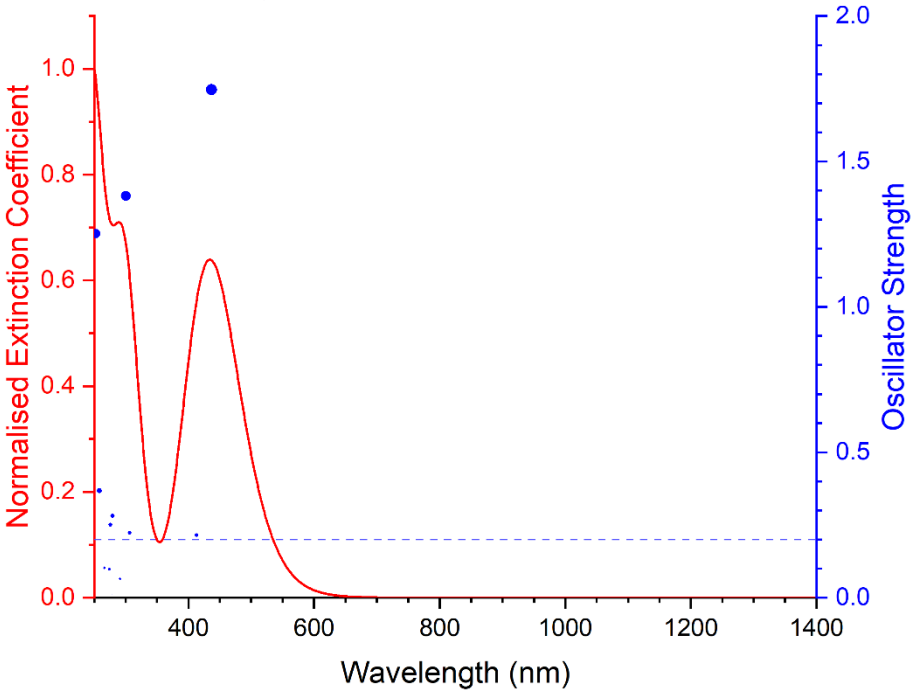

*Figure C-24 Excited states and normalised absorption spectra from TD-DFT calculations of **OTPB-BZN-221** in **EB** state. The areas of excited state dots are proportional to their oscillator strengths.*

Excited State 1: Singlet-A 2.7159 eV 456.52 nm f=0.0000 <S**2>=0.000

199→216	0.11335	213→215	0.44528	214→216	0.48834

Excited State 2:	**Singlet-B**	**2.8391 eV**	**436.70 nm**	**f=1.7473**	**<S**2>=0.000**				
199→215	0.13436		**213→216**	**0.43787**					
210→216	-0.10077		**214→215**	**0.48736**					
Excited State 3:	**Singlet-B**	**3.0042 eV**	**412.70 nm**	**f=0.2149**	**<S**2>=0.000**				
194→215	-0.10420		200→216	-0.21705		**211→215**	**0.35353**		
198→215	-0.11790		209→215	-0.27274		**212→216**	**0.44532**		
Excited State 4:	Singlet-A	3.0214 eV	410.35 nm	f=0.0023	<S**2>=0.000				
194→216	-0.10886		200→215	-0.21958		211→216	0.35056		
198→216	-0.12310		209→216	-0.27654		212→215	0.44112		
Excited State 5:	Singlet-A	4.0110 eV	309.11 nm	f=0.0000	<S**2>=0.000				
213→215	0.47648		214→216	-0.46893					
Excited State 6:	**Singlet-B**	**4.0417 eV**	**306.76 nm**	**f=0.2225**	**<S**2>=0.000**				
199→215	-0.14269		**213→216**	**-0.44718**					
201→216	-0.12249		**214→215**	**0.48309**					
Excited State 7:	Singlet-A	4.0621 eV	305.22 nm	f=0.0000	<S**2>=0.000				
191→216	0.12653		199→216	0.36710		208→216	0.22647		
192→215	0.15162		201→215	0.32354		213→215	-0.16499		
197→215	-0.22652		205→215	0.14557		213→220	0.10333		
Excited State 8:	**Singlet-B**	**4.1274 eV**	**300.39 nm**	**f=1.3809**	**<S**2>=0.000**				
191→215	0.11140		**199→215**	**0.34414**		208→215	0.23757		
192→216	0.13615		**201→216**	**0.32054**		213→216	-0.27654		
197→216	-0.21860		205→216	0.12545					
Excited State 9:	Singlet-A	4.2515 eV	291.62 nm	f=0.0000	<S**2>=0.000				
195→215	0.39313		201→215	0.10043		205→215	-0.25511		
196→216	0.40127		204→216	-0.26900					

Excited State 10:	Singlet-B	4.2549 eV	291.39 nm	f=0.0638	<S**2>=0.000
195→216	0.39183	204→215	-0.27924		
196→215	0.39410	205→216	-0.27212		
Excited State 11:	Singlet-B	4.2685 eV	290.46 nm	f=0.0008	<S**2>=0.000
211→215	0.47319	212→216	-0.41248	213→217	0.12265
211→220	-0.11706	212→219	0.11613	214→218	0.12778
Excited State 12:	Singlet-A	4.3533 eV	284.80 nm	f=0.0016	<S**2>=0.000
200→215	0.14906	211→216	-0.42697	212→215	0.50475
Excited State 13:	**Singlet-B**	**4.4372 eV**	**279.42 nm**	**f=0.2814**	**<S**2>=0.000**
193→216	0.16113	200→216	0.23538	209→215	0.16475
194→215	0.17556	202→216	-0.30784	211→215	0.17533
198→215	0.15624	**203→215**	**0.32617**	212→216	0.21457
Excited State 14:	Singlet-A	4.4565 eV	278.21 nm	f=0.0089	<S**2>=0.000
200→215	0.13330	203→216	0.41380		
202→215	-0.40174	211→216	0.23213		
Excited State 15:	Singlet-B	4.4992 eV	275.57 nm	f=0.2505	<S**2>=0.000
193→216	0.15537	200→216	0.18467	209→215	0.19088
194→215	0.16608	202→216	0.33493	211→215	0.18197
198→215	0.15375	203→215	-0.32281	212→216	0.17114
Excited State 16:	Singlet-A	4.5168 eV	274.50 nm	f=0.0000	<S**2>=0.000
195→215	0.27183	201→215	-0.10756	205→215	0.34489
196→216	0.27606	204→216	0.35185	214→222	0.11553
Excited State 17:	Singlet-B	4.5192 eV	274.35 nm	f=0.0978	<S**2>=0.000
195→216	0.27985	196→215	0.28215	201→216	-0.12477

204→215	0.35026	213→222	0.10806		
205→216	0.33585	214→223	-0.10351		

Excited State 18:	Singlet-A	4.5259 eV	273.94 nm	f=0.0000	<S**2>=0.000
193→215	0.18619	200→215	0.23683	209→216	0.22682
194→216	0.20222	202→215	0.21173	211→216	0.34973
198→216	0.19171	203→216	-0.19027	212→215	0.13645

Excited State 19:	Singlet-A	4.5824 eV	270.57 nm	f=0.0000	<S**2>=0.000
197→215	0.11082	210→215	0.53113	212→218	0.15068
208→216	0.11294	210→220	-0.13369	214→216	0.16434
209→217	0.10977	211→217	0.15687	214→219	0.14943

Excited State 20:	Singlet-B	4.6551 eV	266.34 nm	f=0.1023	<S**2>=0.000
192→216	-0.10162	208→215	0.21616	213→216	0.10702
197→216	0.12931	210→216	0.59052	214→215	0.11415

Excited State 21:	**Singlet-B**	**4.8011 eV**	**258.24 nm**	**f=0.3672**	**<S**2>=0.000**
200→219	0.11073	210→217	0.16348	**212→219**	**0.31755**
208→218	0.14196	211→215	-0.19171	**214→218**	**0.39846**
209→215	0.13918	211→220	-0.10279		
209→220	-0.11067	212→216	0.20069		

Excited State 22:	Singlet-A	4.8030 eV	258.14 nm	f=0.0000	<S**2>=0.000
192→215	-0.11889	208→219	-0.13181	212→218	-0.25509
199→216	-0.10409	210→215	0.22887	213→215	0.15822
200→218	-0.12504	210→220	0.11431	213→220	0.15491
208→216	0.29983	211→217	-0.17756	214→219	-0.25692

Excited State 23:	Singlet-A	4.8891 eV	253.59 nm	f=0.0000	<S**2>=0.000
211→219	-0.12126	212→220	-0.30820	213→218	-0.23500

213→221	0.15250	214→217	0.48866

Excited State 24: Singlet-B 4.9078 eV 252.63 nm f=1.2512 <S2>=0.000**

211→215	-0.17341	**213→217**	**0.47302**	214→221	0.20438
211→220	-0.29956	214→218	-0.19238		

C.2.7 Electronic Transitions in **OTPB-FLR-210** Oligomers

*Table C-11 Attributes of **OTPB-FLR-210** in **LEB**, **ES** (singlet and triplet), and **EB** states related to electronic structures*

Attribute	LEB State	^{1}ES State	^{3}ES State	EB State
Molecular Formula	$C_{61}H_{44}N_2$	$C_{61}H_{44}N_2^{2+}$	$C_{61}H_{44}N_2^{2+}$	$C_{61}H_{42}N_2$
Number of Atoms	107	107	107	105
Number of Electrons	424	422	422	422
HOMO	MO 212	MO 211	MOs 212A, 210B	MO 211
LUMO	MO 213	MO 212	MOs 213A, 211B	MO 212

*C.2.7.1 **OTPB-FLR-210**, **LEB** State*

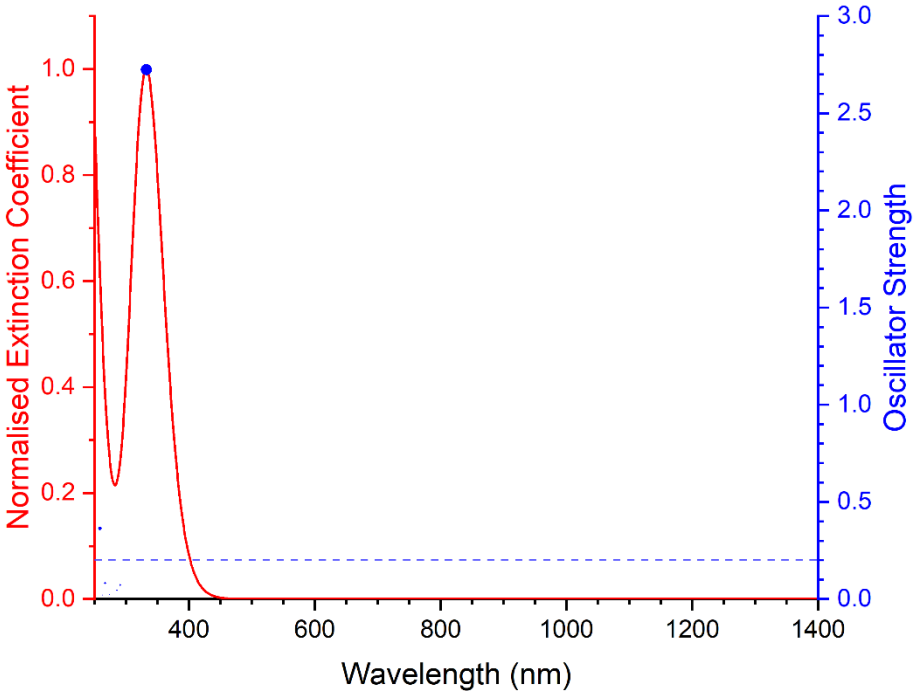

*Figure C-25 Excited states and normalised absorption spectra from TD-DFT calculations of **OTPB-FLR-210** in **LEB** state. The areas of excited state dots are proportional to their oscillator strengths.*

Excited State 1: Singlet-A 3.7294 eV 332.45 nm f=2.7240 <S2>=0.000**

211→216	-0.19259	**212→213**	**0.58636**
211→219	-0.11920	212→217	0.26054

Excited State 2:	Singlet-A	4.2564 eV	291.29 nm	f=0.0711	<S**2>=0.000	
210→216	0.10127	212→216	-0.40245	212→219	-0.17730	
211→213	0.41667	212→218	0.23314			

Excited State 3:	Singlet-A	4.3360 eV	285.94 nm	f=0.0442	<S**2>=0.000	
210→218	0.12033	212→216	0.13767	212→219	0.12033	
211→213	-0.15951	212→217	-0.16156			
211→227	0.12434	212→218	0.55891			

Excited State 4:	Singlet-A	4.5229 eV	274.12 nm	f=0.0212	<S**2>=0.000	
207→214	-0.13459	210→214	-0.20717	212→214	0.33715	
208→213	0.12755	211→214	-0.30522	212→220	-0.22393	
208→216	0.14745	211→220	0.11042			
209→214	-0.10079	211→221	-0.14752			

Excited State 5:	Singlet-A	4.5347 eV	273.42 nm	f=0.0136	<S**2>=0.000	
207→215	0.13844	210→215	-0.20271	211→221	0.12149	
209→213	-0.10900	211→215	0.30037	212→215	0.32752	
209→216	0.15467	211→220	0.13348	212→221	0.21078	

Excited State 6:	Singlet-A	4.6480 eV	266.75 nm	f=0.0814	<S**2>=0.000	
211→214	-0.10470	211→221	0.24851	212→220	0.36827	
211→215	-0.10058	212→214	0.10330	212→227	0.20673	
211→218	0.17329	212→215	-0.10559			

Excited State 7:	Singlet-A	4.6740 eV	265.26 nm	f=0.0010	<S**2>=0.000	
198→213	-0.10709	211→220	0.33603			
209→216	-0.10627	212→221	0.42121			

Excited State 8:	Singlet-A	4.7228 eV	262.52 nm	f=0.0201	<S**2>=0.000
205→213	-0.15554	211→218	0.17222	212→220	-0.14302
205→217	-0.13277	211→221	-0.17945	212→226	-0.16204
211→216	-0.15465	212→217	-0.19084	212→227	0.43374

Excited State 9:	**Singlet-A**	**4.7918 eV**	**258.74 nm**	**f=0.3629**	**<S**2>=0.000**
210→213	0.20268	**212→217**	**0.36696**	212→227	0.21473
211→216	**0.31648**	212→218	0.11859		
211→221	-0.13146	212→226	0.21839		

*C.2.7.2 **OTPB-FLR-210**, **^{1}ES** State*

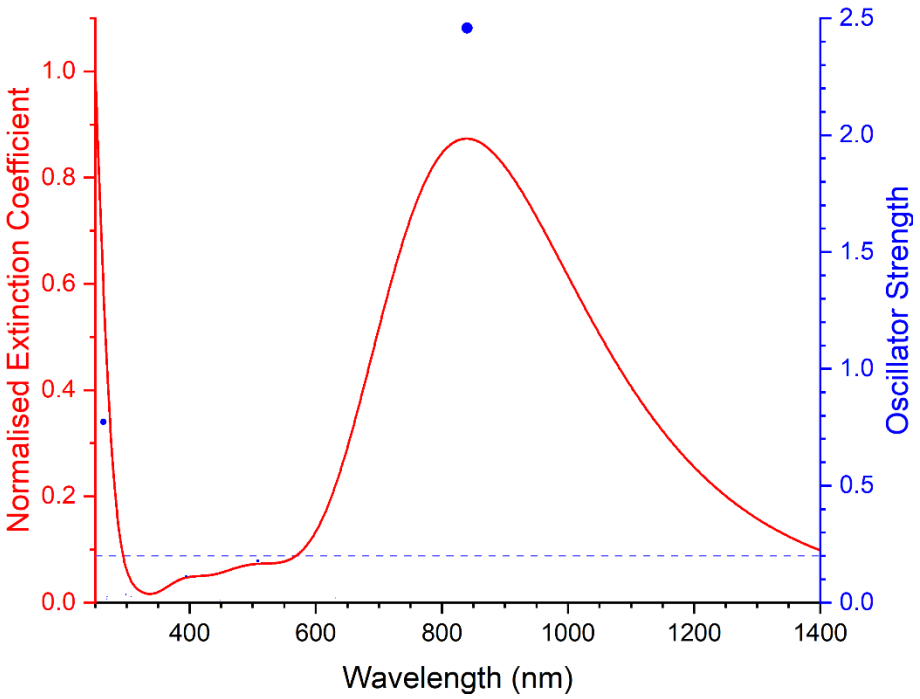

*Figure C-26 Excited states and normalised absorption spectra from TD-DFT calculations of **OTPB-FLR-210** in **^{1}ES** state. The areas of excited state dots are proportional to their oscillator strengths.*

Excited State 1:	**Singlet-A**	**1.4763 eV**	**839.83 nm**	**f=2.4576**	**<S**2>=0.000**
207→212	0.16691	**211→212**	**0.68155**		

Excited State 2:	Singlet-A	1.9625 eV	631.77 nm	f=0.0194	<S**2>=0.000
202→212	-0.21573	208→212	0.59132	210→212	0.30652

Excited State 3:	Singlet-A	1.9854 eV	624.47 nm	f=0.0039	<S**2>=0.000
202→212	0.11140	208→212	-0.28208	210→212	0.63164

Excited State 4:	Singlet-A	1.9998 eV	619.98 nm	f=0.0003	<S**2>=0.000
209→212	0.70093				
Excited State 5:	Singlet-A	2.4391 eV	508.33 nm	f=0.1777	<S**2>=0.000
201→212	0.16696	207→212	0.65992	211→212	-0.17199
Excited State 6:	Singlet-A	2.6841 eV	461.91 nm	f=0.0058	<S**2>=0.000
196→212	0.15774	202→212	0.62831	208→212	0.25752
Excited State 7:	Singlet-A	2.7635 eV	448.65 nm	f=0.0095	<S**2>=0.000
195→212	0.68695				
Excited State 8:	Singlet-A	2.9296 eV	423.21 nm	f=0.0000	<S**2>=0.000
203→212	0.70398				
Excited State 9:	Singlet-A	2.9335 eV	422.66 nm	f=0.0000	<S**2>=0.000
204→212	0.70134				
Excited State 10:	Singlet-A	2.9756 eV	416.67 nm	f=0.0005	<S**2>=0.000
199→212	0.14849	200→212	0.31415	206→212	0.59759
Excited State 11:	Singlet-A	2.9764 eV	416.56 nm	f=0.0001	<S**2>=0.000
205→212	0.69521				
Excited State 12:	Singlet-A	2.9788 eV	416.23 nm	f=0.0021	<S**2>=0.000
193→212	0.10107	199→212	0.26489	206→212	-0.36058
198→212	-0.11156	200→212	0.50960		
Excited State 13:	Singlet-A	2.9869 eV	415.09 nm	f=0.0017	<S**2>=0.000
199→212	0.60518	200→212	-0.31237		

Excited State 14:	Singlet-A	3.0782 eV	402.79 nm	f=0.0022	<S**2>=0.000	
193→212	0.68261	199→212	-0.11540			
Excited State 15:	Singlet-A	3.1433 eV	394.44 nm	f=0.1131	<S**2>=0.000	
194→212	0.19906	201→212	0.65027	207→212	-0.16747	
Excited State 16:	Singlet-A	3.7042 eV	334.71 nm	f=0.0013	<S**2>=0.000	
196→212	0.66018	202→212	-0.17273			
Excited State 17:	Singlet-A	3.8532 eV	321.77 nm	f=0.0031	<S**2>=0.000	
198→212	0.68042	200→212	0.12473			
Excited State 18:	Singlet-A	3.8890 eV	318.80 nm	f=0.0023	<S**2>=0.000	
197→212	0.69477					
Excited State 19:	Singlet-A	4.0370 eV	307.12 nm	f=0.0252	<S**2>=0.000	
194→212	0.64996	201→212	-0.20079			
Excited State 20:	Singlet-A	4.1460 eV	299.05 nm	f=0.0350	<S**2>=0.000	
201→213	0.11049	208→215	0.12560			
207→213	0.23451	211→213	0.61666			
Excited State 21:	Singlet-A	4.6021 eV	269.41 nm	f=0.0254	<S**2>=0.000	
208→218	0.16473	210→215	0.32610	210→222	0.11404	
210→213	0.33398	210→216	-0.27110	211→218	0.16987	
210→214	-0.14838	210→219	0.12558			
Excited State 22:	Singlet-A	4.6125 eV	268.80 nm	f=0.0148	<S**2>=0.000	
208→217	-0.19056	209→215	-0.31935	211→217	0.20382	
209→213	0.33619	209→216	-0.30830			
209→214	0.10399	209→222	-0.11971			

Excited State 23:	**Singlet-A**	**4.7116 eV**	**263.15 nm**	**f=0.7725**	**<S**2>=0.000**				
202→213	-0.22123		208→216	-0.19093		**211→215**	**0.35703**		
208→213	**0.42924**		211→214	-0.21649					
Excited State 24:	Singlet-A	4.8024 eV	258.17 nm	f=0.0003	<S**2>=0.000				
172→212	0.53995		182→212	-0.13490		192→212	-0.10043		
178→212	-0.13424		184→212	0.29489					
Excited State 25:	Singlet-A	4.9381 eV	251.08 nm	f=0.0028	<S**2>=0.000				
172→212	0.35770		184→212	-0.31378		207→213	-0.11050		
178→212	0.10629		188→212	0.11252		208→215	0.15958		
182→212	0.16198		192→212	0.16201		211→216	-0.21729		

*C.2.7.3 **OTPB-FLR-210**, **^{3}ES** State*

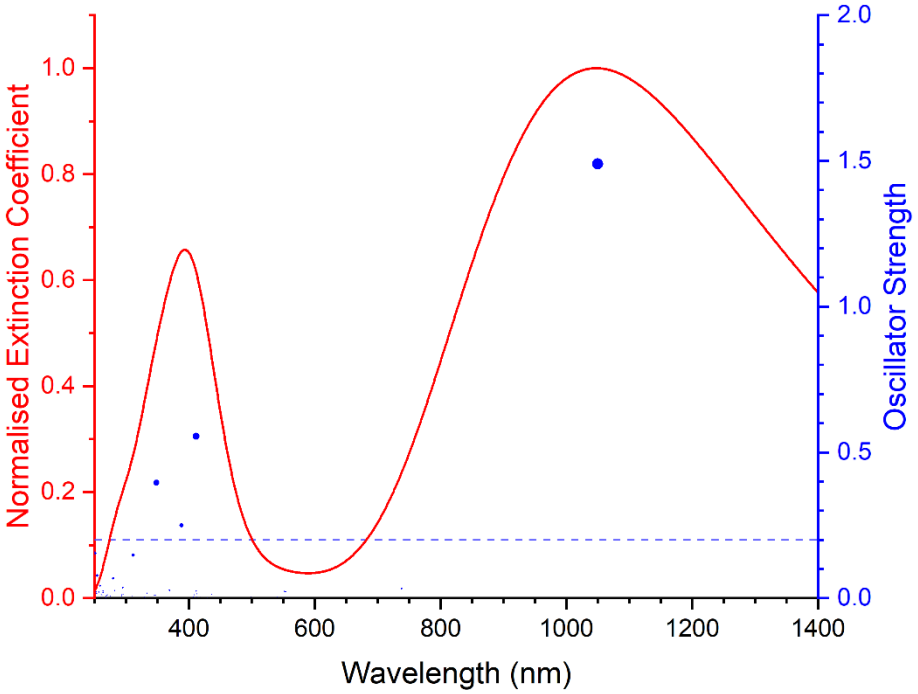

*Figure C-27 Excited states and normalised absorption spectra from TD-DFT calculations of **OTPB-FLR-210** in **^{3}ES** state. The areas of excited state dots are proportional to their oscillator strengths.*

Excited State 1:	**3.094-A**	**1.1813 eV**	**1049.58 nm**	**f=1.4902**	**<S**2>=2.144**				
193B→212B	-0.12839		**206B→211B**	**0.36958**		**209B→211B**	**0.44790**		
201B→212B	0.27404		207B→212B	-0.23628		**210B→211B**	**0.70227**		

Excited State 2:	3.080-A	1.6802 eV	737.89 nm	f=0.0324	<S**2>=2.122			
193B→211B	-0.12266	206B→212B	0.19042	209B→212B	0.34882			
201B→211B	0.41056	207B→211B	-0.51653	210B→212B	0.56990			
Excited State 3:	3.096-A	1.7494 eV	708.73 nm	f=0.0000	<S**2>=2.146			
196B→211B	0.15182	208B→211B	0.82516					
196B→212B	-0.11961	208B→212B	-0.49433					
Excited State 4:	3.095-A	1.7498 eV	708.55 nm	f=0.0000	<S**2>=2.145			
197B→211B	-0.14928	209B→211B	0.69160	210B→211B	-0.44685			
197B→212B	-0.11918	209B→212B	0.43135	210B→212B	-0.25383			
Excited State 5:	3.115-A	2.2390 eV	553.74 nm	f=0.0219	<S**2>=2.175			
193B→212B	-0.10648	195B→212B	0.41713	207B→212B	0.27839			
194B→211B	0.32936	199B→211B	0.27664	209B→211B	-0.10113			
194B→212B	-0.18988	200B→212B	0.10809					
195B→211B	0.47089	206B→211B	0.42939					
Excited State 6:	3.080-A	2.2399 eV	553.53 nm	f=0.0035	<S**2>=2.122			
194B→211B	0.60558	195B→212B	-0.25845	200B→211B	-0.14120			
194B→212B	-0.51467	196B→211B	-0.13292					
195B→211B	-0.43424	198B→212B	-0.11365					
Excited State 7:	3.136-A	2.2462 eV	551.98 nm	f=0.0232	<S**2>=2.208			
193B→212B	-0.13930	195B→212B	-0.32477	207B→212B	0.34685			
194B→211B	-0.28375	198B→211B	-0.16908	210B→211B	-0.14022			
194B→212B	0.18657	199B→211B	0.24281					
195B→211B	-0.37691	206B→211B	0.53552					
Excited State 8:	3.082-A	2.2937 eV	540.55 nm	f=0.0035	<S**2>=2.125			
193B→211B	-0.22113	199B→212B	0.25112	200B→211B	0.10762			

206B→212B	0.55700	209B→212B	0.16445		
207B→211B	0.63912	210B→212B	0.27096		

Excited State 9:	3.128-A	2.4823 eV	499.46 nm	f=0.0048	<S**2>=2.197
195B→211B	-0.11524	199B→212B	0.15772	200B→213B	0.12072
198B→212B	0.39225	200B→211B	0.84744		

Excited State 10:	3.118-A	2.5954 eV	477.70 nm	f=0.0027	<S**2>=2.180
194B→211B	-0.11308	199B→211B	0.30501		
198B→211B	0.66629	200B→212B	0.60812		

Excited State 11:	3.426-A	2.8396 eV	436.62 nm	f=0.0120	<S**2>=2.684
202A→213A	-0.11144	212A→215A	-0.17131	207B→212B	-0.12103
208A→213A	-0.12282	198B→211B	0.17967	208B→215B	-0.16786
209A→214A	0.14154	199B→211B	-0.30474	209B→211B	-0.19155
210A→216A	0.16655	201B→211B	-0.13063	209B→216B	0.10079
210A→219A	-0.10774	201B→212B	0.41099	210B→211B	-0.30414
211A→217A	-0.10729	206B→211B	0.40386	210B→213B	-0.13238

Excited State 12:	3.181-A	2.8852 eV	429.72 nm	f=0.0010	<S**2>=2.280
193B→211B	-0.10720	206B→212B	0.10509	210B→212B	-0.38929
199B→212B	-0.25018	207B→211B	0.17899		
201B→211B	0.70311	209B→212B	-0.24469		

Excited State 13:	3.903-A	2.9578 eV	419.18 nm	f=0.0048	<S**2>=3.558
202A→214A	0.10928	210A→216A	-0.20081	193B→211B	0.25834
208A→214A	0.15821	210A→219A	0.13065	201B→211B	-0.18517
208A→222A	-0.13397	211A→217A	-0.22102	201B→213B	-0.10583
209A→213A	-0.15423	211A→218A	0.11538	206B→222B	0.11287
209A→215A	-0.16483	211A→220A	-0.15665	207B→211B	0.22597
209A→223A	-0.11600	212A→214A	0.13878	207B→213B	0.13058

207B→218B	0.12394	209B→214B	0.10958	210B→214B	0.16413
207B→223B	0.11122	209B→216B	0.22966	210B→216B	-0.15227
208B→215B	0.22682	210B→212B	0.17632		

Excited State 14:	3.079-A	2.9977 eV	413.60 nm	f=0.0041	<S**2>=2.119
202B→211B	0.88676	202B→212B	-0.37937	204B→211B	-0.19940

Excited State 15:	3.093-A	3.0014 eV	413.08 nm	f=0.0145	<S**2>=2.142
203B→211B	0.73952	204B→211B	-0.47923	205B→211B	0.13535
203B→212B	0.33390	204B→212B	0.22069		

Excited State 16:	3.082-A	3.0023 eV	412.97 nm	f=0.0041	<S**2>=2.124
202B→211B	0.18971	203B→212B	0.21996	204B→212B	-0.33578
203B→211B	0.48781	204B→211B	0.72907		

Excited State 17:	3.105-A	3.0119 eV	411.64 nm	f=0.0237	<S**2>=2.160
203B→211B	-0.17128	205B→211B	0.86535	205B→212B	0.40067

Excited State 18:	**3.759-A**	**3.0133 eV**	**411.45 nm**	**f=0.5553**	**<S**2>=3.282**
202A→215A	0.12760	199B→211B	-0.10154	207B→214B	0.11347
208A→215A	0.18925	201B→212B	0.17485	207B→222B	-0.12527
209A→214A	-0.21142	202B→211B	0.10306	208B→215B	0.22221
210A→216A	-0.18798	204B→211B	0.12138	209B→216B	-0.16408
210A→219A	0.11887	205B→211B	-0.20401	210B→216B	0.10821
211A→217A	0.14701	206B→211B	0.10244	210B→218B	0.15120
211A→220A	0.10406	206B→223B	-0.11205		
212A→213A	**0.43221**	207B→212B	-0.10458		

Excited State 19:	3.104-A	3.0332 eV	408.75 nm	f=0.0114	<S**2>=2.159
209B→211B	-0.45352	210B→211B	0.30034		
209B→212B	0.67738	210B→212B	-0.43547		

Excited State 20:	3.098-A	3.0433 eV	407.40 nm	f=0.0039	<S**2>=2.149
208B→211B	0.54092	208B→212B	0.81145		

Excited State 21:	**3.557-A**	**3.1912 eV**	**388.52 nm**	**f=0.2493**	**<S**2>=2.912**
198A→218A	0.13330	212A→215A	-0.16874	208B→215B	-0.13178
201A→221A	-0.14823	198B→217B	-0.11431	209B→211B	0.18751
208A→213A	-0.18405	200B→221B	-0.12212	210B→211B	0.24746
210A→216A	0.13398	201B→212B	-0.18313	210B→213B	-0.12701
211A→217A	-0.10135	206B→213B	-0.11461		
212A→213A	**0.38403**	**207B→212B**	**0.49673**		

Excited State 22:	3.335-A	3.2732 eV	378.78 nm	f=0.0009	<S**2>=2.531
210A→216A	0.10909	199B→212B	-0.34090	209B→212B	0.21331
211A→217A	0.10834	201B→211B	0.22014	209B→216B	-0.11196
183B→211B	-0.10742	206B→212B	-0.32747	210B→212B	0.26872
193B→211B	0.38720	207B→211B	0.40636		
198B→212B	0.16313	208B→215B	-0.12243		

Excited State 23:	3.247-A	3.3555 eV	369.49 nm	f=0.0273	<S**2>=2.386
212A→213A	-0.17632	199B→211B	-0.52798	210B→211B	0.12736
193B→212B	0.26067	201B→212B	0.13503		
198B→211B	0.22867	207B→212B	0.58452		

Excited State 24:	4.149-A	3.3680 eV	368.12 nm	f=0.0001	<S**2>=4.053
203A→224A	0.27772	209A→216A	0.17259	202B→224B	0.27822
205A→226A	0.28275	209A→219A	-0.11297	204B→226B	0.28337
207A→216A	-0.13016	210A→214A	0.10135	206B→215B	-0.15847
207A→231A	0.10304	210A→215A	0.10322	206B→230B	0.10188
208A→216A	-0.18254	210A→222A	-0.21876	207B→215B	0.20863
208A→219A	0.12430	210A→223A	0.20218	207B→230B	-0.10707

208B→214B	0.10820	208B→222B	-0.21527	210B→215B	0.12802
208B→218B	0.10267	208B→223B	0.19771		

Excited State 25: 4.108-A 3.3690 eV 368.01 nm f=0.0010 <S**2>=3.970

204A→225A	0.26894	211A→214A	-0.10977	207B→212B	-0.13496
206A→227A	-0.25941	211A→222A	0.19298	207B→216B	0.19601
207A→217A	-0.11661	211A→223A	0.21564	209B→214B	-0.10004
207A→232A	-0.10374	199B→211B	0.11503	209B→222B	0.16532
208A→217A	0.16102	203B→225B	0.27322	209B→223B	0.16223
208A→220A	0.12335	205B→227B	-0.26341	210B→216B	-0.12148
209A→217A	0.13362	206B→216B	0.16201	210B→222B	-0.10518
209A→220A	0.10175	206B→231B	-0.10140	210B→223B	-0.11830

Excited State 26: 3.723-A 3.5567 eV 348.59 nm f=0.3964 <S2>=3.216**

195A→219A	0.12290	**209A→214A**	**0.32276**	203B→225B	-0.10398
196A→220A	-0.12983	212A→213A	-0.25762	204B→226B	0.11278
202A→213A	-0.22509	212A→215A	-0.21130	205B→227B	-0.10875
202A→215A	-0.11498	193B→212B	-0.19142	206B→213B	-0.16527
203A→224A	-0.10774	194B→219B	0.10214	207B→212B	0.13900
205A→226A	0.10679	195B→220B	0.10870	209B→213B	-0.13032
206A→227A	-0.10138	199B→211B	0.18495	210B→213B	-0.20283
207A→214A	0.23868	201B→214B	0.11427		
208A→213A	-0.10668	202B→224B	-0.11376		

Excited State 27: 3.731-A 3.5763 eV 346.68 nm f=0.0104 <S**2>=3.230

195A→219A	-0.10447	206A→227A	-0.11825	212A→214A	0.31178
202A→214A	0.22753	207A→213A	-0.18382	193B→211B	0.15475
203A→224A	0.12870	207A→215A	-0.12235	201B→213B	-0.12286
204A→225A	-0.12135	209A→213A	-0.27446	202B→224B	0.13355
205A→226A	-0.12834	209A→215A	-0.15983	203B→225B	-0.12731

204B→226B	-0.13299	206B→212B	0.31479	210B→212B	-0.14718
205B→227B	-0.12402	209B→212B	-0.10181	210B→214B	0.12070

Excited State 28: 3.333-A 3.5890 eV 345.45 nm f=0.0101 <S**2>=2.527

198A→221A	-0.12767	212A→214A	-0.25001	200B→217B	-0.10843
201A→218A	0.13766	193B→211B	0.41919	206B→212B	0.55955
207A→213A	0.15626	198B→212B	0.15090	207B→211B	-0.19640
209A→213A	0.18996	198B→221B	-0.10598	210B→212B	-0.11994

Excited State 29: 3.194-A 3.6198 eV 342.51 nm f=0.0007 <S**2>=2.300

193B→212B	-0.19443	199B→211B	-0.13407	201B→212B	0.23731
198B→211B	-0.49206	199B→213B	-0.10029	206B→211B	-0.19595
198B→213B	-0.13002	200B→212B	0.66438	207B→212B	0.12860

Excited State 30: 3.276-A 3.7152 eV 333.72 nm f=0.0165 <S**2>=2.434

186B→211B	-0.12100	197B→212B	0.31261	206B→211B	0.23421
188B→211B	0.13678	198B→211B	-0.16425	207B→212B	-0.12521
193B→212B	0.24810	199B→211B	-0.17139	209B→212B	0.14492
195B→211B	0.10032	200B→212B	0.25730		
197B→211B	0.51809	201B→212B	-0.27379		

Excited State 31: 3.263-A 3.7277 eV 332.61 nm f=0.0113 <S**2>=2.412

186B→211B	0.10476	197B→212B	0.32161	201B→212B	0.27665
188B→211B	-0.13019	198B→211B	0.12164	206B→211B	-0.22832
193B→212B	-0.25766	199B→211B	0.13823	207B→212B	0.11868
197B→211B	0.56471	200B→212B	-0.21574	209B→212B	0.14699

Excited State 32: 3.205-A 3.7444 eV 331.12 nm f=0.0012 <S**2>=2.317

198B→212B	0.75871	200B→211B	-0.40349	200B→217B	0.12847
199B→212B	0.35168	200B→213B	-0.17788		

Excited State 33:	3.198-A	3.7567 eV	330.03 nm	f=0.0035	<S**2>=2.308	
194B→211B	0.15710	196B→212B	-0.43123	208B→211B	-0.10961	
194B→212B	-0.10114	196B→213B	-0.10338	208B→212B	0.24455	
196B→211B	0.75589	196B→214B	-0.11138			
Excited State 34:	3.069-A	3.8800 eV	319.55 nm	f=0.0000	<S**2>=2.104	
202B→211B	0.39530	202B→212B	0.91258			
Excited State 35:	3.069-A	3.9015 eV	317.79 nm	f=0.0000	<S**2>=2.104	
203B→211B	-0.40955	203B→212B	0.89711	205B→212B	0.13942	
Excited State 36:	3.069-A	3.9379 eV	314.85 nm	f=0.0000	<S**2>=2.105	
203B→212B	-0.13893	205B→211B	-0.41832	205B→212B	0.89303	
Excited State 37:	3.069-A	3.9404 eV	314.65 nm	f=0.0000	<S**2>=2.105	
204B→211B	0.41995	204B→212B	0.90145			
Excited State 38:	3.825-A	3.9810 eV	311.44 nm	f=0.1472	<S**2>=3.409	
194A→213A	0.11646	209A→214A	-0.13931	202B→224B	-0.15685	
197A→216A	0.15069	210A→216A	0.15121	203B→225B	-0.11452	
197A→219A	-0.10872	210A→231A	0.14528	204B→226B	0.15418	
199A→217A	-0.11311	211A→217A	-0.10907	205B→227B	-0.11351	
203A→224A	-0.16009	211A→232A	0.11519	206B→211B	-0.15780	
204A→225A	-0.11497	212A→213A	0.23403	207B→212B	0.10717	
205A→226A	0.15731	196B→215B	-0.14787	208B→215B	-0.14326	
206A→227A	-0.11410	197B→216B	-0.12377	208B→230B	-0.15176	
207A→214A	-0.12720	199B→211B	0.17202	209B→216B	0.10179	
207A→222A	-0.10427	201B→212B	0.26608			
Excited State 39:	3.861-A	3.9909 eV	310.67 nm	f=0.0060	<S**2>=3.476	
193A→213A	-0.12130	194A→214A	0.15797	197A→216A	0.11775	

199A→217A	0.13505	209A→229A	-0.10733	199B→214B	0.11103
199A→220A	0.10955	210A→216A	0.11625	202B→224B	-0.12685
202A→214A	0.11159	210A→231A	0.11334	203B→225B	0.14427
202A→222A	0.10285	211A→217A	0.13332	204B→226B	0.12495
203A→224A	-0.13006	211A→232A	-0.14122	205B→227B	0.14521
204A→225A	0.14554	212A→214A	0.24487	208B→215B	-0.11518
205A→226A	0.12797	212A→230A	0.11352	208B→230B	-0.12133
206A→227A	0.14656	183B→211B	-0.13759	209B→216B	-0.12270
207A→213A	-0.14947	193B→213B	0.13385	209B→231B	-0.12594
207A→223A	0.12921	196B→215B	-0.11903		
209A→213A	-0.16727	197B→216B	0.15646		

Excited State 40: 3.699-A 4.0425 eV 306.70 nm f=0.0017 <S**2>=3.171

193A→213A	0.10879	212A→221A	-0.11929	193B→213B	-0.11493
198A→221A	0.23167	212A→228A	0.17172	198B→221B	0.18405
200A→213A	-0.11828	181B→211B	-0.13024	199B→212B	-0.21335
201A→215A	0.11970	183B→211B	0.14235	199B→221B	0.11452
201A→217A	-0.10407	186B→212B	-0.11411	200B→217B	0.21476
201A→218A	-0.25634	188B→212B	0.14816	200B→218B	-0.16188
212A→214A	0.10451	193B→211B	0.38520	206B→212B	0.19992

Excited State 41: 3.550-A 4.1979 eV 295.35 nm f=0.0125 <S**2>=2.900

195A→216A	-0.15264	183B→211B	0.26648	194B→219B	-0.16637
195A→219A	-0.20143	183B→212B	-0.10160	199B→212B	0.26222
198A→221A	-0.13053	186B→212B	-0.15539	201B→211B	0.33434
201A→218A	0.13586	188B→211B	-0.18325	201B→212B	-0.16456
210A→216A	0.13665	188B→212B	0.23175	206B→212B	-0.11855
181B→211B	-0.10259	190B→212B	0.10017	208B→215B	-0.13173

Excited State 42:	3.591-A	4.2061 eV	294.78 nm	f=0.0361	<S**2>=2.974				
196A→217A	0.14185	183B→212B	0.17126	201B→211B	0.18038				
196A→220A	-0.16703	186B→211B	-0.21321	201B→212B	0.32406				
208A→213A	-0.10421	186B→212B	-0.12726	207B→214B	-0.11872				
208A→218A	-0.11336	188B→211B	0.22011	209B→216B	-0.12167				
211A→217A	0.14346	190B→211B	0.13467	209B→218B	-0.10370				
212A→213A	0.11489	192B→211B	-0.14556	210B→216B	0.10284				
212A→218A	0.16668	195B→220B	0.13492						
183B→211B	0.13420	199B→212B	0.14705						

Excited State 43:	4.006-A	4.2217 eV	293.68 nm	f=0.0067	<S**2>=3.763				
199A→213A	-0.12082	211A→215A	-0.26556	205B→227B	-0.13119				
199A→214A	0.17155	211A→218A	-0.10435	209B→213B	-0.18382				
199A→215A	-0.11597	211A→222A	-0.10055	209B→214B	0.23850				
204A→225A	0.12087	211A→229A	0.14430	209B→218B	-0.13696				
206A→227A	-0.13045	197B→211B	0.29587	210B→213B	0.12945				
211A→213A	-0.34984	197B→214B	-0.10941	210B→214B	-0.16729				
211A→214A	0.44427	203B→225B	0.12076	210B→218B	0.11145				

Excited State 44:	3.998-A	4.2284 eV	293.22 nm	f=0.0106	<S**2>=3.745				
197A→213A	0.12804	210A→215A	0.28431	204B→226B	-0.11946				
197A→214A	0.16353	210A→222A	-0.12269	208B→213B	0.22924				
197A→215A	0.12124	210A→229A	-0.11215	208B→214B	0.28218				
203A→224A	-0.12247	210A→230A	-0.12223	208B→217B	0.14298				
205A→226A	-0.12114	196B→211B	0.30465	208B→218B	0.15571				
210A→213A	0.37451	196B→214B	0.10210						
210A→214A	0.42953	202B→224B	-0.12071						

Excited State 45:	3.570-A	4.2522 eV	291.58 nm	f=0.0070	<S**2>=2.935				
198A→218A	-0.11168	200A→221A	-0.10769	201A→221A	0.13652				

202A→218A	-0.17269	212A→217A	0.21301	201B→212B	-0.33450
208A→215A	0.15191	212A→218A	0.47593	206B→217B	0.10041
208A→218A	-0.23178	188B→211B	-0.12933	210B→217B	0.13315
212A→213A	0.11581	199B→211B	-0.16888		
212A→215A	-0.31920	200B→221B	0.13868		

Excited State 46: 3.906-A 4.3778 eV 283.21 nm f=0.0027 <S**2>=3.564

194A→214A	0.14621	210A→216A	-0.14310	207B→213B	-0.20117
195A→219A	-0.15503	211A→217A	-0.15411	207B→217B	-0.10056
196A→217A	0.10576	212A→222A	0.15514	207B→218B	-0.14124
196A→220A	-0.14467	181B→211B	-0.12252	208B→215B	0.15705
200A→213A	-0.14106	193B→211B	0.22631	209B→214B	-0.12472
207A→213A	-0.14726	194B→219B	-0.13935	209B→216B	0.15747
208A→214A	-0.22135	195B→220B	0.13421	210B→214B	-0.18903
209A→215A	0.15370	199B→214B	0.12671	210B→216B	-0.11339
209A→223A	0.13923	201B→211B	0.11423		
209A→229A	-0.10767	206B→212B	-0.10177		

Excited State 47: 3.946-A 4.3972 eV 281.96 nm f=0.0254 <S**2>=3.643

195A→216A	0.18740	210A→216A	0.14204	194B→219B	0.23889
195A→219A	0.27449	211A→217A	-0.10823	194B→220B	0.10520
196A→217A	0.19352	212A→215A	0.10046	195B→216B	0.10873
196A→220A	-0.25204	181B→212B	-0.12061	195B→220B	0.22164
208A→213A	0.14178	182B→211B	-0.11043	199B→211B	-0.14264
208A→215A	0.11863	188B→211B	0.12349	207B→214B	0.17822
209A→214A	-0.19332	192B→211B	-0.11033	208B→215B	-0.15933
209A→222A	0.13737	194B→215B	0.10818	209B→216B	0.11234

Excited State 48: 3.756-A 4.4340 eV 279.62 nm f=0.0679 <S**2>=3.278

196A→217A	-0.12883	196A→220A	0.17858	198A→215A	-0.14333

198A→217A	0.11212	212A→217A	0.18028	198B→211B	-0.16038
198A→218A	0.23424	212A→218A	0.30978	198B→217B	-0.23509
201A→221A	-0.25530	181B→212B	-0.10335	198B→218B	0.12091
208A→213A	0.12187	182B→211B	-0.12105	200B→221B	-0.24810
208A→218A	-0.14367	188B→211B	0.10633	201B→212B	0.18433
212A→213A	-0.23664	195B→220B	-0.16439		

Excited State 49: 3.602-A 4.4867 eV 276.34 nm f=0.0038 <S**2>=2.994

194A→219A	-0.10440	207A→216A	0.11371	212A→216A	-0.34820
195A→216A	-0.10728	207A→219A	0.11498	212A→219A	-0.11161
195A→219A	-0.15159	208A→216A	-0.18349	194B→219B	-0.14621
196A→217A	0.10211	209A→213A	0.12403	195B→220B	0.13359
196A→220A	-0.13227	209A→216A	0.37492	199B→212B	-0.15675
202A→216A	-0.16766	209A→217A	-0.10391	202B→224B	-0.12743
203A→224A	-0.12296	210A→213A	-0.15029	204B→226B	-0.11574
205A→226A	-0.11752	210A→214A	-0.14988		
207A→213A	0.10237	212A→214A	-0.14260		

Excited State 50: 3.644-A 4.4974 eV 275.68 nm f=0.0065 <S**2>=3.069

195A→216A	0.13284	209A→213A	-0.14751	212A→216A	-0.18692
195A→219A	0.19264	209A→216A	0.30080	212A→217A	0.21404
196A→220A	0.12619	209A→217A	0.17472	212A→218A	-0.12292
202A→217A	0.12164	210A→214A	-0.11327	194B→219B	0.18615
208A→216A	-0.11899	211A→214A	0.10331	195B→220B	-0.13103
208A→217A	0.15190	212A→214A	0.16475	199B→212B	0.18365

Excited State 51: 3.620-A 4.5027 eV 275.35 nm f=0.0062 <S**2>=3.025

194A→220A	-0.10414	202A→217A	0.15668	207A→217A	0.11720
195A→219A	-0.11043	204A→225A	-0.13426	207A→220A	-0.10731
196A→220A	-0.11814	206A→227A	0.13028	208A→217A	0.20676

208A→218A	-0.10015	212A→214A	-0.12398	199B→212B	-0.12545
209A→217A	0.40667	212A→216A	0.15037	203B→225B	-0.13438
209A→218A	-0.13158	212A→217A	0.32315	205B→227B	0.13460
211A→213A	-0.16523	212A→218A	-0.10899	207B→216B	0.10614
211A→214A	0.18683	194B→219B	-0.10831		
211A→215A	-0.11210	195B→220B	0.11760		

Excited State 52: 3.271-A 4.5708 eV 271.25 nm f=0.0105 <S**2>=2.425

198A→218A	0.10190	172B→212B	0.12276	182B→211B	0.24011
201A→221A	-0.11162	178B→211B	0.26575	191B→211B	-0.26974
212A→215A	0.11302	178B→212B	-0.20852	191B→212B	0.20055
212A→218A	0.12395	179B→211B	0.19720	192B→211B	0.16583
171B→211B	-0.25951	180B→211B	-0.20704	198B→217B	-0.11934
171B→212B	0.21852	181B→211B	-0.14883	199B→211B	-0.11416
172B→211B	0.15377	181B→212B	0.28474	200B→221B	-0.12419

Excited State 53: 3.173-A 4.5981 eV 269.64 nm f=0.0094 <S**2>=2.267

212A→220A	-0.12289	179B→211B	0.14516	191B→211B	0.18853
212A→221A	-0.14895	179B→212B	0.18504	192B→211B	0.25641
169B→211B	0.10702	180B→211B	-0.16212	192B→212B	0.18664
171B→211B	0.14579	180B→212B	-0.20863	193B→211B	0.23309
172B→211B	0.23924	181B→211B	0.36343	199B→212B	0.19225
172B→212B	0.19219	182B→211B	0.12464	201B→211B	0.11210
178B→211B	-0.13267	182B→212B	0.18126		
178B→212B	0.12734	187B→211B	-0.10452		

Excited State 54: 3.555-A 4.6162 eV 268.58 nm f=0.0071 <S**2>=2.909

202A→219A	0.14993	207A→216A	-0.19189	209A→219A	-0.33788
203A→224A	-0.18758	207A→219A	-0.17441	212A→216A	0.13912
205A→226A	-0.18759	208A→216A	-0.11601	212A→219A	0.37319

212A→220A	0.13627	194B→212B	0.16862	207B→215B	0.12667
212A→221A	0.16365	202B→224B	-0.18903		
194B→211B	0.17036	204B→226B	-0.18778		

Excited State 55: 3.714-A 4.6256 eV 268.04 nm f=0.0013 <S**2>=3.199

202A→217A	-0.10301	207A→220A	0.14035	203B→216B	-0.12977
202A→220A	0.12104	209A→220A	0.28413	203B→223B	-0.10179
204A→217A	0.11878	211A→225A	-0.14576	203B→225B	-0.15109
204A→222A	-0.10217	212A→217A	-0.14165	205B→227B	0.16135
204A→223A	-0.11768	212A→219A	-0.12024	207B→216B	0.11317
204A→225A	-0.14337	212A→220A	0.30707	209B→225B	-0.10804
206A→227A	0.16088	195B→211B	-0.15649	210B→225B	0.11774
207A→217A	-0.18835	195B→212B	0.16228		

Excited State 56: 4.090-A 4.6298 eV 267.80 nm f=0.0003 <S**2>=3.931

203A→216A	-0.22280	208A→225A	-0.10116	203B→218B	0.12958
203A→219A	0.13697	209A→220A	0.10668	203B→222B	0.13707
203A→222A	0.14184	210A→224A	-0.14139	203B→223B	0.14946
203A→223A	-0.13654	211A→225A	0.16361	203B→231B	-0.11757
203A→231A	0.10884	212A→220A	0.12595	206B→225B	0.10780
204A→217A	-0.21737	202B→215B	0.18418	207B→224B	0.11629
204A→218A	0.14627	202B→217B	-0.11619	207B→225B	0.12050
204A→220A	-0.16177	202B→222B	0.12852	208B→224B	-0.17354
204A→222A	0.14453	202B→223B	-0.12638	209B→225B	0.11024
204A→223A	0.16889	202B→230B	-0.10119	210B→225B	-0.16877
204A→232A	-0.13372	203B→216B	0.23288		

Excited State 57: 4.080-A 4.6304 eV 267.76 nm f=0.0005 <S**2>=3.912

203A→216A	0.25134	203A→222A	-0.14770	203A→231A	-0.12369
203A→219A	-0.15556	203A→223A	0.14311	204A→217A	-0.14493

204A→220A	-0.10770	210A→224A	0.12193	203B→216B	0.15550
204A→223A	0.10181	210A→226A	-0.14999	204B→215B	-0.13339
205A→216A	0.12155	212A→220A	0.10429	204B→222B	0.10441
205A→222A	0.11348	202B→215B	-0.21002	206B→224B	0.11970
205A→223A	-0.10514	202B→217B	0.12775	207B→224B	-0.14571
208A→224A	-0.11821	202B→222B	-0.13370	208B→224B	0.15585
209A→220A	0.10520	202B→223B	0.13200	208B→226B	-0.16742
209A→224A	0.11294	202B→230B	0.11492		

Excited State 58: 4.120-A 4.6311 eV 267.72 nm f=0.0005 <S**2>=3.993

203A→216A	0.11459	208A→226A	0.13000	204B→230B	-0.14637
205A→215A	0.10855	209A→226A	-0.10177	206B→226B	-0.13406
205A→216A	-0.27347	210A→224A	0.14286	207B→226B	0.16638
205A→219A	0.20364	210A→226A	0.19189	208B→224B	0.16338
205A→222A	-0.19676	204B→215B	0.29096	208B→226B	0.19866
205A→223A	0.18141	204B→219B	-0.12626	210B→226B	0.10052
205A→231A	0.15465	204B→222B	-0.18090		
207A→226A	0.11513	204B→223B	0.16525		

Excited State 59: 4.107-A 4.6316 eV 267.69 nm f=0.0005 <S**2>=3.968

205A→216A	0.10163	208A→227A	0.12070	205B→223B	-0.19096
206A→217A	-0.27271	209A→227A	0.11548	205B→231B	-0.14788
206A→220A	-0.21008	211A→227A	0.21108	206B→227B	-0.12920
206A→222A	-0.19496	204B→215B	-0.10852	207B→227B	-0.14969
206A→223A	-0.21986	205B→216B	0.28325	209B→225B	0.10395
206A→229A	-0.11458	205B→217B	-0.12674	209B→227B	0.26284
206A→232A	-0.15503	205B→220B	-0.10950		
207A→227A	-0.10648	205B→222B	-0.18380		

Excited State 60:	3.578-A	4.6514 eV	266.55 nm	f=0.0075	<S**2>=2.950				
193A→218A	0.10386	209A→219A	0.11019	194B→212B	-0.10476				
200A→215A	0.10774	212A→221A	0.54716	199B→212B	-0.16239				
200A→218A	-0.13611	212A→222A	0.17015	200B→211B	0.12027				
202A→221A	-0.17701	212A→228A	0.10549	200B→213B	-0.14516				
207A→218A	-0.10461	178B→211B	-0.11270	206B→221B	-0.12746				
208A→221A	-0.26345	191B→211B	0.10818	210B→221B	-0.14790				

Excited State 61:	3.532-A	4.6968 eV	263.98 nm	f=0.0238	<S**2>=2.868				
202A→220A	-0.11275	211A→223A	0.14370	209B→213B	-0.27875				
204A→225A	-0.20423	212A→220A	-0.11371	209B→214B	0.30579				
206A→227A	0.20160	197B→211B	0.15891	209B→216B	-0.10853				
207A→220A	-0.12319	197B→214B	-0.12403	209B→218B	-0.17432				
211A→213A	0.17455	203B→225B	-0.20577	210B→213B	0.17660				
211A→214A	-0.21907	205B→227B	0.20474	210B→214B	-0.20133				
211A→215A	0.13970	206B→216B	0.10578	210B→216B	-0.16707				
211A→222A	0.14101	207B→216B	0.21398	210B→217B	0.10433				

Excited State 62:	3.509-A	4.7016 eV	263.71 nm	f=0.0180	<S**2>=2.829				
202A→219A	0.12362	210A→223A	-0.13041	208B→213B	0.32814				
203A→224A	0.21294	212A→219A	0.13071	208B→214B	0.34666				
205A→226A	0.20427	194B→211B	0.10291	208B→217B	0.14893				
207A→219A	-0.13162	196B→211B	0.13318	208B→218B	0.16114				
210A→213A	-0.18628	196B→214B	0.11302	208B→228B	-0.11306				
210A→214A	-0.21076	202B→224B	0.20949	208B→229B	-0.10659				
210A→215A	-0.14854	204B→226B	0.20240	209B→215B	-0.10745				
210A→222A	0.15555	207B→215B	-0.20976	210B→215B	-0.16106				

Excited State 63:	3.535-A	4.7334 eV	261.94 nm	f=0.0088	<S**2>=2.875				
198A→221A	0.16555	201A→213A	-0.10102	201A→215A	0.13356				

201A→218A	-0.17080	193B→212B	0.13438	198B→221B	0.15895
212A→221A	0.17855	193B→213B	0.13476	199B→212B	0.41344
212A→228A	-0.11662	195B→211B	0.12857	200B→213B	-0.12652
183B→211B	-0.13922	195B→212B	-0.15925	200B→217B	0.20175
193B→211B	0.26606	198B→212B	-0.29964	201B→211B	0.16317

Excited State 64: 3.616-A 4.7526 eV 260.88 nm f=0.0130 <S**2>=3.018

202A→213A	-0.10844	183B→212B	-0.11899	202B→224B	0.12862
203A→224A	0.13099	193B→211B	-0.11084	203B→225B	0.12177
204A→225A	0.12091	193B→212B	0.30674	204B→226B	-0.16590
205A→226A	-0.16821	194B→211B	-0.21577	205B→227B	0.12475
206A→227A	0.12434	194B→212B	-0.30178	206B→218B	-0.10708
207A→214A	0.10932	198B→211B	-0.11748	207B→214B	0.10991
208A→223A	0.11456	199B→211B	0.19061	207B→222B	-0.11967
209A→222A	0.10268	199B→212B	-0.14946	210B→213B	0.15738
212A→213A	0.10214	201B→212B	0.13025		

Excited State 65: 3.321-A 4.7578 eV 260.59 nm f=0.0035 <S**2>=2.507

212A→217A	0.10227	195B→211B	-0.45623	197B→212B	-0.16549
194B→211B	0.19786	195B→212B	0.50847	203B→225B	0.10017
194B→212B	0.33346	197B→211B	0.11997		

Excited State 66: 3.301-A 4.7592 eV 260.51 nm f=0.0006 <S**2>=2.475

212A→219A	-0.10408	195B→211B	0.26565	196B→212B	-0.17779
194B→211B	0.41973	195B→212B	-0.40633	197B→212B	0.12214
194B→212B	0.45984	196B→211B	-0.12489	202B→224B	0.10091

Excited State 67: 4.145-A 4.7750 eV 259.65 nm f=0.0002 <S**2>=4.046

197A→216A	-0.14361	202A→222A	-0.10479	204A→225A	0.20697
199A→217A	-0.13376	203A→224A	-0.22389	204A→227A	-0.12854

205A→226A	0.22793	211A→232A	0.15213	205B→225B	0.12081
206A→225A	0.12413	196B→215B	0.14459	205B→227B	0.21191
206A→227A	0.20801	197B→216B	-0.15113	206B→222B	-0.14483
207A→223A	-0.15195	202B→224B	-0.22592	207B→223B	-0.17502
208A→222A	0.16018	203B→225B	0.21133	208B→230B	0.15799
209A→223A	0.12765	203B→227B	-0.12415	209B→231B	0.13257
210A→231A	-0.15031	204B→226B	0.23029		

Excited State 68: 3.467-A 4.7855 eV 259.08 nm f=0.0416 <S**2>=2.755

198A→218A	0.10830	212A→215A	-0.18372	201B→212B	0.10718
201A→221A	-0.10267	183B→212B	-0.10522	204B→226B	0.11126
205A→226A	0.10206	193B→212B	0.22459	205B→227B	-0.11742
206A→227A	-0.10782	194B→211B	0.12403	206B→213B	0.25694
208A→213A	-0.17247	194B→212B	0.15371	209B→213B	0.25239
209A→214A	0.18067	199B→211B	0.10369	210B→213B	0.42963

Excited State 69: 3.704-A 4.8250 eV 256.96 nm f=0.0212 <S**2>=3.180

198A→218A	-0.10558	186B→211B	-0.13313	201B→222B	0.11085
201A→221A	0.12107	193B→212B	0.38028	202B→224B	-0.12303
203A→224A	-0.12602	193B→214B	-0.11278	203B→225B	-0.10456
204A→225A	-0.10628	198B→217B	0.12900	204B→226B	0.10481
205A→226A	0.10730	199B→211B	0.20957	206B→213B	-0.20811
207A→222A	0.10065	199B→213B	-0.10007	209B→213B	-0.14591
170B→211B	-0.11365	200B→221B	0.12680	210B→213B	-0.23022
180B→211B	-0.11015	201B→212B	0.13763		

Excited State 70: 3.806-A 4.8701 eV 254.58 nm f=0.0771 <S**2>=3.372

194A→217A	-0.11890	202A→220A	0.16429	207A→220A	0.16307
200A→217A	-0.13183	204A→225A	0.15990	208A→232A	-0.11057
202A→217A	0.10011	206A→227A	-0.15297	209A→217A	0.11551

209A→220A	0.22729	199B→216B	0.17950	209B→218B	-0.15746
209A→232A	-0.12268	201B→216B	-0.20275	209B→222B	-0.14132
211A→213A	0.12835	203B→225B	0.15996	209B→223B	-0.13135
211A→214A	-0.12440	205B→227B	-0.15439	210B→214B	-0.13862
211A→223A	-0.10244	207B→216B	0.12058	210B→216B	-0.15717
212A→220A	0.24641	207B→231B	0.14577	210B→217B	0.10824
190B→211B	0.11326	209B→213B	-0.14508	210B→231B	-0.10783
193B→216B	-0.11229	209B→214B	0.17773		

Excited State 71: 3.687-A 4.8763 eV 254.26 nm f=0.0772 <S**2>=3.148

194A→216A	-0.11255	210A→214A	-0.11717	207B→230B	-0.13723
200A→216A	0.13219	212A→219A	-0.22938	208B→213B	0.16640
202A→216A	0.11521	177B→211B	-0.14202	208B→214B	0.20354
202A→219A	-0.15455	177B→212B	0.11292	208B→217B	0.10751
203A→224A	-0.14457	184B→211B	0.12543	208B→218B	0.13134
205A→226A	-0.14914	189B→211B	0.23208	208B→222B	-0.17025
207A→219A	0.15533	189B→212B	-0.14544	208B→223B	0.13904
209A→216A	-0.12620	199B→215B	0.16377	210B→215B	-0.13294
209A→219A	0.20426	201B→215B	0.18791	210B→230B	-0.10290
209A→231A	-0.12070	202B→224B	-0.14454		
210A→213A	-0.13157	204B→226B	-0.14671		

Excited State 72: 3.229-A 4.8977 eV 253.15 nm f=0.0162 <S**2>=2.356

164B→211B	0.16521	176B→211B	-0.17539	184B→211B	0.16286
165B→212B	0.10998	176B→212B	-0.12937	184B→212B	-0.10901
167B→212B	-0.11357	177B→211B	-0.11225	185B→211B	-0.17431
168B→211B	-0.10284	177B→212B	0.16539	185B→212B	-0.13849
174B→211B	-0.13141	179B→211B	-0.18394	186B→211B	-0.15529
174B→212B	-0.10253	180B→211B	-0.19011	188B→211B	0.15790

189B→211B	0.31364	190B→211B	-0.27132	196B→211B	-0.10923
189B→212B	-0.15795	190B→212B	-0.20754	196B→212B	-0.10683

Excited State 73: 3.194-A 4.9016 eV 252.95 nm f=0.0217 <S**2>=2.300

164B→212B	-0.14367	179B→212B	0.12695	189B→212B	-0.21148
165B→211B	-0.13846	184B→211B	0.16403	190B→211B	0.37875
167B→211B	0.12860	184B→212B	-0.11872	190B→212B	0.21190
174B→211B	0.12071	185B→211B	0.20432	192B→211B	-0.10033
176B→211B	0.17701	185B→212B	0.12763	196B→211B	-0.12283
176B→212B	0.16391	188B→211B	-0.12472	196B→212B	-0.12810
177B→211B	-0.23933	189B→211B	0.26479		

Excited State 74: 3.248-A 4.9455 eV 250.70 nm f=0.1543 <S**2>=2.388

201A→213A	-0.13857	182B→211B	-0.11661	197B→211B	0.12087
202A→213A	-0.13228	183B→212B	0.21052	197B→212B	-0.22689
208A→213A	-0.14876	186B→211B	-0.22188	199B→211B	-0.13657
209A→214A	0.18454	188B→211B	0.27862	201B→214B	-0.10617
212A→215A	-0.13560	189B→211B	-0.13888	207B→214B	0.20114
177B→211B	0.10307	190B→211B	0.14217	209B→213B	0.16350
177B→212B	-0.11033	193B→212B	-0.24446	210B→213B	0.18812
178B→212B	-0.10216	194B→219B	-0.10061		
180B→211B	-0.24962	195B→220B	-0.10425		

Excited State 75: 3.584-A 4.9575 eV 250.09 nm f=0.0009 <S**2>=2.961

198A→228A	0.14918	212A→221A	-0.12569	200B→211B	0.11251
201A→213A	-0.47617	195B→212B	0.13841	200B→213B	-0.24507
201A→215A	0.24617	197B→211B	-0.30464	200B→218B	0.14484
201A→218A	0.16385	197B→212B	0.54083		

*C.2.7.4 **OTPB-FLR-210, EB** State*

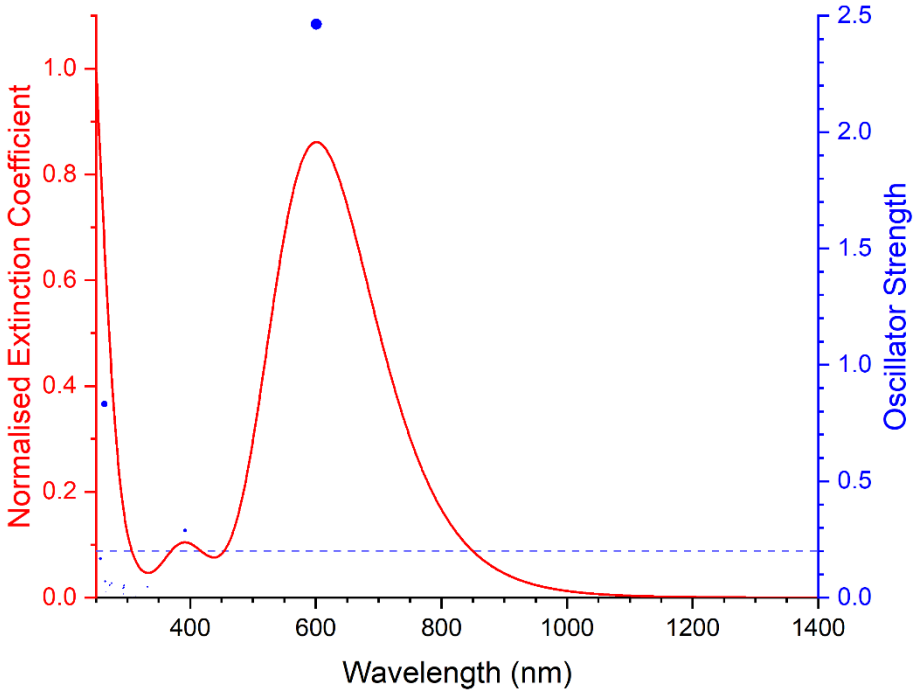

*Figure C-28 Excited states and normalised absorption spectra from TD-DFT calculations of **OTPB-FLR-210** in **EB** state. The areas of excited state dots are proportional to their oscillator strengths.*

Excited State 1:	**Singlet-A**	**2.0622 eV**	**601.21 nm**	**f=2.4635**	**<S**2>=0.000**	
210→213	0.10059	**211→212**	**0.68983**			
Excited State 2:	Singlet-A	2.7018 eV	458.89 nm	f=0.0115	<S**2>=0.000	
197→212	0.14089	206→212	0.20135	210→212	0.62907	
Excited State 3:	**Singlet-A**	**3.1624 eV**	**392.06 nm**	**f=0.2882**	**<S**2>=0.000**	
196→212	0.20326	**205→212**	**0.35731**	**207→212**	**0.52216**	
Excited State 4:	Singlet-A	3.7298 eV	332.41 nm	f=0.0464	<S**2>=0.000	
197→212	-0.12735	198→212	0.66477	200→212	0.12971	
Excited State 5:	Singlet-A	3.9568 eV	313.35 nm	f=0.0077	<S**2>=0.000	
194→212	-0.12234	195→212	0.65231	199→212	-0.14233	
Excited State 6:	Singlet-A	4.0275 eV	307.84 nm	f=0.0026	<S**2>=0.000	
194→212	-0.22768	206→212	-0.13979	209→212	0.54237	
197→212	-0.13435	208→212	0.15408	210→212	0.14628	

211→213	-0.14979							

Excited State 7:	Singlet-A	4.0415 eV	306.78 nm	f=0.0042	<S**2>=0.000

194→212	-0.10702	208→212	0.58719	209→212	-0.29592

Excited State 8:	Singlet-A	4.0586 eV	305.48 nm	f=0.0001	<S**2>=0.000

194→212	0.30104	208→212	0.30550	211→213	0.25037
197→212	0.20720	209→212	0.29654	211→217	-0.11236
206→212	0.16078	210→212	-0.18427		

Excited State 9:	Singlet-A	4.2053 eV	294.83 nm	f=0.0527	<S**2>=0.000

191→212	0.16037	199→212	-0.18145	207→212	-0.30171
196→212	0.17082	200→212	0.36876	211→213	-0.17840
197→212	0.17979	205→212	0.21018		

Excited State 10:	Singlet-A	4.2115 eV	294.40 nm	f=0.0430	<S**2>=0.000

191→212	-0.15993	200→212	0.45436	207→212	0.29727
196→212	-0.24286	205→212	-0.22260		

Excited State 11:	Singlet-A	4.2154 eV	294.12 nm	f=0.0151	<S**2>=0.000

195→212	0.13732	200→213	0.10463		
199→212	0.58864	211→213	-0.21024		

Excited State 12:	Singlet-A	4.2300 eV	293.11 nm	f=0.0406	<S**2>=0.000

194→212	-0.12572	199→212	0.15674	210→216	-0.14437
196→212	0.11343	200→212	0.26961	211→213	0.45617
197→212	-0.10183	206→212	-0.20209	211→217	-0.12119

Excited State 13:	Singlet-A	4.5118 eV	274.80 nm	f=0.0612	<S**2>=0.000

194→212	-0.23621	207→218	-0.11398	211→218	0.50769
206→212	0.26663	211→216	-0.19457		

Excited State 14:	Singlet-A	4.5590 eV	271.95 nm	f=0.0535	<S**2>=0.000	
194→212	-0.32610	206→212	0.44236	211→218	-0.29234	
195→212	-0.11299	211→216	0.16130			
Excited State 15:	Singlet-A	4.6703 eV	265.48 nm	f=0.0230	<S**2>=0.000	
197→214	-0.12560	208→212	-0.12520	208→217	0.12469	
206→214	-0.11704	208→213	0.17659	210→214	0.34014	
207→214	0.26412	208→216	-0.20428	211→214	0.34067	
Excited State 16:	Singlet-A	4.6797 eV	264.94 nm	f=0.0696	<S**2>=0.000	
196→215	-0.11988	209→212	-0.12460	209→217	-0.10861	
206→215	0.11729	209→213	-0.18949	210→215	-0.31480	
207→215	0.26125	209→216	-0.22524	211→215	0.33055	
Excited State 17:	**Singlet-A**	**4.7094 eV**	**263.27 nm**	**f=0.8316**	**<S**2>=0.000**	
207→216	0.15318	**211→216**	**0.41136**	211→219	-0.22379	
210→213	**-0.32631**	211→218	0.23893			
Excited State 18:	Singlet-A	4.8216 eV	257.14 nm	f=0.1667	<S**2>=0.000	
191→212	-0.33531	197→212	-0.11056	207→212	-0.11357	
196→212	-0.28831	205→212	0.48781			

C.2.8 Electronic Transitions in **OTPB-FLR-221** Oligomers

*Table C-12 Attributes of **OTPB-FLR-221** in **LEB**, **ES** (singlet and quintet), and **EB** states related to electronic structures*

Attribute	LEB State	^{1}ES State	^{5}ES State	EB State
Molecular Formula	$C_{74}H_{52}N_4$	$C_{74}H_{52}N_4^{4+}$	$C_{74}H_{52}N_4^{4+}$	$C_{74}H_{48}N_4$
Number of Atoms	130	130	130	126
Number of Electrons	524	520	520	520
HOMO	MO 262	MO 260	MOs 262A, 258B	MO 260
LUMO	MO 263	MO 261	MOs 263A, 259B	MO 261

*C.2.8.1 **OTPB-FLR-221**, **LEB** State*

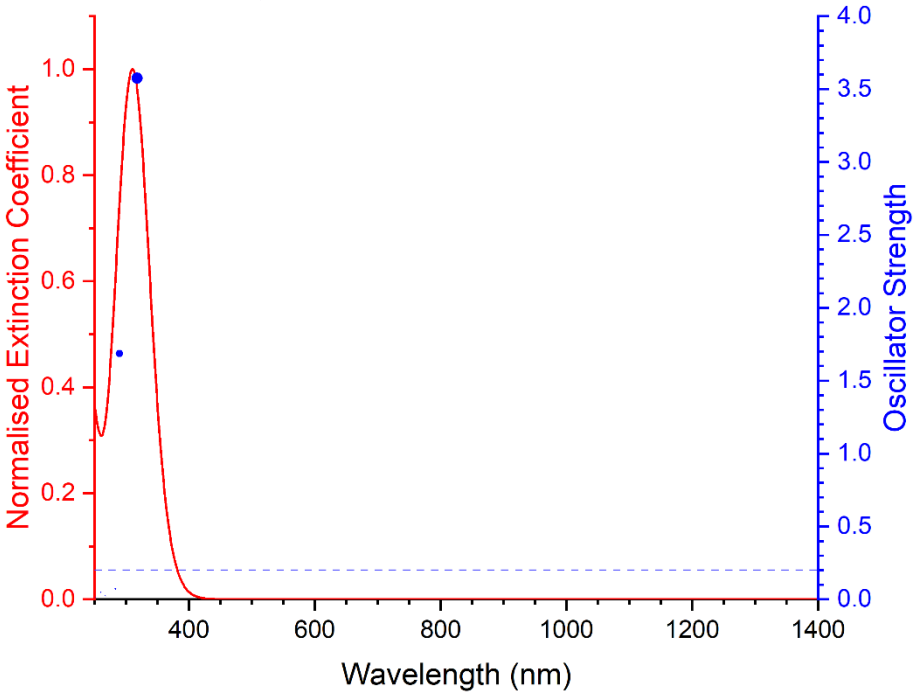

*Figure C-29 Excited states and normalised absorption spectra from TD-DFT calculations of **OTPB-FLR-221** in **LEB** state. The areas of excited state dots are proportional to their oscillator strengths.*

Excited State 1:	Singlet-A	3.7865 eV	327.43 nm	f=0.0000	<S**2>=0.000			
259→266	0.17637		261→263	0.43466		262→264	0.40320	
260→265	0.12382		261→268	-0.10827		262→267	-0.17705	
Excited State 2:	**Singlet-B**	**3.9048 eV**	**317.52 nm**	**f=3.5745**	**<S**2>=0.000**			
260→266	0.17184		261→267	-0.21038		262→268	-0.11736	
261→264	**0.37943**		**262→263**	**0.45432**				
Excited State 3:	**Singlet-B**	**4.2830 eV**	**289.48 nm**	**f=1.6855**	**<S**2>=0.000**			
259→263	**0.33427**		**261→266**	**0.31964**		262→271	0.17098	
260→264	**0.32378**		262→265	0.24313		262→273	0.11751	
Excited State 4:	Singlet-A	4.3759 eV	283.33 nm	f=0.0719	<S**2>=0.000			
257→266	0.12340		260→263	0.38037		261→271	0.18009	
259→264	0.23571		261→265	0.15236		262→266	0.37943	
Excited State 5:	Singlet-A	4.4048 eV	281.48 nm	f=0.0005	<S**2>=0.000			
259→272	-0.14692		260→271	-0.14094		261→268	-0.23398	

261→270	-0.34785	262→269	0.41287		

Excited State 6:	Singlet-B	4.4062 eV	281.38 nm	f=0.0130	<S**2>=0.000
259→271	-0.13596	261→269	0.41545	262→270	-0.35448
260→272	-0.15373	262→268	-0.24085		

Excited State 7:	Singlet-B	4.5073 eV	275.08 nm	f=0.0011	<S**2>=0.000
252→264	-0.10533	259→263	-0.17190	261→266	-0.19771
256→263	-0.11269	259→268	-0.15280	261→272	-0.13266
257→265	0.19250	260→264	0.22332	262→265	0.28529
258→266	0.19647	260→267	0.19213	262→271	-0.12475

Excited State 8:	Singlet-A	4.5199 eV	274.31 nm	f=0.0001	<S**2>=0.000
252→265	-0.14541	258→263	0.14512	261→263	-0.16871
256→266	-0.15864	258→268	0.13532	262→264	0.23090
257→264	0.17624	259→266	-0.16504	262→267	0.23886
257→267	0.13057	260→265	0.33566		

Excited State 9:	Singlet-A	4.6131 eV	268.76 nm	f=0.0216	<S**2>=0.000
254→263	0.10671	260→268	0.12601	261→273	-0.22511
259→264	-0.13401	260→270	0.18766	262→272	0.34249
259→269	-0.20726	260→277	0.15194		
259→276	-0.13300	261→271	0.23171		

Excited State 10:	Singlet-B	4.6364 eV	267.42 nm	f=0.0254	<S**2>=0.000
253→263	-0.10498	259→270	0.19419	260→276	-0.11356
254→264	0.10771	259→277	0.11994	261→272	0.30957
258→266	0.11545	260→267	0.11639	262→271	0.23859
259→263	-0.14282	260→269	-0.20574	262→273	-0.20690

Excited State 11:	Singlet-B	4.7675 eV	260.06 nm	f=0.0473	<S**2>=0.000	
257→263	0.18570	261→267	0.15570	262→268	0.28998	
260→266	0.33418	261→278	0.18966	262→270	-0.21591	
261→264	-0.12384	262→263	0.13971	262→277	0.14365	

Excited State 12:	Singlet-A	4.7767 eV	259.56 nm	f=0.0001	<S**2>=0.000	
257→264	0.10750	260→265	0.13583	261→277	-0.13752	
258→263	-0.17531	260→273	0.14353	262→267	0.23417	
259→266	0.28724	261→268	0.29253	262→276	0.19036	
259→272	-0.12963	261→270	-0.17973			

Excited State 13:	Singlet-B	4.7830 eV	259.22 nm	f=0.0299	<S**2>=0.000	
259→265	-0.16880	260→266	-0.11038	261→276	-0.27145	
259→271	0.11398	260→272	0.22012	262→268	-0.13370	
259→273	-0.16681	260→279	0.11809	262→277	0.28896	
259→280	-0.10872	261→267	-0.18524			

Excited State 14:	Singlet-A	4.8156 eV	257.47 nm	f=0.0001	<S**2>=0.000	
257→269	-0.13338	260→271	0.18003	261→277	0.28427	
259→266	0.11739	260→273	-0.11826	262→267	0.12772	
259→272	0.18655	260→280	-0.12933	262→276	-0.22693	
259→279	0.11886	261→268	0.12548	262→278	0.22724	
260→265	0.11055	261→270	-0.12397			

Excited State 15:	Singlet-A	4.9069 eV	252.67 nm	f=0.0027	<S**2>=0.000	
246→263	-0.10109	257→272	0.11421	261→265	-0.17942	
253→264	0.11876	259→267	-0.14782	261→280	-0.29334	
253→267	-0.10716	259→276	-0.17479	262→279	0.29986	
254→263	-0.12044	260→263	0.10097			
254→268	0.11395	260→277	0.19776			

Excited State 16:	Singlet-B	4.9246 eV	251.77 nm	f=0.0114	<S**2>=0.000
247→263	0.11183	254→267	-0.11403	261→279	-0.30558
253→263	-0.11748	257→271	-0.10318	262→280	0.30989
253→268	0.10899	259→277	-0.21066		
254→264	0.11847	260→276	0.20398		

*C.2.8.2 **OTPB-FLR-221**, **^{1}ES** State*

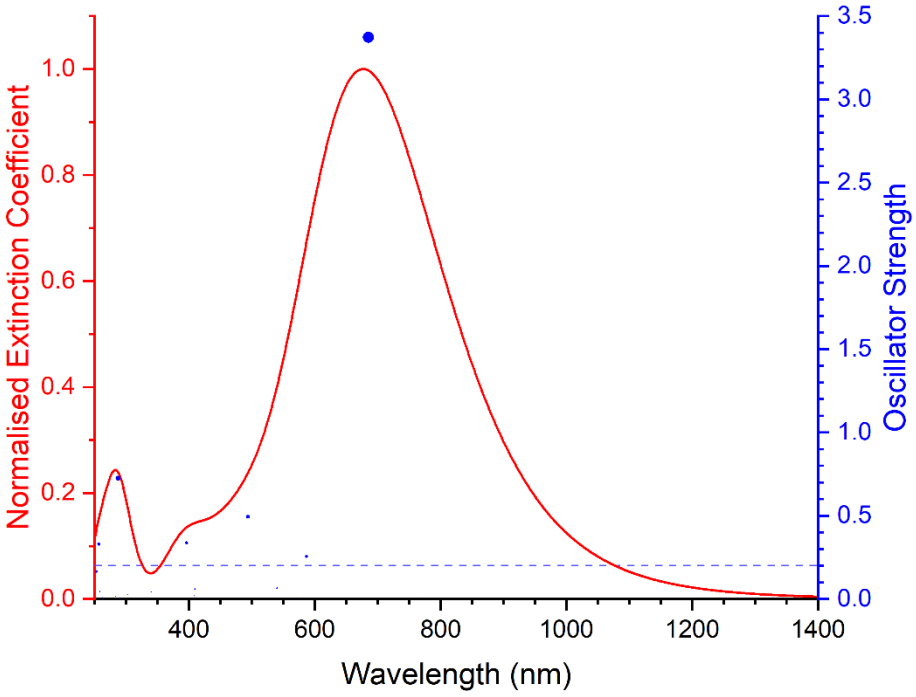

*Figure C-30 Excited states and normalised absorption spectra from TD-DFT calculations of **OTPB-FLR-221** in **^{1}ES** state. The areas of excited state dots are proportional to their oscillator strengths.*

Excited State 1:	Singlet-A	1.6046 eV	772.68 nm	f=0.0003	<S**2>=0.000
256→262	0.27198	259→261	0.54915	260→262	-0.30107

Excited State 2:	**Singlet-B**	**1.8094 eV**	**685.21 nm**	**f=3.3711**	**<S**2>=0.000**
256→261	0.26327	**259→262**	**0.55200**	**260→261**	**-0.31771**

Excited State 3:	Singlet-B	2.1114 eV	587.22 nm	f=0.2558	<S**2>=0.000
253→262	0.21661	258→262	0.50607		
257→261	-0.40598	259→262	-0.10022		

Excited State 4:	Singlet-A	2.1372 eV	580.13 nm	f=0.0000	<S**2>=0.000
259→261	0.35642	260→262	0.60463		

Excited State 5:	Singlet-B	2.1425 eV	578.69 nm	f=0.0015	<S**2>=0.000	
259→262	0.35592	260→261	0.60502			
Excited State 6:	Singlet-A	2.1548 eV	575.38 nm	f=0.0055	<S**2>=0.000	
253→261	0.19123	257→262	-0.31194	258→261	0.58468	
Excited State 7:	Singlet-B	2.2937 eV	540.53 nm	f=0.0657	<S**2>=0.000	
256→261	0.11353	257→261	0.50105	258→262	0.46464	
Excited State 8:	Singlet-A	2.3210 eV	534.18 nm	f=0.0045	<S**2>=0.000	
253→261	-0.12174	257→262	0.56759			
256→262	0.12389	258→261	0.36646			
Excited State 9:	**Singlet-B**	**2.5099 eV**	**493.98 nm**	**f=0.4937**	**<S**2>=0.000**	
252→262	0.15148	257→261	-0.13718	260→261	0.16619	
256→261	**0.60452**	259→262	-0.22840			
Excited State 10:	Singlet-A	2.5180 eV	492.40 nm	f=0.0005	<S**2>=0.000	
252→261	0.15742	257→262	-0.12749	260→262	0.17521	
256→262	0.59732	259→261	-0.24028			
Excited State 11:	Singlet-A	2.7822 eV	445.63 nm	f=0.0000	<S**2>=0.000	
242→262	-0.40644	247→262	0.14034	250→261	0.12629	
243→261	0.43273	248→261	-0.21159			
244→262	-0.13452	249→262	0.19290			
Excited State 12:	Singlet-B	2.7824 eV	445.60 nm	f=0.0002	<S**2>=0.000	
242→261	-0.41207	247→261	0.14268	250→262	0.12401	
243→262	0.42674	248→262	-0.20779			
244→261	-0.13681	249→261	0.19618			

Excited State 13:	Singlet-B	2.9577 eV	419.20 nm	f=0.0023	<S**2>=0.000			
239→261	0.20079		247→261	0.37782		249→261	-0.24888	
240→262	-0.19791		248→262	-0.25304		250→262	-0.37125	
Excited State 14:	Singlet-A	2.9579 eV	419.17 nm	f=0.0035	<S**2>=0.000			
239→262	-0.19790		247→262	-0.37069		249→262	0.24328	
240→261	0.20043		248→261	0.25854		250→261	0.37746	
Excited State 15:	Singlet-A	3.0213 eV	410.36 nm	f=0.0000	<S**2>=0.000			
242→262	0.15400		248→261	-0.27707		252→261	0.33603	
243→261	-0.18541		249→262	0.26175		255→261	0.10411	
244→262	0.13166		250→261	0.21035		256→262	-0.11635	
247→262	0.14032		251→262	0.24226				
Excited State 16:	Singlet-B	3.0268 eV	409.62 nm	f=0.0591	<S**2>=0.000			
242→261	-0.17357		248→262	0.29140		252→262	-0.28764	
243→262	0.19740		249→261	-0.28861		256→261	0.10150	
244→261	-0.12633		250→262	-0.21756				
247→261	-0.15950		251→261	-0.23881				
Excited State 17:	Singlet-A	3.0272 eV	409.57 nm	f=0.0045	<S**2>=0.000			
245→262	-0.13111		253→261	0.62526		258→261	-0.10078	
246→261	0.11415		257→262	0.21665				
Excited State 18:	Singlet-B	3.0320 eV	408.92 nm	f=0.0190	<S**2>=0.000			
245→261	-0.13093		253→262	0.61666		257→261	0.21904	
246→262	0.10540		254→261	-0.14152		258→262	-0.10825	
Excited State 19:	Singlet-A	3.0390 eV	407.98 nm	f=0.0000	<S**2>=0.000			
254→262	-0.31188		255→261	0.62395				

Excited State 20:	Singlet-B	3.0391 eV	407.96 nm	f=0.0006	<S**2>=0.000	
253→262	0.10899	254→261	0.61179	255→262	-0.32398	
Excited State 21:	Singlet-B	3.0455 eV	407.10 nm	f=0.0003	<S**2>=0.000	
254→261	0.32158	255→262	0.61837			
Excited State 22:	Singlet-A	3.0455 eV	407.10 nm	f=0.0001	<S**2>=0.000	
254→262	0.62967	255→261	0.30950			
Excited State 23:	Singlet-A	3.1122 eV	398.38 nm	f=0.0005	<S**2>=0.000	
241→261	0.10974	248→261	0.20322	252→261	0.49269	
242→262	-0.18328	249→262	-0.22592	256→262	-0.14151	
243→261	0.15399	250→261	-0.12818			
247→262	-0.15979	251→262	0.12099			
Excited State 24:	**Singlet-B**	**3.1269 eV**	**396.51 nm**	**f=0.3367**	**<S**2>=0.000**	
241→262	0.11356	247→261	-0.14652	251→261	0.15253	
242→261	-0.17107	248→262	0.17060	**252→262**	**0.51965**	
243→262	0.13361	249→261	-0.20625	256→261	-0.14434	
244→261	0.10597	250→262	-0.10779			
Excited State 25:	Singlet-B	3.1785 eV	390.08 nm	f=0.0053	<S**2>=0.000	
239→261	0.45592	247→261	-0.16917	249→261	0.10256	
240→262	-0.44969	248→262	0.11524	250→262	0.16089	
Excited State 26:	Singlet-A	3.1788 eV	390.04 nm	f=0.0010	<S**2>=0.000	
239→262	-0.44964	247→262	0.16468	249→262	-0.10106	
240→261	0.45623	248→261	-0.11696	250→261	-0.16478	
Excited State 27:	Singlet-A	3.6402 eV	340.60 nm	f=0.0000	<S**2>=0.000	
241→261	0.14164	251→262	0.58011			
244→262	0.12947	252→261	-0.31200			

Excited State 28:	Singlet-B	3.6415 eV	340.47 nm	f=0.0423	<S**2>=0.000
241→262	0.13877	251→261	0.57404		
244→261	0.13510	252→262	-0.32599		
Excited State 29:	Singlet-A	3.8519 eV	321.88 nm	f=0.0001	<S**2>=0.000
247→262	-0.13878	249→262	0.48453	250→261	-0.48431
Excited State 30:	Singlet-B	3.8520 eV	321.87 nm	f=0.0003	<S**2>=0.000
247→261	0.14176	249→261	-0.47365	250→262	0.49470
Excited State 31:	Singlet-A	3.8676 eV	320.57 nm	f=0.0003	<S**2>=0.000
245→262	0.10322	247→262	0.46883	249→262	0.13197
246→261	-0.12093	248→261	0.47284		
Excited State 32:	Singlet-B	3.8677 eV	320.57 nm	f=0.0010	<S**2>=0.000
245→261	0.11466	247→261	0.45610	249→261	0.13482
246→262	-0.12583	248→262	0.48051		
Excited State 33:	Singlet-B	3.8949 eV	318.32 nm	f=0.0017	<S**2>=0.000
245→261	-0.43524	247→261	0.12765	253→262	-0.19284
246→262	0.45410	248→262	0.13177		
Excited State 34:	Singlet-A	3.8987 eV	318.01 nm	f=0.0046	<S**2>=0.000
245→262	-0.42312	247→262	0.12233	253→261	-0.19783
246→261	0.46878	248→261	0.12061		
Excited State 35:	Singlet-B	4.0932 eV	302.90 nm	f=0.0269	<S**2>=0.000
241→262	0.36436	244→261	0.48285		
242→261	-0.13736	251→261	-0.25774		

Excited State 36:	Singlet-A	4.0937 eV	302.87 nm	f=0.0001	<S**2>=0.000
241→261	0.37585	244→262	0.47663		
242→262	-0.13535	251→262	-0.25074		
Excited State 37:	Singlet-B	4.2499 eV	291.73 nm	f=0.0004	<S**2>=0.000
245→261	0.48475	246→262	0.48578		
Excited State 38:	Singlet-A	4.2670 eV	290.57 nm	f=0.0001	<S**2>=0.000
245→262	0.50401	246→261	0.48082		
Excited State 39:	**Singlet-B**	**4.3140 eV**	**287.40 nm**	**f=0.7238**	**<S**2>=0.000**
252→264	0.14162	257→263	-0.10098	**259→264**	**0.45531**
253→265	-0.10278	257→268	0.12379	260→263	-0.29167
256→263	0.30963	258→265	-0.10107		
Excited State 40:	Singlet-A	4.3672 eV	283.90 nm	f=0.0168	<S**2>=0.000
252→263	0.13758	257→264	-0.10380	259→263	0.48386
256→264	0.31111	257→265	0.14254	260→264	-0.25094
Excited State 41:	Singlet-A	4.5698 eV	271.32 nm	f=0.0004	<S**2>=0.000
241→261	0.11777	258→263	0.30181	260→265	0.36926
251→265	0.10234	258→269	-0.28416		
257→270	0.16140	259→268	0.13265		
Excited State 42:	Singlet-B	4.5816 eV	270.61 nm	f=0.0113	<S**2>=0.000
246→262	0.10046	258→265	0.32810	260→263	0.26890
252→270	-0.10547	259→264	0.18878	260→269	-0.28342
257→268	0.17998	259→270	0.18070		
Excited State 43:	Singlet-B	4.6921 eV	264.24 nm	f=0.0006	<S**2>=0.000
242→261	0.44316	243→262	0.50065	244→261	0.21702

Excited State 44:	Singlet-A	4.6922 eV	264.24 nm	f=0.0000	<S**2>=0.000			
242→262	0.44782		243→261	0.49281		244→262	0.22171	
Excited State 45:	Singlet-A	4.7188 eV	262.75 nm	f=0.0001	<S**2>=0.000			
241→261	0.52089		244→262	-0.37380				
242→262	0.21817		260→265	-0.10144				
Excited State 46:	Singlet-B	4.7221 eV	262.56 nm	f=0.0123	<S**2>=0.000			
241→262	0.54813		242→261	0.21189		244→261	-0.37390	
Excited State 47:	Singlet-A	4.7979 eV	258.41 nm	f=0.0026	<S**2>=0.000			
220→261	0.27532		233→262	0.30145		245→262	0.11041	
221→262	0.25314		234→261	0.32644				
231→262	0.14546		236→261	-0.15735				
Excited State 48:	Singlet-B	4.8004 eV	258.28 nm	f=0.0433	<S**2>=0.000			
220→262	0.27542		233→261	0.31297		245→261	0.11131	
221→261	0.25835		234→262	0.32399				
231→261	0.14971		236→262	-0.15614				
Excited State 49:	**Singlet-B**	**4.8244 eV**	**256.99 nm**	**f=0.3300**	**<S**2>=0.000**			
253→264	-0.14719		258→264	-0.18705		260→268	-0.19166	
257→263	**0.34548**		258→270	-0.10720				
257→269	-0.21136		**259→265**	**0.37439**				
Excited State 50:	Singlet-A	4.8257 eV	256.93 nm	f=0.0009	<S**2>=0.000			
253→263	-0.16743		257→264	0.35311		259→268	0.37630	
256→264	0.10188		257→270	0.23305		260→265	-0.13582	
256→265	0.14263		258→263	-0.13608				
Excited State 51:	Singlet-A	4.8939 eV	253.34 nm	f=0.0042	<S**2>=0.000			
220→261	0.32455		221→262	0.36736		224→261	-0.19118	

233→262	-0.21736	257→265	0.14461		
234→261	-0.19171	259→269	-0.14317		

Excited State 52: Singlet-B 4.8944 eV 253.32 nm f=0.1656 <S**2>=0.000

220→262	0.31966	233→261	-0.24745	259→270	0.11977
221→261	0.37653	234→262	-0.20882		
224→262	-0.19740	257→268	0.11239		

*C.2.8.3 **OTPB-FLR-221**, **^{5}ES** State*

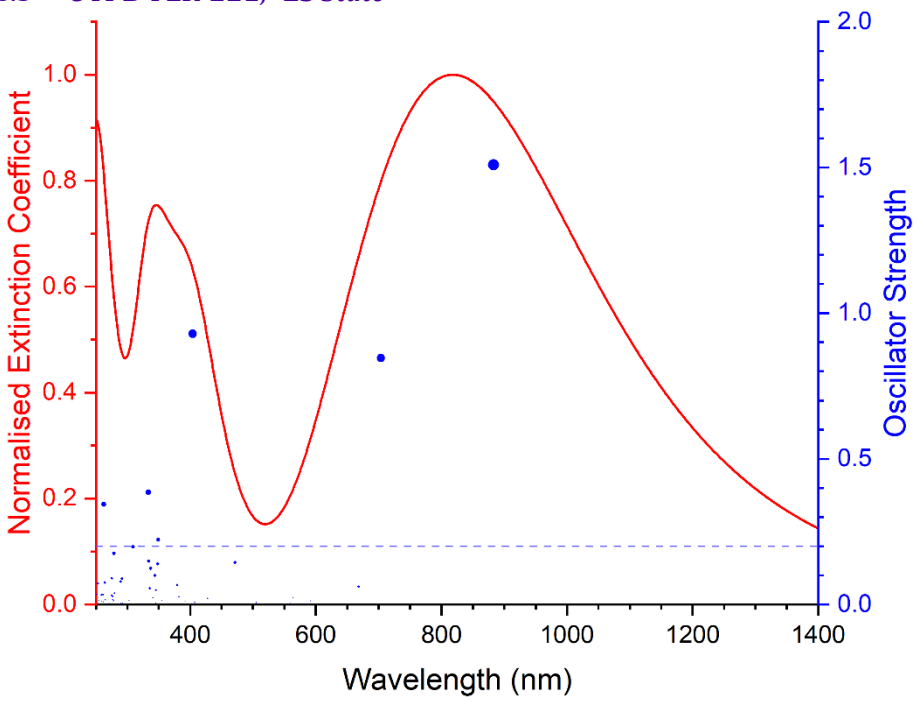

*Figure C-31 Excited states and normalised absorption spectra from TD-DFT calculations of **OTPB-FLR-221** in **^{5}ES** state. The areas of excited state dots are proportional to their oscillator strengths.*

Excited State 1: 5.104-A 1.1783 eV 1052.24 nm f=0.0000 <S**2>=6.262

240B→262B	-0.10180	255B→260B	0.40717	257B→262B	-0.10461
249B→262B	-0.18647	256B→259B	0.60031	258B→260B	0.40827
252B→261B	0.26683	257B→259B	0.39475		

Excited State 2: 5.112-B 1.4040 eV 883.09 nm f=1.5092 <S2>=6.283**

240B→261B	-0.11181	**255B→259B**	**0.46682**	257B→261B	-0.10074
249B→261B	-0.18150	**256B→260B**	**0.53094**	**258B→259B**	**0.45408**
252B→262B	0.22537	**257B→260B**	**0.35346**		

Excited State 3:	**5.082-B**	**1.7615 eV**	**703.87 nm**	**f=0.8459**	**<S**2>=6.206**	
239B→259B	-0.10808	255B→262B	0.27989	257B→261B	0.30400	
240B→260B	-0.10356	256B→260B	0.19141	**258B→262B**	**0.42240**	
249B→260B	-0.27200	**256B→261B**	**0.47224**			
252B→259B	**0.40766**	257B→260B	-0.27711			

Excited State 4:	5.095-A	1.8545 eV	668.55 nm	f=0.0612	<S**2>=6.239	
240B→259B	-0.10759	255B→261B	0.30078	257B→259B	-0.31606	
249B→259B	-0.28159	256B→259B	0.21137	257B→262B	0.27215	
252B→260B	0.34274	256B→262B	0.42199	258B→261B	0.45110	

Excited State 5:	5.106-A	2.0519 eV	604.23 nm	f=0.0001	<S**2>=6.269	
245B→260B	-0.17525	256B→262B	0.22728	258B→260B	0.71305	
255B→260B	-0.24008	257B→259B	-0.22076	258B→263B	-0.10806	
256B→259B	-0.25081	257B→262B	-0.40547			

Excited State 6:	5.101-B	2.0950 eV	591.80 nm	f=0.0126	<S**2>=6.255	
245B→259B	-0.16610	257B→260B	-0.44577	258B→262B	0.14930	
255B→259B	-0.23879	257B→261B	-0.40837			
255B→262B	-0.13368	258B→259B	0.63864			

Excited State 7:	5.102-B	2.1146 eV	586.31 nm	f=0.0088	<S**2>=6.258	
240B→260B	0.13878	255B→262B	-0.27735	258B→259B	-0.31503	
245B→262B	-0.11898	256B→260B	0.48086	258B→262B	0.28360	
252B→259B	-0.17226	256B→261B	-0.38938			
255B→259B	0.12911	257B→260B	-0.45532			

Excited State 8:	5.090-A	2.1634 eV	573.10 nm	f=0.0090	<S**2>=6.228	
240B→259B	-0.16285	244B→259B	0.12752	252B→260B	0.18754	
243B→260B	0.10624	245B→261B	0.13730	255B→261B	0.34194	

256B→259B	-0.40239	257B→259B	0.58847	258B→261B	-0.21559
256B→262B	0.35702	257B→262B	0.19559		

Excited State 9: 5.096-B 2.1999 eV 563.58 nm f=0.0234 <S**2>=6.243

241B→260B	0.21975	243B→259B	0.40119	250B→259B	0.28117
241B→261B	0.36500	244B→260B	0.39234	251B→260B	-0.24612
242B→259B	-0.27773	247B→262B	-0.20113		
242B→262B	-0.34957	248B→261B	-0.20309		

Excited State 10: 5.097-A 2.2015 eV 563.19 nm f=0.0000 <S**2>=6.244

241B→259B	0.28759	244B→259B	0.38572	248B→262B	-0.18253
241B→262B	0.32860	244B→262B	0.10828	250B→260B	0.23761
242B→260B	-0.29335	247B→260B	-0.10423	251B→259B	-0.25783
242B→261B	-0.36102	247B→261B	-0.20126	257B→259B	-0.15318
243B→260B	0.32528	248B→259B	-0.10935		

Excited State 11: 5.095-A 2.2117 eV 560.59 nm f=0.0000 <S**2>=6.241

241B→259B	0.38924	244B→262B	0.36528	250B→261B	0.16466
242B→260B	-0.33390	246B→259B	0.10568	251B→259B	0.12470
243B→260B	-0.28796	247B→260B	-0.23273	251B→262B	-0.15014
243B→261B	0.39113	248B→259B	-0.24064		
244B→259B	-0.28076	250B→260B	-0.11598		

Excited State 12: 5.096-B 2.2128 eV 560.30 nm f=0.0038 <S**2>=6.241

241B→260B	0.37826	244B→260B	-0.21828	250B→262B	0.16007
242B→259B	-0.39317	244B→261B	0.39439	251B→261B	-0.16717
243B→259B	-0.27366	247B→259B	-0.26642	258B→259B	0.13594
243B→262B	0.37175	248B→260B	-0.22922		

Excited State 13: 5.122-B 2.4527 eV 505.50 nm f=0.0070 <S**2>=6.309

241B→261B	-0.22745	242B→262B	0.20804	243B→259B	-0.27543

244B→260B	-0.25048	248B→261B	-0.20447	251B→260B	-0.48637
246B→261B	0.16757	249B→260B	-0.13660		
247B→262B	-0.24426	250B→259B	0.56760		

Excited State 14: 5.122-A 2.4530 eV 505.44 nm f=0.0051 <S**2>=6.309

241B→262B	0.21389	246B→262B	-0.15251	250B→260B	-0.50393
242B→261B	-0.22152	247B→261B	0.26190	251B→259B	0.54795
243B→260B	0.25051	248B→262B	0.19317		
244B→259B	0.27479	249B→259B	0.14988		

Excited State 15: 5.164-B 2.4586 eV 504.28 nm f=0.0062 <S**2>=6.416

255A→263A	0.12051	246B→260B	0.28030	256B→263B	0.10485
258A→265A	0.13226	248B→260B	0.28047	257B→260B	-0.20954
262A→267A	-0.11818	252B→262B	-0.34940	257B→261B	0.13490
239B→262B	-0.12821	255B→259B	0.51904	258B→259B	0.19257
245B→259B	0.15514	256B→260B	-0.33702		

Excited State 16: 5.131-A 2.5345 eV 489.19 nm f=0.0000 <S**2>=6.331

241B→259B	0.22403	247B→260B	0.25635	255B→260B	0.43397
242B→260B	-0.15888	248B→259B	0.44075	256B→259B	-0.22124
243B→261B	0.11933	250B→261B	-0.27889	257B→259B	-0.13807
244B→262B	0.11099	251B→262B	0.23344	258B→260B	0.17111
245B→260B	0.12674	252B→261B	-0.25297		

Excited State 17: 5.120-B 2.5458 eV 487.01 nm f=0.0006 <S**2>=6.304

241B→260B	0.23843	246B→260B	-0.32099	250B→262B	-0.38873
242B→259B	-0.26937	247B→259B	0.47796	251B→261B	0.41225
243B→262B	0.15444	248B→260B	0.29262		
244B→261B	0.16645	249B→261B	0.10152		

Excited State 18:	5.144-A	2.5511 eV	486.01 nm	f=0.0000	<S**2>=6.366				
241B→259B	-0.17022	247B→260B	-0.34456	255B→260B	0.34511				
242B→260B	0.19009	248B→259B	-0.11029	256B→259B	-0.18047				
243B→261B	-0.11990	250B→261B	0.32169	257B→259B	-0.10804				
244B→262B	-0.11549	251B→262B	-0.30111	258B→260B	0.11523				
246B→259B	0.46693	252B→261B	-0.22535						

Excited State 19:	5.134-A	2.5976 eV	477.30 nm	f=0.0001	<S**2>=6.339				
255A→265A	-0.10135	245B→261B	-0.11951	252B→260B	0.59549				
258A→263A	-0.10305	246B→262B	-0.30996	255B→261B	-0.40105				
239B→260B	0.16531	248B→262B	-0.23608	258B→261B	-0.37602				

Excited State 20:	5.096-B	2.6290 eV	471.60 nm	f=0.1443	<S**2>=6.242				
238B→262B	-0.10764	246B→261B	-0.31432	255B→262B	-0.36804				
239B→259B	0.14503	248B→261B	-0.24633	256B→261B	-0.13918				
245B→262B	-0.12159	252B→259B	0.66718	258B→262B	-0.33593				

Excited State 21:	5.199-A	2.8958 eV	428.15 nm	f=0.0000	<S**2>=6.508				
261A→263A	0.17386	245B→260B	-0.15315	255B→260B	0.51278				
261A→267A	0.16161	246B→259B	-0.20971	255B→263B	-0.11282				
262A→264A	-0.18874	248B→259B	-0.18503	256B→259B	-0.34829				
262A→268A	-0.12358	249B→262B	-0.24293	257B→259B	-0.24053				
238B→260B	-0.15210	252B→261B	0.32073						

Excited State 22:	5.250-B	2.8984 eV	427.77 nm	f=0.0205	<S**2>=6.640				
255A→263A	-0.14090	238B→259B	-0.13810	252B→262B	0.25592				
258A→265A	-0.11745	245B→259B	-0.16561	255B→259B	0.52577				
260A→266A	0.11058	246B→260B	-0.17621	255B→264B	-0.10998				
261A→268A	-0.15337	248B→260B	-0.15639	256B→260B	-0.35865				
262A→267A	0.16697	249B→261B	-0.24055	256B→263B	-0.12694				

257B→260B	-0.23520	258B→259B	-0.12238	258B→264B	-0.10749

Excited State 23:	5.090-A	3.0299 eV	409.20 nm	f=0.0001	<S**2>=6.226
253B→259B	0.88225	254B→260B	-0.24000		
253B→262B	0.12494	254B→261B	-0.37428		

Excited State 24:	5.088-B	3.0300 eV	409.19 nm	f=0.0001	<S**2>=6.222
253B→260B	-0.21303	254B→259B	0.89162		
253B→261B	-0.37839	254B→262B	0.11091		

Excited State 25:	5.135-A	3.0358 eV	408.41 nm	f=0.0010	<S**2>=6.341
253B→259B	0.25534	254B→260B	0.79108	257B→259B	-0.10875
253B→262B	-0.40479	254B→261B	-0.10516	258B→261B	-0.16685

Excited State 26:	5.096-B	3.0368 eV	408.27 nm	f=0.0073	<S**2>=6.243
253B→260B	0.85372	254B→259B	0.22385	254B→262B	-0.43587

Excited State 27:	5.350-A	3.0450 eV	407.17 nm	f=0.0082	<S**2>=6.907
255A→265A	-0.12265	239B→260B	0.13728	256B→262B	-0.12983
258A→263A	-0.11703	240B→259B	0.15979	257B→259B	0.32948
259A→266A	-0.14590	245B→261B	-0.11636	257B→267B	0.13012
259A→275A	-0.13334	252B→260B	-0.10127	258B→261B	0.46900
260A→264A	0.10835	253B→262B	-0.15824	258B→266B	0.19070
260A→268A	-0.15744	254B→260B	0.31351	258B→275B	0.10441
260A→276A	-0.12237	256B→259B	-0.22176		

Excited State 28:	**5.521-B**	**3.0679 eV**	**404.13 nm**	**f=0.9285**	**<S**2>=7.371**
253A→268A	0.11100	260A→266A	0.15495	**262A→263A**	**-0.38883**
255A→267A	0.20602	260A→275A	0.10896	262A→267A	-0.17555
258A→265A	-0.19024	**261A→264A**	**0.38933**	255B→264B	0.14285
259A→268A	0.17726	261A→268A	0.13484	256B→260B	-0.11926

257B→261B	-0.11033	257B→275B	-0.10359	258B→267B	-0.17567
257B→266B	-0.12578	258B→259B	-0.15048		

Excited State 29: 5.178-A 3.1050 eV 399.30 nm f=0.0022 <S**2>=6.454

233B→262B	0.11080	249B→259B	0.47549	256B→259B	0.11911
238B→261B	0.12268	251B→259B	-0.14379	256B→262B	0.47320
239B→260B	0.18580	252B→260B	-0.22717	257B→259B	-0.18402
240B→259B	0.17999	252B→263B	-0.11166	257B→262B	0.35436
245B→261B	0.12939	255B→261B	-0.13913	258B→261B	-0.16991

Excited State 30: 5.103-B 3.1054 eV 399.25 nm f=0.0021 <S**2>=6.261

239B→259B	0.15767	251B→260B	-0.10741	256B→261B	0.44529
240B→260B	0.10361	252B→259B	-0.12700	257B→260B	-0.28371
245B→262B	0.12881	255B→262B	-0.28419	257B→261B	0.44041
249B→260B	0.38353	256B→260B	0.16877	258B→262B	-0.36182

Excited State 31: 5.367-A 3.1505 eV 393.54 nm f=0.0000 <S**2>=6.952

249A→269A	-0.10144	261A→263A	-0.35873	252B→261B	0.28370
251A→277A	0.11081	261A→267A	-0.19678	255B→263B	0.12373
252A→278A	-0.11281	262A→264A	0.38089	256B→259B	-0.18051
253A→267A	-0.11532	262A→268A	0.14149	256B→264B	0.11974
254A→265A	0.11001	239B→261B	0.10391	257B→259B	-0.10622
255A→264A	-0.10602	245B→260B	-0.12411	258B→260B	-0.12093
255A→268A	-0.13550	246B→259B	-0.24131		
258A→266A	0.12092	248B→259B	-0.21487		

Excited State 32: 5.115-B 3.1621 eV 392.10 nm f=0.0097 <S**2>=6.290

246B→260B	-0.13947	255B→259B	-0.12542	258B→259B	0.41568
248B→260B	-0.10519	256B→261B	-0.52659		
249B→261B	0.12216	257B→261B	0.62748		

Excited State 33:	5.362-A	3.2389 eV	382.80 nm	f=0.0030	<S**2>=6.938	
256A→280A	0.14320	239B→260B	0.12319	257B→259B	0.18356	
257A→281A	0.14276	249B→259B	0.22025	257B→262B	0.12972	
259A→266A	0.14048	252B→260B	0.17892	257B→267B	-0.13568	
259A→275A	0.16511	253B→279B	-0.12935	258B→261B	0.51359	
260A→264A	-0.11126	254B→280B	-0.14004	258B→266B	-0.15355	
260A→268A	0.15769	255B→261B	-0.36101	258B→275B	-0.14694	
260A→276A	0.15023	256B→259B	-0.12373			

Excited State 34:	5.150-B	3.2436 eV	382.25 nm	f=0.0260	<S**2>=6.381	
239B→259B	0.27365	249B→260B	0.21117	256B→261B	0.11476	
240B→260B	0.21762	255B→262B	-0.31860	257B→260B	0.38217	
246B→261B	-0.15400	256B→260B	-0.22186	258B→262B	0.60079	

Excited State 35:	5.107-A	3.2454 eV	382.03 nm	f=0.0000	<S**2>=6.270	
239B→261B	0.11111	249B→262B	0.14183	257B→262B	0.61576	
246B→259B	-0.17852	255B→260B	-0.20474	258B→260B	0.49130	
248B→259B	-0.13414	256B→262B	-0.45086			

Excited State 36:	5.557-B	3.2693 eV	379.24 nm	f=0.0664	<S**2>=7.470	
256A→281A	-0.17764	262A→263A	-0.15804	256B→266B	-0.10335	
257A→280A	-0.17769	238B→259B	-0.11362	256B→275B	-0.10277	
259A→264A	0.14583	246B→260B	-0.22078	257B→266B	0.17509	
259A→268A	-0.13910	248B→260B	-0.20871	257B→275B	0.15857	
259A→276A	-0.19253	252B→262B	0.29215	258B→264B	0.14140	
260A→266A	-0.15904	253B→280B	0.17699	258B→267B	0.15060	
260A→275A	-0.20639	254B→279B	0.16370	258B→277B	0.12916	
261A→264A	0.13948	255B→267B	-0.11768			
261A→268A	0.13532	256B→260B	-0.19924			

Excited State 37:	5.523-A	3.4962 eV	354.63 nm	f=0.0134	<S**2>=7.375				
253A→266A	-0.14286	259A→286A	-0.12926	254B→280B	-0.20640				
254A→264A	-0.10530	260A→276A	0.15596	255B→261B	0.37103				
254A→268A	0.10898	260A→285A	0.13019	255B→266B	0.11443				
255A→265A	-0.19475	262A→265A	-0.18510	256B→262B	-0.11940				
256A→280A	0.19978	239B→260B	0.17936	256B→265B	0.11039				
257A→281A	0.19960	240B→259B	0.15514	257B→284B	0.10089				
258A→263A	-0.21919	252B→260B	-0.11622	258B→261B	-0.13624				
258A→267A	0.13930	252B→263B	-0.12497	258B→275B	-0.13313				
259A→275A	0.14306	253B→279B	-0.19093						

Excited State 38:	**5.539-B**	**3.5486 eV**	**349.39 nm**	**f=0.2225**	**<S**2>=7.419**				
253A→264A	0.12487	260A→286A	-0.11380	252B→262B	0.17506				
254A→266A	0.14592	262A→263A	0.17816	252B→265B	-0.15055				
255A→263A	0.20866	262A→267A	-0.12512	253B→280B	-0.18226				
256A→281A	0.17178	245B→259B	-0.12072	254B→279B	-0.16850				
257A→280A	0.17123	247B→259B	-0.15196	255B→264B	0.11807				
258A→265A	0.28894	248B→260B	-0.18496	256B→263B	0.15968				
259A→276A	0.11322	249B→266B	0.10339	257B→263B	0.10627				
259A→285A	0.12233	250B→262B	-0.16526						
260A→275A	0.11898	251B→261B	0.22004						

Excited State 39:	5.228-B	3.5594 eV	348.32 nm	f=0.1387	<S**2>=6.582				
232B→260B	-0.14778	246B→261B	-0.20011	255B→262B	0.38438				
239B→259B	0.31387	249B→260B	-0.32376	258B→262B	-0.20876				
240B→260B	0.32455	249B→263B	0.10549						
245B→262B	-0.28801	252B→259B	-0.21979						

Excited State 40:	5.177-A	3.5715 eV	347.15 nm	f=0.0004	<S**2>=6.450	
254A→265A	0.12765	240B→262B	-0.20087	250B→261B	-0.38664	
258A→266A	0.13919	245B→260B	0.13265	251B→262B	0.35536	
233B→259B	-0.12439	246B→259B	0.40241	252B→261B	0.22892	
239B→261B	-0.23415	247B→260B	-0.26197	255B→260B	-0.20934	

Excited State 41:	5.191-B	3.5855 eV	345.79 nm	f=0.0491	<S**2>=6.487	
258A→265A	-0.11138	246B→260B	0.36548	250B→262B	-0.41363	
239B→262B	-0.14001	247B→259B	-0.39273	251B→261B	0.49124	
240B→261B	-0.12005	247B→264B	-0.10699	255B→259B	-0.13248	
245B→259B	0.10216	248B→260B	-0.10309			

Excited State 42:	5.147-A	3.5871 eV	345.64 nm	f=0.0053	<S**2>=6.372	
239B→260B	0.15610	251B→259B	-0.17844	257B→259B	-0.11745	
245B→261B	0.17860	252B→260B	0.42201	257B→262B	-0.20430	
246B→262B	-0.10789	255B→261B	0.47756			
249B→259B	0.43563	256B→262B	-0.27559			

Excited State 43:	5.219-A	3.6017 eV	344.23 nm	f=0.0008	<S**2>=6.559	
253A→263A	0.14657	262A→264A	0.19810	249B→262B	-0.18160	
254A→265A	0.20287	233B→259B	-0.11875	250B→261B	0.37268	
255A→264A	0.11685	239B→261B	-0.15356	251B→262B	-0.29257	
258A→266A	0.23190	240B→262B	-0.10724	255B→263B	-0.10445	
260A→265A	-0.12564	247B→260B	0.23492	256B→264B	-0.10376	
261A→263A	-0.19912	248B→259B	0.34287			

Excited State 44:	5.152-B	3.6092 eV	343.52 nm	f=0.0988	<S**2>=6.386	
254A→263A	-0.13173	261A→265A	0.15828	239B→259B	0.15925	
258A→264A	-0.14260	262A→266A	-0.14713	245B→262B	0.24177	
260A→263A	0.10584	233B→261B	0.10306	249B→260B	0.45422	

251B→260B	-0.16367	256B→261B	-0.21602	258B→262B	0.10511
252B→259B	0.33237	257B→260B	-0.14766		
255B→262B	0.44493	257B→261B	-0.16188		

Excited State 45: 5.317-A 3.6374 eV 340.86 nm f=0.0232 <S**2>=6.817

248A→267A	0.10199	261A→266A	0.10392	246B→262B	0.16448
251A→269A	0.10229	262A→265A	-0.22196	249B→259B	0.33869
252A→270A	0.10100	232B→259B	0.16104	252B→260B	0.13102
254A→264A	-0.13378	239B→260B	-0.22356	255B→261B	-0.15800
255A→265A	-0.13694	240B→259B	-0.30744	256B→262B	-0.12875
258A→263A	-0.24701	245B→261B	0.27142	258B→261B	0.10840

Excited State 46: 5.142-B 3.6768 eV 337.20 nm f=0.1238 <S**2>=6.360

254A→266A	0.10559	245B→259B	0.25680	249B→261B	0.46017
261A→264A	-0.12029	246B→260B	-0.18838	250B→262B	-0.13469
233B→260B	0.21751	247B→259B	-0.11481	255B→259B	0.27110
238B→259B	0.18255	247B→262B	0.12070	256B→261B	0.11428
239B→262B	0.28145	248B→260B	-0.31474	257B→261B	-0.15165
240B→261B	0.16793	248B→261B	0.10280		

Excited State 47: 5.155-A 3.6848 eV 336.47 nm f=0.0005 <S**2>=6.393

260A→265A	0.10860	248B→262B	-0.19147	252B→261B	0.40597
240B→262B	-0.25100	249B→262B	0.18483	256B→259B	-0.13904
245B→260B	0.52315	250B→261B	0.10292	256B→262B	0.10898
246B→262B	0.15154	251B→259B	0.17455	257B→262B	-0.15618
247B→261B	-0.27230	251B→262B	-0.12328		

Excited State 48: 5.165-B 3.6905 eV 335.95 nm f=0.0553 <S**2>=6.420

258A→264A	0.10638	241B→261B	0.10446	246B→261B	-0.37235
262A→266A	0.10349	245B→259B	-0.14903	247B→262B	0.50374

248B→261B	0.43025	250B→259B	0.33573	251B→260B	-0.21960
249B→261B	-0.13084	250B→264B	0.11918	251B→263B	-0.10759

Excited State 49: 5.165-A 3.6949 eV 335.55 nm f=0.0021 <S**2>=6.418

240B→262B	-0.12435	248B→262B	0.38493	251B→259B	-0.30497
242B→261B	-0.10257	249B→259B	-0.10954	251B→262B	-0.10133
245B→260B	0.25473	250B→260B	0.19574	251B→264B	-0.10778
246B→262B	-0.29562	250B→261B	0.10045	252B→261B	0.19524
247B→261B	0.54288	250B→263B	0.10513		

Excited State 50: 5.196-B 3.7098 eV 334.21 nm f=0.1487 <S**2>=6.500

253A→265A	0.10687	239B→262B	-0.14140	252B→262B	0.40186
254A→263A	0.12727	240B→261B	-0.29106	255B→259B	-0.11844
258A→264A	0.14929	245B→259B	0.53302	256B→260B	-0.14182
261A→265A	-0.14022	247B→259B	0.10555	257B→260B	-0.11318
262A→266A	0.14839	251B→261B	-0.11856	257B→261B	-0.13600

Excited State 51: 5.271-B 3.7169 eV 333.57 nm f=0.3855 <S2>=6.696**

253A→265A	-0.18910	262A→266A	-0.24536	250B→259B	0.12318
254A→263A	-0.21878	239B→259B	-0.12317	252B→262B	0.20147
255A→266A	-0.18131	240B→261B	-0.14124	255B→262B	-0.23444
258A→264A	-0.25796	245B→259B	0.25988	256B→260B	-0.10775
258A→268A	0.14056	247B→262B	0.16359	256B→261B	0.12113
260A→263A	0.15275	248B→261B	0.17551		
261A→265A	0.23216	249B→260B	-0.22553		

Excited State 52: 5.241-A 3.7974 eV 326.50 nm f=0.0000 <S**2>=6.617

253A→263A	0.11838	258A→266A	0.18591	262A→264A	0.12392
254A→265A	0.12759	260A→265A	-0.10700	233B→259B	0.12817
255A→264A	0.12108	261A→263A	-0.11165	239B→261B	0.20507

245B→260B	0.34559	249B→262B	0.41869	255B→260B	0.27582
246B→259B	-0.22445	252B→261B	-0.13957	256B→264B	-0.12593
248B→259B	-0.30166	252B→266B	0.10468	257B→262B	-0.13815

Excited State 53: 5.087-B 3.8420 eV 322.71 nm f=0.0000 <S**2>=6.219

253B→261B	0.91903	254B→259B	0.39092		

Excited State 54: 5.087-A 3.8420 eV 322.71 nm f=0.0000 <S**2>=6.219

253B→259B	0.39079	254B→261B	0.91847		

Excited State 55: 5.095-B 3.8959 eV 318.24 nm f=0.0020 <S**2>=6.239

248B→261B	-0.11118	250B→259B	0.62772		
249B→260B	0.19630	251B→260B	0.71900		

Excited State 56: 5.095-A 3.8959 eV 318.24 nm f=0.0001 <S**2>=6.241

247B→261B	0.11237	250B→260B	0.74471		
249B→259B	0.16325	251B→259B	0.61332		

Excited State 57: 5.090-A 3.9342 eV 315.14 nm f=0.0000 <S**2>=6.226

253B→262B	0.88448	254B→260B	0.46022		

Excited State 58: 5.090-B 3.9342 eV 315.14 nm f=0.0000 <S**2>=6.226

253B→260B	0.46018	254B→262B	0.88450		

Excited State 59: 5.435-A 3.9878 eV 310.91 nm f=0.0023 <S**2>=7.134

239A→263A	-0.10717	251A→269A	0.12356	258A→263A	0.11827
240A→264A	-0.11674	252A→270A	0.11419	261A→282A	0.11712
242A→266A	0.11856	252A→273A	0.10084	262A→265A	0.13727
247A→268A	-0.10102	254A→276A	0.11599	262A→284A	0.12405
249A→277A	-0.11467	256A→280A	0.10016	231B→260B	0.20522
250A→278A	0.11943	257A→281A	0.10030	232B→259B	0.19362

233B→262B	0.20602	240B→264B	-0.13395	250B→270B	-0.10035
238B→261B	0.22139	245B→261B	-0.10671	251B→269B	0.12530
239B→263B	-0.11955	245B→266B	-0.11106	255B→261B	0.13384
240B→259B	0.28749	247B→278B	-0.11445		

Excited State 60: 5.400-B 4.0002 eV 309.95 nm f=0.0003 <S**2>=7.039

240A→263A	0.10621	260A→263A	-0.13428	239B→259B	0.18005
247A→267A	0.10326	261A→284A	0.11728	240B→260B	0.34904
249A→278A	0.11850	262A→282A	0.13209	240B→263B	-0.12331
250A→277A	-0.11343	231B→259B	0.22382	245B→262B	-0.12831
251A→270A	0.12659	232B→260B	0.19291	250B→269B	-0.14168
252A→269A	0.13619	233B→261B	0.22870	251B→270B	0.12241
259A→265A	0.13478	238B→262B	0.24184	255B→262B	0.19893

Excited State 61: 5.340-B 4.0085 eV 309.30 nm f=0.1982 <S**2>=6.878

241A→263A	-0.10242	261A→264A	-0.13545	246B→260B	0.19342
242A→264A	0.10953	262A→263A	0.21927	248B→260B	0.24002
247A→266A	0.11674	231B→262B	0.11663	249B→261B	-0.15718
254A→266A	0.11683	232B→261B	0.12585	252B→262B	0.38133
256A→281A	-0.13245	233B→260B	0.15751	253B→280B	0.12831
257A→280A	-0.13181	238B→259B	0.21652	254B→279B	0.11855
258A→265A	0.15208	240B→266B	0.11260	255B→264B	0.10349

Excited State 62: 5.317-A 4.0440 eV 306.59 nm f=0.0001 <S**2>=6.817

242A→263A	-0.10601	232B→262B	0.16517	248B→259B	0.17150
247A→265A	-0.12448	233B→259B	0.27978	252B→261B	0.46564
259A→263A	0.20286	236B→260B	0.10334	257B→262B	0.10606
259A→267A	-0.12836	238B→260B	0.33553	257B→265B	-0.14254
260A→265A	-0.21685	240B→262B	0.19530	258B→263B	-0.13360
231B→261B	0.16152	246B→259B	0.13904		

Excited State 63:	5.408-B	4.0556 eV	305.71 nm	f=0.0005	<S**2>=7.061				
247A→263A	-0.10072	260A→263A	-0.13355	250B→259B	0.10039				
249A→278A	-0.13583	232B→260B	0.14590	250B→269B	0.13119				
250A→277A	0.13091	238B→262B	0.16218	251B→270B	-0.10203				
251A→270A	-0.12584	239B→259B	-0.22545	252B→259B	0.31476				
251A→273A	-0.11383	240B→260B	0.13631	255B→262B	-0.11919				
252A→269A	-0.14018	246B→261B	0.31904	257B→263B	0.11214				
252A→274A	0.10843	248B→261B	0.31251	258B→262B	-0.12876				
259A→265A	0.17868	249B→260B	-0.11367	258B→265B	0.15765				

Excited State 64:	5.444-A	4.0910 eV	303.07 nm	f=0.0133	<S**2>=7.158				
242A→266A	0.11274	258A→263A	0.13663	247B→278B	0.11163				
247A→264A	0.11406	259A→266A	-0.13303	248B→262B	0.24364				
248A→263A	-0.10072	261A→271A	-0.11789	250B→270B	0.11226				
249A→277A	0.12893	262A→265A	0.17834	251B→269B	-0.13708				
250A→278A	-0.13233	232B→259B	0.13482	252B→260B	0.23292				
251A→269A	-0.14419	238B→261B	0.10100	253B→279B	-0.11462				
251A→274A	0.10416	239B→260B	-0.23907	254B→280B	-0.12394				
252A→270A	-0.13534	240B→259B	-0.14259	255B→261B	-0.16429				
252A→273A	-0.10998	245B→261B	0.11556	258B→266B	0.12543				
256A→280A	0.12426	245B→266B	-0.10969						
257A→281A	0.12351	246B→262B	0.23060						

Excited State 65:	5.094-B	4.1360 eV	299.77 nm	f=0.0026	<S**2>=6.236				
241B→260B	0.24305	244B→261B	-0.11843	248B→260B	-0.50207				
242B→259B	0.22401	246B→260B	0.39994	250B→262B	0.17988				
243B→262B	0.14806	247B→259B	0.58774	251B→261B	0.18302				

Excited State 66:	5.092-A	4.1375 eV	299.66 nm	f=0.0000	<S**2>=6.232	
241B→259B	0.24170	244B→262B	-0.15232	248B→259B	-0.44209	
242B→260B	0.22283	246B→259B	0.38373	250B→261B	0.17819	
243B→261B	0.11203	247B→260B	0.64914	251B→262B	0.17817	

Excited State 67:	5.346-A	4.2409 eV	292.35 nm	f=0.0044	<S**2>=6.894	
243A→272A	0.13344	232B→259B	0.13653	244B→259B	-0.24402	
244A→271A	-0.11953	233B→262B	0.14666	246B→262B	0.20750	
256A→280A	-0.10567	238B→261B	0.21243	248B→262B	0.13147	
257A→281A	-0.10524	240B→259B	0.37103	249B→259B	-0.23451	
259A→266A	0.11028	241B→262B	0.14719	252B→260B	0.23324	
260A→268A	0.10363	241B→272B	-0.10863	254B→280B	0.10659	
231B→260B	0.13079	243B→260B	0.25689			

Excited State 68:	5.383-B	4.2541 eV	291.45 nm	f=0.0891	<S**2>=6.995	
251A→278A	0.10016	262A→263A	-0.14838	246B→260B	0.18549	
256A→281A	0.12548	262A→270A	0.12163	248B→260B	0.18992	
257A→280A	0.12530	233B→260B	0.17229	252B→262B	0.36225	
259A→264A	0.12757	238B→259B	0.24133	253B→280B	-0.12795	
260A→266A	-0.16016	240B→261B	0.17541	254B→279B	-0.11841	
261A→268A	0.10897	241B→260B	0.10018	258B→267B	0.11541	
261A→269A	0.14885	245B→259B	-0.34732			

Excited State 69:	5.487-A	4.2605 eV	291.01 nm	f=0.0000	<S**2>=7.277	
249A→269A	0.13238	259A→263A	-0.21640	262A→264A	0.23110	
250A→270A	0.12021	259A→270A	0.10312	262A→269A	0.29852	
251A→277A	-0.12573	260A→265A	0.22804	262A→274A	-0.13889	
252A→278A	0.13513	261A→267A	-0.21058	245B→260B	-0.13581	
255A→269A	-0.12667	261A→270A	0.25938	246B→259B	0.13790	
258A→266A	0.11302	261A→273A	0.15106	247B→270B	-0.11864	

248B→259B	0.17401	250B→278B	-0.12025	252B→261B	0.20008
248B→269B	-0.12925	251B→276B	0.10981		

Excited State 70: 5.099-B 4.2735 eV 290.12 nm f=0.0033 <S**2>=6.249

241B→261B	-0.21799	243B→259B	-0.60718	247B→262B	-0.11196
242B→259B	0.11408	243B→262B	-0.10203	249B→260B	0.10361
242B→262B	-0.26099	244B→260B	0.62716		

Excited State 71: 5.124-A 4.2739 eV 290.10 nm f=0.0035 <S**2>=6.313

240B→259B	-0.28532	242B→261B	0.18920	248B→262B	-0.20281
241B→262B	0.22806	243B→260B	0.54943	250B→260B	-0.10804
242B→260B	-0.11839	244B→259B	-0.54637	252B→260B	-0.12707

Excited State 72: 5.463-B 4.2863 eV 289.26 nm f=0.0789 <S**2>=7.210

246A→272A	-0.10091	261A→264A	0.19554	241B→260B	-0.18146
249A→270A	0.10371	261A→269A	0.33753	242B→259B	-0.19391
250A→269A	0.10996	261A→274A	-0.16073	245B→259B	0.18406
255A→270A	-0.11831	262A→267A	-0.18006	246B→260B	0.10128
255A→273A	-0.11599	262A→270A	0.30547	247B→259B	0.16452
259A→269A	0.10564	262A→273A	0.15803	247B→269B	-0.10219
260A→266A	0.10750	238B→259B	-0.11781		

Excited State 73: 5.455-B 4.3013 eV 288.25 nm f=0.0001 <S**2>=7.189

242A→265A	-0.13519	260A→267A	0.22842	239B→259B	-0.10436
247A→263A	-0.13832	260A→283A	-0.11431	240B→260B	-0.23855
255A→266A	-0.15299	261A→265A	-0.17705	246B→261B	-0.13561
258A→264A	-0.19358	262A→266A	-0.17590	248B→261B	-0.14008
258A→268A	0.12813	231B→259B	-0.11739	249B→260B	0.15954
259A→265A	0.36931	233B→261B	-0.13789	252B→259B	-0.11330
260A→263A	-0.36267	238B→262B	-0.13176	257B→263B	0.11119

258B→265B	0.14036				

Excited State 74:	5.491-A	4.3163 eV	287.24 nm	f=0.0000	<S**2>=7.289
245A→272A	0.11851	259A→267A	0.18875	262A→274A	0.10210
246A→271A	-0.11278	260A→265A	0.35777	233B→259B	0.16539
247A→265A	0.11854	261A→263A	0.22659	238B→260B	0.14651
255A→264A	0.14594	261A→270A	-0.18955	240B→262B	0.10720
255A→268A	-0.10339	261A→273A	-0.13138	242B→260B	-0.10775
258A→266A	0.19349	262A→268A	-0.11255	245B→260B	-0.18236
259A→263A	-0.26106	262A→269A	-0.19867		

Excited State 75:	5.107-A	4.3250 eV	286.67 nm	f=0.0000	<S**2>=6.269
241B→259B	0.56363	243B→261B	0.18379	247B→260B	-0.30951
242B→260B	0.57641	244B→262B	-0.24814	248B→259B	0.15743
243B→260B	0.12116	246B→259B	-0.21307		

Excited State 76:	5.144-B	4.3288 eV	286.42 nm	f=0.0022	<S**2>=6.365
261A→269A	0.11556	242B→259B	0.53620	246B→260B	-0.26430
262A→270A	0.10290	243B→262B	0.22359	247B→259B	-0.22287
241B→260B	0.55685	244B→261B	-0.18169	248B→260B	0.18128

Excited State 77:	5.378-A	4.3409 eV	285.62 nm	f=0.0004	<S**2>=6.982
241A→265A	0.13168	259A→266A	-0.12888	239B→260B	-0.10703
248A→263A	0.12689	260A→264A	0.18344	240B→259B	0.21707
253A→266A	-0.14043	260A→268A	-0.14552	243B→260B	0.14366
254A→264A	-0.14039	261A→266A	0.23874	244B→259B	-0.13604
255A→265A	0.17282	231B→260B	-0.14802	245B→261B	-0.21871
258A→263A	0.12185	232B→259B	-0.15355	246B→262B	0.16590
258A→267A	-0.10859	233B→262B	-0.14507	246B→265B	0.12420
258A→283A	0.12450	238B→261B	-0.10651	248B→265B	0.10262

249B→259B	0.32035	252B→263B	0.13845	256B→265B	-0.11597
252B→260B	0.17050	252B→268B	0.10200	258B→266B	0.11745

Excited State 78: 5.420-A 4.4211 eV 280.44 nm f=0.0000 <S**2>=7.095

243A→274A	0.10728	261A→263A	0.16397	246B→269B	-0.10423
245A→272A	0.11796	261A→270A	0.29455	247B→268B	0.12034
246A→271A	-0.11015	261A→273A	0.14880	249B→262B	-0.18077
249A→269A	-0.13449	262A→269A	0.31894	250B→261B	0.21332
250A→270A	-0.12307	262A→274A	-0.12793	251B→262B	0.19031
255A→269A	-0.10871	242B→273B	-0.10424	252B→261B	-0.13329
255A→274A	0.10515	244B→272B	-0.10058		
258A→271A	-0.10369	246B→259B	-0.25220		

Excited State 79: 5.489-B 4.4339 eV 279.63 nm f=0.0377 <S**2>=7.283

243A→270A	-0.10767	261A→269A	-0.24608	242B→259B	0.12481
243A→273A	0.15472	261A→274A	0.10441	242B→274B	-0.14590
244A→274A	-0.14088	262A→263A	-0.16299	243B→272B	0.16030
245A→271A	0.17638	262A→267A	0.10933	244B→271B	-0.14772
246A→272A	-0.18983	262A→270A	-0.22291	246B→260B	0.31093
249A→270A	0.12004	262A→273A	-0.10364	247B→269B	-0.10905
250A→269A	0.12735	238B→259B	-0.11540	248B→260B	0.12453
258A→265A	-0.13781	241B→273B	-0.15570	249B→261B	0.20889

Excited State 80: 5.232-B 4.4500 eV 278.62 nm f=0.0128 <S**2>=6.593

258A→265A	-0.12623	247B→259B	-0.10452	251B→261B	0.52634
260A→266A	-0.12571	248B→260B	0.10922	252B→262B	-0.20946
245B→259B	0.12262	249B→261B	-0.22820		
246B→260B	-0.12024	250B→262B	0.53182		

Excited State 81:	5.417-B	4.4521 eV	278.49 nm	f=0.1750	<S**2>=7.087				
243A→271A	0.18111	261A→265A	-0.16407	243B→274B	0.15219				
244A→272A	-0.19651	262A→266A	0.15953	244B→273B	-0.16218				
245A→270A	-0.13268	212B→261B	-0.10904	245B→262B	-0.13976				
245A→273A	0.15387	231B→259B	-0.14508	246B→261B	0.30674				
246A→269A	-0.12350	232B→260B	-0.12750	248B→261B	0.26175				
246A→274A	-0.15094	240B→260B	0.25559	249B→260B	0.19393				
254A→263A	0.12574	241B→271B	-0.15683	252B→259B	0.10772				
258A→264A	0.12179	242B→272B	-0.16526	252B→264B	0.10306				

Excited State 82:	5.443-B	4.4619 eV	277.87 nm	f=0.0101	<S**2>=7.158				
248A→265A	0.11929	261A→274A	0.11963	247B→269B	-0.13959				
250A→269A	0.11069	262A→267A	-0.11841	248B→260B	-0.10445				
251A→278A	0.12291	262A→270A	-0.19476	250B→262B	0.19874				
252A→277A	-0.11547	262A→273A	-0.13636	250B→276B	-0.10524				
255A→263A	0.18117	226B→259B	-0.10212	251B→261B	0.25134				
258A→265A	0.18780	233B→260B	0.13551	251B→278B	0.11921				
260A→266A	0.12673	238B→259B	0.13553	252B→262B	0.10956				
261A→264A	0.24785	245B→259B	0.12372	252B→265B	-0.10309				
261A→269A	-0.18213	246B→263B	-0.10255	256B→268B	0.11956				

Excited State 83:	5.132-A	4.4655 eV	277.65 nm	f=0.0000	<S**2>=6.334				
261A→270A	-0.10624	247B→260B	-0.20011	251B→262B	0.68541				
262A→269A	-0.10072	250B→261B	0.56742						

Excited State 84:	5.287-B	4.4754 eV	277.04 nm	f=0.0162	<S**2>=6.738				
248A→264A	-0.13312	258A→268A	0.29252	261A→272A	-0.10903				
254A→263A	0.15892	258A→276A	0.11480	262A→266A	-0.13559				
255A→266A	-0.23000	260A→263A	-0.15241	262A→271A	0.21616				
258A→264A	-0.10833	261A→265A	-0.22695	226B→262B	-0.10164				

231B→259B	0.11163	245B→262B	0.14420	258B→265B	-0.20712
233B→261B	0.14863	249B→260B	-0.20075		
239B→259B	0.21191	257B→263B	-0.16429		

Excited State 85: 5.527-A 4.4862 eV 276.37 nm f=0.0284 <S**2>=7.388

243A→272A	0.19893	251A→269A	0.12819	242B→271B	-0.15829
244A→271A	-0.17438	252A→270A	0.11417	243B→273B	0.17982
245A→269A	0.11651	254A→264A	0.13104	244B→267B	0.10737
245A→274A	0.15743	258A→263A	0.21363	244B→274B	-0.17500
246A→270A	0.13003	261A→266A	-0.14149	246B→262B	-0.19221
246A→273A	-0.16918	262A→265A	0.24800	248B→262B	-0.18551
249A→272A	-0.10300	241B→272B	-0.18045	251B→269B	0.11014

Excited State 86: 5.442-A 4.4888 eV 276.21 nm f=0.0000 <S**2>=7.153

243A→269A	-0.10199	258A→266A	0.33838	243B→271B	-0.13438
244A→270A	-0.12037	258A→271A	-0.18758	244B→272B	0.13970
244A→273A	0.10929	258A→275A	0.12501	245B→260B	0.13195
245A→272A	-0.15845	261A→263A	0.14740	256B→265B	0.11279
246A→271A	0.14306	262A→264A	0.11456	257B→265B	-0.16819
248A→266A	0.12321	262A→268A	-0.27637	258B→263B	-0.16445
255A→264A	0.19415	241B→274B	0.11101		
255A→268A	-0.21537	242B→273B	0.10687		

Excited State 87: 5.387-B 4.5005 eV 275.49 nm f=0.0896 <S**2>=7.005

244A→272A	0.10438	258A→268A	0.15120	240B→260B	0.32118
245A→273A	-0.10132	262A→266A	-0.18626	243B→274B	-0.10036
251A→270A	0.10675	262A→271A	0.12634	244B→273B	0.10437
252A→269A	0.12017	231B→259B	-0.17466	245B→262B	-0.26027
255A→266A	-0.13351	232B→260B	-0.10751	246B→261B	0.13302
258A→264A	-0.18994	233B→261B	-0.17307	249B→260B	0.17656

249B→261B	-0.11425	252B→259B	0.11174		

Excited State 88:	5.156-B	4.5065 eV	275.12 nm	f=0.0319	<S**2>=6.396
231B→262B	-0.11746	245B→259B	-0.21724	250B→262B	0.42661
233B→260B	-0.15646	248B→260B	0.20742	251B→261B	0.24302
238B→259B	-0.13942	249B→261B	0.57831	252B→262B	0.21112

Excited State 89:	5.184-A	4.5333 eV	273.50 nm	f=0.0000	<S**2>=6.467
261A→267A	0.11701	238B→260B	-0.14898	248B→259B	0.20765
262A→264A	-0.14677	239B→261B	0.13926	249B→262B	0.56660
231B→261B	-0.16014	240B→262B	0.16487	250B→261B	0.20941
232B→262B	-0.13806	245B→260B	-0.28377	252B→261B	0.16833
233B→259B	-0.18088	246B→259B	0.17238		

Excited State 90:	5.257-A	4.5534 eV	272.29 nm	f=0.0032	<S**2>=6.659
248A→263A	-0.10935	220B→260B	0.16698	239B→260B	-0.25681
254A→264A	0.10848	225B→259B	-0.18414	240B→259B	0.25783
255A→265A	-0.14533	226B→261B	0.17941	244B→259B	-0.10529
258A→267A	0.13006	227B→260B	-0.16671	245B→261B	-0.21749
260A→264A	-0.12163	228B→259B	-0.18194	246B→262B	0.21659
261A→266A	-0.15892	231B→260B	-0.15683	248B→262B	0.14173
217B→259B	0.12313	233B→262B	-0.16158	249B→259B	0.11655
219B→262B	-0.15190	235B→259B	-0.12709		

Excited State 91:	5.801-A	4.5803 eV	270.69 nm	f=0.0001	<S**2>=8.162
256A→266A	0.24923	257A→268A	0.26335	253B→267B	-0.22460
256A→271A	-0.12130	257A→276A	0.32639	253B→269B	-0.10622
256A→275A	0.34000	257A→285A	0.19701	253B→276B	0.11134
256A→286A	-0.18707	259A→280A	0.17073	253B→277B	-0.20191
257A→264A	-0.14296	260A→281A	0.17108	253B→284B	0.15855

254B→266B	-0.21927	254B→285B	0.13017	257B→279B	-0.17781
254B→275B	-0.26763	255B→280B	0.12008	258B→280B	-0.19952
254B→282B	-0.12402	256B→279B	0.11277		

Excited State 92: 5.801-B 4.5805 eV 270.68 nm f=0.0013 <S**2>=8.162

256A→264A	-0.14479	259A→281A	0.17227	254B→276B	0.11156
256A→268A	0.26526	260A→280A	0.16961	254B→277B	-0.20236
256A→276A	0.32813	253B→266B	-0.21996	254B→284B	0.15901
256A→285A	0.19759	253B→275B	-0.26831	255B→279B	0.11181
257A→266A	0.24845	253B→282B	-0.12433	256B→280B	0.12215
257A→271A	-0.12084	253B→285B	0.13049	257B→280B	-0.19274
257A→275A	0.34000	254B→267B	-0.22502	258B→279B	-0.18286
257A→286A	-0.18761	254B→269B	-0.10638		

Excited State 93: 5.277-A 4.6074 eV 269.10 nm f=0.0000 <S**2>=6.711

253A→263A	-0.10611	220B→261B	0.20982	227B→261B	-0.12057
254A→265A	-0.11138	221B→261B	0.13419	228B→262B	-0.15181
261A→267A	-0.12400	222B→259B	-0.18293	233B→259B	-0.16857
214B→260B	0.13099	223B→259B	0.13274	234B→260B	-0.14237
217B→262B	0.11991	224B→260B	0.11678	235B→262B	-0.10908
218B→260B	-0.13460	225B→262B	-0.19324	249B→262B	0.11194
219B→259B	-0.28264	226B→260B	0.30236	250B→278B	-0.10747

Excited State 94: 5.218-B 4.6084 eV 269.04 nm f=0.0125 <S**2>=6.556

253A→264A	0.10454	217B→261B	0.12278	223B→260B	0.11033
254A→266A	0.12452	218B→259B	-0.13807	224B→259B	0.13924
261A→268A	0.15605	219B→260B	-0.28772	225B→261B	-0.20745
262A→270A	-0.11760	220B→262B	0.22163	226B→259B	0.34084
213B→261B	-0.10654	221B→262B	0.14483	227B→259B	-0.11497
214B→259B	0.15274	222B→260B	-0.18059	227B→262B	-0.12828

228B→261B	-0.18086	233B→260B	-0.10519	235B→261B	-0.11463
229B→260B	-0.10477	234B→259B	-0.17221	248B→260B	-0.10271

Excited State 95: 5.330-A 4.6453 eV 266.90 nm f=0.0032 <S**2>=6.851

248A→270A	-0.10696	257A→281A	-0.11611	242B→261B	0.14843
253A→271A	0.10554	258A→270A	0.25159	243B→260B	0.12933
253A→278A	-0.11327	258A→273A	-0.14678	244B→259B	0.14428
254A→268A	0.11319	261A→271A	-0.32990	245B→261B	-0.10190
254A→269A	-0.20681	261A→275A	-0.12004	250B→263B	0.11670
254A→274A	-0.10216	261A→278A	-0.20552	251B→264B	-0.12359
255A→277A	-0.15180	262A→272A	0.38671	253B→279B	0.10665
256A→280A	-0.11665	262A→277A	0.19032	254B→280B	0.11522

Excited State 96: 5.241-B 4.6702 eV 265.48 nm f=0.0002 <S**2>=6.618

254A→270A	-0.18129	262A→275A	-0.14679	228B→260B	0.14924
255A→278A	0.12439	262A→278A	-0.14567	235B→260B	0.10192
258A→269A	0.18348	219B→261B	0.14536	241B→261B	-0.21316
258A→274A	0.11852	220B→259B	-0.16534	242B→262B	0.13956
258A→276A	0.10867	221B→259B	-0.10808	243B→259B	0.18758
261A→272A	0.28442	225B→260B	0.13359	244B→260B	0.17518
261A→277A	0.16093	226B→262B	-0.14437	245B→262B	-0.10432
262A→271A	-0.27900	227B→259B	0.11927	250B→264B	0.10201

Excited State 97: 5.252-B 4.6833 eV 264.74 nm f=0.0165 <S**2>=6.646

253A→268A	-0.10063	258A→272A	-0.26482	242B→259B	0.27640
253A→269A	0.11599	261A→274A	-0.19072	243B→262B	0.22817
254A→271A	-0.21332	262A→270A	-0.13085	244B→261B	0.38032
255A→270A	-0.13581	262A→273A	0.22843	253B→280B	0.13158
256A→281A	-0.13133	241B→260B	-0.26633	254B→279B	0.12184
257A→280A	-0.13138	241B→263B	-0.10635		

Excited State 98:	5.274-B	4.6888 eV	264.43 nm	f=0.0749	<S**2>=6.704				
255A→278A	0.11835	221B→259B	0.15280	239B→259B	0.12877				
261A→272A	0.16031	222B→261B	-0.13616	240B→260B	0.10500				
261A→277A	0.20942	224B→262B	0.10445	248B→261B	-0.11262				
262A→271A	-0.13720	225B→260B	-0.16674	250B→264B	0.13526				
262A→278A	-0.21555	226B→262B	0.18695	251B→263B	-0.11513				
213B→260B	-0.11832	227B→259B	-0.16156	257B→263B	-0.13372				
214B→262B	0.11839	228B→260B	-0.20955	258B→265B	-0.14878				
219B→261B	-0.20101	234B→262B	-0.11646						
220B→259B	0.22864	235B→260B	-0.14707						

Excited State 99:	5.238-A	4.6917 eV	264.26 nm	f=0.0000	<S**2>=6.609				
253A→270A	0.11877	261A→273A	0.16943	242B→261B	-0.11802				
254A→272A	0.19593	262A→269A	-0.10563	243B→261B	0.37253				
255A→269A	-0.10904	262A→274A	-0.18205	244B→262B	0.24821				
258A→271A	0.21084	241B→259B	-0.30615	255B→263B	-0.12633				
258A→275A	0.11004	241B→264B	-0.11109	256B→264B	-0.14703				
261A→270A	-0.10642	242B→260B	0.24510	258B→263B	-0.13003				

Excited State 100:	5.263-A	4.7005 eV	263.77 nm	f=0.0028	<S**2>=6.674				
248A→263A	-0.10710	219B→262B	0.20377	227B→260B	0.14546				
254A→264A	0.10362	220B→260B	-0.22902	228B→259B	0.23038				
258A→267A	0.10967	221B→260B	-0.15958	234B→261B	0.12682				
261A→266A	-0.11002	222B→262B	0.14538	235B→259B	0.16461				
261A→282A	-0.12488	223B→259B	0.10763	239B→260B	-0.16638				
262A→279A	0.13752	223B→262B	-0.10202	245B→261B	-0.16527				
213B→259B	0.14203	224B→261B	-0.11544	246B→262B	0.12851				
214B→261B	-0.14774	225B→259B	0.22136	248B→262B	0.14676				
217B→259B	-0.10144	226B→261B	-0.22030	254B→280B	0.10234				

Excited State 101:	5.315-A	4.7040 eV	263.57 nm	f=0.0029	<S**2>=6.813	
251A→264A	-0.13570	242B→261B	0.40780	250B→263B	-0.14040	
252A→263A	0.11846	243B→260B	0.23673	250B→268B	0.10669	
252A→267A	0.12213	243B→261B	0.12625	251B→259B	-0.11286	
261A→278A	0.18264	244B→259B	0.34423	251B→264B	0.14594	
262A→277A	-0.17969	245B→261B	-0.13084			
241B→262B	-0.27705	247B→261B	0.31885			

Excited State 102:	5.274-B	4.7046 eV	263.54 nm	f=0.0001	<S**2>=6.703	
251A→263A	-0.11642	221B→259B	-0.10065	244B→260B	-0.22880	
251A→267A	-0.11458	225B→260B	0.11705	246B→261B	0.15551	
252A→264A	0.13396	226B→262B	-0.11368	248B→261B	-0.20495	
261A→277A	0.14916	228B→260B	0.10022	250B→264B	0.12006	
262A→278A	-0.14517	241B→261B	0.40960	251B→263B	-0.12197	
219B→261B	0.11437	242B→262B	-0.25880			
220B→259B	-0.13217	243B→259B	-0.33787			

Excited State 103:	**5.380-B**	**4.7272 eV**	**262.28 nm**	**f=0.3443**	**<S**2>=6.985**	
246A→272A	0.10841	232B→261B	-0.13790	255B→264B	0.31504	
249A→273A	0.10198	238B→259B	-0.14038	255B→267B	-0.10545	
251A→278A	0.11325	239B→262B	0.12781	**256B→263B**	**0.32468**	
252A→277A	-0.10865	244B→261B	-0.12614	256B→268B	-0.13489	
261A→264A	-0.17420	245B→259B	0.10141	256B→270B	0.10499	
262A→267A	0.11213	248B→263B	0.11403	257B→263B	0.21560	
230B→259B	0.10919	249B→261B	-0.16222	258B→264B	0.26210	

Excited State 104:	5.306-A	4.7307 eV	262.09 nm	f=0.0000	<S**2>=6.787	
219B→259B	0.14769	226B→260B	-0.11840	229B→259B	0.13444	
220B→261B	-0.10666	228B→262B	0.13666	230B→260B	0.14253	

233B→259B	-0.13048	242B→261B	-0.11145	257B→264B	0.15979
234B→260B	0.11518	243B→261B	0.33367	257B→265B	-0.13279
238B→260B	-0.12143	244B→262B	0.20516	258B→268B	-0.11480
241B→259B	-0.24824	255B→263B	0.24296	258B→270B	0.11666
242B→260B	0.22719	256B→264B	0.24408		

Excited State 105: 5.258-B 4.7352 eV 261.84 nm f=0.0084 <S**2>=6.661

251A→263A	-0.10856	240B→260B	-0.11746	249B→260B	-0.19142
251A→267A	-0.10588	245B→262B	0.30504	250B→269B	-0.10839
252A→264A	0.12587	247B→262B	-0.37847	251B→260B	0.10268
239B→259B	0.41952	248B→261B	0.44972		

Excited State 106: 5.535-B 4.7424 eV 261.44 nm f=0.0332 <S**2>=7.410

247A→266A	0.10169	262A→263A	0.10703	254B→279B	-0.24707
253A→268A	0.11209	241B→260B	-0.21991	254B→281B	0.10135
256A→281A	0.26287	242B→259B	0.25786	255B→267B	-0.11817
257A→280A	0.26285	243B→262B	0.21790	257B→275B	0.12627
259A→276A	-0.13661	244B→261B	0.35201	258B→277B	0.11854
259A→285A	-0.12267	245B→259B	0.10851	258B→284B	-0.11115
260A→275A	-0.11908	249B→266B	-0.10452		
260A→286A	0.12326	253B→280B	-0.26680		

Excited State 107: 5.248-A 4.7462 eV 261.23 nm f=0.0000 <S**2>=6.635

256A→280A	-0.11896	239B→260B	0.14243	248B→262B	0.51328
257A→281A	-0.11872	245B→261B	0.16223	250B→260B	0.10699
261A→278A	0.14151	246B→262B	-0.32934	253B→279B	0.11075
262A→277A	-0.13952	247B→261B	-0.48890	254B→280B	0.11956

Excited State 108: 5.527-A 4.7498 eV 261.03 nm f=0.0000 <S**2>=7.387

256A→280A	0.24548	257A→281A	0.24459	259A→275A	-0.12210

259A→286A	0.10969	243B→260B	0.21288	249B→267B	-0.10282
260A→276A	-0.11764	244B→259B	0.17996	253B→279B	-0.23214
260A→285A	-0.12595	245B→261B	0.12119	254B→280B	-0.25070
240B→259B	0.10481	245B→266B	0.11091	257B→277B	0.10793
241B→262B	-0.15598	247B→261B	-0.18222	257B→284B	-0.10354
242B→261B	0.27140	248B→262B	0.30116	258B→275B	0.10742

Excited State 109: 5.139-B 4.7561 eV 260.68 nm f=0.0001 <S**2>=6.354

262A→278A	0.10887	245B→262B	0.14588	248B→261B	-0.25384
239B→259B	0.25049	246B→261B	0.51631	249B→260B	-0.14875
244B→260B	0.16398	247B→262B	0.62502		

Excited State 110: 5.229-A 4.7717 eV 259.83 nm f=0.0006 <S**2>=6.584

258A→273A	-0.11938	239B→260B	0.30848	247B→261B	0.27174
261A→278A	0.13965	242B→261B	-0.13077	249B→259B	-0.19694
262A→277A	-0.12769	245B→261B	0.44284		
232B→259B	-0.10674	246B→262B	0.42779		

Excited State 111: 5.352-B 4.7816 eV 259.29 nm f=0.0102 <S**2>=6.912

251A→263A	0.22904	255A→271A	-0.11666	243B→259B	-0.21465
251A→267A	0.15778	258A→269A	0.15743	244B→260B	-0.22727
252A→264A	-0.24716	258A→274A	0.16778	250B→264B	-0.15222
252A→268A	-0.13107	261A→272A	0.17897	251B→263B	0.14996
253A→272A	-0.13717	262A→271A	-0.19702	251B→270B	0.10033
254A→270A	-0.12851	241B→261B	0.36471		
254A→273A	0.14051	242B→262B	-0.21293		

Excited State 112: 5.189-A 4.7853 eV 259.09 nm f=0.0000 <S**2>=6.481

253A→270A	-0.12663	254A→272A	-0.23004	258A→271A	-0.25150
253A→273A	0.10549	255A→269A	0.12443	258A→275A	-0.13833

260A→272A	0.11151	241B→259B	-0.19846	255B→268B	0.11084
261A→270A	0.13868	242B→260B	0.14923	256B→264B	-0.12949
261A→273A	-0.19374	243B→261B	0.29158	256B→269B	0.10843
262A→269A	0.16519	244B→262B	0.19597	257B→265B	0.14325
262A→274A	0.22545	245B→260B	-0.18330	258B→263B	0.10267
232B→262B	0.10467	249B→262B	0.11407	258B→268B	0.16111
239B→261B	-0.15837	255B→263B	-0.11819		

Excited State 113: 5.318-B 4.7866 eV 259.02 nm f=0.0324 <S**2>=6.819

246A→265A	0.10223	257A→280A	-0.11197	242B→259B	0.15361
249A→263A	-0.10142	258A→272A	0.29710	243B→262B	0.16409
250A→264A	0.10630	260A→271A	-0.13516	244B→261B	0.31620
253A→269A	-0.13397	261A→269A	0.13392	245B→259B	-0.13883
253A→274A	-0.11451	261A→274A	0.19915	253B→280B	0.11764
254A→271A	0.21392	262A→270A	0.18691	254B→279B	0.10881
254A→275A	0.12265	262A→273A	-0.23182	255B→269B	0.10980
255A→270A	0.13687	240B→261B	-0.13696	256B→270B	0.10013
256A→281A	-0.11234	241B→260B	-0.16910		

Excited State 114: 5.469-A 4.7960 eV 258.52 nm f=0.0005 <S**2>=7.228

251A→264A	0.29452	258A→270A	-0.13903	243B→260B	0.15070
251A→268A	0.15384	258A→273A	0.10652	244B→259B	0.15561
252A→263A	-0.26118	261A→271A	0.15359	245B→261B	0.15215
252A→267A	-0.19831	262A→272A	-0.18392	250B→263B	0.16411
254A→269A	0.10687	239B→260B	0.22678	251B→264B	-0.17571
256A→280A	-0.11131	241B→262B	-0.14453	253B→279B	0.10400
257A→281A	-0.11096	242B→261B	0.22464	254B→280B	0.11232

Excited State 115: 5.163-A 4.8103 eV 257.75 nm f=0.0001 <S**2>=6.413

255A→264A	-0.12119	258A→266A	-0.11315	259A→263A	-0.13106

260A→265A	0.13373	233B→259B	-0.11994	255B→268B	0.12844
261A→267A	-0.14582	239B→261B	-0.25079	256B→264B	-0.15145
262A→268A	0.12673	240B→262B	-0.12826	256B→265B	0.13163
214B→260B	-0.10345	243B→261B	-0.14775	256B→267B	0.11448
219B→259B	0.11978	245B→260B	-0.21219	257B→264B	-0.10069
222B→259B	0.10894	249B→262B	0.36315	257B→265B	-0.21863
226B→260B	-0.10456	255B→263B	-0.10195	258B→263B	-0.35630

Excited State 116: 5.259-B 4.8598 eV 255.12 nm f=0.0009 <S**2>=6.665

250A→264A	-0.10062	229B→260B	-0.10055	240B→261B	0.37588
261A→268A	-0.12372	230B→259B	-0.12829	243B→262B	0.11124
262A→267A	0.10686	233B→260B	0.10727	244B→261B	0.10279
214B→259B	0.12258	234B→259B	-0.11437	245B→259B	0.25462
226B→259B	0.10563	238B→259B	0.13236	249B→261B	-0.26256
228B→261B	-0.11684	239B→262B	0.26113		

Excited State 117: 5.417-B 4.8640 eV 254.90 nm f=0.0137 <S**2>=7.085

251A→263A	-0.26678	255A→271A	-0.13956	240B→260B	0.12357
251A→267A	-0.20339	258A→268A	-0.10155	256B→263B	0.11000
252A→264A	0.29165	258A→274A	0.14291	257B→263B	-0.15518
252A→268A	0.17679	261A→277A	-0.27605	258B→265B	-0.22096
253A→272A	-0.12386	262A→278A	0.29059		
254A→273A	0.13329	239B→259B	-0.20944		

Excited State 118: 5.469-A 4.8773 eV 254.21 nm f=0.0001 <S**2>=7.226

250A→282A	-0.10533	252A→270A	-0.11871	258A→270A	0.10571
251A→264A	0.29440	253A→271A	0.14682	258A→273A	-0.18858
251A→268A	0.18605	254A→274A	-0.15584	261A→278A	0.31443
252A→263A	-0.27405	255A→272A	0.17247	262A→277A	-0.31248
252A→267A	-0.21127	255A→277A	0.10517	239B→260B	-0.18664

242B→261B	-0.10507	245B→261B	-0.10530		

Excited State 119: 5.425-B 4.8985 eV 253.11 nm f=0.0717 <S**2>=7.107

248A→264A	-0.12098	262A→282A	0.10210	256B→266B	-0.16213
251A→263A	-0.13226	231B→259B	-0.13177	257B→263B	0.22201
251A→267A	-0.11043	232B→260B	-0.12013	257B→266B	-0.10377
252A→264A	0.14266	239B→259B	0.27387	257B→268B	0.11891
255A→266A	-0.13350	240B→260B	-0.15032	257B→270B	-0.10242
258A→274A	0.10064	252B→264B	0.16921	258B→265B	0.24739
259A→265A	-0.12282	255B→265B	-0.13121		
261A→277A	-0.12409	256B→263B	-0.12254		

Excited State 120: 5.202-A 4.9083 eV 252.60 nm f=0.0002 <S**2>=6.515

255A→264A	-0.11436	262A→274A	0.13476	248B→259B	0.10799
258A→266A	-0.15214	232B→262B	-0.17749	249B→262B	-0.21037
258A→275A	-0.12607	238B→260B	-0.16058	249B→265B	-0.10957
259A→263A	-0.10641	239B→261B	0.38205	255B→263B	-0.17523
260A→265A	0.10958	240B→262B	0.20356	256B→264B	-0.18323
261A→267A	-0.10337	243B→261B	0.13066	257B→264B	-0.12727
261A→273A	-0.10757	245B→260B	0.25705	257B→265B	-0.13229
262A→268A	0.11780	246B→259B	0.12449	258B→263B	-0.29843

Excited State 121: 5.151-B 4.9255 eV 251.72 nm f=0.0350 <S**2>=6.383

255A→263A	-0.11498	229B→260B	-0.18934	240B→261B	-0.20729
258A→265A	-0.14656	230B→259B	-0.21119	245B→259B	-0.14761
259A→264A	-0.18327	231B→262B	0.11757	246B→260B	-0.12785
259A→268A	0.10211	232B→261B	0.17509	248B→260B	-0.10089
260A→266A	0.23564	233B→260B	0.11319	249B→261B	0.14292
261A→268A	-0.15810	238B→259B	0.22226	252B→265B	-0.18183
262A→267A	0.14853	239B→262B	-0.23445	255B→264B	0.12133

256B→263B	0.28629	257B→266B	0.15903	258B→267B	0.12371
257B→263B	0.16432	258B→264B	0.23380		

*C.2.8.4 **OTPB-FLR-221**, **EB** State*

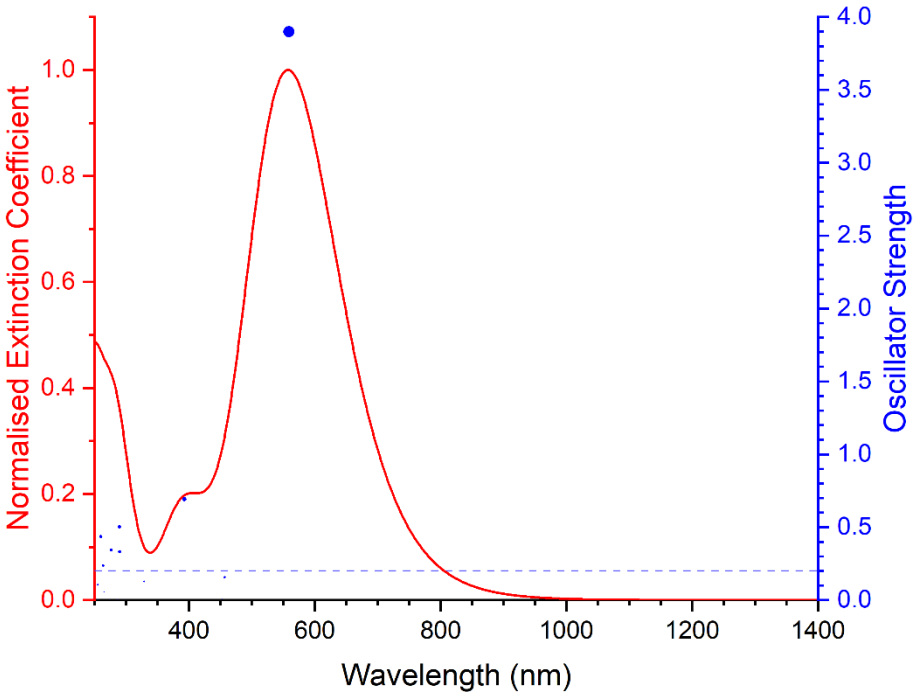

*Figure C-32 Excited states and normalised absorption spectra from TD-DFT calculations of **OTPB-FLR-221** in **EB** state. The areas of excited state dots are proportional to their oscillator strengths.*

Excited State 1:	Singlet-A	2.0645 eV	600.55 nm	f=0.0000	<S**2>=0.000
259→262	0.47010	260→261	0.50054		
Excited State 2:	**Singlet-B**	**2.2182 eV**	**558.94 nm**	**f=3.8979**	**<S**2>=0.000**
259→261	**0.47009**	**260→262**	**0.50322**		
Excited State 3:	Singlet-B	2.7130 eV	457.00 nm	f=0.1565	<S**2>=0.000
246→261	0.14847	257→262	-0.40676		
254→262	0.19181	258→261	0.47877		
Excited State 4:	Singlet-A	2.7379 eV	452.85 nm	f=0.0080	<S**2>=0.000
246→262	0.15127	257→261	-0.40615		
254→261	0.19508	258→262	0.47633		

Excited State 5:	Singlet-A	2.9752 eV	416.72 nm	f=0.0000	<S**2>=0.000			
259→262	0.51624		260→261	-0.47719				
Excited State 6:	Singlet-B	2.9777 eV	416.38 nm	f=0.0122	<S**2>=0.000			
259→261	0.51954		260→262	-0.47541				
Excited State 7:	Singlet-A	3.1456 eV	394.15 nm	f=0.0000	<S**2>=0.000			
245→261	0.20707		255→261	0.44162		260→261	-0.10549	
253→262	0.32728		256→262	-0.30813				
Excited State 8:	**Singlet-B**	**3.1548 eV**	**393.00 nm**	**f=0.6913**	**<S**2>=0.000**			
245→262	0.20462		**255→262**	**0.43945**		260→262	-0.11552	
253→261	**0.32692**		256→261	-0.31080				
Excited State 9:	Singlet-B	3.7525 eV	330.41 nm	f=0.0000	<S**2>=0.000			
257→262	0.50976		258→261	0.47090				
Excited State 10:	Singlet-A	3.7663 eV	329.20 nm	f=0.0000	<S**2>=0.000			
243→261	0.42850		245→261	-0.12067		250→262	-0.20465	
244→262	0.43818		249→261	0.20212				
Excited State 11:	Singlet-A	3.7693 eV	328.93 nm	f=0.0001	<S**2>=0.000			
257→261	0.50600		258→262	0.47627				
Excited State 12:	Singlet-B	3.7697 eV	328.90 nm	f=0.1270	<S**2>=0.000			
243→262	0.42898		245→262	-0.12200		250→261	-0.20667	
244→261	0.44268		249→262	0.20232				
Excited State 13:	Singlet-B	3.9569 eV	313.34 nm	f=0.0002	<S**2>=0.000			
240→262	0.40894		242→262	-0.13475		248→262	0.21160	
241→261	0.42632		247→261	0.20297				

Excited State 14:	Singlet-A	3.9575 eV	313.29 nm	f=0.0000	<S**2>=0.000			
237→262	-0.10224		241→262	0.42416		248→261	0.21272	
238→261	-0.10220		242→261	-0.13702				
240→261	0.40930		247→262	0.20326				
Excited State 15:	Singlet-A	4.0739 eV	304.34 nm	f=0.0000	<S**2>=0.000			
255→261	0.35741		256→262	0.58079				
Excited State 16:	Singlet-B	4.1062 eV	301.94 nm	f=0.0058	<S**2>=0.000			
255→262	0.38035		256→261	0.58838				
Excited State 17:	Singlet-B	4.1658 eV	297.62 nm	f=0.0010	<S**2>=0.000			
237→261	0.20358		246→261	0.18535		258→261	-0.16886	
238→262	0.20712		247→261	-0.12350		259→263	0.18162	
240→262	0.11130		254→262	0.33729		260→264	0.17690	
242→262	0.11169		257→262	0.21706		260→267	-0.10331	
Excited State 18:	Singlet-A	4.1697 eV	297.34 nm	f=0.0009	<S**2>=0.000			
237→262	0.20218		246→262	0.18263		258→262	-0.15770	
238→261	0.20817		247→262	-0.12804		259→264	0.17335	
240→261	0.11510		254→261	0.31403		259→267	-0.12194	
242→261	0.10585		257→261	0.22327		260→263	0.21577	
Excited State 19:	Singlet-A	4.2469 eV	291.94 nm	f=0.0000	<S**2>=0.000			
243→261	-0.17763		249→261	0.41368		253→262	0.11499	
244→262	-0.19451		250→262	-0.40719		255→261	-0.10486	
Excited State 20:	Singlet-B	4.2475 eV	291.90 nm	f=0.0070	<S**2>=0.000			
243→262	-0.18517		249→262	0.41847				
244→261	-0.19786		250→261	-0.41685				

Excited State 21:	Singlet-B	4.2544 eV	291.43 nm	f=0.0403	<S**2>=0.000	
240→262	-0.15695	246→261	0.14472	254→262	0.15765	
241→261	-0.18957	247→261	0.35796	259→263	-0.10035	
242→262	0.11828	248→262	0.38569	260→269	0.10507	

Excited State 22:	Singlet-A	4.2560 eV	291.32 nm	f=0.0055	<S**2>=0.000	
240→261	-0.16364	246→262	0.13543	254→261	0.11526	
241→262	-0.19194	247→262	0.37655			
242→261	0.10934	248→261	0.40450			

Excited State 23:	Singlet-A	4.2676 eV	290.52 nm	f=0.0002	<S**2>=0.000	
234→261	-0.14527	243→261	-0.12042	253→262	-0.31667	
236→262	-0.16260	245→261	-0.26205	255→261	0.36909	
239→262	-0.17492	250→262	-0.12900	256→262	-0.17833	

Excited State 24:	**Singlet-B**	**4.2724 eV**	**290.20 nm**	**f=0.3308**	**<S**2>=0.000**	
234→262	-0.10856	248→262	0.12356	259→263	0.24727	
236→261	-0.12558	253→261	-0.25168	260→264	0.21524	
239→261	-0.13775	254→262	-0.13904	260→267	-0.11357	
245→262	-0.20245	255→262	0.28153			
247→261	0.13169	256→261	-0.15463			

Excited State 25:	**Singlet-B**	**4.2774 eV**	**289.86 nm**	**f=0.5014**	**<S**2>=0.000**	
236→261	0.10351	253→261	0.21477	257→266	-0.11377	
239→261	0.11025	254→262	-0.22123	259→263	0.29590	
245→262	0.17080	255→262	-0.23287	260→264	0.25400	
247→261	0.10415	256→261	0.13004	260→267	-0.13160	

Excited State 26:	Singlet-A	4.3285 eV	286.44 nm	f=0.0036	<S**2>=0.000	
254→261	-0.37443	259→264	0.28086	260→263	0.37946	
258→266	0.12809	259→267	-0.17143	260→270	-0.10019	

Excited State 27:	**Singlet-B**	**4.4845 eV**	**276.47 nm**	**f=0.3444**	**<S**2>=0.000**	
237→261	-0.28395	246→261	-0.15631	258→265	0.14448	
238→262	-0.29628	**254→262**	**0.42097**	260→264	0.15341	

Excited State 28:	Singlet-A	4.5376 eV	273.23 nm	f=0.0019	<S**2>=0.000	
237→262	-0.28001	254→261	0.39371	260→263	0.21426	
238→261	-0.29407	258→266	0.12937			
246→262	-0.16972	259→264	0.13184			

Excited State 29:	Singlet-B	4.5546 eV	272.21 nm	f=0.0000	<S**2>=0.000	
255→269	-0.10169	259→270	0.12522			
259→268	-0.43748	260→269	0.45119			

Excited State 30:	Singlet-A	4.5551 eV	272.19 nm	f=0.0123	<S**2>=0.000	
259→269	0.44724	260→268	-0.44064	260→270	0.12408	

Excited State 31:	Singlet-A	4.6647 eV	265.79 nm	f=0.0000	<S**2>=0.000	
245→261	-0.12786	254→263	0.11636	258→264	0.30359	
245→265	-0.10366	255→265	0.22987	258→267	0.14743	
246→264	-0.10397	256→262	-0.10586	260→265	0.34897	
253→262	0.16646	256→266	0.15268			

Excited State 32:	Singlet-B	4.6712 eV	265.42 nm	f=0.0546	<S**2>=0.000	
237→261	0.10889	255→267	0.10533	258→265	0.24812	
238→262	0.10473	256→263	0.19757	259→263	-0.20119	
246→265	-0.11575	256→270	0.11024	259→270	-0.10090	
254→262	-0.12699	257→262	-0.10268	260→264	0.22268	
255→264	0.15673	257→266	0.25024	260→267	0.12471	

Excited State 33:	Singlet-A	4.6827 eV	264.77 nm	f=0.0001	<S**2>=0.000			
253→262	-0.13779	258→264	0.13681	260→271	0.22960			
256→266	-0.15987	259→266	0.39679					
257→263	-0.28472	260→265	0.16145					
Excited State 34:	**Singlet-B**	**4.6984 eV**	**263.89 nm**	**f=0.2352**	**<S**2>=0.000**			
234→262	0.11179	255→266	0.11596	259→271	0.19540			
236→261	0.13227	257→264	-0.12218	**260→266**	**0.36435**			
245→262	0.12366	258→263	0.24302					
253→261	-0.25622	259→265	0.14205					
Excited State 35:	Singlet-A	4.7580 eV	260.58 nm	f=0.0000	<S**2>=0.000			
234→261	-0.18163	245→261	-0.25045	257→263	-0.13172			
236→262	-0.21341	253→262	0.45431	259→266	0.14329			
239→262	-0.13957	256→266	-0.11946					
Excited State 36:	**Singlet-B**	**4.7648 eV**	**260.21 nm**	**f=0.4350**	**<S**2>=0.000**			
234→262	-0.16332	245→262	-0.26986	260→266	0.23387			
236→261	-0.20010	**253→261**	**0.42647**					
239→261	-0.11860	258→263	0.15809					
Excited State 37:	Singlet-A	4.8519 eV	255.54 nm	f=0.0070	<S**2>=0.000			
233→262	0.16245	242→261	0.14612	260→263	0.10413			
235→261	0.20898	246→262	0.38544	260→270	0.14789			
237→262	-0.22345	254→261	-0.18537					
238→261	-0.20181	258→266	0.14967					
Excited State 38:	Singlet-B	4.8537 eV	255.44 nm	f=0.1046	<S**2>=0.000			
233→261	0.16590	238→262	-0.18707	254→262	-0.20943			
235→262	0.20758	242→262	0.15154	258→265	0.13905			
237→261	-0.21000	246→261	0.39435	259→270	0.10578			

260→267	0.12745				

Excited State 39:	Singlet-B	4.9505 eV	250.45 nm	f=0.0003	<S**2>=0.000
250→261	0.10683	257→276	0.12663	259→265	-0.15138
256→265	0.13223	258→263	-0.10760	259→271	0.23526
257→264	0.16424	258→268	0.13048	259→273	-0.21327
257→269	0.12721	258→277	-0.15229	260→272	0.34111

Excited State 40:	Singlet-A	4.9582 eV	250.06 nm	f=0.0000	<S**2>=0.000
249→261	-0.12090	257→277	0.13709	259→272	0.34507
257→263	0.13734	258→269	-0.14877	260→271	0.26344
257→268	-0.11296	258→276	-0.15123	260→273	-0.24002

C.2.9 Electronic Transitions in **OTPT-BZN-210** Oligomers

*Table C-13 Attributes of **OTPT-BZN-210** in **LEB**, **ES** (singlet and triplet), and **EB** states related to electronic structures*

Attribute	**LEB State**	**^{1}ES State**	**^{3}ES State**	**EB State**
Molecular Formula	$C_{48}H_{34}N_8$	$C_{48}H_{34}N_8^{2+}$	$C_{48}H_{34}N_8^{2+}$	$C_{48}H_{30}N_8$
Number of Atoms	90	90	90	88
Number of Electrons	378	376	376	376
HOMO	MO 189	MO 188	MOs 189A, 187B	MO 188
LUMO	MO 190	MO 189	MOs 190A, 188B	MO 189

*C.2.9.1 **OTPT-BZN-210, LEB** State*

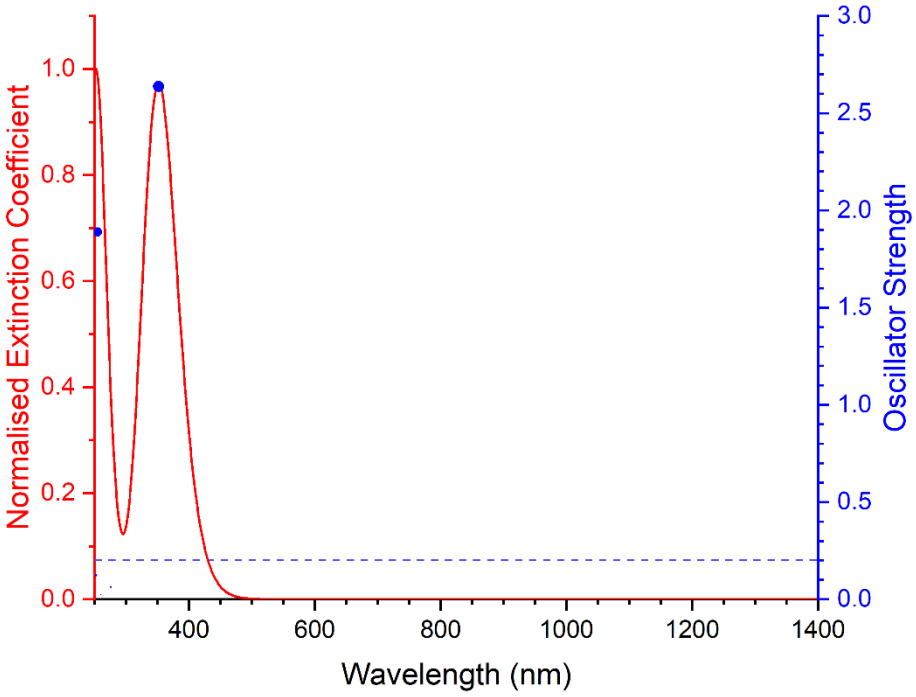

*Figure C-33 Excited states and normalised absorption spectra from TD-DFT calculations of **OTPT-BZN-210** in **LEB** state. The areas of excited state dots are proportional to their oscillator strengths.*

Excited State 1:	**Singlet-AU**	**3.5243 eV**	**351.80 nm**	**f=2.6379**	**<S**2>=0.000**	
188→193	0.26300		**189→190**	**0.58476**	189→194	-0.22448
Excited State 2:	Singlet-AG	3.8997 eV	317.94 nm	f=0.0000	<S**2>=0.000	
188→190	0.35626		189→193	0.56152	189→195	0.13420
Excited State 3:	Singlet-AU	4.1139 eV	301.38 nm	f=0.0038	<S**2>=0.000	
185→191	0.10542		188→192	0.32172	189→191	0.57589
Excited State 4:	Singlet-AG	4.1149 eV	301.31 nm	f=0.0000	<S**2>=0.000	
185→192	0.10578		188→191	0.32232	189→192	0.57671
Excited State 5:	Singlet-AU	4.4900 eV	276.13 nm	f=0.0632	<S**2>=0.000	
176→203	-0.10405		189→196	0.64917		
Excited State 6:	Singlet-AU	4.5495 eV	272.52 nm	f=0.0006	<S**2>=0.000	
172→191	0.41809		174→190	-0.24345		
173→192	0.41929		175→193	-0.24265		

Excited State 7:	Singlet-AG	4.5496 eV	272.52 nm	f=0.0000	<S**2>=0.000
172→192	0.41843	174→193	-0.24190		
173→191	0.41966	175→190	-0.24307		
Excited State 8:	Singlet-AG	4.5982 eV	269.64 nm	f=0.0000	<S**2>=0.000
172→193	-0.11973	174→192	0.46756	175→191	0.46786
173→190	-0.11706	174→204	-0.10297	175→205	-0.10301
Excited State 9:	Singlet-AU	4.5982 eV	269.63 nm	f=0.0044	<S**2>=0.000
172→190	-0.11717	174→191	0.46748	175→192	0.46775
173→193	-0.12005	174→205	-0.10294	175→204	-0.10301
Excited State 10:	Singlet-AU	4.6589 eV	266.12 nm	f=0.0010	<S**2>=0.000
172→191	0.24186	174→190	0.41953		
173→192	0.24234	175→193	0.41061		
Excited State 11:	Singlet-AG	4.6592 eV	266.10 nm	f=0.0000	<S**2>=0.000
172→192	0.24127	174→193	0.41092		
173→191	0.24171	175→190	0.42032		
Excited State 12:	Singlet-AG	4.7111 eV	263.18 nm	f=0.0000	<S**2>=0.000
172→193	0.46264	174→192	0.12004		
173→190	0.46682	175→191	0.12019		
Excited State 13:	Singlet-AU	4.7112 eV	263.17 nm	f=0.0125	<S**2>=0.000
172→190	0.46546	174→191	0.12024		
173→193	0.46431	175→192	0.12031		
Excited State 14:	Singlet-AU	4.7644 eV	260.23 nm	f=0.0239	<S**2>=0.000
176→190	0.11633	178→190	0.17368	188→198	-0.29154
177→193	-0.18928	188→193	-0.11323	189→194	-0.18773

189→197	0.41048	189→199	-0.10955	189→201	0.16972

Excited State 15:	Singlet-AG	4.7716 eV	259.84 nm	f=0.0000	<S**2>=0.000
177→190	0.23956	188→196	0.10428	188→201	-0.12460
178→193	-0.18813	188→197	-0.25930	189→198	0.45452

Excited State 16:	Singlet-AG	4.8634 eV	254.93 nm	f=0.0000	<S**2>=0.000
183→192	0.14466	185→192	-0.33152	186→194	0.11910
184→191	0.35413	186→190	0.30191	187→193	0.30329

Excited State 17:	**Singlet-AU**	**4.8652 eV**	**254.84 nm**	**f=1.8891**	**<S**2>=0.000**
183→191	0.14290	**185→191**	**-0.33335**	187→190	0.30223
184→192	**0.35567**	186→193	0.30335	187→194	0.11763

Excited State 18:	Singlet-AU	4.9097 eV	252.53 nm	f=0.1239	<S**2>=0.000
177→193	-0.10426	186→192	0.15714	188→198	-0.11795
178→190	0.13255	187→191	0.15707	189→194	0.33074
183→190	0.15762	188→193	0.32827	189→203	0.28553

Excited State 19:	Singlet-AG	4.9199 eV	252.01 nm	f=0.0000	<S**2>=0.000
179→192	-0.16181	182→195	0.11198	187→193	0.23683
180→191	-0.22315	183→192	0.13791	187→202	-0.10117
181→190	0.12023	184→191	-0.21541	189→192	-0.20609
181→194	0.10800	185→192	0.24004		
182→193	-0.12638	186→190	0.24247		

Excited State 20:	Singlet-AU	4.9201 eV	251.99 nm	f=0.0003	<S**2>=0.000
179→191	-0.16244	182→190	-0.11973	184→200	-0.10085
180→192	-0.22380	182→194	-0.10848	185→191	0.24072
181→193	0.12674	183→191	0.13819	186→193	0.23774
181→195	-0.11251	184→192	-0.21604	186→202	-0.10141

187→190	0.24359	189→191	-0.20862		

Excited State 21:	Singlet-AG	4.9406 eV	250.95 nm	f=0.0000	<S**2>=0.000
183→193	0.15589	187→192	0.18955	188→194	-0.14842
186→191	0.18947	188→190	0.42850	189→193	-0.37995

*C.2.9.2 **OTPT-BZN-210**, **^{1}ES** State*

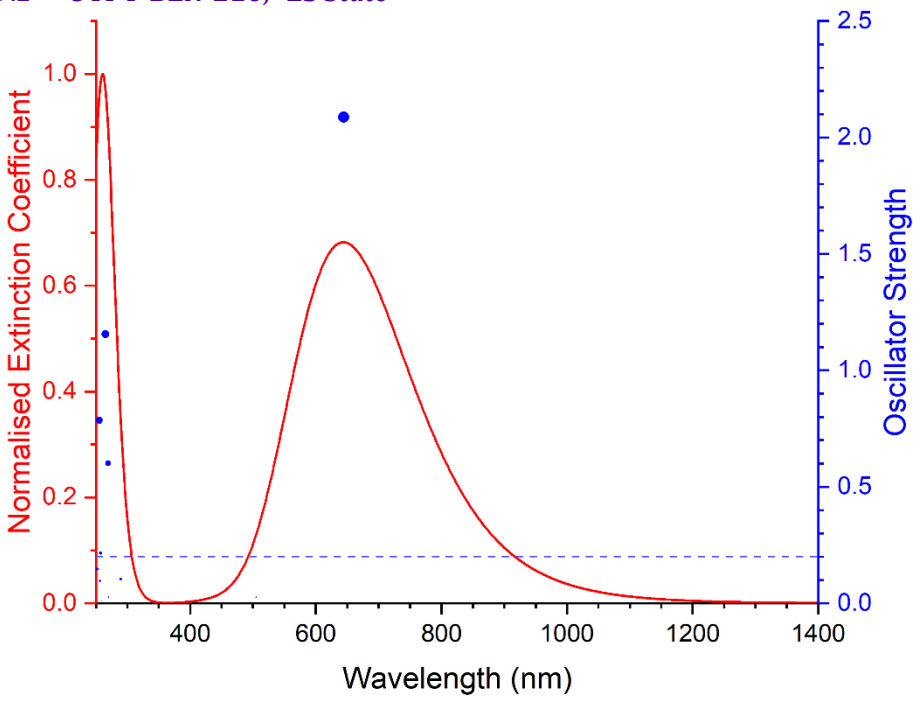

*Figure C-34 Excited states and normalised absorption spectra from TD-DFT calculations of **OTPT-BZN-210** in **^{1}ES** state. The areas of excited state dots are proportional to their oscillator strengths.*

Excited State 1:	**Singlet-AU**	**1.9237 eV**	**644.50 nm**	**f=2.0870**	**<S**2>=0.000**
180→189	**0.61401**	184→189	0.14999		
182→189	-0.14149	186→189	0.26137		

Excited State 2:	Singlet-AG	2.3069 eV	537.44 nm	f=0.0000	<S**2>=0.000
185→189	-0.15265	187→189	0.67986		

Excited State 3:	Singlet-AU	2.3071 eV	537.40 nm	f=0.0036	<S**2>=0.000
186→189	-0.17938	188→189	0.67287		

Excited State 4:	Singlet-AG	2.4295 eV	510.32 nm	f=0.0000	<S**2>=0.000
175→189	-0.11121	185→189	0.67845	187→189	0.15128

Excited State 5:	Singlet-AU	2.4548 eV	505.08 nm	f=0.0260	<S**2>=0.000
180→189	-0.22617	186→189	0.62542		
184→189	-0.12897	188→189	0.17775		
Excited State 6:	Singlet-AG	2.6336 eV	470.79 nm	f=0.0000	<S**2>=0.000
174→189	0.11042	181→189	0.68715		
Excited State 7:	Singlet-AU	2.6381 eV	469.97 nm	f=0.0027	<S**2>=0.000
173→189	0.10741	180→189	0.16681	182→189	0.67654
Excited State 8:	Singlet-AG	2.6620 eV	465.75 nm	f=0.0000	<S**2>=0.000
174→189	-0.28280	175→189	0.13670	183→189	0.61973
Excited State 9:	Singlet-AU	2.6695 eV	464.45 nm	f=0.0022	<S**2>=0.000
173→189	0.28531	180→189	-0.17119	184→189	0.61486
Excited State 10:	Singlet-AG	2.6778 eV	463.00 nm	f=0.0000	<S**2>=0.000
174→189	0.62258	183→189	0.30405		
Excited State 11:	Singlet-AU	2.6841 eV	461.92 nm	f=0.0113	<S**2>=0.000
173→189	0.62411	182→189	-0.11888	184→189	-0.28027
Excited State 12:	Singlet-AG	2.7783 eV	446.26 nm	f=0.0000	<S**2>=0.000
166→189	-0.10304	177→189	0.19679	183→189	-0.12411
175→189	0.63124	181→189	-0.11303	185→189	0.11528
Excited State 13:	Singlet-AG	3.0280 eV	409.46 nm	f=0.0000	<S**2>=0.000
175→189	-0.15337	177→189	0.57311		
176→190	-0.10365	179→189	-0.33727		
Excited State 14:	Singlet-AU	3.0286 eV	409.38 nm	f=0.0018	<S**2>=0.000
176→189	0.61703	177→190	-0.10257	178→189	-0.30360

Excited State 15:	Singlet-AG	3.0453 eV	407.13 nm	f=0.0000	<S**2>=0.000
169→189	-0.11057	177→189	0.32218		
175→189	-0.13546	179→189	0.58193		
Excited State 16:	Singlet-AU	3.0467 eV	406.95 nm	f=0.0006	<S**2>=0.000
176→189	0.30294	178→189	0.61740		
Excited State 17:	Singlet-AG	3.1039 eV	399.45 nm	f=0.0000	<S**2>=0.000
167→189	0.10851	169→189	0.67814	179→189	0.14067
Excited State 18:	Singlet-AU	4.2831 eV	289.47 nm	f=0.1043	<S**2>=0.000
157→189	-0.10270	159→189	-0.26061	172→189	0.63161
Excited State 19:	Singlet-AG	4.5446 eV	272.81 nm	f=0.0000	<S**2>=0.000
176→190	-0.10842	178→192	-0.46326		
177→191	0.12478	179→193	0.46467		
Excited State 20:	Singlet-AU	4.5449 eV	272.80 nm	f=0.0002	<S**2>=0.000
176→191	0.12275	178→193	0.46623		
177→190	-0.10356	179→192	-0.46478		
Excited State 21:	Singlet-AG	4.5887 eV	270.19 nm	f=0.0000	<S**2>=0.000
178→190	-0.39098	179→189	-0.14206	179→198	-0.11466
178→195	0.26584	179→191	0.43759		
Excited State 22:	Singlet-AU	4.5888 eV	270.19 nm	f=0.0253	<S**2>=0.000
178→189	-0.14249	178→198	-0.11494	179→195	0.26658
178→191	0.43879	179→190	-0.39209		
Excited State 23:	Singlet-AG	4.6012 eV	269.46 nm	f=0.0000	<S**2>=0.000
171→189	-0.19984	187→191	-0.38666	188→190	0.39448

188→195	-0.20452				

Excited State 24:	**Singlet-AU**	**4.6022 eV**	**269.40 nm**	**f=0.6011**	**<S**2>=0.000**
170→189	0.20188	187→195	-0.20634		
187→190	**0.39953**	**188→191**	**-0.38408**		

Excited State 25:	Singlet-AG	4.6399 eV	267.21 nm	f=0.0000	<S**2>=0.000
176→190	-0.38804	177→191	0.42101	179→193	-0.13509
176→195	0.22540	177→204	-0.10118	180→190	0.13606
177→189	-0.13903	178→192	0.13462		

Excited State 26:	Singlet-AU	4.6448 eV	266.93 nm	f=0.0014	<S**2>=0.000
176→189	-0.14793	177→190	-0.39200	179→192	0.12952
176→191	0.43422	177→195	0.22404		
176→204	-0.10761	178→193	-0.12983		

Excited State 27:	Singlet-AG	4.6721 eV	265.37 nm	f=0.0000	<S**2>=0.000
171→189	-0.11286	185→193	0.44542	186→192	-0.44518

Excited State 28:	**Singlet-AU**	**4.6735 eV**	**265.29 nm**	**f=1.1558**	**<S**2>=0.000**
170→189	0.10918	**185→192**	**-0.44434**	**186→193**	**0.44641**

Excited State 29:	Singlet-AG	4.7446 eV	261.31 nm	f=0.0000	<S**2>=0.000
148→189	0.11495	175→191	0.15166	188→192	-0.22052
158→189	-0.15241	180→190	0.27290		
166→189	0.41798	187→193	0.22354		

Excited State 30:	Singlet-AG	4.7635 eV	260.28 nm	f=0.0000	<S**2>=0.000
148→189	0.11945	175→191	-0.13676	187→193	-0.18076
158→189	-0.14574	180→190	-0.32316	188→192	0.17866
166→189	0.43014	184→190	-0.10493		

Excited State 31:	Singlet-AG	4.7806 eV	259.35 nm	f=0.0000	<S**2>=0.000			
175→193	0.13040		176→192	0.47802		177→193	-0.46292	
Excited State 32:	Singlet-AU	4.7806 eV	259.35 nm	f=0.0083	<S**2>=0.000			
175→192	0.13026		176→193	0.47975		177→192	-0.46191	
Excited State 33:	**Singlet-AU**	**4.8177 eV**	**257.35 nm**	**f=0.2153**	**<S**2>=0.000**			
170→189	-0.18430		183→192	0.23613		184→198	-0.11513	
182→193	0.13866		184→191	0.16979		187→192	0.28670	
183→190	0.10726		184→193	0.19926		188→193	-0.28299	
Excited State 34:	Singlet-AG	4.8241 eV	257.01 nm	f=0.0000	<S**2>=0.000			
171→189	0.55121		183→191	-0.10171		184→192	-0.19285	
181→193	-0.14676		183→193	-0.16512				
Excited State 35:	Singlet-AU	4.8255 eV	256.94 nm	f=0.0957	<S**2>=0.000			
170→189	0.52671		182→193	0.17920		188→193	-0.11384	
181→192	-0.20674		184→193	-0.10277				
182→191	-0.11706		187→192	0.11103				
Excited State 36:	Singlet-AG	4.8432 eV	256.00 nm	f=0.0000	<S**2>=0.000			
180→190	-0.17458		182→195	0.10427		185→200	-0.12253	
181→191	0.16332		183→191	0.11050		186→201	-0.11332	
181→193	-0.23022		183→193	0.27950		187→202	0.10888	
181→198	-0.12621		184→192	0.20869		188→203	-0.10370	
182→192	0.29352		184→195	-0.10477				
Excited State 37:	**Singlet-AU**	**4.8564 eV**	**255.30 nm**	**f=0.7852**	**<S**2>=0.000**			
180→191	0.15242		182→193	-0.21723		185→190	0.13527	
181→190	-0.10506		183→192	-0.22721		185→195	-0.10261	
181→192	0.15784		184→193	-0.17252		186→191	-0.12233	

186→198	0.10072	187→192	0.27278	188→193	-0.26998

Excited State 38: Singlet-AG 4.9113 eV 252.45 nm f=0.0000 <S**2>=0.000

171→189	0.32634	182→195	-0.10145	186→190	0.10100
180→192	-0.11025	183→191	0.12523	186→192	-0.11178
181→193	0.23193	183→193	0.16622	187→191	-0.12995
182→190	0.10166	184→192	0.21551	188→190	0.15891
182→192	-0.16041	185→193	0.11082		

Excited State 39: Singlet-AU 4.9120 eV 252.41 nm f=0.1464 <S**2>=0.000

170→189	0.34725	182→193	-0.17959	185→192	0.10473
180→193	-0.11528	183→190	0.11602	186→193	-0.10346
181→192	0.24467	183→192	0.17009	187→190	-0.14824
182→191	0.13263	184→193	0.21846	188→191	0.12467

Excited State 40: Singlet-AG 4.9154 eV 252.23 nm f=0.0000 <S**2>=0.000

171→189	-0.12446	185→191	-0.27001	187→193	-0.25563
175→191	0.10212	186→190	0.36261	188→192	0.25458
180→190	0.21548	186→195	-0.12638		

*C.2.9.3 **OTPT-BZN-210**, **^{3}ES** State*

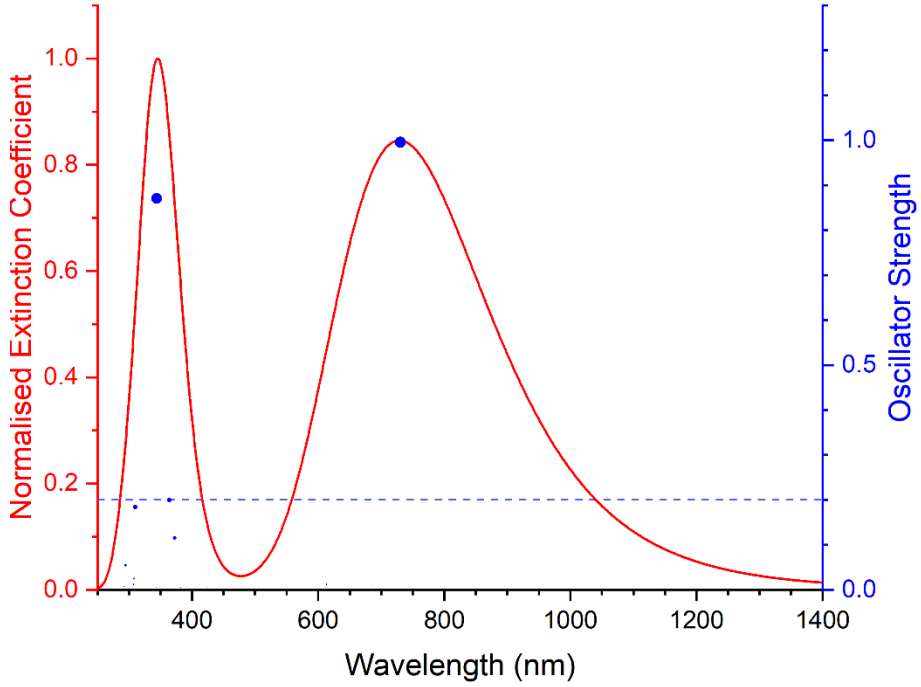

*Figure C-35 Excited states and normalised absorption spectra from TD-DFT calculations of **OTPT-BZN-210** in **^{3}ES** state. The areas of excited state dots are proportional to their oscillator strengths.*

Excited State 1:	**3.122-AU**	**1.6969 eV**	**730.64 nm**	**f=0.9955**	**<S**2>=2.186**	
159B→189B	-0.11687	**179B→188B**	**0.89616**			
171B→189B	0.22602	185B→188B	-0.22461			
Excited State 2:	3.068-AU	1.8035 eV	687.45 nm	f=0.0100	<S**2>=2.103	
172B→188B	0.55129	174B→188B	0.50810	187B→188B	0.30892	
173B→189B	0.52451	186B→189B	0.15835			
Excited State 3:	3.067-AG	1.8040 eV	687.29 nm	f=0.0000	<S**2>=2.101	
172B→189B	0.39829	174B→189B	0.34783	187B→189B	0.16080	
173B→188B	0.75190	186B→188B	0.31587			
Excited State 4:	3.095-AU	2.0202 eV	613.72 nm	f=0.0116	<S**2>=2.145	
170B→188B	0.12810	174B→188B	-0.20115	187B→188B	0.81836	
172B→188B	-0.20918	185B→188B	-0.10060			
173B→189B	-0.19985	186B→189B	0.37130			

Excited State 5:	3.095-AG	2.0204 eV	613.67 nm	f=0.0000	<S**2>=2.145
169B→188B	-0.12908	173B→188B	-0.29105	186B→188B	0.81876
172B→189B	-0.15096	174B→189B	-0.13418	187B→189B	0.37026
Excited State 6:	3.128-AG	2.2127 eV	560.32 nm	f=0.0000	<S**2>=2.195
171B→188B	-0.17375	184B→188B	0.85818		
179B→189B	-0.15685	185B→189B	0.36374		
Excited State 7:	3.121-AU	2.2527 eV	550.37 nm	f=0.0076	<S**2>=2.185
168B→188B	-0.10238	184B→189B	0.34760	187B→188B	0.10711
179B→188B	0.23126	185B→188B	0.86041		
Excited State 8:	3.144-AU	2.3984 eV	516.95 nm	f=0.0005	<S**2>=2.221
175B→188B	0.80023	176B→189B	0.51855		
175B→190B	0.19250	176B→191B	-0.13426		
Excited State 9:	3.144-AG	2.3984 eV	516.95 nm	f=0.0000	<S**2>=2.221
175B→189B	0.51748	176B→188B	0.80131		
175B→191B	-0.13369	176B→190B	0.19319		
Excited State 10:	3.180-AU	2.4494 eV	506.19 nm	f=0.0023	<S**2>=2.278
177B→188B	0.78857	178B→189B	0.48897	178B→193B	-0.11384
177B→190B	0.21126	178B→191B	-0.16047		
Excited State 11:	3.179-AG	2.4495 eV	506.17 nm	f=0.0000	<S**2>=2.277
177B→189B	0.47843	177B→193B	-0.11278	178B→190B	0.21372
177B→191B	-0.16054	178B→188B	0.79019	179B→189B	0.13360
Excited State 12:	3.076-AG	2.5287 eV	490.31 nm	f=0.0000	<S**2>=2.115
159B→188B	-0.15351	180B→188B	0.61353	183B→189B	0.11603
171B→188B	0.28766	181B→189B	0.22546	184B→188B	0.15231
179B→189B	0.53374	182B→188B	0.27474		

Excited State 13:	3.075-AU	2.5431 eV	487.53 nm	f=0.0009	<S**2>=2.114
180B→189B	0.28413	182B→189B	-0.11860		
181B→188B	0.87963	183B→188B	-0.34059		
Excited State 14:	3.076-AG	2.5452 eV	487.12 nm	f=0.0000	<S**2>=2.115
179B→189B	0.15896	181B→189B	-0.17036	183B→189B	0.25809
180B→188B	-0.54294	182B→188B	0.74619		
Excited State 15:	3.075-AU	2.5507 eV	486.07 nm	f=0.0007	<S**2>=2.114
180B→189B	0.11967	182B→189B	0.30431	185B→188B	-0.10118
181B→188B	0.33327	183B→188B	0.86967		
Excited State 16:	3.073-AG	2.5632 eV	483.70 nm	f=0.0000	<S**2>=2.111
159B→188B	-0.11996	180B→188B	-0.46996	183B→189B	-0.16580
171B→188B	0.26075	181B→189B	-0.12934	184B→188B	0.25761
179B→189B	0.53174	182B→188B	-0.49511		
Excited State 17:	3.160-AU	2.5823 eV	480.12 nm	f=0.0037	<S**2>=2.246
172B→188B	-0.63825	174B→188B	0.72459	174B→190B	-0.11966
Excited State 18:	4.046-AU	2.9272 eV	423.56 nm	f=0.0044	<S**2>=3.842
181A→201A	-0.12163	188A→191A	0.11957	182B→202B	-0.12374
182A→200A	-0.11571	188A→193A	0.21352	183B→203B	-0.11393
183A→203A	0.12235	188A→198A	-0.13501	184B→189B	-0.10975
184A→202A	-0.11399	189A→190A	-0.14162	184B→191B	0.11592
185A→199A	-0.11593	189A→195A	-0.12414	184B→193B	0.12448
186A→191A	0.10722	168B→188B	0.14904	184B→198B	0.17236
186A→193A	-0.22700	171B→189B	0.12297	185B→188B	0.23255
186A→198A	-0.12544	180B→200B	-0.12349	185B→190B	-0.15059
187A→192A	0.30607	181B→201B	0.11331	185B→195B	-0.13646

185B→199B	0.12621	186B→193B	-0.26089		
186B→191B	0.20407	187B→192B	0.33058		

Excited State 19: 4.062-AG 2.9553 eV 419.53 nm f=0.0000 <S**2>=3.876

181A→200A	-0.12534	188A→199A	-0.10181	184B→190B	-0.14393
182A→201A	-0.12410	189A→191A	-0.13565	184B→195B	-0.14207
183A→202A	0.12699	189A→198A	0.15545	184B→199B	0.13288
184A→203A	-0.12331	179B→189B	-0.20501	185B→191B	0.11734
185A→198A	-0.10961	180B→201B	0.11713	185B→193B	0.13178
186A→192A	0.22406	181B→200B	-0.12843	185B→198B	0.17634
186A→195A	0.10282	182B→203B	-0.11808	186B→192B	0.33950
187A→193A	-0.30917	183B→202B	-0.12889	187B→191B	0.21124
188A→192A	-0.21912	184B→188B	0.18369	187B→193B	-0.26561

Excited State 20: 3.970-AU 3.1444 eV 394.30 nm f=0.0004 <S**2>=3.691

182A→200A	-0.10063	188A→198A	0.11947	186B→189B	0.36589
184A→202A	0.10445	189A→192A	-0.21741	186B→191B	-0.16068
185A→192A	0.17144	180B→200B	-0.11692	186B→198B	-0.16514
186A→193A	-0.18244	181B→201B	0.13094	187B→188B	-0.23705
186A→198A	-0.12253	182B→202B	0.11942	187B→190B	0.16220
187A→190A	0.11473	183B→203B	0.13438	187B→195B	0.12585
187A→195A	0.11675	184B→191B	-0.13876	187B→199B	-0.12818
187A→199A	-0.13165	184B→193B	0.23067		
188A→193A	-0.20094	185B→192B	-0.26623		

Excited State 21: 3.970-AG 3.1444 eV 394.30 nm f=0.0000 <S**2>=3.691

182A→201A	-0.10946	187A→191A	0.13427	180B→201B	0.13189
184A→203A	0.11052	187A→198A	-0.16852	181B→200B	-0.11831
185A→193A	-0.17196	188A→192A	0.20333	182B→203B	0.13390
186A→192A	0.17959	189A→193A	0.21666	183B→202B	0.11944

184B→192B	-0.26802	186B→190B	0.16256	187B→191B	-0.16148
185B→191B	-0.13559	186B→195B	0.12616	187B→198B	-0.16481
185B→193B	0.23129	186B→199B	-0.12835		
186B→188B	-0.23772	187B→189B	0.36522		

Excited State 22:	3.346-AU	3.2448 eV	382.10 nm	f=0.0060	<S**2>=2.549
185A→192A	-0.10480	184B→189B	-0.19987	186B→189B	0.75566
186A→193A	0.11063	184B→193B	-0.12937	187B→188B	-0.36779
189A→192A	0.10402	185B→192B	0.15548		

Excited State 23:	3.344-AG	3.2449 eV	382.09 nm	f=0.0000	<S**2>=2.546
185A→193A	0.10517	184B→192B	0.15545	186B→188B	-0.37078
186A→192A	-0.10572	185B→189B	-0.19786	187B→189B	0.75652
189A→193A	-0.10457	185B→193B	-0.12703		

Excited State 24:	3.081-AG	3.3035 eV	375.31 nm	f=0.0000	<S**2>=2.123
171B→188B	-0.14154	174B→189B	0.75036		
172B→189B	-0.59229	179B→189B	0.11364		

Excited State 25:	3.347-AU	3.3268 eV	372.69 nm	f=0.1156	<S**2>=2.551
174A→194A	0.10128	171B→189B	-0.30950	186B→189B	0.17397
175A→190A	0.11630	174B→194B	0.10523	186B→193B	-0.10859
185A→195A	0.15059	179B→190B	-0.11973	187B→192B	0.12798
158B→188B	0.18435	184B→189B	0.58938		
168B→188B	-0.33327	185B→188B	-0.27054		

Excited State 26:	3.096-AG	3.3605 eV	368.95 nm	f=0.0000	<S**2>=2.147
158B→189B	-0.11019	171B→188B	0.33205	185B→189B	0.80934
159B→188B	-0.11266	174B→189B	0.11823	187B→189B	0.18452
168B→189B	0.12958	184B→188B	-0.27215		

Excited State 27:	3.186-AG	3.3992 eV	364.74 nm	f=0.0000	<S**2>=2.287
144B→188B	-0.10967	171B→188B	0.56495	184B→188B	0.20511
158B→189B	-0.16918	174B→189B	0.12533	185B→189B	-0.33156
168B→189B	0.33198	179B→189B	-0.42253		
Excited State 28:	3.316-AU	3.4057 eV	364.05 nm	f=0.1998	<S**2>=2.500
174A→194A	-0.15131	189A→195A	-0.11227	179B→190B	0.14316
175A→190A	-0.12175	158B→188B	-0.21673	179B→195B	-0.11545
175A→195A	0.11881	168B→188B	0.32254	184B→189B	0.64001
185A→190A	0.10455	171B→189B	0.27044	185B→188B	-0.20036
185A→195A	-0.16352	172B→194B	0.10608	186B→189B	0.12572
185A→199A	-0.10726	174B→194B	-0.14868		
Excited State 29:	3.090-AU	3.5655 eV	347.73 nm	f=0.0009	<S**2>=2.136
180B→189B	0.90958	181B→188B	-0.30676	182B→189B	-0.23304
Excited State 30:	3.089-AG	3.5659 eV	347.69 nm	f=0.0000	<S**2>=2.135
180B→188B	-0.30446	181B→189B	0.91015	183B→189B	-0.22895
Excited State 31:	**3.354-AU**	**3.6063 eV**	**343.80 nm**	**f=0.8708**	**<S**2>=2.563**
172A→194A	-0.11066	181A→190A	0.11278	171B→189B	-0.17395
174A→194A	-0.17446	**185A→190A**	**0.50154**	172B→194B	0.10480
175A→195A	0.15887	185A→195A	-0.14334	174B→194B	-0.15297
175A→199A	0.10513	**189A→190A**	**0.38597**	179B→188B	0.15757
180A→191A	**0.38524**	189A→195A	-0.11851	184B→189B	-0.13418
180A→198A	0.10363	168B→188B	-0.18165		
Excited State 32:	3.094-AU	3.6079 eV	343.65 nm	f=0.0049	<S**2>=2.143
180B→189B	0.23108	182B→189B	0.89768	183B→188B	-0.32452
Excited State 33:	3.091-AG	3.6085 eV	343.59 nm	f=0.0000	<S**2>=2.138

181B→189B	0.22225	182B→188B	-0.32334	183B→189B	0.89995

Excited State 34: 3.618-AG 3.9277 eV 315.66 nm f=0.0000 <S**2>=3.023

172A→196A	-0.18716	185A→191A	0.30987	172B→196B	-0.13976
173A→197A	0.22465	189A→191A	0.29903	173B→197B	-0.17031
174A→196A	0.15288	159B→188B	-0.11191	174B→196B	-0.11890
175A→191A	0.25382	171B→188B	0.15669	179B→191B	0.12801
180A→190A	0.47914	171B→190B	-0.13197		

Excited State 35: 3.860-AU 4.0005 eV 309.92 nm f=0.1841 <S**2>=3.475

172A→194A	0.25329	183A→192A	0.11721	172B→197B	-0.11556
172A→197A	0.15130	184A→193A	0.10545	173B→196B	-0.20518
173A→196A	-0.25647	185A→190A	0.10199	174B→194B	0.19148
174A→194A	0.21126	189A→190A	0.12909	174B→197B	-0.15875
174A→195A	0.11328	158B→188B	-0.11432	179B→188B	-0.12242
174A→197A	-0.19280	168B→188B	0.27524	179B→190B	-0.19300
175A→190A	0.19450	171B→189B	0.18931	179B→195B	0.12939
180A→191A	0.22041	172B→194B	-0.22274	183B→192B	0.11189

Excited State 36: 4.142-AG 4.0238 eV 308.13 nm f=0.0000 <S**2>=4.038

183A→191A	0.16086	184A→197A	-0.12334	182B→197B	0.10431
183A→193A	0.34848	184A→199A	0.15822	182B→199B	-0.14092
183A→198A	-0.19217	186A→192A	-0.12754	183B→191B	-0.32298
184A→190A	-0.13571	182B→190B	0.12107	183B→193B	0.18859
184A→192A	0.36832	182B→192B	-0.34320	183B→198B	-0.18615
184A→195A	-0.12284	182B→195B	0.12514		

Excited State 37: 4.119-AU 4.0246 eV 308.06 nm f=0.0246 <S**2>=3.992

181A→192A	0.12192	183A→192A	0.33333	183A→197A	-0.11332
183A→190A	-0.13327	183A→195A	-0.11724	183A→199A	0.14265

184A→191A	0.15883	182B→191B	0.31114	183B→192B	0.32752
184A→193A	0.34862	182B→193B	-0.17620	183B→195B	-0.12477
184A→198A	-0.20404	182B→198B	0.18332	183B→197B	-0.10246
186A→193A	-0.11855	183B→190B	-0.11841	183B→199B	0.13976

Excited State 38: 4.142-AG 4.0322 eV 307.49 nm f=0.0000 <S**2>=4.040

181A→191A	-0.15489	182A→199A	0.17116	180B→195B	-0.15311
181A→193A	0.35556	183A→193A	-0.10223	180B→199B	0.15117
181A→198A	0.19194	188A→192A	-0.11369	181B→193B	0.37248
182A→190A	-0.14115	189A→193A	-0.11920	181B→198B	0.18736
182A→192A	-0.36633	180B→190B	-0.13371		
182A→195A	-0.16299	180B→192B	-0.33871		

Excited State 39: 4.129-AU 4.0323 eV 307.47 nm f=0.0120 <S**2>=4.012

181A→190A	-0.13745	182A→198A	0.21033	181B→190B	-0.13096
181A→192A	-0.34017	183A→192A	0.10932	181B→192B	-0.33159
181A→195A	-0.15217	188A→193A	0.11203	181B→195B	-0.15258
181A→199A	0.14982	189A→192A	0.11330	181B→199B	0.15069
182A→191A	-0.15470	180B→193B	0.36485		
182A→193A	0.36630	180B→198B	0.18508		

Excited State 40: 3.522-AG 4.0392 eV 306.95 nm f=0.0000 <S**2>=2.852

178A→190A	0.20791	177B→189B	-0.55953	178B→188B	0.56490
178A→195A	0.11347	177B→191B	0.22582	178B→190B	-0.29260
179A→191A	0.22454	177B→193B	0.15342	178B→195B	-0.11682

Excited State 41: 3.526-AU 4.0396 eV 306.92 nm f=0.0026 <S**2>=2.859

178A→191A	-0.22296	177B→188B	-0.55997	178B→189B	0.55893
179A→190A	-0.20682	177B→190B	0.28654	178B→191B	-0.22425
179A→195A	-0.11248	177B→195B	0.11637	178B→193B	-0.15550

Excited State 42:	3.472-AU	4.1702 eV	297.31 nm	f=0.0019	<S**2>=2.764	
176A→191A	-0.15984	154B→188B	-0.14425	176B→191B	-0.18573	
177A→190A	-0.15366	175B→188B	-0.53307	176B→193B	-0.13723	
178A→193A	0.13982	175B→190B	0.26825	177B→192B	0.15645	
179A→192A	-0.13884	176B→189B	0.58662	178B→193B	-0.14075	

Excited State 43:	3.470-AG	4.1721 eV	297.17 nm	f=0.0000	<S**2>=2.760	
176A→190A	-0.15557	151B→188B	0.12531	176B→188B	-0.54260	
177A→191A	-0.16204	175B→189B	0.59369	176B→190B	0.26986	
178A→192A	-0.14125	175B→191B	-0.18555	177B→193B	-0.14196	
179A→193A	0.14225	175B→193B	-0.13927	178B→192B	0.16001	

Excited State 44:	3.690-AG	4.1949 eV	295.56 nm	f=0.0000	<S**2>=3.154	
164A→191A	-0.11737	184A→203A	0.16082	169B→192B	-0.11197	
169A→190A	-0.13211	185A→191A	0.22544	171B→190B	0.14512	
170A→193A	-0.10637	185A→198A	0.11376	179B→189B	0.17104	
171A→192A	-0.10616	154B→189B	0.16257	180B→201B	-0.15747	
180A→190A	0.17253	157B→188B	-0.24197	181B→200B	0.16926	
181A→200A	0.16564	159B→188B	0.34558	182B→203B	0.15540	
182A→201A	0.15924	168B→189B	0.19062	183B→202B	0.16914	
183A→202A	-0.16866	168B→191B	-0.11026			

Excited State 45:	3.840-AU	4.2083 eV	294.62 nm	f=0.0548	<S**2>=3.436	
164A→190A	0.12010	182A→200A	-0.17790	154B→188B	-0.21963	
169A→191A	0.14756	183A→203A	0.20023	157B→189B	0.15449	
170A→192A	-0.11764	184A→202A	-0.18405	158B→188B	-0.15427	
171A→193A	-0.11760	185A→190A	-0.18504	159B→189B	-0.23404	
180A→198A	-0.11311	189A→205A	0.10315	168B→188B	-0.15611	
181A→201A	-0.19513	150B→188B	-0.11835	168B→190B	-0.15126	

169B→193B	-0.10591	176B→189B	-0.11171	183B→203B	-0.18504
170B→192B	-0.12856	180B→200B	-0.19690	187B→192B	-0.10143
171B→191B	0.12780	181B→201B	0.18417		
175B→188B	0.10751	182B→202B	-0.20046		

Excited State 46: 3.663-AG 4.2346 eV 292.79 nm f=0.0000 <S**2>=3.105

170A→191A	-0.12881	152B→188B	0.10353	186B→190B	-0.23173
171A→190A	0.12003	169B→188B	0.52235	187B→189B	0.24828
186A→190A	-0.22543	169B→190B	0.16274	187B→191B	0.17782
187A→191A	-0.30578	170B→189B	-0.30698	187B→193B	0.12907
188A→190A	0.21666	170B→191B	0.12841		

Excited State 47: 3.663-AU 4.2346 eV 292.79 nm f=0.0072 <S**2>=3.105

170A→190A	0.12004	153B→188B	-0.10444	186B→189B	-0.24853
171A→191A	-0.12870	169B→189B	-0.30840	186B→191B	-0.17697
186A→191A	0.22364	169B→191B	0.12643	186B→193B	-0.13080
187A→190A	0.30814	170B→188B	0.52044	187B→190B	0.23135
188A→191A	-0.21440	170B→190B	0.16209		

Excited State 48: 3.535-AU 4.3149 eV 287.34 nm f=0.0019 <S**2>=2.874

176A→193A	-0.10874	150B→188B	0.16718	176B→189B	-0.15983
177A→192A	0.11066	151B→189B	0.18920	177B→188B	-0.13463
178A→191A	0.39757	154B→188B	-0.22998	177B→192B	0.11973
178A→198A	-0.14310	172B→188B	-0.14844	178B→189B	0.39286
179A→190A	0.37058	173B→189B	0.25538	178B→191B	0.12915
179A→192A	-0.10552	174B→188B	-0.11800		
179A→195A	0.18777	175B→192B	-0.11005		

Excited State 49: 3.575-AG 4.3165 eV 287.23 nm f=0.0000 <S**2>=2.944

176A→192A	0.12005	177A→193A	-0.11828	178A→190A	0.41034

178A→195A	0.20863	151B→188B	0.16076	177B→189B	0.43886
178A→205A	0.10248	172B→189B	0.17690	177B→191B	0.11863
179A→191A	0.43955	173B→188B	-0.17851	178B→188B	-0.15456
179A→198A	-0.15799	174B→189B	0.16374		
179A→204A	0.10217	176B→192B	-0.12008		

Excited State 50:	3.508-AG	4.3237 eV	286.75 nm	f=0.0000	<S**2>=2.826

176A→190A	-0.12329	150B→189B	0.22721	176B→188B	0.20151
177A→191A	-0.12343	151B→188B	0.44940	177B→189B	-0.17353
178A→190A	-0.16488	152B→188B	0.11619	177B→191B	0.11802
178A→192A	-0.20148	154B→189B	-0.25631	177B→193B	-0.20783
179A→191A	-0.17186	157B→188B	0.12842	178B→192B	0.23963
179A→193A	0.20718	175B→189B	-0.32333		

*C.2.9.4 **OTPT-BZN-210, EB** State*

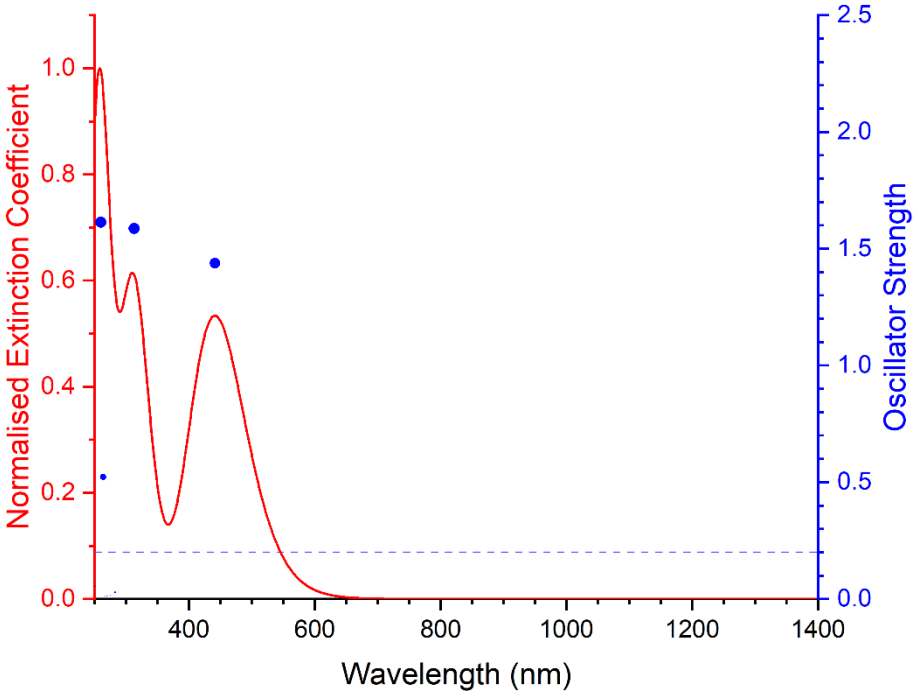

*Figure C-36 Excited states and normalised absorption spectra from TD-DFT calculations of **OTPT-BZN-210** in **EB** state. The areas of excited state dots are proportional to their oscillator strengths.*

Excited State 1:	**Singlet-AU**	**2.8090 eV**	**441.37 nm**	**f=1.4379**	**<S**2>=0.000**

169→189	0.14182	187→190	0.10488
176→189	-0.10323	**188→189**	**0.65936**

Excited State 2:	Singlet-AG	3.0856 eV	401.81 nm	f=0.0000	<S**2>=0.000
170→189	-0.23614	187→189	0.63110		
Excited State 3:	**Singlet-AU**	**3.9629 eV**	**312.86 nm**	**f=1.5861**	**<S**2>=0.000**
169→189	-0.25817	176→193	-0.10538	188→189	0.14655
172→189	-0.10619	**178→189**	**0.32120**	188→193	0.19063
176→189	**0.42029**	187→190	0.15045		
Excited State 4:	Singlet-AG	4.2393 eV	292.46 nm	f=0.0000	<S**2>=0.000
171→189	0.59919	171→193	-0.11466	177→189	0.31580
Excited State 5:	Singlet-AU	4.3811 eV	283.00 nm	f=0.0280	<S**2>=0.000
176→189	-0.30841	178→189	0.49852	188→192	0.11507
177→190	0.15445	186→189	0.17211	188→197	-0.13114
Excited State 6:	Singlet-AG	4.3895 eV	282.46 nm	f=0.0000	<S**2>=0.000
170→189	-0.14451	178→190	0.12128	188→190	-0.30382
171→189	-0.27547	185→189	0.12675		
177→189	0.40458	187→193	-0.19002		
Excited State 7:	Singlet-AG	4.4322 eV	279.74 nm	f=0.0000	<S**2>=0.000
170→189	0.12597	185→189	0.10361	188→191	-0.10175
171→189	-0.17382	187→193	0.26720		
177→189	0.30038	188→190	0.42200		
Excited State 8:	Singlet-AU	4.5018 eV	275.41 nm	f=0.0146	<S**2>=0.000
172→189	0.25850	174→192	0.21873	176→193	0.12314
172→193	0.32801	175→190	0.19189		
173→190	0.35457	175→191	-0.20585		

Excited State 9:	Singlet-AG	4.5019 eV	275.40 nm	f=0.0000	<S**2>=0.000	
172→190	0.37905	173→193	0.30562	175→192	0.19076	
173→189	0.23951	174→191	-0.22420	175→193	0.18486	
173→192	-0.11429	175→189	0.14148	176→190	0.13344	

Excited State 10:	Singlet-AU	4.5842 eV	270.46 nm	f=0.0117	<S**2>=0.000	
172→189	0.13012	174→189	-0.16964	175→190	-0.16041	
172→193	0.14005	174→192	-0.32071	175→191	0.32951	
173→190	0.26397	174→193	-0.25068			

Excited State 11:	Singlet-AG	4.5852 eV	270.40 nm	f=0.0000	<S**2>=0.000	
172→190	0.17675	174→190	-0.26669	175→192	-0.30837	
173→189	0.20116	174→191	0.33146	175→193	-0.18571	
173→193	0.24583	175→189	-0.11112			

Excited State 12:	Singlet-AG	4.5881 eV	270.23 nm	f=0.0000	<S**2>=0.000	
172→191	-0.15451	174→191	0.26104	175→193	0.29678	
173→192	0.25472	175→189	0.21987			
174→190	0.34127	175→192	-0.20597			

Excited State 13:	Singlet-AU	4.5882 eV	270.22 nm	f=0.0035	<S**2>=0.000	
172→192	0.15157	174→192	-0.27207	175→191	0.16153	
173→191	-0.24790	174→193	0.30076			
174→189	0.21095	175→190	0.35642			

Excited State 14:	Singlet-AU	4.6097 eV	268.96 nm	f=0.0049	<S**2>=0.000	
176→189	0.10264	184→192	-0.15913	186→193	0.18407	
178→189	-0.19665	185→190	0.20897	187→191	-0.29636	
183→191	0.13378	186→189	0.17680	188→192	0.36568	

Excited State 15:	Singlet-AG	4.6103 eV	268.93 nm	f=0.0000	<S**2>=0.000			
177→189	0.23051		185→189	-0.17306		187→192	-0.29486	
183→192	0.13481		185→193	-0.18268		188→191	0.36537	
184→191	-0.15946		186→190	-0.20820				
Excited State 16:	Singlet-AU	4.6368 eV	267.39 nm	f=0.0116	<S**2>=0.000			
172→192	0.42704		174→193	-0.12198		176→192	0.13432	
173→191	-0.39037		175→190	-0.14603				
174→189	-0.10836		175→191	-0.23255				
Excited State 17:	Singlet-AG	4.6368 eV	267.39 nm	f=0.0000	<S**2>=0.000			
172→191	0.42702		174→190	0.14956		175→193	0.10813	
173→192	-0.38733		175→192	-0.24204		176→191	0.13622	
Excited State 18:	**Singlet-AU**	**4.7004 eV**	**263.78 nm**	**f=0.5226**	**<S**2>=0.000**			
176→189	-0.23406		186→192	0.13175		188→189	-0.13163	
185→191	-0.13177		**187→190**	**0.35562**		**188→193**	**0.42209**	
Excited State 19:	Singlet-AG	4.7653 eV	260.18 nm	f=0.0000	<S**2>=0.000			
183→192	-0.29642		185→193	-0.25476		188→191	-0.13821	
184→191	0.30240		186→190	-0.28630				
185→189	-0.29035		187→192	0.12273				
Excited State 20:	**Singlet-AU**	**4.7683 eV**	**260.02 nm**	**f=1.6129**	**<S**2>=0.000**			
183→191	-0.29706		186→189	0.29043		188→192	-0.14020	
184→192	0.30458		186→193	0.25488				
185→190	0.28704		187→191	0.12567				
Excited State 21:	Singlet-AG	4.8084 eV	257.85 nm	f=0.0000	<S**2>=0.000			
168→189	-0.14629		187→189	0.25700				
170→189	0.54016		188→190	-0.19604				

Excited State 22:	Singlet-AG	4.9524 eV	250.35 nm	f=0.0000	<S**2>=0.000	
179→192	0.24248	182→190	0.18088	185→201	0.11508	
180→191	-0.21764	182→191	-0.20298	186→200	0.10487	
181→189	0.11855	182→194	-0.13128	187→192	0.10611	
181→192	0.16643	183→192	0.16270	188→191	-0.20230	
181→193	0.18632	184→191	-0.15754			
181→195	-0.12474	184→200	0.11062			

Excited State 23:	Singlet-AU	4.9525 eV	250.35 nm	f=0.0074	<S**2>=0.000	
179→191	0.26995	182→192	-0.12999	184→199	-0.10493	
180→192	-0.24907	182→193	-0.18901	186→201	-0.11859	
181→190	-0.18552	182→195	0.12692	187→191	0.11320	
181→191	0.12126	183→191	0.17186	188→192	-0.21286	
181→194	0.13237	183→200	-0.10299			
182→189	-0.11925	184→192	-0.16859			

Excited State 24:	Singlet-AG	4.9552 eV	250.21 nm	f=0.0000	<S**2>=0.000	
179→189	0.12647	180→191	0.17267	184→198	0.12467	
179→192	-0.16230	180→194	-0.14396	185→192	-0.10493	
179→193	0.19392	181→192	0.29537	185→199	0.12541	
179→195	-0.13436	182→191	-0.27618	186→191	0.10359	
180→190	0.21685	183→201	0.11681	186→198	-0.10393	

Excited State 25:	Singlet-AU	4.9566 eV	250.14 nm	f=0.0558	<S**2>=0.000	
179→190	-0.21811	180→193	-0.20001	183→198	-0.11815	
179→194	0.14520	180→195	0.13631	184→201	-0.12812	
180→189	-0.13451	181→191	0.32850	186→199	-0.13146	
180→192	0.14436	182→192	-0.31578			

C.2.10 Electronic Transition in **OTPT-BZN-221** Oligomers

*Table C-14 Attributes of **OTPT-BZN-221** in **LEB**, **ES** (singlet and quintet), and **EB** states related to electronic structures*

Attribute	LEB State	^{1}ES State	^{5}ES State	EB State
Molecular Formula	$C_{54}H_{38}N_{10}$	$C_{54}H_{38}N_{10}^{4+}$	$C_{54}H_{38}N_{10}^{4+}$	$C_{54}H_{34}N_{10}$
Number of Atoms	102	102	102	98
Number of Electrons	432	428	428	428
HOMO	MO 216	MO 214	MOs 216A, 212B	MO 214
LUMO	MO 217	MO 215	MOs 217A, 213B	MO 215

*C.2.10.1 **OTPT-BZN-221**, **LEB** State*

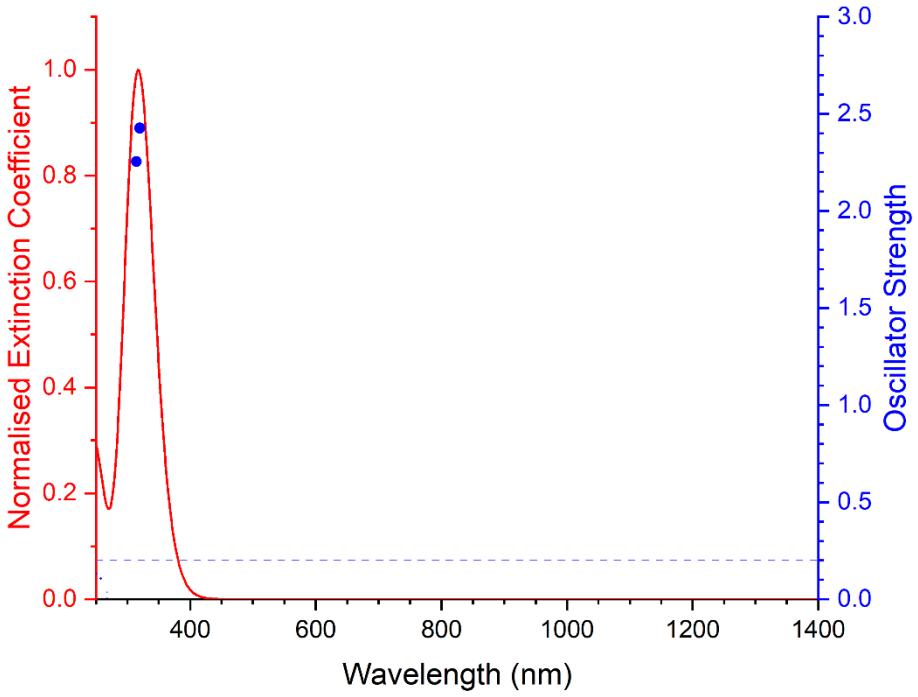

*Figure C-37 Excited states and normalised absorption spectra from TD-DFT calculations of **OTPT-BZN-221** in **LEB** state. The areas of excited state dots are proportional to their oscillator strengths.*

Excited State 1:	Singlet-A"	3.5842 eV	345.92 nm	f=0.0000	<S**2>=0.000
213→219	-0.16213	215→217	-0.27426	216→218	0.48375
214→220	0.27084	215→221	-0.21690		
Excited State 2:	**Singlet-A'**	**3.8738 eV**	**320.06 nm**	**f=2.4266**	**<S**2>=0.000**
213→220	0.24168	**215→218**	**0.49092**	216→217	-0.27498
214→219	-0.12527	215→225	-0.11251	216→221	-0.23733

Excited State 3:	**Singlet-A"**	**3.9418 eV**	**314.54 nm**	**f=2.2549**	**<S**2>=0.000**	
213→217	-0.22162	215→219	-0.28502	**216→220**	**0.44523**	
214→218	**0.33820**	215→224	0.12047			
Excited State 4:	Singlet-A'	4.1617 eV	297.92 nm	f=0.0000	<S**2>=0.000	
213→218	0.32575	215→220	0.45595	216→224	0.11806	
214→217	-0.18856	216→219	-0.29037			
Excited State 5:	Singlet-A"	4.2071 eV	294.70 nm	f=0.0000	<S**2>=0.000	
210→217	0.13932	213→219	0.32505	215→217	0.45888	
212→218	-0.10045	214→220	0.16174	216→218	0.26829	
Excited State 6:	Singlet-A"	4.2205 eV	293.77 nm	f=0.0087	<S**2>=0.000	
210→219	0.13364	213→217	0.31099	215→219	0.43714	
212→220	-0.10557	214→218	0.20988	216→220	0.27418	
Excited State 7:	Singlet-A'	4.3910 eV	282.36 nm	f=0.0013	<S**2>=0.000	
213→220	0.13549	215→218	0.26582	216→226	0.10752	
214→219	0.28753	216→217	0.51478			
Excited State 8:	Singlet-A'	4.3999 eV	281.79 nm	f=0.0032	<S**2>=0.000	
213→218	0.18633	215→220	0.26029	216→219	0.47828	
214→217	0.26131	215→223	0.14446	216→222	0.13571	
Excited State 9:	Singlet-A"	4.5816 eV	270.61 nm	f=0.0000	<S**2>=0.000	
197→219	0.39139	199→218	-0.28077			
198→217	0.39252	200→220	-0.27655			
Excited State 10:	Singlet-A"	4.5819 eV	270.60 nm	f=0.0017	<S**2>=0.000	
197→217	0.39317	199→220	-0.27672			
198→219	0.39328	200→218	-0.27658			

Excited State 11:	Singlet-A"	4.6082 eV	269.05 nm	f=0.0060	<S**2>=0.000			
215→222	0.39651		215→224	0.16818		216→223	0.44405	
Excited State 12:	Singlet-A'	4.6132 eV	268.76 nm	f=0.0020	<S**2>=0.000			
199→219	0.38685		215→223	-0.24924				
200→217	0.38792		216→222	-0.23733				
Excited State 13:	Singlet-A'	4.6189 eV	268.43 nm	f=0.0015	<S**2>=0.000			
199→217	0.47715		200→219	0.46982		200→233	-0.10201	
Excited State 14:	Singlet-A'	4.6312 eV	267.72 nm	f=0.0355	<S**2>=0.000			
199→219	0.27271		215→223	0.32837		216→224	0.13811	
200→217	0.27249		216→219	-0.15488				
214→217	-0.10606		216→222	0.31090				
Excited State 15:	Singlet-A"	4.6533 eV	266.44 nm	f=0.0000	<S**2>=0.000			
197→219	0.28068		199→218	0.38952				
198→217	0.27927		200→220	0.38296				
Excited State 16:	Singlet-A"	4.6539 eV	266.41 nm	f=0.0054	<S**2>=0.000			
197→217	0.27596		199→220	0.38684				
198→219	0.27849		200→218	0.38806				
Excited State 17:	Singlet-A'	4.7838 eV	259.18 nm	f=0.0012	<S**2>=0.000			
197→220	0.47316		197→235	0.10071		198→218	0.47811	
Excited State 18:	Singlet-A'	4.7839 eV	259.17 nm	f=0.0087	<S**2>=0.000			
197→218	0.47792		198→220	0.47451		198→235	0.10097	
Excited State 19:	Singlet-A"	4.8147 eV	257.51 nm	f=0.0000	<S**2>=0.000			
203→218	0.19264		213→222	0.14060		214→220	-0.13403	
205→220	0.15513		213→230	-0.16751		214→223	0.15869	

214→231	-0.17541	215→226	0.28203	216→227	-0.22351
215→221	-0.17595	216→225	-0.25997		

Excited State 20: Singlet-A' 4.8149 eV 257.50 nm f=0.1062 <S**2>=0.000

204→218	0.16560	213→223	0.13796	215→225	-0.24111
206→220	0.15776	213→231	-0.15210	215→227	-0.18919
211→219	0.12180	214→222	0.13142	216→217	-0.13522
212→217	0.11657	214→230	-0.16039	216→221	-0.19397
213→220	-0.14743	215→218	-0.10775	216→226	0.26969

Excited State 21: Singlet-A" 4.8962 eV 253.22 nm f=0.0109 <S**2>=0.000

201→218	0.13085	205→218	-0.17382	214→227	0.18066
203→220	-0.19622	206→217	0.10284	215→230	0.29987
204→219	0.10766	213→226	-0.20188	216→231	0.31856
204→224	-0.11227	214→225	0.12135		

Excited State 22: Singlet-A' 4.9004 eV 253.01 nm f=0.0037 <S**2>=0.000

202→218	0.12786	213→225	0.10725	216→219	0.12270
203→219	0.10703	213→227	0.17238	216→230	0.29993
204→220	-0.19865	214→226	-0.20193		
206→218	-0.18692	215→231	0.29218		

Excited State 23: Singlet-A" 4.9441 eV 250.77 nm f=0.0000 <S**2>=0.000

208→218	0.14842	215→221	0.29369	216→227	-0.12930
213→219	-0.17226	215→232	0.19450	216→229	0.19700
214→220	0.30216	216→225	0.23369		

Excited State 24: Singlet-A' 4.9540 eV 250.27 nm f=0.1313 <S**2>=0.000

204→218	0.14234	212→217	-0.20421	215→225	0.16221
208→217	-0.14082	213→220	0.22772	215→227	-0.14221
211→219	-0.23514	214→219	-0.12817	215→229	0.17738

216→221 0.23803 216→232 0.18183

*C.2.10.2 **OTPT-BZN-221**, **¹ES** State*

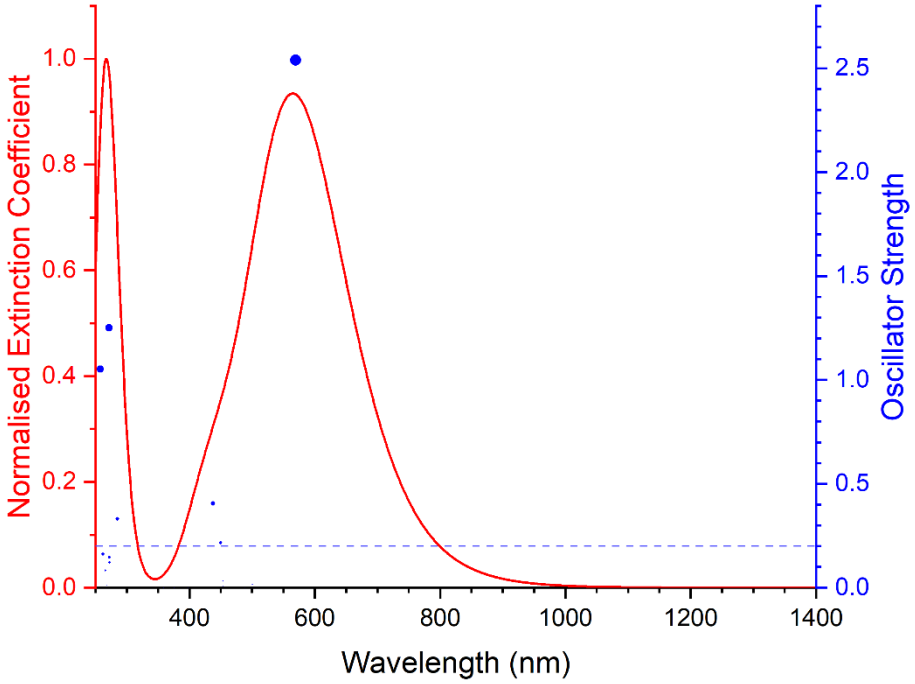

*Figure C-38 Excited states and normalised absorption spectra from TD-DFT calculations of **OTPT-BZN-221** in **¹ES** state. The areas of excited state dots are proportional to their oscillator strengths.*

Excited State 1:	Singlet-A"	1.9424 eV	638.29 nm	f=0.0000	<S**2>=0.000	
209→215	0.48347	210→216	-0.47103	212→216	-0.14588	
Excited State 2:	**Singlet-A'**	**2.1762 eV**	**569.73 nm**	**f=2.5389**	**<S**2>=0.000**	
209→216	**-0.46107**	**210→215**	**0.49648**	212→215	0.16900	
Excited State 3:	Singlet-A"	2.4746 eV	501.03 nm	f=0.0000	<S**2>=0.000	
210→216	0.11229	214→215	0.67566			
Excited State 4:	Singlet-A"	2.4768 eV	500.59 nm	f=0.0159	<S**2>=0.000	
207→215	0.10216	213→215	0.68798			
Excited State 5:	Singlet-A'	2.5271 eV	490.61 nm	f=0.0057	<S**2>=0.000	
203→215	-0.12622	214→216	0.67142			

Excited State 6:	Singlet-A'	2.5356 eV	488.98 nm	f=0.0001	<S**2>=0.000
201→215	0.10385	213→216	0.68650		
Excited State 7:	Singlet-A"	2.6990 eV	459.37 nm	f=0.0000	<S**2>=0.000
200→215	-0.35446	204→215	0.31421		
203→216	0.46494	214→215	0.14976		
Excited State 8:	Singlet-A'	2.7040 eV	458.53 nm	f=0.0139	<S**2>=0.000
200→216	-0.34543	204→216	0.30355		
203→215	0.46702	214→216	0.18917		
Excited State 9:	Singlet-A'	2.7202 eV	455.79 nm	f=0.0019	<S**2>=0.000
201→215	-0.12014	208→215	-0.13468		
207→216	-0.15051	211→215	0.65794		
Excited State 10:	Singlet-A'	2.7308 eV	454.01 nm	f=0.0087	<S**2>=0.000
209→216	0.13809	210→215	-0.10792	212→215	0.67940
Excited State 11:	Singlet-A"	2.7335 eV	453.57 nm	f=0.0319	<S**2>=0.000
199→215	0.33729	207→215	0.32675	211→216	-0.22106
201→216	0.43126	208→216	0.13559	213→215	-0.12487
Excited State 12:	Singlet-A'	2.7432 eV	451.96 nm	f=0.0038	<S**2>=0.000
199→216	0.40556	207→216	0.22649	213→216	-0.15178
201→215	0.46795	211→215	0.18182		
Excited State 13:	**Singlet-A"**	**2.7563 eV**	**449.82 nm**	**f=0.2153**	**<S**2>=0.000**
199→215	0.26982	202→215	0.10201	**211→216**	**0.53602**
201→216	0.20855	208→216	-0.26739		
Excited State 14:	Singlet-A"	2.7739 eV	446.97 nm	f=0.0000	<S**2>=0.000
209→215	0.17292	212→216	0.68024		

Excited State 15:	**Singlet-A"**	**2.8336 eV**	**437.55 nm**	**f=0.4055**	**<S**2>=0.000**	
199→215	-0.17656	207→215	0.29192	**211→216**	**0.40269**	
202→215	-0.15540	**208→216**	**0.42404**			
Excited State 16:	Singlet-A'	2.8627 eV	433.11 nm	f=0.0012	<S**2>=0.000	
199→216	-0.19140	207→216	0.33308	211→215	0.17577	
202→216	-0.18477	208→215	0.51496			
Excited State 17:	Singlet-A"	2.9038 eV	426.97 nm	f=0.0000	<S**2>=0.000	
209→215	0.46399	210→216	0.50255	212→216	-0.10118	
Excited State 18:	Singlet-A'	2.9131 eV	425.62 nm	f=0.0029	<S**2>=0.000	
209→216	0.50407	210→215	0.47663			
Excited State 19:	Singlet-A'	3.1187 eV	397.55 nm	f=0.0005	<S**2>=0.000	
195→215	0.48039	196→216	0.48149			
Excited State 20:	Singlet-A"	3.1189 eV	397.52 nm	f=0.0000	<S**2>=0.000	
195→216	0.47824	196→215	0.48500			
Excited State 21:	Singlet-A'	3.3015 eV	375.54 nm	f=0.0006	<S**2>=0.000	
202→216	-0.23363	205→219	0.12158	207→216	-0.10785	
205→215	0.61890	206→217	-0.14448			
Excited State 22:	Singlet-A'	3.3026 eV	375.41 nm	f=0.0003	<S**2>=0.000	
200→216	0.15316	205→217	-0.14410	206→219	0.12247	
204→216	0.20497	206→215	0.62075			
Excited State 23:	Singlet-A"	3.3349 eV	371.78 nm	f=0.0035	<S**2>=0.000	
199→215	-0.12703	204→217	0.10181	207→215	0.27255	
202→215	0.52701	205→216	-0.30294			

Excited State 24:	Singlet-A"	3.3421 eV	370.98 nm	f=0.0000	<S**2>=0.000
200→215	0.37365	204→215	0.46620		
202→217	0.11936	206→216	0.32049		
Excited State 25:	Singlet-A'	3.4565 eV	358.69 nm	f=0.0010	<S**2>=0.000
199→216	-0.14579	205→215	0.23928	208→215	-0.10747
202→216	0.51439	207→216	0.33325		
Excited State 26:	Singlet-A'	3.4688 eV	357.43 nm	f=0.0015	<S**2>=0.000
200→216	0.39710	204→216	0.49668	206→215	-0.24626
Excited State 27:	Singlet-A"	3.4836 eV	355.91 nm	f=0.0028	<S**2>=0.000
202→215	0.20914	207→215	0.18522		
205→216	0.60700	208→216	-0.13829		
Excited State 28:	Singlet-A"	3.4902 eV	355.24 nm	f=0.0000	<S**2>=0.000
200→215	-0.20116	204→215	-0.23932	206→216	0.61227
Excited State 29:	Singlet-A"	3.6014 eV	344.27 nm	f=0.0048	<S**2>=0.000
199→215	0.10621	202→215	0.32149	207→215	-0.39050
201→216	0.10427	205→216	0.13095	208→216	0.43858
Excited State 30:	Singlet-A'	3.6267 eV	341.86 nm	f=0.0012	<S**2>=0.000
201→215	0.10969	207→216	-0.39959		
202→216	0.34296	208→215	0.43139		
Excited State 31:	Singlet-A'	3.8488 eV	322.13 nm	f=0.0051	<S**2>=0.000
200→216	0.40918	203→215	0.49306	204→216	-0.29285
Excited State 32:	Singlet-A"	3.8497 eV	322.06 nm	f=0.0000	<S**2>=0.000
200→215	0.39818	203→216	0.50219	204→215	-0.29360

Excited State 33:	Singlet-A"	3.8772 eV	319.78 nm	f=0.0000	<S**2>=0.000
199→215	-0.48436	201→216	0.49059	207→215	-0.11904
Excited State 34:	Singlet-A'	3.8780 eV	319.71 nm	f=0.0000	<S**2>=0.000
199→216	0.49661	201→215	-0.48002	207→216	0.10862
Excited State 35:	**Singlet-A'**	**4.3507 eV**	**284.98 nm**	**f=0.3307**	**<S**2>=0.000**
187→215	0.15660	197→216	-0.30947		
188→216	-0.28170	**198→215**	**0.50964**		
Excited State 36:	Singlet-A"	4.3522 eV	284.87 nm	f=0.0000	<S**2>=0.000
187→216	0.16017	197→215	-0.31945		
188→215	-0.28787	198→216	0.49660		
Excited State 37:	Singlet-A"	4.5459 eV	272.74 nm	f=0.0000	<S**2>=0.000
197→215	-0.12563	211→221	0.10318	213→224	0.13806
207→217	0.11054	212→220	0.16343	214→219	-0.35875
211→218	-0.12089	213→217	0.41096		
Excited State 38:	Singlet-A"	4.5476 eV	272.64 nm	f=0.1220	<S**2>=0.000
207→219	-0.12828	212→218	-0.11179	214→217	0.41675
209→217	0.14820	212→221	0.10777	214→224	0.13734
211→220	0.13589	213→219	-0.34929		
Excited State 39:	Singlet-A'	4.5550 eV	272.19 nm	f=0.1462	<S**2>=0.000
209→218	0.12405	213→220	0.42890	214→218	-0.35719
210→217	0.18912	213→225	0.12023	214→221	0.28294
Excited State 40:	**Singlet-A'**	**4.5661 eV**	**271.53 nm**	**f=1.2506**	**<S**2>=0.000**
213→218	**-0.38254**	**214→220**	**0.44425**		
213→221	0.29170	214→225	0.12428		

Excited State 41:	Singlet-A"	4.6142 eV	268.70 nm	f=0.0106	<S**2>=0.000			
200→217	0.10996		205→220	0.37394		212→218	-0.11210	
202→219	0.14742		206→218	-0.31230		214→217	0.10696	
204→217	0.12373		206→221	0.24269				
205→216	0.10034		211→220	0.11083				
Excited State 42:	Singlet-A"	4.6173 eV	268.52 nm	f=0.0000	<S**2>=0.000			
200→219	-0.10822		205→218	-0.33137		206→220	0.40947	
202→217	-0.14719		205→221	0.25868				
204→219	-0.12915		206→216	0.10919				
Excited State 43:	Singlet-A'	4.6499 eV	266.64 nm	f=0.0024	<S**2>=0.000			
202→220	0.10475		205→219	0.41041		206→224	-0.20046	
205→215	-0.20565		206→217	-0.40881				
Excited State 44:	Singlet-A'	4.6513 eV	266.56 nm	f=0.0081	<S**2>=0.000			
205→217	-0.40859		206→215	-0.20820				
205→224	-0.20043		206→219	0.41679				
Excited State 45:	Singlet-A"	4.6674 eV	265.64 nm	f=0.0823	<S**2>=0.000			
205→220	-0.15768		209→217	-0.19984		212→221	0.23231	
206→218	0.12619		211→220	0.35167		214→217	-0.13748	
206→221	-0.10488		211→225	0.12722				
207→219	0.10843		212→218	-0.30759				
Excited State 46:	Singlet-A"	4.6795 eV	264.95 nm	f=0.0000	<S**2>=0.000			
211→218	-0.31855		212→225	0.13905		214→219	0.12850	
211→221	0.27776		213→217	-0.15541				
212→220	0.38202		213→232	-0.10805				

Excited State 47:	Singlet-A"	4.7351 eV	261.84 nm	f=0.1610	<S**2>=0.000			
200→217	0.18306		205→220	-0.18599		210→218	-0.17990	
202→215	-0.11892		206→218	0.13924		211→220	-0.15663	
202→219	0.24792		206→221	-0.13143		212→221	-0.11483	
204→217	0.22198		207→219	0.16459		213→219	-0.12533	
204→224	0.11474		209→217	-0.19944		214→217	0.14001	
Excited State 48:	Singlet-A"	4.7465 eV	261.21 nm	f=0.0000	<S**2>=0.000			
200→215	-0.10954		204→215	-0.12953		206→220	0.18315	
200→219	0.22978		204→219	0.29830		207→217	0.17220	
202→217	0.33195		205→218	-0.14005				
202→224	0.16309		205→221	0.13756				
Excited State 49:	Singlet-A'	4.7801 eV	259.38 nm	f=0.0089	<S**2>=0.000			
200→218	0.21357		204→218	0.27124		207→220	0.20984	
200→221	-0.14746		204→221	-0.19531		209→218	-0.16946	
202→216	0.10935		205→219	-0.12263		210→217	-0.13893	
202→220	0.35198		206→217	0.12020				
Excited State 50:	**Singlet-A"**	**4.8095 eV**	**257.79 nm**	**f=1.0519**	**<S**2>=0.000**			
200→217	0.13319		204→217	0.21322		**209→217**	**0.35790**	
202→219	0.26577		208→220	0.16330		**210→218**	**0.37007**	

*C.2.10.3 **OTPT-BZN-221**, **^{5}ES** State*

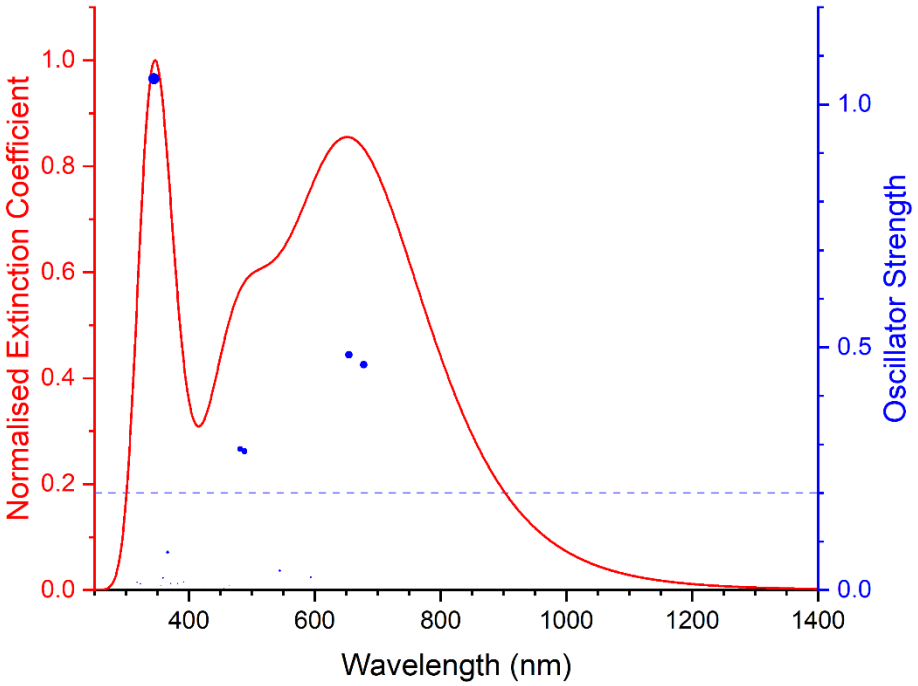

*Figure C-39 Excited states and normalised absorption spectra from TD-DFT calculations of **OTPT-BZN-221** in **^{5}ES** state. The areas of excited state dots are proportional to their oscillator strengths.*

Excited State 1:	5.115-A"	1.7318 eV	715.95 nm	f=0.0000	<S**2>=6.290
195B→215B	-0.14863	199B→213B	-0.11417	208B→214B	0.62110
196B→216B	0.17588	200B→214B	0.16459	212B→213B	-0.19756
197B→215B	0.11080	207B→213B	0.62410		
Excited State 2:	**5.101-A'**	**1.8290 eV**	**677.87 nm**	**f=0.4641**	**<S**2>=6.256**
196B→215B	0.14035	**200B→213B**	**0.41993**	**208B→213B**	**0.42286**
197B→216B	0.25616	203B→215B	-0.16859	212B→214B	-0.15211
198B→215B	0.23677	204B→216B	-0.17771		
199B→214B	**-0.37689**	**207B→214B**	**0.45972**		
Excited State 3:	5.087-A"	1.8429 eV	672.77 nm	f=0.0004	<S**2>=6.218
197B→213B	0.42620	200B→216B	0.39221	211B→213B	-0.20383
198B→214B	0.42519	203B→214B	-0.33880	212B→215B	-0.11736
199B→215B	-0.38083	204B→213B	-0.34306		

Excited State 4:	5.086-A'	1.8493 eV	670.44 nm	f=0.0002	<S**2>=6.216			
197B→214B	0.43339	200B→215B	0.40005	211B→214B	-0.12344			
198B→213B	0.43397	203B→213B	-0.34631					
199B→216B	-0.38807	204B→214B	-0.34905					
Excited State 5:	5.091-A"	1.8657 eV	664.56 nm	f=0.0000	<S**2>=6.229			
197B→215B	-0.30524	200B→214B	-0.52416	207B→213B	0.14944			
198B→216B	-0.31838	203B→216B	0.21802	208B→214B	0.23995			
199B→213B	0.52887	204B→215B	0.21436	212B→213B	0.13063			
Excited State 6:	**5.111-A'**	**1.8948 eV**	**654.35 nm**	**f=0.4844**	**<S**2>=6.279**			
195B→216B	-0.12653	**199B→214B**	**0.39681**	**207B→214B**	**0.43207**			
196B→215B	0.11426	**200B→213B**	**-0.36899**	**208B→213B**	**0.51993**			
197B→216B	-0.20691	203B→215B	0.15882					
198B→215B	-0.23390	204B→216B	0.14696					
Excited State 7:	5.113-A"	2.0869 eV	594.12 nm	f=0.0261	<S**2>=6.286			
195B→213B	0.10765	211B→213B	0.83524	212B→215B	0.43090			
198B→214B	0.10530	211B→217B	0.12236	212B→220B	0.10638			
Excited State 8:	5.114-A"	2.0931 eV	592.34 nm	f=0.0000	<S**2>=6.288			
194B→213B	0.10823	208B→214B	0.13213	212B→213B	0.82969			
199B→213B	-0.11291	211B→215B	0.42601	212B→217B	0.12200			
200B→214B	0.12472	211B→220B	0.10530					
Excited State 9:	5.137-A'	2.2702 eV	546.14 nm	f=0.0002	<S**2>=6.348			
195B→214B	0.13263	211B→218B	-0.12434	212B→219B	-0.11672			
211B→214B	0.85512	212B→216B	0.37738					
Excited State 10:	5.130-A'	2.2777 eV	544.34 nm	f=0.0397	<S**2>=6.329			
194B→214B	0.11214	208B→213B	0.10543	211B→216B	0.37583			

211B→219B	-0.11273	212B→214B	0.86841	212B→218B	-0.12190

Excited State 11:	5.174-A'	2.4858 eV	498.76 nm	f=0.0014	<S**2>=6.442
196B→213B	0.10001	205B→220B	-0.21076	208B→215B	0.21477
201B→214B	-0.12473	206B→213B	0.65062	209B→213B	0.24500
204B→214B	-0.10556	206B→217B	0.21846	210B→215B	0.11925
205B→215B	-0.45710	207B→216B	0.15452		

Excited State 12:	5.189-A'	2.4889 eV	498.15 nm	f=0.0001	<S**2>=6.482
201B→216B	0.11127	205B→213B	0.71122	206B→220B	-0.22687
202B→214B	-0.15988	205B→217B	0.25686	210B→213B	0.11664
203B→215B	-0.12429	206B→215B	-0.50489		

Excited State 13:	5.120-A'	2.4926 eV	497.40 nm	f=0.0004	<S**2>=6.302
195B→214B	-0.10778	206B→213B	-0.27642	209B→213B	0.70893
196B→213B	0.17225	206B→217B	-0.10589	210B→215B	0.32211
203B→213B	-0.10692	207B→216B	0.21711	211B→214B	0.10167
205B→215B	0.22992	208B→215B	0.24032		

Excited State 14:	5.102-A'	2.5118 eV	493.60 nm	f=0.0005	<S**2>=6.257
209B→215B	0.38075	210B→213B	0.90085		

Excited State 15:	**5.103-A"**	**2.5371 eV**	**488.69 nm**	**f=0.2855**	**<S**2>=6.261**
190B→213B	0.12514	198B→214B	-0.29593	**207B→215B**	**0.42169**
195B→213B	-0.19968	**203B→214B**	**-0.33389**	**208B→216B**	**0.44801**
196B→214B	0.22104	**204B→213B**	**-0.37272**	209B→214B	0.11258
197B→213B	-0.24191	206B→214B	0.11493		

Excited State 16:	5.115-A'	2.5447 eV	487.23 nm	f=0.0017	<S**2>=6.290
195B→214B	0.13655	197B→214B	0.22274	203B→213B	0.35883
196B→213B	-0.17548	198B→213B	0.27778	204B→214B	0.35970

205B→215B	-0.11281	208B→215B	-0.34866	210B→215B	0.16235
207B→216B	-0.29652	209B→213B	0.45884	211B→214B	-0.10809

Excited State 17:	5.122-A'	2.5728 eV	481.91 nm	f=0.0037	<S**2>=6.310
195B→214B	-0.13229	203B→213B	0.41962	208B→215B	0.36929
196B→213B	0.22472	204B→214B	0.41952	209B→213B	-0.25092
197B→214B	0.29709	206B→213B	-0.10005	211B→214B	0.12695
198B→213B	0.26409	207B→216B	0.31864		

Excited State 18:	**5.113-A"**	**2.5730 eV**	**481.87 nm**	**f=0.2903**	**<S**2>=6.287**
190B→213B	0.10650	198B→214B	0.25989	**207B→215B**	**0.37739**
195B→213B	-0.16344	**203B→214B**	**0.41559**	**208B→216B**	**0.38797**
196B→214B	0.22705	**204B→213B**	**0.42451**	209B→214B	0.12495
197B→213B	0.29351	206B→214B	-0.12847		

Excited State 19:	5.095-A"	2.6701 eV	464.35 nm	f=0.0000	<S**2>=6.239
209B→216B	0.31936	210B→214B	0.93959		

Excited State 20:	5.094-A"	2.6729 eV	463.85 nm	f=0.0085	<S**2>=6.236
207B→215B	-0.12147	209B→214B	0.92733		
208B→216B	-0.12787	210B→216B	0.30408		

Excited State 21:	5.146-A"	2.7158 eV	456.53 nm	f=0.0000	<S**2>=6.370
199B→213B	0.11842	202B→213B	0.73072	206B→216B	0.14707
201B→215B	-0.51120	202B→217B	0.21071		
201B→220B	-0.18640	205B→214B	-0.23717		

Excited State 22:	5.146-A"	2.7165 eV	456.40 nm	f=0.0033	<S**2>=6.370
197B→213B	0.11285	202B→215B	-0.50687	206B→214B	-0.23830
201B→213B	0.73013	202B→220B	-0.18556		
201B→217B	0.21145	205B→216B	0.15539		

Excited State 23:	5.167-A'	2.8696 eV	432.06 nm	f=0.0009	<S**2>=6.425	
199B→214B	0.11618	201B→219B	0.19388	202B→218B	-0.21961	
201B→216B	-0.49278	202B→214B	0.74917	205B→213B	0.13425	

Excited State 24:	5.168-A'	2.8709 eV	431.86 nm	f=0.0009	<S**2>=6.427	
197B→214B	0.11266	201B→218B	-0.22069	202B→219B	0.19319	
201B→214B	0.74921	202B→216B	-0.48891	206B→213B	0.12428	

Excited State 25:	5.652-A'	2.9312 eV	422.98 nm	f=0.0044	<S**2>=7.736	
210A→218A	0.10284	216A→230A	-0.10207	211B→219B	0.33629	
213A→233A	0.13358	216A→236A	-0.10259	211B→227B	0.15443	
215A→220A	-0.30416	193B→213B	0.18844	212B→214B	0.28291	
215A→225A	-0.19624	196B→215B	0.15512	212B→218B	0.31160	
215A→235A	-0.10464	207B→214B	-0.13384	212B→221B	-0.17588	
216A→219A	-0.26008	209B→231B	-0.14778	212B→226B	-0.10340	
216A→221A	-0.21155	210B→232B	-0.15213			
216A→227A	0.11595	211B→216B	-0.13598			

Excited State 26:	5.687-A'	2.9738 eV	416.93 nm	f=0.0000	<S**2>=7.835	
211A→233A	-0.10150	216A→220A	0.31360	211B→221B	0.18907	
213A→232A	-0.12582	216A→225A	0.20199	211B→226B	0.11073	
213A→234A	-0.11416	216A→235A	0.11636	211B→230B	-0.10828	
214A→233A	-0.10911	207B→216B	0.18500	212B→216B	0.12775	
215A→219A	0.27661	208B→215B	0.14884	212B→219B	-0.35768	
215A→221A	0.22448	209B→232B	0.16632	212B→227B	-0.16486	
215A→227A	-0.12039	210B→231B	0.16117	212B→235B	-0.10394	
215A→230A	0.10195	211B→214B	-0.26816			
215A→236A	0.11335	211B→218B	-0.32766			

Excited State 27:	5.120-A"	3.0989 eV	400.09 nm	f=0.0000	<S**2>=6.303
201B→215B	-0.14288	205B→214B	0.77450	206B→219B	0.13316
202B→213B	0.21576	205B→218B	-0.16150		
204B→215B	0.11967	206B→216B	-0.47445		
Excited State 28:	5.121-A"	3.1026 eV	399.62 nm	f=0.0012	<S**2>=6.307
201B→213B	0.22206	205B→216B	-0.46376	206B→218B	-0.16101
202B→215B	-0.14164	205B→219B	0.14379		
203B→214B	0.21006	206B→214B	0.76090		
Excited State 29:	5.113-A"	3.1644 eV	391.81 nm	f=0.0000	<S**2>=6.286
197B→215B	0.30439	204B→215B	0.57933	212B→213B	-0.12164
198B→216B	0.31842	205B→214B	-0.14575		
203B→216B	0.55453	211B→215B	0.20580		
Excited State 30:	5.115-A'	3.1656 eV	391.67 nm	f=0.0168	<S**2>=6.291
197B→216B	0.31724	203B→215B	0.57650	206B→215B	-0.16090
198B→215B	0.33691	204B→216B	0.59072		
Excited State 31:	5.113-A"	3.1975 eV	387.76 nm	f=0.0007	<S**2>=6.287
211B→213B	-0.48495	211B→217B	0.11517	212B→215B	0.84494
Excited State 32:	5.113-A"	3.2003 eV	387.41 nm	f=0.0000	<S**2>=6.285
197B→215B	-0.10055	204B→215B	-0.14728	212B→213B	-0.47335
203B→216B	-0.15062	211B→215B	0.81708	212B→217B	0.11192
Excited State 33:	5.293-A'	3.2442 eV	382.17 nm	f=0.0133	<S**2>=6.755
202A→217A	0.13595	215A→220A	0.11288	194B→214B	-0.13272
210A→218A	0.16780	216A→219A	0.10091	195B→216B	-0.12650
211A→224A	0.11540	187B→214B	-0.19280	196B→215B	0.33981
212A→230A	-0.11756	193B→213B	0.39489	203B→215B	0.10838

207B→214B	-0.36133	211B→216B	0.15590	212B→218B	-0.12187
208B→213B	0.30251	211B→219B	-0.13319		
208B→217B	0.14958	212B→214B	-0.11256		

Excited State 34: 5.117-A' 3.2999 eV 375.72 nm f=0.0008 <S**2>=6.296

210A→217A	-0.12221	195B→214B	-0.20148	211B→214B	-0.21796
187B→216B	-0.15408	196B→213B	0.45068	212B→216B	0.57382
190B→214B	0.10440	207B→216B	-0.32904		
193B→215B	0.29603	208B→215B	-0.16239		

Excited State 35: 5.280-A" 3.3291 eV 372.42 nm f=0.0000 <S**2>=6.719

202A→221A	-0.10581	185B→214B	-0.11506	203B→222B	-0.12352
205A→222A	0.10919	187B→213B	-0.24661	204B→223B	-0.12704
206A→223A	0.11752	190B→215B	0.10143	207B→213B	-0.31172
211A→221A	-0.12736	193B→214B	0.39921	207B→224B	-0.11035
211A→230A	0.11650	194B→213B	-0.17107	208B→214B	0.30028
212A→224A	-0.21157	195B→215B	-0.18189	208B→218B	-0.10426
214A→221A	0.10238	196B→216B	0.33302	208B→221B	-0.12002

Excited State 36: 5.160-A' 3.3413 eV 371.06 nm f=0.0132 <S**2>=6.405

215A→220A	-0.10836	211B→216B	0.85293		
195B→216B	0.11064	212B→214B	-0.34690		

Excited State 37: 5.182-A' 3.3585 eV 369.17 nm f=0.0000 <S**2>=6.464

216A→220A	-0.11831	195B→214B	0.20714	210B→215B	0.11889
187B→216B	0.10976	196B→213B	-0.27378	211B→214B	-0.28386
193B→215B	-0.18845	207B→216B	0.19853	212B→216B	0.67220
194B→216B	0.15012	208B→215B	0.20088		

Excited State 38: 5.112-A" 3.3835 eV 366.44 nm f=0.0778 <S**2>=6.283

187B→215B	-0.21421	190B→213B	0.15529	193B→216B	0.32159

194B→215B	-0.18454	196B→214B	0.54399	208B→216B	-0.25848
195B→213B	-0.37897	207B→215B	-0.35952		

Excited State 39:	5.153-A"	3.4386 eV	360.57 nm	f=0.0000	<S**2>=6.389
212A→224A	-0.12086	194B→213B	-0.16343	207B→213B	0.63498
187B→213B	-0.13808	195B→215B	-0.19032	208B→214B	-0.58332

Excited State 40:	5.135-A'	3.4561 eV	358.74 nm	f=0.0248	<S**2>=6.342
187B→214B	-0.16151	196B→215B	0.10262	210B→213B	-0.20559
193B→213B	0.11537	207B→214B	0.51281	211B→216B	0.15722
194B→214B	-0.14881	208B→213B	-0.48243		
195B→216B	-0.18663	209B→215B	0.45321		

Excited State 41:	5.100-A'	3.4814 eV	356.14 nm	f=0.0000	<S**2>=6.253
209B→213B	-0.39106	210B→215B	0.90309		

Excited State 42:	5.119-A'	3.4876 eV	355.50 nm	f=0.0095	<S**2>=6.301
195B→216B	0.10299	208B→213B	0.26827	210B→213B	-0.33552
207B→214B	-0.28048	209B→215B	0.79085	211B→216B	-0.12332

Excited State 43:	5.163-A"	3.5684 eV	347.45 nm	f=0.0000	<S**2>=6.413
212A→217A	0.12834	209B→216B	0.87153	210B→214B	-0.31845
214A→219A	0.12747	209B→219B	-0.12826	210B→218B	-0.13864

Excited State 44:	5.150-A"	3.5697 eV	347.32 nm	f=0.0000	<S**2>=6.381
209B→214B	-0.33007	210B→216B	0.90230		
209B→218B	-0.14268	210B→219B	-0.13173		

Excited State 45:	**5.376-A'**	**3.6002 eV**	**344.38 nm**	**f=1.0531**	**<S**2>=6.977**
197A→230A	0.10010	205A→223A	0.17233	209A→220A	-0.15806
202A→224A	0.17842	206A→222A	0.15140	210A→218A	-0.25452

211A→217A	**0.33643**	214A→217A	-0.29877	204B→222B	-0.16161
211A→224A	0.16459	214A→224A	-0.13133	207B→221B	-0.10480
212A→219A	**-0.33150**	216A→219A	-0.10422	208B→213B	0.24384
212A→221A	0.27029	203B→223B	-0.15513	208B→224B	-0.13685

Excited State 46:	5.173-A"	3.6086 eV	343.58 nm	f=0.0000	<S**2>=6.440
209A→218A	-0.31717	212A→224A	0.11415	195B→215B	-0.16441
210A→220A	-0.22775	214A→219A	0.24096	196B→216B	0.17558
210A→225A	0.11732	214A→221A	-0.13865	208B→214B	-0.14715
211A→219A	-0.28909	187B→213B	-0.15552	209B→216B	-0.23078
211A→221A	0.15188	193B→214B	0.18562		
212A→217A	0.48089	194B→213B	-0.12534		

Excited State 47:	5.318-A'	3.8380 eV	323.04 nm	f=0.0004	<S**2>=6.821
189A→218A	-0.10189	186B→213B	-0.23968	197B→214B	-0.10537
193A→217A	0.12348	187B→216B	0.11150	203B→213B	-0.13338
202A→218A	-0.17684	190B→214B	-0.17899	204B→214B	0.15160
210A→217A	-0.22977	193B→215B	0.10408	207B→216B	-0.27630
211A→218A	0.12166	193B→220B	0.12872	208B→215B	0.36630
214A→218A	-0.12193	195B→214B	0.41782	208B→220B	0.15430
185B→215B	0.12533	196B→217B	0.18525		

Excited State 48:	5.734-A"	3.8393 eV	322.93 nm	f=0.0130	<S**2>=7.971
211A→220A	0.23577	214A→220A	0.36425	209B→236B	-0.10707
211A→225A	0.17285	214A→225A	0.18653	210B→216B	-0.25630
213A→219A	0.38492	214A→235A	0.10342	210B→219B	-0.34497
213A→221A	0.28706	209B→218B	-0.30851	210B→227B	-0.16977
213A→227A	-0.14655	209B→221B	0.19164	210B→235B	-0.11335
213A→230A	0.12374	209B→226B	0.11095		
213A→236A	0.13004	209B→230B	-0.11246		

Excited State 49:	5.743-A"	3.8406 eV	322.83 nm	f=0.0000	<S**2>=7.995

211A→219A	0.23686	214A→221A	0.23532	209B→235B	-0.11437
211A→221A	0.17066	214A→227A	-0.11425	210B→218B	-0.31190
213A→220A	0.43226	214A→236A	0.10127	210B→221B	0.19241
213A→225A	0.25547	209B→216B	-0.25811	210B→226B	0.11184
213A→235A	0.13374	209B→219B	-0.34799	210B→230B	-0.11359
214A→219A	0.30131	209B→227B	-0.17160	210B→236B	-0.10786

Excited State 50:	5.097-A"	3.9003 eV	317.89 nm	f=0.0156	<S**2>=6.244

195B→213B	0.15722	199B→215B	0.14648	206B→214B	0.11662
196B→214B	0.20407	200B→216B	0.15047	207B→215B	-0.22944
197B→213B	-0.32203	203B→214B	-0.51408	208B→216B	0.19309
198B→214B	0.29987	204B→213B	0.53073		

*C.2.10.4 **OTPT-BZN-221**, **EB** State*

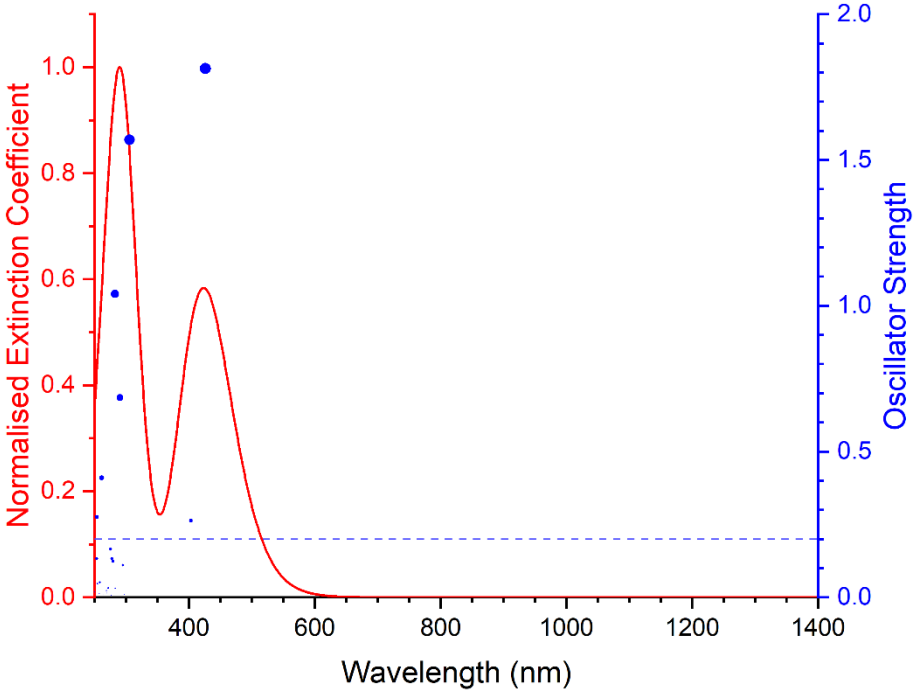

*Figure C-40 Excited states and normalised absorption spectra from TD-DFT calculations of **OTPT-BZN-221** in **EB** state. The areas of excited state dots are proportional to their oscillator strengths.*

Excited State 1:	Singlet-A"	2.7506 eV	450.76 nm	f=0.0000	<S**2>=0.000

211→217	-0.11289	213→216	0.44442	214→215	0.49787

Excited State 2:	**Singlet-A'**	**2.9092 eV**	**426.18 nm**	**f=1.8131**	**<S**2>=0.000**	
192→215	-0.11053	**213→215**	**0.47433**	**214→216**	**0.46040**	
Excited State 3:	**Singlet-A"**	**3.0749 eV**	**403.21 nm**	**f=0.2625**	**<S**2>=0.000**	
193→215	-0.14797	**211→215**	**0.46346**			
194→216	0.17253	**212→216**	**0.43940**			
Excited State 4:	Singlet-A'	3.0959 eV	400.48 nm	f=0.0006	<S**2>=0.000	
193→216	-0.15923	211→216	0.44785			
194→215	0.17579	212→215	0.44828			
Excited State 5:	Singlet-A"	3.9774 eV	311.72 nm	f=0.0000	<S**2>=0.000	
191→215	0.19796	202→216	0.33125	211→217	-0.14408	
192→216	0.20946	205→216	-0.12257	214→215	0.17275	
201→215	0.32741	206→215	0.13956	214→220	0.19103	
Excited State 6:	**Singlet-A'**	**4.0578 eV**	**305.54 nm**	**f=1.5692**	**<S**2>=0.000**	
191→216	0.16438	202→215	0.30730	212→217	-0.11137	
192→215	0.20182	205→215	-0.15283	213→215	0.27928	
201→216	**0.32089**	206→216	0.16709	213→220	0.14498	
Excited State 7:	Singlet-A"	4.1164 eV	301.20 nm	f=0.0000	<S**2>=0.000	
195→215	-0.12607	206→215	0.20912	213→216	0.42441	
196→216	0.12280	210→215	0.10262	213→219	-0.12849	
205→216	-0.19692	212→218	0.12401	214→215	-0.34185	
Excited State 8:	Singlet-A'	4.1661 eV	297.61 nm	f=0.0096	<S**2>=0.000	
195→216	-0.34523	201→216	-0.16073	206→216	0.22643	
196→215	0.35771	202→215	-0.16947	213→215	0.12799	
197→216	-0.10066	205→215	-0.25764	214→216	-0.15948	

Excited State 9:	Singlet-A"	4.1832 eV	296.39 nm	f=0.0000	<S**2>=0.000			
195→215	-0.35370		201→215	-0.14634		206→215	0.20147	
196→216	0.36144		202→216	-0.12383		213→216	-0.22150	
197→215	-0.11805		205→216	-0.20506		214→215	0.18338	
Excited State 10:	Singlet-A'	4.2017 eV	295.08 nm	f=0.1100	<S**2>=0.000			
195→216	-0.11160		205→215	-0.15093		214→216	0.48437	
196→215	0.10606		206→216	0.14488				
202→215	0.10603		213→215	-0.37440				
Excited State 11:	**Singlet-A"**	**4.2672 eV**	**290.55 nm**	**f=0.6846**	**<S**2>=0.000**			
197→217	-0.11204		209→215	0.12270		212→216	0.14164	
203→215	-0.26227		211→215	-0.21859		**214→217**	**0.37180**	
204→216	0.22926		211→220	-0.23176				
Excited State 12:	Singlet-A'	4.3762 eV	283.31 nm	f=0.0304	<S**2>=0.000			
203→216	-0.41995		205→217	0.13511				
204→215	0.46252		213→217	0.10052				
Excited State 13:	**Singlet-A"**	**4.3881 eV**	**282.54 nm**	**f=1.0405**	**<S**2>=0.000**			
203→215	-0.22795		212→216	0.11242		214→217	-0.24574	
204→216	0.22494		212→219	-0.23844				
211→220	0.12438		**213→218**	**0.35953**				
Excited State 14:	Singlet-A"	4.4326 eV	279.71 nm	f=0.0000	<S**2>=0.000			
195→215	0.25066		201→215	-0.11745		213→216	-0.11787	
196→216	-0.25594		203→217	0.13832		214→215	0.12499	
197→215	0.11726		205→216	-0.27311		214→220	-0.10146	
197→220	0.10967		206→215	0.30870				
200→217	-0.13920		210→215	0.10040				

Excited State 15:	Singlet-A'	4.4410 eV	279.18 nm	f=0.1236	<S**2>=0.000			
195→216	-0.29850		201→216	0.11776		205→215	0.33068	
196→215	0.30109		204→217	0.13037		206→216	-0.28001	
Excited State 16:	Singlet-A'	4.4675 eV	277.52 nm	f=0.1327	<S**2>=0.000			
194→215	0.10190		211→216	0.20378		213→217	0.43981	
209→219	0.14131		212→215	-0.25717		214→218	-0.14439	
210→218	-0.14432		212→220	-0.24798		214→221	0.10016	
Excited State 17:	Singlet-A"	4.4762 eV	276.99 nm	f=0.0057	<S**2>=0.000			
197→217	0.16529		203→215	-0.28024		212→216	-0.21806	
200→215	-0.16857		204→216	0.28394		212→219	0.17859	
200→220	-0.14265		211→215	0.17307		213→218	-0.25296	
Excited State 18:	Singlet-A"	4.4953 eV	275.81 nm	f=0.0000	<S**2>=0.000			
195→215	0.13560		198→216	0.12007		201→220	0.15384	
196→216	-0.10230		198→219	-0.19428		205→216	-0.12040	
197→215	-0.27075		199→218	-0.21398		206→215	0.10421	
197→220	-0.26125		200→217	0.35788				
Excited State 19:	Singlet-A"	4.5013 eV	275.44 nm	f=0.1655	<S**2>=0.000			
197→217	0.27958		200→215	-0.25898		211→215	-0.12728	
198→218	0.19572		200→220	-0.26962		211→220	-0.11920	
199→216	-0.10961		201→217	-0.19395		212→216	0.15456	
199→219	0.17934		203→215	0.15970		214→217	0.17605	
Excited State 20:	Singlet-A'	4.5500 eV	272.49 nm	f=0.0000	<S**2>=0.000			
197→218	0.32628		199→220	0.18930		201→218	-0.15147	
198→217	0.22340		200→216	0.22933		211→216	-0.12691	
199→215	0.18717		200→219	-0.32079		214→218	-0.13914	

Excited State 21:	Singlet-A'	4.5635 eV	271.69 nm	f=0.0314	<S**2>=0.000			
197→216	0.19478		198→220	-0.24504		201→219	0.13825	
197→219	-0.26150		199→217	-0.29855				
198→215	-0.24669		200→218	0.32603				
Excited State 22:	Singlet-A"	4.5840 eV	270.47 nm	f=0.0000	<S**2>=0.000			
197→215	-0.14212		198→219	0.38774		213→219	0.10215	
197→220	-0.13806		199→218	0.40730				
198→216	-0.17674		200→217	0.18954				
Excited State 23:	Singlet-A"	4.5872 eV	270.28 nm	f=0.0004	<S**2>=0.000			
197→217	-0.16629		199→216	-0.18338		200→215	0.16572	
198→218	0.41486		199→219	0.39922		200→220	0.15387	
Excited State 24:	Singlet-A'	4.6001 eV	269.52 nm	f=0.0149	<S**2>=0.000			
197→218	-0.20137		199→220	0.31500		214→218	0.11982	
198→217	0.37356		200→216	-0.11350				
199→215	0.31112		200→219	0.20424				
Excited State 25:	Singlet-A'	4.6063 eV	269.16 nm	f=0.0228	<S**2>=0.000			
197→216	0.14880		198→220	0.27034		201→219	0.12765	
197→219	-0.25597		199→217	0.32554				
198→215	0.26182		200→218	0.30470				
Excited State 26:	Singlet-A"	4.6581 eV	266.17 nm	f=0.0000	<S**2>=0.000			
202→216	0.14163		210→220	-0.10593		213→219	0.38526	
209→217	0.13747		212→218	-0.33492		214→220	-0.11511	
210→215	-0.14301		213→216	0.18240				
Excited State 27:	Singlet-A'	4.6800 eV	264.92 nm	f=0.0087	<S**2>=0.000			
197→218	-0.12589		200→219	0.13873		201→218	0.11970	

211→216	-0.35174	212→215	0.35474	214→218	-0.31767
211→219	0.17094	213→217	0.14516		

Excited State 28: Singlet-A' 4.7439 eV 261.36 nm f=0.4097 <S2>=0.000**

201→216	-0.10923	210→219	-0.24446	213→220	0.29698
202→215	-0.13409	211→218	0.14032	214→219	-0.19948
209→218	0.27328	212→217	-0.29136		
210→216	0.15197	213→215	-0.13712		

Excited State 29: Singlet-A" 4.7456 eV 261.26 nm f=0.0000 <S**2>=0.000

201→215	0.17378	210→220	0.14812	214→220	-0.32916
209→217	-0.14891	211→217	0.35280		
210→215	0.22321	214→215	0.19683		

Excited State 30: Singlet-A" 4.8008 eV 258.26 nm f=0.0515 <S**2>=0.000

190→216	-0.11490	209→215	-0.13464	214→217	0.19094
193→215	0.38294	211→215	0.18987		
194→216	-0.37429	212→216	0.16291		

Excited State 31: Singlet-A' 4.8097 eV 257.78 nm f=0.0124 <S**2>=0.000

190→215	0.11467	194→215	0.39735	212→215	-0.15742
193→216	-0.38879	211→216	-0.20063	213→217	-0.15170

Excited State 32: Singlet-A" 4.8709 eV 254.54 nm f=0.0458 <S**2>=0.000

207→219	0.16807	210→217	0.17764	213→218	-0.11433
208→218	-0.17571	211→215	-0.32579	214→217	-0.16463
209→215	-0.24129	212→216	0.34129		
209→220	-0.13870	212→219	0.10394		

Excited State 33: Singlet-A' 4.8877 eV 253.66 nm f=0.1323 <S**2>=0.000

209→216	0.29007	209→219	-0.36585	210→218	0.39842

211→219	0.13573	212→215	-0.14845	214→218	-0.16326

Excited State 34:	**Singlet-A'**	**4.8902 eV**	**253.54 nm**	**f=0.2758**	**<S**2>=0.000**
209→218	0.29712	211→218	-0.27223	214→219	0.31387
210→216	0.24573	212→217	0.11806		
210→219	-0.30072	213→220	-0.14001		

Excited State 35:	Singlet-A"	4.9496 eV	250.50 nm	f=0.0000	<S**2>=0.000
207→218	0.39730	208→219	-0.38387	210→228	-0.17580
207→221	0.14300	208→224	0.11742	213→219	0.12025
208→216	0.18114	209→227	0.17256		

Excited State 36:	Singlet-A"	4.9558 eV	250.18 nm	f=0.0175	<S**2>=0.000
207→216	0.17105	208→221	0.12786	212→216	0.17390
207→219	-0.35417	209→228	-0.15899	213→218	-0.17270
207→224	0.10601	210→227	0.15297	214→217	-0.12455
208→218	0.35561	211→215	-0.14448		

C.2.11 Electronic Transitions in **OTPT-FLR-210** Oligomers

*Table C-15 Attributes of **OTPT-FLR-210** in **LEB**, **ES** (singlet and triplet), and **EB** states related to electronic structures*

Attribute	**LEB State**	**^{1}ES State**	**^{3}ES State**	**EB State**
Molecular Formula	$C_{55}H_{38}N_8$	$C_{55}H_{38}N_8^{2+}$	$C_{55}H_{38}N_8^{2+}$	$C_{55}H_{36}N_8$
Number of Atoms	101	101	101	99
Number of Electrons	424	422	422	422
HOMO	MO 212	MO 211	MOs 212A, 210B	MO 211
LUMO	MO 213	MO 212	MOs 213A, 211B	MO 212

*C.2.11.1 **OTPT-FLR-210, LEB** State*

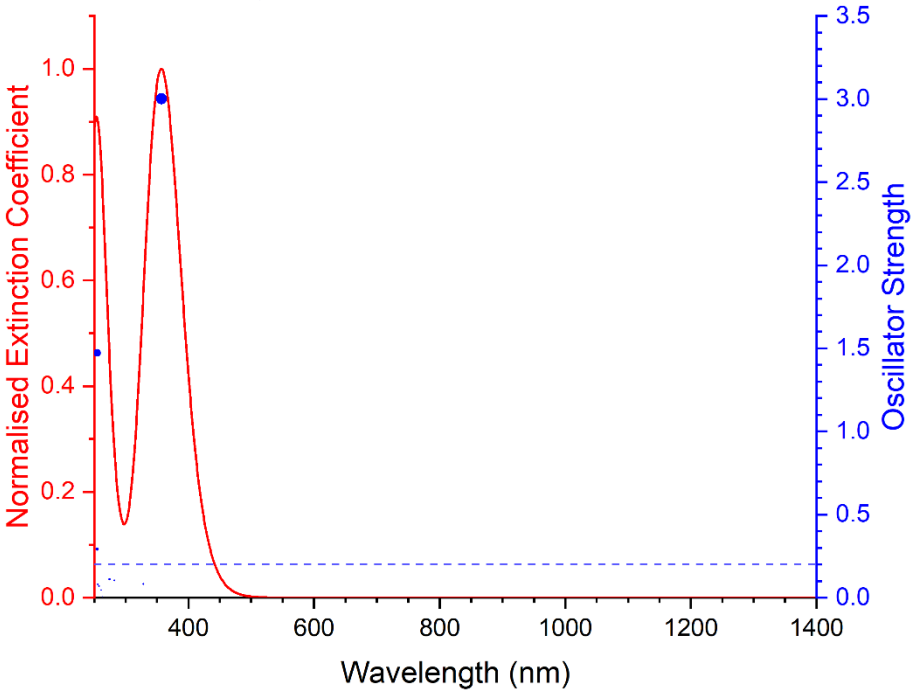

*Figure C-41 Excited states and normalised absorption spectra from TD-DFT calculations of **OTPT-FLR-210** in **LEB** state. The areas of excited state dots are proportional to their oscillator strengths.*

Excited State 1:	**Singlet-A**	**3.4693 eV**	**357.37 nm**	**f=3.0018**	**<S**2>=0.000**	
211→216	-0.28560	**212→213**	**0.53881**	212→217	-0.28525	
Excited State 2:	Singlet-A	3.7783 eV	328.15 nm	f=0.0825	<S**2>=0.000	
210→216	-0.14966	212→216	0.50483			
211→213	-0.40647	212→218	0.12900			
Excited State 3:	Singlet-A	4.1124 eV	301.49 nm	f=0.0021	<S**2>=0.000	
210→214	-0.17928	211→214	0.35922	212→214	0.53737	
Excited State 4:	Singlet-A	4.1144 eV	301.34 nm	f=0.0017	<S**2>=0.000	
210→215	-0.17930	211→215	-0.36316	212→215	0.53476	
Excited State 5:	Singlet-A	4.3925 eV	282.27 nm	f=0.1037	<S**2>=0.000	
200→217	-0.10629	211→227	-0.10957	212→219	0.41793	
210→213	-0.11451	212→217	0.37883			
211→216	-0.18025	212→218	0.22243			

Excited State 6:	Singlet-A	4.5195 eV	274.33 nm	f=0.1106	<S**2>=0.000			
210→213	-0.14668		212→217	0.35798		212→219	-0.31838	
211→216	-0.23497		212→218	-0.18310		212→220	-0.27099	
Excited State 7:	Singlet-A	4.5492 eV	272.54 nm	f=0.0000	<S**2>=0.000			
193→214	0.19356		194→215	-0.20274		196→213	0.14073	
193→215	0.10920		195→214	0.19823		196→216	-0.22698	
194→214	0.37499		195→215	0.26754		197→213	0.18690	
Excited State 8:	Singlet-A	4.5500 eV	272.49 nm	f=0.0043	<S**2>=0.000			
193→214	-0.14569		194→215	-0.26372		196→213	-0.19733	
193→215	0.14228		195→214	-0.14927		197→213	0.12577	
194→214	-0.28428		195→215	0.35174		197→216	0.22658	
Excited State 9:	Singlet-A	4.5987 eV	269.61 nm	f=0.0019	<S**2>=0.000			
195→215	-0.11189		197→215	0.60972				
196→215	-0.21889		197→230	-0.13418				
Excited State 10:	Singlet-A	4.5994 eV	269.57 nm	f=0.0022	<S**2>=0.000			
193→214	0.10296		195→214	-0.14438		196→229	-0.13374	
194→213	0.10024		196→214	0.60773		197→214	0.18063	
Excited State 11:	Singlet-A	4.6560 eV	266.29 nm	f=0.0007	<S**2>=0.000			
193→214	0.14140		195→214	0.13875		197→213	-0.21563	
194→214	0.26830		196→213	-0.33848				
195→213	0.10116		196→216	0.38736				
Excited State 12:	Singlet-A	4.6567 eV	266.25 nm	f=0.0020	<S**2>=0.000			
193→215	-0.10370		195→215	-0.25044		197→213	0.31354	
194→215	0.18982		196→213	-0.23509		197→216	0.41209	

Excited State 13:	Singlet-A	4.7074 eV	263.38 nm	f=0.0049	<S**2>=0.000	
193→213	-0.20588	194→216	0.38237	196→214	0.16071	
193→216	0.16610	195→213	-0.23506			
194→213	-0.35530	195→216	0.15176			

Excited State 14:	Singlet-A	4.7083 eV	263.33 nm	f=0.0073	<S**2>=0.000	
193→213	0.10983	194→216	-0.23617	197→215	-0.15814	
193→216	0.16234	195→213	0.30995			
194→213	-0.28404	195→216	0.38577			

Excited State 15:	Singlet-A	4.7457 eV	261.26 nm	f=0.0459	<S**2>=0.000	
198→216	0.12738	211→217	0.12774	212→221	0.30570	
199→213	0.11743	211→219	0.17112	212→222	0.13009	
207→213	0.11001	211→221	0.17030	212→226	0.10187	
207→217	-0.16114	211→222	-0.14517	212→227	-0.28783	
211→213	-0.11576	212→216	-0.11364			

Excited State 16:	Singlet-A	4.7674 eV	260.07 nm	f=0.0020	<S**2>=0.000	
198→213	0.17254	211→213	0.11212	211→222	-0.20909	
199→213	0.11903	211→217	-0.13056	212→216	0.14524	
199→216	0.20478	211→220	0.11784	212→221	-0.12241	
210→222	-0.13354	211→221	-0.20445	212→222	0.36412	

Excited State 17:	Singlet-A	4.8075 eV	257.90 nm	f=0.0688	<S**2>=0.000	
198→213	-0.13057	210→221	-0.11548	211→222	-0.16391	
198→216	0.16211	211→213	0.18450	212→216	0.19689	
199→213	0.13866	211→217	-0.12643	212→221	0.21192	
207→217	0.14152	211→221	0.19794	212→227	0.31899	

Excited State 18:	Singlet-A	4.8422 eV	256.05 nm	f=0.0804	<S**2>=0.000	
207→217	-0.12128	210→216	0.14178	211→213	0.30520	

211→217	-0.15459	211→222	0.12896	212→227	-0.26595
211→219	0.10817	212→216	0.36215		

Excited State 19:	**Singlet-A**	**4.8614 eV**	**255.04 nm**	**f=0.2925**	**<S**2>=0.000**
205→214	**0.36155**	206→215	0.15252	208→217	-0.10283
205→215	-0.11714	208→213	-0.27739	209→213	0.10340
206→214	0.28087	208→216	0.25660	209→216	0.12714

Excited State 20:	**Singlet-A**	**4.8630 eV**	**254.95 nm**	**f=1.4713**	**<S**2>=0.000**
205→214	-0.16079	**206→215**	**0.35970**	209→213	0.25474
205→215	-0.27361	208→213	0.11351	209→216	0.27939
206→214	-0.12403	208→216	-0.11810		

Excited State 21:	Singlet-A	4.9009 eV	252.98 nm	f=0.0006	<S**2>=0.000
201→214	0.26230	205→223	0.10066	210→214	0.14300
203→213	0.10293	206→214	0.18521	211→214	-0.12096
203→216	-0.10076	208→213	0.26146	212→214	0.27007
205→214	0.21154	208→216	-0.24121		

Excited State 22:	Singlet-A	4.9051 eV	252.77 nm	f=0.0004	<S**2>=0.000
202→215	0.26770	206→215	0.23907	210→215	-0.13865
204→216	-0.11278	206→224	0.10191	211→215	-0.10610
204→218	0.10334	209→213	-0.23627	212→215	-0.26212
205→215	-0.16118	209→216	-0.25860		

C.2.11.2 ***OTPT-FLR-210****,* ***¹ES*** *State*

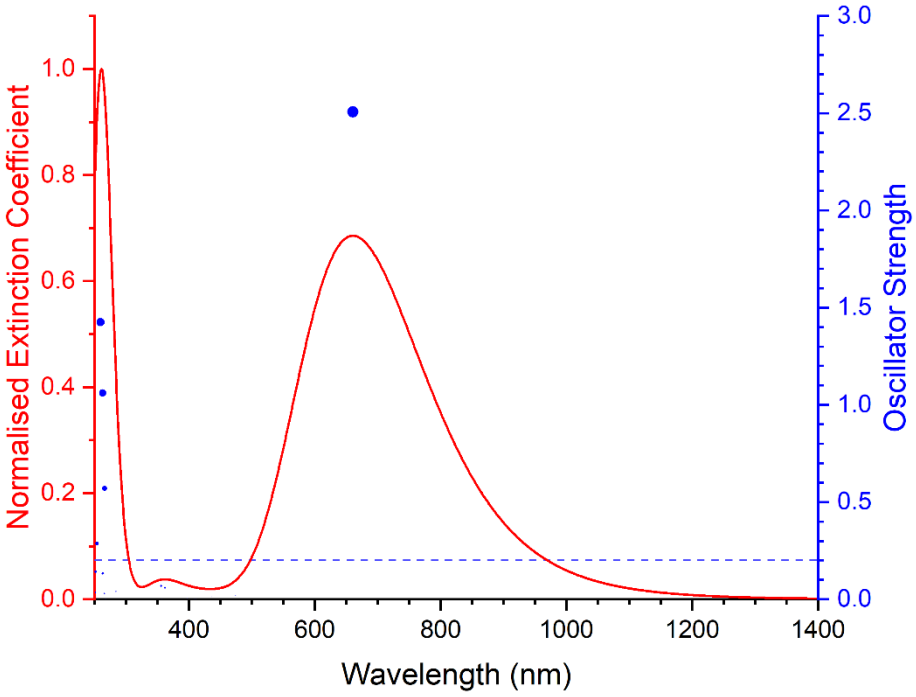

Figure C-42 Excited states and normalised absorption spectra from TD-DFT calculations of ***OTPT-FLR-210*** *in* ***¹ES*** *state. The areas of excited state dots are proportional to their oscillator strengths.*

Excited State 1:	**Singlet-A**	**1.8762 eV**	**660.83 nm**	**f=2.5056**	**<S**2>=0.000**
207→212	0.12007	**211→212**	**0.68808**		
Excited State 2:	Singlet-A	2.6133 eV	474.44 nm	f=0.0207	<S**2>=0.000
202→212	0.61650	208→212	-0.29954		
Excited State 3:	Singlet-A	2.7087 eV	457.72 nm	f=0.0001	<S**2>=0.000
197→212	0.10155	209→212	-0.36621		
208→212	-0.12519	210→212	0.57257		
Excited State 4:	Singlet-A	2.7091 eV	457.66 nm	f=0.0022	<S**2>=0.000
207→212	-0.13509	209→212	0.57133	210→212	0.37173
Excited State 5:	Singlet-A	2.7928 eV	443.95 nm	f=0.0091	<S**2>=0.000
194→212	0.68382				
Excited State 6:	Singlet-A	2.8410 eV	436.41 nm	f=0.0121	<S**2>=0.000
207→212	0.67012	209→212	0.10582	211→212	-0.12268

Excited State 7:	Singlet-A	2.8661 eV	432.59 nm	f=0.0021	<S**2>=0.000
202→212	0.28189	208→212	0.61508		
Excited State 8:	Singlet-A	3.0064 eV	412.40 nm	f=0.0070	<S**2>=0.000
193→212	0.14287	197→212	0.55108		
196→212	0.33416	204→212	0.13653		
Excited State 9:	Singlet-A	3.0150 eV	411.22 nm	f=0.0011	<S**2>=0.000
196→212	0.52821	203→212	0.22425	205→212	-0.10118
197→212	-0.32905	204→212	-0.10843		
Excited State 10:	Singlet-A	3.0318 eV	408.94 nm	f=0.0003	<S**2>=0.000
196→212	-0.21915	203→212	0.62470	204→212	0.19564
Excited State 11:	Singlet-A	3.0346 eV	408.57 nm	f=0.0001	<S**2>=0.000
197→212	-0.19438	204→212	0.63286		
203→212	-0.18099	206→212	-0.10286		
Excited State 12:	Singlet-A	3.0697 eV	403.89 nm	f=0.0011	<S**2>=0.000
203→212	0.10306	205→212	0.51059		
204→212	0.13597	206→212	0.44628		
Excited State 13:	Singlet-A	3.0725 eV	403.53 nm	f=0.0000	<S**2>=0.000
202→212	-0.10353	205→212	-0.45216	206→212	0.51314
Excited State 14:	Singlet-A	3.1185 eV	397.58 nm	f=0.0047	<S**2>=0.000
193→212	0.67591	196→212	-0.12800		
Excited State 15:	Singlet-A	3.4229 eV	362.22 nm	f=0.0589	<S**2>=0.000
195→212	0.43013	199→212	-0.36537	201→212	-0.11509
198→212	-0.35485	200→212	-0.10656		

Excited State 16:	Singlet-A	3.4482 eV	359.56 nm	f=0.0000	<S**2>=0.000
198→212	-0.45362	200→212	-0.16640		
199→212	0.45427	201→212	0.17537		
Excited State 17:	Singlet-A	3.4701 eV	357.29 nm	f=0.0032	<S**2>=0.000
198→212	-0.14075	200→212	0.60790	201→212	0.27463
Excited State 18:	Singlet-A	3.4705 eV	357.25 nm	f=0.0002	<S**2>=0.000
198→212	0.11573	200→212	-0.25302		
199→212	-0.20431	201→212	0.59406		
Excited State 19:	Singlet-A	3.4833 eV	355.94 nm	f=0.0677	<S**2>=0.000
195→212	0.52272	198→212	0.32484	199→212	0.29617
Excited State 20:	Singlet-A	4.3589 eV	284.44 nm	f=0.0399	<S**2>=0.000
195→217	-0.10553	207→213	0.12743		
202→214	-0.19232	211→213	0.62790		
Excited State 21:	Singlet-A	4.5408 eV	273.04 nm	f=0.0001	<S**2>=0.000
198→213	-0.10944	198→217	0.13702	200→231	0.12932
198→214	-0.15989	200→215	0.62111	201→216	-0.14194
Excited State 22:	Singlet-A	4.5413 eV	273.01 nm	f=0.0003	<S**2>=0.000
199→213	-0.10813	199→217	0.13163	201→216	0.61951
199→214	0.16709	200→215	0.14383	201→232	0.12909
Excited State 23:	Singlet-A	4.5940 eV	269.88 nm	f=0.0031	<S**2>=0.000
200→212	0.14945	200→214	0.43908	200→220	-0.12311
200→213	0.30635	200→217	-0.36879		

Excited State 24:	Singlet-A	4.5947 eV	269.84 nm	f=0.0031	<S**2>=0.000	
201→212	0.15006	201→214	0.45173	201→220	-0.11052	
201→213	-0.29820	201→217	0.34957			
Excited State 25:	Singlet-A	4.6247 eV	268.09 nm	f=0.0050	<S**2>=0.000	
199→212	0.14636	199→214	0.41149	201→216	-0.24880	
199→213	-0.28165	199→217	0.30255			
Excited State 26:	Singlet-A	4.6259 eV	268.02 nm	f=0.0012	<S**2>=0.000	
190→212	0.10562	198→213	0.28919	198→217	-0.31817	
198→212	0.14473	198→214	0.39911	200→215	0.24102	
Excited State 27:	Singlet-A	4.6537 eV	266.42 nm	f=0.0009	<S**2>=0.000	
173→212	-0.22735	190→212	0.46295	210→214	-0.13335	
174→212	0.10098	209→214	0.10930			
180→212	0.27652	210→213	0.10209			
Excited State 28:	**Singlet-A**	**4.6613 eV**	**265.99 nm**	**f=0.5701**	**<S**2>=0.000**	
209→213	0.19470	209→217	-0.18393	**210→214**	**0.33468**	
209→214	0.24316	210→213	-0.26589	210→217	0.24471	
Excited State 29:	Singlet-A	4.6623 eV	265.93 nm	f=0.0293	<S**2>=0.000	
173→212	0.10224	209→213	0.25802	210→213	0.16502	
180→212	-0.12516	209→214	0.30668	210→214	-0.21597	
190→212	-0.20006	209→217	-0.24461	210→217	-0.15221	
Excited State 30:	Singlet-A	4.7122 eV	263.11 nm	f=0.1325	<S**2>=0.000	
207→215	0.42132	208→215	-0.33980	211→215	-0.17672	
207→216	0.15750	208→216	0.23447			
Excited State 31:	**Singlet-A**	**4.7132 eV**	**263.06 nm**	**f=1.0612**	**<S**2>=0.000**	
207→215	-0.22084	207→216	0.29451	208→215	0.17253	

208→216	**0.45223**	211→216	-0.18128		

Excited State 32:	Singlet-A	4.7324 eV	261.99 nm	f=0.0087	<S**2>=0.000
199→216	0.67806	199→232	0.13923		

Excited State 33:	Singlet-A	4.7334 eV	261.94 nm	f=0.0057	<S**2>=0.000
198→215	0.68069	198→231	0.13973		

Excited State 34:	**Singlet-A**	**4.7755 eV**	**259.62 nm**	**f=1.4252**	**<S**2>=0.000**
195→214	0.10295	207→214	0.13038	**211→214**	**0.35602**
202→213	-0.26302	209→215	0.29600		
202→217	0.15515	210→216	-0.30331		

Excited State 35:	Singlet-A	4.8506 eV	255.60 nm	f=0.0054	<S**2>=0.000
169→212	0.19257	190→212	0.18369	211→217	0.10324
173→212	0.51983	209→215	-0.15845		
180→212	0.10813	210→216	-0.17405		

Excited State 36:	Singlet-A	4.8732 eV	254.42 nm	f=0.0010	<S**2>=0.000
173→212	0.23290	203→217	-0.10168	206→216	0.25290
190→212	0.10281	204→216	-0.15483	209→215	0.14507
203→215	-0.17254	205→215	0.27264	210→216	0.13335

Excited State 37:	**Singlet-A**	**4.8825 eV**	**253.94 nm**	**f=0.2858**	**<S**2>=0.000**
203→214	-0.12282	204→214	-0.11205	205→215	-0.29398
203→215	0.18741	204→216	-0.19765	206→216	0.31413

Excited State 38:	Singlet-A	4.9135 eV	252.34 nm	f=0.0173	<S**2>=0.000
173→212	0.14422	207→213	0.11161	209→215	0.35795
205→215	-0.14372	207→217	-0.15330	210→216	0.34420
206→216	-0.13444	208→214	-0.17669	211→213	-0.13065

Excited State 39:	Singlet-A	4.9253 eV	251.73 nm	f=0.0345	<S**2>=0.000
203→215	0.14207	204→216	0.39355	206→216	0.25729
204→214	0.12798	206→214	-0.13986	206→217	-0.10814

Excited State 40:	Singlet-A	4.9256 eV	251.71 nm	f=0.1408	<S**2>=0.000
203→214	-0.12549	203→217	0.10979	205→214	0.13595
203→215	0.39701	204→216	-0.14130	205→215	0.25557

*C.2.11.3 **OTPT-FLR-210**, **^{3}ES** State*

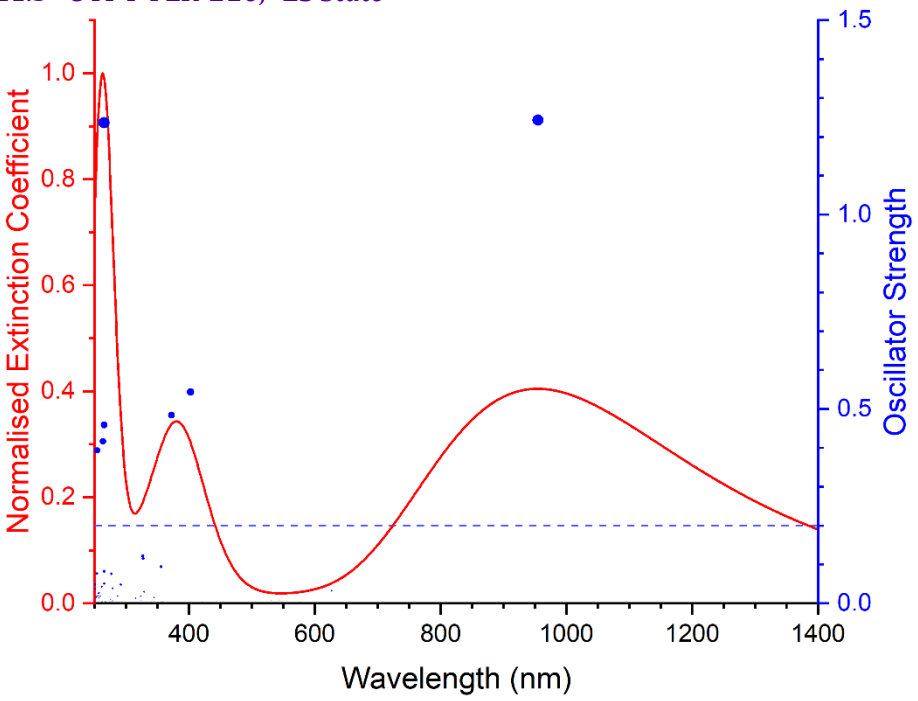

*Figure C-43 Excited states and normalised absorption spectra from TD-DFT calculations of **OTPT-FLR-210** in **^{3}ES** state. The areas of excited state dots are proportional to their oscillator strengths.*

Excited State 1:	**3.093-A**	**1.2981 eV**	**955.10 nm**	**f=1.2434**	**<S**2>=2.142**
196B→212B	0.30752	**208B→211B**	**0.52991**		
206B→211B	**0.73654**	209B→211B	0.11222		

Excited State 2:	3.074-A	1.9777 eV	626.91 nm	f=0.0319	<S**2>=2.112
189B→211B	0.10572	199B→211B	-0.26491	207B→211B	0.12981
196B→211B	0.53275	206B→212B	0.56924	208B→212B	0.43777

Excited State 3:	3.082-A	2.0485 eV	605.25 nm	f=0.0017	<S**2>=2.125
193B→211B	-0.11342	193B→212B	0.29033	194B→211B	0.69064

194B→212B	-0.19153	196B→211B	0.12929	210B→212B	0.10241
195B→211B	0.15064	199B→211B	0.27191		
195B→212B	-0.40257	210B→211B	-0.21043		

Excited State 4:	3.081-A	2.0551 eV	603.31 nm	f=0.0009	<S**2>=2.123
193B→211B	-0.50306	195B→211B	0.55208	209B→211B	-0.21310
193B→212B	-0.11926	195B→212B	0.14222	209B→212B	-0.10112
194B→211B	-0.15622	199B→211B	-0.10913	210B→211B	-0.11160
194B→212B	-0.49113	199B→212B	-0.11215		

Excited State 5:	3.122-A	2.1497 eV	576.76 nm	f=0.0031	<S**2>=2.186
193B→212B	-0.37312	195B→212B	-0.19947	199B→211B	0.76769
194B→211B	-0.30104	196B→211B	0.24246	199B→213B	-0.10320

Excited State 6:	3.117-A	2.2829 eV	543.10 nm	f=0.0079	<S**2>=2.179
193B→211B	0.55492	195B→211B	0.55226	199B→212B	-0.52150
194B→212B	0.10643	196B→212B	-0.14588	210B→211B	0.10133

Excited State 7:	3.113-A	2.3322 eV	531.62 nm	f=0.0067	<S**2>=2.172
191B→211B	0.10324	194B→212B	-0.12354	210B→212B	-0.36527
193B→211B	-0.15185	208B→211B	0.11853		
194B→211B	0.18797	210B→211B	0.84046		

Excited State 8:	3.112-A	2.3386 eV	530.17 nm	f=0.0050	<S**2>=2.172
190B→211B	0.10248	194B→212B	-0.11747	209B→211B	0.82581
193B→211B	-0.19457	207B→211B	-0.10129	209B→212B	0.34869
194B→211B	-0.14074	208B→211B	-0.18907		

Excited State 9:	3.174-A	2.5171 eV	492.57 nm	f=0.0020	<S**2>=2.269
206B→211B	-0.47824	207B→211B	-0.32258	208B→211B	0.64587
206B→212B	0.14393	207B→212B	0.30087	208B→212B	-0.11392

209B→211B	0.12612	210B→211B	-0.11040		

Excited State 10:	3.162-A	2.5234 eV	491.34 nm	f=0.0001	<S**2>=2.249
206B→211B	-0.25906	207B→212B	0.15108	209B→211B	0.14801
206B→212B	-0.30576	208B→211B	0.19269		
207B→211B	0.80575	208B→212B	0.12146		

Excited State 11:	3.178-A	2.7431 eV	451.99 nm	f=0.0002	<S**2>=2.275
198B→211B	0.79683	198B→213B	0.20842		
198B→212B	-0.49909	198B→214B	0.19548		

Excited State 12:	3.178-A	2.7529 eV	450.38 nm	f=0.0000	<S**2>=2.275
197B→211B	0.79846	197B→213B	0.21061		
197B→212B	0.49354	197B→214B	-0.18965		

Excited State 13:	3.213-A	2.7988 eV	442.99 nm	f=0.0004	<S**2>=2.330
201B→211B	0.75770	201B→213B	0.21581	203B→211B	-0.19377
201B→212B	-0.45146	201B→214B	0.21852	205B→211B	-0.14419

Excited State 14:	3.096-A	2.8061 eV	441.84 nm	f=0.0006	<S**2>=2.146
201B→211B	0.18358	202B→212B	0.13793	204B→211B	-0.10796
201B→212B	-0.10566	203B→211B	0.84658	205B→211B	0.22218
202B→211B	0.22009	203B→212B	-0.25405		

Excited State 15:	3.130-A	2.8078 eV	441.56 nm	f=0.0008	<S**2>=2.199
200B→211B	-0.43520	202B→211B	0.72404	204B→211B	0.22896
200B→212B	-0.25051	202B→212B	0.20477	205B→211B	-0.13317
200B→213B	-0.12600	203B→211B	-0.15435		
200B→214B	0.11981	203B→212B	0.12734		

Excited State 16:	3.181-A	2.8097 eV	441.27 nm	f=0.0011	<S**2>=2.280	
200B→211B	0.65286	200B→213B	0.18872	202B→211B	0.51288	
200B→212B	0.38429	200B→214B	-0.18351	202B→212B	0.15378	

Excited State 17:	3.090-A	2.8200 eV	439.67 nm	f=0.0006	<S**2>=2.137	
203B→211B	-0.23398	204B→211B	0.17153	205B→212B	-0.28913	
203B→212B	0.10998	205B→211B	0.87812			

Excited State 18:	3.090-A	2.8232 eV	439.16 nm	f=0.0016	<S**2>=2.137	
202B→211B	-0.21031	204B→211B	0.87985			
203B→211B	0.20076	204B→212B	0.29546			

Excited State 19:	3.958-A	2.9397 eV	421.76 nm	f=0.0027	<S**2>=3.666	
202A→213A	0.11678	210A→215A	-0.29074	207B→221B	0.12451	
204A→225A	-0.10602	211A→216A	0.28301	208B→211B	0.27197	
208A→213A	0.10410	212A→217A	-0.12851	208B→213B	-0.15626	
208A→217A	0.10135	192B→211B	-0.20074	208B→223B	0.10132	
208A→223A	-0.12223	196B→212B	-0.18471	209B→215B	0.30555	
209A→214A	-0.13406	206B→211B	-0.11641	210B→216B	-0.29450	
209A→221A	-0.10146	207B→214B	0.14256			

Excited State 20:	3.322-A	2.9452 eV	420.97 nm	f=0.0001	<S**2>=2.510	
210A→215A	0.11499	199B→211B	-0.16162	209B→215B	-0.11761	
211A→216A	0.16032	206B→212B	-0.38688	210B→216B	-0.16421	
192B→212B	0.25333	207B→211B	-0.20475			
196B→211B	0.57225	208B→212B	-0.33468			

Excited State 21:	3.944-A	2.9658 eV	418.05 nm	f=0.0007	<S**2>=3.639	
208A→214A	-0.12001	209A→223A	-0.12715	196B→211B	0.32207	
208A→222A	-0.10420	210A→215A	-0.27505	202B→224B	-0.10875	
209A→217A	0.10010	211A→216A	-0.28194	203B→225B	-0.10299	

204B→226B	0.10549	207B→213B	-0.12390	208B→214B	0.14737
205B→227B	0.11066	207B→217B	-0.12521	209B→215B	0.30108
206B→212B	-0.16362	207B→223B	0.13439	210B→216B	0.30518
207B→211B	0.18445	208B→212B	-0.17093		

Excited State 22: 3.590-A 3.0799 eV 402.56 nm f=0.5432 <S2>=2.971**

202A→213A	0.14416	212A→223A	-0.11093	206B→217B	0.10595
202A→217A	-0.13122	181B→211B	0.14610	208B→217B	0.13457
211A→216A	-0.10147	192B→211B	-0.31848	209B→215B	-0.13661
212A→213A	**0.41521**	**196B→212B**	**-0.37761**	210B→216B	0.14221
212A→217A	**-0.40222**	206B→213B	-0.19676		

Excited State 23: 4.142-A 3.1759 eV 390.39 nm f=0.0001 <S**2>=4.040

204A→215A	-0.10359	210A→215A	0.13892	207B→215B	-0.32196
204A→225A	-0.17470	210A→217A	-0.11457	207B→231B	-0.10630
206A→215A	0.10451	210A→221A	0.10459	208B→215B	-0.20254
206A→226A	0.12221	210A→222A	0.15958	209B→211B	-0.11229
206A→228A	0.11342	210A→223A	0.14832	209B→213B	0.12499
208A→215A	0.38696	210A→224A	-0.10062	209B→214B	-0.15273
208A→231A	0.12501	202B→224B	-0.15964	209B→217B	0.13377
209A→215A	0.10009	202B→225B	-0.12803	209B→221B	-0.12795
210A→213A	-0.10569	204B→226B	-0.15531	209B→222B	-0.13847
210A→214A	0.13700	206B→215B	0.18405	209B→223B	-0.14799

Excited State 24: 4.144-A 3.1760 eV 390.38 nm f=0.0000 <S**2>=4.043

205A→216A	-0.10795	207A→228A	-0.13979	211A→214A	-0.14614
205A→226A	0.11983	208A→216A	-0.12331	211A→217A	-0.11502
205A→227A	-0.12701	209A→216A	0.39592	211A→221A	-0.16121
207A→216A	0.10265	209A→232A	-0.12729	211A→223A	0.18447
207A→227A	0.12996	211A→213A	-0.10598	203B→225B	-0.13084

203B→226B	-0.12823	208B→216B	0.28080	210B→217B	0.12986
205B→227B	-0.17084	210B→211B	-0.11309	210B→221B	0.17214
206B→216B	-0.17004	210B→213B	0.12396	210B→223B	-0.17488
207B→216B	-0.27614	210B→214B	0.15985		

Excited State 25:	**3.352-A**	**3.3288 eV**	**372.46 nm**	**f=0.4843**	**<S**2>=2.559**
194A→218A	-0.10570	212A→217A	-0.15578	**199B→212B**	**-0.33166**
202A→213A	-0.10944	181B→211B	-0.11428	206B→211B	-0.12272
202A→217A	-0.14813	192B→211B	0.30596	207B→212B	0.11968
203A→214A	-0.28519	195B→211B	-0.12605	208B→211B	-0.16116
212A→213A	**0.48217**	196B→212B	0.27682		

Excited State 26:	3.144-A	3.4523 eV	359.13 nm	f=0.0053	<S**2>=2.221
207B→212B	-0.18452	208B→212B	-0.26412	209B→212B	0.80783
208B→211B	0.10013	209B→211B	-0.38685	209B→213B	0.10010

Excited State 27:	3.142-A	3.4647 eV	357.85 nm	f=0.0032	<S**2>=2.218
207B→212B	-0.10264	210B→211B	0.40995	210B→213B	-0.10241
208B→212B	0.15601	210B→212B	0.84112		

Excited State 28:	3.184-A	3.4870 eV	355.56 nm	f=0.0936	<S**2>=2.284
203A→214A	-0.13820	193B→211B	0.31043	199B→212B	0.70452
212A→213A	0.21600	195B→211B	0.39304	210B→212B	0.10185
212A→218A	0.10442	195B→213B	-0.10195		
192B→211B	0.11117	196B→212B	0.16051		

Excited State 29:	3.309-A	3.5593 eV	348.34 nm	f=0.0015	<S**2>=2.487
202A→214A	0.17507	179B→211B	0.12466	206B→212B	-0.39047
203A→213A	0.16039	189B→211B	-0.23111	207B→211B	-0.29745
203A→217A	0.10761	192B→212B	0.20217	207B→212B	0.12872
212A→214A	-0.13450	196B→213B	0.12315	208B→212B	0.52270

209B→212B	0.24491	210B→212B	-0.12755		

Excited State 30:	3.119-A	3.5919 eV	345.18 nm	f=0.0144	<S**2>=2.182
206B→211B	0.18344	208B→212B	-0.14854	210B→212B	0.10916
207B→212B	0.86449	209B→211B	-0.10262		
208B→211B	-0.24814	209B→212B	0.14274		

Excited State 31:	3.164-A	3.6069 eV	343.74 nm	f=0.0018	<S**2>=2.253
193B→212B	0.51236	199B→213B	-0.13099	208B→212B	-0.17145
195B→212B	0.64710	199B→217B	0.13793		
199B→211B	0.35747	206B→212B	0.11141		

Excited State 32:	3.452-A	3.6455 eV	340.10 nm	f=0.0045	<S**2>=2.728
193A→213A	0.12039	179B→211B	-0.15455	196B→213B	-0.20250
202A→214A	-0.27403	189B→211B	0.22814	206B→212B	-0.30931
203A→213A	-0.28360	192B→212B	-0.16139	206B→214B	0.16861
203A→217A	-0.14292	193B→212B	0.13750	207B→211B	-0.14460
203A→223A	-0.10718	195B→212B	0.17362	208B→212B	0.39476
212A→214A	0.23400	196B→211B	0.11540	209B→212B	0.13075

Excited State 33:	3.187-A	3.7707 eV	328.81 nm	f=0.0292	<S**2>=2.289
202B→211B	-0.27502	203B→212B	0.23823		
202B→212B	0.84009	204B→212B	0.13533		

Excited State 34:	3.402-A	3.7847 eV	327.59 nm	f=0.1152	<S**2>=2.644
195A→219A	-0.14432	194B→219B	0.12141	203B→212B	0.55784
196A→220A	0.11221	196B→212B	-0.16011	204B→212B	-0.25771
202A→213A	-0.18243	196B→214B	-0.11461	205B→212B	0.12533
203A→214A	-0.18232	202B→212B	-0.32589	206B→213B	0.14736
192B→211B	-0.19341	203B→211B	0.22782	208B→213B	0.12303

Excited State 35:	3.405-A	3.7947 eV	326.73 nm	f=0.1214	<S**2>=2.649	
195A→219A	0.14195	194B→219B	-0.12449	205B→211B	0.10933	
196A→220A	-0.12698	196B→212B	0.14358	205B→212B	0.34500	
202A→213A	0.17910	196B→214B	0.10815	206B→213B	-0.15798	
203A→214A	0.17550	203B→211B	0.18330	208B→213B	-0.12384	
192B→211B	0.22948	203B→212B	0.61110			

Excited State 36:	3.229-A	3.8210 eV	324.48 nm	f=0.0070	<S**2>=2.356	
203A→213A	-0.16230	192B→212B	0.12658	204B→212B	0.68538	
212A→214A	0.13769	202B→212B	-0.14608	205B→211B	-0.17481	
179B→211B	0.11945	203B→212B	0.16575	205B→212B	-0.33404	
189B→211B	-0.16954	204B→211B	-0.22279	206B→212B	0.13145	

Excited State 37:	3.169-A	3.8253 eV	324.12 nm	f=0.0183	<S**2>=2.261	
192B→211B	-0.13898	204B→211B	-0.18242	205B→212B	0.71559	
203B→211B	-0.10313	204B→212B	0.46644			
203B→212B	-0.19323	205B→211B	0.21350			

Excited State 38:	3.457-A	3.8341 eV	323.38 nm	f=0.0183	<S**2>=2.738	
193A→217A	0.12286	212A→221A	-0.13040	199B→218B	-0.17371	
194A→222A	-0.10452	212A→224A	-0.14335	202B→212B	0.15950	
195A→220A	0.16819	179B→211B	0.18906	203B→212B	-0.22462	
196A→219A	-0.16233	189B→211B	-0.29324	204B→212B	-0.28266	
197A→218A	0.17793	192B→212B	0.20038	205B→211B	0.12800	
202A→214A	-0.11744	193B→222B	-0.10060	205B→212B	0.30709	
203A→213A	-0.27085	194B→220B	-0.13900			
212A→214A	0.23827	195B→219B	0.13249			

Excited State 39:	3.292-A	3.9316 eV	315.35 nm	f=0.0131	<S**2>=2.460	
195A→219A	-0.10663	212A→218A	0.10786	166B→211B	-0.14273	

176B→211B	0.12251	189B→212B	0.37691	196B→212B	0.53012
179B→212B	-0.15290	192B→211B	-0.44310	206B→211B	-0.23870

Excited State 40: 4.139-A 4.0642 eV 305.07 nm f=0.0003 <S**2>=4.033

205A→215A	0.14096	206A→223A	0.15102	204B→217B	-0.12212
206A→213A	-0.11164	206A→231A	0.12246	204B→221B	0.12451
206A→214A	0.15159	208A→215A	-0.14166	204B→222B	0.14318
206A→215A	0.47662	204B→212B	0.13318	204B→223B	0.14179
206A→217A	-0.10986	204B→213B	-0.10488	204B→231B	0.12771
206A→221A	0.11297	204B→214B	0.14309		
206A→222A	0.17411	204B→215B	0.47669		

Excited State 41: 4.138-A 4.0655 eV 304.96 nm f=0.0006 <S**2>=4.031

206A→216A	-0.12067	207A→223A	0.18042	205B→216B	0.48033
207A→213A	-0.10765	207A→232A	-0.12521	205B→217B	-0.10701
207A→214A	-0.15932	209A→216A	-0.11886	205B→221B	-0.17378
207A→216A	0.49020	211A→216A	0.10091	205B→223B	0.14639
207A→217A	-0.10696	205B→212B	-0.12522	205B→232B	-0.12744
207A→221A	-0.19144	205B→214B	-0.13481		

Excited State 42: 4.146-A 4.0720 eV 304.48 nm f=0.0002 <S**2>=4.046

205A→213A	0.11736	205A→232A	-0.12489	203B→216B	0.47830
205A→214A	0.15265	206A→216A	-0.11110	203B→217B	0.12105
205A→216A	0.48628	209A→216A	0.13406	203B→221B	0.12534
205A→217A	0.13522	203B→212B	0.10112	203B→223B	-0.15867
205A→221A	0.13176	203B→213B	0.10326	203B→232B	-0.12810
205A→223A	-0.19489	203B→214B	0.13772		

Excited State 43: 4.147-A 4.0741 eV 304.32 nm f=0.0003 <S**2>=4.050

204A→213A	0.13071	204A→214A	-0.15933	204A→215A	0.50594

204A→217A	0.15770	210A→215A	0.11513	202B→221B	-0.13084
204A→221A	-0.12061	202B→212B	-0.10857	202B→222B	-0.12655
204A→222A	-0.17117	202B→213B	0.12062	202B→223B	-0.15402
204A→223A	-0.17447	202B→214B	-0.14906	202B→231B	0.12867
204A→231A	0.12956	202B→215B	0.48472		
208A→215A	0.10652	202B→217B	0.14798		

Excited State 44: 3.798-A 4.1399 eV 299.48 nm f=0.0001 <S**2>=3.357

198A→215A	-0.18326	197B→215B	0.19564	200B→214B	0.30023
200A→213A	0.29087	200B→211B	0.49935	200B→217B	-0.17757
200A→214A	-0.33794	200B→212B	-0.35253		
200A→217A	0.22067	200B→213B	-0.28955		

Excited State 45: 3.819-A 4.1471 eV 298.96 nm f=0.0001 <S**2>=3.397

199A→216A	-0.18853	201A→221A	0.11686	201B→213B	-0.28016
201A→213A	0.28933	198B→216B	0.20151	201B→214B	-0.30964
201A→214A	0.35957	201B→211B	0.49238	201B→217B	-0.16811
201A→217A	0.21543	201B→212B	0.33007		

Excited State 46: 3.901-A 4.1916 eV 295.79 nm f=0.0001 <S**2>=3.554

194A→219A	0.19041	212A→224A	-0.10503	195B→221B	0.11259
194A→222A	-0.12957	189B→211B	0.27918	195B→222B	-0.17852
195A→220A	-0.19547	189B→213B	0.10067	196B→211B	0.19305
196A→221A	-0.13873	192B→212B	-0.17907	199B→218B	-0.28793
196A→222A	0.14765	193B→219B	0.19654	206B→212B	-0.17815
197A→218A	0.31003	194B→220B	0.18286		

Excited State 47: 3.957-A 4.2453 eV 292.05 nm f=0.0483 <S**2>=3.664

191A→215A	-0.12867	200A→215A	-0.11689	205A→226A	0.16076
192A→216A	0.12007	204A→225A	0.18834	206A→226A	0.10688

206A→227A	0.14343	190B→215B	0.13413	203B→225B	-0.12131
207A→227A	-0.12116	191B→216B	-0.12540	203B→226B	-0.10813
207A→228A	0.14002	192B→213B	-0.10841	204B→225B	0.11108
210A→215A	-0.11760	196B→212B	-0.12029	204B→226B	-0.14536
211A→216A	0.11173	197B→211B	0.11920	205B→227B	0.16698
212A→213A	0.16022	197B→212B	-0.10582	209B→215B	0.13014
212A→218A	-0.17838	200B→215B	0.12476	210B→216B	-0.12328
181B→211B	-0.14496	202B→224B	0.16721		
189B→214B	-0.11374	202B→225B	0.11473		

Excited State 48: 3.898-A 4.2600 eV 291.04 nm f=0.0019 <S**2>=3.550

198A→213A	0.20419	201A→216A	-0.11266	197B→214B	0.19667
198A→214A	-0.22697	197B→211B	0.36765	198B→211B	0.10691
198A→217A	0.12863	197B→212B	-0.29584	200B→215B	0.40542
200A→215A	-0.37989	197B→213B	-0.20546	201B→216B	0.12037

Excited State 49: 3.923-A 4.2652 eV 290.69 nm f=0.0006 <S**2>=3.598

199A→213A	0.19714	197B→211B	-0.12977	200B→215B	-0.12746
199A→214A	0.23517	198B→211B	0.34657	201B→216B	0.40805
199A→217A	0.12298	198B→212B	0.26316	202B→224B	0.10307
200A→215A	0.11950	198B→213B	-0.18797		
201A→216A	-0.38192	198B→214B	-0.19375		

Excited State 50: 3.953-A 4.2712 eV 290.28 nm f=0.0007 <S**2>=3.656

191A→215A	0.10555	205A→227A	-0.12632	211A→216A	0.13451
192A→216A	0.12390	206A→226A	-0.15066	212A→214A	0.12755
197A→218A	0.12398	206A→228A	-0.10088	171B→211B	0.11710
201A→216A	-0.16691	207A→227A	-0.16863	179B→211B	-0.17157
204A→225A	-0.13445	207A→228A	0.10980	181B→212B	0.10492
205A→225A	-0.10755	210A→215A	0.10889	190B→215B	-0.11154

191B→216B	-0.13073	199B→218B	-0.10111	205B→227B	0.20344
192B→212B	-0.12441	201B→216B	0.17898	209B→215B	-0.13210
196B→211B	0.11171	202B→224B	-0.16877	210B→216B	-0.15937
198B→211B	0.15430	203B→225B	-0.18425		
198B→212B	0.11644	204B→226B	0.16853		

Excited State 51: 3.606-A 4.3244 eV 286.71 nm f=0.0192 <S**2>=3.001

194A→218A	-0.10295	212A→217A	0.26265	196B→212B	-0.26296
197A→222A	0.12425	212A→218A	0.62960	199B→222B	-0.12834
202A→218A	0.19407	193B→218B	-0.10623	206B→218B	-0.14185
212A→213A	-0.14839	195B→218B	-0.14506		

Excited State 52: 4.100-A 4.3262 eV 286.59 nm f=0.0004 <S**2>=3.952

198A→215A	-0.59789	197B→231B	-0.15062	200B→213B	0.10756
198A→231A	0.13924	200B→211B	-0.10199	200B→214B	-0.11787
197B→215B	0.65002	200B→212B	0.18581		

Excited State 53: 4.116-A 4.3280 eV 286.47 nm f=0.0001 <S**2>=3.985

199A→216A	-0.60258	198B→232B	0.15261	201B→213B	0.10730
199A→232A	-0.14026	201B→211B	-0.10059	201B→214B	0.12531
198B→216B	0.65862	201B→212B	-0.17518		

Excited State 54: 3.976-A 4.3512 eV 284.94 nm f=0.0049 <S**2>=3.702

192A→213A	0.10715	211A→214A	0.35717	203B→226B	-0.13792
192A→214A	0.13247	211A→217A	0.18050	203B→227B	0.10202
205A→226A	0.12686	191B→211B	-0.27584	205B→227B	-0.18413
205A→227A	-0.14030	191B→212B	0.17516	210B→212B	-0.21744
207A→227A	0.14629	191B→213B	-0.13344	210B→213B	-0.26337
207A→228A	-0.14624	191B→214B	-0.14396	210B→214B	-0.28283
211A→213A	0.30910	203B→225B	-0.13840	210B→217B	-0.12232

Excited State 55:	3.981-A	4.3533 eV	284.80 nm	f=0.0045	<S**2>=3.711	
191A→213A	-0.11022	210A→214A	0.33275	202B→225B	0.13892	
191A→214A	0.12727	210A→217A	-0.18241	204B→226B	0.17034	
204A→225A	0.18674	190B→211B	0.26983	209B→212B	-0.20995	
204A→226A	0.11043	190B→212B	0.16951	209B→213B	0.26391	
206A→226A	-0.13903	190B→213B	0.13488	209B→214B	-0.26786	
206A→228A	-0.11970	190B→214B	-0.13863	209B→217B	0.12469	
210A→213A	-0.30814	202B→224B	0.17086			

Excited State 56:	3.613-A	4.3886 eV	282.52 nm	f=0.0002	<S**2>=3.014	
200A→213A	0.17784	197B→211B	-0.34170	200B→211B	-0.12000	
200A→214A	-0.20935	197B→212B	0.48079	200B→212B	0.25536	
200A→215A	-0.39514	197B→213B	0.17855	200B→215B	0.42727	
200A→217A	0.12365	197B→214B	-0.16198			

Excited State 57:	3.593-A	4.3979 eV	281.91 nm	f=0.0002	<S**2>=2.977	
201A→213A	-0.16607	198B→211B	0.36611	201B→211B	0.13370	
201A→214A	-0.20763	198B→212B	0.49179	201B→212B	0.26315	
201A→216A	0.38283	198B→213B	-0.18975	201B→216B	-0.41481	
201A→217A	-0.11573	198B→214B	-0.18492			

Excited State 58:	3.415-A	4.3992 eV	281.83 nm	f=0.0011	<S**2>=2.665	
200A→213A	0.32686	193B→211B	-0.10151	197B→212B	-0.24771	
200A→214A	-0.37591	193B→212B	0.13481	197B→213B	-0.10343	
200A→215A	0.18709	194B→211B	-0.10747	200B→211B	-0.25891	
200A→217A	0.25187	194B→212B	0.12746	200B→212B	0.50276	
200A→222A	-0.11530	197B→211B	0.18563	200B→215B	-0.21194	

Excited State 59:	3.392-A	4.4067 eV	281.35 nm	f=0.0012	<S**2>=2.626	
201A→213A	-0.32895	201A→214A	-0.40526	201A→216A	-0.17886	

201A→217A	-0.24631	198B→211B	-0.18547	201B→211B	0.28943
201A→221A	-0.12925	198B→212B	-0.23895	201B→212B	0.53790
201A→223A	0.10242	198B→213B	0.10064	201B→216B	0.20093

Excited State 60: 3.327-A 4.4200 eV 280.51 nm f=0.0028 <S**2>=2.517

200A→213A	-0.11890	193B→212B	0.42348	195B→211B	0.16547
200A→214A	0.13679	194B→211B	-0.37495	195B→212B	-0.34047
212A→218A	0.12343	194B→212B	0.33089	196B→212B	0.11115
193B→211B	-0.26498	194B→213B	0.15033	200B→212B	-0.17973

Excited State 61: 3.343-A 4.4343 eV 279.60 nm f=0.0070 <S**2>=2.544

212A→218A	-0.14446	193B→213B	0.14757	194B→214B	-0.10869
193B→211B	-0.32129	194B→211B	0.25210	195B→211B	0.30434
193B→212B	-0.15974	194B→212B	0.61502	195B→212B	0.17621

Excited State 62: 3.627-A 4.4448 eV 278.94 nm f=0.0387 <S**2>=3.038

194A→218A	-0.13668	212A→213A	-0.17005	194B→219B	0.13575
195A→219A	-0.15484	212A→214A	-0.14546	195B→212B	-0.19016
196A→218A	0.13511	212A→218A	-0.24252	195B→218B	-0.15174
196A→219A	-0.11092	175B→211B	-0.13064	196B→212B	-0.14610
197A→218A	0.11987	193B→212B	0.31180	199B→218B	-0.10255
197A→222A	0.13488	194B→211B	-0.28429	199B→222B	-0.13774
203A→213A	0.10625	194B→212B	-0.12030		
211A→216A	-0.10624	194B→213B	0.10734		

Excited State 63: 3.726-A 4.4553 eV 278.29 nm f=0.0055 <S**2>=3.222

193A→217A	-0.11669	203A→213A	0.16150	212A→218A	0.22776
195A→220A	0.16028	208A→214A	0.11387	212A→224A	0.10268
196A→219A	-0.11063	210A→215A	-0.19348	175B→211B	-0.19650
197A→218A	0.17291	212A→214A	-0.16159	176B→212B	-0.12597

179B→211B	-0.17010	194B→212B	0.11049	199B→218B	-0.14402
181B→212B	0.16591	194B→220B	-0.14818	209B→215B	0.14818
192B→212B	-0.11748	195B→212B	0.10575		
193B→220B	-0.10445	195B→219B	0.12459		

Excited State 64: 3.902-A 4.4817 eV 276.65 nm f=0.0754 <S**2>=3.556

185A→214A	0.10653	211A→216A	-0.20140	199B→222B	0.10528
190A→213A	0.11254	212A→213A	0.15978	207B→212B	0.11131
193A→214A	-0.10221	212A→218A	0.23868	207B→214B	0.16868
194A→218A	0.11109	181B→211B	-0.18108	208B→213B	-0.16113
208A→213A	0.14629	182B→211B	0.10624	208B→217B	-0.11958
209A→213A	-0.12857	189B→214B	-0.13436	209B→215B	-0.16985
209A→214A	-0.20071	192B→213B	-0.14098	210B→216B	0.27111
210A→215A	0.12278	195B→218B	0.10951		

Excited State 65: 3.800-A 4.5106 eV 274.87 nm f=0.0101 <S**2>=3.360

190A→214A	0.11089	199A→217A	-0.10495	194B→220B	0.11792
195A→220A	-0.11839	200A→215A	-0.15693	195B→219B	-0.10059
196A→219A	0.10038	201A→216A	-0.13854	196B→213B	0.10272
197A→218A	-0.10717	203A→213A	-0.17957	197B→212B	-0.10784
198A→213A	-0.19878	208A→214A	0.15637	199B→218B	0.10446
198A→214A	0.22318	210A→215A	-0.11842	207B→213B	0.13713
198A→217A	-0.13457	212A→214A	0.22300	208B→214B	-0.16256
199A→213A	-0.15802	212A→218A	-0.11849	209B→215B	0.22013
199A→214A	-0.19199	192B→214B	-0.11911	210B→216B	0.16207

Excited State 66: 4.067-A 4.5146 eV 274.63 nm f=0.0005 <S**2>=3.886

205A→225A	0.12688	207A→227A	-0.19336	209A→227A	0.11309
205A→226A	-0.18037	207A→228A	0.20851	211A→213A	0.12324
205A→227A	0.18509	209A→216A	0.33198	211A→214A	0.13165

191B→211B	-0.24699	203B→227B	-0.12997	207B→216B	-0.24588
191B→212B	0.14653	205B→224B	-0.10872	208B→216B	0.26654
191B→214B	-0.10004	205B→225B	0.15135	210B→212B	-0.10081
203B→225B	0.19533	205B→227B	0.25391	210B→213B	-0.10118
203B→226B	0.18684	206B→216B	-0.12454		

Excited State 67: 4.044-A 4.5163 eV 274.52 nm f=0.0015 <S**2>=3.839

199A→214A	-0.10571	210A→213A	0.11404	204B→226B	0.21068
204A→225A	0.26417	210A→214A	-0.11319	204B→227B	0.12132
204A→226A	0.14041	190B→211B	-0.23747	206B→215B	0.13491
206A→226A	-0.16664	190B→212B	-0.13960	207B→215B	-0.28827
206A→227A	-0.12350	202B→224B	0.24144	208B→215B	-0.20244
206A→228A	-0.15395	202B→225B	0.18277		
208A→215A	0.32090	204B→224B	0.13787		

Excited State 68: 3.633-A 4.5190 eV 274.36 nm f=0.0008 <S**2>=3.050

198A→213A	-0.37918	199A→213A	0.27892	201A→216A	0.24913
198A→214A	0.42921	199A→214A	0.33474	197B→212B	-0.19440
198A→217A	-0.25657	199A→217A	0.18578	198B→212B	-0.16118
198A→229A	-0.11278	200A→215A	-0.33436		

Excited State 69: 3.686-A 4.5217 eV 274.20 nm f=0.0037 <S**2>=3.146

198A→213A	0.22564	200A→215A	0.20676	198B→212B	-0.18661
198A→214A	-0.25304	201A→216A	0.29568	207B→213B	0.10494
198A→217A	0.15257	203A→213A	-0.10002	208B→214B	-0.11926
199A→213A	0.32452	208A→214A	0.11744	209B→215B	0.12635
199A→214A	0.39350	212A→214A	0.12532	210B→216B	0.11269
199A→217A	0.21626	197B→212B	0.11901		

Excited State 70:	3.137-A	4.5710 eV	271.24 nm	f=0.0003	<S**2>=2.210	
198A→213A	-0.14624	200A→231A	-0.12242	200B→231B	-0.14103	
198A→214A	0.15997	197B→212B	-0.11894			
200A→215A	0.60313	200B→215B	0.69485			

Excited State 71:	3.134-A	4.5721 eV	271.17 nm	f=0.0000	<S**2>=2.205	
199A→213A	-0.14168	201A→232A	0.12257	201B→232B	0.14062	
199A→214A	-0.16600	198B→212B	0.12365			
201A→216A	0.60430	201B→216B	0.69323			

Excited State 72:	3.304-A	4.6135 eV	268.74 nm	f=0.0038	<S**2>=2.479	
203A→214A	0.10879	171B→212B	0.24351	175B→212B	0.35349	
212A→217A	-0.12251	172B→211B	0.52443	176B→211B	0.14270	
212A→218A	0.10830	172B→212B	0.11310	177B→211B	0.25420	
171B→211B	-0.11306	175B→211B	-0.13473	178B→211B	-0.18849	

Excited State 73:	3.201-A	4.6433 eV	267.02 nm	f=0.0052	<S**2>=2.312	
212A→214A	-0.10572	172B→211B	0.18640	175B→212B	-0.10385	
171B→211B	0.32872	172B→212B	0.42534	176B→212B	0.12824	
171B→212B	-0.10157	175B→211B	0.57078	177B→212B	0.14107	

Excited State 74:	3.181-A	4.6678 eV	265.61 nm	f=0.0824	<S**2>=2.279	
190A→216A	-0.11344	211A→213A	0.23692	203B→216B	-0.12883	
193A→216A	0.10254	211A→214A	0.26845	206B→216B	0.10762	
202A→216A	-0.15672	211A→217A	0.13254	207B→216B	0.25993	
203A→216A	-0.14589	212A→216A	0.19285	208B→216B	-0.28842	
208A→216A	-0.13711	191B→211B	0.22638			
209A→216A	0.52602	191B→212B	-0.12232			

Excited State 75:	3.151-A	4.6687 eV	265.56 nm	f=0.0507	<S**2>=2.233	
190A→215A	0.10011	202A→215A	0.13443	203A→215A	-0.11905	

208A→215A	0.53186	210A→215A	0.18553	208B→215B	0.23971
209A→215A	0.16326	212A→215A	-0.17427	208B→216B	-0.10458
209A→216A	0.12915	190B→211B	0.17684	209B→215B	0.10202
210A→213A	0.17046	206B→215B	-0.15146		
210A→214A	-0.16818	207B→215B	0.35477		

Excited State 76: 3.106-A 4.6699 eV 265.50 nm f=0.4587 <S2>=2.162**

209A→216A	-0.27865	211A→221A	0.12224	208B→216B	0.24909
210A→213A	0.14663	211A→223A	-0.11177	209B→213B	0.11611
210A→214A	-0.18472	190B→211B	0.12395	210B→213B	0.24952
211A→213A	0.27566	191B→211B	0.17385	210B→214B	0.27959
211A→214A	0.31586	206B→216B	-0.14560	210B→217B	0.14396
211A→217A	0.17996	207B→216B	-0.24275		

Excited State 77: 3.090-A 4.6718 eV 265.39 nm f=1.2360 <S2>=2.138**

208A→215A	0.26670	210A→222A	0.11862	208B→215B	0.17571
209A→216A	-0.14347	190B→211B	-0.18902	208B→216B	0.11018
210A→213A	-0.29700	190B→212B	-0.10366	209B→213B	-0.26659
210A→214A	**0.31887**	206B→215B	-0.15956	209B→214B	0.28531
210A→215A	0.12586	207B→215B	0.28191	209B→215B	0.10183
210A→217A	-0.19499	207B→216B	-0.10741	209B→217B	-0.15522

Excited State 78: 3.488-A 4.7072 eV 263.39 nm f=0.4170 <S2>=2.792**

194A→220A	-0.12371	212A→217A	0.22636	192B→211B	-0.22287
195A→219A	0.19495	212A→218A	-0.10921	193B→218B	-0.11320
196A→220A	-0.16783	172B→211B	0.25028	193B→220B	-0.15348
202A→213A	-0.17494	175B→212B	0.21199	194B→219B	-0.21032
203A→214A	-0.20517	176B→211B	0.19106	195B→220B	0.15965
210A→215A	-0.12111	177B→212B	-0.11517	196B→212B	-0.11304
211A→216A	0.12485	**178B→211B**	**0.33893**	199B→222B	-0.11160

209B→215B	-0.12012	210B→216B	0.12817		

Excited State 79:	3.779-A	4.7215 eV	262.60 nm	f=0.0052	<S**2>=3.319
192A→216A	0.14239	212A→221A	-0.25944	199B→213B	-0.10769
193A→218A	-0.13443	212A→222A	0.34091	205B→227B	-0.12205
203A→218A	-0.13183	178B→211B	-0.14060	206B→213B	-0.11979
208A→213A	-0.12999	181B→211B	-0.13855	207B→214B	-0.13164
209A→214A	0.18076	190B→215B	0.10437		
212A→219A	-0.19973	191B→216B	-0.15574		

Excited State 80:	3.910-A	4.7355 eV	261.82 nm	f=0.0033	<S**2>=3.571
191A→215A	-0.20076	212A→214A	-0.11054	191B→216B	0.10375
204A→225A	-0.14672	171B→211B	-0.18548	202B→224B	-0.16878
206A→226A	-0.12375	172B→211B	-0.14581	204B→226B	0.15928
208A→213A	-0.13022	172B→212B	-0.15036	206B→214B	0.12576
208A→214A	0.19655	179B→211B	0.10365	207B→213B	0.12840
208A→217A	-0.10155	181B→212B	-0.12355	207B→217B	0.10294
209A→213A	-0.11409	189B→211B	0.20697	207B→223B	-0.10255
210A→231A	0.11169	190B→215B	0.21757	209B→231B	-0.12356

Excited State 81:	3.671-A	4.7412 eV	261.50 nm	f=0.0427	<S**2>=3.119
192A→216A	-0.14397	212A→219A	-0.24363	181B→211B	0.11101
193A→218A	-0.17076	212A→221A	-0.30607	189B→211B	0.10868
202A→221A	-0.10975	212A→222A	0.40282	191B→216B	0.15209
202A→222A	0.10899	212A→223A	-0.15645	199B→213B	-0.12391
203A→218A	-0.15541	171B→211B	-0.10018	199B→217B	0.12172
209A→214A	-0.12521	172B→211B	0.10521	205B→227B	0.11748

Excited State 82:	3.112-A	4.7765 eV	259.57 nm	f=0.0038	<S**2>=2.171
198A→215A	0.56137	198A→231A	-0.11221	199A→216A	-0.11338

200A→213A	0.12606	197B→215B	0.47325	200B→214B	-0.27821
200A→214A	-0.14670	200B→212B	-0.25518	200B→217B	0.18099
178B→211B	0.14714	200B→213B	0.22871		

Excited State 83: 3.100-A 4.7783 eV 259.47 nm f=0.0015 <S**2>=2.153

198A→215A	0.14530	201A→214A	0.14856	201B→213B	0.21928
199A→216A	0.57725	197B→215B	0.12383	201B→214B	0.28139
199A→232A	0.11538	198B→216B	0.48781	201B→217B	0.17147
201A→213A	0.12030	201B→212B	0.25543	201B→221B	0.10596

Excited State 84: 3.274-A 4.7896 eV 258.86 nm f=0.0179 <S**2>=2.430

195A→219A	-0.10687	177B→211B	-0.21627	194B→219B	0.10880
198A→215A	-0.19864	177B→212B	-0.23807	197B→215B	-0.18067
199A→216A	0.14171	178B→211B	0.63453	198B→216B	0.12778
211A→216A	-0.11432	178B→212B	0.11644	210B→216B	-0.10975
176B→211B	0.16963	192B→211B	0.15895		

Excited State 85: 3.148-A 4.8185 eV 257.31 nm f=0.0004 <S**2>=2.227

198A→215A	-0.24051	177B→211B	-0.13721	200B→214B	-0.22849
199A→216A	-0.26067	191B→211B	0.10806	200B→217B	0.16235
200A→213A	0.11755	197B→215B	-0.25371	201B→212B	0.28366
200A→214A	-0.13259	198B→216B	-0.27949	201B→213B	0.21171
201A→213A	0.12502	200B→212B	-0.22993	201B→214B	0.28545
201A→214A	0.14624	200B→213B	0.22618	201B→217B	0.14888

Excited State 86: 3.147-A 4.8213 eV 257.16 nm f=0.0140 <S**2>=2.226

198A→215A	0.26532	201A→213A	0.11098	197B→215B	0.28327
199A→216A	-0.22000	201A→214A	0.13436	198B→216B	-0.23991
200A→213A	-0.13996	178B→211B	0.18631	200B→212B	0.30647
200A→214A	0.15095	191B→211B	0.10134	200B→213B	-0.23724

200B→214B	0.30440	201B→212B	0.23149	201B→214B	0.23273
200B→217B	-0.17052	201B→213B	0.21553	201B→217B	0.15253

Excited State 87: 3.299-A 4.8243 eV 257.00 nm f=0.0138 <S**2>=2.472

199A→216A	0.13214	191B→212B	-0.16266	207B→216B	-0.10258
202A→216A	-0.10368	198B→216B	0.12701	208B→216B	0.15649
203A→216A	-0.14526	201B→212B	-0.12284	210B→213B	-0.19154
205A→216A	-0.16145	201B→213B	-0.10465	210B→214B	-0.22277
206A→215A	0.11880	201B→214B	-0.12495	210B→217B	-0.12432
207A→216A	0.24450	203B→216B	0.20775	210B→227B	0.10992
190B→211B	0.13215	204B→215B	-0.13393		
191B→211B	0.36514	205B→216B	-0.21385		

Excited State 88: 3.290-A 4.8245 eV 256.99 nm f=0.0271 <S**2>=2.456

202A→215A	0.10024	190B→211B	0.32984	207B→226B	0.10579
203A→215A	-0.13582	190B→212B	0.14272	208B→215B	-0.14238
205A→216A	0.10926	191B→211B	-0.15285	209B→213B	-0.16562
206A→213A	-0.10954	202B→215B	0.10487	209B→214B	0.19422
206A→215A	0.27377	203B→216B	-0.12833	209B→215B	0.10308
210A→215A	0.16249	204B→215B	-0.29713	209B→217B	-0.11197
177B→211B	0.15171	207B→215B	-0.13667	209B→226B	0.11304

Excited State 89: 3.261-A 4.8258 eV 256.92 nm f=0.0254 <S**2>=2.409

203A→215A	0.11751	212A→224A	0.10090	202B→215B	-0.24725
203A→217A	-0.10005	177B→211B	0.30007	209B→213B	0.13014
204A→214A	-0.10627	178B→211B	0.17458	209B→214B	-0.12593
204A→215A	0.21746	178B→212B	-0.18297	209B→215B	0.22707
210A→215A	0.22006	189B→211B	-0.16675	210B→216B	0.10404
211A→216A	0.11404	190B→211B	-0.21240		

Excited State 90:	3.155-A	4.8381 eV	256.27 nm	f=0.0019	<S**2>=2.239	
204A→215A	0.10944	211A→216A	-0.25138	203B→223B	-0.10918	
205A→214A	-0.11553	211A→227A	0.10892	204B→215B	-0.13309	
205A→216A	-0.25612	177B→211B	0.11195	205B→216B	0.38151	
205A→223A	0.10184	202B→215B	-0.10436	206B→213B	0.19560	
206A→216A	0.12035	203B→214B	0.15282	210B→216B	-0.21549	
207A→214A	0.10047	203B→216B	0.22131	210B→227B	-0.10188	
207A→216A	-0.25931	203B→217B	0.10703			
210A→215A	0.10296	203B→221B	0.10728			

Excited State 91:	3.158-A	4.8476 eV	255.76 nm	f=0.0188	<S**2>=2.243	
204A→214A	0.10537	177B→211B	0.38976	202B→214B	-0.12952	
204A→215A	-0.27127	178B→211B	0.14575	202B→215B	0.24753	
206A→215A	-0.22278	178B→212B	-0.23061	204B→215B	0.29898	
172B→211B	-0.14241	202B→213B	0.10452	205B→216B	0.12016	

Excited State 92:	**3.262-A**	**4.8772 eV**	**254.21 nm**	**f=0.3936**	**<S**2>=2.410**	
205A→216A	-0.16873	177B→211B	-0.12018	207B→214B	-0.12634	
207A→216A	-0.19879	203B→216B	0.11100	208B→217B	0.11398	
210A→215A	-0.14559	205B→216B	0.21545	209B→215B	-0.13759	
211A→216A	**0.42119**	206B→213B	-0.24789	**210B→216B**	**0.37766**	

Excited State 93:	3.253-A	4.8854 eV	253.79 nm	f=0.0764	<S**2>=2.395	
195A→214A	0.14658	210A→215A	0.39935	204B→215B	0.15481	
196A→213A	0.10574	211A→216A	0.13225	206B→213B	0.13066	
204A→215A	-0.14519	172B→211B	0.13841	207B→213B	-0.12638	
206A→215A	-0.15327	177B→211B	-0.30532	208B→214B	0.10166	
208A→214A	0.10142	178B→212B	0.17016	209B→215B	0.35928	
208A→215A	-0.11224	202B→215B	0.10478	210B→216B	0.11252	

Excited State 94:	3.912-A	4.8927 eV	253.41 nm	f=0.0155	<S**2>=3.576				
194A→213A	-0.20384	196A→213A	-0.25346	194B→212B	0.16091				
194A→214A	0.21688	196A→214A	0.28053	194B→213B	-0.18926				
195A→213A	0.34156	197A→213A	0.10388	194B→214B	0.17322				
195A→214A	-0.29305	211A→216A	0.14856	195B→212B	-0.12389				
195A→217A	0.10516	193B→212B	0.15580	195B→213B	0.13093				
195A→222A	0.10512	193B→213B	-0.15650	195B→214B	-0.14537				
195A→223A	0.12422	193B→214B	0.16447	210B→216B	0.13306				

Excited State 95:	3.886-A	4.8950 eV	253.29 nm	f=0.0182	<S**2>=3.525				
194A→213A	0.18627	196A→223A	0.10912	194B→213B	-0.18716				
194A→214A	0.17951	210A→215A	-0.14111	194B→214B	-0.22421				
195A→213A	0.30970	177B→211B	0.14442	195B→212B	-0.11237				
195A→214A	0.35702	193B→212B	0.11164	195B→213B	-0.13731				
195A→223A	0.13743	193B→213B	0.12825	195B→214B	-0.12672				
196A→213A	0.27365	193B→214B	0.12010	209B→215B	-0.13049				
196A→214A	0.25423	194B→212B	-0.19662						

Excited State 96:	3.323-A	4.9283 eV	251.57 nm	f=0.0115	<S**2>=2.511				
195A→213A	0.10083	203A→220A	0.33811	190B→211B	-0.30102				
202A→215A	0.12907	203A→221A	0.10126	190B→212B	-0.11734				
202A→216A	0.13127	212A→215A	-0.17113	191B→211B	0.32268				
202A→219A	-0.23384	212A→216A	-0.17283	191B→212B	-0.13273				
203A→215A	-0.17077	212A→219A	0.28500	193B→212B	-0.11412				
203A→216A	0.18860	212A→220A	0.12053						
203A→219A	-0.11457	212A→221A	-0.13419						

Excited State 97:	3.321-A	4.9293 eV	251.53 nm	f=0.0005	<S**2>=2.508				
195A→214A	-0.11367	202A→216A	-0.12842	203A→215A	-0.19023				
202A→215A	0.13322	202A→220A	-0.24862	203A→216A	-0.17506				

203A→219A	0.31737	212A→216A	0.16747	191B→211B	-0.31543
203A→220A	0.15105	212A→220A	0.32585	191B→212B	0.12580
203A→221A	-0.10834	190B→211B	-0.31973	194B→212B	-0.13120
212A→215A	-0.17595	190B→212B	-0.12879		

Excited State 98: 3.239-A 4.9402 eV 250.97 nm f=0.0485 <S**2>=2.372

203A→219A	-0.11546	211A→228A	0.10160	205B→214B	0.12816
205A→216A	-0.28189	189B→216B	-0.11304	205B→216B	-0.18394
207A→214A	-0.10533	191B→211B	-0.18367	207B→216B	0.15872
207A→216A	0.24694	192B→216B	-0.12558	208B→216B	-0.22232
209A→227A	-0.11289	196B→216B	0.11174	210B→213B	0.25736
211A→213A	0.13275	203B→216B	0.36776	210B→214B	0.26621
211A→214A	0.13183	205B→213B	0.10798	210B→217B	0.11949

Excited State 99: 3.223-A 4.9406 eV 250.95 nm f=0.0369 <S**2>=2.347

204A→215A	-0.28673	192B→215B	0.11889	207B→215B	0.20504
206A→215A	0.24114	196B→215B	0.10713	208B→215B	0.17505
210A→213A	0.12882	202B→215B	0.35559	209B→213B	0.27445
210A→214A	-0.12033	204B→213B	0.10308	209B→214B	-0.26526
189B→215B	-0.11082	204B→214B	-0.11884	209B→217B	0.12717
190B→211B	-0.23455	204B→215B	-0.22671		

Excited State 100: 3.545-A 4.9469 eV 250.63 nm f=0.0027 <S**2>=2.892

195A→220A	0.11522	189B→211B	0.31005	198B→214B	0.10378
197A→213A	0.23185	194B→220B	-0.13633	199B→213B	-0.13948
197A→217A	-0.20168	197B→212B	-0.25831	199B→217B	0.10076
210A→215A	0.12767	197B→213B	0.25098	206B→214B	-0.14751
211A→216A	0.15716	197B→214B	-0.27647	209B→215B	0.12493
177B→211B	0.17951	197B→217B	0.15450	210B→216B	0.15351

Excited State 101:	3.293-A	4.9528 eV	250.33 nm	f=0.0004	<S**2>=2.461	
199A→214A	0.11496	197B→213B	-0.19254	198B→213B	0.41136	
172B→211B	-0.13914	197B→214B	0.20325	198B→214B	0.49465	
175B→212B	-0.10352	197B→217B	-0.11925	198B→217B	0.25689	
197B→212B	0.19037	198B→212B	0.45310	198B→229B	-0.11895	

Excited State 102:	3.454-A	4.9554 eV	250.20 nm	f=0.0013	<S**2>=2.733	
197A→213A	0.24570	197B→212B	0.35653	198B→214B	-0.19578	
197A→217A	-0.20833	197B→213B	-0.33543	198B→217B	-0.10530	
172B→211B	-0.12573	197B→214B	0.38412	199B→213B	-0.13431	
175B→211B	-0.13181	197B→217B	-0.21031	199B→217B	0.10591	
177B→211B	0.15350	198B→212B	-0.17893			
189B→211B	0.16111	198B→213B	-0.17294			

*C.2.11.4 **OTPT-FLR-210, EB** State*

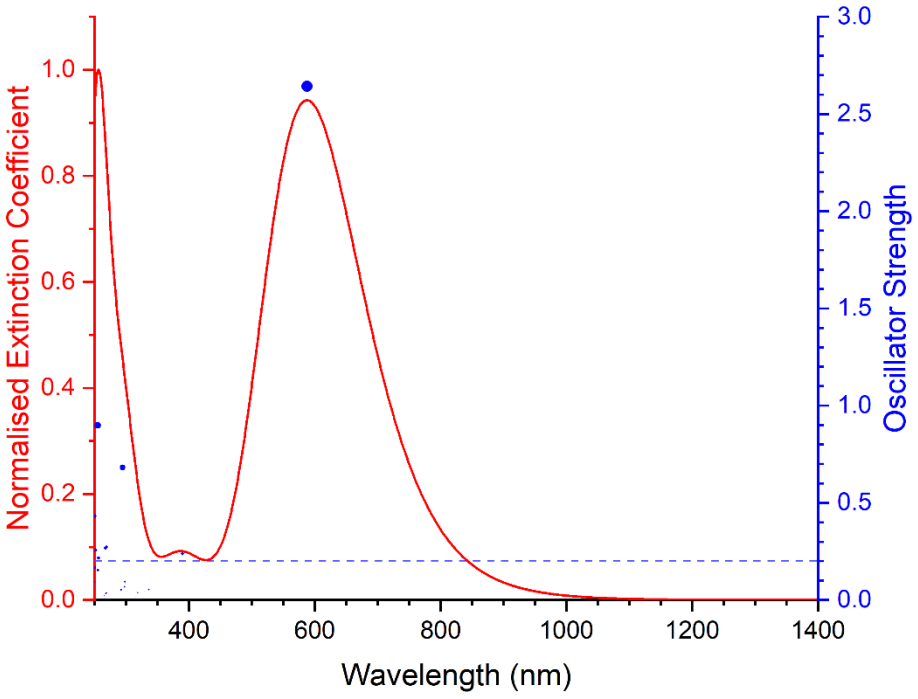

*Figure C-44 Excited states and normalised absorption spectra from TD-DFT calculations of **OTPT-FLR-210** in **EB** state. The areas of excited state dots are proportional to their oscillator strengths.*

Excited State 1:	**Singlet-A**	**2.1092 eV**	**587.82 nm**	**f=2.6422**	**<S**2>=0.000**
210→213	-0.10311	**211→212**	**0.68720**		

Excited State 2:	Singlet-A	2.7974 eV	443.21 nm	f=0.0113	<S**2>=0.000
192→212	0.14703	210→212	0.65599		
Excited State 3:	**Singlet-A**	**3.1779 eV**	**390.14 nm**	**f=0.2373**	**<S**2>=0.000**
191→212	0.19895	**209→212**	**0.63285**		
Excited State 4:	Singlet-A	3.6835 eV	336.59 nm	f=0.0534	<S**2>=0.000
198→212	0.66865	200→212	0.14643		
Excited State 5:	Singlet-A	3.8874 eV	318.94 nm	f=0.0376	<S**2>=0.000
193→212	-0.24145	211→213	0.55943		
210→216	0.21014	211→217	-0.20155		
Excited State 6:	Singlet-A	3.9218 eV	316.14 nm	f=0.0135	<S**2>=0.000
192→212	0.10024	199→212	-0.14572		
193→212	0.60539	211→213	0.22523		
Excited State 7:	Singlet-A	4.1529 eV	298.55 nm	f=0.0944	<S**2>=0.000
198→212	0.10575	200→212	-0.33872	211→215	-0.11698
199→212	0.43757	207→212	0.14545	211→216	0.18127
199→213	-0.10513	210→213	0.10312		
Excited State 8:	Singlet-A	4.1641 eV	297.75 nm	f=0.0667	<S**2>=0.000
193→212	0.10531	200→212	0.47807	211→216	0.15248
198→212	-0.10134	208→212	0.16245		
199→212	0.29321	211→214	0.12286		
Excited State 9:	**Singlet-A**	**4.2094 eV**	**294.54 nm**	**f=0.6805**	**<S**2>=0.000**
193→212	-0.10374	209→216	-0.11753	**211→216**	**0.50573**
199→212	-0.23705	210→213	0.26824		

Excited State 10:	Singlet-A	4.2389 eV	292.49 nm	f=0.0519	<S**2>=0.000			
192→212	0.55993		210→212	-0.17249		211→217	0.12185	
197→212	-0.19858		210→216	0.10933				
Excited State 11:	Singlet-A	4.3581 eV	284.49 nm	f=0.0000	<S**2>=0.000			
200→212	-0.19674		210→214	-0.21533		211→215	0.37140	
209→214	-0.12230		210→215	0.18686				
209→215	-0.12242		211→214	0.37974				
Excited State 12:	Singlet-A	4.3585 eV	284.46 nm	f=0.0009	<S**2>=0.000			
199→212	0.20432		210→214	0.18563		211→215	0.37692	
209→214	0.11968		210→215	0.21509				
209→215	-0.12408		211→214	-0.37191				
Excited State 13:	Singlet-A	4.4853 eV	276.42 nm	f=0.0021	<S**2>=0.000			
195→215	-0.22762		196→216	0.34476		197→216	0.15233	
196→212	-0.26692		197→212	-0.10967				
196→213	0.14444		197→213	0.36383				
Excited State 14:	Singlet-A	4.4874 eV	276.29 nm	f=0.0007	<S**2>=0.000			
194→214	-0.23349		196→216	-0.15160		197→216	0.33491	
196→212	0.11643		197→212	-0.24108				
196→213	0.36945		197→213	-0.14402				
Excited State 15:	Singlet-A	4.5773 eV	270.87 nm	f=0.0022	<S**2>=0.000			
195→212	-0.26130		195→215	0.18708		196→215	-0.16218	
195→213	0.37846		195→216	0.38275		197→215	-0.12943	
Excited State 16:	Singlet-A	4.5787 eV	270.79 nm	f=0.0008	<S**2>=0.000			
194→212	0.25500		194→214	0.19668		195→213	0.10509	
194→213	0.37804		194→216	-0.37631		196→214	-0.17248	

197→214	0.12511							

Excited State 17:	Singlet-A	4.5834 eV	270.50 nm	f=0.0001	<S**2>=0.000			
195→213	-0.11777	195→229	-0.12127	196→216	0.10872			
195→215	0.59453	196→212	-0.11029	197→215	0.10330			
195→216	-0.11381	196→213	0.10235					

Excited State 18:	Singlet-A	4.5838 eV	270.48 nm	f=0.0003	<S**2>=0.000			
194→213	-0.12841	194→216	0.12190	196→213	0.12536			
194→214	0.58870	194→230	0.12040	197→214	-0.10519			

Excited State 19:	**Singlet-A**	**4.6097 eV**	**268.97 nm**	**f=0.2727**	**<S**2>=0.000**			
199→212	-0.10764	208→212	0.28471	211→218	-0.17591			
207→212	**0.43910**	208→213	0.21212					
207→216	-0.15522	211→214	-0.13685					

Excited State 20:	Singlet-A	4.6128 eV	268.78 nm	f=0.0358	<S**2>=0.000			
196→215	-0.12136	207→212	-0.26730	208→216	-0.16331			
197→215	-0.11898	207→213	0.21702	211→215	-0.14071			
200→212	-0.12044	208→212	0.45911					

Excited State 21:	Singlet-A	4.6263 eV	268.00 nm	f=0.0319	<S**2>=0.000			
195→213	0.10477	196→215	0.35042	207→212	-0.11877			
195→216	0.11295	197→214	0.20041	211→218	0.10740			
196→214	-0.24124	197→215	0.36717					

Excited State 22:	Singlet-A	4.6269 eV	267.96 nm	f=0.0014	<S**2>=0.000			
194→212	0.10313	196→214	0.36775	197→215	0.20376			
194→213	0.10746	196→215	0.22500	208→212	0.16817			
194→216	-0.11411	197→214	-0.35240					

Excited State 23:	**Singlet-A**	**4.6357 eV**	**267.45 nm**	**f=0.2678**	**<S**2>=0.000**						
191→212	**0.38781**		207→212	0.19549		**211→218**	**0.36202**				
205→212	-0.14537		209→212	-0.17685		211→219	0.13991				
Excited State 24:	Singlet-A	4.6689 eV	265.55 nm	f=0.0210	<S**2>=0.000						
191→212	-0.36727		209→212	0.17238		211→219	0.21660				
205→212	0.16197		211→218	0.41738							
Excited State 25:	Singlet-A	4.8049 eV	258.04 nm	f=0.0043	<S**2>=0.000						
190→212	-0.13468		206→212	0.59325		210→216	-0.10225				
205→213	-0.15989		206→216	-0.12350		211→217	-0.13612				
Excited State 26:	**Singlet-A**	**4.8368 eV**	**256.34 nm**	**f=0.2165**	**<S**2>=0.000**						
191→212	0.16376		206→213	-0.16032		211→216	0.10010				
205→212	**0.57815**		207→215	-0.11695							
205→216	-0.14012		208→214	0.10097							
Excited State 27:	Singlet-A	4.8567 eV	255.28 nm	f=0.1529	<S**2>=0.000						
204→212	-0.11228		205→215	-0.17242		208→212	0.10844				
204→216	0.10818		206→214	0.38100		211→214	-0.15257				
205→214	-0.35368		206→215	-0.14747							
Excited State 28:	**Singlet-A**	**4.8601 eV**	**255.11 nm**	**f=0.8971**	**<S**2>=0.000**						
203→212	-0.11987		**205→215**	**0.36216**		207→212	0.11031				
203→216	0.11224		206→214	0.14689		211→215	0.15117				
205→214	-0.16282		**206→215**	**0.36805**							
Excited State 29:	Singlet-A	4.8898 eV	253.56 nm	f=0.0018	<S**2>=0.000						
190→212	0.12202		209→213	-0.29804		211→220	-0.11893				
192→212	-0.18135		210→216	0.30599							
206→212	0.28339		211→217	0.27981							

Excited State 30:	**Singlet-A**	**4.9281 eV**	**251.59 nm**	**f=0.2566**	**<S**2>=0.000**	
191→212	0.11647	208→214	-0.12437	211→216	-0.31109	
205→212	0.17687	209→216	-0.27083			
207→215	0.13538	**210→213**	**0.34927**			

Excited State 31:	Singlet-A	4.9446 eV	250.75 nm	f=0.0019	<S**2>=0.000	
201→213	0.17671	203→215	0.25749	207→223	0.10673	
202→212	0.31120	204→214	0.30799			
202→216	-0.18013	205→226	-0.10004			

Excited State 32:	Singlet-A	4.9487 eV	250.54 nm	f=0.1666	<S**2>=0.000	
201→212	-0.29943	203→215	0.31142	208→223	-0.10906	
201→216	0.18218	204→214	-0.25408			
202→213	-0.17605	204→215	-0.10486			

Excited State 33:	Singlet-A	4.9561 eV	250.16 nm	f=0.0928	<S**2>=0.000	
201→214	0.16623	204→213	0.10270	208→213	-0.11290	
201→215	0.14355	204→216	-0.12856	208→216	0.18894	
202→214	0.33550	207→213	-0.13700			
204→212	0.19457	208→212	0.21563			

Excited State 34:	**Singlet-A**	**4.9587 eV**	**250.03 nm**	**f=0.4307**	**<S**2>=0.000**	
201→212	0.10331	203→212	-0.19070	207→216	-0.18412	
201→215	**0.33723**	203→216	0.12787	208→213	0.13027	
202→214	-0.12250	207→212	-0.21125			
202→215	-0.17618	207→213	-0.10696			

C.2.12 Electronic Transitions in **OTPT-FLR-221** Oligomers

*Table C-16 Attributes of **OTPT-FLR-221** in **LEB**, **ES** (singlet and quintet), and **EB** states related to electronic structures*

Attribute	LEB State	^{1}ES State	^{5}ES State	EB State
Molecular Formula	$C_{68}H_{46}N_{10}$	$C_{68}H_{46}N_{10}^{4+}$	$C_{68}H_{46}N_{10}^{4+}$	$C_{68}H_{42}N_{10}$
Number of Atoms	124	124	124	120
Number of Electrons	524	520	520	520
HOMO	MO 262	MO 260	MOs 262A, 258B	MO 260
LUMO	MO 263	MO 261	MOs 263A, 259B	MO 261

*C.2.12.1 **OTPT-FLR-221**, **LEB** State*

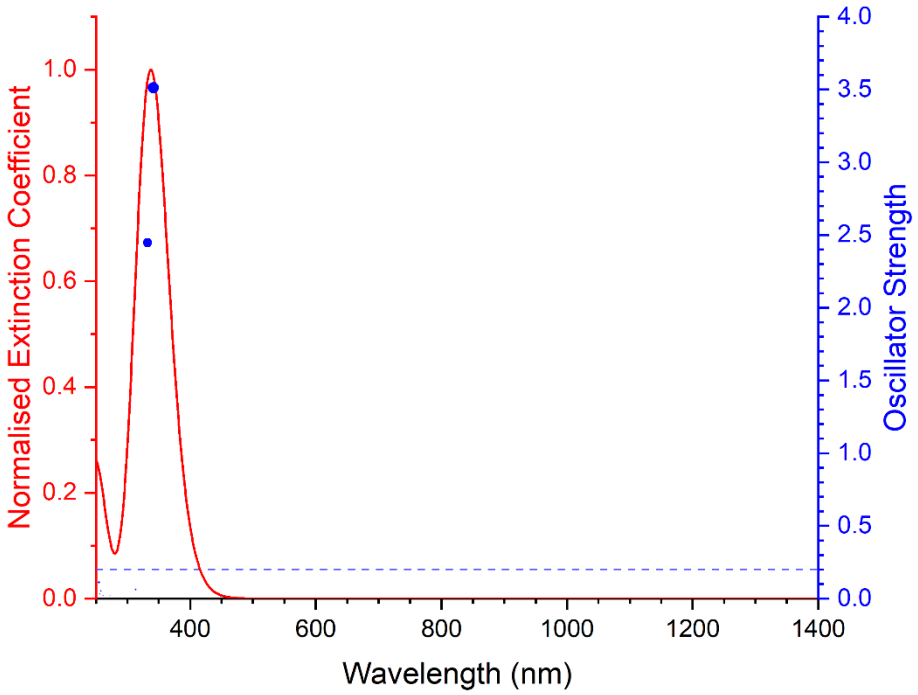

*Figure C-45 Excited states and normalised absorption spectra from TD-DFT calculations of **OTPT-FLR-221** in **LEB** state. The areas of excited state dots are proportional to their oscillator strengths.*

Excited State 1:	Singlet-A2	3.3918 eV	365.54 nm	f=0.0000	<S**2>=0.000			
259→265	-0.15344		261→264	-0.26632		262→268	0.13861	
259→271	0.11009		261→267	-0.24820				
260→266	0.26138		262→263	0.45789				
Excited State 2:	**Singlet-B2**	**3.6325 eV**	**341.32 nm**	**f=3.5126**	**<S**2>=0.000**			
259→266	0.22412		**261→263**	**0.45828**		262→267	-0.28660	
260→265	-0.11870		261→268	0.17317				
260→271	0.10171		262→264	-0.26635				

Excited State 3:	**Singlet-B1**	**3.7299 eV**	**332.41 nm**	**f=2.4461**	**<S**2>=0.000**	
257→266	-0.13964	**260→263**	**0.35598**	261→271	0.13607	
259→264	-0.22440	261→265	-0.25288	**262→266**	**0.42205**	
Excited State 4:	Singlet-A1	3.9596 eV	313.12 nm	f=0.0626	<S**2>=0.000	
258→266	-0.12401	260→267	-0.10071	262→271	0.13854	
259→263	0.34534	261→266	0.43843			
260→264	-0.19860	262→265	-0.25840			
Excited State 5:	Singlet-A2	4.1239 eV	300.65 nm	f=0.0000	<S**2>=0.000	
258→264	-0.17617	260→266	0.15331	262→263	0.25616	
259→265	0.33117	261→264	0.44757			
Excited State 6:	Singlet-B1	4.1384 eV	299.59 nm	f=0.0016	<S**2>=0.000	
257→266	-0.10436	259→264	0.31976	261→265	0.43633	
258→265	-0.17267	260→263	0.19649	262→266	0.25751	
Excited State 7:	Singlet-B2	4.2782 eV	289.80 nm	f=0.0000	<S**2>=0.000	
257→264	-0.12204	260→265	0.29887	262→264	0.50691	
259→266	0.12843	261→263	0.25463			
Excited State 8:	Singlet-A1	4.2979 eV	288.47 nm	f=0.0001	<S**2>=0.000	
257→265	-0.12195	260→264	0.28994	262→265	0.49900	
259→263	0.17936	261→266	0.25600			
Excited State 9:	Singlet-A2	4.3946 eV	282.13 nm	f=0.0000	<S**2>=0.000	
257→263	0.11916	261→267	-0.27277	262→268	0.33401	
260→266	-0.18193	261→269	-0.31635	262→270	-0.26933	
Excited State 10:	Singlet-B2	4.4167 eV	280.71 nm	f=0.0000	<S**2>=0.000	
259→266	0.16511	261→263	0.14458	261→268	-0.27744	

261→270	0.31287	262→267	0.21620	262→269	0.36135

Excited State 11:	Singlet-A2	4.5297 eV	273.72 nm	f=0.0000	<S**2>=0.000
257→263	0.12050	261→267	-0.25359	262→268	0.21656
259→265	0.11130	261→269	0.29039	262→270	0.35047
260→266	-0.19312	261→272	0.13876		

Excited State 12:	Singlet-B2	4.5549 eV	272.20 nm	f=0.0195	<S**2>=0.000
258→263	0.13475	261→263	-0.11499	262→267	-0.29613
259→266	-0.22251	261→268	0.25214	262→269	0.24305
260→265	0.12416	261→270	0.29994	262→272	0.14903

Excited State 13:	Singlet-B1	4.5793 eV	270.75 nm	f=0.0018	<S**2>=0.000
240→264	0.20968	242→264	0.35547	244→263	-0.23446
241→265	0.41745	243→266	-0.24139		

Excited State 14:	Singlet-A2	4.5814 eV	270.62 nm	f=0.0000	<S**2>=0.000
240→265	0.21763	242→265	0.35701	244→266	-0.22328
241→264	0.41279	243→263	-0.21720		

Excited State 15:	Singlet-A1	4.6363 eV	267.42 nm	f=0.0027	<S**2>=0.000
243→265	0.47291	244→264	0.46934		

Excited State 16:	Singlet-B2	4.6372 eV	267.37 nm	f=0.0042	<S**2>=0.000
243→264	0.46792	244→265	0.46865		

Excited State 17:	Singlet-B1	4.6603 eV	266.04 nm	f=0.0049	<S**2>=0.000
240→264	0.12162	242→264	0.20299	244→263	0.40074
241→265	0.24200	243→266	0.41147	244→268	-0.12335

Excited State 18:	Singlet-A2	4.6620 eV	265.95 nm	f=0.0000	<S**2>=0.000
240→265	0.11818	241→264	0.22899	242→265	0.20287

243→263	0.40374	243→268	-0.12426	244→266	0.41249

Excited State 19:	Singlet-B1	4.7364 eV	261.77 nm	f=0.0003	<S**2>=0.000

247→263	0.11672	259→278	0.11436	261→279	0.18684
253→268	0.10041	260→268	-0.13248	262→266	0.15105
254→267	-0.11948	260→270	0.13517	262→273	0.27286
259→267	0.12645	260→275	0.15963	262→280	0.17304
259→269	0.14757	261→274	0.25401		

Excited State 20:	Singlet-A1	4.7437 eV	261.37 nm	f=0.0214	<S**2>=0.000

248→263	-0.11674	259→275	0.14323	261→273	0.25267
253→267	-0.12319	260→267	0.13094	261→280	0.18438
254→268	0.10754	260→269	0.15485	262→274	0.25310
259→268	-0.12530	260→278	0.11169	262→279	0.20257
259→270	0.13495	261→266	0.15418		

Excited State 21:	Singlet-A1	4.7622 eV	260.35 nm	f=0.0082	<S**2>=0.000

240→263	0.23548	242→263	0.39816
241→266	0.47255	242→268	-0.12319

Excited State 22:	Singlet-B2	4.7622 eV	260.35 nm	f=0.0031	<S**2>=0.000

240→266	0.24208	241→268	-0.14122
241→263	0.46274	242→266	0.40705

Excited State 23:	Singlet-A2	4.7972 eV	258.45 nm	f=0.0000	<S**2>=0.000

245→263	-0.18070	248→271	-0.10841	261→272	-0.18978
246→264	0.11132	257→275	-0.11455	261→278	0.20379
247→266	0.19096	259→274	0.24363	262→275	0.29275
248→265	0.10944	260→273	0.25099		

Excited State 24:	Singlet-B2	4.8036 eV	258.11 nm	f=0.0516	<S**2>=0.000	
245→264	0.11004	248→266	-0.19029	261→275	0.27122	
246→263	-0.18266	258→275	-0.11291	262→264	0.15023	
247→265	-0.11216	259→273	0.23736	262→272	-0.18045	
247→271	0.10657	260→274	0.24533	262→278	0.21508	

Excited State 25:	Singlet-B1	4.8353 eV	256.41 nm	f=0.0307	<S**2>=0.000	
245→266	0.13167	259→272	0.14559	261→279	0.30368	
247→263	-0.14931	259→278	-0.11303	262→273	-0.11038	
253→268	0.14129	260→270	0.10831	262→280	0.31800	
254→267	-0.15108	260→275	-0.18765			
259→269	0.10021	261→274	-0.11400			

Excited State 26:	Singlet-A1	4.8368 eV	256.34 nm	f=0.0015	<S**2>=0.000	
246→266	0.14247	259→275	-0.18602	261→280	0.29818	
248→263	0.16414	260→272	0.15054	262→274	-0.13099	
253→267	-0.14289	260→278	-0.12415	262→279	0.29605	
254→268	0.13720	261→273	-0.11162			

Excited State 27:	Singlet-B1	4.8622 eV	255.00 nm	f=0.1114	<S**2>=0.000	
257→266	0.13219	260→263	-0.33672	262→266	0.37872	
259→264	0.17365	260→268	-0.13543			
259→267	0.20236	261→265	-0.23034			

Excited State 28:	Singlet-A1	4.8718 eV	254.49 nm	f=0.0166	<S**2>=0.000	
255→265	0.10934	259→263	-0.31112	260→267	0.22311	
256→264	0.10238	259→268	-0.14348	261→266	0.37966	
258→266	0.12982	260→264	0.19785	262→265	-0.20963	

*C.2.12.2 **OTPT-FLR-221**, **¹ES** State*

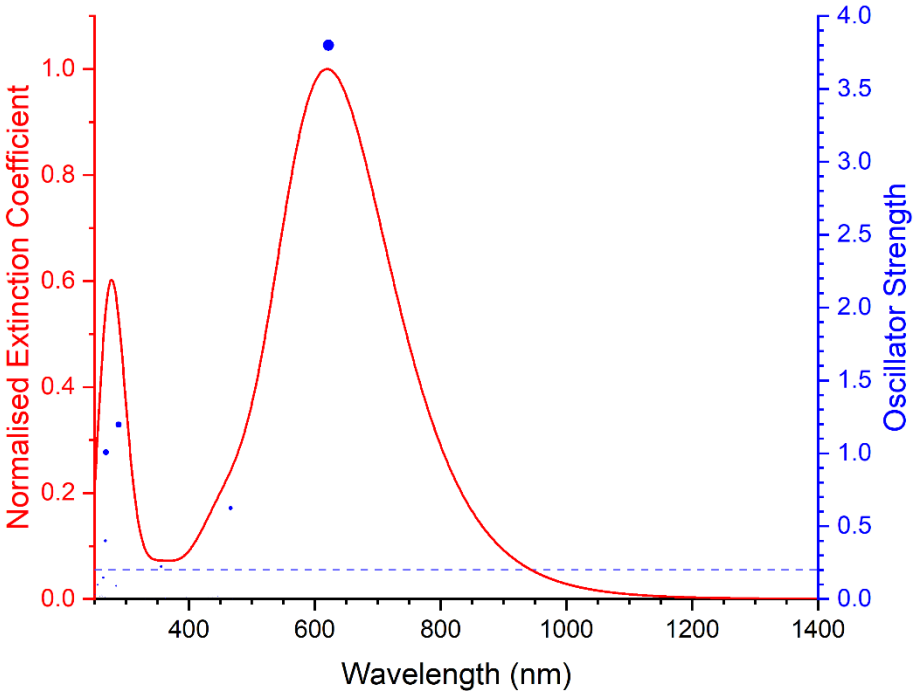

*Figure C-46 Excited states and normalised absorption spectra from TD-DFT calculations of **OTPT-FLR-221** in **¹ES** state. The areas of excited state dots are proportional to their oscillator strengths.*

Excited State 1:	Singlet-A2	1.8098 eV	685.07 nm	f=0.0000	<S**2>=0.000
259→261	0.49334	260→262	0.48765		
Excited State 2:	**Singlet-B2**	**1.9929 eV**	**622.13 nm**	**f=3.7983**	**<S**2>=0.000**
259→262	**0.47760**	**260→261**	**0.50952**		
Excited State 3:	Singlet-A2	2.6336 eV	470.78 nm	f=0.0000	<S**2>=0.000
259→261	0.49479	260→262	-0.49167		
Excited State 4:	Singlet-B2	2.6413 eV	469.40 nm	f=0.0018	<S**2>=0.000
259→262	0.51645	260→261	-0.47545		
Excited State 5:	**Singlet-B1**	**2.6568 eV**	**466.67 nm**	**f=0.6250**	**<S**2>=0.000**
253→261	**-0.45295**	256→262	0.12891		
254→262	**0.48357**	258→261	-0.15567		
Excited State 6:	Singlet-A1	2.7052 eV	458.31 nm	f=0.0170	<S**2>=0.000
253→262	-0.44031	254→261	0.50120	256→261	0.14659

258→262	-0.11229				

Excited State 7:	Singlet-A2	2.7774 eV	446.41 nm	f=0.0000	<S**2>=0.000
241→261	0.47690	250→261	0.11564		
242→262	0.47374	257→261	0.10018		

Excited State 8:	Singlet-B2	2.7781 eV	446.29 nm	f=0.0169	<S**2>=0.000
241→262	0.47788	242→261	0.47998	250→262	0.11261

Excited State 9:	Singlet-B1	2.8265 eV	438.65 nm	f=0.0099	<S**2>=0.000
249→261	0.10763	254→262	0.13959	258→261	0.66822

Excited State 10:	Singlet-A2	2.8414 eV	436.35 nm	f=0.0000	<S**2>=0.000
257→261	0.67958				

Excited State 11:	Singlet-A1	2.8570 eV	433.97 nm	f=0.0007	<S**2>=0.000
249→262	0.11981	254→261	0.10377	258→262	0.67369

Excited State 12:	Singlet-B2	2.8718 eV	431.73 nm	f=0.0110	<S**2>=0.000
257→262	0.68384				

Excited State 13:	Singlet-B1	3.0241 eV	409.98 nm	f=0.0008	<S**2>=0.000
239→261	0.22632	249→261	0.41734	258→261	-0.13630
240→262	0.22672	251→262	0.23045		
247→262	-0.35129	253→261	0.11019		

Excited State 14:	Singlet-A1	3.0266 eV	409.65 nm	f=0.0061	<S**2>=0.000
239→262	0.22864	249→262	0.40338	258→262	-0.15815
240→261	0.23111	251→261	0.23050		
247→261	-0.35100	253→262	0.10293		

Excited State 15:	Singlet-A2	3.0577 eV	405.48 nm	f=0.0000	<S**2>=0.000			
241→261	-0.10677	248→262	-0.37489	252→262	0.28134			
242→262	-0.10539	250→261	0.47439	257→261	-0.10869			
Excited State 16:	Singlet-B2	3.0589 eV	405.33 nm	f=0.0136	<S**2>=0.000			
241→262	-0.10413	250→262	0.45839	257→262	-0.12977			
242→261	-0.10399	252→261	0.28271					
248→261	-0.37497	255→261	-0.11752					
Excited State 17:	Singlet-A1	3.0806 eV	402.47 nm	f=0.0001	<S**2>=0.000			
253→262	0.11461	254→261	-0.10831	256→261	0.68205			
Excited State 18:	Singlet-B2	3.0807 eV	402.45 nm	f=0.0049	<S**2>=0.000			
255→261	0.69354							
Excited State 19:	Singlet-B1	3.1070 eV	399.05 nm	f=0.0029	<S**2>=0.000			
253→261	0.11502	256→262	0.67606					
Excited State 20:	Singlet-A2	3.1090 eV	398.79 nm	f=0.0000	<S**2>=0.000			
255→262	0.70171							
Excited State 21:	Singlet-B1	3.1257 eV	396.66 nm	f=0.0106	<S**2>=0.000			
239→261	0.43120	247→262	0.17007	251→262	-0.13021			
240→262	0.42740	249→261	-0.21641	256→262	0.13833			
Excited State 22:	Singlet-A1	3.1258 eV	396.65 nm	f=0.0001	<S**2>=0.000			
239→262	0.43413	247→261	0.18041	251→261	-0.13961			
240→261	0.43487	249→262	-0.21991					
Excited State 23:	Singlet-B1	3.4174 eV	362.81 nm	f=0.0078	<S**2>=0.000			
253→261	0.50319	254→262	0.47249					

Excited State 24:	Singlet-A1	3.4283 eV	361.65 nm	f=0.0002	<S**2>=0.000
253→262	0.51927	254→261	0.46041		
Excited State 25:	Singlet-A2	3.4810 eV	356.18 nm	f=0.0000	<S**2>=0.000
243→261	-0.45088	244→262	0.50915		
Excited State 26:	**Singlet-B2**	**3.4823 eV**	**356.05 nm**	**f=0.2234**	**<S**2>=0.000**
243→262	**-0.44266**	**244→261**	**0.51512**		
Excited State 27:	Singlet-A1	3.6040 eV	344.02 nm	f=0.0004	<S**2>=0.000
245→262	0.23559	251→261	0.52978	252→263	-0.11121
247→261	0.33284	251→265	0.11318		
Excited State 28:	Singlet-B2	3.6042 eV	344.00 nm	f=0.0000	<S**2>=0.000
246→262	0.23152	251→263	-0.11485	252→265	0.11039
248→261	0.35273	252→261	0.51832		
Excited State 29:	Singlet-B1	3.6384 eV	340.76 nm	f=0.0007	<S**2>=0.000
245→261	0.56589	246→263	-0.12039	251→262	0.31089
245→265	0.11485	247→262	0.17687		
Excited State 30:	Singlet-A2	3.6385 eV	340.75 nm	f=0.0000	<S**2>=0.000
245→263	-0.12091	246→265	0.11558	250→261	-0.10213
246→261	0.56424	248→262	0.17909	252→262	0.30966
Excited State 31:	Singlet-B2	3.7405 eV	331.46 nm	f=0.0004	<S**2>=0.000
246→262	0.63273	250→262	-0.11337		
248→261	-0.17194	252→261	-0.16345		
Excited State 32:	Singlet-A1	3.7409 eV	331.43 nm	f=0.0014	<S**2>=0.000
245→262	0.63560	247→261	-0.15334	251→261	-0.18175

Excited State 33:	Singlet-A2	3.7448 eV	331.08 nm	f=0.0000	<S**2>=0.000	
246→261	-0.34598	248→262	0.35796	252→262	0.47403	
Excited State 34:	Singlet-B1	3.7455 eV	331.03 nm	f=0.0003	<S**2>=0.000	
245→261	-0.34944	247→262	0.32897	251→262	0.49348	
Excited State 35:	Singlet-A2	3.9027 eV	317.69 nm	f=0.0000	<S**2>=0.000	
248→262	0.41228	250→261	0.48171	252→262	-0.27740	
Excited State 36:	Singlet-B2	3.9032 eV	317.65 nm	f=0.0000	<S**2>=0.000	
246→262	0.11570	250→262	0.48755			
248→261	0.39899	252→261	-0.27789			
Excited State 37:	Singlet-A1	3.9044 eV	317.55 nm	f=0.0000	<S**2>=0.000	
247→261	0.41607	249→262	0.49446	251→261	-0.26225	
Excited State 38:	Singlet-B1	3.9045 eV	317.54 nm	f=0.0000	<S**2>=0.000	
247→262	0.42909	249→261	0.48725	251→262	-0.25992	
Excited State 39:	Singlet-A2	4.2937 eV	288.76 nm	f=0.0000	<S**2>=0.000	
243→261	0.51187	244→262	0.45593			
Excited State 40:	**Singlet-B1**	**4.2969 eV**	**288.54 nm**	**f=1.1966**	**<S**2>=0.000**	
253→265	0.17523	**259→263**	**0.49209**			
254→266	0.11682	**260→264**	**0.41261**			
Excited State 41:	Singlet-B2	4.3131 eV	287.46 nm	f=0.0121	<S**2>=0.000	
243→262	0.52362	244→261	0.45944			
Excited State 42:	Singlet-A1	4.3599 eV	284.37 nm	f=0.0908	<S**2>=0.000	
254→265	-0.16092	258→266	0.11896	260→263	0.48634	
257→264	0.12514	259→264	0.37934			

Excited State 43:	Singlet-A2	4.5828 eV	270.54 nm	f=0.0000	<S**2>=0.000	
245→263	0.15163	247→267	0.18694	252→266	0.32571	
245→268	-0.13021	248→266	0.23578	259→265	-0.10186	
246→265	-0.19278	251→264	0.19624			
247→264	0.13274	251→267	0.28196			

Excited State 44:	Singlet-B1	4.5894 eV	270.16 nm	f=0.0063	<S**2>=0.000	
245→265	-0.17552	247→266	0.23069	251→266	0.35442	
246→263	0.13928	248→264	0.14498	252→264	0.20338	
246→268	-0.11839	248→267	0.20701	252→267	0.29058	

Excited State 45:	**Singlet-B2**	**4.6243 eV**	**268.11 nm**	**f=1.0069**	**<S**2>=0.000**	
248→265	-0.12186	252→265	-0.19648	258→264	0.20510	
251→263	0.15729	254→263	0.14061	258→267	0.28509	
251→268	-0.12971	**257→266**	**0.34610**	260→265	-0.18550	

Excited State 46:	Singlet-B1	4.6318 eV	267.68 nm	f=0.0051	<S**2>=0.000	
254→266	-0.13849	257→268	0.18286	260→264	-0.17017	
255→267	-0.13023	258→265	0.33415	260→267	-0.13533	
256→266	-0.18324	259→263	0.12427			
257→263	-0.30199	259→268	-0.10248			

Excited State 47:	Singlet-A1	4.6337 eV	267.57 nm	f=0.0109	<S**2>=0.000	
245→266	-0.11765	248→263	-0.19505	251→265	0.35525	
247→261	-0.11835	248→268	0.16266	252→263	-0.27917	
247→265	0.22768	251→261	-0.17794	252→268	0.23041	

Excited State 48:	**Singlet-B2**	**4.6362 eV**	**267.43 nm**	**f=0.3998**	**<S**2>=0.000**	
246→266	-0.10074	248→261	-0.10693	251→268	0.19952	
247→263	-0.15845	248→265	0.21039	252→261	-0.14464	
247→268	0.13062	251→263	-0.24099	252→265	0.28676	

257→266	0.24088	258→264	0.14827	258→267	0.20266

Excited State 49: Singlet-A2 4.6424 eV 267.07 nm f=0.0000 <S**2>=0.000

252→266	0.11082	256→267	0.14412	258→268	-0.19820
253→263	0.10909	257→265	-0.30248	259→265	0.20887
255→266	0.13952	258→263	0.32084	260→266	0.12457

Excited State 50: Singlet-A1 4.6718 eV 265.39 nm f=0.0000 <S**2>=0.000

216→261	0.10243	224→261	-0.13250	237→261	0.41958
221→262	0.21485	229→261	0.14085	238→262	-0.25278
223→261	0.19167	230→262	-0.28192		

Excited State 51: Singlet-B1 4.6740 eV 265.26 nm f=0.0045 <S**2>=0.000

216→262	0.10376	224→262	-0.13230	237→262	0.40738
221→261	0.21812	229→262	0.14197	238→261	-0.26321
223→262	0.19305	230→261	-0.28314		

Excited State 52: Singlet-A1 4.6965 eV 263.99 nm f=0.1471 <S**2>=0.000

257→264	0.24497	258→266	0.42133	259→264	-0.18944
257→267	0.35558	258→271	0.11496	260→263	-0.10325

Excited State 53: Singlet-A2 4.6987 eV 263.87 nm f=0.0000 <S**2>=0.000

245→263	-0.22423	251→267	0.14410	256→264	-0.11351
245→268	0.18700	252→266	0.15249	256→267	-0.15334
246→261	-0.13499	253→263	0.14142	259→265	0.17814
246→265	0.28043	254→264	-0.10303	260→266	-0.18427
248→266	0.10895	255→266	-0.14858		

Excited State 54: Singlet-B1 4.7181 eV 262.78 nm f=0.0168 <S**2>=0.000

245→261	-0.18203	246→263	-0.31480	251→266	0.14332
245→265	0.38902	246→268	0.25892	252→267	0.12532

Excited State 55:	Singlet-A2	4.7454 eV	261.27 nm	f=0.0000	<S**2>=0.000
241→261	-0.49522	242→262	0.49872		
Excited State 56:	Singlet-B2	4.7455 eV	261.26 nm	f=0.0000	<S**2>=0.000
241→262	0.49809	242→261	-0.49708		
Excited State 57:	Singlet-B2	4.7511 eV	260.96 nm	f=0.0019	<S**2>=0.000
245→264	0.27003	246→262	0.13507		
245→267	0.35457	246→266	0.43443		
Excited State 58:	Singlet-A1	4.7569 eV	260.64 nm	f=0.0270	<S**2>=0.000
245→262	0.13774	246→264	0.27132		
245→266	0.43316	246→267	0.35311		
Excited State 59:	Singlet-A2	4.7597 eV	260.49 nm	f=0.0000	<S**2>=0.000
245→263	0.21286	253→263	0.16091	256→267	-0.18515
245→268	-0.17145	254→264	-0.10629	258→263	0.13513
246→261	0.11273	255→266	-0.18825	259→265	0.25991
246→265	-0.25758	256→264	-0.13786	260→266	-0.18473
Excited State 60:	Singlet-B1	4.7908 eV	258.80 nm	f=0.0198	<S**2>=0.000
254→266	-0.10710	256→266	0.36897	258→265	0.15440
255→264	0.22725	256→271	0.14157	258→282	0.12851
255→267	0.33522	257→263	-0.15349		
255→274	-0.10312	257→281	0.12148		
Excited State 61:	Singlet-A2	4.8204 eV	257.21 nm	f=0.0000	<S**2>=0.000
244→266	-0.10555	254→267	-0.16500	256→264	0.14232
253→263	0.12425	255→266	0.31843	256→267	0.24223
254→264	-0.20327	255→271	0.10972	257→265	0.14100

257→282	0.10745	258→281	0.10129	260→266	-0.22763
258→263	-0.11455	259→265	0.16492		

Excited State 62: Singlet-B1 4.8637 eV 254.92 nm f=0.0957 <S**2>=0.000

216→262	0.15355	223→262	0.39081	237→262	-0.19484
221→261	0.39993	229→262	-0.11665	238→261	0.13817
222→261	-0.10660	230→261	0.14041		

Excited State 63: Singlet-A1 4.8697 eV 254.60 nm f=0.0005 <S**2>=0.000

216→261	0.15574	223→261	0.39531	237→261	-0.20624
221→262	0.40146	229→261	-0.10922	238→262	0.12839
222→262	-0.10533	230→262	0.13737		

Excited State 64: Singlet-B2 4.9381 eV 251.08 nm f=0.0317 <S**2>=0.000

244→265	0.10182	256→263	-0.12123	259→266	-0.21581
253→264	0.14769	257→266	0.16525	260→265	0.41349
254→263	-0.28063	258→264	0.14581		
254→268	0.12314	258→267	0.15749		

*C.2.12.3 **OTPT-FLR-221**, ^{5}**ES** State*

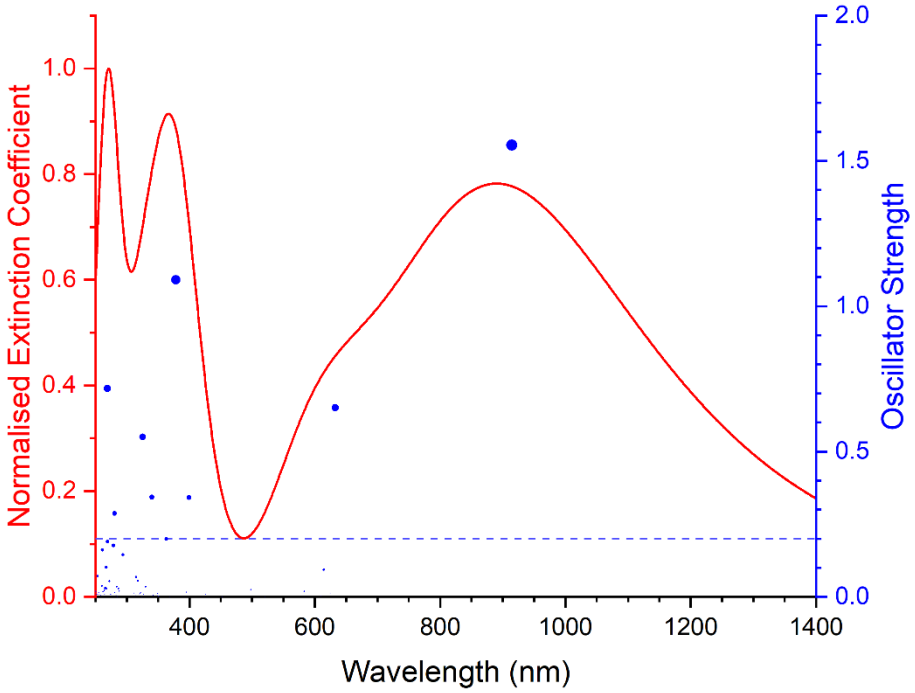

*Figure C-47 Excited states and normalised absorption spectra from TD-DFT calculations of **OTPT-FLR-221** in ^{5}**ES** state. The areas of excited state dots are proportional to their oscillator strengths.*

Excited State 1:	5.094-A2	1.1974 eV	1035.42 nm	f=0.0000	<S**2>=6.237
249B→261B	0.20346	253B→260B	-0.16992	258B→259B	-0.20275
250B→262B	0.20100	255B→259B	-0.62887		
252B→262B	0.11233	256B→260B	0.64726		
Excited State 2:	**5.099-B2**	**1.3560 eV**	**914.31 nm**	**f=1.5538**	**<S**2>=6.250**
249B→262B	0.18755	253B→259B	-0.16840	258B→260B	-0.18379
250B→261B	0.19349	**255B→260B**	**-0.61489**		
252B→261B	0.11382	**256B→259B**	**0.65172**		
Excited State 3:	**5.088-B1**	**1.9593 eV**	**632.80 nm**	**f=0.6506**	**<S**2>=6.223**
242B→259B	-0.13913	250B→260B	0.24256	**255B→261B**	**-0.43205**
245B→262B	0.10673	**251B→259B**	**0.37352**	**256B→262B**	**0.44469**
246B→261B	0.11596	**252B→260B**	**0.43307**	258B→261B	-0.14712
249B→259B	0.28616	253B→262B	-0.11556		

Excited State 4:	5.104-A1	1.9842 eV	624.85 nm	f=0.0117	<S**2>=6.264
242B→260B	-0.12152	249B→260B	0.13352	255B→262B	-0.31794
245B→261B	0.19598	251B→260B	0.51094	256B→261B	0.35176
246B→262B	0.20430	252B→259B	0.55228		

Excited State 5:	5.104-B1	2.0172 eV	614.65 nm	f=0.0929	<S**2>=6.263
244B→260B	0.18553	250B→260B	-0.37441	256B→262B	-0.20637
245B→262B	0.27557	251B→259B	0.46858	257B→259B	0.10885
246B→261B	0.27822	252B→260B	0.40325	258B→261B	0.11029
249B→259B	-0.35728	255B→261B	0.20447		

Excited State 6:	5.102-A1	2.0329 eV	609.89 nm	f=0.0031	<S**2>=6.258
244B→259B	-0.18360	250B→259B	0.44356	256B→261B	0.36071
245B→261B	-0.22070	251B→260B	-0.31001	258B→262B	-0.13535
246B→262B	-0.22051	252B→259B	-0.22513		
249B→260B	0.42068	255B→262B	-0.32820		

Excited State 7:	5.095-A2	2.0851 eV	594.63 nm	f=0.0000	<S**2>=6.240
239B→259B	0.19770	243B→259B	-0.15631	249B→261B	-0.19556
240B→261B	0.17585	244B→262B	0.31302	251B→261B	0.19659
241B→260B	-0.24343	245B→260B	0.50387	252B→262B	0.19743
242B→261B	-0.19176	246B→259B	0.51123	258B→259B	0.17561

Excited State 8:	5.095-B2	2.0884 eV	593.68 nm	f=0.0154	<S**2>=6.240
239B→260B	0.19466	243B→260B	-0.15244	249B→262B	-0.19612
240B→262B	0.17522	244B→261B	0.31732	251B→262B	0.19919
241B→259B	-0.24560	245B→259B	0.51443	252B→261B	0.20034
242B→262B	-0.18999	246B→260B	0.51362	258B→260B	0.13241

Excited State 9:	5.096-B1	2.1268 eV	582.96 nm	f=0.0184	<S**2>=6.243
239B→261B	0.25842	240B→259B	0.33854	241B→262B	-0.33603

242B→259B	-0.39961	246B→261B	0.12260	252B→260B	-0.12448
243B→261B	-0.22293	249B→259B	-0.15429	257B→259B	0.16190
244B→260B	0.53038	250B→260B	0.18297		
245B→262B	0.12513	251B→259B	-0.17974		

Excited State 10: 5.096-A1 2.1295 eV 582.23 nm f=0.0018 <S**2>=6.242

239B→262B	0.25846	244B→259B	0.54339	251B→260B	-0.17342
240B→260B	0.33883	245B→261B	0.13318	252B→259B	-0.11775
241B→261B	-0.34085	246B→262B	0.12545	257B→260B	0.11404
242B→260B	-0.39866	249B→260B	-0.15826		
243B→262B	-0.22224	250B→259B	0.18231		

Excited State 11: 5.109-A2 2.1940 eV 565.10 nm f=0.0000 <S**2>=6.275

239B→259B	-0.37663	243B→259B	0.33846	250B→262B	-0.17177
240B→261B	-0.13812	244B→262B	-0.19950	251B→261B	0.32092
241B→260B	0.50494	245B→260B	0.24178	252B→262B	0.28333
242B→261B	0.16773	246B→259B	0.25720	258B→259B	-0.10063

Excited State 12: 5.109-B2 2.1948 eV 564.90 nm f=0.0055 <S**2>=6.275

239B→260B	-0.37987	243B→260B	0.33999	250B→261B	-0.17371
240B→262B	-0.14159	244B→261B	-0.20832	251B→262B	0.31695
241B→259B	0.51504	245B→259B	0.23107	252B→261B	0.28026
242B→262B	0.17081	246B→260B	0.24855		

Excited State 13: 5.113-A2 2.3754 eV 521.96 nm f=0.0000 <S**2>=6.286

241B→260B	0.11193	257B→261B	0.34641	258B→263B	0.11482
255B→259B	-0.13759	257B→265B	0.10239		
256B→260B	0.13810	258B→259B	0.86091		

Excited State 14: 5.113-B1 2.3831 eV 520.27 nm f=0.0005 <S**2>=6.287

244B→260B	-0.12803	255B→261B	-0.11880	257B→259B	0.88040

257B→263B	0.11531	258B→261B	0.33043	258B→265B	0.10279

Excited State 15:	5.141-B2	2.4892 eV	498.08 nm	f=0.0235	<S**2>=6.358
256B→259B	0.17053	257B→266B	-0.12200	258B→264B	-0.12578
257B→262B	0.30429	258B→260B	0.87244		

Excited State 16:	5.142-A1	2.5008 eV	495.77 nm	f=0.0019	<S**2>=6.361
255B→262B	-0.12069	257B→264B	-0.12631	258B→266B	-0.12550
257B→260B	0.88879	258B→262B	0.28649		

Excited State 17:	5.145-B2	2.7005 eV	459.11 nm	f=0.0000	<S**2>=6.369
238B→259B	0.13731	254B→261B	0.18951	256B→259B	0.60557
253B→259B	0.41297	255B→260B	0.55001		

Excited State 18:	5.105-A1	2.7414 eV	452.26 nm	f=0.0003	<S**2>=6.266
253B→261B	0.30855	254B→259B	0.92640	255B→262B	0.10779

Excited State 19:	5.087-A2	2.7480 eV	451.19 nm	f=0.0000	<S**2>=6.218
255B→259B	0.69312	256B→260B	0.69378		

Excited State 20:	5.102-B2	2.7739 eV	446.96 nm	f=0.0017	<S**2>=6.258
253B→259B	0.82719	255B→260B	-0.41879		
254B→261B	0.23910	256B→259B	-0.17770		

Excited State 21:	5.214-A1	2.8074 eV	441.63 nm	f=0.0007	<S**2>=6.545
240B→260B	0.12386	247B→263B	0.27296	248B→265B	0.25788
242B→260B	0.11082	247B→268B	-0.10134		
247B→259B	0.73369	248B→261B	0.45708		

Excited State 22:	5.212-B2	2.8079 eV	441.56 nm	f=0.0003	<S**2>=6.541
239B→260B	0.10390	245B→259B	0.12473	247B→265B	0.25778
243B→260B	0.13296	247B→261B	0.45889	248B→259B	0.72092

248B→263B	0.26845	253B→259B	0.10894		

Excited State 23:	5.100-B1	2.8389 eV	436.73 nm	f=0.0029	<S**2>=6.252
249B→259B	0.12114	253B→262B	0.27217	255B→261B	0.20549
250B→260B	0.16230	254B→260B	0.88449		

Excited State 24:	5.094-A2	2.8592 eV	433.63 nm	f=0.0000	<S**2>=6.238
253B→260B	0.94182	254B→262B	0.25399	255B→259B	-0.18274

Excited State 25:	5.134-A1	2.8961 eV	428.10 nm	f=0.0001	<S**2>=6.338
232B→262B	-0.10331	249B→260B	0.34191	254B→259B	-0.15166
237B→262B	-0.15188	250B→259B	0.45411	255B→262B	0.41766
238B→261B	0.21548	251B→260B	0.10956	256B→261B	-0.42180
242B→260B	-0.13635	252B→259B	0.23810	258B→262B	0.15064

Excited State 26:	5.128-B1	2.9086 eV	426.27 nm	f=0.0089	<S**2>=6.324
237B→261B	-0.13721	250B→260B	0.42633	255B→261B	0.39697
238B→262B	0.18061	251B→259B	0.10970	256B→262B	-0.38891
242B→259B	-0.14805	252B→260B	0.22354	258B→261B	0.14856
249B→259B	0.34983	254B→260B	-0.37044		

Excited State 27:	5.526-B2	2.9629 eV	418.46 nm	f=0.0004	<S**2>=7.383
254A→263A	-0.13489	261A→268A	-0.13386	256B→259B	-0.26154
256A→265A	-0.12402	262A→267A	0.10114	256B→263B	0.13277
257A→280A	0.11622	237B→260B	-0.15935	257B→266B	0.26160
258A→282A	0.11750	238B→259B	0.22411	257B→271B	-0.10966
259A→264A	-0.20235	249B→262B	0.15737	258B→260B	0.26713
259A→267A	-0.18750	250B→261B	0.18631	258B→264B	0.24037
259A→276A	-0.13668	253B→280B	-0.12264	258B→267B	0.14814
260A→266A	-0.25696	254B→281B	-0.10624		
260A→271A	-0.14518	255B→260B	-0.22045		

Excited State 28:	5.704-A1	2.9966 eV	413.75 nm	f=0.0002	<S**2>=7.883	
257A→282A	0.16512	260A→276A	-0.17507	257B→260B	0.26406	
258A→280A	0.15270	260A→285A	-0.10516	257B→264B	0.29114	
259A→266A	-0.31543	235B→259B	0.11228	257B→267B	0.22020	
259A→271A	-0.18576	249B→260B	-0.13905	257B→278B	0.12842	
259A→286A	-0.10008	253B→281B	-0.13600	258B→266B	0.34030	
260A→264A	-0.24797	254B→259B	-0.10215	258B→271B	-0.13400	
260A→267A	-0.23443	254B→280B	-0.16877	258B→273B	-0.11348	

Excited State 29:	5.161-B1	2.9976 eV	413.61 nm	f=0.0015	<S**2>=6.409	
239B→261B	0.29256	242B→259B	0.47029	247B→260B	0.26272	
239B→265B	0.13563	242B→263B	0.14503	248B→262B	0.14377	
240B→259B	0.58493	243B→261B	0.34802	249B→259B	0.10689	
240B→263B	0.17696	243B→265B	0.16398			

Excited State 30:	5.161-A2	2.9981 eV	413.54 nm	f=0.0000	<S**2>=6.409	
239B→259B	0.48372	242B→261B	0.29451	247B→262B	0.14846	
239B→263B	0.14563	242B→265B	0.13390	248B→260B	0.26260	
240B→261B	0.34402	243B→259B	0.57963			
240B→265B	0.16204	243B→263B	0.17738			

Excited State 31:	5.327-A2	3.0560 eV	405.71 nm	f=0.0000	<S**2>=6.844	
253A→268A	-0.10459	262A→268A	0.34148	250B→262B	-0.27478	
254A→267A	0.10392	228B→260B	-0.10932	252B→262B	-0.10862	
261A→264A	0.27900	232B→259B	0.15986	255B→263B	0.15280	
261A→267A	-0.31718	237B→259B	0.23564	255B→268B	0.11206	
261A→276A	0.12005	238B→260B	-0.28604	256B→264B	0.13047	
262A→263A	-0.29078	249B→261B	-0.25525	256B→267B	-0.13211	

Excited State 32:	**5.462-B2**	**3.1041 eV**	**399.42 nm**	**f=0.3418**	**<S**2>=7.208**	
257A→280A	0.10491	262A→264A	0.20188	249B→262B	-0.20537	
258A→282A	0.11397	262A→267A	-0.25570	250B→261B	-0.25510	
259A→264A	-0.13296	262A→276A	0.10531	252B→261B	-0.10813	
259A→267A	-0.13123	228B→259B	-0.10573	253B→280B	-0.10796	
259A→276A	-0.10208	232B→260B	0.14521	255B→264B	-0.14711	
260A→266A	-0.17157	237B→260B	0.18898	256B→263B	-0.12621	
260A→271A	-0.10687	238B→259B	-0.23851	257B→266B	0.21192	
261A→263A	-0.19914	239B→260B	0.10487	258B→264B	0.14559	
261A→268A	0.27713	242B→262B	0.14345	258B→267B	0.16478	

Excited State 33:	5.183-A1	3.1375 eV	395.17 nm	f=0.0011	<S**2>=6.466	
239B→262B	0.28158	242B→260B	0.48469	247B→259B	-0.13470	
239B→266B	-0.13910	242B→264B	-0.14862	249B→260B	0.12298	
240B→260B	0.61007	243B→262B	0.33483			
240B→264B	-0.18148	243B→266B	-0.16894			

Excited State 34:	5.195-B2	3.1398 eV	394.87 nm	f=0.0157	<S**2>=6.497	
239B→260B	0.49354	240B→266B	-0.16527	243B→260B	0.59907	
239B→264B	-0.14928	242B→262B	0.25603	243B→264B	-0.17880	
240B→262B	0.33877	242B→266B	-0.13553	248B→259B	-0.13519	

Excited State 35:	**5.313-B2**	**3.2789 eV**	**378.12 nm**	**f=1.0905**	**<S**2>=6.808**	
254A→268A	0.13121	**261A→263A**	**0.38888**	238B→259B	-0.17749	
255A→266A	-0.14928	261A→268A	-0.18001	246B→260B	0.11818	
255A→271A	0.11707	**262A→264A**	**-0.32733**	251B→262B	-0.24363	
256A→265A	0.22900	262A→267A	0.21997	252B→261B	-0.28268	
260A→266A	-0.10885	237B→260B	0.11622	256B→259B	0.15344	

Excited State 36:	5.144-A2	3.2948 eV	376.30 nm	f=0.0000	<S**2>=6.365	
255A→265A	0.10124	241B→260B	0.10828	248B→260B	0.71713	
261A→264A	-0.12336	243B→259B	-0.15045	248B→264B	-0.15854	
262A→263A	0.14720	245B→260B	0.17044	251B→261B	-0.12988	
239B→259B	-0.17868	247B→262B	0.36264	252B→262B	-0.14617	
240B→261B	-0.10779	247B→266B	-0.14524			

Excited State 37:	5.131-B1	3.2949 eV	376.29 nm	f=0.0002	<S**2>=6.333	
240B→259B	-0.19607	247B→260B	0.80978	248B→266B	-0.15732	
242B→259B	-0.13943	247B→264B	-0.17220	250B→260B	0.12268	
243B→261B	-0.10074	248B→262B	0.39145			

Excited State 38:	5.178-A2	3.3015 eV	375.54 nm	f=0.0000	<S**2>=6.453	
253A→263A	-0.10627	232B→259B	-0.11578	249B→261B	0.16202	
255A→265A	-0.20628	237B→259B	-0.16700	250B→262B	0.14290	
256A→266A	0.14367	238B→260B	0.19500	251B→261B	0.31729	
256A→271A	-0.11043	243B→259B	-0.12354	252B→262B	0.34006	
261A→264A	0.24608	246B→259B	-0.12883	256B→260B	-0.12567	
261A→267A	-0.12158	247B→262B	0.15497			
262A→263A	-0.29369	248B→260B	0.37422			

Excited State 39:	5.310-A1	3.3673 eV	368.20 nm	f=0.0001	<S**2>=6.800	
240A→263A	-0.10213	238B→261B	0.19645	255B→262B	0.31389	
254A→265A	-0.18992	242B→260B	0.17617	256B→261B	0.38269	
256A→263A	-0.17848	249B→260B	-0.33038	256B→265B	0.16638	
259A→266A	0.10039	250B→259B	0.20521	257B→260B	-0.10821	
261A→265A	-0.12595	250B→263B	0.16493	258B→262B	0.20592	
235B→259B	0.26026	251B→260B	-0.11077			

Excited State 40:	5.173-B2	3.4134 eV	363.23 nm	f=0.1985	<S**2>=6.440	
256A→265A	0.13407	241B→259B	-0.18482	250B→261B	-0.19005	
261A→263A	0.19025	243B→260B	-0.13052	251B→262B	0.50182	
262A→264A	-0.15351	245B→259B	-0.28034	252B→261B	0.48414	
239B→260B	0.15916	246B→260B	-0.27367			

Excited State 41:	5.157-A2	3.4279 eV	361.69 nm	f=0.0000	<S**2>=6.399	
255A→265A	0.16773	239B→259B	0.14135	250B→262B	-0.24507	
256A→266A	-0.11846	241B→260B	-0.17931	251B→261B	0.46545	
261A→264A	-0.18801	243B→259B	-0.12643	252B→262B	0.40583	
262A→263A	0.22610	245B→260B	-0.26315	257B→261B	0.12524	
237B→259B	0.11474	246B→259B	-0.27014			
238B→260B	-0.13286	249B→261B	-0.13118			

Excited State 42:	5.119-B1	3.4473 eV	359.65 nm	f=0.0024	<S**2>=6.300	
242B→259B	0.13447	251B→259B	-0.11029	257B→259B	-0.32923	
249B→259B	-0.25331	255B→261B	0.20102	257B→263B	0.10816	
250B→260B	0.22133	256B→262B	0.43171	258B→261B	0.64884	

Excited State 43:	5.134-A2	3.4977 eV	354.47 nm	f=0.0000	<S**2>=6.341	
257B→261B	0.86295	258B→259B	-0.38953			
257B→265B	0.12025	258B→263B	0.14184			

Excited State 44:	5.122-B1	3.5379 eV	350.44 nm	f=0.0020	<S**2>=6.309	
235B→260B	-0.13246	245B→262B	-0.21428	255B→261B	-0.42069	
238B→262B	-0.11655	246B→261B	-0.23213	256B→262B	-0.29540	
239B→261B	0.12521	249B→259B	0.20981	257B→259B	-0.23116	
241B→262B	-0.16852	250B→260B	-0.27498	258B→261B	0.49289	
243B→261B	-0.12863	251B→259B	0.21648			

Excited State 45:	5.194-A1	3.5423 eV	350.01 nm	f=0.0054	<S**2>=6.495	
253A→266A	-0.10062	236B→260B	0.11237	249B→260B	-0.15475	
254A→265A	0.12168	237B→262B	0.13293	251B→260B	0.13092	
255A→264A	-0.11477	239B→262B	0.19358	252B→259B	0.24193	
256A→263A	0.13657	241B→261B	-0.22769	255B→262B	0.15010	
261A→265A	0.11149	243B→262B	-0.15836	256B→261B	0.27221	
229B→260B	0.10777	245B→261B	-0.35217	257B→260B	-0.15360	
235B→259B	-0.10675	246B→262B	-0.32863	258B→262B	0.35282	

Excited State 46:	5.140-B1	3.5470 eV	349.55 nm	f=0.0109	<S**2>=6.355	
239B→261B	-0.23280	246B→261B	0.44606	252B→260B	-0.27514	
241B→262B	0.29599	249B→259B	0.21805	255B→261B	-0.24884	
243B→261B	0.20059	251B→259B	-0.17911	256B→262B	-0.23366	
245B→262B	0.43001	251B→268B	0.10066	258B→261B	0.21949	

Excited State 47:	5.237-A1	3.5488 eV	349.37 nm	f=0.0018	<S**2>=6.607	
253A→266A	-0.10167	241B→261B	0.27062	251B→260B	-0.20898	
254A→265A	0.13082	243B→262B	0.16843	252B→259B	-0.11288	
255A→264A	-0.11528	245B→261B	0.34814	256B→261B	0.17279	
256A→263A	0.14238	246B→262B	0.36862	257B→260B	-0.14987	
261A→265A	0.10619	250B→259B	0.22353	258B→262B	0.37321	
239B→262B	-0.17106	250B→263B	-0.10776			

Excited State 48:	5.115-B2	3.6207 eV	342.43 nm	f=0.0050	<S**2>=6.291	
257B→262B	0.91825	258B→260B	-0.30248			

Excited State 49:	**5.381-B1**	**3.6449 eV**	**340.16 nm**	**f=0.3423**	**<S**2>=6.990**	
239A→263A	-0.11256	254A→266A	-0.20547	255A→268A	0.12097	
243A→273A	-0.10135	254A→271A	0.13369	256A→264A	-0.26069	
253A→265A	0.28379	**255A→263A**	**0.34549**	256A→276A	0.15627	

261A→266A	-0.20311	236B→259B	0.10669	255B→265B	0.17598
261A→271A	0.11245	237B→261B	0.12267	256B→266B	0.13012
262A→265A	0.28672	238B→262B	-0.14524	256B→271B	0.11328
229B→259B	0.16651	249B→263B	-0.13921	258B→261B	-0.11787
235B→260B	-0.18570	250B→264B	0.12776		

Excited State 50: 5.141-A1 3.6636 eV 338.42 nm f=0.0003 <S**2>=6.358

254A→265A	-0.11004	250B→259B	-0.18600	256B→261B	-0.19852
256A→263A	-0.12689	251B→260B	0.12733	257B→260B	-0.21288
261A→265A	-0.10295	252B→259B	-0.15636	258B→262B	0.71184
249B→260B	0.15473	255B→262B	-0.39435		

Excited State 51: 5.090-B1 3.7193 eV 333.35 nm f=0.0018 <S**2>=6.227

244B→260B	-0.10992	250B→260B	0.20583	252B→260B	-0.65938
249B→259B	-0.11608	251B→259B	0.67511	255B→261B	0.11425

Excited State 52: 5.089-A1 3.7199 eV 333.30 nm f=0.0000 <S**2>=6.224

244B→259B	-0.10336	251B→260B	0.68061	256B→261B	0.10364
249B→260B	-0.12229	252B→259B	-0.64729		
250B→259B	0.21754	255B→262B	0.12327		

Excited State 53: 5.427-B2 3.7566 eV 330.05 nm f=0.0346 <S**2>=7.113

240A→265A	0.10511	253A→264A	-0.13182	244B→272B	0.10084
242A→269A	-0.10677	254A→263A	0.19519	249B→262B	0.22548
243A→274A	0.11306	255A→266A	-0.10678	250B→261B	0.24145
244A→272A	0.12683	256A→265A	0.18070	250B→265B	-0.15534
245A→273A	0.10899	228B→259B	0.12744	253B→259B	-0.11477
246A→275A	-0.10027	232B→260B	-0.14488	254B→261B	0.40164
251A→278A	0.11562	237B→260B	-0.16821	255B→260B	0.11181
252A→277A	0.11813	238B→259B	0.18069	255B→264B	-0.14085

256B→259B	-0.10434	256B→263B	-0.19980		

Excited State 54:	5.499-A2	3.7659 eV	329.23 nm	f=0.0000	<S**2>=7.310
241A→269A	-0.10479	255A→265A	0.19919	244B→273B	-0.12793
242A→270A	-0.10404	256A→266A	-0.14186	245B→260B	0.15672
243A→272A	-0.16854	262A→268A	0.11257	245B→275B	-0.10165
244A→274A	-0.15564	232B→259B	-0.11186	246B→259B	-0.10352
245A→275A	0.13258	235B→262B	0.11265	246B→274B	0.10767
246A→273A	-0.14146	237B→259B	-0.21687	250B→262B	0.13243
251A→277A	0.11633	238B→260B	0.31003	255B→263B	0.21284
252A→278A	0.11404	239B→259B	-0.12522	256B→264B	0.16732
253A→263A	0.20281	241B→260B	-0.13514	256B→267B	-0.10592
254A→264A	-0.16701	243B→259B	0.10072		

Excited State 55:	5.103-A1	3.7832 eV	327.72 nm	f=0.0000	<S**2>=6.259
249B→260B	0.16293	253B→261B	0.85772	256B→261B	0.30464
250B→259B	-0.13001	254B→259B	-0.30634		

Excited State 56:	5.179-B2	3.7905 eV	327.09 nm	f=0.0085	<S**2>=6.456
237B→260B	0.13580	253B→259B	-0.27134	256B→263B	0.12475
238B→259B	-0.15454	254B→261B	0.84023		

Excited State 57:	5.322-B1	3.8098 eV	325.43 nm	f=0.5500	<S**2>=6.831
239A→268A	-0.10648	246A→272A	-0.11086	261A→281A	-0.14263
240A→267A	-0.10053	251A→269A	-0.13627	262A→265A	0.16320
241A→277A	0.10090	252A→270A	-0.13640	262A→279A	-0.15453
242A→278A	0.10627	255A→263A	0.17827	229B→259B	-0.24865
243A→273A	-0.11646	256A→264A	-0.14466	235B→260B	0.32915
244A→275A	0.11100	261A→266A	-0.11227	236B→259B	-0.19566
245A→274A	-0.10827	261A→271A	0.12590	237B→261B	-0.16006

238B→262B	0.20609	244B→260B	0.19286	251B→270B	0.13538
240B→259B	-0.12189	250B→260B	0.17099	252B→269B	0.13490
242B→259B	0.12723	251B→259B	0.10445	255B→261B	-0.23385

Excited State 58: 5.291-B1 3.8230 eV 324.31 nm f=0.0003 <S**2>=6.748

257A→266A	0.18593	244B→260B	0.13724	254B→260B	-0.23695
257A→271A	0.10765	249B→259B	0.25751	254B→264B	-0.21032
258A→264A	0.14324	250B→260B	-0.19312	254B→267B	-0.11898
258A→267A	0.13444	253B→262B	0.66225	255B→261B	0.13740
258A→276A	0.10038	253B→266B	-0.21450	256B→262B	0.32137

Excited State 59: 5.337-A2 3.8272 eV 323.96 nm f=0.0000 <S**2>=6.871

257A→264A	0.16513	258A→271A	0.11966	254B→262B	0.77840
257A→267A	0.15282	253B→260B	-0.23745	254B→266B	-0.24635
257A→276A	0.11287	253B→264B	-0.22291		
258A→266A	0.20342	253B→267B	-0.12682		

Excited State 60: 5.250-A1 3.8497 eV 322.06 nm f=0.0139 <S**2>=6.641

243A→275A	0.10083	261A→265A	-0.13970	250B→259B	-0.36100
244A→273A	-0.10946	261A→279A	0.11449	251B→269B	-0.10987
245A→272A	-0.10135	262A→271A	-0.10545	252B→270B	-0.10561
251A→270A	0.11391	229B→260B	0.14886	253B→261B	-0.23260
252A→269A	0.11354	235B→259B	-0.23995	255B→262B	0.41820
255A→264A	0.13679	238B→261B	-0.13886	256B→261B	0.23338
256A→263A	-0.15070	249B→260B	0.28549		

Excited State 61: 5.107-B2 3.8600 eV 321.20 nm f=0.0124 <S**2>=6.269

235B→261B	-0.12127	239B→260B	0.31681	242B→262B	-0.14643
237B→260B	0.10168	240B→262B	0.12139	243B→260B	-0.23395
238B→259B	-0.12824	241B→259B	0.40152	244B→261B	-0.16330

245B→259B	-0.45904	246B→260B	0.50803	250B→261B	0.16243

Excited State 62: 5.151-B1 3.8650 eV 320.79 nm f=0.0006 <S**2>=6.383

257A→266A	-0.10972	249B→259B	0.48142	253B→266B	0.11600
240B→259B	-0.18979	250B→260B	-0.30766	254B→264B	0.11045
242B→259B	0.14574	252B→260B	-0.13718	255B→261B	0.31839
244B→260B	0.42404	253B→262B	-0.34991	256B→262B	0.24650

Excited State 63: 5.144-A2 3.8674 eV 320.59 nm f=0.0000 <S**2>=6.366

239B→259B	0.28911	242B→261B	-0.13642	245B→260B	-0.47738
240B→261B	0.11743	243B→259B	-0.21576	246B→259B	0.51504
241B→260B	0.38437	244B→262B	-0.15044	250B→262B	0.17848

Excited State 64: 5.171-A1 3.8720 eV 320.21 nm f=0.0071 <S**2>=6.434

255A→264A	-0.10625	236B→260B	-0.11034	249B→260B	0.43081
256A→263A	0.13784	240B→260B	-0.27223	251B→260B	0.10910
261A→265A	0.12595	241B→261B	-0.11031	253B→261B	-0.18519
229B→260B	-0.13338	242B→260B	0.24821	255B→262B	0.12705
235B→259B	0.13674	244B→259B	0.50883	256B→261B	0.15843

Excited State 65: 5.221-B2 3.9019 eV 317.75 nm f=0.0544 <S**2>=6.564

243A→274A	0.10017	237B→260B	-0.18437	249B→262B	-0.37135
244A→272A	0.11404	238B→259B	0.41582	250B→261B	-0.24888
229B→262B	-0.12745	239B→260B	0.10425	255B→260B	-0.19860
235B→261B	0.29073	245B→259B	-0.30075		
236B→262B	-0.14360	246B→260B	0.21850		

Excited State 66: 5.159-B1 3.9350 eV 315.08 nm f=0.0671 <S**2>=6.404

229B→259B	0.10235	242B→259B	0.46020	250B→260B	0.34221
237B→261B	0.11012	244B→260B	0.46838	255B→261B	-0.17725
240B→259B	-0.36076	249B→259B	-0.16027	256B→262B	-0.19261

Excited State 67:	5.161-A1	3.9386 eV	314.79 nm	f=0.0032	<S**2>=6.410	
229B→260B	0.14937	240B→260B	-0.34220	250B→259B	0.34699	
235B→259B	-0.12639	242B→260B	0.44120	253B→261B	0.14365	
236B→260B	0.12627	244B→259B	0.40418	255B→262B	-0.18007	
237B→262B	0.13863	249B→260B	-0.19686	256B→261B	-0.18939	

Excited State 68:	5.212-A2	3.9477 eV	314.07 nm	f=0.0000	<S**2>=6.540	
257A→264A	-0.11208	237B→259B	0.23119	250B→262B	0.31001	
257A→267A	-0.10077	238B→260B	-0.37659	254B→262B	0.14089	
258A→266A	-0.14975	242B→261B	-0.11208	254B→266B	0.11528	
229B→261B	0.14806	245B→260B	0.24641	255B→259B	0.19159	
235B→262B	-0.25441	246B→259B	-0.15337	256B→260B	-0.14478	
236B→261B	0.15105	249B→261B	0.38550			

Excited State 69:	5.533-B1	3.9783 eV	311.65 nm	f=0.0118	<S**2>=7.403	
257A→266A	-0.35574	258A→276A	-0.18182	254B→260B	-0.10069	
257A→271A	-0.19686	258A→285A	-0.10572	254B→264B	0.21597	
257A→274A	0.10210	253B→262B	0.55675	254B→267B	0.19398	
257A→286A	-0.10281	253B→266B	0.26099	254B→278B	0.11671	
258A→264A	-0.27371	253B→271B	-0.12706			
258A→267A	-0.25528	253B→273B	-0.10060			

Excited State 70:	5.508-A2	3.9803 eV	311.50 nm	f=0.0000	<S**2>=7.335	
257A→264A	-0.27132	238B→260B	0.10584	253B→278B	0.10417	
257A→267A	-0.24702	249B→261B	-0.16001	254B→262B	0.53056	
257A→276A	-0.17781	250B→262B	-0.13867	254B→266B	0.26235	
257A→285A	-0.10503	253B→260B	-0.11564	254B→271B	-0.12849	
258A→266A	-0.32984	253B→264B	0.20367	254B→273B	-0.10108	
258A→271A	-0.19090	253B→267B	0.17965			

Excited State 71:	5.094-B2	4.0827 eV	303.68 nm	f=0.0011	<S**2>=6.236			
237B→260B	-0.10178	243B→260B	-0.36273	248B→259B	-0.11995			
239B→260B	0.41186	245B→259B	0.39539	250B→261B	-0.10855			
241B→259B	0.54623	246B→260B	-0.42342					
Excited State 72:	5.091-A2	4.0847 eV	303.53 nm	f=0.0000	<S**2>=6.229			
239B→259B	0.41231	243B→259B	-0.36425	246B→259B	-0.42608			
241B→260B	0.56043	245B→260B	0.39039	248B→260B	-0.10781			
Excited State 73:	5.625-A1	4.1987 eV	295.29 nm	f=0.0004	<S**2>=7.659			
241A→274A	0.15317	252A→269A	0.21696	245B→276B	-0.15562			
242A→272A	-0.15536	235B→259B	0.22562	246B→277B	-0.16070			
243A→275A	-0.16006	236B→260B	-0.13946	250B→259B	-0.16723			
244A→273A	0.17175	238B→261B	0.15574	251B→269B	-0.20717			
245A→277A	-0.15144	239B→273B	-0.10914	252B→270B	-0.19002			
246A→278A	0.16120	241B→272B	-0.15709	255B→262B	-0.16559			
251A→270A	0.22078	244B→274B	0.15216					
Excited State 74:	5.389-B2	4.2155 eV	294.11 nm	f=0.1445	<S**2>=7.010			
231A→265A	-0.12046	262A→264A	-0.15991	238B→263B	0.16955			
235A→263A	-0.12030	262A→270A	-0.13364	250B→261B	0.36401			
255A→266A	-0.10266	223B→261B	0.10185	250B→265B	0.10643			
255A→271A	0.10076	228B→259B	-0.26461	252B→261B	0.16574			
257A→280A	-0.13641	229B→262B	0.12148	253B→280B	0.14358			
258A→282A	-0.14403	232B→260B	0.20074	254B→281B	0.12622			
261A→263A	0.12233	235B→265B	0.15120	256B→259B	-0.11298			
261A→269A	-0.13378	237B→260B	0.28998					
Excited State 75:	5.563-B1	4.2172 eV	294.00 nm	f=0.0013	<S**2>=7.486			
241A→272A	-0.15159	241A→277A	-0.10620	242A→274A	0.15417			

242A→278A	-0.10206	229B→259B	-0.13832	245B→277B	-0.16051
243A→273A	-0.15902	235B→260B	0.23412	246B→276B	-0.16507
244A→275A	0.15347	236B→259B	-0.16927	249B→259B	-0.15483
245A→278A	-0.16269	237B→261B	-0.15128	250B→260B	-0.17770
246A→277A	0.16412	238B→262B	0.18111	251B→270B	-0.20827
251A→269A	0.23515	239B→272B	0.11553	252B→269B	-0.20553
252A→270A	0.23804	241B→273B	0.13604	255B→261B	-0.15056
262A→265A	-0.11097	244B→275B	-0.13693	256B→262B	0.10572

Excited State 76: 5.572-A1 4.2814 eV 289.59 nm f=0.0000 <S**2>=7.512

249A→263A	0.29889	229B→260B	0.12804	253B→279B	0.10511
249A→268A	0.15140	247B→259B	0.40445	253B→281B	0.14358
250A→265A	0.32610	247B→263B	-0.21309	254B→280B	0.18198
257A→282A	-0.17782	248B→261B	-0.22443	258B→266B	0.10247
258A→280A	-0.15877	248B→265B	-0.20932		

Excited State 77: 5.540-B2 4.2837 eV 289.43 nm f=0.0018 <S**2>=7.424

249A→265A	0.39442	250A→283A	0.10573	248B→263B	-0.24860
249A→279A	0.10933	247B→261B	-0.26311	248B→268B	0.11291
250A→263A	0.36251	247B→265B	-0.25128	250B→261B	-0.11411
250A→268A	0.18537	248B→259B	0.49684		

Excited State 78: 5.582-A1 4.2920 eV 288.87 nm f=0.0007 <S**2>=7.539

249A→263A	0.23952	260A→264A	0.11013	248B→261B	-0.16933
249A→268A	0.12554	261A→265A	-0.10506	248B→265B	-0.16014
250A→265A	0.26207	228B→261B	0.10527	253B→279B	-0.13290
257A→282A	0.22240	229B→260B	-0.16030	253B→281B	-0.17874
258A→280A	0.19863	232B→262B	-0.11953	254B→280B	-0.22771
258A→283A	0.11020	247B→259B	0.33713	257B→264B	-0.11626
259A→266A	0.12335	247B→263B	-0.15910	258B→266B	-0.12402

Excited State 79:	5.518-B2	4.3033 eV	288.12 nm	f=0.0195	<S**2>=7.362	
249A→265A	0.13830	262A→267A	-0.11706	252B→261B	0.13882	
250A→263A	0.12633	262A→270A	0.19956	253B→280B	-0.19973	
255A→266A	-0.10129	236B→262B	0.10506	254B→279B	-0.12167	
257A→280A	0.19031	237B→260B	0.24520	254B→281B	-0.17343	
258A→282A	0.19634	238B→259B	0.12383	257B→262B	-0.13772	
259A→264A	0.13830	247B→261B	-0.11723	257B→266B	-0.13395	
260A→266A	0.15143	248B→259B	0.13932	258B→264B	-0.14910	
261A→263A	-0.15923	249B→262B	-0.12307			
261A→269A	0.19923	250B→261B	0.27591			

Excited State 80:	5.443-A2	4.3160 eV	287.26 nm	f=0.0000	<S**2>=7.158	
242A→270A	0.10734	261A→267A	-0.15256	246B→270B	0.14152	
246A→269A	-0.10803	261A→270A	0.39608	249B→261B	0.13028	
251A→277A	-0.13631	262A→263A	-0.17220	250B→262B	0.23535	
252A→278A	-0.13319	262A→268A	0.14830	251B→276B	0.14813	
253A→269A	-0.12015	262A→269A	0.39683	252B→277B	0.14251	
254A→270A	-0.12602	237B→259B	0.14502	255B→270B	-0.10758	
261A→264A	0.13830	245B→269B	0.13473	256B→269B	0.10496	

Excited State 81:	5.460-B2	4.3233 eV	286.78 nm	f=0.0276	<S**2>=7.204	
251A→278A	-0.10252	262A→264A	0.14516	246B→260B	0.12855	
252A→277A	-0.10601	262A→267A	-0.10375	246B→269B	0.11235	
254A→269A	-0.10581	262A→270A	0.33164	249B→262B	0.28770	
257A→280A	-0.12899	238B→259B	-0.12180	250B→261B	0.10115	
258A→282A	-0.13228	241B→259B	-0.12618	251B→277B	0.11427	
260A→266A	-0.10120	244B→261B	-0.22260	252B→276B	0.11311	
261A→268A	0.13492	245B→259B	0.10743	253B→280B	0.13801	
261A→269A	0.32254	245B→270B	0.10848	254B→281B	0.11750	

Excited State 82:	5.427-A2	4.3334 eV	286.11 nm	f=0.0000	<S**2>=7.114	
259A→263A	0.27404	237B→263B	-0.10703	246B→259B	0.16555	
259A→268A	0.11595	238B→260B	-0.17518	249B→261B	0.36290	
260A→265A	0.28496	240B→261B	-0.11478	250B→262B	-0.13345	
232B→259B	0.13966	241B→260B	-0.13409	257B→261B	0.22607	
236B→261B	-0.14678	242B→261B	0.14072	257B→265B	-0.21341	
236B→265B	-0.11735	243B→259B	-0.14840	258B→263B	-0.22358	
237B→259B	-0.23556	244B→262B	-0.22914			

Excited State 83:	5.257-A1	4.3517 eV	284.91 nm	f=0.0006	<S**2>=6.660	
244A→263A	-0.10856	242B→260B	-0.26045	244B→263B	-0.17638	
239B→262B	-0.26010	242B→264B	-0.11790	245B→261B	-0.30309	
240B→260B	0.14517	243B→262B	0.27513	246B→262B	-0.25697	
241B→261B	0.43836	244B→259B	0.38486	249B→260B	-0.16270	

Excited State 84:	5.289-B1	4.3538 eV	284.77 nm	f=0.0004	<S**2>=6.744	
243A→263A	0.10564	241B→262B	0.36968	244B→264B	0.12927	
259A→265A	0.13306	242B→259B	-0.31320	245B→262B	-0.24249	
260A→263A	0.12895	242B→263B	0.13811	246B→261B	-0.29127	
239B→261B	-0.29178	243B→261B	0.31599	249B→259B	-0.14004	
240B→259B	0.16961	244B→260B	0.31175			

Excited State 85:	5.280-B2	4.3597 eV	284.39 nm	f=0.0065	<S**2>=6.720	
257A→280A	-0.10594	241B→259B	0.30345	245B→259B	-0.20766	
258A→282A	-0.10862	241B→263B	-0.12221	245B→263B	0.10028	
261A→269A	0.13938	242B→262B	-0.33408	246B→260B	-0.15009	
262A→270A	0.14168	243B→260B	0.20501	249B→262B	-0.10434	
239B→260B	-0.20530	244B→261B	0.50455	253B→280B	0.11210	
240B→262B	0.25164	244B→265B	0.10217			

Excited State 86:	5.309-A2	4.3635 eV	284.14 nm	f=0.0000	<S**2>=6.796	
259A→263A	-0.17636	239B→259B	0.17659	245B→260B	0.18743	
260A→265A	-0.18397	240B→261B	-0.25164	246B→259B	0.14364	
261A→270A	-0.12062	241B→260B	-0.24150	257B→261B	-0.11765	
262A→269A	-0.12194	242B→261B	0.38751	257B→265B	0.13461	
237B→259B	0.16653	243B→259B	-0.23797	258B→263B	0.13226	
238B→260B	0.13866	244B→262B	-0.38664			

Excited State 87:	5.562-B1	4.3701 eV	283.71 nm	f=0.0349	<S**2>=7.483	
234A→263A	0.11432	229B→259B	0.12708	243B→261B	-0.10211	
238A→265A	0.12756	232B→261B	0.17558	244B→260B	-0.13956	
255A→263A	-0.11005	236B→259B	-0.18230	245B→262B	0.10022	
259A→265A	0.37962	236B→263B	-0.12337	246B→261B	0.10827	
260A→263A	0.36713	237B→265B	-0.10168	257B→263B	-0.24160	
260A→268A	0.15498	238B→262B	-0.11558	258B→261B	0.19192	
262A→265A	-0.11981	241B→262B	-0.10384	258B→265B	-0.22908	

Excited State 88:	5.640-A2	4.3799 eV	283.08 nm	f=0.0000	<S**2>=7.703	
247A→263A	-0.21036	239B→259B	-0.25230	247B→262B	-0.16193	
247A→268A	-0.10942	239B→263B	0.12753	247B→266B	0.34172	
248A→265A	-0.22720	240B→261B	0.19710	248B→260B	0.22047	
249A→266A	-0.30702	240B→265B	0.13939	248B→264B	0.30558	
249A→271A	-0.12709	243B→259B	-0.17373	248B→267B	0.18722	
250A→264A	-0.24931	243B→263B	0.10485			
250A→267A	-0.20714	244B→262B	0.11107			

Excited State 89:	5.642-B1	4.3803 eV	283.05 nm	f=0.0019	<S**2>=7.709	
247A→265A	-0.23189	248A→268A	-0.10935	249A→267A	-0.20674	
248A→263A	-0.21016	249A→264A	-0.24923	250A→266A	-0.30862	

250A→271A	-0.12739	240B→263B	0.14440	247B→264B	0.30574
239B→261B	0.17858	242B→259B	-0.12332	247B→267B	0.18975
239B→265B	0.11718	243B→265B	0.11282	248B→262B	-0.17070
240B→259B	-0.28163	247B→260B	0.21706	248B→266B	0.34444

Excited State 90: 5.543-A1 4.3977 eV 281.93 nm f=0.0040 <S**2>=7.430

247A→266A	-0.28854	261A→265A	-0.16729	240B→260B	0.31074
248A→264A	-0.24933	219B→260B	0.11088	240B→264B	0.22354
248A→267A	-0.15526	223B→259B	0.11746	241B→261B	0.14298
251A→270A	-0.10637	225B→259B	-0.12261	242B→264B	0.14259
252A→269A	-0.10514	228B→261B	-0.12448	242B→267B	0.10908
256A→263A	-0.13240	239B→262B	-0.18499	243B→266B	0.22023
259A→266A	0.10842	239B→266B	0.17708	244B→259B	0.10406

Excited State 91: 5.608-B2 4.4085 eV 281.24 nm f=0.0023 <S**2>=7.612

247A→264A	0.34154	239B→264B	-0.23594	242B→266B	-0.22925
247A→267A	0.20760	240B→262B	0.20736	243B→260B	-0.31947
248A→266A	0.39070	240B→266B	-0.28785	243B→264B	-0.26461
239B→260B	-0.30245	242B→262B	0.15212	243B→267B	-0.11870

Excited State 92: 5.540-A1 4.4178 eV 280.65 nm f=0.0148 <S**2>=7.424

243A→275A	-0.10722	255A→264A	0.10337	240B→260B	-0.22244
244A→273A	0.11817	256A→263A	-0.15532	240B→264B	-0.17131
245A→272A	0.10971	259A→266A	0.13213	242B→260B	-0.21455
246A→274A	0.10570	260A→264A	0.11099	242B→264B	-0.14772
247A→266A	0.26457	261A→265A	-0.21043	243B→262B	0.14102
248A→264A	0.22698	262A→266A	0.10915	243B→266B	-0.16355
248A→267A	0.13537	228B→261B	-0.12158	244B→274B	0.12192
251A→270A	-0.13229	239B→262B	0.10187	245B→272B	0.10079
252A→269A	-0.13152	239B→266B	-0.16289	251B→269B	0.11575

252B→270B	0.10253				

Excited State 93:	**5.531-B1**	**4.4198 eV**	**280.52 nm**	**f=0.2868**	**<S**2>=7.397**
241A→277A	-0.11880	259A→265A	0.19893	242B→274B	0.10464
242A→278A	-0.12484	260A→263A	0.18901	244B→275B	0.15343
243A→273A	0.15858	261A→266A	-0.19490	245B→273B	0.11887
244A→275A	-0.15069	261A→271A	0.13279	246B→272B	-0.13040
245A→274A	0.13949	262A→265A	0.27246	251B→270B	-0.13755
246A→272A	0.14471	262A→279A	-0.11043	252B→269B	-0.13640
251A→269A	0.15977	210B→259B	-0.10676	257B→263B	-0.15356
252A→270A	0.16014	228B→262B	0.10683	258B→261B	0.10076
255A→263A	0.18353	237B→261B	-0.13578	258B→265B	-0.17145
256A→264A	-0.16178	241B→277B	-0.10951		

Excited State 94:	5.388-A2	4.4322 eV	279.73 nm	f=0.0000	<S**2>=7.007
243A→272A	0.11937	260A→265A	-0.11369	237B→259B	-0.22119
244A→274A	0.10269	261A→270A	0.36928	241B→275B	-0.10030
245A→270A	-0.10771	262A→263A	0.12159	249B→261B	0.11074
246A→269A	0.10676	262A→269A	0.37074	250B→262B	-0.26498
251A→277A	0.10588	228B→260B	0.18736	252B→262B	-0.19684
259A→263A	-0.10937	232B→259B	-0.12667		

Excited State 95:	5.467-B2	4.4521 eV	278.49 nm	f=0.1763	<S**2>=7.221
241A→270A	-0.11288	246A→270A	0.12684	238B→259B	0.14184
241A→275A	0.10298	251A→278A	0.12797	241B→274B	0.12298
242A→269A	-0.10305	252A→277A	0.13232	244B→272B	-0.12685
242A→273A	0.11033	261A→263A	0.16458	245B→270B	-0.11955
243A→274A	-0.12166	261A→269A	0.38876	246B→269B	-0.12909
244A→272A	-0.13390	262A→264A	-0.13955	249B→262B	-0.12640
245A→269A	-0.13545	262A→270A	0.39299	251B→277B	-0.11619

252B→276B	-0.10239				

Excited State 96: 5.375-A2 4.4824 eV 276.60 nm f=0.0000 <S**2>=6.974

259A→263A	-0.26745	237B→259B	-0.22821	248B→264B	-0.10207
259A→268A	-0.10980	238B→260B	-0.20883	249B→261B	0.30511
260A→265A	-0.27509	240B→261B	0.16425	250B→262B	-0.27605
261A→264A	0.10319	243B→259B	-0.11256	251B→261B	0.17818
261A→270A	-0.17757	247B→262B	0.14114	252B→262B	-0.19793
262A→269A	-0.17803	247B→266B	-0.11535		

Excited State 97: 5.438-B1 4.4909 eV 276.08 nm f=0.0033 <S**2>=7.143

247A→265A	0.20550	240B→259B	0.32756	247B→260B	0.27371
248A→263A	0.18801	240B→263B	-0.20149	247B→264B	0.24785
249A→264A	-0.13523	242B→259B	0.24368	248B→262B	-0.32468
250A→266A	-0.15754	242B→263B	-0.16287	248B→266B	0.24908
239B→261B	-0.27417	243B→261B	-0.32197		
239B→265B	-0.16082	243B→265B	-0.19062		

Excited State 98: 5.422-A2 4.4920 eV 276.01 nm f=0.0000 <S**2>=7.099

247A→263A	-0.18058	239B→259B	-0.26360	243B→263B	0.19075
248A→265A	-0.19667	239B→263B	0.15209	247B→262B	0.29943
249A→266A	0.13508	240B→261B	0.28790	247B→266B	-0.22578
250A→264A	0.11834	240B→265B	0.17790	248B→260B	-0.25725
259A→263A	0.11582	242B→261B	0.29016	248B→264B	-0.22430
260A→265A	0.11925	242B→265B	0.14953	250B→262B	0.14964
237B→259B	0.10367	243B→259B	-0.27954		

Excited State 99: 5.444-A1 4.5158 eV 274.56 nm f=0.0089 <S**2>=7.158

231A→263A	0.11106	240A→263A	0.12911	250A→265A	-0.14356
235A→265A	0.13985	249A→263A	-0.12599	255A→264A	0.19058

257A→282A	-0.16209	235B→259B	-0.10926	249B→260B	-0.10303
258A→280A	-0.16383	235B→263B	-0.14857	250B→263B	-0.15047
261A→265A	-0.17525	238B→261B	-0.10105	253B→281B	0.13462
262A→266A	0.23962	238B→265B	-0.17379	254B→280B	0.16667
262A→271A	-0.13654	242B→260B	0.16890	256B→265B	-0.17317
225B→259B	0.15833	243B→262B	-0.10602	257B→264B	0.14986
228B→261B	0.14430	247B→259B	0.11342	258B→266B	0.15417
229B→260B	-0.16209	248B→261B	-0.17565		

Excited State 100: 5.157-B2 4.5249 eV 274.00 nm f=0.0000 <S**2>=6.398

249A→265A	0.46280	250A→268A	0.21323	247B→265B	0.15530
249A→279A	0.11927	250A→283A	0.11400	248B→259B	-0.36119
250A→263A	0.42844	247B→261B	0.51901	248B→263B	0.17418

Excited State 101: 5.194-A1 4.5261 eV 273.93 nm f=0.0090 <S**2>=6.495

249A→263A	0.40855	250A→265A	0.44111	247B→263B	0.17132
249A→268A	0.20213	250A→279A	0.11388	248B→261B	0.48728
249A→283A	0.10852	247B→259B	-0.34929	248B→265B	0.14691

Excited State 102: 5.429-B2 4.5579 eV 272.02 nm f=0.0538 <S**2>=7.118

257A→280A	0.15035	262A→270A	0.15855	238B→259B	-0.19866
258A→282A	0.15299	221B→260B	0.11738	249B→262B	0.16887
259A→264A	0.17494	222B→259B	0.10222	251B→262B	0.14071
259A→267A	0.14400	225B→261B	-0.11018	251B→277B	-0.10361
260A→266A	0.21276	226B→259B	-0.14194	252B→261B	-0.19087
260A→271A	0.10075	227B→260B	-0.18630	253B→280B	-0.17037
261A→268A	-0.10280	228B→259B	-0.16297	254B→279B	-0.10725
261A→269A	0.15790	232B→260B	0.16051	254B→281B	-0.14526
262A→267A	0.11114	237B→260B	-0.12403		

Excited State 103:	5.262-A2	4.5729 eV	271.13 nm	f=0.0000	<S**2>=6.672	
247A→263A	-0.32584	250A→264A	0.39673	248B→260B	0.18161	
247A→268A	-0.16271	250A→267A	0.26539	248B→264B	0.13991	
248A→265A	-0.35278	247B→262B	-0.26802			
249A→266A	0.46391	247B→266B	0.13695			

Excited State 104:	5.256-B1	4.5750 eV	271.00 nm	f=0.0002	<S**2>=6.656	
247A→265A	-0.34635	249A→267A	0.26728	247B→260B	0.19345	
248A→263A	-0.31922	250A→266A	0.47272	247B→264B	0.14313	
248A→268A	-0.15920	250A→271A	0.10010	248B→262B	-0.28273	
249A→264A	0.40111	243B→261B	-0.10189	248B→266B	0.14209	

Excited State 105:	5.314-A2	4.6023 eV	269.40 nm	f=0.0000	<S**2>=6.810	
243A→272A	0.10365	261A→270A	-0.11212	226B→260B	0.24573	
254A→264A	-0.17577	262A→268A	0.12679	227B→259B	0.30714	
256A→266A	-0.19602	262A→269A	-0.11171	228B→260B	0.22100	
258A→266A	-0.12134	221B→259B	-0.17831	232B→259B	-0.13419	
259A→263A	0.15341	222B→260B	-0.19339	238B→260B	0.10655	
260A→265A	0.15592	224B→261B	-0.15443	251B→261B	0.10311	
261A→267A	-0.18525	225B→262B	0.16636	251B→276B	0.10848	

Excited State 106:	5.100-B2	4.6053 eV	269.22 nm	f=0.1894	<S**2>=6.253	
259A→264A	-0.12594	251B→262B	0.64600	258B→264B	-0.15195	
260A→266A	-0.14747	252B→261B	-0.58776			
250B→261B	0.19892	257B→266B	-0.17743			

Excited State 107:	5.097-A2	4.6071 eV	269.11 nm	f=0.0000	<S**2>=6.245	
237B→259B	0.10326	250B→262B	0.25549	252B→262B	-0.63691	
249B→261B	-0.12214	251B→261B	0.65257			

Excited State 108:	**5.225-B2**	**4.6120 eV**	**268.83 nm**	**f=0.7172**	**<S**2>=6.575**
256A→265A	-0.11143	221B→260B	-0.12174	252B→261B	-0.23181
257A→280A	-0.14812	226B→259B	-0.13087	253B→280B	0.11424
258A→282A	-0.15297	232B→260B	-0.13305	255B→264B	-0.16124
259A→264A	0.22673	236B→262B	0.11028	**257B→266B**	**0.36776**
259A→267A	0.13516	237B→260B	0.16624	257B→271B	-0.12333
260A→266A	0.25636	249B→262B	-0.18088	258B→264B	0.29286
261A→263A	-0.10162	250B→261B	0.10938	258B→267B	0.20080
261A→268A	-0.10005	251B→262B	0.23652	258B→278B	0.10099

Excited State 109:	5.148-B1	4.6297 eV	267.80 nm	f=0.0275	<S**2>=6.375
247A→265A	-0.20017	258A→264A	-0.13868	242B→259B	0.12710
248A→263A	-0.19049	258A→267A	-0.10164	243B→261B	-0.22351
249A→264A	-0.15034	259A→265A	0.19961	247B→260B	-0.13899
249A→267A	-0.11807	260A→263A	0.19804	247B→264B	-0.10244
250A→266A	-0.17592	261A→266A	-0.16183	248B→262B	0.24259
254A→266A	-0.17693	262A→265A	-0.14946	253B→266B	-0.14926
255A→263A	-0.11572	225B→260B	0.11497	254B→264B	-0.13344
256A→264A	-0.14198	236B→259B	0.14009	257B→263B	0.17216
256A→267A	-0.11067	239B→261B	-0.19853	258B→265B	0.17007
257A→266A	-0.12763	240B→259B	0.16257		

Excited State 110:	5.165-A2	4.6359 eV	267.44 nm	f=0.0000	<S**2>=6.420
247A→263A	-0.27267	262A→263A	-0.12593	247B→262B	0.33932
247A→268A	-0.13483	226B→260B	-0.12892	247B→266B	-0.12902
248A→265A	-0.29780	227B→259B	-0.11482	248B→260B	-0.18702
249A→266A	-0.22300	239B→259B	0.15865	248B→264B	-0.12430
250A→264A	-0.17969	240B→261B	-0.28142	257B→265B	0.10607
250A→267A	-0.14599	242B→261B	-0.23927	258B→263B	0.11257
255A→265A	-0.12842	243B→259B	0.18698		

Excited State 111:	5.106-A1	4.6434 eV	267.01 nm	f=0.1013	<S**2>=6.267	
259A→266A	0.40771	220B→259B	0.10668	257B→264B	0.37461	
259A→271A	0.12782	221B→262B	-0.11912	257B→267B	0.20761	
260A→264A	0.35119	222B→261B	-0.11197	258B→266B	0.39127	
260A→267A	0.24010	223B→259B	-0.13193			
219B→260B	-0.17344	255B→266B	-0.12311			

Excited State 112:	5.166-B1	4.6521 eV	266.51 nm	f=0.0301	<S**2>=6.423	
247A→265A	0.35053	259A→265A	0.16537	247B→260B	0.15393	
248A→263A	0.31922	260A→263A	0.16379	248B→262B	-0.25937	
248A→268A	0.15888	261A→266A	-0.10538	253B→266B	-0.17316	
250A→266A	0.12032	262A→265A	-0.10098	254B→264B	-0.15850	
254A→266A	-0.10888	239B→261B	0.19846	254B→267B	-0.10313	
257A→266A	-0.15186	240B→259B	-0.14545	257B→263B	0.15493	
258A→264A	-0.14394	242B→259B	-0.12388	258B→265B	0.14905	
258A→267A	-0.11360	243B→261B	0.24825			

Excited State 113:	5.169-A2	4.6586 eV	266.14 nm	f=0.0000	<S**2>=6.431	
247A→263A	-0.24044	260A→265A	-0.14819	247B→262B	0.14977	
247A→268A	-0.11968	261A→264A	0.10896	250B→262B	0.16730	
248A→265A	-0.25435	262A→263A	0.14395	253B→264B	0.17385	
255A→265A	0.11160	224B→261B	-0.10198	253B→267B	0.11750	
257A→264A	0.13803	226B→260B	0.29585	254B→266B	0.19804	
257A→267A	0.10553	227B→259B	0.28981	257B→265B	-0.17648	
258A→266A	0.18722	240B→261B	-0.16482	258B→263B	-0.18206	
259A→263A	-0.14485	242B→261B	-0.11008			

Excited State 114:	5.174-B2	4.6668 eV	265.67 nm	f=0.0275	<S**2>=6.443	
259A→264A	0.18044	259A→267A	0.13869	260A→266A	0.21638	

261A→263A	0.10044	226B→259B	0.47047	257B→266B	0.16966
222B→259B	-0.12072	227B→260B	0.49550	258B→264B	0.15305
224B→262B	-0.20130	228B→259B	0.14276		
225B→261B	0.17566	249B→262B	0.12376		

Excited State 115: 5.135-B1 4.6765 eV 265.12 nm f=0.0299 <S**2>=6.341

257A→266A	0.12249	221B→261B	-0.21479	228B→262B	0.13816
258A→264A	0.11231	222B→262B	-0.25697	229B→259B	-0.13501
217B→259B	0.12171	223B→260B	-0.12280	253B→266B	0.12544
218B→261B	0.15550	224B→259B	-0.36509	254B→264B	0.13842
219B→259B	-0.29645	225B→260B	0.42913	256B→266B	0.11647
220B→260B	0.26040	227B→261B	0.12789		

Excited State 116: 5.155-A2 4.6785 eV 265.01 nm f=0.0000 <S**2>=6.393

257A→264A	-0.11806	222B→260B	0.29862	253B→267B	-0.10112
258A→266A	-0.15226	223B→262B	0.21875	254B→266B	-0.17868
218B→259B	-0.15747	226B→260B	0.39772	255B→263B	-0.10906
219B→261B	0.24123	227B→259B	0.34973	256B→264B	-0.10307
220B→262B	-0.15045	249B→261B	0.15124	257B→265B	0.11479
221B→259B	0.29392	253B→264B	-0.13512		

Excited State 117: 5.341-A1 4.6834 eV 264.73 nm f=0.0084 <S**2>=6.881

238A→266A	0.10143	258A→280A	-0.11342	224B→260B	-0.24805
247A→266A	-0.14721	259A→271A	-0.10297	225B→259B	0.23901
248A→264A	-0.13492	261A→265A	-0.16312	235B→259B	0.11372
253A→266A	-0.17436	262A→266A	-0.16438	236B→260B	0.27787
255A→264A	-0.15187	219B→260B	-0.14702	236B→264B	-0.11889
255A→267A	-0.13463	220B→259B	0.16715	237B→262B	0.13653
256A→263A	-0.14865	221B→262B	-0.12264	237B→266B	-0.11881
257A→282A	-0.12788	222B→261B	-0.13666	242B→260B	-0.10994

243B→262B	0.15342	253B→281B	0.11049	254B→280B	0.14446

Excited State 118: 5.223-B2 4.6930 eV 264.19 nm f=0.0223 <S**2>=6.570

256A→265A	-0.10718	221B→260B	0.29008	239B→260B	-0.14715
261A→268A	-0.10895	222B→259B	0.37512	240B→262B	0.22249
217B→262B	-0.11176	223B→261B	0.18722	242B→262B	0.19146
218B→260B	-0.22902	226B→259B	0.27062	243B→260B	-0.15237
219B→262B	0.24253	227B→260B	0.23509		
220B→261B	-0.21081	237B→260B	0.11109		

Excited State 119: 5.178-A1 4.6986 eV 263.88 nm f=0.0000 <S**2>=6.454

247A→266A	-0.25623	220B→259B	-0.24983	239B→262B	0.27991
248A→264A	-0.22293	221B→262B	0.12325	240B→260B	-0.22604
248A→267A	-0.13872	222B→261B	0.19935	242B→260B	-0.16442
217B→260B	-0.13686	224B→260B	0.29881	243B→262B	0.33335
218B→262B	-0.13554	225B→259B	-0.28869		
219B→260B	0.16418	227B→262B	-0.11168		

Excited State 120: 5.175-B2 4.7037 eV 263.59 nm f=0.0054 <S**2>=6.446

247A→264A	0.38446	227B→260B	0.13469	242B→262B	-0.32075
247A→267A	0.23711	239B→260B	0.16068	243B→260B	0.22865
248A→266A	0.44180	239B→264B	0.11070	243B→264B	0.12527
222B→259B	0.10144	240B→262B	-0.34535	247B→261B	0.11852
226B→259B	0.13988	240B→266B	0.11670	249B→262B	-0.16218

Excited State 121: 5.290-A1 4.7176 eV 262.81 nm f=0.0018 <S**2>=6.746

247A→266A	0.33415	223B→259B	-0.10041	227B→262B	-0.12068
248A→264A	0.28384	224B→260B	0.25005	236B→260B	0.24111
248A→267A	0.17636	225B→259B	-0.23347	236B→264B	-0.10239
257A→282A	-0.10128	226B→261B	-0.11866	237B→266B	-0.10081

239B→262B	-0.21805	242B→260B	0.11318	254B→280B	0.10241
240B→260B	0.15322	243B→262B	-0.27224		

Excited State 122: 5.179-A2 4.7217 eV 262.58 nm f=0.0000 <S**2>=6.454

253A→263A	-0.12090	259A→263A	0.14109	236B→261B	0.10271
254A→267A	-0.11411	260A→265A	0.14155	237B→259B	0.14236
255A→265A	-0.16521	261A→264A	-0.11816	253B→264B	0.26787
256A→266A	-0.16845	262A→263A	-0.16696	253B→267B	0.16584
256A→271A	-0.10295	262A→268A	-0.13776	254B→266B	0.33155
257A→264A	0.23714	226B→260B	0.11808	254B→271B	-0.10185
257A→267A	0.17597	227B→259B	0.14201	256B→264B	0.12870
257A→276A	0.10472	228B→260B	0.12345	258B→280B	0.10393
258A→266A	0.25356	232B→259B	-0.15057		

Excited State 123: 5.157-B1 4.7274 eV 262.27 nm f=0.0172 <S**2>=6.399

254A→266A	-0.14879	260A→263A	0.14217	236B→259B	0.17031
256A→264A	-0.19408	261A→266A	-0.13544	253B→266B	0.31691
256A→267A	-0.12308	261A→278A	0.10699	254B→264B	0.30043
257A→266A	0.28978	262A→265A	-0.11612	254B→267B	0.19186
257A→271A	0.11951	262A→272A	0.10102	256B→266B	0.12419
258A→264A	0.20693	262A→277A	0.11625	257B→280B	0.11245
258A→267A	0.16568	224B→259B	0.16315	258B→281B	0.10079
259A→265A	0.13968	225B→260B	-0.12517		

Excited State 124: 5.172-B1 4.7478 eV 261.14 nm f=0.1614 <S**2>=6.438

261A→274A	-0.14601	220B→260B	-0.11423	225B→260B	0.24649
261A→278A	0.22459	221B→261B	0.14229	226B→262B	0.24072
262A→272A	0.13234	222B→262B	0.13894	227B→261B	0.21882
262A→277A	0.23562	223B→260B	0.38645		
219B→259B	0.30415	224B→259B	-0.34377		

Excited State 125:	5.325-A2	4.7573 eV	260.62 nm	f=0.0000	<S**2>=6.840	
243A→272A	0.12884	218B→259B	-0.17650	227B→259B	-0.20394	
244A→266A	0.10092	219B→261B	0.17751	228B→260B	-0.15298	
244A→274A	0.11837	220B→262B	-0.13908	237B→259B	-0.16539	
246A→273A	0.11002	221B→259B	0.25999	238B→260B	0.16939	
254A→264A	-0.15898	222B→260B	0.31860	244B→273B	0.12076	
256A→266A	-0.19997	224B→261B	0.13109	256B→264B	0.11397	
261A→267A	-0.15502	225B→262B	-0.16286			
262A→268A	0.10800	226B→260B	-0.14715			

Excited State 126:	5.302-A1	4.7586 eV	260.55 nm	f=0.0053	<S**2>=6.779	
239A→270A	0.14759	261A→277A	0.48098	251B→267B	0.12367	
240A→269A	-0.15275	262A→274A	-0.25290	252B→263B	0.11253	
253A→278A	-0.13244	262A→278A	0.46585	252B→268B	0.10732	
254A→277A	-0.13911	223B→259B	0.10342	255B→277B	-0.10356	
255A→270A	0.15858	224B→260B	-0.13396	256B→276B	0.10443	
256A→269A	0.14606	225B→259B	0.11288			
261A→272A	0.20977	251B→264B	-0.10137			

Excited State 127:	5.411-B2	4.7608 eV	260.43 nm	f=0.0367	<S**2>=7.071	
243A→266A	-0.14059	256A→265A	0.16229	225B→261B	-0.11715	
243A→274A	-0.10828	260A→266A	0.10495	238B→259B	0.18800	
244A→265A	-0.15292	261A→263A	0.12530	240B→262B	0.11123	
244A→272A	-0.11843	218B→260B	-0.15592	244B→272B	-0.12949	
245A→263A	-0.12507	219B→262B	0.15162	249B→262B	-0.14380	
245A→273A	-0.10270	220B→261B	-0.12382	250B→261B	0.18177	
246A→264A	-0.12860	221B→260B	0.20815	256B→263B	-0.16843	
254A→263A	0.15014	222B→259B	0.27248	257B→266B	0.12015	

Excited State 128:	5.256-B1	4.7618 eV	260.37 nm	f=0.0003	<S**2>=6.657	
239A→269A	0.13129	261A→278A	0.41788	223B→260B	-0.21627	
240A→270A	-0.13436	262A→272A	0.15407	224B→259B	0.11612	
253A→277A	-0.11258	262A→277A	0.43667	226B→262B	-0.11420	
254A→278A	-0.11399	219B→259B	-0.20273	251B→263B	0.10561	
255A→269A	0.13410	220B→260B	0.11270	251B→268B	0.10195	
256A→270A	0.12871	221B→261B	-0.10860	252B→267B	0.10040	
261A→274A	-0.19343	222B→262B	-0.11228			

Excited State 129:	5.162-A1	4.7698 eV	259.93 nm	f=0.0029	<S**2>=6.412	
247A→266A	0.13531	218B→262B	-0.13866	223B→259B	0.40459	
248A→264A	0.10958	219B→260B	0.37422	224B→260B	-0.27132	
261A→277A	-0.11648	220B→259B	-0.23952	225B→259B	0.18311	
262A→278A	-0.11326	221B→262B	0.18046	226B→261B	0.21959	
217B→260B	-0.12263	222B→261B	0.22601	227B→262B	0.19424	

Excited State 130:	5.476-B2	4.7902 eV	258.83 nm	f=0.0016	<S**2>=7.246	
241A→264A	0.14307	246A→264A	0.15910	242B→262B	0.16066	
242A→263A	-0.19759	222B→259B	0.13259	244B→265B	0.19898	
243A→266A	0.19308	238B→259B	0.19070	245B→263B	0.11794	
243A→271A	-0.16440	239B→260B	0.12811	249B→262B	0.33350	
244A→265A	0.30122	240B→262B	-0.22615	250B→261B	-0.10796	
245A→263A	0.23590	241B→263B	-0.15678	255B→264B	-0.10055	

Excited State 131:	5.550-A1	4.7948 eV	258.58 nm	f=0.0040	<S**2>=7.449	
241A→266A	0.16103	244A→263A	0.35873	239B→262B	-0.19368	
241A→271A	-0.10763	244A→268A	0.10380	241B→265B	-0.15576	
242A→265A	-0.22581	245A→265A	0.28994	243B→262B	0.14360	
243A→264A	0.26749	246A→266A	0.19817	244B→263B	0.19631	
243A→276A	-0.16587	246A→271A	-0.14055	245B→265B	0.14161	

246B→262B	-0.28022				

Excited State 132: 5.558-B1 4.7971 eV 258.46 nm f=0.0062 <S**2>=7.473

241A→265A	0.22414	245A→271A	-0.14095	242B→263B	0.13788
242A→266A	-0.15252	246A→265A	0.27874	243B→265B	0.10802
242A→271A	0.10384	259A→265A	-0.14683	244B→260B	-0.16894
243A→263A	0.34375	260A→263A	-0.14460	244B→264B	0.13694
243A→268A	0.10205	239B→265B	-0.13187	244B→278B	-0.10692
244A→264A	0.26642	240B→263B	-0.12426	245B→262B	0.28993
244A→276A	-0.16269	241B→262B	-0.26231	246B→265B	-0.14718
245A→266A	0.19853	241B→266B	-0.10594	249B→263B	0.10506

Excited State 133: 5.582-A2 4.8010 eV 258.25 nm f=0.0000 <S**2>=7.540

241A→263A	0.23143	246A→263A	0.28850	243B→263B	0.11842
242A→264A	-0.16557	259A→263A	-0.12194	244B→262B	0.32699
242A→276A	0.10186	260A→265A	-0.12395	244B→266B	0.13532
243A→265A	0.36008	239B→263B	-0.12959	244B→271B	0.12517
244A→266A	0.24017	240B→265B	-0.13165	246B→263B	-0.14891
244A→271A	-0.18820	241B→260B	0.12838	249B→265B	0.11065
245A→264A	0.22171	241B→264B	-0.10882		
245A→276A	-0.11908	242B→265B	0.16160		

Excited State 134: 5.259-B2 4.8321 eV 256.58 nm f=0.0000 <S**2>=6.665

241A→264A	-0.10278	248A→266A	0.10286	262A→264A	-0.20170
242A→263A	0.13043	255A→266A	-0.17097	262A→275A	0.10552
243A→266A	-0.14034	255A→274A	-0.10934	237B→260B	0.12783
243A→271A	0.10955	256A→265A	-0.10133	238B→259B	0.13882
244A→265A	-0.22047	256A→272A	0.12469	240B→262B	-0.11034
245A→263A	-0.19225	261A→263A	-0.14093	244B→261B	0.35007
246A→264A	-0.14167	261A→273A	0.12518	249B→262B	0.42800

250B→261B	-0.30630							

Excited State 135:	5.146-A1	4.8406 eV	256.13 nm	f=0.0011	<S**2>=6.371			
244A→263A	-0.12179	241B→261B	-0.29340	245B→261B	0.57377			
239B→262B	-0.25183	243B→262B	0.16015	246B→262B	-0.55837			
240B→260B	0.10711	244B→259B	-0.14257					

Excited State 136:	5.138-B1	4.8408 eV	256.12 nm	f=0.0018	<S**2>=6.351			
243A→263A	-0.11030	243B→261B	0.17408	246B→261B	-0.55933			
239B→261B	-0.24346	244B→260B	-0.13959					
241B→262B	-0.25921	245B→262B	0.57222					

Excited State 137:	5.191-A2	4.8464 eV	255.83 nm	f=0.0000	<S**2>=6.487			
248A→265A	0.10245	228B→260B	0.18650	248B→260B	-0.12691			
249A→266A	0.10654	232B→259B	-0.12131	248B→264B	0.22707			
256A→266A	0.10534	235B→262B	-0.10524	248B→267B	0.17178			
261A→264A	0.11166	238B→260B	-0.15309	249B→261B	-0.28139			
261A→267A	0.11942	240B→261B	0.11695	250B→262B	0.11854			
262A→268A	-0.10879	244B→262B	-0.27880	250B→266B	0.13430			
218B→259B	-0.10723	247B→262B	0.41153	255B→263B	0.18774			
222B→260B	0.10834	247B→266B	0.27116	256B→264B	0.14068			

Excited State 138:	5.192-B1	4.8487 eV	255.71 nm	f=0.0070	<S**2>=6.488			
247A→265A	0.11968	236B→259B	0.16842	247B→267B	0.22845			
248A→263A	0.10648	246B→261B	0.17348	248B→262B	0.57964			
249A→264A	0.12594	247B→260B	-0.15811	248B→266B	0.36724			
250A→266A	0.14884	247B→264B	0.31070	248B→271B	-0.10322			

Excited State 139:	5.148-A2	4.8520 eV	255.53 nm	f=0.0000	<S**2>=6.375			
249A→266A	0.12346	222B→260B	-0.11238	237B→259B	0.12071			
250A→264A	0.10539	228B→260B	-0.11010	238B→260B	0.16477			

240B→261B	-0.21373	247B→266B	0.30169	248B→267B	0.17888
244B→262B	0.34204	248B→260B	-0.12445	249B→261B	0.29067
247B→262B	0.47948	248B→264B	0.24019	255B→263B	-0.12010

Excited State 140: 5.301-B1 4.8629 eV 254.96 nm f=0.0139 <S**2>=6.776

254A→266A	0.17844	262A→265A	0.22198	241B→262B	-0.14655
255A→273A	-0.12236	220B→260B	0.12299	248B→262B	-0.21516
256A→264A	0.15988	224B→259B	-0.10158	248B→266B	-0.14649
256A→267A	0.13817	235B→260B	0.19551	250B→264B	-0.16923
256A→275A	-0.11947	235B→264B	-0.12552	250B→267B	-0.10663
259A→265A	0.18854	236B→259B	0.26040	253B→266B	0.10015
260A→263A	0.18958	237B→261B	0.16366	256B→266B	-0.20407
261A→266A	0.16202	238B→262B	0.10945	257B→263B	0.16882
261A→271A	0.11584	238B→266B	-0.16072	258B→265B	0.14607

Excited State 141: 5.225-A2 4.8719 eV 254.49 nm f=0.0000 <S**2>=6.575

253A→273A	-0.10579	262A→273A	-0.13822	249B→261B	0.16692
255A→272A	-0.14870	218B→259B	-0.12125	249B→265B	-0.10722
256A→266A	0.18361	222B→260B	0.11250	255B→263B	0.26333
256A→274A	0.11135	228B→260B	0.11734	256B→264B	0.15410
259A→263A	0.14568	232B→259B	-0.13170	256B→267B	-0.10640
260A→265A	0.14500	240B→261B	-0.16062	258B→263B	0.12721
261A→264A	0.19427	242B→261B	0.23087		
261A→267A	0.17946	244B→262B	0.43260		

Excited State 142: 5.264-B1 4.8945 eV 253.31 nm f=0.0709 <S**2>=6.676

256A→267A	0.11877	217B→259B	-0.17098	222B→262B	0.13399
261A→266A	0.14270	218B→261B	-0.14494	224B→259B	-0.11580
261A→281A	-0.12413	219B→259B	0.11065	225B→260B	0.16145
262A→265A	-0.10717	220B→260B	-0.21688	228B→262B	0.19294

232B→261B	-0.16538	236B→259B	0.35079	257B→263B	-0.20099
235B→260B	-0.32286	246B→261B	0.10184	258B→265B	-0.17558

Excited State 143: 5.152-B2 4.8948 eV 253.30 nm f=0.0081 <S**2>=6.385

255A→266A	0.13587	241B→259B	0.11112	250B→261B	0.23685
262A→264A	0.14726	242B→262B	0.47816		
240B→262B	-0.36919	244B→261B	0.56408		

Excited State 144: 5.176-A2 4.9122 eV 252.40 nm f=0.0000 <S**2>=6.447

218B→259B	-0.12651	238B→260B	0.37177	250B→262B	-0.32929
232B→259B	-0.19366	240B→261B	0.12976	257B→265B	-0.30337
236B→261B	0.18558	242B→261B	-0.20505	258B→263B	-0.35051
237B→259B	0.46893	249B→261B	0.16677		

Excited State 145: 5.197-A2 4.9183 eV 252.09 nm f=0.0000 <S**2>=6.503

255A→272A	0.11217	261A→275A	0.11109	244B→262B	0.23705
256A→266A	-0.13508	262A→263A	-0.18820	250B→262B	0.22521
259A→263A	-0.19828	262A→273A	0.10158	250B→266B	0.10148
260A→265A	-0.19258	240B→261B	-0.29813	257B→265B	-0.27198
261A→264A	-0.14769	242B→261B	0.39972	258B→263B	-0.29873

Excited State 146: 5.564-A1 4.9365 eV 251.16 nm f=0.0005 <S**2>=7.490

244A→263A	-0.10393	225B→259B	0.10339	251B→264B	-0.14720
251A→264A	0.25722	235B→259B	-0.26549	251B→267B	0.15999
251A→267A	-0.26518	236B→260B	0.15570	252B→263B	0.18715
252A→263A	-0.26516	239B→262B	0.10164	252B→268B	0.14234
252A→268A	0.27937	244B→274B	0.10821	256B→265B	0.13119
261A→279A	-0.10206	245B→261B	0.14153		
224B→260B	-0.12456	246B→262B	-0.15922		

Excited State 147:	5.156-B2	4.9425 eV	250.85 nm	f=0.0091	<S**2>=6.395	
253A→275A	-0.13560	261A→273A	-0.19260	238B→259B	0.34829	
254A→273A	-0.14885	262A→264A	0.21319	240B→262B	0.17802	
255A→266A	0.16460	262A→267A	0.10876	242B→262B	-0.23412	
255A→274A	0.17804	262A→275A	-0.17665	249B→262B	0.17809	
256A→272A	-0.20035	236B→262B	0.13024	250B→261B	-0.25372	
261A→263A	0.13375	237B→260B	0.47811			

Excited State 148:	5.617-B1	4.9491 eV	250.52 nm	f=0.0180	<S**2>=7.638	
241A→279A	-0.10358	252A→267A	-0.32558	251B→268B	0.16073	
242A→281A	-0.10078	252A→276A	0.10328	252B→260B	0.10635	
243A→263A	0.10809	261A→266A	-0.13336	252B→264B	-0.17566	
245A→281A	-0.10170	261A→278A	-0.10379	252B→267B	0.17316	
251A→263A	-0.32809	262A→277A	-0.10086	255B→265B	-0.11814	
251A→268A	0.33893	220B→260B	0.14174			
252A→264A	0.31166	251B→263B	0.20940			

*C.2.12.4 **OTPT-FLR-221**, **EB** State*

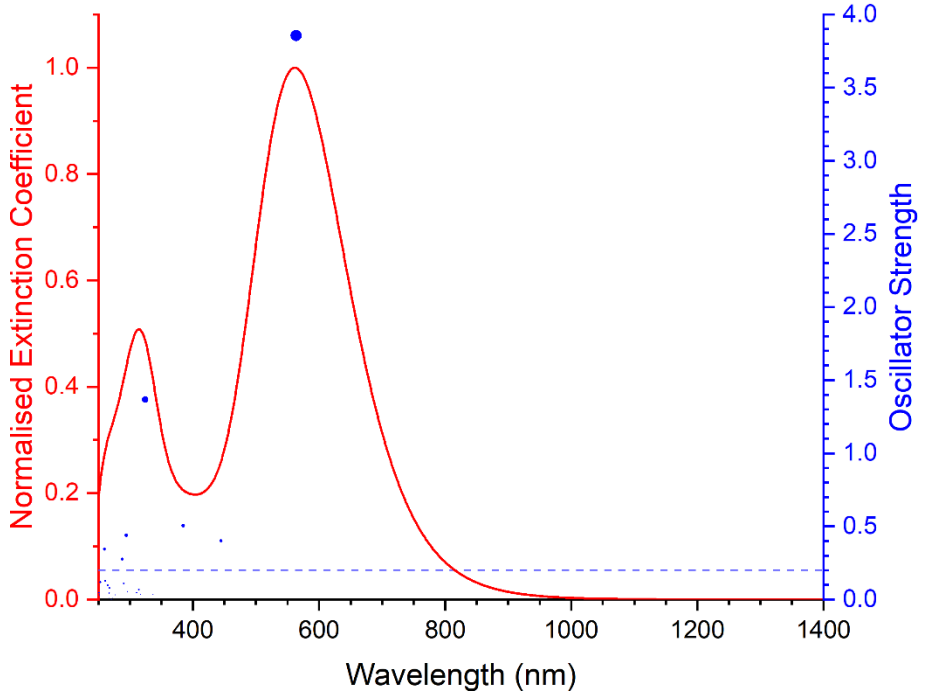

*Figure C-48 Excited states and normalised absorption spectra from TD-DFT calculations of **OTPT-FLR-221** in **EB** state. The areas of excited state dots are proportional to their oscillator strengths.*

Excited State 1:	Singlet-A2	2.0095 eV	617.00 nm	f=0.0000	<S**2>=0.000
259→262	0.45786	260→261	0.50802		
Excited State 2:	**Singlet-B2**	**2.1996 eV**	**563.67 nm**	**f=3.8554**	**<S**2>=0.000**
259→261	**0.49411**	**260→262**	**0.48285**		
Excited State 3:	**Singlet-B1**	**2.7876 eV**	**444.77 nm**	**f=0.4019**	**<S**2>=0.000**
238→262	-0.11655	**257→261**	**0.47996**	**258→262**	**-0.44952**
Excited State 4:	Singlet-A1	2.8175 eV	440.04 nm	f=0.0140	<S**2>=0.000
237→262	-0.10201	257→262	0.46409		
238→261	-0.12419	258→261	-0.46341		
Excited State 5:	Singlet-A2	3.0206 eV	410.46 nm	f=0.0000	<S**2>=0.000
259→262	0.52335	260→261	-0.47118		
Excited State 6:	Singlet-B2	3.0211 eV	410.40 nm	f=0.0052	<S**2>=0.000
259→261	-0.49589	260→262	0.49784		
Excited State 7:	Singlet-A2	3.2180 eV	385.28 nm	f=0.0000	<S**2>=0.000
234→261	0.13553	253→261	-0.10012	256→262	0.44452
236→262	0.15617	255→261	0.44963		
Excited State 8:	**Singlet-B2**	**3.2247 eV**	**384.48 nm**	**f=0.5038**	**<S**2>=0.000**
234→262	0.13366	**255→262**	**0.44195**	260→262	0.11428
236→261	0.15233	**256→261**	**0.44967**		
Excited State 9:	Singlet-A2	3.6806 eV	336.86 nm	f=0.0000	<S**2>=0.000
245→261	0.46516	247→261	0.13910		
246→262	0.46604	250→262	-0.12919		

Excited State 10:	Singlet-B2	3.6813 eV	336.80 nm	f=0.0345	<S**2>=0.000
245→262	0.46030	247→262	0.13587		
246→261	0.47184	250→261	-0.13163		
Excited State 11:	**Singlet-B1**	**3.8221 eV**	**324.39 nm**	**f=1.3661**	**<S**2>=0.000**
257→266	0.20706	258→265	0.10572	259→267	-0.19074
258→262	0.14356	259→264	-0.27039	**260→263**	**0.51352**
Excited State 12:	Singlet-A1	3.9141 eV	316.76 nm	f=0.0367	<S**2>=0.000
239→262	0.38071	249→261	0.13292	260→264	0.14153
240→261	0.38409	257→262	0.12689	260→267	0.11498
248→262	-0.12405	259→263	-0.27500		
Excited State 13:	Singlet-B1	3.9214 eV	316.17 nm	f=0.0000	<S**2>=0.000
239→261	0.43905	248→261	-0.17236	257→261	0.10871
240→262	0.43584	249→262	0.16925	258→262	0.12005
Excited State 14:	Singlet-A1	3.9455 eV	314.25 nm	f=0.0683	<S**2>=0.000
239→262	0.25320	258→261	-0.10764	260→264	-0.20766
240→261	0.26142	258→266	-0.14099	260→267	-0.17256
257→262	-0.17019	259→263	0.41973		
Excited State 15:	Singlet-B1	3.9880 eV	310.89 nm	f=0.0464	<S**2>=0.000
239→261	-0.14252	257→261	0.41998	258→265	-0.13014
240→262	-0.14418	258→262	0.40419	259→264	0.24141
Excited State 16:	Singlet-A1	4.0352 eV	307.26 nm	f=0.0013	<S**2>=0.000
257→262	0.41398	259→263	0.11813	260→267	-0.10426
258→261	0.47246	260→264	-0.19812		
Excited State 17:	Singlet-A2	4.1441 eV	299.18 nm	f=0.0000	<S**2>=0.000
245→261	-0.11860	246→262	-0.11236	247→261	0.36249

250→262	-0.35215	255→261	0.15918	257→263	-0.17786
253→261	0.11342	255→266	0.10146	260→266	-0.26010

Excited State 18:	Singlet-B2	4.1689 eV	297.40 nm	f=0.0106	<S**2>=0.000
245→262	0.12356	247→262	-0.41548	250→261	0.45897
246→261	0.12681	249→263	0.11501		

Excited State 19:	Singlet-A2	4.1782 eV	296.74 nm	f=0.0000	<S**2>=0.000
247→261	-0.18741	257→263	-0.18149	259→271	-0.10659
250→262	0.17644	258→264	-0.22385	260→266	-0.35482
256→265	-0.12004	259→265	0.36510		

Excited State 20:	Singlet-A1	4.1794 eV	296.65 nm	f=0.0068	<S**2>=0.000
239→262	-0.15276	248→262	-0.40336	250→263	0.11153
240→261	-0.15595	249→261	0.44249	254→262	-0.10974

Excited State 21:	Singlet-B1	4.1883 eV	296.02 nm	f=0.0535	<S**2>=0.000
239→261	0.15047	248→261	0.42336	257→261	0.13540
240→262	0.13993	249→262	-0.40760	258→262	0.12617
247→263	0.10464	254→261	0.10688		

Excited State 22:	**Singlet-B1**	**4.2093 eV**	**294.55 nm**	**f=0.4390**	**<S**2>=0.000**
237→261	**0.37469**	244→261	0.20893	259→267	0.10080
238→262	**0.41175**	258→262	-0.16615	260→268	0.11722

Excited State 23:	Singlet-A1	4.2644 eV	290.74 nm	f=0.1093	<S**2>=0.000
237→262	0.37634	244→262	0.18975	259→263	0.10459
238→261	0.41694	257→262	0.19665		

Excited State 24:	**Singlet-B2**	**4.3016 eV**	**288.23 nm**	**f=0.2764**	**<S**2>=0.000**
256→266	-0.10728	257→264	-0.13811	258→263	-0.24537

259→266	**0.47724**	**260→265**	**-0.32329**	260→271	0.12895

Excited State 25:	Singlet-A2	4.3403 eV	285.66 nm	f=0.0000	<S**2>=0.000
247→261	0.20043	256→262	0.20936	259→265	0.31942
250→262	-0.18851	256→265	-0.13295	260→266	0.24594
255→261	-0.20949	257→263	0.17793		
255→266	-0.11296	258→264	-0.20916		

Excited State 26:	Singlet-B1	4.3736 eV	283.48 nm	f=0.0000	<S**2>=0.000
256→264	-0.14075	258→262	-0.19126	259→264	0.42652
257→261	-0.17215	258→265	-0.22535	260→263	0.28456

Excited State 27:	Singlet-A2	4.4575 eV	278.15 nm	f=0.0000	<S**2>=0.000
241→265	-0.15865	243→261	0.32517	244→263	0.36483
242→264	-0.16722	243→266	0.33707	256→262	-0.10996

Excited State 28:	Singlet-B1	4.4704 eV	277.35 nm	f=0.0308	<S**2>=0.000
237→261	-0.14809	242→265	-0.19059	244→261	0.27991
241→264	-0.19411	243→263	0.35154	244→266	0.33252

Excited State 29:	Singlet-B2	4.4730 eV	277.18 nm	f=0.0321	<S**2>=0.000
255→262	-0.36025	257→264	-0.15845	259→266	-0.10780
256→261	0.37077	258→263	0.12383	260→265	-0.35860

Excited State 30:	Singlet-A1	4.4871 eV	276.31 nm	f=0.0003	<S**2>=0.000
243→264	0.17136	257→265	0.16399	259→263	0.28990
244→265	0.16698	258→261	0.10840	260→264	0.49399

Excited State 31:	Singlet-B2	4.5346 eV	273.42 nm	f=0.0002	<S**2>=0.000
241→261	-0.24221	242→263	-0.27451	243→265	0.26966
241→266	-0.25266	243→262	-0.21133	244→264	0.28648

256→261	0.15775							

Excited State 32:	Singlet-A1	4.5440 eV	272.85 nm	f=0.0098	<S**2>=0.000

241→263	0.35668	243→264	-0.17633	260→264	0.12742
242→261	0.31083	244→262	0.12157		
242→266	0.33743	244→265	-0.16523		

Excited State 33:	Singlet-A2	4.5586 eV	271.98 nm	f=0.0000	<S**2>=0.000

241→262	-0.16045	255→261	0.22909	260→266	0.13339
241→265	0.36590	256→262	-0.22897		
242→264	0.37118	259→265	0.11798		

Excited State 34:	Singlet-B2	4.5675 eV	271.45 nm	f=0.0019	<S**2>=0.000

241→261	0.25336	243→265	0.21266	259→266	0.15153
241→266	0.27242	244→264	0.21767	260→265	0.19264
242→263	0.29331	255→262	-0.12823		
243→262	-0.12321	256→261	0.18063		

Excited State 35:	Singlet-B1	4.5714 eV	271.22 nm	f=0.0004	<S**2>=0.000

241→264	0.40884	242→265	0.41050	244→261	0.15148
242→262	-0.17752	243→263	0.16350	244→266	0.15282

Excited State 36:	Singlet-A2	4.5953 eV	269.80 nm	f=0.0000	<S**2>=0.000

234→261	-0.11566	243→261	-0.13280	256→262	-0.25554
236→262	-0.11019	244→263	-0.10162	259→265	0.19560
241→265	-0.20289	253→261	0.10839	260→266	0.21700
242→264	-0.20351	255→261	0.36751		

Excited State 37:	Singlet-A1	4.5980 eV	269.65 nm	f=0.0003	<S**2>=0.000

237→265	-0.10173	242→261	0.18526	243→264	0.34581
241→263	0.20003	242→266	0.18728	244→262	-0.19765

244→265	0.33398	260→264	-0.15373		

Excited State 38:	Singlet-B1	4.6278 eV	267.91 nm	f=0.0789	<S**2>=0.000
254→261	0.20706	260→268	0.11381		
259→269	0.43921	260→270	0.43454		

Excited State 39:	Singlet-B2	4.6395 eV	267.23 nm	f=0.0083	<S**2>=0.000
243→262	0.13256	255→262	-0.19685	259→266	0.25747
243→265	-0.20821	256→261	0.24431	260→265	0.34703
244→264	-0.21323	257→264	0.12829		

Excited State 40:	Singlet-A1	4.6399 eV	267.21 nm	f=0.0436	<S**2>=0.000
259→268	0.10710	260→264	-0.10809		
259→270	0.44087	260→269	0.45830		

Excited State 41:	Singlet-A2	4.6422 eV	267.08 nm	f=0.0000	<S**2>=0.000
234→261	-0.31664	253→261	0.31993		
236→262	-0.31134	256→262	0.31971		

Excited State 42:	Singlet-B2	4.6789 eV	264.99 nm	f=0.0975	<S**2>=0.000
232→261	0.10715	236→261	0.38482	255→262	-0.27747
234→262	0.37000	253→262	-0.16292		

Excited State 43:	Singlet-B1	4.6948 eV	264.09 nm	f=0.0038	<S**2>=0.000
253→263	0.15257	259→264	0.15664	260→270	-0.15185
254→261	0.58696	259→269	-0.14114		
254→266	0.12239	260→263	0.11029		

Excited State 44:	Singlet-A2	4.7458 eV	261.25 nm	f=0.0000	<S**2>=0.000
234→261	0.23002	253→261	0.52725	254→263	0.12889
236→262	0.23851	253→266	0.10982	259→265	0.14883

Excited State 45:	Singlet-A1	4.7486 eV	261.10 nm	f=0.1269	<S**2>=0.000			
253→264	-0.24267		254→262	0.57616		254→265	-0.22803	
Excited State 46:	**Singlet-B2**	**4.7730 eV**	**259.76 nm**	**f=0.3428**	**<S**2>=0.000**			
253→262	**0.55258**		254→264	-0.25857				
253→265	-0.24242		259→266	-0.11040				
Excited State 47:	Singlet-B1	4.8926 eV	253.41 nm	f=0.1182	<S**2>=0.000			
233→261	0.14345		255→263	-0.26136		259→267	0.27945	
235→262	0.14100		256→264	0.17062		260→268	0.25553	
237→261	-0.10469		257→266	0.27097				
238→262	-0.13090		258→265	0.17951				
Excited State 48:	Singlet-A1	4.9204 eV	251.98 nm	f=0.0302	<S**2>=0.000			
233→262	0.15488		255→264	0.13481		259→268	0.26390	
235→261	0.14432		256→263	-0.22669		260→267	0.31025	
238→261	-0.11389		257→265	-0.16029				
254→262	-0.19518		258→266	-0.24547				
Excited State 49:	Singlet-B1	4.9352 eV	251.22 nm	f=0.0457	<S**2>=0.000			
251→264	0.35849		252→265	0.36132		254→276	0.16052	
251→267	-0.12620		252→271	0.11317				
252→262	-0.32825		253→277	0.12939				
Excited State 50:	Singlet-A2	4.9366 eV	251.15 nm	f=0.0000	<S**2>=0.000			
251→262	-0.25360		253→276	0.12972		258→264	-0.14897	
251→265	0.30155		254→277	0.11149		259→265	-0.13523	
251→271	0.10214		255→266	0.13339		260→266	0.15369	
252→264	0.30214		256→265	-0.12635				
252→267	-0.11318		257→263	-0.19293				

Excited State 51:	Singlet-A2	4.9486 eV	250.55 nm	f=0.0000	<S**2>=0.000	
251→262	-0.19314	256→265	0.12294	259→265	0.12008	
251→265	0.21043	256→271	-0.10468	260→266	-0.26822	
252→264	0.20657	257→263	0.30362			
255→266	-0.22364	258→264	0.18718			

Appendix D Adsorption Isotherms and Other Related Data

D.1 Nitrogen Adsorption Isotherm Analyses of PANI-CMPs at 77 K

D.1.1 Isotherm Plots

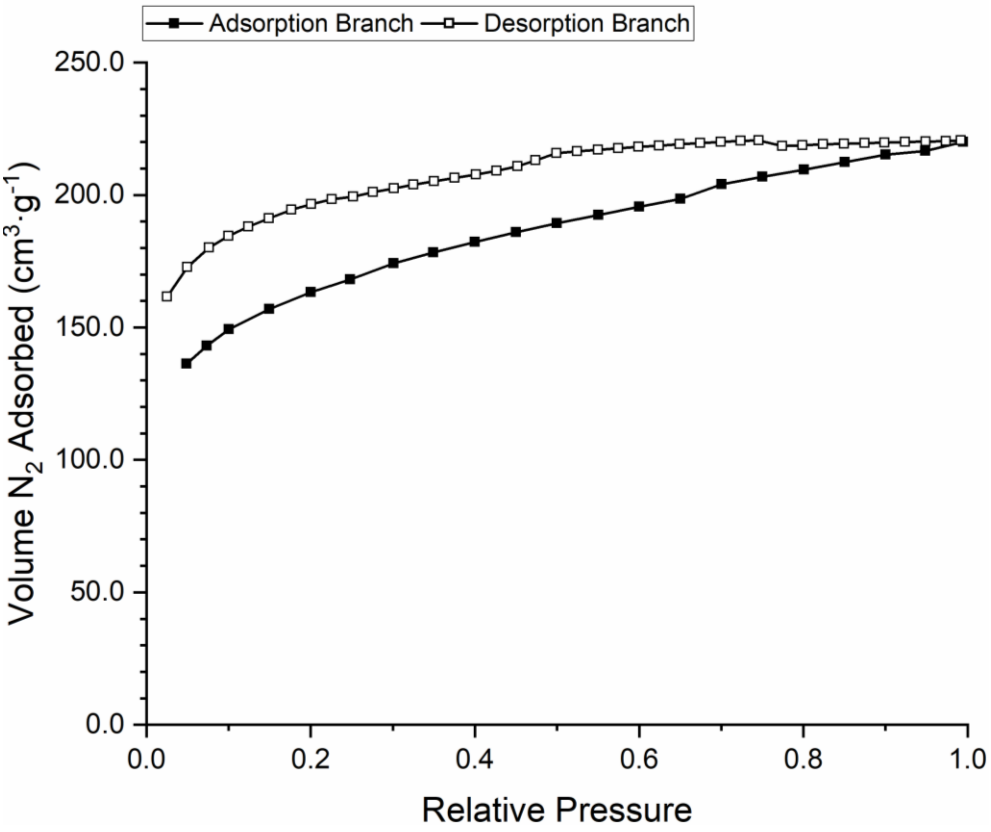

*Figure D-1 Nitrogen adsorption isotherm at 77 K of **PTPA-FLR-SN***

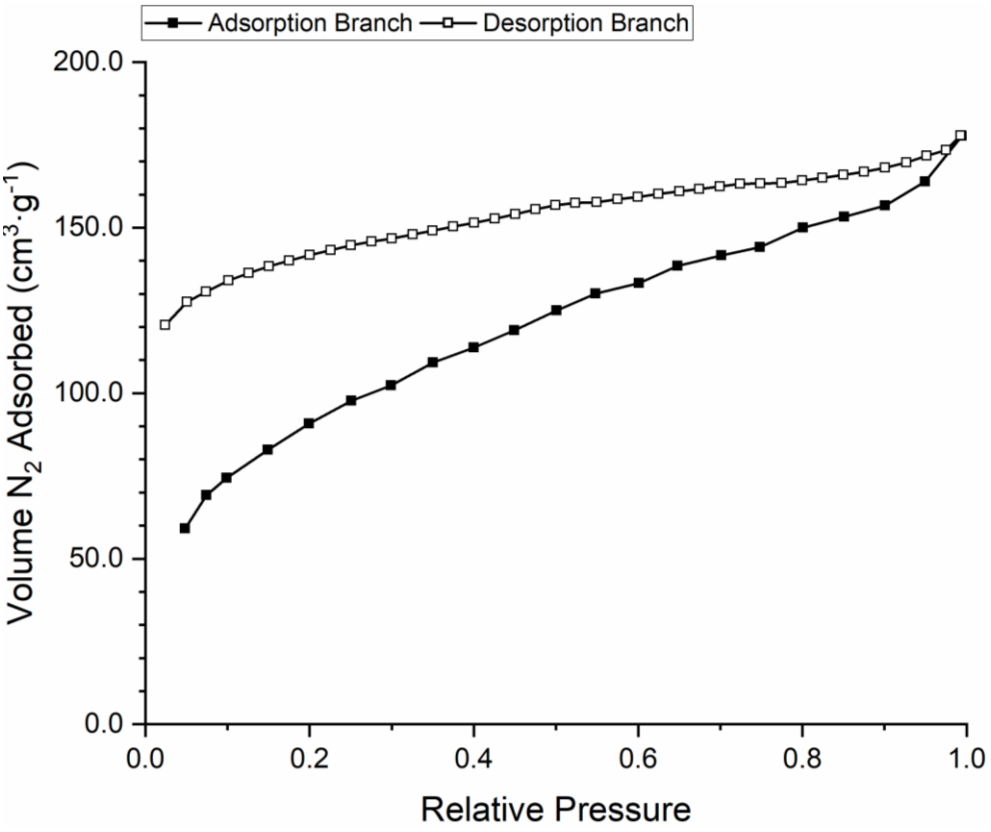

*Figure D-2 Nitrogen adsorption isotherm at 77 K of **PTPA-FLR-SNx***

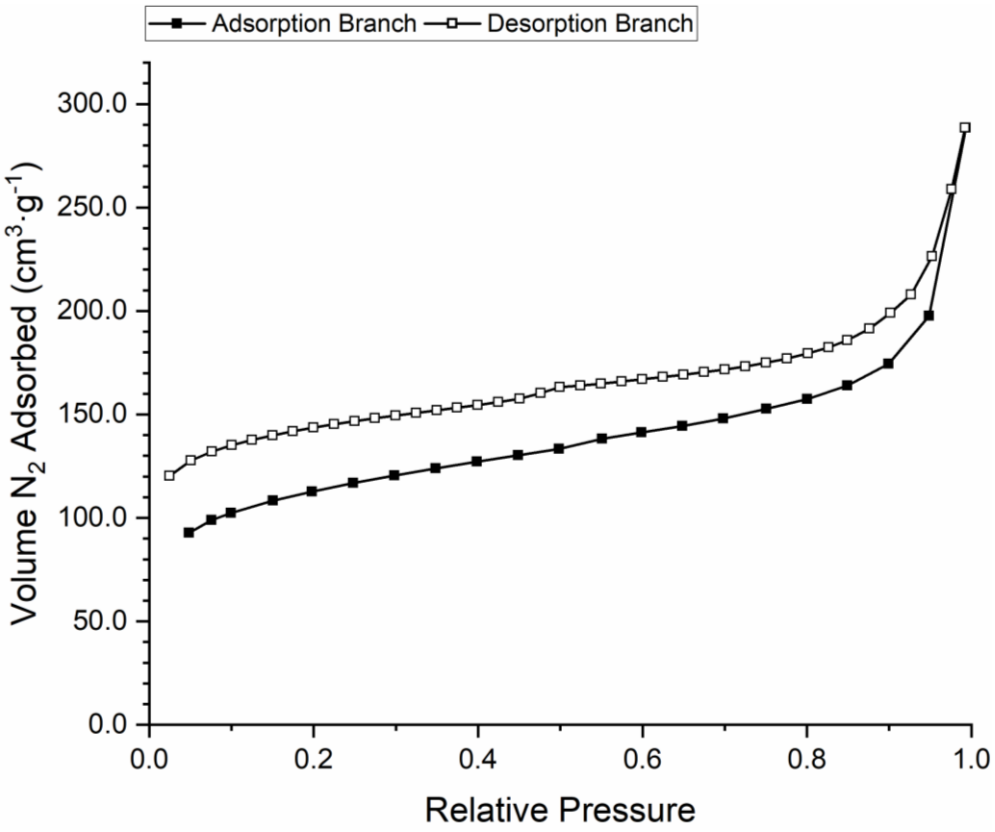

*Figure D-3 Nitrogen adsorption isotherm at 77 K of **PTPA-FLR-SR***

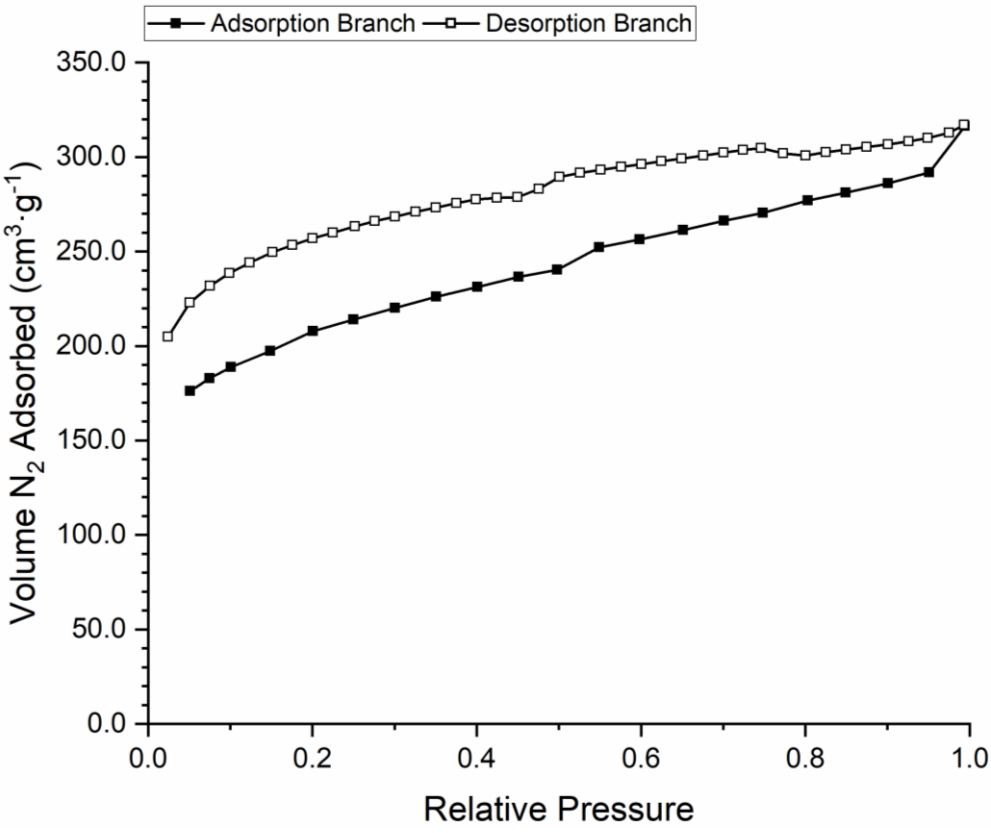

*Figure D-4 Nitrogen adsorption isotherm at 77 K of **PTPB-FLR-SN***

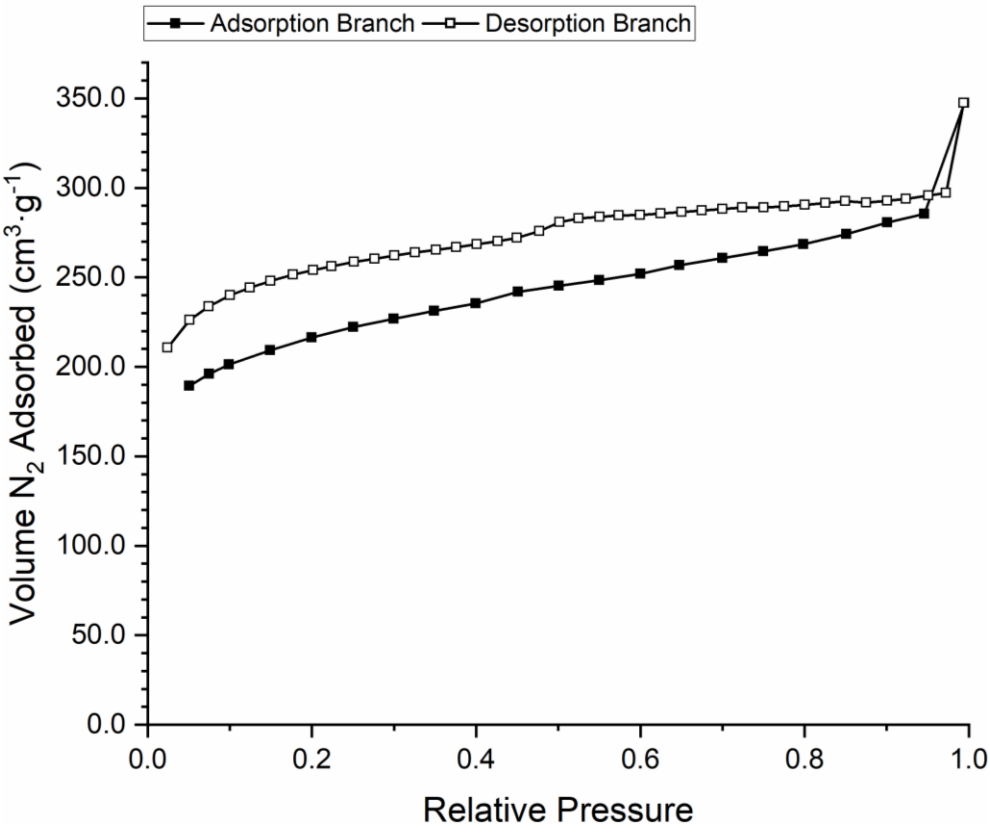

*Figure D-5 Nitrogen adsorption isotherm at 77 K of **PTPB-FLR-SNx***

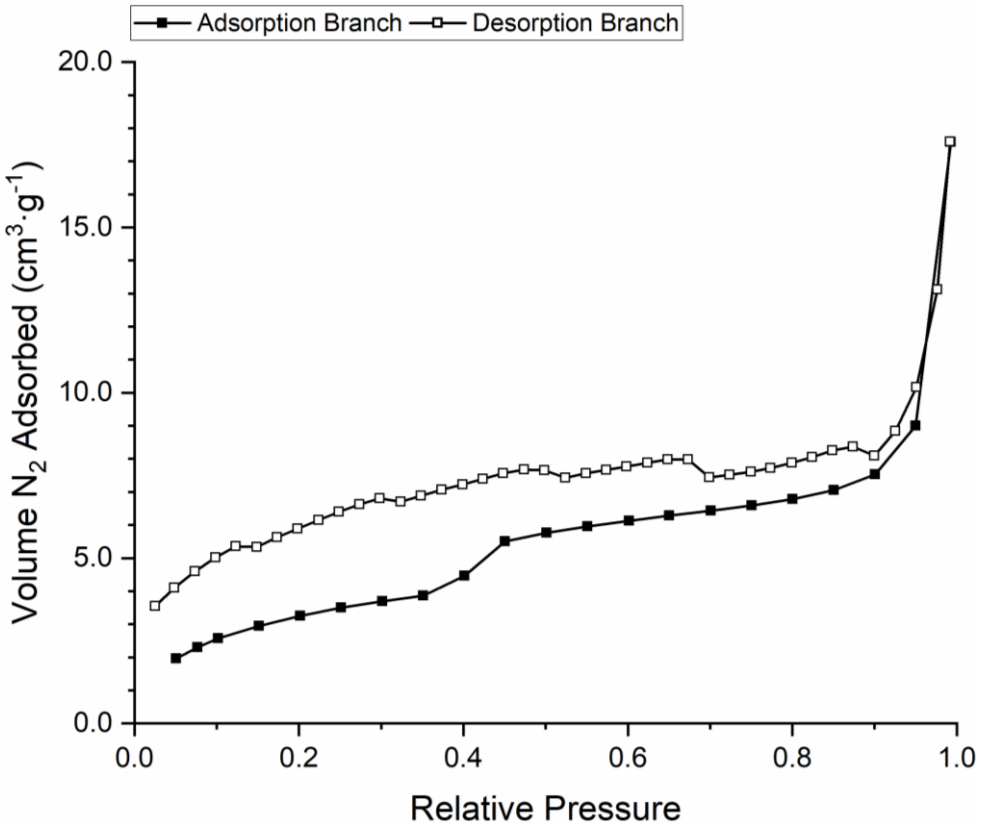

Figure D-6 Nitrogen adsorption isotherm at 77 K of ***PTPB-FLR-SR***

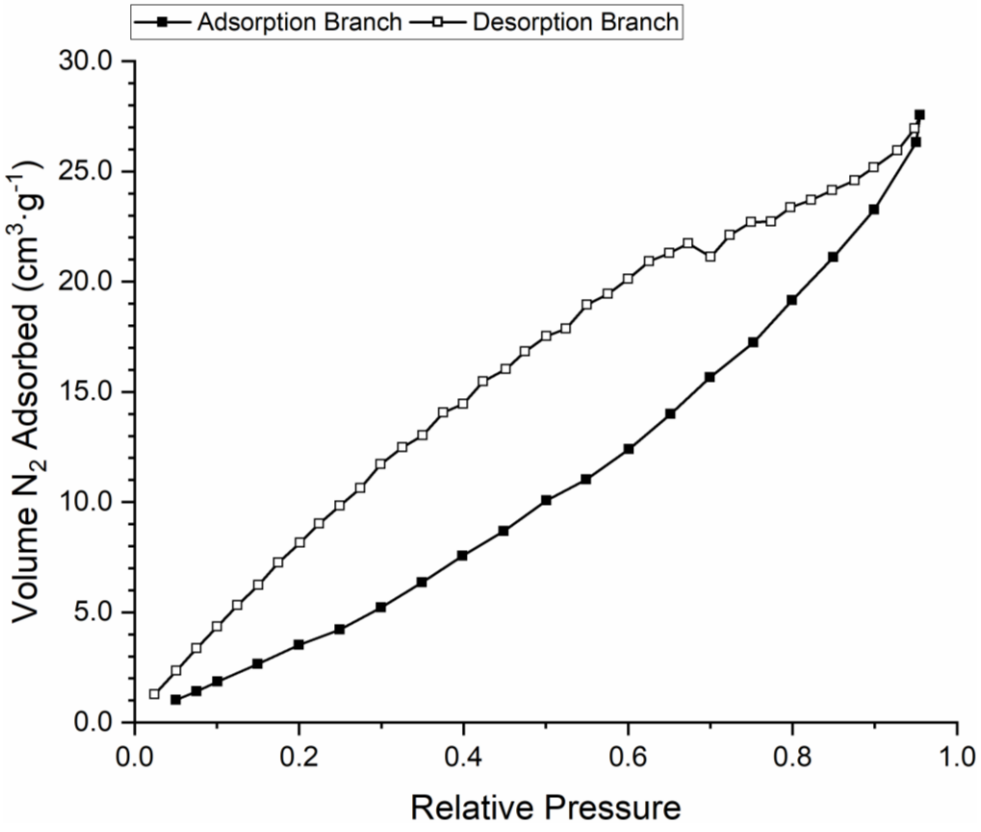

Figure D-7 Nitrogen adsorption isotherm at 77 K of ***PTPB-FLR-SRx***

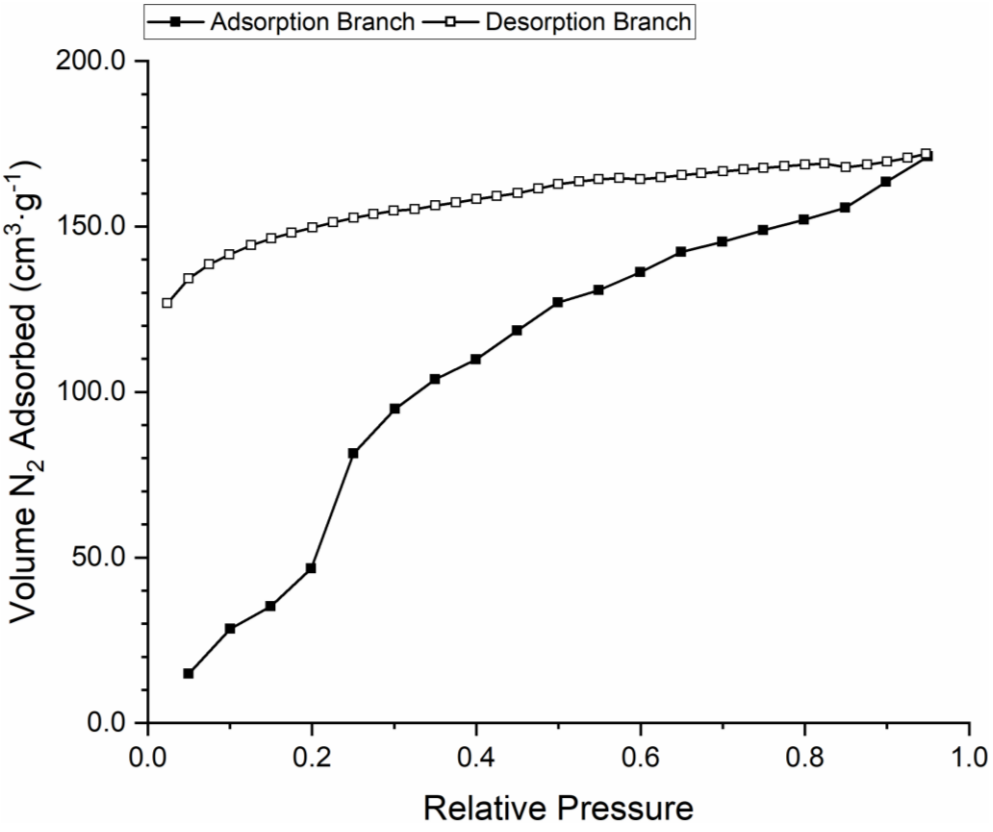

Figure D-8 Nitrogen adsorption isotherm at 77 K of ***PTPT-BZN-SN***

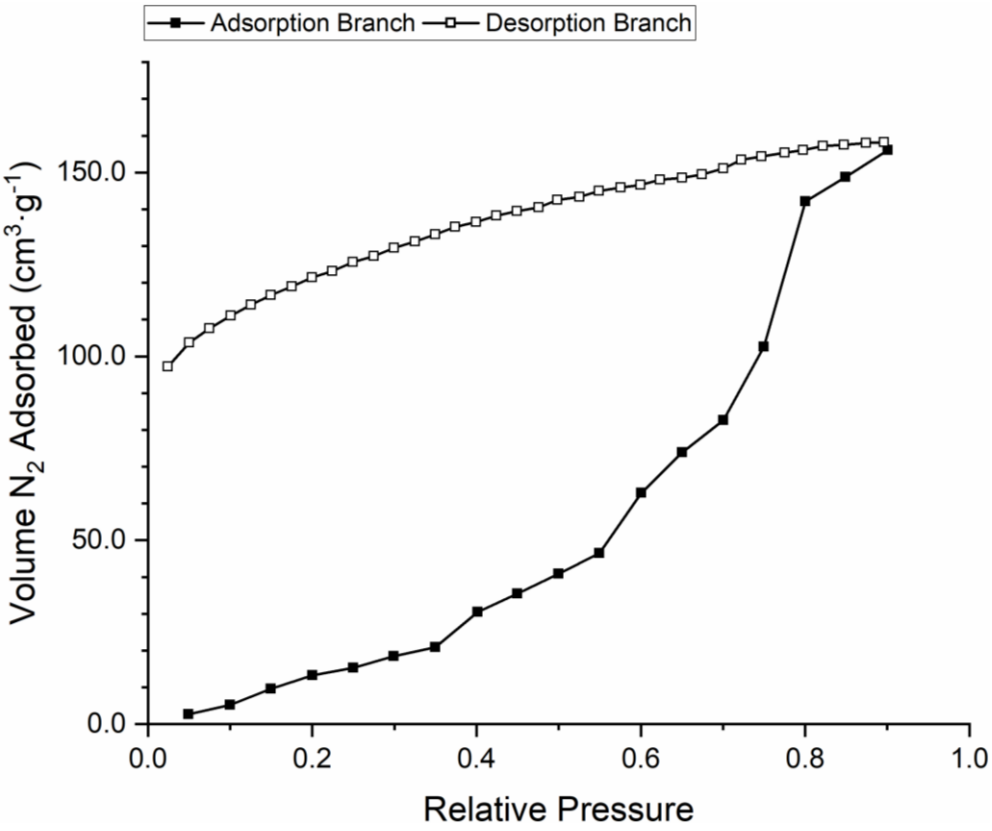

Figure D-9 Nitrogen adsorption isotherm at 77 K of ***PTPT-BZN-SNx***

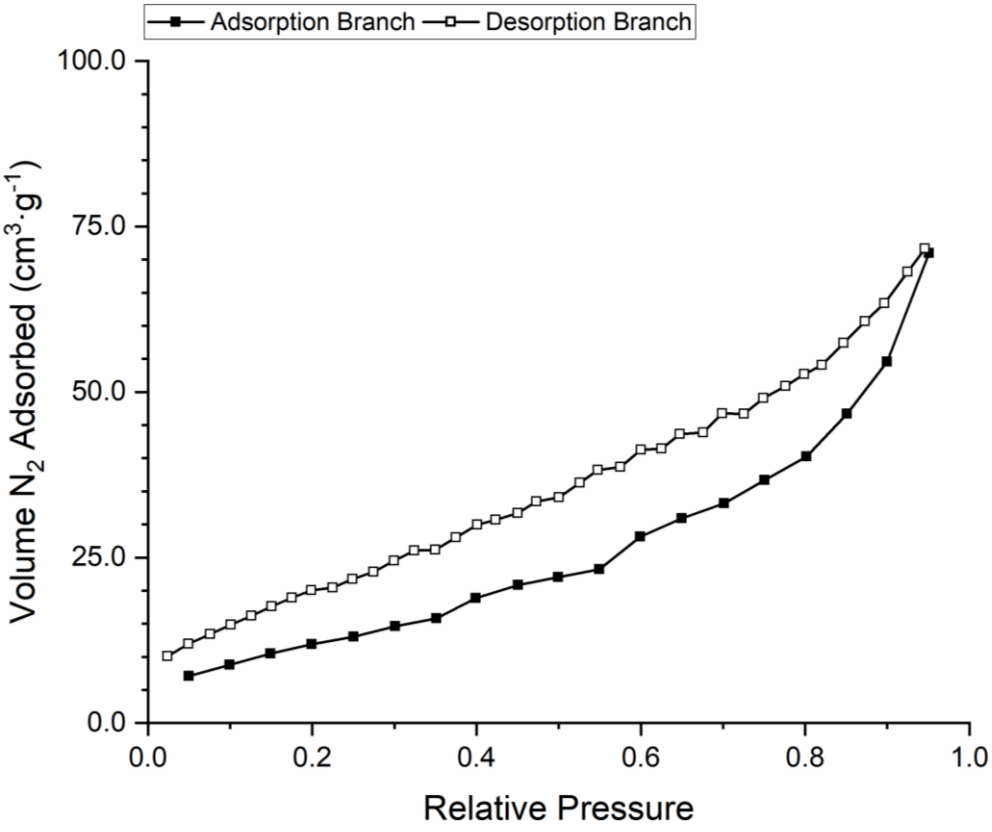

*Figure D-10 Nitrogen adsorption isotherm at 77 K of **PTPT-BZN-SR***

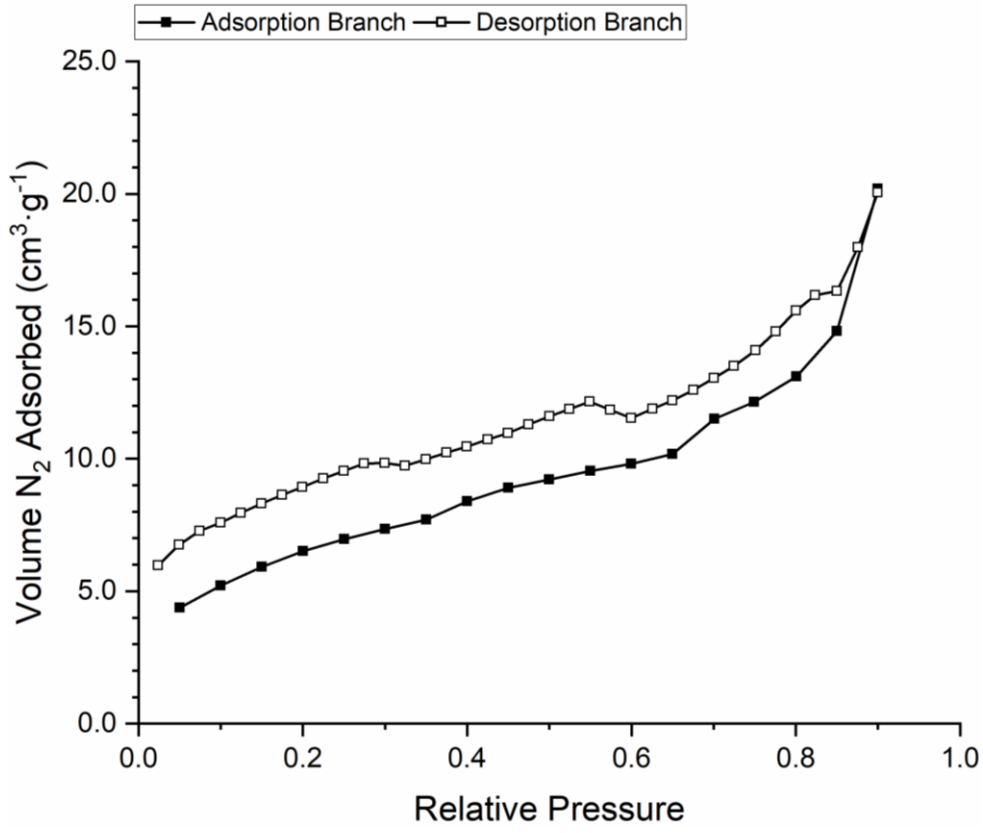

*Figure D-11 Nitrogen adsorption isotherm at 77 K of **PTPT-BZN-SRx***

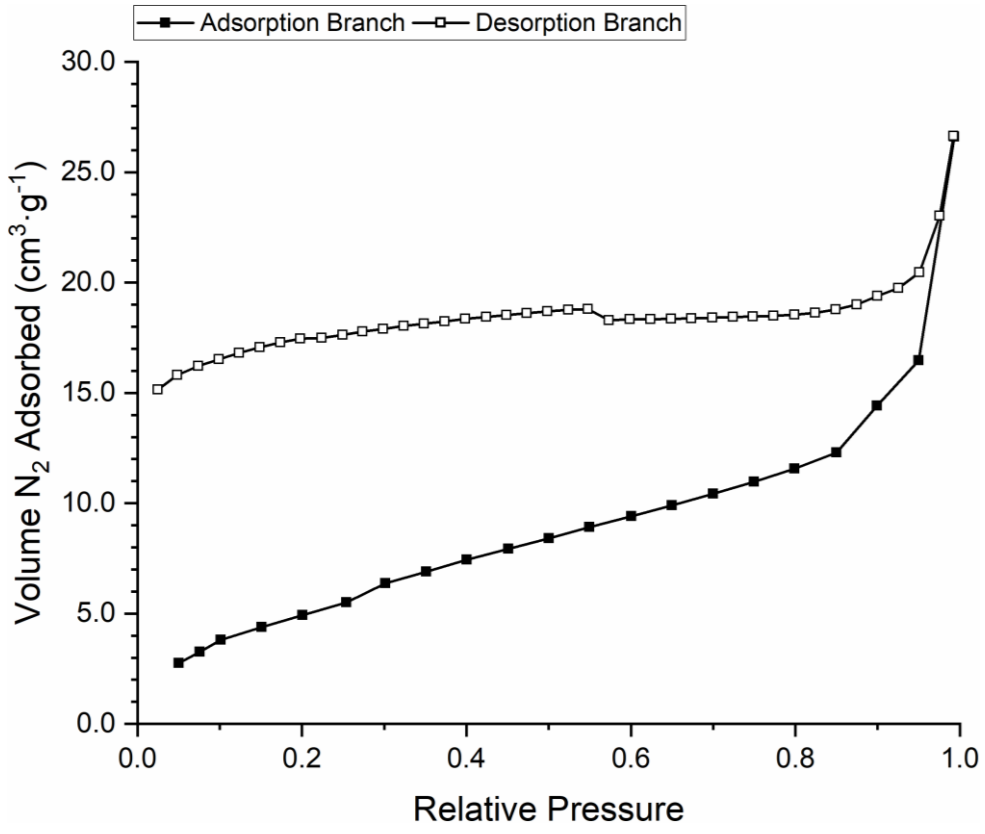

*Figure D-12 Nitrogen adsorption isotherm at 77 K of **PTPT-FLR-SN***

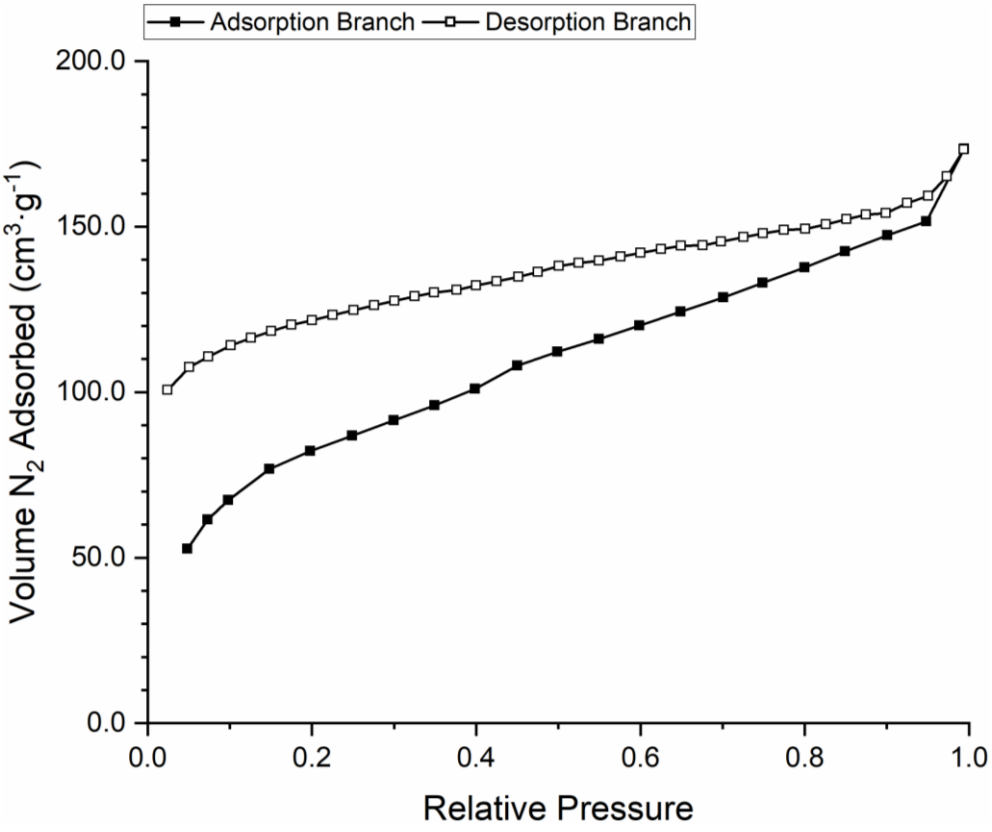

*Figure D-13 Nitrogen adsorption isotherm at 77 K of **PTPT-FLR-SNx***

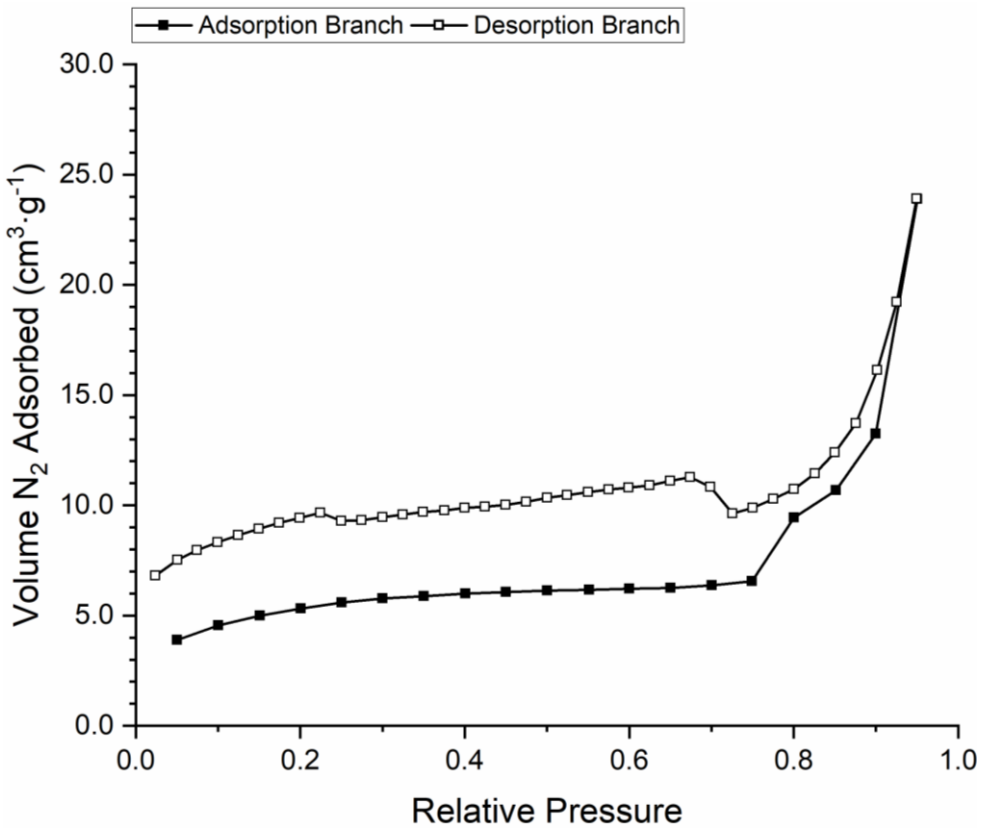

*Figure D-14 Nitrogen adsorption isotherm at 77 K of **PTPT-FLR-SR***

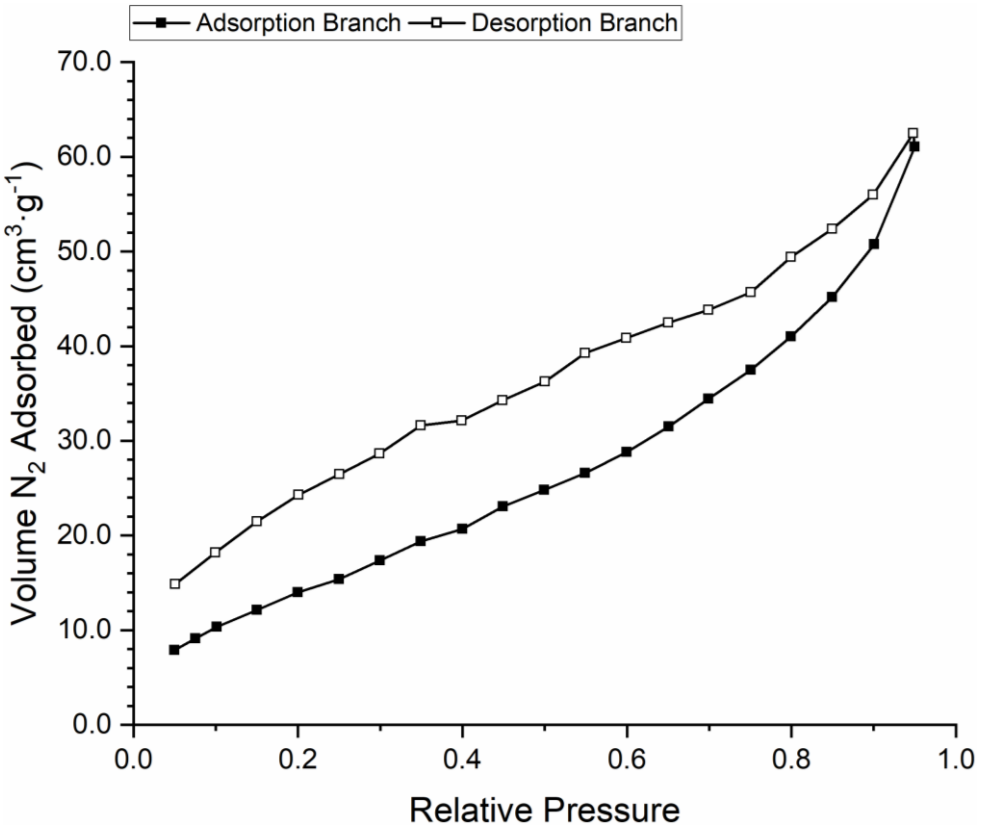

*Figure D-15 Nitrogen adsorption isotherm at 77 K of **PTPT-FLR-SRx***

D.1.2 BET Analysis Plots

Table D-1 Parameters related to the BET analysis of nitrogen adsorption isotherm data at 77 K of PANI-CMPs

Material	Number of Points	Slope	Intercept	R^2	*c* Constant	Specific Surface Area ($m^2 \cdot g^{-1}$)
PTPA-FLR-SN	5	6.106	-0.005754	0.999645	-1060.173	570.9
PTPA-FLR-SNx	5	10.027	0.1938	0.999917	52.726	340.7
PTPA-FLR-SR	5	8.786	-7.433e-5	0.999697	-1.182e+5	396.4
PTPB-FLR-SN	5	4.838	-0.007758	0.999881	-622.603	721.0
PTPB-FLR-SNx	5	4.681	-0.01966	0.999617	-237.137	747.1
PTPB-FLR-SR	5	266.759	8.231	0.999935	33.409	12.7
PTPB-FLR-SRx	7	94.929	38.28	0.993845	3.480	26.1
PTPT-BZN-SN	4	10.442	2.250	0.975585	5.640	274.4
PTPT-BZN-SNx	6	9.617	14.69	0.599394	1.655	143.3
PTPT-BZN-SR	7	70.035	2.792	0.999460	26.083	47.8
PTPT-BZN-SRx	5	141.959	2.627	0.999810	55.034	24.1
PTPT-FLR-SN	6	167.310	7.101	0.999810	24.561	20.0
PTPT-FLR-SNx	4	10.469	0.2637	0.999989	40.705	324.5
PTPT-FLR-SR	3	174.758	2.064	0.999997	85.671	19.7
PTPT-FLR-SRx	7	57.745	2.773	0.999067	21.726	57.8

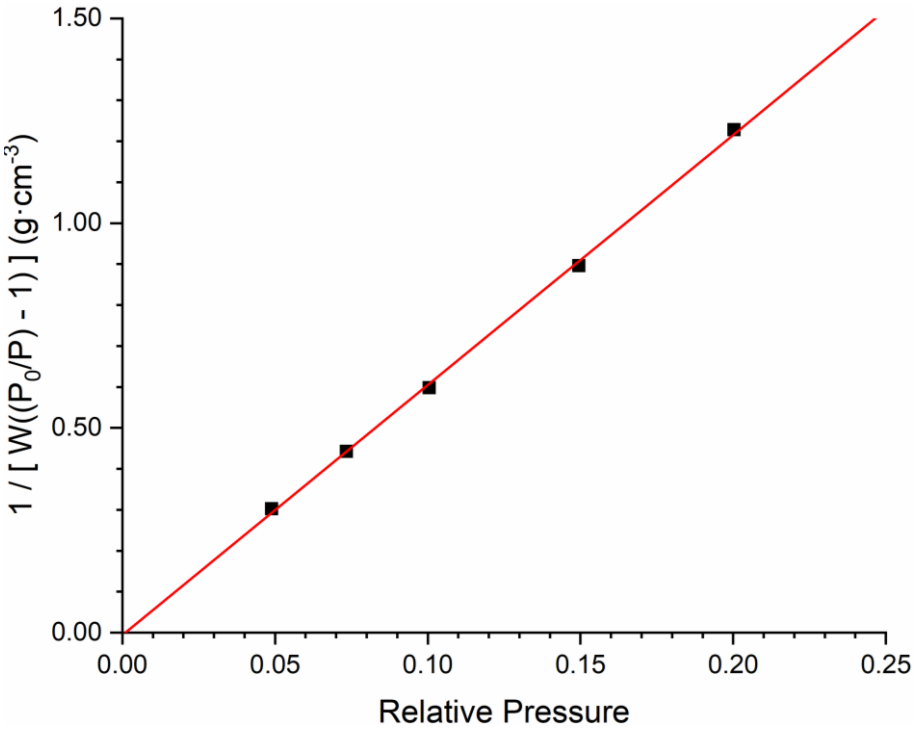

*Figure D-16 BET analysis plot for **PTPA-FLR-SN***

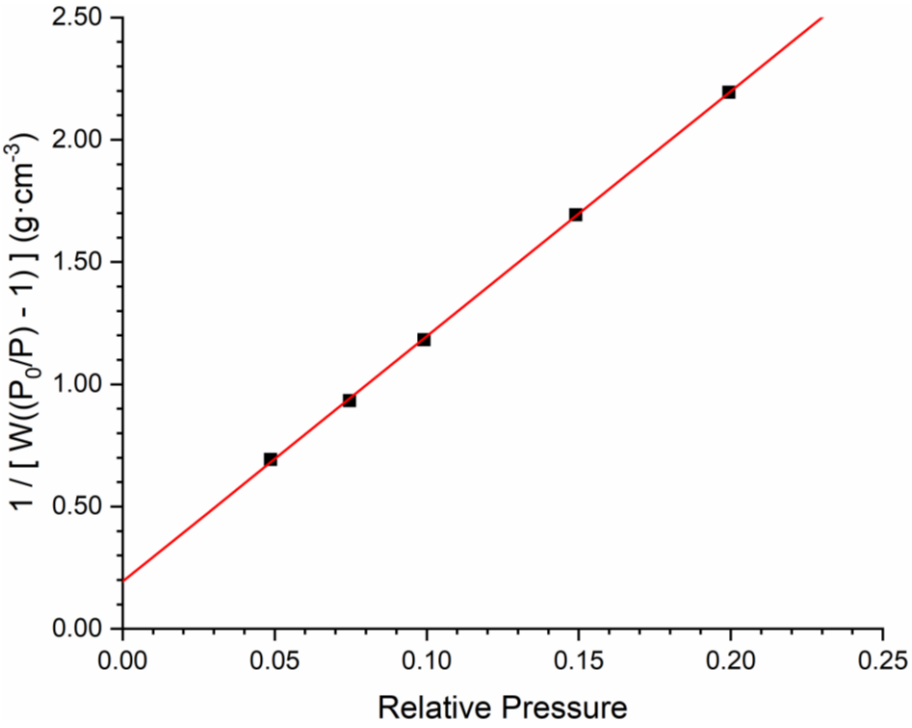

*Figure D-17 BET analysis plot for **PTPA-FLR-SNx***

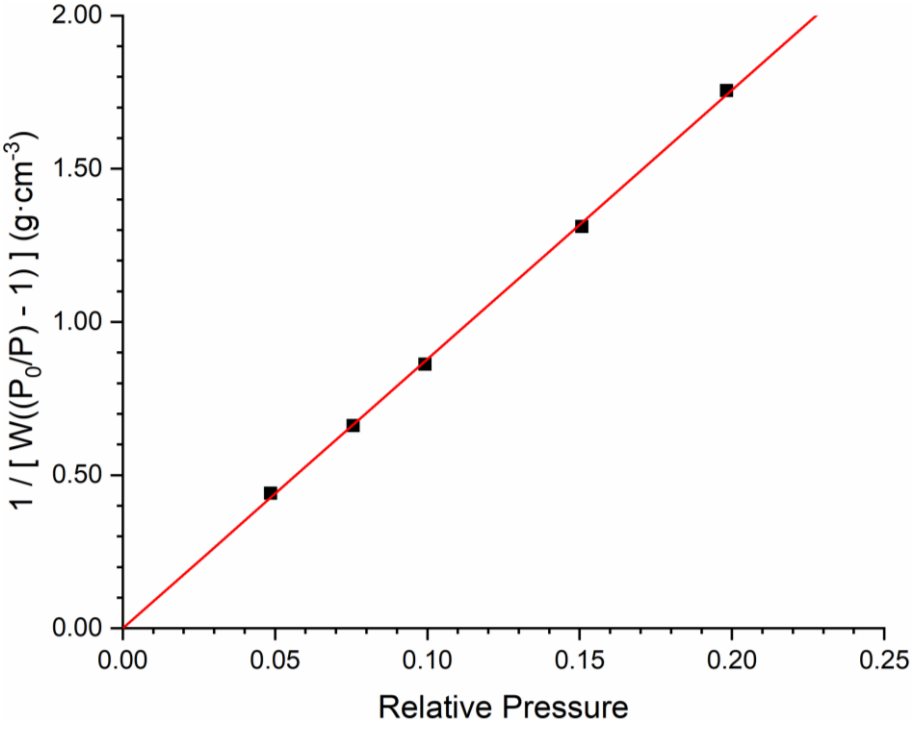

*Figure D-18 BET analysis plot for **PTPA-FLR-SR***

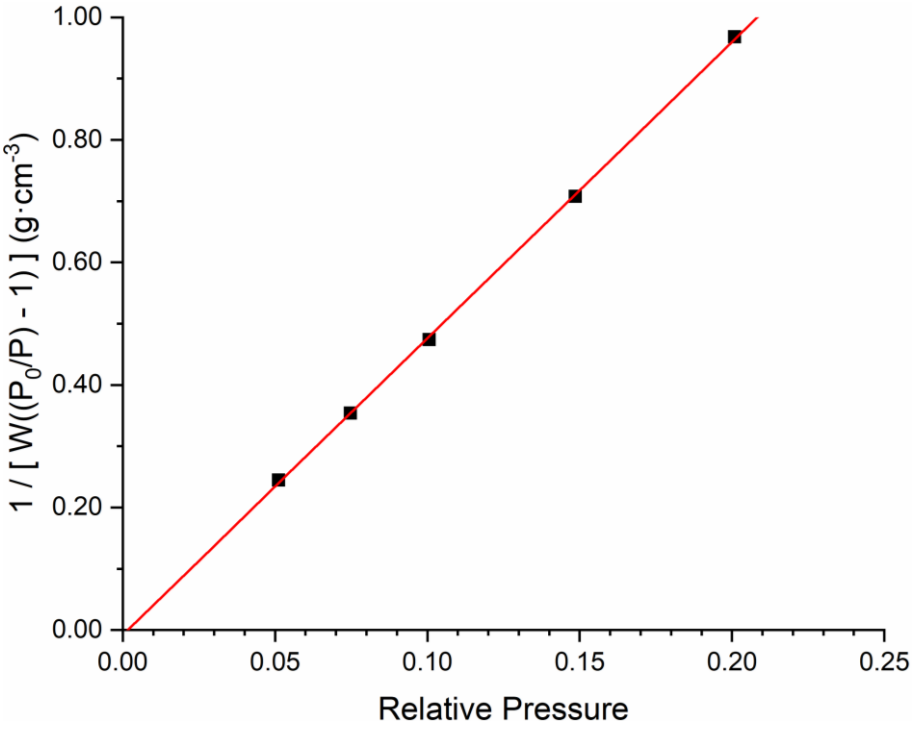

*Figure D-19 BET analysis plot for **PTPB-FLR-SN***

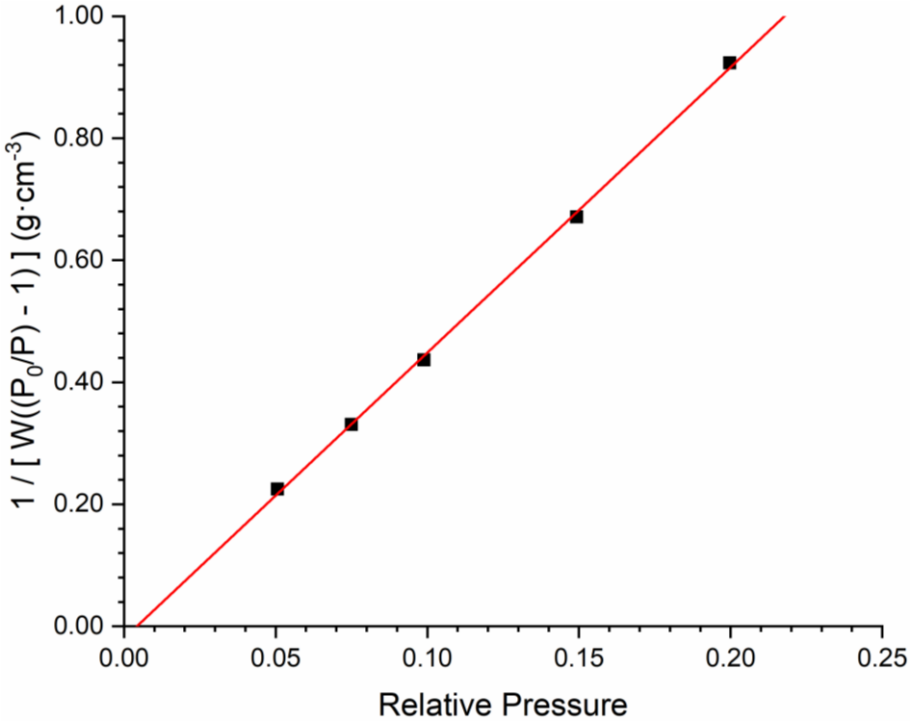

*Figure D-20 BET analysis plot for **PTPB-FLR-SNx***

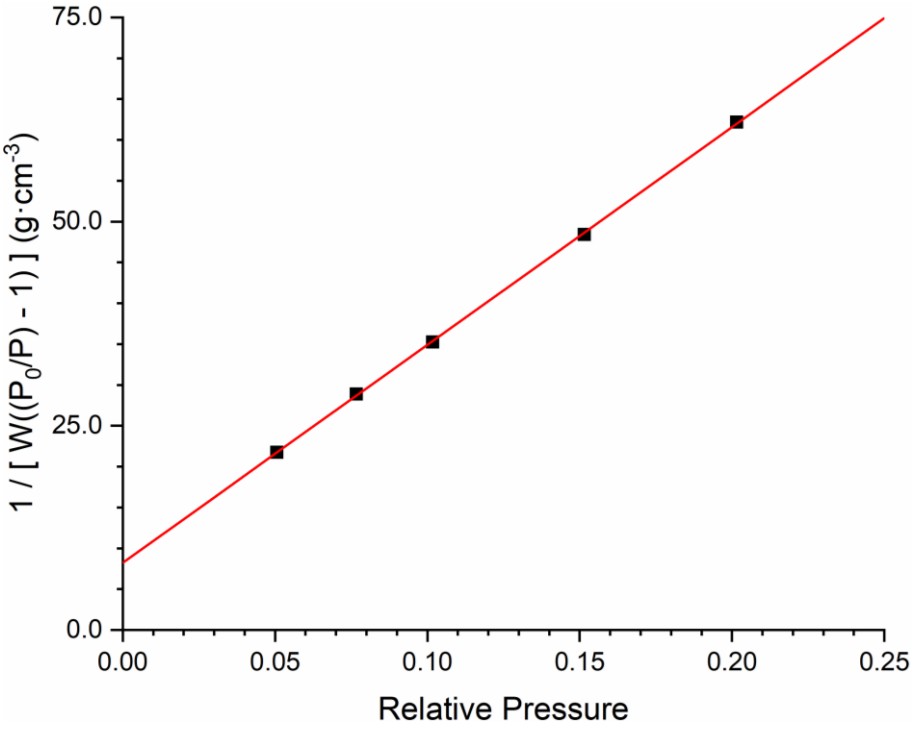

*Figure D-21 BET analysis plot for **PTPB-FLR-SR***

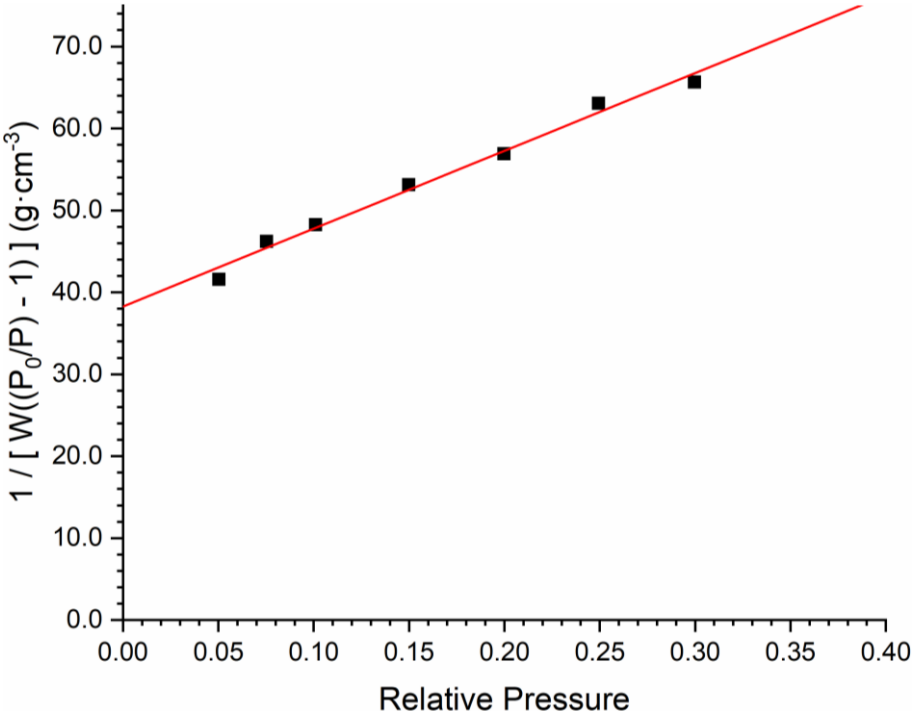

*Figure D-22 BET analysis plot for **PTPB-FLR-SRx***

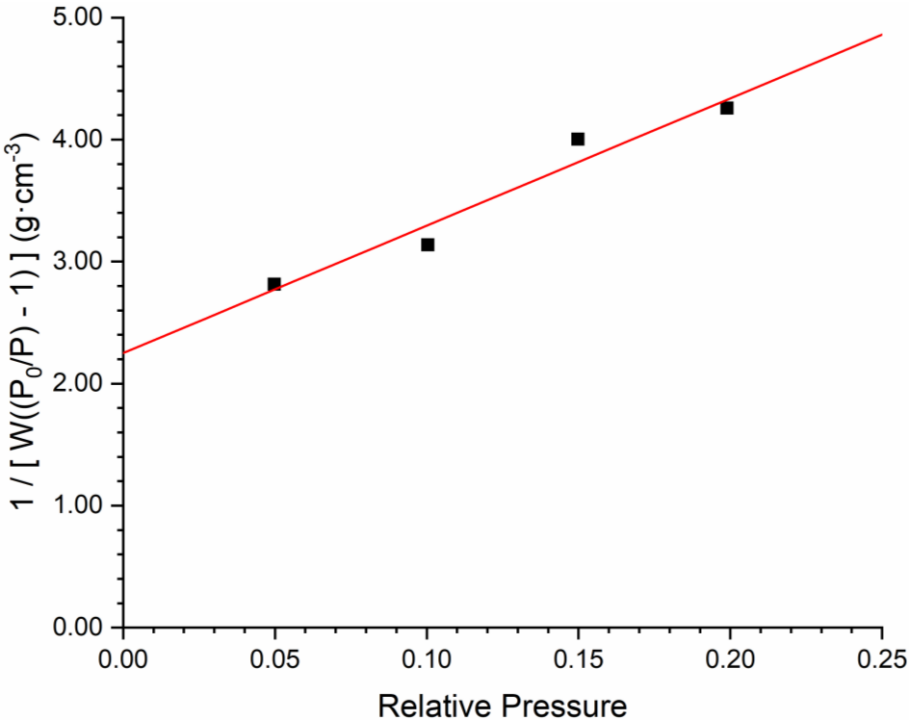

*Figure D-23 BET analysis plot for **PTPT-BZN-SN***

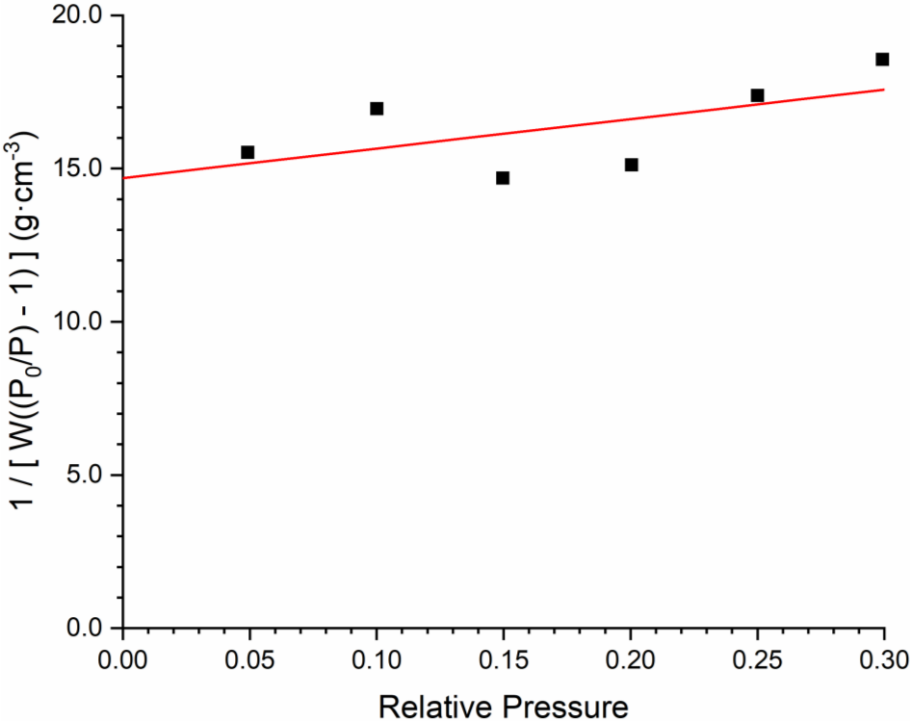

*Figure D-24 BET analysis plot for **PTPT-BZN-SNx***

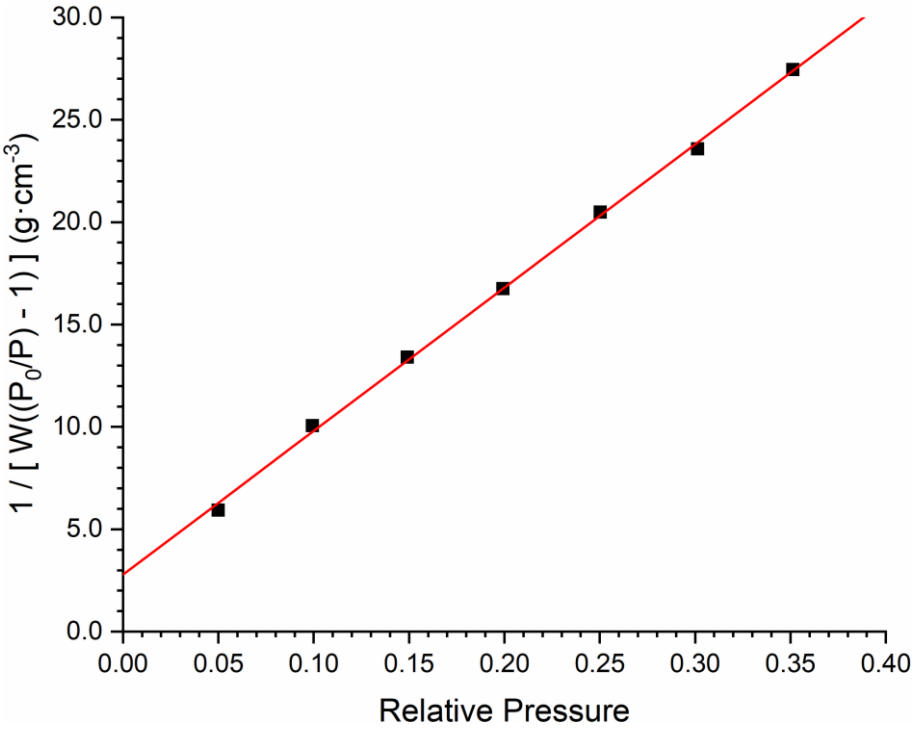

*Figure D-25 BET analysis plot for **PTPT-BZN-SR***

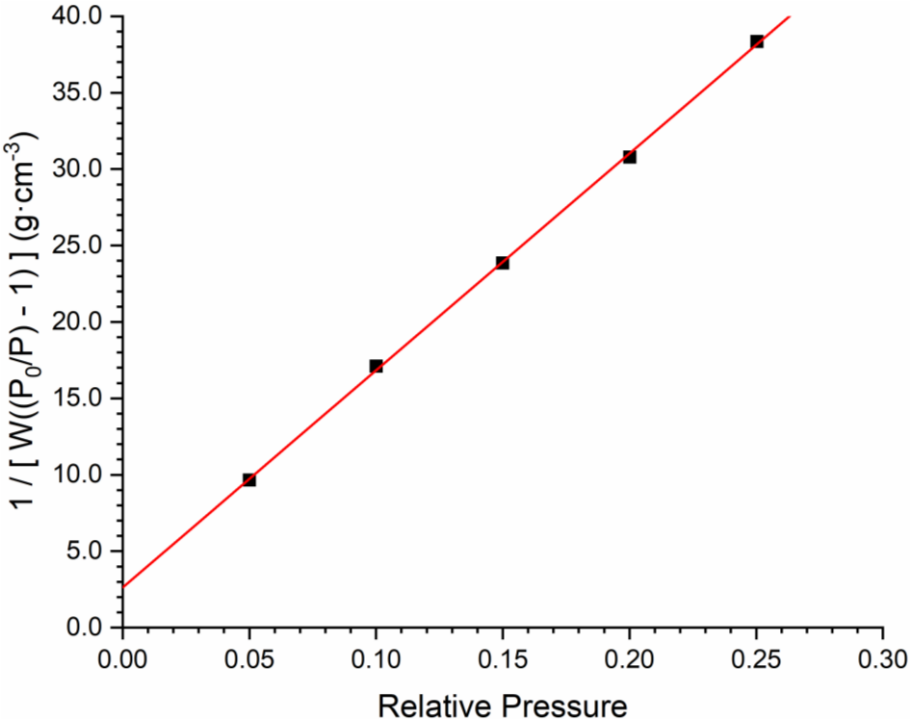

*Figure D-26 BET analysis plot for **PTPT-BZN-SRx***

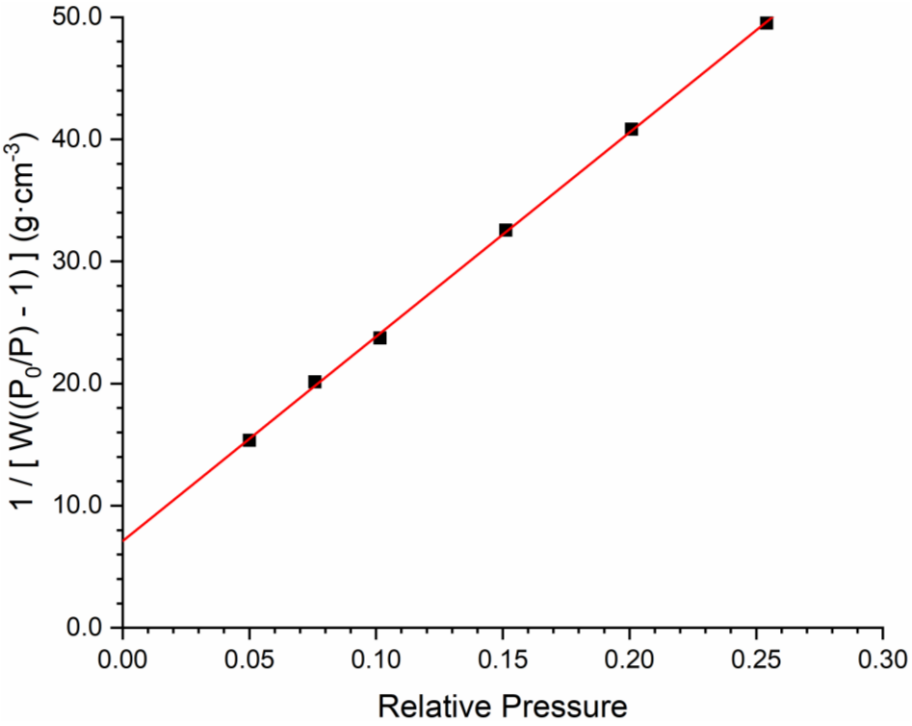

*Figure D-27 BET analysis plot for **PTPT-FLR-SN***

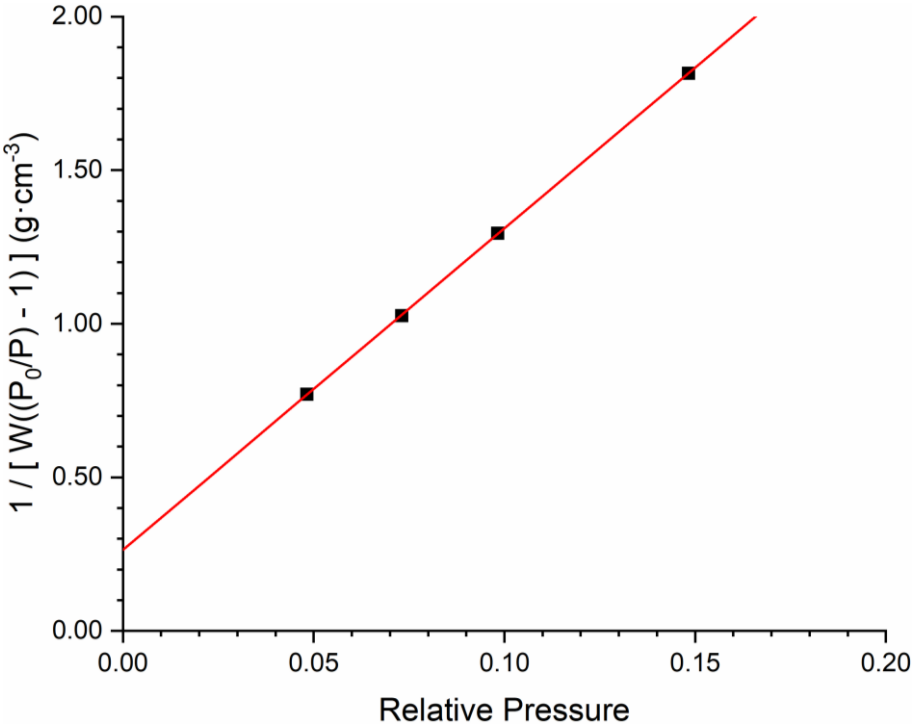

*Figure D-28 BET analysis plot for **PTPT-FLR-SNx***

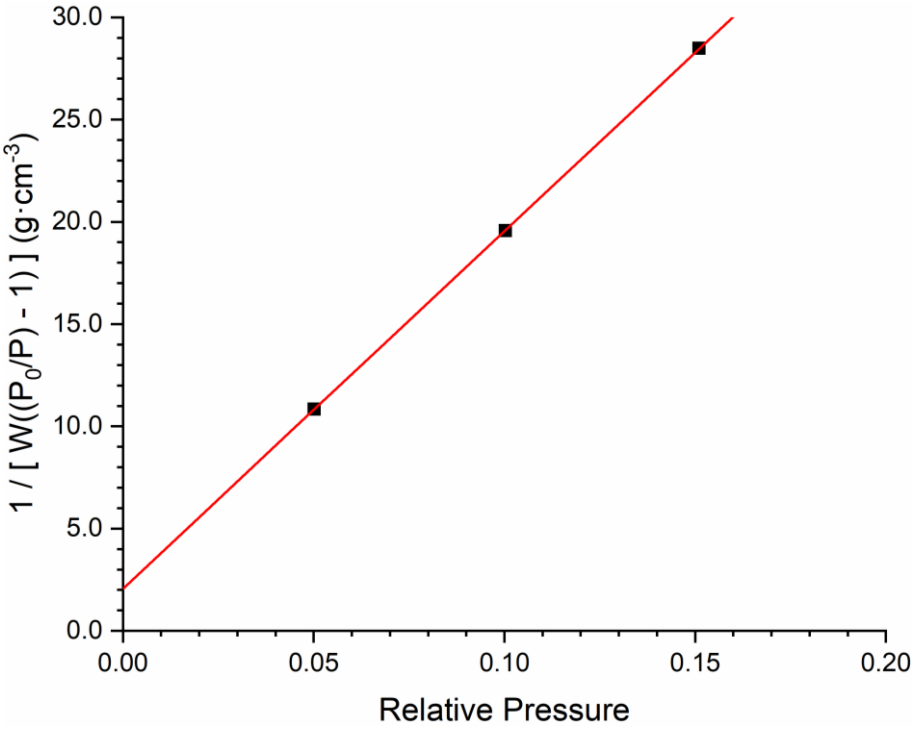

*Figure D-29 BET analysis plot for **PTPT-FLR-SR***

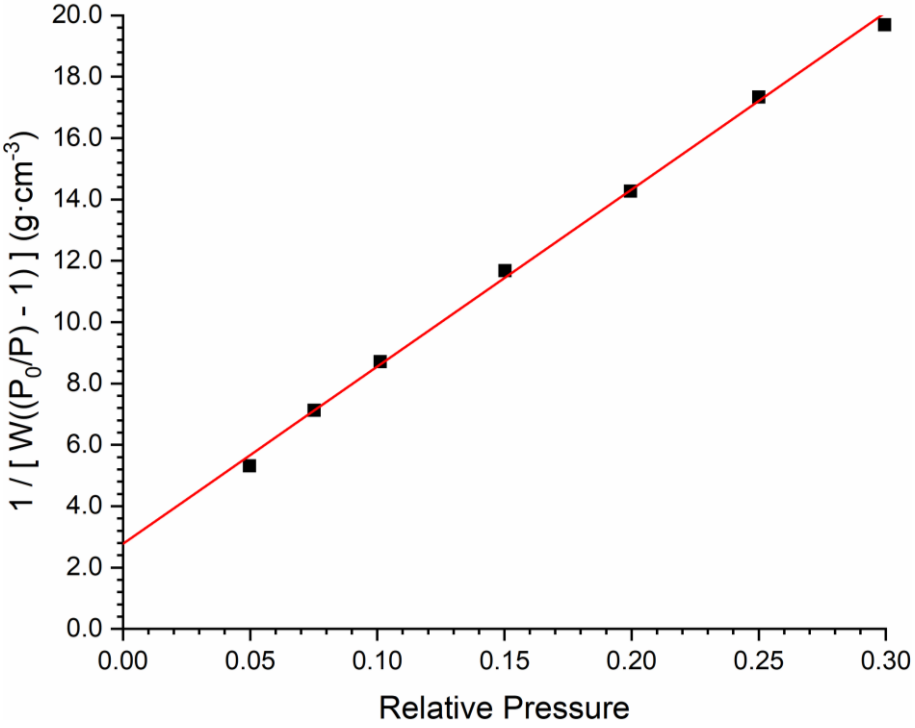

*Figure D-30 BET analysis plot for **PTPT-FLR-SRx***

D.1.3 NLDFT Pore Size Distribution Plots

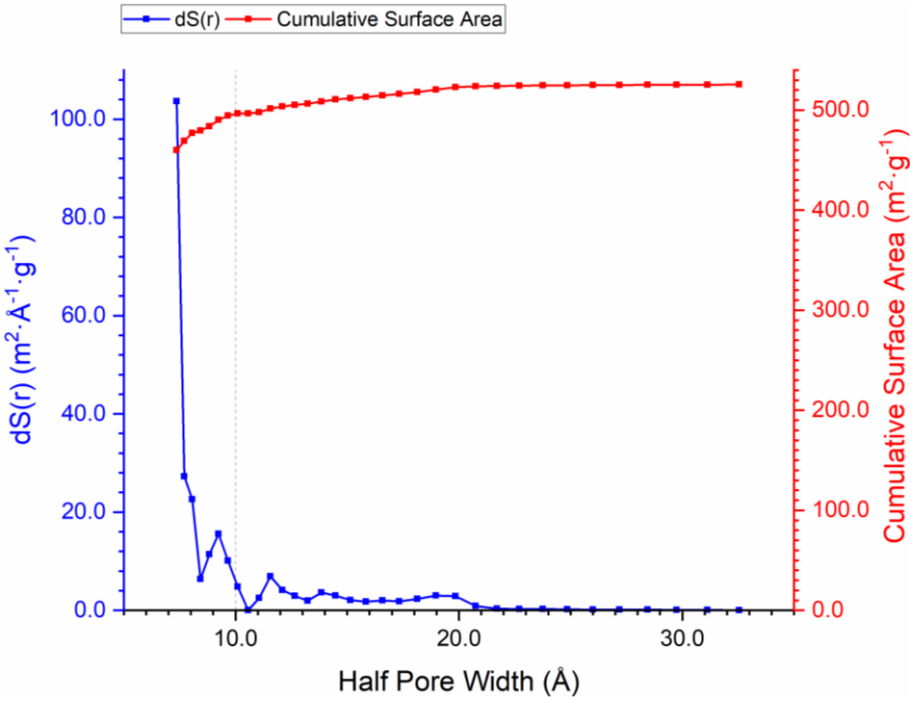

*Figure D-31 NLDFT pore size distributions in **PTPA-FLR-SN**, analysed from surface area, and cumulative surface area plot*

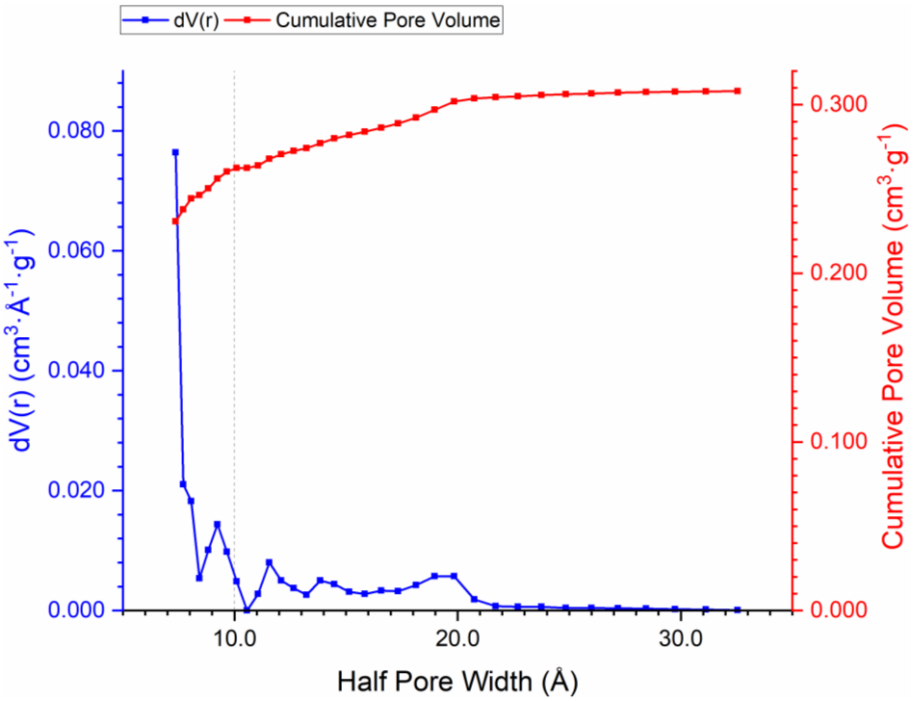

*Figure D-32 NLDFT pore size distributions in **PTPA-FLR-SN**, analysed from pore volume, and cumulative pore volume plot*

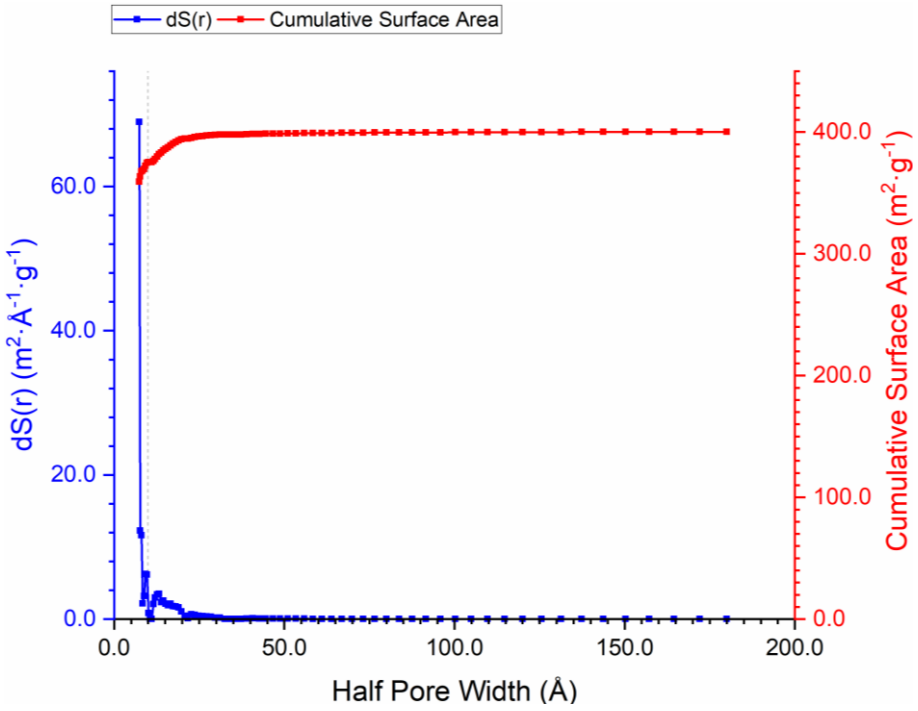

*Figure D-33 NLDFT pore size distributions in **PTPA-FLR-SNx**, analysed from surface area, and cumulative surface area plot*

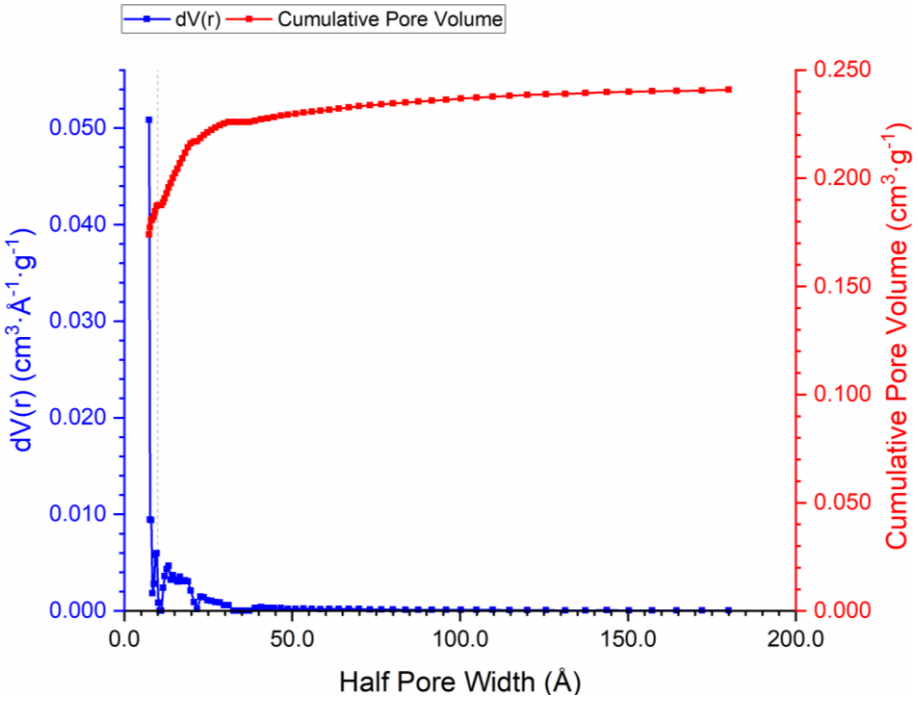

*Figure D-34 NLDFT pore size distributions in **PTPA-FLR-SNx**, analysed from pore volume, and cumulative pore volume plot*

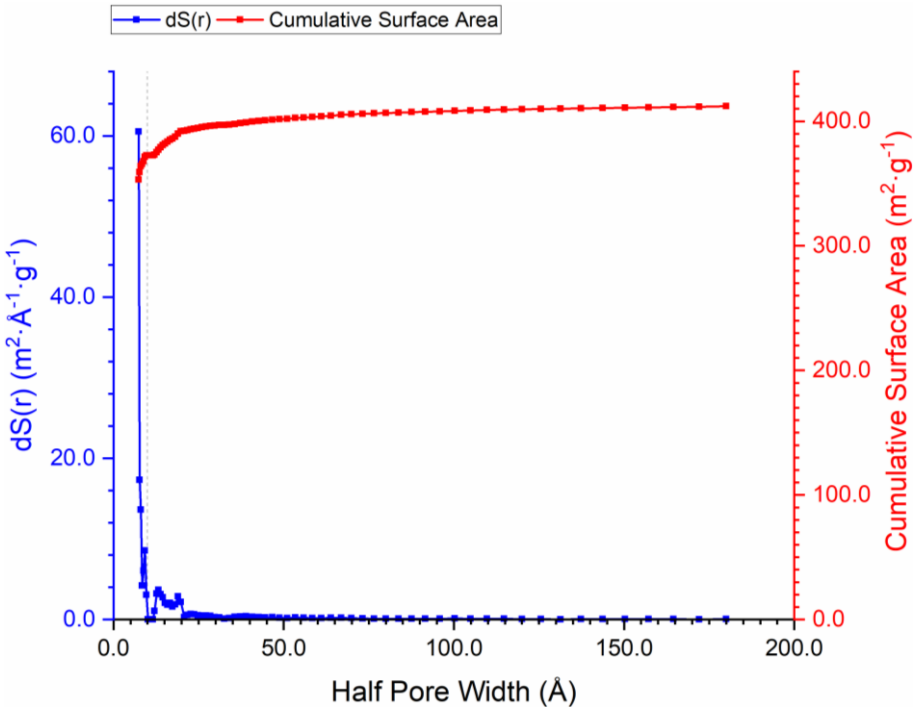

*Figure D-35 NLDFT pore size distributions in **PTPA-FLR-SR**, analysed from surface area, and cumulative surface area plot*

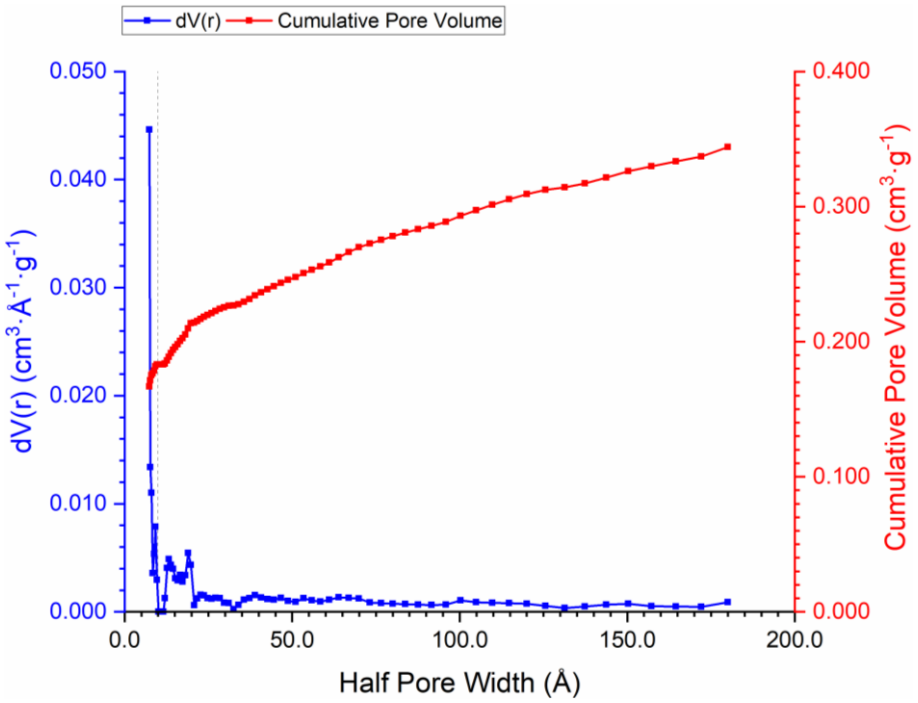

*Figure D-36 NLDFT pore size distributions in **PTPA-FLR-SR**, analysed from pore volume, and cumulative pore volume plot*

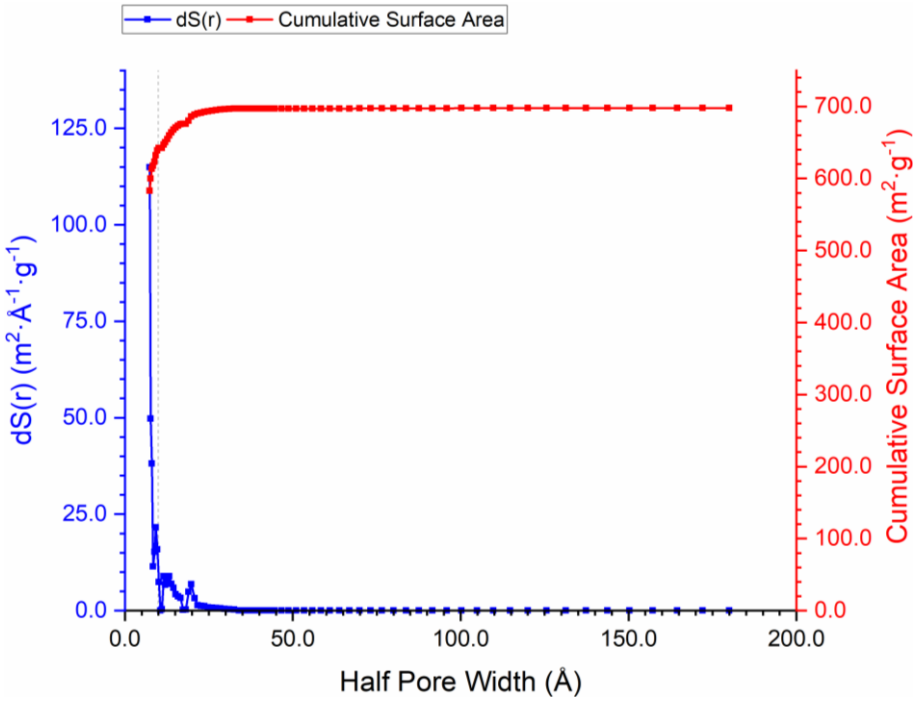

*Figure D-37 NLDFT pore size distributions in **PTPB-FLR-SN**, analysed from surface area, and cumulative surface area plot*

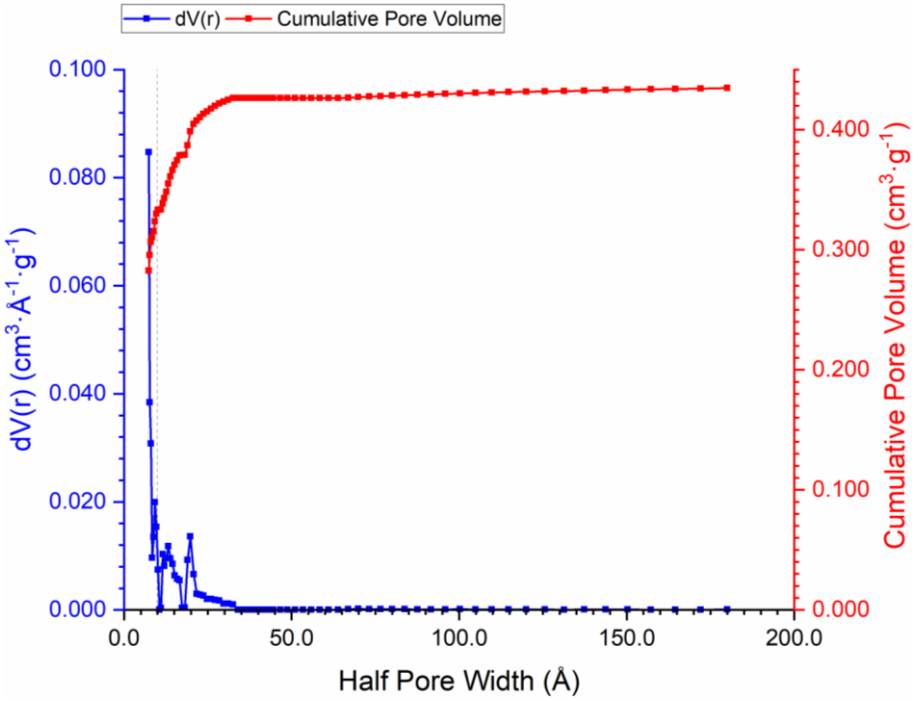

*Figure D-38 NLDFT pore size distributions in **PTPB-FLR-SN**, analysed from pore volume, and cumulative pore volume plot*

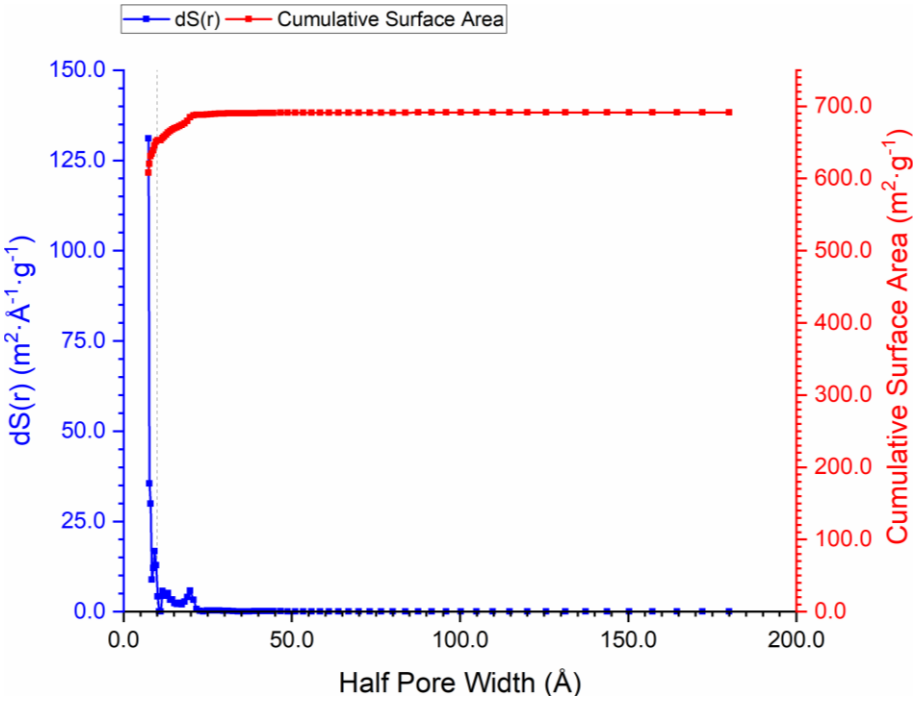

*Figure D-39 NLDFT pore size distributions in **PTPB-FLR-SNx**, analysed from surface area, and cumulative surface area plot*

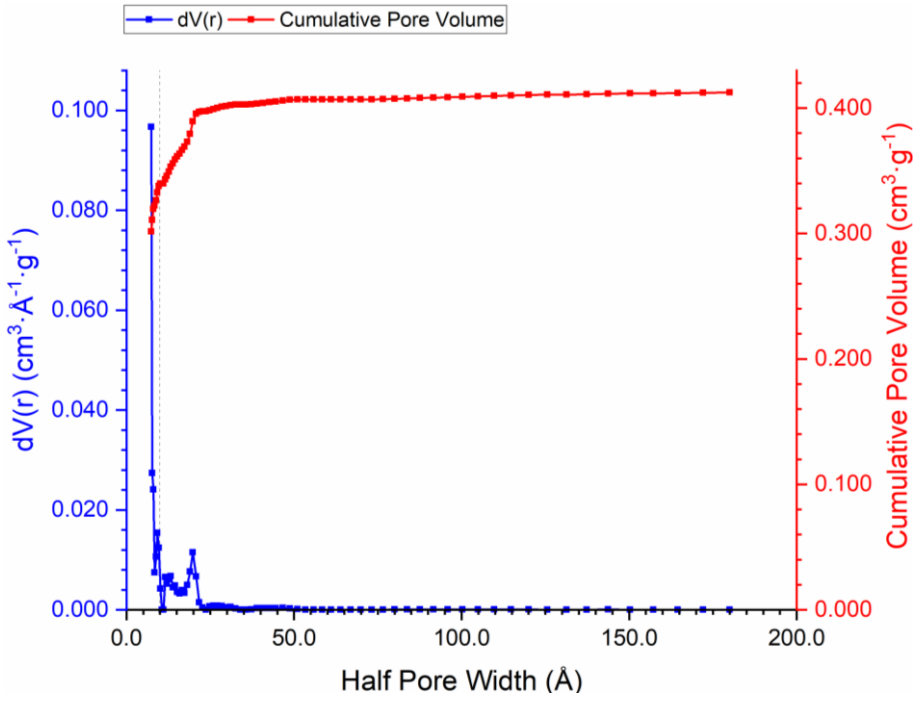

*Figure D-40 NLDFT pore size distributions in **PTPB-FLR-SNx**, analysed from pore volume, and cumulative pore volume plot*

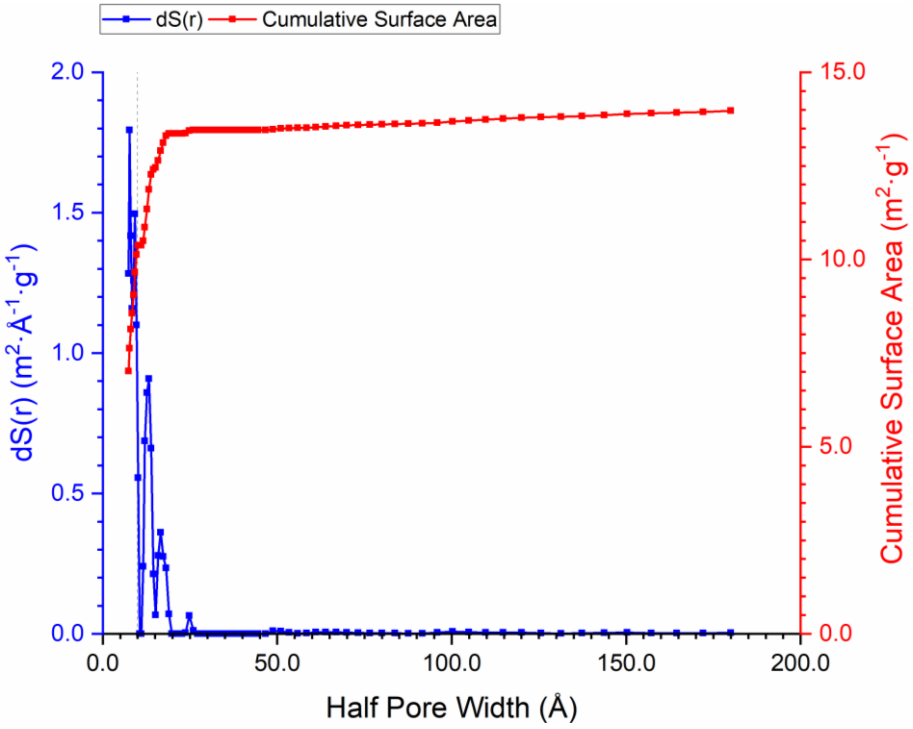

*Figure D-41 NLDFT pore size distributions in **PTPB-FLR-SR**, analysed from surface area, and cumulative surface area plot*

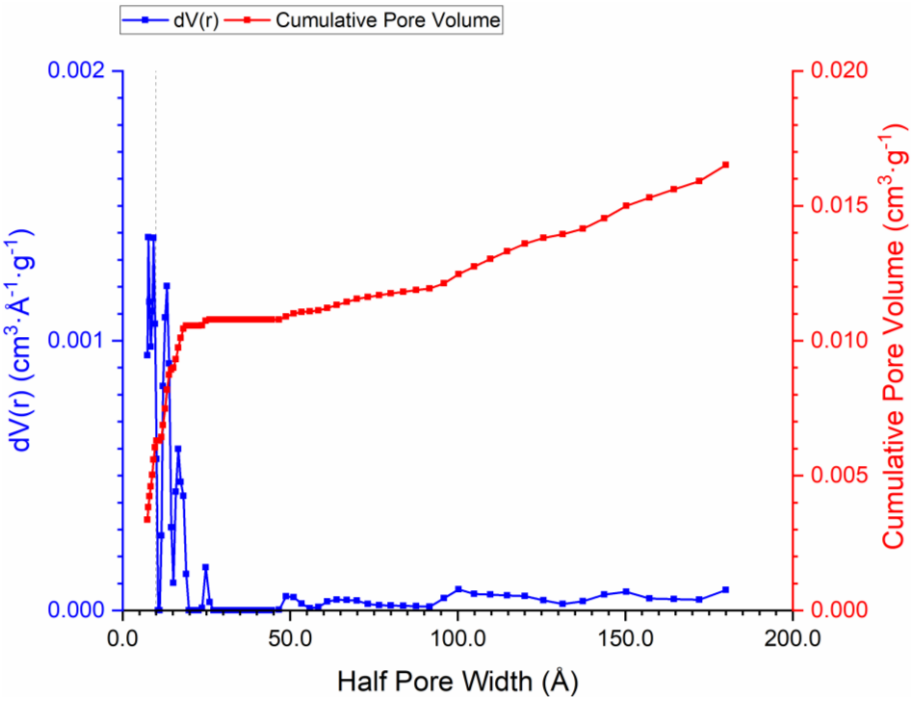

*Figure D-42 NLDFT pore size distributions in **PTPB-FLR-SR**, analysed from pore volume, and cumulative pore volume plot*

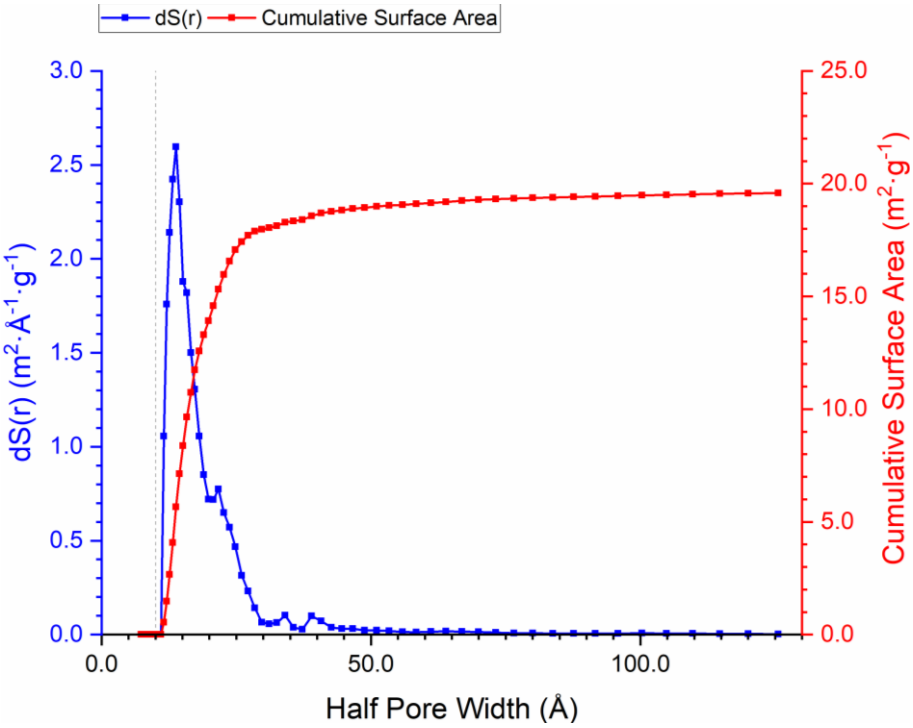

*Figure D-43 NLDFT pore size distributions in **PTPB-FLR-SRx**, analysed from surface area, and cumulative surface area plot*

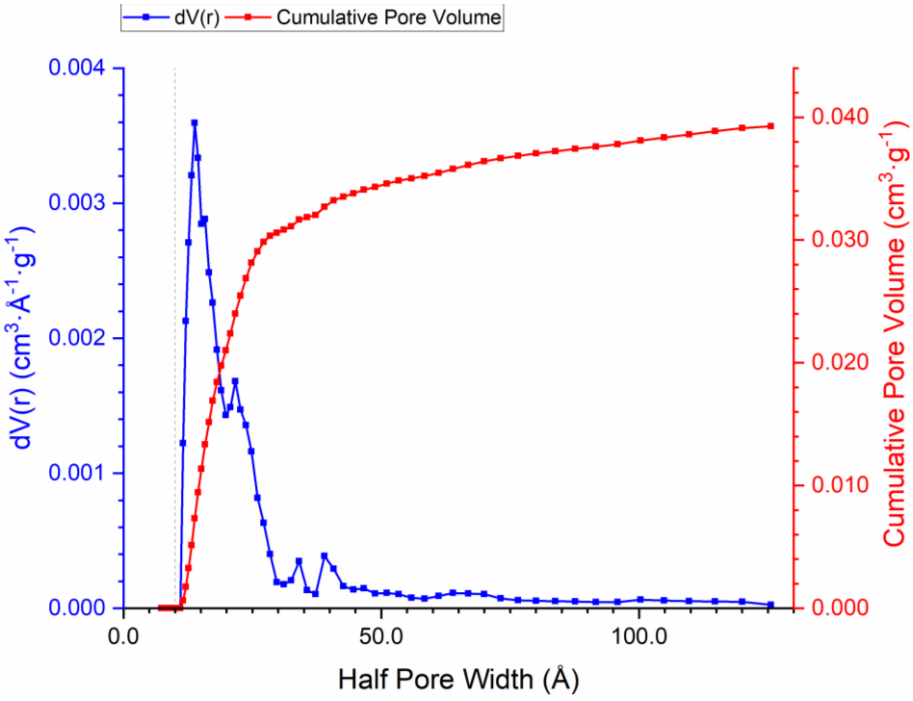

*Figure D-44 NLDFT pore size distributions in **PTPB-FLR-SRx**, analysed from pore volume, and cumulative pore volume plot*

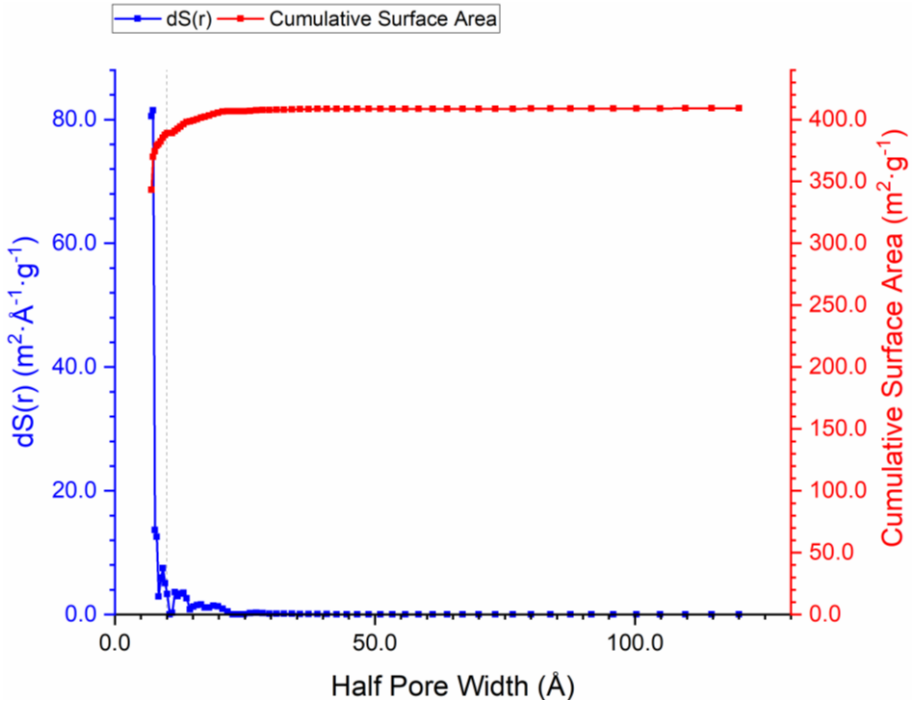

*Figure D-45 NLDFT pore size distributions in **PTPT-BZN-SN**, analysed from surface area, and cumulative surface area plot*

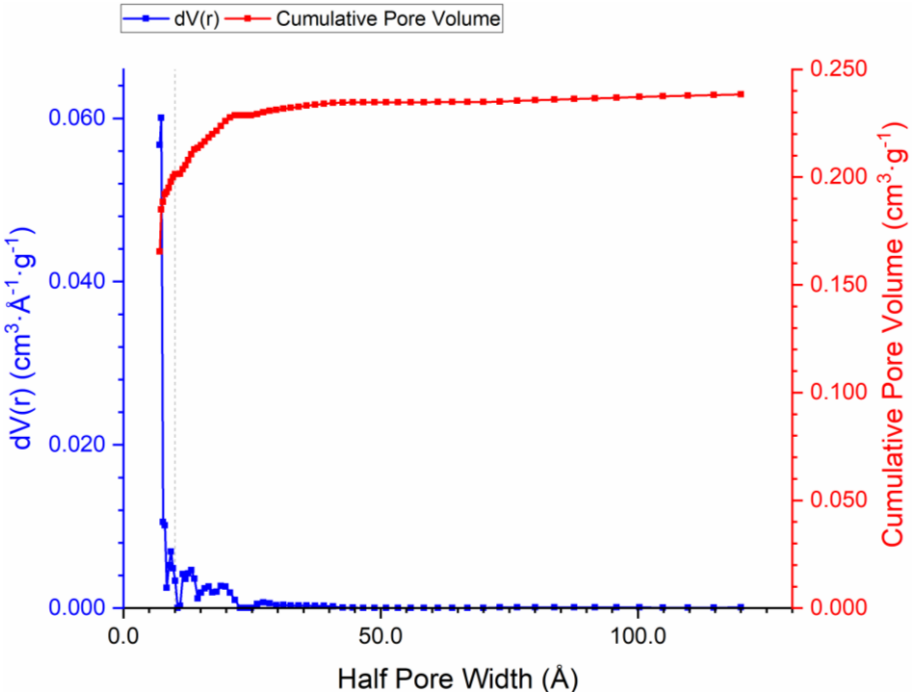

*Figure D-46 NLDFT pore size distributions in **PTPT-BZN-SN**, analysed from pore volume, and cumulative pore volume plot*

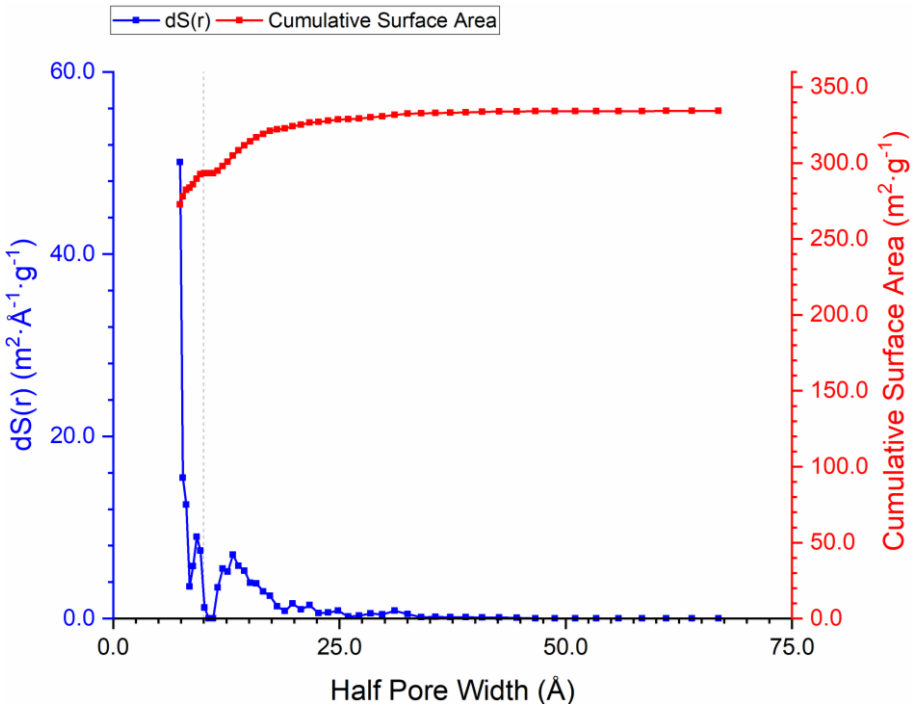

*Figure D-47 NLDFT pore size distributions in **PTPT-BZN-SNx**, analysed from surface area, and cumulative surface area plot*

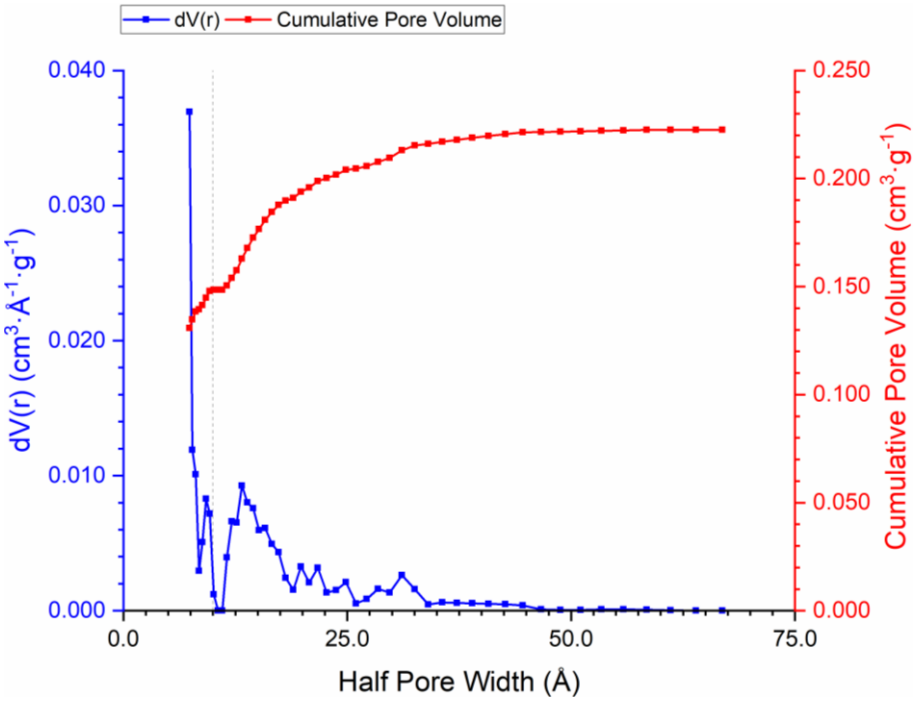

*Figure D-48 NLDFT pore size distributions in **PTPT-BZN-SNx**, analysed from pore volume, and cumulative pore volume plot*

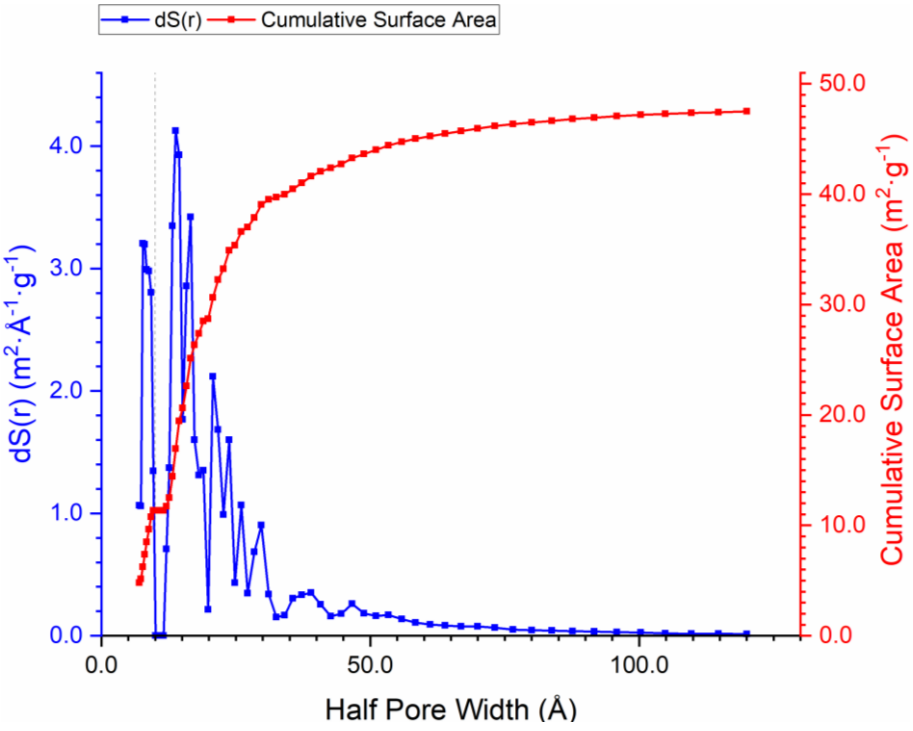

*Figure D-49 NLDFT pore size distributions in **PTPT-BZN-SR**, analysed from surface area, and cumulative surface area plot*

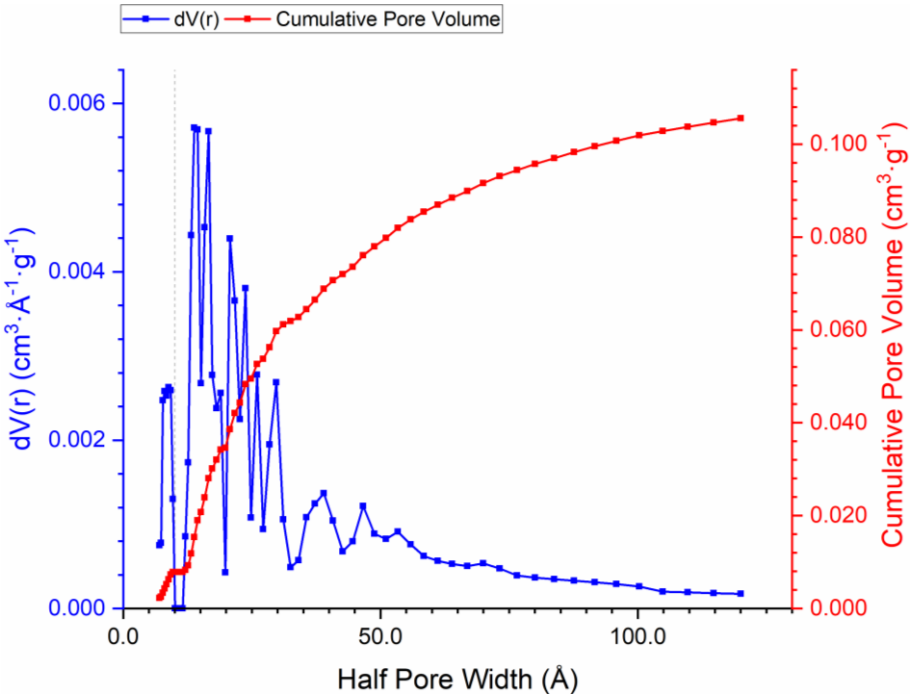

*Figure D-50 NLDFT pore size distributions in **PTPT-BZN-SR**, analysed from pore volume, and cumulative pore volume plot*

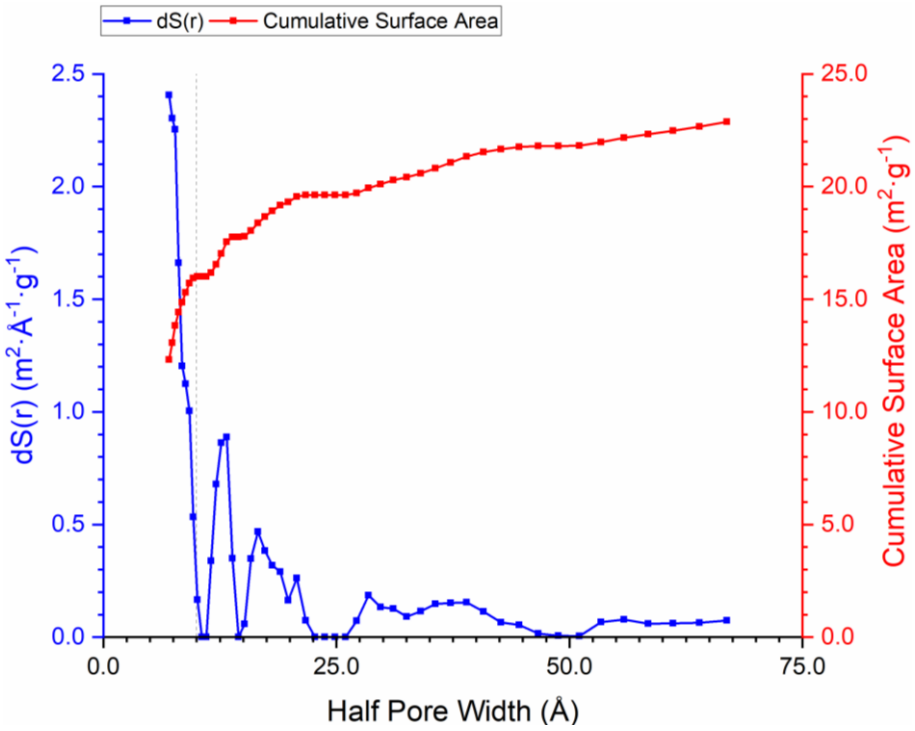

*Figure D-51 NLDFT pore size distributions in **PTPT-BZN-SRx**, analysed from surface area, and cumulative surface area plot*

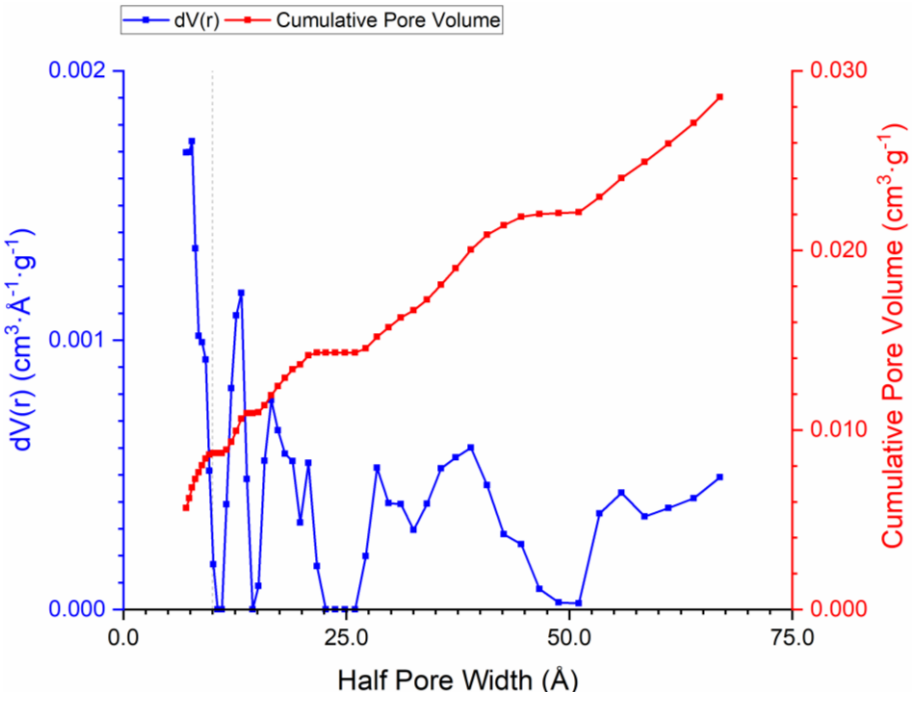

*Figure D-52 NLDFT pore size distributions in **PTPT-BZN-SRx**, analysed from pore volume, and cumulative volume plot*

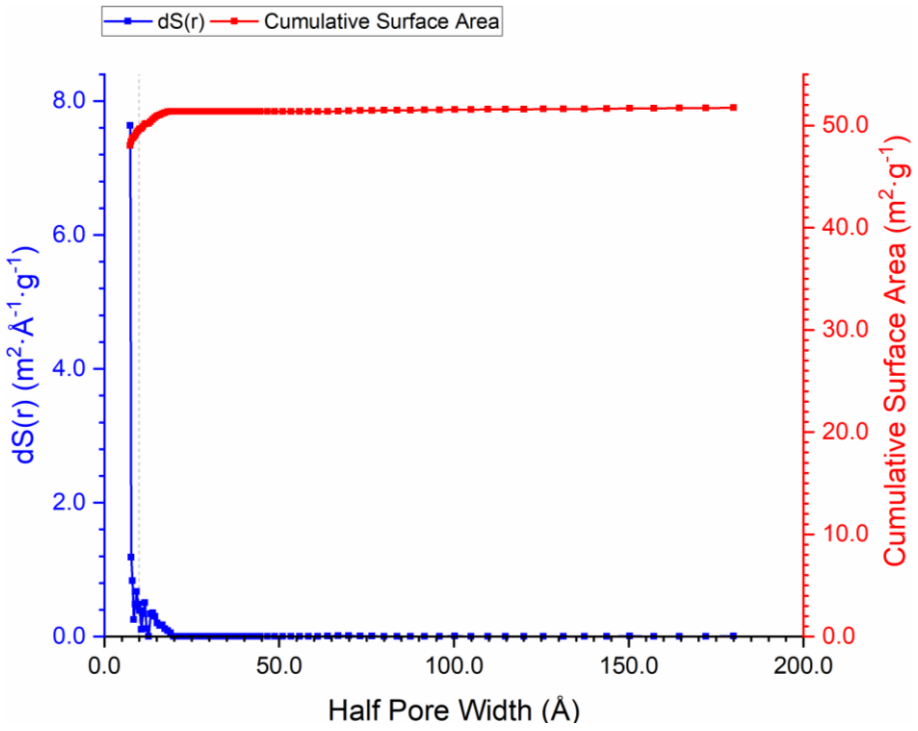

*Figure D-53 NLDFT pore size distributions in **PTPT-FLR-SN**, analysed from surface area, and cumulative surface area plot*

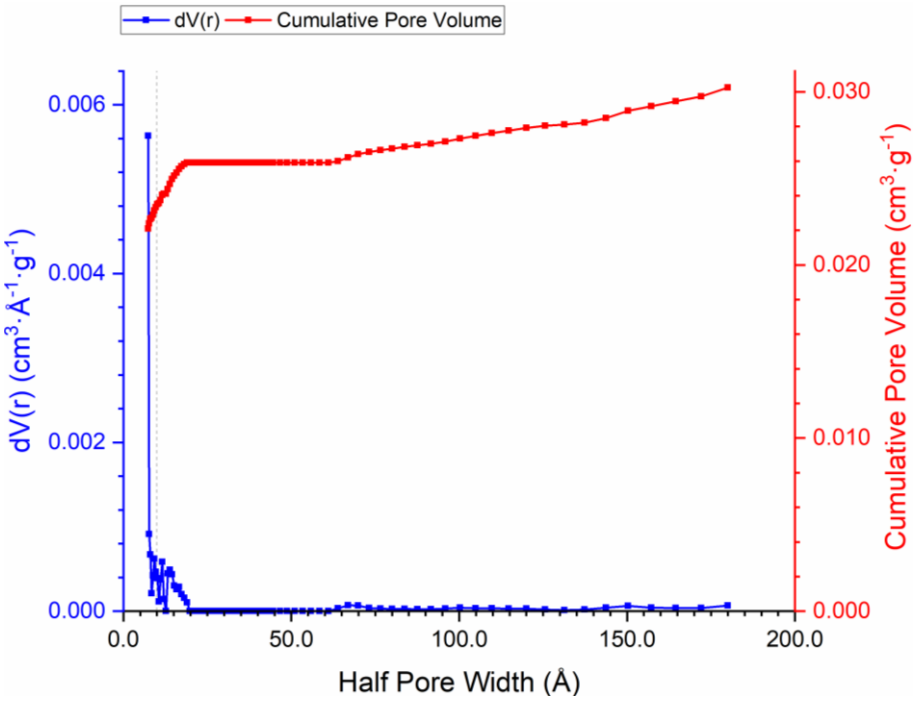

*Figure D-54 NLDFT pore size distributions in **PTPT-FLR-SN**, analysed from pore volume, and cumulative pore volume plot*

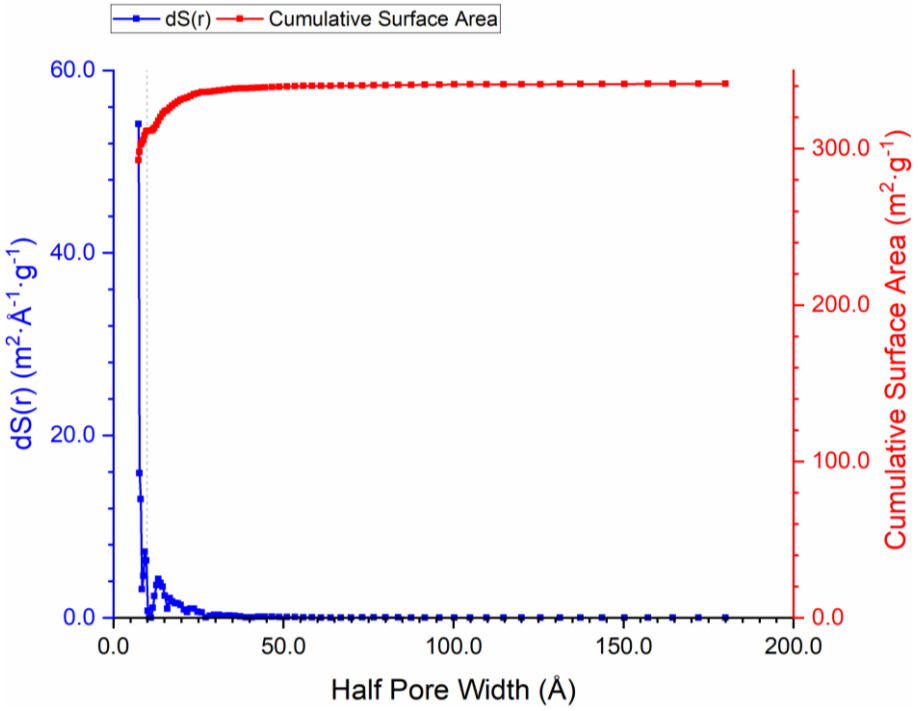

*Figure D-55 NLDFT pore size distributions in **PTPT-FLR-SNx**, analysed from surface area, and cumulative surface area plot*

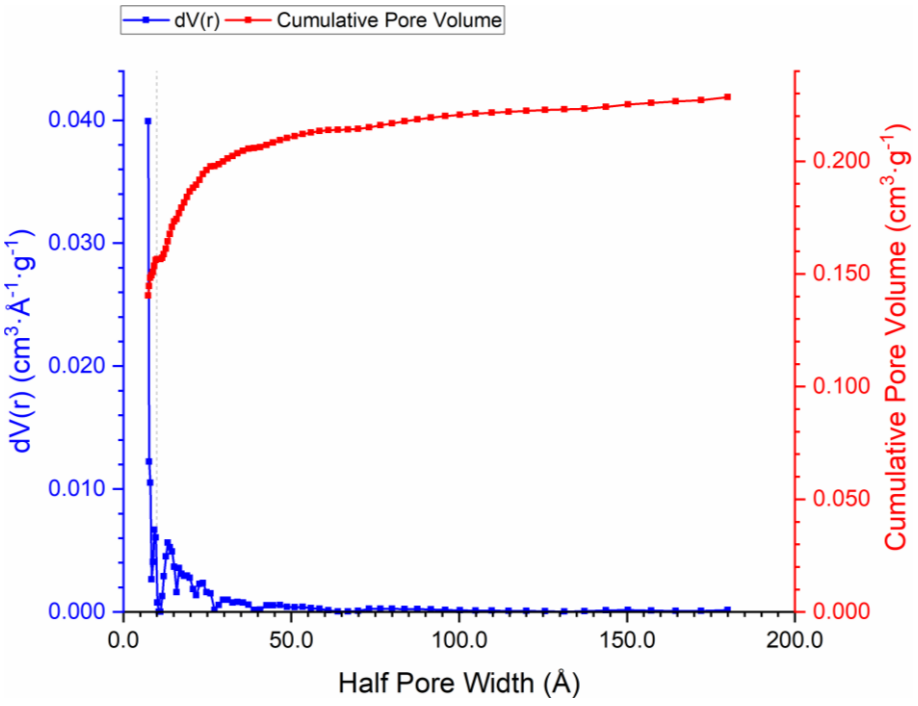

*Figure D-56 NLDFT pore size distributions in **PTPT-FLR-SNx**, analysed from pore volume, and cumulative pore volume plot*

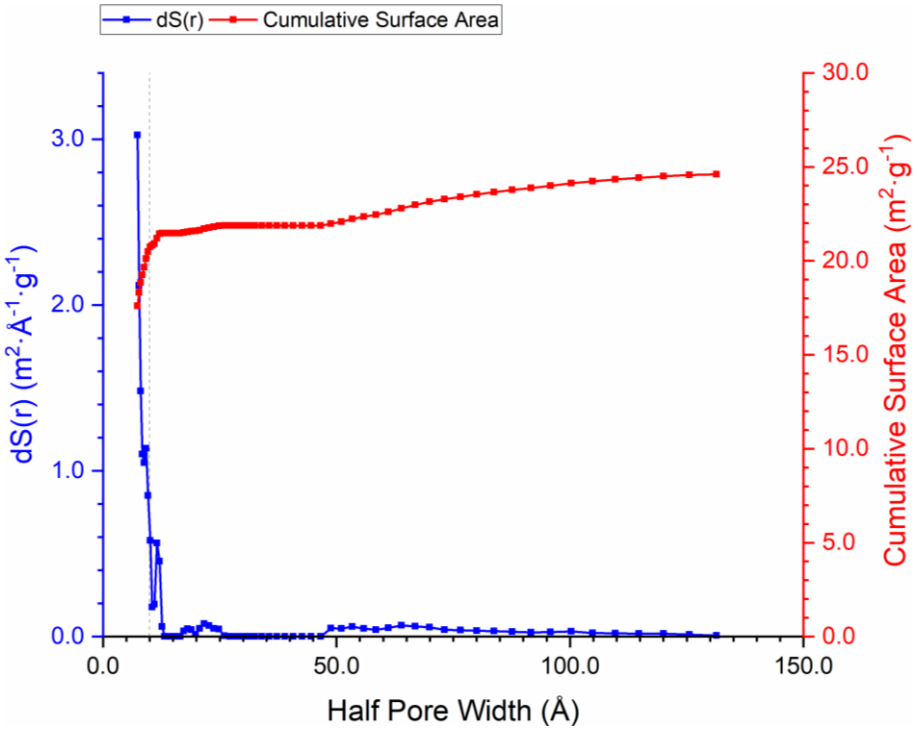

*Figure D-57 NLDFT pore size distributions in **PTPT-FLR-SR**, analysed from surface area, and cumulative surface area plot*

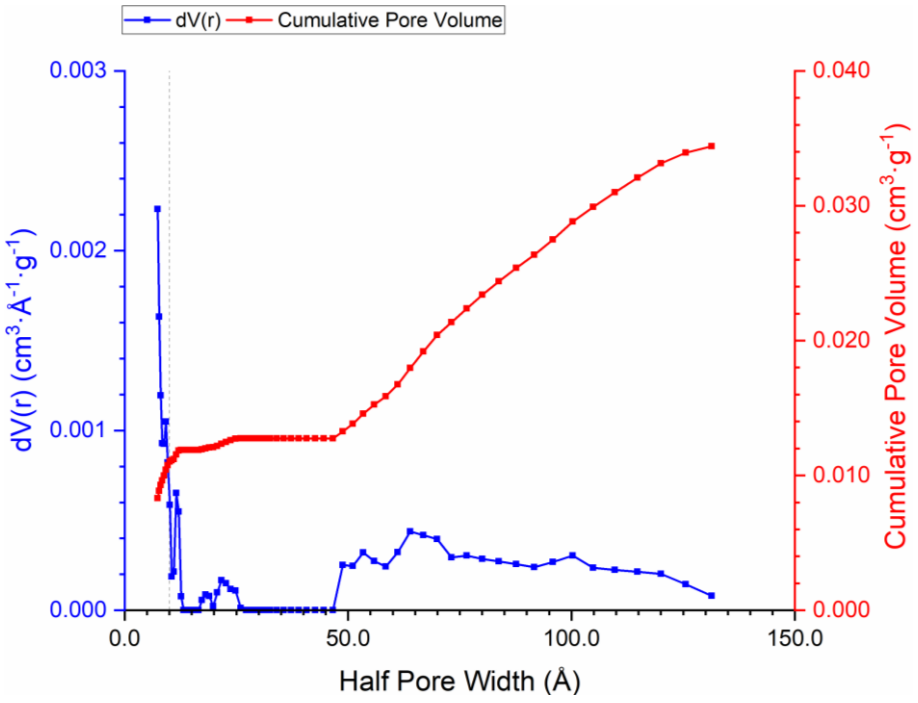

*Figure D-58 NLDFT pore size distributions in **PTPT-FLR-SR**, analysed from pore volume, and cumulative pore volume plot*

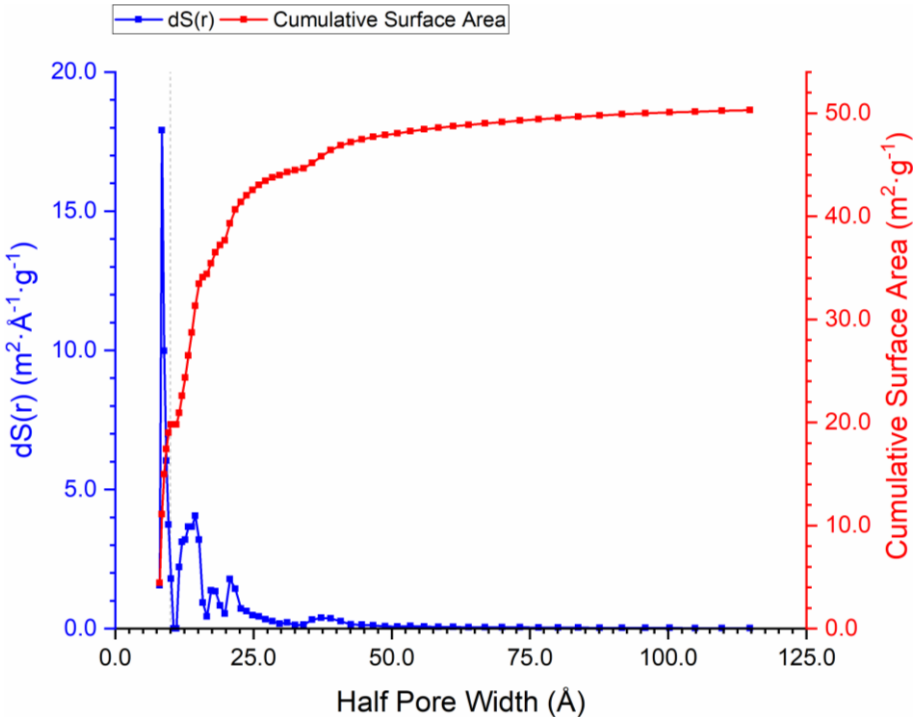

*Figure D-59 NLDFT pore size distributions in **PTPT-FLR-SRx**, analysed from surface area, and cumulative surface area plot*

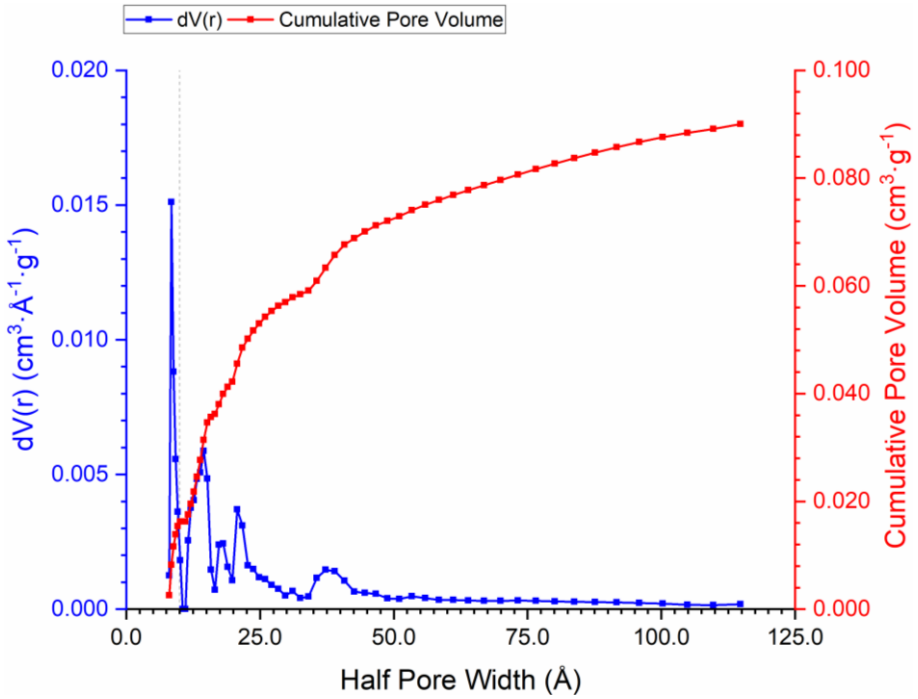

*Figure D-60 NLDFT pore size distributions in **PTPT-FLR-SRx**, analysed from pore volume, and cumulative pore volume plot*

D.2 Carbon Dioxide Adsorption Isotherm Analyses of PANI-CMPs

D.2.1 Isotherm Plots

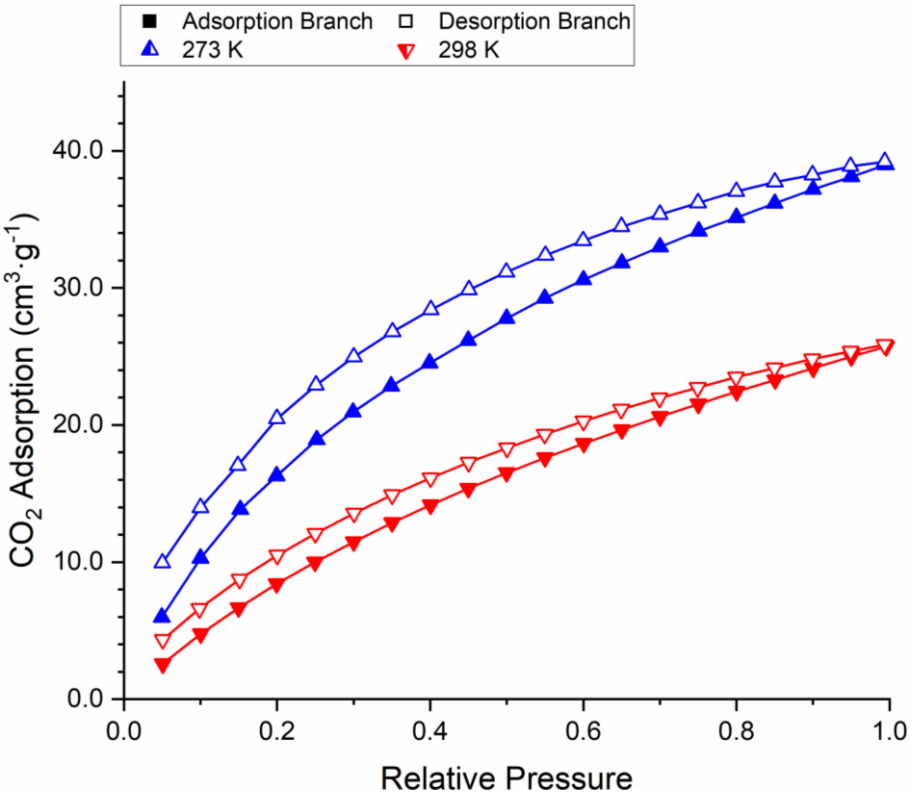

*Figure D-61 Carbon dioxide adsorption isotherm at 273 K (blue) and 298 K (red) of **PTPA-FLR-SN***

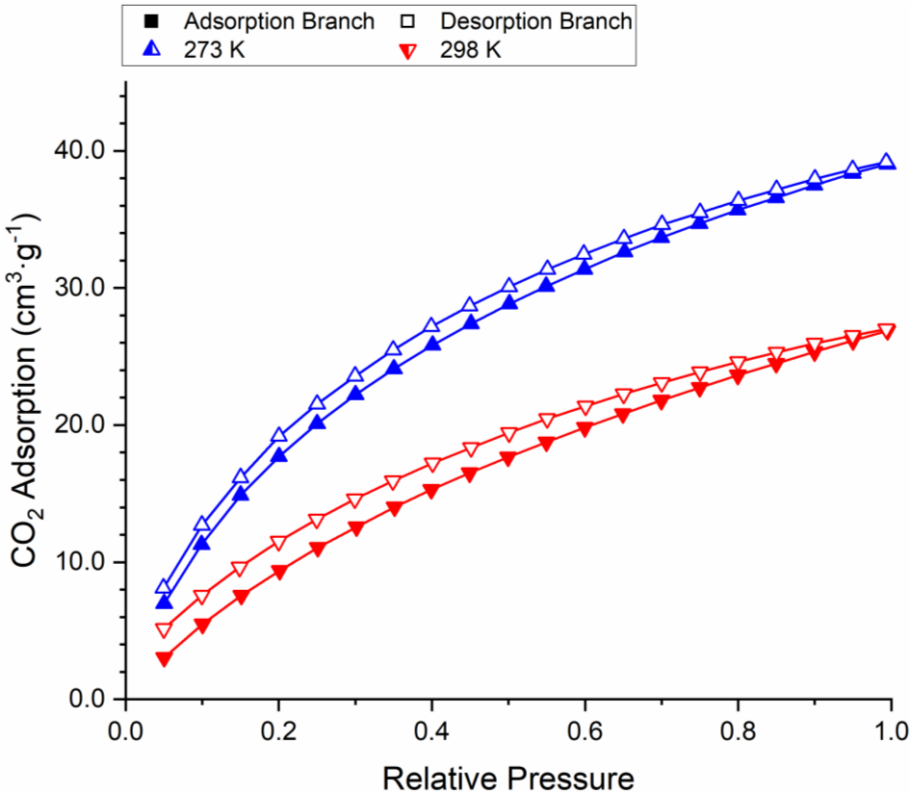

*Figure D-62 Carbon dioxide adsorption isotherm at 273 K (blue) and 298 K (red) of **PTPA-FLR-SNx***

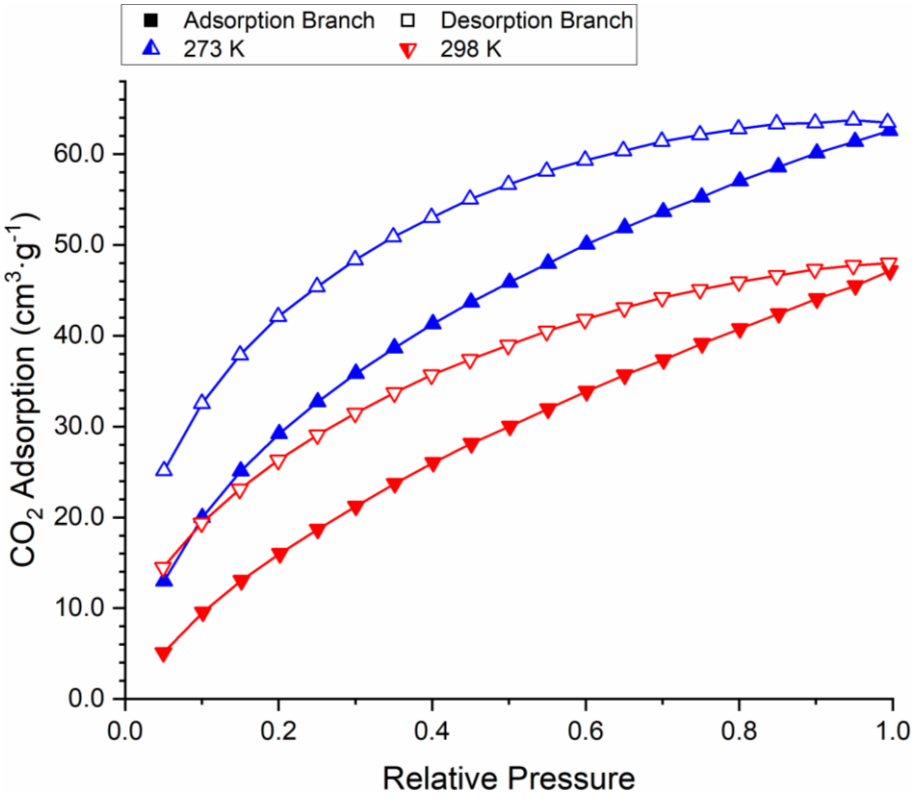

Figure D-63 Carbon dioxide adsorption isotherm at 273 K (blue) and 298 K (red) of ***PTPA-FLR-SR***

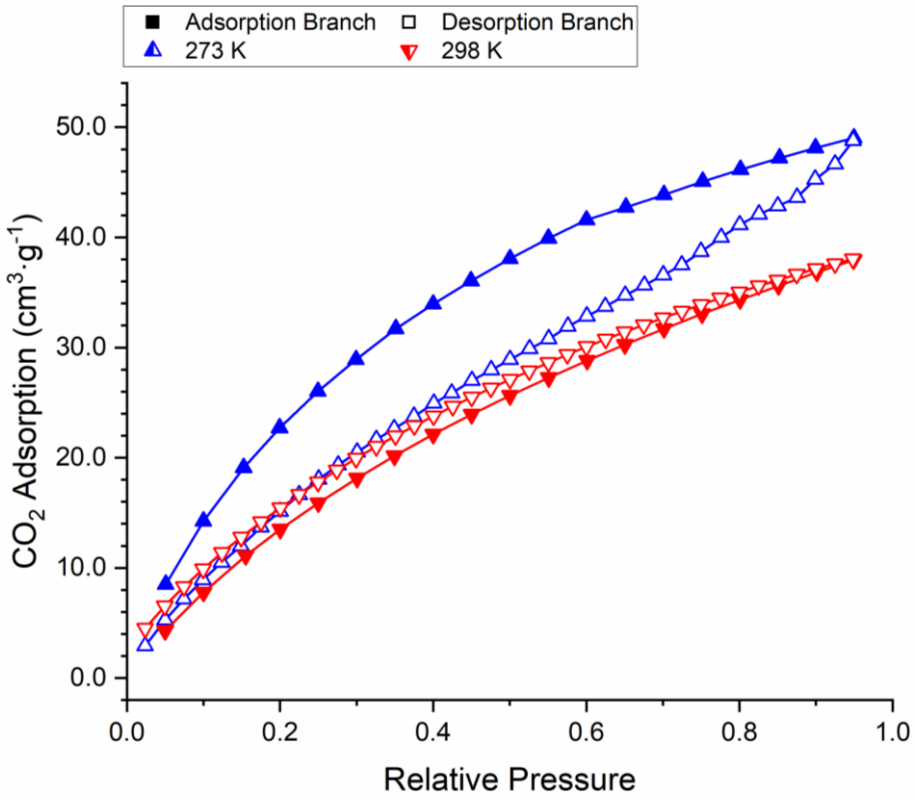

Figure D-64 Carbon dioxide adsorption isotherm at 273 K (blue) and 298 K (red) of ***PTPB-FLR-SN***

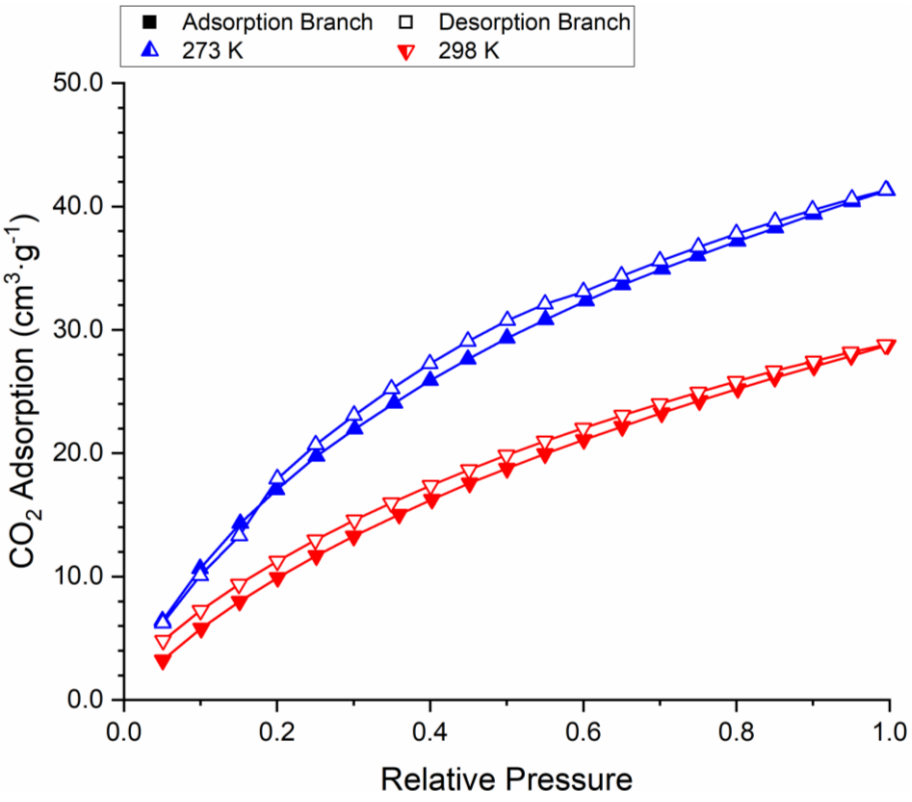

Figure D-65 Carbon dioxide adsorption isotherm at 273 K (blue) and 298 K (red) of ***PTPB-FLR-SNx***

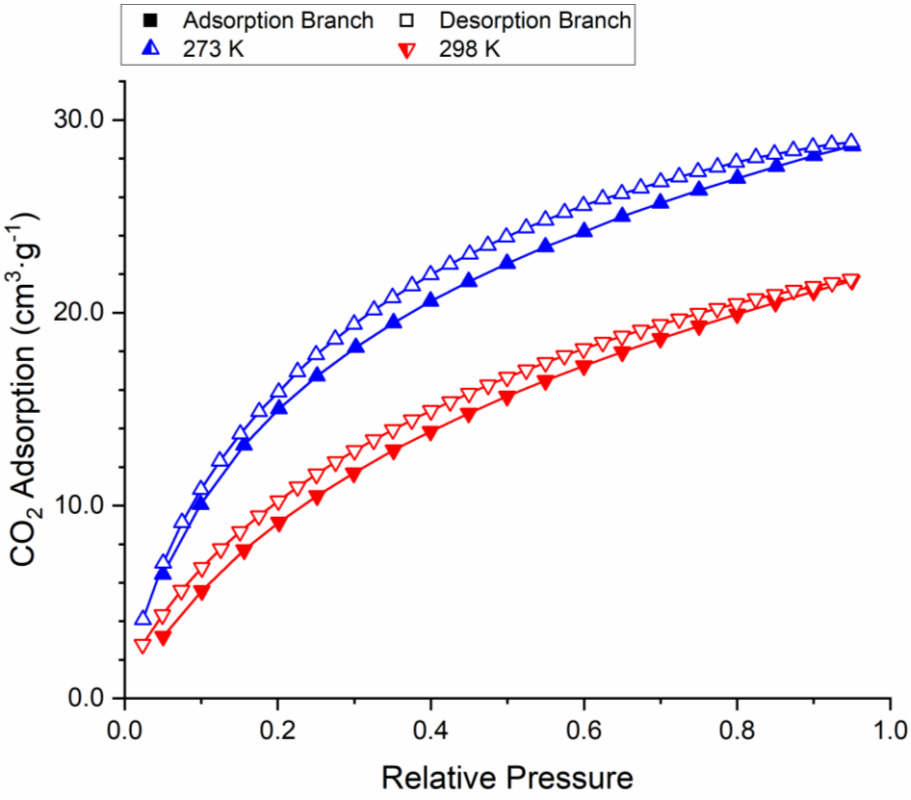

Figure D-66 Carbon dioxide adsorption isotherm at 273 K (blue) and 298 K (red) of ***PTPB-FLR-SR***

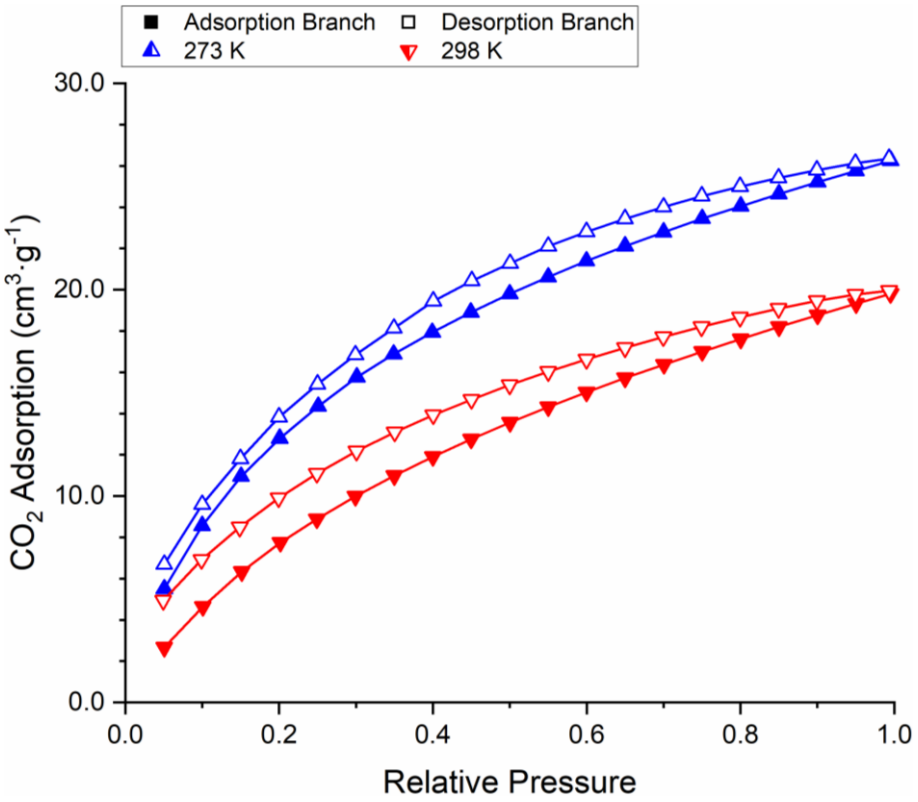

Figure D-67 Carbon dioxide adsorption isotherm at 273 K (blue) and 298 K (red) of ***PTPB-FLR-SRx***

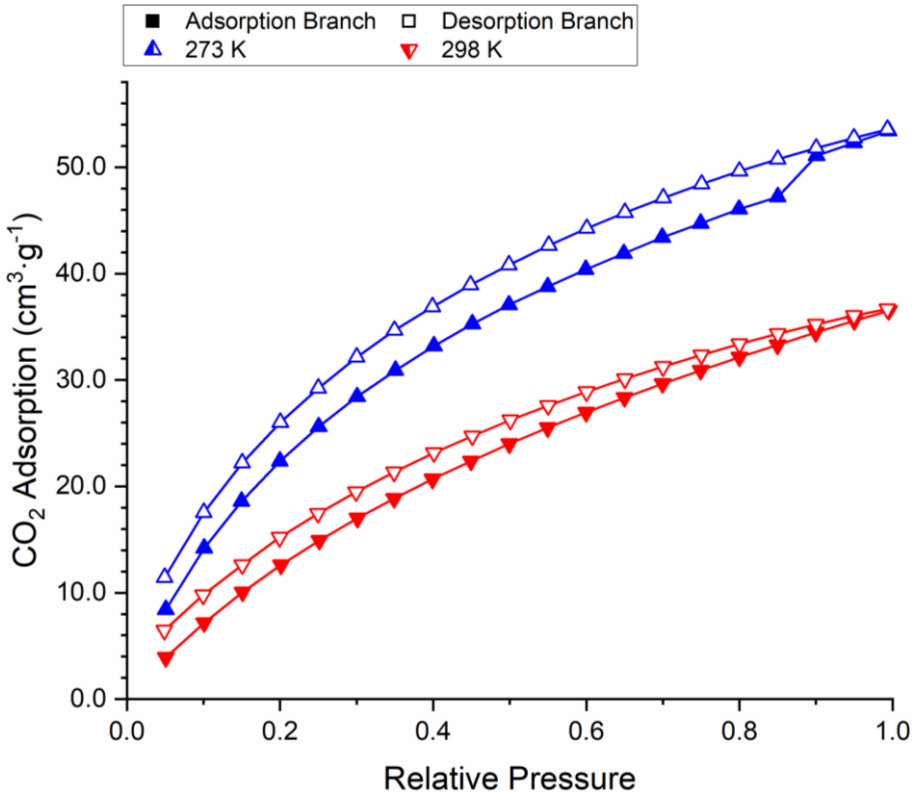

Figure D-68 Carbon dioxide adsorption isotherm at 273 K (blue) and 298 K (red) of ***PTPT-BZN-SN***

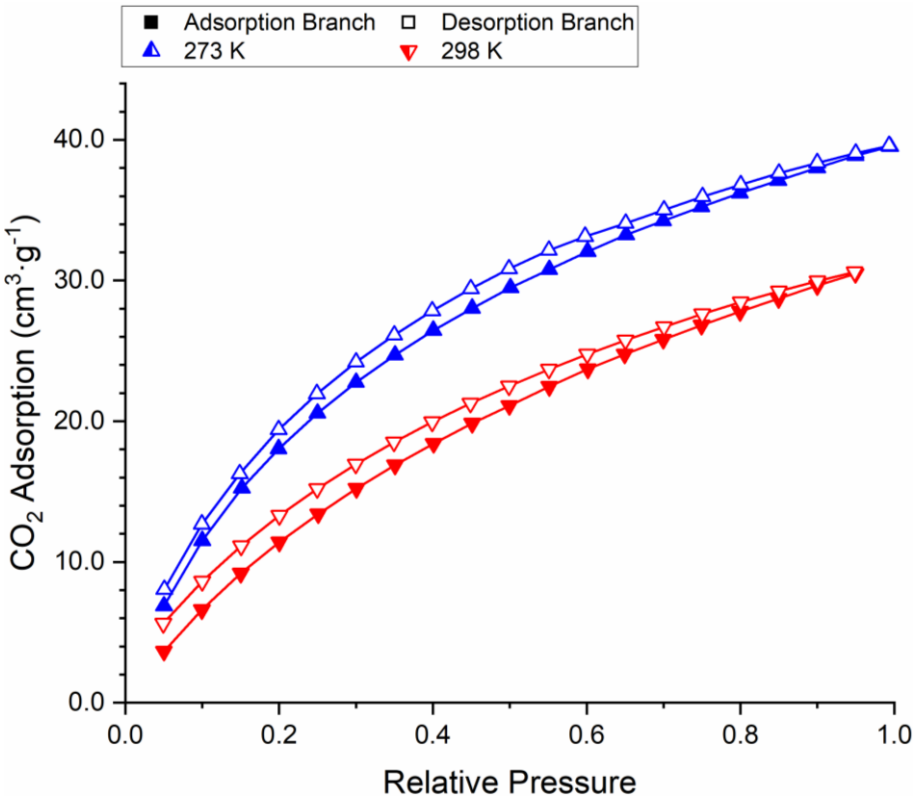

Figure D-69 Carbon dioxide adsorption isotherm at 273 K (blue) and 298 K (red) of ***PTPT-BZN-SNx***

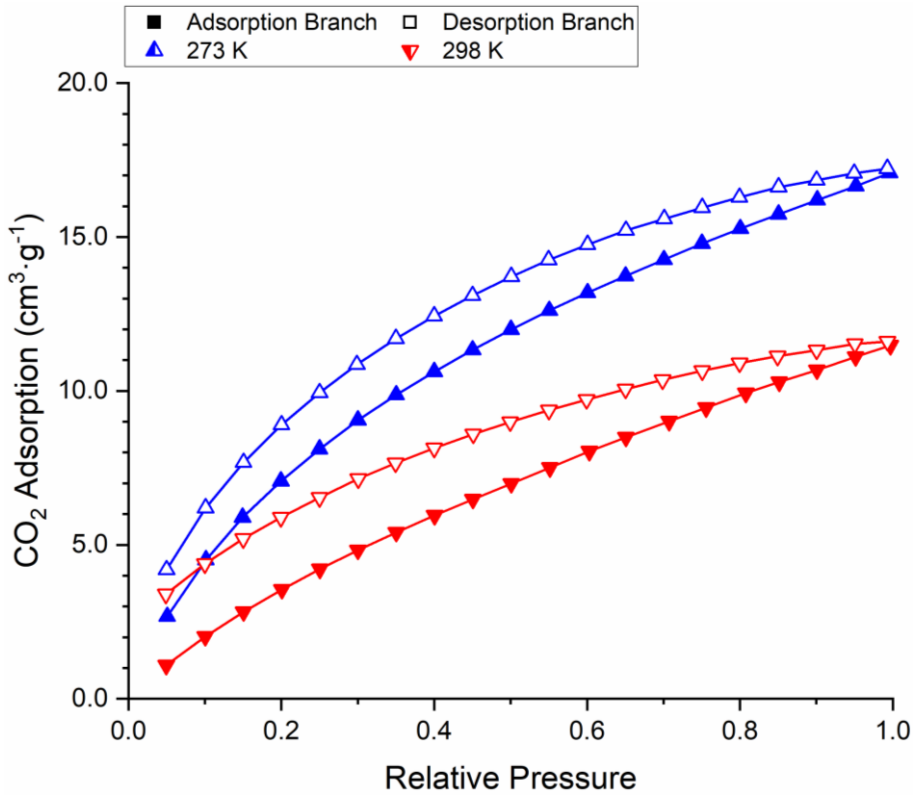

Figure D-70 Carbon dioxide adsorption isotherm at 273 K (blue) and 298 K (red) of ***PTPT-BZN-SR***

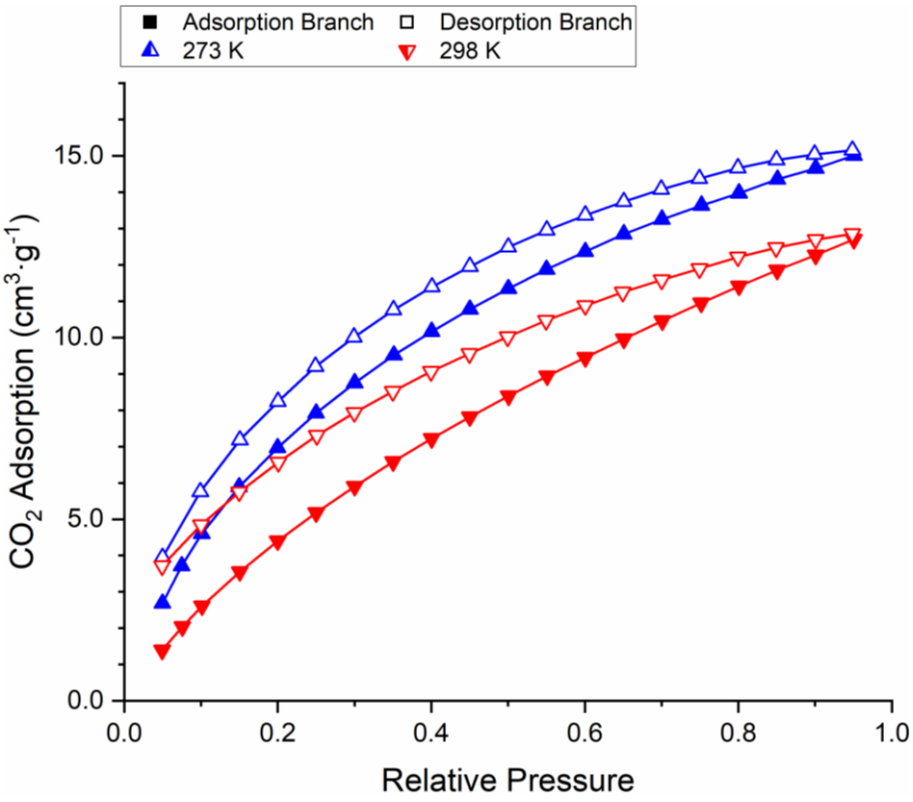

Figure D-71 Carbon dioxide adsorption isotherm at 273 K (blue) and 298 K (red) of ***PTPT-BZN-SRx***

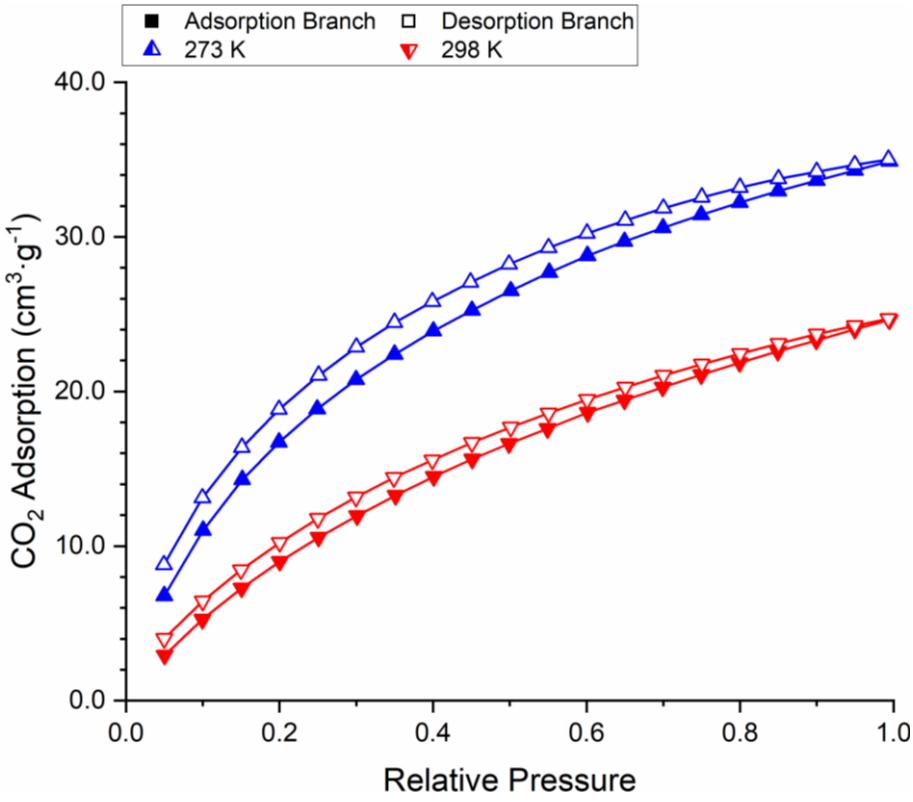

Figure D-72 Carbon dioxide adsorption isotherm at 273 K (blue) and 298 K (red) of ***PTPT-FLR-SN***

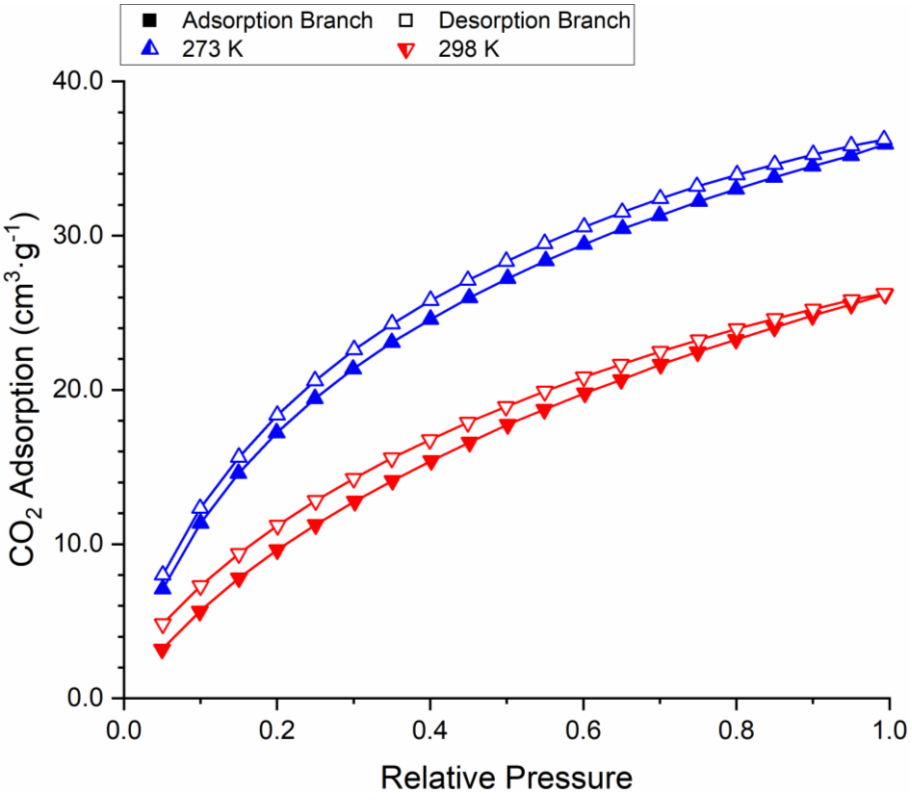

Figure D-73 Carbon dioxide adsorption isotherm at 273 K (blue) and 298 K (red) of ***PTPT-FLR-SNx***

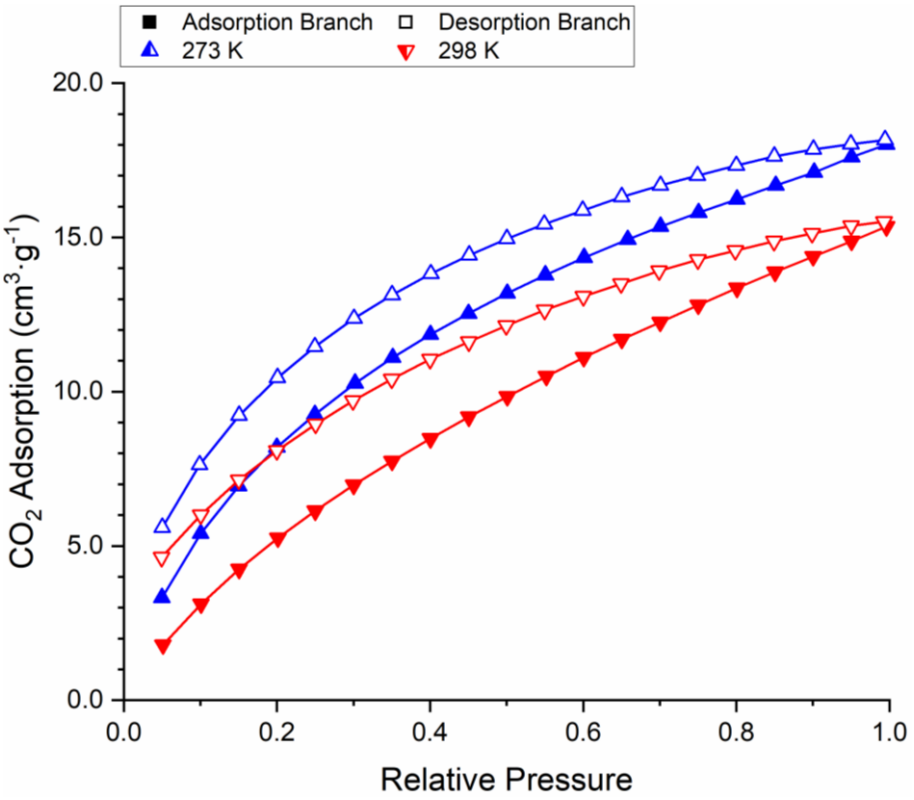

Figure D-74 Carbon dioxide adsorption isotherm at 273 K (blue) and 298 K (red) of ***PTPT-FLR-SR***

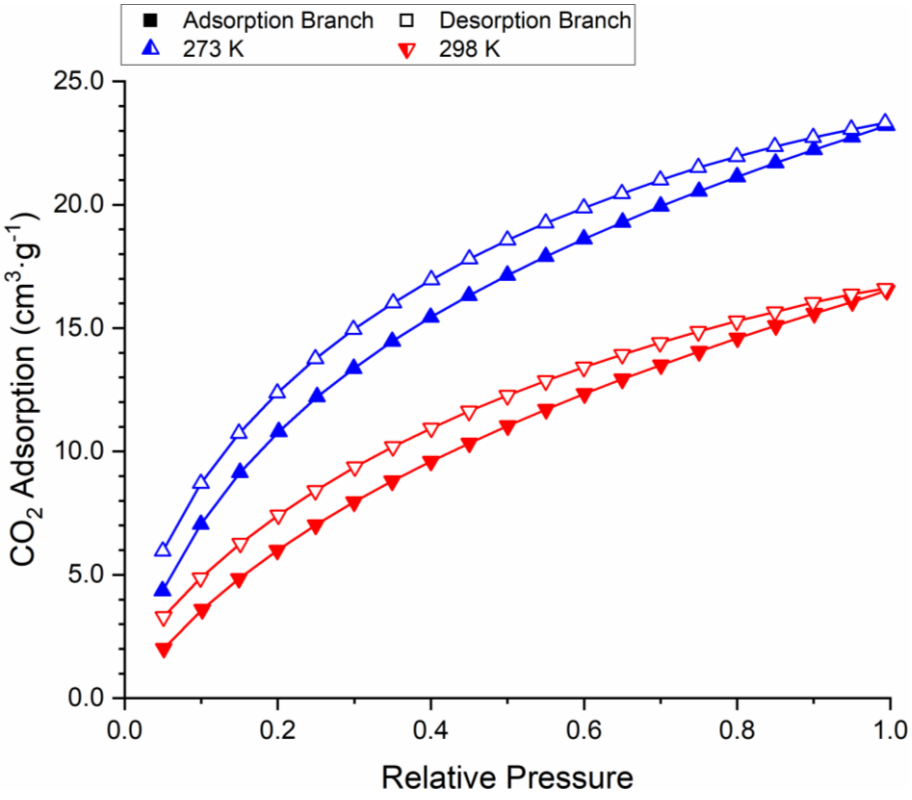

Figure D-75 Carbon dioxide adsorption isotherm at 273 K (blue) and 298 K (red) of ***PTPT-FLR-SRx***

D.2.2 Langmuir Fitting Plots

Table D-2 Fitting parameters for Langmuir isotherm adsorption models of PANI-CMPs for CO_2 adsorption

Material			At 273 K			At 298 K		
Core-Linker	**Approach**	**Added NaBr**	**a**	**b**	**c**	**a**	**b**	**c**
TPA-FLR	Normal	Yes	3.93691	0.79017	0.77731	3.36188	0.51767	0.88212
		No	3.54431	0.96832	0.76175	3.45682	0.53125	0.84327
	Reversed	Yes	8.31525	0.50695	0.62971	9.43621	0.28535	0.78421
TPB-FLR	Normal	Yes	3.52556	1.72234	0.89701	4.79500	0.56954	0.86026
		No	4.27152	0.75752	0.77872	3.87818	0.49333	0.83987
	Reversed	Yes	2.26570	1.33472	0.72918	2.11846	0.86986	0.81487
		No	2.36663	0.97452	0.70291	2.31354	0.61608	0.79284
TPT-BZN	Normal	Yes	7.85019	0.42622	0.67860	4.27312	0.61646	0.87915
		No	3.23536	1.19760	0.80225	3.20583	0.76925	0.87743
	Reversed	Yes	2.01144	0.60615	0.73870	3.20500	0.19052	0.81453
		No	1.32026	1.06694	0.77361	2.12475	0.37804	0.82001
TPT-FLR	Normal	Yes	2.82770	1.22873	0.76808	2.69218	0.68992	0.85610
		No	2.93990	1.19288	0.75826	2.96782	0.65077	0.84169
	Reversed	Yes	1.79276	0.80186	0.71346	3.02547	0.29240	0.78230
		No	2.23055	0.86216	0.71739	2.04928	0.56059	0.82204

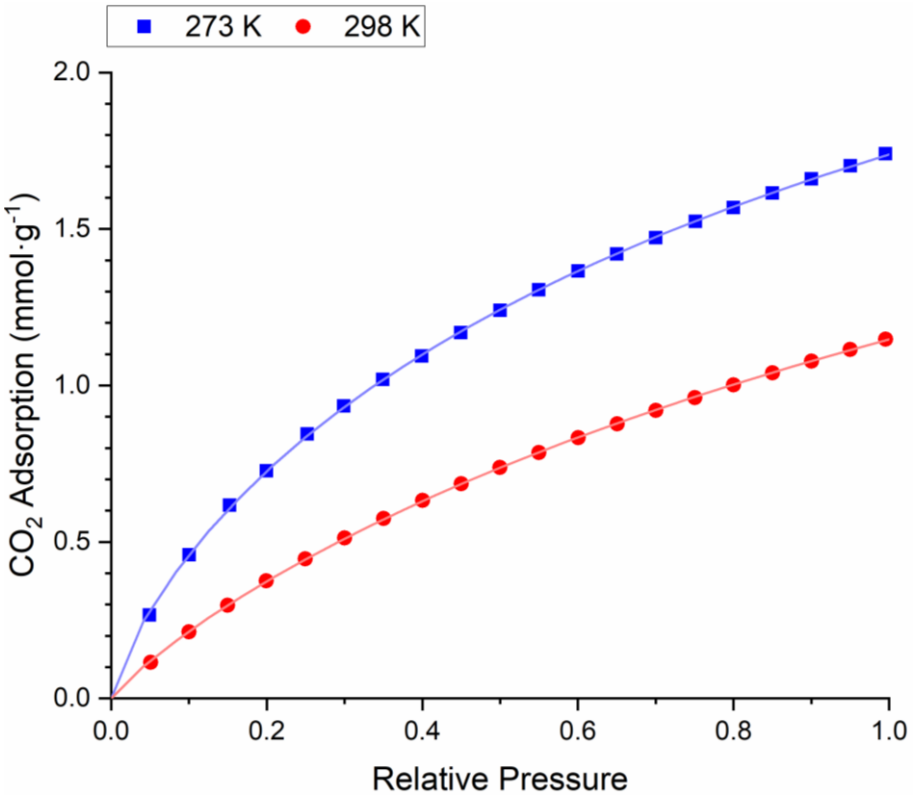

*Figure D-76 Langmuir fitting plot for **PTPA-FLR-SN** CO_2 adsorption isotherm*

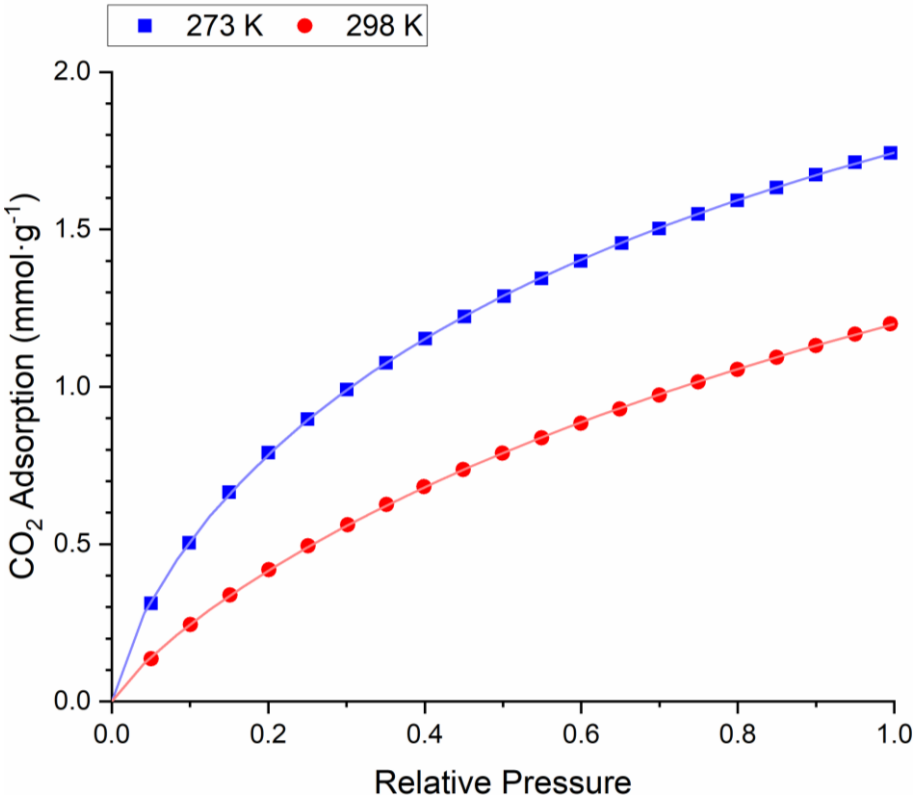

*Figure D-77 Langmuir fitting plot for **PTPA-FLR-SNx** CO_2 adsorption isotherm*

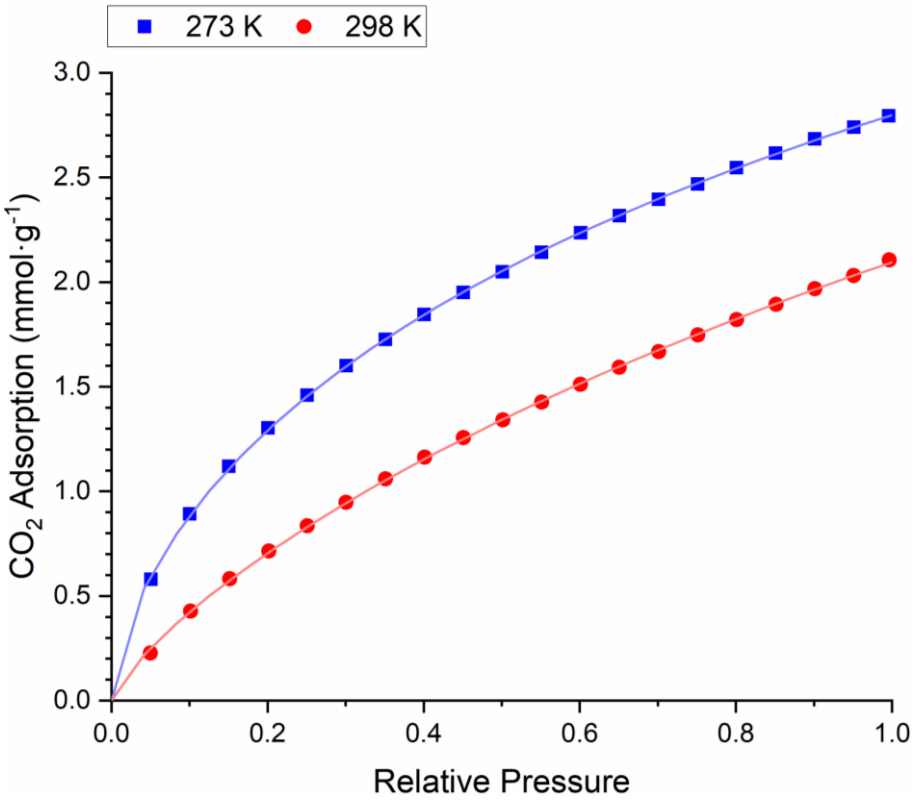

*Figure D-78 Langmuir fitting plot for **PTPA-FLR-SR** CO_2 adsorption isotherm*

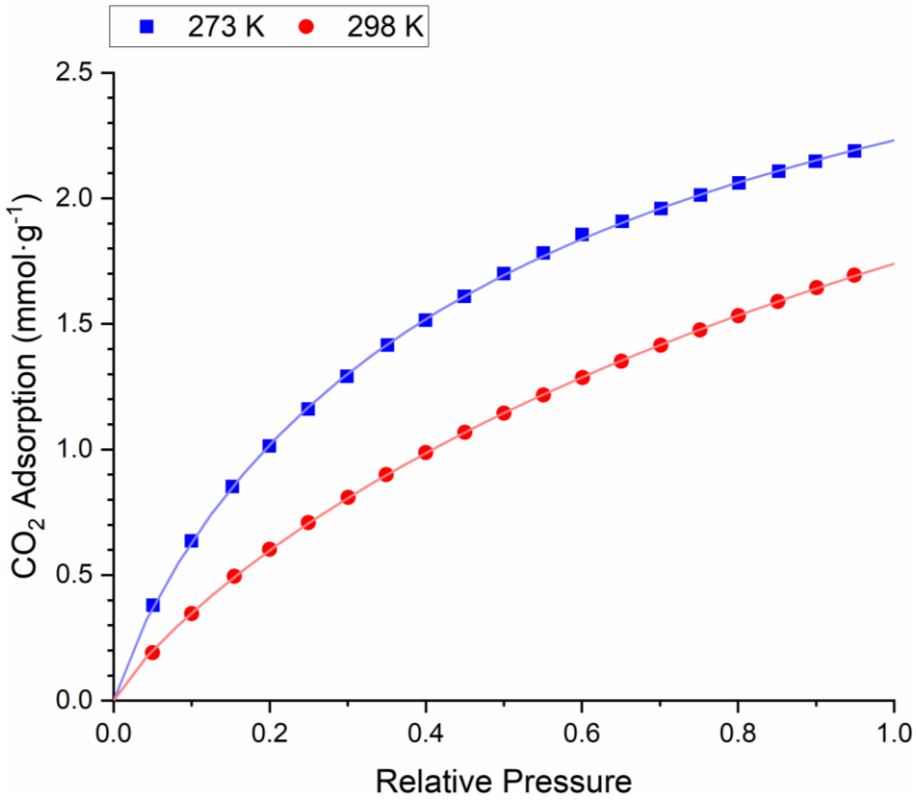

*Figure D-79 Langmuir fitting plot for **PTPB-FLR-SN** CO_2 adsorption isotherm*

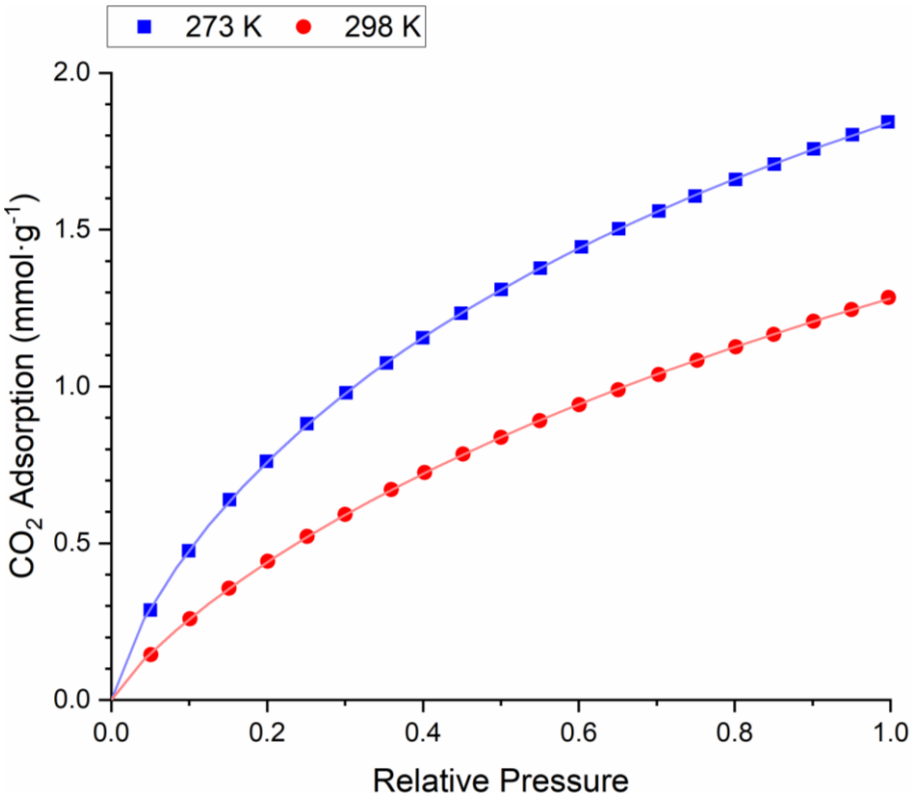

*Figure D-80 Langmuir fitting plot for **PTPB-FLR-SNx** CO_2 adsorption isotherm*

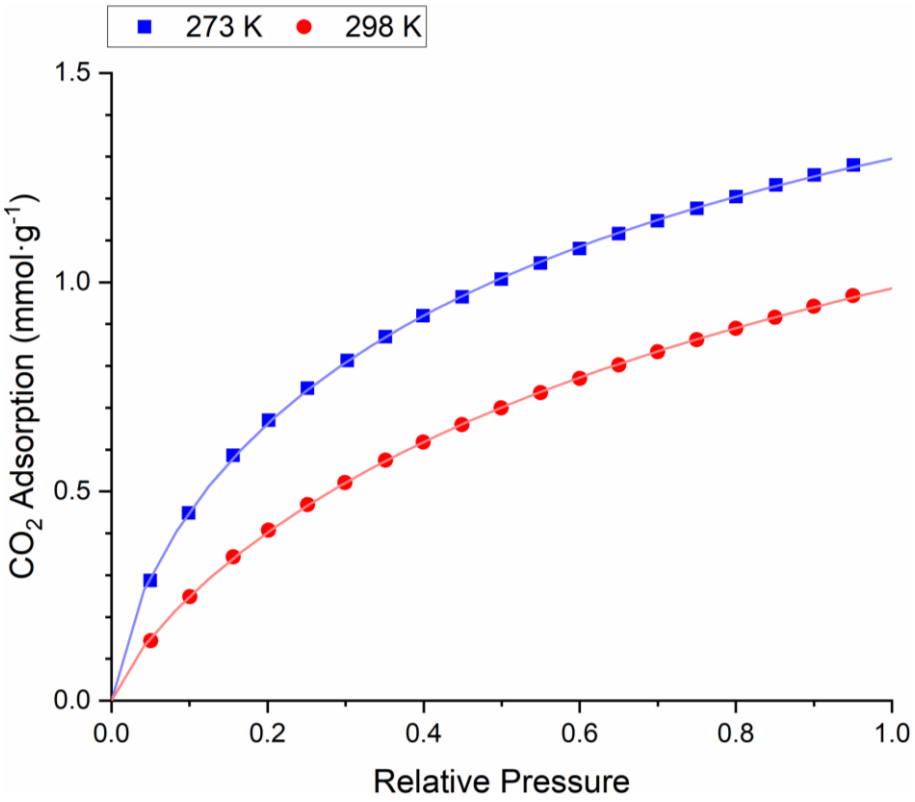

*Figure D-81 Langmuir fitting plot for **PTPB-FLR-SR** CO_2 adsorption isotherm*

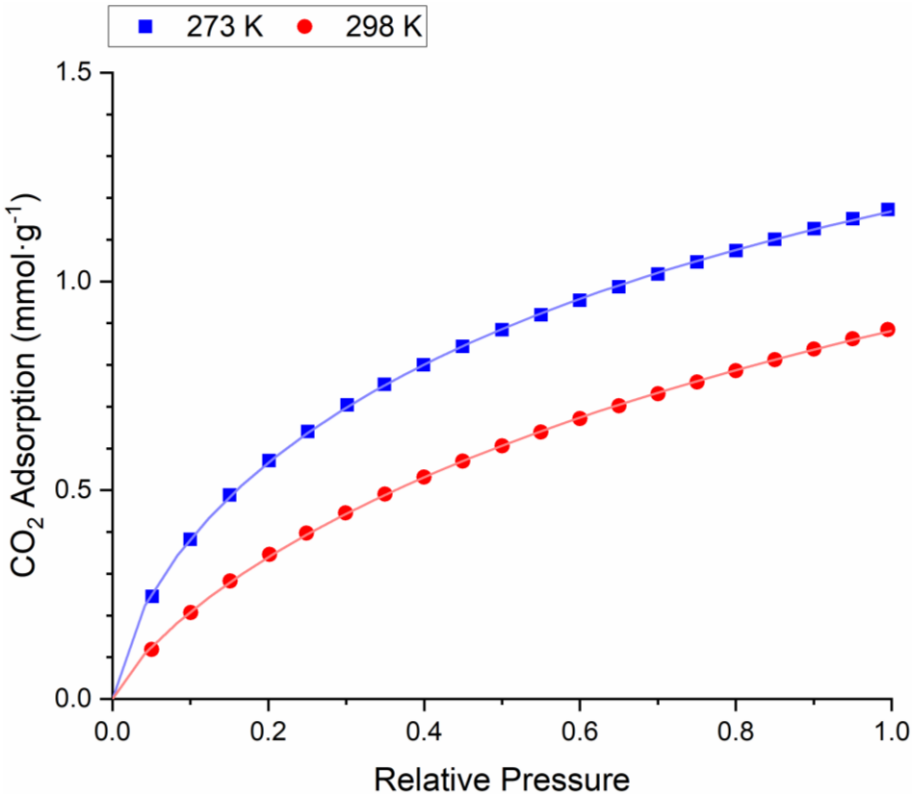

*Figure D-82 Langmuir fitting plot for **PTPB-FLR-SRx** CO_2 adsorption isotherm*

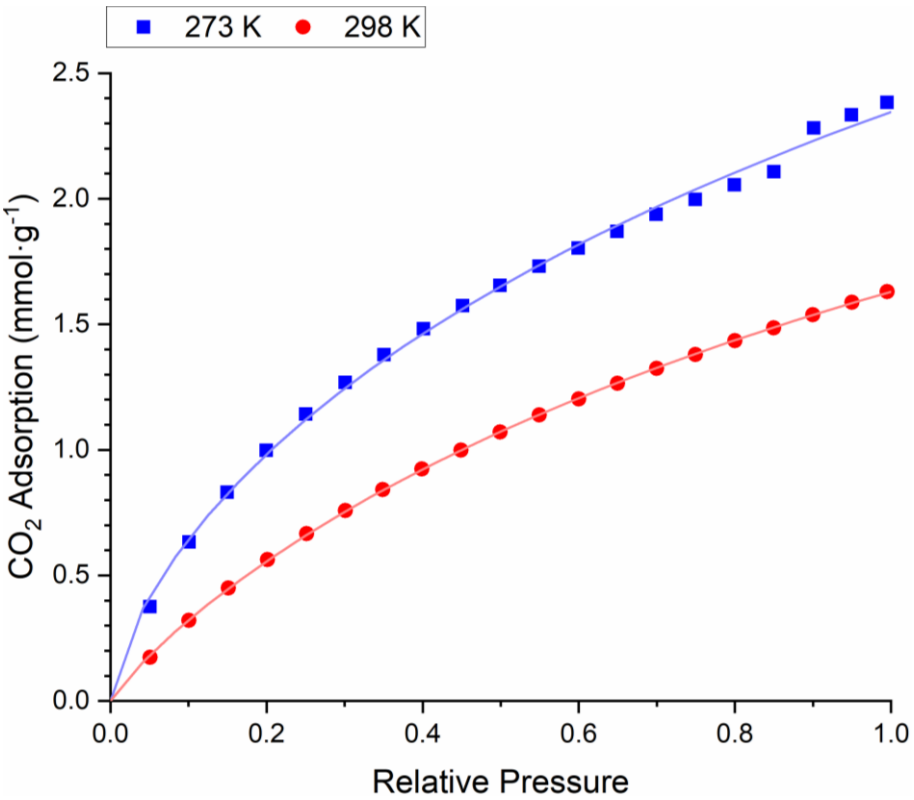

*Figure D-83 Langmuir fitting plot for **PTPT-BZN-SN** CO_2 adsorption isotherm*

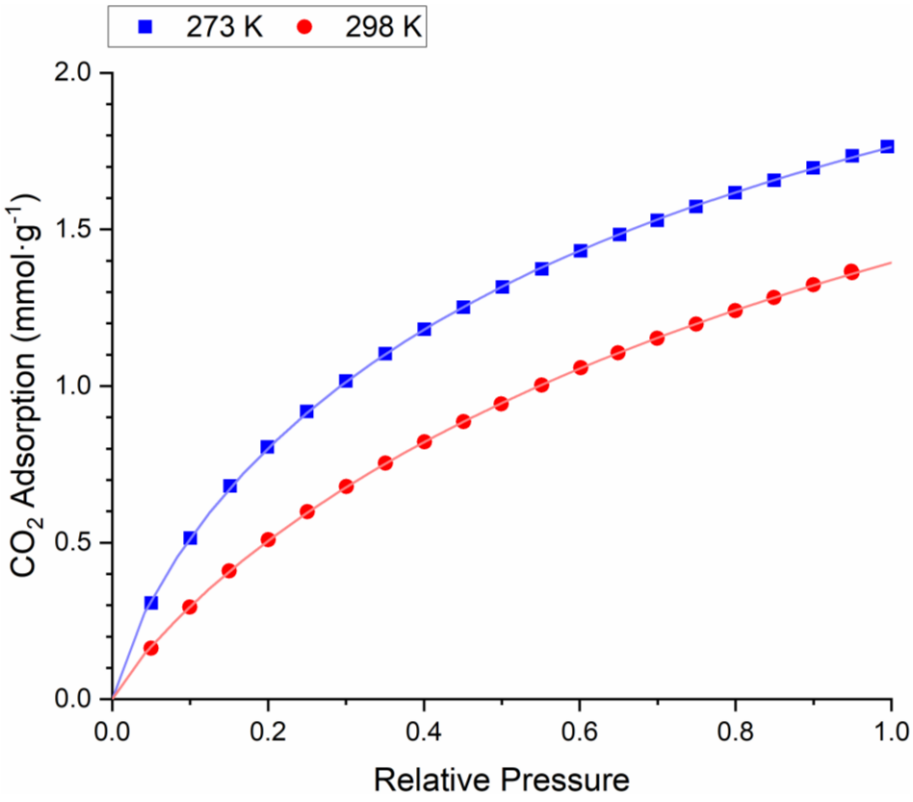

*Figure D-84 Langmuir fitting plot for **PTPT-BZN-SNx** CO_2 adsorption isotherm*

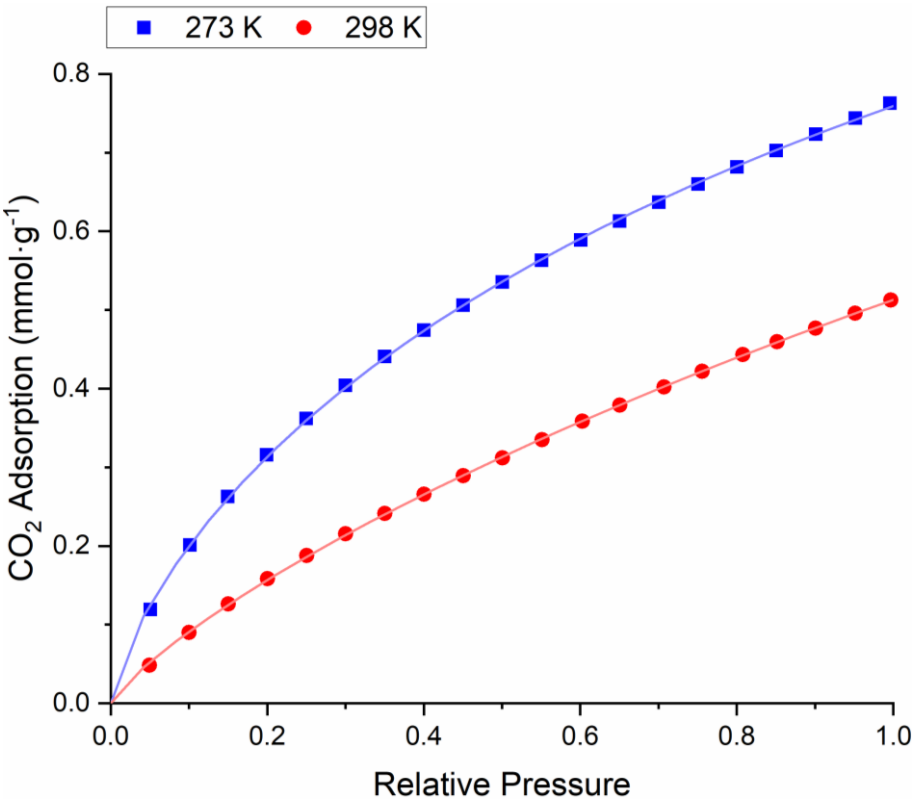

*Figure D-85 Langmuir fitting plot for **PTPT-BZN-SR** CO_2 adsorption isotherm*

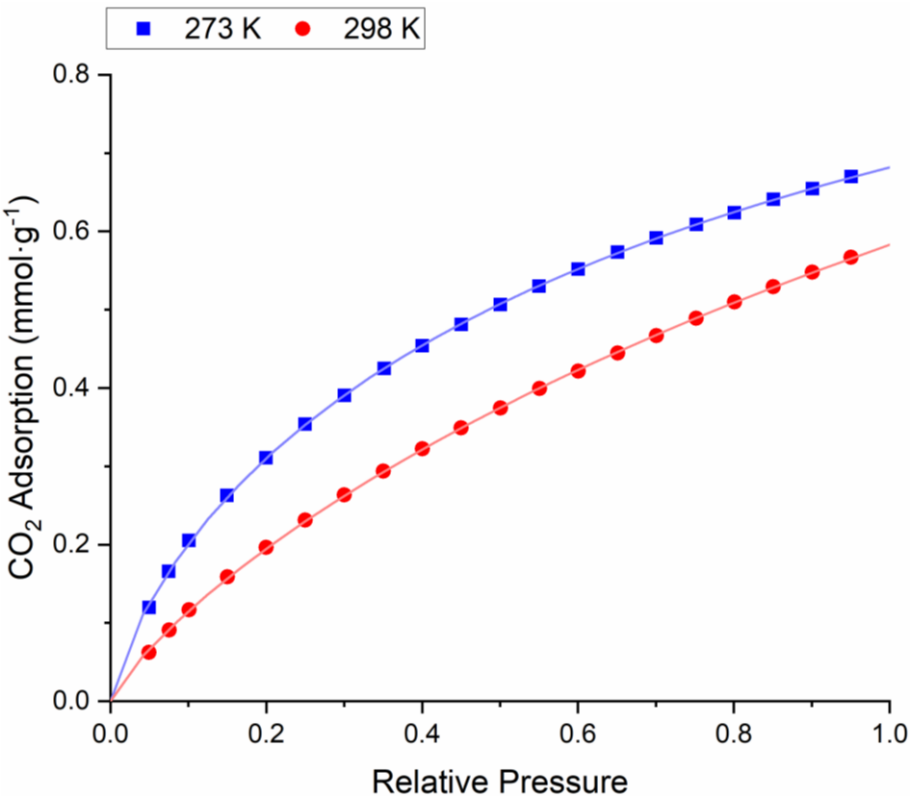

*Figure D-86 Langmuir fitting plot for **PTPT-BZN-SRx** CO_2 adsorption isotherm*

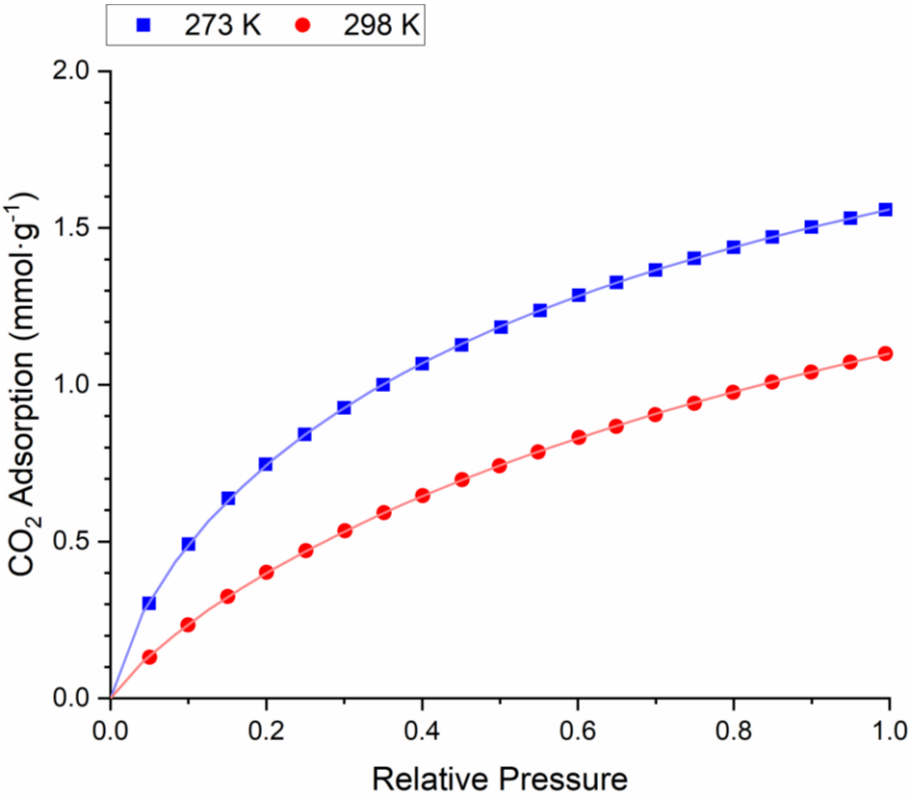

*Figure D-87 Langmuir fitting plot for **PTPT-FLR-SN** CO_2 adsorption isotherm*

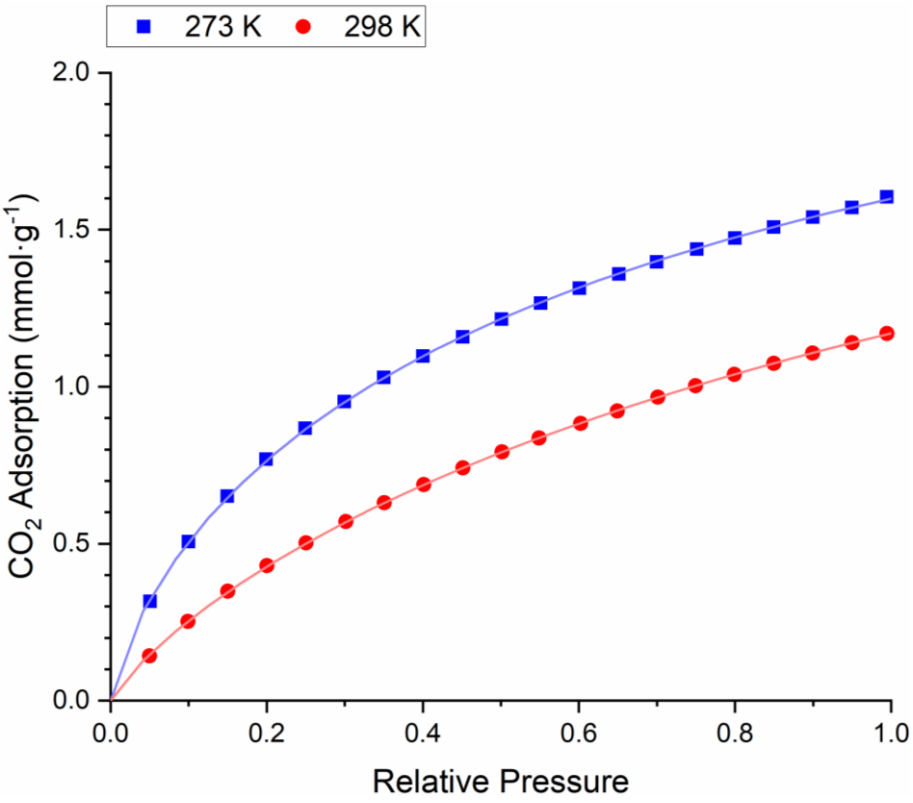

*Figure D-88 Langmuir fitting plot for **PTPT-FLR-SNx** CO_2 adsorption isotherm*

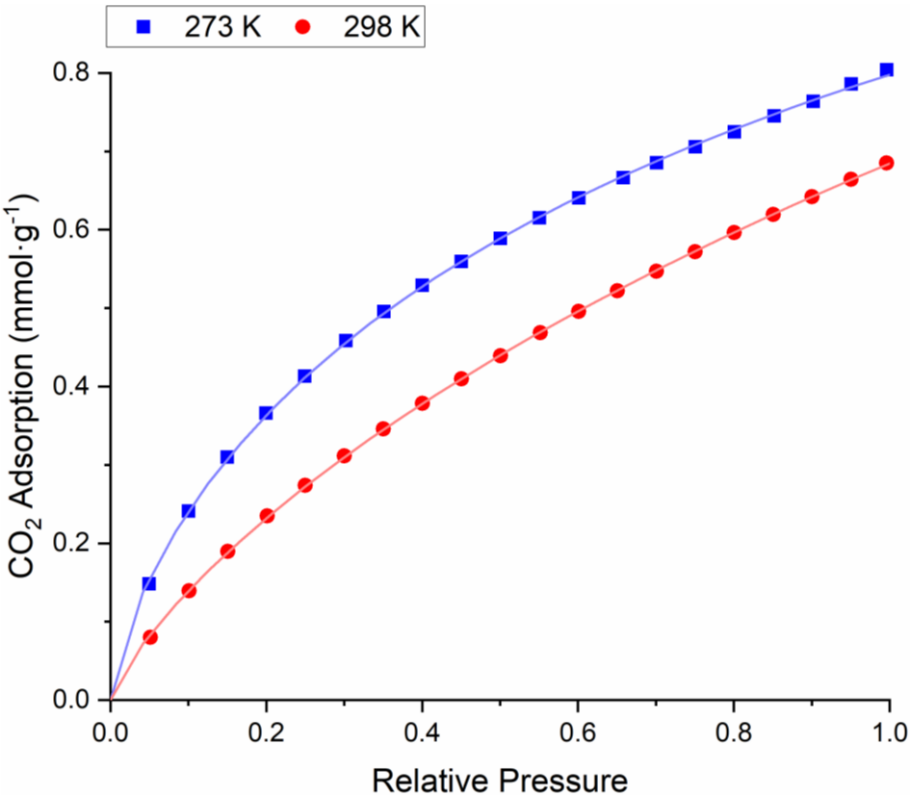

*Figure D-89 Langmuir fitting plot for **PTPT-FLR-SR** CO_2 adsorption isotherm*

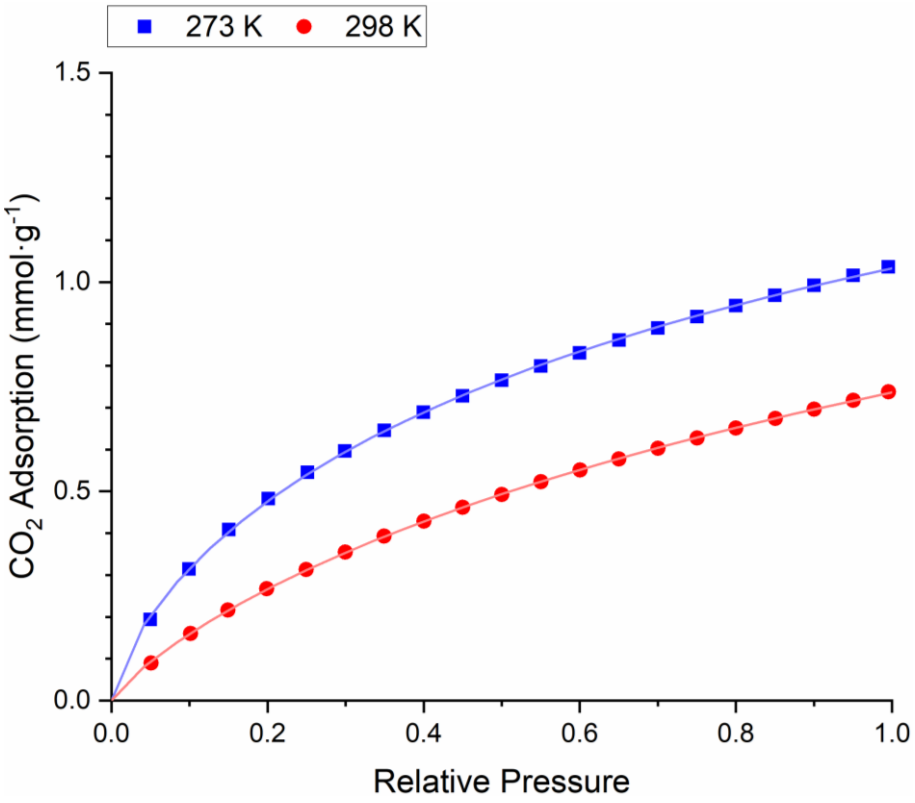

*Figure D-90 Langmuir fitting plot for **PTPT-FLR-SRx** CO_2 adsorption isotherm*

D.2.3 Virial Analysis Fitting Plots

Table D-3 Fitting parameters for virial analyses of PANI-CMPs CO_2 adsorption isotherms

Material			Parameters						
Core-Linker	**Approach**	**Added NaBr**	**a_0**	**a_1**	**a_2**	**a_3**	**a_4**	**b_0**	**b_1**
TPA-FLR	Normal	Yes	-3337.91584	552.61362	0.45127	-20.96176	6.51015	10.30196	-1.13383
		No	-3468.77915	716.54272	-141.68795	65.70355	-11.29792	10.50762	-1.29335
	Reversed	Yes	-4156.28293	1012.72908	30.33122	-28.72932	4.86656	12.30806	-2.913
TPB-FLR	Normal	Yes	-2744.96956	382.86916	11.91172	-39.32126	14.27476	7.75798	-0.68494
		No	-2787.93212	422.65765	-124.96918	48.09848	-7.08146	8.16713	-0.36354
	Reversed	Yes	-3158.26889	813.59437	-199.76842	162.90679	-45.37727	9.33713	-1.16069
		No	-3257.00354	1201.53199	-161.80587	78.06338	-16.88956	9.88719	-2.39211
TPT-BZN	Normal	Yes	-3071.33341	542.33684	-180.1137	116.82238	-26.12586	8.9265	-0.94614
		No	-2572.86045	548.34261	-41.72214	20.63505	-2.57466	7.33284	-1.06184
	Reversed	Yes	-3732.6558	2719.93454	-1561.76153	2006.15564	-1020.07202	12.41445	-6.21329
		No	-2930.71217	2860.7612	168.45791	-1235.2422	1166.72392	9.49006	-7.75706
TPT-FLR	Normal	Yes	-3524.71149	725.9362	-51.71082	0.2411	8.89785	10.73537	-1.38057
		No	-3431.60993	888.27464	-214.76895	128.40193	-26.73916	10.29593	-1.67449
	Reversed	Yes	-3113.19578	3241.15438	-1433.46545	1660.45122	-761.56076	9.78814	-7.84618
		No	-3418.92069	1357.13171	-396.75791	354.3948	-135.01778	10.74048	-2.62529

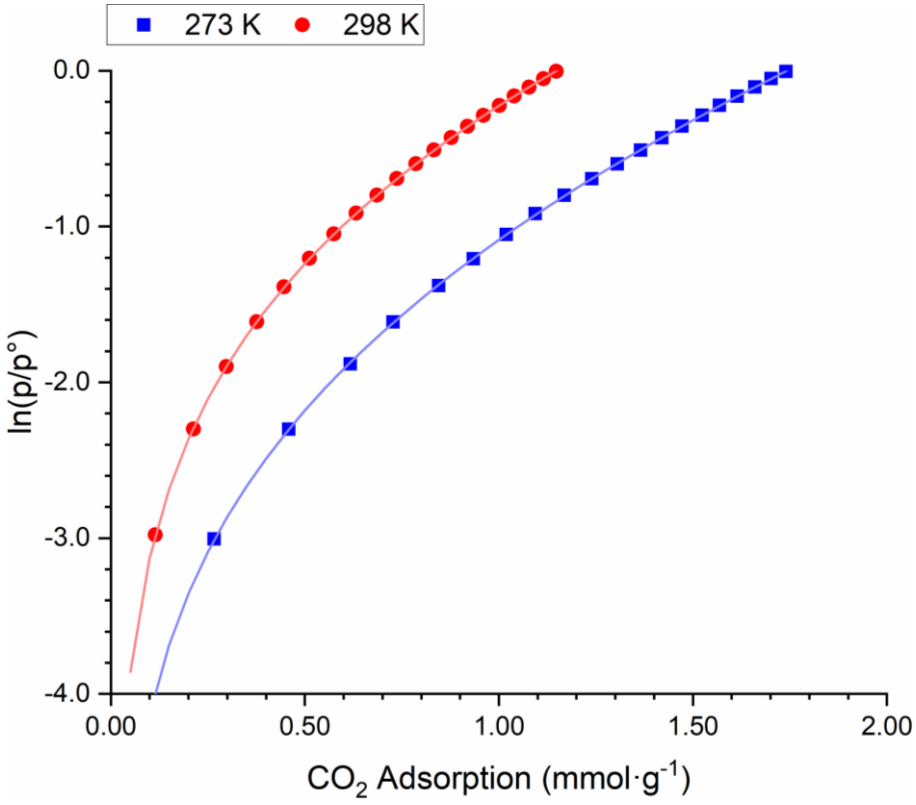

*Figure D-91 Virial analysis fitting plot for **PTPA-FLR-SN** CO_2 adsorption isotherm*

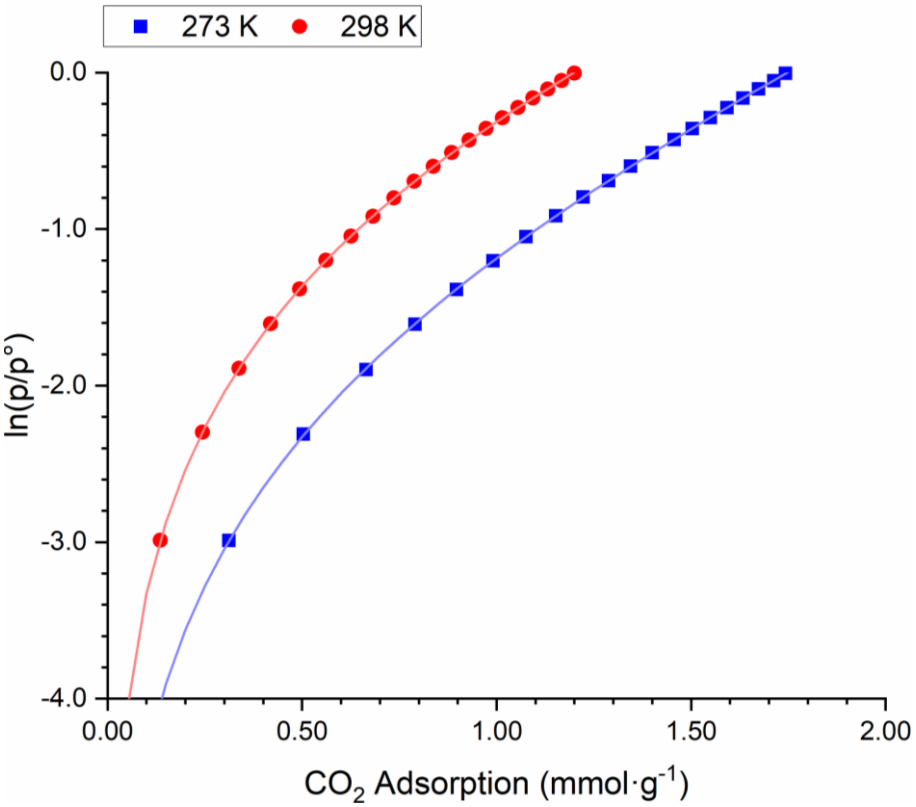

*Figure D-92 Virial analysis fitting plot for **PTPA-FLR-SNx** CO_2 adsorption isotherm*

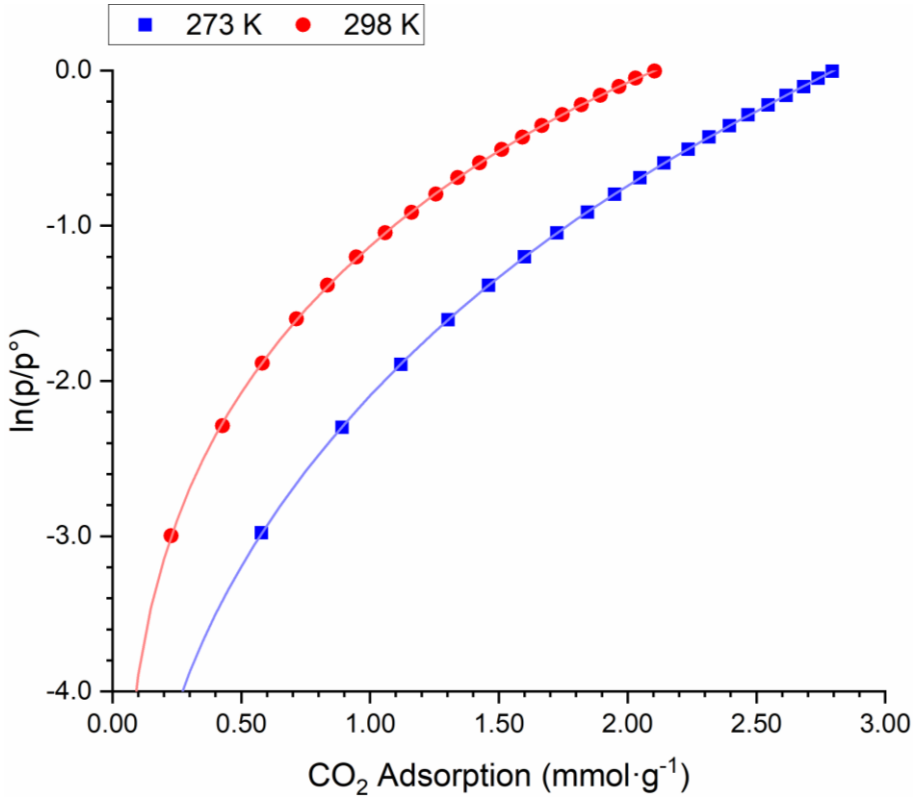

*Figure D-93 Virial analysis fitting plot for **PTPA-FLR-SR** CO_2 adsorption isotherm*

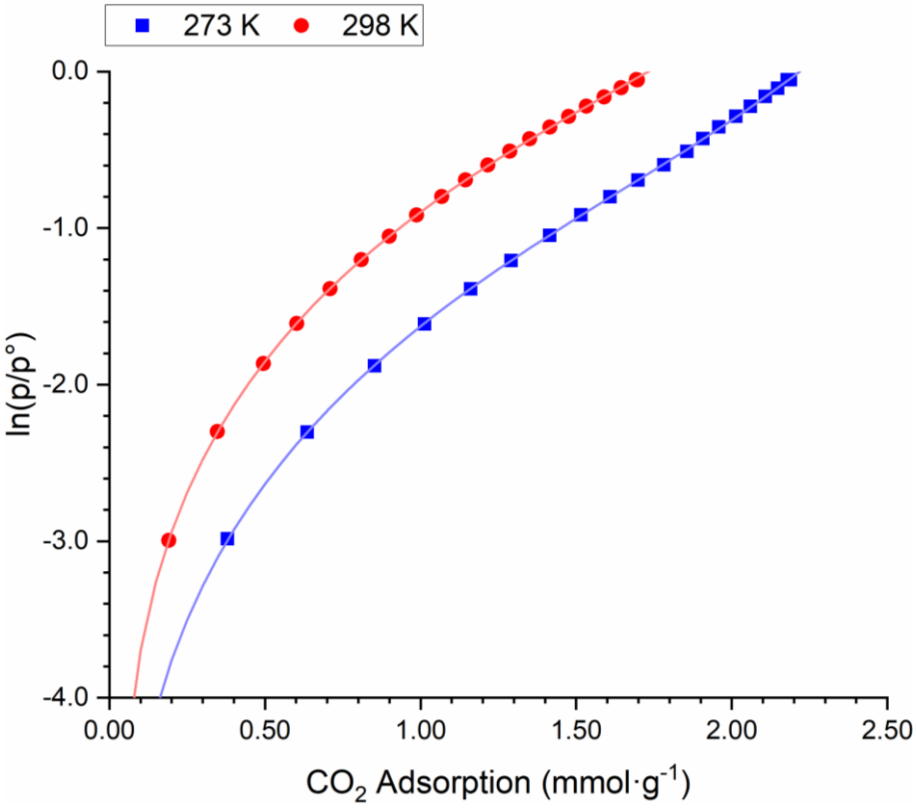

*Figure D-94 Virial analysis fitting plot for **PTPB-FLR-SN** CO_2 adsorption isotherm*

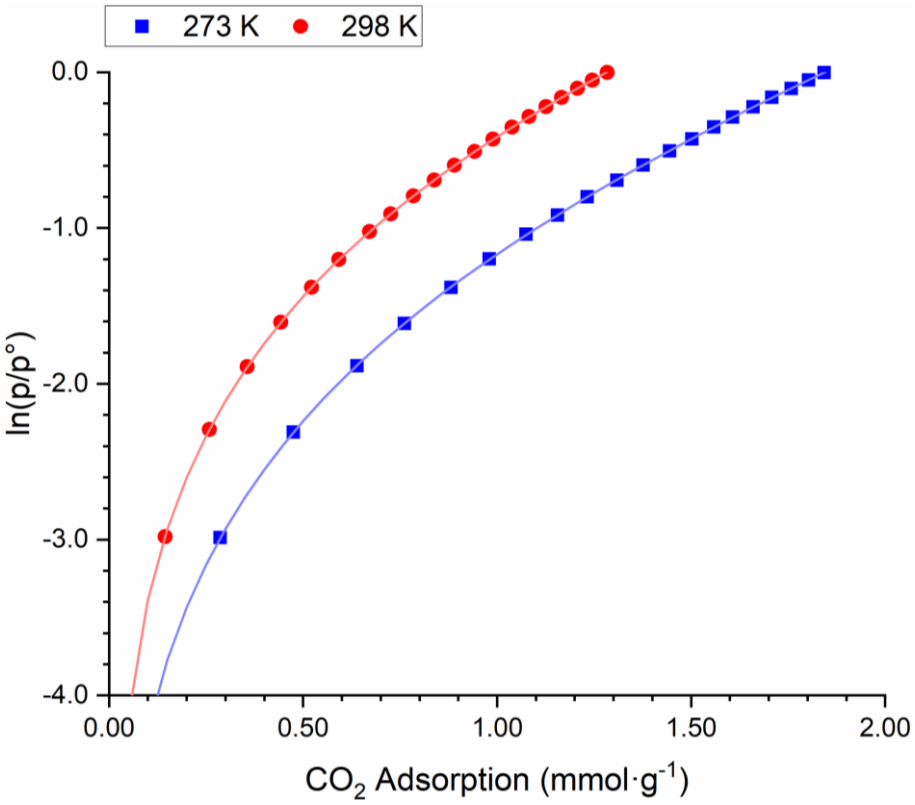

*Figure D-95 Virial analysis fitting plot for **PTPB-FLR-SNx** CO_2 adsorption isotherm*

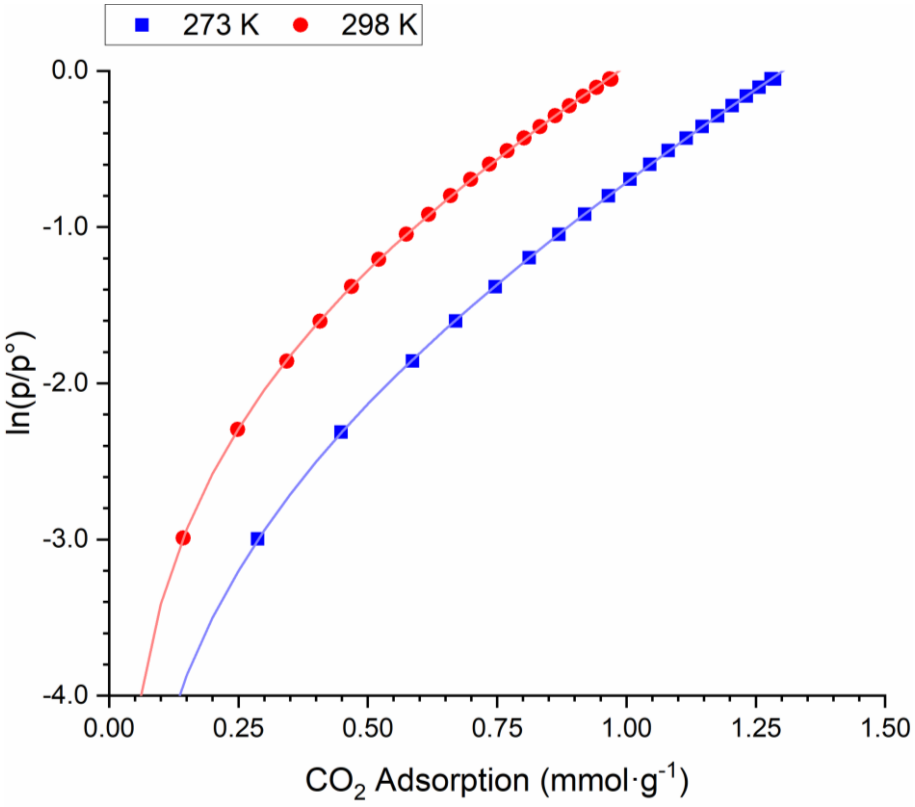

*Figure D-96 Virial analysis fitting plot for **PTPB-FLR-SR** CO_2 adsorption isotherm*

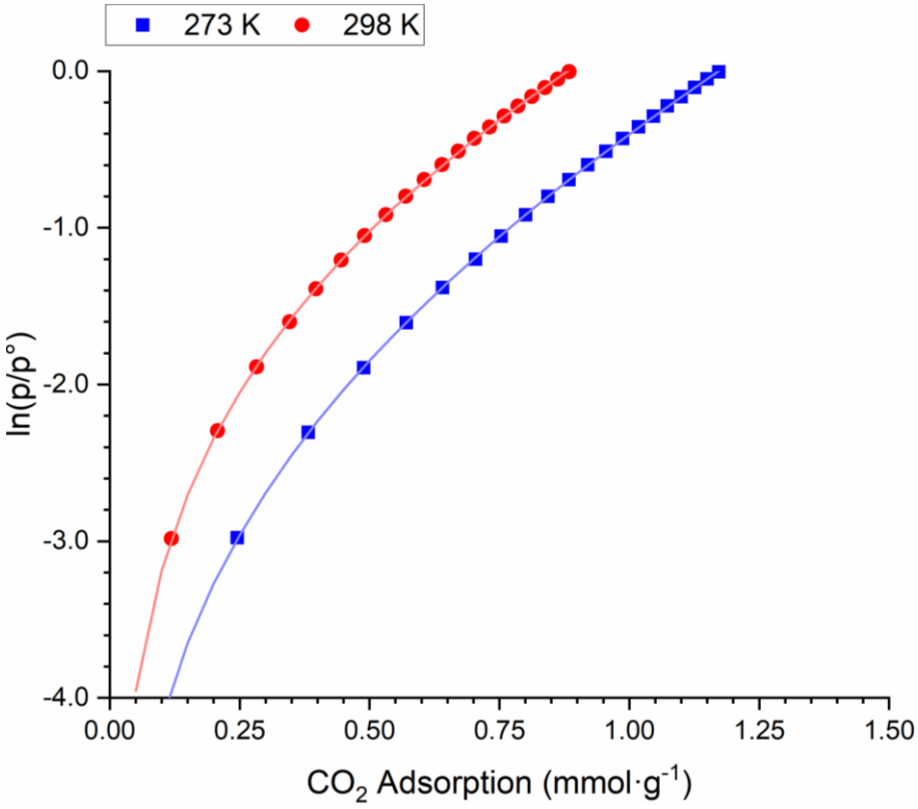

*Figure D-97 Virial analysis fitting plot for **PTPB-FLR-SRx** CO_2 adsorption isotherm*

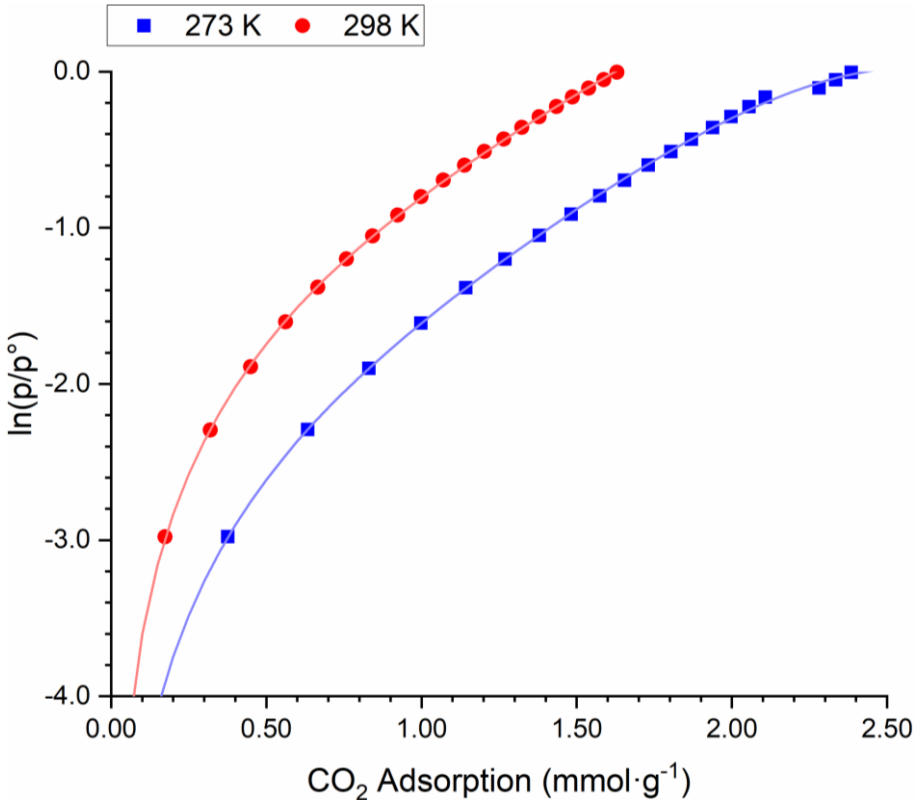

*Figure D-98 Virial analysis fitting plot for **PTPT-BZN-SN** CO_2 adsorption isotherm*

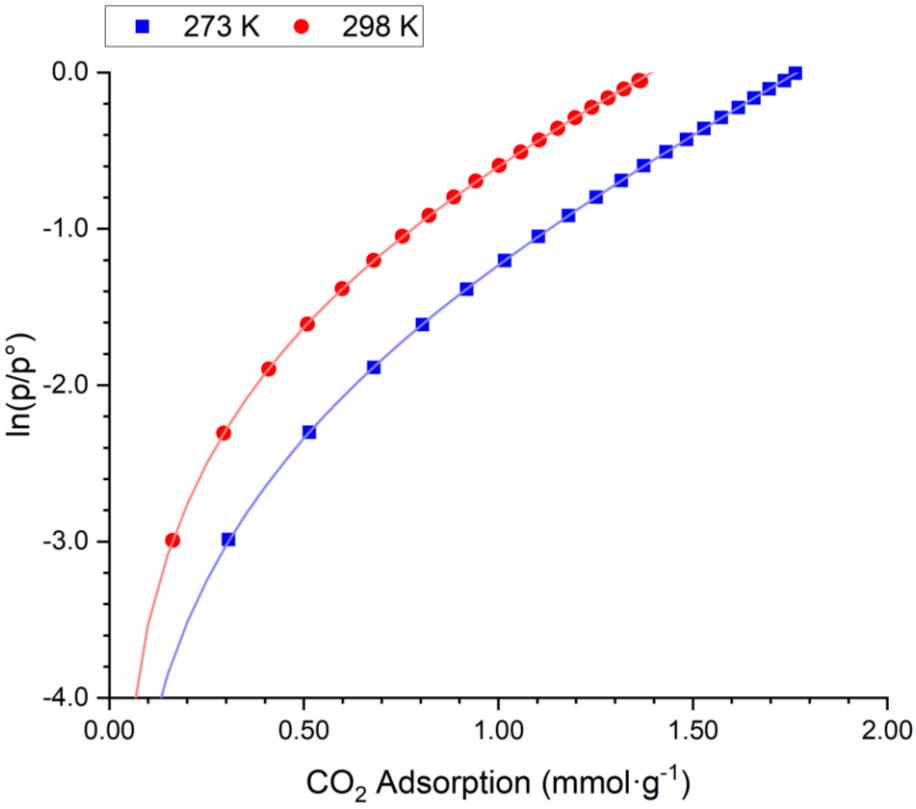

*Figure D-99 Virial analysis fitting plot for **PTPT-BZN-SNx** CO_2 adsorption isotherm*

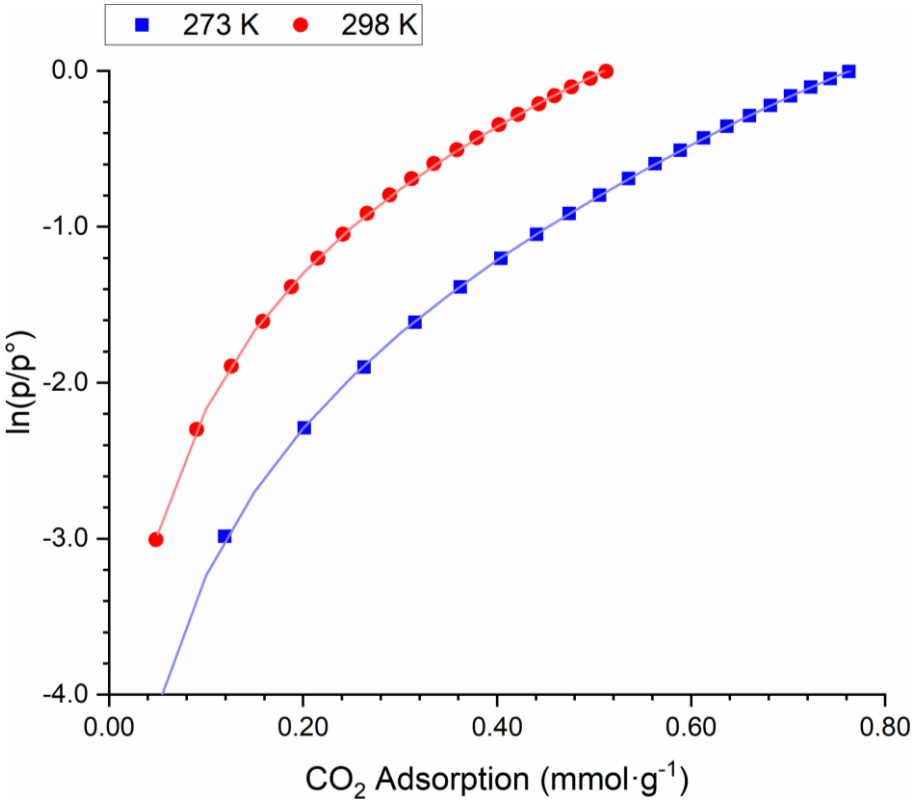

*Figure D-100 Virial analysis fitting plot for **PTPT-BZN-SR** CO_2 adsorption isotherm*

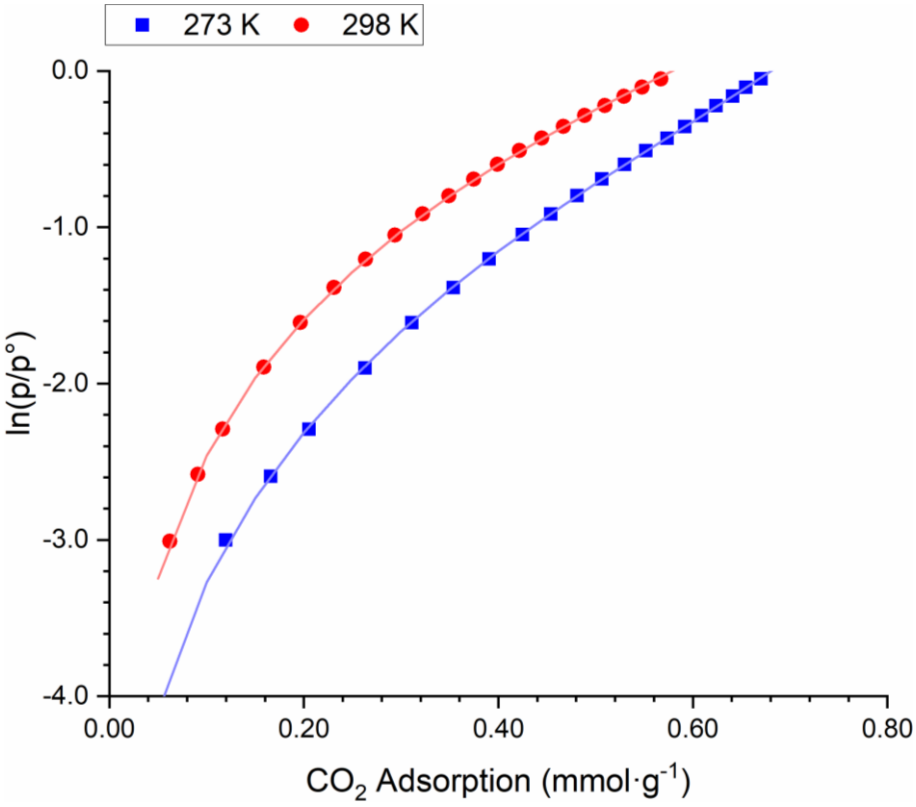

*Figure D-101 Virial analysis fitting plot for **PTPT-BZN-SRx** CO_2 adsorption isotherm*

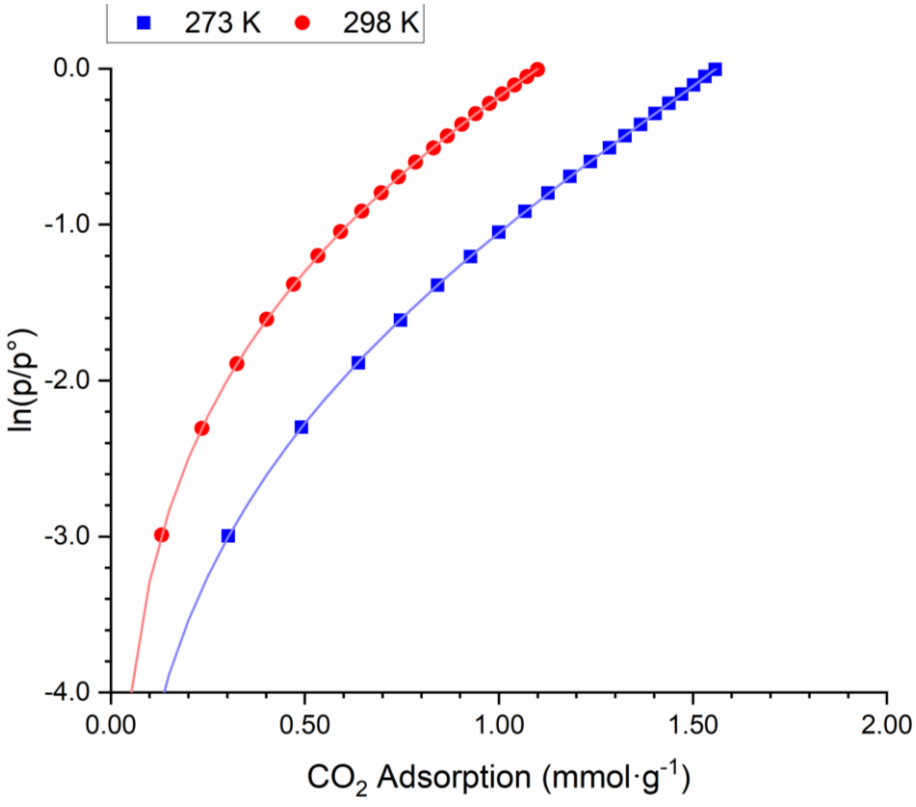

*Figure D-102 Virial analysis fitting plot for **PTPT-FLR-SN** CO_2 adsorption isotherm*

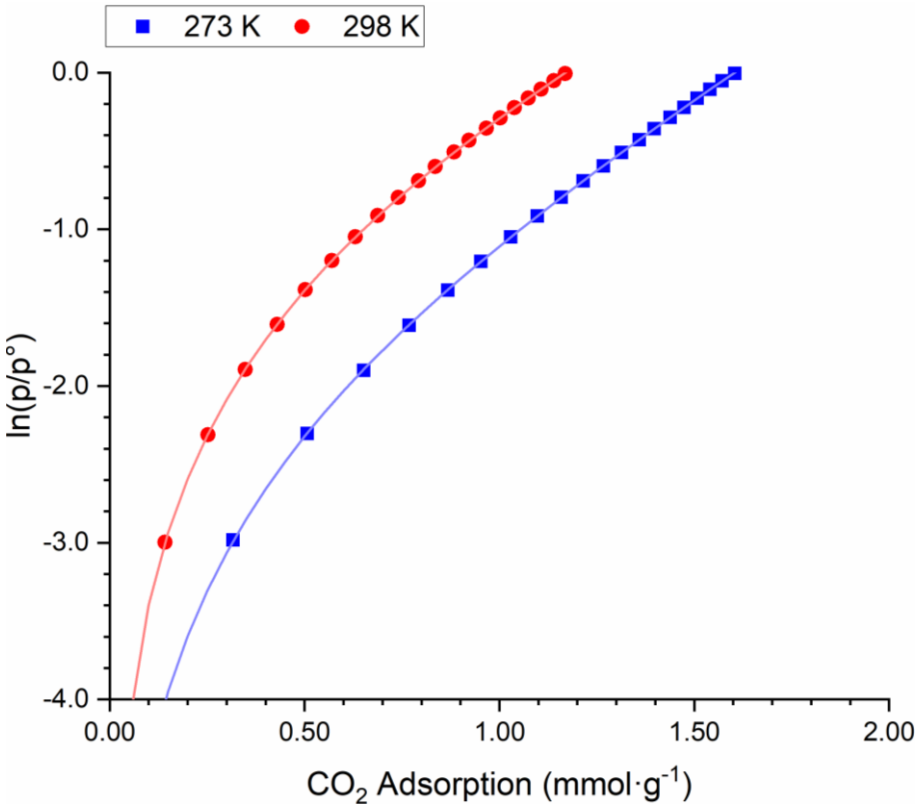

*Figure D-103 Virial analysis fitting plot for **PTPT-FLR-SNx** CO_2 adsorption isotherm*

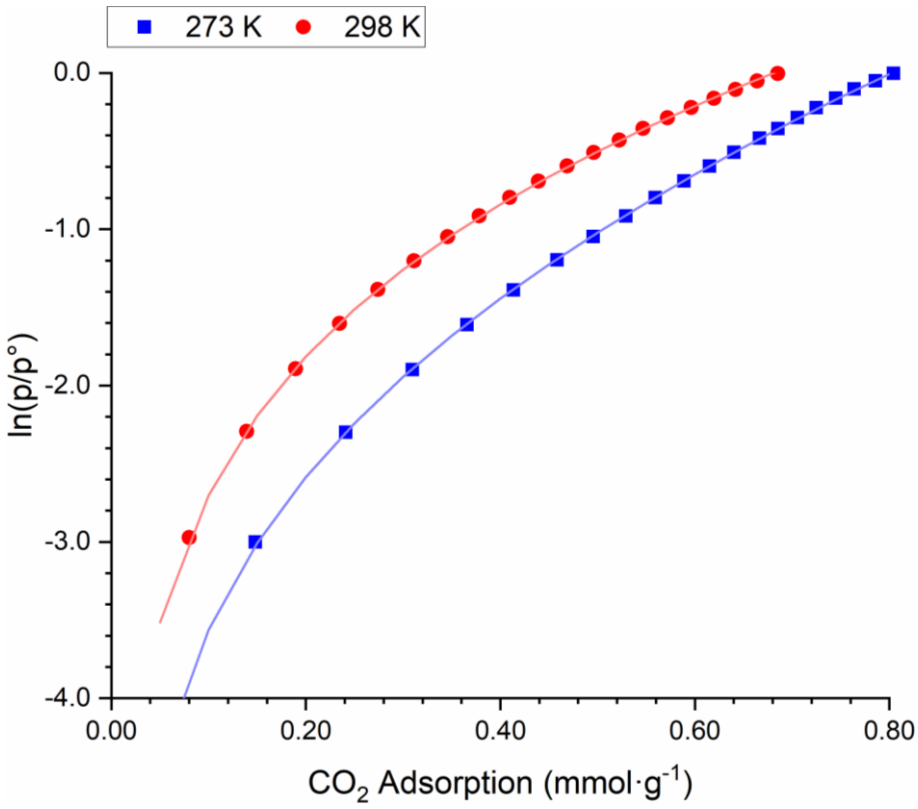

*Figure D-104 Virial analysis fitting plot for **PTPT-FLR-SR** CO_2 adsorption isotherm*

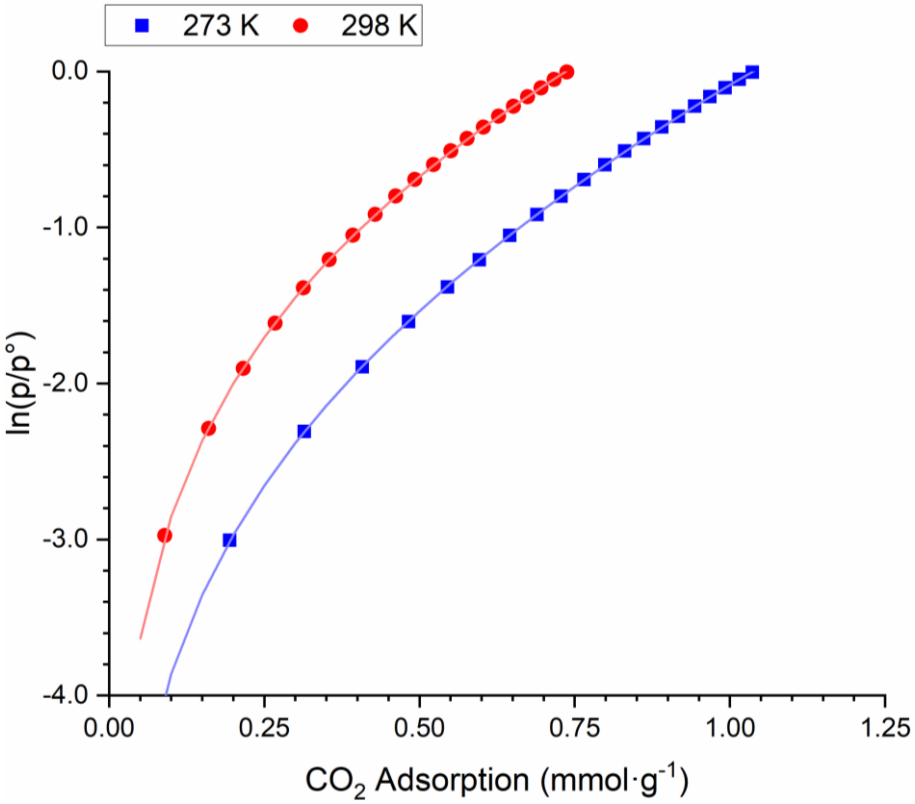

*Figure D-105 Virial analysis fitting plot for **PTPT-FLR-SNx** CO_2 adsorption isotherm*

D.2.4 Isosteric Enthalpy of Adsorption Plots

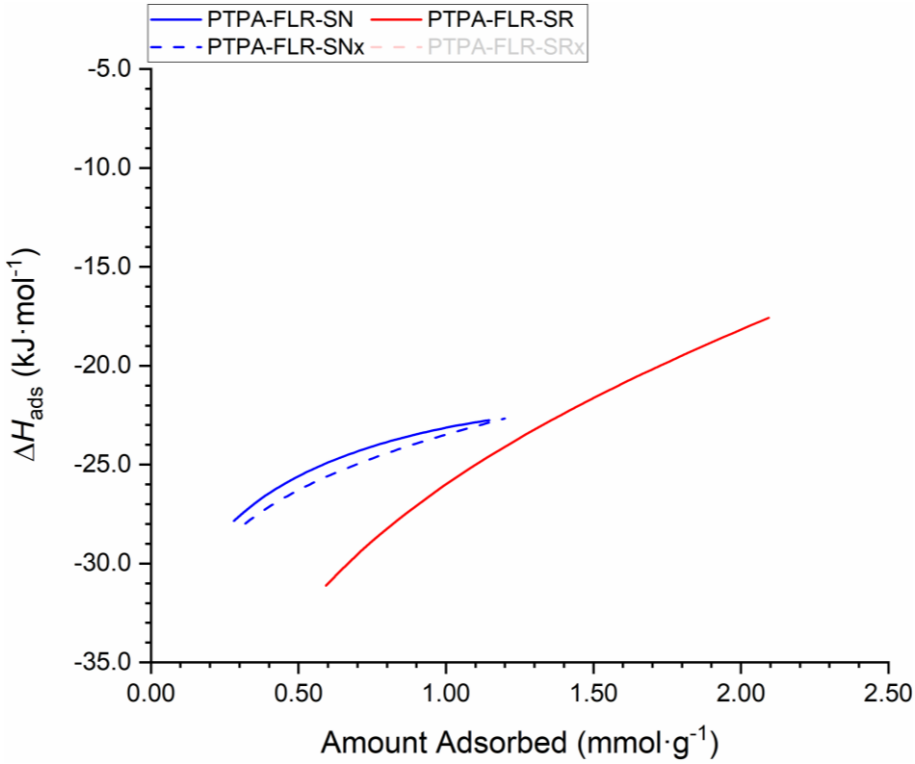

*Figure D-106 Isosteric enthalpy of adsorption over the valid range of **PTPA-FLR** from different approaches. **SN** and **SR** refer to normal and reversed approaches, respectively, and letter **x** refers to the syntheses without added sodium bromide.*

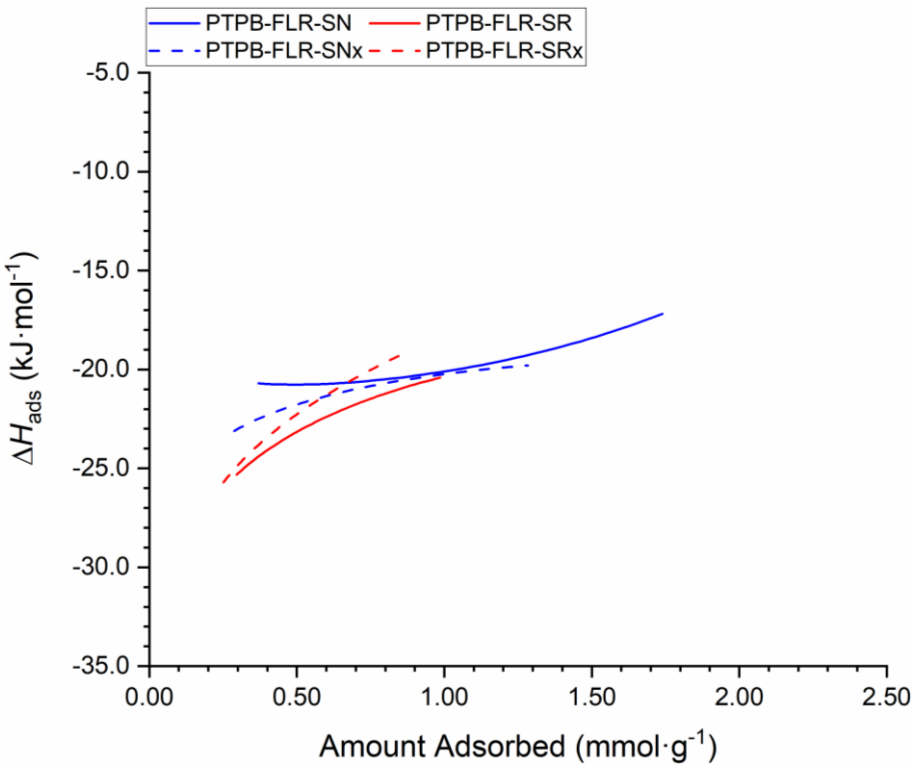

*Figure D-107 Isosteric enthalpy of adsorption over the valid range of **PTPB-FLR** from different approaches. **SN** and **SR** refer to normal and reversed approaches, respectively, and letter **x** refers to the syntheses without added sodium bromide.*

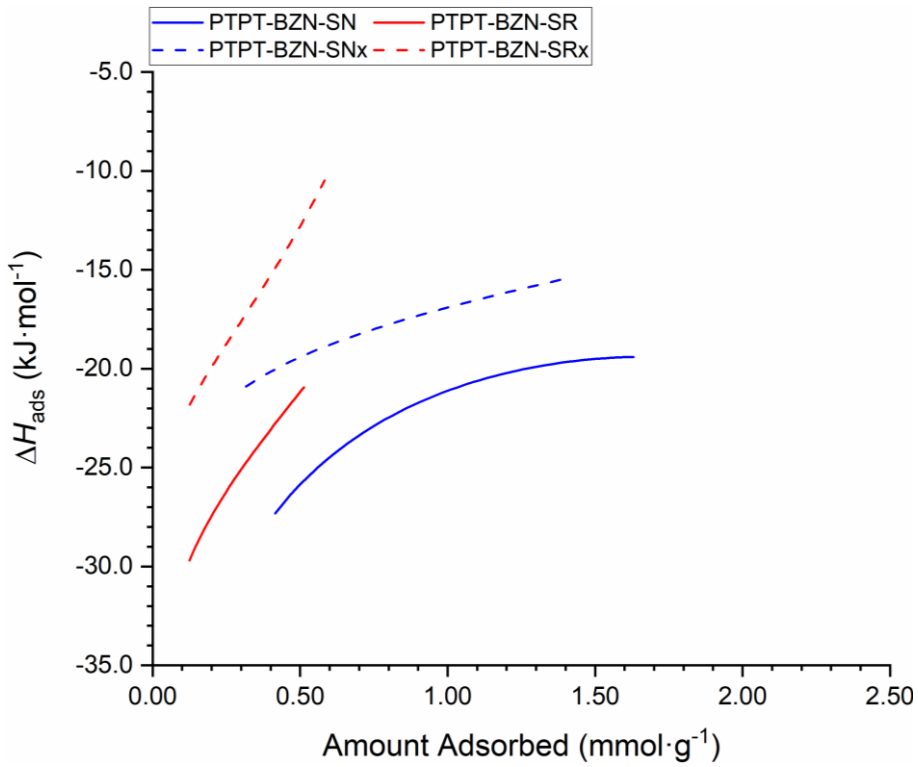

*Figure D-108 Isosteric enthalpy of adsorption over the valid range of **PTPT-BZN** from different approaches. **SN** and **SR** refer to normal and reversed approaches, respectively, and letter **x** refers to the syntheses without added sodium bromide.*

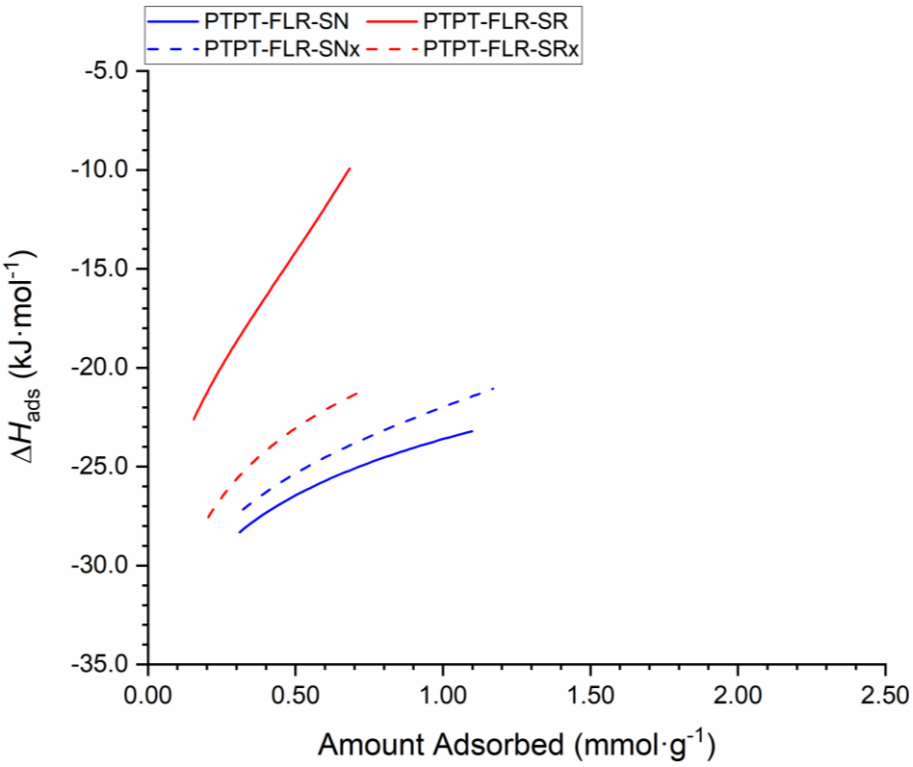

*Figure D-109 Isosteric enthalpy of adsorption over the valid range of **PTPT-FLR** from different approaches. **SN** and **SR** refer to normal and reversed approaches, respectively, and letter **x** refers to the syntheses without added sodium bromide.*

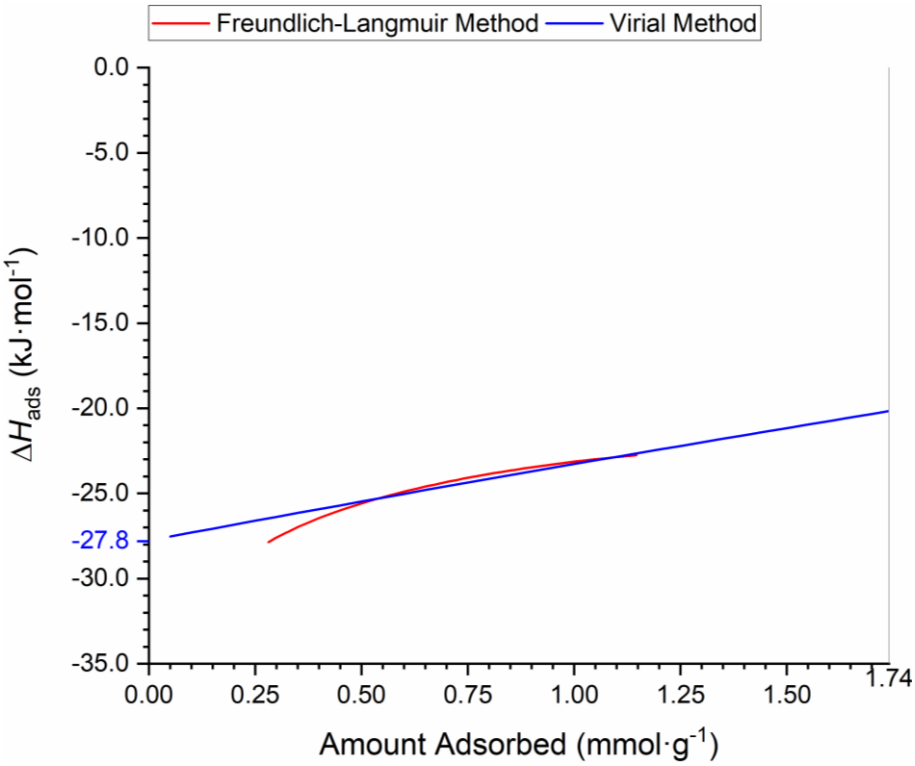

*Figure D-110 Comparison between isosteric enthalpies of adsorption from Langmuir model (red) and virial analysis (blue) in the range from zero adsorption to maximum adsorption at relative pressure 0.95 and 273 K (grey line) for **PTPA-FLR-SN**. The blue number on the y-axis is the estimated isosteric enthalpy of adsorption at zero coverage ($\Delta H°_{ads}$).*

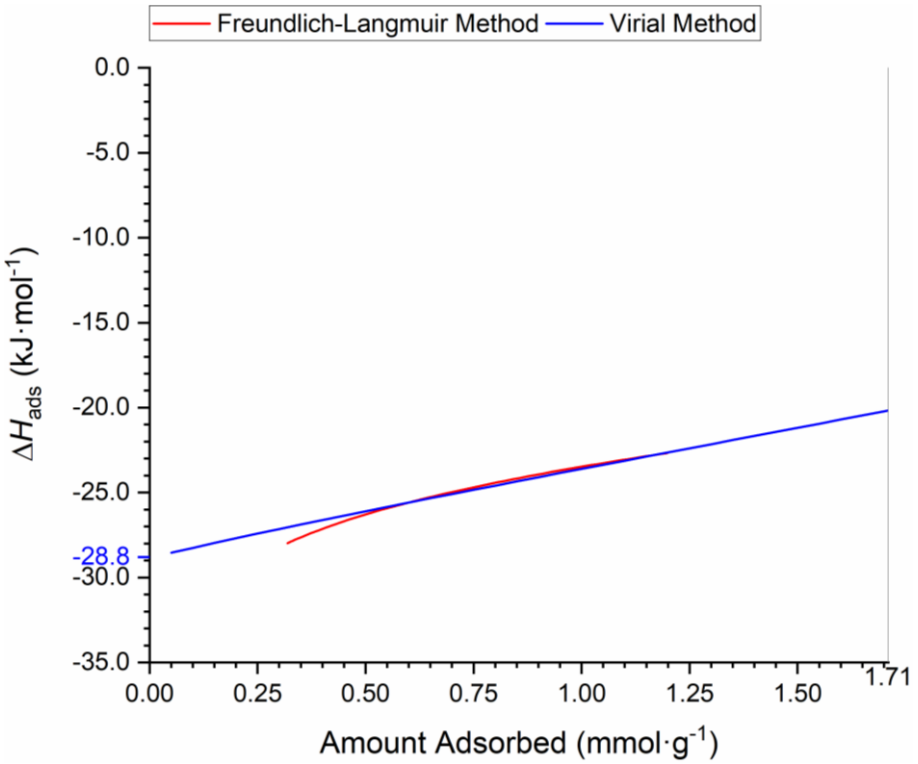

*Figure D-111 Comparison between isosteric enthalpies of adsorption from Langmuir model (red) and virial analysis (blue) in the range from zero adsorption to maximum adsorption at relative pressure 0.95 and 273 K (grey line) for **PTPA-FLR-SNx**. The blue number on the y-axis is the estimated isosteric enthalpy of adsorption at zero coverage ($\Delta H°_{ads}$).*

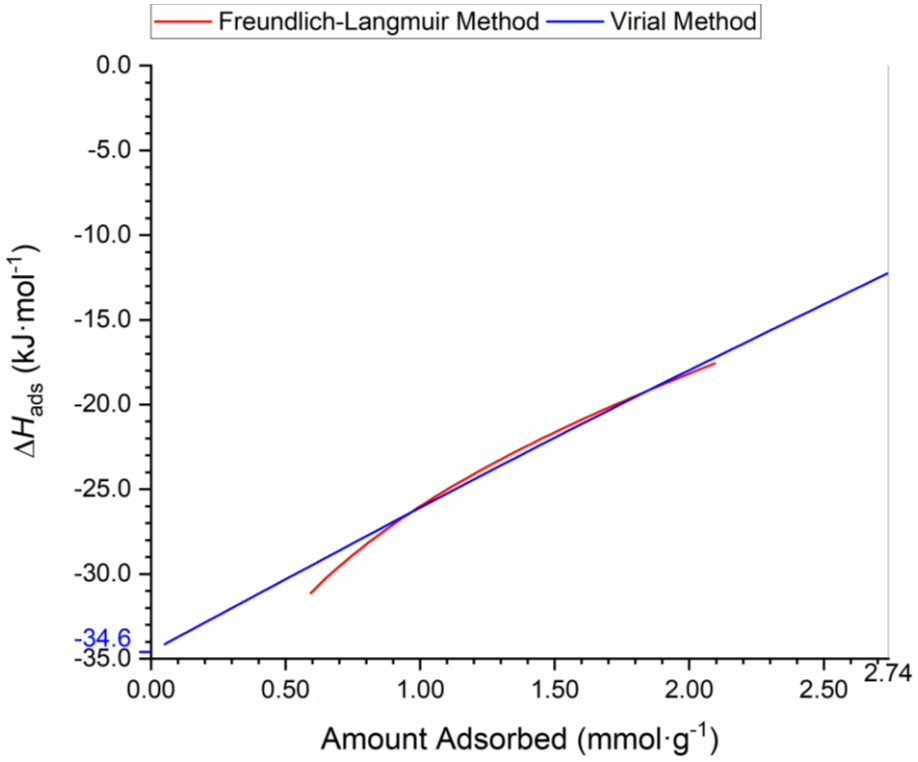

*Figure D-112 Comparison between isosteric enthalpies of adsorption from Langmuir model (red) and virial analysis (blue) in the range from zero adsorption to maximum adsorption at relative pressure 0.95 and 273 K (grey line) for **PTPA-FLR-SR**. The blue number on the y-axis is the estimated isosteric enthalpy of adsorption at zero coverage ($\Delta H°_{ads}$).*

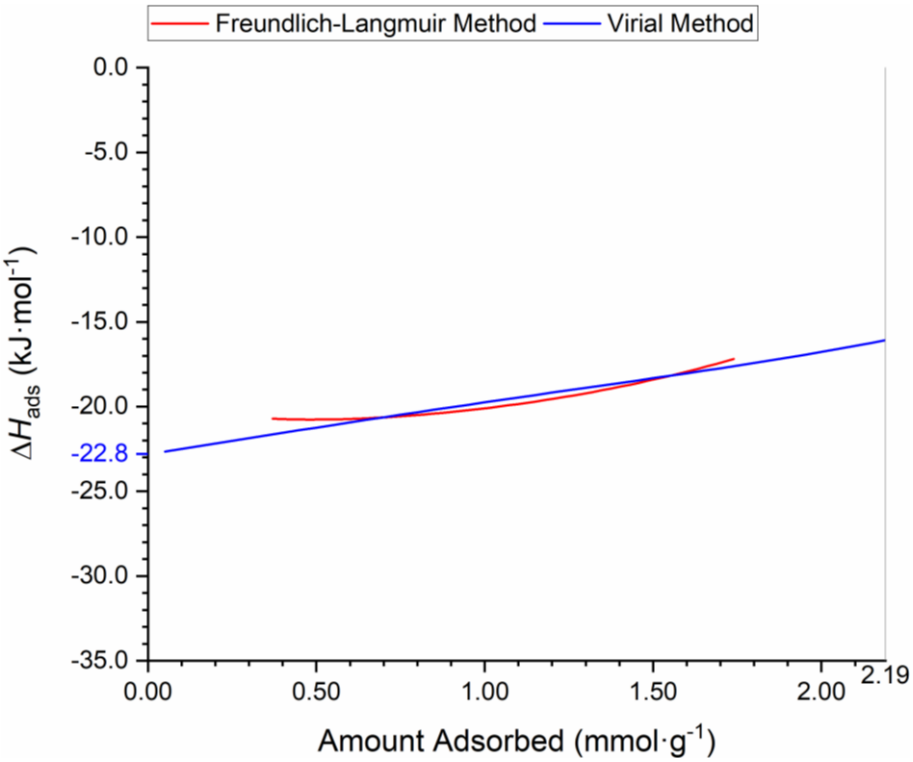

*Figure D-113 Comparison between isosteric enthalpies of adsorption from Langmuir model (red) and virial analysis (blue) in the range from zero adsorption to maximum adsorption at relative pressure 0.95 and 273 K (grey line) for **PTPB-FLR-SN**. The blue number on the y-axis is the estimated isosteric enthalpy of adsorption at zero coverage ($\Delta H°_{ads}$).*

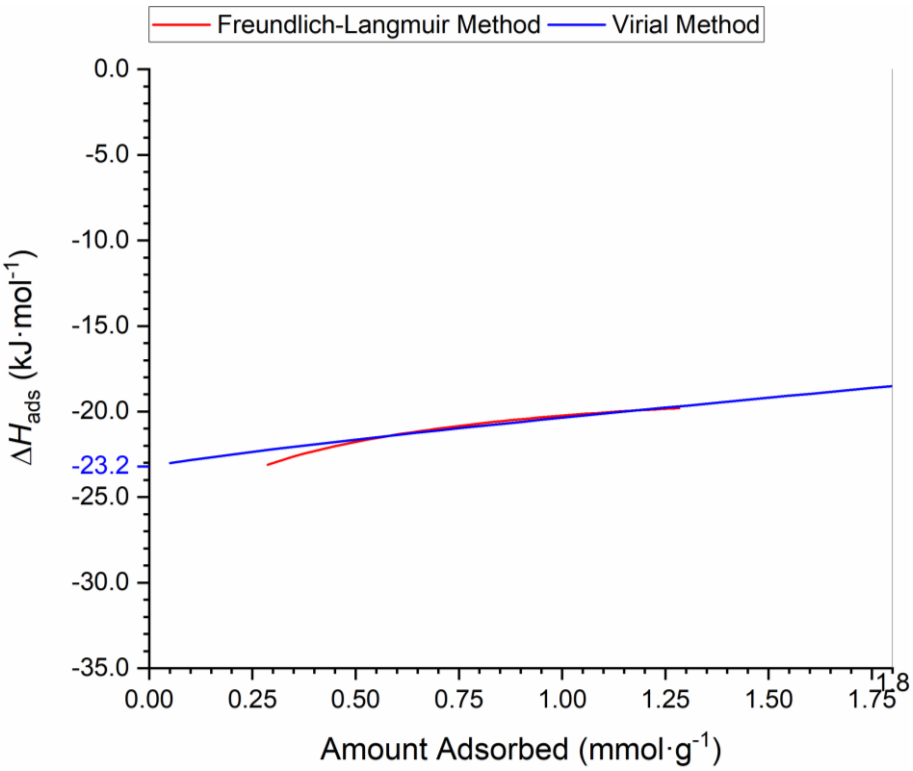

*Figure D-114 Comparison between isosteric enthalpies of adsorption from Langmuir model (red) and virial analysis (blue) in the range from zero adsorption to maximum adsorption at relative pressure 0.95 and 273 K (grey line) for **PTPB-FLR-SNx**. The blue number on the y-axis is the estimated isosteric enthalpy of adsorption at zero coverage ($\Delta H°_{ads}$).*

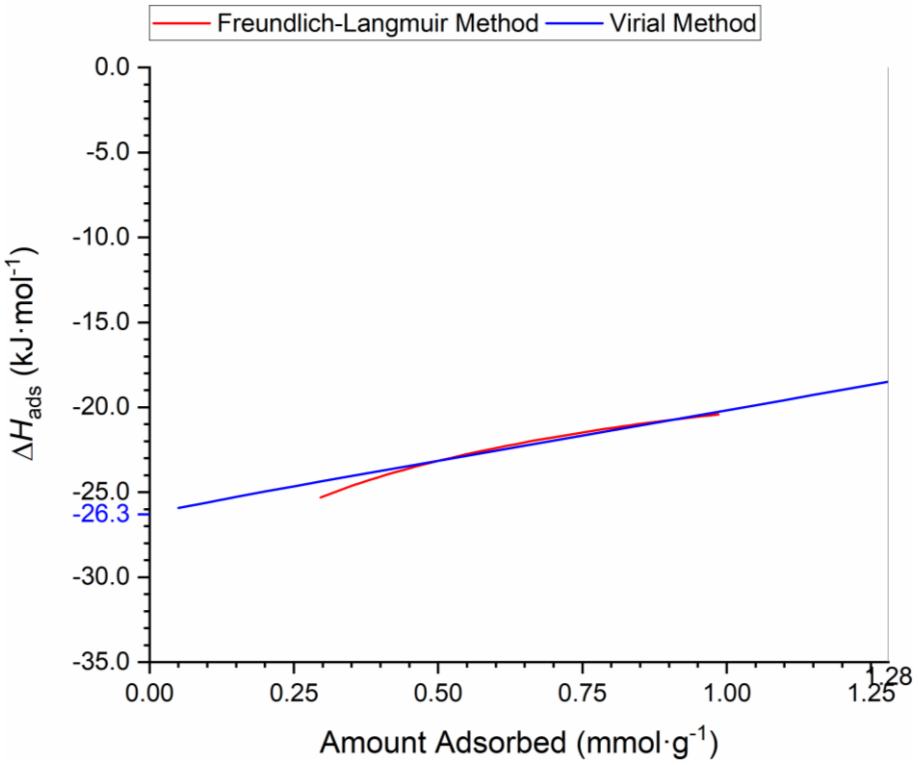

*Figure D-115 Comparison between isosteric enthalpies of adsorption from Langmuir model (red) and virial analysis (blue) in the range from zero adsorption to maximum adsorption at relative pressure 0.95 and 273 K (grey line) for **PTPB-FLR-SR**. The blue number on the y-axis is the estimated isosteric enthalpy of adsorption at zero coverage ($\Delta H°_{ads}$).*

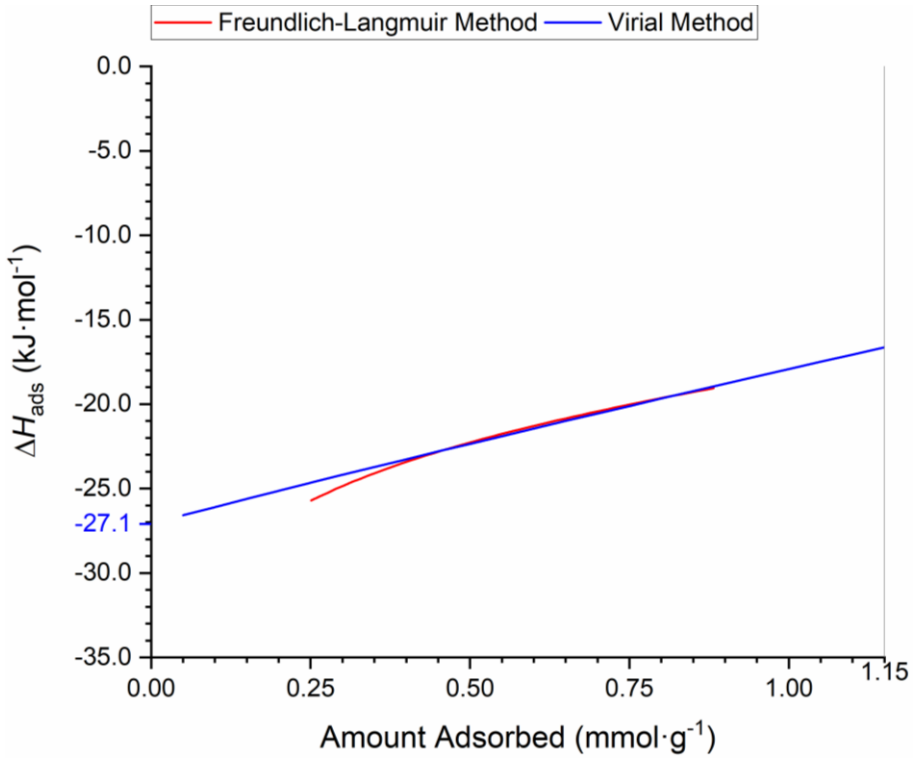

*Figure D-116 Comparison between isosteric enthalpies of adsorption from Langmuir model (red) and virial analysis (blue) in the range from zero adsorption to maximum adsorption at relative pressure 0.95 and 273 K (grey line) for **PTPB-FLR-SRx**. The blue number on the y-axis is the estimated isosteric enthalpy of adsorption at zero coverage ($\Delta H°_{ads}$).*

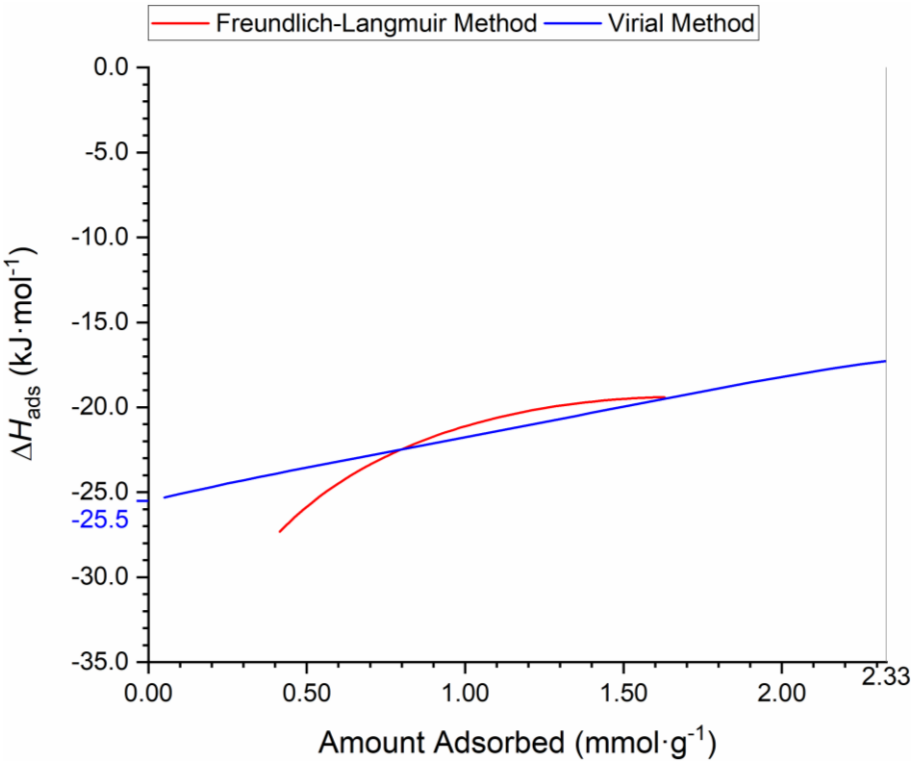

*Figure D-117 Comparison between isosteric enthalpies of adsorption from Langmuir model (red) and virial analysis (blue) in the range from zero adsorption to maximum adsorption at relative pressure 0.95 and 273 K (grey line) for **PTPT-BZN-SN**. The blue number on the y-axis is the estimated isosteric enthalpy of adsorption at zero coverage ($\Delta H°_{ads}$).*

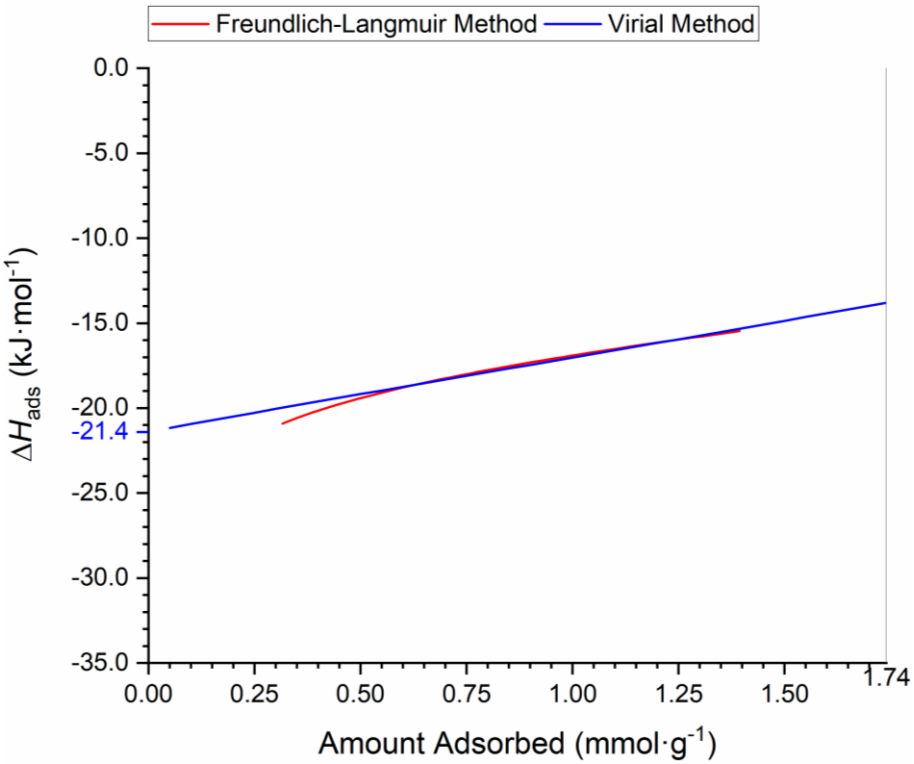

*Figure D-118 Comparison between isosteric enthalpies of adsorption from Langmuir model (red) and virial analysis (blue) in the range from zero adsorption to maximum adsorption at relative pressure 0.95 and 273 K (grey line) for **PTPT-BZN-SNx**. The blue number on the y-axis is the estimated isosteric enthalpy of adsorption at zero coverage ($\Delta H°_{ads}$).*

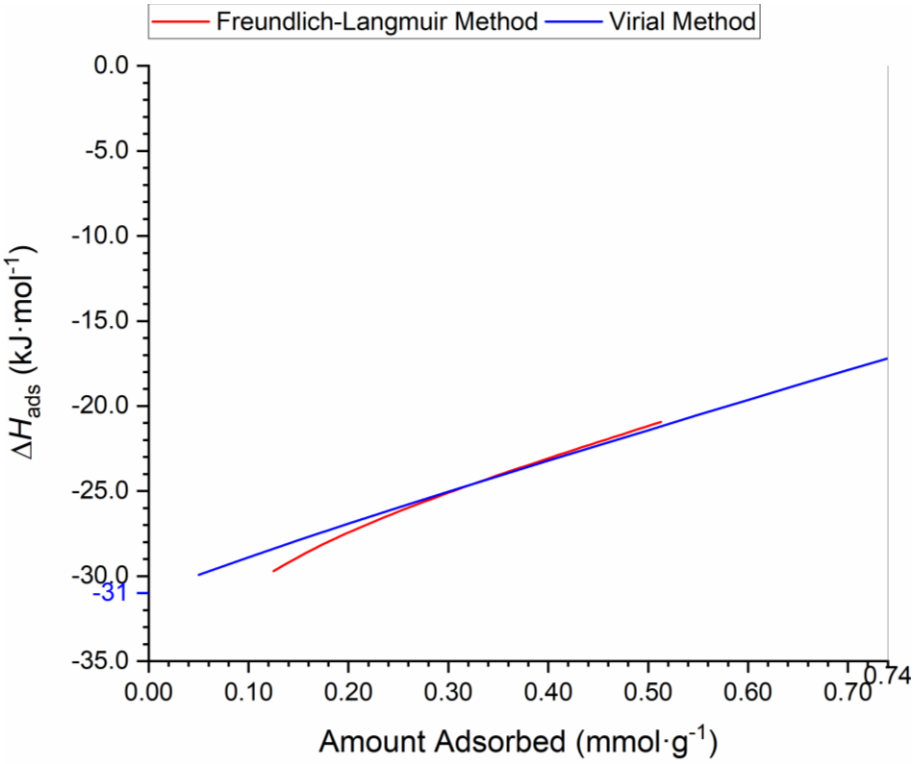

*Figure D-119 Comparison between isosteric enthalpies of adsorption from Langmuir model (red) and virial analysis (blue) in the range from zero adsorption to maximum adsorption at relative pressure 0.95 and 273 K (grey line) for **PTPT-BZN-SR**. The blue number on the y-axis is the estimated isosteric enthalpy of adsorption at zero coverage ($\Delta H°_{ads}$).*

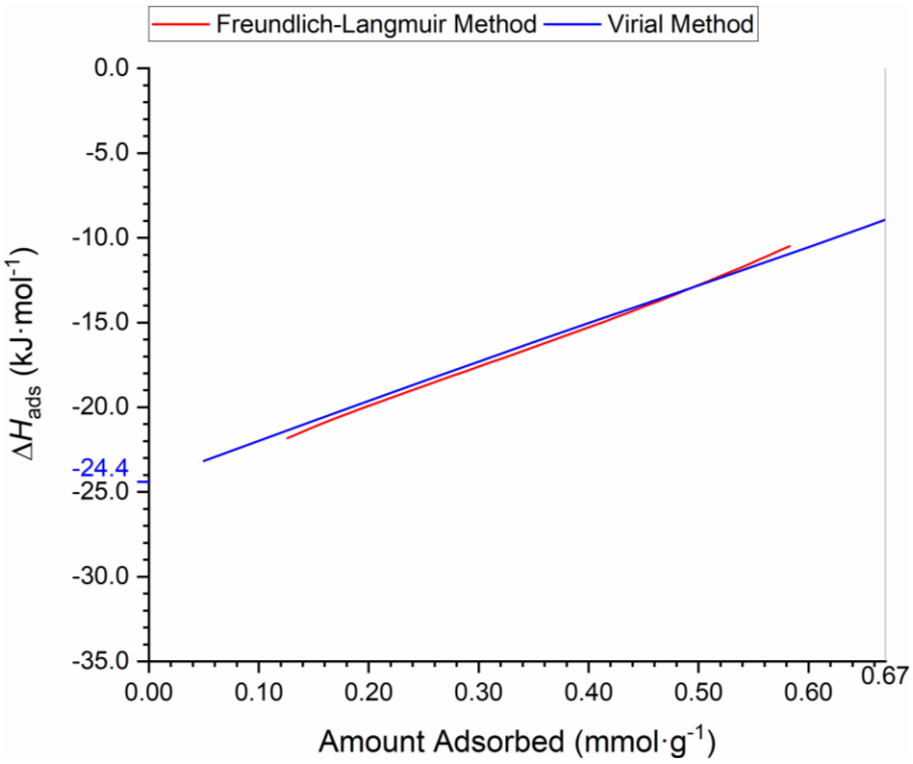

*Figure D-120 Comparison between isosteric enthalpies of adsorption from Langmuir model (red) and virial analysis (blue) in the range from zero adsorption to maximum adsorption at relative pressure 0.95 and 273 K (grey line) for **PTPT-BZN-SRx**. The blue number on the y-axis is the estimated isosteric enthalpy of adsorption at zero coverage ($\Delta H°_{ads}$).*

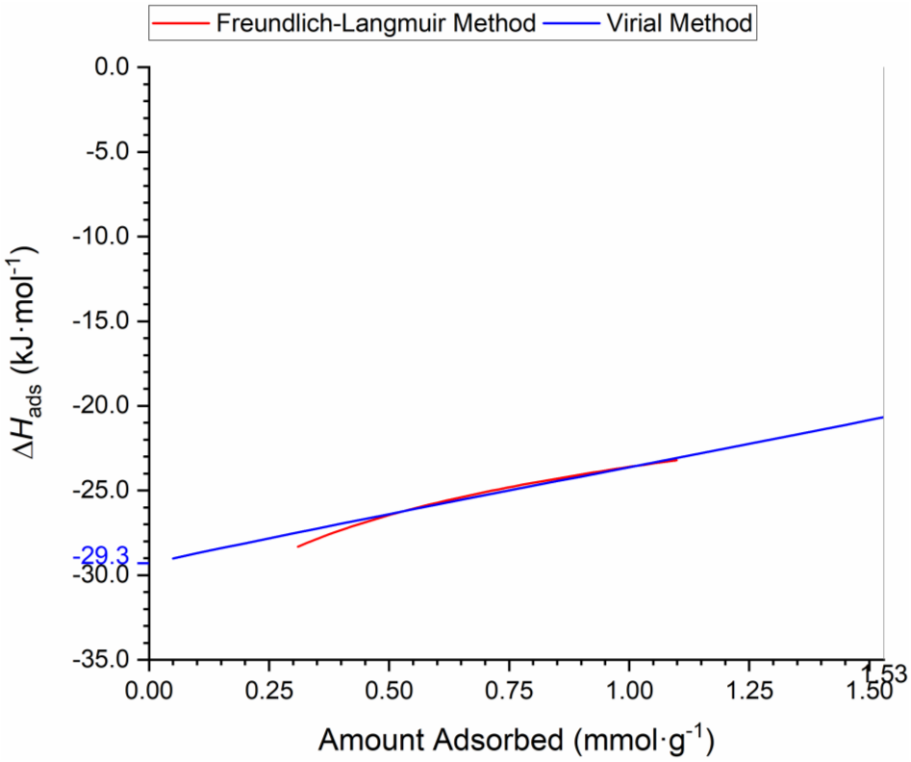

Figure D-121 Comparison between isosteric enthalpies of adsorption from Langmuir model (red) and virial analysis (blue) in the range from zero adsorption to maximum adsorption at relative pressure 0.95 and 273 K (grey line) for ***PTPT-FLR-SN****. The blue number on the y-axis is the estimated isosteric enthalpy of adsorption at zero coverage ($\Delta H°_{ads}$).*

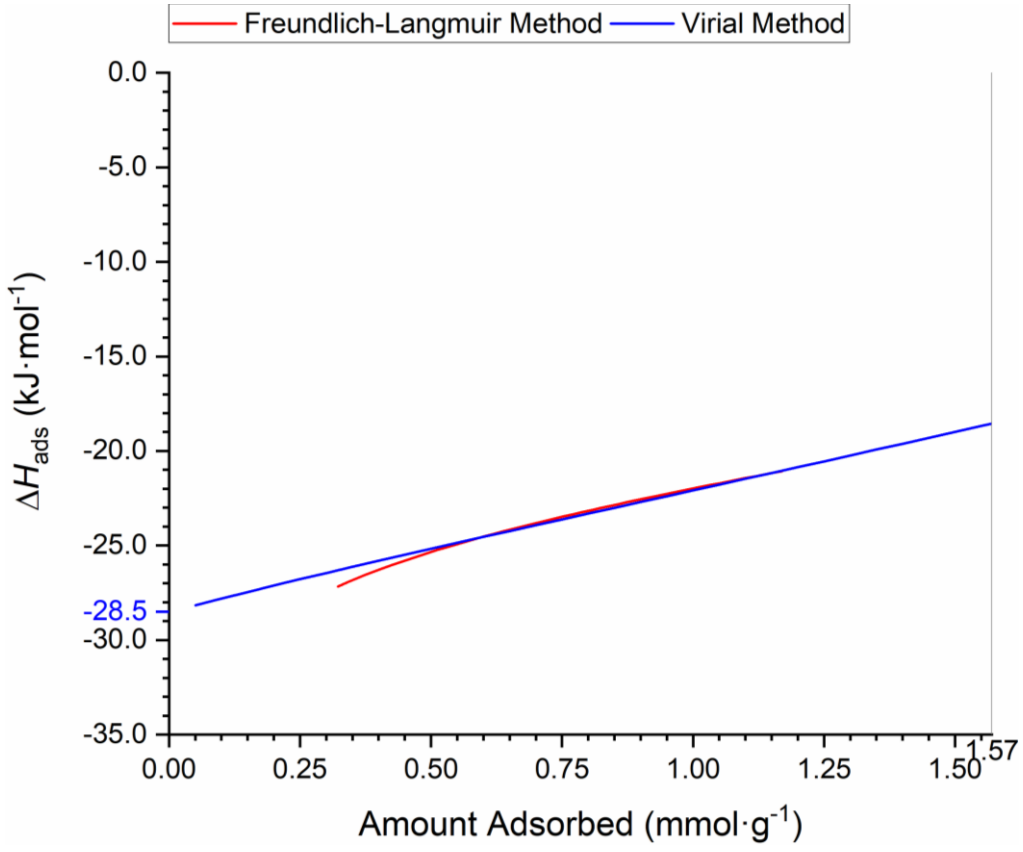

Figure D-122 Comparison between isosteric enthalpies of adsorption from Langmuir model (red) and virial analysis (blue) in the range from zero adsorption to maximum adsorption at relative pressure 0.95 and 273 K (grey line) for

***PTPT-FLR-SNx**. The blue number on the y-axis is the estimated isosteric enthalpy of adsorption at zero coverage ($\Delta H°_{ads}$).*

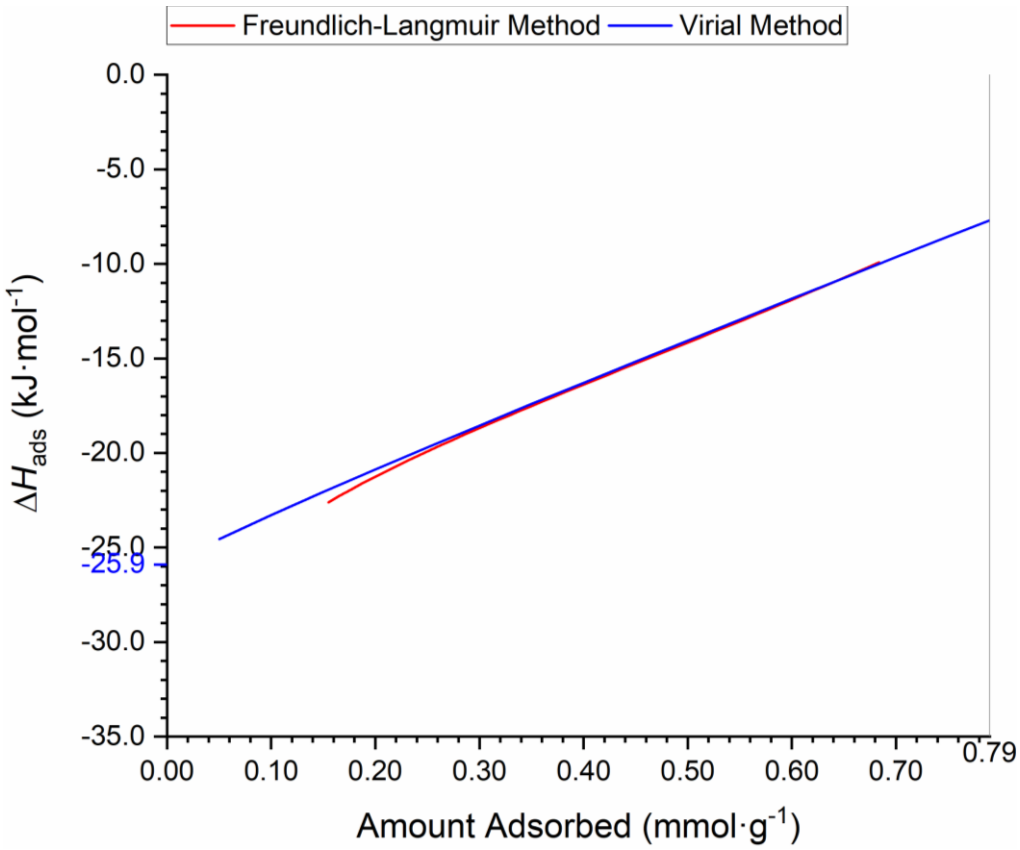

*Figure D-123 Comparison between isosteric enthalpies of adsorption from Langmuir model (red) and virial analysis (blue) in the range from zero adsorption to maximum adsorption at relative pressure 0.95 and 273 K (grey line) for **PTPT-FLR-SR**. The blue number on the y-axis is the estimated isosteric enthalpy of adsorption at zero coverage ($\Delta H°_{ads}$).*

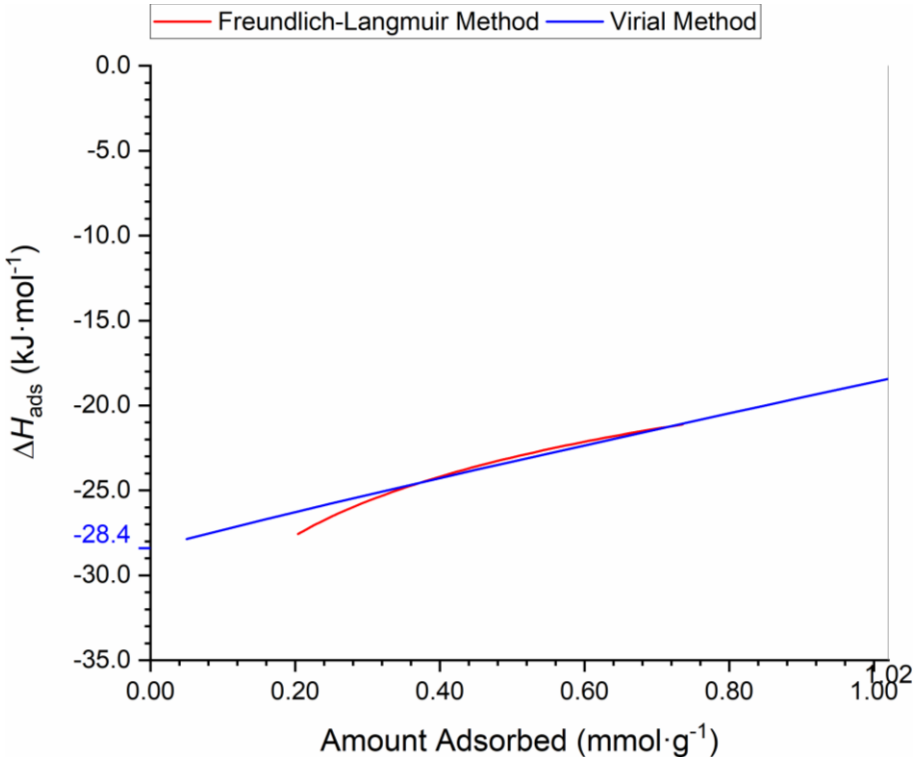

Figure D-124 Comparison between isosteric enthalpies of adsorption from Langmuir model (red) and virial analysis (blue) in the range from zero adsorption to maximum adsorption at relative pressure 0.95 and 273 K (grey line) for ***PTPT-FLR-SRx****. The blue number on the y-axis is the estimated isosteric enthalpy of adsorption at zero coverage ($\Delta H°_{ads}$).*

Appendix E Miscellaneous Data

E.1 Material Appearances

E.1.1 Polymers

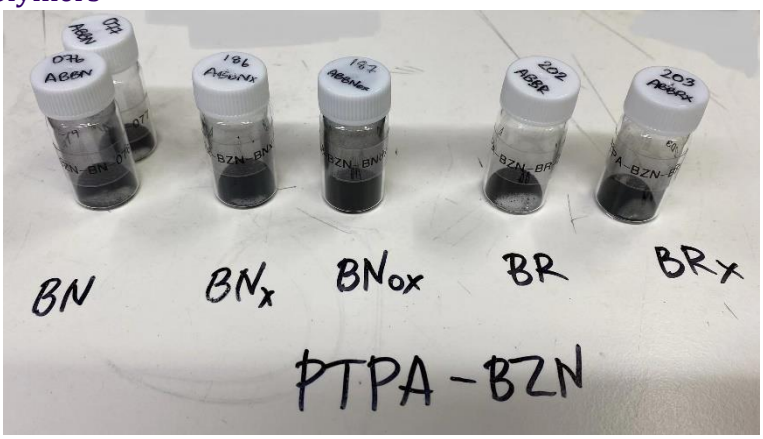

*Figure E-1 Appearances of **PTPA-BZN** materials. **PTPA-BZN-BNox** refers to a failed batch of **PTPA-BZN-BNx** in which material was accidentally oxidised during synthesis.*

*Figure E-2 Appearances of **PTPA-FLR** materials*

*Figure E-3 Appearances of **PTPB-BZN** materials*

*Figure E-4 Appearances of **PTPB-FLR** materials*

*Figure E-5 Appearances of **PTPT-BZN** materials*

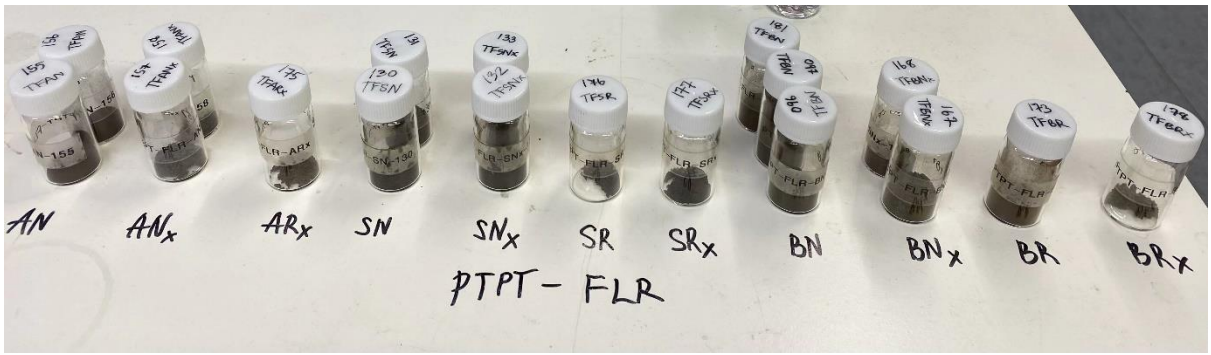

*Figure E-6 Appearances of **PTPT-FLR** materials*

E.1.2 Oligomers

*Figure E-7 Appearances of **OTPA-BZN** materials. **OTPA-BZN-BNox** refers to a failed batch of **OTPA-BZN-BNx** in which material was accidentally oxidised during synthesis.*

*Figure E-8 Appearances of **OTPA-FLR** materials*

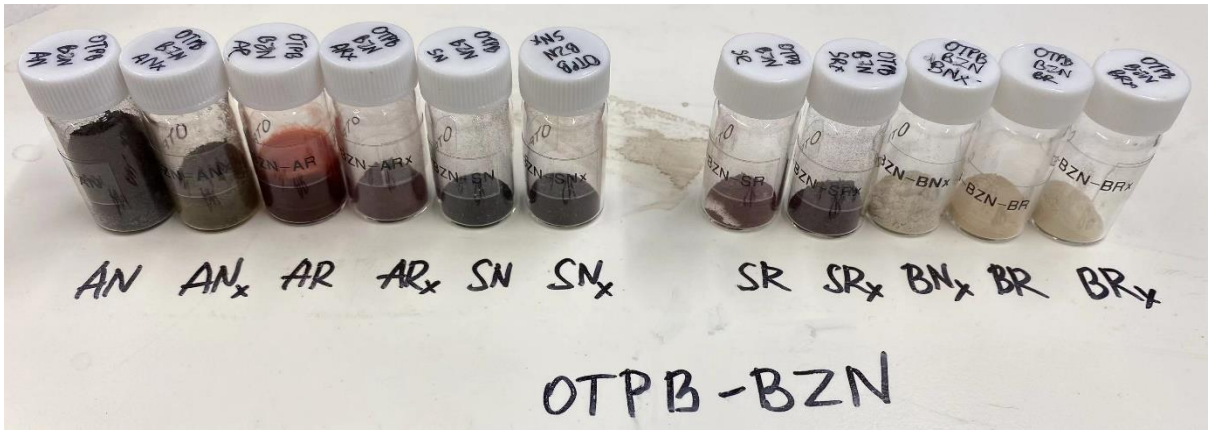

*Figure E-9 Appearances of **OTPB-BZN** materials*

*Figure E-10 Appearances of **OTPB-FLR** materials*

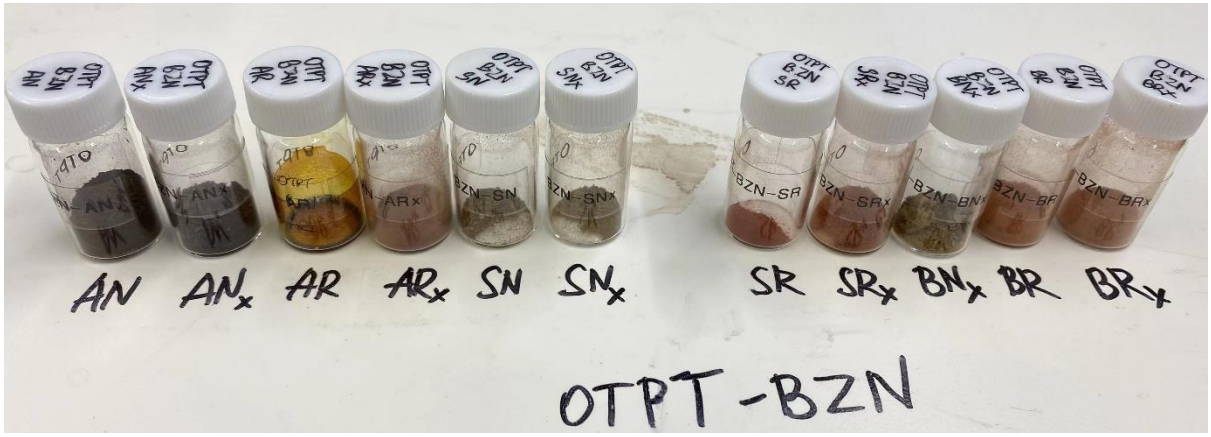

*Figure E-11 Appearances of **OTPT-BZN** materials*

*Figure E-12 Appearances of **OTPT-FLR** materials*

E.2 Additional Powder XRD Analysis Results

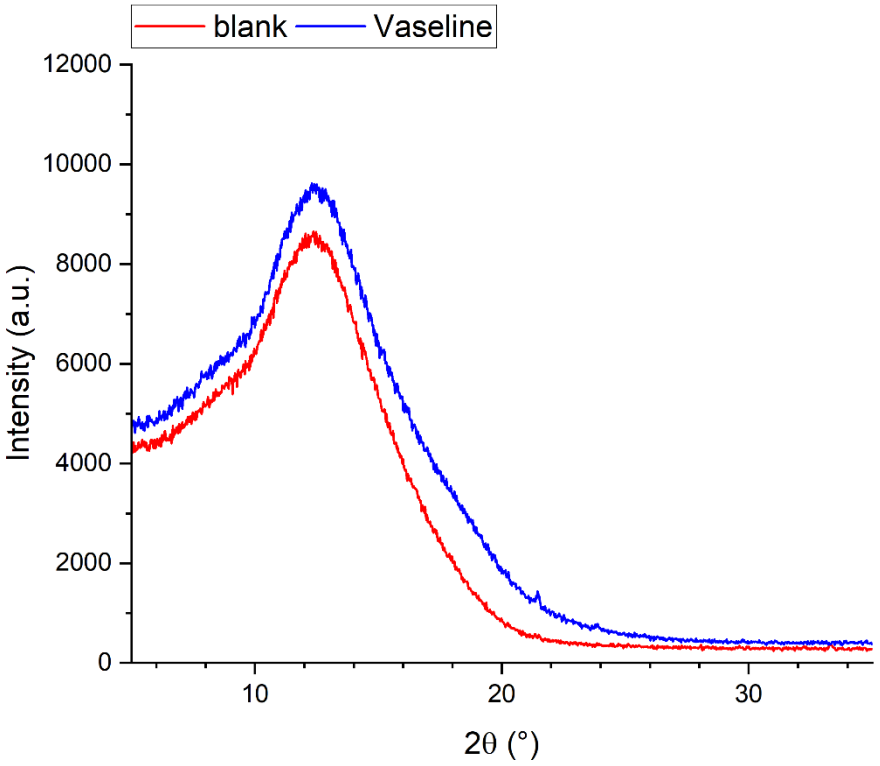

Figure E-13 XRD analysis result of an empty amorphous silicon sample holder (red) and a sample holder with vaseline (blue) from the 2θ of 5° to 35°

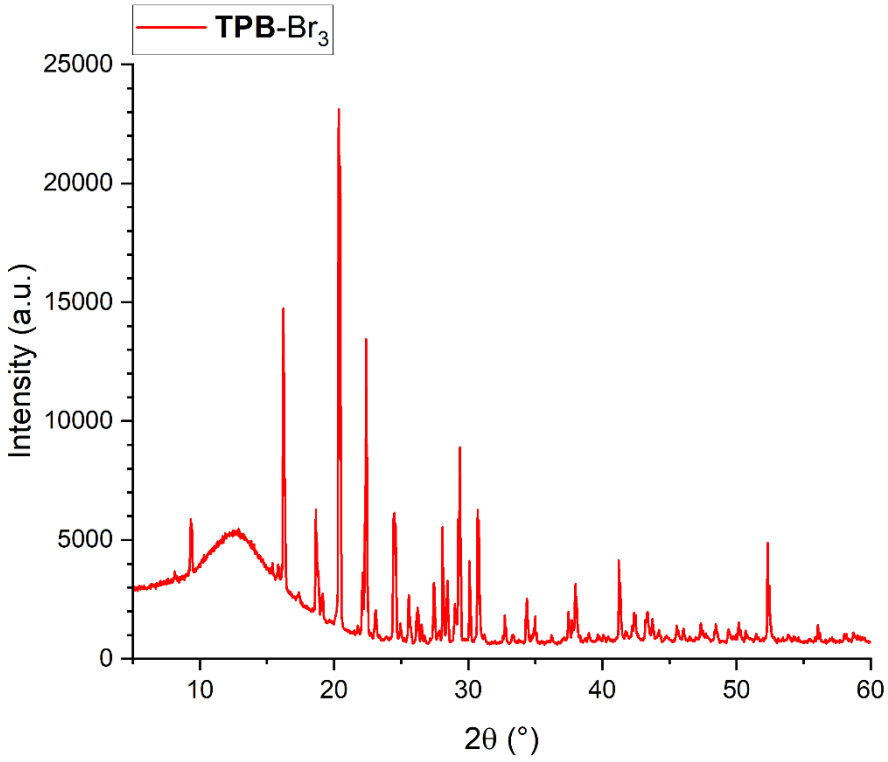

*Figure E-14 XRD analysis result of **TPB**-Br_3 core monomer from the 2θ of 5° to 60°*

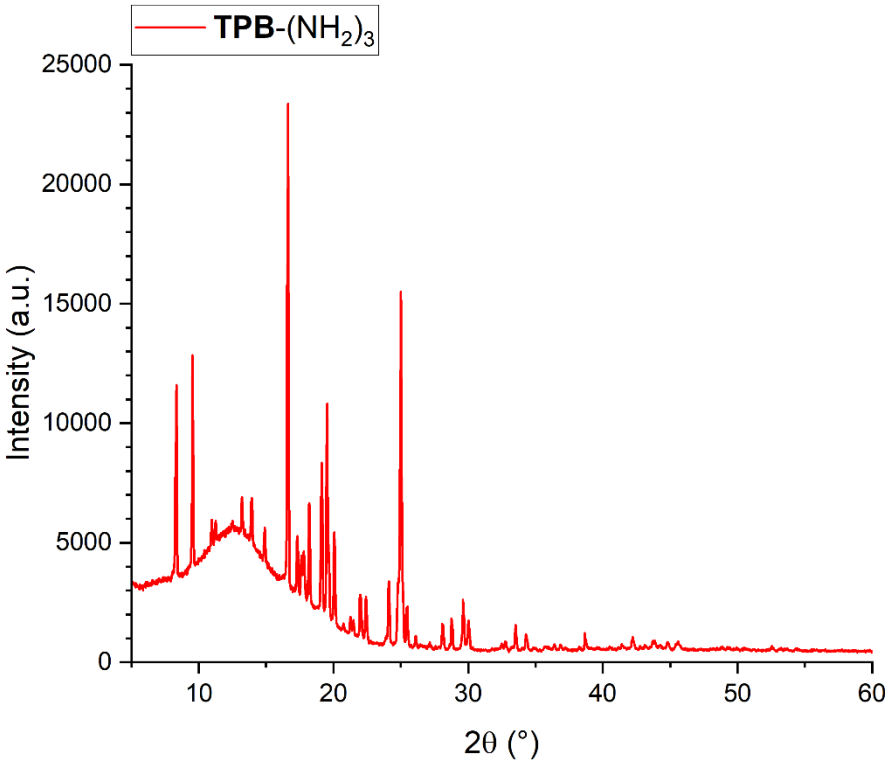

*Figure E-15 XRD analysis result of **TPB**-$(NH_2)_3$ core monomer from the 2θ of 5° to 60°*

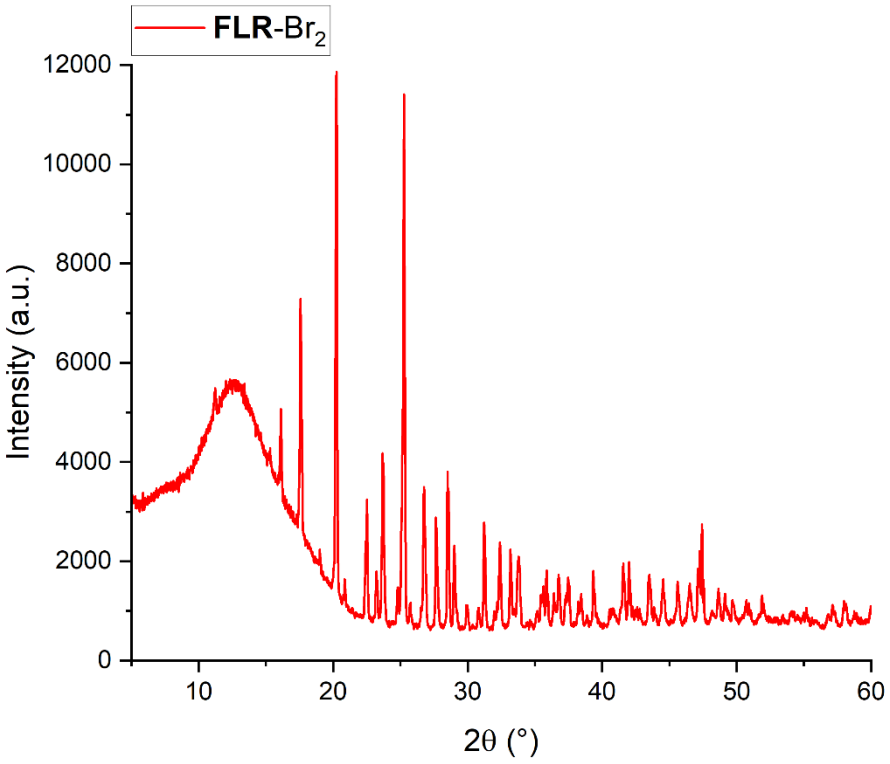

*Figure E-16 XRD analysis result of **FLR**-Br_2 linker monomer from the 2θ of 5° to 60°*

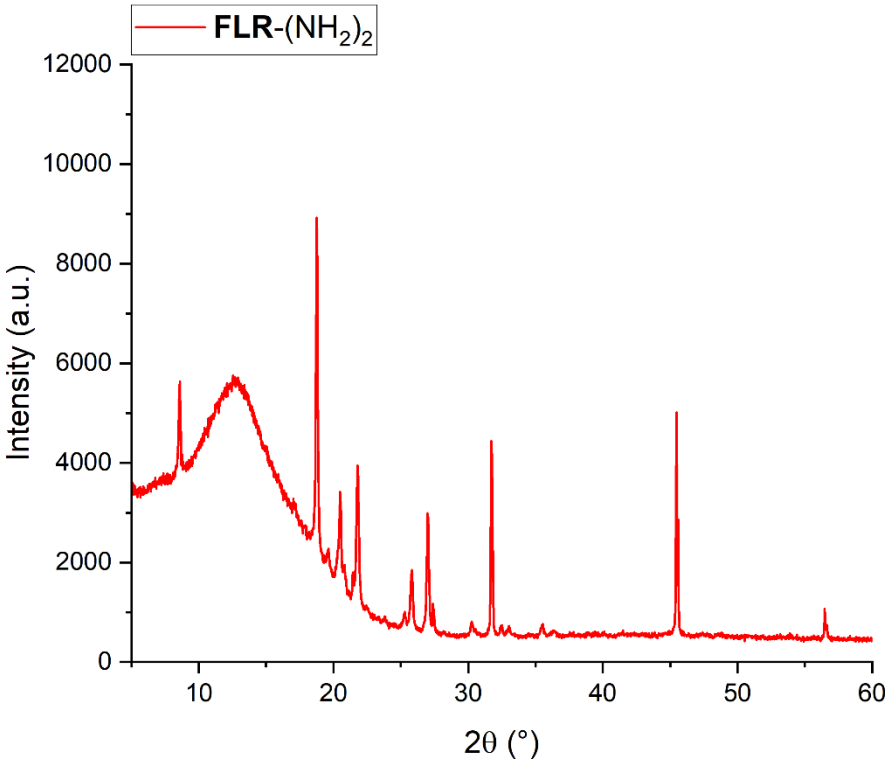

*Figure E-17 XRD analysis result of **FLR**-$(NH_2)_2$ linker monomer from the 2θ of 5° to 60°*